Title
Response of Liquefiable Sites in the Central Business District of Christchurch, New Zealand

Author
Markham, Christopher Stephen

Publication Date
2015

Response of Liquefiable Sites in the Central Business District of Christchurch, New Zealand

By

Christopher Stephen Markham

A dissertation submitted in partial satisfaction of the

requirements for the degree of

Doctor of Philosophy

in

Engineering – Civil and Environmental Engineering

in the

Graduate Division

of the

University of California, Berkeley

Committee in charge:

Professor Jonathan D. Bray, Chair
Professor Raymond B. Seed
Professor Misko Cubrinovski
Professor Douglas S. Dreger

Fall 2015

Abstract

Response of Liquefiable Sites in the
Central Business District of Christchurch, New Zealand

by

Christopher Stephen Markham

Doctor of Philosophy in Engineering – Civil and Environmental Engineering

University of California, Berkeley

Professor Jonathan D. Bray, Chair

The strong shaking of the 2010-2011 Canterbury earthquake sequence caused widespread liquefaction in much of the city of Christchurch, NZ, including large parts of the central business district (CBD). The most intense event of the earthquake sequence with regards to shaking in the CBD was the 22 FEB 2011 M_w6.2 Christchurch event. A reported 185 casualties were caused by the destruction from this event. The financial damage was immense as many of the structures, especially in the CBD, had to be demolished due to damage sustained from the Christchurch earthquake as well as some of the other less intense events. The performance of structures during these events was often related to liquefaction of foundation soils. Understanding the effects of liquefaction on soil and building response is an area of earthquake engineering that continues to challenge practitioners and researchers. This challenging topic makes the study of case histories, such as those provided by the Canterbury earthquakes, an essential component to characterizing and understanding the effects of soil liquefaction on building performance. This thesis focuses on providing insights regarding the seismic response of liquefiable soils through the use of information and data collected in Christchurch, NZ following the Canterbury earthquake sequence.

Nonlinear effective stress site response analyses are often used by engineers to model the dynamic response of potentially liquefiable soils during strong shaking. For the presented research, a widely used one-dimensional nonlinear effective stress site response analysis program is used to perform this modelling. Ground motions recorded during six events of the 2010-11 Canterbury earthquake sequence are used in conjunction with the extensive site investigation data that has been obtained in Christchurch to complete site response analyses at several strong motion station sites in the greater Christchurch area. Deconvolved Riccarton Gravel input motions were generated, because representative, recorded rock or firm layer base-motions were not available in the Christchurch area. Nonlinear effective stress seismic site response analyses are shown to capture key aspects of the observed soil response through the comparison of acceleration response spectra of calculated surface motions to those of recorded surface motions; however, equivalent-linear and total stress nonlinear analyses are shown to capture these aspects as well. Biases in the computed motions compared to recorded motions were realized for some

cases, but they can be attributed primarily to the uncertainty in the development of the input motions used in the analyses.

The study of the consequences of liquefaction on building performance is a complex soil-structure interaction problem that requires the use of well-documented case histories for validation purposes. An extensive site investigation and advanced laboratory testing program was carried out in Christchurch, NZ from April to October of 2014. The aim of this work was to provide characterization of the liquefaction resistance of foundation soils from building sites affected by liquefaction during the Canterbury earthquakes. In-situ penetration tests, such as CPT, are valuable methods for gaining an initial understanding of a site's characteristics and the expected performance of critical soil layers. However, to understand fully the complex response of soil at the element level, laboratory testing of relatively undisturbed soil specimens provide unique insights. To accomplish these goals, "undisturbed" sampling and triaxial testing (monotonic and cyclic) were performed on soils from key building sites in Christchurch's CBD. High quality sampling and testing could be achieved for most of the predominantly silty and sandy soils in the CBD. Test results indicate, though, that loose clean sand specimens were densified significantly during the sampling with the Dames & Moore hydraulic fixed-piston sampler (an Osterberg-type thin-walled sampler). The cyclic resistances measured in the tests on "undisturbed" specimens were generally consistent with those estimated using empirical simplified liquefaction triggering procedures.

Important insights regarding the cyclic response of the shallow CBD soils were obtained through the laboratory testing carried out as a part of the research presented in this thesis. Triaxial testing of "undisturbed" soil specimens proved important in understanding not only the stress-strain response of the studied soils, but also allowed for further knowledge regarding the pore water pressure response of the tested soils during both cyclic and monotonic loading. Importantly, insights into how various soil types of the CBD responded to cyclic loading were gained through comparisons of cyclic triaxial (CTX) tests performed on a variety of sand and silty sand soils. It was seen through CTX results comparisons that silty sands (soils classified as SM) and clean sands (SP and SP-SM) responded similarly in cyclic loading, even when the fines content of the tested specimens differed. Monotonic triaxial testing was also performed on reconstituted specimens to characterize the steady state response of several soil units in the CBD. The extensive insight garnered from laboratory testing is critical for informing researchers and engineers studying the case histories provided by the Canterbury earthquakes of buildings founded on liquefiable soils, especially those using numerical-based soil-structure interaction analyses. The results of the monotonic and cyclic tests performed as part of this study provide useful data for calibrating advanced numerical models.

Appendices are included as a part of this dissertation to provide supporting information and data not included in the main body of the thesis. A majority of these appendices are included at the end of this thesis; however, there are several additional appendices included as electronic attachments to this dissertation, which provide supplementary information regarding the work presented in Chapters 2 through 4 of this dissertation. Electronic appendices that support the work presented in Chapter 2 include: rotated (fault normal and fault parallel) seismic records for events studied at the strong motion station sites of interest (zip file that contains text files), deconvolved Riccarton Gravel motions for all events studied (zip file that contains text files), and selected results for completed site response analyses (PDF file). Electronic appendices that support the work presented in Chapters 3 and 4 include triaxial test data and results for "undisturbed" soil specimens (zip file that contains text, data, and PDF files).

TABLE OF CONTENTS

ACKNOWLEDGEMENTS

The research presented in Chapter 2 of this thesis was supported by the U.S. Geological Survey (U.S.G.S.), Department of Interior, under USGS award number G13AP00029. The research presented in Chapters 3 and 4 of this thesis was supported by the U.S. National Science Foundation (NSF) under award number CMMI-1332501. The financial support of both the USGS and the NSF is greatly acknowledged. Any opinions, findings, and conclusions or recommendations expressed in this thesis do not necessarily reflect the views of either the USGS or the NSF.

The guidance my adviser, Prof. Jonathan Bray, has provided throughout my academic career at UC Berkeley has been invaluable not only to my progression as a researcher and student, but also to my development as an engineer. His insights and support regarding the research presented in this thesis are greatly appreciated. Prof. Misko Cubrinovski was a most outstanding academic host during the time I spent in Christchurch, New Zealand. His willing collaboration and support have been vital to the research presented, and the comments and suggestions he provided during the review of this thesis were very constructive. Profs. Raymond Seed and Douglas Dreger provided very helpful comments and suggestions during their reviews of this thesis and their efforts are appreciated. Prof. Michael Riemer provided many helpful insights regarding the laboratory work presented in Chapters 3 and 4 of this thesis. His assistance was crucial to the presented research and his efforts are very much appreciated.

The assistance of several collaborators has been vital to the work presented in this thesis. Jorge Macedo and Roberto Luque provided valuable assistance with the work completed in Chapter 2. Profs. Brendon Bradley (Univ. of Canterbury) and Liam Wotherspoon (Univ. of Auckland) provided information regarding the Canterbury earthquakes and strong motion station site characterizations. Christine Beyzaei provided assistance with the sampling and laboratory testing work. Dr. Mark Stringer, Siale Faitotonu, and Nicole van de Weerd were very helpful with the work completed at the geomechanics laboratory at the University of Canterbury. Dr. Merrick Taylor provided important insights, especially with regards to the sampling and laboratory testing work presented. Dr. Josh Zupan shared data and insights regarding the sites where sampling was completed. McMillan Drilling Ltd. assisted during the sampling process, especially Mr. Iain Haycock and Mr. Richard Wise.

Several individuals and organizations were vital in providing access to the sites examined in the Christchurch CBD for the sampling and laboratory test work presented in this dissertation. These individuals include: Jan Kupec and James Parker with the Canterbury Earthquake Recovery Authority (CTUC, AM, and VT sites), David Shackleton (FTG-7 site), Mike Jacka and the Christchurch City Council (CTH site), Sharon Blackburn with Carter Group (PWC site), John Cleary with Kiwis STAT (LS-II site), and Annette Gamble with Tectra (SA site).

All of my colleagues and friends on the fourth floor of Davis Hall have been extremely supportive during my years at UC Berkeley. A special thanks to my officemates Roberto Luque, Christine Beyzaei, and Nick Oettle. My friends and family provided a great amount of support during these past few years. My parents have always been more than willing to provide their advice and support during my entire academic career—for that I will always be grateful. Lastly, and most importantly, I would like to thank my best friend and partner, Amelia. Her untiring support has been crucial during my PhD career and I cannot express enough gratitude for the patience and encouragement she has readily provided during my entire academic career.

LIST OF FIGURES

LIST OF TABLES

CHAPTER 1: INTRODUCTION

1.1 OVERVIEW

Understanding the effects of liquefaction on both soil and building response has been a challenging topic of engineering research for the past few decades. The devastation witnessed during the Niigata and Great Alaskan earthquakes of 1964 was pivotal in bringing soil liquefaction to the attention of engineers and researchers alike. More recent earthquakes, such as the 27 FEB 2010 M_w8.8 Maule, Chile event (Bray et al. 2012, Hayden 2014), multiple events from the 2010-11 Canterbury (Christchurch, New Zealand) earthquake sequence (Green and Cubrinovski 2010, Cubrinovski et al. 2011b), and the 11 MAR 2011 M_w9.0 Tohoku Pacific (Japan) Earthquake (Tokimatsu et al 2012), have focused attention currently to evaluating the consequences of soil liquefaction in geotechnical and structural engineering design. Damage to several types of infrastructure during these events was attributed to the cyclic softening of foundation soils due to the generation of excess pore water pressure during earthquake strong shaking. The objective of this thesis is to provide insights and information regarding the dynamic response of liquefiable soils. Specifically, the information and data collected in Christchurch, New Zealand following the 2010-11 Canterbury earthquake sequence provide motivation for this research. Its primary objective is to characterize the cyclic response of key soil layers that liquefied and affected building performance within the central business district (CBD) of Christchurch through advanced testing of retrieved soil samples.

An important precursor to examining the effects of soil liquefaction on infrastructure is being able to understand the free-field response of soils vulnerable to potential softening due to the development of excess pore water pressure during strong shaking. Several researchers have studied the effects of soil liquefaction on ground response during earthquake loading (e.g., Matasovic and Vucetic 1993a, Zehgal and Elgamal 1994, Youd and Carter 2005, Kramer et al. 2011, and Gingery et al. 2014). With building codes often requiring the development of site specific ground motions for sites with potentially liquefiable soils, there is a need to evaluate the capabilities of commonly used site response analysis procedures. This evaluation is challenging due to the fact that there are relatively few recordings of ground motions at liquefied sites that could be used for verification purposes. Seismic recordings from the Canterbury earthquakes were taken on both sites that liquefied (sometimes multiple times) and sites that did not show signs of liquefaction during these events. These recordings coupled with the extensive site investigation data that has been collected in the greater Christchurch area following the Canterbury earthquake sequence provide an exceptional opportunity to evaluate effective stress analyses' capabilities to model the response of liquefiable soils during strong shaking.

Modelling the response of structures on liquefiable soils through effective stress analyses is critical to gaining knowledge of the effects of soil liquefaction. Similar to using information from free-field sites that experienced liquefaction during strong shaking to verify techniques commonly used in modelling soil response, studying case histories of buildings affected by liquefaction is a vital component to exploring and expanding engineers' abilities to model the complex interaction of buildings with liquefiable foundation soils during earthquake loading. The effects of liquefaction on buildings during the 2010-11 Canterbury earthquake sequence were devastating, especially in the CBD of Christchurch, New Zealand (NZ). Over a third of the approximate 4,000 buildings in Christchurch's CBD were demolished following these events,

while most of the high-rise structures were also demolished due to sustained damage. Liquefaction of foundation soils was a major contributing factor in the damage sustained by many of the buildings in Christchurch's CBD, making the information from these events vital to researchers.

Thorough documentation of the effects of liquefaction on structures was made by post-earthquake reconnaissance teams, which are discussed by Cubrinovski et al. (2011a, 2011b, 2011c), Bray et al. (2014), and Zupan (2014). This work allowed for the development of important case histories of buildings of various footprint area and height affected by the liquefaction of foundation soils. Furthermore, in-situ investigations were carried out to characterize the subsurface soils of several building sites affected by liquefaction. The data and information from these in-situ investigations were important for gaining a better understanding of these soils; however, laboratory testing of "undisturbed" soil samples is essential in fully characterizing the properties of these soils. By obtaining "undisturbed" soil samples at a select number of case history sites, advanced laboratory testing (specifically in the form of cyclic and monotonic triaxial testing) was carried out as a part of the research presented in this thesis. The results from this study assist in characterizing the strength characteristics and liquefaction susceptibility of key soils, which can then be used by future researchers and practitioners studying the case histories of the Canterbury earthquakes.

1.2 ORGANIZATION

This thesis is organized in the following chapters:

- Chapter 2 describes research that was conducted to examine the modelling of the seismic response of liquefiable soil using 1D nonlinear effective stress site response analysis procedures. Seismic records from the 2010-11 Canterbury earthquake sequence in Christchurch, NZ were used to assist in this evaluation. A deconvolution procedure for generating input motions for site response analyses in Christchurch is described, which is followed by an explanation of the selection of analyses parameters and the assumptions made for the conducted analyses. In addition to 1D nonlinear effective stress analyses, nonlinear total stress and equivalent linear site response analyses were conducted. Representative comparisons of calculated surface motions from analyses to recorded surface motions are made followed by a discussion of analyses results.
- Chapter 3 describes an extensive site investigation and advanced laboratory testing program that was carried out in Christchurch, NZ. One of the components of this work was obtaining "undisturbed" samples of silty and sandy soils that comprised the foundation material of key building sites in the CBD of Christchurch. The buildings located at these sites suffered immense damage due to the liquefaction of these subsurface materials. The ultimate motivation of this research was to characterize the liquefaction resistance of these soils. Sampling and testing procedures are described, with an emphasis on the triaxial testing that was carried out on the "undisturbed" soil specimens. An explanation is provided regarding the assessment of sample disturbance, and representative results are examined and discussed.
- Chapter 4 incorporates the various testing results described in Chapter 3 by delving more into examining the insights provided through the laboratory testing program. Laboratory

test results from cyclic triaxial (CTX) testing are compared to a CPT based liquefaction triggering correlation. Additional information provided by laboratory testing is discussed with an emphasis on the cyclic loading response of soil specimens and how this information is critical for fully characterizing case histories of buildings affected by soil liquefaction during the Canterbury earthquake sequence. The results of large strain monotonic triaxial testing on reconstituted specimens to characterize the steady state response of critical soil units in the CBD of Christchurch are provided and discussed. In addition to the material presented in Chapter 4, Appendix B provides further insights regarding the triaxial testing of "undisturbed" soil specimens; these insights include summary tables containing interpreted "undisturbed" triaxial specimen data, a site-by-site examination of CTX test results, further comparisons of CTX results with CPT-based liquefaction triggering analyses, and comparisons of information obtained from the sampling and testing of "undisturbed" soil specimens to relevant information obtained from CPT data.

- Chapter 5 provides a synopsis and the conclusions of the presented research with a focus on important insights and recommendations for future work and research.

CHAPTER 2: NONLINEAR EFFECTIVE STRESS SITE RESPONSE ANALYSES

The contents of this chapter are primarily from a journal article accepted for publication to the Soil Dynamics and Earthquake Engineering journal by Markham, C.S., Bray, J.D., Macedo, J., and Luque, R. entitled: "Evaluating Nonlinear Effective Stress Site Response Analyses using Records from the Canterbury Earthquake Sequence."

2.1 INTRODUCTION

The 2010-11 Canterbury earthquake sequence devastated much of Christchurch, New Zealand and its surrounding areas. Liquefaction during the 4 SEP 10 (moment magnitude, M_w7.1) Darfield event affected approximately 10% of the Christchurch area; whereas the 22 FEB 11 (M_w6.2) Christchurch event affected over 50% of the developed land (see Figure 2.1). Including these two events, there were a total of seven events with moment magnitude (M_w) greater than or equal to 5.5 between 4 SEP 2010 and 23 DEC 2011 which caused varying degrees of liquefaction in and around Christchurch.

The Canterbury earthquake sequence provides a great opportunity to examine soil response during strong seismic shaking, particularly as it relates to the effects of liquefaction. During the events discussed above, some sites within Christchurch liquefied as many as five times, other sites only liquefied once or twice, and other sites never experienced soil liquefaction. By taking advantage of the dataset provided by these earthquakes, our understanding of the performance of critical infrastructure during major shaking events with extensive and damaging liquefaction can be improved. Understanding the effects of liquefaction, however, starts with being able to capture reliably the seismic response of free-field sites that develop significant pore water pressures during earthquake shaking. Moreover, building codes commonly require that seismic site response analyses be performed to develop design earthquake ground motions at liquefiable sites. Improved methods for estimating earthquake ground motions at sites that contain liquefiable soils are required. However, there are relatively few recordings of ground motions at liquefied sites to evaluate current or new methods. Thus, the Canterbury earthquake sequence dataset is invaluable.

Previous studies, such as those by Matasovic and Vucetic (1993a), Zehgal and Elgamal (1994), Youd and Carter (2005), Kramer et al. (2011), and Gingery et al. (2014), have provided useful insights regarding the effects of soil liquefaction on ground response during strong shaking. This research focuses on evaluating the capabilities of one-dimensional (1D), nonlinear effective stress seismic site response analytical procedures to capture the seismic response of sites with and without significant earthquake-induced pore water pressure generation. The goal of the presented work is to provide insights into procedures and methods commonly used to perform seismic site response analyses in U.S. based earthquake engineering practice. Specifically, the widely used seismic site response program *DEEPSOIL* (Hashash 2012) was utilized to perform the analyses for this evaluation. The research capitalizes on the data provided by the GeoNet network of strong motion station recordings taken throughout the greater Christchurch area during the Canterbury earthquake sequence (GeoNet Database 2014). The site investigation data that have been collected by researchers and practitioners throughout

Christchurch over the past several years were used in the estimation and selection of soil properties for the analyses presented in this chapter. More in-depth information and results are presented in Appendix A of this thesis, which provides all characterization data considered for each strong motion station site, input parameters for seismic site response analyses, and analytical results.

2.2 CANTERBURY EARTHQUAKE SEQUENCE

Seven events between 4 SEP 10 and 23 DEC 2011 had a M_w greater than or equal to 5.5 during the Canterbury earthquake sequence. Of these seven events, seismic records from five earthquakes were examined in this study. In addition to these events with $M_w \geq 5.5$, the M_w4.7 earthquake that occurred on 26 DEC 2010 was included in this study, because the shaking intensities resulting from this event were such that soil response was largely linear. Table 2.1 provides relevant information for each of the events studied. The horizontal acceleration records and respective 5% damped pseudo-acceleration response spectra from each event at each strong motion station were employed to evaluate the results of the seismic site response analyses presented in this chapter. All records were rotated to fault normal and fault parallel components based on the strike values listed in Table 2.1. Uniformly processed acceleration records for the 4 SEP 10 Darfield and 22 FEB 11 Christchurch events were available from the Pacific Earthquake Engineering Research (PEER) center (PEER Ground Motion Database 2014). Processed records for the remaining events were obtained from the GeoNet strong motion acceleration-time series database (GeoNet Dabase 2014) as records for these events are not included in the PEER Ground Motion Database. These motions are included as an electronic appendix to this dissertation.

Figure 2.1 provides a map overview of the locations of the strong motion stations from which the seismic records for this study were obtained. Some of these sites showed signs of liquefaction in multiple events, which was evident in surface manifestation (i.e., sediment ejecta—see Wotherspoon et al. 2013) or distinct features of the surface recording (e.g., dilation spikes within the acceleration time series—see Bradley and Cubrinovski 2011). Table 2.2 provides a detailed overview of relevant parameters for each strong motion station for the events studied. The 4 SEP 10 Darfield event had the largest moment magnitude of all the events shown in Table 2.1. However, it was the 22 FEB 11 Christchurch event that caused the most intense shaking in the greater Christchurch area, which is evidenced by the generally higher recorded peak ground accelerations for the stations presented in Table 2.2. The relatively lower source-to-site distances of the Christchurch event compared to the Darfield event is the primary cause of its more intense shaking, which is illustrated in Table 2.2 (see Kaiser et al. 2012 for further discussion).

2.3 SUBSURFACE CHARACTERIZATION OF STRONG MOTION STATION SITES

Over 18,000 cone penetration tests (CPT) have been completed in the greater Christchurch area. Much of these site investigation data can be obtained directly through the Canterbury Geotechnical Database (2013). In addition to these data, much of the site investigation information necessary to characterize the strong motion stations of interest was obtained through the work of other researchers, particularly Prof. Wotherspoon of the Univ. of Auckland and his

research collaborators (Wotherspoon et al. 2013). Table 2.3 provides a summary of the site investigation data for each site. The information obtained from CPT data was crucial in defining the stratigraphy of the sites and in estimating the engineering properties of the subsurface materials through established correlations. The McGann et al. (2014) Christchurch specific CPT-V_s correlation provided the primary means for estimating the shear wave velocity (V_s) profiles of the strong motion station sites. Table 2.3 shows that no CPT data were available at the time of writing for the strong motion station sites at CACS, RHSC, SMTC and KPOC (primarily due to the presence of near surface gravelly soil). For such cases, V_s profiles calculated and presented in Wotherspoon et al. (2013), which were based on the surface wave testing results of Wood et al. (2011), were used for site characterization purposes. All site characterization data and information, including CPTs, considered V_s profiles, and assumed soil properties for analyses presented subsequently can be found in Appendix A.

A simplified subsurface profile for Christchurch is shown in Figure 2.2. The subsurface is comprised generally of surficial deposits varying in thickness from less than 10 m to over 40 m. These materials form the Springston Formation (primarily alluvial gravels, sands, and silts) in the western area of Christchurch and the Christchurch Formation (comprised of estuarine, lagoon, beach, dune, and coastal swamp deposits of sand, silt, and some clay, and peat) in the eastern part of the city (Cubrinovski et al. 2011b). Below these deposits lies the dense, well-graded Riccarton Gravel layer (Brown and Weeber 1992). Most site investigations characterize only the soils that overlie the dense Riccarton Gravel. The estimated depth to the Riccarton Gravel layer at each site studied is also listed in Table 2.3.

2.4 SELECTION OF INPUT GROUND MOTIONS FOR SITE RESPONSE ANALYSES

All of the strong motion station sites of interest are situated within the Canterbury Plains. The general geology of this area comprises distinct layers of gravels interbedded with layers of primarily sands and silts, with some pockets of clays and peats, to a depth of over 500 m below the ground surface (Brown and Wilson 1988; Brown and Weeber 1992; Forsyth et al. 2008). Figure 2.2 provides a simplified geologic profile of the Christchurch region. The depth to "basement" rock for soils underlying the Canterbury Plains can be over 2 km below the ground surface (Brown et al. 1995; Hicks 1989). These deep sediment deposits coupled with the presence of the volcanic rock that makes up the Port Hills and Banks Peninsula to the southeast of central Christchurch create a basin structure.

The deep basin structure that underlies the studied sites makes the selection of representative "rock" input motions difficult due to the absence of outcropping "rock" recordings on the north side of the Port Hills (i.e., within Canterbury Plains side of the Port Hills). The Lyttelton Port strong motion station (LPCC) has a V_{s30} of about 792 m/s according to the work of Wood et al. (2011), placing it in the category of engineering bedrock (i.e., B/C rock boundary for $V_s \approx 760$ m/s; ASCE 7-10). However, the location of LPCC with respect to the locations of the events of interest and seismic energy propagation from these events make it a non-ideal input motion for seismic site response analyses in the Christchurch area (e.g., LPCC is located on the southern side of the Port Hills as opposed to the northern side, it is a significant distance from downtown Christchurch, and it is on the hanging wall as opposed to the footwall for several events).

2.4.1 Deconvolution of Surface Motions

With the lack of representative "rock" input motions, as well as the difficulty in reliably characterizing the stratigraphy beneath the studied sites to the depth of engineering bedrock, deconvolving recorded surface motions to obtain input motions for a "firm" base material is required. An alternative would be to use synthetic "rock" motions for each event, but they are not currently available, and they will contain significant uncertainty when produced. Deconvolution consists of inputting an outcropping motion at the surface of a 1D soil column and using an equivalent-linear analysis to calculate the acceleration-time history at a point beneath the ground surface (see Kramer 1996; Silva 1988; Idriss and Akky 1979). This *within* motion can be converted to an *outcropping* motion for use in subsequent convolution analyses.

Silva (1988) outlines a procedure to help avoid the situation of unrealistic motions being calculated at depth due to the propagation of the total surface motion via an equivalent-linear analysis during the deconvolution process. These steps were adhered to and are as follows:

1. A low pass (LP) filter was applied to the recorded surface motion to be used for the deconvolution analysis at 15 Hz and scaled by 0.87; SeismoSignal™ was used to perform a 4th order, LP Butterworth filter.
2. The filtered and scaled motion from step 1 was input at the surface of a 1D soil column.
3. This motion is transferred through the soil column to a predetermined half-space.
4. The final iteration values of shear modulus reduction (G/G_{max}) and material damping (λ) for each layer during the deconvolution process is obtained.
5. The deconvolution process was performed again by using a linear analysis with the final values of G/G_{max} and λ from step 4 for each layer of the 1D soil column and inputting the LP filtered (15 Hz) full surface motion (i.e., not scaled by 0.87) at the top of the column to obtain a final *within* motion. This *within* motion was then converted to a final *outcropping* deconvolved motion for use as an input motion in convolution analyses.

SHAKE2000 was utilized to perform all deconvolution analyses (Ordonez 2000).

The dense Riccarton Gravel unit (see Figure 2.2b) was used as the "firm" half-space for deconvolution analyses and subsequent seismic site response analyses. The impedance contrast between the Riccarton Gravel and the softer overlying surficial deposits was on average two for the sites studied. The presence of this firm layer below the potentially liquefiable soils in the Christchurch area supported using the Riccarton Gravel unit as the half-space for deconvolution.

2.4.1.1 Deconvolution at Selected Strong Motion Station Sites (CACS and RHSC) and Scaling of Input Motions

The Canterbury Aero Club (CACS) and the Riccarton High School (RHSC) strong motion sites were used for the deconvolution procedure (see Figure 2.1). These sites are located on sites that did not show surface manifestations of liquefaction during any of the events of interest and are believed to have shown low nonlinearity in the soil response during strong shaking. These points are important, because the required equivalent-linear approach to deconvolution cannot capture fully the nonlinear response of soils. Furthermore, as can be seen in Table 2.3, the depth to the Riccarton Gravel layer for these sites is the lowest among the 13 strong motion station sites studied, which requires the surface motion to be deconvolved over a relatively shallow profile.

For the deconvolution process, the strain-dependent normalized shear modulus reduction and material damping relationships presented by Darendeli (2001) were used for all material above the Riccarton Gravel. Two different V_s profiles were initially considered for both the CACS and RHSC sites to account for the epistemic uncertainty in the site characterization of these stations. For CACS, both V_s profiles were assumed based on the information presented by Wotherspoon et al. (2013) and mostly differed by the assumed depth and V_s of the Riccarton Gravel (see Figure 2.3a). For RHSC, one V_s profile was estimated based on the work of Wood et al. (2011) while the other was assumed from the work presented by Wotherspoon et al. (2013). Figure 2.3 provides the estimated V_s profiles for the deconvolution sites. It was found that for a given deconvolution site, the input motions generated from the consideration of two different V_s profiles yielded similar results for subsequent convolution analyses. Wotherspoon (2013) combined the surface wave testing results described by Wood et al. (2011), as well as additional surface wave testing results, with in-situ site investigation data (e.g., borings and CPT data) to inform the inversion process for developing V_s profiles at strong motion station sites in Christchurch. Also, a shear wave velocity of the Riccarton Gravel at the CACS site of 360 m/s (*Woth1* profile) was deemed more appropriate than V_s of 700 m/s (*Woth2* profile) based on data from other strong motion station sites in Christchurch. For these reasons, the *Woth1* V_s profiles for both the CACS and RHSC sites were considered to be more representative of field conditions than the alternative V_s profiles. Consequently, results presented hereafter are based on the use of input motions *CACS_Woth1* and *RHSC_Woth1*, which are named based on their respective V_s profiles.

Deconvolved ground motions were scaled to account for differences in the site-to-source distance and V_s of the Riccarton Gravel between the deconvolution sites and the sites where convolution analyses were performed. This scaling was completed using the New Zealand specific ground motion prediction equation outlined in Bradley (2013)—referred to as Bradley GMPE herein. This model uses source, path, and site input parameters to generate period dependent pseudo-spectral acceleration (S_a) values. For a given event the source parameters (e.g., M_w, Z_{tor}, dip) were the same; however, the shortest distance between sites and the event rupture plane (path parameter R_{rup}) varied between deconvolution and convolution sites, as did the shear wave velocity of the Riccarton Gravel due to its differing depth across Christchurch. To account for these differences, a single scale factor was calculated to transfer *outcropping* deconvolved Riccarton Gravel motions from deconvolution sites to convolution sites. This scale factor was calculated by averaging (arithmetic mean) the period dependent factors of median S_a at convolution sites to deconvolution sites predicted by the Bradley GMPE across all periods considered in the GMPE. A single factor was used to scale input motions as opposed to spectrally matching deconvolved motions to a smooth target response spectrum to retain the event-specific characteristics of the input acceleration-time series.

As stated previously, the only parameters that were varied in the Bradley GMPE between the convolution sites and the deconvolution sites for a given event were R_{rup} and V_{s30}, where V_{s30} was used as a proxy to account for the varying V_s of the Riccarton Gravel. Shear wave velocity values for the Riccarton Gravel were estimated based on the work of Wotherspoon et al. (2013) and ranged from 300 to 460 m/s for the sites studied. Representative deconvolved input motions are provided in Figure 2.4. These motions represent *outcropping* Riccarton Gravel motions that were used as input motions for analyses completed at the Christchurch Hospital (CHHC) strong motion station site; the scale factors used for this site were 2.61 and 1.47 for the input motions that resulted from the deconvolution process at the CACS and RHSC sites, respectively. All

scale factors used for the various sites and events are provided in Table 2.4, while the unscaled deconvolved Riccarton Gravel motions for all events are included as an electronic appendix to this dissertation.

Equivalent linear analyses were carried out at the deconvolution sites for the events studied to examine the ability of the deconvolution process to generate input motions capable of capturing key characteristics of recorded surface motions. The input motions for these analyses corresponded to deconvolved Riccarton Gravel motions from the other deconvolution site (e.g., CACS deconvolved motion was used as the input motion for a convolution analysis at RHSC). Figure 2.5 provides representative results of analyses completed for the 13 JUN 2011 M_w6.0 event at the deconvolution sites. As will be discussed further in Section 2.6, residuals can be calculated to compare the pseudo-spectral acceleration (S_a) values of recorded motions ($S_{a\text{-}Recorded}$) to those of calculated surface motions ($S_{a\text{-}Predicted}$) using equivalent linear analyses. These residuals are defined as the difference between the natural logarithm of $S_{a\text{-}Recorded}$ and $S_{a\text{-}Predicted}$ (i.e., $\delta=\ln(S_{a\text{-}Recorded}) - \ln(S_{a\text{-}Predicted})$). Based on average residual (μ_δ) values and standard deviation of residuals (σ_δ), the results of the equivalent linear analyses generally capture the key characteristics of the recorded surface motion. The response spectra presented in Figure 2.5 and in Section 2.6 are plotted from periods of 0.067 s to 10 s, because a low-pass filter at 15 Hz was applied during the deconvolution procedure. The maximum shear strains calculated during the deconvolution analyses were less than about 0.1% for the Christchurch event and lower for the other events. Hence, the use of equivalent-linear analysis was judged to be acceptable for the deconvolution.

2.5 SEISMIC SITE RESPONSE ANALYSES OVERVIEW

Nonlinear effective stress, nonlinear total stress, and equivalent-linear 1D seismic site response analyses were performed for each station listed in Table 2.2 that recorded shaking for each event of interest (see Table 2.1). The seismic site response program *DEEPSOIL* was used to perform these analyses (Hashash 2012). It is a widely used nonlinear time domain site response analysis program that utilizes a discretized multi-degree-of-freedom lumped parameter model of the 1D soil column. The hysteretic soil response is captured by a pressure-dependent hyperbolic model that represents the backbone curve of the soil along with the modified extended unload-reload Masing rules (Hashash 2012). Some additional pertinent details are discussed below.

2.5.1 Representation of Strain Dependent Soil Response

Correlations proposed by Darendeli (2001) were used to obtain initial estimates of normalized shear modulus reduction (G/G_{max}) and material damping (λ) curves for each site where seismic site response analyses were completed. In general, the soils for each subsurface profile were considered to be non-plastic (PI=0) and normally consolidated (OCR=1). The mean confining pressure for each layer (σ'_m) was estimated based on assumed unit weights of 17.3 kN/m^3 for all soils above the groundwater table and 19.6 kN/m^3 for all soils below the groundwater table and an assumed K_o value of 0.5 (i.e., $\sigma'_m = 2/3\sigma'_v$). Event specific groundwater table depths for each strong motion station site were estimated from the Canterbury Geotechnical Database (2013).

The Darendeli (2001) relationship tended to underestimate the assumed shear strength of the soils studied. The procedure proposed by Yee et al. (2013) was utilized to remedy the potential

misrepresentation of a soil's shear strength. This procedure allowed for the calculation of a "strength corrected" hybrid shear modulus reduction curve that transitions from the G/G_{max} curve computed from the Darendeli (2001) relationship to a strength based G/G_{max} curve at a specific strain level. Due to a lack of published guidance in correcting the material damping curve to capture large strain response, a hybrid damping curve was calculated that transitioned from the damping curve calculated from the Darendeli (2001) relationship to a strength based material damping curve using a linear (in semi-log space) approximation. Figure 2.6 illustrates the corrections made to the target shear modulus reduction and material damping curves for the performed seismic site response analyses. Shear strength estimates for the subsurface soils at the strong motion sites were primarily based on correlations from in-situ site investigation data (i.e., CPT and SPT data from Wotherspoon et al. 2013 and the Canterbury Geotechnical Databse 2013). Appendix A.4 provides the assumed values of shear strength used at each strong motion station site.

The MRDF-UIUC pressure dependent, hyperbolic fitting procedure proposed by Phillips and Hashash (2009), which is implemented in *DEEPSOIL*, was used to fit the target (corrected) shear modulus reduction and material damping curves for all nonlinear (effective and total stress) analyses. The procedure proposed by Hashash et al. (2010) was followed for all nonlinear site response analyses to ensure that the implied shear strength of the fitted shear modulus reduction curve for a given material was approximately equal to the assumed shear strength. This procedure requires an iterative adjustment of the target shear modulus reduction curve to capture the assumed shear strength for a given material. The frequency independent small strain damping formulation proposed by Phillips and Hashash (2009) was used to calculate viscous damping for all nonlinear site response analyses.

Normalized shear modulus reduction values calculated via the procedure outlined in Yee et al. (2013) were used directly at discrete values of shear strain for each layer of a given 1D soil profile for equivalent-linear analyses. The final material damping curves that resulted from the MRDF-UIUC fitting procedure discussed above for nonlinear analyses were used to define values of material damping at discrete values of shear strain for equivalent-linear seismic site response analyses. The reason for the use of the fitted material damping curve versus the material damping curve obtained directly from the strength correction procedure is due primarily to the hyperbolic representation of the material damping curve that the fitted procedure provides as well as a better representation of material damping at large strains via the fitting procedure implemented in *DEEPSOIL*. The effective shear strain ratio (γ_{ref}) proposed by Idriss and Sun (1992) and the frequency independent complex shear modulus discussed in Hashash (2012) were used for all equivalent-linear analyses.

2.5.2 Parameters for Nonlinear Effective Stress Analyses

This study consisted of primarily non-plastic, cohesionless soils. These soils were modelled using the pore water pressure generation model for sands originally developed by Dobry et al. (1985), modified by Vucetic and Dobry (1988), and presented in Matasovic and Vucetic (1993a). Equation 1.1 provides the governing equation of this model:

$$u_N^* = \frac{p * f * F * N * \left(\gamma_c - \gamma_{tvp}\right)^s}{1 + f * F * N * \left(\gamma_c - \gamma_{tvp}\right)} \quad (1.1)$$

The parameters for the pore water pressure generation model would ideally be selected based on curve fitting site specific, undrained, cyclic test results. Due to a lack of site specific information for the strong motion stations sites, the *D-MOD2000* manual (see Matasovic and Ordonez 2012) and the work of Carlton (2014) were used in the selection of parameters. Based on this information, the following logic was used in the selection of parameters:

- f was assumed to be 2 for all analyses; this value was used to better represent 2D shaking in the pore water pressure generation model (analyses were also performed with f = 1 and 1.5 to evaluate the sensitivity of the results to this parameter); the maximum r_u value was set to 0.99
- p was assumed to be 1 for all analyses
- γ_{tvp} was chosen based on the value of shear strain (γ) at G/G_{max}=0.65
- In general, F was chosen based on the guidance of the correlation presented by Carlton (2014) that uses the soil information from Matasovic and Ordonez (2012) to correlate F to shear wave velocity (V_s in m/s). In some cases F was adjusted to prevent unrealistic large shear strains or unexpected high pore water pressure generation (e.g., in a layer of silty clay material directly above the Riccarton Gravel). The correlation used for F is:

$$F = 3810 * V_s^{-1.55} \quad (1.2)$$

- s was chosen based on a similar correlation from Carlton (2014) which relates this parameter to fines content (FC in percent):

$$s = (FC + 1)^{0.1252} \quad (1.3)$$

where FC was correlated from CPT data using the average CPT I_c-FC correlation proposed by Robertson and Wride (1998), which largely enveloped the Christchurch data presented by Robinson et al. (2013).

The degradation of both the stiffness and strength of a liquefied soil is then represented through the modification of the MKZ hyperbolic model as proposed by Matasovic and Vucetic (1993a) and Matasovic and Vucetic (1993b) through the use of the above pore water pressure generation model. The additional exponent v considered by Matasovic and Vucetic (1993a) in the calculation of the degradation parameter was incorporated into the analyses. A value of v equal to 3.8 was assumed for all materials based on the recommendation of Matasovic and Vucetic (1993a).

Excess pore water pressure dissipation and redistribution can be accounted for simultaneously with the generation of excess pore water pressure in a nonlinear effective stress analysis. The dissipation and redistribution of excess pore water pressure is modeled using Terzaghi's 1D consolidation theory. The solution process of *DEEPSOIL* assumes dissipation only in the vertical direction (Hashash 2012). This model requires only the specification of the coefficient of consolidation (c_v), which was estimated based on CPT correlations. Additionally, since the half-space used for all analyses was the Riccarton Gravel, a permeable boundary was used for the

bottom layer within *DEEPSOIL*. Its c_v value is set by the program to be that of the bottom soil layer, which was at least 0.1 ft^2/s for all sites.

Appendix A.4 provides the parameters used at each of the strong motion station sites analyzed in this study. Parameters are tabulated for effective stress analyses; however, the same normalized shear modulus reduction and material damping curve fitting parameters apply for nonlinear total stress analyses. Appendix A.2 provides summaries of the CPT investigations used at each of the studied strong motion station sites as well as the assumed V_s profile for each site.

2.6 RESULTS AND DISCUSSIONS

The results presented and discussed herein correspond to analyses completed using input motions from the deconvolution of the CACS and RHSC surface motions using the V_s profiles named *Woth1*, as discussed in Section 2.4.1.1. Analyses were completed for each event and SMS site listed in Table 2.2. No analyses were completed for cases where there were no recordings for a particular station (e.g., CCCC for the 13 JUN 2011 earthquake—Table 2.2). For the 26 Dec 2010 event only input motions generated from deconvolution at the CACS site were considered as no recordings were taken at the RHSC site for this event.

The recordings at each station for each event provide a means for assessing the results of the calculated surface motions from the seismic site response analyses completed at each site. Pseudo-acceleration response spectra (5% damped; abbreviated as *acceleration response spectra* hereafter) were used to simplify the comparisons between recorded surface motions and those calculated from analyses. As a low-pass filter was applied at 15 Hz to the motions used in the deconvolution process (see Section 2.4.1), response spectra are plotted with a minimum period of 0.067 s when comparing analytical results to the response spectra of recorded motions. Spectral acceleration residuals (referred to as *residuals* hereafter) were considered on a period-by-period basis to quantify the "fit" of acceleration response spectra calculated from analyses to those of recorded surface motions. The residuals are calculated as:

$$\delta(T_i) = \ln\left(S_{a_{recorded}}\right)_{T_i} - \ln\left(S_{a_{predicted}}\right)_{T_i} \tag{1.4}$$

Figure 2.7 shows the calculated surface acceleration-time series for analyses completed at the CHHC strong motion station site using the fault normal component (FN) of the *CACS Woth1* input motion for the Christchurch event. The recorded motion is also shown. Figure 2.8 shows the calculated acceleration response spectra of these motions as well as those from the effective stress analysis completed using the *RHSC Woth1* input motion. The plots on the right-hand side of Figure 2.8 show the period dependent residuals for each analysis. Also displayed is the average (arithmetic mean) residual across all periods as well as the standard deviation of residuals for each analysis. Based on the average residual, it can be seen that the analyses resulting from the use of the *CACS Woth1* input motion compare better to the recorded surface motion (as opposed to those from the use of the *RHSC Woth1* input motion). This better matching with input motions that were a result of deconvolution at the CACS site was not always necessarily true for the other events studied; however, it was the general trend for the Christchurch event.

Interestingly, the acceleration response spectra of the surface motions calculated at the CHHC site by the equivalent-linear (EQL), total stress (TS), and effective stress (ES) nonlinear analyses

were similar, as shown in Figure 2.8. Figure 2.9 shows plots of the maximum calculated shear strain, maximum pore water pressure ratio (r_u), and maximum acceleration with depth for each analysis of the CHHC site in the fault normal direction using the *CACS Woth1* input motion. The excess pore water pressure ratios calculated with the effective stress analysis are in excess of 0.94 at depths of 17-19 m. The calculated maximum shear strain at these depths of higher maximum r_u are considerably larger than maximum shear strains calculated using the total stress nonlinear analysis and the equivalent-linear analysis.

Sensitivity analyses were completed to examine the effects of pore water pressure generation on the calculated soil response by using values of *f* (see Section 2.5.2) equal to 1 and 1.5 for the pore water pressure model implemented in *DEEPSOIL*. Lower values of *f* yielded lower values of r_u and lower shear strains but did not have an appreciable effect on the calculated response spectra. Furthermore, as was typical for analyses conducted in this study, there were only slight differences between the acceleration response spectra of calculated surface motions that resulted from nonlinear total stress and effective stress analyses, as well as equivalent-linear analyses, for a given 1D soil column using the same input motion.

Figure 2.10 provides a comparison of response spectra of surface motions from analyses completed at the PPHS site for the Darfield event and the recorded surface motion in the fault parallel direction. On average analyses from both input motions result in underestimations when compared to the acceleration response spectrum of the recorded motion, though again the *CACS Woth1* input motion resulted in average residuals being closer to zero. The spectral acceleration values are generally slightly higher for the TS analysis compared to the ES analysis for periods between 0.067 and 0.2 s, while both are higher than the EQL analysis in this period range. Beyond this period range there is not a significant difference between the spectral acceleration values for the three types of analyses for the same input motion. Though the acceleration response spectra of the surface motions calculated from effective stress and total stress analyses are similar, it can be seen from Figure 2.11 that significant excess pore water pressures are indicated at a depth of about 3-5 m, with a max r_u of 0.95 calculated at a depth of 4 m. The Boulanger and Idriss (2014) CPT-based simplified liquefaction triggering procedure generally agreed well with the effective stress analyses' calculated excess pore water pressure with depth (i.e., layers with r_u values over 0.5 to 0.6 generally had $FS_{liq} \leq 1$).

To examine trends in the results of seismic site response analyses performed for a given event, one can examine plots of residuals as a function of period for all stations where analyses were completed for a particular event. Figure 2.12 summarizes the results of the nonlinear effective stress analyses of all sites for the Christchurch event using the *CACS Woth1* input in the fault normal direction. As was previously mentioned, residuals are only presented for periods greater than 0.067 s due to the use of a low-pass filter during the deconvolution process. In general, the results of the effective stress analyses compared well with the recorded motions at the sites studied, which can be seen in Figure 2.12 via the fact that most of the residuals are between +/- 0.5 across the period range of interest.

In addition to effective stress analyses completed using *DEEPSOIL*, a series of 1D analyses were completed using the finite-difference code *FLAC* (Fast Lagrangian Analysis of Continua—see Itasca 2009). The constitutive model *PM4Sand* developed by Boulanger and Ziotopoulou (2012) was utilized to model the dynamic response of the soil. This model is a critical-state compatible, stress-ratio based, bounding-surface plasticity model for sands that modifies the model outlined in Manzari and Dafalias (1997) and Dafalias and Manzari (2004) to better capture the response of liquefiable soils. These analyses were completed only for a selection of

sites for the Christchurch event to further examine the capability of the generated input motions to capture soil response using a different analysis procedure.

Figure 2.13 shows the computed response spectra for the calculated surface motions from the analyses completed using *DEEPSOIL* and *FLAC* at the Christchurch Botanical Gardens strong motion station (CBGS) using the *CACS Woth1 FN* input motion. As can be seen for this case, the *FLAC* analysis resulted in a better match of both the shape and amplitude of the recorded motion's response spectrum, especially from 0.1 to 1 s. The variation in the calculated response spectra presented in Figure 2.13 could be due to the representation of the soil's stress-strain behavior via the *PM4Sand* constitutive model implemented in *FLAC* versus the *MKZ* model implemented in *DEEPSOIL*. A comparison of shear stress vs. shear strain response of a soil layer due to the differing pore water pressure models is shown in Figure 2.14. The layers chosen for comparison correspond to the layers from each analysis that generated the maximum amount of excess pore water pressure (i.e., max r_u). The more advanced *PM4Sand* model appears to capture the nonlinear response of the liquefied soil better. However, a more exhaustive study would need to be completed to confirm the reasons for these differences.

Figure 2.15a shows a plot of residuals for all nonlinear effective stress analyses using the *CACS Woth1* input motion for the Darfield event. There is a consistent positive "bump" in the residuals across all stations for periods between 1 s and approximately 6 s. The consistent underestimation of the spectral accelerations within this period range is most likely due to the input motion's inability to fully replicate the forward directivity effects or basin response experienced at the strong motion stations in the eastern stations during the Darfield event. Figure 2.15b presents the residuals for the effective stress analyses completed using the *RHSC Woth1 FN* input motion. Now there is a general underestimation of the spectral acceleration values for periods greater than 1 s, but on a much less pronounced scale compared to those shown in Figure 2.15a. The RHSC recording is classified as a velocity-pulse-type motion for the Darfield event based on the Hayden et al. (2014) procedure; whereas, the CACS recording is not. Consequently, the *RHSC Woth1* motion should be superior to the *CACS Woth1* motion at estimating the response for periods in the 1 to 6 s range for those sites that were also identified as having velocity-pulse-type motion for the Darfield event. A proper characterization of the input motion is thus critical for calculating reasonable responses at the ground surface.

2.7 CONCLUSIONS

The 2010-11 Canterbury earthquake sequence provides an exceptional opportunity to investigate how the same ground responded to several significant earthquakes that delivered different intensities and durations of strong shaking. The ground near some of these strong motion station sites liquefied multiple times during the sequence; whereas other sites never liquefied. The seismic recordings at these sites were utilized to evaluate the capabilities of nonlinear 1D effective stress seismic site response analyses.

One of the greatest sources of uncertainty with most seismic site response analyses is the characterization of input motions. The deep basin structure that underlies much of Christchurch and the lack of recorded "rock" motions in the area of interest makes the selection of input motions for site response analyses in Christchurch challenging. This study generated deconvolved surface motions from two firm soil sites to provide input motions at the top of the dense Riccarton Gravel unit for the analyses. With the uncertainty introduced by using this

procedure for generating input motions, some consistent biases were evident in the results of analyses compared to recorded surface motions for some events using a particular input motion; however, reasonable trends in the seismic response of sites that did or did not liquefy during the Canterbury earthquake sequence were observed.

Effective stress analyses did capture the generation of pore water pressure during strong shaking in critical layers. The generation of substantial excess pore water pressures in key layers generally agreed with the results of the empirical CPT-based liquefaction triggering procedures. However, even for cases where substantial excess pore water pressures were indicated within the subsurface of a given 1D soil column (i.e., r_u values in excess of 0.95), there were typically only minor differences between the acceleration response spectra of surface motions calculated using nonlinear total stress and effective stress analyses.

Given the wealth of subsurface data available, it would be advantageous to install at least one down-hole array in Christchurch to measure accelerations at various depths within a soil profile (including the top of the Riccarton Gravel layer and in bedrock) as well as pore water pressures in the shallow liquefiable soils to assist in the calibration of input parameters for future analyses. Also, the generation of synthetic "rock" or "Riccarton Gravel" motions for Christchurch to be used as representative input motions for seismic site response analyses would be beneficial to future studies.

Table 2.1: Information for events examined from Canterbury earthquake sequence

Event	Date	NZ Local Time	M_w	Hypocentral Latitude	Hypocentral Longitude	Strike (°)	Dip (°)	Z_{tor} (km)
1	4 SEP 10	04:35:46	7.1	-43.5382	172.1635	85	82	0.0
2	26 DEC 10	10:30:15	4.7	-43.5544	172.6615	74	84	2.0
3	22 FEB 11	12:51:42	6.2	-43.5644	172.6915	50	64	0.5
4	13 JUN 11	14:20:50	6.0	-43.5638	172.7431	162	67	1.4
5	23 DEC 11	12:58:36	5.8	-43.4862	172.7957	45	63	0.0
6	23 DEC 11	14:18:02	5.9	-43.5300	172.7428	57	51	1.5

Notes:

1) Moment magnitudes obtained from GeoNet (www.geonet.org.nz) regional Centroid Moment Tensor (CMT) solutions (Ristau 2008)
2) Strike, dip, and Z_{tor} values are based on Metadata received from Bradley (2013) via personal communication, except for the 22 FEB 11 event; the 22 FEB 11 values are based on Bradley and Cubrinovski (2011)

Table 2.2: Characteristics of event parameters at strong motion stations

Station	4 SEP 10 M_w7.1		26 DEC 10 M_w4.7		22 FEB 11 M_w6.2		13 JUN 11 M_w6.0		23 DEC 11 M_w5.8		23 DEC 11 M_w5.9	
	PGA (g)	R_{rup} (km)	PGA (g)	R_{rup} (km)	PGA (g)	R_{rup} (km)	PGA (g)	R_{rup} (km)	PGA (g)	R_{rup} (km)	PGA (g)	R_{rup} (km)
CACS	0.2	11.7	0.02	13.1	0.21	12.8	0.14	16.2	0.07	19.4	0.08	16.7
CBGS	0.16	14.4	0.27	4.4	0.5	4.7	0.16	7.6	0.16	12.9	0.21	10.2
CCCC	0.22	16.2	0.23	2.6	0.43	2.8	-	-	0.13	11.1	0.18	8.7
CHHC	0.17	14.7	0.16	3.5	0.37	3.8	0.22	6.8	0.17	12.5	0.22	10.0
HPSC	0.15	21.7	0.05	6.6	0.22	3.9	0.26	5.5	0.2	6.12	0.26	3.2
KPOC	0.34	27.6	0.01	19.8	0.2	17.4	0.1	19.4	-	-	-	-
NNBS	0.21	23.1	0.04	7.8	0.67	3.8	0.2	5.6	-	-	-	-
PPHS	0.22	15.3	0.09	8.2	0.21	8.6	0.12	10.4	0.12	13.4	0.14	10.5
PRPC	0.21	19.3	0.09	3.7	0.63	2.5	0.34	3.7	0.29	8.1	-	-
REHS	0.25	15.8	0.25	4.4	0.52	4.7	0.26	6.8	0.2	11.5	0.25	8.8
RHSC	0.21	10.0	-	-	0.28	6.5	0.19	11.8	0.16	17.2	0.16	14.6
SHLC	0.18	18.6	0.16	5.6	0.33	5.1	0.18	6.3	0.26	9.1	0.28	6.1
SMTC	0.18	17.5	0.03	10.5	0.16	10.8	0.09	12.0	0.07	13.2	0.15	10.4

Notes:

1) PGA values from Bradley et al. (2014) for Darfield, Christchurch, 13 JUN 11, and 23 DEC 11 (M_w5.9) events; values for 23 DEC 11 (M_w5.8) and 26 DEC 10 events are from metadata provided by Bradley (2013) pers. comm.
2) R_{rup} values from Bradley et al. (2014) for Darfield, Christchurch, 13 JUN 11, and 23 DEC 11 (M_w5.9) events; values for 23 DEC 11 (M_w5.8) and 26 DEC 10 events are from metadata provided by Bradley (2013) pers. comm.

Table 2.3: Site investigation information for strong motion station sites

Station name	Station Lat.	Station Long.	Depth to Riccarton Gravel[1] (m)	Available Site Investigation Data		
				Geophysical Testing[4]	CPTu [5]	Boreholes [5]
CACS	-43.4832	172.5300	6/14	SW[2]	--	BH-11529A
CBGS	-43.5293	172.6199	21.0	SW[2]	CBGS_CPT1[2]	CBGS_BH1[2], BH11793(CGD)
CCCC	-43.5381	172.6474	25.0	SW[2]	CPT484(CGD), CPT24862(CGD), CPT24865(CGD)	BH1759(CGD)
CHHC	-43.5359	172.6275	22.0	SW[2]	CPT425(CGD), CPT12257(CGD), CPT12258(CGD)	BH1756 (CGD), BH12255(CGD), BH26682 (CGD)
HPSC	-43.5016	172.7022	36.0	SW [3]	CPT47(CGD), CPT89(CGD), CPT18940(CGD)	BH16910 (CGD)
KPOC	-43.3764	172.6637	18.5	SW[2]	--	KPOC_BH1[2]
NNBS	-43.4954	172.7180	41.0	SW[2]	CPT33695(CGD), CPT1461(CGD) CPT17254(CGD)	BH30210 (CGD), BH2685 (CGD), BH30211(CGD)
PPHS	-43.4928	172.6069	20.0	SW[2]	CPT1497(CGD)	BH34717(CGD),
PRPC	-43.5258	172.6828	28.0	SW[2]	CPT1396(CGD), PRPC_CPT2[2]	BH23529 (CGD)
REHS	-43.5219	172.6351	20.0	SW[2]	REHS_CPT1[2], REHS_CPT2[2],CPT386(CGD), CPT9215(CGD),CPT9217(CGD)	BH1735 (CGD), BH21735 (CGD)
RHSC	-43.5362	172.5644	11/16	SW[2], SW[3]	--	BH11529 (CGD)
SHLC	-43.5053	172.6634	27.0	SW[2]	CPT626(CGD),CPT17584(CGD)	BH20985(CGD), BH20992(CGD), BH23531(CGD)
SMTC	-43.4675	172.6139	28.0	SW[2]	--	BH14315(CGD)

Notes:

1) Depth to Riccarton Gravel estimated from the site investigation data presented by Wotherspoon et al. (2013) and Bradley (2014) pers. comm.
2) Data and results from Wotherspoon et al. (2013)
3) Data and results from Wood et al. (2011)
4) SW = surface wave testing
5) CPT and borehole data from Canterbury Geotechnical Database (2013) unless otherwise noted

Table 2.4: Scale factors for deconvolved Riccarton Gravel motions

Station	4 SEP 10 M_w7.1		22 FEB 11 M_w6.2		13 JUN 11 M_w6.0		23 DEC 11 M_w5.8		23 DEC 11 M_w5.9		26 DEC 10 M_w4.7	
	CACS	**RHSC**	**CACS**	**RHSC**	**CACS**	**RHSC**	**CACS**	**RHSC**	**CACS**	**RHSC**	**CACS**	**RHSC**
CBGS	0.85	0.76	2.15	1.22	2.08	1.48	1.61	1.40	1.69	1.45	3.20	--
CCCC	0.78	0.69	2.74	1.55	--	--	1.90	1.65	1.98	1.70	4.59	--
CHHC	0.93	0.83	2.61	1.47	2.53	1.79	1.90	1.65	1.94	1.67	4.32	--
HPSC	0.63	0.56	2.48	1.40	2.80	1.98	3.37	2.92	3.96	3.39	2.42	--
KPOC	0.47	0.42	0.73	0.42	0.82	0.58	--	--	--	--	0.47	--
NNBS	0.61	0.54	2.57	1.45	2.83	2.00	--	--	--	--	2.11	--
PPHS	0.81	0.73	1.44	0.82	1.69	1.19	1.57	1.36	1.75	1.50	1.93	--
PRPC	0.78	0.70	3.16	1.78	3.77	2.67	3.05	2.64	--	--	4.55	--
REHS	0.92	0.82	2.45	1.38	2.66	1.89	2.21	1.92	2.30	1.97	3.98	--
SHLC	0.68	0.61	2.07	1.17	2.42	1.71	2.31	2.01	2.62	2.25	2.65	--
SMTC	0.76	0.68	1.25	0.71	1.47	1.04	1.69	1.46	1.77	1.52	1.44	--

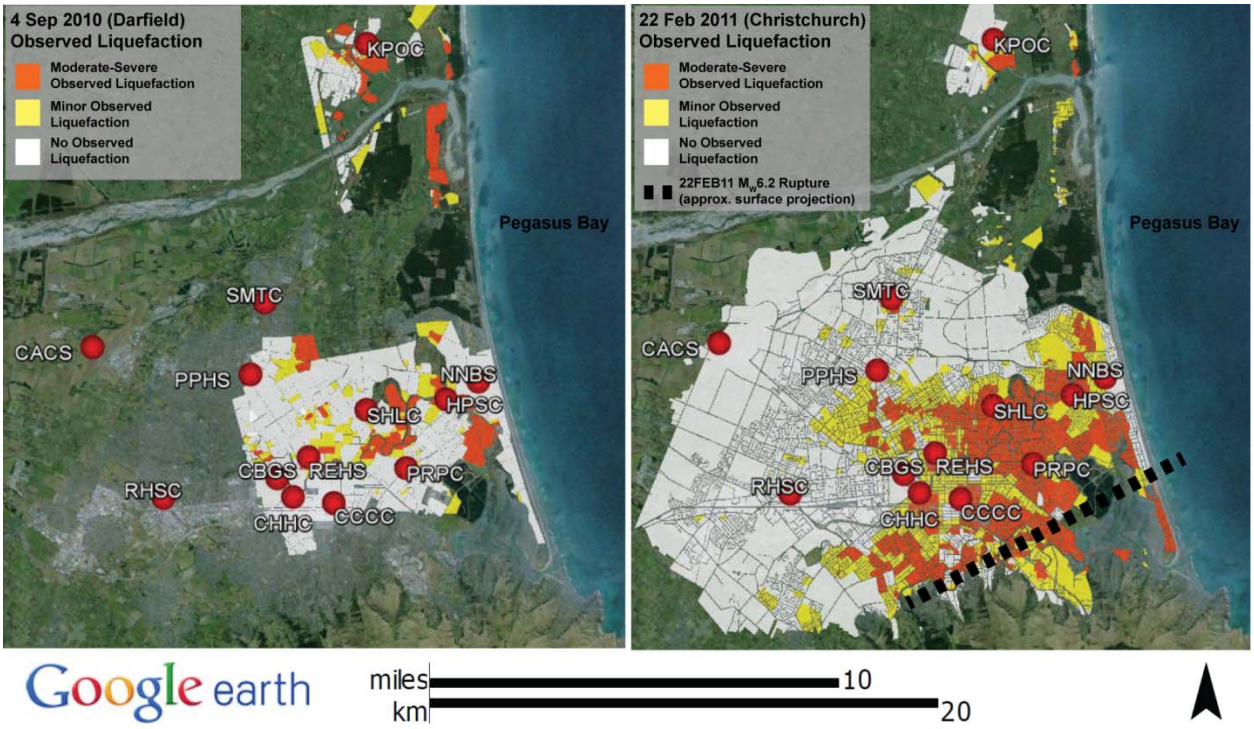

Figure 2.1: Observed liquefaction maps for the 4 SEP 10 and 22 FEB 11 events (Canterbury Geotechnical Database 2013)

Figure 1 was created from maps or data extracted from the Canterbury Geotechnical Database (https://canterburygeotechnicaldatabase.projectorbit.com), which were prepared or compiled for the Earthquake Commission (EQC) to assist in assessing insurance claims made under the Earthquake Commission Act 1993. The source maps and data were not intended for any other purpose. EQC and its engineers, Tonkin & Taylor, have no liability for any use of the maps and data or for the consequences of any person relying on them in any way.

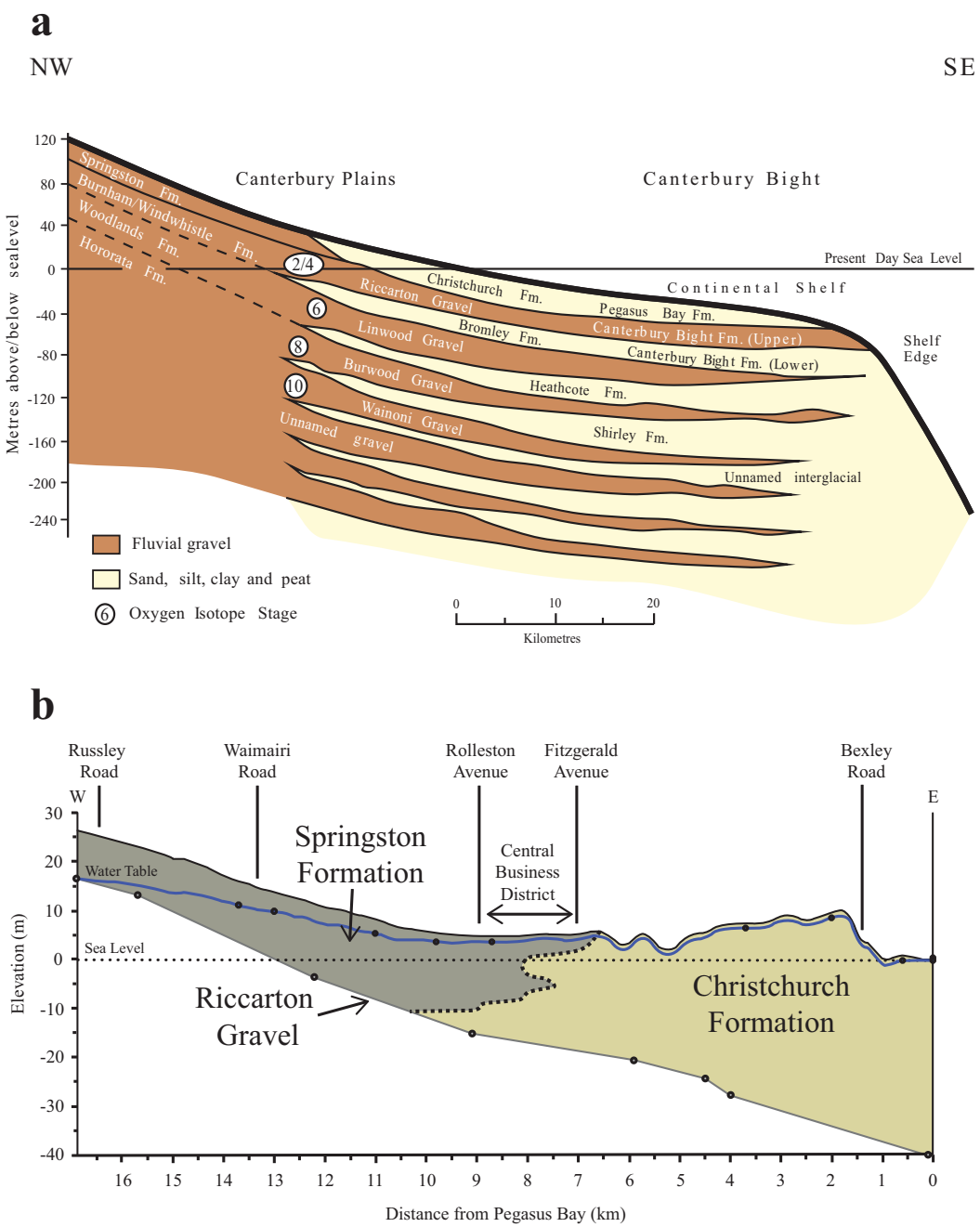

Figure 2.2: a) Geologic cross section of the Christchurch area (modified after Forsyth et al. 2008—originally from Brown and Weeber 1992 and Browne and Naish 2003) and b) Simplified subsurface profile for Christchurch (modified after Cubrinovski et al. 2011b)

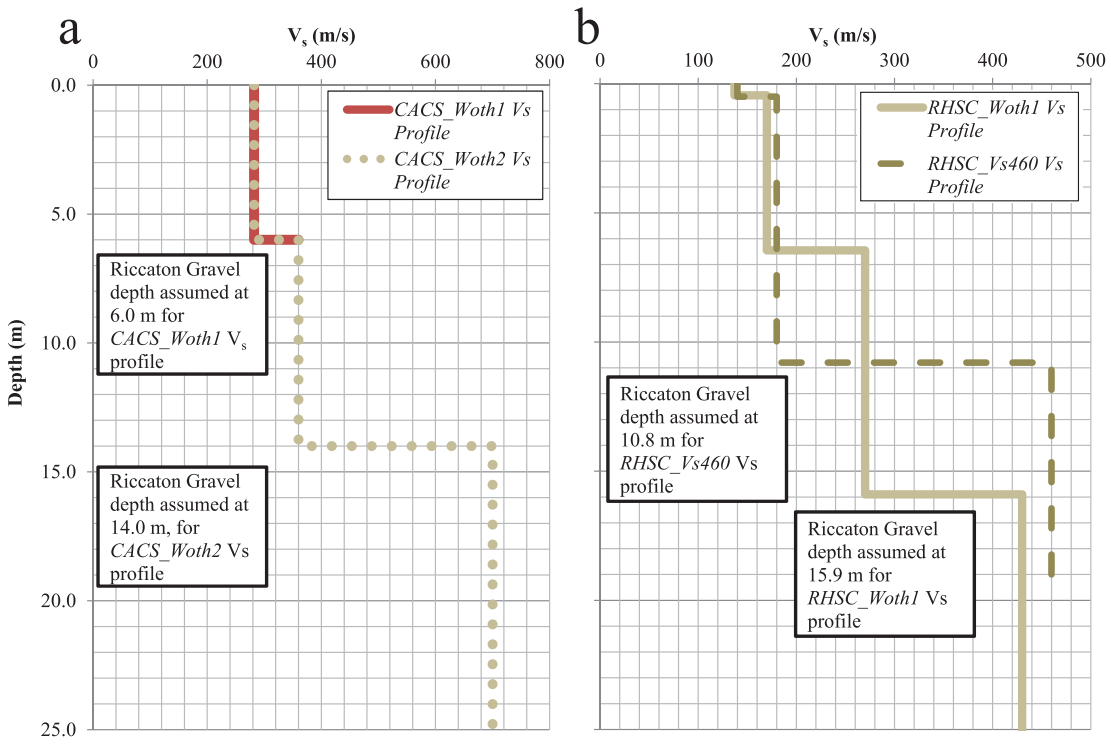

Figure 2.3: Assumed V_s profiles for a) CACS and b) RHSC

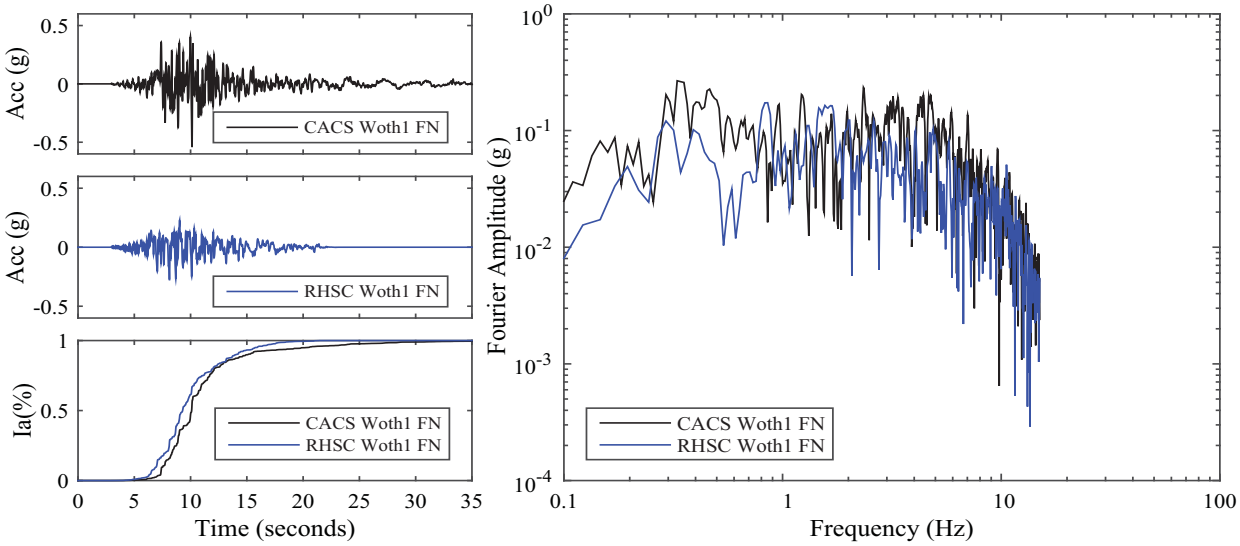

Figure 2.4: Input motions for site response analyses completed at CHHC for the 22 FEB 11 Mw6.2 Christchurch event; includes Husid plot and Fourier amplitude spectra

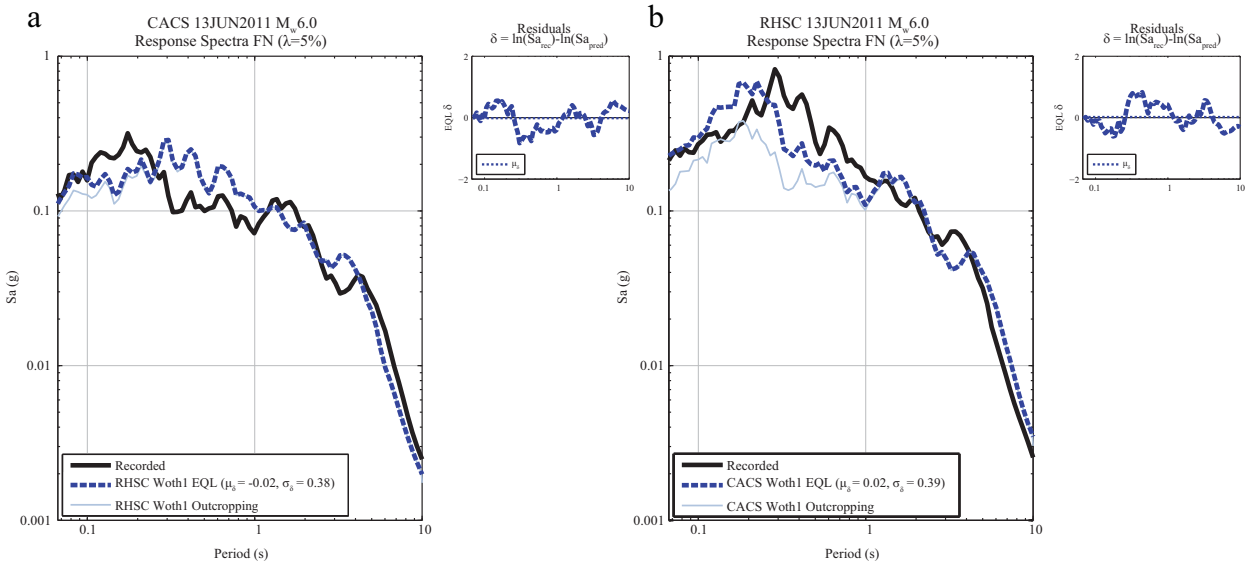

Figure 2.5: Results of equivalent linear analyses conducted at a) CACS using *RHSC Woth1* input motion and b) RHSC using *CACS Woth1* input motion in the fault normal (FN) direction for the 13 JUN 2011 M_w6.0 event

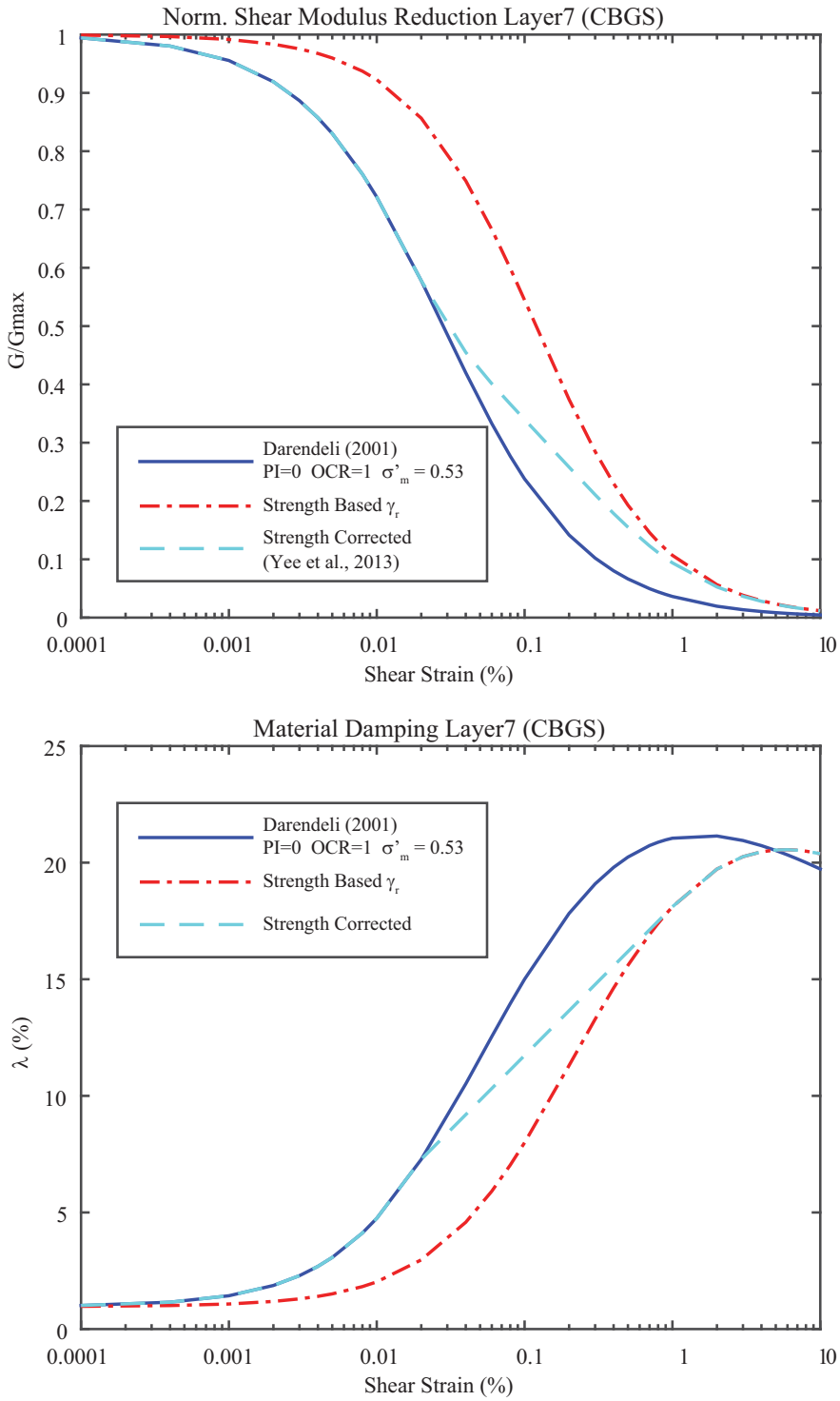

Figure 2.6: Adjustment of target curves for shear modulus reduction and material damping

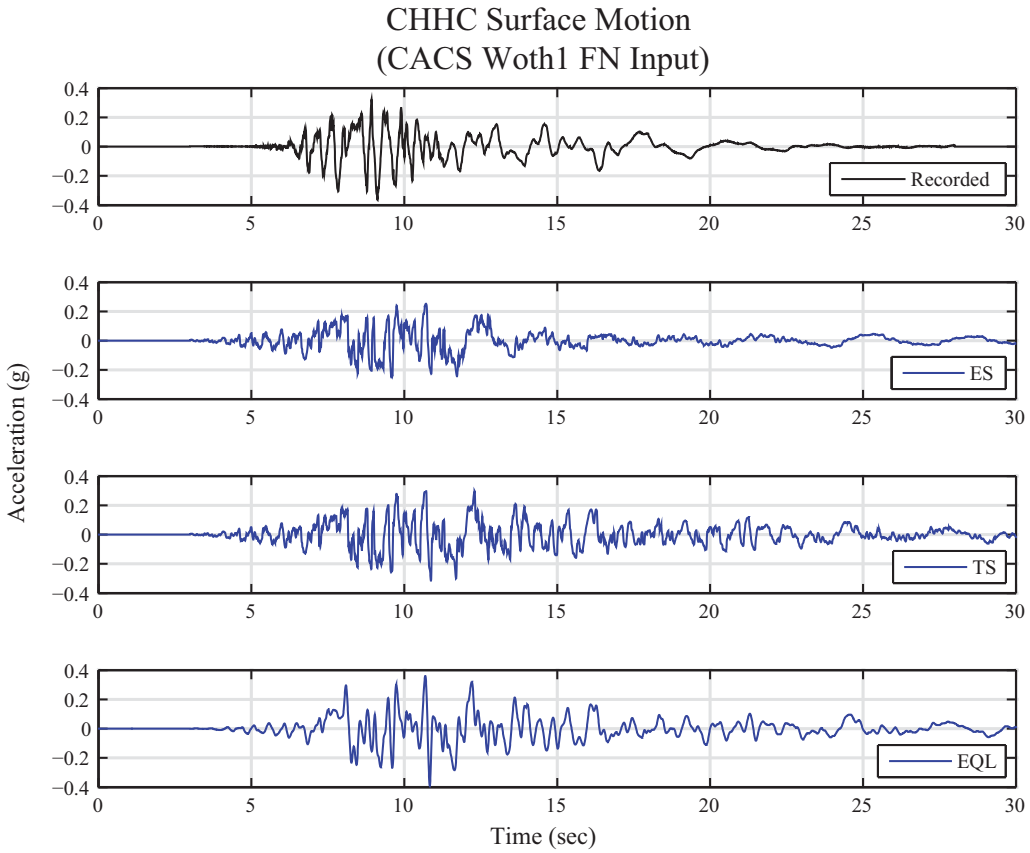

Figure 2.7: Acceleration-time series for analyses at CHHC using *CACS Woth1* input motion in the FN direction for the Christchurch earthquake

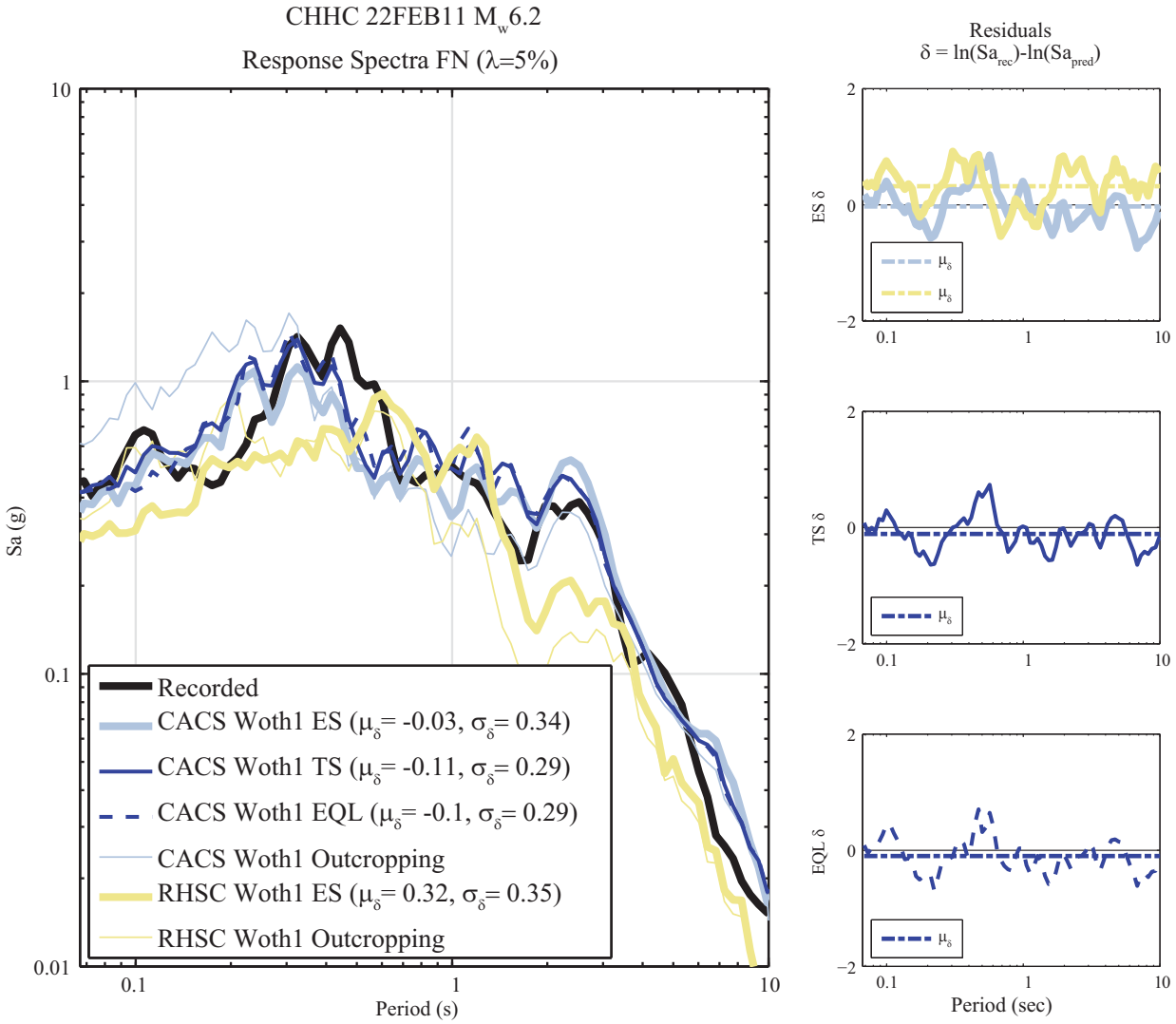

Figure 2.8: Acceleration response spectra comparisons for CHHC (FN) site for the Christchurch earthquake

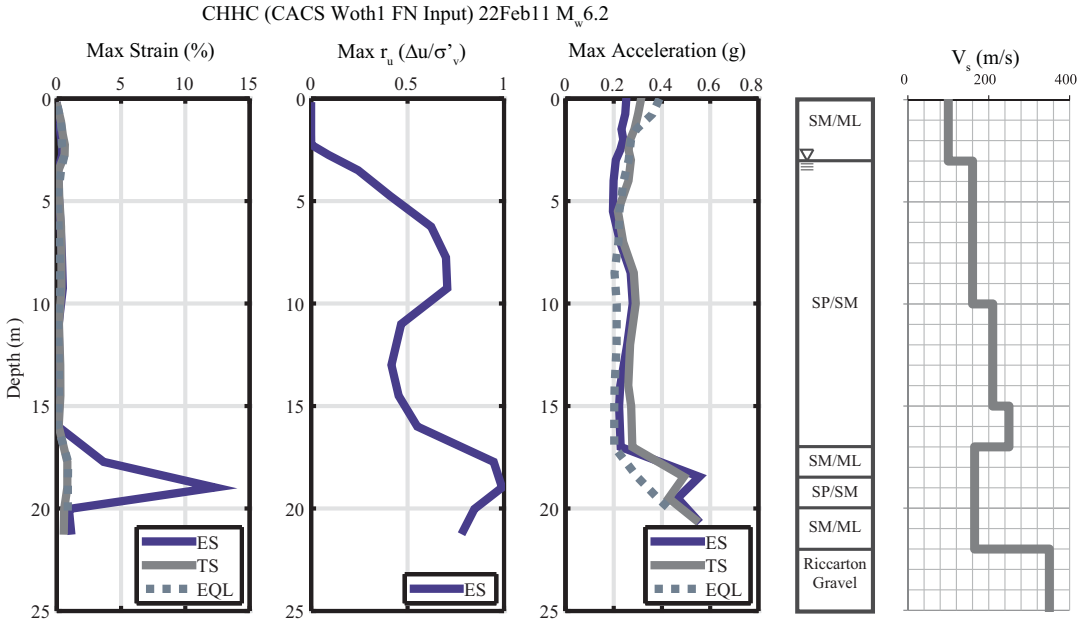

Figure 2.9: Maximum shear strain, pore pressure ratio, and acceleration values with depth for analyses completed at CHHC for the Christchurch earthquake using *CACS Woth1 FN* input motion

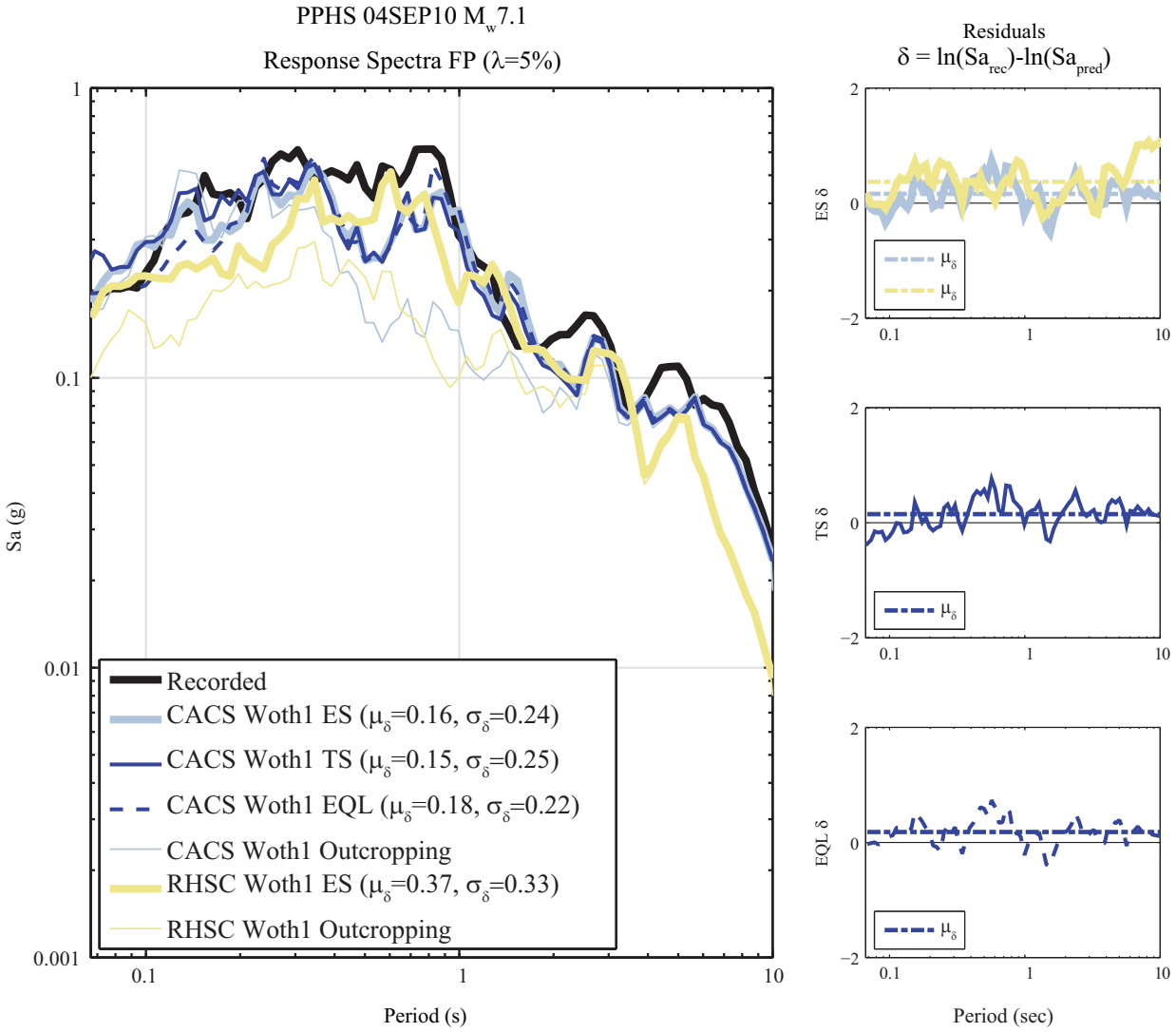

Figure 2.10: Acceleration response spectra comparisons for PPHS (FP) for the Darfield earthquake

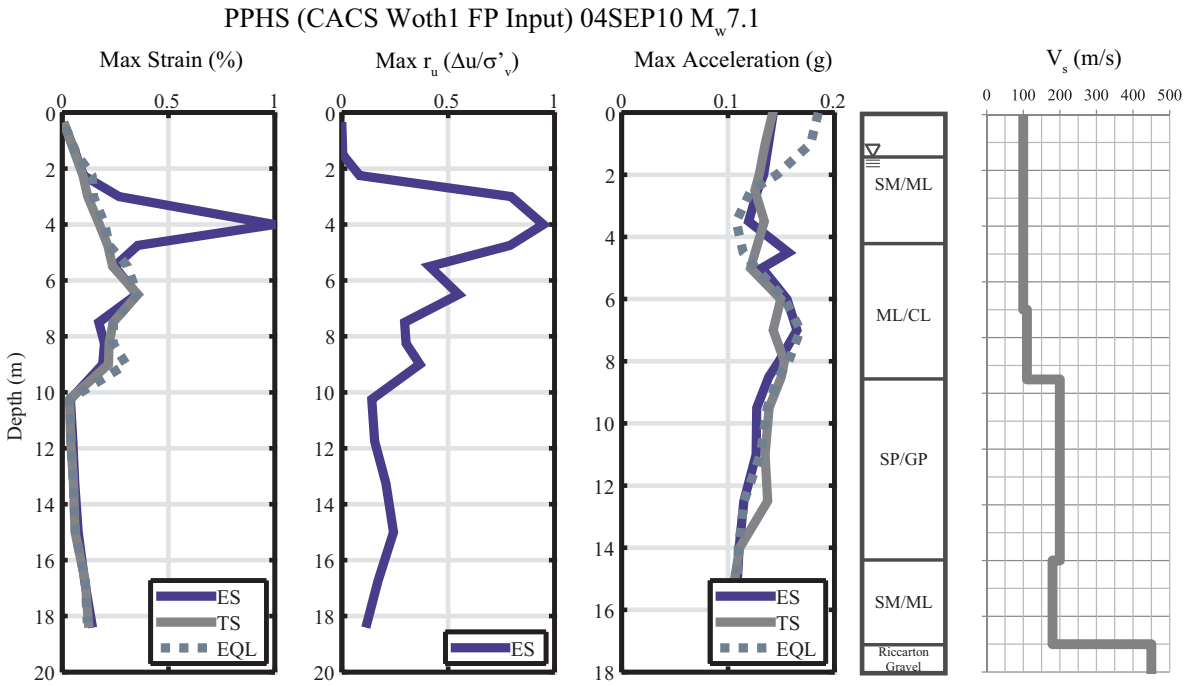

Figure 2.11: Maximum shear strain, pore pressure ratio, and acceleration values with depth for analyses completed at PPHS for the Darfield earthquake using the *CACS Woth1 FP* input motion

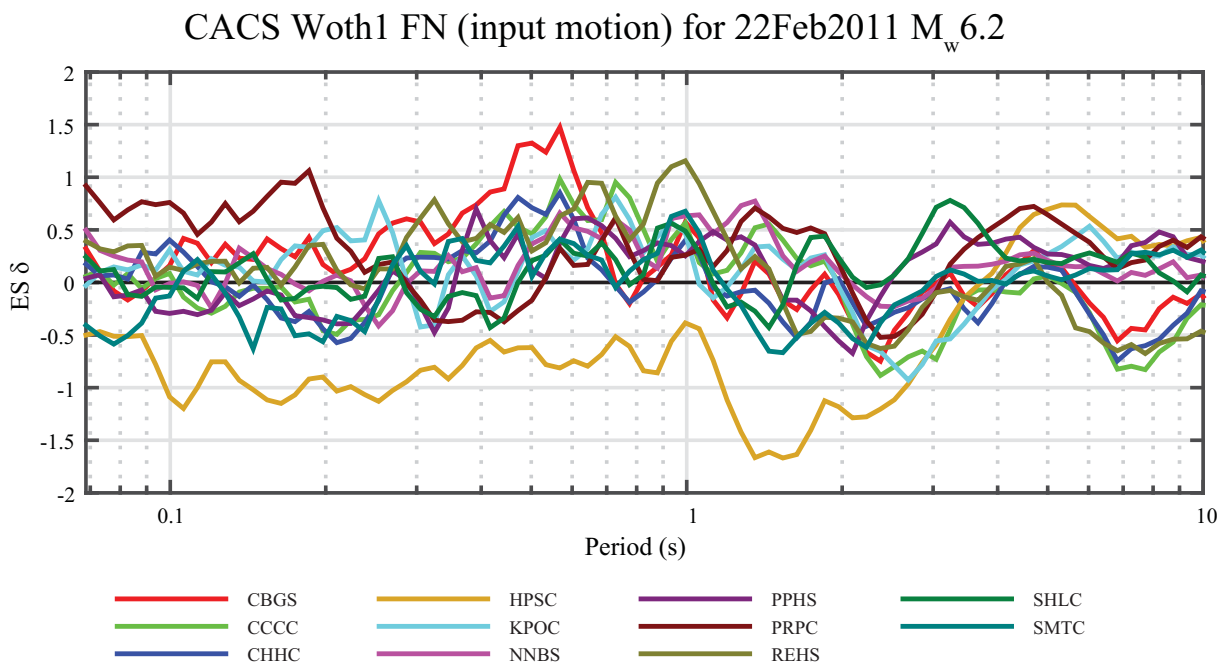

Figure 2.12: Residuals for effective stress analyses completed using the *CACS Woth1* input motion (FN component) for the Christchurch event

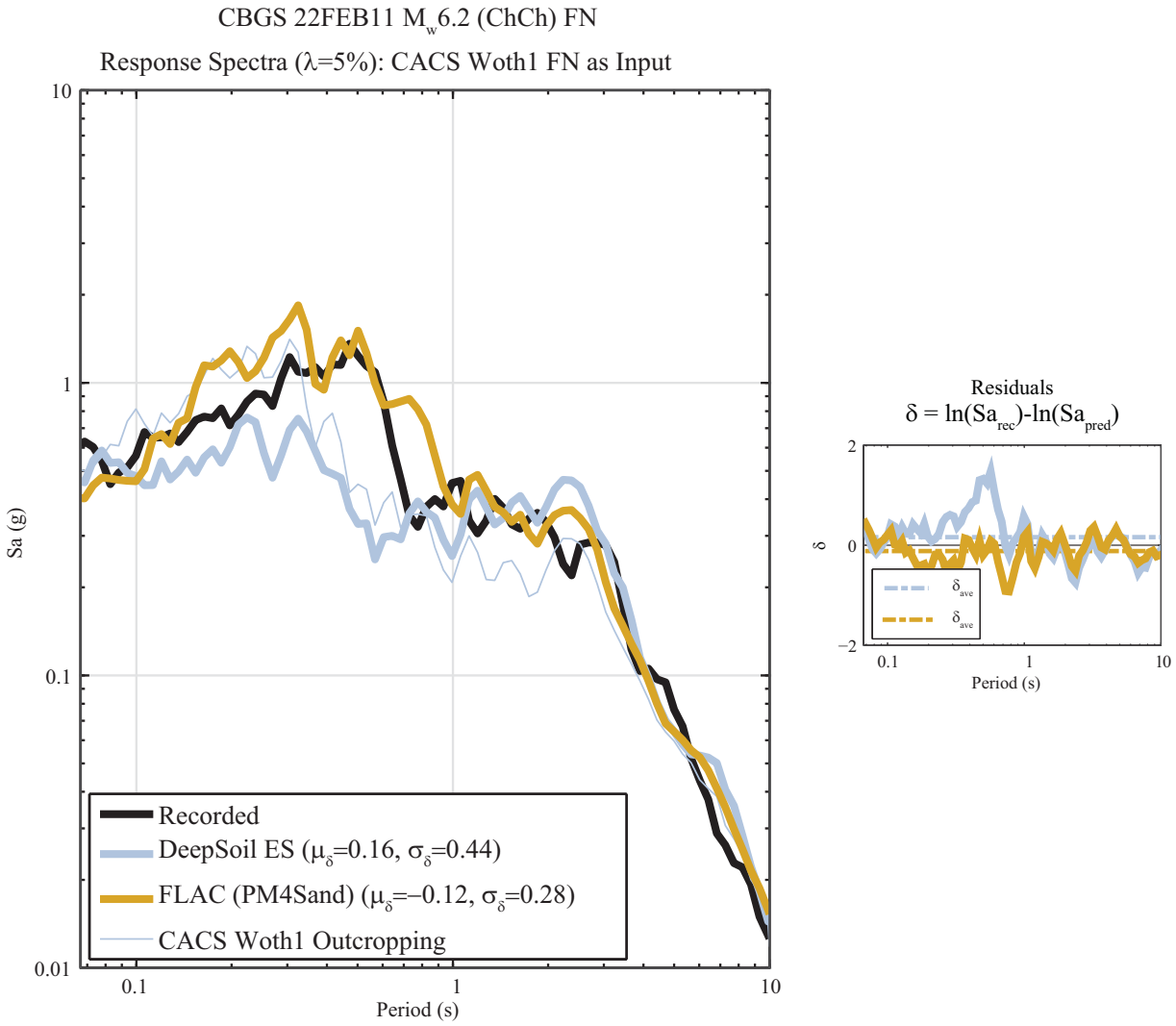

Figure 2.13: Comparison of acceleration response spectra for calculated surface motions using DEEPSOIL and FLAC (with PM4SAND) for CBGS using the *CACS Woth1 FN* input motion for the Christchurch event

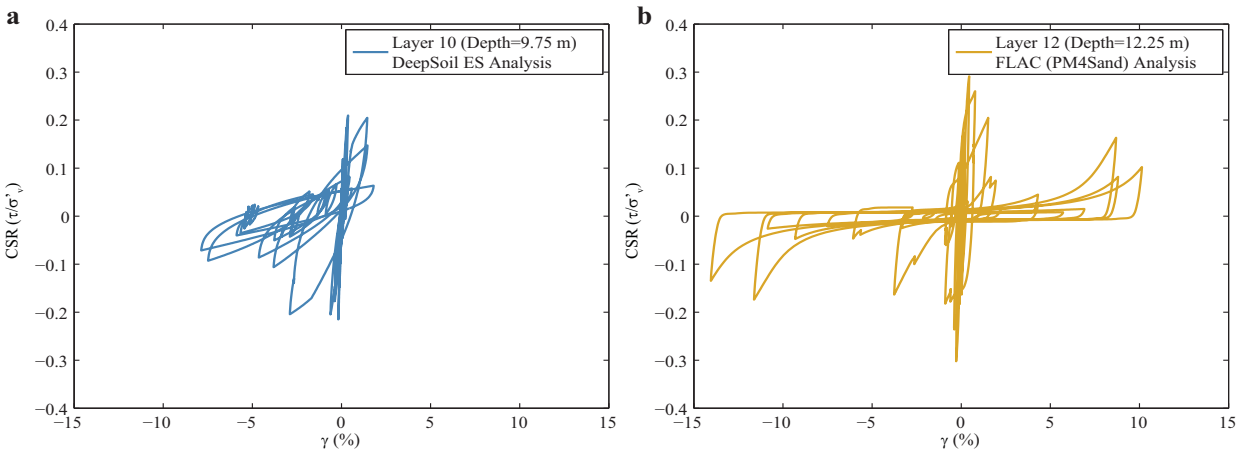

Figure 2.14: CSR vs. shear strain for a) Layer 10 of the nonlinear effective stress analysis completed using DEEPSOIL and b) Layer 12 of the analysis completed using FLAC (with PM4Sand) at CBGS for the Christchurch earthquake using the *CACS Woth1 FN* input motion

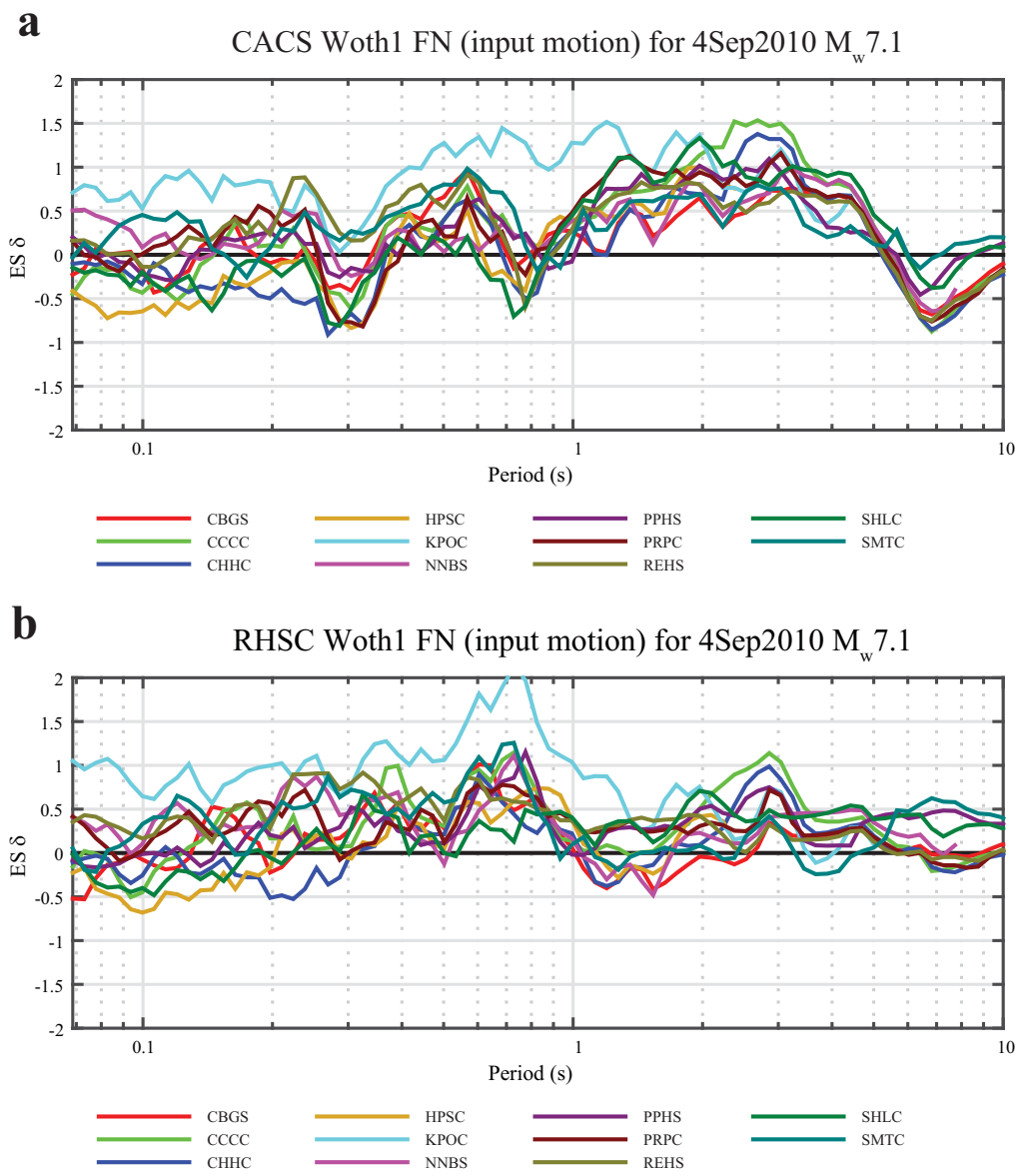

Figure 2.15: Residuals for effective stress analyses completed using the a) *CACS Woth1* non-pulse-type input motion and b) *RHSC Woth1* pulse-type input motions (FN component) for the Darfield event

CHAPTER 3: CHARACTERIZATION OF SHALLOW SOILS IN THE CENTRAL BUSINESS DISTRICT OF CHRISTCHURCH, NEW ZEALAND

The contents of this chapter are primarily from a journal article submitted to the ASTM Geotechnical Testing Journal by Markham, C.S., Bray, J.D., Riemer, M.F., and Cubrinovski, M. entitled: "Characterization of Shallow Soils in the Central Business District of Christchurch, New Zealand," which is under review.

3.1 INTRODUCTION

Christchurch, New Zealand (NZ) experienced intense shaking from numerous events of the 2010-11 Canterbury earthquake sequence. Of these events, the 22 FEB 2011 M_w6.2 Christchurch event was the most destructive. The Christchurch earthquake caused 185 casualties and left many individuals seriously injured (Cubrinovski et al. 2011a). Most of the high-rise buildings within the central business district (CBD) have been demolished, and over a third of its approximate 4,000 buildings have been demolished due to damage from the Christchurch earthquake. Liquefaction of foundation soils was a major contributing factor in the damage sustained by many of the buildings in the CBD.

Christchurch is situated on the eastern coast of the Canterbury Plains, which is comprised primarily of Quaternary deposits of alluvial material interlayered with marine deposits. Regular flooding of the Waimakariri River, which is now channelized north of the city, led to the deposition of gravels and sands in flood channels throughout the Canterbury Plains as well as overbank deposits of silts (Brown and Weeber 1992). The Springston Formation makes up the shallowest subsurface deposits of much of the CBD and comprises layers of postglacial fluvial sands, silts, and gravels that have been deposited within the last 3,000 years. This formation overlies and interfingers with deposits of the Christchurch Formation in the CBD. The Christchurch formation consists of sands, silts, and gravels, as well as clays, peats, and shells originating from beach, estuarine, lagoonal, dune, and coastal swamp sediments that have been deposited within the last 6,500 years (Brown and Weeber 1992). The water table in the CBD is generally within 1-3 m of the ground surface.

The spatial extent of observed liquefaction was widespread during the Christchurch earthquake as well as the 4 SEP 2010 M_w7.1 Darfield event and 13 JUN 2011 M_w6.0 event. Figure 3.1 shows the areas in the CBD that were affected by liquefaction. The zone of *severe* liquefaction observed in the northern part of the CBD was most critical with regards to the seismic performance of foundation soils and consequently the overlying structures during the Christchurch event. Cubrinovski et al. (2011a, 2011b, 2011c), Bray et al. (2014), and Zupan (2014) document several observations of the adverse effects of liquefaction on the performance of structures throughout the CBD. The varying performance of structures during the Canterbury earthquake sequence provides an exceptional opportunity to investigate the effects of liquefaction on buildings during seismic events with varying magnitudes and levels of strong shaking. To understand the effects of liquefaction on the performance of structures, though, understanding the response of their respective foundation soils is critically important.

This chapter describes a comprehensive field sampling and advanced laboratory testing program that characterized the subsurface soils at several sites within and adjacent to the CBD of Christchurch. The nature of the silty and sandy soils investigated allowed for "undisturbed" samples to be obtained and high-quality laboratory testing to be completed to characterize the liquefaction resistance of these soils. In addition to monotonic and cyclic triaxial testing being employed to characterize the monotonic and dynamic response of the examined soils, various index tests were completed. The responses of these soils were critical with regards to the performance of structures during the Canterbury earthquake sequence. The data and results obtained from this study provide vital information to engineers and researchers performing advanced analyses (e.g., soil-structure interaction analyses) to study the effects of liquefaction on buildings.

3.2 CBD SITE INVESTIGATIONS

3.2.1 Previous Investigations

Christchurch's CBD is delineated by four avenues: Bealey Ave. (to the north), Moorehouse Ave. (to the south), Deans Ave. (to the west) and Fitzgerald Ave. (to the east) and covers an area of approximately 6 km^2. Following the Darfield and Christchurch events, teams of researchers and practitioners surveyed and documented ground conditions and the performance of structures throughout the CBD as part of the Geotechnical Extreme Events Reconnaissance (GEER) Association efforts. These efforts included the documentation of the effects of liquefaction with regards to building settlements and movements as well as observations of sediment ejecta at various sites. Green and Cubrinovski (2010) provides an overview of the GEER team investigations following the Darfield earthquake, while Cubrinovski et al. (2011a,b,c) provide synopses of the findings following the Christchurch event.

A joint site investigation program completed by researchers from the University of California, Berkeley (UCB) and University of Canterbury (UC) focused on characterizing shallow subsurface soils at sites within Christchurch's CBD where liquefaction of foundation soils caused varying degrees of damage to overlying structures during the Canterbury earthquake sequence. These studies were completed between July 2011 and April 2013 and primarily consisted of cone penetration tests (CPTs) as well as two boreholes where "undisturbed" soil samples were obtained via the Gel-push piston sampler. This work built on the previously discussed post-earthquake studies and is detailed by Taylor et al. (2012a,b), Bray et al. (2014), and Zupan (2014).

3.2.2 Overview of Investigations at Sites Selected for Further Study

From April to June 2014 and September to October 2014 a subsurface investigation program was undertaken to characterize the engineering properties of soils at key building sites within Christchurch. These investigations included exploratory boreholes with "undisturbed" sampling of critical soil layers. Figure 3.2 shows the locations of these boreholes, and Table 3.1 provides their GPS coordinates. All but one of the boreholes correspond to sites located in the CBD; the lone exception being the LS-II site, which is located approximately half a kilometer southeast of the CBD. Structures of varying height (2 to 22-story buildings) and footprint area were located at

these sites during the Canterbury earthquakes; all but one of the buildings—CTH building—were demolished following the Canterbury events. These sites also consist of soils that are representative of ground conditions throughout the CBD, especially with regards to zones of liquefiable material.

The adverse effects of liquefaction on the performance of foundation soils at each of the sites listed in Table 3.1 varied and was documented in Cubrinovski et al. (2011a,b,c) as well as other post-event studies (e.g., Kam et al. 2011). The identification of problematic soils with regards to liquefaction susceptibility at each of these sites was examined via CPT investigations and subsequent interpretation of the resulting data by the aforementioned UCB-UC site investigation studies. "Undisturbed" sampling of shallow foundation soils focused on soil strata that were deemed to have been critical layers with regards to the effects of liquefaction on buildings. The use of CPT-based empirical liquefaction evaluation procedures (e.g., Robertson and Wride 1998) were the primary means of identifying soil layers to be sampled (i.e., shallow soils with factor of safety against liquefaction triggering less than or equal to one, $FS_l \leq 1$).

3.2.3 Undisturbed Sampling

Block sampling or ground freezing sampling techniques have been shown to provide high-quality laboratory specimens (e.g., Yoshimi et al. 1978, and Yoshimi et al. 1994) of cohesionless soils. However, the use of block sampling on the soils well below the shallow groundwater table in Christchurch was impractical, and ground freezing sampling technology was not available in New Zealand. Consequently, the Dames and Moore (D&M) Osterberg-type hydraulic piston sampler, which has been successful in retrieving high-quality samples in silty soils (Bray and Sancio 2006), was used to obtain "undisturbed" samples of soils in this UCB-led study. In a companion study led by UC researchers, the Gel-Push sampler was employed (Taylor et al. 2012b).

Figure 3.3 illustrates the general set-up and operation of an Osterberg-type hydraulic piston sampler. Soil exploratory borings were advanced using a tri-cone side-discharge drill bit in a cased borehole with drilling mud. The D&M sampler uses thin walled brass tubes of constant internal diameter, ID = 61.2 mm, and outside diameter, OD = 63.5 mm. The tubes are only pushed into the soil a length of 45 cm using the pressure provided by the circulation mud to minimize soil plugging within the tube. Friction between the soil and the tube is minimized by using smooth brass tubes. The area ratio, defined by Hvorslev (1949) as $C_a = 100 \cdot (OD^2 - ID^2)/ID^2$, is 7.6% for the D&M brass tubes. Following sampling, the tops of tubes were sealed and free draining caps were placed at the bottom of the tubes to allow for pore water to partially drain from the sampled soil. This drainage was important for coarser materials (e.g., sandy soils) as it helped minimize the chance of these soils liquefying in the tubes during transport; the drainage caps had negligible effect on the finer materials (e.g., silty soils). The samples were then placed upright in a specially designed box, and carefully transported to the UC laboratory in Christchurch for testing. Upon arrival to the lab, the free draining caps were replaced with non-draining caps and sealed to prevent excessive drying of the sample soil during storage.

3.3 SHALLOW GROUND CONDITIONS IN THE CBD

3.3.1 Overview

There are five soil types of interest with regards to liquefaction susceptibility and its effects on the performance of structures in the CBD of Christchurch. Four of these soil types (using the Unified Soil Classification System, USCS, ASTM D2487-11) are poorly graded clean sands (SP), poorly graded sands with silt (SP-SM), silty sands (SM), and silts (ML). The fifth soil type includes gravelly soil horizons (GP or GW) that are present at various sites throughout the CBD at various depths within the shallow subsurface.

Triaxial testing of "undisturbed" soil specimens was performed on all of these soil types except for the gravelly soils. Additionally, index testing was performed on each soil specimen (e.g., grain size distribution, Atterberg limits, and maximum and minimum void ratio). Advanced laboratory testing (i.e., triaxial testing) was not performed on the gravelly soils, because the D&M sampler is unable to obtain "undisturbed" samples of this coarse material (i.e., the brass tube warps and deforms due to the high stresses required to advance the sampling tube and the relatively large particle sizes of the gravel). Grain size distribution testing of this gravelly material was performed at one of the sites studied using material obtained through bulk sampling via sonic coring.

Figure 3.4 provides an overview of the grain size distribution (GSD) curves for soil specimens that were studied using either monotonic or cyclic triaxial testing. The sand materials (SP, SP-SM, and SM) are for the most part fine sands (passing the No. 40 sieve and retained on the No. 200 sieve) with a minimum of 87% by mass passing the No. 40 sieve for all soils tested. The maximum plasticity index (PI) for the ML soil specimens was a PI=5, which actually corresponded to a specimen that fell within the CL-ML zone of the classification chart (ASTM D2487-11). In general, though, the PI of the silts ranged from 0 to 4.

Figure 3.5 shows the grain size distribution of soil obtained via sonic coring from a depth of approximately 3.19 m to 5.0 m at the PWC building site (see Figure 3.2 for location). A gravel horizon starting from approximately 3 m and extending to a maximum depth of about 10 m (below ground surface) is present at this site. Bulk samples of this gravelly material were obtained for classification purposes by use of a plastic liner in conjunction with a 1.5 m long sonic coring barrel. The diameter of the sample obtained via this sampling technique is on the order of 82.5 mm. Therefore, coarse gravel particles have the potential to be broken as the sampler advances or pushed either away from or into the advancing sampler. Nonetheless, the grain size distribution chart shown in Figure 3.5 is informative in that it provides insights into the characteristics of the gravelly soil that is present in the shallow subsurface of several building sites in the CBD that were affected by liquefaction during the Canterbury earthquakes (e.g., VT and CTH sites in addition to the PWC building site). The tests suggest that the gravelly soil contains 30%-40% sand-sized particles and about 10% fines. Even considering the limitations of the sampling procedure, it is likely that this soil is actually a sandy gravel where the sand fraction contributes significantly to the deposit's response. Additional investigation is warranted to further characterize the engineering properties of the gravelly soils in Christchurch.

3.3.2 Representative Sites for Subsurface Characterization in the CBD

This study focused on characterizing four predominant soil types that are present throughout Christchurch's CBD, especially with regards to their cyclic response. The following sites are chosen to provide representative illustrations of the subsurface soil conditions in the CBD. Representative test results will also be shown in the results section of this chapter from triaxial testing that was performed on soils from these sites.

3.3.2.1 CTH Building Site

Figure 3.6a provides an overview of the portion of the CTH site that was investigated as a part of this study, while Figure 3.6b shows an east-west subsurface cross-section of the southern portion of the site. The auditorium of the CTH building sustained severe structural damage during the Christchurch earthquake (Zupan 2014). Differential settlement of shallow foundations that supported the main load bearing columns of the structure led to angular distortion and subsequent damage to structural elements throughout the building. The performance of the auditorium structure at the CTH site during the strong shaking of the Christchurch event was directly related to the performance of the underlying foundation soils.

Based on the CPT data provided by the work of Zupan (2014) and the corresponding soil behavior type index (I_c; Robertson and Wride 1998), which are presented in Figure 3.6b, a layer of silty sand and silt (I_c ranging from 1.75 to 2.6) is in the upper portion of the site. This layer is underlain by a layer of gravelly and sandy material (I_c ranging from 1 to 1.7), and finally a layer of cleaner sand (I_c < 2.05). These layers, excluding the dense layer of gravelly soil, predominantly had a $FS_l < 1$ (as computed by Zupan 2014 using the Robertson and Wride 1998 procedure). Sampling and testing of these soil layers (excluding the gravelly material from a depth of about 5 to 12 m) indicated that the upper portion of the soil profile comprises a layer of ML soil (to a depth of just under 4 m) overlying a layer of SP-SM material (to a depth of about 4.5 m). Below the layer of gravelly soil is another layer of SP-SM soil. Figure 3.7 shows the grain size distribution plots for the triaxial test specimens that were obtained from samples taken at various depths from the CTH site (see Figure 3.6b for sample depths).

3.3.2.2 FTG-7 Building Site

Figure 3.8a provides an overview of the FTG-7 site (with the adjacent *FTG-4* building shown). The FTG-7 building was a seven-story steel-framed building measuring approximately 29 m in the E-W direction by 32 m in the N-S direction. The building was founded on a system of shallow, reinforced concrete strip footings interconnected by tie-beams. Following the Christchurch event, it was reported that the southeast and southwest corners of the building had settled about 10 cm and 7 cm, respectively, relative to the northwest corner of the building, which caused an overall tilt of the building to the southeast (Zupan 2014).

Figure 3.8b shows an interpreted east-west cross-section for the FTG-7 site. Silty and sandy material (I_c generally ranging from 1.7 to 2.5) with $FS_l < 1$ is identified in the upper 7 to 9 m of the subsurface based on the CPT investigations performed by Zupan (2014). Below this material is a layer of liquefiable cleaner sandy material ($1.4 \leq I_c \leq 2.05$). The CPT interpretations shown in Figure 3.8b suggest that the upper silty material is variable (i.e., varying I_c values), which was supported by the classification of the triaxial test specimens from the upper portion of the FTG-7

subsurface. Nevertheless, relatively homogeneous specimens were able to be tested from this upper material and typically classified as SM or ML material. Additionally, triaxial testing of specimens from the lower, sandier material was also completed; these soils classified as SP or SP-SM.

3.4 TRIAXIAL TESTING OVERVIEW

Cyclic triaxial (CTX) tests were performed on specimens obtained from the sites to examine the cyclic response of critical soil layers in the CBD. In addition to cyclic testing, monotonic triaxial tests were performed on some soil specimens to examine their response to monotonic loading. All triaxial tests were performed using the CKC electropneumatic triaxial device with the Automated Triaxial Testing System software developed by Li et al. (1988). All testing on "undisturbed" soil specimens was performed at the UC Geomechanics Laboratory in Christchurch, NZ to minimize disturbance due to transportation.

Test specimens were prepared from sample tubes with high recovery (typically ≥ 95%). The bottom 50 mm and upper 100 mm of each tube sample were assumed to be too disturbed for testing, so that a maximum of two 135-140-mm-high test specimens were obtained from each tube. Extrusion length was minimized by cutting tubes to the desired height. After installing stiffening rings on the tube above and below the location of the intended cut, a large-diameter pipe cutter was slowly rotated around the sample tube to cut it. The test specimen was extruded from the tube in the same direction as the soil first entered the tube using a hydraulic jack. It was visually inspected to ensure it was relatively undisturbed. Following the placement and sealing of a flexible latex membrane around each specimen, an internal vacuum of 10-15 kPa was applied to each specimen to allow for set-up of the triaxial chamber. Flushing of de-aired water through each specimen was attempted using differential vacuum, which was necessary for the saturation of the coarser-grained sand specimens. Subsequent specimen saturation was achieved through vacuum saturation (extraction) followed by back pressure saturation so that B-values larger than 0.95 were achieved (most B-values were ≥ 0.97).

Specimens were isotropically consolidated to reasonably conservative estimates of the field vertical effective stresses, which included estimates of geostatic overburden stresses, pore water pressure, and net pressure increases due to building loads using Westergaard theory. Stress-controlled cyclic triaxial tests were performed using a sinusoidal loading pattern at a frequency of 0.1 Hz under undrained conditions. Cyclic triaxial tests were generally terminated once a double amplitude (compression peak-to-extension trough or vice versa) axial strain of 5% was reached. Post-liquefaction reconsolidation or monotonic compression tests were conducted following cyclic triaxial tests. Undrained monotonic triaxial tests were also stress-controlled with loading rates determined so that time to failure was greater than $4*t_{50}$, where t_{50} was the time to 50% consolidation estimated from the consolidation phase. Monotonic tests were generally run to the limit of the pressure supplied to the triaxial testing device (a resulting deviator stress on the order of 350 kPa) or 10% axial strain.

3.4.1 Disturbance Assessment of Triaxial Specimens

High quality samples of silts and clays have been obtained previously using the D&M sampler as described by Bray and Sancio (2006). Sample quality was evaluated in this earlier

study using the ratio of the change in void ratio to the soil's initial void ratio upon recompression to the in situ effective stress state criteria developed by Lunne et al. (1997) (i.e., $\Delta e/e_o < 0.04$ indicates very good to excellent specimen quality for OCR < 2). The Lunne et al. criteria were developed for plastic clays, so it cannot be applied to nonplastic to slightly plastic silty sands and sands.

In this study, three specimen quality evaluation approaches were primarily employed: 1) drilling and sampling notes relevant to disturbance and visual inspection of samples, 2) comparison of field measured and lab measured shear wave velocity (V_s), and 3) comparison of laboratory relative density (D_r) with estimates from CPT correlations. Laboratory test results were examined for signs of disturbance as well. Additionally, the lab-measured cyclic resistance ratios (CRR) were compared with those estimated using CPT liquefaction triggering correlations to discern if the cyclic responses of the lab specimens were consistent with those expected based on established CPT-based procedures. In evaluating sample disturbance in Christchurch it is important to remember that the soils that liquefied in the 22 FEB 2011 and later earthquakes had likely liquefied in the 4 SEP 2010 earthquake, so that samples retrieved in 2014 were not older than 3 years in terms of their cyclic response. Although shallow soils in the CBD were deposited within the past few thousand years, their seismic age was only a few months at the time of the Christchurch and later events of the Canterbury earthquake sequence. CPTs performed after the Canterbury earthquake sequence which were adjacent to CPTs performed before the earthquakes showed no significant change in the relative density of the soils that liquefied (S. van Ballegooy, personal communication). Thus, the tests on these soil specimens likely reflected the cyclic response of soils of similar type and density during the Christchurch and later earthquakes of the sequence.

Shear wave velocity was measured in five of the laboratory specimens using bender elements. Direct field measurements of V_s were not available at most of the CBD sites. However, a robust Christchurch-specific CPT-V_s correlation developed by McGann et al. (2014) was used to obtain an estimate of $V_{s\text{-}Field}$. The difference between lab and field Vs values was about 10% (i.e., $V_{s\text{-}Lab}/V_{s\text{-}Field}$ values were between 1.09 and 1.11). This indicates "medium to low" levels of sample disturbance according to Chiara and Stokoe (2006). A more comprehensive companion study by Beyzaei et al. (2015 & personnel communication) that focused on soil samples retrieved from the suburbs of Christchurch using the same sampling and testing procedures as this study also found good agreement between $V_{s\text{-}Lab}$ and $V_{s\text{-}Field}$ measurements in samples retrieved below the water table, where $V_{s\text{-}Field}$ was measured using cross-hole seismic testing (which was completed by the Univ. of Texas at Austin research team led by K. Stokoe and B. Cox, personnel communication).

Estimated field and laboratory relative density (D_r) values of test specimens were also compared when FC were less than 15% to gain insights into possible volumetric strains induced during the sampling and specimen preparation process. The minimum and maximum void ratio (e_{min} and e_{max}) for soil specimens were found using the Japanese Standard method (JIS A 1224:2000) so that $D_{r\text{-}Lab}$ could be calculated. $D_{r\text{-}Field}$ was estimated from various CPT-D_r correlations (e.g., Baldi et al. 1986, Salgado et al. 1997, and Jamiolkowski et al. 2001). These correlations require the use of a normalized equivalent clean-sand penetration resistance (e.g., q_{c1Ncs}, Boulanger and Idriss 2014), which were estimated based on the CPT data obtained near each borehole. Figure 3.9 shows a plot of $D_{r\text{-}Lab}$ versus q_{c1Ncs} for the tested triaxial specimens with FC < 12%. Also shown in Figure 3.9 are the various correlations for D_r from q_{c1Ncs}, which would represent $D_{r\text{-}Field}$. The estimated values of $D_{r\text{-}Lab}$ tended to be significantly higher than values of $D_{r\text{-}Field}$ for SP and SP-SM soil specimens with low equivalent penetration resistance

(i.e., $q_{c1Ncs} < 80$), while the remaining specimens' $D_{r\text{-}Lab}$ are close to or within the range of $D_{r\text{-}Field}$ as calculated from the correlations. The discrepancy for the looser specimens suggests that the sampling and specimen preparation procedures potentially densified these nonplastic sandy soils prior to testing.

Considering these three approaches to evaluating specimen quality, as well as examination of the laboratory tests and comparisons with CPT-based liquefaction triggering procedures, which are shown later, we judge that the D&M Osterberg-type hydraulic piston sampler could not retrieve "undisturbed" samples of very loose and loose SP and SP-SM soils (i.e., when $q_{c1N} < 60$ or $D_r < 50\%$). Conversely, relatively "undisturbed" samples of medium density SP and SP-SM soils could be obtained, and "undisturbed" samples of silty soils (SM and ML) could be obtained with the D&M sampler. Therefore, sound insights could be garnered from testing soils in the latter cases. An alternative method (i.e., block sampling or freezing) would be required to retrieve high-quality samples of very loose and loose sands.

3.5 RESULTS AND DISCUSSION

Soil samples from eleven boreholes at eight different sites were obtained using the D&M hydraulic piston sampler (see Table 3.1 and Figure 3.2). Laboratory testing was completed on specimens from seven of these eight different sites (no specimens were tested from samples obtained from borehole *DM_Z4_BH2* at the AM building site). Representative results from this testing are discussed below. These results include monotonic triaxial compression and cyclic triaxial test data from single specimen tests on a range of soil types (e.g., sands, silty sands, and silts) as well as collated data from multiple tests in the form of deviatoric ($q=\sigma_1-\sigma_3$) vs. mean effective stress [$p'=(\sigma'_1+2\sigma'_3)/3$] and liquefaction resistance curves (in the form of CSR vs. N_c, where $CSR=q/(2\sigma'_c)$ and N_c is the number of cyles of loading; σ'_c is the isotropic consolidation stress).

3.5.1 Monotonic Triaxial Compression Testing

Four isotropically consolidated undrained (ICU) monotonic triaxial compression tests were completed on "undisturbed" soil specimens from four different sites. Figure 3.10 provides the results from testing a specimen located at a depth of 3.83 m at the CTH building site. This specimen was a low-plasticity (PI=4) silt tested at an isotropic effective confining pressure of approximately 55 kPa. As can be seen from the plots in Figure 3.10, an initial contractive response of the soil is followed by a dilative response. From the plot of excess pore water pressure ratio ($r_u=\Delta u/\sigma'_{3o}$) vs. axial strain ($\varepsilon_{ax}$), the contractive response (increasing r_u) occurs up to a strain of approximately 0.55%, at which point the specimen starts to dilate (decreasing r_u) with further loading. Based on the plot of stress ratio (σ'_1/σ'_3) a peak effective friction angle (ϕ') of about 42° was measured for this specimen (based on $\sigma'_1/\sigma'_{3\text{-}max} \approx 5$).

Figure 3.11 provides the stress paths (q vs. p') for all monotonic triaxial compression tests completed in this study. Similar to the results shown in Figure 3.10, all of the specimens exhibit an initial contractive response followed by a dilative response as deviatoric loading increases. This type of response was expected for the shallow soils sampled in the CBD and tested under confining pressures representative of field conditions. Furthermore, CPT data for the sites studied supports the laboratory data in that negative values of the state parameter (i.e., $\psi \approx -0.2$ to

0) were estimated using the Robertson (2010) CPT-ψ correlation.

A limitation of the stress-controlled monotonic compression tests was the maximum magnitude of deviatoric stress (q) that could be applied to the specimen during a test. As pneumatic controls were used to apply the vertical load, the maximum pressure that can be applied during a test is directly related to the pressure being supplied to the triaxial apparatus and the cross-sectional area of both the loading piston and specimen. A maximum deviatoric stress of about 350 kPa was typically achievable for the set-up and diameters of the tested specimens. Consequently, the maximum achievable axial strain depended on the stiffness properties of the tested soil specimens. Figure 3.10 shows the results of a test where the maximum strain reached was 5%. The maximum axial strains for all monotonic triaxial tests ranged from 3.5 to 10%. This limitation of specimen supply pressure can be overcome by simply using a larger diameter loading piston, which was not available in NZ at the time of testing. Future triaxial strength testing (e.g., monotonic testing to generate critical state lines from reconstituted soil specimens) will be completed to larger strains.

3.5.2 Cyclic Triaxial Testing

Stress-controlled cyclic triaxial (CTX) testing was performed on soil specimens from all of the sites studied (excluding the *AM* building site). The goal of this testing was to characterize the cyclic response of the silty and sandy soils of Christchurch's CBD. To this extent, the results of individual tests can provide insights into the undrained, dynamic response of these soils, while a collation of test results for an assumed soil horizon can then be examined in the form of applied cyclic stress ratio (CSR) compared to the number of cycles of loading (N_c). These combined results can then provide valuable insight into the liquefaction resistance of a given soil via an interpreted cyclic resistance ratio (CRR) curve. A single amplitude axial strain (S.A. ε_{ax}) of 3% was adopted as the criteria for failure of the CTX tests (e.g., similar to that used in Bray and Sancio 2006), so that $N_{c\text{-}3\%\ S.A.\ \varepsilon ax}$ is reported hereafter to describe the cyclic loading resistance of a particular specimen.

Figure 3.12 through Figure 3.14 provide a summary of the results obtained from CTX testing on a range of different soil types including plots of applied deviator stress (q) vs. mean effective stress (p'), q vs. ε_{ax}, and q, ε_{ax}, and r_u vs. number of loading cycles. Figure 3.12 shows the results for a specimen from the CTH site at a depth of 4.27 m. This specimen is classified as SP-SM with a fines content of 5.9% (FC=5.9). A cyclic stress ratio (CSR) of 0.365 was applied to this specimen, which resulted in $N_{c\text{-}3\%\ S.A.\ \varepsilon ax}$ of 6. Figure 3.13 provides the results for a soil specimen that classified as SM from the FTG-7 site at a depth of 4.77 m. The $N_{c\text{-}3\%\ S.A.\ \varepsilon ax}$ was 13 for a CSR of about 0.36 for this specimen. Figure 3.14 shows the results of CTX testing for a silt (ML) specimen that was obtained from the FTG-7 site at depth of 3.72 m. A CSR of 0.296 led to a $N_{c\text{-}3\%\ S.A.\ \varepsilon ax}$ value of 17 for this specimen.

The CTX results presented in Figure 3.12 to Figure 3.14 share some similarities with regards to the salient features of the soil's response to cyclic loading. One prominent characteristic feature is the relationship between the applied deviator stress and the subsequent pore water pressure response of the presented soils. As the excess pore water pressure ratio ($r_u=\Delta u/\sigma'_3$) approaches a value of unity, an "inverted s-shape" or "banana loop" in the q vs. ε_{ax} plot starts to develop, which also corresponds to the point at which p' approaches zero. This type of stress-strain response is occurring due to the soil alternating between dilative (during loading above the phase transformation state) and contractive (during unloading) responses after the soil has

reached p'≈0, which leads to an alternating sequence of soil stiffening and softening, respectively. This response is typical of a soil that is dense of critical state, which as stated previously, is expected for the shallow soils sampled and tested in this study. The results presented in Figure 3.12 to Figure 3.14 are indicative of a soil that is undergoing a "cyclic mobility" type of response. The limited strain potential of the soil is due to the temporary stiffening of the soil as the specimen dilates under peak loading conditions, which leads to local minimums in the excess pore water pressure response (r_u vs. N_c).

Another noticeable attribute of the presented CTX results is the bias towards extension in the developed axial strains (i.e., larger magnitudes of negative ε_{ax} compared to positive ε_{ax}), which can be seen in both the ε_{ax} vs. N_c and q vs. ε_{ax} plots. This bias towards extensional loading would most likely not have been as evident in the results of CTX testing on reconstituted specimens of similar soils, had this type of testing been completed. Ghionna and Porcino (2006) report similar asymmetric patterns toward extensional versus compressional axial strain for CTX testing of "undisturbed" sand specimens sampled using freezing techniques. When CTX test results of reconstituted specimens were compared to "undisturbed" testing of similar soils there was practically no perceivable bias towards extensional strain for the reconstituted specimen testing. Ghionna and Porcino (2006) attributed this difference to the fabric dependency of the "undisturbed" soil specimens' response to cyclic loading. Taylor (2015) also reports similar bias towards extensional loading for CTX testing of "undisturbed" soil specimens from the CBD of Christchurch, which was not necessarily observed for testing of reconstituted CTX specimens. Realizing a similar tendency for the CTX specimens tested in this study to strain more in extension compared to compression supports the notion that the sampling, specimen preparation, and testing procedures were able to maintain much of the natural depositional fabric of the examined soils.

A large portion of the cyclic triaxial testing in this study was carried out on sand specimens. These soils classified as SP or SP-SM. By compiling the CTX results from multiple sites, trends were observed with regards to the cyclic response of these soils. Figure 3.15 illustrates these trends via a plot of CSR versus $N_{c\text{-}3\%\ S.A.\ \varepsilon ax}$. It should be noted that the CSR values reported in Figure 3.15 are not adjusted to field conditions (i.e., no correction factor is applied to account for isotropic vs. anisotropic stress state and one-dimensional vs. two-dimensional loading; Idriss and Boulanger 2008). However, the values are corrected using the overburden correction factor (K_σ) recommended by Idriss and Boulanger (2008) to normalize the results to atmospheric pressure. The normalized clean-sand equivalent cone penetration resistance (q_{c1Ncs}; Idriss and Boulanger 2008) was used in the calculation of K_σ for each test specimen. The raw data from the closest CPT to each borehole over the depth range of each specimen was used in conjunction with the confining stress for each CTX test (σ'_c) and the fines content (FC) for each soil specimen to calculate representative values of q_{c1Ncs}.

Figure 3.15 is organized into six subsets of data. Each subset represents a range of q_{c1N} values for soil specimens that classified as either SP or SP-SM. Within the loose to medium dense subset of specimens, distinct trends for specimens with $60 < q_{c1N} < 100$ and $100 < q_{c1N} < 140$ were found; therefore, these results were split into two subgroups with regards to plotting the results. The curves drawn in Figure 3.15 represent the interpreted cyclic resistance ratio (CRR) for each subset of soil and are drawn so that they incorporate the data for both SP and SP-SM soils for a given range of q_{c1N} values (i.e., one CRR curve is drawn for the results from both SP and SP-SM soil specimens for $60 < q_{c1N} < 100$ and another for $100 < q_{c1N} < 140$). The CRR curves are drawn based on a regression of the CTX data for each subset using a power function (i.e., $CRR = a \cdot N^{-b}$).

There is a large spread of the CTX results shown in Figure 3.15 for the very loose to loose sand specimens ($q_{c1N} < 60$). In contrast to the relatively well-defined trends for the previously discussed sand specimen results when $q_{c1N} > 60$, the very loose to loose sand results do not exhibit a clear tendency for values of $N_{c\text{-}3\%\ S.A.\ \varepsilon ax}$ to increase with decreasing values of applied CSR. Additionally, several of the data points for the very loose to loose sand specimens plot above the interpreted CRR curves for the denser sand specimens, which would infer a stronger liquefaction resistance for the looser soils.

The discrepancy in the observed trends versus the expected trends for the very loose to loose sand specimens is believed to be due to a densification of these soils during sampling. Conversely, the results for the medium dense sands reflect the expected trends in that the results from slightly denser ($100 < q_{c1N} < 140$) specimens reflect a higher liquefaction resistance than the slightly looser ($60 < q_{c1N} < 100$) specimens' results, and a clear increase in $N_{c\text{-}3\%\ S.A.\ \varepsilon ax}$ with decreasing CSR is defined via the power function regression to represent the CRR curve. Based on these observations and similar observations for the siltier soils examined in this study, it is judged that the sampling, specimen preparation, and testing procedures employed in this study allowed for high-quality specimens to be tested for all soils except the loose sands with $q_{c1N} < 60$.

3.6 CONCLUSIONS

The cyclic response of foundation soils was critical to the seismic performance of structures in Christchurch's CBD, especially with regards to the softening of these soils due to the generation of excess pore water pressure during the strong shaking of the major events in the Canterbury earthquake sequence. Extensive investigations were carried out by researchers to document the effects of liquefaction on buildings in relation to settlements and deformations following the Canterbury earthquakes. Additionally, a considerable amount of site investigation, mostly in the form of CPTs, was conducted following these events to characterize key sites within Christchurch's CBD. This study focused on obtaining "undisturbed" samples of key soils at several building sites within the CBD and performing triaxial testing to characterize both the monotonic and dynamic undrained loading response of soils that most likely underwent liquefaction.

The sampling and testing program undertaken in this study adds to the advancement of practice with regards to procedural details for "undisturbed" sampling of sandy and silty soils. The D&M Osterberg-type hydraulic fixed-piston sampler allows for the use of a constant inner diameter, smooth, brass tube with a relatively low area ratio of 7.6%. These features of the sampling tube coupled with the relatively short advancement length (45 cm) provided a means for retrieving high quality "undisturbed" samples of silty soils and medium dense sands. Shear wave velocity (V_s) testing of a select number of specimens was completed in this study and a parallel study (where the same sampling procedures were employed on similar soil types) to compare $V_{s\text{-}Lab}$ and $V_{s\text{-}Field}$. The results from these comparisons yielded reasonable trends with regards to $V_{s\text{-}Lab}/V_{s\text{-}Field}$ ratios. In addition to the quantitatively agreeable comparisons of V_s measurements in the laboratory and field, the comparison of $D_{r\text{-}Lab}$ to $D_{r\text{-}Field}$ for the tested specimens, and the observed trends from both monotonic and cyclic triaxial testing results lend confidence with regards to the quality of sampling, specimen preparation, and laboratory testing. The exception to this observation was the sampling and testing of very loose and loose, relatively

clean sands (SP and SP-SM), wherein test results indicated that the sampling and testing procedures densified these soils.

The data and results obtained from the advanced laboratory testing of critical soils from Christchurch's CBD contributes significant insight and information regarding soils that were affected by liquefaction during the Canterbury earthquake sequence. The triaxial specimens tested monotonically exhibited initially a contractive response followed by a dilative response as the applied deviatoric stress increased. This type of response was expected for the shallow soils tested under confining pressures representative of field conditions. The cyclic triaxial tests generated positive pore water pressure initially and then displayed a cyclic mobility type of response that is typical of a soil that is dense of critical state. These test results support analytical studies that examine the consequences and effects of liquefaction on buildings and infrastructure (e.g., numerical soil-structure interaction analyses with soil constitutive models calibrated by this data set). The data set also provides insights for understanding the monotonic and cyclic response of fine sands, silty sands, and silt soils.

Table 3.1: Soil exploratory locations for "undisturbed" soil sampling

Borehole ID	Building Site[1]	Latitude (°)	Longitude (°)
DM_Z1_BH1	FTG-7	-43.52647	172.63854
DM_Z1_BH2	FTG-7	-43.52647	172.63835
DM_Z2_BH1a	PWC	-43.52860	172.63749
DM_Z2_BH1b	PWC	-43.52848	172.63749
DM_Z2_BH2	VT/VSA	-43.52889	172.63537
DM_Z4_BH1	CTUC	-43.52866	172.64248
DM_Z4_BH2	AM	-43.52889	172.64210
DM_Z5_BH1	CTH	-43.52719	172.63524
GP_Z5_BH1	CTH	-43.52719	172.63530
DM_Z8_BH1	SA	-43.52537	172.64198
DM_Z9_BH1	LS-II	-43.54407	172.65298

1. Building site names correspond to those delineated in Zupan (2014)

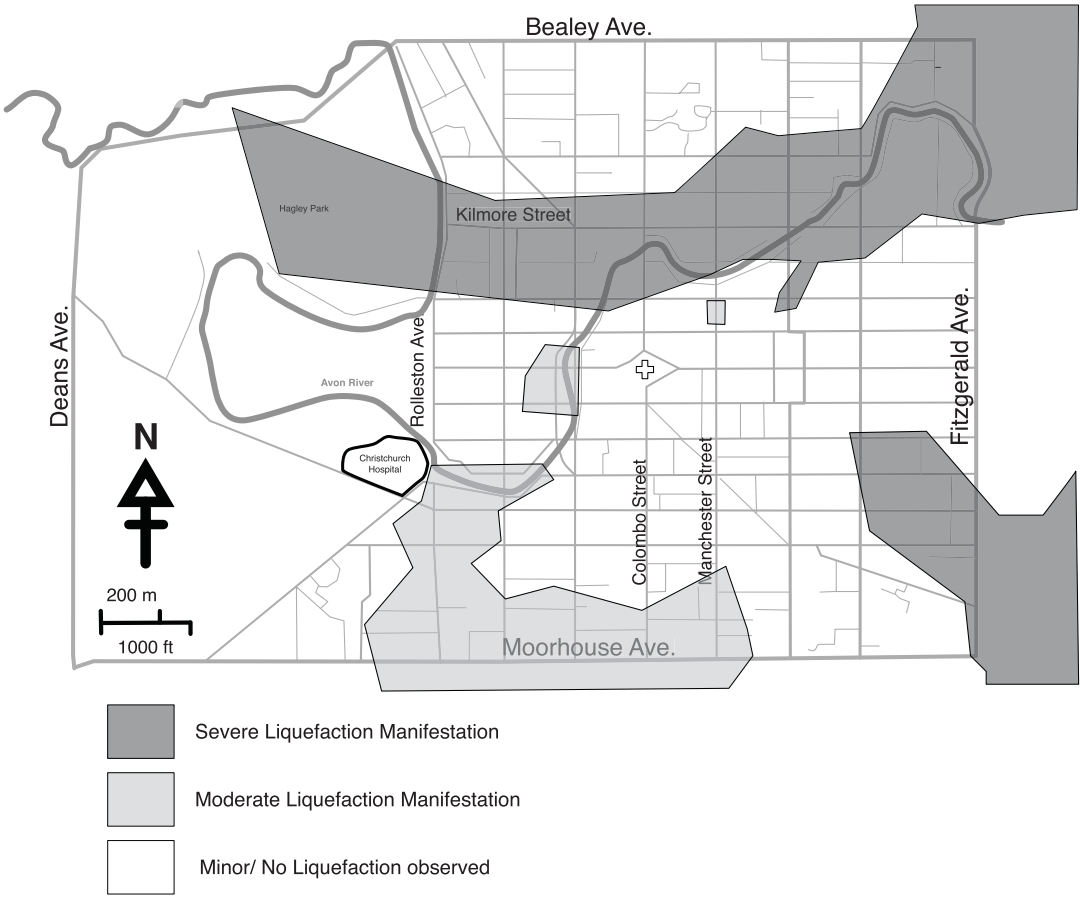

Figure 3.1: Observed liquefaction in the CBD following the 22 FEB 2011 Christchurch earthquake (from Taylor et al. 2012a)

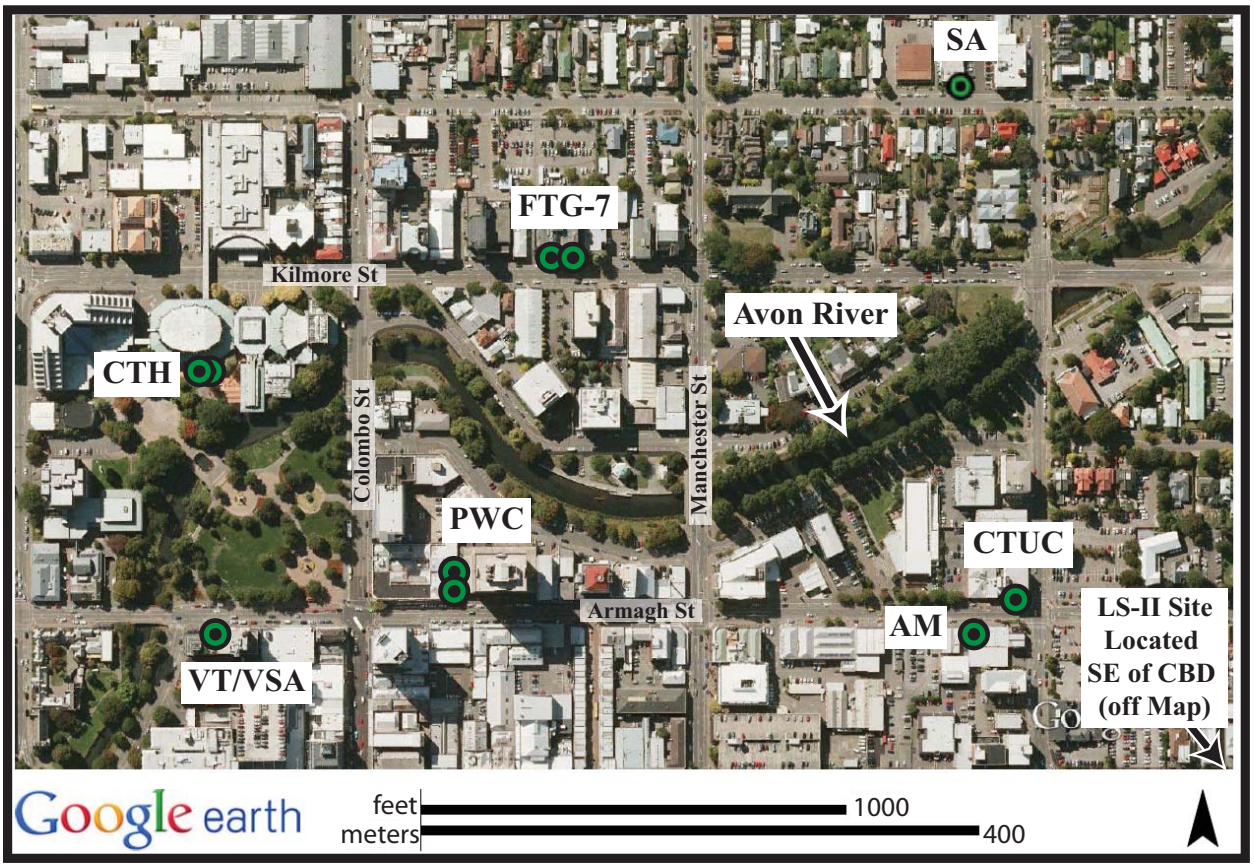

Figure 3.2: Locations of boreholes used for "undisturbed" sampling in this study; background historical Google Earth map dated 3 Mar 2009 is used to illustrate site investigation locations with relation to building locations

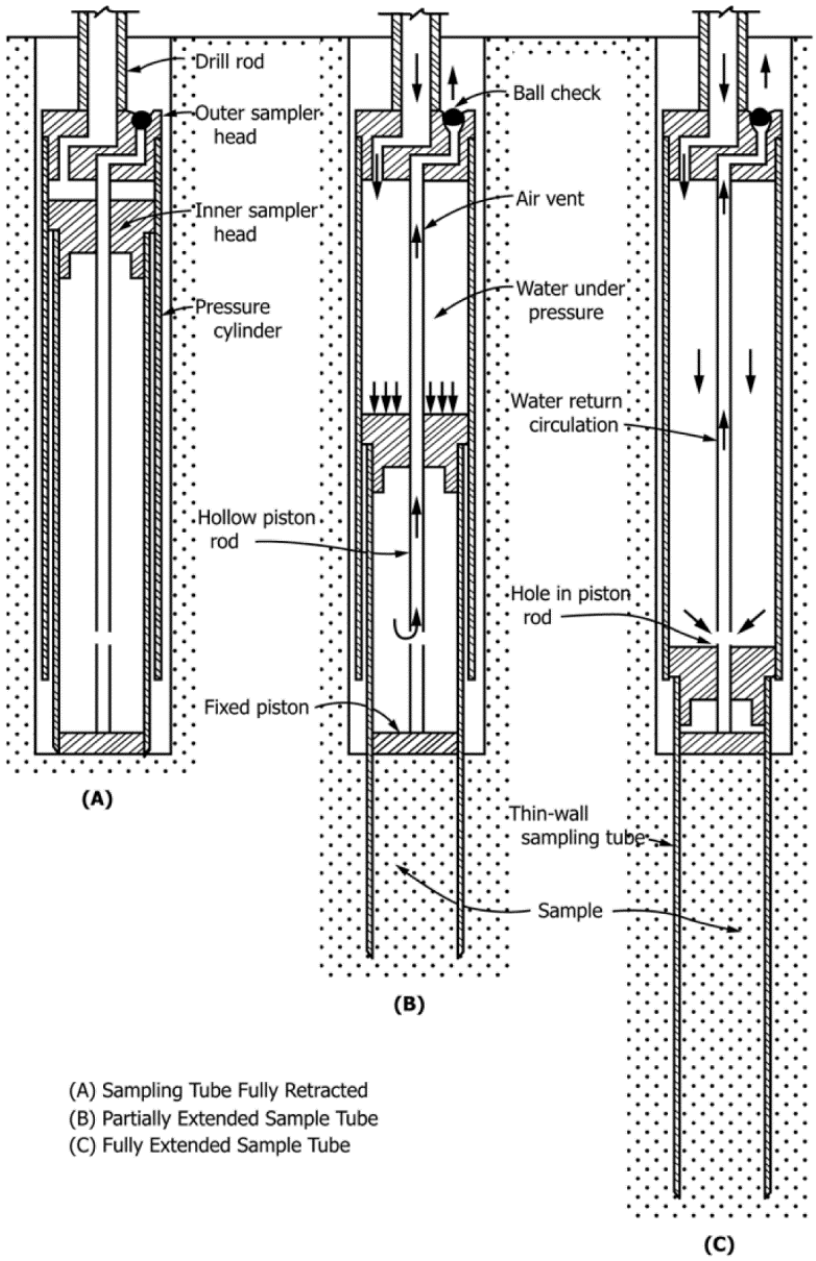

Figure 3.3: Schematic of hydraulic piston sampler operation using a thin-walled sampling tube (from ASTM D6519-08)

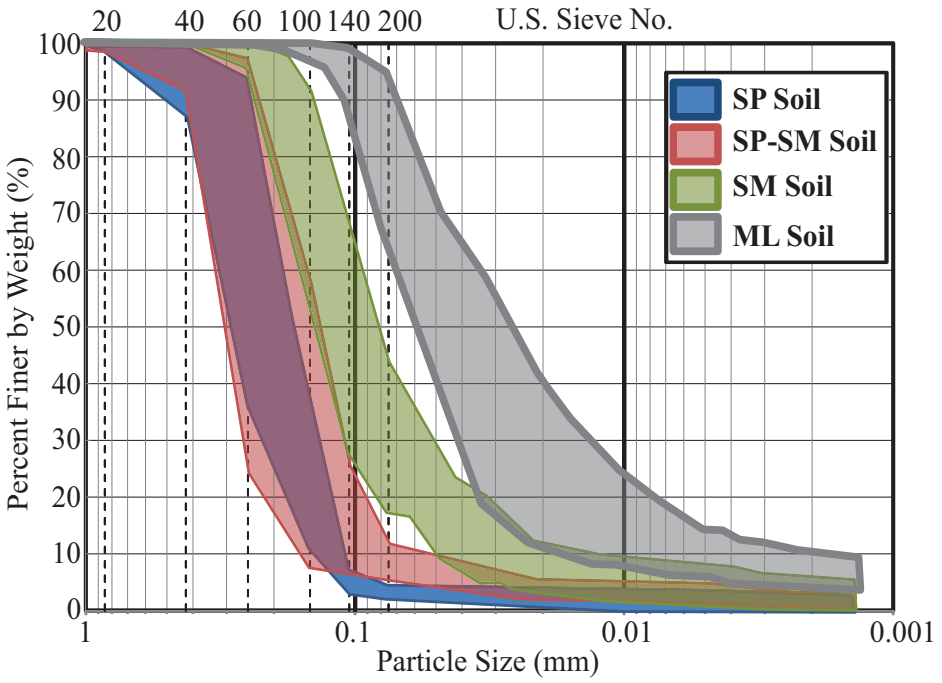

Figure 3.4: Summary of grain size distributions for all triaxial test soil specimens

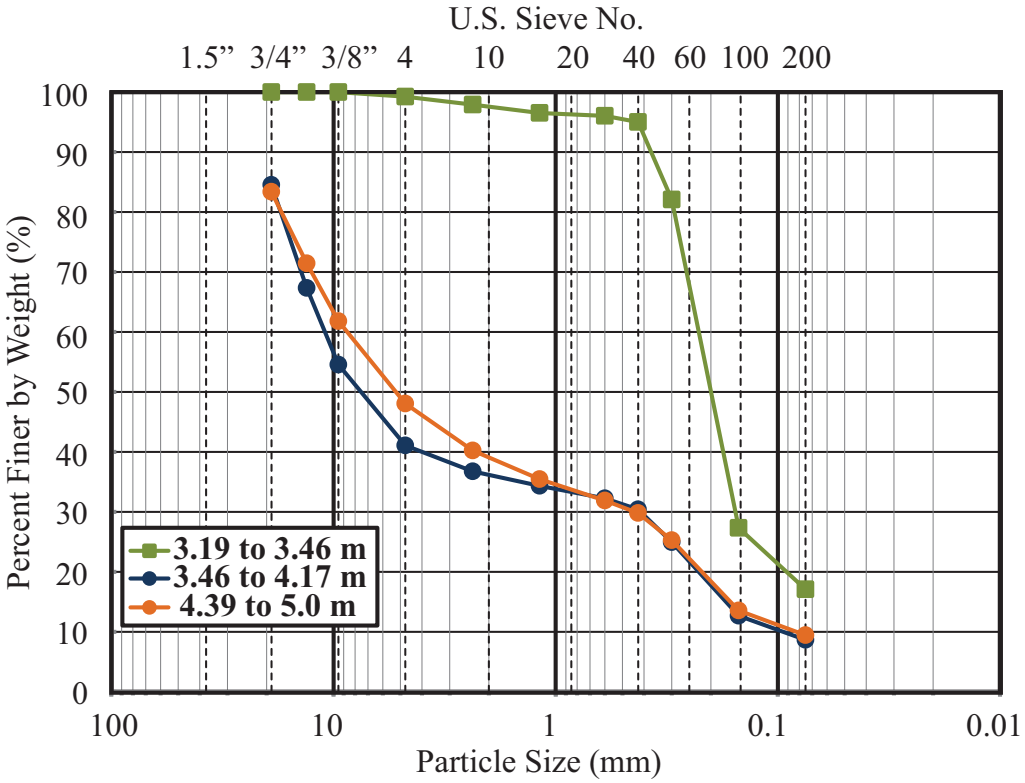

Figure 3.5: Grain size distribution for shallow soil at PWC building site

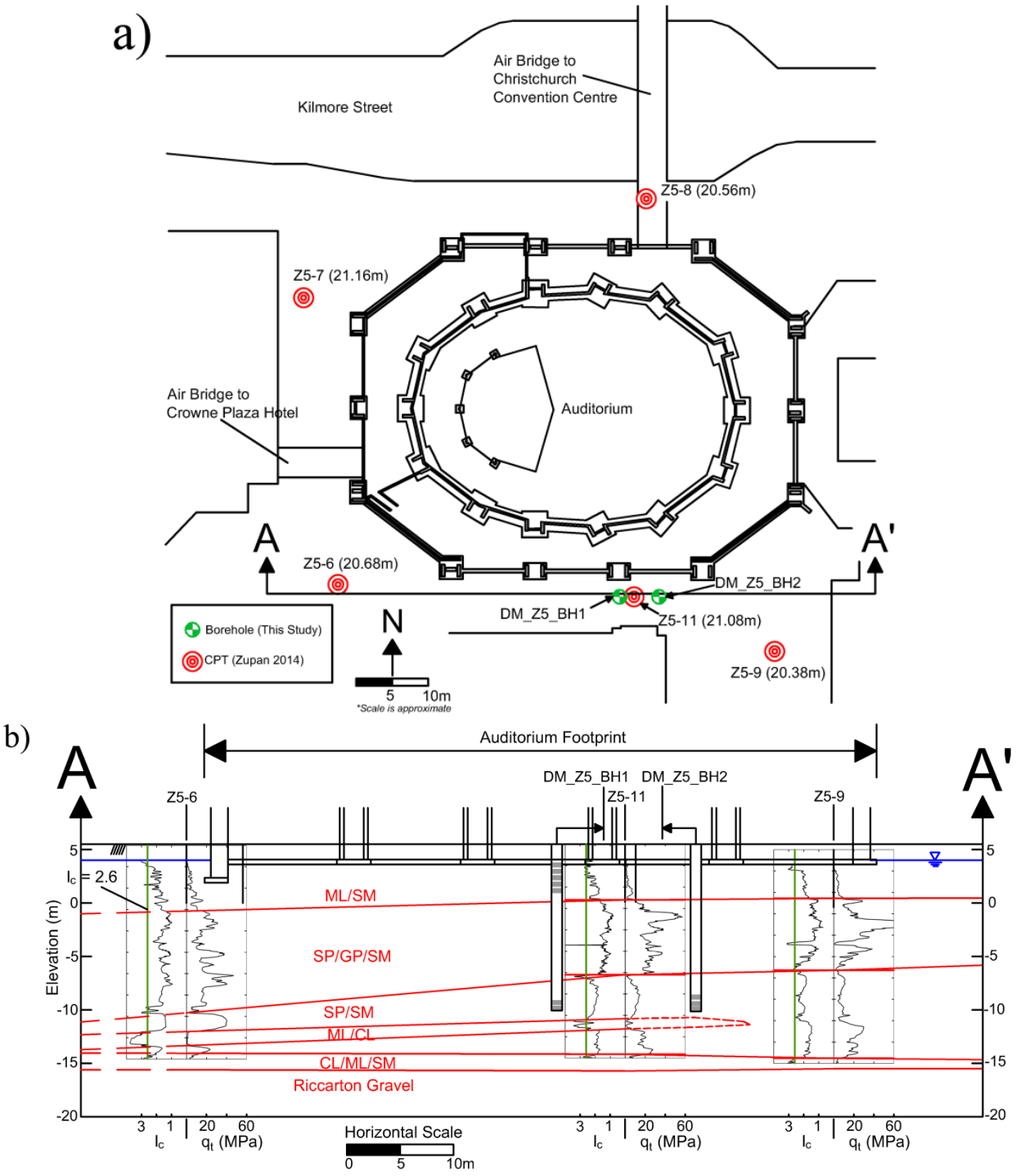

Figure 3.6: a) Site overview and building footprint for CTH Auditorium with locations of CPTs detailed by Zupan (2014) and boreholes completed in this study; b) representative E-W subsurface profile; note that "undisturbed" sample depths are shown in grey (modified from Zupan 2014)

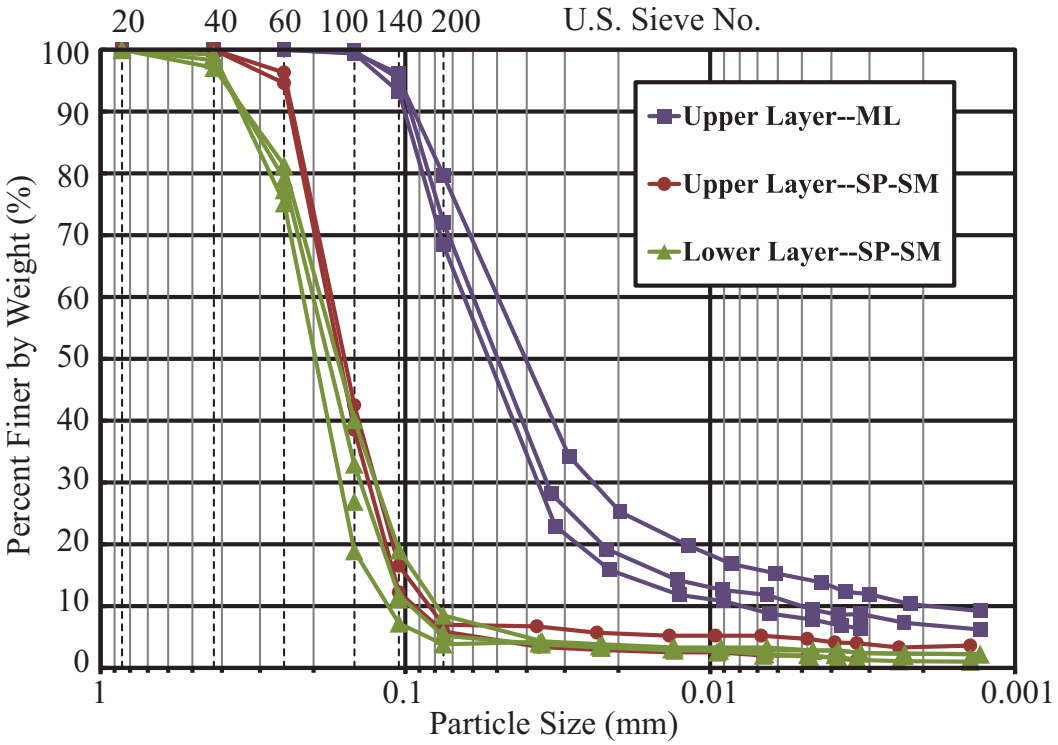

Figure 3.7: Grain size distribution for triaxial test soil specimens from CTH building site

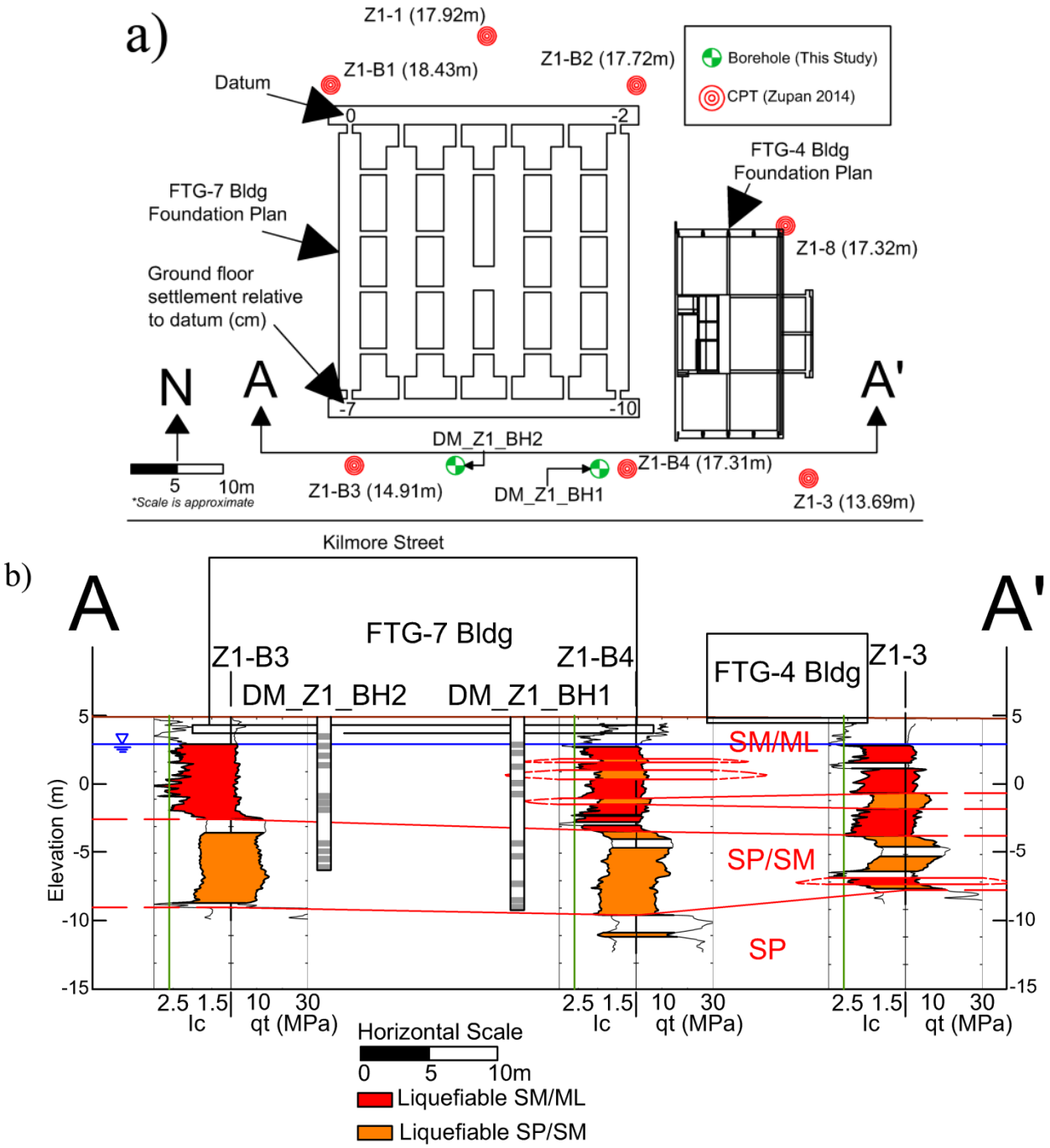

Figure 3.8: a) Site overview and building footprint for FTG-7 site with locations of CPTs detailed by Zupan (2014) and boreholes completed in this study; b) representative E-W subsurface profile; note that "undisturbed" sample locations are shown in grey (modified from Zupan 2014)

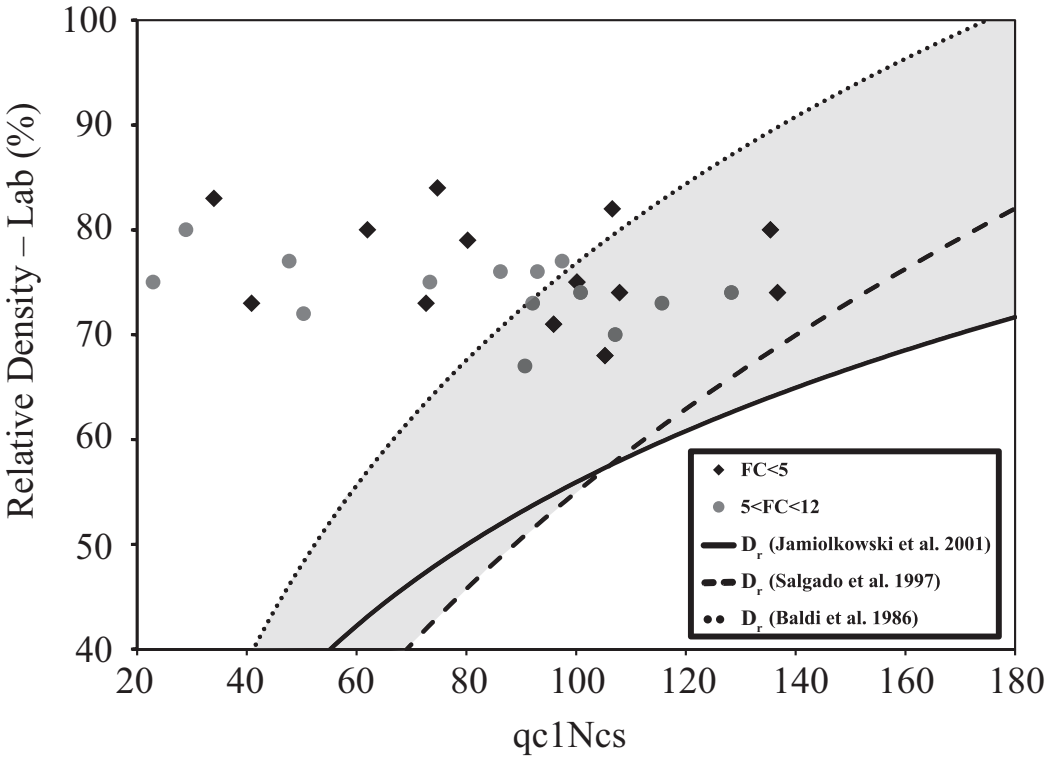

Figure 3.9: Relative density (Dr) calculated via lab testing vs. qc1Ncs (Boulanger and Idriss 2014) for all SP and SP-SM soils; correlations for qc1Ncs to Dr are also shown

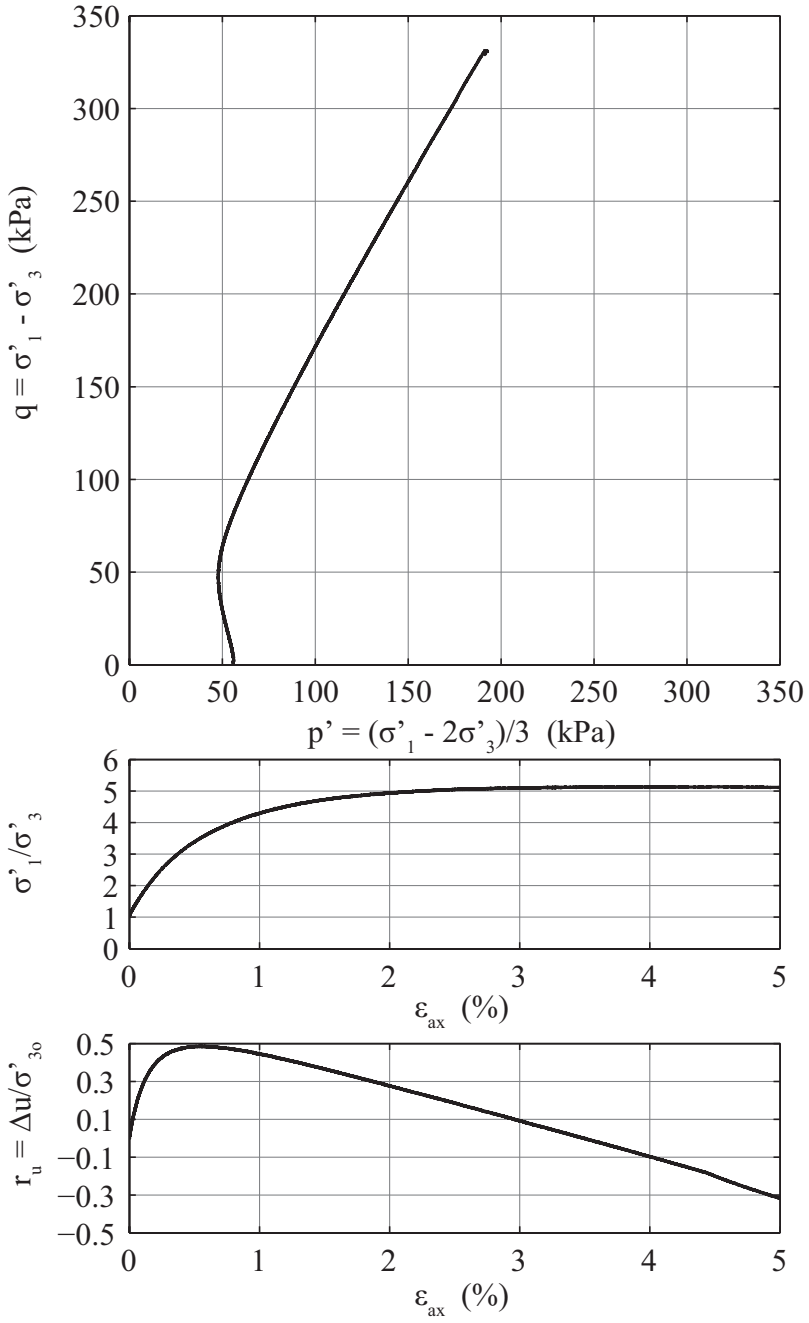

Figure 3.10: Monotonic triaxial test results; CTH site, DM_Z1_BH1, 3.83 m depth, USCS: ML, PI=4, e_o=0.76, σ'_{30} = 55.3 kPa, Specimen Height=137.9 mm, Specimen Diameter=61.0 mm, G_s=2.67, Load Rate=2 kPa/min

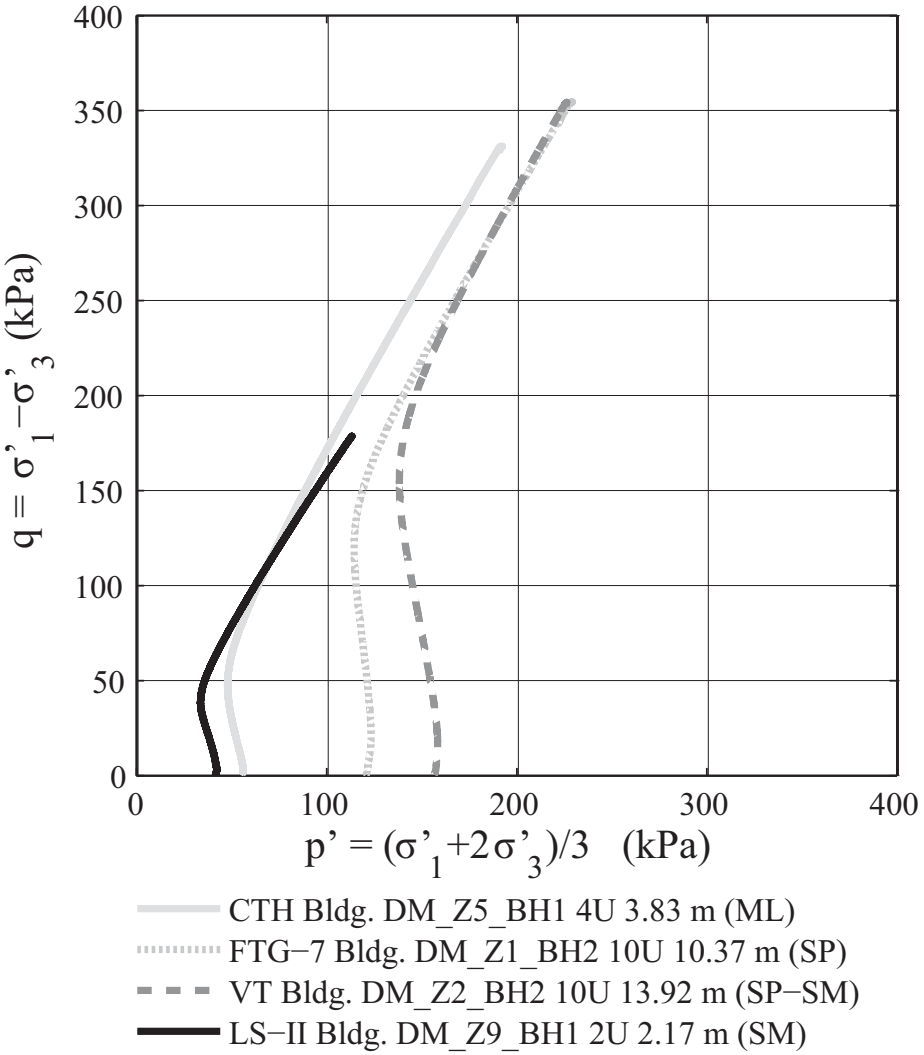

Figure 3.11: Deviatoric stress (q) vs. mean effective stress (p') for ICU monotonic triaxial compression tests

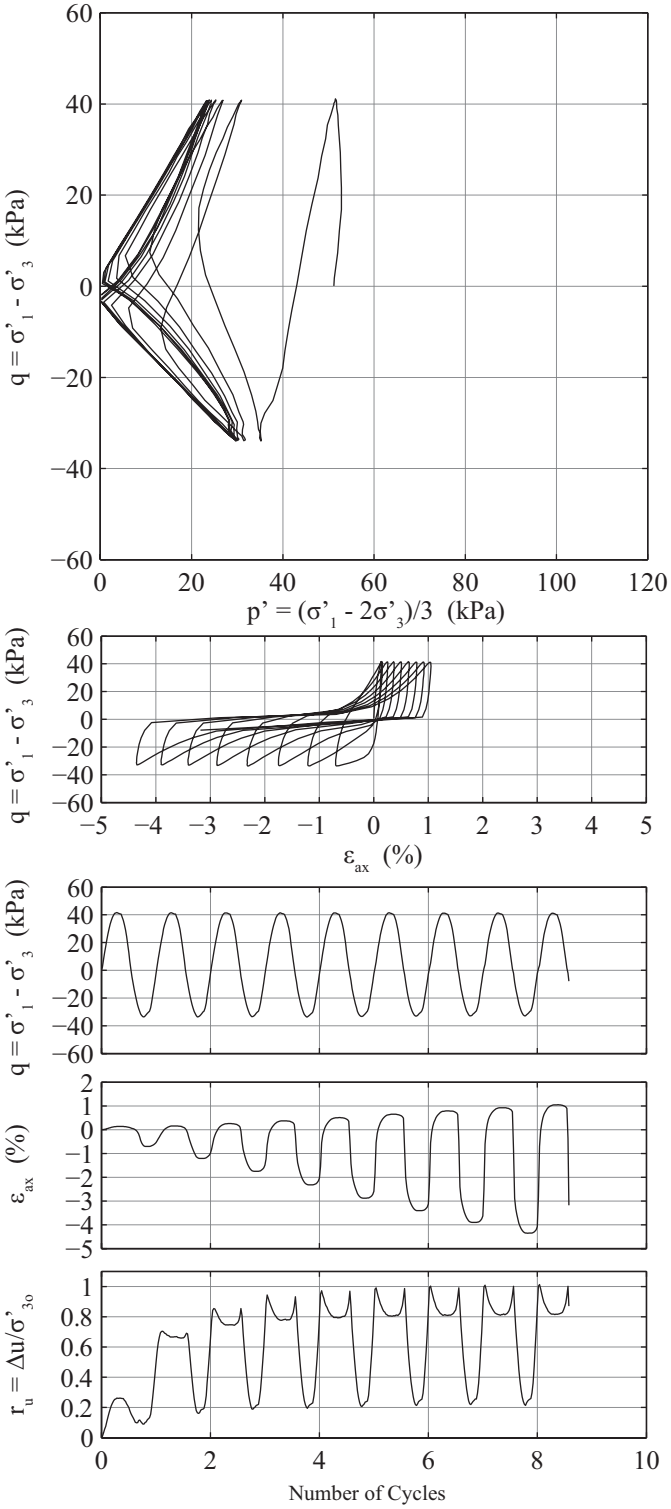

Figure 3.12: CTX results; CTH site, DM_BH1, 4.27 m depth, USCS: SP-SM, PI=Non-Plastic (NP), e_o=0.77, σ'_{3o}=51.0 kPa, Specimen Height=140.4 mm, Specimen Diameter=60.9 mm, G_s=2.69, Load Frequency=0.1 Hz, CSR=0.365, N to S.A. $\varepsilon_{ax=3\%}$=6

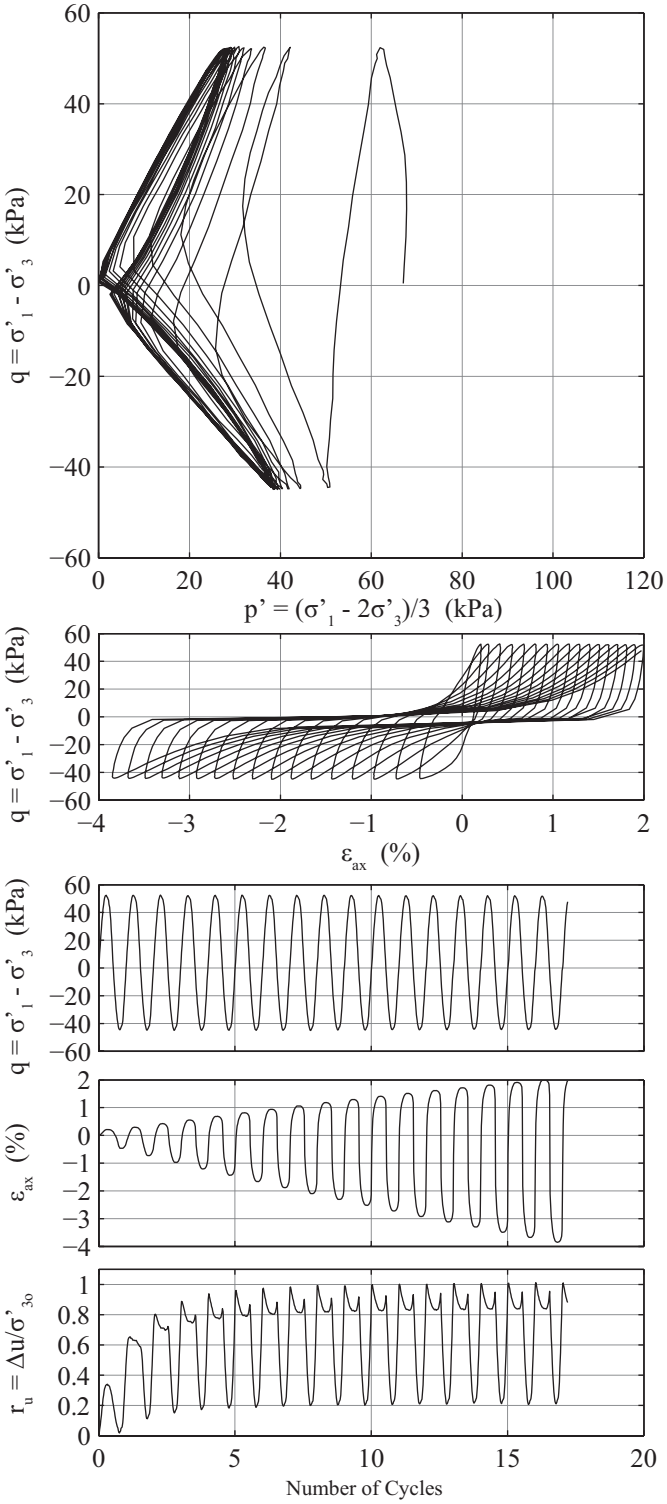

Figure 3.13: CTX results; FTG-7 site, DM_BH1, 4.77 m depth, USCS: SM, PI=4, e_o=0.73, σ'_{3o}=66.9 kPa, Specimen Height=138.8 mm, Specimen Diameter=61.0 mm, G_s=2.71, Load Frequency=0.1 Hz, CSR=0.360, N to S.A. ε_{ax}=3%=13

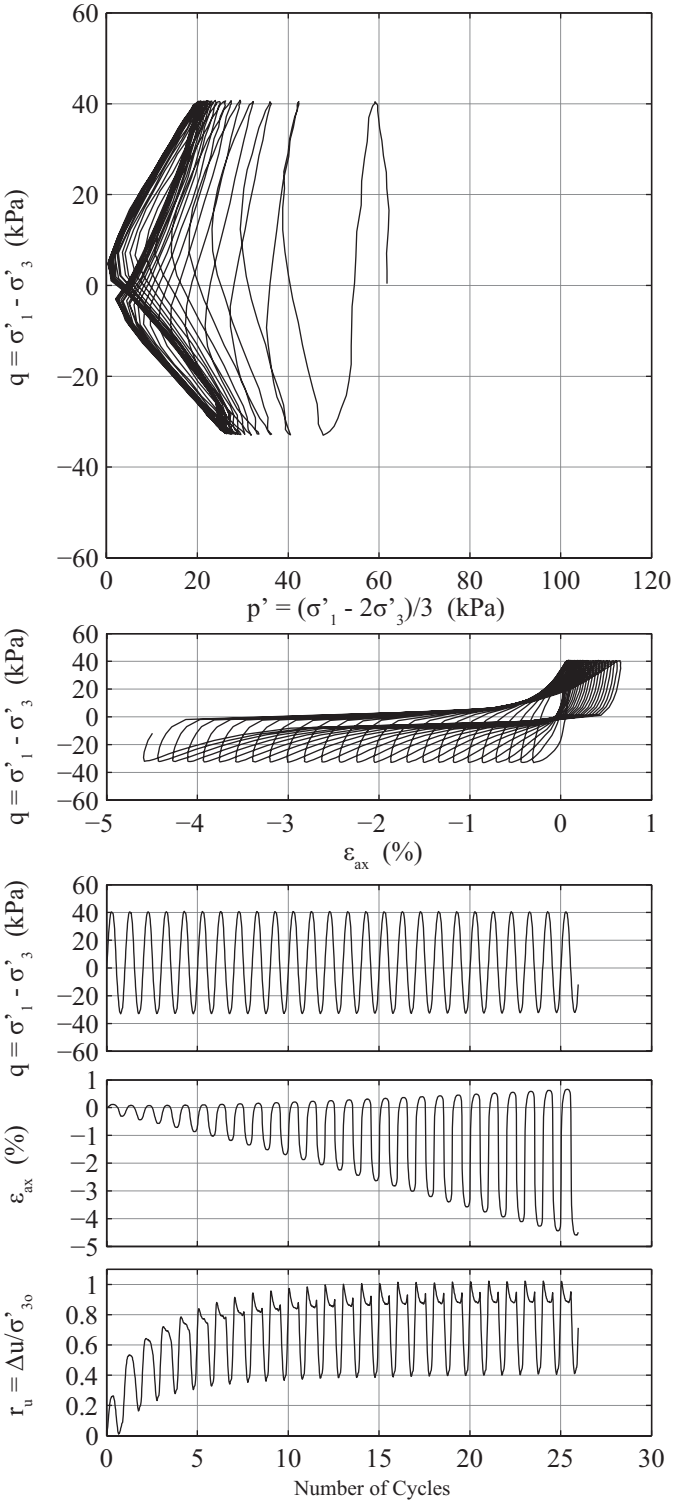

Figure 3.14: CTX results; FTG-7 site, DM_BH1, 3.72 m depth, USCS: ML, PI=2, e_o=0.67, σ'_{3o}=61.6 kPa, Specimen Height=135.2 mm, Specimen Diameter=61.0 mm, G_s=2.75, Load Frequency=0.1 Hz, CSR=0.296, N to S.A. $\varepsilon_{ax=3\%}$=17

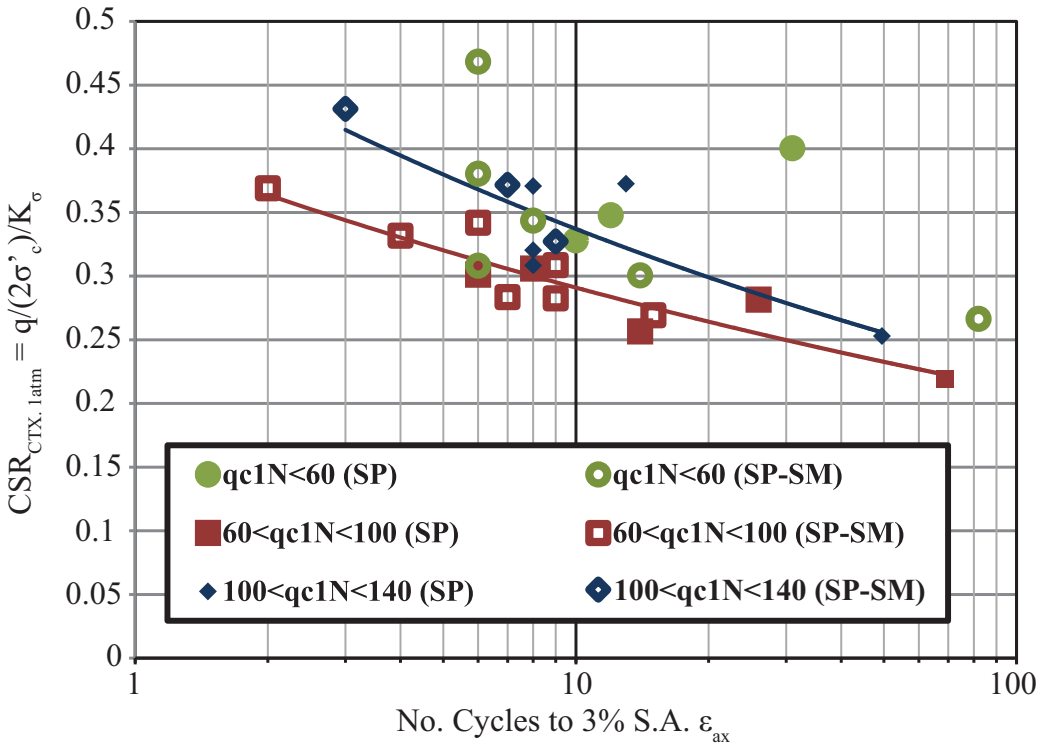

Figure 3.15: CSR vs. $N_{c\text{-}3\%\ S.A.\ \varepsilon ax}$ SP and SP-SM specimens

CHAPTER 4: LIQUEFACTION RESISTANCE AND STEADY STATE CHARACTERIZATION OF SHALLOW SOILS WITHIN THE CHRISTCHURCH CENTRAL BUSINESS DISTRICT

The contents of this chapter are primarily from a journal article to be submitted to the ASCE Journal of Geotechnical and Geoenvironmental Engineering by Markham, C.S., Bray, J.D., Cubrinovski, M., and Riemer, M.F. entitled: "Liquefaction Resistance and Steady State Characterization of Shallow Soils within the Christchurch Central Business District," which is under preparation.

4.1 INTRODUCTION

Understanding the potential effects of soil liquefaction below structures strongly shaken by an earthquake is an important design consideration in performance based earthquake engineering (PBEE). Consequently, well documented case histories of structures founded on liquefiable soils help advance analytical procedures that evaluate this complex soil-structure interaction problem. Recent earthquakes such as the 27 FEB 2010 M_w 8.8 Maule, Chile event (Bray et al. 2012), the 11 MAR 2011 M_w9.0 Tohoku Pacific (Japan) event (Tokimatsu et al. 2012), and the 2010-11 Canterbury (New Zealand) events (Bray et al. 2014) proved devastating for many buildings founded on liquefiable soils. However, there were also numerous cases of limited building damage at liquefiable soil sites. These case histories should be documented and investigated fully to advance practice.

Characterizing critical soil units at building sites affected by liquefaction during the 2010-11 Canterbury earthquake sequence (CES) is the focus of this paper. As highlighted by Bray et al. (2014), seven events of the CES sequence had $M_w \geq 5.5$, three of which had $M_w \geq 6.0$. The shaking intensity of these larger events was significant, especially in the CBD. Median peak ground accelerations (PGA) for the 22 FEB 2011 M_w6.2 Christchurch event were close to 0.5 g in the CBD; whereas recorded PGA values for the 04 SEP 2010 M_w7.1 Darfield and 13 JUN 2011 M_w6.0 events were slightly above 0.2 g in the CBD. This strong shaking coupled with the ground conditions in the CBD led to widespread liquefaction, as shown in Figure 4.1. Over a third of the approximate 4,000 buildings in the CBD were demolished following the CES due to sustained damage, with most of the high rise buildings in the CBD included in this count. Liquefaction led to deformation of building foundations at several sites in the CBD, which had a devastating impact on the buildings' seismic performance. Figure 4.2 provides an illustration of the effects of liquefaction on buildings where differential settlement across both the CTUC and FTG-7 building footprints led to structural damage.

The observations of building performance in the CBD during the CES present opportunities for developing insightful case histories of the seismic performance of buildings founded on liquefiable soils. To date, only a limited amount of cyclic testing has been performed on Christchurch soils. Characterizing and understanding the cyclic response of the key soil units at these sites becomes crucial for describing fully these case histories. This paper presents research that examines both the dynamic and monotonic response of key soil units at several building sites in the CBD of Christchurch with the specific goal of understanding the liquefaction resistance and cyclic response of these soils. Soil characterization is accomplished principally

through the use of "undisturbed" sampling and subsequent laboratory testing of sampled soils (primarily through the use of cyclic and monotonic triaxial testing). Comparisons of information obtained from laboratory testing and in-situ testing are discussed as well as considerations regarding the additional insights and knowledge that laboratory testing provides when used in conjunction with in-situ testing. Further insights regarding the interpretation of results from triaxial testing of "undisturbed" soils specimens from the Christchurch CBD are provided in Appendix B of this dissertation. These insights include further examination of CTX test results as well as comparisons of data obtained from "undisturbed" specimen testing to information interpreted from CPT data.

4.2 CHRISTCHURCH GEOLOGY AND CBD GROUND CONDITIONS

Christchurch is situated on the eastern coast of the northern part of the Canterbury Plains directly adjacent to Pegasus Bay. The upper 300-500 m of the Canterbury Plains' subsurface is composed primarily of Quaternary deposits of alluvial material interlayered with marine deposits (Forsyth et al. 2008; Brown and Weeber 1992). Most of Christchurch is located within the floodplain of the Waimakariri River, the course of which was only recently altered via levee construction to flow just north of the city following the settlement of Christchurch in the 1850s (Brown et al. 1995). Regular flooding of the Waimakariri River led to the deposition of gravels and sands in flood channels throughout the Canterbury Plains as well as overbank deposits of silts (Brown and Weeber 1992). The Springston Formation makes up the shallowest subsurface deposits of the western part of Christchurch and much of the CBD and comprises layers of postglacial fluvial sands, silts, and gravels that have been deposited within the last 3,000 years. This formation overlies and interfingers with deposits of the Christchurch Formation in the CBD. The Christchurch formation consists of sands, silts, and gravels, as well as clays, peats, and shells originating from beach, estuarine, lagoonal, dune, and coastal swamp sediments that have been deposited within the last 6,500 years (Brown and Weeber 1992). Together, the Christchurch and Springston Formations are on the order of 20 to 30 m thick in the CBD and can range in thickness from under 10 m in the western part of Christchurch to over 40 m near the coastline. Directly below these surface deposits lies the Riccarton Gravels, which is a well graded, dense gravel that comprises the uppermost confined aquifer beneath much of Christchurch. The water table in the CBD is generally within 1-3 m of the ground surface.

Although soil conditions can vary significantly over short distances in this fluvial depositional environment, general trends are apparent from examining available cone penetration tests (CPT) and soil exploratory borings. Figure 4.3 provides interpretive soil profiles at two representative CBD sites investigated as a part of this study, the *CTH* and *FTG-7* building sites (see Figure 4.1 for locations), with soil units labelled based on their Unified Soil Classification (USCS; ASTM D2487-11). The interpreted profiles are based on both CPT that were performed as a part of an earlier site investigation program (see Bray et al. 2014 and Zupan 2014) and classification of "undisturbed" samples obtained as a part of this study. The boreholes labeled in Figure 4.3 (*DM_Z5_BH1* and *DM_Z1_BH1*) show the depths of samples taken at the CTH and FTG-7 site and are shown with the closest corresponding CPT soundings (*Z5-11* and *Z1-B4*). Note that the distance between the boreholes and the CPT soundings in Figure 4.3 are not shown to scale; they are shown so that details can be distinguished.

For the CTH site (Figure 4.3a) it can be seen that the profile consists of silt (ML) in the upper 4 m followed by a thin layer of sand (SP-SM), which is underlain by a layer of sandy gravel followed by a layer of sand (SP and SP-SM). The sandy gravel at the CTH site was not sampled or tested; however, a similar shallow soil unit was sampled via sonic drilling techniques and tested from the PWC site (see Figure 4.1 for location). This gravelly soil from the PWC site contained 50-60% gravel, 30-40% sand, and about 10% nonplastic fines. Above the Riccarton Gravel, which is a confined aquifer, lies a layer of fine-grained material, which is typical for several areas of the CBD. The upper portion of the FTG-7 site (Figure 4.3b) is made up of interbedded layers of silt and silty sand (SM), which overly a layer of cleaner sands. The CPT shown was terminated at a depth of about 15 m (most likely due to the stiffness of the lower SP layer), but based on other CPTs at this site the Riccarton Gravel was located at a depth of approximately 20 m.

4.3 FIELD SAMPLING AND LABORATORY TESTING OF CBD SOILS

Figure 4.1 shows the location of the building sites investigated as a part of this study along with the locations of boreholes used for "undisturbed" soil sampling. Taylor et al. (2012a,b), Bray et al. (2014), and Zupan (2014) describe a collaborative project of the Univ. of California, Berkeley (UCB) and the Univ. of Canterbury (UC) that focused on characterizing the shallow subsurface at the sites shown in Figure 4.1 as well as several other sites in and near the CBD through the use of in-situ testing (e.g., CPTs) from July 2011 to April 2013. Boreholes used for "undisturbed" sampling discussed in this paper were located within about 2 m of previously advanced CPTs to enable comparisons of CPT data (and relevant CPT correlations) and laboratory test data. The selection of sites shown in Figure 4.1 was based on the presence of buildings of various footprint area and height that were affected by the liquefaction of shallow foundation soils during the CES as well as the presence of representative subsurface soils in the CBD. Additionally, the performance of buildings during the CES at these sites was well documented through various reconnaissance efforts (see Green and Cubrinovski 2010 and Cubrinovski et al. 2011), which makes these exceptional case histories for examining the effects of liquefaction on buildings.

"Undisturbed" soil sampling at the building sites was achieved through the advancement of boreholes using mud rotary drilling techniques in conjunction with the Dames & Moore (D&M) hydraulic fixed-piston thin-walled Osterberg-type sampler. Markham et al. (2015) provides details regarding the sampling, testing, and evaluation of the quality of soil samples obtained through this study. They found that loose sands were densified during sampling and specimen preparation, whereas medium dense sands, silty sands, and silts were relatively undisturbed by the sampling and specimen preparation procedures. Loose sands were SP and SP-SM soils with $q_{c1N}<60$, where q_{c1N} is the normalized cone penetration resistance (Boulanger and Idriss 2015) obtained from adjacent CPTs over the depth range of individual specimens. Discussions of "undisturbed" sample test results in this paper are limited to tests performed on medium dense sands, silty sands, and silts that exhibited minimal effects of sample disturbance.

Index testing (grain size distribution, void ratio limits, Atterberg limits, and specific gravity testing) was also carried out on the soil specimens after the completion of triaxial testing. Figure 4.4 provides a summary of the grain size distributions of retrieved soil specimens. The soils in

this plot are grouped based on their classification via the USCS, which is used in referring to various soil types throughout this paper. An interesting feature of the plot in Figure 4.4 is the similarity in the shapes of the various soil types, especially when comparing the silty sands (SM) to the cleaner sands (SP and SP-SM). Although the fines content (FC) of these two soil groups varied significantly (i.e., 20-40% for SM and 0-12% for SP and SP-SM), their median C_u and C_c values were similar (i.e., 3.8 and 1.4, respectively, for SM; and 2.1 and 1.1, respectively, for SP and SP-SM). The potential impact of the similarity in the two soil groups' particle shape distributions can be investigated through advanced laboratory testing to more fully characterize the response of these soils as a FC correction may not discern adequately their differing (or similar) seismic response.

In addition to the triaxial testing of "undisturbed" soil specimens, large-strain monotonic triaxial testing of reconstituted specimens was carried out to characterize the steady state response of specific soil types in the CBD. Soil types for this testing were identified via index testing (Figure 4.4) and the grouping of CTX results for interpreted cyclic resistance curves.

4.4 LIQUEFACTION RESISTANCE OF CBD SOILS FROM LABORATORY TESTING

Cyclic testing forms the primary basis for evaluating the liquefaction resistance of the Christchurch CBD soils in this study. For this reason, a majority of the tests performed on "undisturbed" specimens were CTX tests. Figure 4.5 provides representative results from a CTX test on a sand (SP-SM) specimen from a depth of 4.43 m at the CTH site (see Figure 4.3 for the subsurface profile). A single amplitude axial strain of 3% was adopted as the threshold of liquefaction in the CTX tests (similar to that used in Bray and Sancio 2006), so that $N_{c\text{-}3\%\ S.A.\varepsilon}$ is reported hereafter to describe the cyclic resistance ratio (CRR) of soil specimens. This criterion is illustrated by the star in the plot of ε_{axial} vs. number of cycles (N_c) in Figure 4.5. For this case 3% S.A.ε occurs just before the completion of the fifteenth cycle of loading; cycles of loading were rounded up to the nearest half cycle, so $N_{c\text{-}3\%\ S.A.\varepsilon} = 15$ for this test. The applied cyclic stress ratio ($CSR = q/(2\sigma'_c)$ where $q = \sigma_1\text{-}\sigma_3$ and σ'_c is the effective isotropic consolidation pressure in CTX conditions) was 0.289. By combining the results of multiple CTX tests in the form of CSR vs. $N_{c\text{-}3\%\ S.A.\varepsilon}$, cyclic resistance curves can be interpreted for specific soil units to define the liquefaction resistance of the CBD subsurface soils. The CSR required to reach 3% S.A.ε in a specific number of cycles defines the cyclic triaxial (CTX) test specimen's CRR. This lab CTX CRR value is then adjusted to field conditions to enable comparisons of soil units at different depths and in-situ stress conditions.

For example, Figure 4.6 shows the interpreted CRR curves for several soils tested from the CTH site. The soil units that were tested correspond to the layers shown in Figure 4.3a; i.e., specimens tested from the *upper layer of silt* correspond to the shallowest ML layer in Figure 4.3a, while the *upper layer of sand* specimens correspond to the layer of SP-SM directly above the sandy gravel layer, and *lower layer of sand* specimens correspond to the layer of SP/SP-SM directly below the sandy gravel. The CSR values shown in Figure 4.6 (and shown in subsequent plots of CSR vs. $N_{c\text{-}3\%\ S.A.\varepsilon}$) are normalized to atmospheric pressure by using their respective σ'_c values to calculate the overburden correction factor (K_σ) recommended by Idriss and Boulanger (2008). Data from the closest CPT to each borehole over the depth range of each CTX specimen (see Figure 4.3 for an illustration) was used in conjunction with σ'_c and fines content (FC) for

each CTX specimen to calculate the normalized clean-sand equivalent cone penetration resistance (q_{c1Ncs}; Idriss and Boulanger 2008), which is used in the calculation of K_σ.

To correct the CTX results to "field" conditions, a correction factor C_r was applied to the CSR_{CTX} values. This correction factor takes into account 1) a factor to convert from isotropic to anisotropic consolidation stress conditions (all CTX specimens were tested under isotropic conditions) and 2) a factor to estimate bi-directional field loading from uniaxial CTX loading. Ishihara et al. (1985) recommended

$$CSR_{K_o \neq 1} = \frac{1 + 2K_o}{3} CSR_{K_o = 1} \tag{4.1}$$

to convert from isotropic to anisotropic conditions (i.e., the C_r factor where K_o is the coefficient of lateral earth pressure), and Seed (1979) recommended an additional factor of 0.9 to adjust for bi-directional loading. Adopting these recommendations, the following C_r' values (i.e., $0.9C_r$) were assumed based on soil type: 0.57 for SP and SP-SM soils (K_o=0.45), 0.60 for SM soils (K_o=0.5), and 0.66 for ML soils (K_o=0.6). The higher C_r' value for fine-grained soils is consistent with recommendations made by Bray and Sancio (2006) based on comparisons between cyclic simple shear (CSS) tests and CTX tests on Adapazari silt and recommendations made by Boulanger et al. (1998). A direct comparison of CSS and CTX testing on Christchurch soils is not currently available, but future testing will address this issue.

The grouping of results in Figure 4.6 to form CRR curves was based on combining results from CTX testing of specimens of similar depth as well as similar soil types at a particular site. A more holistic perspective of the CTX results across the CBD can also be taken by looking at grouping results for similar soil types at multiple sites. The primary studied sites are located less than a kilometer apart within the CBD and the soils are similar in composition and depositional environment. Figure 4.7a shows a plot of $CSR_{Field,\ 1atm}$ vs. $N_{c\text{-}3\%\ S.A.\varepsilon}$ for all CTX tested sand (SP and SP-SM) specimens, and Figure 4.7b provides similar plots for all silt (ML) and silty sand (SM) specimens. Scatter in the data presented in Figure 4.7 can be partly explained by the fact that though similar soils are being examined, they are from different sites within the CBD. When examining soils from the same site there is typically inherent variability in the CTX test results; therefore, this variability would be expected to increase when examining results from different sites. Although there is scatter in the results, clear trends in the plots of CSR vs. $N_{c\text{-}3\%\ S.A.\varepsilon}$ are apparent. Thus, cyclic resistance curves can be interpreted for the individual soil types. The data for the sandy soils are separated into results for two different ranges of corresponding q_{c1N} values for CTX specimens: q_{c1N} between 60 and 100 and q_{c1N} between 100 and 140. This separation of results was applied because a distinct difference in the implied liquefaction resistance for specimens within these ranges of q_{c1N} was evident. Additionally, though the data points are presented separately for SP and SP-SM in Figure 4.7a, the cyclic resistance curves are drawn to incorporate results from both SP and SP-SM soil specimens, because there is little difference in their respective responses. Lastly, the ML soil displays a flatter CRR curve than the coarser-grained soils, which is an expected trend (e.g., Boulanger and Idriss 2015).

The subsurface profiles shown in Figure 4.3 present soil units commonly encountered within the shallow subsurface of the CBD and consequently represent conditions that must be accounted for by engineers in the design of structures and their respective foundation systems. The data presented in Figure 4.7 provide cyclic resistance curves for the critical shallow layers shown in Figure 4.3 (with the exception of the gravelly soils shown in Figure 4.3a), which provide

valuable insights into the response of these soils that proved problematic for buildings in the CBD during the CES. Importantly, the individual test results, such as those presented in Figure 4.5, document key attributes of cyclic soil response for these soils, which are invaluable for calibrating soil constitutive models.

4.4.1 CPT Triggering Comparisons and Additional Insights from Laboratory Testing

The data that resulted from the CPT investigations completed as a part of the earlier stages of the UCB-UC project allow for the use of simplified procedures to evaluate liquefaction triggering in the various soil units of the CBD. The probabilistic CPT-based liquefaction triggering procedure proposed by Boulanger and Idriss (2015)—hereafter referred to as BI15—was used to provide comparisons between the liquefaction resistances measured using CTX tests and those implied from in-situ CPT testing. To enable these comparisons, CRR curves were fitted to the $CSR_{Field,\ 1atm}$ vs. $N_{c\text{-}3\%\ S.A.\varepsilon}$ for the various soil units tested using a power function regression (i.e., $CRR=a\cdot N^{-b}$). Examples of this power function fit are shown Figure 4.6 for multiple layers of the CTH subsurface, where a=0.38 and b=0.36 for the upper silt layer, a=0.31 and b=0.26 for the upper sand layer, and a=0.28 and b=0.19 for the lower sand layer.

Liquefaction resistances defined by correlations from in-situ soil testing, such as those calculated using the BI15 procedure, use empirical data based on case histories of sites that did or did not show surface manifestations of liquefaction during historical earthquakes. To account for duration effects in the calculation of the liquefaction resistance, simplified methods such as the BI15 procedure use a scaling factor that is a function of an earthquake's magnitude (magnitude being a proxy for number of load cycles). In this way, CRR calculations for critical soil layers from earthquakes of differing magnitude are scaled to a magnitude 7.5 (M7.5) event using a magnitude scaling factor, which allows for the calculation of "standardized" $CRR_{M7.5}$ values. To compare CRR values from CTX test data to the CRR values calculated using BI15, cyclic stress ratios required to cause liquefaction in 15 cycles of uniform loading were used as this approximately represents the duration of loading for a M7.5 event (Idriss & Boulanger 2008).

Figure 4.8 shows a plot of $CRR_{M7.5,\ 1atm}$ vs. q_{c1N} for several soil units tested in this study from Christchurch's CBD and a plot of the corresponding triggering correlation of BI15. Multiple curves are plotted for various considerations of fines content (FC), which correspond to the average FC of the soil units tested (the FC values reported for the CTX results in Figure 4.8 are an average of the FC for the individual specimens included in the CRR curves). A probability of liquefaction (P_L) of 50% was considered in the calculation of the CPT-based curves shown in Figure 4.8 to provide a better estimate of CRR for comparison purposes (i.e., a P_L higher or lower than 50% would be biased to lower or higher implied CRR values, respectively).

The results depicted in Figure 4.8 show that there is generally good agreement between the CTX test results and the BI15 correlation for $CRR_{M7.5,\ 1atm}$ and importantly no apparent bias for laboratory based CRR values to be greater or less than the field-based CRR values. Data for clean sands is again only plotted for specimens with corresponding q_{c1N}>60, because loose sands with q_{c1N}<60 were most likely disturbed during the sampling and testing process. The plotted interpreted CRR values for clean sands do not show a particular bias when compared to the BI15 CRR values as data plots slightly above or below and sometimes on the BI15 triggering curves. Comparatively fewer data are available for the silty sands, but both data points (for average FC=24% and FC=39%) plot above the BI15 triggering curve. Data representing the $CRR_{M7.5,\ 1atm}$

for a tested unit of silt with FC=64% shows a cyclic resistance below the BI15 triggering curve for FC=64%, while the silt unit with average FC=91% plots close to the BI15 triggering curve. There are multiple potential reasons for differences in the CRR calculations from CTX testing and the BI15 procedure, including but not limited to: 1) CPT-based liquefaction triggering correlations are based on case histories where there was (or was not) post-earthquake surface manifestation of liquefaction, which may not directly relate to the cyclic mobility-type of failure witnessed in the CTX testing; 2) the simplification of reducing CRR results from CTX testing to the CSR required to reach 3% S.A.ε in 15 cycles to represent a M7.5 event may lead to biases of the liquefaction resistance calculated from CTX testing; 3) there are inherent differences in the methods for calculating CSR for the BI15 procedure and the CTX testing (based on the known shear stress and effective confining pressure); and 4) C_r' values used to convert CSR_{CTX} to CSR_{Field} were based on assumptions as opposed to site-specific testing and could be high or low.

The results from CTX testing provide information regarding soil response that is unable to be obtained from current, conventional in-situ testing methods. These results include the stress-strain response as well as the pore water pressure response of the tested soil when subjected to dynamic loading (e.g., see Figure 4.5). Insights into the similarities and differences of the response of various soil types can also be explored using CTX test data, which provide information to engineers and researchers that would not be available without the use of laboratory testing. Figure 4.9 shows a comparison of results from CTX testing on two soil specimens from the FTG-7 site (see Figure 4.3b for specimen depths). The specimen from a depth of 4.77 m classified as a silty sand (SM) based on the USCS while the specimen from a depth of 10.97 m classified as a poorly-graded clean sand (SP). The fines contents of the SM specimen was significantly higher than the SP specimen (FC=44% compared to FC=4%), while q_{c1Ncs}=86.1 for the SM specimen and q_{c1Ncs}=107.9 for the SP specimen. Interestingly, even with these different soil characteristics, the CTX test results illustrate a similar response of the two soil specimens both in pore water pressure response and stress-strain response during cyclic loading.

In a similar fashion as the comparison shown in Figure 4.9 between a silty sand and clean sand, Figure 4.10a presents a comparison of CTX results from a silty sand and silt specimen tested from the FTG-7 site. Results are shown again for the SM specimen tested from a depth of 4.77 m but now plotted with the results from a silt specimen tested from a depth of 3.72 m. The fines content of the ML specimen was 89%, while the q_{c1Ncs}=93.3. Based on the CPT data, the soil behavior type index (I_c; Robertson and Wride 1998) was 2.22 and 2.43 for the specimens from 4.77 m and 3.72 m, respectively. A noticeable difference between the CTX results displayed in Figure 4.10a is the much more pronounced bias towards extensional loading for the ML specimen from a depth of 3.72 m compared to the SM specimen from a depth of 4.77 m. It is difficult to draw conclusions regarding the implied liquefaction resistance of these soils based on the data presented in Figure 4.10a alone, but Figure 4.10b shows the liquefaction resistance curves (corrected using C_r' and K_σ) for the soil units where these specimens originate. The curves in Figure 4.10b indicate similar CRR values for these two specimens, which is supported by the CPT data in that q_{c1Ncs} values range from 91 to 93 for the ML layer and 72 to 87 for the SM layer (i.e., fairly similar q_{c1Ncs} values suggest similar cyclic resistances).

4.5 STEADY STATE TESTING OF RECONSTITUTED SPECIMENS

Steady state testing was performed on reconstituted specimens comprised of the soils that were tested as a part of the "undisturbed" sampling and testing program. Defining steady state lines for multiple soil types is an important part of characterizing the soils of Christchurch's CBD, as it provides insights regarding the dilative or contractive tendencies as well as the large strain response of specific soils. Moreover, constitutive models often rely on knowledge regarding the steady state response of a soil to enable accurate representation of a soil's loading response. Multiple soil units were tested to describe the steady state response of various soil types in the CBD. All steady state testing was performed using strain-controlled, monotonic triaxial testing procedures. Due to the size of the mold used for building reconstituted triaxial specimens, soil from specimens tested in the previously described "undisturbed" sampling and testing program were selectively combined for steady state testing. Specimens of soil were only mixed if they corresponded to a particular unit of soil at a given site; the selection of soil specimens to be mixed for steady state testing was based on two criteria: 1) the similarity of soil specimens with regards to index properties (e.g., grain size distribution, void ratio limits, and specific gravity of solids) and 2) the matching of CTX test results of "undisturbed" specimens selected for mixing to a CRR curve at a given site. In this way, steady state lines were developed for a majority of the units represented by CRR curves at the various test sites.

Reconstituted specimens were built using a moist-tamping technique based on an undercompaction method similar to that described by Ladd (1978) for steady state testing, including tested silt specimens. Lubricated end caps were used for all tests, except in the case of tested silt specimens; full specimen diameter sized porous stones had to be used for the silts to inhibit the loss of fines through the drain lines during triaxial testing, which disallowed the use of lubricated end caps. The rate of strain was determined so that time to failure was greater than $4*t_{50}$ for istrotropically consolidated undrained (ICU) monotonic triaxial tests and $32*t_{50}$ for isotropically consolidated drained (CD) monotonic triaxial tests, where t_{50} is the time to 50% consolidation. This rate of strain was chosen to ensure accurate measurement of pore water pressure during undrained tests and free-draining conditions during drained tests.

Steady state testing was completed on units of soil from multiple sites across the CBD, which correspond to the soil types described by the CRR curves in Figure 4.7. As a majority of the "undisturbed" sampling and testing focused on sands (SP and SP-SM), multiple units of this soil were tested from various sites in the CBD. Only one unit of silt (ML) and one unit of silty sand (SM) were tested due to a lack of further soil that met the mixing criteria. Figure 4.11 shows the results for steady state testing of the lower unit of sand at the FTG-7 site (SP/SP-SM unit from a depth of approximately 8 to 14 m—see Figure 4.3b). An area-correction was applied to the raw test data, with an assumption that the soil specimen remained as a constant right-cylinder during shearing (Germaine and Ladd 1988). This area-correction does not necessarily capture the true cross-sectional area of the specimen, especially at large strains as the deformed specimen shape becomes non-uniform. Based on the plot of principal effective stress-ratio (σ'_1/σ'_3) vs. ε_{ax}, a constant value of σ'_1/σ'_3 of just over three is reached for *Test 1*, while σ'_1/σ'_3 continues to decrease for *Test 2* and *Test 3*, even at strains beyond 30%. This continuing decrease of σ'_1/σ'_3 at large strains is believed to be an artifact of the area-correction previously mentioned, and a steady state stress-ratio ($\sigma'_1/\sigma'_{3\text{-ss}}$) of 3.1 was used for all specimens for this set of tests.

By combining the results of multiple tests (typically three tests were run per tested soil unit)

steady state lines (SSL) could be deduced for each tested soil unit. Figure 4.12 provides plots of the void ratio vs. mean effective stress at steady state ($p'_{ss} = (\sigma'_{1\text{-}ss}+2\sigma'_{3\text{-}ss})/3$) for the soil units tested. The functional form of the SSL suggested by Cubrinovski and Ishihara (2000) was fit to the data for each set of tests shown using a least-squares fit; the form of this fit is

$$e_{ss} = e_{10-ss} + \lambda(1 - log_{10}p'_{ss}) \tag{4.2}$$

where $e_{10\text{-}ss}$ is the steady state void ratio at p'_{ss} = 10 kPa and λ is the slope of the fitted line (in semi-log space). A summary of e_{10} and λ for each tested soil unit is provided in Figure 4.12, pertinent information is provided in Table 1. All the data shown in Figure 4.12 corresponds to ICU tests except for the point corresponding to the largest value of p'_{ss} for the silt layer at the CTH site, which was a CD test. The determination of p'_{ss} was based on an examination of the trend of σ'_1/σ'_3 and σ'_3 with strain. The lateral effective stress during shearing (σ'_3) was not sensitive to the area-correction as it was directly measured via a differential pressure transducer during shearing and interpretations of σ'_1/σ'_3 at steady state were more stable compared to interpretations of deviator stress ($q=\sigma_1-\sigma_3$).

An alternative means for examining the steady state response of tested soils is provided in Figure 4.13 where the relative density (D_r) is plotted against p'_{ss}. Void ratio limits (e_{min} and e_{max}) for the tested soils were found using the Japanese Standard method (JIS A 1224:2000). This method is specified for soils with FC < 5%, but Cubrinovski and Ishihara (2002) found it to be reliable for FC ≤ 30%. Plotting the test data in D_r vs. p' space allowed for the grouping of all SP and SP-SM specimen results in the determination of a single steady state line for "clean" sands. The functional form of the fitted steady state lines shown in Figure 4.13 is based on the recommendations of Bolton (1986) so that

$$D_{r-ss} = \frac{R}{Q - \ln\left(100 * \left(\frac{p'_{ss}}{p_{atm}}\right)\right)} \tag{4.3}$$

where R and Q are fitting parameters and p_{atm} is atmospheric pressure in the same units as p'_{ss}. The values of R and Q for the SP and SP-SM material were found to be 0.98 and 7.90, respectively. When the Bolton (1986) functional form of the steady state line was fitted to the SM material shown in Figure 4.12, the R and Q parameters were found to be 3.73 and 9.79, respectively; however, the tested SM specimens had FC ≥ 30% making the calculation of D_r from void ratio limits determined from the Japanese standard likely inappropriate for this material. The Bolton (1986) relationship does not appear to be reasonable for the SM soils.

Data corresponding to the initial states prior to shearing for the sand CTX specimens tested as a part of the previously discussed "undisturbed" testing program are plotted with the steady state testing data in Figure 4.13. As can be seen, all of the CTX test specimens of this study were located below the SSL, which is consistent with the cyclic mobility-type of failure witnessed in all of the CTX tests. The information provided by the steady state testing completed as a part of this study provides details that supplement the "undisturbed" CTX and monotonic triaxial testing results and helps in the characterization of the Christchurch CBD soils.

4.6 CONCLUSIONS

There is limited cyclic test data currently available for Christchurch soils. A comprehensive sampling and laboratory testing program was executed to characterize key soil units in the Christchurch CBD. These soil units were located beneath buildings that were damaged due to the liquefaction of foundation materials during the strong seismic shaking of the CES. Characterizing these shallow soils through advanced laboratory testing provides information to researchers and engineers studying the effects of soil liquefaction on buildings during these events. Insights and observations are provided based on the testing of both "undisturbed" and reconstituted soil specimens. An emphasis is placed on examining the liquefaction resistance of tested soils via cyclic triaxial testing of "undisturbed" specimens and the large strain steady state response of tested soils using monotonic triaxial testing of reconstituted specimens.

Cyclic triaxial test results were compiled in the form of cyclic resistance curves for various tested units on a site-by-site basis. An overburden correction factor and a CTX to field conditions (anisotropic and 2D shaking effects) correction factor were applied to cyclic resistance ratios and the CSR required to reach 3% single amplitude axial strain in 15 cycles of uniform loading (representative of a M7.5 event) was estimated and compared to $CRR_{M7.5,\ 1atm}$ values estimated using the Boulanger and Idriss (2015) CPT-based liquefaction procedure. These comparisons were completed for sand specimens with $q_{c1N}>60$ (as sands with $q_{c1N}<60$ have been shown previously to be disturbed from the employed sampling procedures), silty sand specimens, and silt specimens. There was relatively good agreement between liquefaction triggering estimated via CTX testing and the CPT-based correlation.

The results of both "undisturbed" and reconstituted specimen testing provide information regarding key soils from the CBD of Christchurch. This information includes individual specimen results as well as liquefaction resistance curves and steady state lines for specific units of soil that were pivotal in the response of overlying structures. This information is crucial for PBEE design in that advanced numerical analyses are required, which rely on laboratory test data for the calibration of constitutive models. Information such as the similarity in cyclic response of soils with significantly different fines contents (e.g., SM vs SP soil) could not necessarily be discerned from in-situ testing. The benefits of high quality sampling and advanced laboratory testing are highlighted by insights garnered through the presented test results.

Table 4.1: Steady state tested soil characteristics

Site	Unit	FC	D_{50} (mm)	C_u	C_c	PI	e_{min}	e_{max}
FTG-7	Lower Sand	5.8	0.24	2.39	1.04	NP	0.58	1.04
CTH	Upper Sand	6.5	0.17	2.07	1.04	NP	0.65	1.14
CTH	Lower Sand	5.5	0.19	2.16	1.04	NP	0.62	1.09
CTUC	Upper Sand	7.1	0.18	2.26	1.17	NP	0.62	1.11
PWC	Lower Sand	5.2	0.17	1.95	0.96	NP	0.65	1.12
VT	Upper Sand	4.6	0.20	1.91	1.11	NP	0.65	1.11
FTG-7	Upper SM	38.0	0.09	4.23	1.37	NP	--	--
CTH	Upper ML	73.6	0.05	--	--	4	--	--

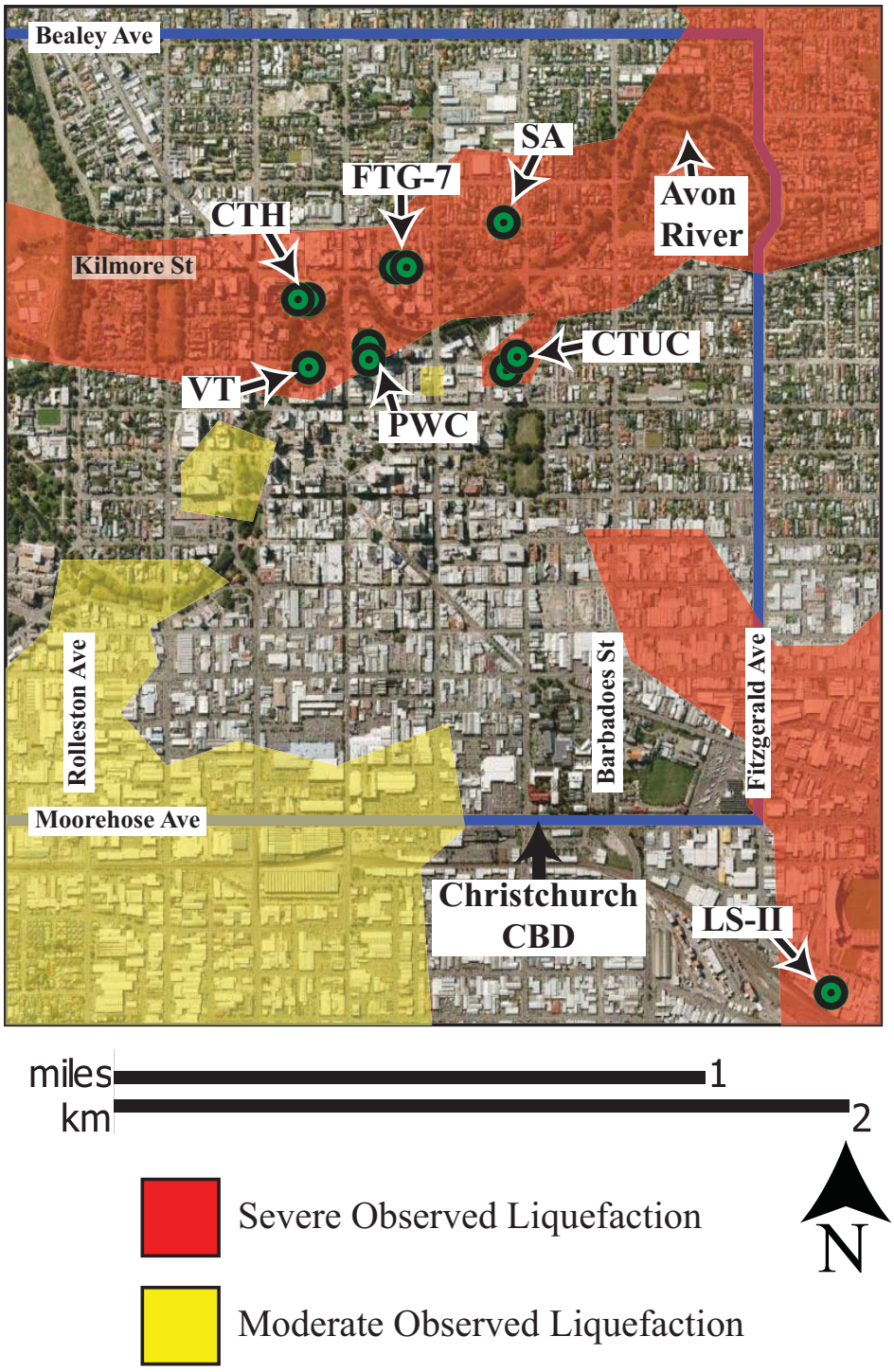

Figure 4.1: Observed liquefaction in the CBD from CES (based on Cubrinovski and Taylor 2011 observed liquefaction map) and locations of boreholes used in this study for "undisturbed" sampling (indicated by green circles); background map from Google Earth™

a) b)

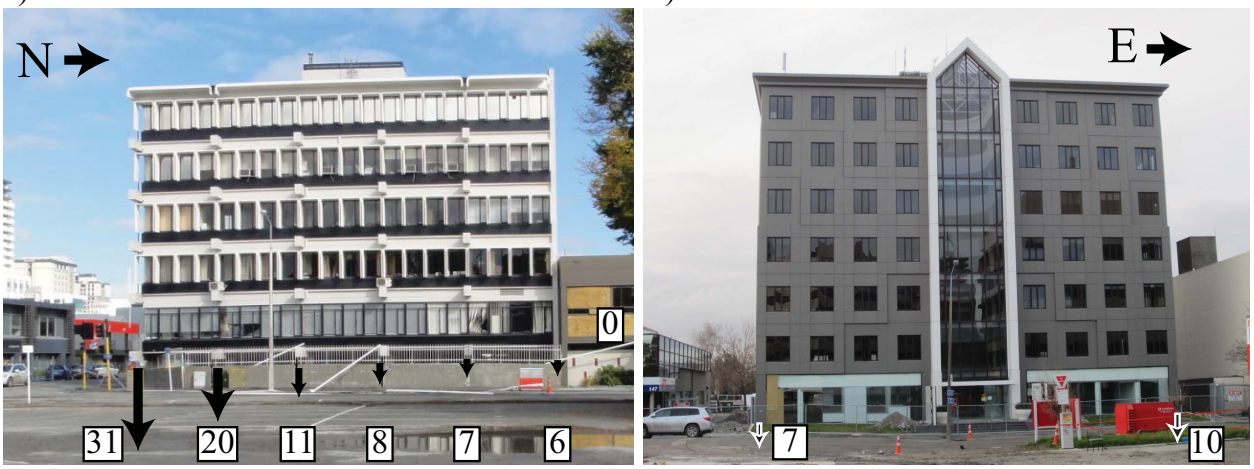

Figure 4.2: a) East side of CTUC building following Canterbury earthquakes; settlements (cm) relative to adjacent building to the north; b) south-side of FTG-7 building; settlements (cm) relative to NW corner of building following 22 FEB 11 M_w6.2 shown

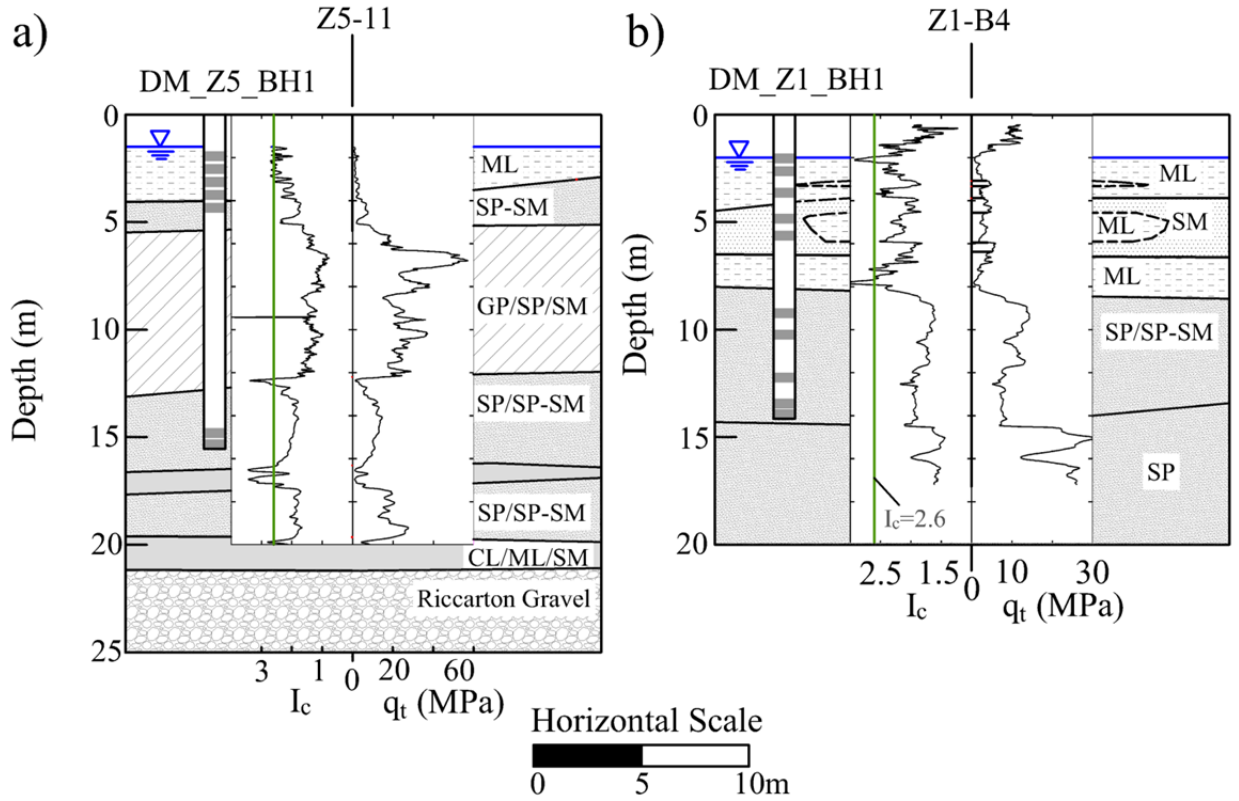

Figure 4.3: Simplified subsurface profile for a) CTH site and b) FTG-7 site with "undisturbed" boreholes and sample depths (this study) and CPT investigations (Zupan 2014); note that spacing of boreholes and CPTs are not to scale

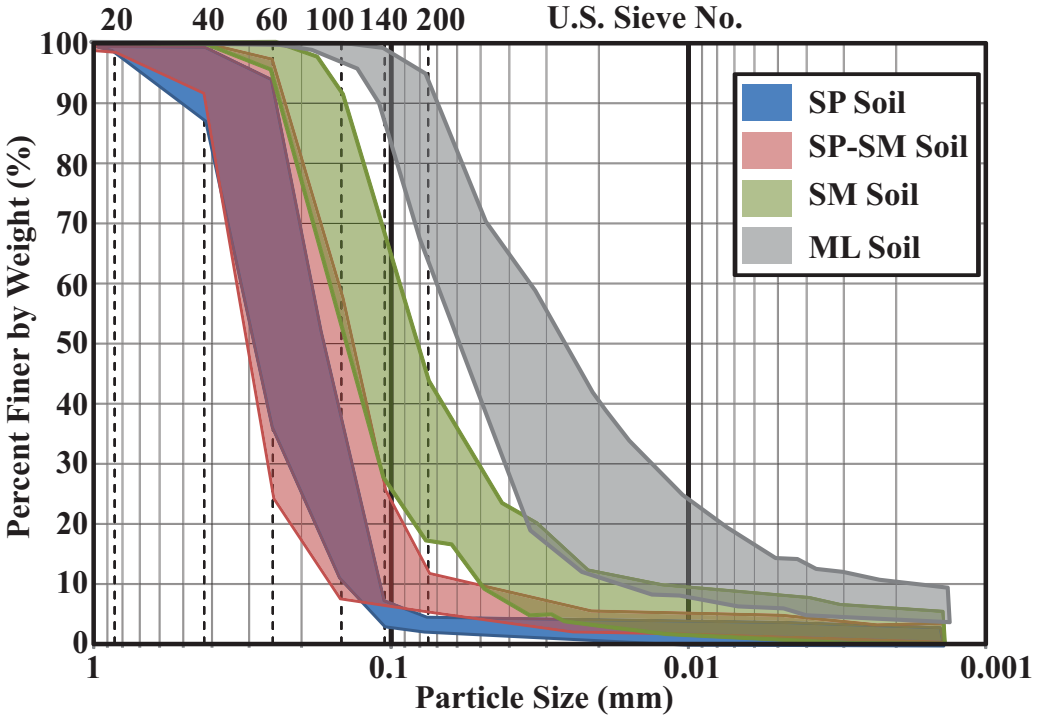

Figure 4.4: Summary of grain size distribution for retrieved CBD soils

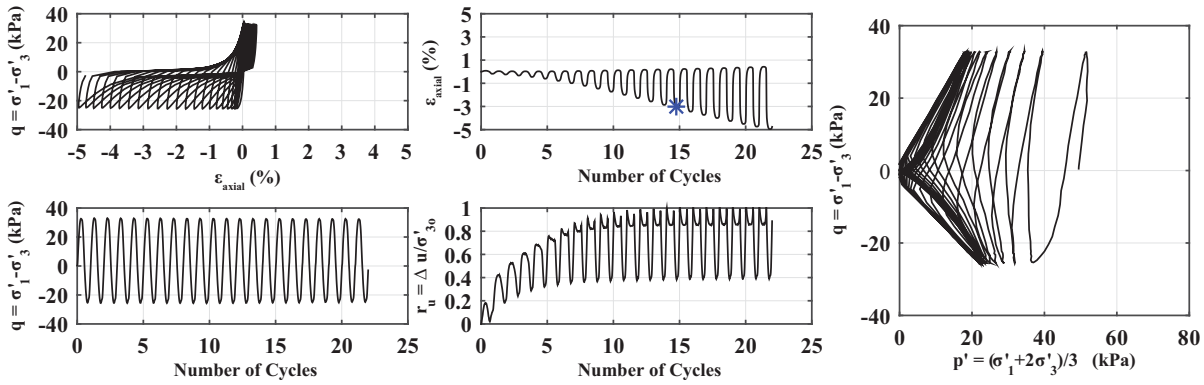

Figure 4.5: CTX test results for CTH site specimen; 4.43 m depth, USCS: SP-SM, PI=Non-Plastic (NP), e_o=0.76, σ'_{3o}=49.3 kPa, Load Frequency=0.1 Hz, CSR_{CTX}=0.289, $Nc_{-3\%\ S.A.\varepsilon}$ =15

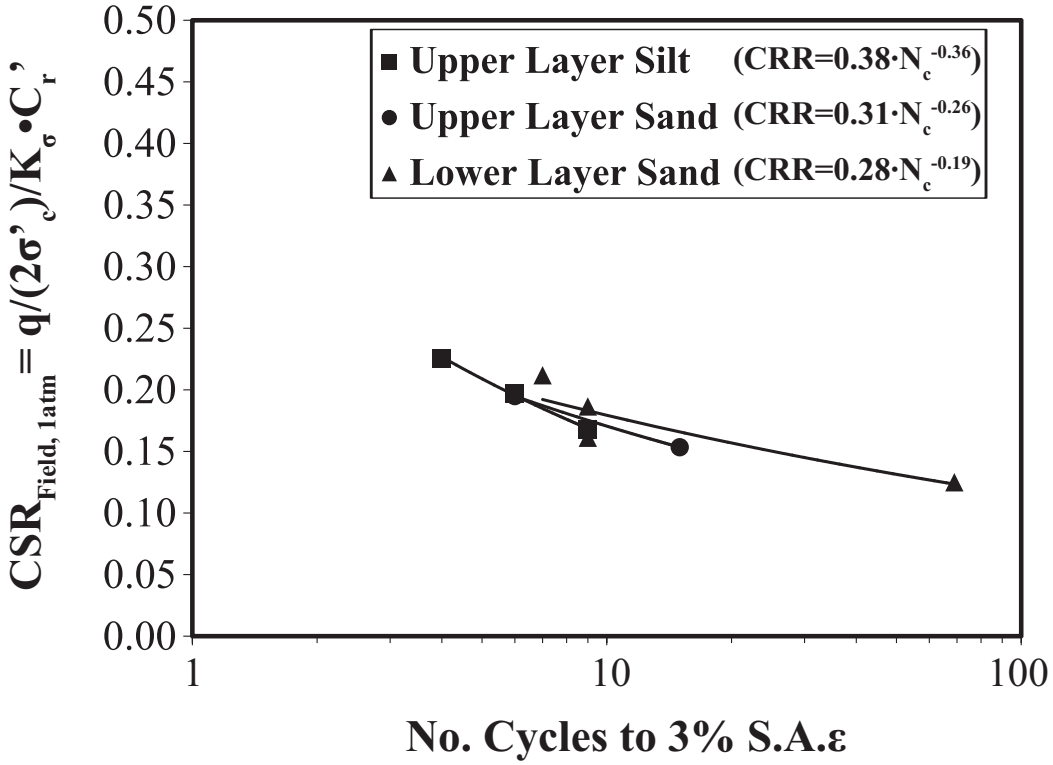

Figure 4.6: Cyclic resistance curves for CTH soil unit

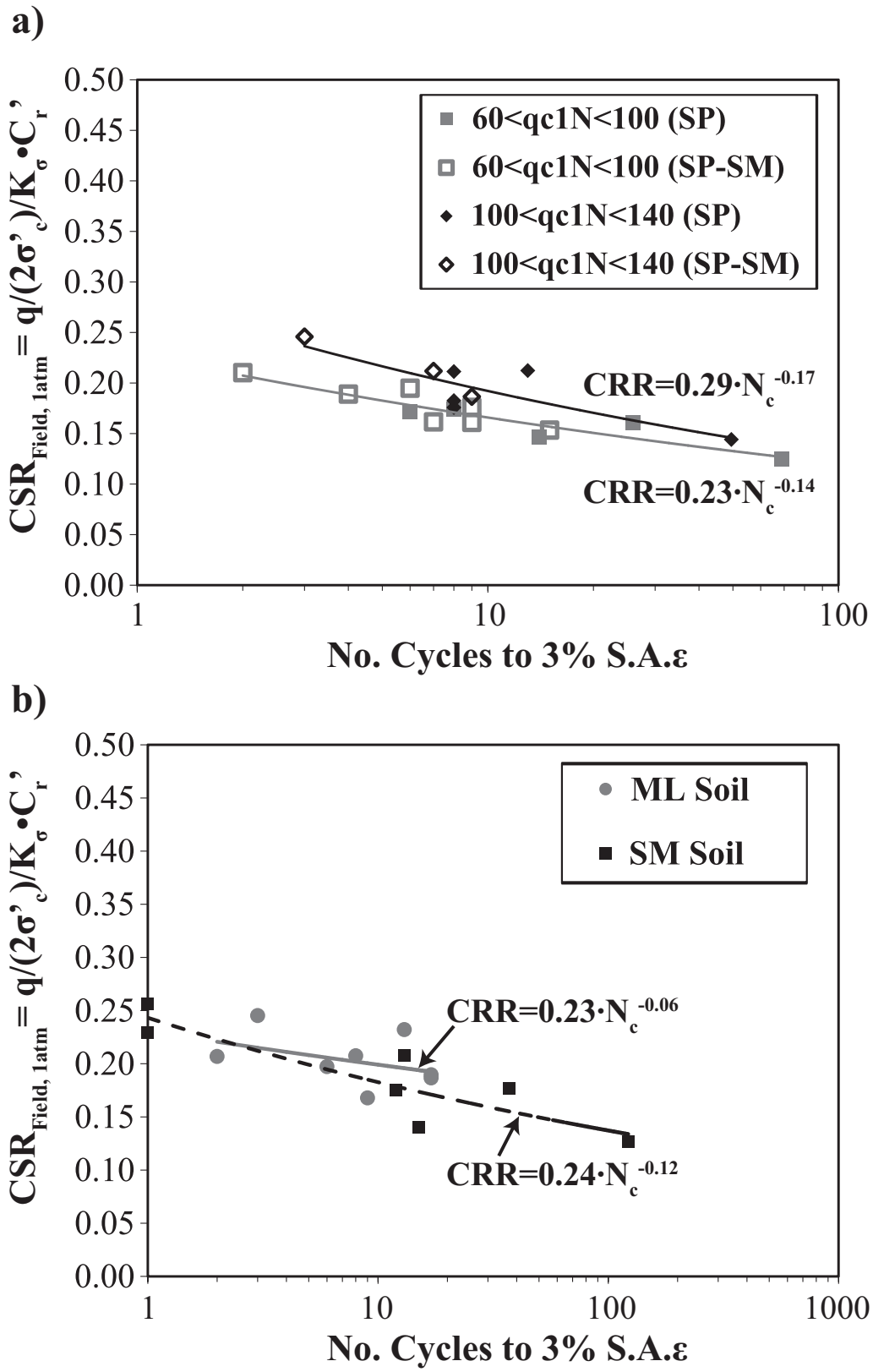

Figure 4.7: CSR vs. $N_{c\text{-}3\%\ S.A.\varepsilon}$ for a) SP and SP-SM soils and b) ML and SM soils

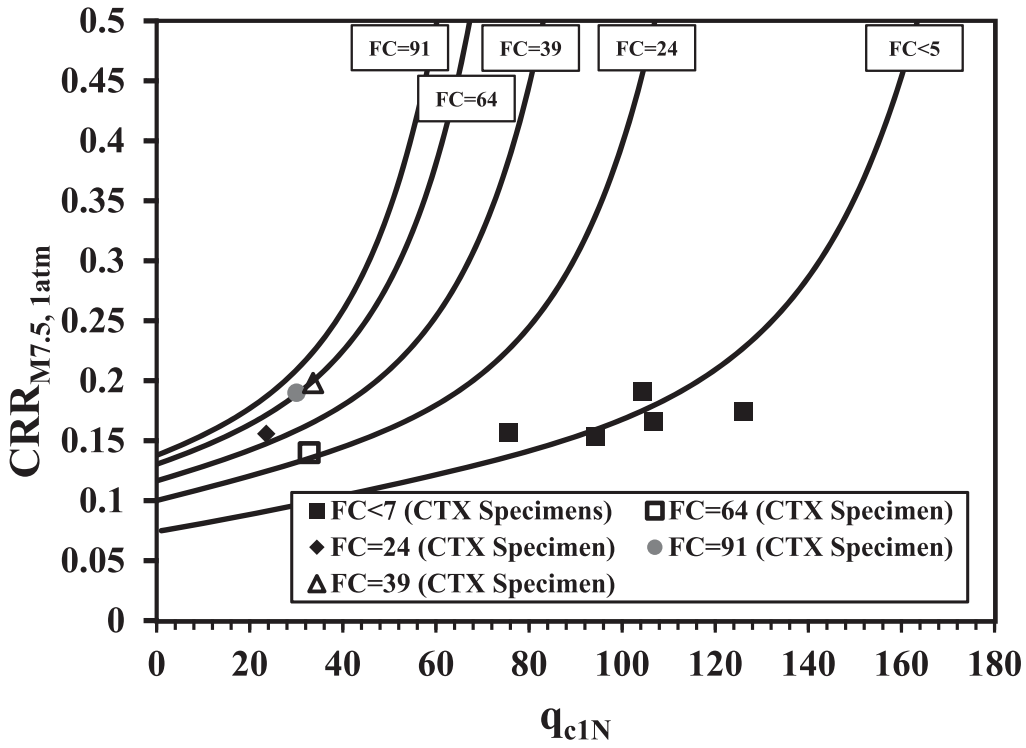

Figure 4.8: CRR vs. qc1N for CTX specimens with correlations from Boulanger and Idriss (2015) CPT based liquefaction triggering correlation for P_L=50%

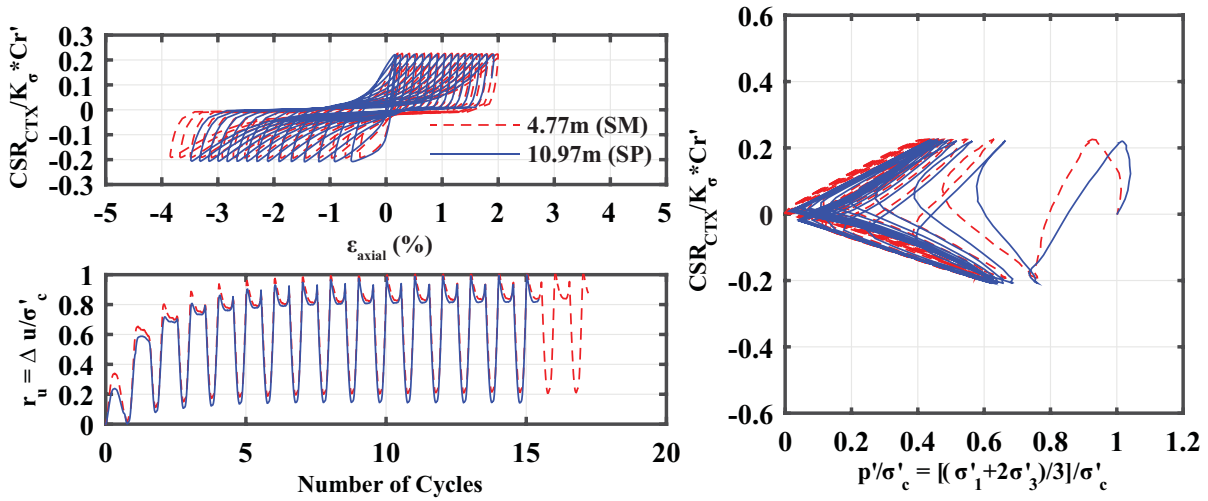

Figure 4.9: CTX test results for FTG-7 site specimens; 1) 4.77 m depth, USCS: SM, FC=44%, PI=4, e_o=0.73, σ'_c=66.9 kPa, K_σ=1.04, C_r'=0.6 and 2) 10.97 m depth, USCS: SP, FC=4%, Non-Plastic, e_o=0.72, σ'_c=125.2 kPa, K_σ=0.97, C_r'=0.57; $N_{c\text{-}3\%\ S.A.\varepsilon}$ =13 for both tests

a)

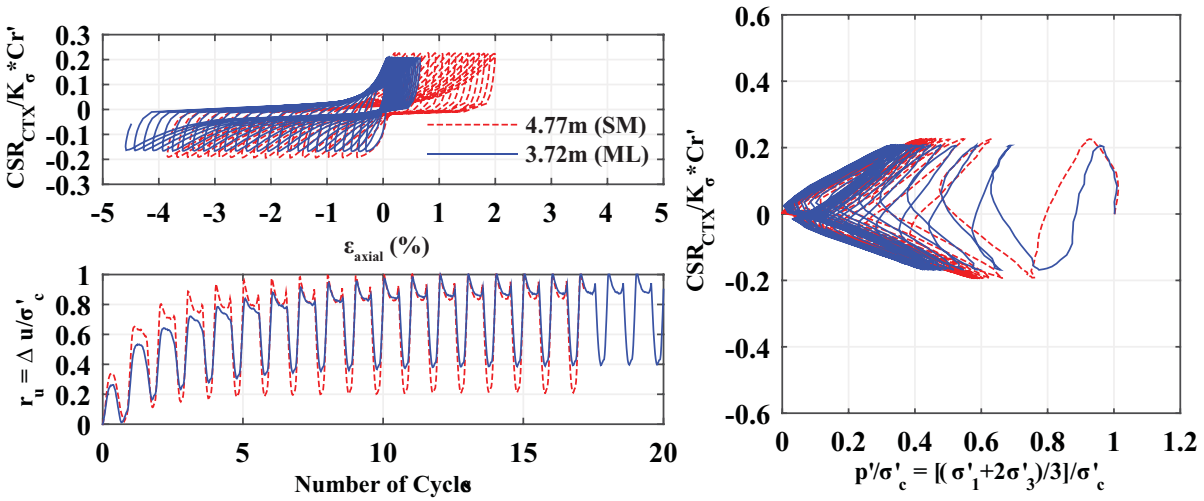

b)

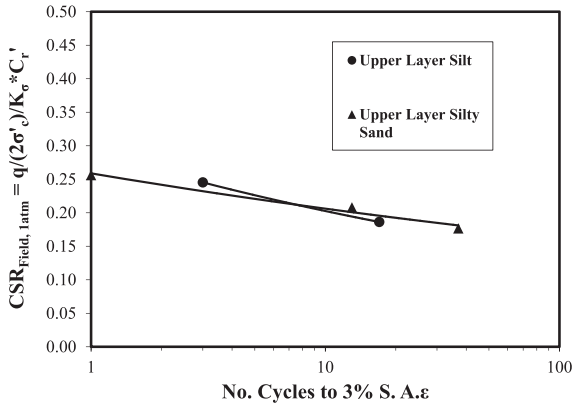

Figure 4.10: a) CTX test results for FTG-7 site specimens; 1) 4.77 m depth, USCS: SM, FC=44%, PI=4, e_o=0.73, σ'_c=66.9 kPa, $N_{c\text{-}3\%\ S.A.\ \varepsilon ax}$ =13, K_σ=1.04, C_r'=0.6 and 2) 3.72 m depth, USCS: ML, FC=89%, PI=2, e_o=0.67, σ'_c=61.6 kPa, $N_{c\text{-}3\%\ S.A.\ \varepsilon ax}$ =17, K_σ=1.05, C_r'=0.66; b) CRR curves for upper ML and SM layer at FTG-7 site

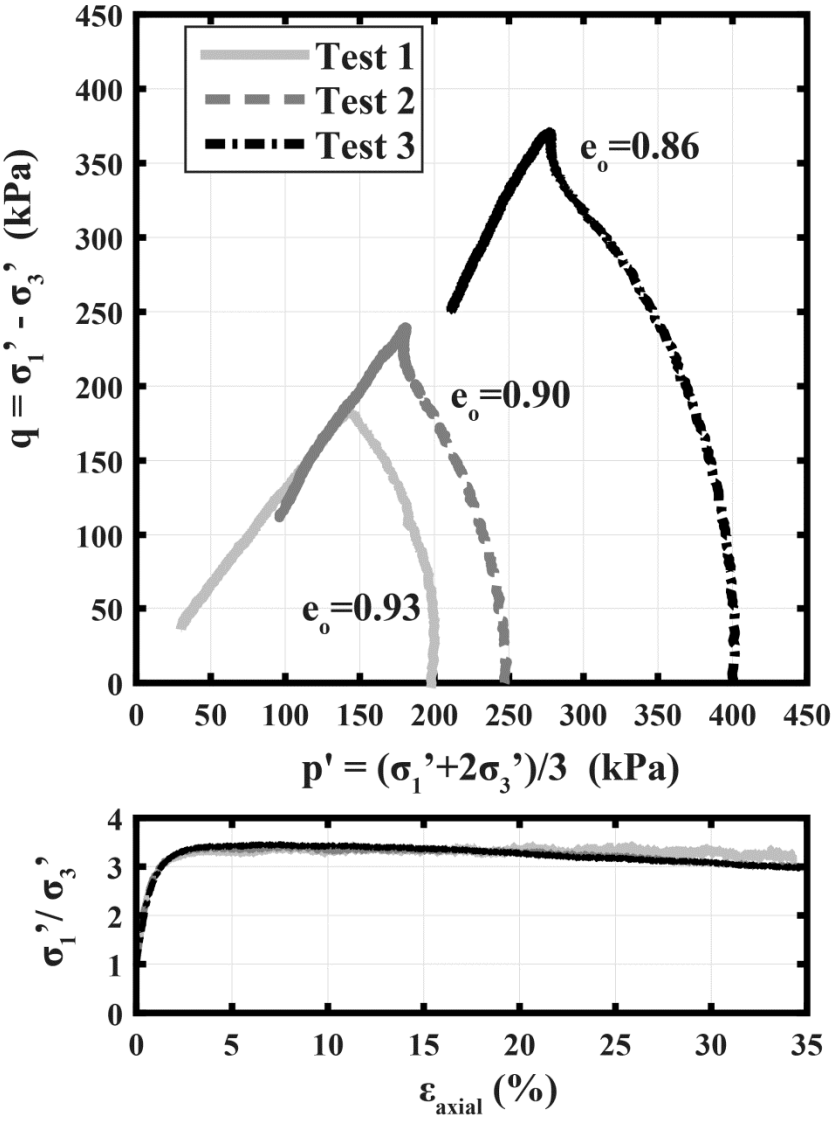

Figure 4.11: Steady state test results of lower sand at FTG-7 site; void ratios labelled for each test (e_{min}=0.58 and e_{max}=1.04)

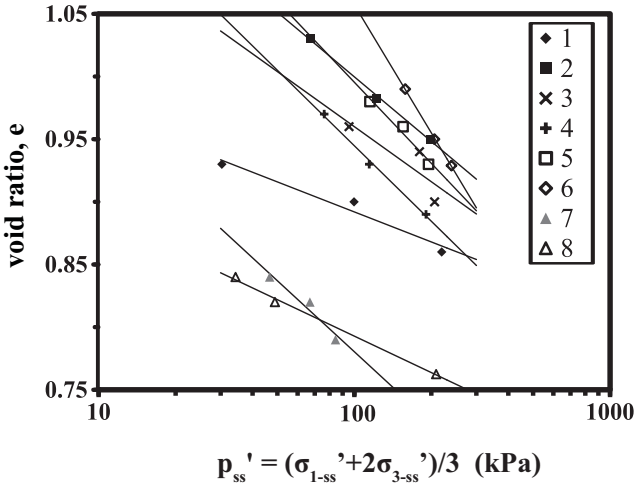

Legend No.	Site	Unit	e_{10}	λ
1	FTG-7	Lower Sand	0.97	0.08
2	CTH	Upper Sand	1.17	0.17
3	CTH	Lower Sand	1.11	0.15
4	CTUC	Upper Sand	1.14	0.20
5	PWC	Lower Sand	1.21	0.21
6	VT	Upper Sand	1.40	0.34
7	FTG-7	Upper SM	0.97	0.19
8	CTH	Upper ML	0.89	0.10

Figure 4.12: e vs. p'_{ss} for steady state testing of soils; e_{10} and λ are fitting parameters used by the Cubrinovski and Ishihara (2000) functional representation of the steady state line

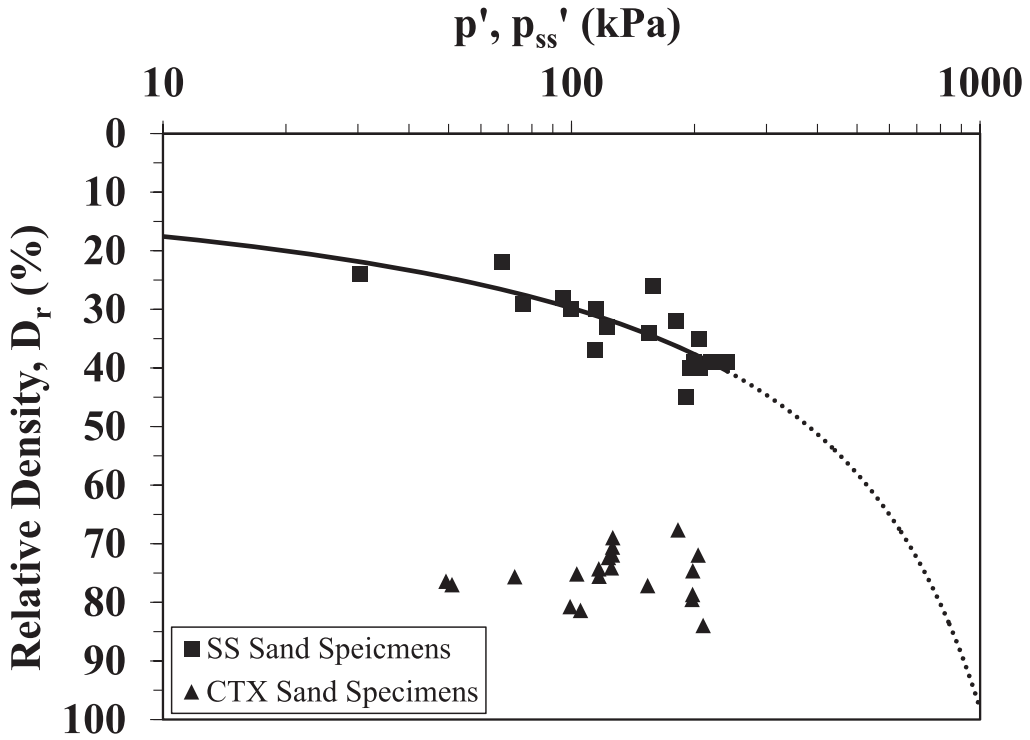

Figure 4.13: D_r vs. p'_{ss} for steady state (SS) testing of sand plotted with initial state of "undisturbed" CTX sand specimens and steady state relationship proposed by Bolton (1986); dotted portion of the curve demarcates the limit of test data

CHAPTER 5: CONCLUSIONS

5.1 SUMMARY

Evaluating the consequences and effects of soil liquefaction on structures and other infrastructure is a key area of performance based earthquake engineering (PBEE). The damage caused by liquefaction to buildings and infrastructure during recent large earthquakes has highlighted the importance of advancing this particular field of engineering. Engineers should learn from the data and information that these devastating events present through studying the case histories of buildings founded on liquefiable soils. This thesis provides information and insights regarding the seismic response of liquefiable soils by examining data collected during and after the 2010-11 Canterbury earthquake sequence in Christchurch, NZ.

A study that focused on examining a widely utilized 1D nonlinear effective stress seismic site response analysis program to model the response of liquefiable soils during strong shaking in the free-field is presented. The data from the Canterbury earthquakes provides an exceptional opportunity to study how the same ground responded to different levels of shaking intensity and duration. Ground near some of the seismic recording station sites in the CBD and greater Christchurch area liquefied multiple times during the Canterbury earthquakes, while some sites did not experience any liquefaction. The seismic recordings from these strong motion station sites and the substantial amount of soil data collected through site investigations were relied on to conduct seismic site response analyses for several strong motion station sites for six events of the Canterbury earthquakes. An emphasis was placed on evaluating the capabilities of nonlinear 1D effective stress seismic site response analyses, though nonlinear total stress and equivalent linear analyses were also carried out.

An extensive site investigation and advanced laboratory testing program that focused on characterizing shallow foundation soils at key building sites in the Christchurch CBD affected by liquefaction during the Canterbury events is described and discussed. Relatively "undisturbed" samples of most soil types were retrieved using the Dames & Moore hydraulic piston sampler to enable a program of advanced laboratory testing. Cyclic and monotonic triaxial testing of "undisturbed" soil specimens was performed (with an emphasis on cyclic testing) to characterize the liquefaction resistance of these soils. Strain controlled monotonic triaxial testing was also performed on reconstituted specimens to characterize the steady state response of the studied soils. Cyclic resistance curves and steady state lines of tested soil units were developed based on the laboratory testing results and an examination of the cyclic resistances is compared to the implied resistances from a CPT-based liquefaction triggering procedure. The advanced laboratory testing in conjunction with index testing (e.g., grain size distribution, Atterberg limits, void ratio limits, and specific gravity) of retrieved soils provides information necessary to characterize soil units that were critical to the seismic performance of structures in Christchurch's CBD during the Canterbury earthquakes. This information is important for performance based earthquake engineering in that advanced numerical soil-structure interaction analyses can be performed, which often rely on laboratory test data to calibrate constitutive models.

5.2 FINDINGS

Engineers often rely on the capabilities of 1D seismic site response analyses, especially nonlinear effective stress analyses, to model the response of liquefiable sites during strong shaking. The results of these analyses are greatly dependent on the selection of input ground motions, the soil properties used in the modeling process, the model used to track the generation of excess pore water pressure, and the constitutive relationships used to model the stress-strain response of the soil during dynamic loading. Site response analyses were completed for several strong motions station sites in Christchurch, NZ for a selection of the large shaking events of the 2010-11 Canterbury earthquake sequence using the procedures outlined in Chapter 2. The following key findings were a result of this work:

- The CBD and most of the greater Christchurch area is located in a deep basin structure within the Canterbury Plains that has over 500 m of sediment and a depth to "basement" rock of over 2 km below the ground surface in some areas. This deep basin structure makes it difficult to locate a half-space with a shear wave velocity close to engineering bedrock (or B/C rock boundary of V_s=760 m/s). Furthermore, characterizing the soil to a depth of bedrock is difficult as in-situ investigations rarely extend to these depths.
- A strong motion station located within the Lyttleton Port (LPCC station) has a V_{s30} of approximately 792 m/s, making it an outcropping "rock" motion; however, the LPCC station is located on the southern side of the Port Hills, which are part of an extinct volcanic complex. Christchurch is located on the northern side of the Port Hills. The location of LPCC with respect to the locations of the events of interest and seismic energy propagation from these events, as well as the fact that it is located on the hanging wall as opposed to the footwall (Christchurch is located on the footwall) for several events, make the recordings from this station non-ideal as input motions for seismic site response analyses in the Christchurch area for the Canterbury earthquakes. Furthermore, for the reasons highlighted above, locating a proper half-space to place input "rock" motions is difficult.
- Due to the lack of representative "rock" input motions, as well as the difficulty in characterizing the subsurface soils that make up the deep basin structure beneath Christchurch, deconvolution of recorded surface motions was completed at two stiff soil sites to generate input motions for site response analyses. The two sites used for deconvolution were the Canterbury Aero Club (CACS) and the Riccarton High School (RHSC) strong motion station sites.
- The relative stiffness of the Riccarton Gravel compared to the overlying, softer materials located just below the ground surface for much of Christchurch make it an ideal half-space for both deconvolution and subsequent convolution analyses. The Riccaron Gravel formation is located at a depth of 10 to 40 m beneath the ground surface for most of Christchurch.
- The empirically based shear modulus reduction (G/G_{max}) and material damping (λ) curve correlations developed by Darendeli (2001) were used to represent the strain dependent properties of the modeled soil. This relationship tended to underestimate the assumed shear strength for the studied soils at large strains. The procedure outlined by Yee et al.

(2013) was used to correct the large strain stiffness of the soil to better represent the shear strength.

- The seismic site response program *DeepSoil* was able to represent the corrected modulus reduction and damping curves through its implementation of the MRDF-UIUC pressure dependent, hyperbolic fitting procedure proposed by Phillips and Hashash (2009). The fitted curves were used for total stress and effective stress nonlinear analyses.
- Effective stress site response analyses carried out using the 1D site response analysis program *DeepSoil* were able to capture the generation of excess pore water pressure during strong shaking in critical layers, which generally agreed with the results of empirical CPT-based liquefaction triggering procedures. These analyses relied on the pore pressure generation model originally proposed by Dobry et al. (1985) and the modified MKZ hyperbolic model developed by Matasovic and Vucetic (1993a,b) to represent the stress-strain response of the modelled soil.
- Similar results with regards to the comparison of pseudo-acceleration response spectra for calculated surface motions from site response analyses completed using nonlinear total stress and nonlinear effective stress analyses were often observed, even for cases where substantial excess pore water pressures were indicated within a given 1D soil column for effective stress analyses.
- The uncertainties introduced by using input motions from the deconvolution procedure resulted in some consistent biases in the results of analyses. One of the noticeable biases was a consistent underestimation of the spectral accelerations at a period range of 1~6 s for analyses completed in the fault normal direction at multiple strong motion station sites that used input motions from deconvolution at the CACS site for the 04 SEP 2010 M_w7.1 Darfield event. This was most likely due to the inability of input motions from the CACS site to replicate the forward directivity effects or basin response experienced at sites, especially in the eastern part of Christchurch. This underestimation of spectral acceleration values in the longer period range was much less pronounced for analyses that used input motions from deconvolution at the RHSC station, which indicates these input motions were better at capturing the near-fault pulses experienced at several sites for the Darfield event.
- Overall, reasonable trends in the calculated seismic response were observed for nonlinear effective stress seismic site response analyses completed at both sites that did and did not liquefy during the Canterbury events; however, nonlinear total stress and equivalent linear analyses often resulted in reasonable trends as well when response spectra of calculated surface motions were compared to recorded motions' response spectra. This similarity in response spectra of calculated surface motions for analyses could be due to the constitutive model employed in the different analyses and the representation of material damping—i.e., the stress-strain model (and calculated material damping) employed in effective stress analyses using *DEEPSOIL* does not always produce an appreciable difference in calculated soil response when comparing the response spectra of calculated surface motions from nonlinear effective stress analyses to nonlinear total stress and equivalent linear analyses, even when large excess pore water pressures are indicated. Though similar response spectra were often calculated for the different analysis types, the added benefit of effective stress analyses is the ability to model the potential generation of excess pore water pressure in critical soil layers during dynamic loading.

Understanding the effects of liquefaction on buildings often relies on the use of analyses to model the complex interaction of buildings and their foundation systems with the ground that supports them. Consequently, understanding the response of the shallow soils that make up this foundation material, especially in cyclic loading, is an important step in the analysis process. The site investigation and laboratory testing program that was completed to characterize soils crucial to the performance of buildings in the Christchurch CBD during the Canterbury earthquakes, especially with regards to damage caused by liquefaction of foundation soils, resulted in the following key findings:

- The Dames and Moore (D&M) Osterberg-type hydraulic fixed-piston sampler was able to retrieve relatively "undisturbed" samples of medium-dense sands, silty sands, and silts. Very loose and loose sands were densified during the sampling and specimen preparation process. Based on CPT data that was obtained adjacent to the boreholes used for "undisturbed" sampling in previous investigations, it was found that soils with a normalized tip resistance less than 60 ($q_{c1N}<60$) and a relative density less than approximately 50% ($D_r<50\%$) were too loose to be sampled and tested via the procedures used in this study.
- As the Lunne et al. (1997) procedure for assessing specimen/sample disturbance was developed for plastic clays, it was not used to assess disturbance levels of the nonplastic to slightly plastic silty sands and sands sampled in this study. Instead, visual inspection of extruded and tested soil specimens, comparisons of field and laboratory based shear wave velocity measurements of tested specimens, comparisons of laboratory D_r to D_r values estimated using CPT-based correlations, and comparisons between laboratory and field estimated CRR values were all used in assessing disturbance levels.
- Consistent cyclic resistance ratio (CRR) curves could be developed for soil units on a site-by-site basis, and by compiling CTX results across several sites in the CBD for three main soil types (defined using the Unified Soil Classification System): ML, SM, and SP/SP-SM, generalized CRR curves could also be developed for the soils of the Christchurch CBD..
- Two CRR curves were used to represent the tested "undisturbed" sand specimens (SP and SP-SM): one corresponding to sands with $60<q_{c1N}<100$ and one corresponding to sands with $100<q_{c1N}<140$ (the latter curve representing a higher cyclic resistance). An examination of the CSR to reach 3% S.A. ε_{ax} for sand specimens with $q_{c1N}<60$ often indicated a higher liquefaction resistance (sometimes significantly higher) than sands specimens with $60<q_{c1N}<140$; furthermore, a similar trend in the CSR vs. $N_{c\text{-}3\%\ S.A.\ \varepsilon ax}$ was not realized for these loose sands as was observed with the medium-dense sands (i.e., a reasonable power function regression could not be completed to fit the data). These observations indicated that the loose SP and SP-SM soils were disturbed.
- After correcting CSR_{CTX} values to CSR_{Field} values based on assumed C_r' values of 0.57, 0.6, and 0.66 for sands, silty sands, and silts, respectively, the implied CRR_{Field} curves for ML and SM soils indicated similar to slightly higher liquefaction resistance for these finer materials compared to the tested sands. However, the slope of the interpreted CRR curve for the silts was flatter than the silty sands and sands.
- Comparisons of $CRR_{M7.5,\ 1atm}$ versus q_{c1N} implied via triaxial testing (where $N_{c\text{-}3\%\ S.A.\ \varepsilon ax}=15$ was used to represent a M7.5 event) to $CRR_{M7.5,\ 1atm}$ versus q_{c1N} from the

Boulanger and Idriss (2015) CPT-based liquefaction triggering procedure (for P_L=50%) for several soil units tested in the CBD showed relatively good agreement.

- Results of individual CTX tests of "undisturbed" specimens of SM soils showed very similar stress-strain and pore water pressure response when compared to sand (SP and SP-SM) specimen results.
- A single steady state line using the equation proposed by Bolton (1986) in $D_{r\text{-}ss}$ vs. p'_{ss} (where $D_{r\text{-}ss}$ is the relative density at steady state and p'_{ss} is the mean effective stress at steady state) was able to be fitted to the results from testing sands from multiple sites in the CBD.
- The functional representation of the steady state line proposed by Cubrinovski and Ishihara (2000) was able to be fitted to results from individually tested soil units in e_{ss} vs. p'_{ss} space (where e_{ss} is the void ratio at steady state).

5.3 FUTURE RESEARCH

The selection of input motions is often a large source of uncertainty for engineers when conducting site response analyses. This uncertainty is accentuated in Christchurch by the deep basin structure that underlies much of Christchurch and the lack of "rock" motions on the northern side of the Port Hills in areas of interest (e.g., the CBD). Deconvolution of surface motions at stiff soil sites was completed using the Riccarton Gravel layer as a half-space to generate input motions for site response analyses completed as a part of the presented research. The installation of at least one down-hole array in Christchurch that extends to the Riccarton Gravel would be advantageous so that accelerometers can be installed to measure accelerations during future shaking events at various depths within the subsurface, including at the top of the Riccarton Gravel. Acceleration records from the down-hole array could then be used to provide input motions for future site response analyses as well as assist in the calibration and verification of site response analyses (especially with the additional installation of piezometers to measure pore pressures during future events). The generation of synthetic "rock" or "Riccarton Gravel" motions for Christchurch would be another means of creating representative input motions for site response analyses.

The results presented in Section 2.6 compare response spectra obtained from 1D nonlinear effective stress site response analyses using *DEEPSOIL* and *FLAC* (using PM4Sand) for the Christchurch Botanical Gardens (CBGS) strong motion station site for the 22 FEB 2011 M_w6.2 Christchurch earthquake. As stated, a more exhaustive study should be completed to better analyze the differences (and underlying reasons for these differences) in results between these two procedures. It was observed that in terms of spectral acceleration values of the calculated surface motions, the FLAC analysis was superior in matching the recorded response spectrum for the presented analyses at the CBGS site for the Christchurch event in the fault normal direction. Further research should be conducted to see whether this superior fit is consistent for other sites and events. Also, effective stress site response analyses could be completed using additional constitutive models and numerical procedures (e.g., finite-element) for the sites and events analyzed in this study to provide a more comprehensive dataset for comparing different analytical procedures.

The presented research that characterizes the liquefaction resistance of critical soil layers in the CBD of Christchurch relied on assumed values of C_r to correct CRR_{CTX} values to CRR_{Field}

values. As CRR_{Field} values are ultimately used to characterize a soil unit's liquefaction resistance during seismic shaking, a more rigorous assessment is needed to estimate correct values of C_r for the various soil types examined. This work would require the use of cyclic simple shear or cyclic torsional shear testing to compare values of $CRR_{Ko\neq1}$ to $CRR_{Ko=1}$ (or CSR_{CTX}). Furthermore, as cyclic simple shear testing applies a horizontal load during shearing as opposed to the vertical deviatoric load applied in CTX testing, it better simulates the loading regime that a soil element would undergo during seismic loading (i.e., vertically propagating horizontal shear waves). For these reasons, it would be very useful to conduct simple shear tests on "undisturbed" soil specimens from all or a selection of the sites presented in this study to both allow for comparisons with the CTX test results from this study and provide further characterization of the case histories of buildings founded on liquefiable soils in the Christchurch CBD.

There is a need to better understand the complex soil-structure interaction problem of buildings founded on liquefiable soils during strong shaking events. Advanced numerical analyses with well calibrated constitutive models have the potential to accurately model case histories of buildings damaged during earthquakes due to both volumetric and shear-induced settlements caused by the liquefaction of shallow foundation soils. Proper characterization and documentation of both affected buildings and subsurface soils is necessary to make these case histories and related analyses as useful as possible to engineers and researchers. The data and insights provided by the presented research coupled with the work of previous researchers regarding the effects of liquefaction on buildings during the 2010-11 Canterbury events (e.g., Cubrinovski et al. 2011a, Bray et al. 2014, and Zupan 2014) document important details of valuable case histories. The natural progression of this work is the completion of numerical-based analyses to model these well-documented cases and provide a means for the variation of soil and structural parameters within these verified analyses to develop useful tools for practicing engineers (e.g., simplified procedures that use a set of key soil and structural-based input parameters).

REFERENCES

ASTM D2487-11, 2011: Standard Practice for Classification of Soils for Engineering Purposes (Unified Soil Classification System), *Annual Book of ASTM Standards*, ASTM International, West Conshohocken, PA.

ASTM D6519-08, 2008: Standard Practice for Sampling of Soil Using the Hydraulically Operated Stationary Piston Sampler, *Annual Book of ASTM Standards,* ASTM International, West Conshohocken, PA.

Baldi, G., Bellotti, R., Ghionna, N., Jamiolkowski, M., and Pasqualini, E. (1986). Interpretation of CPT's and CPTU's, 2nd part, drained penetration of sands. In 4th International Geotechnical Seminar, Singapore.

Beyzaei, C.Z., Bray, J.D., Cubrinovski, M.C, Riemer, Stringer, M.E., Jacka, M.E., and Wentz, R. 2015. Liquefaction resistance of silty soils at the Riccarton Road site, Christchurch, New Zealand. 6th Inter. Conf. on Earthquake Geotechnical Engineering, 6ICEGE, 1-4 November, Christchurch, New Zealand.

Bolton, M. D. (1986). "The strength and dilatancy of sands." *Géotechnique*, 36, No. 1, pp. 65-78.

Boulanger R.W., Meyers M.W., Mejia L.H. and Idriss I.M. (1998). "Behavior of a fine-grained soil during the Loma Prieta earthquake." Canadian Geotechnical Journal, 35, 146-158.

Boulanger RW, Ziotopoulou K. (2012) PM4Sand (Version 2): A sand plasticity model for earthquake engineering applications. Report no. UCD/CGM-12/01, center for Geotechnical Modeling, Department of Civil and Environmental Engineering, University of California, Davis, CA; 2012, 100 pp.

Boulanger, R. W., and Idriss, I. M. (2014). CPT and SPT based liquefaction triggering procedures, Report No. UCD/CGM-14/01, Center for Geotechnical Modeling, Department of Civil and Environmental Engineering, University of California, Davis, CA, 134 pp.

Boulanger, R. and Idriss, I. (2015). "CPT-Based Liquefaction Triggering Procedure." J. Geotech. Geoenviron. Eng., 10.1061/(ASCE)GT.1943-5606.0001388 , 04015065.

Bradley B.A. and Cubrinovski M. (2011). "Near-source strong ground motions observed in the 22 February 2011 Christchurch earthquake." Bulletin of the New Zealand Society for Earthquake Engineering. Vol. 44, No. 4, December 2011.

Bradley, B.A., Quigley, M.C., Van Dissen, R.J., Litchfield, N.J. (2014). "Ground Motion and Seismic Sources Aspects of the Canterbury Earthquake Sequence." Earthquake Spectra. Preprint.

Bradley, B.A. (2013). "A New Zealand-Specific Pseudospectral Acceleration Ground-Motion Prediction Equation for Active Shallow Crustal Earthquakes Based on Foreign Models." Bulletin of the Seismological Society of America. Vol. 103, No. 3, pp. 1801-1822, June 2013.

Bray, J.D., Cubrinovski, M., Zupan, J., and Taylor, M. (2014). Liquefaction Effects on Buildings in the Central Business District of Christchurch. *Earthquake Spectra,* February 2014, Vol. 30, No. 1, pp. 85-109.

Bray, J., Rollins, K., Hutchinson, T., Verdugo, R. Ledezma, C., Mylonakis, G., Assimaki, D., Montalva, G., Arduino, P., Olson, S.M., Kayen, R., Hashash, Y.M.A., and Candia, G. (2012) Effects of Ground Failure on Buildings, Ports, and Industrial Facilities. Earthquake Spectra: June 2012, Vol. 28, No. S1, pp. S97-S118.

Bray, J.D., Sancio, R.B. (2006). Assessment of the Liquefaction Susceptibility of Fine-Grained Soils. J. of Geotech. Geoenviron. Eng., ASCE, Vol. 132, No. 9, pp. 1165-1177.

Brown, L.J., Beetham, R.D., Paterson, B.R., and Weeber, J.H. (1995). "Geology of Christchurch, New Zealand: Environmental and Engineering Geoscience." 1, 427–488.

Brown, L.J. and Weeber, J.H. (1992). "Geology of the Christchurch Urban Area." Scale 1:25000. Institute of Geological and Nuclear Sciences geological map 1.

Brown, L.J., and Wilson, D.D. (1988). "Stratigraphy of late Quaternary deposits of the northern Canterbury Plains, New Zealand." New Zealand Journal of Geology and Geophysics 31: 305–335.

Browne, G.H., and Naish, T.R. (2003). "Facies development and sequence architecture of a Late Quaternary fluvial-marine transition, Canterbury Plains and shelf, New Zealand: implications for forced regressive deposits." Sedimentary Geology 158: 57–86.

Canterbury Geotechnical Database (2013) "Liquefaction Interpreted from Aerial Photography", Map Layer CGD0200 - 11 Feb 2013, retrieved [23 Jan 2015] from https://canterburygeotechnicaldatabase.projectorbit.com/

Canterbury Geotechnical Database (2013). Site Investigation Data. Website accessed June 2014: https://canterburygeotechnicaldatabase.projectorbit.com.

Canterbury Geotechnical Database (2013). "EQC Event Specific Groundwater Surface Elevations." Map Layer CGD0800. 06 Sep 2014. Retrieved 23 Jan 2015 from https://canterburygeotechnicaldatabase.projectorbit.com/

Carlton, B. (2014). "An Improved Description of the Seismic Response of Sites with High Plasticity Soils, Organic Clays, and Deep Soft Soil Deposits." PhD Thesis. University of California, Berkeley.

Chiara, N. and Stokoe, K. H. II. (2006). Sample disturbance in resonant column test measurement of small-strain shear wave velocity. Soil Stress-Strain Behavior: Measurement, Modeling and Analysis Geotechnical Symposium. Roma, 2006. Hoe I. Ling et al. (eds.). pp. 605-613.

Cubrinovski, M., Bray, J.D., Taylor, M., Giorgini, S., Bradley, B., Wotherspoon, L., and Zupan, J. (2011a). Soil Liquefaction Effects in the Central Business District during the February 2011 Christchurch Earthquake. *Seismological Research Letters*, 82(6), 893-904.

Cubrinovski, M., Green, R.A., Wotherspoon, L., [Eds] (2011b). Geotechnical Reconnaissance of the 2011 Christchurch Earthquake. *Technical Report*. Retrieved from: http://geerassociation.org/GEER_Post%20EQ%20Reports/Christchurch_2011/Index_Christchurch_2011.html.

Cubrinovski, M., Bradley, B., Wotherspoon, L., Green, R., Bray, J., Wood, C., Pender, M., Allen, J., Bradshaw, A., Rix, G., Taylor, M., Robinson, K., Henderson, D., Giorgini, S., Ma, K., Winkley, A., Zupan, J., O'Rourke, T., DePascale, G. and Wells, D. (2011c). Geotechnical Aspects of the 22 February 2011 Christchurch earthquake. *Bulletin of the New Zealand Society of Earthquake Engineering*, 44(4), 205-226.

Cubrinosvski, M. and Ishihara, K. (2000). "Flow potential of sandy soils with different grain compositions." Soils and Foundations, 40(4):103-119.

Cubrinovski, M. and Ishihara, K. (2002). "Maximum and minimum void ratio characteristics of sands." Soils and Foundations, 42(6):65–78.

Cubrinovski, M. and Taylor, M. (2011). "Liquefaction map of Christchurch based on drivethrough reconnaissance after the 22 February 2011 earthquake." University of Canterbury.

Dafalias, Y.F., and Manzari, M. T. (2004). “Simple plasticity sand model accounting for fabric change effects.” Journal of Engineering Mechanics, ASCE, 130(6), 622-634.

Darendeli, M. B. (2001). "Development of a new family of normalized modulus reduction and material damping curves," Ph. D., University of Texas at Austin, Austin, Texas.

Dobry, R., Pierce, W. G., Dyvik, R., Thomas, G. E., and Ladd, R. S. (1985). "Pore pressure model for cyclic straining of sand." Rensselaer Polytechnic Institute, Troy, New York.

Forsyth, P.J., Barrell, D.J.A., and Jongens, R. (compilers). (2008). “Geology of the Christchurch area.” Institute of Geological & Nuclear Sciences 1:250 000 geological map 16. 1 sheet + 67 p. Lower Hutt, New Zealand. GNS Science.

GeoNet database of processed strong motion records for New Zealand. Accessed June 2014: ftp://ftp.geonet.org.nz/strong/processed/Proc

Germaine, J.T. and Ladd, C.C. (1988). “Triaxial testing of saturated cohesive soils.” Advanced Triaxial Testing of Soil and Rock, ASTM STP 977, R. T. Donaghe, R.C. Chaney, and M. L. Silver, Eds. Amer. Soc. for Testing and Materials, Philadelphia, 1988. pp. 421-459.

Ghionna, V. and Porcino, D. (2006). Liquefaction Resistance of Undisturbed and Reconstituted Samples of a Natural Coarse Sand from Undrained Cyclic Triaxial Tests. J. Geotech. Geoenviron. Eng., 132(2), 194–202.

Gingery, J.R., Elgamal, A., and Bray, J.D. (2014) “Response Spectra at Liquefaction Sites during Shallow Crustal Earthquakes.” Earthquake Spectra, In-Press, http://dx.doi.org/10.1193/101813EQS272M.

Green, R.A., and Cubrinovski, M. [Eds] (2010). Geotechnical Reconnaissance of the 2010 Darfield (New Zealand) Earthquake. Technical Report. Retrieved from http://geerassociation.org/GEER_Post%20EQ%20Reports/Christchurch_2011/Index_Christchurch_2011.html.

Hashash, Y.M.A. (2012). “DEEPSOIL V5.1, User Manual and Tutorial 2002-2012.” Department of Civil and Environmental Engineering, University of Illinois at Urbana-Champaign.

Hashash, Y.M.A., Groholski, D.R. Phillips, C.A., (2010). “Recent advances in non-linear site response analysis.” In proceedings of Fifth International Conference on Recent Advances in Geotechnical Earthquake Engineering and Soil Dynamics, May 24-29, San Diego, CA.

Hayden, C., Bray, J., and Abrahamson, N. (2014). "Selection of Near-Fault Pulse Motions." J. Geotech. Geoenviron. Eng., 10.1061/(ASCE)GT.1943-5606.0001129, 04014030.

Hayden, C. P. (2014). “Liquefaction-Induced Building Performance and Near-Fault Ground Motions.” PhD dissertation. University of California, Berkeley.

Hicks, S.R. (1989). “Structure of the Canterbury Plains, New Zealand from gravity modelling. “ Geophysics Division, Department of Science and Industrial Research: Wellington.

Hvorslev, M. J. (1949). Subsurface exploration and sampling of soils for civil engineering purposes. Waterways Experiment Station, Vicksburg, Miss.

Idriss, I. M. (1999). “An update to the Seed-Idriss simplified procedure for evaluating liquefaction potential,” in Proceedings, TRB Workshop on New Approaches to Liquefaction. No. FHWA-RD-99-165, Federal Highway Administration, January.

Idriss, I.M. and Akky, M.R. (1979). “Primary Variables Influencing Generation of Earthquake Ground Motions by a Deconvolution Process.” Paper K 1/3. Proceedings of the 5th Annual SMiRT Conference, August 1979.

Idriss, I. M. and Boulanger, R. W. (2008). Soil Liquefaction During Earthquakes. EERIMNO-12. Earthquake Engineering Research Institute, Oakland, CA.

Idriss, I. M., and Sun, J. I. (1992). "SHAKE91: A computer program for conducting equivalent linear seismic response analyses of horizontally layered soil deposits." Department of Civil and Environmental Engineering, University of California Davis.

Ishihara, K., Yamazaki, H., and Haga, K. (1985). "Liquefaction of k0-consolidated sand under cyclic rotation of principal stress direction with lateral constraint." Soils and Foundations, 25(4):63–74.

Itasca (2009). Flac – Fast Lagrangian Analysis of Continua, Version 6.0, Itasca Consulting Group, Inc., Minneapolis, Minnestota.

Jamiolkowski, M., Lo Presti, D., and Manaserro, M. (2001). Evaluation of the relative density and shear strength of sands from CPT and DMT. Soil Behavior and Soft Ground Construction, GSP 119, pages 201–238, Reston, Virginia. ASCE. via Mayne, P.W. 2014. Interpretation of geotechnical parameters from seismic piezocone tests. CPT 2014. Paper No. KN-2.

Kaiser, A., C Holden, J Beavan, D Beetham, R Benites, A Celentano, D Collett, J Cousins, M Cubrinovski, G Dellow, P Denys, E Fielding, B Fry, M Gerstenberger, R Langridge, C Massey, M Motagh, N Pondard, G McVerry, J Ristau, M Stirling, J Thomas, SR Uma & J Zhao (2012)."The Mw 6.2 Christchurch earthquake of February 2011: preliminary report." New Zealand Journal of Geology and Geophysics, 55:1, 67-90.

Kam, W.Y., Pampanin, S., and Elwood, K. (2011). Seismic performance of reinforced concrete buildings in the 22 February Christchurch (Lyttelton) Earhtquake. B. NZEE, V. 44(4), 239-278.

Kramer, S.L., Hartvigsen, A.J., Sideras, S.S., Ozener, P.T. (2011). "Site response modeling in liquefiable soil deposits," 4th IASPEI / IAEE International Symposium, Effects of Surface Geology on Seismic Motions, Santa Barbara, California.

Kramer, S. L. (1996). Geotechnical Earthquake Engineering. Prentice Hall, Upper Saddle River, N.J.

Kulhawy, F.H., and Mayne, P.H. (1990). "Manual on estimating soil properties for foundation design." Report EL-6800 Electric Power Research Institute, EPRI, August 1990.

Ladd, R.S. (1978). "Preparing test specimens using undercompaction." Geotechnical Testing Journal, GTJODJ, Vol. 1, No. 1, March 1978, pp. 16-23.

Li, X.S., Chan C.K., and Shen C.K. (1988). An automated triaxial testing system. In Advanced Triaxial Testing of Soil and Rock; American Society for Testing and Materials, Philadelphia, 95-106.

Lunne, T., Berre, T., Strandvik, S. (1997). Sample disturbance in soft low plastic Norwegian clay. Recent Developments in Soil and Pavement Mechanics, Almedia, Ed., Balkema, Rotterdam, pp. 81-102.

Manzari, M.T., and Dafalias, Y. F. (1997). "A critical state two-surface plasticity model for sand." Geotechnique, 47(2), 255-272.

Matasovic, N. and Ordóñez, G.A. (2012). "D-MOD2000 – A Computer Program for Seismic Site Response Analysis of Horizontally Layered Soil Deposits, Earthfill Dams, and Solid Waste Landfills." GeoMotions, LLC; Lacey, Washington, USA.

Matasovic, N. and Vucetic, M. (1993a). "Seismic response of composite horizontally-layered soil deposits," Research Report, Civil Engineering Dept. Univ. of California, Los Angeles, CA, March.

Matasovic, N., and Vucetic, M. (1993b). "Cyclic Characterization of Liquefiable Sands." ASCE Journal of Geotechnical and Geoenvironmental Engineering, 119(11), 1805-1822.

McGann, C., Bradley, B., Taylor, M., Wotherspoon, L., and Cubrinovski, M. (2014). "Development of an empirical correlation for predicting shear wave velocity of Christchurch soils from cone penetration test data." Soil Dynamics and Earthquake Engineering, 00(0), 15–27.

Minimum Design Loads for Buildings and Other Structures. ASCE 7-10.

Ordonez, G. (2000) "SHAKE2000," commercial software for performing seismic site response analysis.

Pacific Earthquake Engineering Research Center, "PEER Ground Motion Database." Website accessed on June 2014. http://peer.berkeley.edu/nga/

Phillips, C., and Hashash, Y. M. (2009). "Damping formulation for nonlinear 1D site response analyses." Soil Dynamics and Earthquake Engineering, 29(7), 1143–1158.

Ristau, J. 2008. "Implementation of routine regional moment tensor analysis in New Zealand." Seismological research letters, 79(3): 400-415.

Robertson, P.K. (2010). Estimating in-situ state parameter and friction angle in sandy soils from the CPT. *2nd International Symposium on Cone Penetration Testing*, CPT'10, Huntington Beach, CA, USA.

Robertson, P.K. and Wride, C.E. (1998). "Evaluating cyclic liquefaction potential using the cone penetration test." Can. Geotech. J., 35, 442-459.

Robinson, K., Cubrinovski, M., Bradley, B.A. (2013). "Sensitivity of predicted liquefaction-induced lateral displacements from the 2010 Darfield and 2011 Christchurch Earthquakes." 2013 NZSEE Conference.

Sancio, R. B. (2003). "Ground failure and building performance in Adapazari, Turkey." PhD Thesis. University of California, Berkeley.

Salgado, R., Mitchell, J., and Jamiolkowski, M. (1997). Cavity expansion and penetration resistance of sand. Journal of Geotechnical and Geoenvironmental Engineering, 123(4):344–354.

Seed, H.B. (1979). "Soil Liquefaction and cyclic mobility evaluation for level ground during earthquakes," J. Geotech. Eng. Div., ASCE 105(GT2), 201-55.

SeismoSignal. Version 5.1.0. Build 200. SeismoSoft.

Silva, W. J., (1988). "Soil response to earthquake ground motion", EPRI Report NP-5747, Electric Power Research Institute, Palo Alto, California.

Taylor M.L, Cubrinovski M., and Haycock, I. (2012a). Application of new 'Gel push' sampling procedure to obtain high quality laboratory test data for advanced geotechnical analyses. *2012 New Zealand Society for Earthquake Engineering Conference*. Christchurch, New Zealand, NZSEE.

Taylor, M. L., Cubrinovski, M., and Bradley, B. A. (2012b). Characterisation of ground conditions in the Christchurch Central Business District. Australian Geomechanics Journal, 47(4), 43–57.

Taylor, M. L. (2015). "The geotechnical characterisation of Christchurch Sands for Advanced Soil Modelling." PhD thesis. University of Canterbury.

Tokimatsu, K., Tamura, S., Suzuki, H., and Katsumata, K. (2012). "Building damage associated with geotechnical problems in the 2011 Tohoku Pacific Earthquake." Soils and Foundations, 52(5). 956-974.

Vucetic, M., and Dobry, R. (1988). "Cyclic triaxial strain controlled testing of liquefiable sands." Advanced Triaxial Testing of Soil and Rock, ASTM STP 977, American Society for Testing and Materials, Philadelphia, 475-485.

Wood, C.M., Cox, B.R., Wotherspoon, L.M. & Green, R.A. (2011) "Dynamic site characterization of Christchurch strong motion stations" Bulletin of the NZSEE, 44(4): 195-204.

Wotherspoon, L.M., Orense, R.P., Bradley, B.A., Cox, B.R., Wood, C.M. & Green, R.A. (2013). "Geotechnical characterisation of Christchurch strong motion stations." Earthquake Commission Biennial Grant Report, Project No. 12/629; 2013.

Yee, E., Stewart J.P., Tokimatsu K. (2013). "Elastic and Large-Strain Nonlinear Seismic Site Response from Analysis of Vertical Array Recordings." J. Geotech. Geoenviron. Eng.139(10).

Youd, T.L. and Carter, B.L. (2005). "Influence of soil softening and liquefaction on spectral acceleration," J. Geotechnical and Geoenvironmental Engineering, ASCE, 131(7).

Zehgal, M. and Elgamal, A. (1994). "Analysis of site liquefaction using earthquake records," J. Geotech. and Geoenvr. Engr., ASCE, 120(6), pp. 996-1017.

Zupan, J. (2014). Seismic Performance of Buildings Subjected to Soil Liquefaction. PhD Thesis. University of California, Berkeley.

Appendix A

Supporting Data and Information for Site Response Analyses

Appendix A.1

Recorded Motions at CBD Strong Motion Stations used in Site Response Analyses

Recorded surface motions for the following events are included as separate electronic files attached to this dissertation (original sources for these processed ground motions are listed as well):

- 04 SEP 2010 M_w7.1 (PEER)
- 22 FEB 2011 M_w6.2 (PEER)
- 13 JUN 2011 M_w6.0 (GeoNet)
- 23 DEC 2011 M_w5.8 (GeoNet)
- 23 DEC 2011 M_w5.9 (GeoNet)
- 26 DEC 2010 M_w4.7 (GeoNet)

Appendix A.2

Strong Motion Station Site Characterization Data

A.2.1 CPT Profiles

A.2.2 Shear Wave Velocity Profiles

Appendix A.2.1

CPT Profiles at Strong Motion Station Sites

CPT: CBGS_CPT1(Wotherspoon,2013)

Total depth: 21.60 m

Project: **Evaluating Fully Nonlinear Effective Stress Site Resonse Computer Programs using Records from the Canterbury Earthquake Sequence**

Coords: S 43.5293, E 172.6198

Location: **Christchurch, New Zealand**

Cone Operator: Uknown

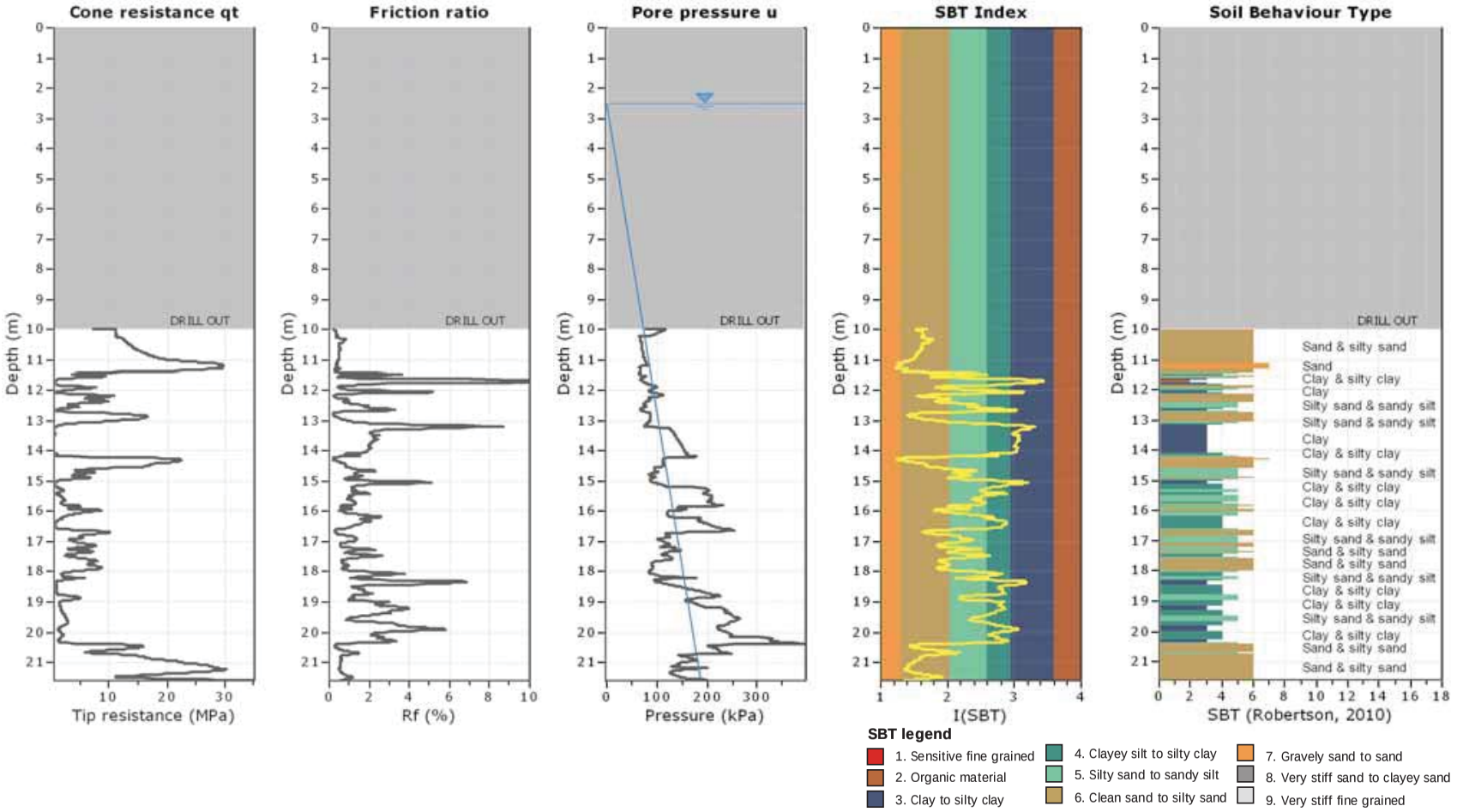

CPeT-IT v.1.7.6.42 - CPTU data presentation & interpretation software - Report created on: 21/08/2014, 01:30:58 a.m.

Project file: C:\Users\User\Desktop\summer\USGS Site Response Project\Soil Profiles and Info\CBGS\Site Investigation Data\CBGS CPT\test_2.cpt

CPT: CBGS_CPT1(Wotherspoon,2013)

Total depth: 21.60 m, Date: 07/07/2014

Coords: S 43.5293, E 172.6198

Cone Operator: Uknown

Project: **Evaluating Fully Nonlinear Effective Stress Site Resonse Computer Programs using Records from the Canterbury Earthquake Sequence**

Location: **Christchurch, New Zealand**

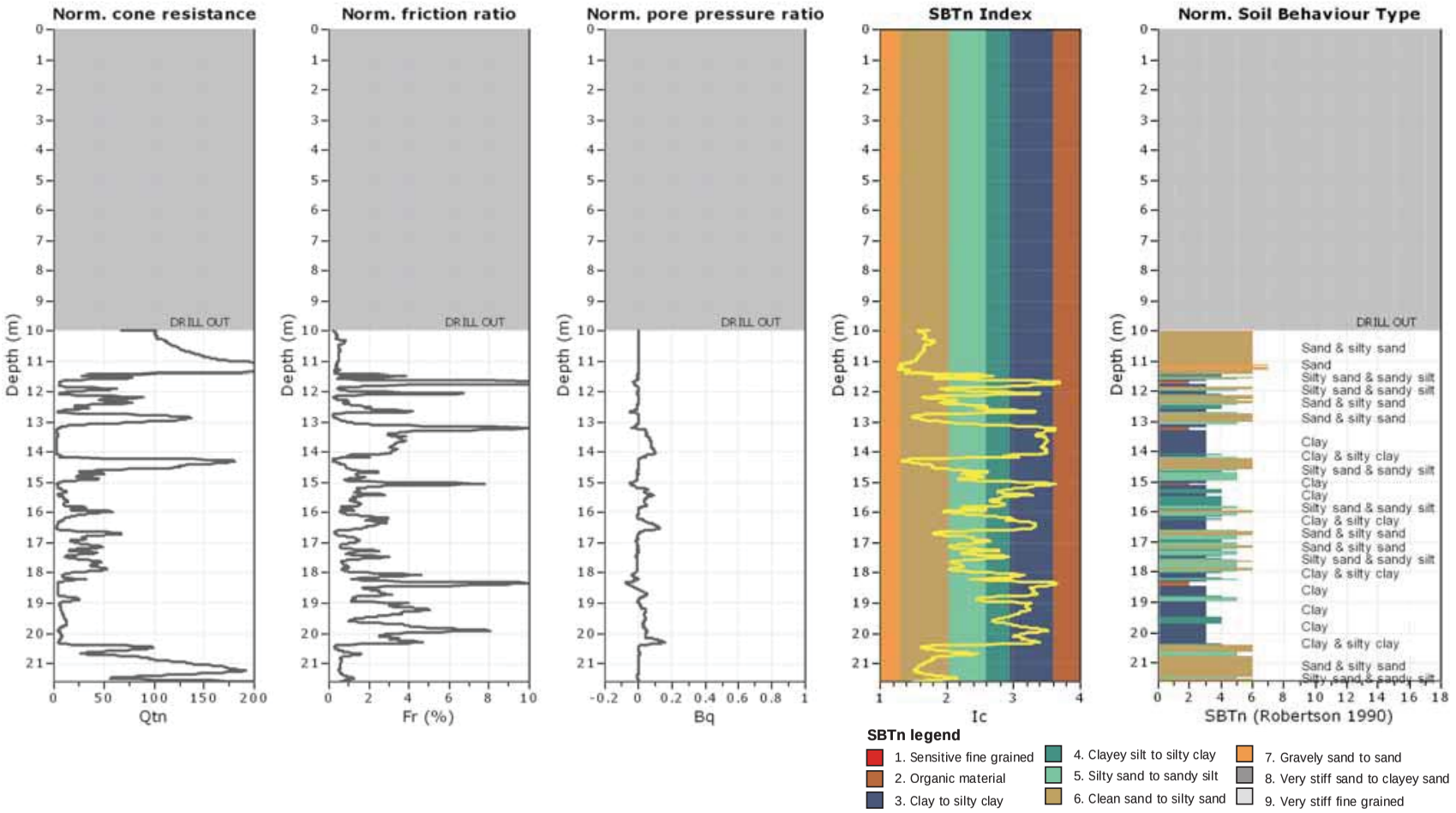

CPeT-IT v.1.7.6.42 - CPTU data presentation & interpretation software - Report created on: 21/08/2014, 01:30:58 a.m.

Project file: C:\Users\User\Desktop\summer\USGS Site Response Project\Soil Profiles and Info\CBGS\Site Investigation Data\CBGS CPT\test_2.cpt

CPT: CCCC_CPT484(CGD)

Total depth: 25.11 m

Project: **Evaluating Fully Nonlinear Effective Stress Site Resonse Computer Programs using Records from the Canterbury Earthquake Sequence**

Coords: S 43.5379, E 172.6479

Location: **Christchurch, New Zealand**

Cone Operator: Uknown

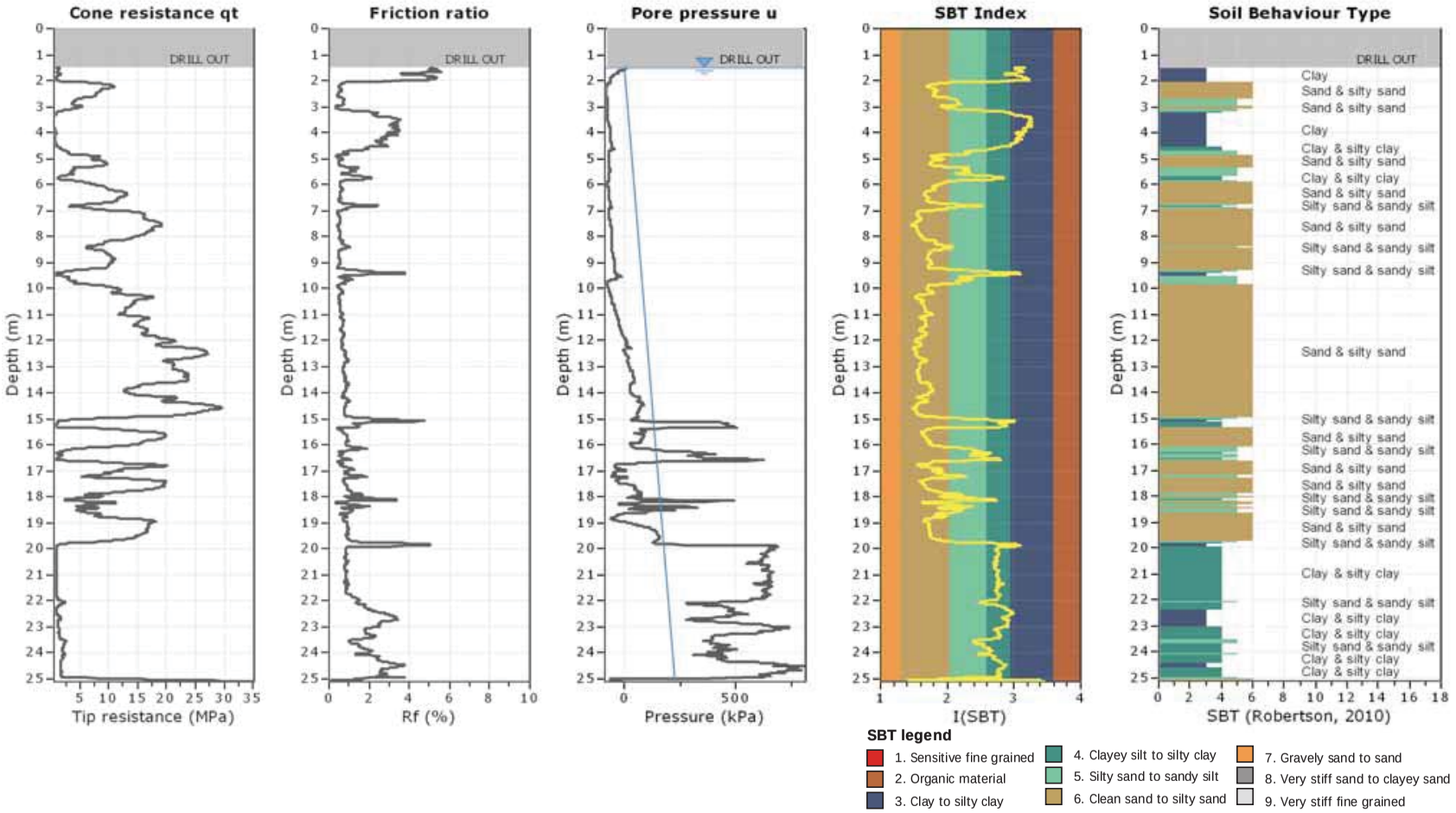

CPeT-IT v.1.7.6.42 - CPTU data presentation & interpretation software - Report created on: 21/08/2014, 11:04:56 a.m.

Project file: C:\Users\User\Desktop\summer\USGS Site Response Project\Soil Profiles and Info\CCCC\Proceced Data\CPT_484\cpt_484_2.cpt

CPT: CCCC_CPT484(CGD)

Total depth: 25.11 m, Date: 05/07/2014

Coords: S 43.5379, E 172.6479

Cone Operator: Uknown

Project: **Evaluating Fully Nonlinear Effective Stress Site Resonse Computer Programs using Records from the Canterbury Earthquake Sequence**

Location: **Christchurch, New Zealand**

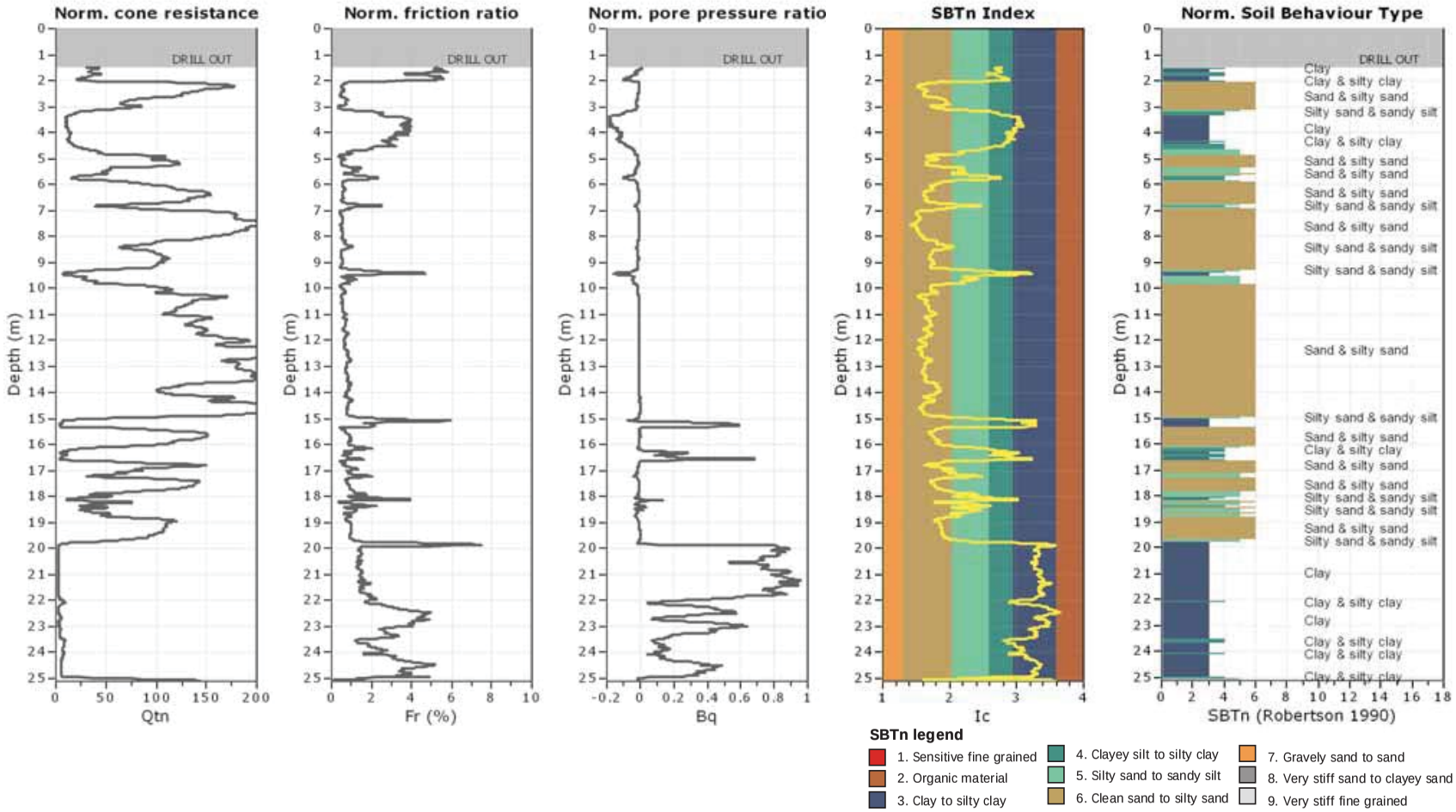

CPeT-IT v.1.7.6.42 - CPTU data presentation & interpretation software - Report created on: 21/08/2014, 11:04:56 a.m.

Project file: C:\Users\User\Desktop\summer\USGS Site Response Project\Soil Profiles and Info\CCCC\Proceced Data\CPT_484\cpt_484_2.cpt

CPT: CHHC_CPT425(CGD)

Total depth: 22.08 m

Coords: S 43.5354, E 172.6275

Cone Operator: Uknown

Project: **Evaluating Fully Nonlinear Effective Stress Site Resonse Computer Programs using Records from the Canterbury Earthquake Sequence**

Location: **Christchurch, New Zealand**

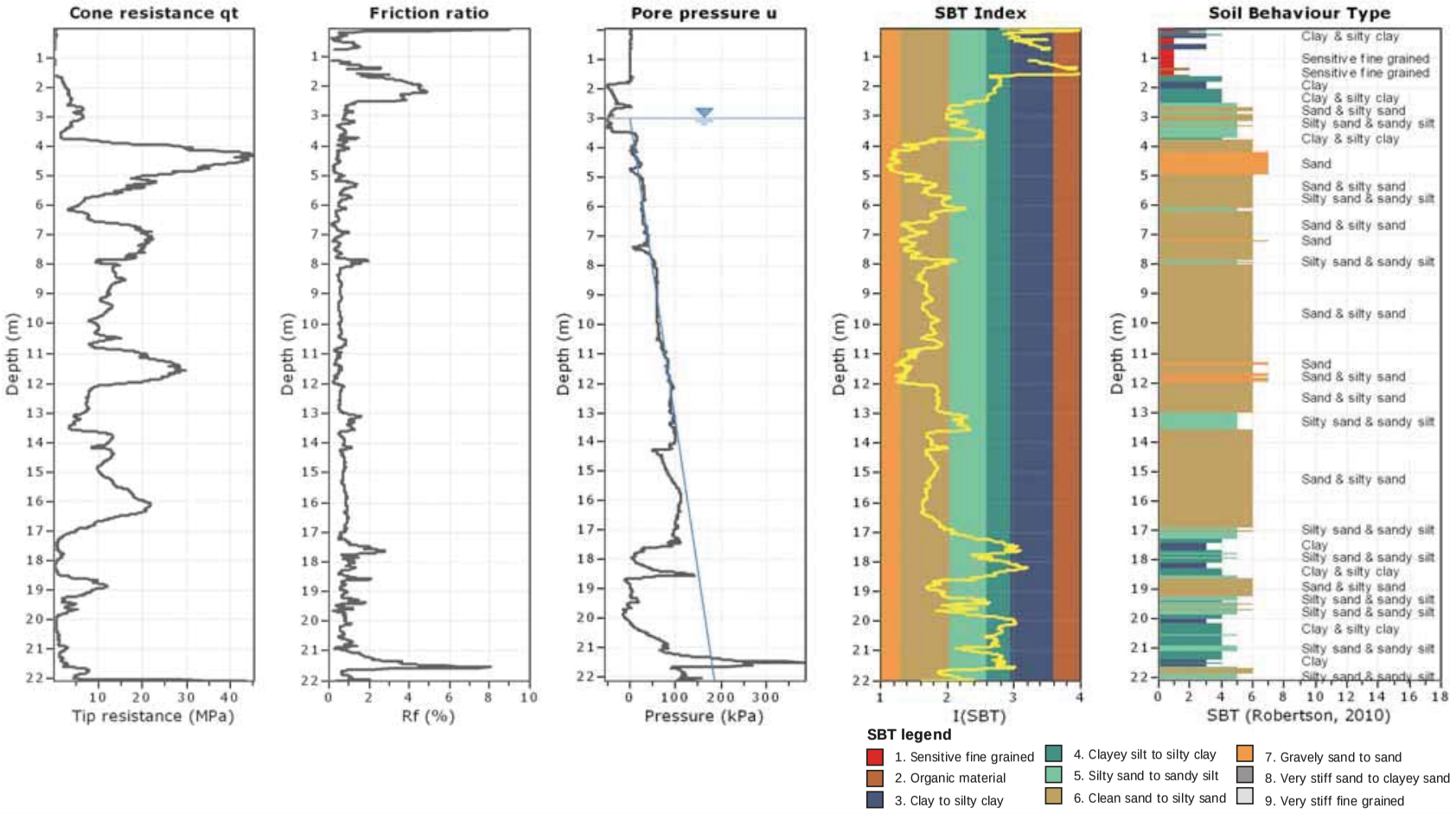

CPeT-IT v.1.7.6.42 - CPTU data presentation & interpretation software - Report created on: 21/08/2014, 01:53:56 a.m.

Project file: C:\Users\User\Desktop\summer\USGS Site Response Project\Soil Profiles and Info\CHHC\Proceed Data\CPT_425\CPT425_2.cpt

CPT: CHHC_CPT425(CGD)

Total depth: 22.08 m, Date: 09/07/2014

Coords: S 43.5354, E 172.6275

Cone Operator: Uknown

Project: **Evaluating Fully Nonlinear Effective Stress Site Resonse Computer Programs using Records from the Canterbury Earthquake Sequence**

Location: **Christchurch, New Zealand**

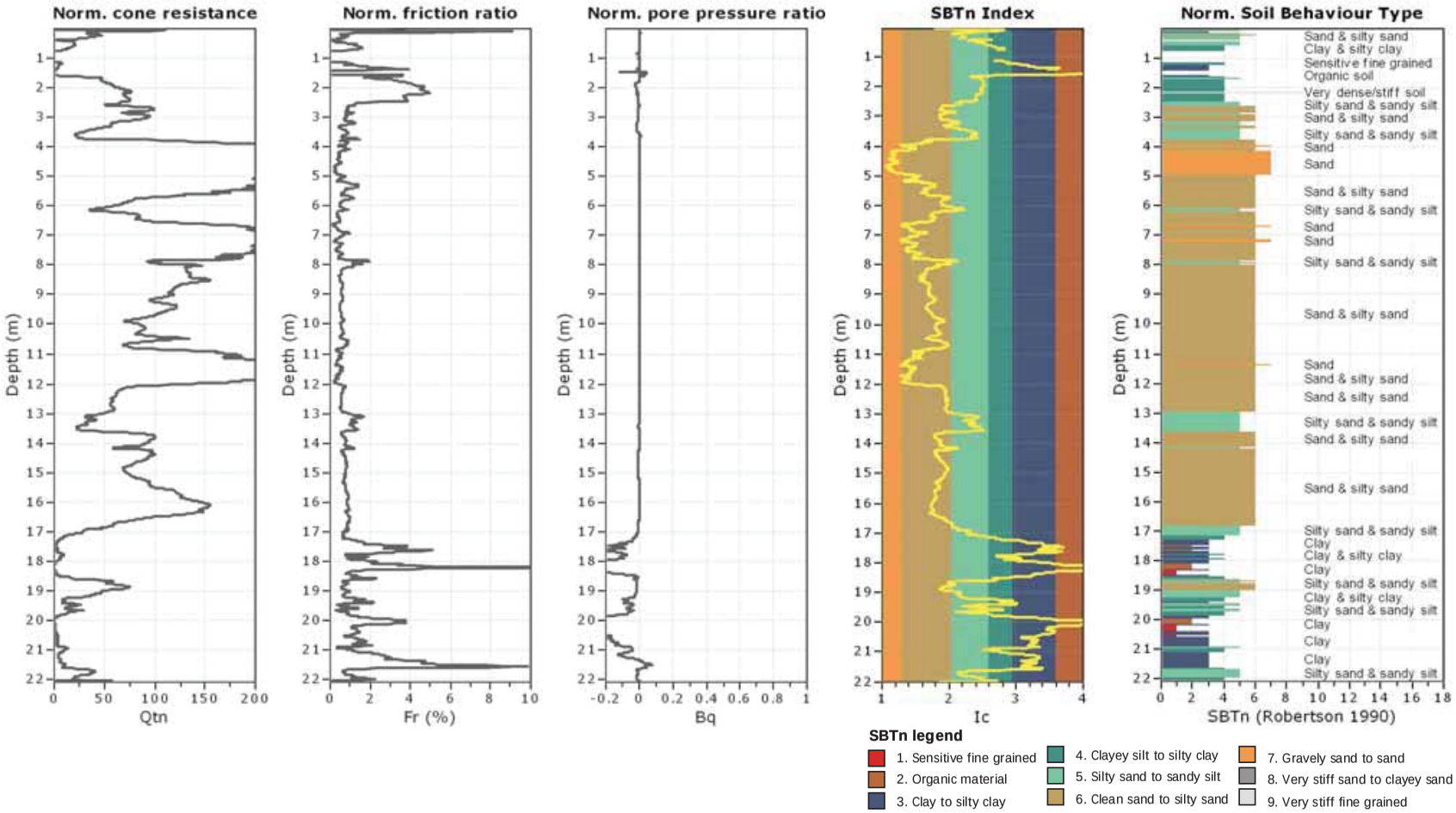

CPeT-IT v.1.7.6.42 - CPTU data presentation & interpretation software - Report created on: 21/08/2014, 01:53:56 a.m.

Project file: C:\Users\User\Desktop\summer\USGS Site Response Project\Soil Profiles and Info\CHHC\Proceed Data\CPT_425\CPT425_2.cpt

CPT: HPSC_CPT89(CGD)

Total depth: 36.23 m

Project: **Evaluating Fully Nonlinear Stress Site Response Computer Programs using Records from the Canterbury Earthquake Sequence**

Coords: S 43.5014, E 172.7021

Location: **Christchurch, New Zealand**

Cone Operator: Uknown

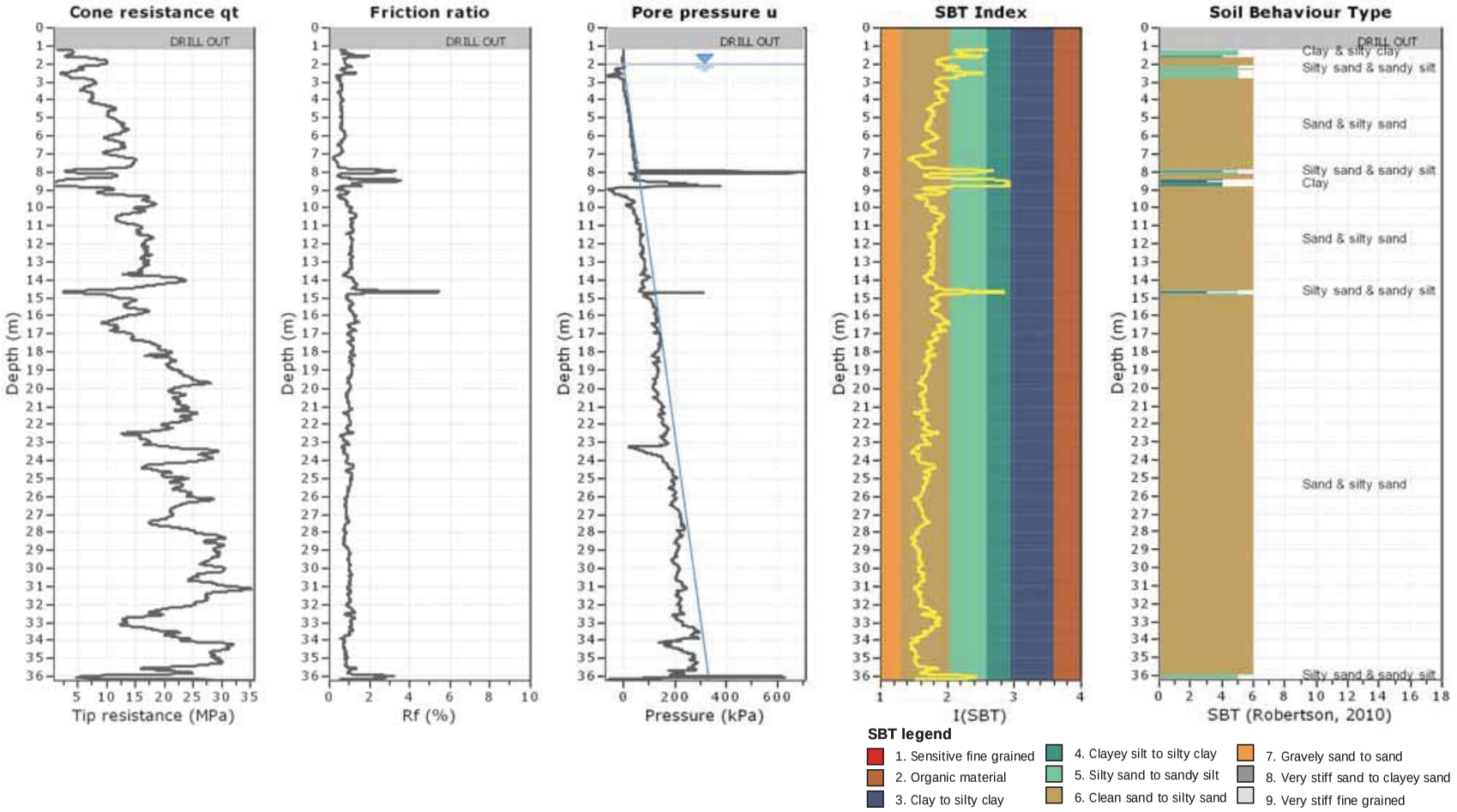

CPeT-IT v.1.7.6.42 - CPTU data presentation & interpretation software - Report created on: 21/08/2014, 04:31:30 p.m.

Project file: C:\Users\User\Desktop\summer\USGS Site Response Project\Soil Profiles and Info\HPSC\Proceeced Data\CPT89(13m)\CPT89(13m)_2.cpt

CPT: HPSC_CPT89(CGD)

Total depth: 36.23 m, Date: 12/07/2014

Project: **Evaluating Fully Nonlinear Stress Site Response Computer Programs using Records from the Canterbury Earthquake Sequence**

Coords: S 43.5014, E 172.7021

Location: **Christchurch, New Zealand**

Cone Operator: Uknown

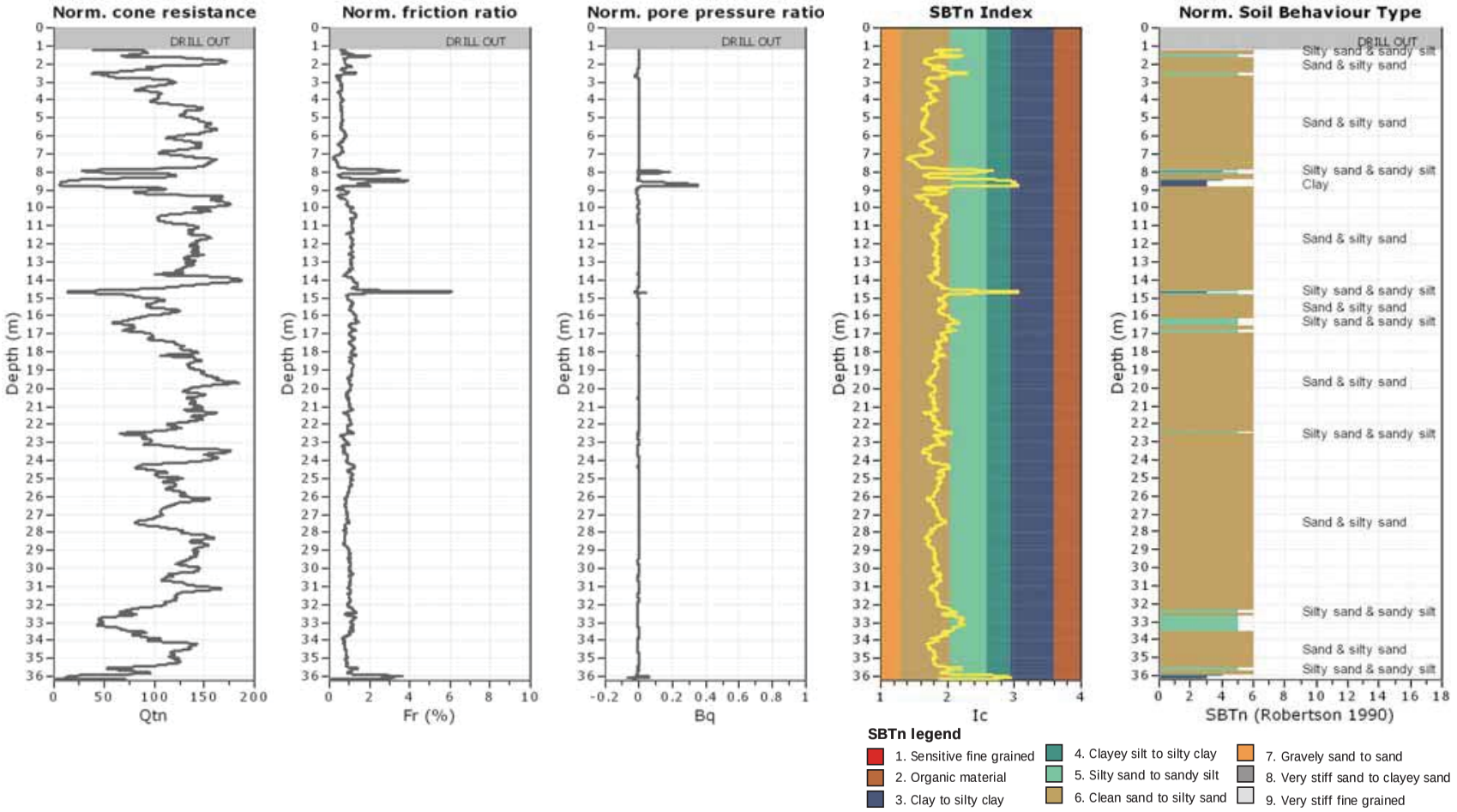

CPeT-IT v.1.7.6.42 - CPTU data presentation & interpretation software - Report created on: 21/08/2014, 04:31:30 p.m.

Project file: C:\Users\User\Desktop\summer\USGS Site Response Project\Soil Profiles and Info\HPSC\Proceeced Data\CPT89(13m)\CPT89(13m)_2.cpt

CPT: NNBS_CPT33695(CGD)

Total depth: 29.59 m

Project: **Evaluating Fully Nonlinear Stress Site Response Computer Programs using Records from the Canterbury Earthquake Sequence**

Coords: S 43.4953, E 172.7181

Location: **Christchurch, New Zealand**

Cone Operator: Uknown

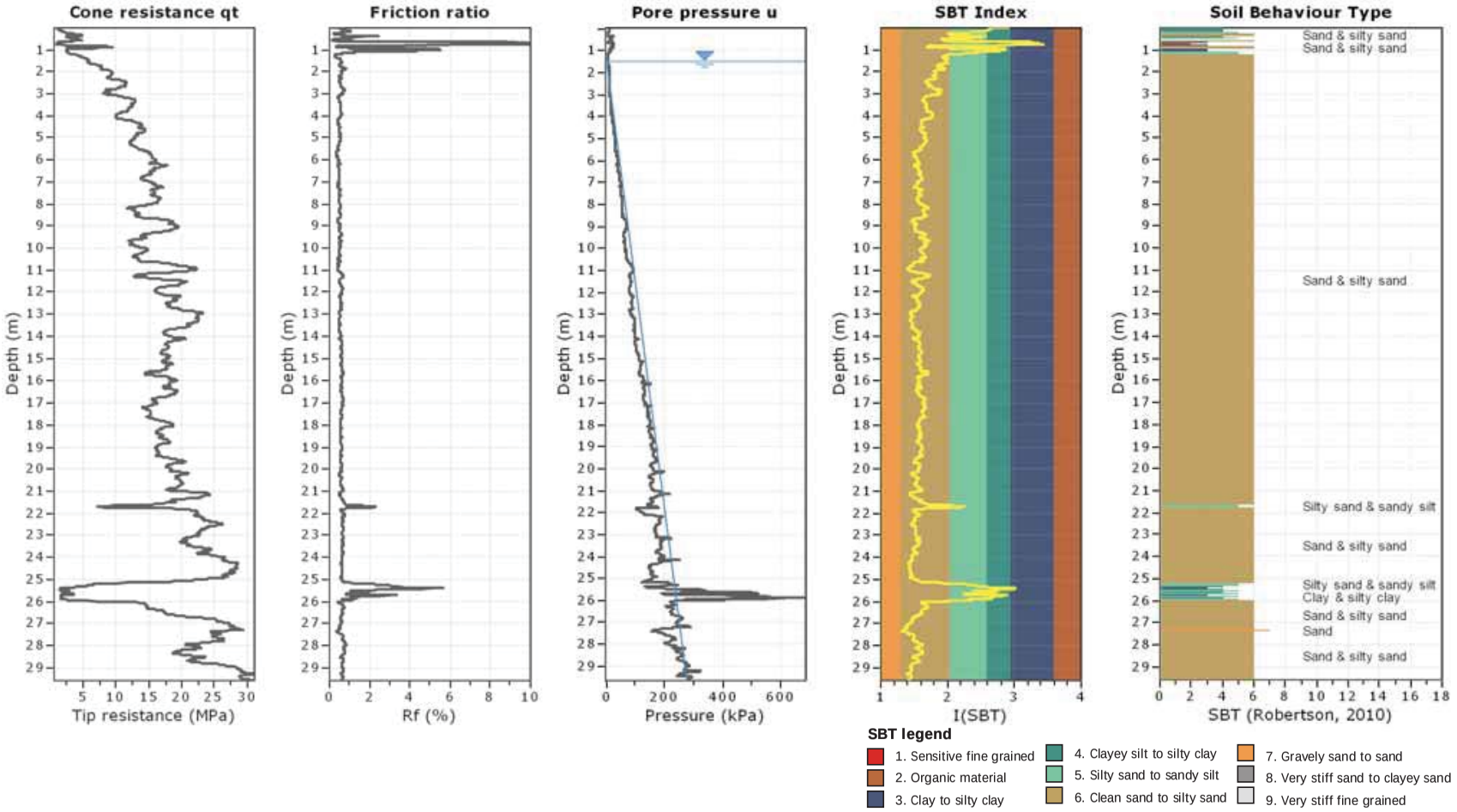

CPT: NNBS_CPT33695(CGD)

Total depth: 29.59 m, Date: 22/07/2014

Coords: S 43.4953, E 172.7181

Cone Operator: Uknown

Project: **Evaluating Fully Nonlinear Stress Site Response Computer Programs using Records from the Canterbury Earthquake Sequence**

Location: **Christchurch, New Zealand**

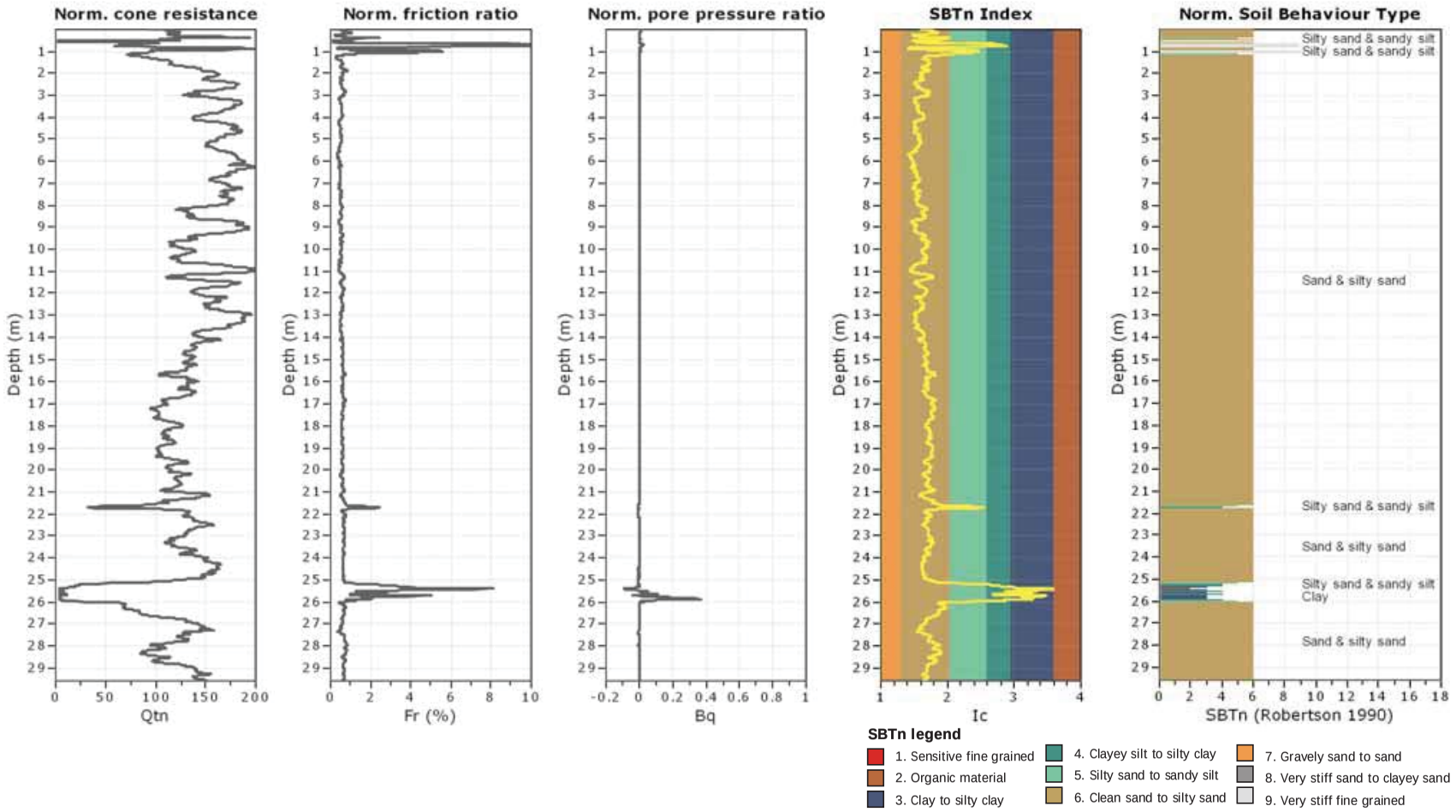

CPT: PPHS_CPT1497(CGD)

Total depth: 10.38 m

Coords: S 43.4932, E 172.6067

Cone Operator: Uknown

Project: **Evaluating Fully Nonlinear Stress Site Response Computer Programs using Records from the Canterbury Earthquake Sequence**

Location: **Christchurch, New Zealand**

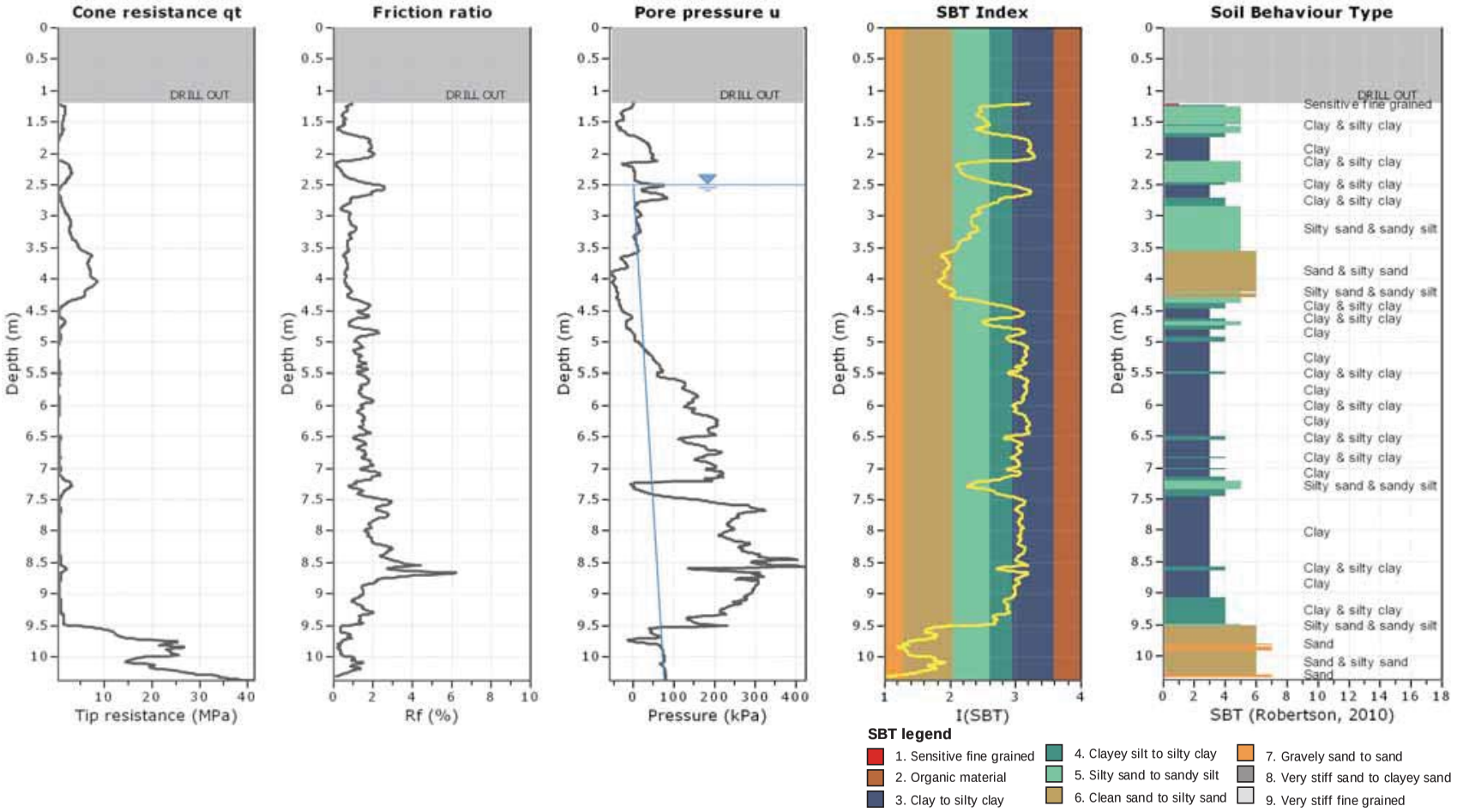

CPeT-IT v.1.7.6.42 - CPTU data presentation & interpretation software - Report created on: 21/08/2014, 04:28:47 p.m.

Project file: C:\Users\User\Desktop\summer\USGS Site Response Project\Soil Profiles and Info\PPHS\Proceed Data\CPT1497(125m)\cpt1497(125m)_2.cpt

CPT: PPHS_CPT1497(CGD)

Total depth: 10.38 m, Date: 13/07/2014

Coords: S 43.4932, E 172.6067

Cone Operator: Uknown

Project: **Evaluating Fully Nonlinear Stress Site Response Computer Programs using Records from the Canterbury Earthquake Sequence**

Location: **Christchurch, New Zealand**

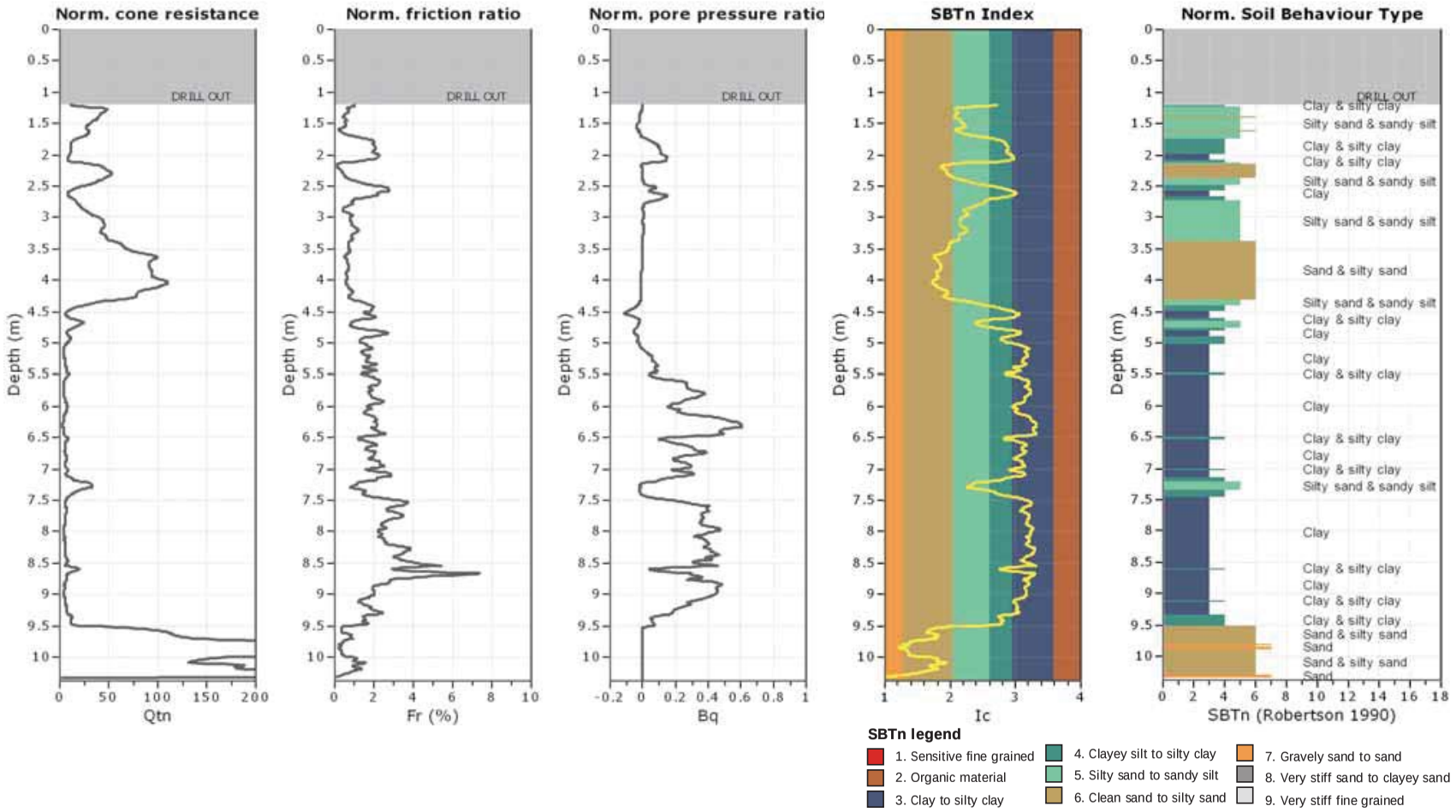

CPeT-IT v.1.7.6.42 - CPTU data presentation & interpretation software - Report created on: 21/08/2014, 04:28:47 p.m.

Project file: C:\Users\User\Desktop\summer\USGS Site Response Project\Soil Profiles and Info\PPHS\Proceed Data\CPT1497(125m)\cpt1497(125m)_2.cpt

CPT: PRPC_CPT1396 (CGD)

Total depth: 28.16 m

Project:

Coords: S 43.5259, E 172.6828

Location:

Cone Operator: Uknown

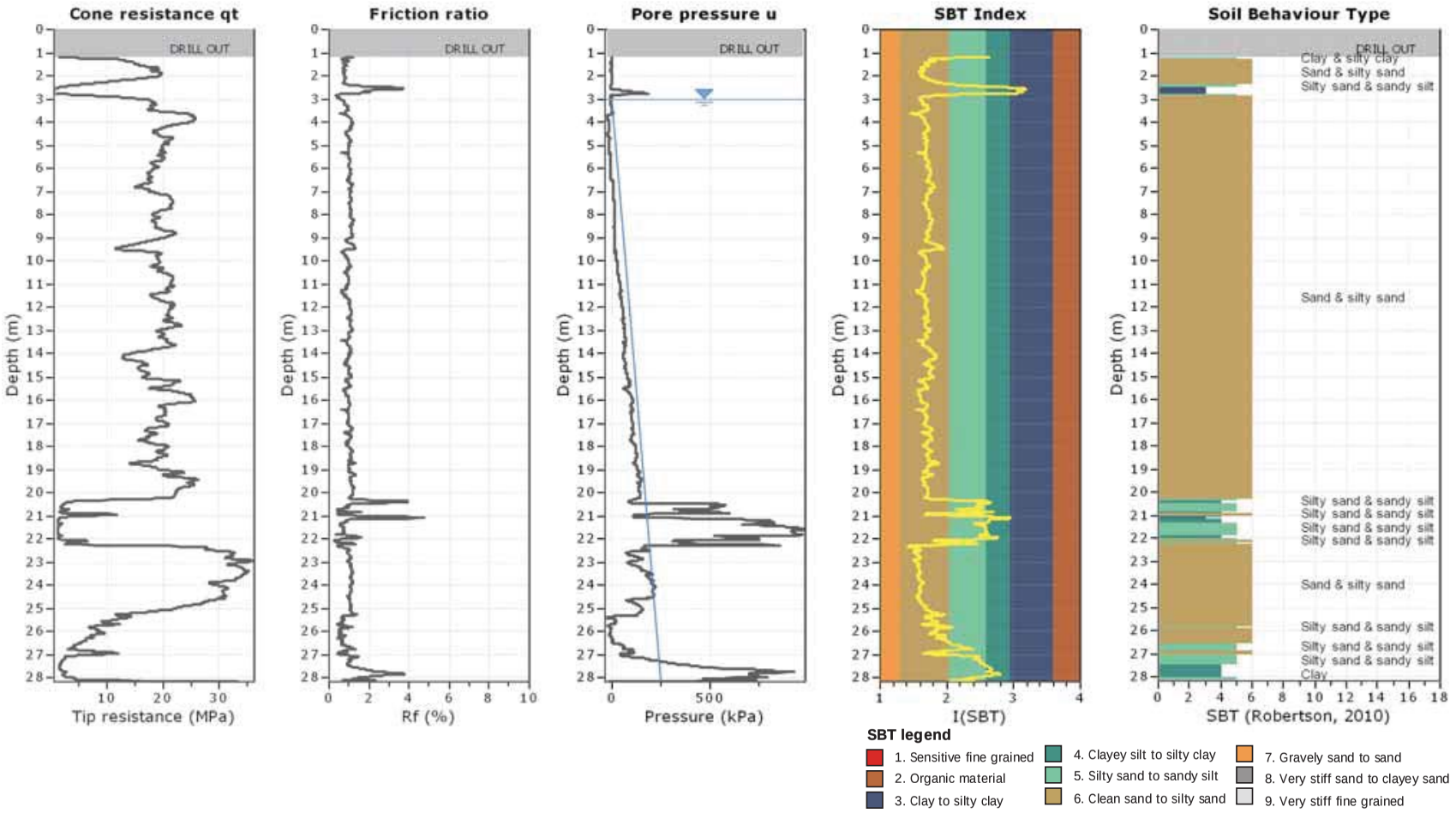

CPeT-IT v.1.7.6.42 - CPTU data presentation & interpretation software - Report created on: 21/08/2014, 04:44:07 p.m.

Project file: C:\Users\User\Desktop\summer\USGS Site Response Project\Soil Profiles and Info\PRPC\Proceed Data\CPT 39 TT\CPT39TT_2.cpt

CPT: PRPC_CPT1396 (CGD)

Total depth: 28.16 m, Date: 18/07/2014

Coords: S 43.5259, E 172.6828

Cone Operator: Uknown

Project:

Location:

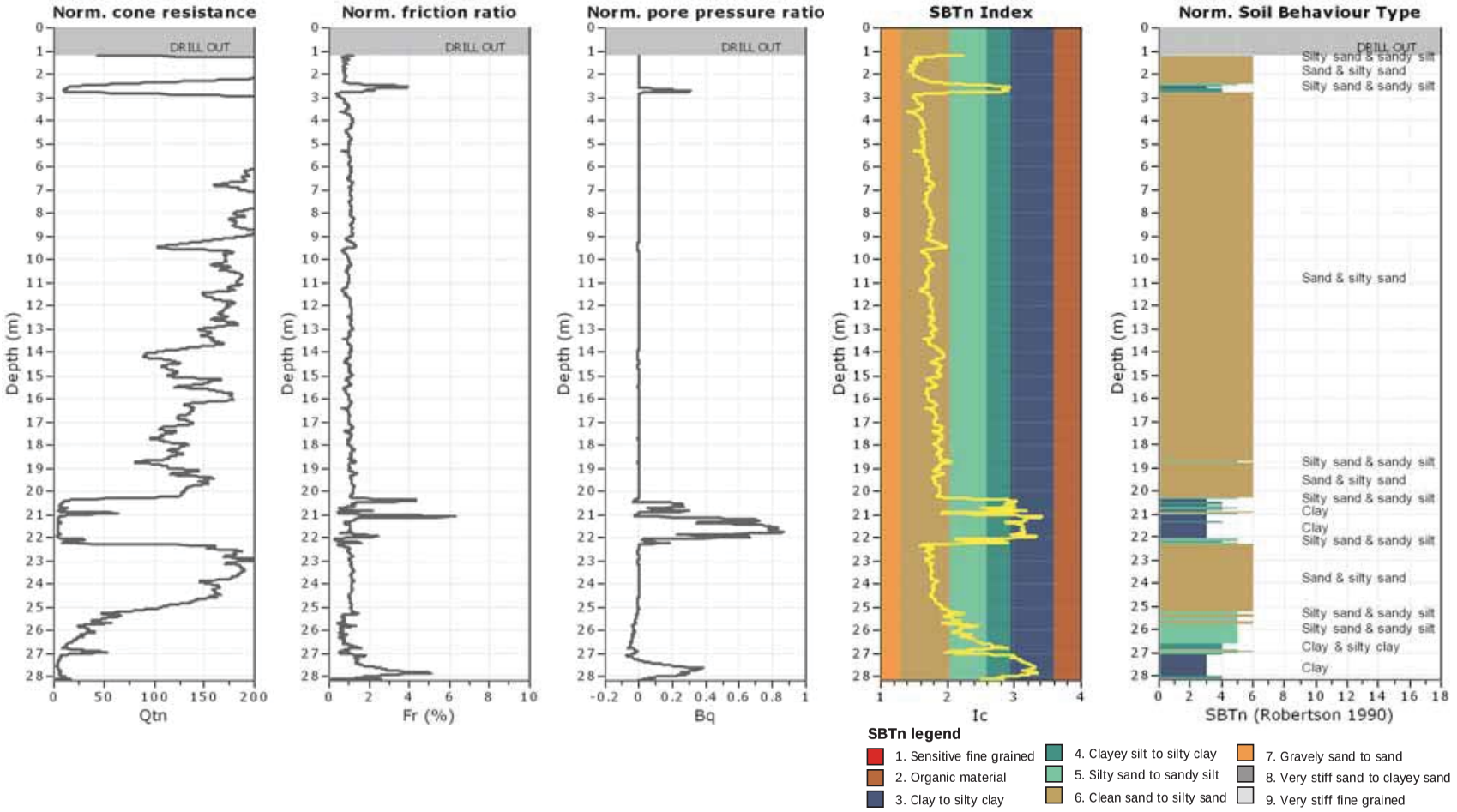

CPeT-IT v.1.7.6.42 - CPTU data presentation & interpretation software - Report created on: 21/08/2014, 04:44:07 p.m.

Project file: C:\Users\User\Desktop\summer\USGS Site Response Project\Soil Profiles and Info\PRPC\Proceed Data\CPT 39 TT\CPT39TT_2.cpt

CPT: REHS_CPT2 (Wotherspoon,2013)

Total depth: 19.76 m

Project: **Evaluating Fully Nonlinear Effective Stress Site Resonse Computer Programs using Records from the Canterbury Earthquake Sequence**

Coords: S 43.5220, E172.6351

Location: **Christchurch, New Zealand**

Cone Operator: Uknown

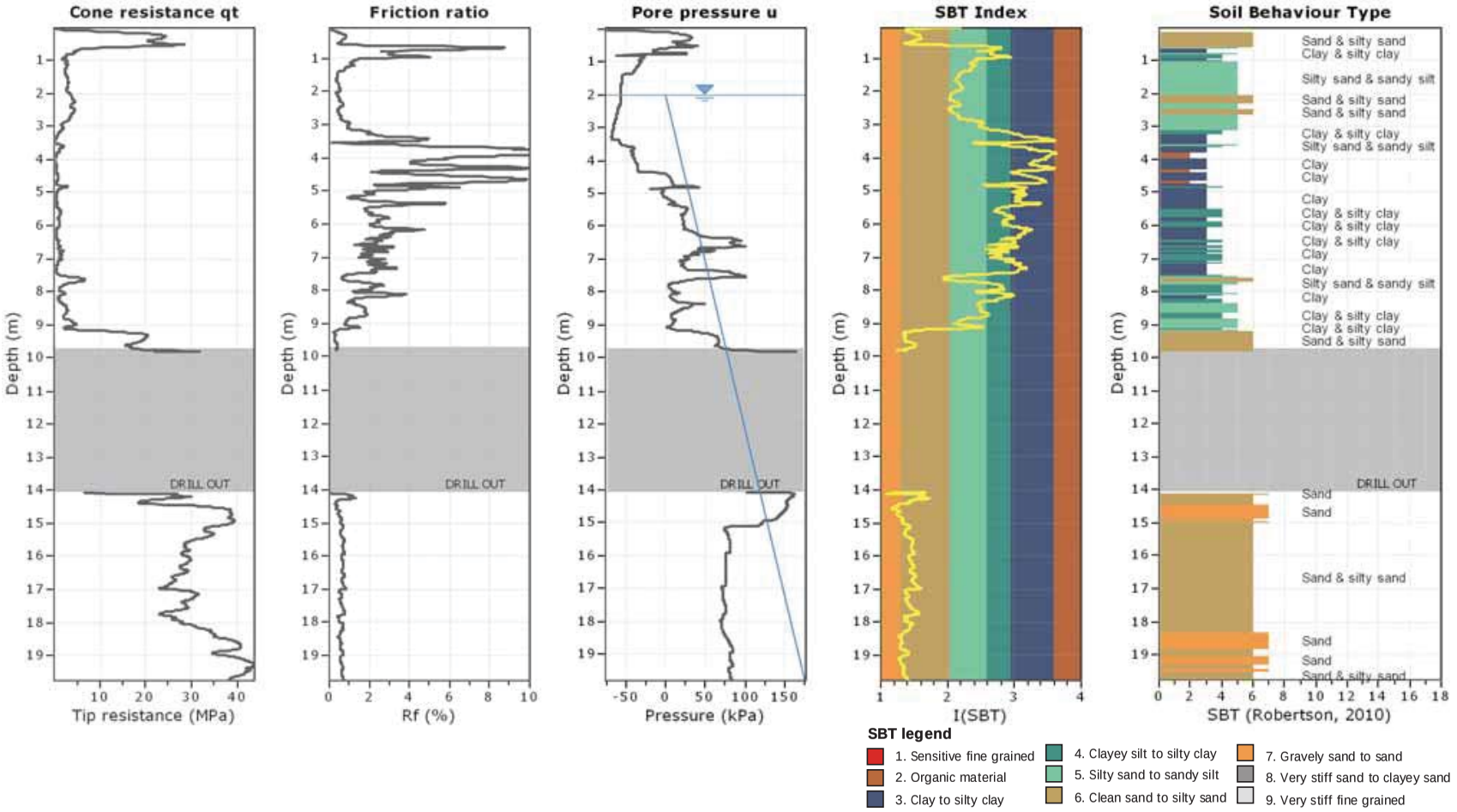

CPeT-IT v.1.7.6.42 - CPTU data presentation & interpretation software - Report created on: 21/08/2014, 01:28:45 a.m.

Project file: C:\Users\User\Desktop\summer\USGS Site Response Project\Soil Profiles and Info\REHS\Proceed Data\Wotherspoon\REHC_CPT1_CPT1a_2.cpt

CPT: REHS_CPT2 (Wotherspoon,2013)

Total depth: 19.76 m, Date: 06/07/2014

Coords: S 43.5220, E172.6351

Cone Operator: Uknown

Project: **Evaluating Fully Nonlinear Effective Stress Site Resonse Computer Programs using Records from the Canterbury Earthquake Sequence**

Location: **Christchurch, New Zealand**

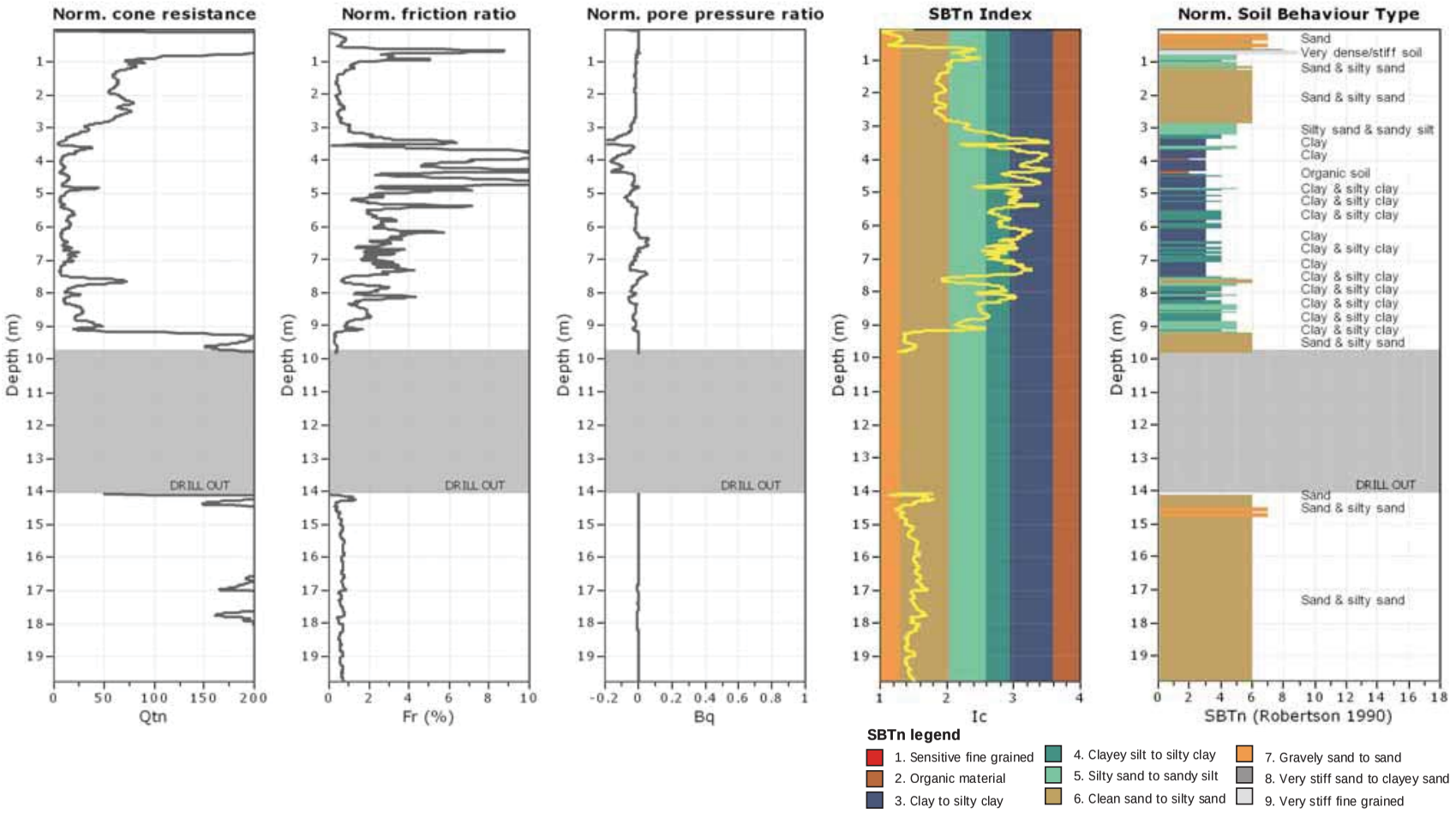

CPeT-IT v.1.7.6.42 - CPTU data presentation & interpretation software - Report created on: 21/08/2014, 01:28:45 a.m.

Project file: C:\Users\User\Desktop\summer\USGS Site Response Project\Soil Profiles and Info\REHS\Proceed Data\Wotherspoon\REHC_CPT1_CPT1a_2.cpt

CPT: SHLC_CPT626(CGD)

Total depth: 27.58 m

Project: **Evaluating Fully Nonlinear Effective Stress Site Resonse Computer Programs using Records from the Canterbury Earthquake Sequence**

Coords: S 43.5054, E 172.6628

Location: **Christchurch, New Zealand**

Cone Operator: Uknown

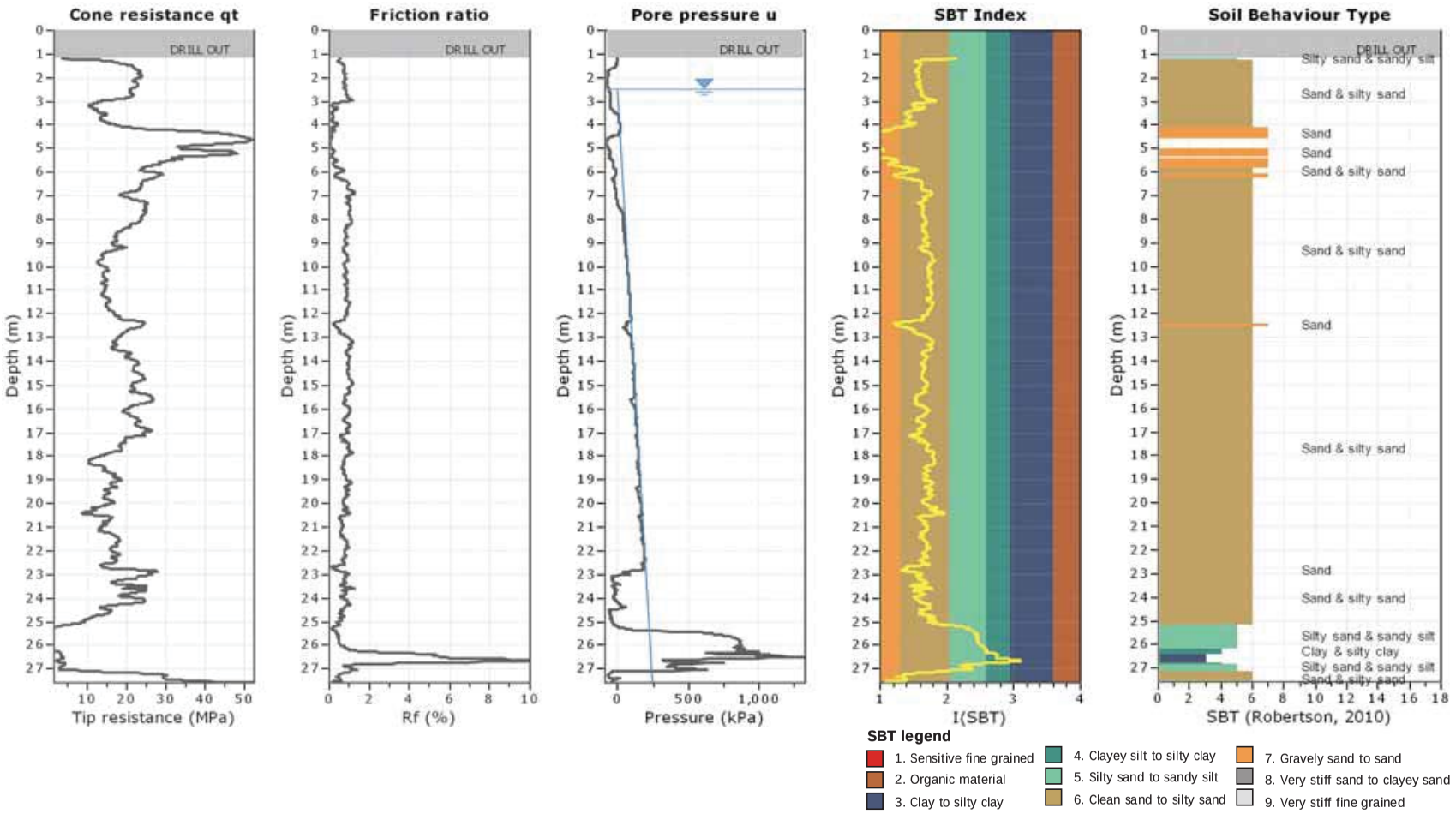

CPeT-IT v.1.7.6.42 - CPTU data presentation & interpretation software - Report created on: 21/08/2014, 04:39:13 p.m.

Project file: C:\Users\User\Desktop\summer\USGS Site Response Project\Soil Profiles and Info\SHLC\Proceed Data\CPT626(50m)\CPT626(50m)_2.cpt

CPT: SHLC_CPT626(CGD)

Total depth: 27.58 m, Date: 11/07/2014

Coords: S 43.5054, E 172.6628

Cone Operator: Uknown

Project: **Evaluating Fully Nonlinear Effective Stress Site Resonse Computer Programs using Records from the Canterbury Earthquake Sequence**

Location: **Christchurch, New Zealand**

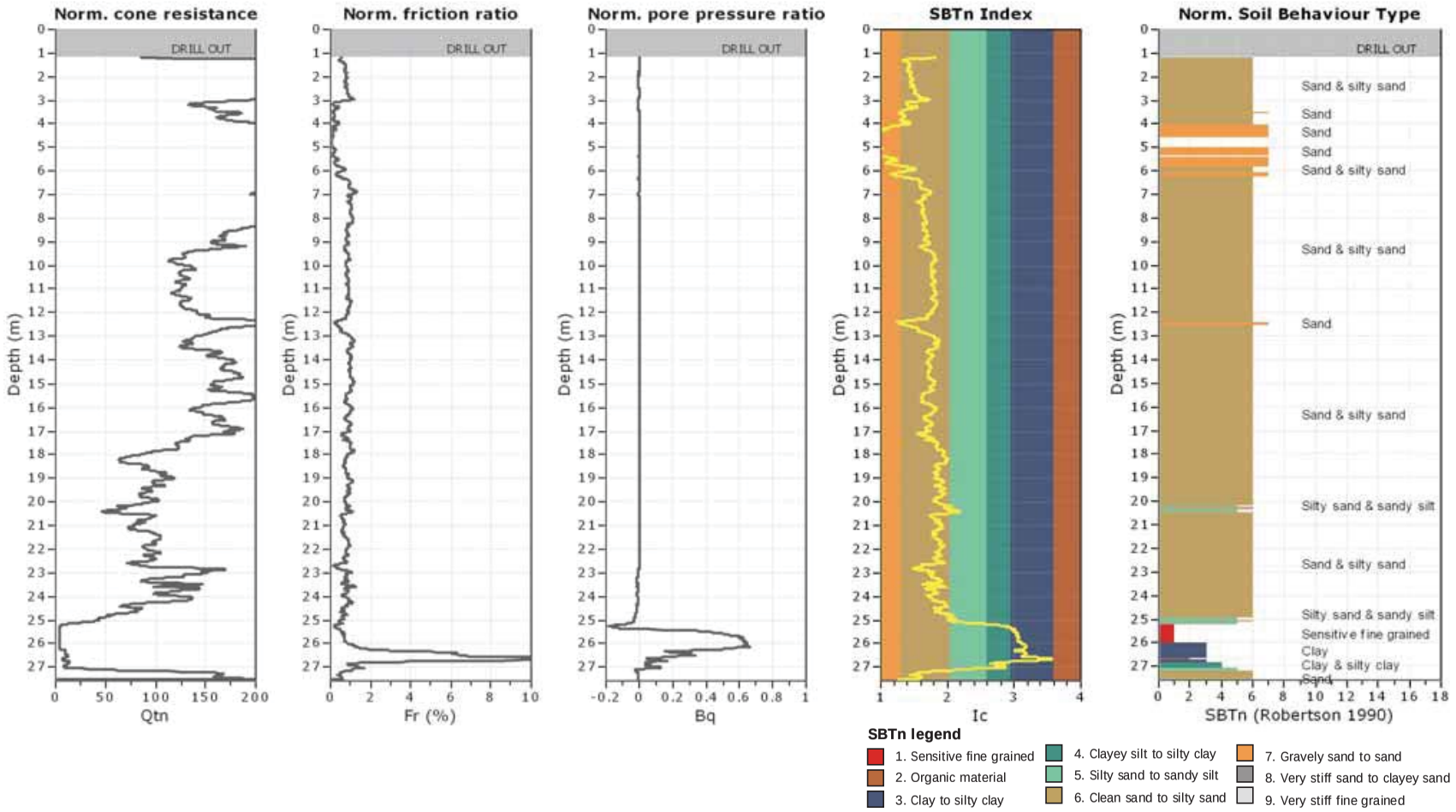

CPeT-IT v.1.7.6.42 - CPTU data presentation & interpretation software - Report created on: 21/08/2014, 04:39:13 p.m.

Project file: C:\Users\User\Desktop\summer\USGS Site Response Project\Soil Profiles and Info\SHLC\Proceed Data\CPT626(50m)\CPT626(50m)_2.cpt

CPT: CBGS_CPT1(Wotherspoon,2013)

Total depth: 21.60 m

Project: **Evaluating Fully Nonlinear Effective Stress Site Resonse Computer Programs using Records from the Canterbury Earthquake Sequence**

Coords: S 43.5293, E 172.6198

Location: **Christchurch, New Zealand**

Cone Operator: Uknown

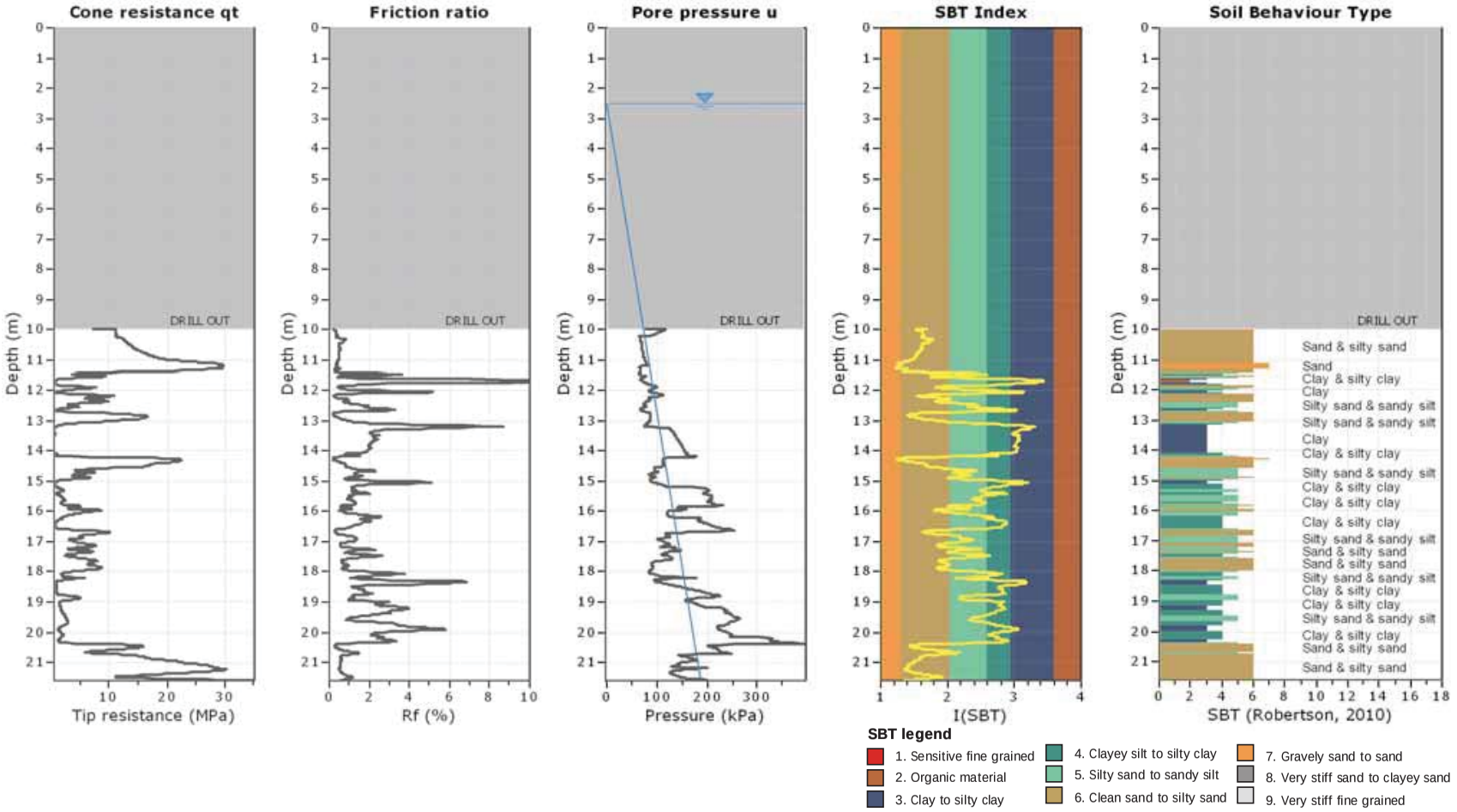

CPeT-IT v.1.7.6.42 - CPTU data presentation & interpretation software - Report created on: 21/08/2014, 01:30:58 a.m.

Project file: C:\Users\User\Desktop\summer\USGS Site Response Project\Soil Profiles and Info\CBGS\Site Investigation Data\CBGS CPT\test_2.cpt

CPT: CBGS_CPT1(Wotherspoon,2013)

Total depth: 21.60 m, Date: 07/07/2014

Coords: S 43.5293, E 172.6198

Cone Operator: Uknown

Project: **Evaluating Fully Nonlinear Effective Stress Site Resonse Computer Programs using Records from the Canterbury Earthquake Sequence**

Location: **Christchurch, New Zealand**

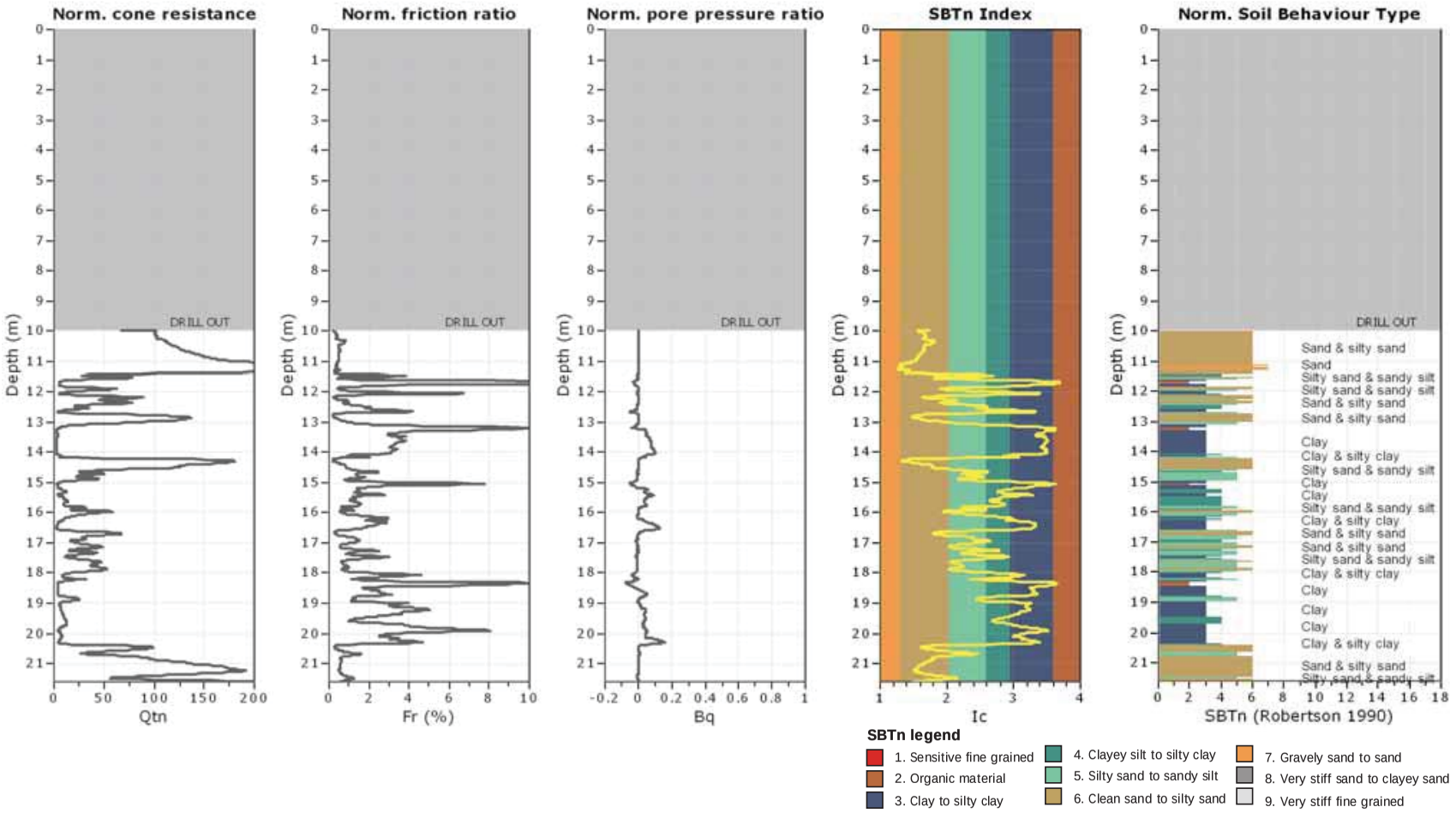

CPeT-IT v.1.7.6.42 - CPTU data presentation & interpretation software - Report created on: 21/08/2014, 01:30:58 a.m.

Project file: C:\Users\User\Desktop\summer\USGS Site Response Project\Soil Profiles and Info\CBGS\Site Investigation Data\CBGS CPT\test_2.cpt

CPT: CCCC_CPT484(CGD)

Total depth: 25.11 m

Project: **Evaluating Fully Nonlinear Effective Stress Site Resonse Computer Programs using Records from the Canterbury Earthquake Sequence**

Coords: S 43.5379, E 172.6479

Location: **Christchurch, New Zealand**

Cone Operator: Uknown

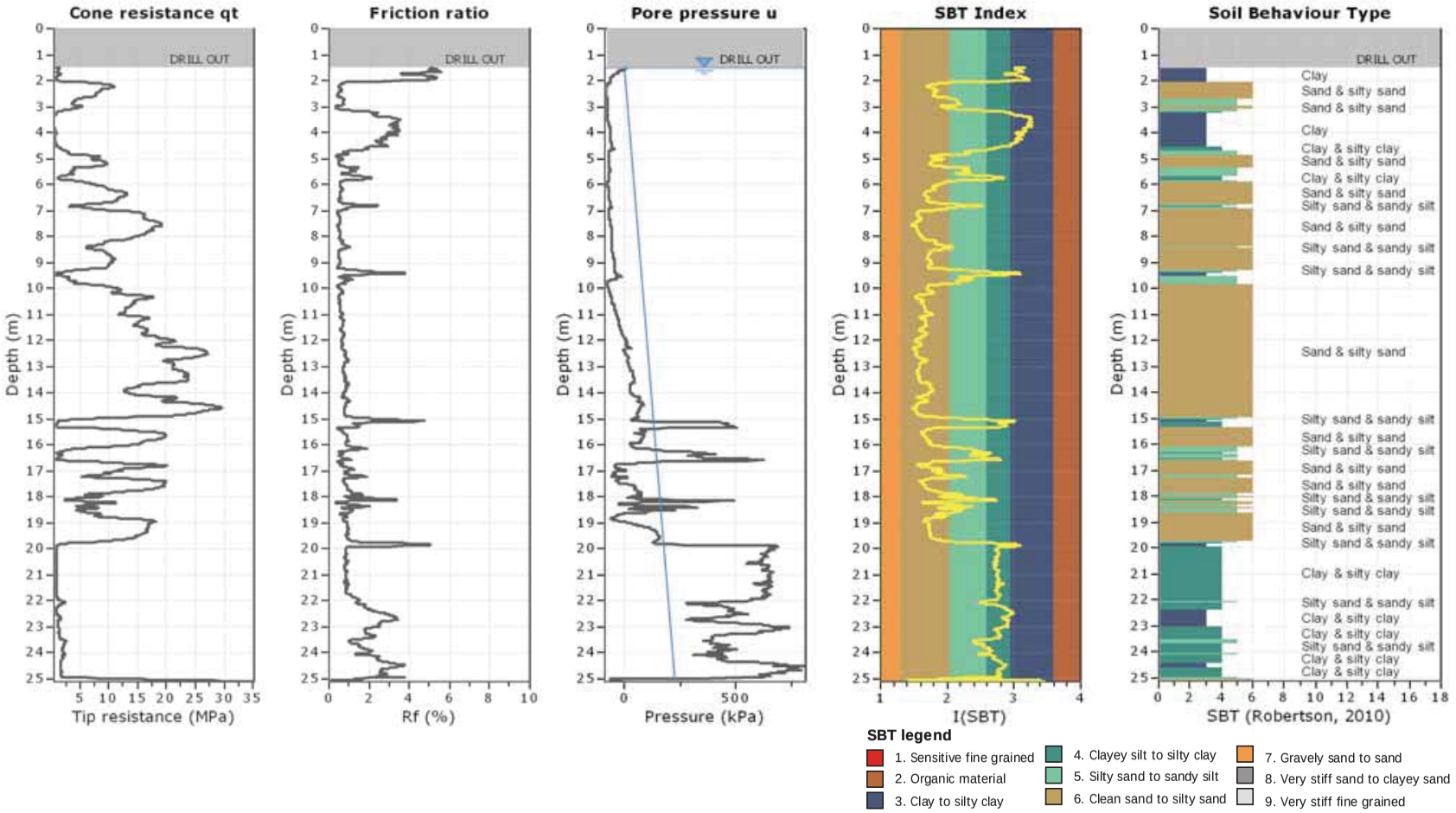

CPeT-IT v.1.7.6.42 - CPTU data presentation & interpretation software - Report created on: 21/08/2014, 11:04:56 a.m.

Project file: C:\Users\User\Desktop\summer\USGS Site Response Project\Soil Profiles and Info\CCCC\Proceced Data\CPT_484\cpt_484_2.cpt

CPT: CCCC_CPT484(CGD)

Total depth: 25.11 m, Date: 05/07/2014

Coords: S 43.5379, E 172.6479

Cone Operator: Uknown

Project: **Evaluating Fully Nonlinear Effective Stress Site Resonse Computer Programs using Records from the Canterbury Earthquake Sequence**

Location: **Christchurch, New Zealand**

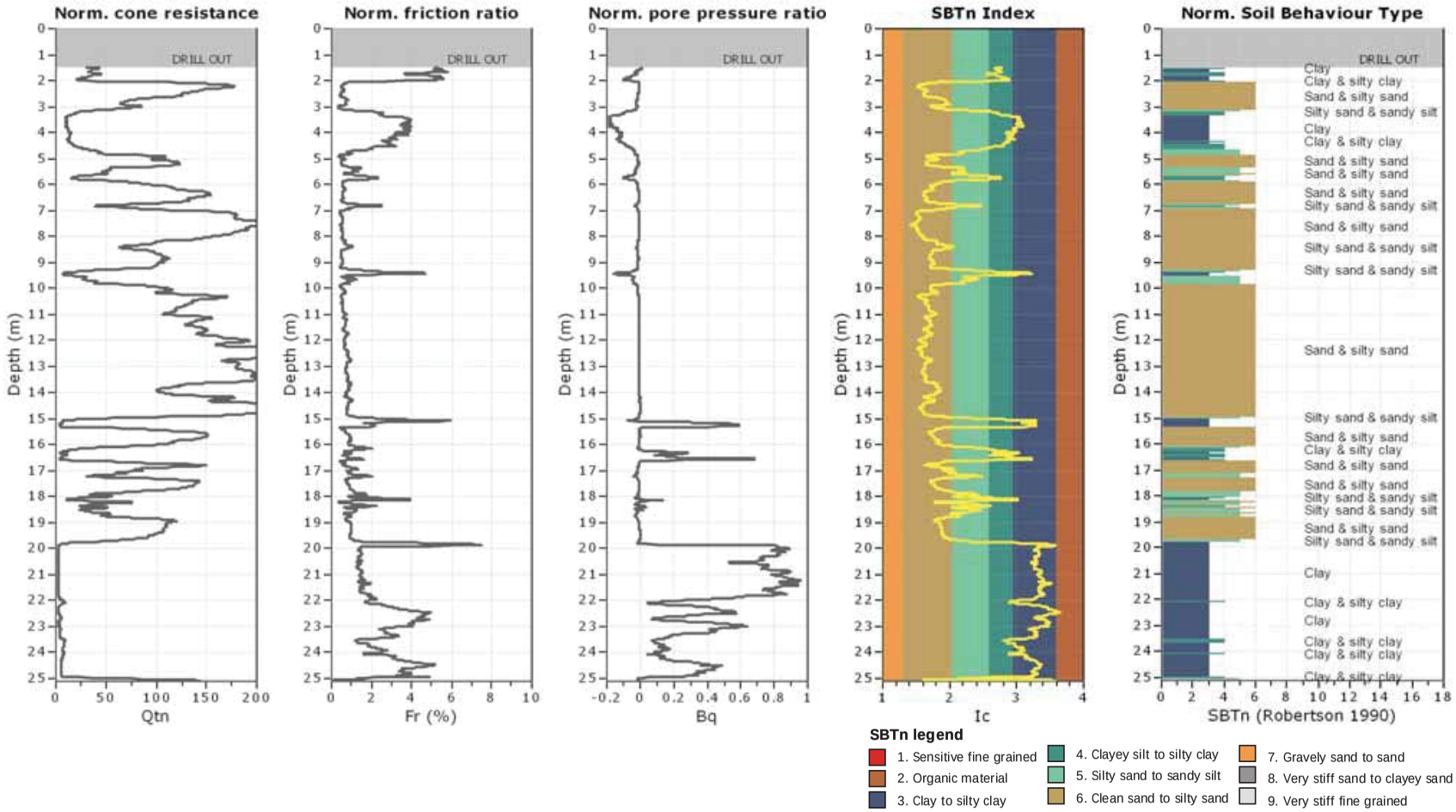

CPeT-IT v.1.7.6.42 - CPTU data presentation & interpretation software - Report created on: 21/08/2014, 11:04:56 a.m.

Project file: C:\Users\User\Desktop\summer\USGS Site Response Project\Soil Profiles and Info\CCCC\Proceced Data\CPT_484\cpt_484_2.cpt

CPT: CHHC_CPT425(CGD)

Total depth: 22.08 m

Coords: S 43.5354, E 172.6275

Cone Operator: Uknown

Project: **Evaluating Fully Nonlinear Effective Stress Site Resonse Computer Programs using Records from the Canterbury Earthquake Sequence**

Location: **Christchurch, New Zealand**

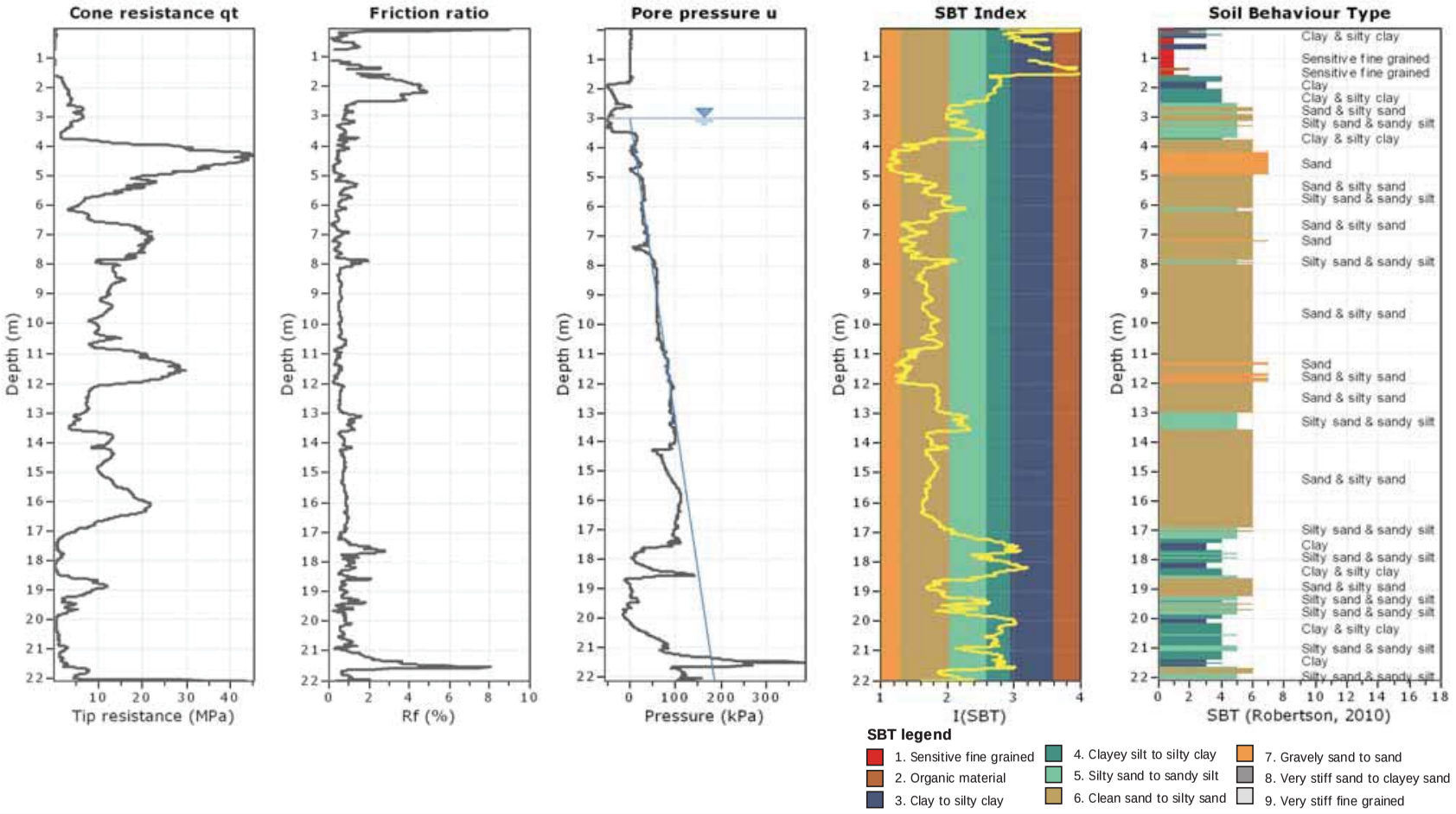

CPeT-IT v.1.7.6.42 - CPTU data presentation & interpretation software - Report created on: 21/08/2014, 01:53:56 a.m.

Project file: C:\Users\User\Desktop\summer\USGS Site Response Project\Soil Profiles and Info\CHHC\Proceed Data\CPT_425\CPT425_2.cpt

CPT: CHHC_CPT425(CGD)

Total depth: 22.08 m, Date: 09/07/2014

Coords: S 43.5354, E 172.6275

Cone Operator: Uknown

Project: **Evaluating Fully Nonlinear Effective Stress Site Resonse Computer Programs using Records from the Canterbury Earthquake Sequence**

Location: **Christchurch, New Zealand**

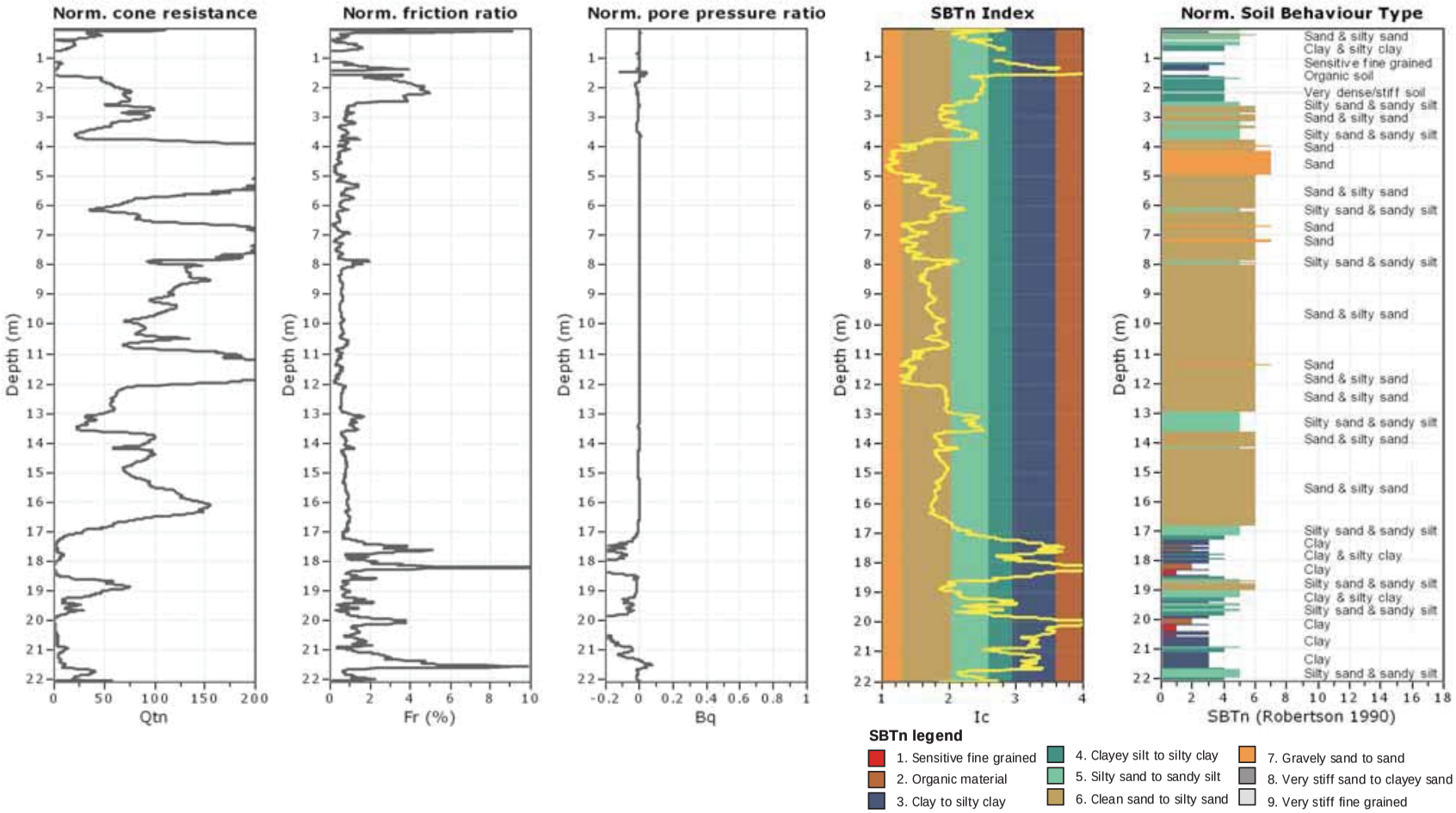

CPeT-IT v.1.7.6.42 - CPTU data presentation & interpretation software - Report created on: 21/08/2014, 01:53:56 a.m.

Project file: C:\Users\User\Desktop\summer\USGS Site Response Project\Soil Profiles and Info\CHHC\Proceed Data\CPT_425\CPT425_2.cpt

CPT: HPSC_CPT89(CGD)

Total depth: 36.23 m

Project: **Evaluating Fully Nonlinear Stress Site Response Computer Programs using Records from the Canterbury Earthquake Sequence**

Coords: S 43.5014, E 172.7021

Location: **Christchurch, New Zealand**

Cone Operator: Uknown

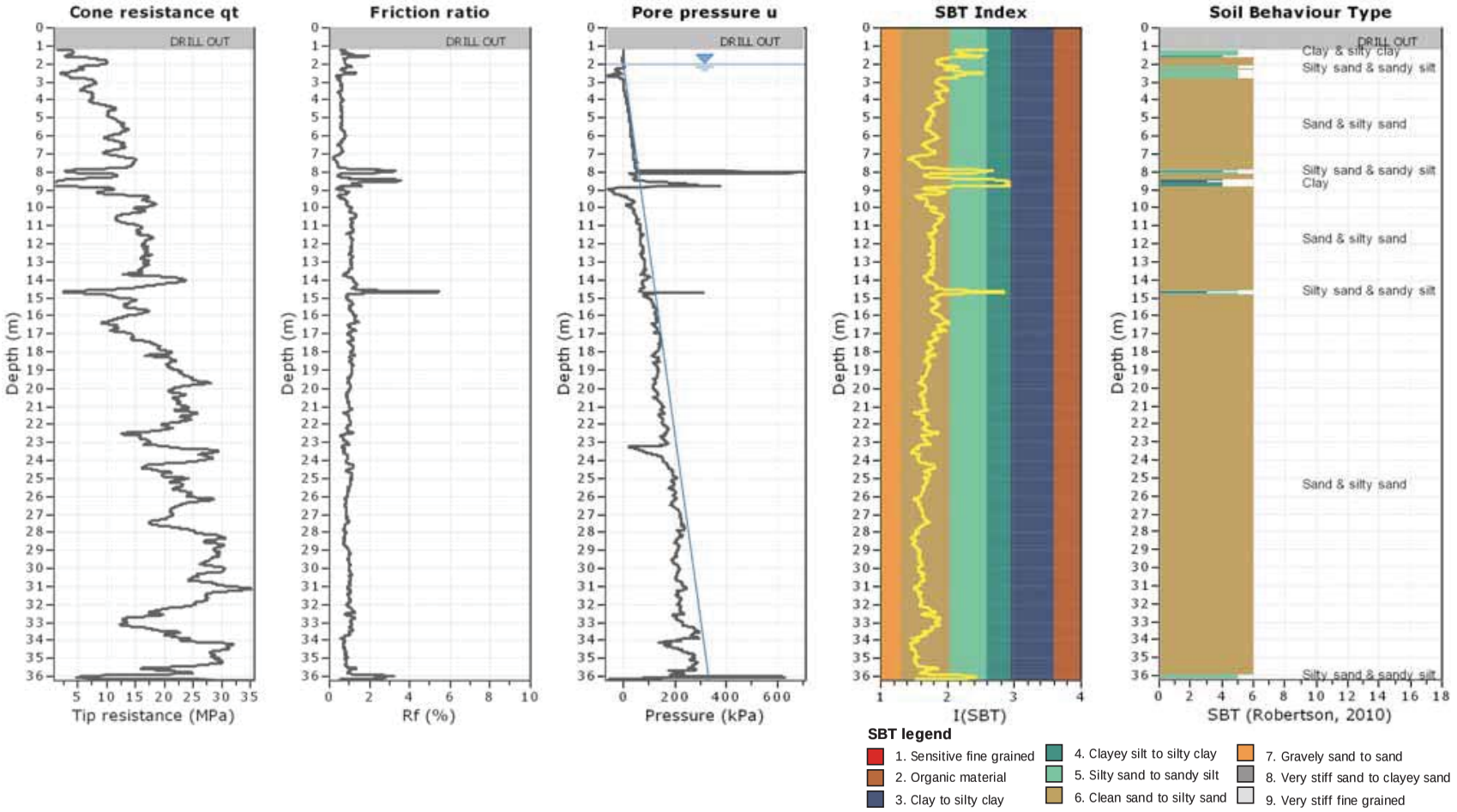

CPeT-IT v.1.7.6.42 - CPTU data presentation & interpretation software - Report created on: 21/08/2014, 04:31:30 p.m.

Project file: C:\Users\User\Desktop\summer\USGS Site Response Project\Soil Profiles and Info\HPSC\Proceeced Data\CPT89(13m)\CPT89(13m)_2.cpt

CPT: HPSC_CPT89(CGD)

Total depth: 36.23 m, Date: 12/07/2014

Coords: S 43.5014, E 172.7021

Cone Operator: Uknown

Project: **Evaluating Fully Nonlinear Stress Site Response Computer Programs using Records from the Canterbury Earthquake Sequence**

Location: **Christchurch, New Zealand**

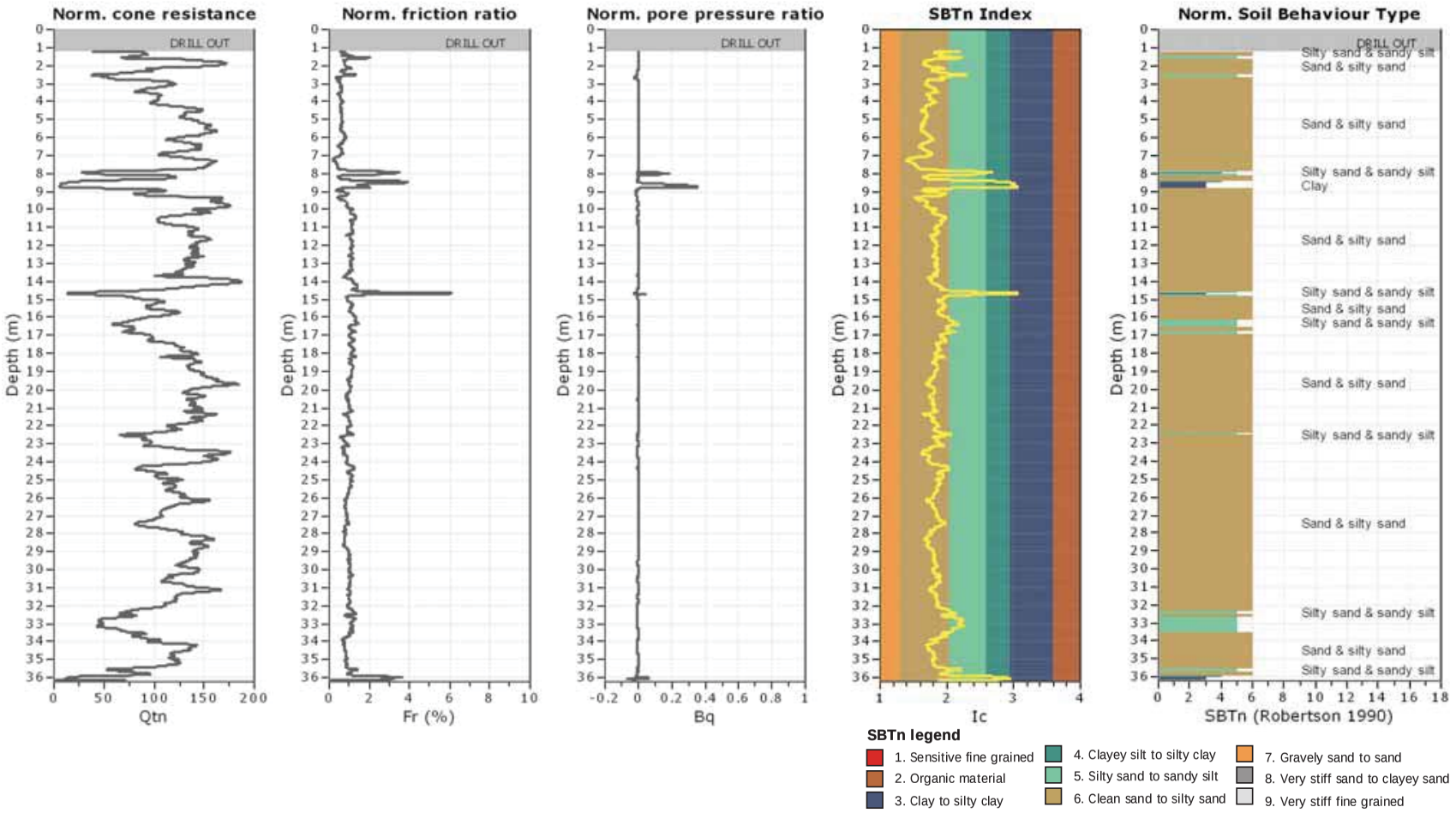

CPeT-IT v.1.7.6.42 - CPTU data presentation & interpretation software - Report created on: 21/08/2014, 04:31:30 p.m.

Project file: C:\Users\User\Desktop\summer\USGS Site Response Project\Soil Profiles and Info\HPSC\Proceeced Data\CPT89(13m)\CPT89(13m)_2.cpt

CPT: NNBS_CPT33695(CGD)

Total depth: 29.59 m

Project: **Evaluating Fully Nonlinear Stress Site Response Computer Programs using Records from the Canterbury Earthquake Sequence**

Coords: S 43.4953, E 172.7181

Location: **Christchurch, New Zealand**

Cone Operator: Uknown

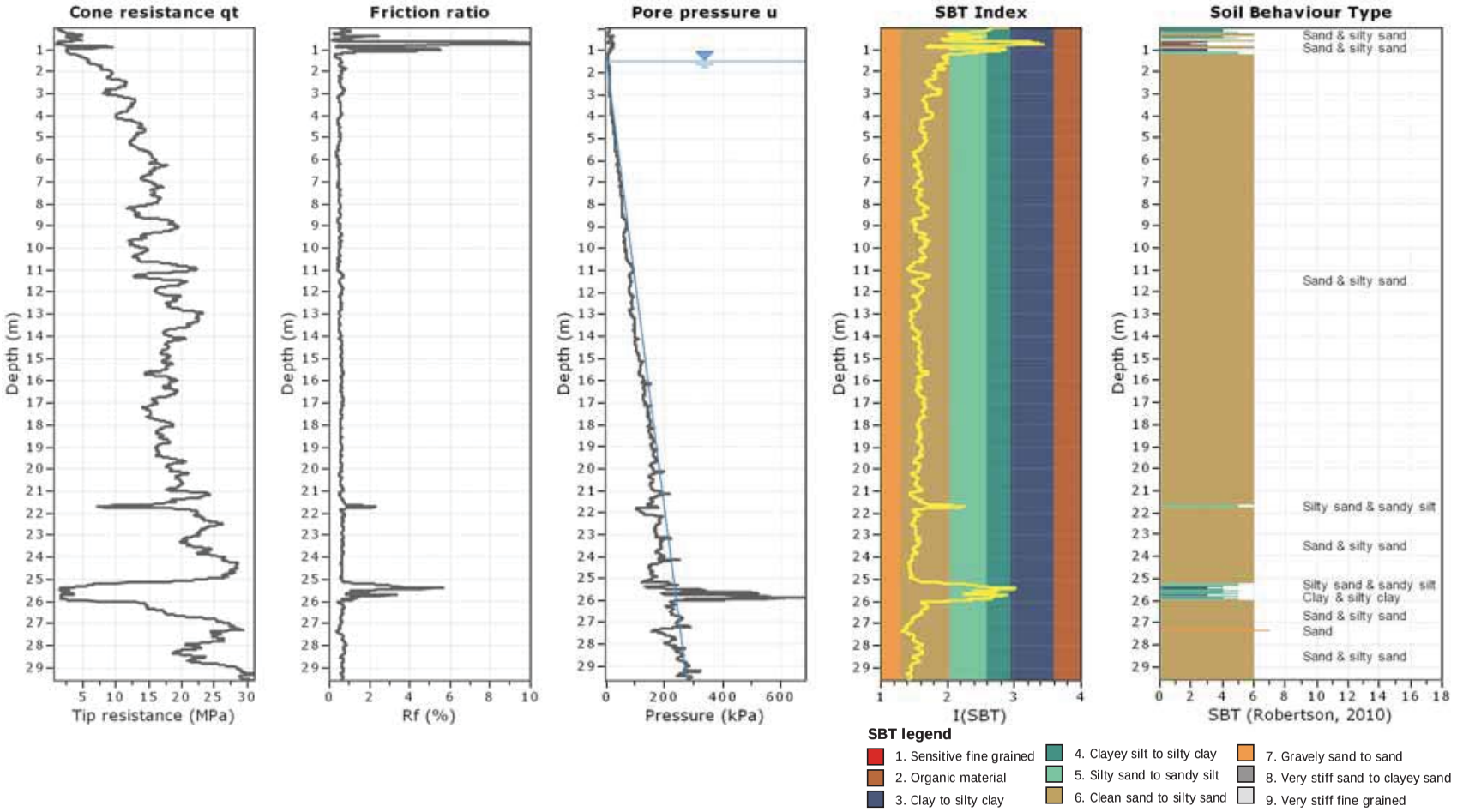

CPT: NNBS_CPT33695(CGD)

Total depth: 29.59 m, Date: 22/07/2014

Coords: S 43.4953, E 172.7181

Cone Operator: Uknown

Project: **Evaluating Fully Nonlinear Stress Site Response Computer Programs using Records from the Canterbury Earthquake Sequence**

Location: **Christchurch, New Zealand**

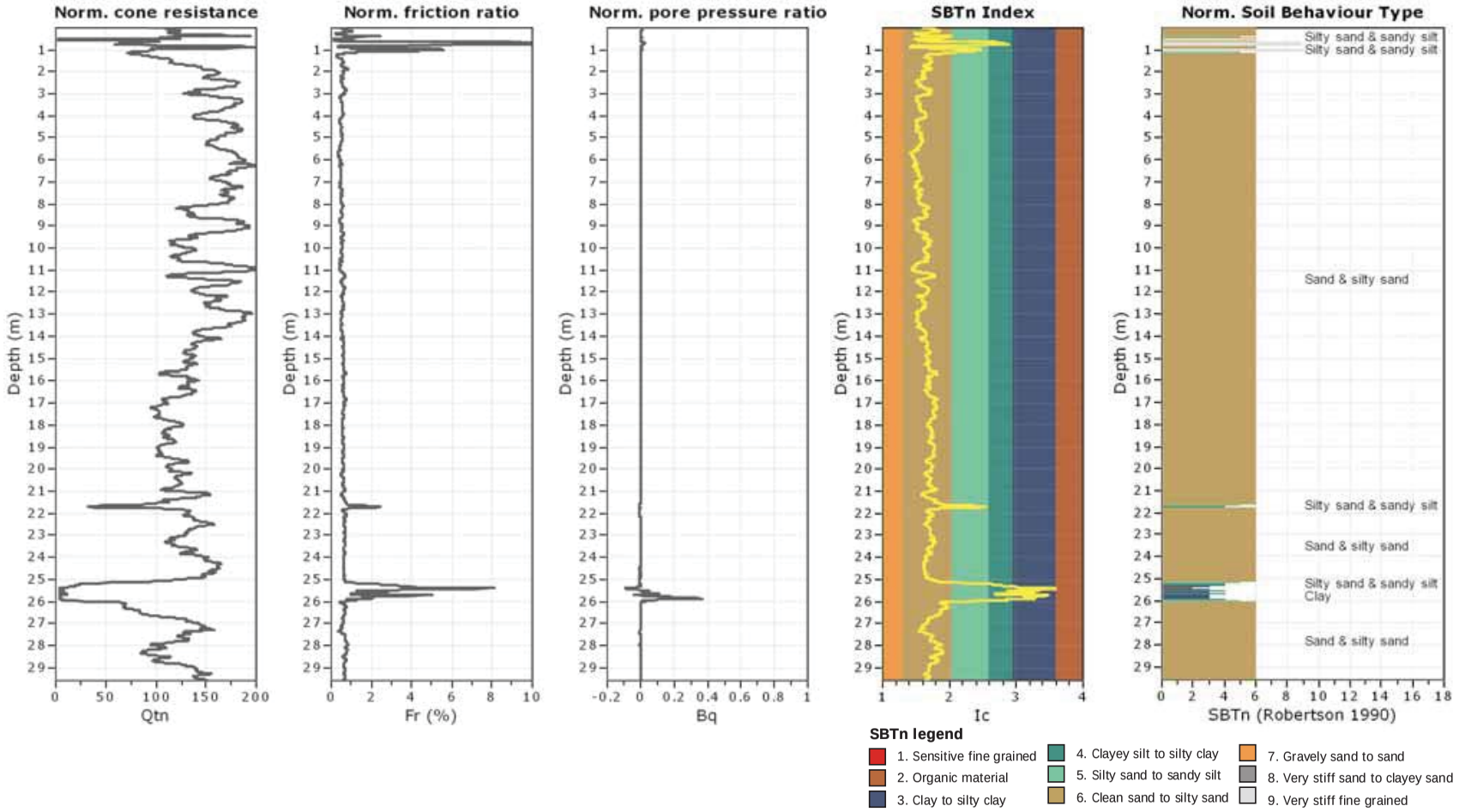

CPT: PPHS_CPT1497(CGD)

Total depth: 10.38 m

Project: **Evaluating Fully Nonlinear Stress Site Response Computer Programs using Records from the Canterbury Earthquake Sequence**

Coords: S 43.4932, E 172.6067

Location: **Christchurch, New Zealand**

Cone Operator: Uknown

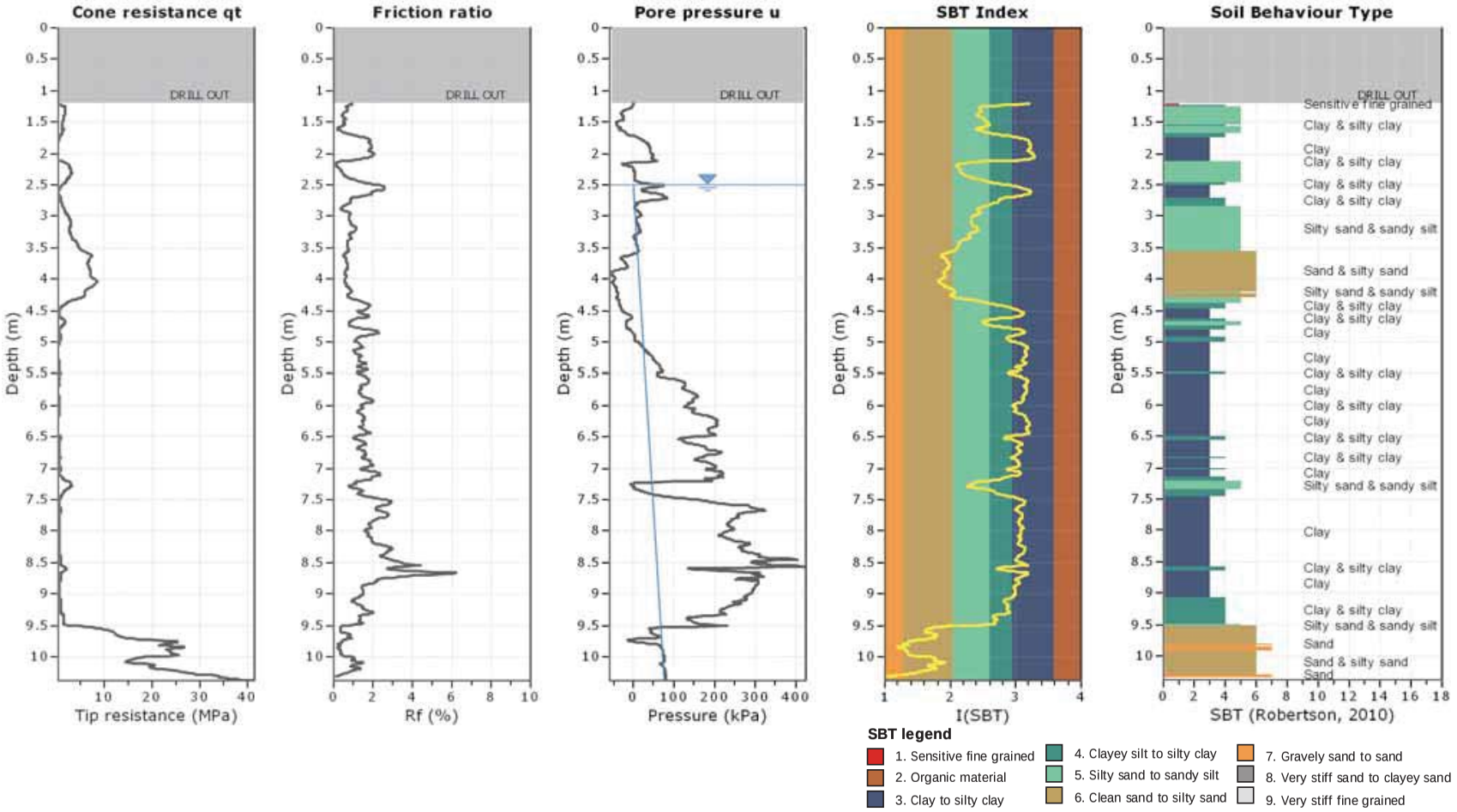

CPeT-IT v.1.7.6.42 - CPTU data presentation & interpretation software - Report created on: 21/08/2014, 04:28:47 p.m.

Project file: C:\Users\User\Desktop\summer\USGS Site Response Project\Soil Profiles and Info\PPHS\Proceed Data\CPT1497(125m)\cpt1497(125m)_2.cpt

CPT: PPHS_CPT1497(CGD)

Total depth: 10.38 m, Date: 13/07/2014

Coords: S 43.4932, E 172.6067

Cone Operator: Uknown

Project: **Evaluating Fully Nonlinear Stress Site Response Computer Programs using Records from the Canterbury Earthquake Sequence**

Location: **Christchurch, New Zealand**

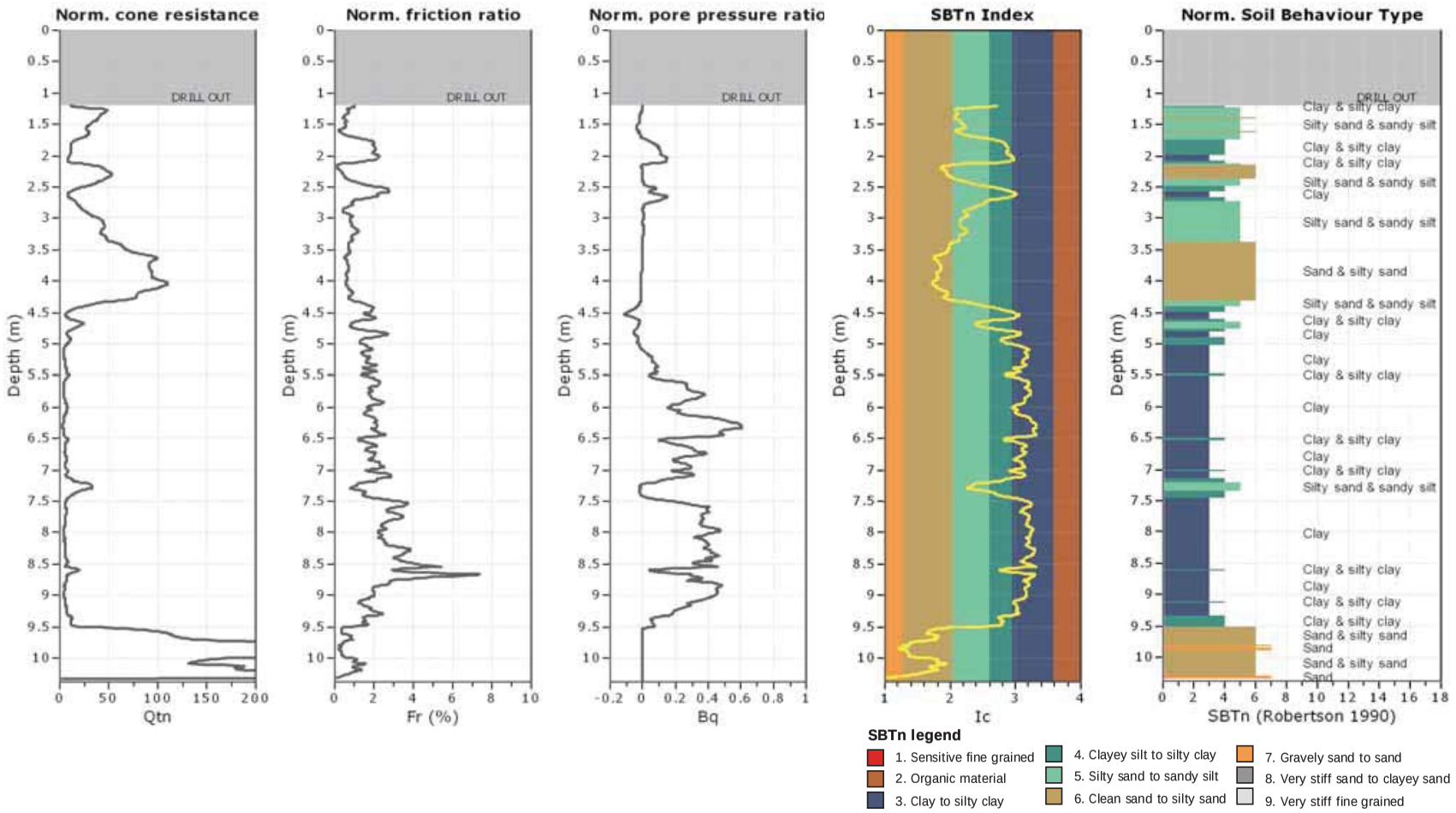

CPeT-IT v.1.7.6.42 - CPTU data presentation & interpretation software - Report created on: 21/08/2014, 04:28:47 p.m.

Project file: C:\Users\User\Desktop\summer\USGS Site Response Project\Soil Profiles and Info\PPHS\Proceed Data\CPT1497(125m)\cpt1497(125m)_2.cpt

CPT: PRPC_CPT1396 (CGD)

Total depth: 28.16 m

Project:

Coords: S 43.5259, E 172.6828

Location:

Cone Operator: Uknown

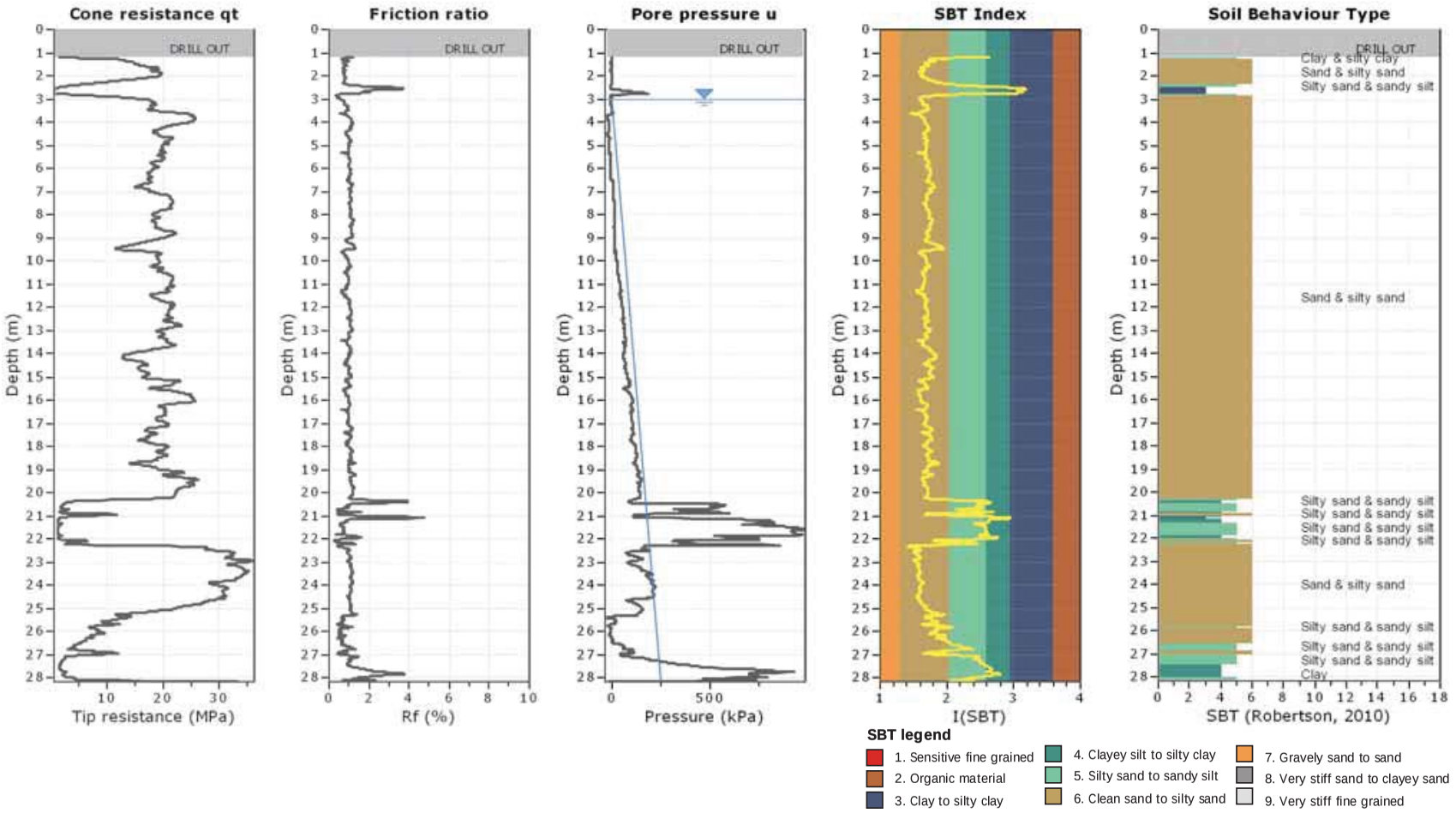

CPeT-IT v.1.7.6.42 - CPTU data presentation & interpretation software - Report created on: 21/08/2014, 04:44:07 p.m.

Project file: C:\Users\User\Desktop\summer\USGS Site Response Project\Soil Profiles and Info\PRPC\Proceced Data\CPT 39 TT\CPT39TT_2.cpt

CPT: PRPC_CPT1396 (CGD)

Total depth: 28.16 m, Date: 18/07/2014

Coords: S 43.5259, E 172.6828

Cone Operator: Uknown

Project:

Location:

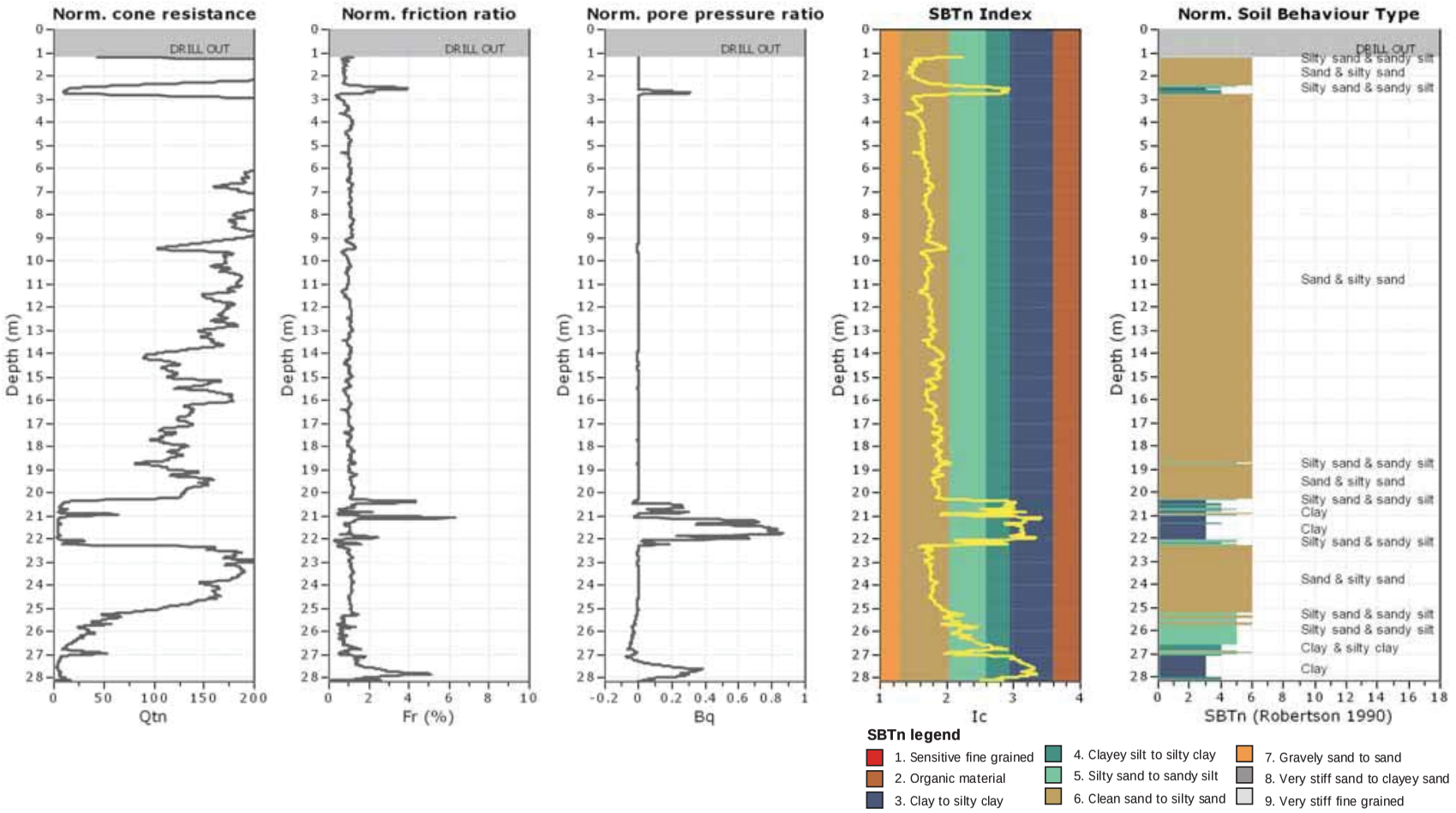

CPeT-IT v.1.7.6.42 - CPTU data presentation & interpretation software - Report created on: 21/08/2014, 04:44:07 p.m.

Project file: C:\Users\User\Desktop\summer\USGS Site Response Project\Soil Profiles and Info\PRPC\Proceed Data\CPT 39 TT\CPT39TT_2.cpt

CPT: REHS_CPT2 (Wotherspoon,2013)

Total depth: 19.76 m

Project: **Evaluating Fully Nonlinear Effective Stress Site Resonse Computer Programs using Records from the Canterbury Earthquake Sequence**

Coords: S 43.5220, E172.6351

Location: **Christchurch, New Zealand**

Cone Operator: Uknown

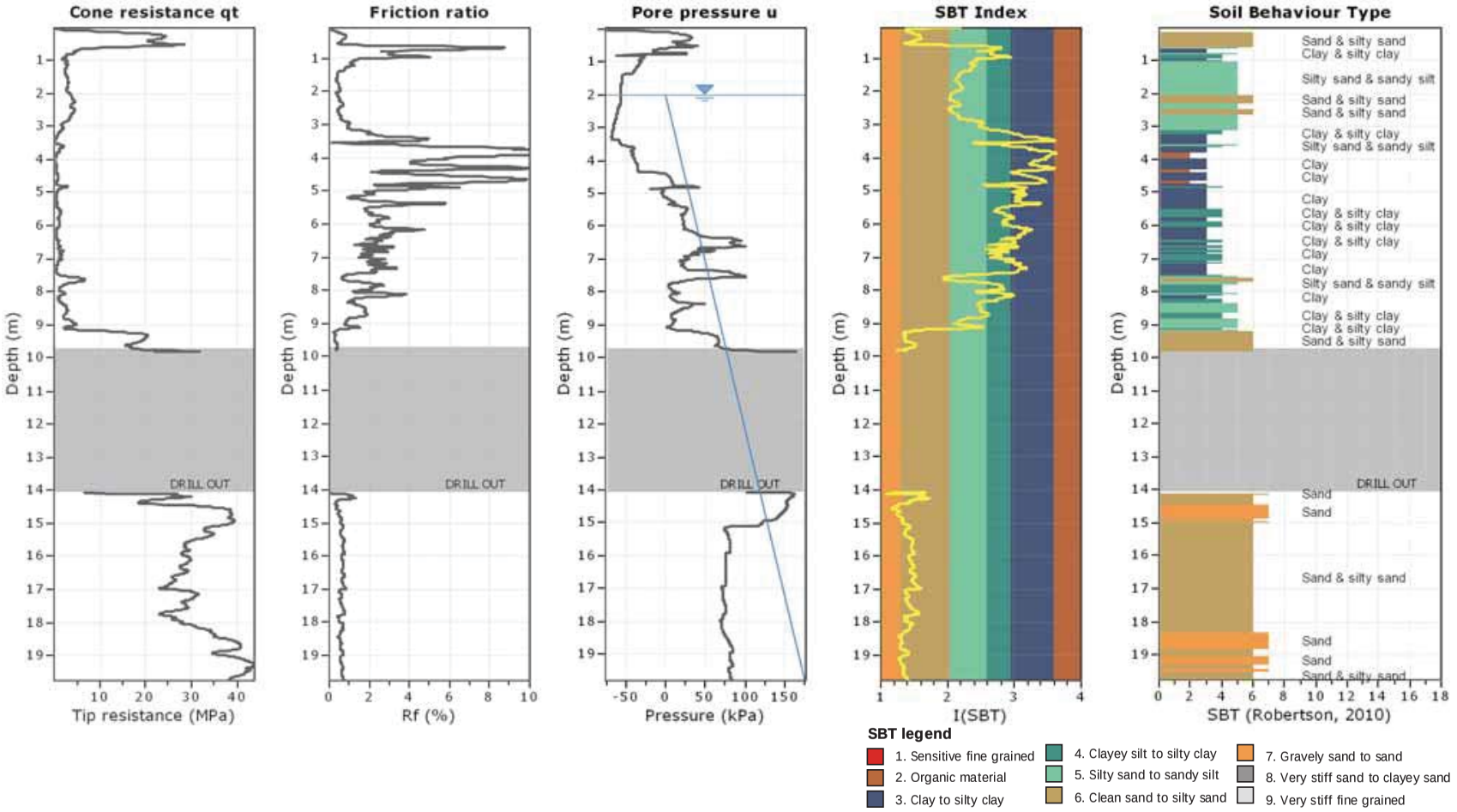

CPeT-IT v.1.7.6.42 - CPTU data presentation & interpretation software - Report created on: 21/08/2014, 01:28:45 a.m.

Project file: C:\Users\User\Desktop\summer\USGS Site Response Project\Soil Profiles and Info\REHS\Proceed Data\Wotherspoon\REHC_CPT1_CPT1a_2.cpt

CPT: REHS_CPT2 (Wotherspoon,2013)

Total depth: 19.76 m, Date: 06/07/2014

Coords: S 43.5220, E172.6351

Cone Operator: Uknown

Project: **Evaluating Fully Nonlinear Effective Stress Site Resonse Computer Programs using Records from the Canterbury Earthquake Sequence**

Location: **Christchurch, New Zealand**

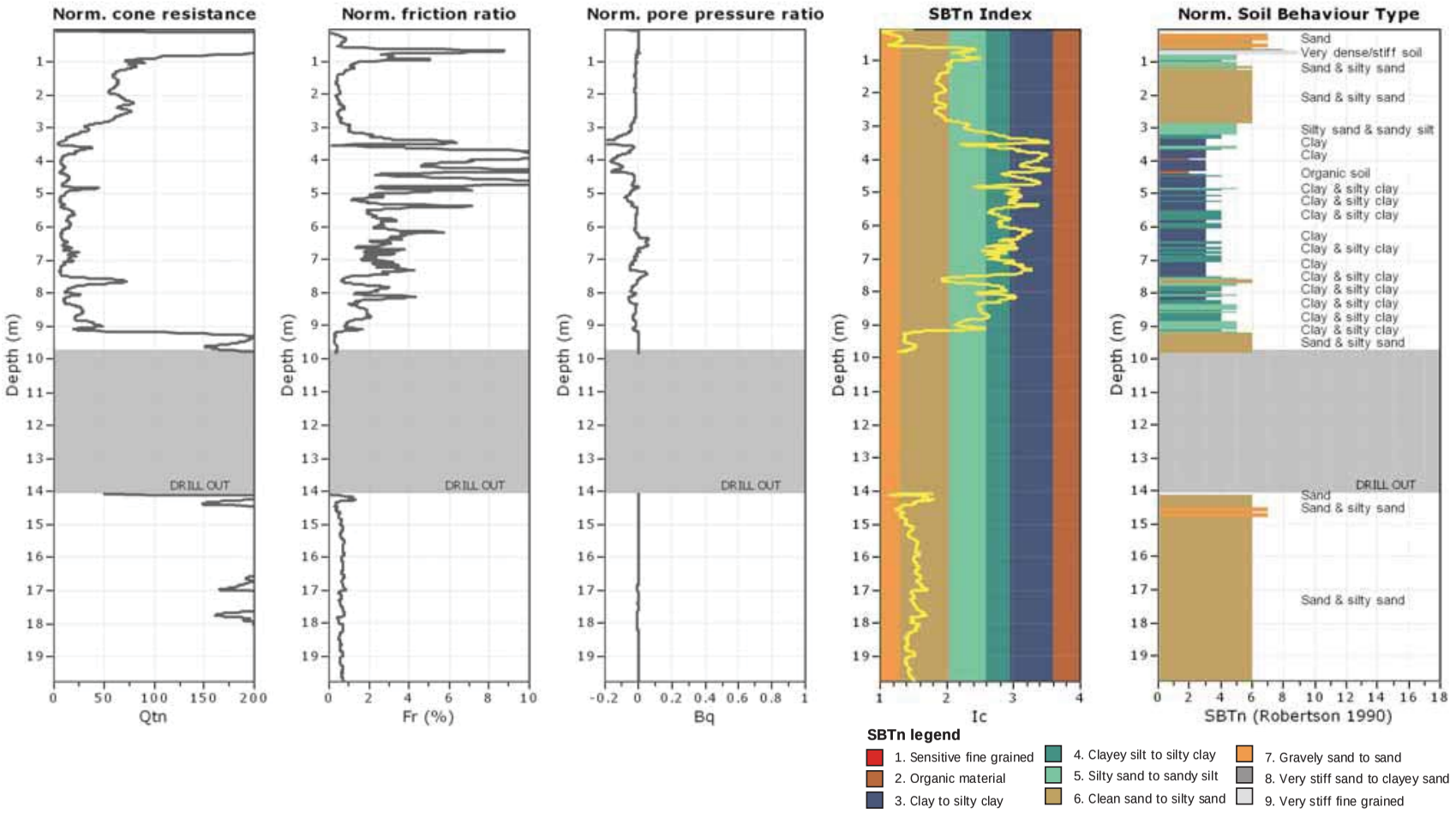

CPeT-IT v.1.7.6.42 - CPTU data presentation & interpretation software - Report created on: 21/08/2014, 01:28:45 a.m.

Project file: C:\Users\User\Desktop\summer\USGS Site Response Project\Soil Profiles and Info\REHS\Proceed Data\Wotherspoon\REHC_CPT1_CPT1a_2.cpt

CPT: SHLC_CPT626(CGD)

Total depth: 27.58 m

Project: **Evaluating Fully Nonlinear Effective Stress Site Resonse Computer Programs using Records from the Canterbury Earthquake Sequence**

Coords: S 43.5054, E 172.6628

Location: **Christchurch, New Zealand**

Cone Operator: Uknown

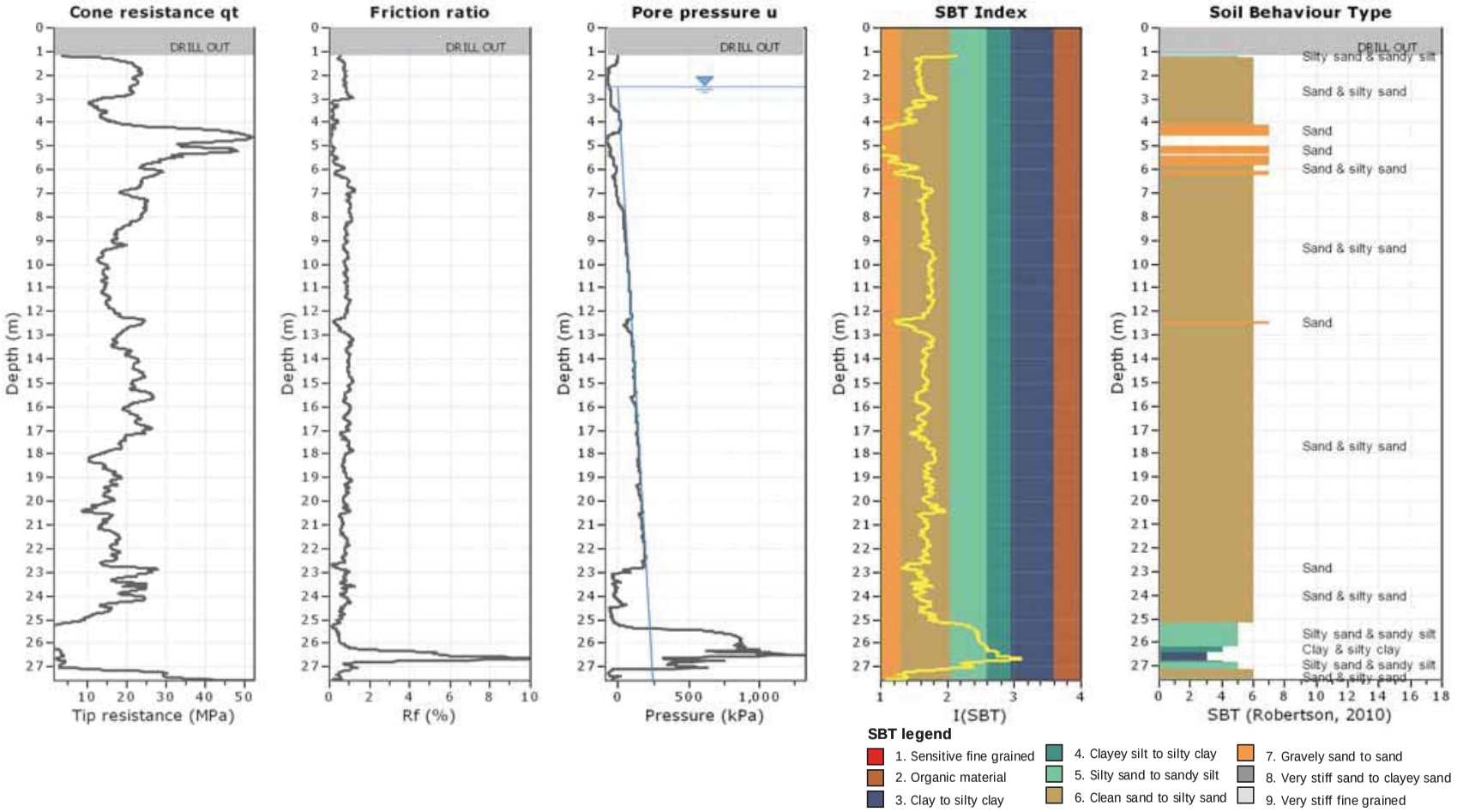

CPeT-IT v.1.7.6.42 - CPTU data presentation & interpretation software - Report created on: 21/08/2014, 04:39:13 p.m.

Project file: C:\Users\User\Desktop\summer\USGS Site Response Project\Soil Profiles and Info\SHLC\Proceed Data\CPT626(50m)\CPT626(50m)_2.cpt

CPT: SHLC_CPT626(CGD)

Total depth: 27.58 m, Date: 11/07/2014

Coords: S 43.5054, E 172.6628

Cone Operator: Uknown

Project: **Evaluating Fully Nonlinear Effective Stress Site Resonse Computer Programs using Records from the Canterbury Earthquake Sequence**

Location: **Christchurch, New Zealand**

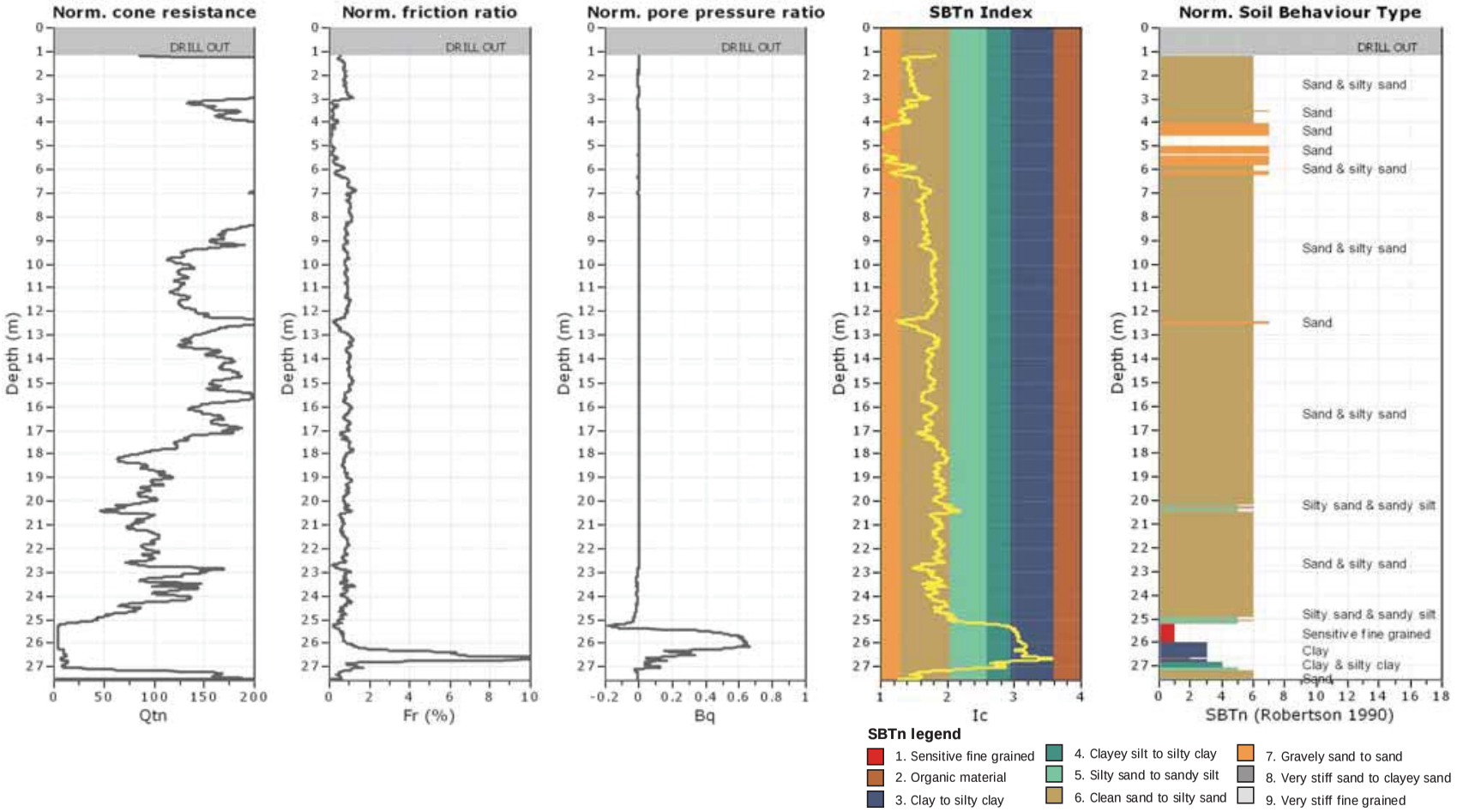

Appendix A.2.2

Shear Wave Velocity Profiles for Strong Motion Station Sites

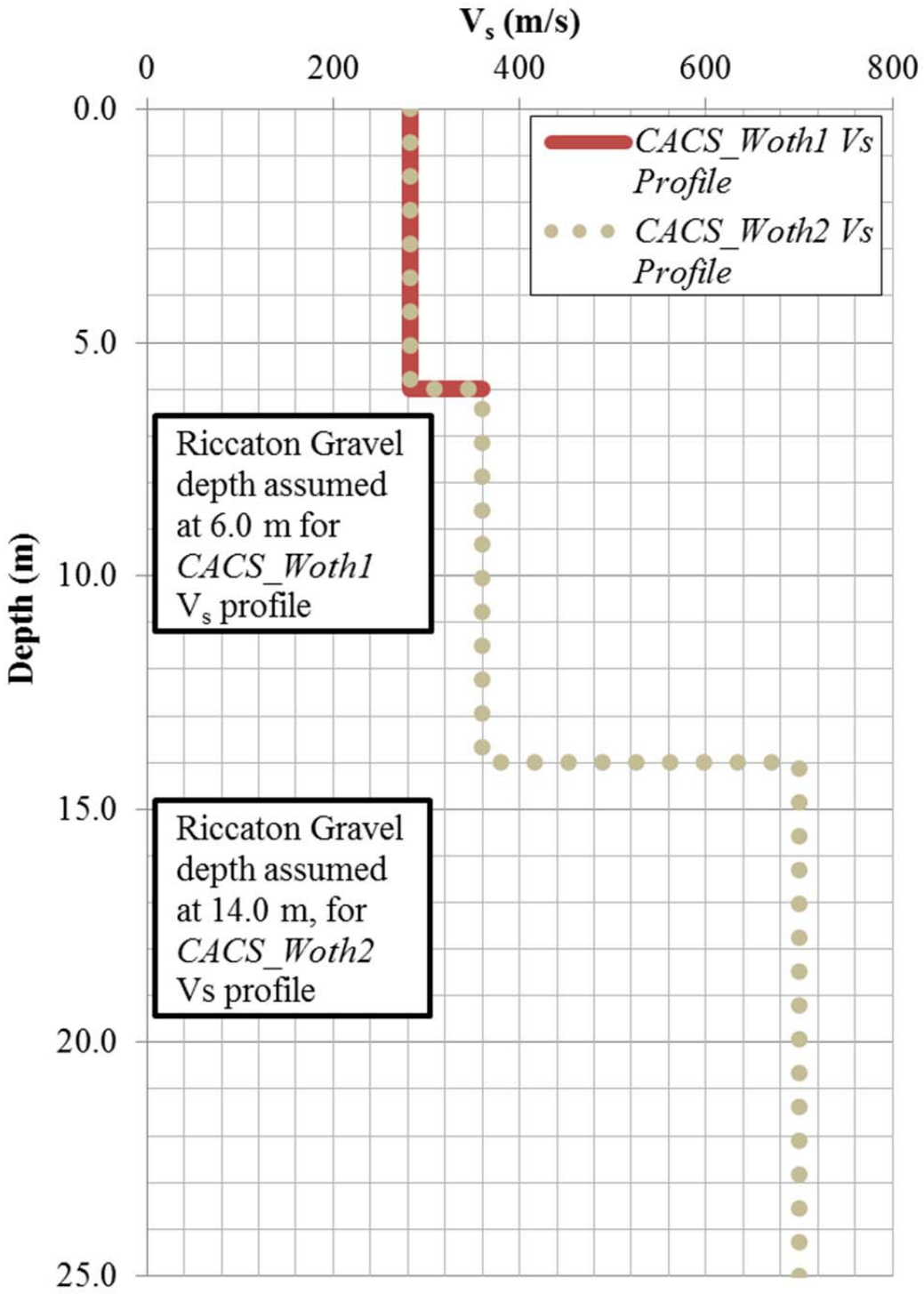

CACS V_s Profile

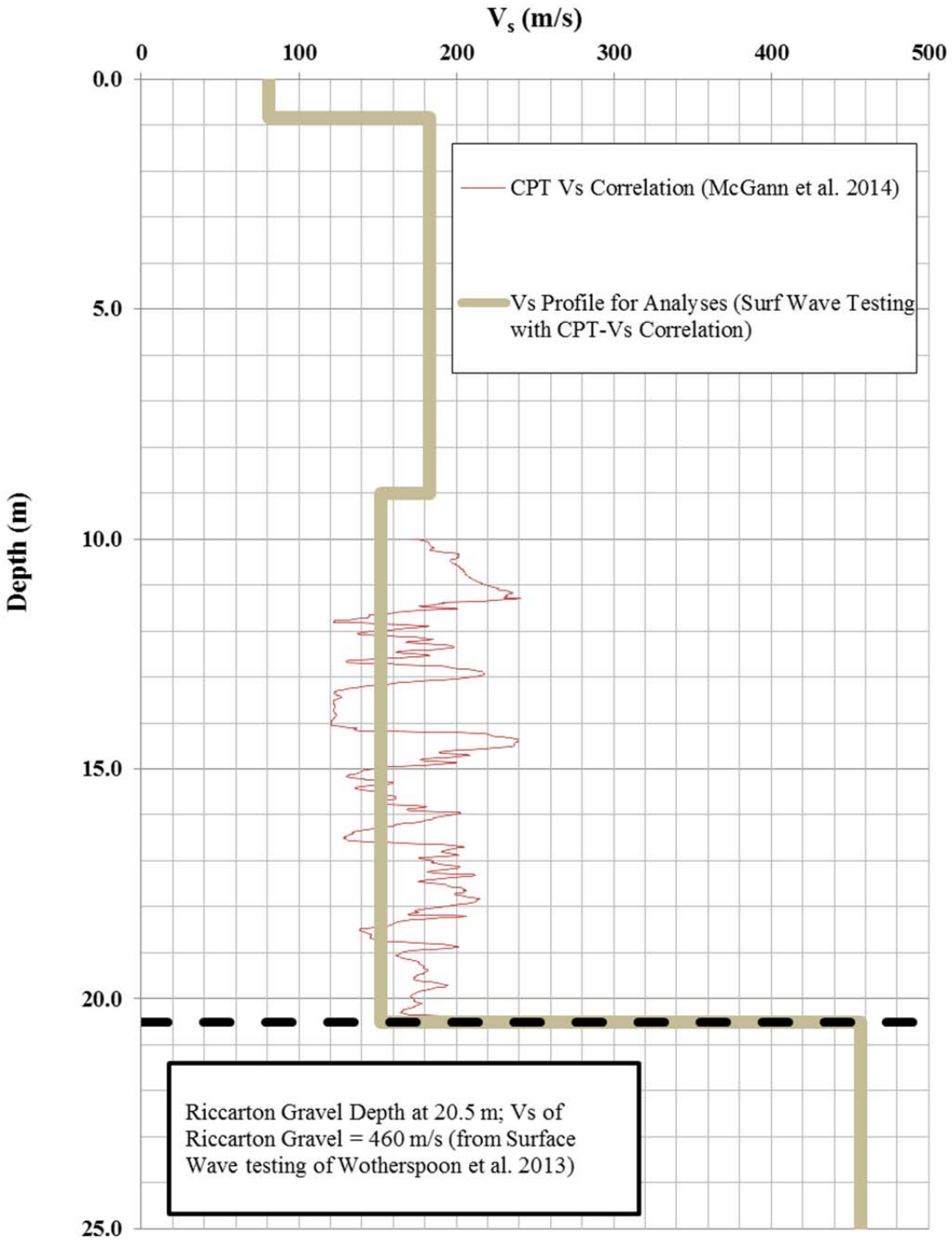

CBGS V_s Profile

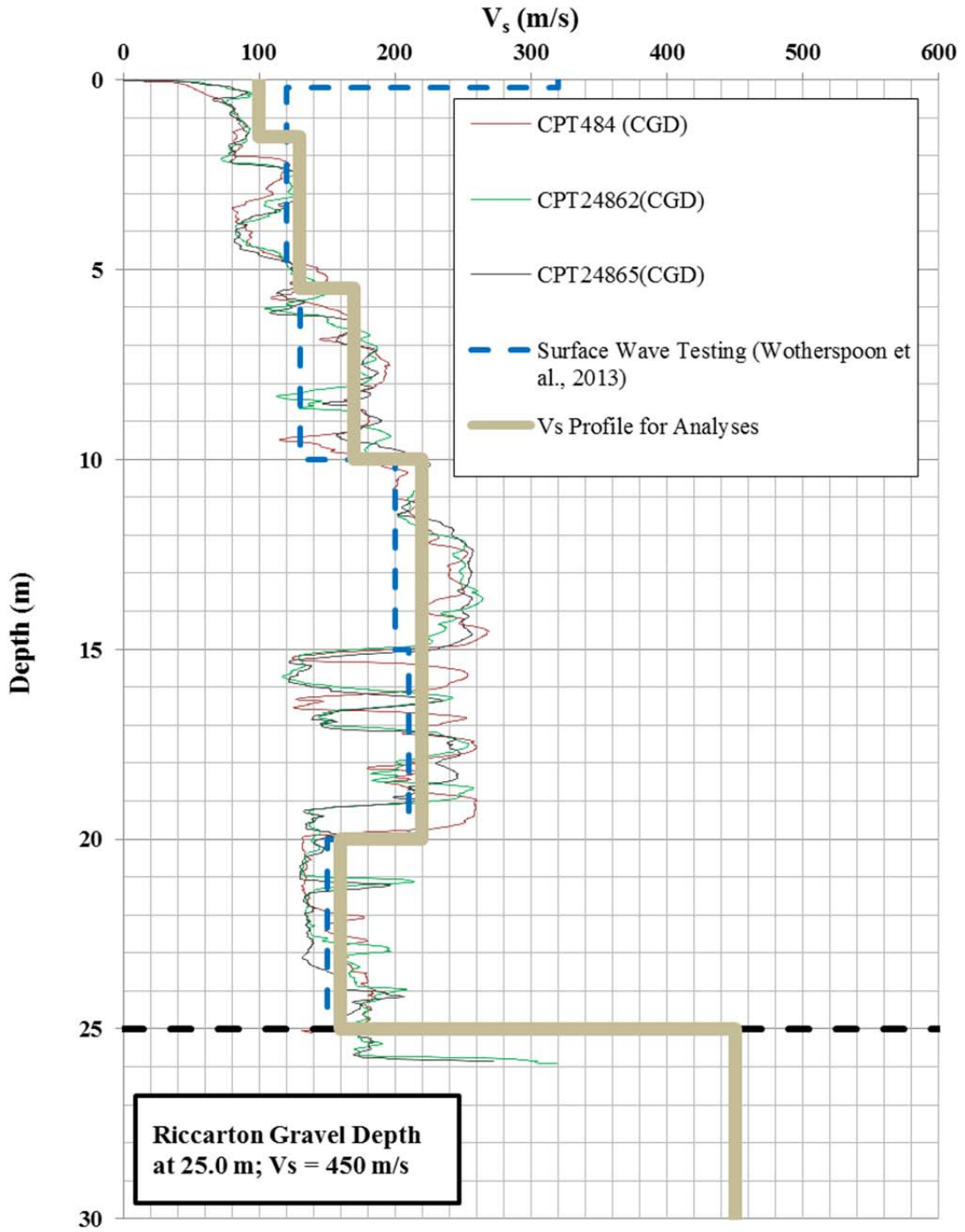

CCCC V_s Profile

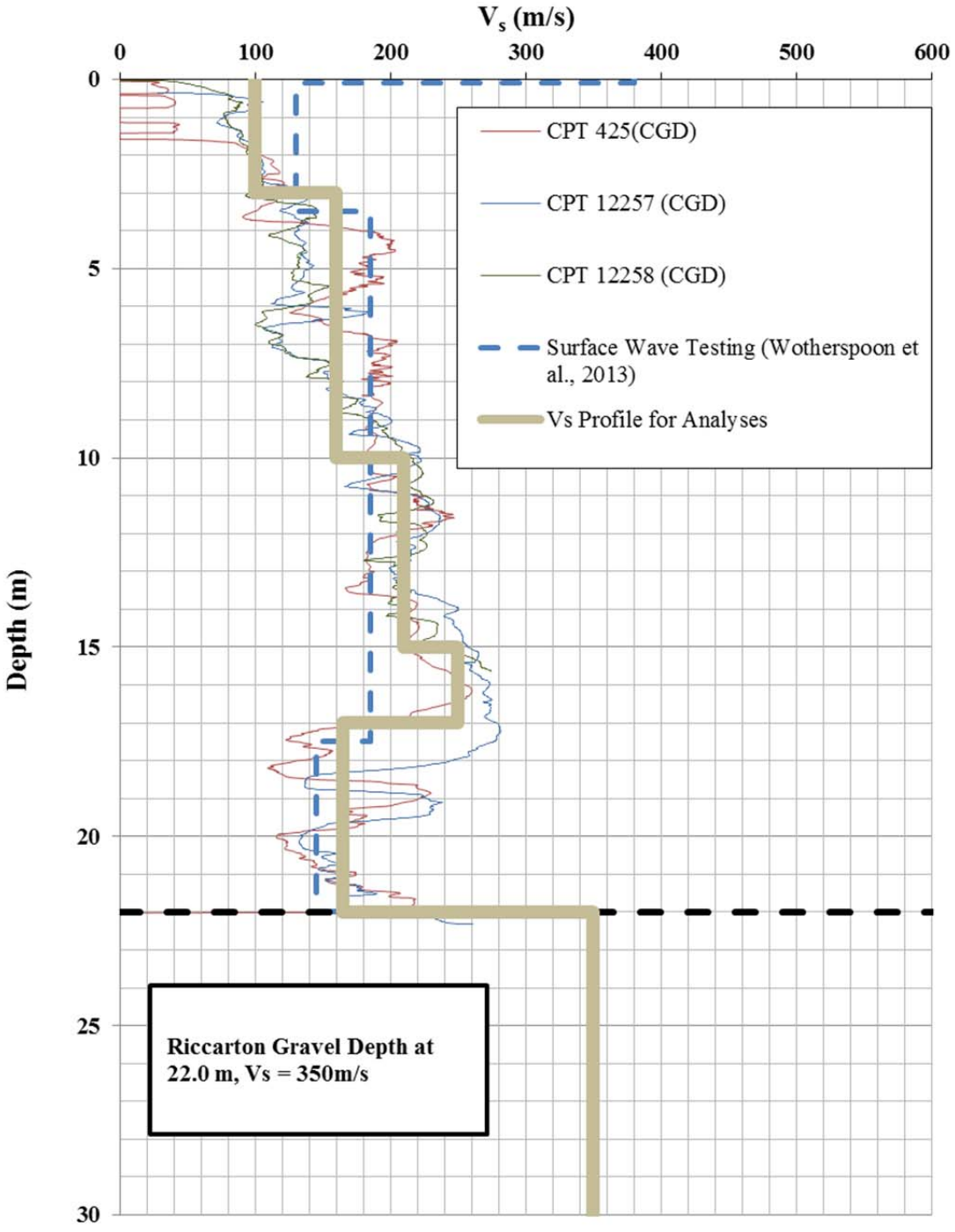

CHHC V_s Profile

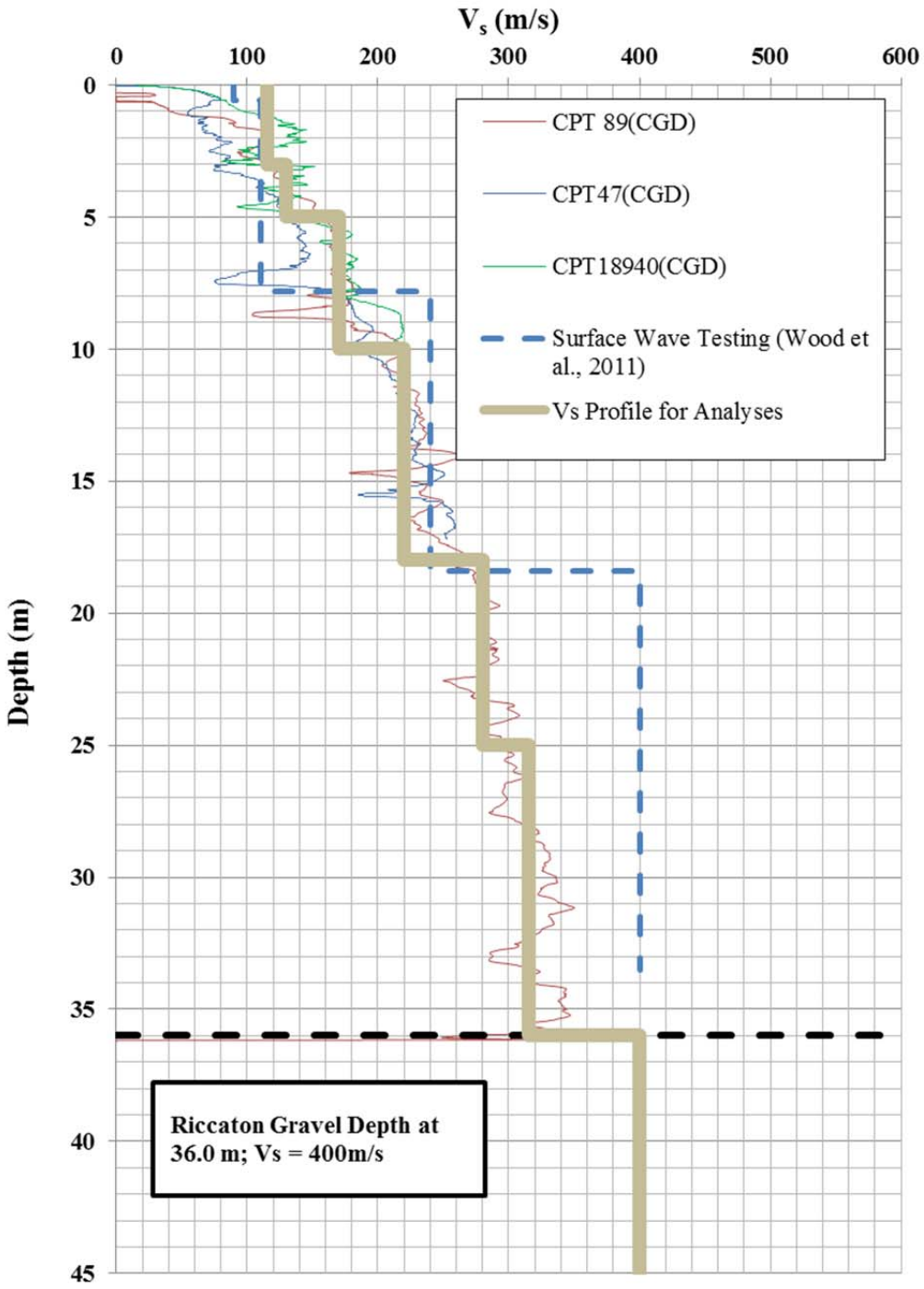

HPSC V_s Profile

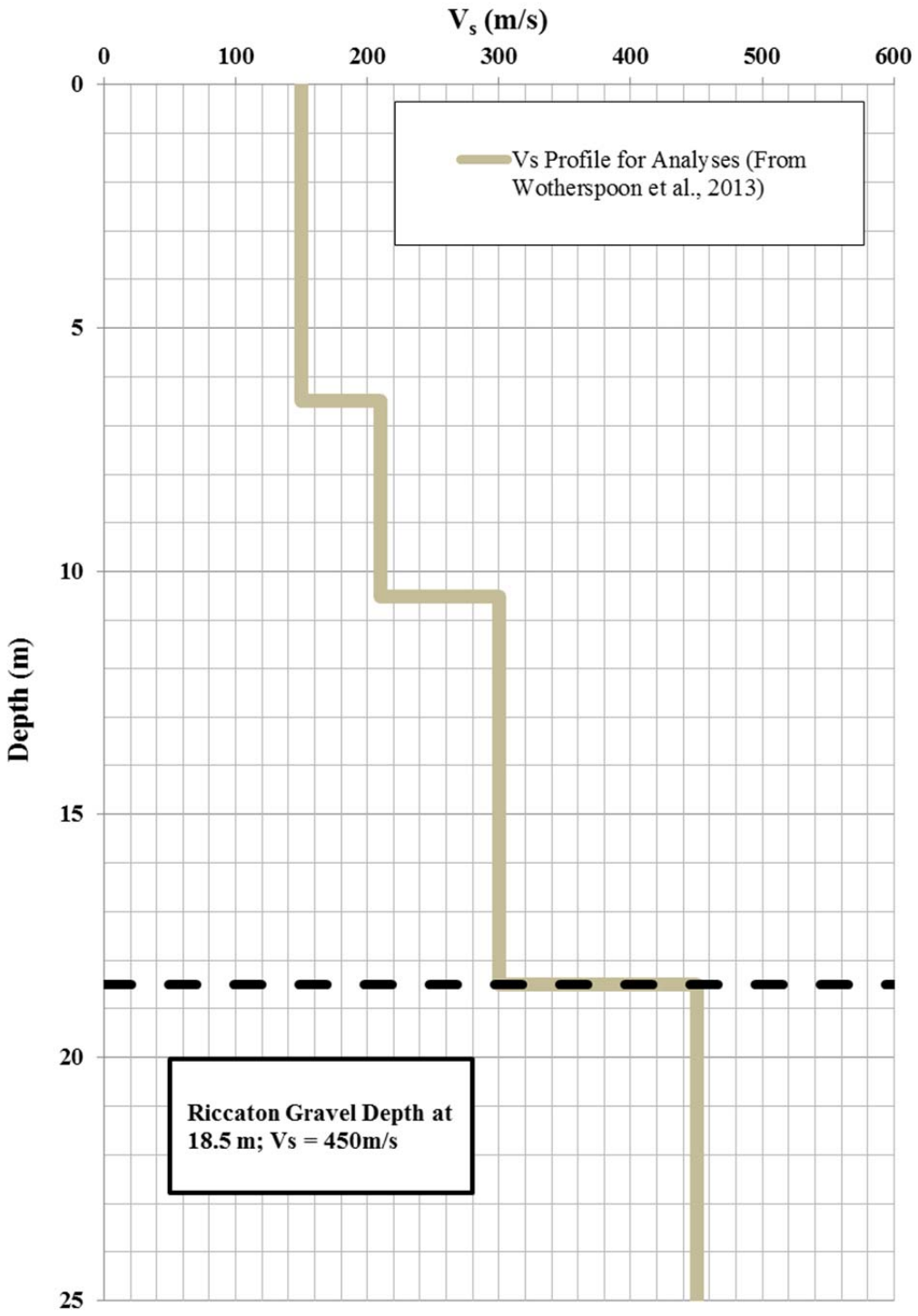

KPOC V_s Profile

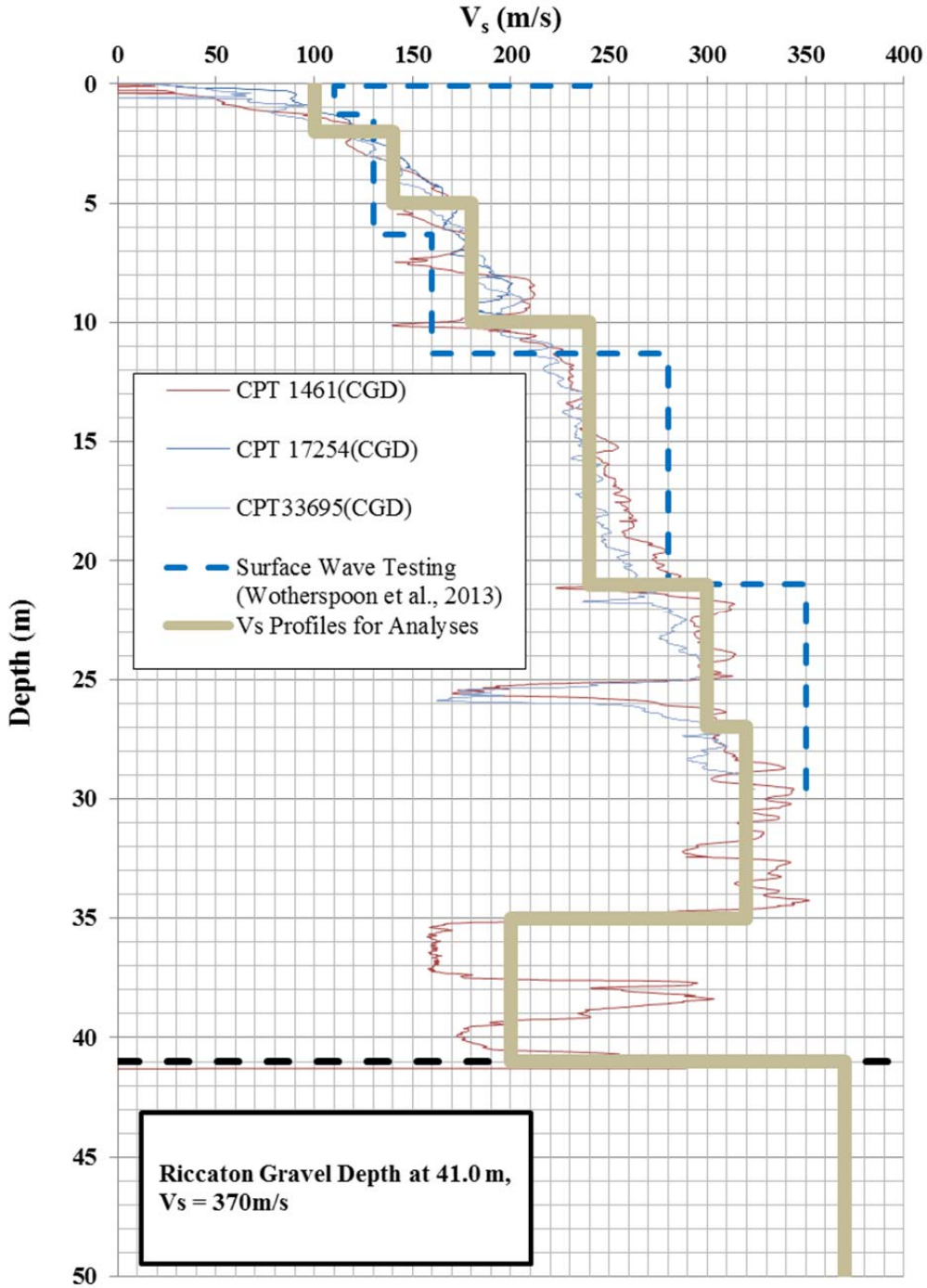

NNBS V_s Profile

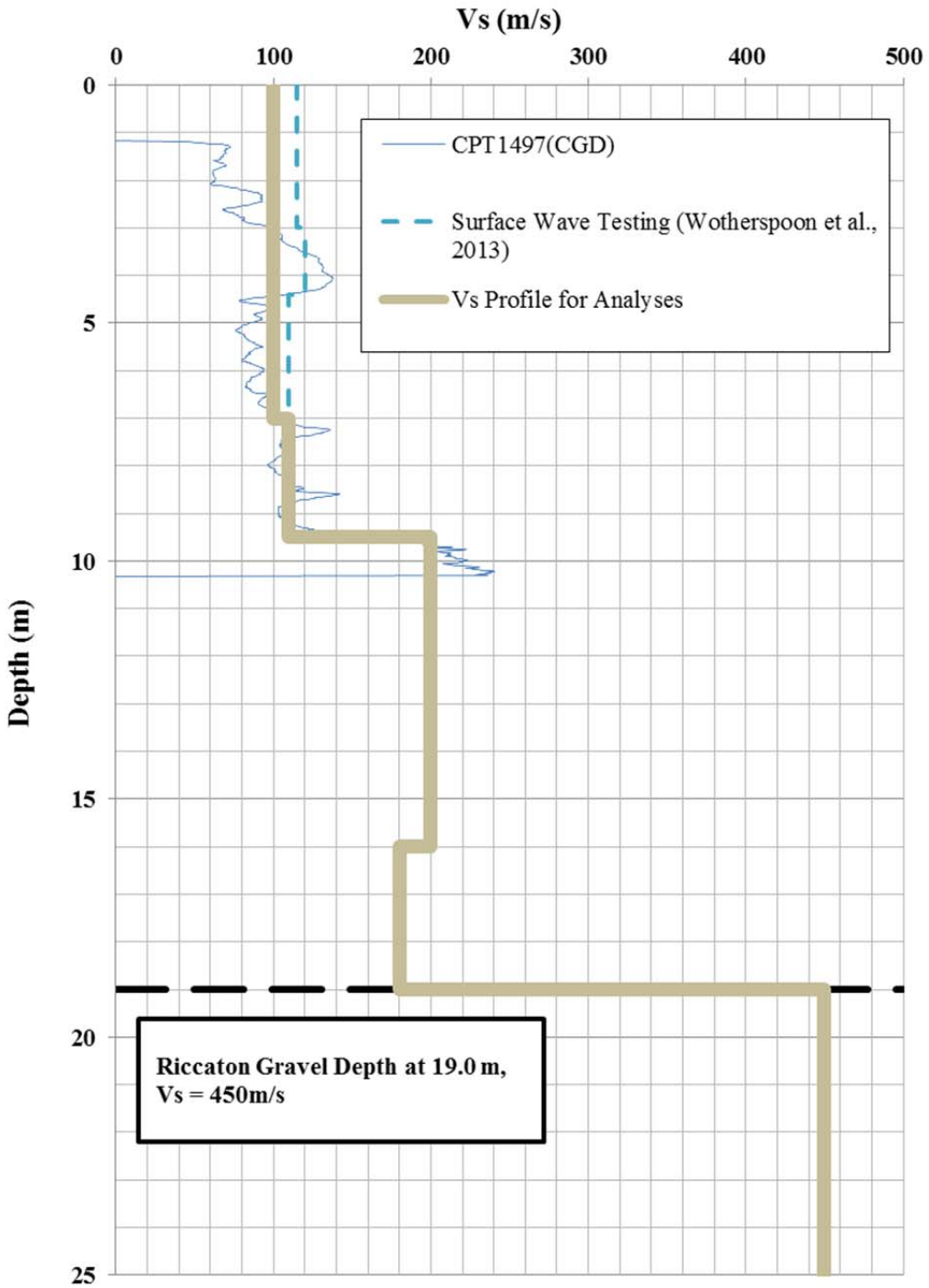

PPHS V_s Profile

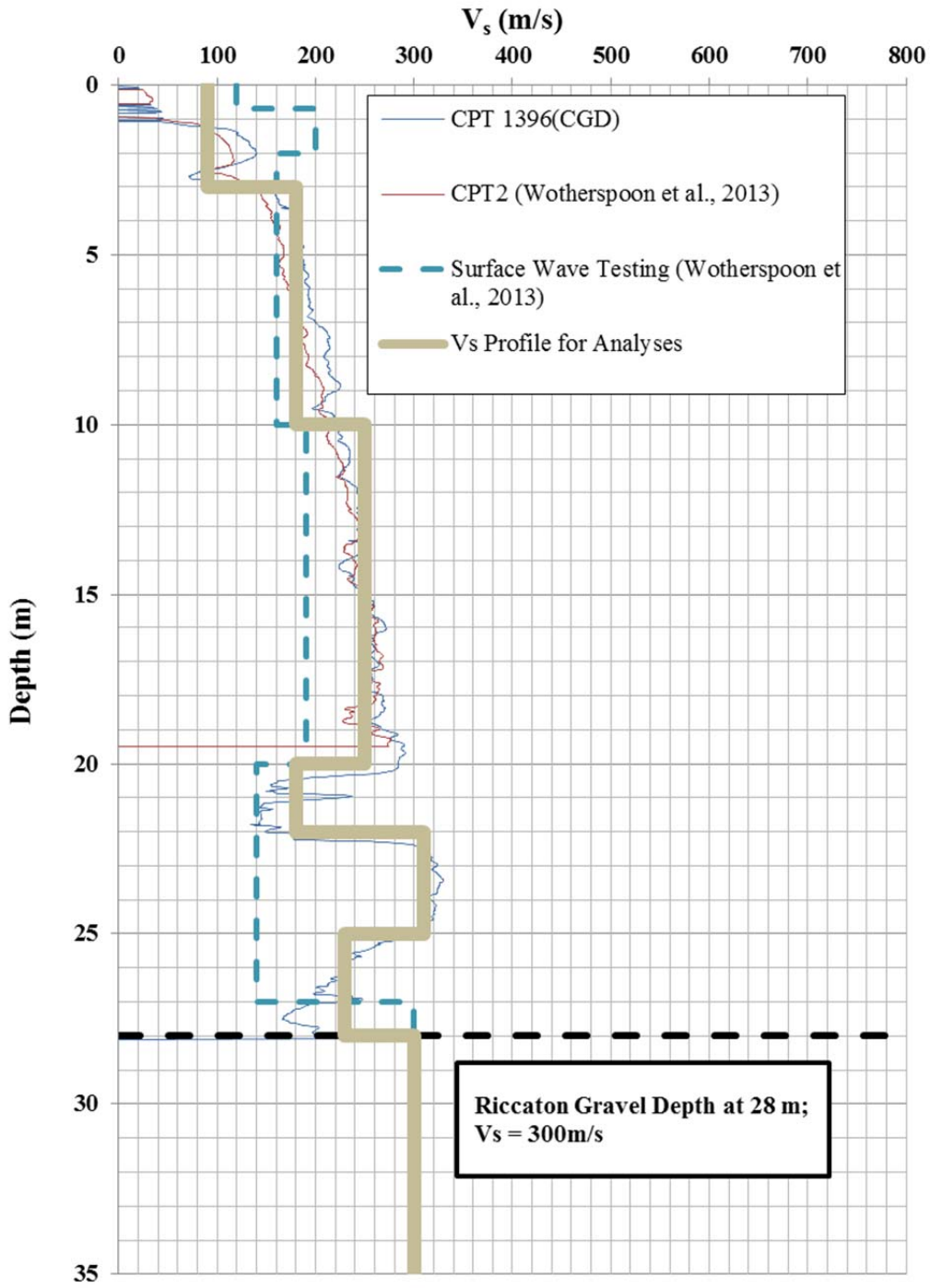

PRPC V_s Profile

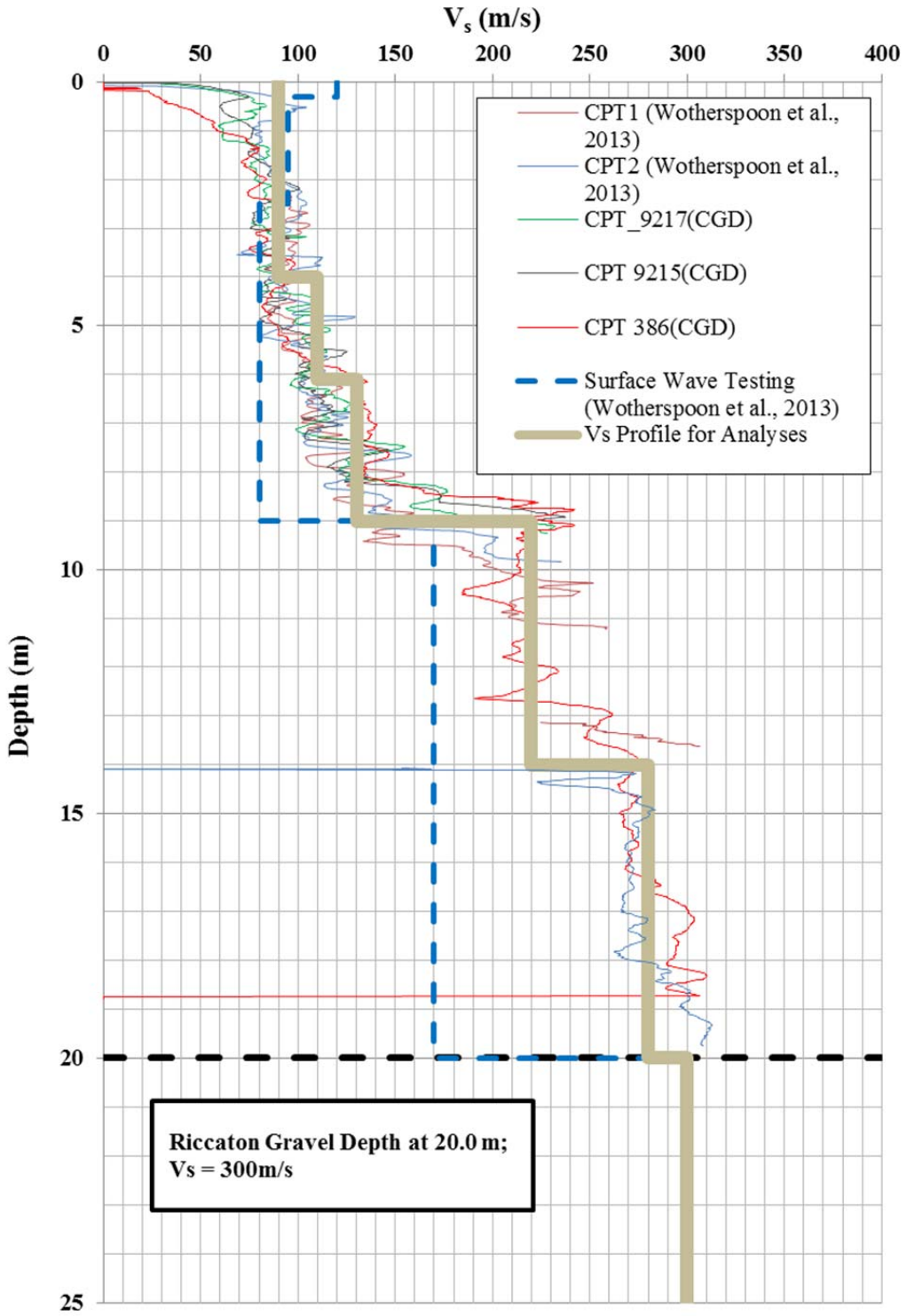

REHS V_s Profile

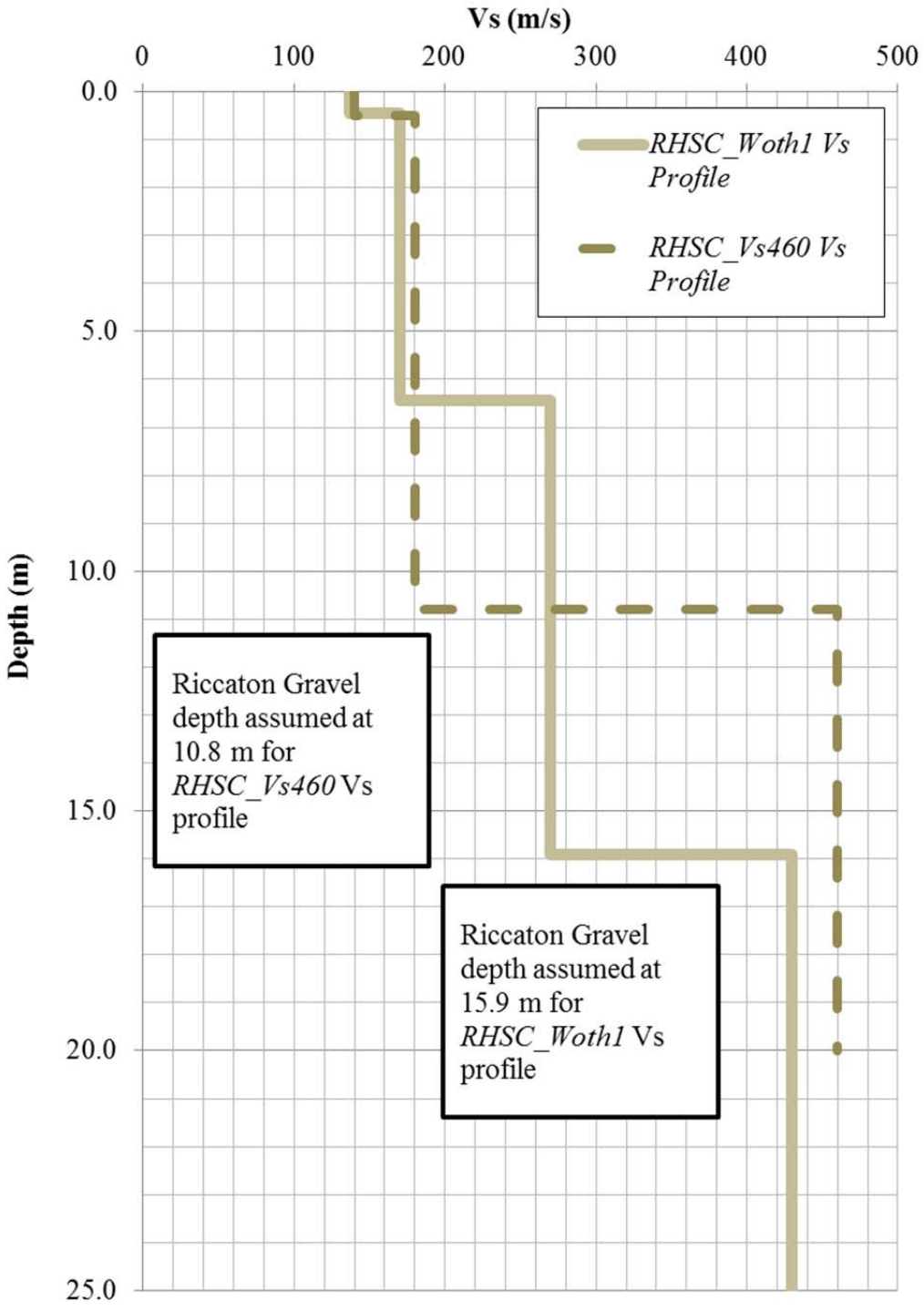

RHSC V_s Profile

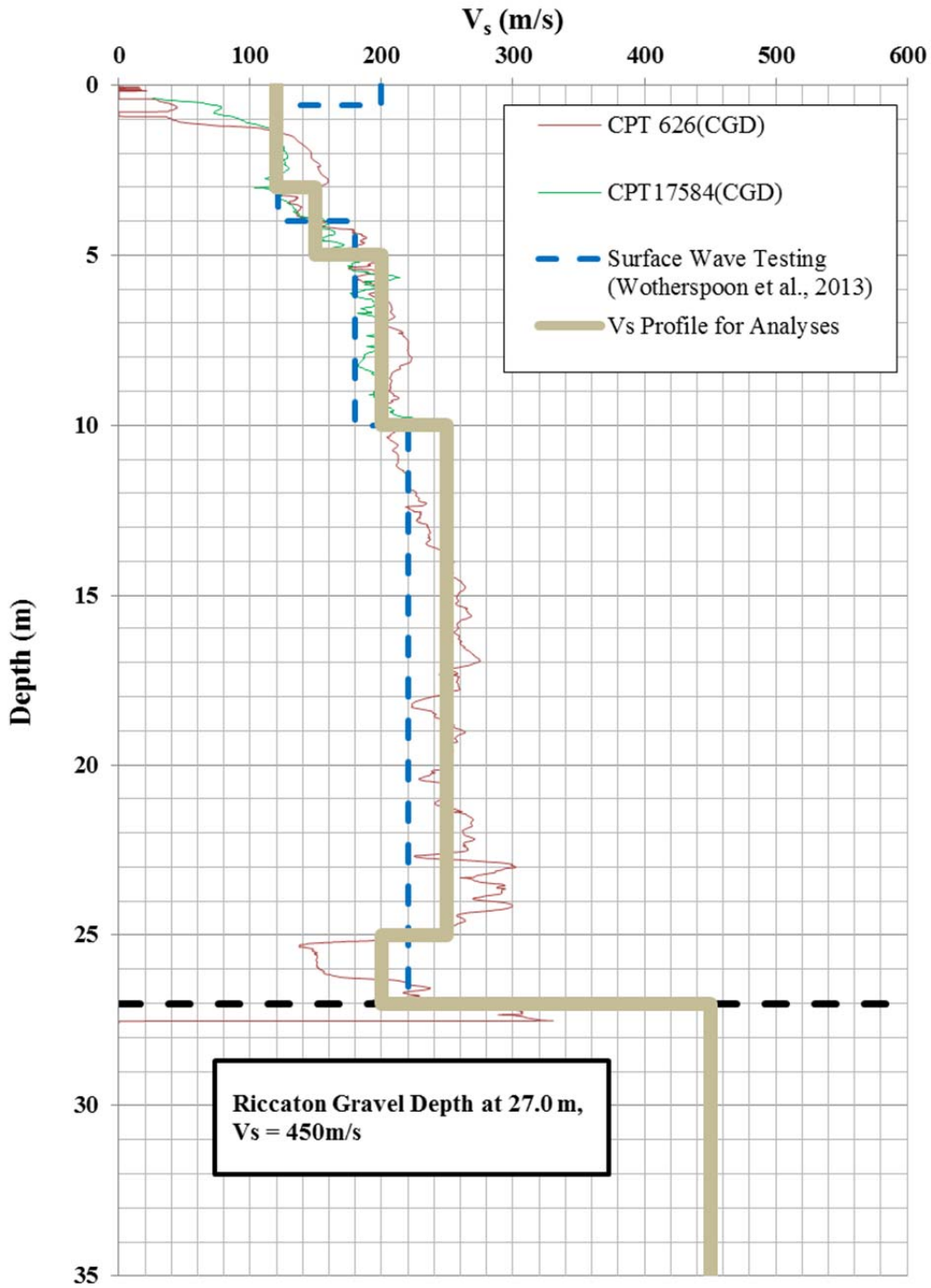

SHLC V_s Profile

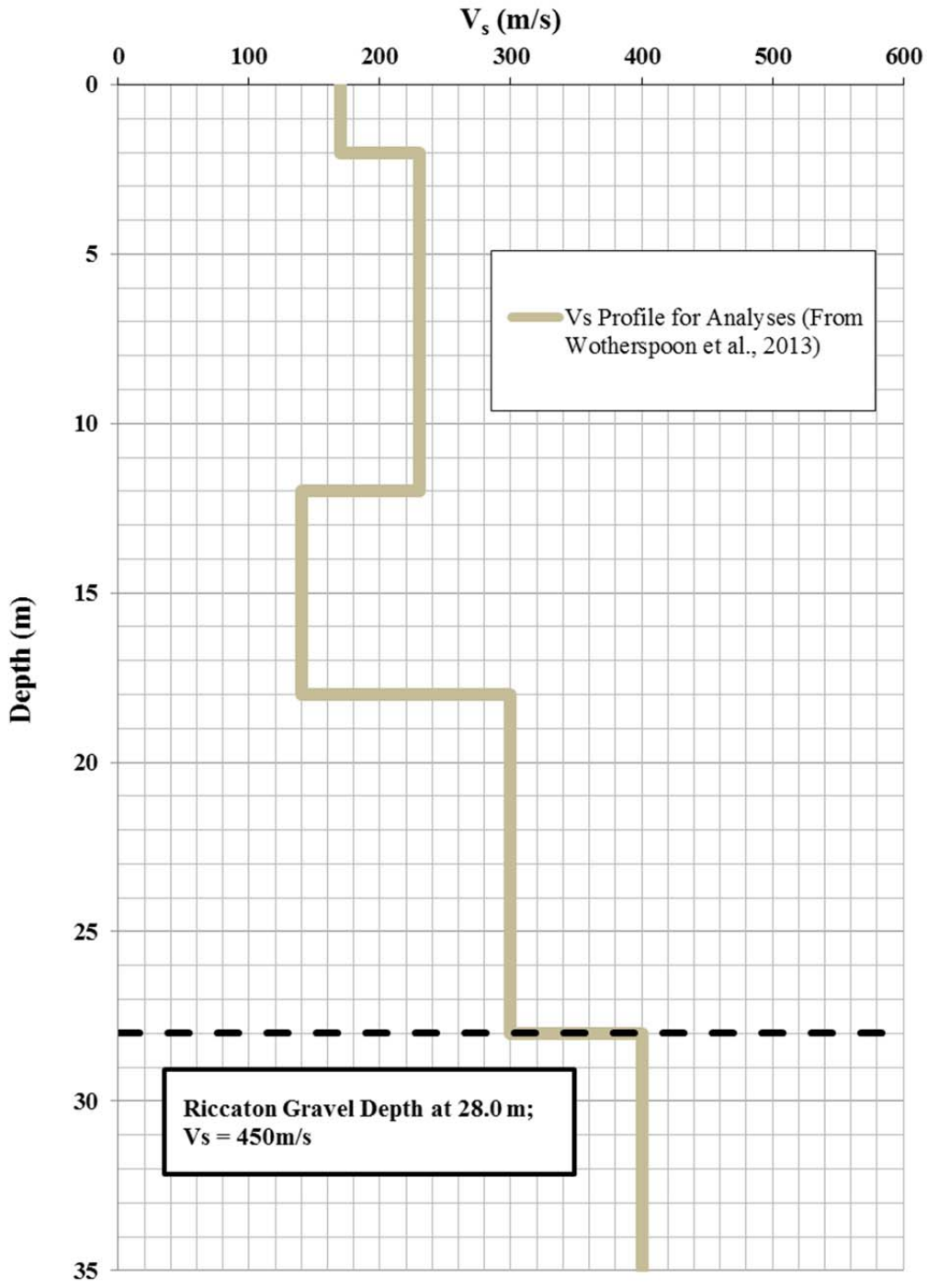

SMTC V_s Profile

Appendix A.3

Deconvolved Riccarton Gravel Motions

Deconvolved Riccarton Gravel motions used as input motions for site response analyses are included as separate electronic files attached to this dissertation

Appendix A.4

Parameters for Site Response Analyses

Notes:

1) Tables include parameters used for effective stress, total stress, and equivalent linear analyses as well as parameters used to calculate the strain dependent soil properties (G/Gmax and λ) based on the Darendeli (2001) model. Also included are the assumed strength values for sublayers, which is used in the strength correction of the modulus reduction and damping curves (using the Yee et al. 2013 procedure).

2) Parameters for site response analyses include:
    - γ: Unit weight of soil
    - V_s: Shear wave velocity
    - C_v: Coefficient of consolidation
    - OCR: Overconsolidation ratio (for Darendeli 2001 model)
    - PI: Plasticity index of soil (for Darendeli 2001 model)
    - σ'_m: Mean effective stress (for Darendeli 2001 model)
    - τ: Assumed shear strength of soil (Yee et al. 2013 procedure)
    - See Hashash (2012). "DeepSoil V5.1, User Manual and Tutorial 2002-2012" for an explanation of the remaining parameters used in nonlinear site response analyses

Table C. 1: Parameters for Nonlinear Seismic Site Response Analyses CBGS

Layer #	Thickness (m)	γ (kN/m^3)	Vs (m/s)	Damping Ratio (%)	Ref Strain (%)	Ref Stress (MPa)	Beta	s	b	d	Max r_u	PWP Model	f/s/f	p/r/Dr(%)	F/A/FC(%)	s/B/-	g/C/-	v/D/v	-/g/-	C_v (m^2/s)	P1	P2	P3
1	0.42	17.3	81	2.2204	0.017	0.18	1.47	0.84	0	0	0.99	1	2	0	1	1	0.0051	3.8		9.30E-03	0.76	0.32	1.15
2	0.42	17.3	81	1.5132	0.031	0.18	1.55	0.74	0	0	0.99	1	2	0	1	1	0.0074	3.8		9.30E-03	0.79	0.24	1.55
3	0.65	17.3	183	1.4087	0.0284	0.18	1.46	0.9	0	0	0.99	1	2	0	1	1	0.0094	3.8		9.30E-03	0.59	0.2	3.25
4	1.00	17.3	183	1.1693	0.0418	0.18	1.55	0.86	0	0	0.99	1	2	0	1	1	0.0122	3.8		9.30E-03	0.76	0.33	1
5	1.50	19.6	183	1.0382	0.045	0.18	1.5	0.83	0	0	0.99	1	2	1	1.1861	1	0.0130	3.8		9.30E-03	0.68	0.22	1.6
6	1.50	19.6	183	0.9331	0.0536	0.18	1.53	0.8	0	0	0.99	1	2	1	1.1861	1	0.0144	3.8		9.30E-03	0.79	0.29	0.85
7	1.50	19.6	183	0.8862	0.0612	0.18	1.55	0.78	0	0	0.99	1	2	1	1.1861	1	0.0158	3.8		9.30E-03	0.71	0.2	1.35
8	1.50	19.6	183	0.8056	0.0632	0.18	1.53	0.75	0	0	0.99	1	2	1	1.1861	1	0.0157	3.8		9.30E-03	0.78	0.24	1.45
9	0.50	19.6	183	0.7694	0.0542	0.18	1.31	0.74	0	0	0.99	1	2	1	1.1861	1	0.0163	3.8		9.30E-03	0.8	0.24	1.35
10	1.50	19.6	152	0.7299	0.0718	0.18	1.52	0.72	0	0	0.99	1	2	1	1.5815	1	0.0171	3.8		9.30E-03	0.85	0.28	1.05
11	1.50	19.6	152	0.6938	0.0546	0.18	1.2	0.71	0	0	0.99	1	2	1	1.5815	1.592	0.0175	3.8		2.79E-06	0.83	0.25	2.1
12	1.50	19.6	152	0.6741	0.0798	0.18	1.5	0.71	0	0	0.99	1	2	1	1.5815	1.592	0.0187	3.8		2.79E-06	0.84	0.25	2.1
13	1.50	19.6	152	0.6372	0.079	0.18	1.44	0.69	0	0	0.99	1	2	1	1.5815	1.592	0.0190	3.8		2.79E-06	0.85	0.25	2
14	1.50	19.6	152	0.5975	0.0872	0.18	1.46	0.68	0	0	0.99	1	2	1	1.5815	1.592	0.0200	3.8		2.79E-06	0.91	0.29	2.34
15	1.50	19.6	152	0.5828	0.0886	0.18	1.43	0.68	0	0	0.99	1	2	1	1.5815	1.592	0.0210	3.8		2.79E-06	0.92	0.3	2.21
16	1.50	19.6	152	0.5518	0.1042	0.18	1.53	0.66	0	0	0.99	1	2	1	1.5815	1.592	0.0214	3.8		2.79E-06	0.94	0.3	2.27
17	1.00	19.6	152	0.5201	0.095	0.18	1.37	0.65	0	0	0.99	1	2	1	1.5815	1.592	0.0225	3.8		9.30E-03	0.99	0.33	2.7

For Use in Strength Correction							
Layer #	Thickness (m)	γ (kN/m^3)	Vs (m/s)	OCR	PI	σ'_m (atm)	τ (kPa)
1	0.42	17.3	81	1.0	0	0.0	3.7
2	0.42	17.3	81	1.0	0	0.1	11.0
3	0.65	17.3	183	1.0	0	0.2	20.3
4	1.00	17.3	183	1.0	0	0.3	34.6
5	1.50	19.6	183	1.0	0	0.5	50.6
6	1.50	19.6	183	1.0	0	0.6	65.3
7	1.50	19.6	183	1.0	0	0.8	80.1
8	1.50	19.6	183	1.0	0	0.9	94.8
9	0.50	19.6	183	1.0	0	1.0	104.7
10	1.50	19.6	152	1.0	0	1.1	89.5
11	1.50	19.6	152	1.0	0	1.3	97.4
12	1.50	19.6	152	1.0	0	1.4	100.8
13	1.50	19.6	152	1.0	0	1.6	111.2
14	1.50	19.6	152	1.0	0	1.7	121.5
15	1.50	19.6	152	1.0	0	1.9	131.8
16	1.50	19.6	152	1.0	0	2.0	142.1
17	1.00	19.6	152	1.0	0	2.1	156.4

Table C. 2: Parameters for Nonlinear Seismic Site Response Analyses CCCC

Layer #	Thickness (m)	γ (kN/m^3)	Vs (m/s)	Damping Ratio (%)	Ref Strain (%)	Ref Stress (MPa)	Beta	s	b	d	Max r_u	PWP Model	f/s/f	p/r/Dr(%)	F/A/FC(%)	s/B/-	g/C/-	v/D/v	-/g/-	C_v (m^2/s)	P1	P2	P3
1	0.85	17.3	100	1.850	0.020	0.18	1.38	0.84	0	0	0.99	1	2	0	1.00	0.00	0.000	3.8		4.6E-03	0.70	0.26	1.60
2	0.65	17.3	100	1.273	0.032	0.18	1.38	0.77	0	0	0.99	1	2	0	1.00	0.00	0.000	3.8		4.6E-03	0.78	0.26	1.20
3	1.00	19.6	130	1.175	0.040	0.18	1.56	0.83	0	0	0.99	1	2	1	2.02	1.59	0.011	3.8		4.6E-03	0.72	0.26	1.35
4	1.00	19.6	130	1.063	0.046	0.18	1.52	0.78	0	0	0.99	1	2	1	2.02	1.64	0.012	3.8		4.6E-03	0.71	0.21	1.45
5	1.00	19.6	130	0.979	0.051	0.18	1.49	0.77	0	0	0.99	1	2	1	2.02	1.46	0.014	3.8		3.7E-02	0.81	0.29	0.80
6	1.00	19.6	130	0.896	0.056	0.18	1.55	0.74	0	0	0.99	1	2	1	2.02	1.46	0.013	3.8		3.7E-02	0.81	0.26	1.45
7	1.00	19.6	170	0.919	0.054	0.18	1.52	0.81	0	0	0.99	1	2	1	1.33	1.35	0.015	3.8		9.3E-04	0.77	0.30	0.90
8	1.00	19.6	170	0.869	0.058	0.18	1.52	0.80	0	0	0.99	1	2	1	1.33	1.35	0.016	3.8		3.7E-01	0.85	0.36	0.60
9	1.00	19.6	170	0.830	0.064	0.18	1.53	0.78	0	0	0.99	1	2	1	1.33	1.35	0.017	3.8		3.7E-02	0.87	0.36	0.55
10	1.50	19.6	170	0.802	0.060	0.18	1.40	0.78	0	0	0.99	1	2	1	1.33	1.35	0.018	3.8		9.3E-03	0.87	0.36	0.55
11	2.00	19.6	220	0.796	0.067	0.18	1.56	0.81	0	0	0.99	1	2	1	0.89	1.25	0.018	3.8		9.3E-01	0.72	0.24	1.05
12	2.00	19.6	220	0.749	0.072	0.18	1.53	0.80	0	0	0.99	1	2	1	0.89	1.25	0.020	3.8		9.3E-01	0.78	0.28	0.80
13	2.00	19.6	220	0.731	0.075	0.18	1.53	0.81	0	0	0.99	1	2	1	0.89	1.25	0.021	3.8		9.3E-04	0.76	0.28	0.85
14	2.00	19.6	220	0.693	0.074	0.18	1.53	0.78	0	0	0.99	1	2	1	0.89	1.42	0.020	3.8		2.8E-03	0.71	0.20	1.60
15	2.00	19.6	220	0.662	0.078	0.18	1.50	0.77	0	0	0.99	1	2	1	0.89	1.42	0.021	3.8		2.8E-04	0.73	0.20	1.45
16	1.50	19.6	160	0.541	0.106	0.18	1.53	0.66	0	0	0.99	1	2	1	0.35	1.78	0.022	3.8		2.8E-06	0.93	0.29	2.29
17	1.50	19.6	160	0.527	0.077	0.18	1.20	0.66	0	0	0.99	1	2	1	0.35	1.78	0.023	3.8		2.8E-06	0.96	0.32	2.50
18	1.00	19.6	160	0.501	0.119	0.18	1.53	0.65	0	0	0.99	1	2	1	0.35	1.78	0.024	3.8		2.8E-06	0.98	0.33	2.65
19	1.00	19.6	160	0.495	0.123	0.18	1.55	0.65	0	0	0.99	1	2	1	0.35	1.78	0.024	3.8		9.3E-03	0.99	0.33	2.59

For Use in Strength Correction							
Layer #	Thickness (m)	γ (kN/m^3)	Vs (m/s)	OCR	PI	σ'_m (atm)	τ (kPa)
1	0.85	17.28	100	1.0	0	0.1	6.6
2	0.65	17.28	100	1.0	0	0.2	15.3
3	1.00	19.636	130	1.0	0	0.3	23.5
4	1.00	19.636	130	1.0	0	0.4	32.4
5	1.00	19.636	130	1.0	0	0.5	40.7
6	1.00	19.636	130	1.0	0	0.6	48.3
7	1.00	19.636	170	1.0	0	0.7	56.0
8	1.00	19.636	170	1.0	0	0.8	63.7
9	1.00	19.636	170	1.0	0	0.9	71.4
10	1.50	19.636	170	1.0	0	1.0	75.3
11	2.00	19.636	220	1.0	0	1.2	105.1
12	2.00	19.636	220	1.0	0	1.4	122.2
13	2.00	19.636	220	1.0	0	1.6	122.9
14	2.00	19.636	220	1.0	0	1.8	138.0
15	2.00	19.636	220	1.0	0	2.0	153.1
16	1.50	19.636	160	1.0	0	2.1	157.5
17	1.50	19.636	160	1.0	0	2.3	168.2
18	1.00	19.636	160	1.0	0	2.4	177.1
19	1.00	19.636	160	1.0	0	2.5	184.3

Table C. 3: Parameters for Nonlinear Seismic Site Response Analyses CHHC

Layer #	Thickness (m)	γ (kN/m^3)	Vs (m/s)	Damping Ratio (%)	Ref Strain (%)	Ref Stress (MPa)	Beta	s	b	d	Max r_u	PWP Model	f/s/f	p/r/Dr(%)	F/A/FC(%)	s/B/-	g/C/-	v/D/v	-/g/-	C_v (m^2/s)	P1	P2	P3
1	0.75	17.3	100	1.946	0.019	0.18	1.44	0.89	0	0	0.99	1	2	0	1.00	0.00	0.000	3.8		1.9E-04	0.63	0.23	2.50
2	0.75	17.3	100	1.324	0.036	0.18	1.58	0.78	0	0	0.99	1	2	0	1.00	0.00	0.000	3.8		1.9E-04	0.76	0.26	1.30
3	0.50	17.3	100	1.096	0.043	0.18	1.46	0.74	0	0	0.99	1	2	0	1.00	0.00	0.000	3.8		1.9E-04	0.93	0.38	0.60
4	0.50	17.3	100	0.998	0.048	0.18	1.49	0.71	0	0	0.99	1	2	0	1.00	0.00	0.000	3.8		1.9E-04	0.83	0.25	1.96
5	0.50	17.3	100	0.837	0.057	0.18	1.46	0.68	0	0	0.99	1	2	0	1.00	0.00	0.000	3.8		4.6E-03	0.90	0.28	2.51
6	1.00	19.6	160	0.978	0.050	0.18	1.53	0.81	0	0	0.99	1	2	1	1.46	1.32	0.014	3.8		9.3E-03	0.77	0.30	0.90
7	1.50	19.6	160	0.920	0.058	0.18	1.55	0.78	0	0	0.99	1	2	1	1.46	1.32	0.015	3.8		9.3E-03	0.71	0.20	1.40
8	1.50	19.6	160	0.869	0.060	0.18	1.49	0.78	0	0	0.99	1	2	1	1.46	1.32	0.016	3.8		9.3E-03	0.73	0.22	1.15
9	1.50	19.6	160	0.780	0.064	0.18	1.49	0.74	0	0	0.99	1	2	1	1.46	1.32	0.016	3.8		9.3E-02	0.81	0.25	1.30
10	1.50	19.6	160	0.734	0.059	0.18	1.32	0.72	0	0	0.99	1	2	1	1.46	1.32	0.017	3.8		9.3E-02	0.83	0.25	1.20
11	2.00	19.6	210	0.758	0.071	0.18	1.53	0.80	0	0	0.99	1	2	1	0.96	1.32	0.019	3.8		9.3E-02	0.84	0.34	0.60
12	2.00	19.6	210	0.727	0.062	0.18	1.37	0.78	0	0	0.99	1	2	1	0.96	1.32	0.019	3.8		9.3E-02	0.73	0.22	1.60
13	1.00	19.6	210	0.697	0.074	0.18	1.50	0.77	0	0	0.99	1	2	1	0.96	1.32	0.020	3.8		9.3E-02	0.75	0.23	1.40
14	2.00	19.6	250	0.710	0.080	0.18	1.56	0.81	0	0	0.99	1	2	1	0.73	1.32	0.022	3.8		9.3E-02	0.72	0.23	1.15
15	1.45	19.6	145	0.519	0.118	0.18	1.55	0.63	0	0	0.99	1	2	1	1.39	1.46	0.022	3.8		9.3E-03	0.99	0.30	2.60
16	1.05	19.6	145	0.511	0.121	0.18	1.53	0.63	0	0	0.99	1	2	1	1.39	1.54	0.023	3.8		9.3E-03	0.99	0.30	2.55
17	1.05	19.6	165	0.536	0.112	0.18	1.56	0.66	0	0	0.99	1	2	1	1.39	1.67	0.022	3.8		9.3E-06	0.94	0.29	2.26
18	1.05	19.6	165	0.530	0.097	0.18	1.40	0.66	0	0	0.99	1	2	1	1.39	1.73	0.023	3.8		9.3E-03	0.94	0.30	2.25

For Use in Strength Correction							
Layer #	Thickness (m)	γ (kN/m^3)	Vs (m/s)	OCR	PI	σ'_m (atm)	τ (kPa)
1	0.75	17.3	100	1.0	0	0.1	4.7
2	0.75	17.3	100	1.0	0	0.2	14.1
3	0.50	17.3	100	1.0	0	0.3	22.0
4	0.50	17.3	100	1.0	0	0.4	28.2
5	0.50	17.3	100	1.0	0	0.5	36.9
6	1.00	19.6	160	1.0	0	0.6	46.9
7	1.50	19.6	160	1.0	0	0.7	56.9
8	1.50	19.6	160	1.0	0	0.8	64.0
9	1.50	19.6	160	1.0	0	1.0	83.7
10	1.50	19.6	160	1.0	0	1.1	96.1
11	2.00	19.6	210	1.0	0	1.3	114.5
12	2.00	19.6	210	1.0	0	1.5	118.3
13	1.00	19.6	210	1.0	0	1.6	134.5
14	2.00	19.6	250	1.0	0	1.8	151.8
15	1.45	19.6	145	1.0	0	2.0	154.6
16	1.05	19.6	145	1.0	0	2.1	165.7
17	1.05	19.6	165	1.0	0	2.2	163.0
18	1.05	19.6	165	1.0	0	2.3	170.5

Table C. 4: Parameters for Nonlinear Seismic Site Response Analyses HPSC

Layer #	Thickness (m)	γ (kN/m^3)	Vs (m/s)	Damping Ratio (%)	Ref Strain (%)	Ref Stress (MPa)	Beta	s	b	d	Max r_u	PWP Model	f/s/f	p/r/Dr(%)	F/A/FC(%)	s/B/-	g/C/-	v/D/v	-/g/-	C_v (m^2/s)	P1	P2	P3
1	1.00	17.3	115	1.811	0.025	0.18	1.64	0.90	0	0	0.99	1	2	0	1.00	0.00	0.000	3.8		9.3E-05	0.60	0.22	3.25
2	1.00	17.3	115	1.206	0.039	0.18	1.52	0.78	0	0	0.99	1	2	0	1.00	0.00	0.000	3.8		9.3E-05	0.74	0.24	1.30
3	0.50	19.6	115	1.018	0.050	0.18	1.52	0.75	0	0	0.99	1	2	1	2.44	1.46	0.013	3.8		9.3E-05	0.89	0.35	0.60
4	0.50	19.6	115	0.968	0.050	0.18	1.49	0.72	0	0	0.99	1	2	1	2.43	1.46	0.012	3.8		9.3E-05	0.79	0.23	2.20
5	1.00	19.6	130	0.930	0.054	0.18	1.55	0.74	0	0	0.99	1	2	1	2.02	1.25	0.013	3.8		9.3E-02	0.83	0.27	1.45
6	1.00	19.6	130	0.868	0.058	0.18	1.52	0.72	0	0	0.99	1	2	1	2.02	1.25	0.014	3.8		9.3E-02	0.85	0.28	1.30
7	1.50	19.6	170	0.884	0.057	0.18	1.52	0.80	0	0	0.99	1	2	1	1.33	1.25	0.016	3.8		9.3E-02	0.87	0.38	0.60
8	1.50	19.6	170	0.829	0.059	0.18	1.50	0.77	0	0	0.99	1	2	1	1.33	1.25	0.016	3.8		9.3E-02	0.77	0.25	1.50
9	1.50	19.6	170	0.796	0.069	0.18	1.56	0.78	0	0	0.99	1	2	1	1.33	1.32	0.018	3.8		9.3E-02	0.87	0.36	0.55
10	0.50	19.6	170	0.747	0.070	0.18	1.52	0.74	0	0	0.99	1	2	1	1.33	1.32	0.017	3.8		9.3E-02	0.81	0.25	1.30
11	2.00	19.6	220	0.784	0.058	0.18	1.35	0.81	0	0	0.99	1	2	1	0.89	1.32	0.019	3.8		9.3E-02	0.72	0.24	1.10
12	2.00	19.6	220	0.741	0.076	0.18	1.55	0.80	0	0	0.99	1	2	1	0.89	1.32	0.020	3.8		9.3E-02	0.77	0.27	0.85
13	2.00	19.6	220	0.714	0.076	0.18	1.50	0.80	0	0	0.99	1	2	1	0.89	1.32	0.021	3.8		9.3E-02	0.77	0.27	0.83
14	2.00	19.6	220	0.675	0.079	0.18	1.55	0.77	0	0	0.99	1	2	1	0.89	1.32	0.020	3.8		9.3E-02	0.73	0.20	1.50
15	2.50	19.6	280	0.686	0.074	0.18	1.49	0.84	0	0	0.99	1	2	1	0.61	1.32	0.022	3.8		9.3E-02	0.76	0.31	0.85
16	2.50	19.6	280	0.650	0.069	0.18	1.32	0.83	0	0	0.99	1	2	1	0.61	1.32	0.023	3.8		9.3E-02	0.87	0.40	0.55
17	2.00	19.6	280	0.635	0.080	0.18	1.52	0.81	0	0	0.99	1	2	1	0.61	1.32	0.022	3.8		9.3E-02	0.73	0.25	1.21
18	3.00	19.6	315	0.633	0.073	0.18	1.32	0.84	0	0	0.99	1	2	1	0.51	1.32	0.025	3.8		9.3E-02	0.73	0.27	1.05
19	3.00	19.6	315	0.603	0.089	0.18	1.49	0.83	0	0	0.99	1	2	1	0.51	1.32	0.026	3.8		9.3E-02	0.82	0.35	0.70
20	3.00	19.6	315	0.599	0.071	0.18	1.23	0.84	0	0	0.99	1	2	1	0.51	1.32	0.027	3.8		9.3E-02	0.73	0.28	1.00
21	2.00	19.6	315	0.574	0.093	0.18	1.55	0.81	0	0	0.99	1	2	1	0.51	1.32	0.025	3.8		9.3E-02	0.71	0.23	1.15

For Use in Strength Correction							
Layer #	Thickness (m)	γ (kN/m^3)	Vs (m/s)	OCR	PI	σ'_m (atm)	τ (kPa)
1	1.00	17.3	115	1.0	0	0.1	6.3
2	1.00	17.3	115	1.0	0	0.3	20.7
3	0.50	19.6	115	1.0	0	0.4	28.0
4	0.50	19.6	115	1.0	0	0.5	32.7
5	1.00	19.6	130	1.0	0	0.6	46.8
6	1.00	19.6	130	1.0	0	0.6	52.5
7	1.50	19.6	170	1.0	0	0.7	60.1
8	1.50	19.6	170	1.0	0	0.8	71.5
9	1.50	19.6	170	1.0	0	1.0	69.2
10	0.50	19.6	170	1.0	0	1.1	90.5
11	2.00	19.6	220	1.0	0	1.2	100.0
12	2.00	19.6	220	1.0	0	1.4	115.2
13	2.00	19.6	220	1.0	0	1.5	117.0
14	2.00	19.6	220	1.0	0	1.7	135.5
15	2.50	19.6	280	1.0	0	1.9	162.6
16	2.50	19.6	280	1.0	0	2.1	182.4
17	2.00	19.6	280	1.0	0	2.4	201.0
18	3.00	19.6	315	1.0	0	2.6	221.6
19	3.00	19.6	315	1.0	0	2.9	246.4
20	3.00	19.6	315	1.0	0	3.2	243.5
21	2.00	19.6	315	1.0	0	3.4	281.5

Table C. 5: Parameters for Nonlinear Seismic Site Response Analyses KPOC

Layer #	Thickness (m)	γ (kN/m^3)	Vs (m/s)	Damping Ratio (%)	Ref Strain (%)	Ref Stress (MPa)	Beta	s	b	d	Max r_u	PWP Model	f/s/f	p/r/Dr(%)	F/A/FC(%)	s/B/-	g/C/-	v/D/v	-/g/-	C_v (m^2/s)	P1	P2	P3
1	1.00	17.3	150	1.752	0.022	0.18	1.53	0.95	0	0	0.99	1	2	0	1.00	0.00	0.000	3.8		9.3E-03	0.62	0.27	3.25
2	1.50	19.6	150	1.280	0.034	0.18	1.46	0.87	0	0	0.99	1	2	1	1.61	1.25	0.011	3.8		9.3E-03	0.64	0.22	2.10
3	1.00	19.6	150	1.113	0.041	0.18	1.49	0.83	0	0	0.99	1	2	1	1.61	1.25	0.012	3.8		9.3E-03	0.71	0.25	1.36
4	1.50	19.6	150	1.004	0.050	0.18	1.50	0.78	0	0	0.99	1	2	1	1.61	1.25	0.014	3.8		9.3E-03	0.73	0.22	1.30
5	1.50	19.6	150	0.892	0.055	0.18	1.52	0.75	0	0	0.99	1	2	1	1.61	1.25	0.014	3.8		9.3E-03	0.80	0.26	1.45
6	2.00	19.6	210	0.902	0.053	0.18	1.47	0.83	0	0	0.99	1	2	1	0.96	1.25	0.016	3.8		9.3E-03	0.66	0.19	1.85
7	2.00	19.6	210	0.832	0.062	0.18	1.52	0.81	0	0	0.99	1	2	1	0.96	1.25	0.017	3.8		9.3E-03	0.74	0.26	1.05
8	2.50	19.6	300	0.827	0.056	0.18	1.50	0.89	0	0	0.99	1	2	1	0.55	1.25	0.018	3.8		9.3E-03	0.59	0.18	3.10
9	2.50	19.6	300	0.780	0.058	0.18	1.40	0.87	0	0	0.99	1	2	1	0.55	1.25	0.019	3.8		9.3E-03	0.61	0.19	2.25
10	3.00	19.6	300	0.732	0.070	0.18	1.52	0.86	0	0	0.99	1	2	1	0.55	1.25	0.021	3.8		9.3E-03	0.68	0.24	1.32

For Use in Strength Correction							
Layer #	Thickness (m)	γ (kN/m^3)	Vs (m/s)	OCR	PI	σ'_m (atm)	τ (kPa)
1	1.00	17.3	150	1.0	0	0.1	7.7
2	1.50	19.6	150	1.0	0	0.3	21.1
3	1.00	19.6	150	1.0	0	0.4	33.0
4	1.50	19.6	150	1.0	0	0.5	46.4
5	1.50	19.6	150	1.0	0	0.7	59.7
6	2.00	19.6	210	1.0	0	0.8	75.2
7	2.00	19.6	210	1.0	0	1.0	92.9
8	2.50	19.6	300	1.0	0	1.2	125.3
9	2.50	19.6	300	1.0	0	1.5	149.9
10	3.00	19.6	300	1.0	0	1.7	176.9

Table C. 6: Parameters for Nonlinear Seismic Site Response Analyses NNBS

Layer #	Thickness (m)	γ (kN/m^3)	Vs (m/s)	Damping Ratio (%)	Ref Strain (%)	Ref Stress (MPa)	Beta	s	b	d	Max r_u	PWP Model	f/s/f	p/r/Dr(%)	F/A/FC(%)	s/B/-	g/C/-	v/D/v	-/g/-	C_v (m^2/s)	P1	P2	P3
1	1.00	17.3	100	1.772	0.018	0.18	1.19	0.86	0	0	0.99	1	2	0	1.00	0.00	0.000	3.8		9.3E-03	0.63	0.21	2.30
2	0.50	17.3	100	1.195	0.034	0.18	1.37	0.74	0	0	0.99	1	2	0	1.00	0.00	0.000	3.8		9.3E-02	0.94	0.39	0.60
3	0.50	19.6	100	1.059	0.045	0.18	1.50	0.71	0	0	0.99	1	2	1	3.03	1.25	0.011	3.8		9.3E-02	0.84	0.25	2.10
4	1.00	19.6	140	1.098	0.045	0.18	1.55	0.80	0	0	0.99	1	2	1	1.80	1.25	0.012	3.8		9.3E-02	0.71	0.22	1.45
5	1.00	19.6	140	0.999	0.053	0.18	1.55	0.77	0	0	0.99	1	2	1	1.80	1.25	0.013	3.8		9.3E-02	0.79	0.26	0.95
6	1.00	19.6	140	0.906	0.046	0.18	1.34	0.74	0	0	0.99	1	2	1	1.80	1.25	0.013	3.8		9.3E-02	0.83	0.28	1.40
7	1.75	19.6	180	0.917	0.055	0.18	1.53	0.81	0	0	0.99	1	2	1	1.22	1.25	0.015	3.8		9.3E-02	0.77	0.30	0.90
8	1.50	19.6	180	0.837	0.063	0.18	1.55	0.78	0	0	0.99	1	2	1	1.22	1.25	0.016	3.8		9.3E-02	0.87	0.36	0.55
9	1.75	19.6	180	0.795	0.062	0.18	1.52	0.77	0	0	0.99	1	2	1	1.22	1.25	0.016	3.8		9.3E-02	0.76	0.24	1.43
10	2.25	19.6	240	0.799	0.055	0.18	1.35	0.84	0	0	0.99	1	2	1	0.78	1.35	0.018	3.8		9.3E-02	0.75	0.29	1.00
11	2.25	19.6	240	0.767	0.063	0.18	1.41	0.83	0	0	0.99	1	2	1	0.78	1.35	0.020	3.8		9.3E-02	0.67	0.20	1.60
12	2.25	19.6	240	0.723	0.077	0.18	1.55	0.81	0	0	0.99	1	2	1	0.78	1.35	0.021	3.8		9.3E-02	0.74	0.25	1.00
13	2.25	19.6	240	0.667	0.077	0.18	1.55	0.78	0	0	0.99	1	2	1	0.78	1.35	0.020	3.8		9.3E-02	0.81	0.30	0.85
14	2.00	19.6	240	0.646	0.080	0.18	1.52	0.78	0	0	0.99	1	2	1	0.78	1.35	0.021	3.8		9.3E-02	0.83	0.32	0.75
15	2.50	19.6	300	0.669	0.078	0.18	1.50	0.84	0	0	0.99	1	2	1	0.55	1.35	0.023	3.8		9.3E-02	0.71	0.26	1.15
16	1.50	19.6	300	0.651	0.079	0.18	1.47	0.84	0	0	0.99	1	2	1	0.55	1.35	0.024	3.8		9.3E-02	0.74	0.28	0.95
17	1.00	19.6	300	0.643	0.081	0.18	1.47	0.84	0	0	0.99	1	2	1	0.55	1.66	0.024	3.8		2.8E-06	0.73	0.27	1.05
18	1.00	19.6	300	0.620	0.078	0.18	1.37	0.83	0	0	0.99	1	2	1	0.55	1.38	0.025	3.8		9.3E-02	0.87	0.39	0.60
19	3.00	19.6	320	0.624	0.074	0.18	1.32	0.84	0	0	0.99	1	2	1	0.50	1.38	0.026	3.8		9.3E-02	0.73	0.27	1.05
20	3.00	19.6	320	0.595	0.090	0.18	1.56	0.81	0	0	0.99	1	2	1	0.50	1.38	0.024	3.8		9.3E-02	0.70	0.21	1.45
21	2.00	19.6	320	0.583	0.091	0.18	1.55	0.81	0	0	0.99	1	2	1	0.50	1.38	0.025	3.8		9.3E-02	0.69	0.21	1.35
22	1.50	19.6	200	0.475	0.086	0.18	1.17	0.68	0	0	0.99	1	2	1	1.03	1.73	0.027	3.8		9.3E-07	0.93	0.31	2.20
23	1.50	19.6	200	0.470	0.118	0.18	1.44	0.68	0	0	0.99	1	2	1	1.03	1.73	0.028	3.8		9.3E-07	0.93	0.31	2.23
24	1.00	19.6	200	0.450	0.140	0.18	1.56	0.66	0	0	0.99	1	2	1	1.03	1.64	0.028	3.8		9.3E-07	0.94	0.30	2.36
25	2.00	19.6	200	0.445	0.141	0.18	1.55	0.66	0	0	0.99	1	2	1	1.03	1.73	0.029	3.8		9.3E-03	0.95	0.31	2.30

For Use in Strength Correction							
Layer #	Thickness (m)	γ (kN/m^3)	Vs (m/s)	OCR	PI	σ'_m (atm)	τ (kPa)
1	1.00	17.3	100	1.0	0	0.1	6.5
2	0.50	17.3	100	1.0	0	0.2	20.0
3	0.50	19.6	100	1.0	0	0.3	29.7
4	1.00	19.6	140	1.0	0	0.4	36.0
5	1.00	19.6	140	1.0	0	0.5	45.0
6	1.00	19.6	140	1.0	0	0.6	54.0
7	1.75	19.6	180	1.0	0	0.7	63.0
8	1.50	19.6	180	1.0	0	0.9	76.9
9	1.75	19.6	180	1.0	0	1.0	90.7
10	2.25	19.6	240	1.0	0	1.2	104.1
11	2.25	19.6	240	1.0	0	1.4	122.7
12	2.25	19.6	240	1.0	0	1.7	141.2
13	2.25	19.6	240	1.0	0	1.9	159.8
14	2.00	19.6	240	1.0	0	2.1	177.3
15	2.50	19.6	300	1.0	0	2.3	195.9
16	1.50	19.6	300	1.0	0	2.5	212.3
17	1.00	19.6	300	1.0	0	2.6	207.3
18	1.00	19.6	300	1.0	0	2.7	230.9
19	3.00	19.6	320	1.0	0	2.9	247.4
20	3.00	19.6	320	1.0	0	3.2	272.1
21	2.00	19.6	320	1.0	0	3.4	292.8
22	1.50	19.6	200	1.0	0	3.6	266.0
23	1.50	19.6	200	1.0	0	3.8	276.7
24	1.00	19.6	200	1.0	0	3.9	285.6
25	2.00	19.6	200	1.0	0	4.0	296.3

Table C. 7: Parameters for Nonlinear Seismic Site Response Analyses PPHS

Layer #	Thickness (m)	γ (kN/m^3)	Vs (m/s)	Damping Ratio (%)	Ref Strain (%)	Ref Stress (MPa)	Beta	s	b	d	Max r_u	PWP Model	f/s/f	p/r/Dr(%)	F/A/FC(%)	s/B/-	g/C/-	v/D/v	-/g/-	C_v (m^2/s)	P1	P2	P3
1	1.00	17.3	100	1.749	0.022	0.18	1.41	0.86	0	0	0.99	1	2	0	1.00	0.00	0.000	3.8		9.3E-04	0.62	0.20	2.85
2	1.00	17.3	100	1.164	0.036	0.18	1.37	0.75	0	0	0.99	1	2	0	1.00	0.00	0.000	3.8		9.3E-04	0.88	0.34	0.75
3	0.50	17.3	100	0.994	0.050	0.18	1.52	0.71	0	0	0.99	1	2	0	1.00	0.00	0.000	3.8		9.3E-04	0.83	0.25	1.95
4	1.00	19.6	100	0.912	0.052	0.18	1.46	0.69	0	0	0.99	1	2	1	3.03	1.42	0.012	3.8		9.3E-04	0.84	0.23	2.00
5	1.00	19.6	100	0.811	0.002	0.18	0.17	0.66	0	0	0.99	1	2	1	3.03	1.42	0.013	3.8		9.3E-04	0.92	0.28	2.63
6	0.50	19.6	100	0.779	0.061	0.18	1.41	0.66	0	0	0.99	1	2	1	3.03	1.71	0.014	3.8		2.8E-06	0.94	0.30	2.35
7	1.00	19.6	100	0.725	0.074	0.18	1.53	0.65	0	0	0.99	1	2	1	1.00	1.71	0.015	3.8		2.8E-06	0.98	0.33	2.95
8	1.00	19.6	100	0.698	0.068	0.18	1.38	0.65	0	0	0.99	1	2	1	1.00	1.71	0.016	3.8		2.8E-06	0.99	0.34	2.80
9	1.00	19.6	110	0.698	0.070	0.18	1.41	0.66	0	0	0.99	1	2	1	1.00	1.71	0.016	3.8		2.8E-06	0.96	0.32	2.60
10	0.50	19.6	110	0.659	0.060	0.18	1.22	0.65	0	0	0.99	1	2	1	1.00	1.71	0.017	3.8		2.8E-06	0.99	0.33	2.68
11	1.00	19.6	110	0.625	0.089	0.18	1.52	0.63	0	0	0.99	1	2	1	1.00	1.71	0.017	3.8		2.8E-06	0.99	0.32	3.05
12	1.50	19.6	200	0.752	0.066	0.18	1.47	0.75	0	0	0.99	1	2	1	1.03	1.00	0.017	3.8		4.6E-02	0.78	0.24	1.39
13	1.50	19.6	200	0.715	0.063	0.18	1.34	0.74	0	0	0.99	1	2	1	1.03	1.00	0.018	3.8		4.6E-02	0.80	0.24	1.35
14	1.50	19.6	200	0.692	0.057	0.18	1.22	0.74	0	0	0.99	1	2	1	1.03	1.00	0.019	3.8		4.6E-02	0.80	0.24	1.15
15	2.00	19.6	200	0.647	0.080	0.18	1.49	0.72	0	0	0.99	1	2	1	1.03	1.00	0.020	3.8		4.6E-02	0.87	0.30	1.40
16	1.50	19.6	180	0.632	0.070	0.18	1.34	0.72	0	0	0.99	1	2	1	1.22	1.64	0.020	3.8		9.3E-07	0.84	0.27	1.50
17	1.50	19.6	180	0.617	0.083	0.18	1.47	0.72	0	0	0.99	1	2	1	1.22	1.64	0.021	3.8		9.3E-03	0.85	0.27	1.45

For Use in Strength Correction							
Layer #	Thickness (m)	γ (kN/m^3)	Vs (m/s)	OCR	PI	σ'_m (atm)	τ (kPa)
1	1.00	17.3	100	1.0	0	0.1	6.3
2	1.00	17.3	100	1.0	0	0.3	18.8
3	0.50	17.3	100	1.0	0	0.4	28.7
4	1.00	19.6	100	1.0	0	0.5	37.1
5	1.00	19.6	100	1.0	0	0.6	44.5
6	0.50	19.6	100	1.0	0	0.7	50.1
7	1.00	19.6	100	1.0	0	0.7	51.7
8	1.00	19.6	100	1.0	0	0.8	58.6
9	1.00	19.6	110	1.0	0	0.9	65.5
10	0.50	19.6	110	1.0	0	1.0	70.6
11	1.00	19.6	110	1.0	0	1.1	75.8
12	1.50	19.6	200	1.0	0	1.2	120.5
13	1.50	19.6	200	1.0	0	1.3	135.3
14	1.50	19.6	200	1.0	0	1.5	150.0
15	2.00	19.6	200	1.0	0	1.7	167.2
16	1.50	19.6	180	1.0	0	1.8	129.1
17	1.50	19.6	180	1.0	0	2.0	139.5

Table C. 8: Parameters for Nonlinear Seismic Site Response Analyses PRPC

Layer #	Thickness (m)	γ (kN/m^3)	Vs (m/s)	Damping Ratio (%)	Ref Strain (%)	Ref Stress (MPa)	Beta	s	b	d	Max r_u	PWP Model	f/s/f	p/r/Dr(%)	F/A/FC(%)	s/B/-	g/C/-	v/D/v	-/g/-	C_v (m^2/s)	P1	P2	P3
1	0.75	17.3	90	1.980	0.019	0.18	1.41	0.87	0	0	0.99	1	2	0	1.00	0.00	0.000	3.8		9.3E-05	0.61	0.20	3.00
2	0.75	17.3	90	1.272	0.037	0.18	1.47	0.72	0	0	0.99	1	2	0	1.00	0.00	0.000	3.8		4.6E-01	0.79	0.22	1.35
3	0.75	17.3	90	0.943	0.005	0.18	0.33	0.65	0	0	0.99	1	2	0	1.00	0.00	0.000	3.8		4.6E-01	0.96	0.31	3.06
4	0.75	17.3	90	0.842	0.004	0.18	0.26	0.65	0	0	0.99	1	2	0	1.00	0.00	0.000	3.8		1.9E-05	0.96	0.30	2.75
5	1.75	19.6	180	0.965	0.054	0.18	1.59	0.81	0	0	0.99	1	2	1	1.22	1.30	0.014	3.8		5.6E-01	0.74	0.26	1.10
6	1.75	19.6	180	0.875	0.043	0.18	1.20	0.80	0	0	0.99	1	2	1	1.22	1.30	0.016	3.8		5.6E-01	0.86	0.37	0.60
7	1.75	19.6	180	0.816	0.062	0.18	1.53	0.77	0	0	0.99	1	2	1	1.22	1.30	0.016	3.8		5.6E-01	0.76	0.24	1.51
8	1.75	19.6	180	0.762	0.058	0.18	1.35	0.75	0	0	0.99	1	2	1	1.22	1.30	0.017	3.8		5.6E-01	0.80	0.26	1.25
9	1.00	19.6	180	0.743	0.069	0.18	1.52	0.74	0	0	0.99	1	2	1	1.22	1.30	0.017	3.8		5.6E-01	0.80	0.24	1.30
10	2.50	19.6	250	0.777	0.056	0.18	1.35	0.84	0	0	0.99	1	2	1	0.73	1.30	0.019	3.8		5.6E-01	0.77	0.32	0.85
11	2.50	19.6	250	0.746	0.066	0.18	1.43	0.83	0	0	0.99	1	2	1	0.73	1.30	0.020	3.8		5.6E-01	0.69	0.22	1.30
12	2.50	19.6	250	0.707	0.080	0.18	1.55	0.81	0	0	0.99	1	2	1	0.73	1.30	0.022	3.8		5.6E-01	0.72	0.23	1.15
13	2.50	19.6	250	0.661	0.077	0.18	1.52	0.80	0	0	0.99	1	2	1	0.73	1.30	0.021	3.8		5.6E-01	0.78	0.29	0.95
14	1.00	19.6	180	0.568	0.096	0.18	1.49	0.69	0	0	0.99	1	2	1	0.52	1.69	0.022	3.8		9.3E-06	0.89	0.27	1.45
15	1.00	19.6	180	0.562	0.092	0.18	1.44	0.69	0	0	0.99	1	2	1	0.35	1.69	0.022	3.8		9.3E-06	0.88	0.27	2.20
16	3.00	19.6	310	0.650	0.072	0.18	1.35	0.84	0	0	0.99	1	2	1	0.52	1.30	0.024	3.8		9.3E-01	0.74	0.28	1.00
17	1.50	19.6	230	0.602	0.089	0.18	1.49	0.77	0	0	0.99	1	2	1	0.83	1.59	0.024	3.8		9.3E-03	0.73	0.21	1.35
18	1.50	19.6	230	0.584	0.095	0.18	1.52	0.75	0	0	0.99	1	2	1	0.83	1.59	0.024	3.8		9.3E-03	0.75	0.20	1.25

For Use in Strength Correction							
Layer #	Thickness (m)	γ (kN/m^3)	Vs (m/s)	OCR	PI	σ'_m (atm)	τ (kPa)
1	0.75	17.3	90	1.0	0	0.1	4.2
2	0.75	17.3	90	1.0	0	0.2	17.5
3	0.75	17.3	90	1.0	0	0.3	30.2
4	0.75	17.3	90	1.0	0	0.5	33.6
5	1.75	19.6	180	1.0	0	0.6	58.0
6	1.75	19.6	180	1.0	0	0.8	71.5
7	1.75	19.6	180	1.0	0	1.0	87.0
8	1.75	19.6	180	1.0	0	1.1	102.5
9	1.00	19.6	180	1.0	0	1.2	105.8
10	2.50	19.6	250	1.0	0	1.3	121.3
11	2.50	19.6	250	1.0	0	1.6	143.4
12	2.50	19.6	250	1.0	0	1.8	154.3
13	2.50	19.6	250	1.0	0	2.1	174.9
14	1.00	19.6	180	1.0	0	2.2	163.9
15	1.00	19.6	180	1.0	0	2.3	171.1
16	3.00	19.6	310	1.0	0	2.5	221.8
17	1.50	19.6	230	1.0	0	2.7	194.1
18	1.50	19.6	230	1.0	0	2.9	204.4

Table C. 9: Parameters for Nonlinear Seismic Site Response Analyses REHS

Layer #	Thickness (m)	γ (kN/m^3)	Vs (m/s)	Damping Ratio (%)	Ref Strain (%)	Ref Stress (MPa)	Beta	s	b	d	Max r_u	PWP Model	f/s/f	p/r/Dr(%)	F/A/FC(%)	s/B/-	g/C/-	v/D/v	-/g/-	C_v (m^2/s)	P1	P2	P3
1	0.30	17.3	90	2.442	0.014	0.18	1.40	0.90	0	0	0.99	1	2	0	1.00	0.00	0.000	3.8		9.3E-03	0.61	0.23	3.25
2	0.55	17.3	90	1.613	0.029	0.18	1.56	0.81	0	0	0.99	1	2	0	1.00	0.00	0.000	3.8		9.3E-03	0.87	0.40	0.65
3	0.65	17.3	90	1.225	0.037	0.18	1.50	0.74	0	0	0.99	1	2	0	1.00	0.00	0.000	3.8		9.3E-03	0.95	0.39	0.60
4	0.50	17.3	90	1.035	0.045	0.18	1.46	0.68	0	0	0.99	1	2	0	1.00	0.00	0.000	3.8		9.3E-03	0.86	0.23	2.45
5	1.00	19.6	90	0.950	0.006	0.18	0.35	0.68	0	0	0.99	1	2	1	2.50	1.35	0.012	3.8		9.3E-03	0.86	0.23	2.30
6	1.00	19.6	90	0.850	0.005	0.18	0.29	0.66	0	0	0.99	1	2	1	1.00	1.67	0.013	3.8		4.6E-05	0.93	0.29	2.70
7	1.00	19.6	110	0.878	0.046	0.18	1.29	0.71	0	0	0.99	1	2	1	1.00	1.71	0.013	3.8		4.6E-05	0.81	0.23	1.90
8	1.10	19.6	110	0.809	0.062	0.18	1.47	0.69	0	0	0.99	1	2	1	1.00	1.67	0.014	3.8		4.6E-05	0.88	0.28	2.31
9	0.90	19.6	130	0.816	0.059	0.18	1.46	0.72	0	0	0.99	1	2	1	1.00	1.67	0.015	3.8		4.6E-05	0.83	0.25	1.35
10	1.00	19.6	130	0.767	0.055	0.18	1.31	0.71	0	0	0.99	1	2	1	2.00	1.59	0.016	3.8		4.6E-05	0.87	0.28	1.10
11	1.00	19.6	130	0.733	0.058	0.18	1.29	0.69	0	0	0.99	1	2	1	2.00	1.57	0.016	3.8		4.6E-05	0.88	0.27	2.15
12	0.70	19.6	220	0.843	0.058	0.18	1.52	0.86	0	0	0.99	1	2	1	0.89	1.35	0.017	3.8		9.3E-01	0.68	0.24	1.40
13	0.90	19.6	220	0.817	0.056	0.18	1.38	0.83	0	0	0.99	1	2	1	0.89	1.15	0.018	3.8		9.3E-01	0.69	0.23	1.30
14	0.90	19.6	220	0.788	0.070	0.18	1.56	0.81	0	0	0.99	1	2	1	0.89	1.15	0.019	3.8		9.3E-01	0.74	0.26	1.00
15	0.90	19.6	220	0.744	0.067	0.18	1.49	0.77	0	0	0.99	1	2	1	0.89	1.15	0.018	3.8		9.3E-01	0.73	0.21	1.60
16	0.90	19.6	220	0.728	0.060	0.18	1.34	0.77	0	0	0.99	1	2	1	0.89	1.15	0.018	3.8		9.3E-01	0.75	0.23	1.40
17	0.70	19.6	220	0.716	0.073	0.18	1.53	0.77	0	0	0.99	1	2	1	0.89	1.15	0.019	3.8		9.3E-01	0.76	0.23	1.30
18	2.50	19.6	280	0.732	0.068	0.18	1.49	0.84	0	0	0.99	1	2	1	0.61	1.15	0.020	3.8		9.3E-01	0.77	0.31	0.85
19	2.50	19.6	280	0.708	0.074	0.18	1.49	0.83	0	0	0.99	1	2	1	0.61	1.15	0.022	3.8		9.3E-01	0.69	0.22	1.30
20	1.00	19.6	280	0.666	0.079	0.18	1.56	0.80	0	0	0.99	1	2	1	0.61	1.15	0.021	3.8		9.3E-01	0.74	0.25	1.20

For Use in Strength Correction							
Layer #	Thickness (m)	γ (kN/m^3)	Vs (m/s)	OCR	PI	σ'_m (atm)	τ (kPa)
1	0.30	17.3	90	1.0	0	0.0	2.6
2	0.55	17.3	90	1.0	0	0.1	8.3
3	0.65	17.3	90	1.0	0	0.2	15.9
4	0.50	17.3	90	1.0	0	0.3	24.1
5	1.00	19.6	90	1.0	0	0.4	29.5
6	1.00	19.6	90	1.0	0	0.5	35.4
7	1.00	19.6	110	1.0	0	0.6	42.2
8	1.10	19.6	110	1.0	0	0.7	49.5
9	0.90	19.6	130	1.0	0	0.8	56.4
10	1.00	19.6	130	1.0	0	0.9	65.3
11	1.00	19.6	130	1.0	0	1.0	72.4
12	0.70	19.6	220	1.0	0	1.1	78.5
13	0.90	19.6	220	1.0	0	1.1	100.7
14	0.90	19.6	220	1.0	0	1.2	108.4
15	0.90	19.6	220	1.0	0	1.3	133.6
16	0.90	19.6	220	1.0	0	1.4	142.4
17	0.70	19.6	220	1.0	0	1.5	150.3
18	2.50	19.6	280	1.0	0	1.6	166.0
19	2.50	19.6	280	1.0	0	1.9	190.6
20	1.00	19.6	280	1.0	0	2.1	207.8

Table C. 10: Parameters for Nonlinear Seismic Site Response Analyses SHLC

Layer #	Thickness (m)	γ (kN/m^3)	Vs (m/s)	Damping Ratio (%)	Ref Strain (%)	Ref Stress (MPa)	Beta	s	b	d	Max r_u	PWP Model	f/s/f	p/r/Dr(%)	F/A/FC(%)	s/B/-	g/C/-	v/D/v	-/g/-	C_v (m^2/s)	P1	P2	P3
1	1.00	17.3	120	1.780	0.019	0.18	1.25	0.92	0	0	0.99	1	2	0	1.00	0.00	0.000	3.8		9.3E-05	0.63	0.26	2.60
2	0.50	17.3	120	1.256	0.038	0.18	1.55	0.77	0	0	0.99	1	2	0	1.00	0.00	0.000	3.8		7.4E+00	0.78	0.26	1.20
3	0.50	19.6	120	1.132	0.042	0.18	1.52	0.77	0	0	0.99	1	2	1	2.28	1.25	0.011	3.8		7.4E+00	0.80	0.28	0.91
4	1.00	19.6	120	1.015	0.041	0.18	1.32	0.74	0	0	0.99	1	2	1	2.28	1.25	0.012	3.8		9.3E-01	0.92	0.37	0.55
5	1.00	19.6	150	1.021	0.048	0.18	1.49	0.78	0	0	0.99	1	2	1	1.61	1.25	0.013	3.8		7.4E+00	0.73	0.22	1.30
6	1.00	19.6	150	0.946	0.054	0.18	1.52	0.77	0	0	0.99	1	2	1	1.61	1.25	0.014	3.8		7.4E+00	0.79	0.27	0.85
7	2.00	19.6	200	0.918	0.055	0.18	1.53	0.81	0	0	0.99	1	2	1	1.03	1.25	0.015	3.8		7.4E+00	0.72	0.24	1.20
8	1.50	19.6	200	0.860	0.060	0.18	1.53	0.81	0	0	0.99	1	2	1	1.03	1.25	0.016	3.8		9.3E-01	0.75	0.27	0.90
9	1.50	19.6	200	0.808	0.067	0.18	1.56	0.80	0	0	0.99	1	2	1	1.03	1.25	0.018	3.8		7.4E-01	0.84	0.35	0.65
10	2.50	19.6	250	0.809	0.061	0.18	1.52	0.86	0	0	0.99	1	2	1	0.73	1.25	0.018	3.8		4.6E-01	0.68	0.24	1.40
11	2.50	19.6	250	0.763	0.059	0.18	1.32	0.83	0	0	0.99	1	2	1	0.73	1.25	0.020	3.8		4.6E-01	0.65	0.18	1.85
12	2.50	19.6	250	0.714	0.076	0.18	1.53	0.81	0	0	0.99	1	2	1	0.73	1.25	0.021	3.8		9.3E-01	0.74	0.26	0.90
13	2.50	19.6	250	0.691	0.072	0.18	1.40	0.81	0	0	0.99	1	2	1	0.73	1.35	0.022	3.8		1.9E-01	0.71	0.23	1.10
14	2.50	19.6	250	0.647	0.078	0.18	1.50	0.80	0	0	0.99	1	2	1	0.73	1.35	0.022	3.8		2.8E-01	0.79	0.29	0.90
15	2.50	19.6	250	0.618	0.074	0.18	1.37	0.78	0	0	0.99	1	2	1	0.73	1.35	0.022	3.8		2.8E-01	0.81	0.30	0.80
16	2.00	19.6	200	0.540	0.098	0.18	1.44	0.69	0	0	0.99	1	2	1	1.03	1.69	0.024	3.8		9.3E-03	0.87	0.27	2.20

For Use in Strength Correction							
Layer #	Thickness (m)	γ (kN/m^3)	Vs (m/s)	OCR	PI	σ'_m (atm)	τ (kPa)
1	1.00	17.3	120	1.0	0	0.1	6.3
2	0.50	17.3	120	1.0	0	0.2	22.2
3	0.50	19.6	120	1.0	0	0.3	29.8
4	1.00	19.6	120	1.0	0	0.4	36.6
5	1.00	19.6	150	1.0	0	0.5	45.8
6	1.00	19.6	150	1.0	0	0.6	55.0
7	2.00	19.6	200	1.0	0	0.7	73.7
8	1.50	19.6	200	1.0	0	0.9	84.8
9	1.50	19.6	200	1.0	0	1.0	95.1
10	2.50	19.6	250	1.0	0	1.2	109.0
11	2.50	19.6	250	1.0	0	1.5	130.3
12	2.50	19.6	250	1.0	0	1.7	159.9
13	2.50	19.6	250	1.0	0	2.0	161.2
14	2.50	19.6	250	1.0	0	2.2	181.1
15	2.50	19.6	250	1.0	0	2.4	201.0
16	2.00	19.6	200	1.0	0	2.7	211.2

Table C. 11: Parameters for Nonlinear Seismic Site Response Analyses SMTC

Layer #	Thickness (m)	γ (kN/m^3)	Vs (m/s)	Damping Ratio (%)	Ref Strain (%)	Ref Stress (MPa)	Beta	s	b	d	Max r_u	PWP Model	f/s/f	p/r/Dr(%)	F/A/FC(%)	s/B/-	g/C/-	v/D/v	-/g/-	C_v (m^2/s)	P1	P2	P3
1	1.25	17.3	170	1.691	0.025	0.18	1.62	0.95	0	0	0.99	1	2	0	1.00	0.00	0.000	3.8		9.3E-02	0.61	0.26	3.25
2	1.25	17.3	170	1.167	0.036	0.18	1.43	0.83	0	0	0.99	1	2	0	1.00	0.00	0.000	3.8		9.3E-02	0.70	0.24	1.49
3	1.00	19.6	230	1.059	0.034	0.18	1.22	0.90	0	0	0.99	1	2	1	0.83	1.25	0.014	3.8		9.3E-02	0.63	0.24	2.15
4	2.00	19.6	230	0.978	0.040	0.18	1.22	0.87	0	0	0.99	1	2	1	0.83	1.25	0.016	3.8		9.3E-02	0.64	0.22	2.15
5	2.25	19.6	230	0.875	0.054	0.18	1.49	0.84	0	0	0.99	1	2	1	0.83	1.25	0.016	3.8		9.3E-02	0.77	0.32	0.85
6	2.25	19.6	230	0.815	0.056	0.18	1.37	0.81	0	0	0.99	1	2	1	0.83	1.25	0.018	3.8		9.3E-02	0.72	0.24	1.10
7	2.00	19.6	230	0.760	0.074	0.18	1.56	0.80	0	0	0.99	1	2	1	0.83	1.25	0.019	3.8		9.3E-02	0.80	0.30	0.75
8	1.00	19.6	140	0.608	0.094	0.18	1.53	0.66	0	0	0.99	1	2	1	1.80	1.59	0.019	3.8		9.3E-04	0.96	0.32	2.35
9	1.00	19.6	140	0.575	0.099	0.18	1.53	0.65	0	0	0.99	1	2	1	1.80	1.59	0.020	3.8		9.3E-04	0.97	0.31	2.45
10	1.00	19.6	140	0.564	0.105	0.18	1.53	0.65	0	0	0.99	1	2	1	1.80	1.59	0.021	3.8		9.3E-04	0.99	0.34	2.87
11	1.00	19.6	140	0.559	0.091	0.18	1.37	0.65	0	0	0.99	1	2	1	1.80	1.25	0.022	3.8		9.3E-02	0.98	0.34	3.15
12	1.00	19.6	140	0.529	0.077	0.18	1.20	0.63	0	0	0.99	1	2	1	1.80	1.25	0.022	3.8		9.3E-02	0.99	0.32	3.15
13	1.00	19.6	140	0.525	0.119	0.18	1.53	0.63	0	0	0.99	1	2	1	1.80	1.59	0.023	3.8		9.3E-04	0.99	0.32	3.19
14	2.50	19.6	300	0.670	0.058	0.18	1.17	0.83	0	0	0.99	1	2	1	0.55	1.25	0.023	3.8		9.3E-02	0.83	0.36	0.65
15	2.50	19.6	300	0.648	0.078	0.18	1.53	0.81	0	0	0.99	1	2	1	0.55	1.25	0.021	3.8		9.3E-02	0.72	0.24	1.25
16	2.50	19.6	300	0.621	0.083	0.18	1.52	0.80	0	0	0.99	1	2	1	0.55	1.25	0.023	3.8		9.3E-02	0.75	0.26	1.00
17	2.50	19.6	300	0.593	0.076	0.18	1.35	0.78	0	0	0.99	1	2	1	0.55	1.25	0.024	3.8		9.3E-02	0.80	0.29	0.80

For Use in Strength Correction							
Layer #	Thickness (m)	γ (kN/m^3)	Vs (m/s)	OCR	PI	σ'_m (atm)	τ (kPa)
1	1.25	17.3	170	1.0	0	0.1	10.8
2	1.25	17.3	170	1.0	0	0.3	33.9
3	1.00	19.6	230	1.0	0	0.5	54.0
4	2.00	19.6	230	1.0	0	0.7	68.7
5	2.25	19.6	230	1.0	0	0.9	89.6
6	2.25	19.6	230	1.0	0	1.1	111.7
7	2.00	19.6	230	1.0	0	1.3	132.6
8	1.00	19.6	140	1.0	0	1.5	115.1
9	1.00	19.6	140	1.0	0	1.6	122.8
10	1.00	19.6	140	1.0	0	1.6	130.5
11	1.00	19.6	140	1.0	0	1.7	138.2
12	1.00	19.6	140	1.0	0	1.8	145.9
13	1.00	19.6	140	1.0	0	1.9	153.5
14	2.50	19.6	300	1.0	0	2.1	213.7
15	2.50	19.6	300	1.0	0	2.4	238.3
16	2.50	19.6	300	1.0	0	2.6	262.9
17	2.50	19.6	300	1.0	0	2.8	287.4

Appendix A.5

Selected Results for Site Response Analyses

Selected results for completed site response analyses are included as separate electronic files attached to this dissertation

Appendix A.6

Liquefaction Triggering Analyses for a Selection of Events at Strong Motion Station Sites

Appendix A.6.1

Liquefaction Triggering Analyses 22 February 2011 Event

GEOLOGISMIKI Geotechnical Software

LIQUEFACTION ANALYSIS REPORT

Project title : G13AP00029 **Location : Christchurch, New Zealand**

CPT file : CBGS_CPT1(Wotherspoon,2013)

Input parameters and analysis data

Analysis method:	B&I (2014)	G.W.T. (in-situ):	2.50 m	Use fill:	No	Clay like behavior applied:	Sands only
Fines correction method:	B&I (2014)	G.W.T. (earthq.):	2.50 m	Fill height:	N/A	Limit depth applied:	No
Points to test:	Based on Ic value	Average results interval:	3	Fill weight:	N/A	Limit depth:	N/A
Earthquake magnitude M_w:	6.20	Ic cut-off value:	2.60	Trans. detect. applied:	No	MSF method:	Method based
Peak ground acceleration:	0.50	Unit weight calculation:	19.00 kN/m³	K_σ applied:	Yes		

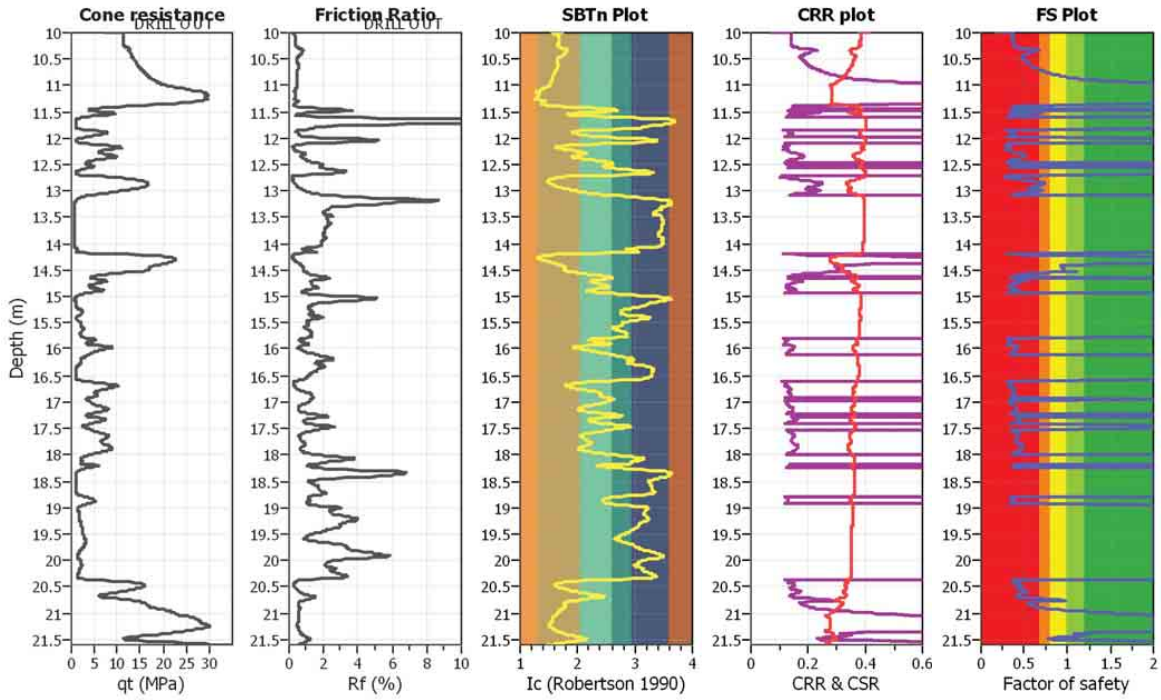

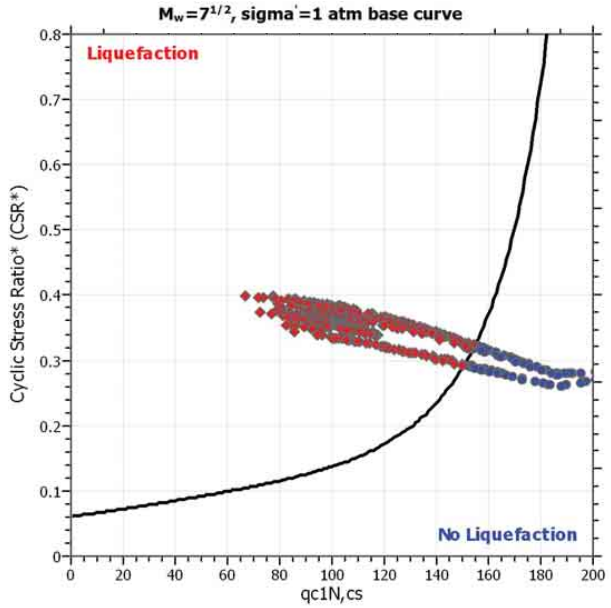

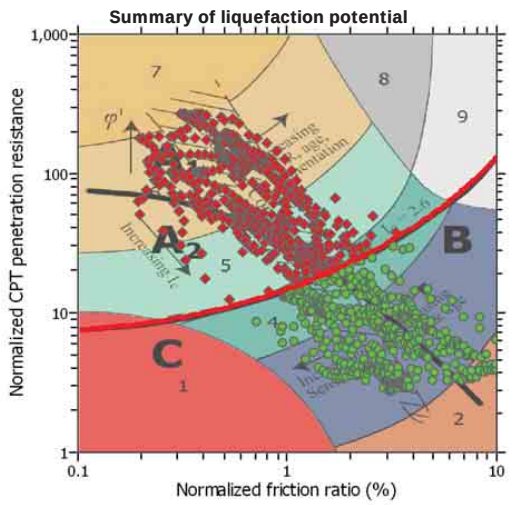

Zone A_1: Cyclic liquefaction likely depending on size and duration of cyclic loading
Zone A_2: Cyclic liquefaction and strength loss likely depending on loading and ground geometry
Zone B: Liquefaction and post-earthquake strength loss unlikely, check cyclic softening
Zone C: Cyclic liquefaction and strength loss possible depending on soil plasticity, brittleness/sensitivity, strain to peak undrained strength and ground geometry

GEOLOGISMIKI Geotechnical Software

LIQUEFACTION ANALYSIS REPORT

Project title : G13AP00029 **Location : Christchurch, New Zealand**

CPT file : CCCC_CPT484(CBD)

Input parameters and analysis data

Analysis method:	B&I (2014)	G.W.T. (in-situ):	1.50 m	Use fill:	No	Clay like behavior applied:	Sands only
Fines correction method:	B&I (2014)	G.W.T. (earthq.):	1.50 m	Fill height:	N/A	Limit depth applied:	No
Points to test:	Based on Ic value	Average results interval:	3	Fill weight:	N/A	Limit depth:	N/A
Earthquake magnitude M_w:	6.20	Ic cut-off value:	2.60	Trans. detect. applied:	No	MSF method:	Method based
Peak ground acceleration:	0.43	Unit weight calculation:	19.00 kN/m³	K_σ applied:	Yes		

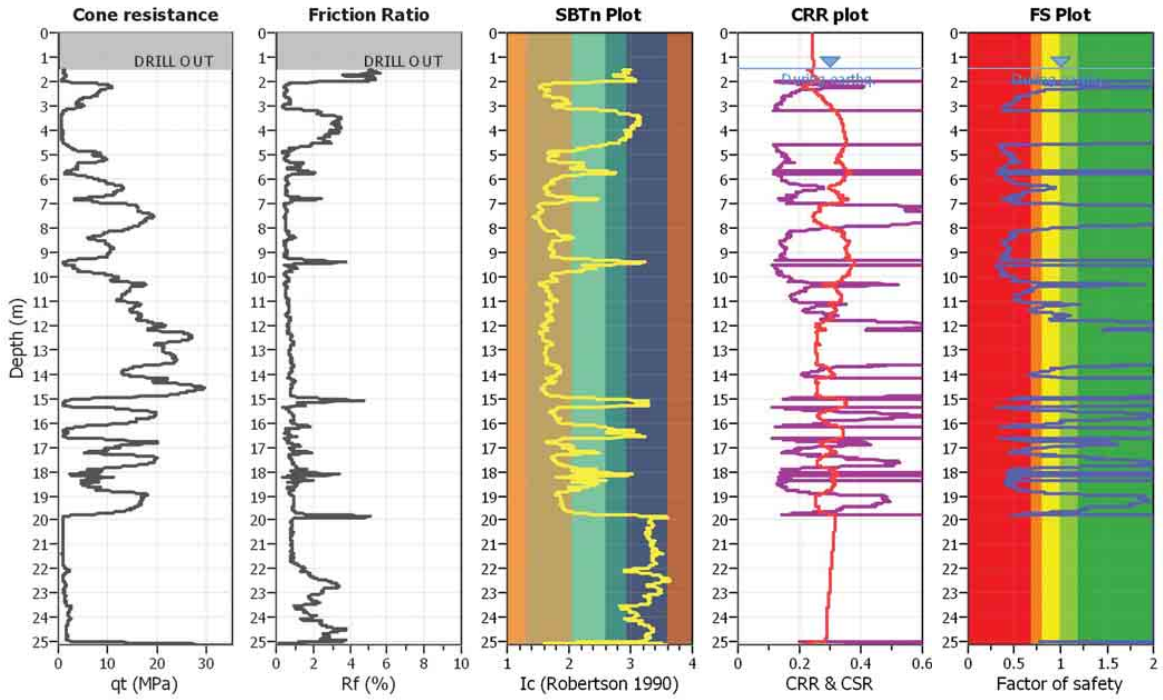

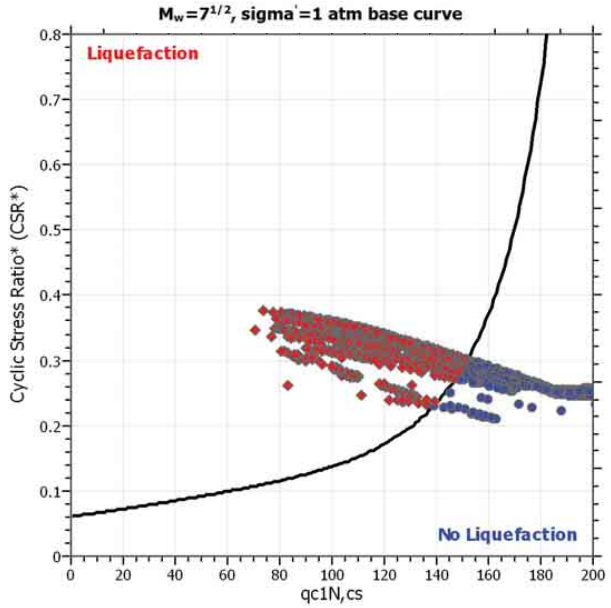

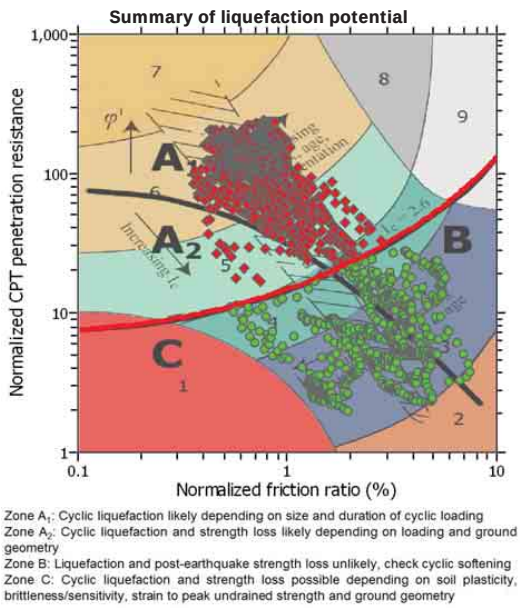

Zone A_1: Cyclic liquefaction likely depending on size and duration of cyclic loading
Zone A_2: Cyclic liquefaction and strength loss likely depending on loading and ground geometry
Zone B: Liquefaction and post-earthquake strength loss unlikely, check cyclic softening
Zone C: Cyclic liquefaction and strength loss possible depending on soil plasticity, brittleness/sensitivity, strain to peak undrained strength and ground geometry

GEOLOGISMIKI Geotechnical Software

LIQUEFACTION ANALYSIS REPORT

Project title : G13AP00029 **Location : Christchurch, New Zealand**

CPT file : CHHC_CPT425(CBD)

Input parameters and analysis data

Analysis method:	B&I (2014)	G.W.T. (in-situ):	3.00 m	Use fill:	No	Clay like behavior applied:	Sands only
Fines correction method:	B&I (2014)	G.W.T. (earthq.):	3.00 m	Fill height:	N/A	Limit depth applied:	No
Points to test:	Based on Ic value	Average results interval:	3	Fill weight:	N/A	Limit depth:	N/A
Earthquake magnitude M_w:	6.20	Ic cut-off value:	2.60	Trans. detect. applied:	No	MSF method:	Method based
Peak ground acceleration:	0.37	Unit weight calculation:	19.00 kN/m³	K_σ applied:	Yes		

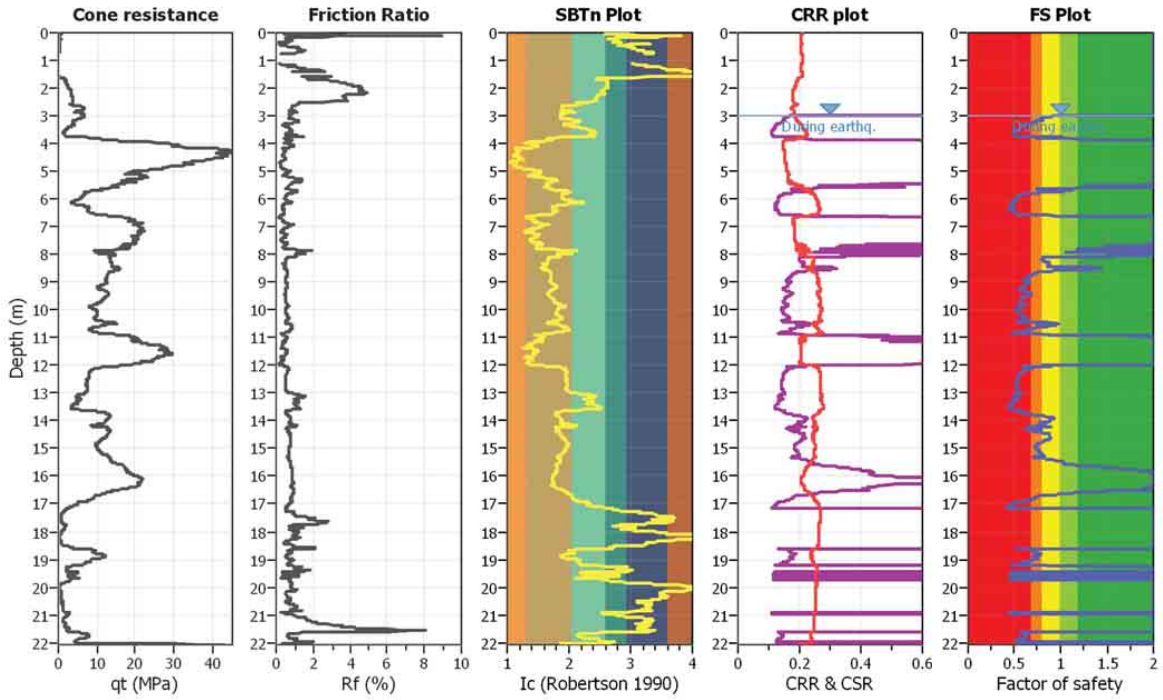

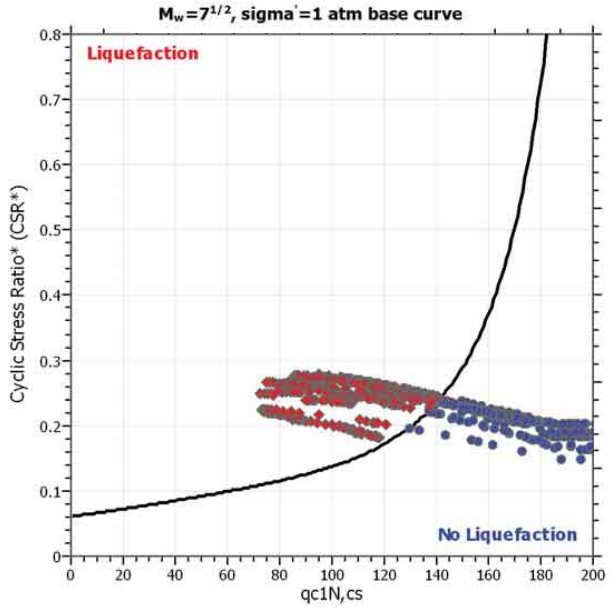

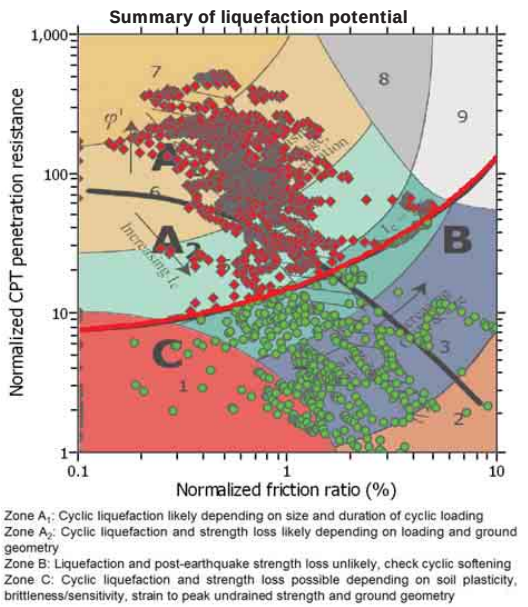

Zone A_1: Cyclic liquefaction likely depending on size and duration of cyclic loading
Zone A_2: Cyclic liquefaction and strength loss likely depending on loading and ground geometry
Zone B: Liquefaction and post-earthquake strength loss unlikely, check cyclic softening
Zone C: Cyclic liquefaction and strength loss possible depending on soil plasticity, brittleness/sensitivity, strain to peak undrained strength and ground geometry

GEOLOGISMIKI Geotechnical Software

LIQUEFACTION ANALYSIS REPORT

Project title : G13AP00029 **Location : Christchurch, New Zealand**

CPT file : HPSC_CPT89(CGD)

Input parameters and analysis data

Analysis method:	B&I (2014)	G.W.T. (in-situ):	2.00 m	Use fill:	No	Clay like behavior applied:	Sands only
Fines correction method:	B&I (2014)	G.W.T. (earthq.):	2.00 m	Fill height:	N/A	Limit depth applied:	No
Points to test:	Based on Ic value	Average results interval:	3	Fill weight:	N/A	Limit depth:	N/A
Earthquake magnitude M_w:	6.20	Ic cut-off value:	2.60	Trans. detect. applied:	No	MSF method:	Method based
Peak ground acceleration:	0.22	Unit weight calculation:	19.00 kN/m³	K_σ applied:	Yes		

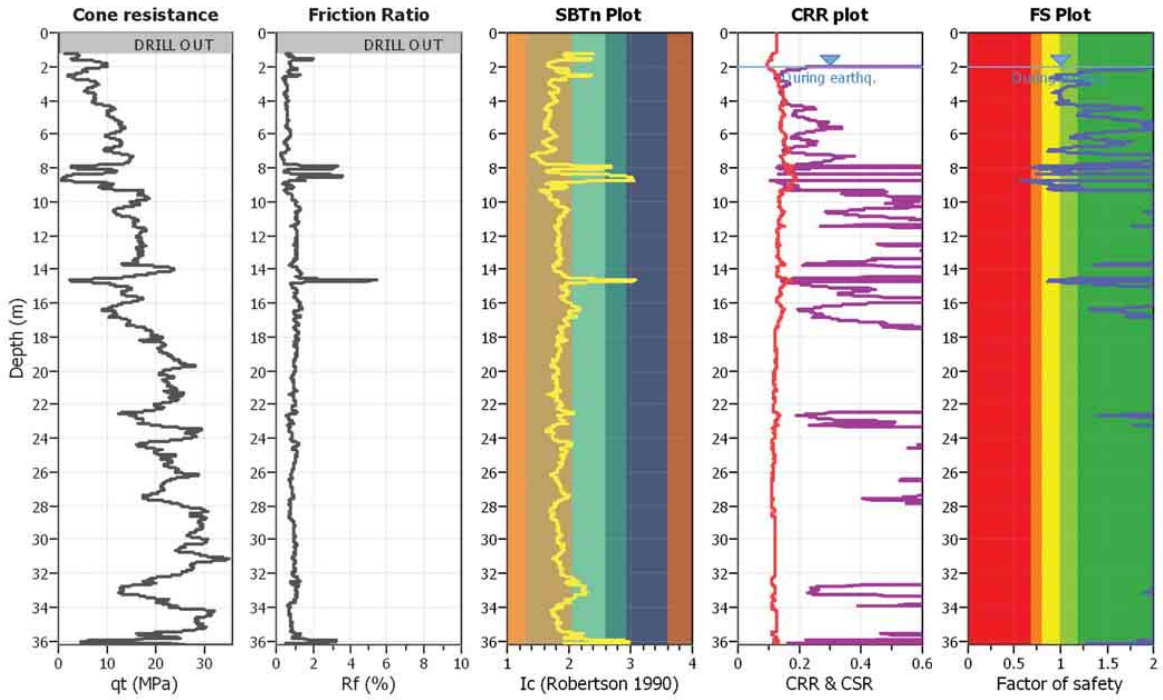

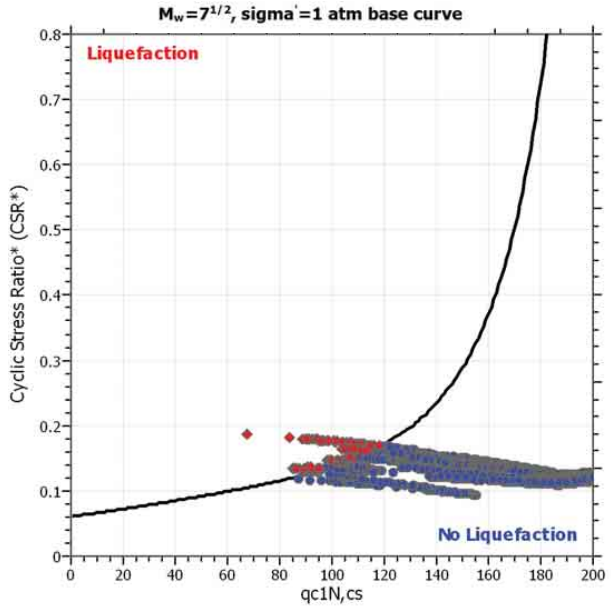

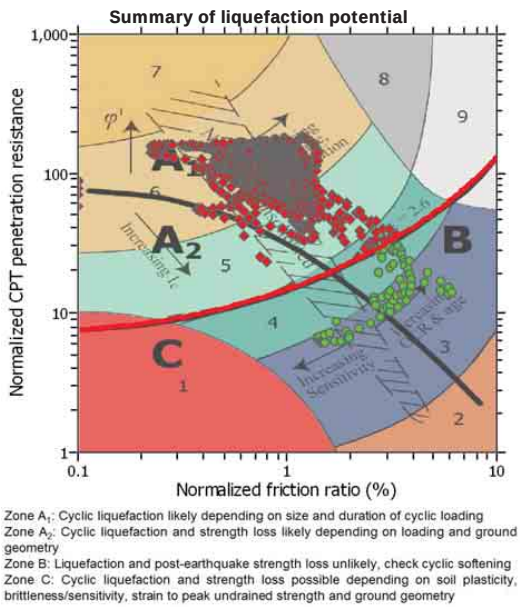

Zone A_1: Cyclic liquefaction likely depending on size and duration of cyclic loading
Zone A_2: Cyclic liquefaction and strength loss likely depending on loading and ground geometry
Zone B: Liquefaction and post-earthquake strength loss unlikely, check cyclic softening
Zone C: Cyclic liquefaction and strength loss possible depending on soil plasticity, brittleness/sensitivity, strain to peak undrained strength and ground geometry

GEOLOGISMIKI Geotechnical Software

LIQUEFACTION ANALYSIS REPORT

Project title : G13AP00029 **Location : Christchurch, New Zealand**

CPT file : NNBS_CPT33695(CGD)

Input parameters and analysis data

Analysis method:	B&I (2014)	G.W.T. (in-situ):	1.50 m	Use fill:	No	Clay like behavior applied:	Sands only
Fines correction method:	B&I (2014)	G.W.T. (earthq.):	1.50 m	Fill height:	N/A	Limit depth applied:	No
Points to test:	Based on Ic value	Average results interval:	3	Fill weight:	N/A	Limit depth:	N/A
Earthquake magnitude M_w:	6.20	Ic cut-off value:	2.60	Trans. detect. applied:	No	MSF method:	Method based
Peak ground acceleration:	0.67	Unit weight calculation:	19.00 kN/m³	K_σ applied:	Yes		

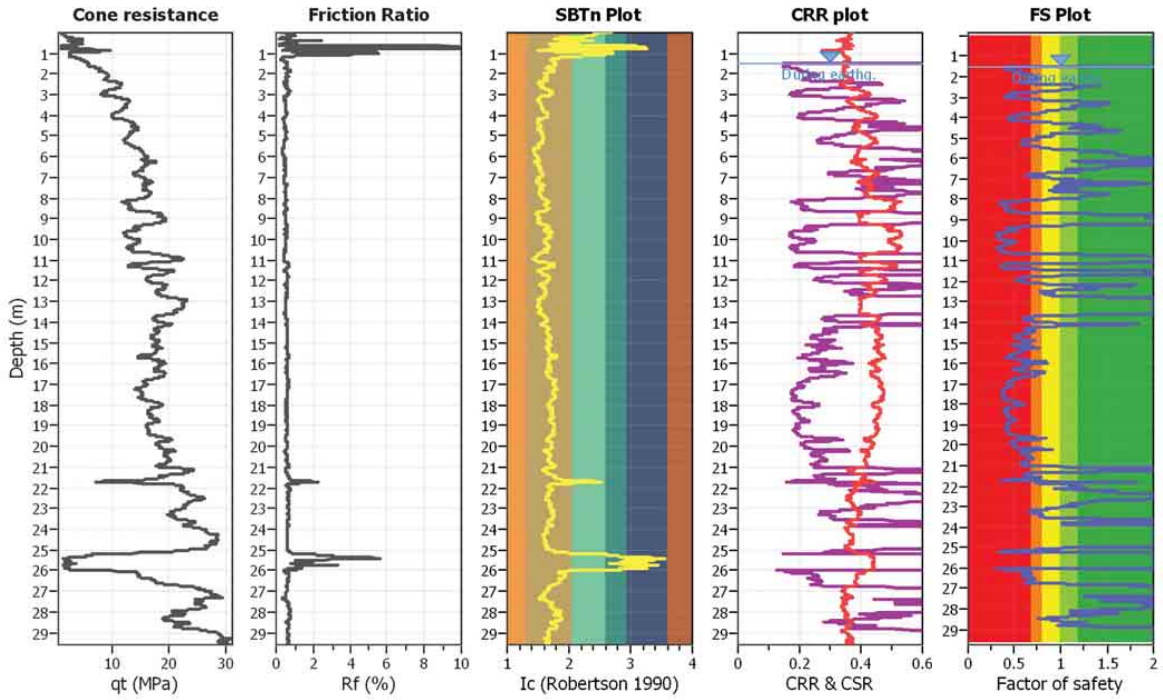

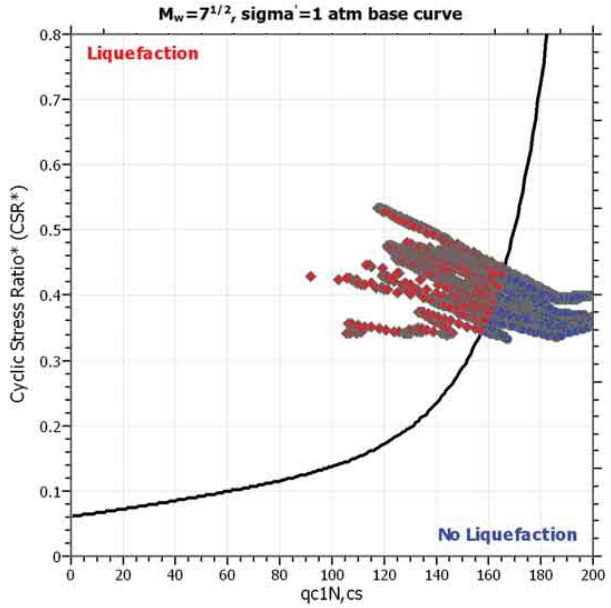

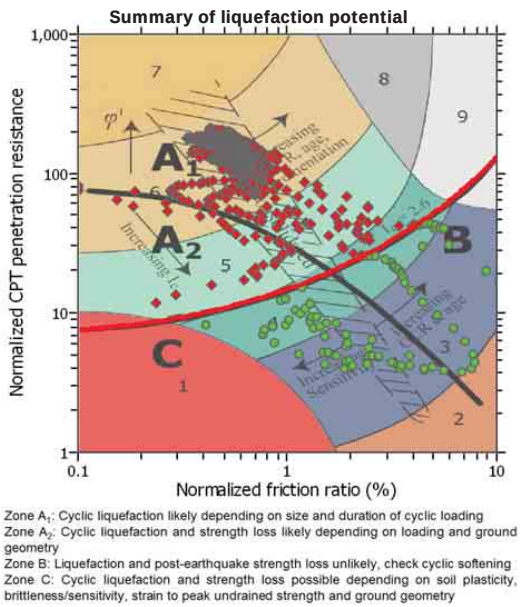

Zone A_1: Cyclic liquefaction likely depending on size and duration of cyclic loading
Zone A_2: Cyclic liquefaction and strength loss likely depending on loading and ground geometry
Zone B: Liquefaction and post-earthquake strength loss unlikely, check cyclic softening
Zone C: Cyclic liquefaction and strength loss possible depending on soil plasticity, brittleness/sensitivity, strain to peak undrained strength and ground geometry

GEOLOGISMIKI Geotechnical Software

LIQUEFACTION ANALYSIS REPORT

Project title : G13AP00029 **Location : Christchurch, New Zealand**

CPT file : PPHS_CPT1497(CGD)

Input parameters and analysis data

Analysis method:	B&I (2014)	G.W.T. (in-situ):	2.50 m	Use fill:	No	Clay like behavior applied:	Sands only
Fines correction method:	B&I (2014)	G.W.T. (earthq.):	2.50 m	Fill height:	N/A	Limit depth applied:	No
Points to test:	Based on Ic value	Average results interval:	3	Fill weight:	N/A	Limit depth:	N/A
Earthquake magnitude M_w:	6.20	Ic cut-off value:	2.60	Trans. detect. applied:	No	MSF method:	Method based
Peak ground acceleration:	0.21	Unit weight calculation:	19.00 kN/m³	K_σ applied:	Yes		

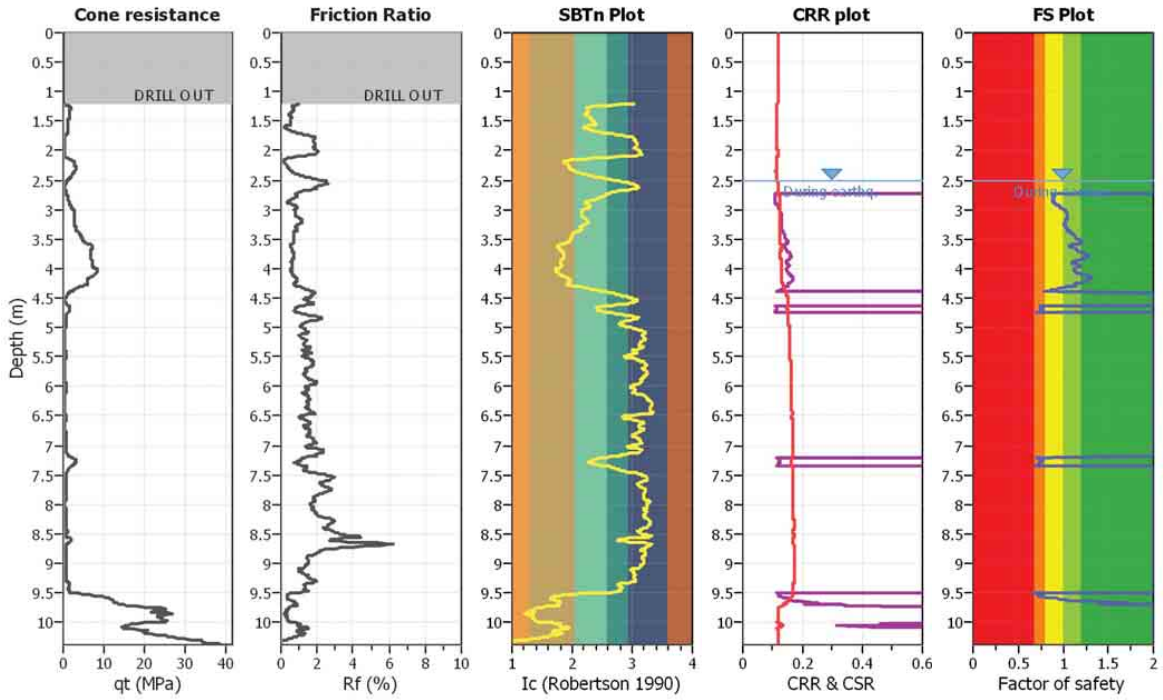

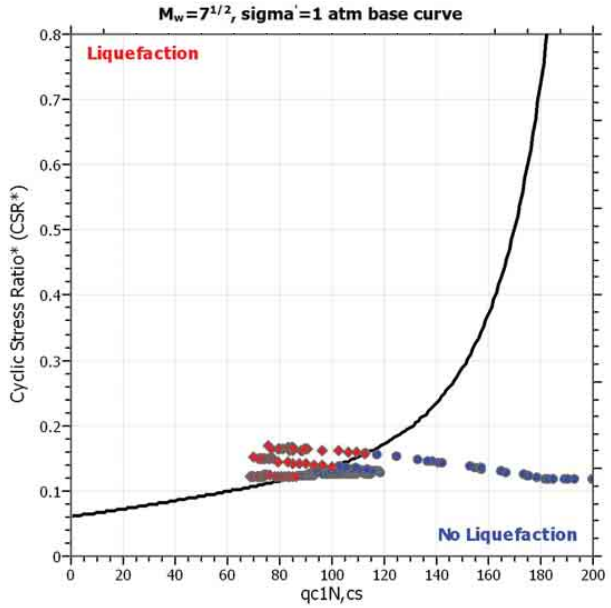

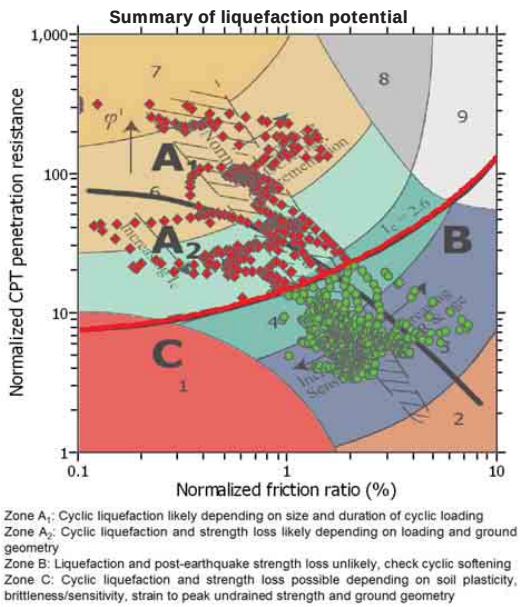

Zone A_1: Cyclic liquefaction likely depending on size and duration of cyclic loading
Zone A_2: Cyclic liquefaction and strength loss likely depending on loading and ground geometry
Zone B: Liquefaction and post-earthquake strength loss unlikely, check cyclic softening
Zone C: Cyclic liquefaction and strength loss possible depending on soil plasticity, brittleness/sensitivity, strain to peak undrained strength and ground geometry

GEOLOGISMIKI Geotechnical Software

LIQUEFACTION ANALYSIS REPORT

Project title : G13AP00029 **Location : Christchurch**

CPT file : PRPC_CPT1396 (CGD)

Input parameters and analysis data

Analysis method:	I&B (2008)	G.W.T. (in-situ):	3.00 m	Use fill:	No	Clay like behavior applied:	Sands only
Fines correction method:	R&W (1998)	G.W.T. (earthq.):	3.00 m	Fill height:	N/A	Limit depth applied:	No
Points to test:	Based on Ic value	Average results interval:	3	Fill weight:	N/A	Limit depth:	N/A
Earthquake magnitude M_w:	6.20	Ic cut-off value:	2.60	Trans. detect. applied:	No	MSF method:	Method based
Peak ground acceleration:	0.63	Unit weight calculation:	19.00 kN/m³	K_σ applied:	Yes		

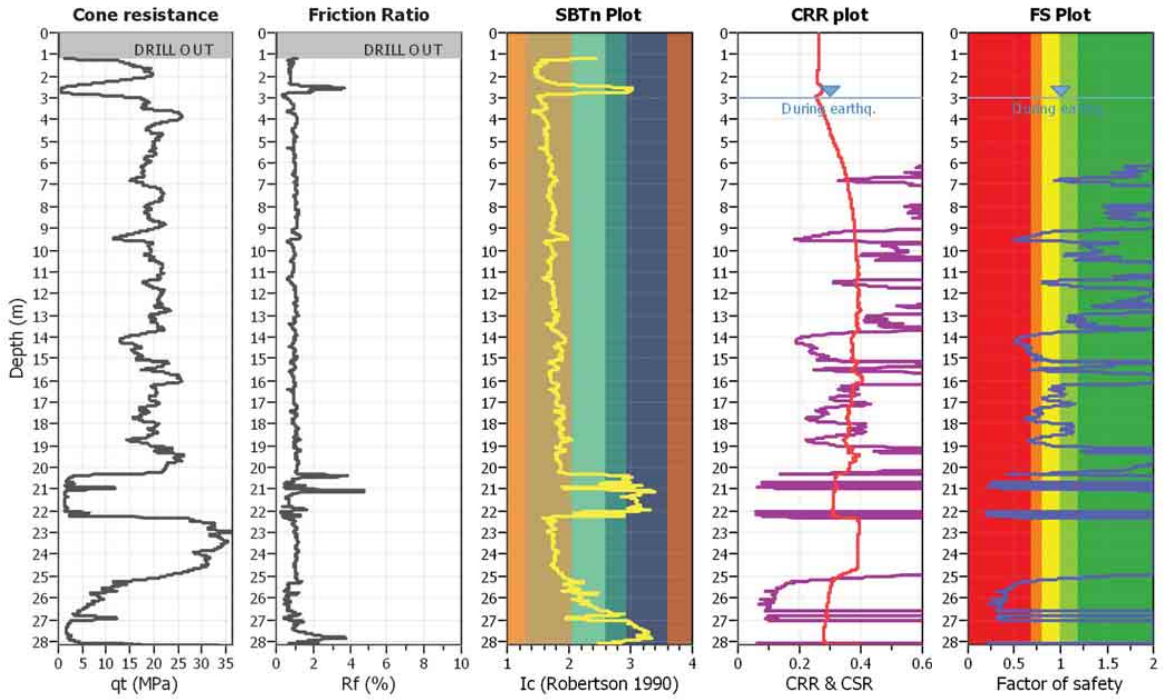

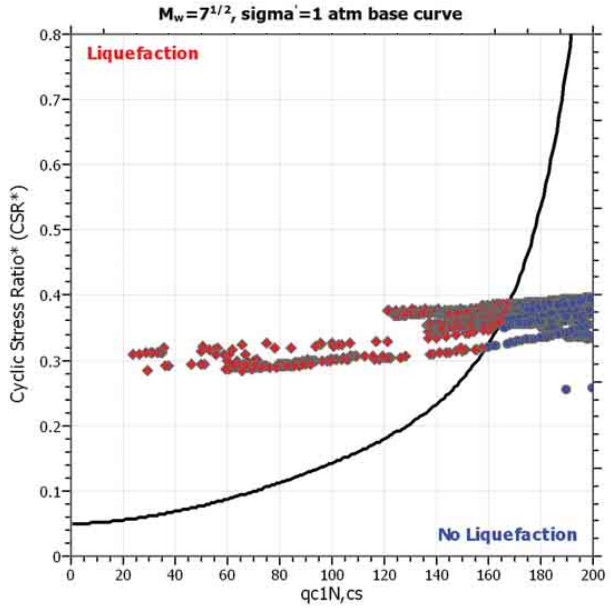

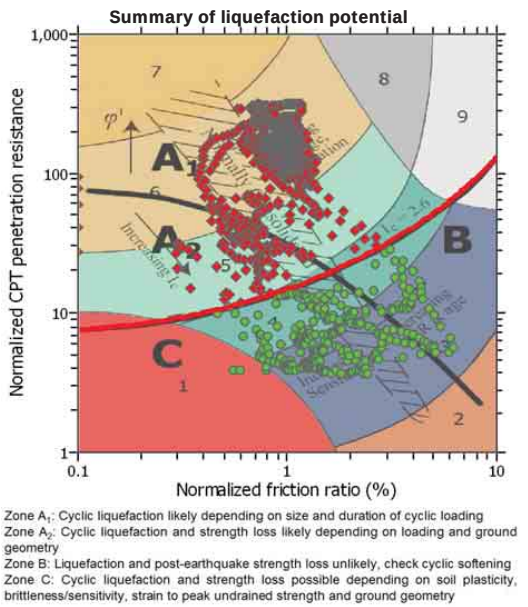

Zone A_1: Cyclic liquefaction likely depending on size and duration of cyclic loading
Zone A_2: Cyclic liquefaction and strength loss likely depending on loading and ground geometry
Zone B: Liquefaction and post-earthquake strength loss unlikely, check cyclic softening
Zone C: Cyclic liquefaction and strength loss possible depending on soil plasticity, brittleness/sensitivity, strain to peak undrained strength and ground geometry

GEOLOGISMIKI Geotechnical Software

LIQUEFACTION ANALYSIS REPORT

Project title : G13AP00029 **Location : Christchurch, New Zealand**

CPT file : REHS_CPT2 (Wotherspoon,2013)

Input parameters and analysis data

Analysis method:	B&I (2014)	G.W.T. (in-situ):	2.00 m	Use fill:	No	Clay like behavior applied:	Sands only
Fines correction method:	B&I (2014)	G.W.T. (earthq.):	2.00 m	Fill height:	N/A	Limit depth applied:	No
Points to test:	Based on Ic value	Average results interval:	3	Fill weight:	N/A	Limit depth:	N/A
Earthquake magnitude M_w:	6.20	Ic cut-off value:	2.60	Trans. detect. applied:	No	MSF method:	Method based
Peak ground acceleration:	0.52	Unit weight calculation:	19.00 kN/m³	K_σ applied:	Yes		

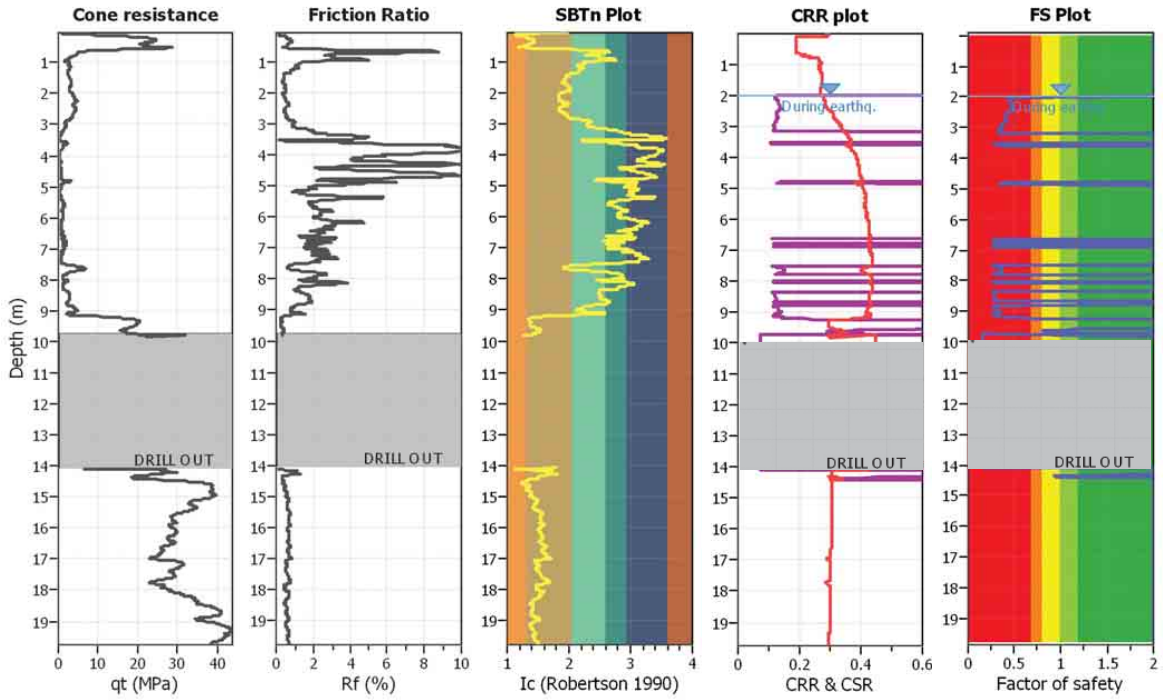

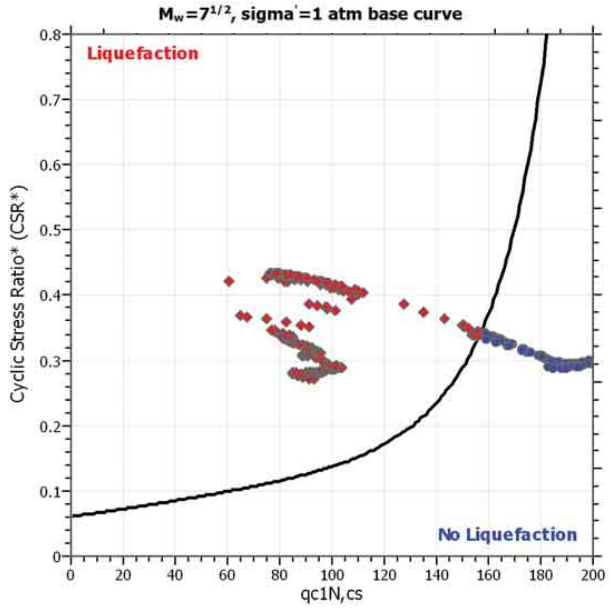

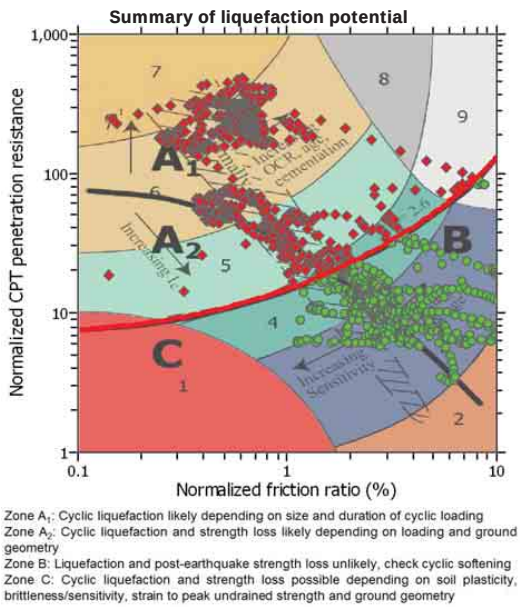

Zone A_1: Cyclic liquefaction likely depending on size and duration of cyclic loading
Zone A_2: Cyclic liquefaction and strength loss likely depending on loading and ground geometry
Zone B: Liquefaction and post-earthquake strength loss unlikely, check cyclic softening
Zone C: Cyclic liquefaction and strength loss possible depending on soil plasticity, brittleness/sensitivity, strain to peak undrained strength and ground geometry

GEOLOGISMIKI Geotechnical Software

LIQUEFACTION ANALYSIS REPORT

Project title : G13AP00029 **Location : Christchurch, New Zealand**

CPT file : SHLC_CPT626(CGD)

Input parameters and analysis data

Analysis method:	B&I (2014)	G.W.T. (in-situ):	1.50 m	Use fill:	No	Clay like behavior applied:	Sands only
Fines correction method:	B&I (2014)	G.W.T. (earthq.):	1.50 m	Fill height:	N/A	Limit depth applied:	No
Points to test:	Based on Ic value	Average results interval:	3	Fill weight:	N/A	Limit depth:	N/A
Earthquake magnitude M_w:	6.20	Ic cut-off value:	2.60	Trans. detect. applied:	No	MSF method:	Method based
Peak ground acceleration:	0.33	Unit weight calculation:	19.00 kN/m³	K_σ applied:	Yes		

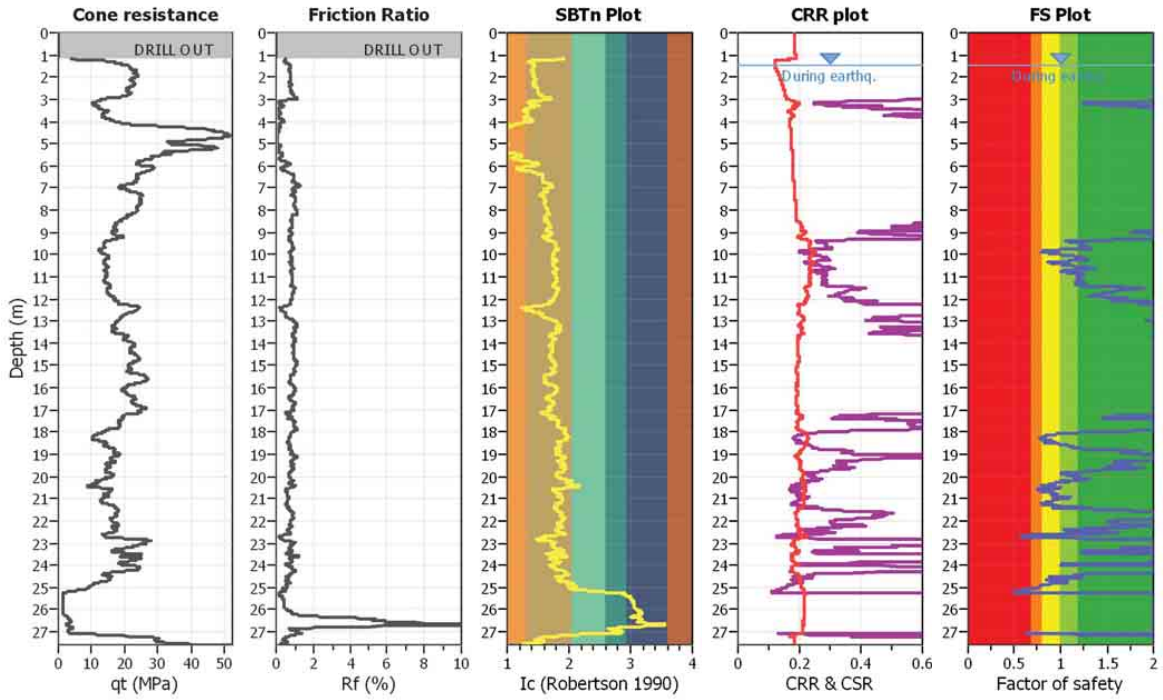

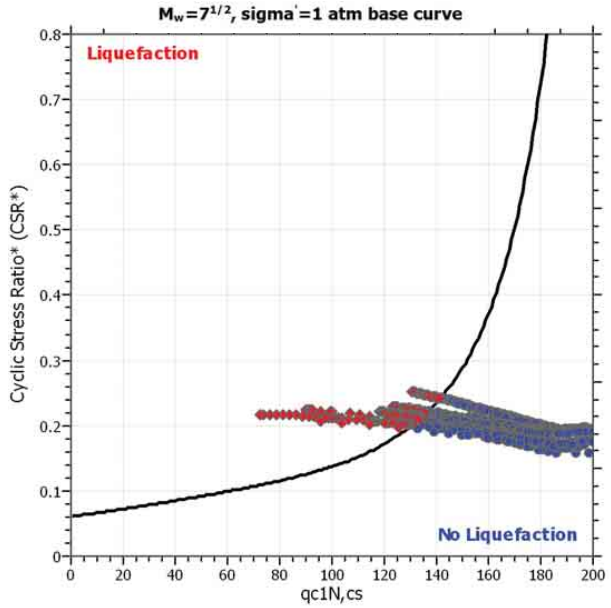

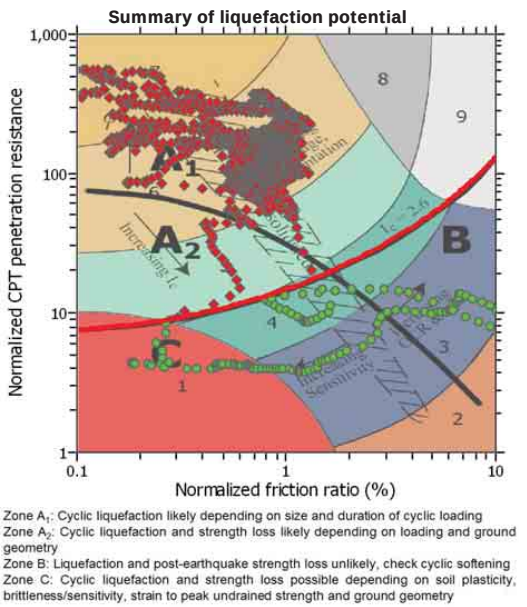

Zone A_1: Cyclic liquefaction likely depending on size and duration of cyclic loading
Zone A_2: Cyclic liquefaction and strength loss likely depending on loading and ground geometry
Zone B: Liquefaction and post-earthquake strength loss unlikely, check cyclic softening
Zone C: Cyclic liquefaction and strength loss possible depending on soil plasticity, brittleness/sensitivity, strain to peak undrained strength and ground geometry

Appendix A.6.2

Liquefaction Triggering Analyses 04 September 2010 Event

GEOLOGISMIKI Geotechnical Software

LIQUEFACTION ANALYSIS REPORT

Project title : G13AP00029 **Location : Christchurch, New Zealand**

CPT file : CBGS_CPT1(Wotherspoon,2013)

Input parameters and analysis data

Analysis method:	B&I (2014)	G.W.T. (in-situ):	2.50 m	Use fill:	No	Clay like behavior applied:	Sands only
Fines correction method:	B&I (2014)	G.W.T. (earthq.):	2.50 m	Fill height:	N/A	Limit depth applied:	No
Points to test:	Based on Ic value	Average results interval:	3	Fill weight:	N/A	Limit depth:	N/A
Earthquake magnitude M_w:	7.10	Ic cut-off value:	2.60	Trans. detect. applied:	No	MSF method:	Method based
Peak ground acceleration:	0.16	Unit weight calculation:	19.00 kN/m³	K_σ applied:	Yes		

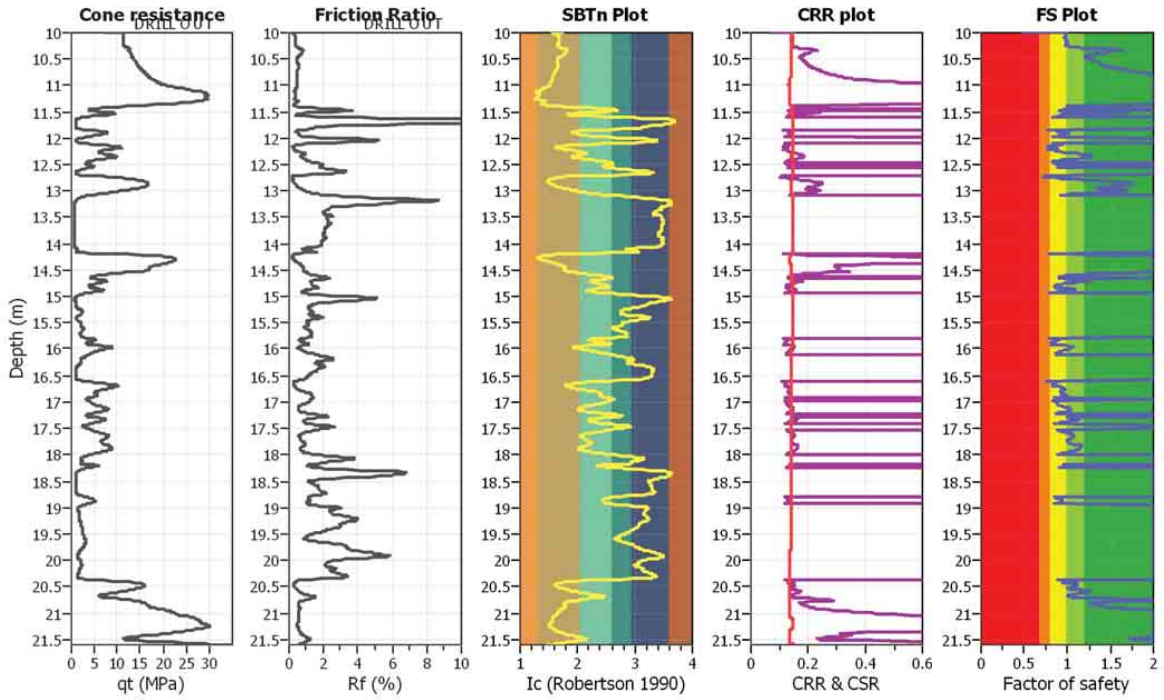

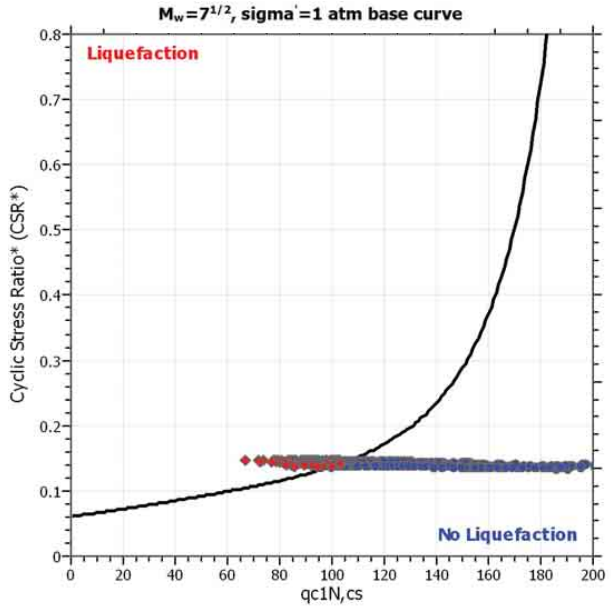

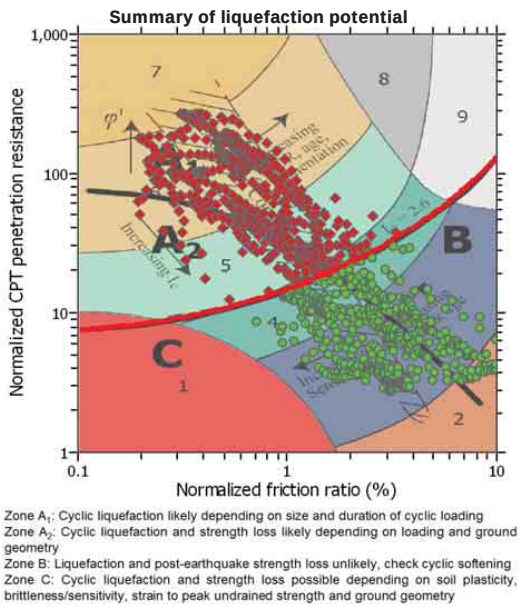

Zone A_1: Cyclic liquefaction likely depending on size and duration of cyclic loading
Zone A_2: Cyclic liquefaction and strength loss likely depending on loading and ground geometry
Zone B: Liquefaction and post-earthquake strength loss unlikely, check cyclic softening
Zone C: Cyclic liquefaction and strength loss possible depending on soil plasticity, brittleness/sensitivity, strain to peak undrained strength and ground geometry

GEOLOGISMIKI Geotechnical Software

LIQUEFACTION ANALYSIS REPORT

Project title : G13AP00029 **Location : Christchurch, New Zealand**

CPT file : CCCC_CPT484(CBD)

Input parameters and analysis data

Analysis method:	B&I (2014)	G.W.T. (in-situ):	1.50 m	Use fill:	No	Clay like behavior applied:	Sands only
Fines correction method:	B&I (2014)	G.W.T. (earthq.):	1.50 m	Fill height:	N/A	Limit depth applied:	No
Points to test:	Based on Ic value	Average results interval:	3	Fill weight:	N/A	Limit depth:	N/A
Earthquake magnitude M_w:	7.10	Ic cut-off value:	2.60	Trans. detect. applied:	No	MSF method:	Method based
Peak ground acceleration:	0.22	Unit weight calculation:	19.00 kN/m³	K_σ applied:	Yes		

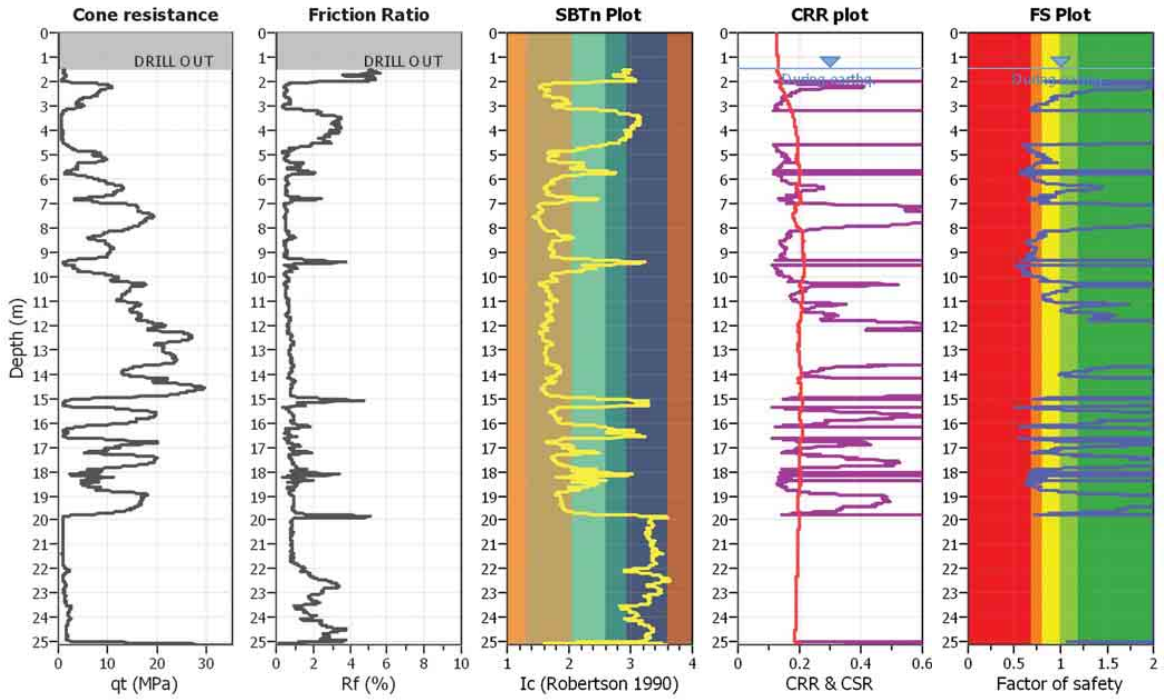

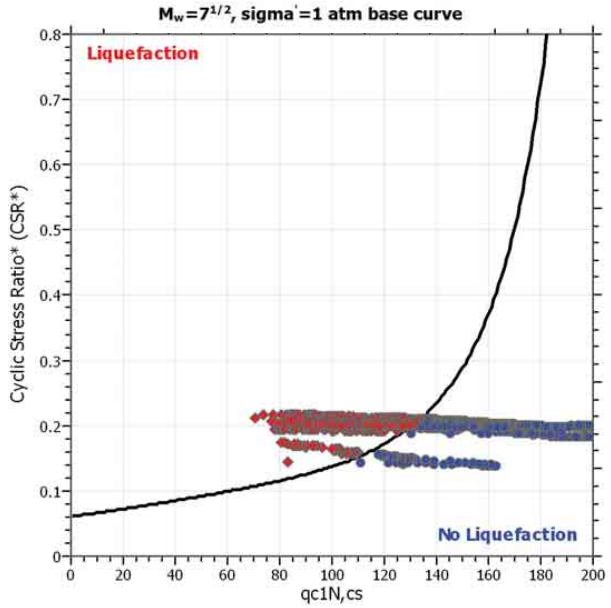

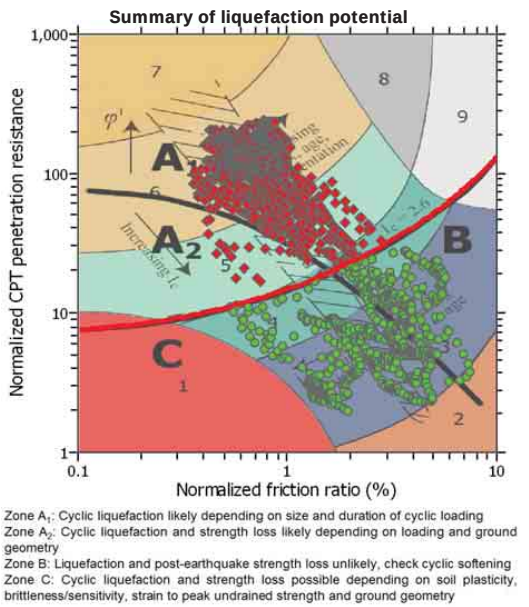

Zone A_1: Cyclic liquefaction likely depending on size and duration of cyclic loading
Zone A_2: Cyclic liquefaction and strength loss likely depending on loading and ground geometry
Zone B: Liquefaction and post-earthquake strength loss unlikely, check cyclic softening
Zone C: Cyclic liquefaction and strength loss possible depending on soil plasticity, brittleness/sensitivity, strain to peak undrained strength and ground geometry

GEOLOGISMIKI Geotechnical Software

LIQUEFACTION ANALYSIS REPORT

Project title : G13AP00029 **Location : Christchurch, New Zealand**

CPT file : CHHC_CPT425(CBD)

Input parameters and analysis data

Analysis method:	B&I (2014)	G.W.T. (in-situ):	3.00 m	Use fill:	No	Clay like behavior applied:	Sands only
Fines correction method:	B&I (2014)	G.W.T. (earthq.):	7.10 m	Fill height:	N/A	Limit depth applied:	No
Points to test:	Based on Ic value	Average results interval:	3	Fill weight:	N/A	Limit depth:	N/A
Earthquake magnitude M_w:	6.20	Ic cut-off value:	2.60	Trans. detect. applied:	No	MSF method:	Method based
Peak ground acceleration:	0.17	Unit weight calculation:	19.00 kN/m³	K_σ applied:	Yes		

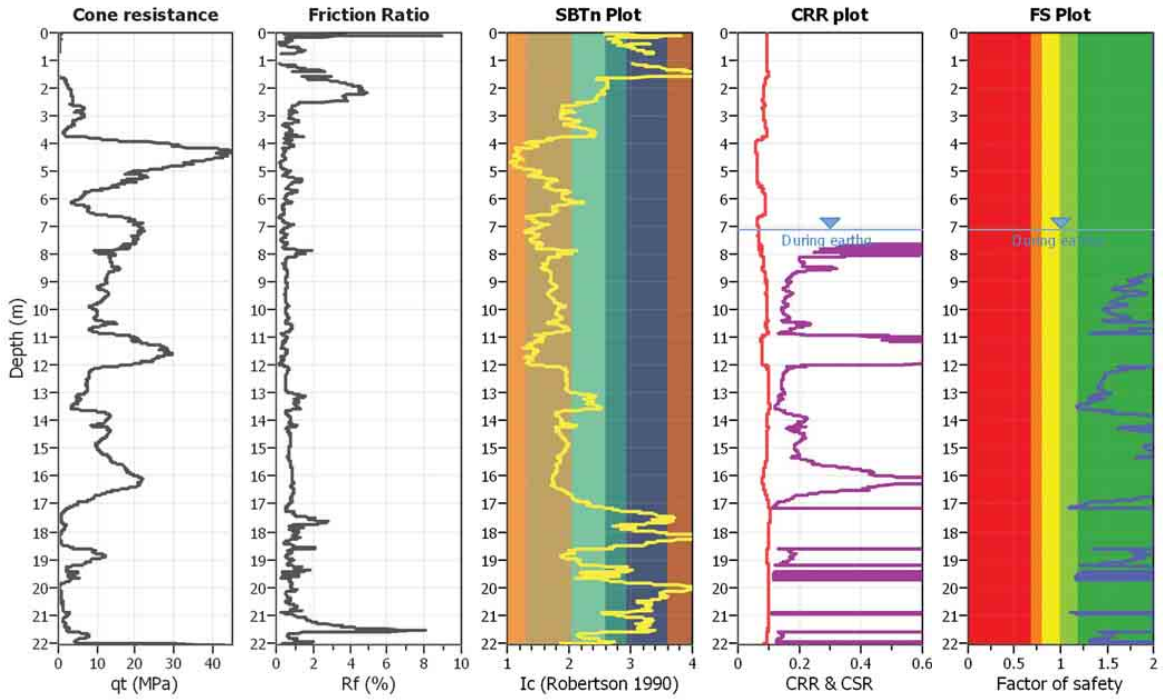

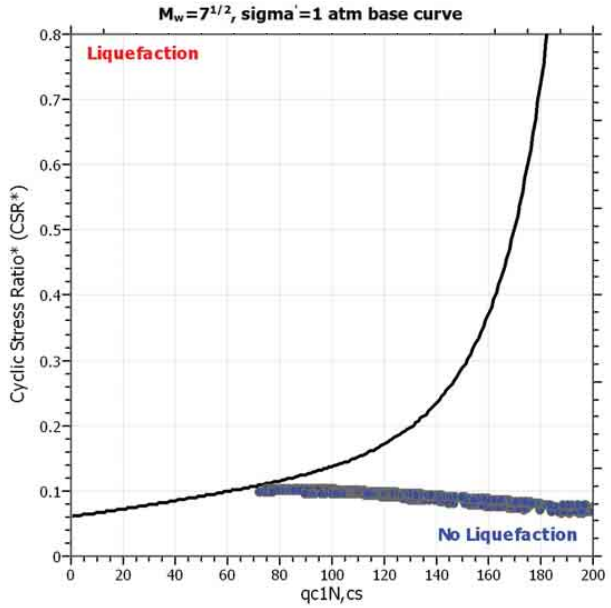

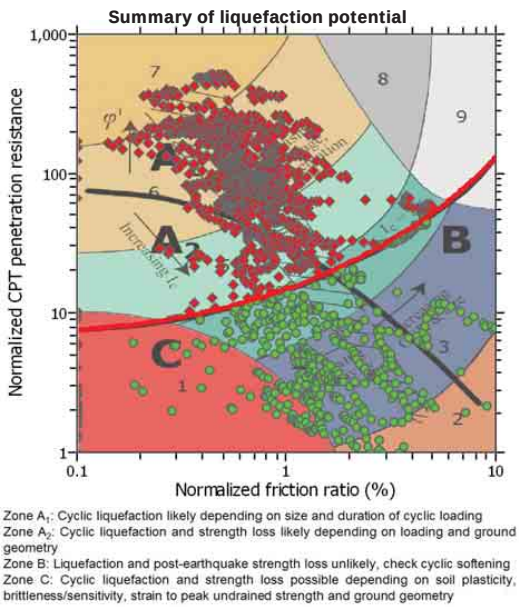

Zone A_1: Cyclic liquefaction likely depending on size and duration of cyclic loading
Zone A_2: Cyclic liquefaction and strength loss likely depending on loading and ground geometry
Zone B: Liquefaction and post-earthquake strength loss unlikely, check cyclic softening
Zone C: Cyclic liquefaction and strength loss possible depending on soil plasticity, brittleness/sensitivity, strain to peak undrained strength and ground geometry

GEOLOGISMIKI Geotechnical Software

LIQUEFACTION ANALYSIS REPORT

Project title : G13AP00029 **Location : Christchurch, New Zealand**

CPT file : HPSC_CPT89(CGD)

Input parameters and analysis data

Analysis method:	B&I (2014)	G.W.T. (in-situ):	2.00 m	Use fill:	No	Clay like behavior applied:	Sands only
Fines correction method:	B&I (2014)	G.W.T. (earthq.):	2.00 m	Fill height:	N/A	Limit depth applied:	No
Points to test:	Based on Ic value	Average results interval:	3	Fill weight:	N/A	Limit depth:	N/A
Earthquake magnitude M_w:	7.10	Ic cut-off value:	2.60	Trans. detect. applied:	No	MSF method:	Method based
Peak ground acceleration:	0.15	Unit weight calculation:	19.00 kN/m³	K_σ applied:	Yes		

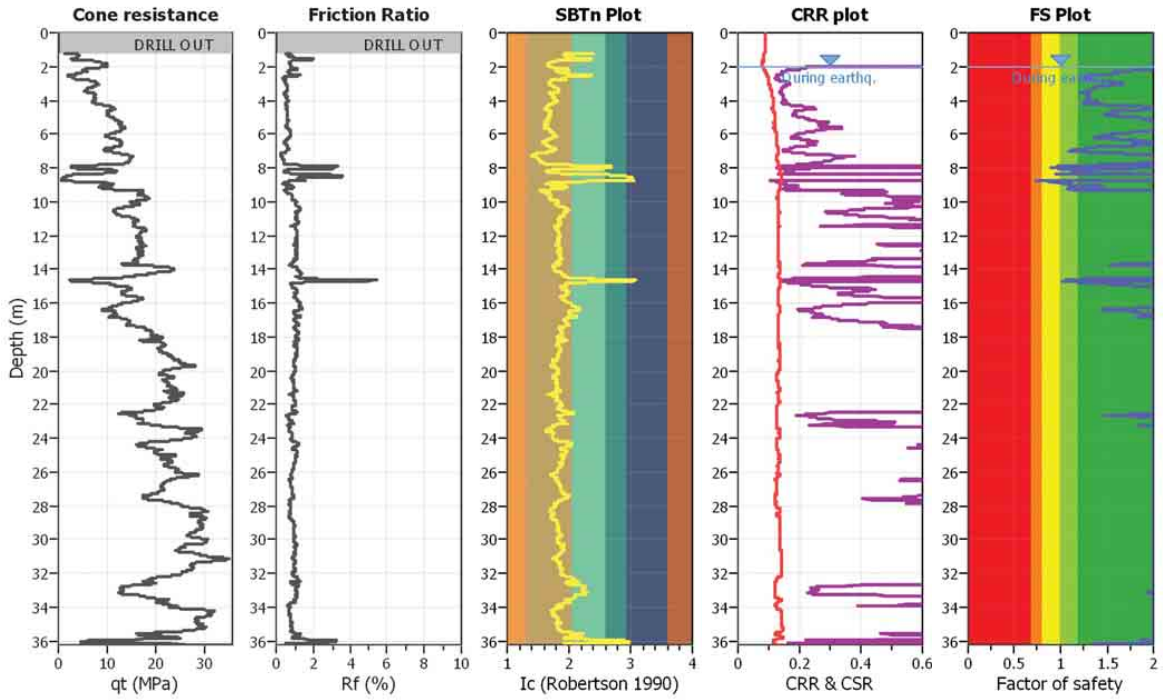

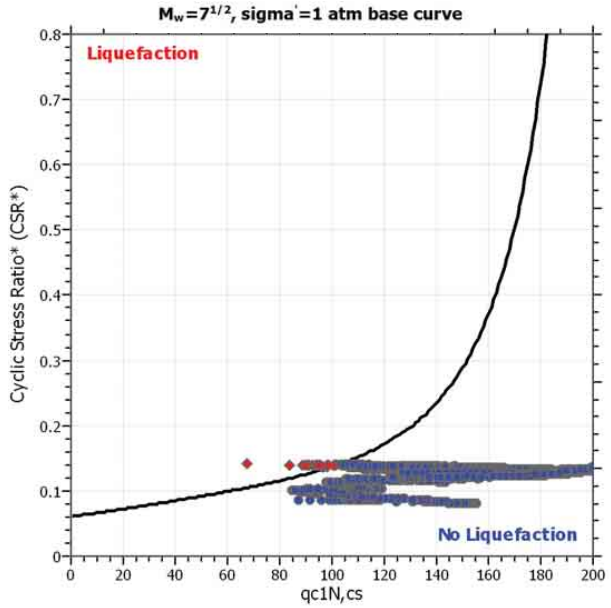

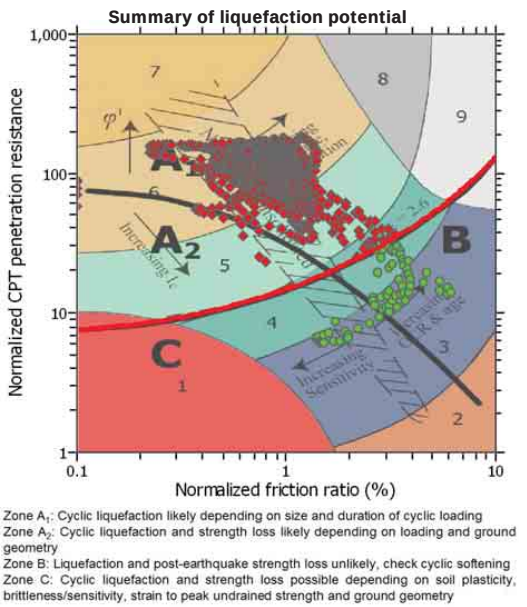

Zone A_1: Cyclic liquefaction likely depending on size and duration of cyclic loading
Zone A_2: Cyclic liquefaction and strength loss likely depending on loading and ground geometry
Zone B: Liquefaction and post-earthquake strength loss unlikely, check cyclic softening
Zone C: Cyclic liquefaction and strength loss possible depending on soil plasticity, brittleness/sensitivity, strain to peak undrained strength and ground geometry

GEOLOGISMIKI Geotechnical Software

LIQUEFACTION ANALYSIS REPORT

Project title : G13AP00029 **Location : Christchurch, New Zealand**

CPT file : NNBS_CPT33695(CGD)

Input parameters and analysis data

Analysis method:	B&I (2014)	G.W.T. (in-situ):	1.50 m	Use fill:	No	Clay like behavior applied:	Sands only
Fines correction method:	B&I (2014)	G.W.T. (earthq.):	1.50 m	Fill height:	N/A	Limit depth applied:	No
Points to test:	Based on Ic value	Average results interval:	3	Fill weight:	N/A	Limit depth:	N/A
Earthquake magnitude M_w:	7.10	Ic cut-off value:	2.60	Trans. detect. applied:	No	MSF method:	Method based
Peak ground acceleration:	0.21	Unit weight calculation:	19.00 kN/m³	K_σ applied:	Yes		

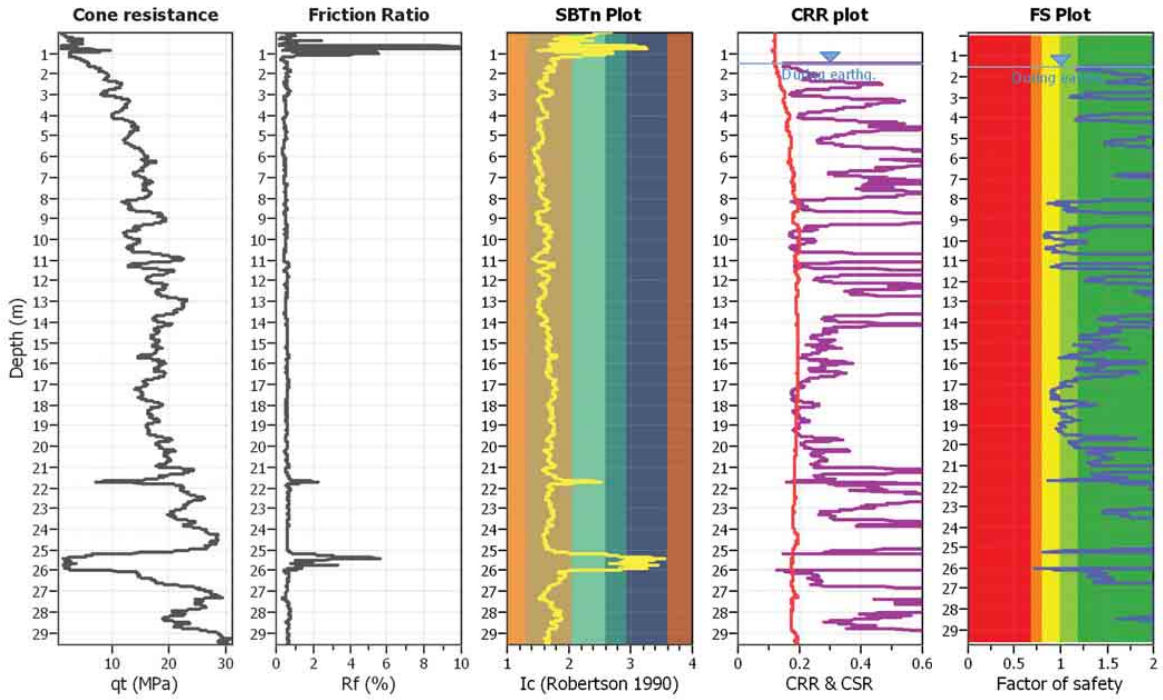

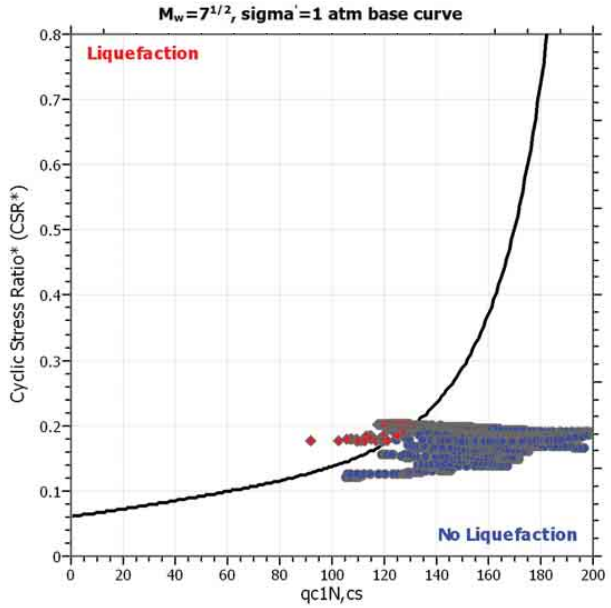

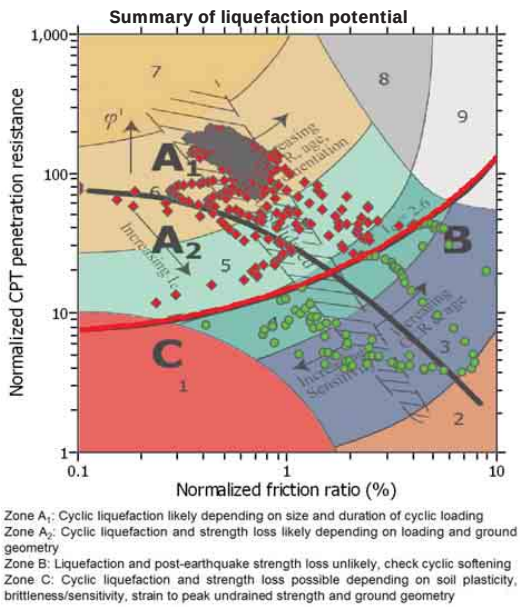

Zone A_1: Cyclic liquefaction likely depending on size and duration of cyclic loading
Zone A_2: Cyclic liquefaction and strength loss likely depending on loading and ground geometry
Zone B: Liquefaction and post-earthquake strength loss unlikely, check cyclic softening
Zone C: Cyclic liquefaction and strength loss possible depending on soil plasticity, brittleness/sensitivity, strain to peak undrained strength and ground geometry

GEOLOGISMIKI Geotechnical Software

LIQUEFACTION ANALYSIS REPORT

Project title : G13AP00029 **Location : Christchurch, New Zealand**

CPT file : PPHS_CPT1497(CGD)

Input parameters and analysis data

Analysis method:	B&I (2014)	G.W.T. (in-situ):	2.50 m	Use fill:	No	Clay like behavior applied:	Sands only
Fines correction method:	B&I (2014)	G.W.T. (earthq.):	2.50 m	Fill height:	N/A	Limit depth applied:	No
Points to test:	Based on Ic value	Average results interval:	3	Fill weight:	N/A	Limit depth:	N/A
Earthquake magnitude M_w:	7.10	Ic cut-off value:	2.60	Trans. detect. applied:	No	MSF method:	Method based
Peak ground acceleration:	0.22	Unit weight calculation:	19.00 kN/m³	K_σ applied:	Yes		

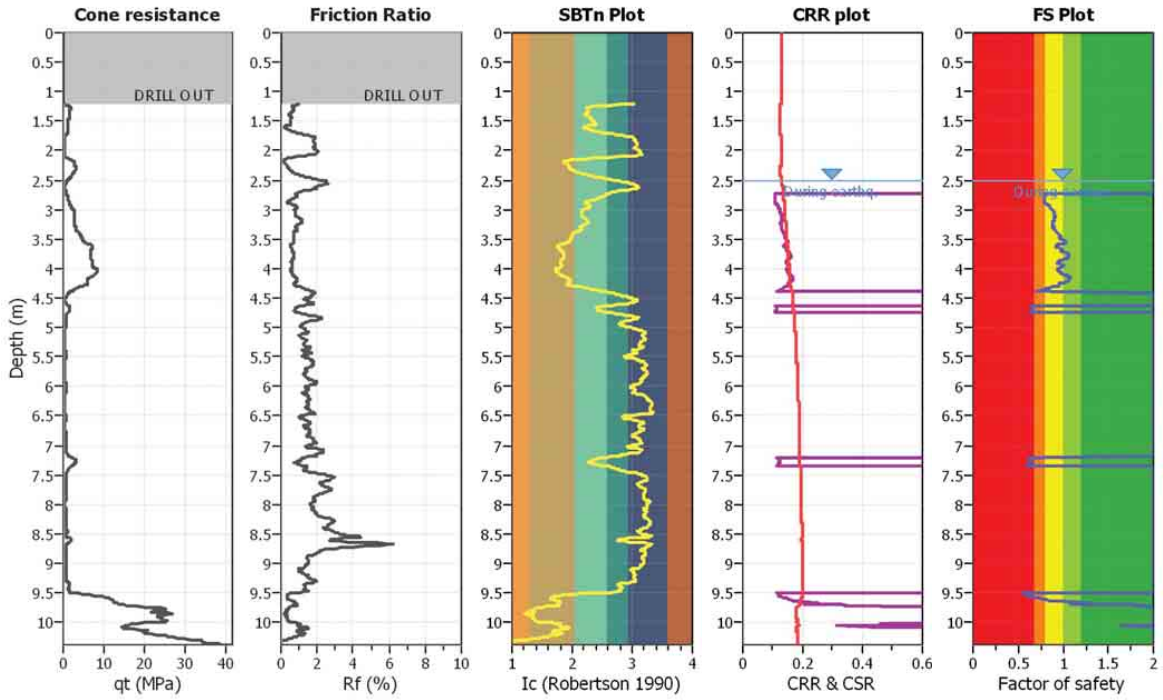

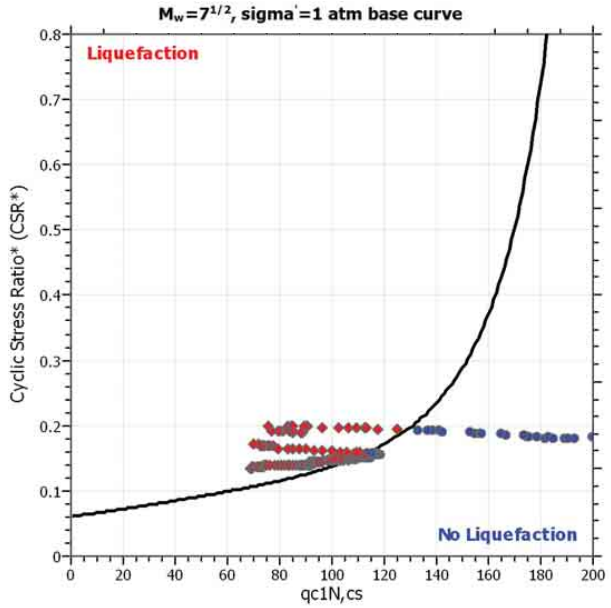

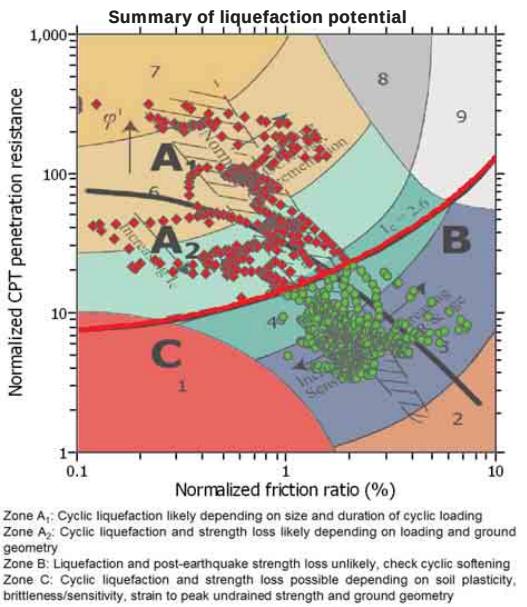

Zone A_1: Cyclic liquefaction likely depending on size and duration of cyclic loading
Zone A_2: Cyclic liquefaction and strength loss likely depending on loading and ground geometry
Zone B: Liquefaction and post-earthquake strength loss unlikely, check cyclic softening
Zone C: Cyclic liquefaction and strength loss possible depending on soil plasticity, brittleness/sensitivity, strain to peak undrained strength and ground geometry

GEOLOGISMIKI Geotechnical Software

LIQUEFACTION ANALYSIS REPORT

Project title : G13AP00029 **Location : Christchurch**

CPT file : PRPC_CPT1396 (CGD)

Input parameters and analysis data

Analysis method:	I&B (2008)	G.W.T. (in-situ):	3.00 m	Use fill:	No	Clay like behavior applied:	Sands only
Fines correction method:	R&W (1998)	G.W.T. (earthq.):	3.00 m	Fill height:	N/A	Limit depth applied:	No
Points to test:	Based on Ic value	Average results interval:	3	Fill weight:	N/A	Limit depth:	N/A
Earthquake magnitude M_w:	7.10	Ic cut-off value:	2.60	Trans. detect. applied:	No	MSF method:	Method based
Peak ground acceleration:	0.21	Unit weight calculation:	19.00 kN/m³	K_σ applied:	Yes		

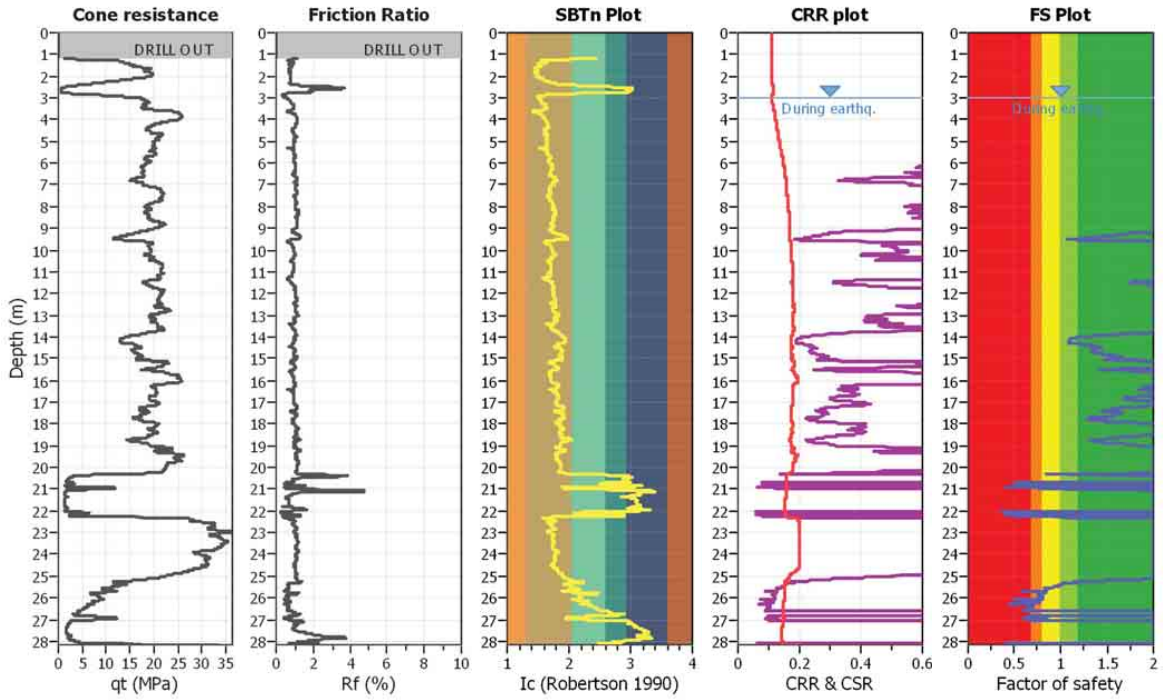

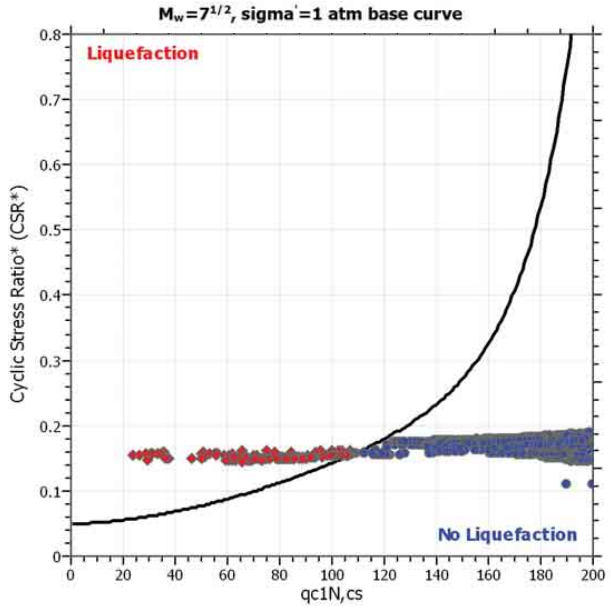

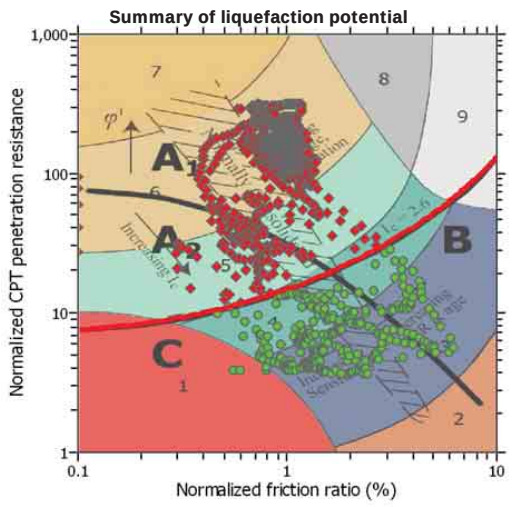

Zone A_1: Cyclic liquefaction likely depending on size and duration of cyclic loading
Zone A_2: Cyclic liquefaction and strength loss likely depending on loading and ground geometry
Zone B: Liquefaction and post-earthquake strength loss unlikely, check cyclic softening
Zone C: Cyclic liquefaction and strength loss possible depending on soil plasticity, brittleness/sensitivity, strain to peak undrained strength and ground geometry

GEOLOGISMIKI Geotechnical Software

LIQUEFACTION ANALYSIS REPORT

Project title : G13AP00029 **Location : Christchurch, New Zealand**

CPT file : REHS_CPT2 (Wotherspoon,2013)

Input parameters and analysis data

Analysis method:	B&I (2014)	G.W.T. (in-situ):	2.00 m	Use fill:	No	Clay like behavior applied:	Sands only
Fines correction method:	B&I (2014)	G.W.T. (earthq.):	2.00 m	Fill height:	N/A	Limit depth applied:	No
Points to test:	Based on Ic value	Average results interval:	3	Fill weight:	N/A	Limit depth:	N/A
Earthquake magnitude M_w:	7.10	Ic cut-off value:	2.60	Trans. detect. applied:	No	MSF method:	Method based
Peak ground acceleration:	0.25	Unit weight calculation:	19.00 kN/m³	K_σ applied:	Yes		

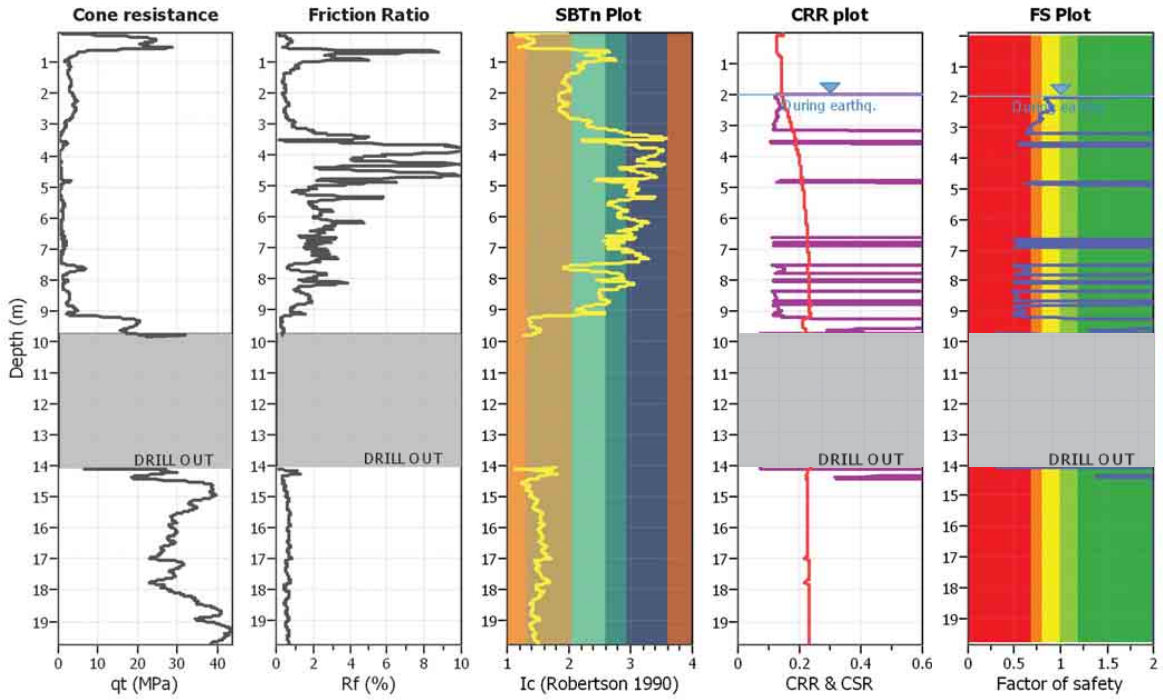

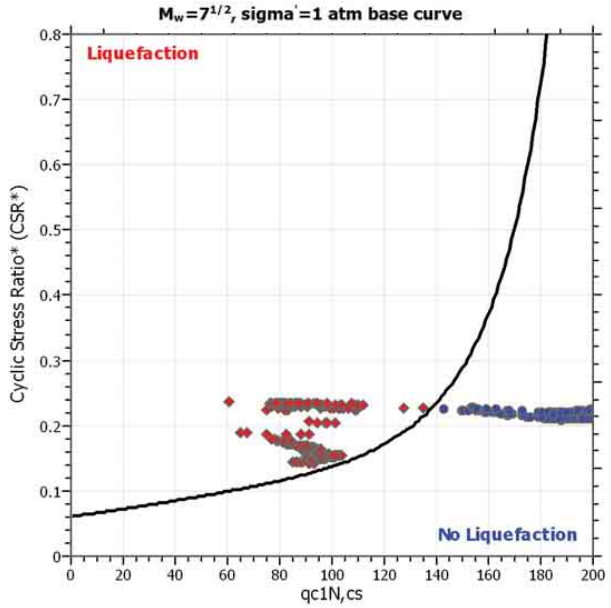

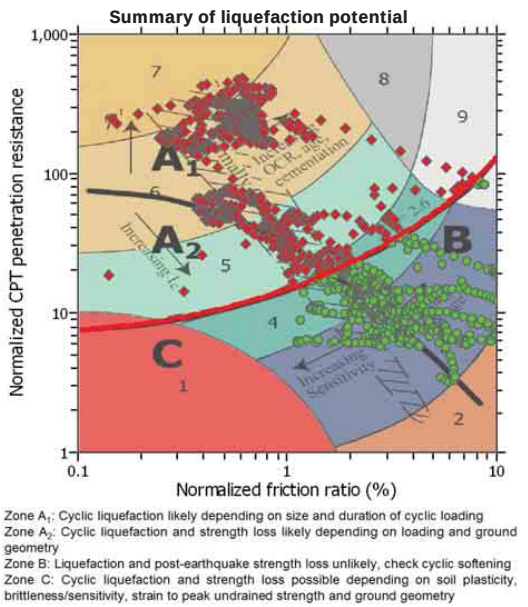

Zone A_1: Cyclic liquefaction likely depending on size and duration of cyclic loading
Zone A_2: Cyclic liquefaction and strength loss likely depending on loading and ground geometry
Zone B: Liquefaction and post-earthquake strength loss unlikely, check cyclic softening
Zone C: Cyclic liquefaction and strength loss possible depending on soil plasticity, brittleness/sensitivity, strain to peak undrained strength and ground geometry

GEOLOGISMIKI Geotechnical Software

LIQUEFACTION ANALYSIS REPORT

Project title : G13AP00029 **Location : Christchurch, New Zealand**

CPT file : SHLC_CPT626(CGD)

Input parameters and analysis data

Analysis method:	B&I (2014)	G.W.T. (in-situ):	1.50 m	Use fill:	No	Clay like behavior applied:	Sands only
Fines correction method:	B&I (2014)	G.W.T. (earthq.):	1.50 m	Fill height:	N/A	Limit depth applied:	No
Points to test:	Based on Ic value	Average results interval:	3	Fill weight:	N/A	Limit depth:	N/A
Earthquake magnitude M_w:	7.10	Ic cut-off value:	2.60	Trans. detect. applied:	No	MSF method:	Method based
Peak ground acceleration:	0.18	Unit weight calculation:	19.00 kN/m³	K_σ applied:	Yes		

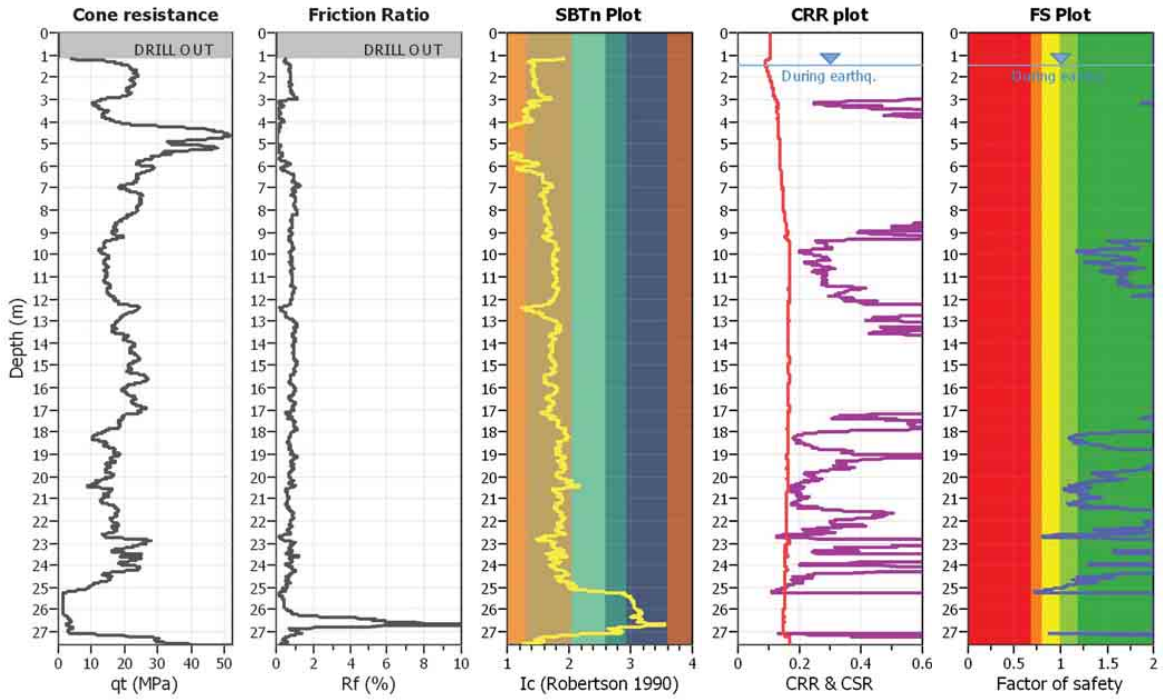

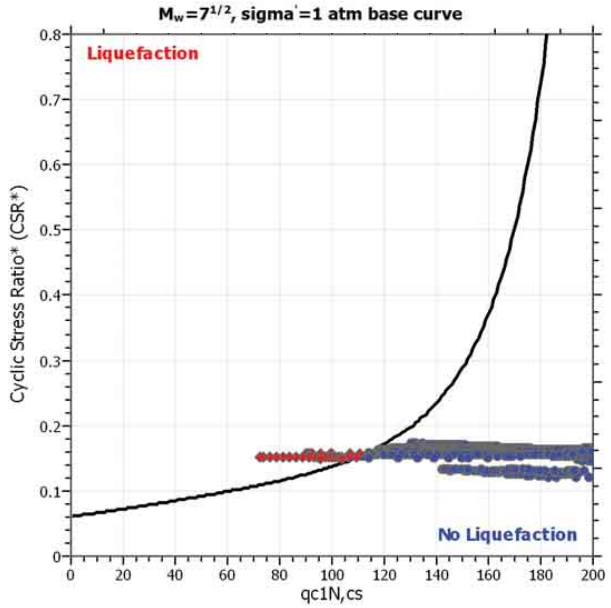

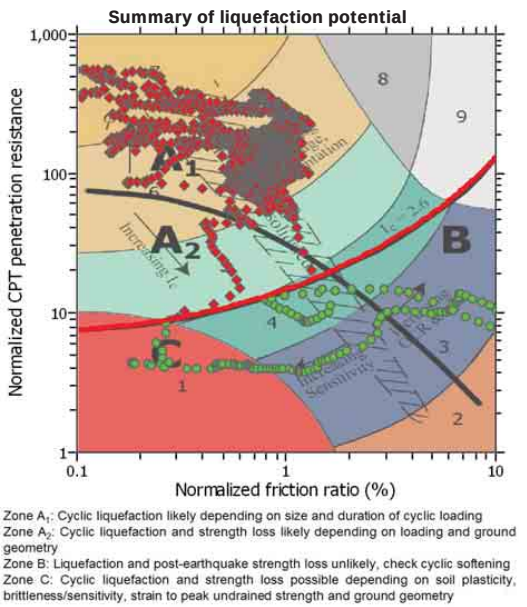

Zone A_1: Cyclic liquefaction likely depending on size and duration of cyclic loading
Zone A_2: Cyclic liquefaction and strength loss likely depending on loading and ground geometry
Zone B: Liquefaction and post-earthquake strength loss unlikely, check cyclic softening
Zone C: Cyclic liquefaction and strength loss possible depending on soil plasticity, brittleness/sensitivity, strain to peak undrained strength and ground geometry

Appendix A.6.3

Liquefaction Triggering Analyses 26 December 2010 Event

GEOLOGISMIKI Geotechnical Software

LIQUEFACTION ANALYSIS REPORT

Project title : G13AP00029 **Location : Christchurch, New Zealand**

CPT file : CBGS_CPT1(Wotherspoon,2013)

Input parameters and analysis data

Analysis method:	B&I (2014)	G.W.T. (in-situ):	1.50 m	Use fill:	No	Clay like behavior applied:	Sands only
Fines correction method:	B&I (2014)	G.W.T. (earthq.):	1.50 m	Fill height:	N/A	Limit depth applied:	No
Points to test:	Based on Ic value	Average results interval:	3	Fill weight:	N/A	Limit depth:	N/A
Earthquake magnitude M_w:	4.70	Ic cut-off value:	2.60	Trans. detect. applied:	No	MSF method:	Method based
Peak ground acceleration:	0.27	Unit weight calculation:	19.00 kN/m³	K_σ applied:	Yes		

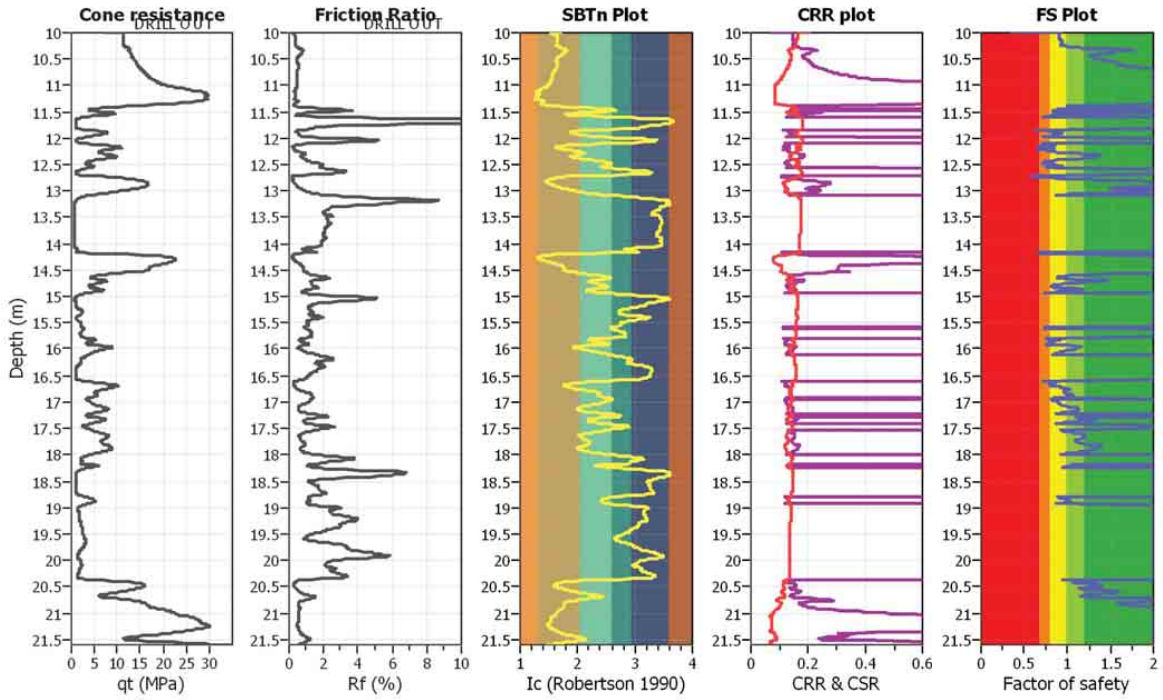

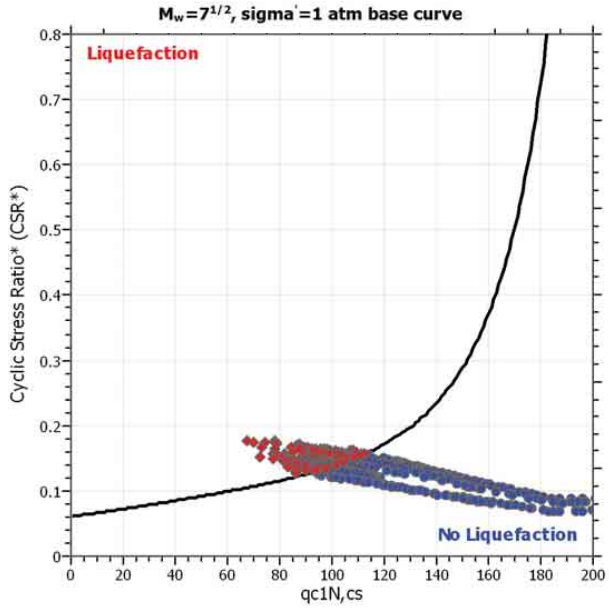

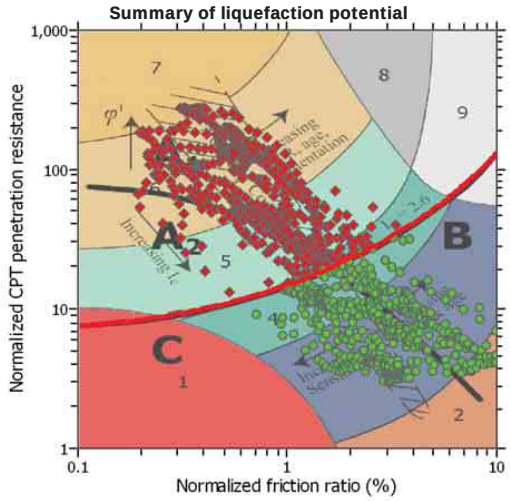

Zone A_1: Cyclic liquefaction likely depending on size and duration of cyclic loading
Zone A_2: Cyclic liquefaction and strength loss likely depending on loading and ground geometry
Zone B: Liquefaction and post-earthquake strength loss unlikely, check cyclic softening
Zone C: Cyclic liquefaction and strength loss possible depending on soil plasticity, brittleness/sensitivity, strain to peak undrained strength and ground geometry

GEOLOGISMIKI Geotechnical Software

LIQUEFACTION ANALYSIS REPORT

Project title : G13AP00029 **Location : Christchurch, New Zealand**

CPT file : CCCC_CPT484(CBD)

Input parameters and analysis data

Analysis method:	B&I (2014)	G.W.T. (in-situ):	1.50 m	Use fill:	No	Clay like behavior applied:	Sands only
Fines correction method:	B&I (2014)	G.W.T. (earthq.):	1.50 m	Fill height:	N/A	Limit depth applied:	No
Points to test:	Based on Ic value	Average results interval:	3	Fill weight:	N/A	Limit depth:	N/A
Earthquake magnitude M_w:	4.70	Ic cut-off value:	2.60	Trans. detect. applied:	No	MSF method:	Method based
Peak ground acceleration:	0.23	Unit weight calculation:	19.00 kN/m³	K_σ applied:	Yes		

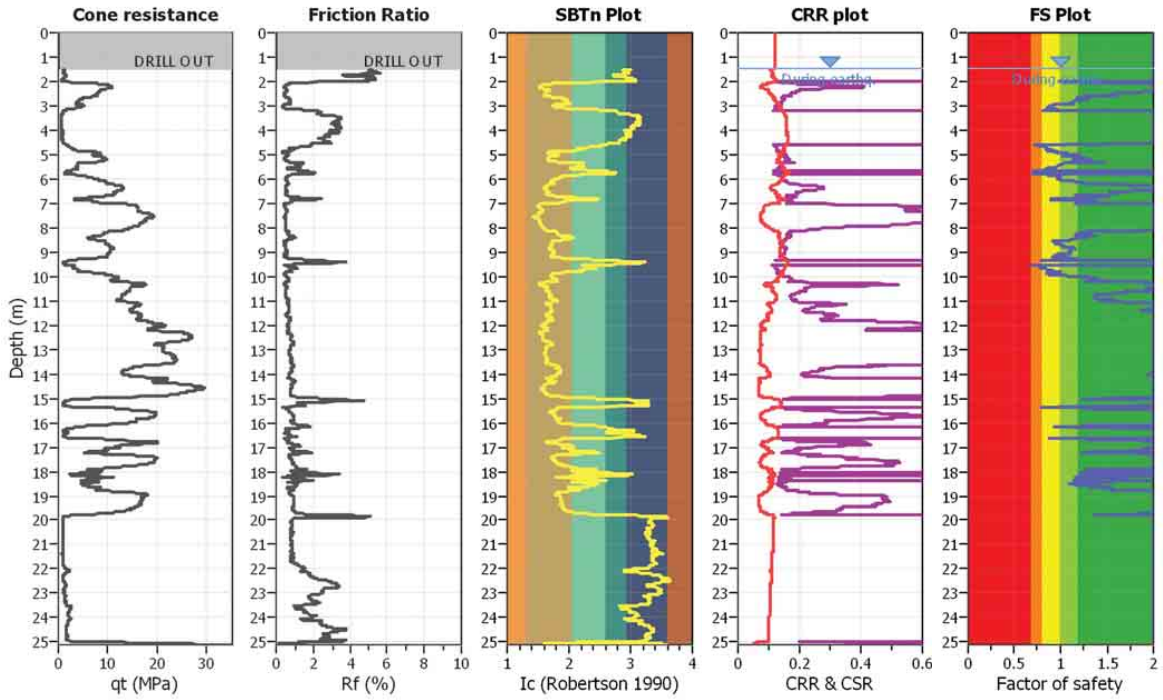

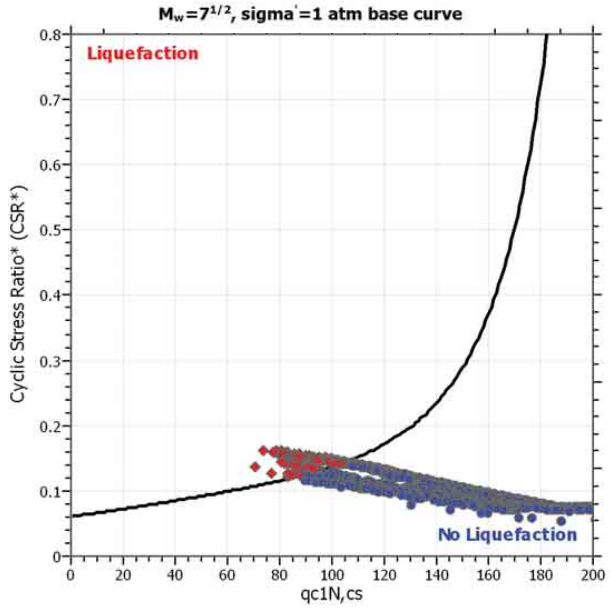

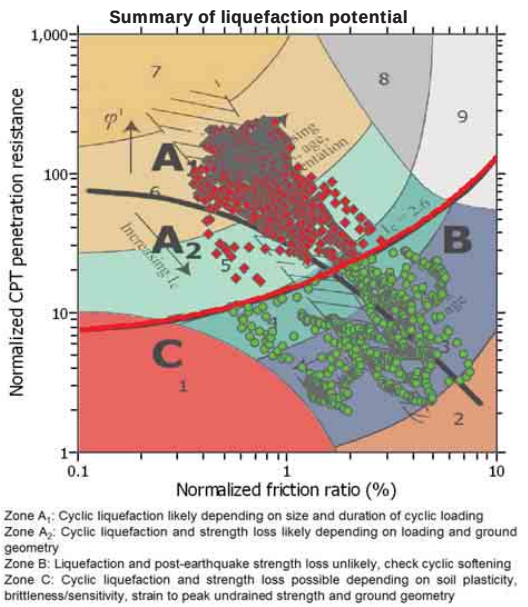

Zone A_1: Cyclic liquefaction likely depending on size and duration of cyclic loading
Zone A_2: Cyclic liquefaction and strength loss likely depending on loading and ground geometry
Zone B: Liquefaction and post-earthquake strength loss unlikely, check cyclic softening
Zone C: Cyclic liquefaction and strength loss possible depending on soil plasticity, brittleness/sensitivity, strain to peak undrained strength and ground geometry

GEOLOGISMIKI Geotechnical Software

LIQUEFACTION ANALYSIS REPORT

Project title : G13AP00029 **Location : Christchurch, New Zealand**

CPT file : CHHC_CPT425(CBD)

Input parameters and analysis data

Analysis method:	B&I (2014)	G.W.T. (in-situ):	3.00 m	Use fill:	No	Clay like behavior applied:	Sands only
Fines correction method:	B&I (2014)	G.W.T. (earthq.):	3.00 m	Fill height:	N/A	Limit depth applied:	No
Points to test:	Based on Ic value	Average results interval:	3	Fill weight:	N/A	Limit depth:	N/A
Earthquake magnitude M_w:	4.70	Ic cut-off value:	2.60	Trans. detect. applied:	No	MSF method:	Method based
Peak ground acceleration:	0.16	Unit weight calculation:	19.00 kN/m³	K_σ applied:	Yes		

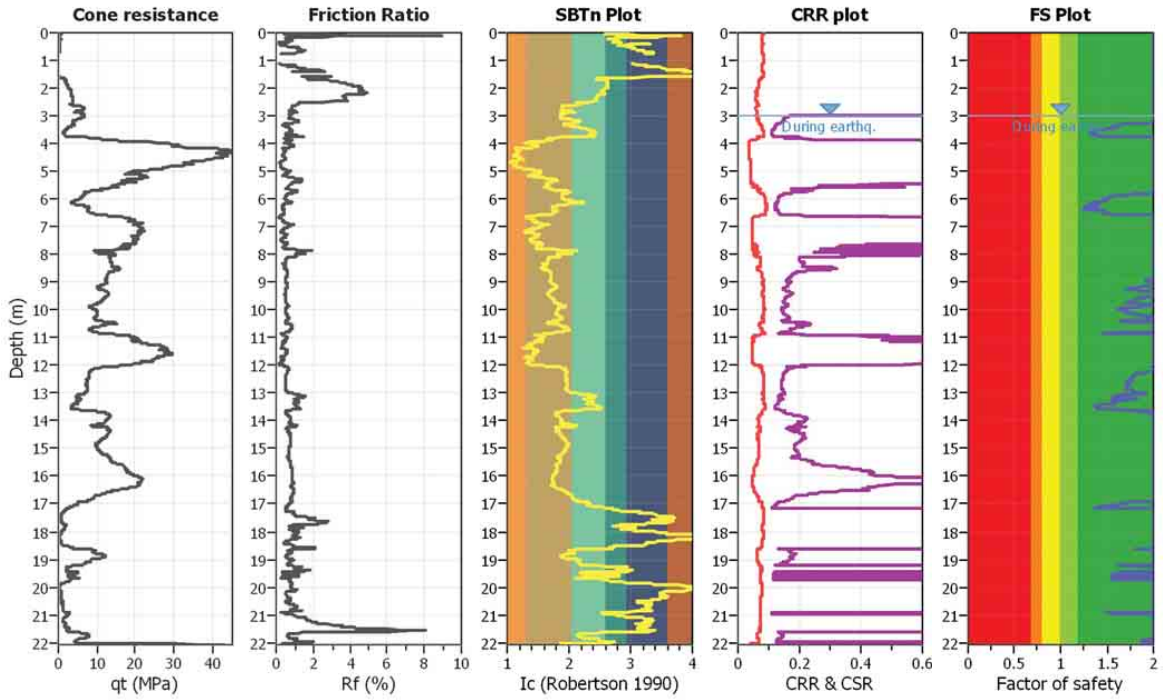

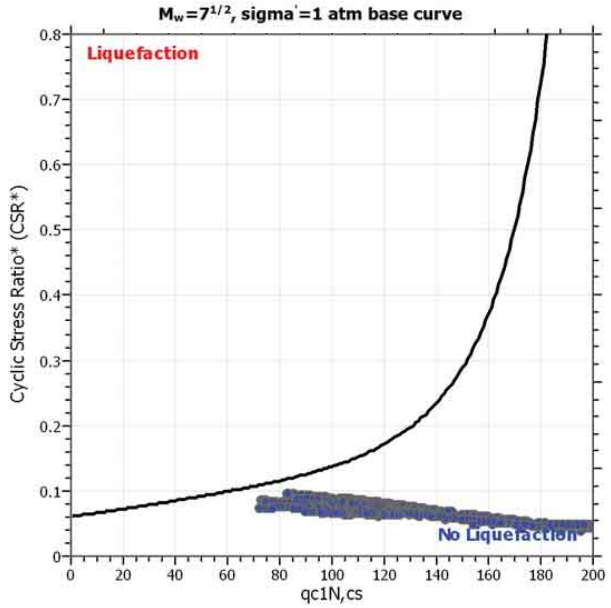

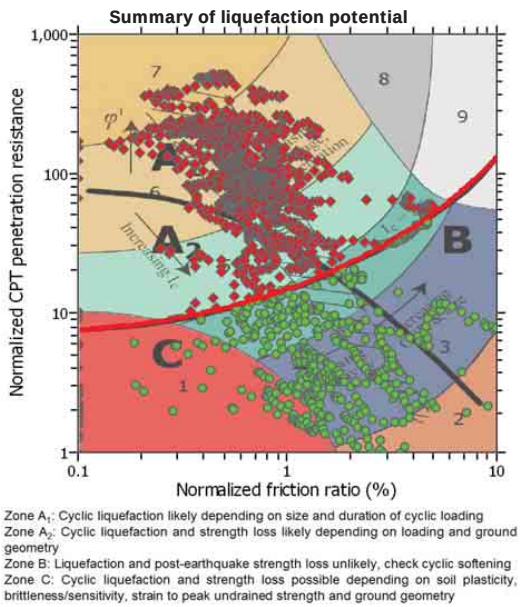

Zone A_1: Cyclic liquefaction likely depending on size and duration of cyclic loading
Zone A_2: Cyclic liquefaction and strength loss likely depending on loading and ground geometry
Zone B: Liquefaction and post-earthquake strength loss unlikely, check cyclic softening
Zone C: Cyclic liquefaction and strength loss possible depending on soil plasticity, brittleness/sensitivity, strain to peak undrained strength and ground geometry

GEOLOGISMIKI Geotechnical Software

LIQUEFACTION ANALYSIS REPORT

Project title : G13AP00029 **Location : Christchurch, New Zealand**

CPT file : HPSC_CPT89(CGD)

Input parameters and analysis data

Analysis method:	B&I (2014)	G.W.T. (in-situ):	2.50 m	Use fill:	No	Clay like behavior applied:	Sands only
Fines correction method:	B&I (2014)	G.W.T. (earthq.):	2.50 m	Fill height:	N/A	Limit depth applied:	No
Points to test:	Based on Ic value	Average results interval:	3	Fill weight:	N/A	Limit depth:	N/A
Earthquake magnitude M_w:	4.70	Ic cut-off value:	2.60	Trans. detect. applied:	No	MSF method:	Method based
Peak ground acceleration:	0.05	Unit weight calculation:	19.00 kN/m³	K_σ applied:	Yes		

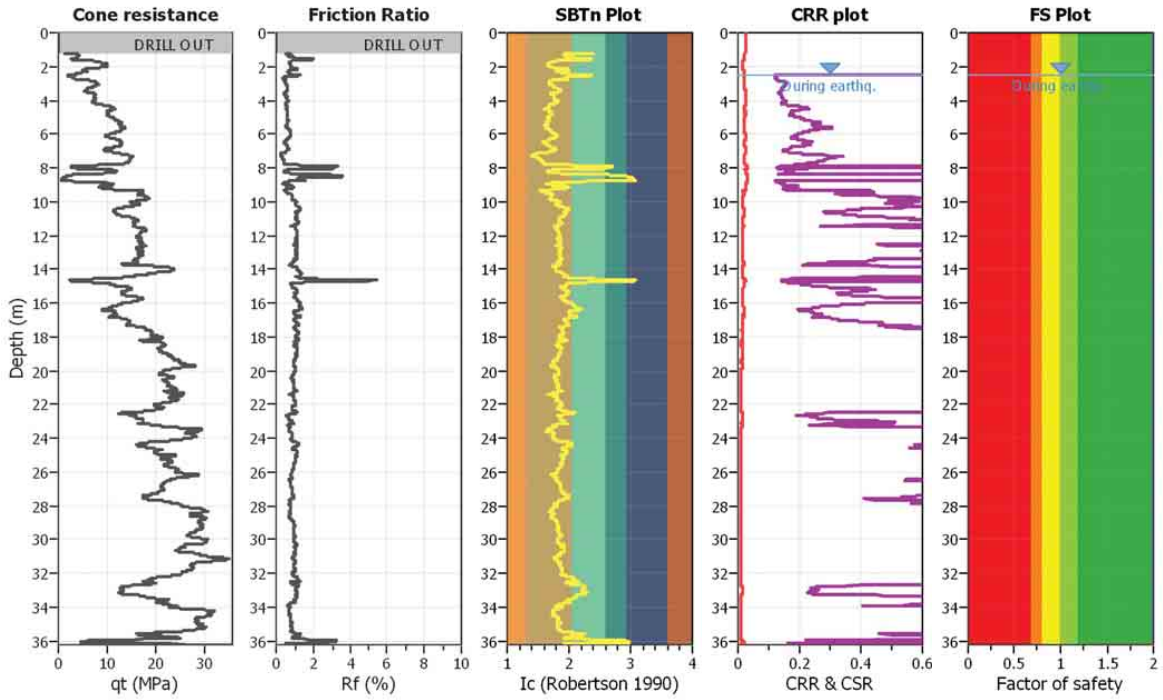

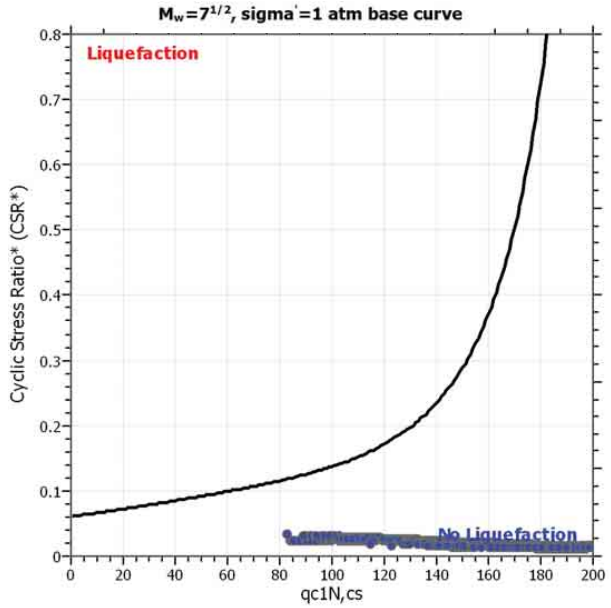

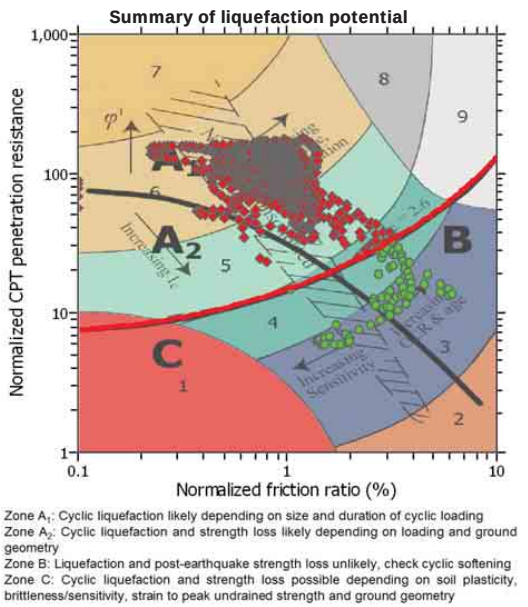

Zone A_1: Cyclic liquefaction likely depending on size and duration of cyclic loading
Zone A_2: Cyclic liquefaction and strength loss likely depending on loading and ground geometry
Zone B: Liquefaction and post-earthquake strength loss unlikely, check cyclic softening
Zone C: Cyclic liquefaction and strength loss possible depending on soil plasticity, brittleness/sensitivity, strain to peak undrained strength and ground geometry

GEOLOGISMIKI Geotechnical Software

LIQUEFACTION ANALYSIS REPORT

Project title : G13AP00029 **Location : Christchurch, New Zealand**

CPT file : NNBS_CPT33695(CGD)

Input parameters and analysis data

Analysis method:	B&I (2014)	G.W.T. (in-situ):	1.50 m	Use fill:	No	Clay like behavior applied:	Sands only
Fines correction method:	B&I (2014)	G.W.T. (earthq.):	1.50 m	Fill height:	N/A	Limit depth applied:	No
Points to test:	Based on Ic value	Average results interval:	3	Fill weight:	N/A	Limit depth:	N/A
Earthquake magnitude M_w:	4.70	Ic cut-off value:	2.60	Trans. detect. applied:	No	MSF method:	Method based
Peak ground acceleration:	0.04	Unit weight calculation:	19.00 kN/m³	K_σ applied:	Yes		

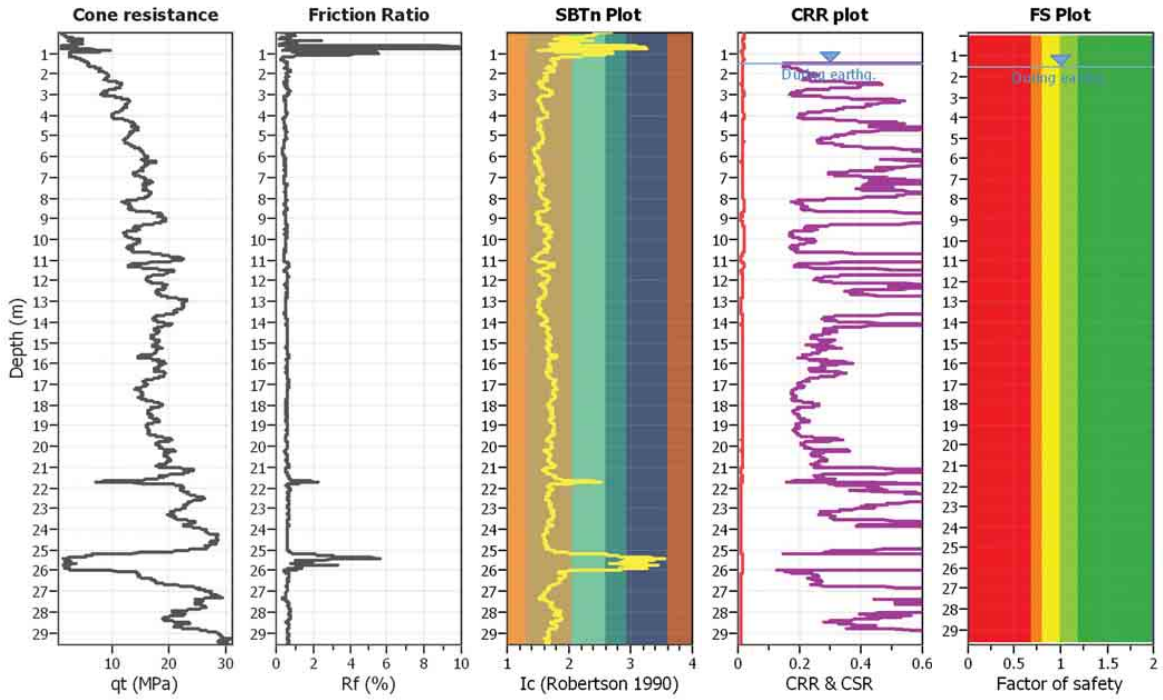

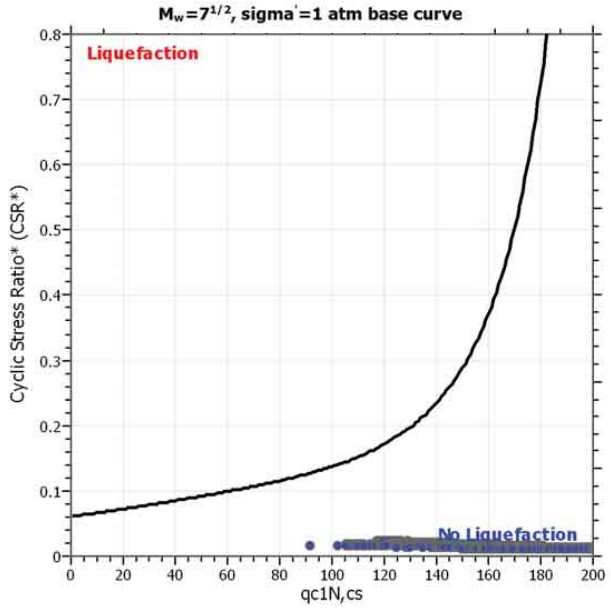

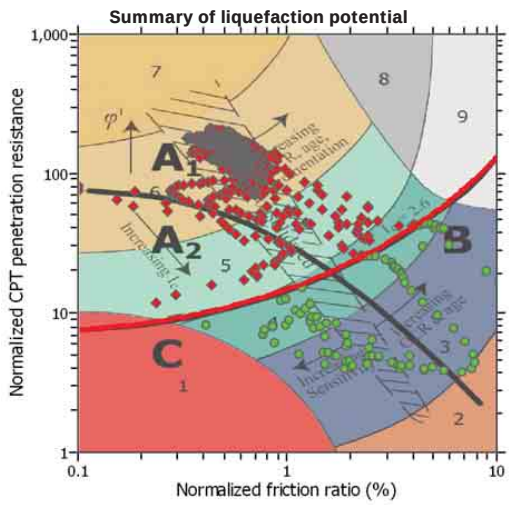

Zone A_1: Cyclic liquefaction likely depending on size and duration of cyclic loading
Zone A_2: Cyclic liquefaction and strength loss likely depending on loading and ground geometry
Zone B: Liquefaction and post-earthquake strength loss unlikely, check cyclic softening
Zone C: Cyclic liquefaction and strength loss possible depending on soil plasticity, brittleness/sensitivity, strain to peak undrained strength and ground geometry

GEOLOGISMIKI Geotechnical Software

LIQUEFACTION ANALYSIS REPORT

Project title : G13AP00029 **Location : Christchurch, New Zealand**

CPT file : PPHS_CPT1497(CGD)

Input parameters and analysis data

Analysis method:	B&I (2014)	G.W.T. (in-situ):	2.50 m	Use fill:	No	Clay like behavior applied:	Sands only
Fines correction method:	B&I (2014)	G.W.T. (earthq.):	2.50 m	Fill height:	N/A	Limit depth applied:	No
Points to test:	Based on Ic value	Average results interval:	3	Fill weight:	N/A	Limit depth:	N/A
Earthquake magnitude M_w:	4.70	Ic cut-off value:	2.60	Trans. detect. applied:	No	MSF method:	Method based
Peak ground acceleration:	0.10	Unit weight calculation:	19.00 kN/m³	K_σ applied:	Yes		

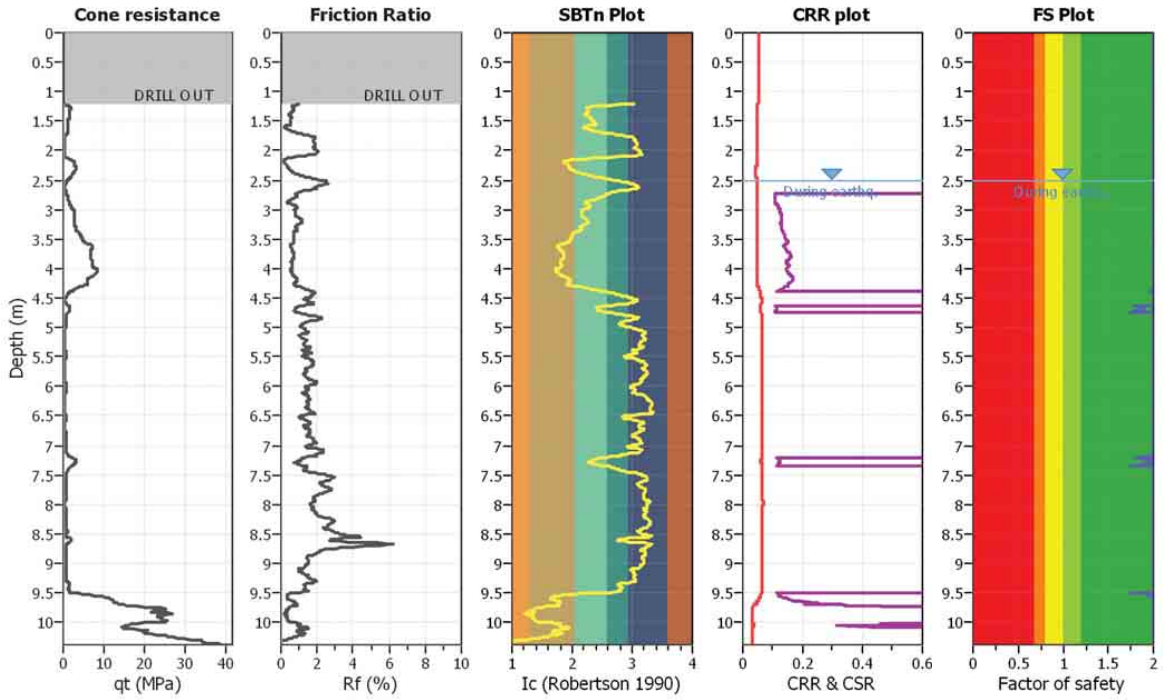

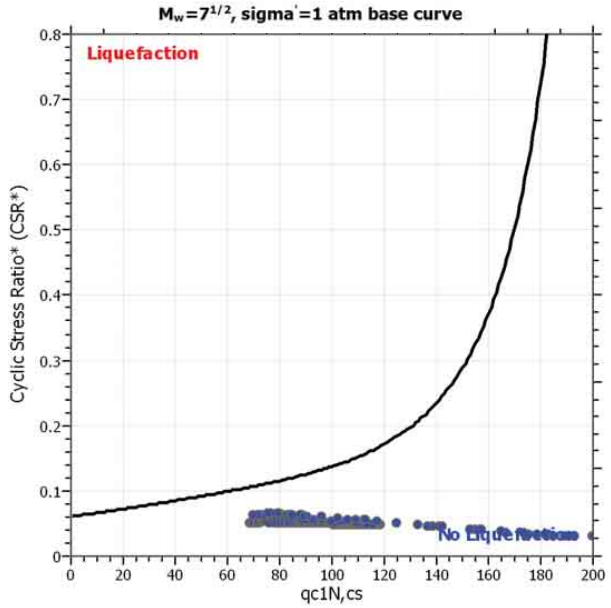

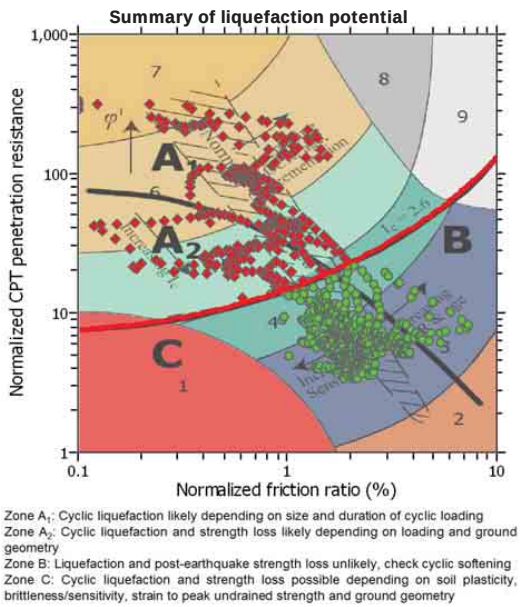

Zone A_1: Cyclic liquefaction likely depending on size and duration of cyclic loading
Zone A_2: Cyclic liquefaction and strength loss likely depending on loading and ground geometry
Zone B: Liquefaction and post-earthquake strength loss unlikely, check cyclic softening
Zone C: Cyclic liquefaction and strength loss possible depending on soil plasticity, brittleness/sensitivity, strain to peak undrained strength and ground geometry

GEOLOGISMIKI Geotechnical Software

LIQUEFACTION ANALYSIS REPORT

Project title : G13AP00029 **Location : Christchurch**

CPT file : PRPC_CPT1396 (CGD)

Input parameters and analysis data

Analysis method:	I&B (2008)	G.W.T. (in-situ):	3.00 m	Use fill:	No	Clay like behavior applied:	Sands only
Fines correction method:	R&W (1998)	G.W.T. (earthq.):	3.00 m	Fill height:	N/A	Limit depth applied:	No
Points to test:	Based on Ic value	Average results interval:	3	Fill weight:	N/A	Limit depth:	N/A
Earthquake magnitude M_w:	4.70	Ic cut-off value:	2.60	Trans. detect. applied:	No	MSF method:	Method based
Peak ground acceleration:	0.09	Unit weight calculation:	19.00 kN/m³	K_σ applied:	Yes		

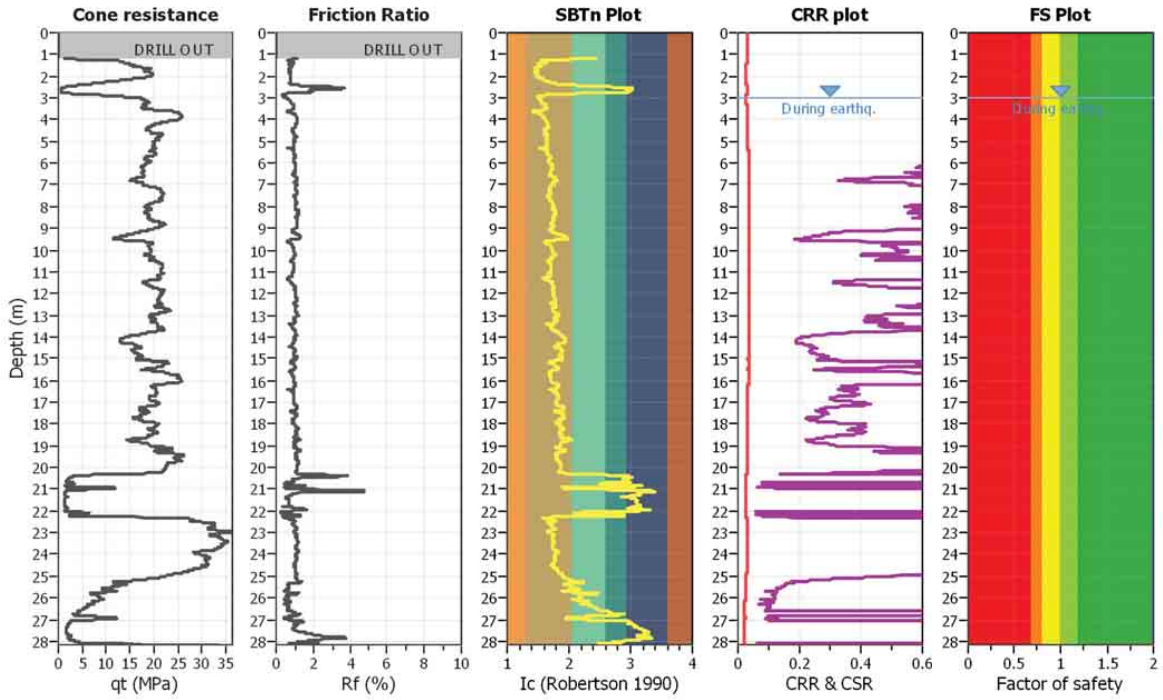

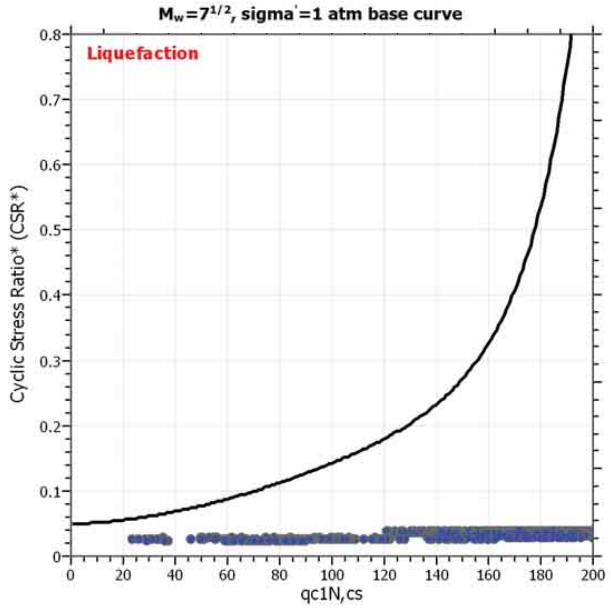

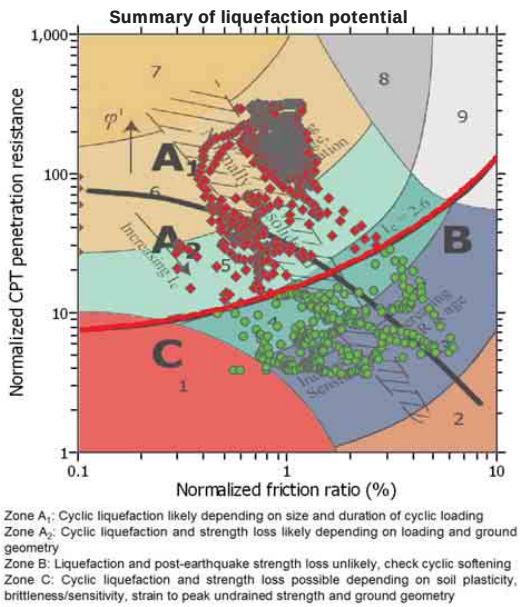

Zone A_1: Cyclic liquefaction likely depending on size and duration of cyclic loading
Zone A_2: Cyclic liquefaction and strength loss likely depending on loading and ground geometry
Zone B: Liquefaction and post-earthquake strength loss unlikely, check cyclic softening
Zone C: Cyclic liquefaction and strength loss possible depending on soil plasticity, brittleness/sensitivity, strain to peak undrained strength and ground geometry

GEOLOGISMIKI Geotechnical Software

LIQUEFACTION ANALYSIS REPORT

Project title : G13AP00029 **Location : Christchurch, New Zealand**

CPT file : REHS_CPT2 (Wotherspoon,2013)

Input parameters and analysis data

Analysis method:	B&I (2014)	G.W.T. (in-situ):	2.00 m	Use fill:	No	Clay like behavior applied:	Sands only
Fines correction method:	B&I (2014)	G.W.T. (earthq.):	2.00 m	Fill height:	N/A	Limit depth applied:	No
Points to test:	Based on Ic value	Average results interval:	3	Fill weight:	N/A	Limit depth:	N/A
Earthquake magnitude M_w:	4.70	Ic cut-off value:	2.60	Trans. detect. applied:	No	MSF method:	Method based
Peak ground acceleration:	0.25	Unit weight calculation:	19.00 kN/m³	K_σ applied:	Yes		

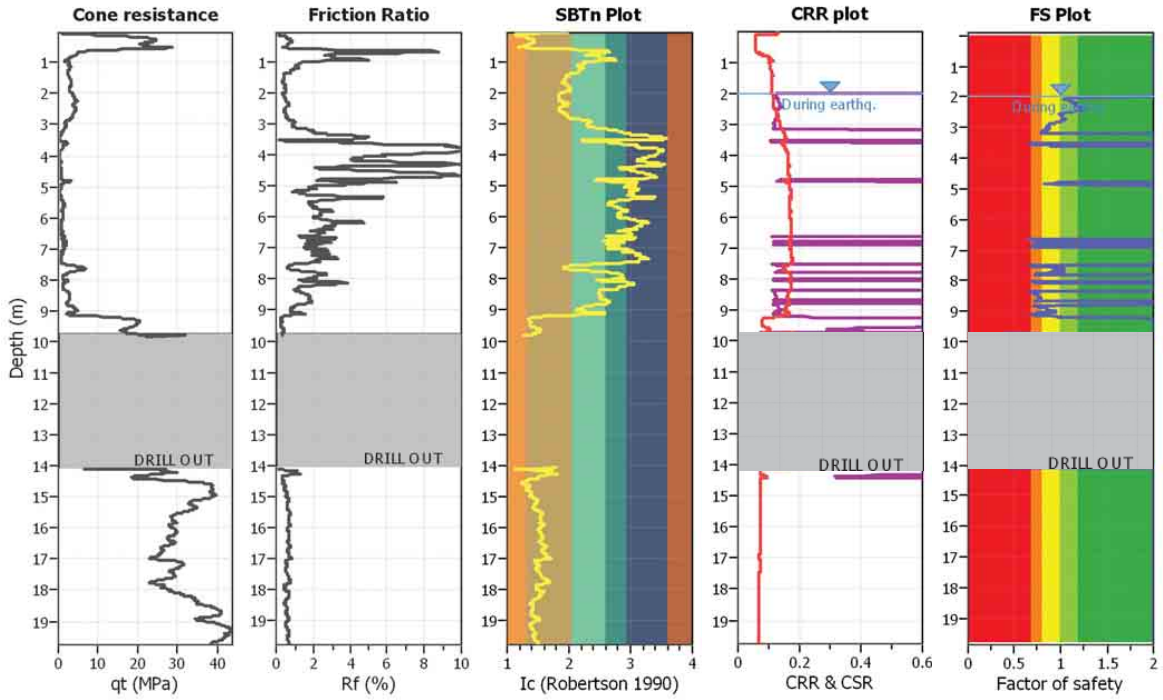

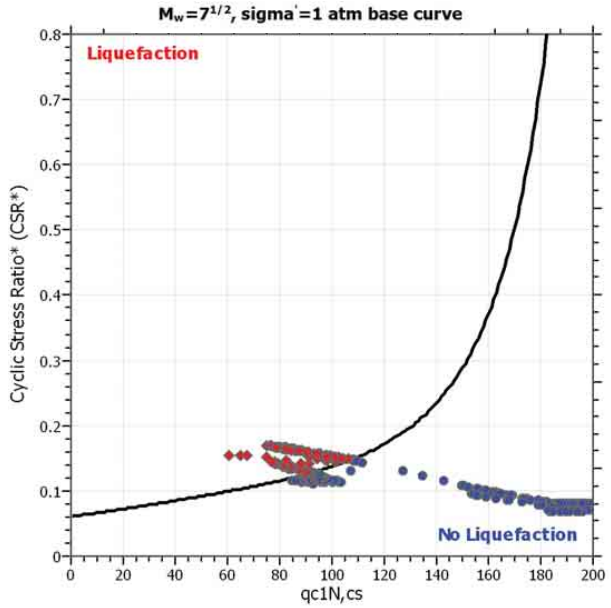

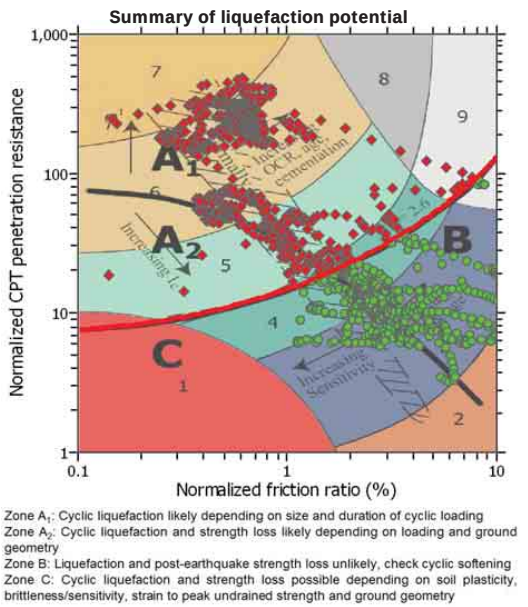

Zone A_1: Cyclic liquefaction likely depending on size and duration of cyclic loading
Zone A_2: Cyclic liquefaction and strength loss likely depending on loading and ground geometry
Zone B: Liquefaction and post-earthquake strength loss unlikely, check cyclic softening
Zone C: Cyclic liquefaction and strength loss possible depending on soil plasticity, brittleness/sensitivity, strain to peak undrained strength and ground geometry

GEOLOGISMIKI Geotechnical Software

LIQUEFACTION ANALYSIS REPORT

Project title : G13AP00029 **Location : Christchurch, New Zealand**

CPT file : SHLC_CPT626(CGD)

Input parameters and analysis data

Analysis method:	B&I (2014)	G.W.T. (in-situ):	1.50 m	Use fill:	No	Clay like behavior applied:	Sands only
Fines correction method:	B&I (2014)	G.W.T. (earthq.):	1.50 m	Fill height:	N/A	Limit depth applied:	No
Points to test:	Based on Ic value	Average results interval:	3	Fill weight:	N/A	Limit depth:	N/A
Earthquake magnitude M_w:	4.70	Ic cut-off value:	2.60	Trans. detect. applied:	No	MSF method:	Method based
Peak ground acceleration:	0.16	Unit weight calculation:	19.00 kN/m³	K_σ applied:	Yes		

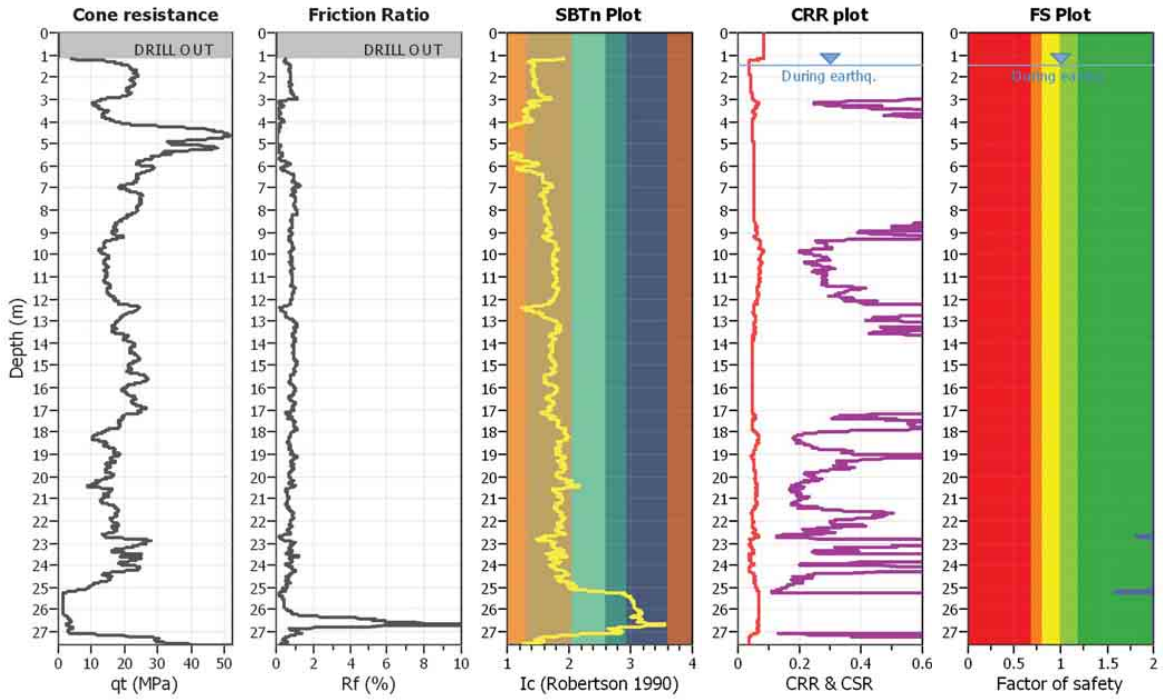

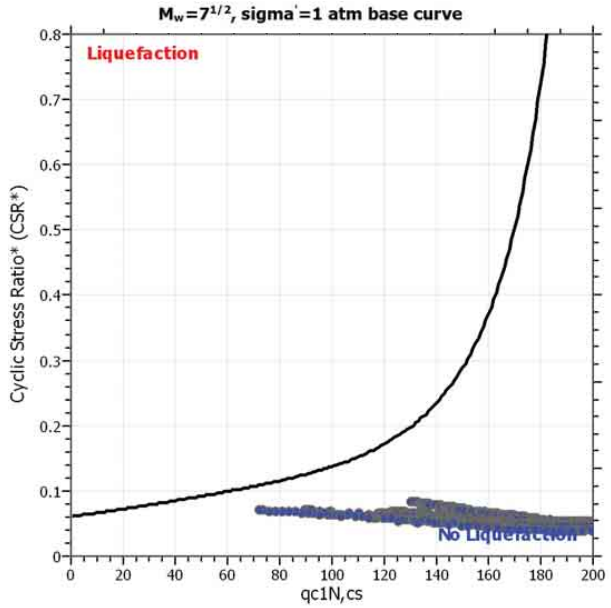

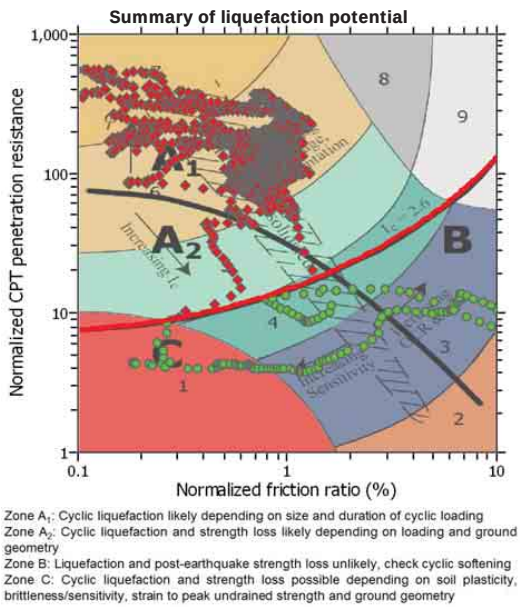

Zone A_1: Cyclic liquefaction likely depending on size and duration of cyclic loading
Zone A_2: Cyclic liquefaction and strength loss likely depending on loading and ground geometry
Zone B: Liquefaction and post-earthquake strength loss unlikely, check cyclic softening
Zone C: Cyclic liquefaction and strength loss possible depending on soil plasticity, brittleness/sensitivity, strain to peak undrained strength and ground geometry

Appendix A.7

Residuals of Calculated Surface Motions from Site Response Analyses Compared to Recorded Surface Motions

A.7.1 Residuals for 22 February 2011 M_w 6.2 Event

A.7.2 Residuals for 04 September 2010 M_w 7.1 Event

A.7.3 Residuals for 13 June 2011 M_w 6.0 Event

A.7.4 Residuals for 23 December 2011 M_w 5.8 Event

A.7.5 Residuals for 23 December 2011 M_w 5.9 Event

A.7.6 Residuals for 26 December 2010 M_w 4.7 Event

Appendix A.7.1

Residuals for 22 February 2011 M_w 6.2 Event

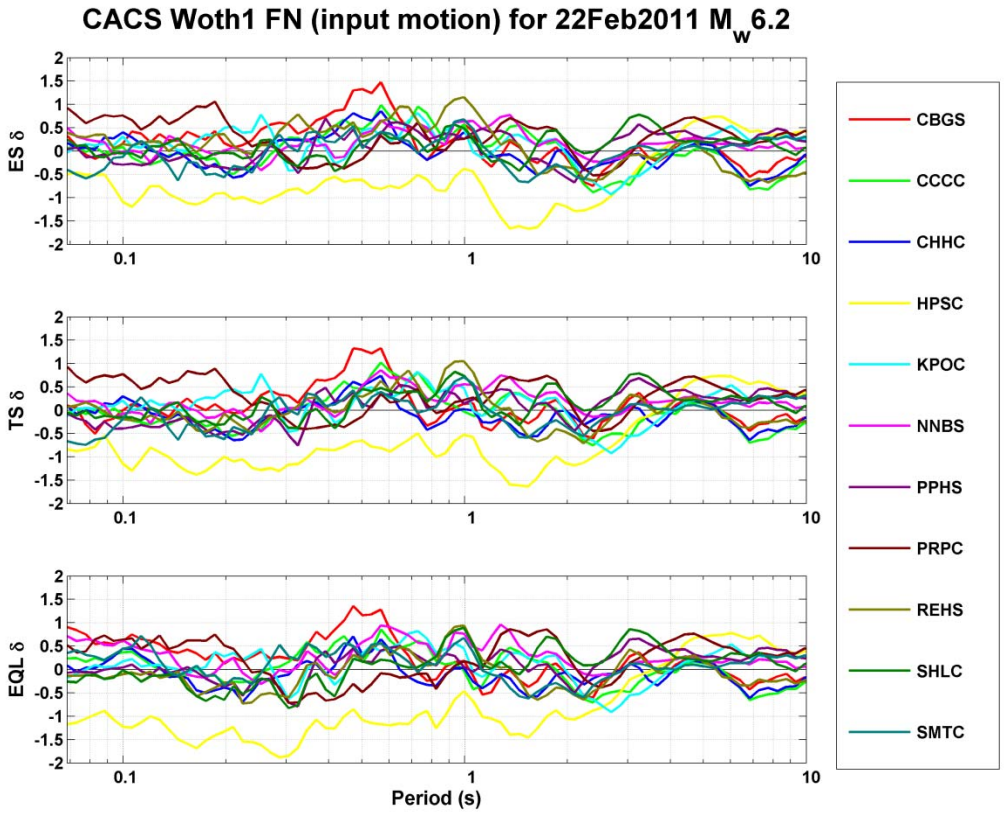
CACS Woth1 FN (input motion) for 22Feb2011 M_w 6.2
ES δ
TS δ
EQL δ
Period (s)
CBGS
CCCC
CHHC
HPSC
KPOC
NNBS
PPHS
PRPC
REHS
SHLC
SMTC

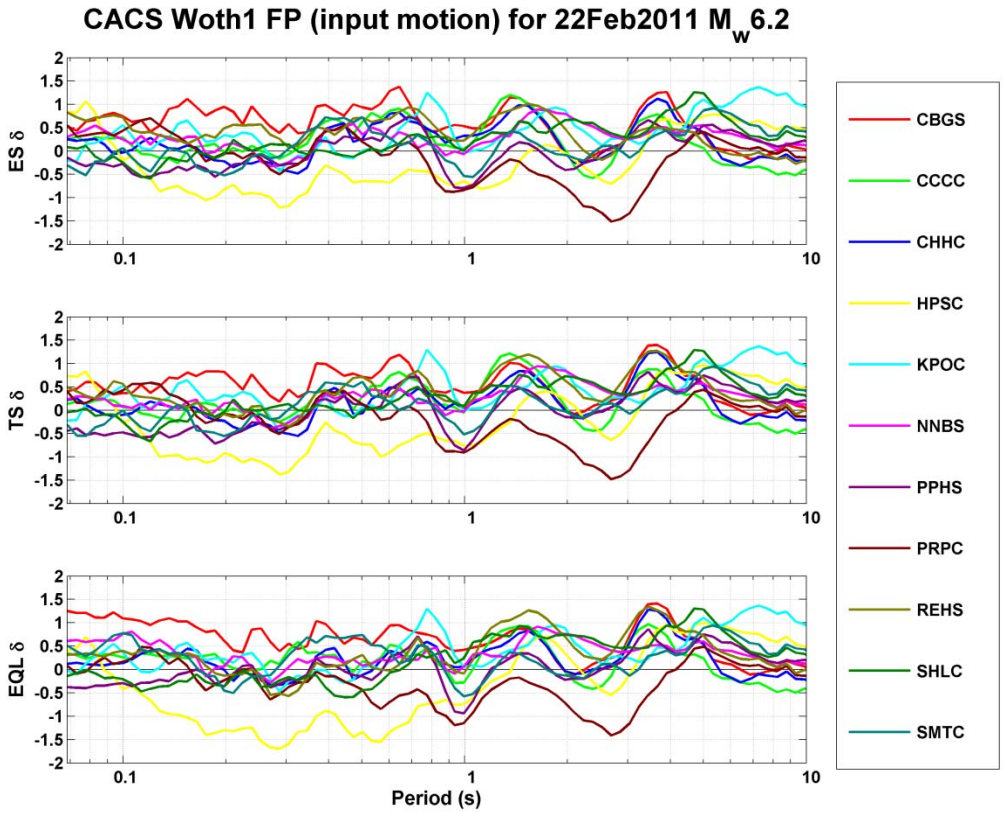
CACS Woth1 FP (input motion) for 22Feb2011 M_w 6.2
ES δ
TS δ
EQL δ
Period (s)
CBGS
CCCC
CHHC
HPSC
KPOC
NNBS
PPHS
PRPC
REHS
SHLC
SMTC

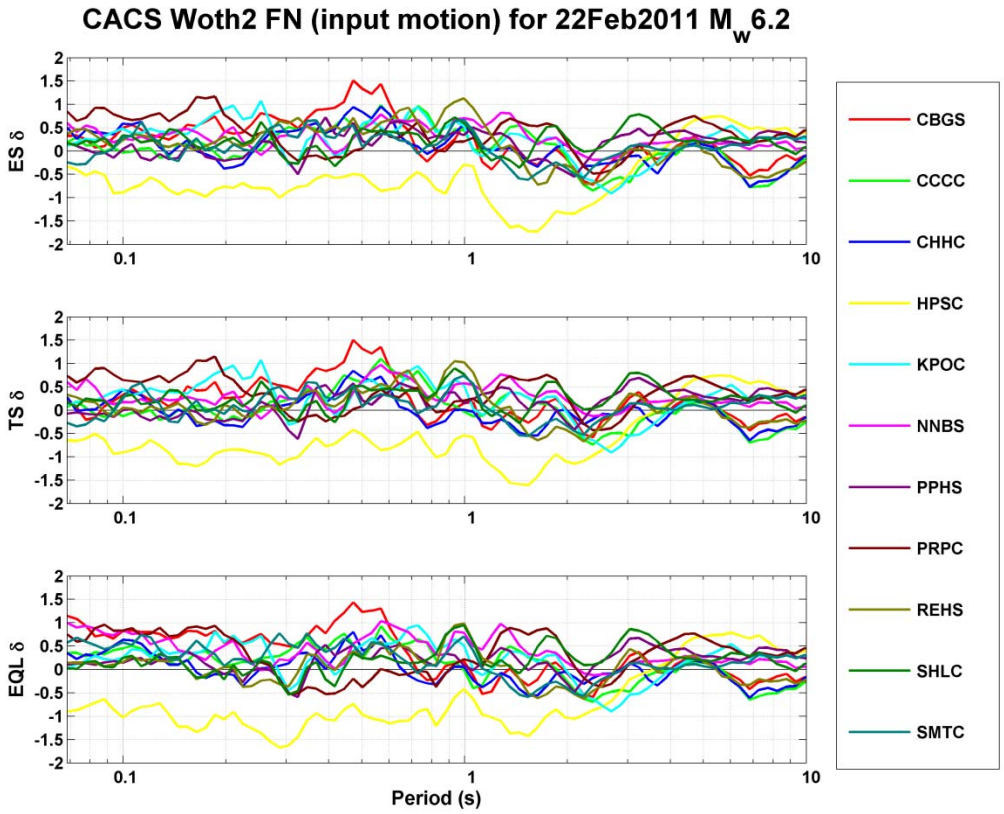
CACS Woth2 FN (input motion) for 22Feb2011 M_w 6.2
ES δ
TS δ
EQL δ
Period (s)
CBGS
CCCC
CHHC
HPSC
KPOC
NNBS
PPHS
PRPC
REHS
SHLC
SMTC

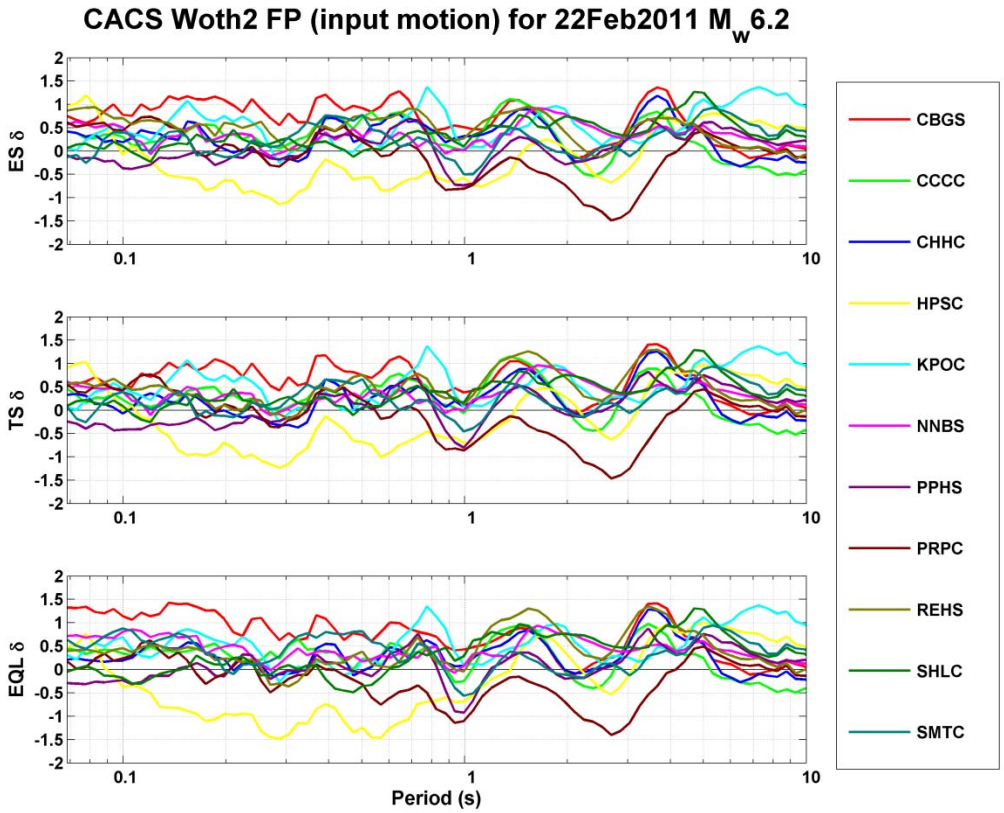
CACS Woth2 FP (input motion) for 22Feb2011 M_w 6.2
ES δ
TS δ
EQL δ
Period (s)
CBGS
CCCC
CHHC
HPSC
KPOC
NNBS
PPHS
PRPC
REHS
SHLC
SMTC

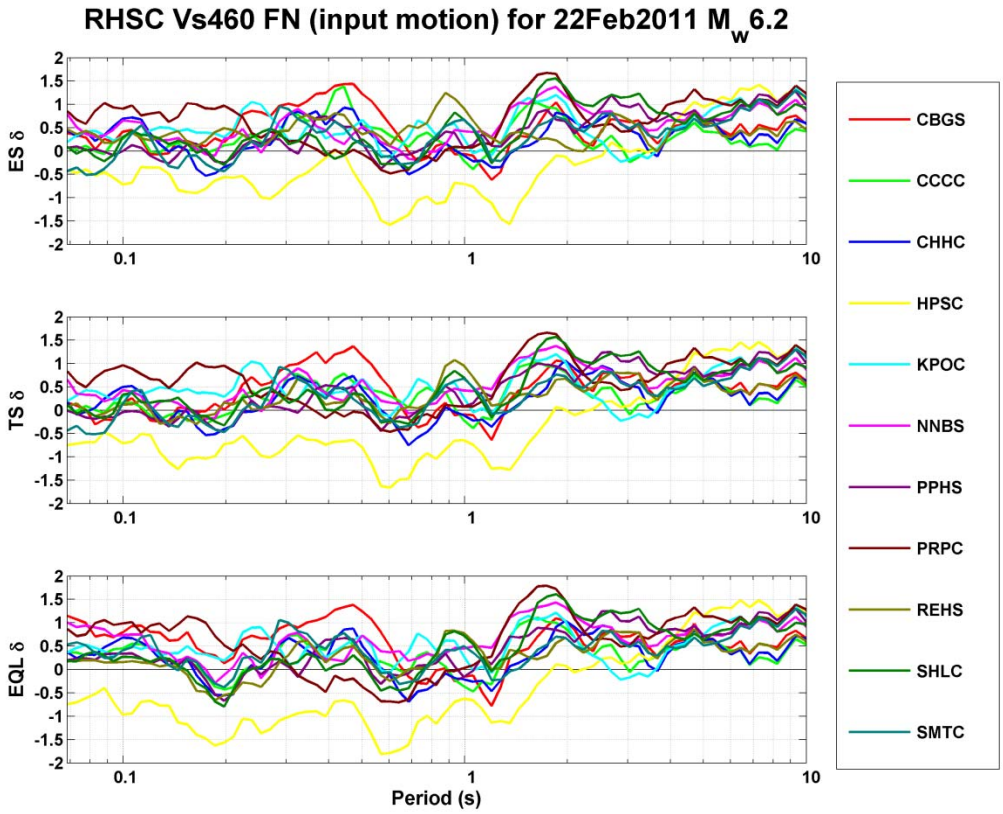
RHSC Vs460 FN (input motion) for 22Feb2011 M_w 6.2
ES δ
TS δ
EQL δ
Period (s)
CBGS
CCCC
CHHC
HPSC
KPOC
NNBS
PPHS
PRPC
REHS
SHLC
SMTC

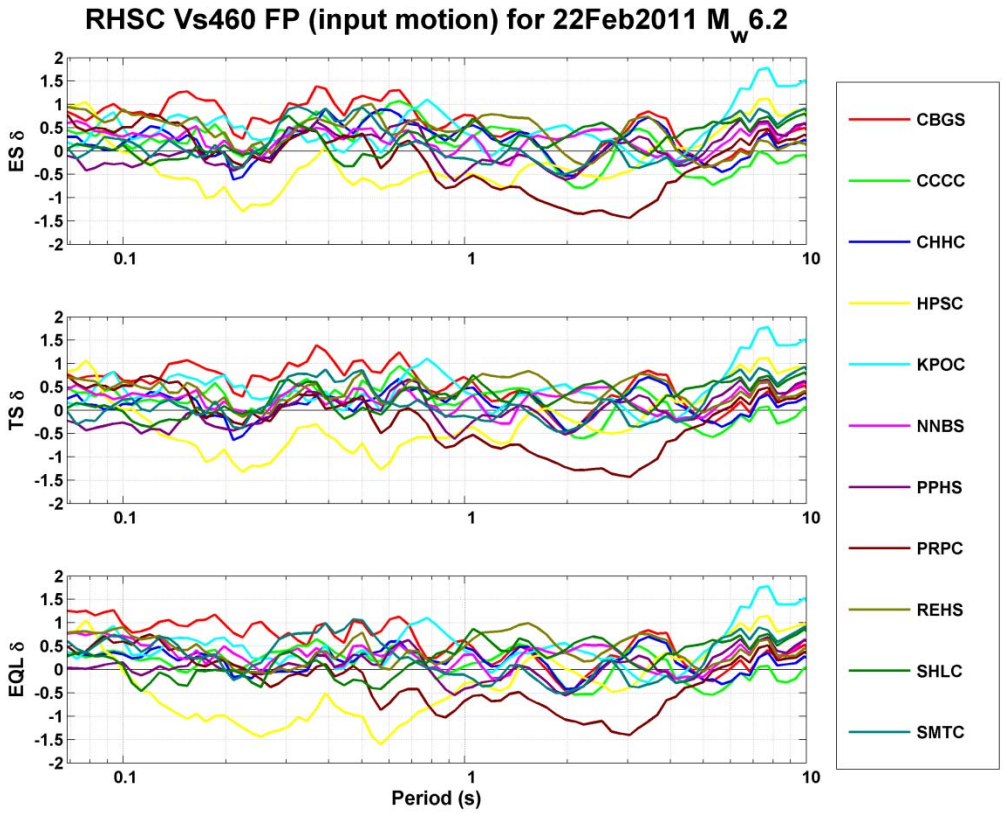
RHSC Vs460 FP (input motion) for 22Feb2011 M_w 6.2
ES δ
TS δ
EQL δ
Period (s)
CBGS
CCCC
CHHC
HPSC
KPOC
NNBS
PPHS
PRPC
REHS
SHLC
SMTC

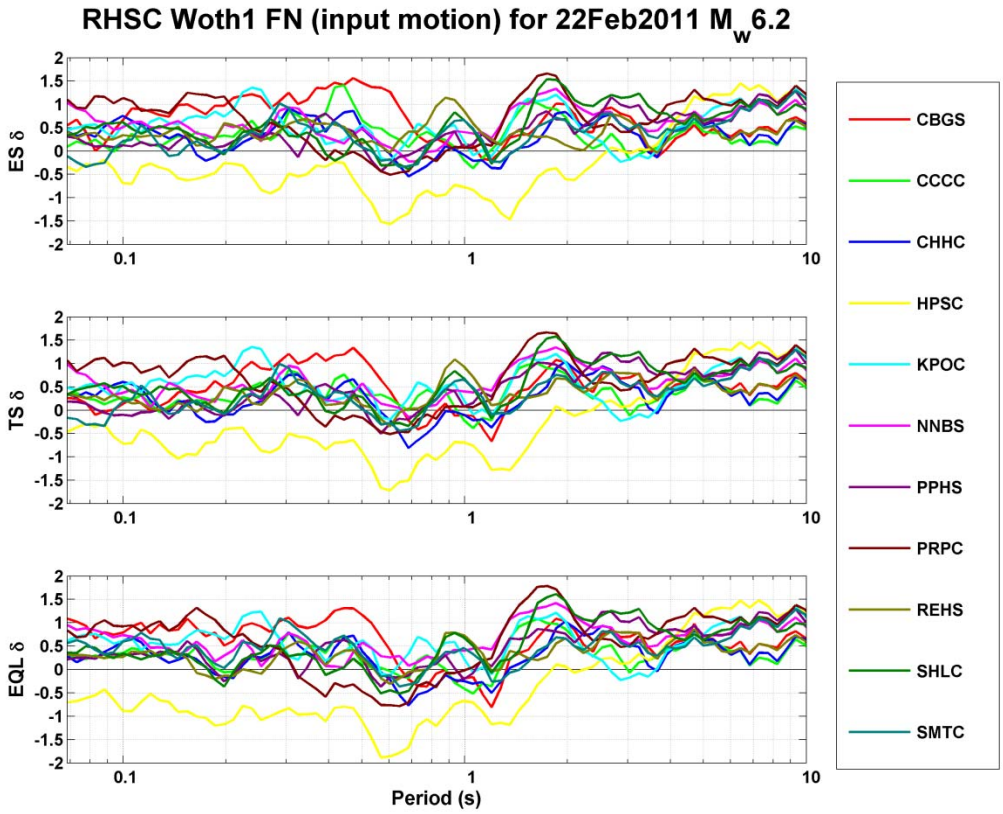
RHSC Woth1 FN (input motion) for 22Feb2011 M_w 6.2
ES δ
TS δ
EQL δ
Period (s)
CBGS
CCCC
CHHC
HPSC
KPOC
NNBS
PPHS
PRPC
REHS
SHLC
SMTC

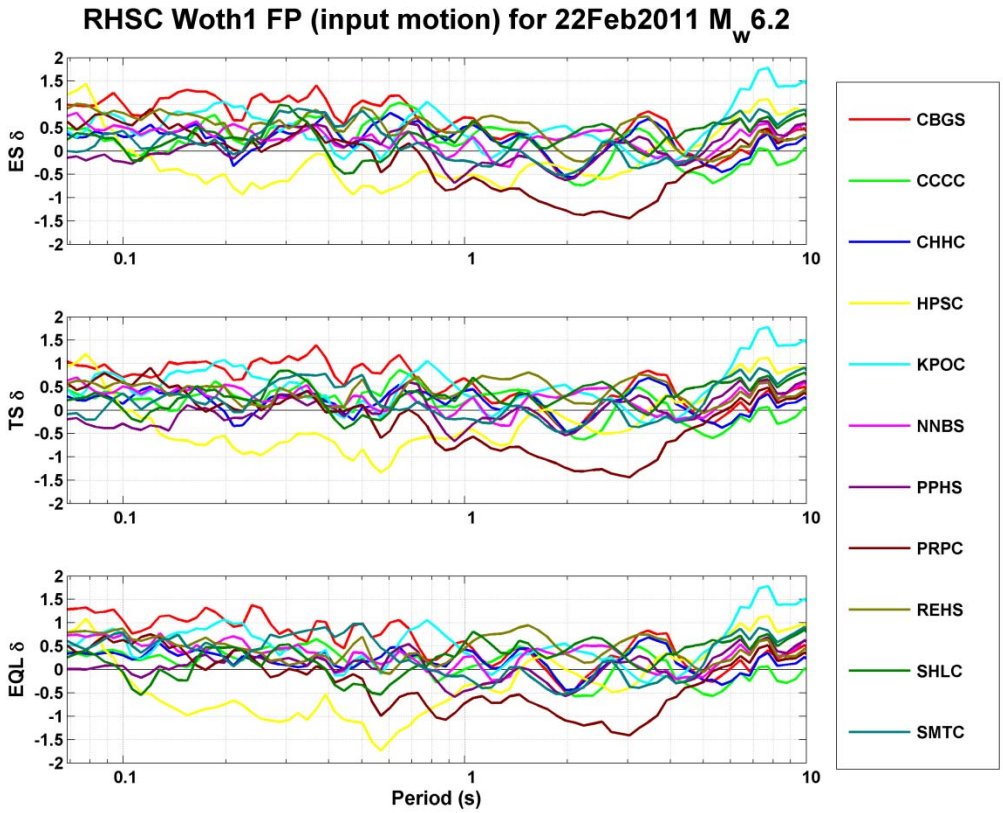
RHSC Woth1 FP (input motion) for 22Feb2011 M_w 6.2
ES δ
TS δ
EQL δ
Period (s)
CBGS
CCCC
CHHC
HPSC
KPOC
NNBS
PPHS
PRPC
REHS
SHLC
SMTC

Appendix A.7.2

Residuals for 04 September 2010 M_w 7.1 Event

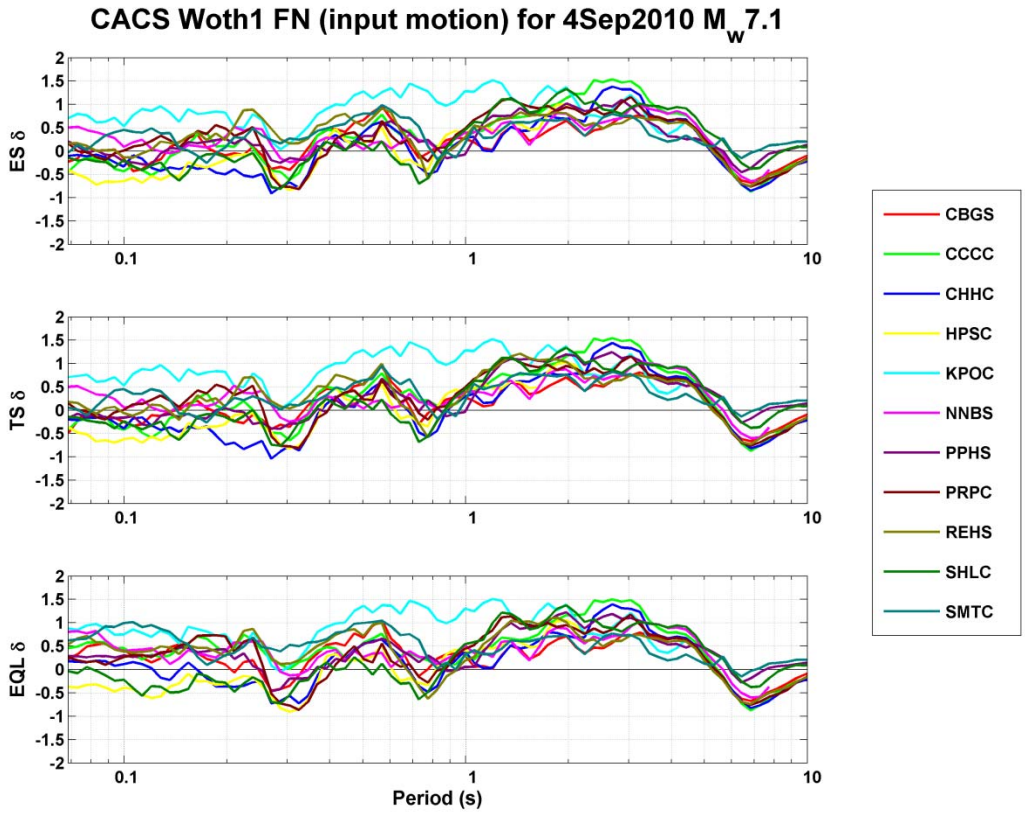
CACS Woth1 FN (input motion) for 4Sep2010 M_w 7.1
ES δ
TS δ
EQL δ
Period (s)
CBGS
CCCC
CHHC
HPSC
KPOC
NNBS
PPHS
PRPC
REHS
SHLC
SMTC

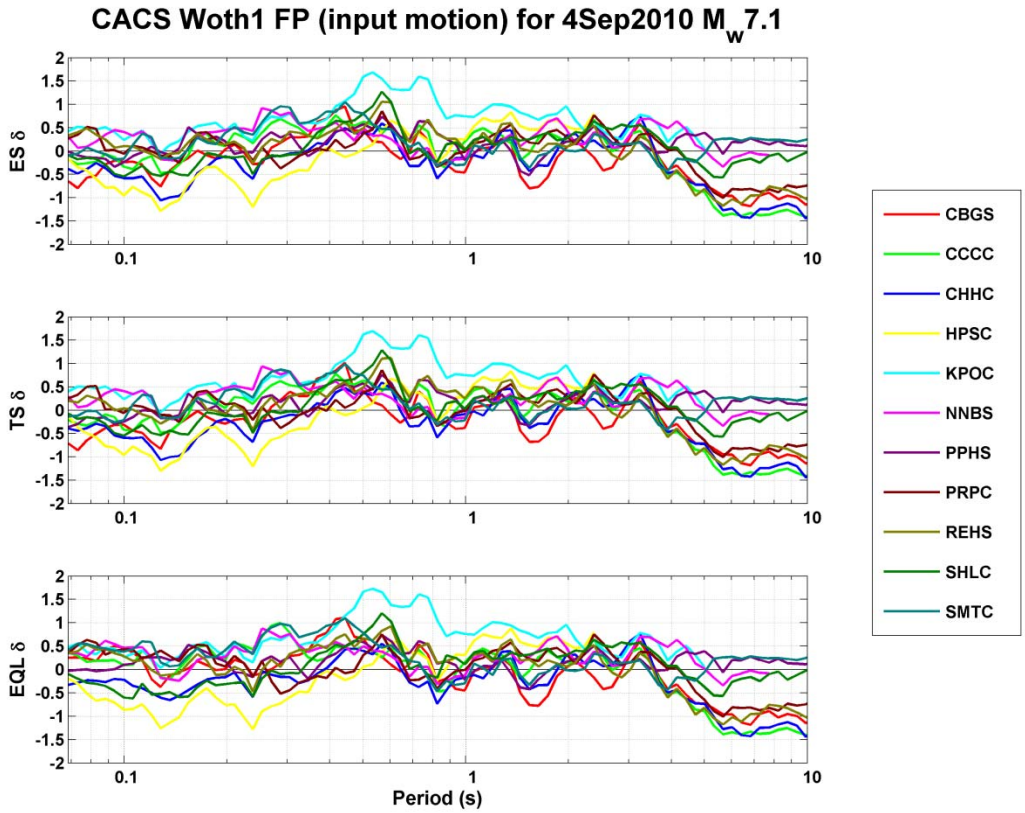
CACS Woth1 FP (input motion) for 4Sep2010 M_w 7.1
ES δ
TS δ
EQL δ
Period (s)
CBGS
CCCC
CHHC
HPSC
KPOC
NNBS
PPHS
PRPC
REHS
SHLC
SMTC

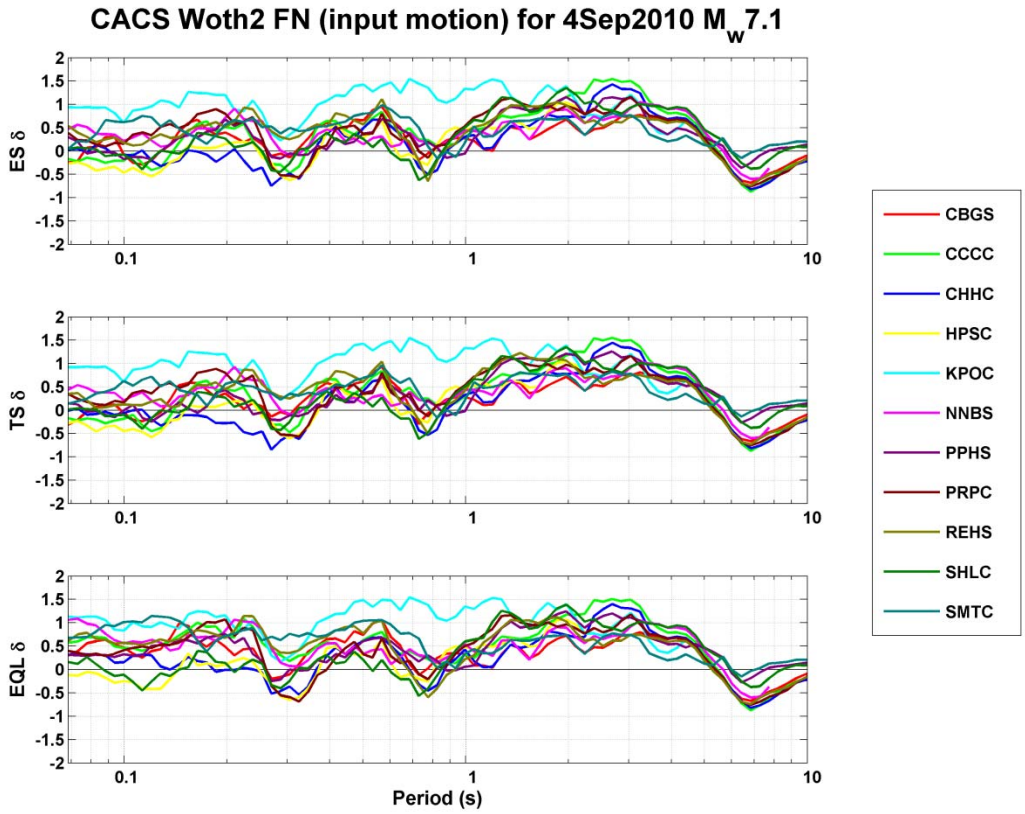
CACS Woth2 FN (input motion) for 4Sep2010 M_w7.1
ES δ
TS δ
EQL δ
Period (s)
CBGS
CCCC
CHHC
HPSC
KPOC
NNBS
PPHS
PRPC
REHS
SHLC
SMTC

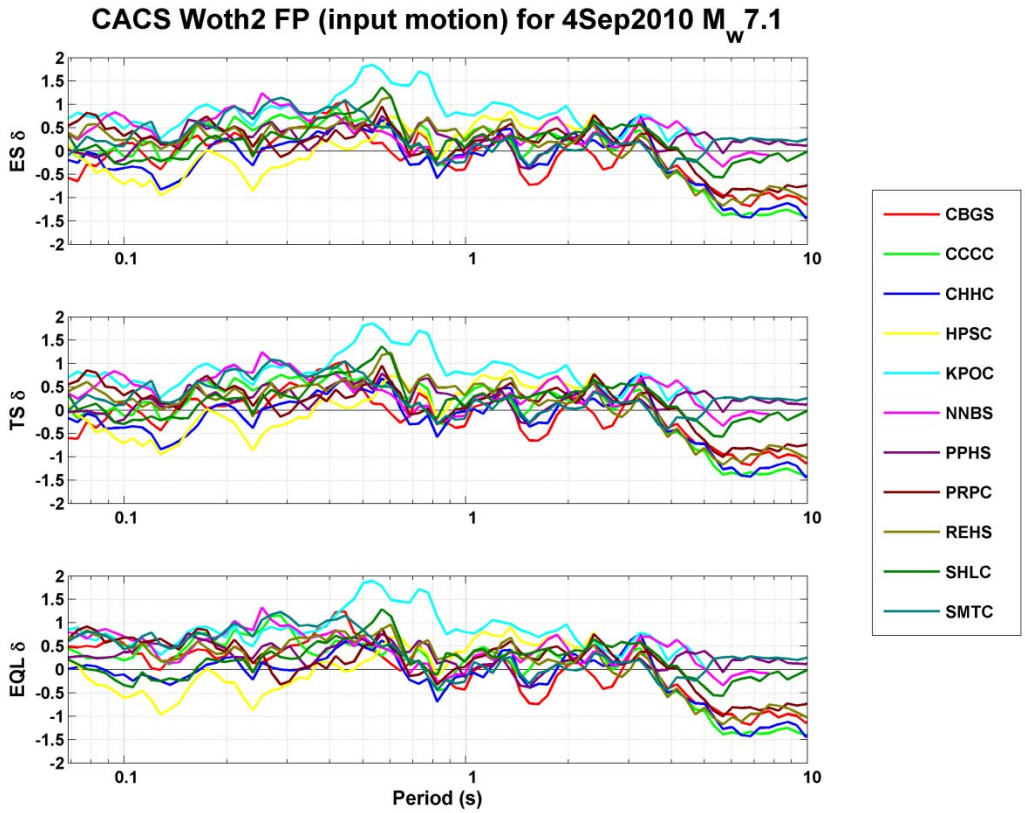
CACS Woth2 FP (input motion) for 4Sep2010 M_w7.1
ES δ
TS δ
EQL δ
Period (s)
CBGS
CCCC
CHHC
HPSC
KPOC
NNBS
PPHS
PRPC
REHS
SHLC
SMTC

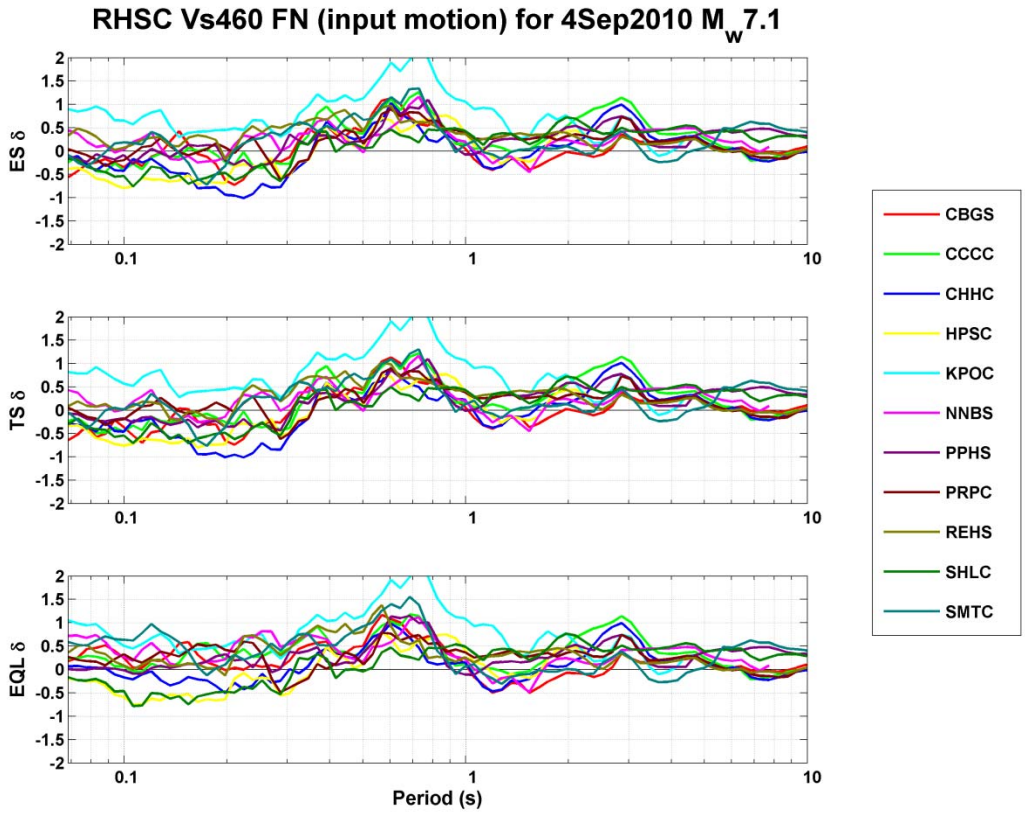
RHSC Vs460 FN (input motion) for 4Sep2010 M_w 7.1
ES δ
TS δ
EQL δ
Period (s)
CBGS
CCCC
CHHC
HPSC
KPOC
NNBS
PPHS
PRPC
REHS
SHLC
SMTC

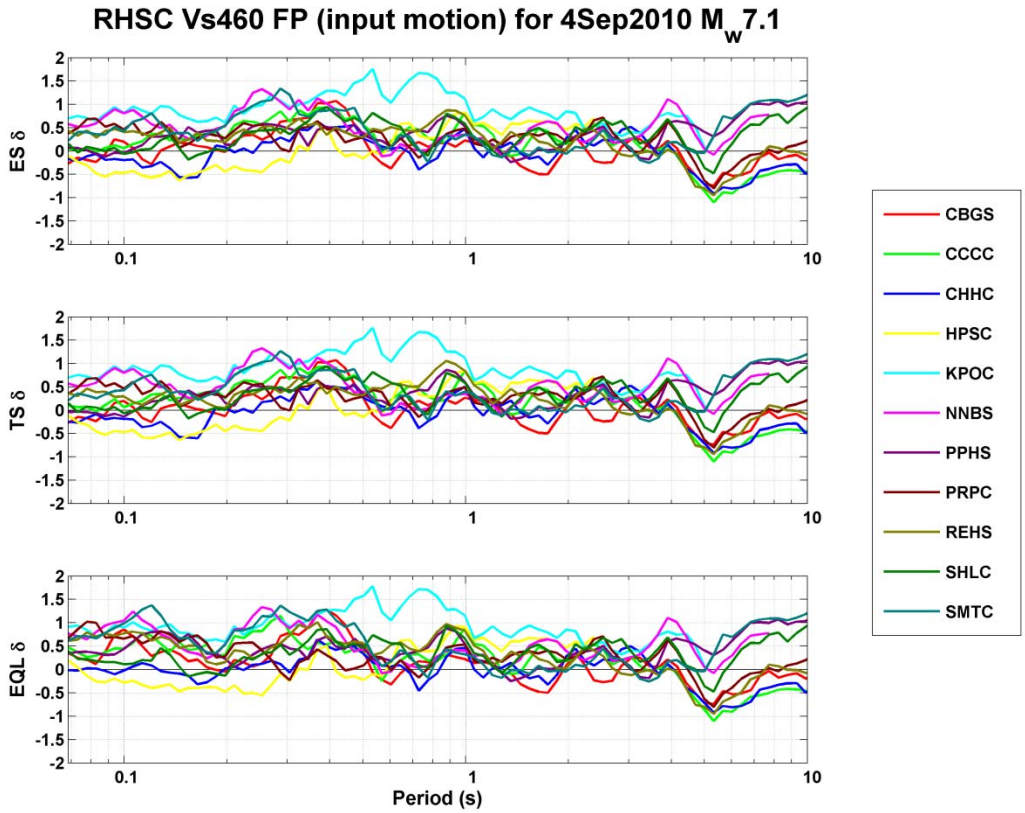
RHSC Vs460 FP (input motion) for 4Sep2010 M_w 7.1
ES δ
TS δ
EQL δ
Period (s)
CBGS
CCCC
CHHC
HPSC
KPOC
NNBS
PPHS
PRPC
REHS
SHLC
SMTC

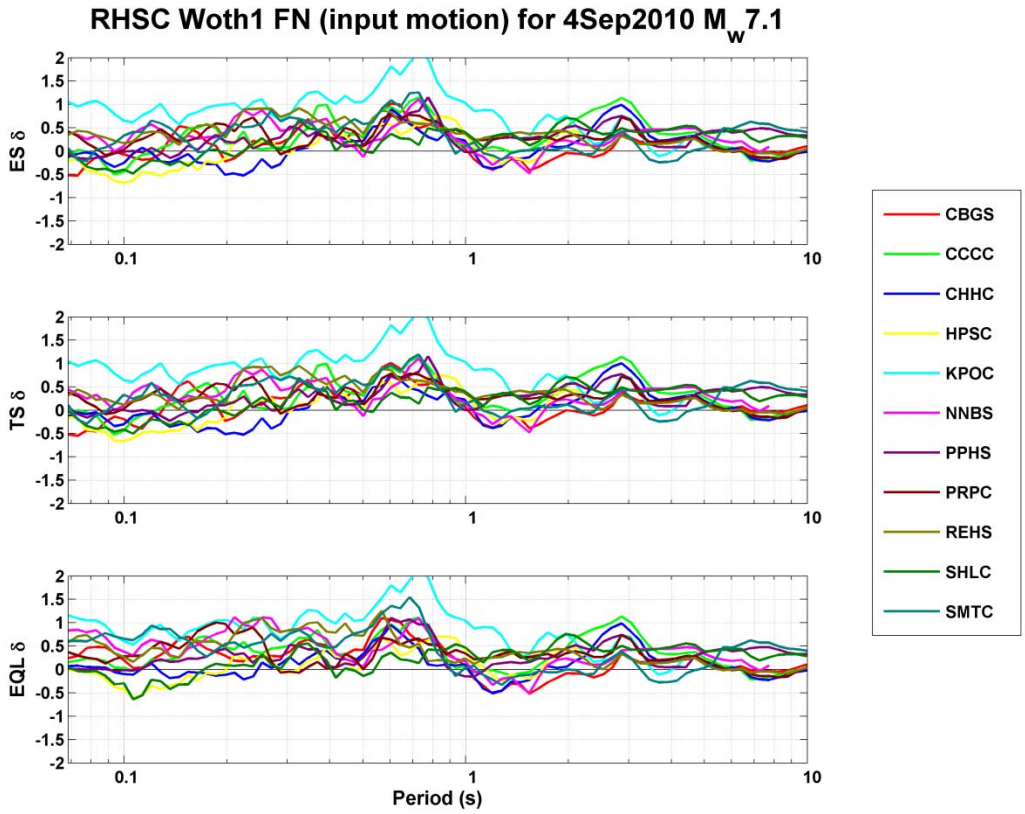
RHSC Woth1 FN (input motion) for 4Sep2010 M_w 7.1
ES δ
TS δ
EQL δ
Period (s)
CBGS
CCCC
CHHC
HPSC
KPOC
NNBS
PPHS
PRPC
REHS
SHLC
SMTC

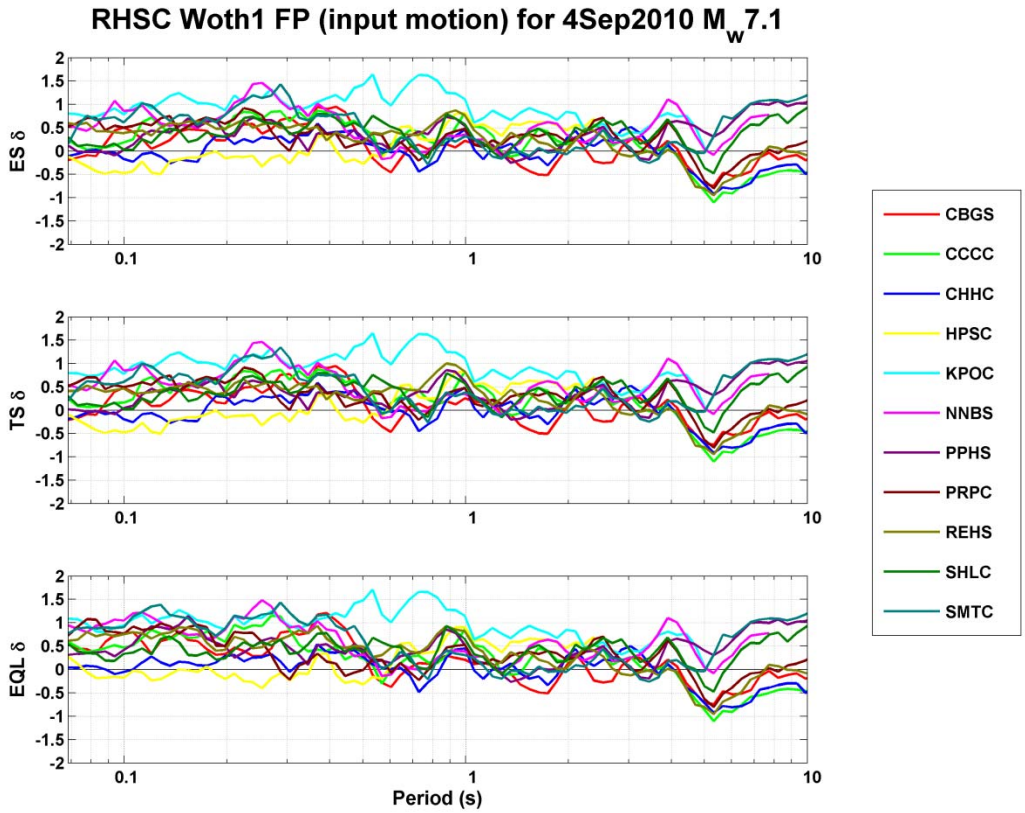
RHSC Woth1 FP (input motion) for 4Sep2010 M_w 7.1
ES δ
TS δ
EQL δ
Period (s)
CBGS
CCCC
CHHC
HPSC
KPOC
NNBS
PPHS
PRPC
REHS
SHLC
SMTC

Appendix A.7.3

Residuals for 13 June 2011 M_w 6.0 Event

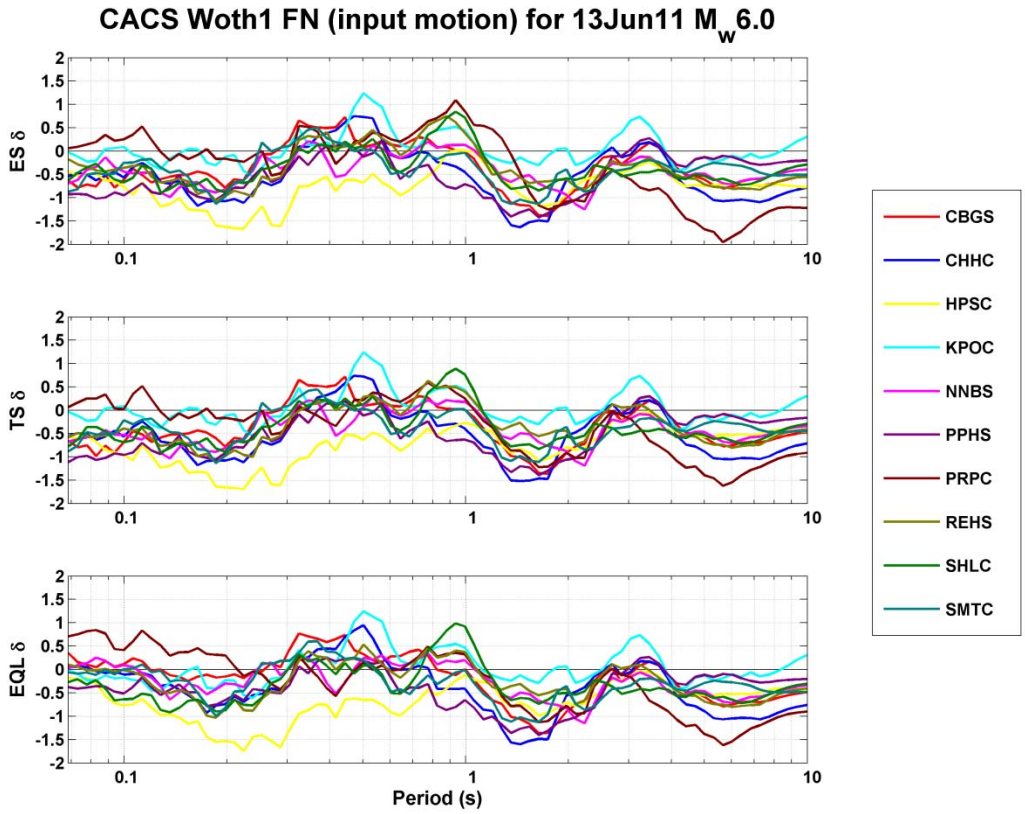
CACS Woth1 FN (input motion) for 13Jun11 M_w6.0
ES δ
TS δ
EQL δ
Period (s)
CBGS
CHHC
HPSC
KPOC
NNBS
PPHS
PRPC
REHS
SHLC
SMTC

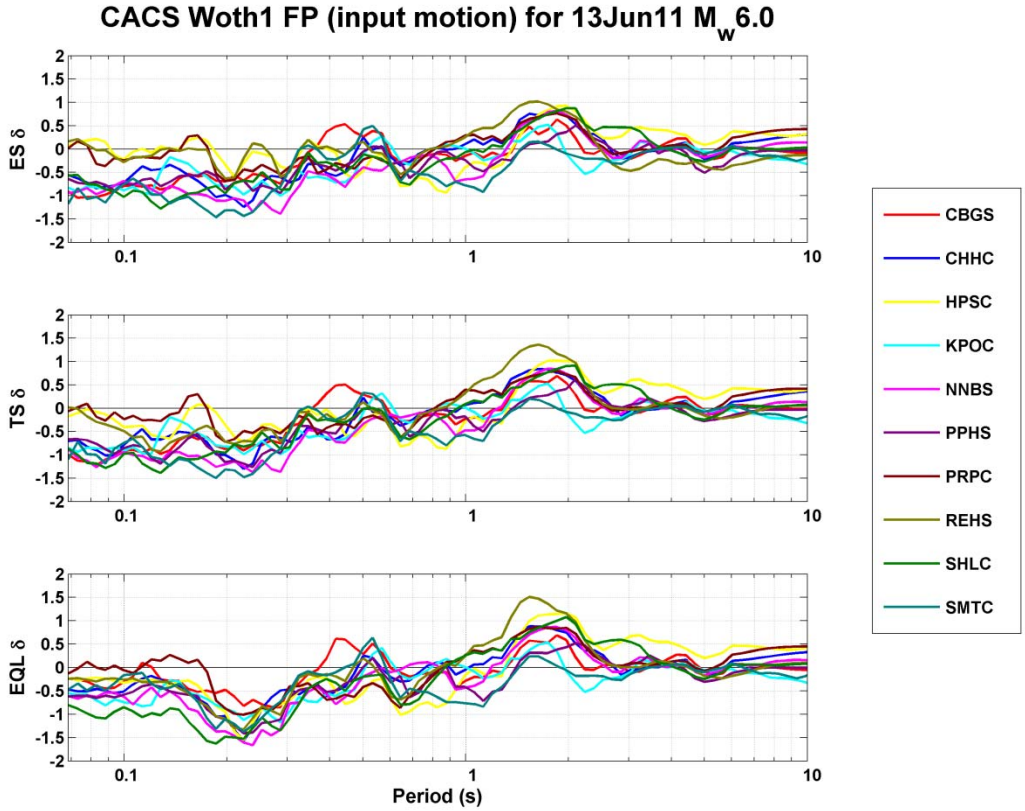
CACS Woth1 FP (input motion) for 13Jun11 M_w6.0
ES δ
TS δ
EQL δ
Period (s)
CBGS
CHHC
HPSC
KPOC
NNBS
PPHS
PRPC
REHS
SHLC
SMTC

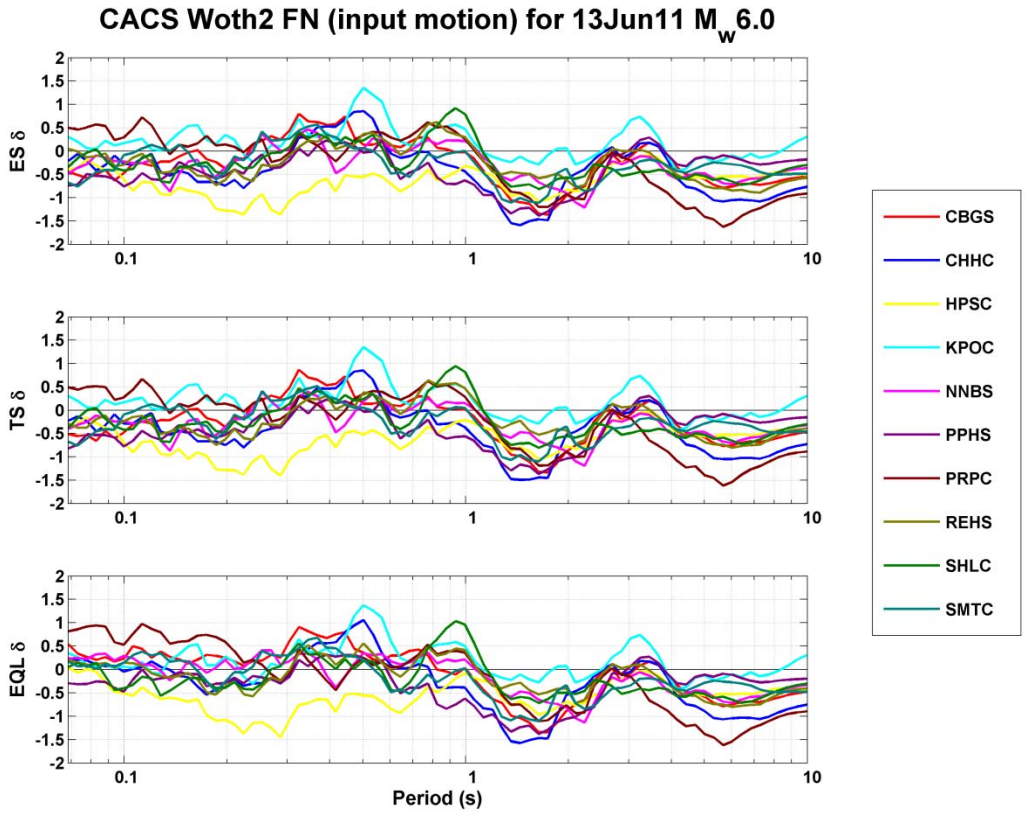
CACS Woth2 FN (input motion) for 13Jun11 M_w6.0
ES δ
TS δ
EQL δ
Period (s)
CBGS
CHHC
HPSC
KPOC
NNBS
PPHS
PRPC
REHS
SHLC
SMTC

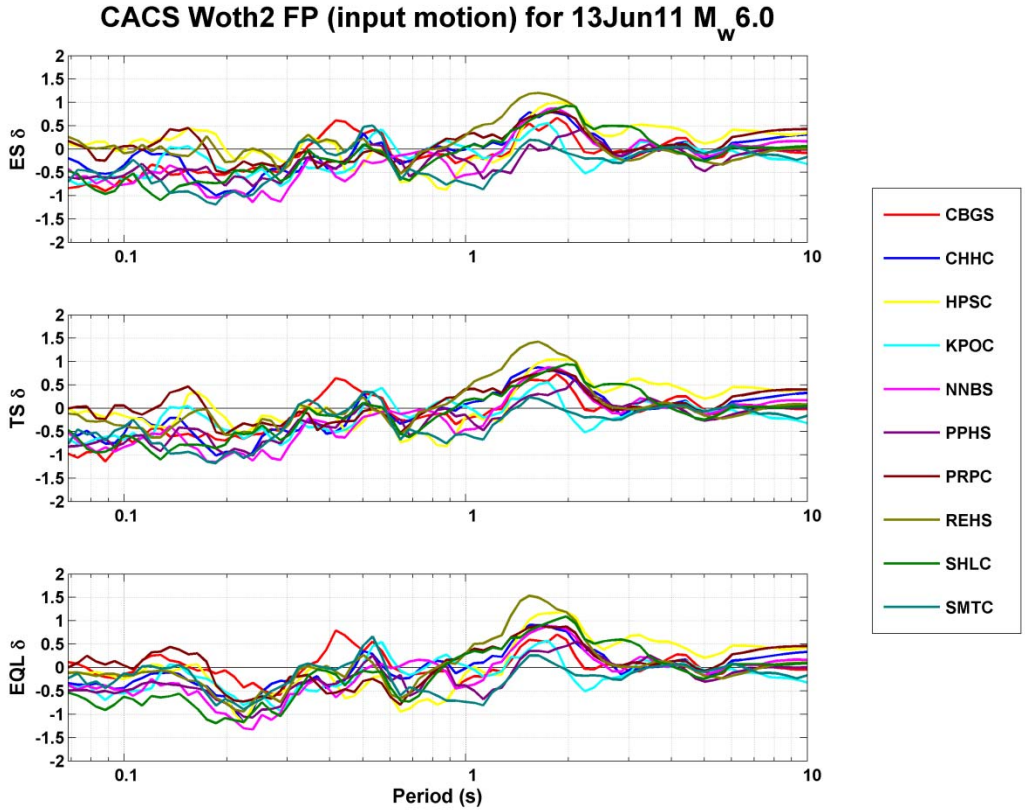
CACS Woth2 FP (input motion) for 13Jun11 M_w6.0
ES δ
TS δ
EQL δ
Period (s)
CBGS
CHHC
HPSC
KPOC
NNBS
PPHS
PRPC
REHS
SHLC
SMTC

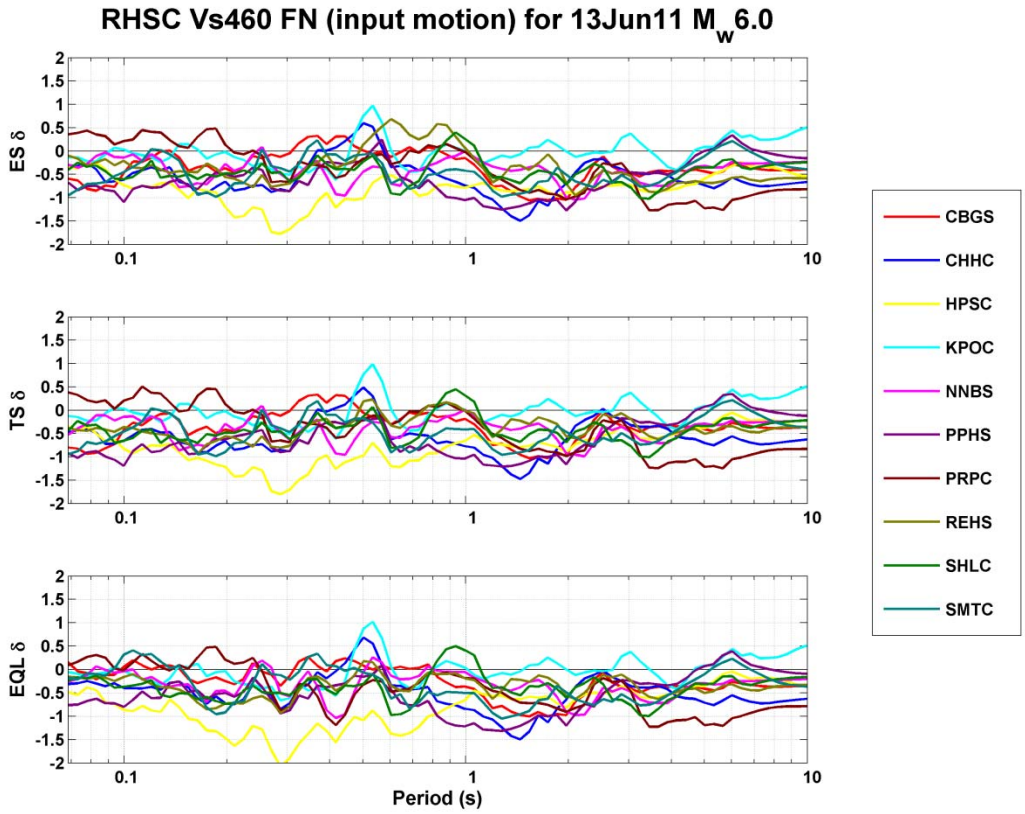
RHSC Vs460 FN (input motion) for 13Jun11 M_w6.0
ES δ
TS δ
EQL δ
Period (s)
CBGS
CHHC
HPSC
KPOC
NNBS
PPHS
PRPC
REHS
SHLC
SMTC

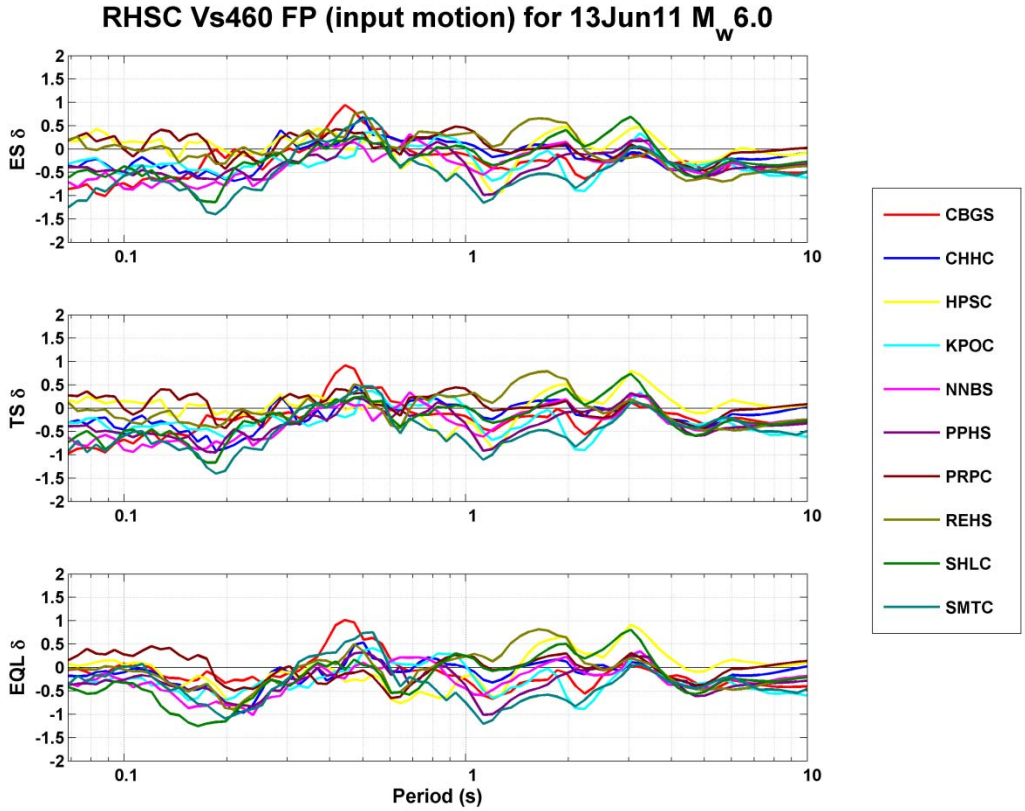
RHSC Vs460 FP (input motion) for 13Jun11 M_w6.0
ES δ
TS δ
EQL δ
Period (s)
CBGS
CHHC
HPSC
KPOC
NNBS
PPHS
PRPC
REHS
SHLC
SMTC

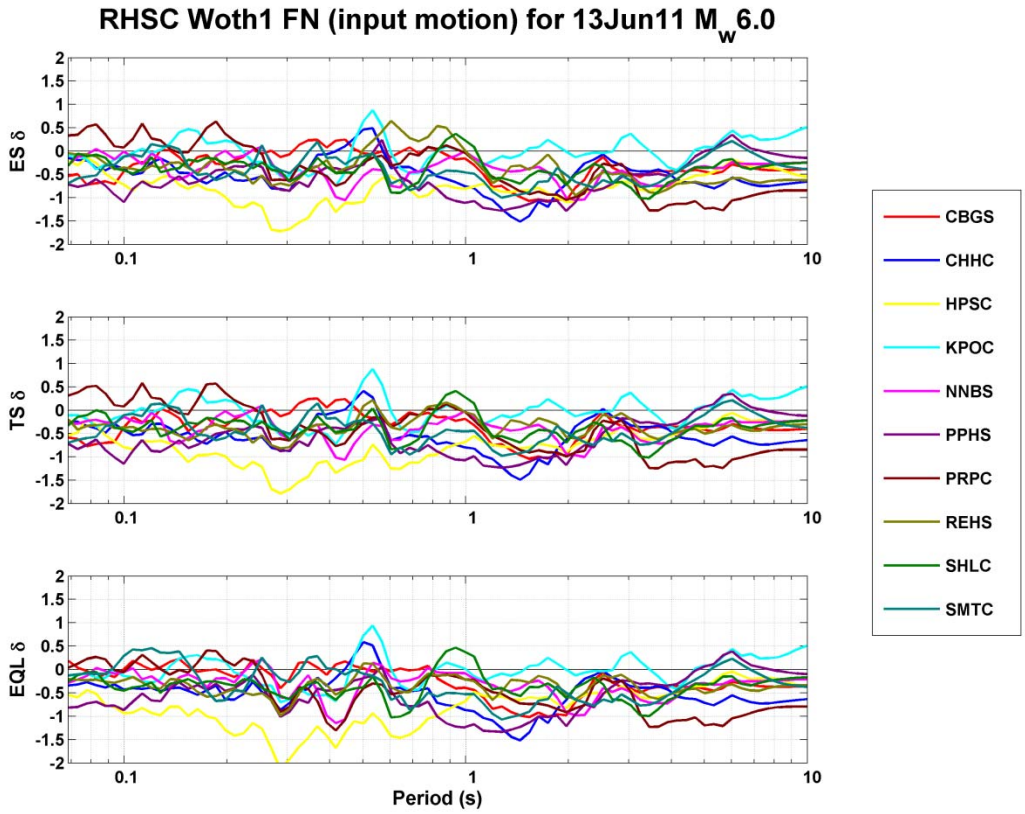
RHSC Woth1 FN (input motion) for 13Jun11 M_w6.0
ES δ
TS δ
EQL δ
Period (s)
CBGS
CHHC
HPSC
KPOC
NNBS
PPHS
PRPC
REHS
SHLC
SMTC

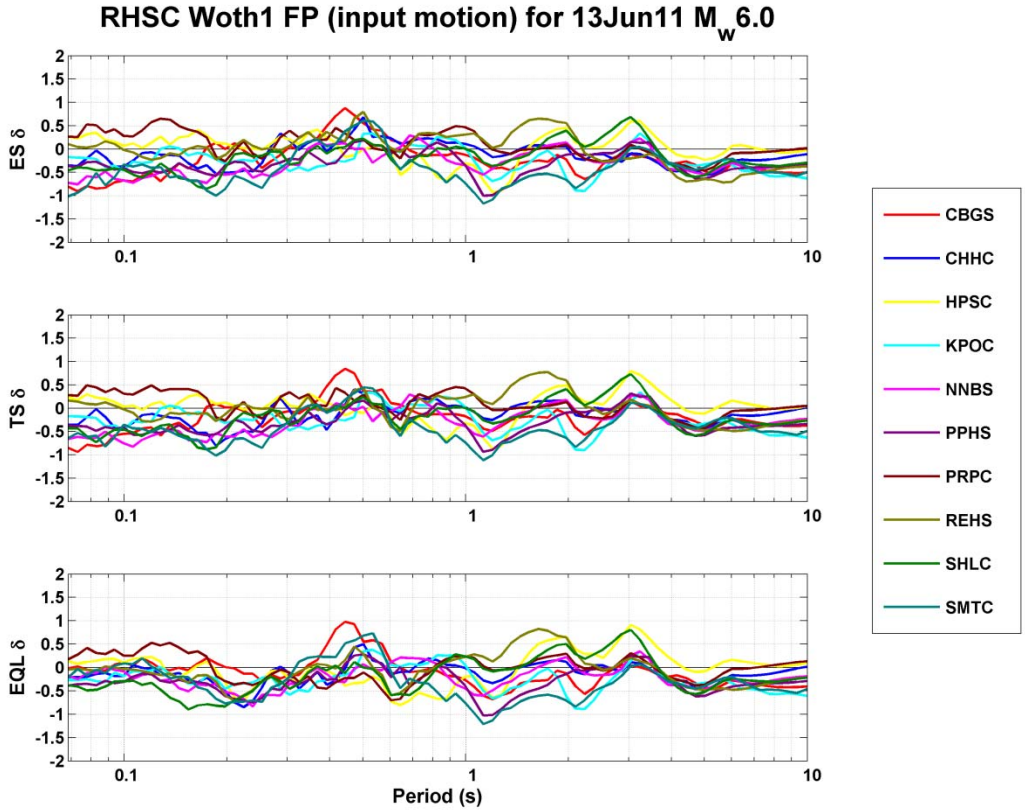
RHSC Woth1 FP (input motion) for 13Jun11 M_w6.0
ES δ
TS δ
EQL δ
Period (s)
CBGS
CHHC
HPSC
KPOC
NNBS
PPHS
PRPC
REHS
SHLC
SMTC

Appendix A.7.4

Residuals for 23 December 2011 M_w 5.8 Event

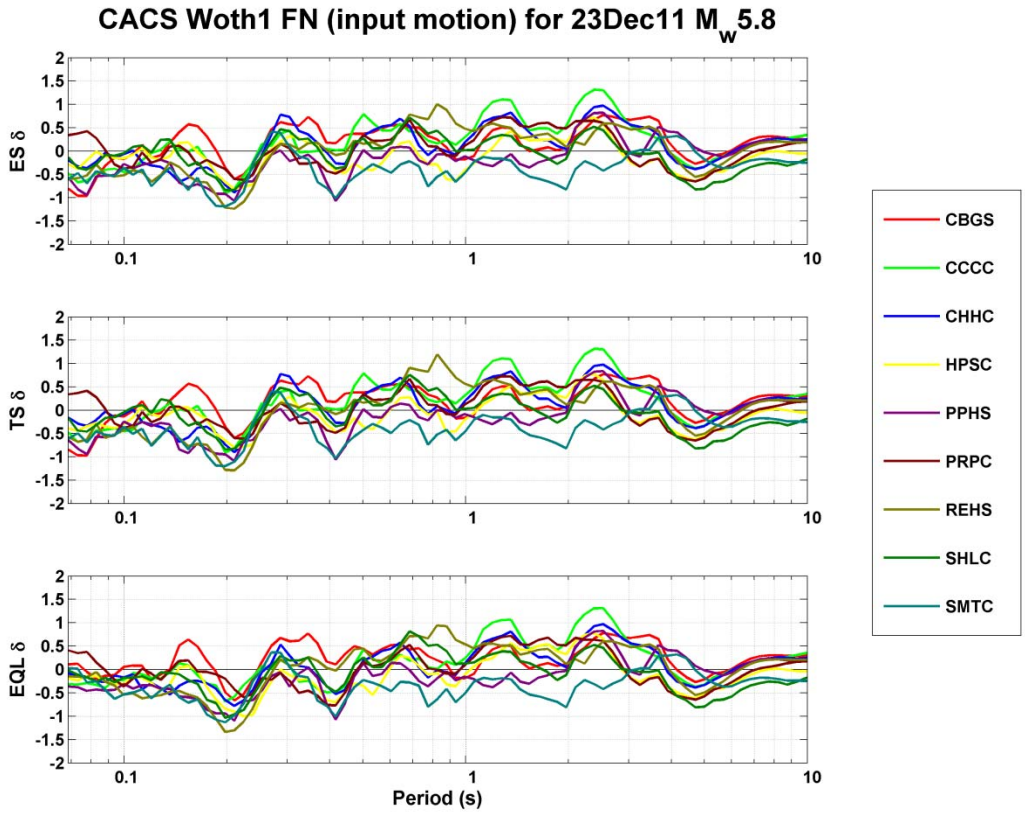
CACS Woth1 FN (input motion) for 23Dec11 M$_w$5.8
ES δ
TS δ
EQL δ
Period (s)
CBGS
CCCC
CHHC
HPSC
PPHS
PRPC
REHS
SHLC
SMTC

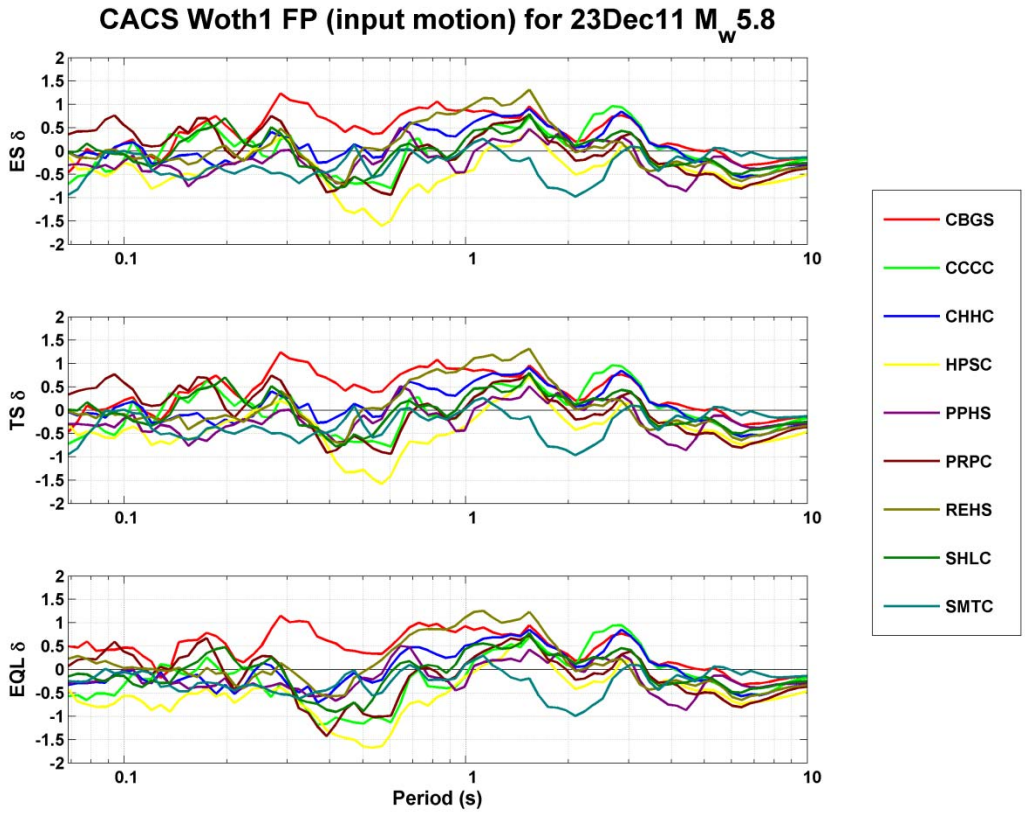
CACS Woth1 FP (input motion) for 23Dec11 M$_w$5.8
ES δ
TS δ
EQL δ
Period (s)
CBGS
CCCC
CHHC
HPSC
PPHS
PRPC
REHS
SHLC
SMTC

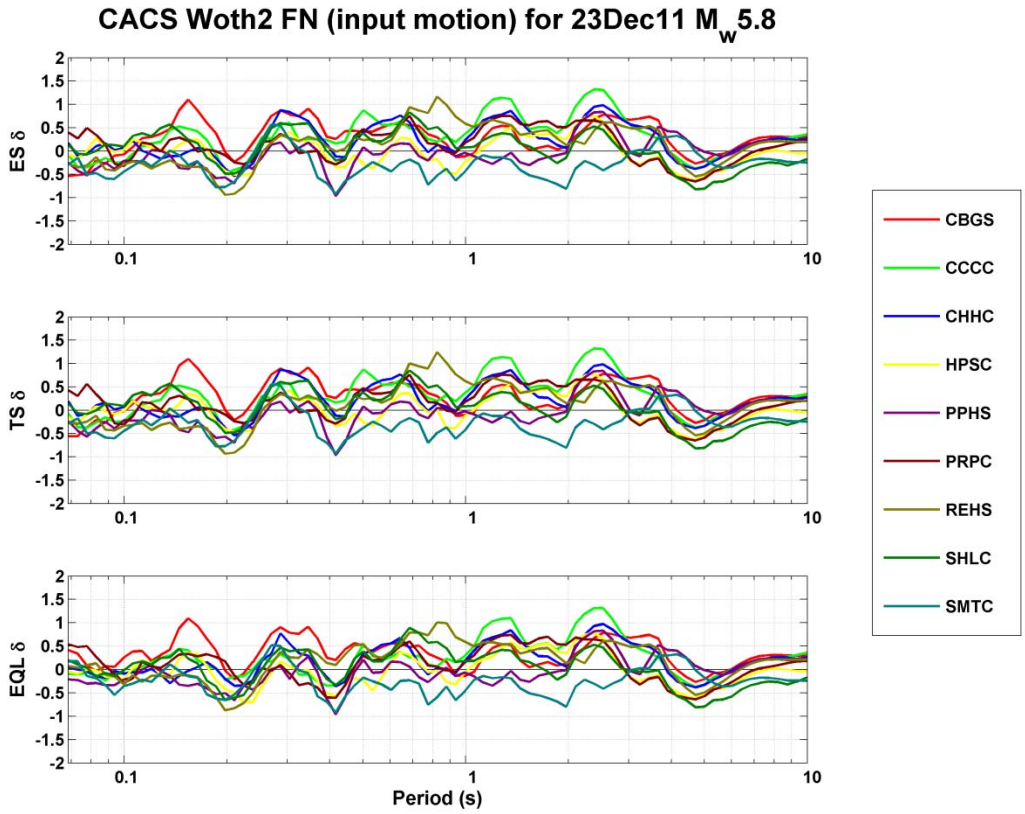
CACS Woth2 FN (input motion) for 23Dec11 M$_w$5.8
ES δ
TS δ
EQL δ
Period (s)
CBGS
CCCC
CHHC
HPSC
PPHS
PRPC
REHS
SHLC
SMTC

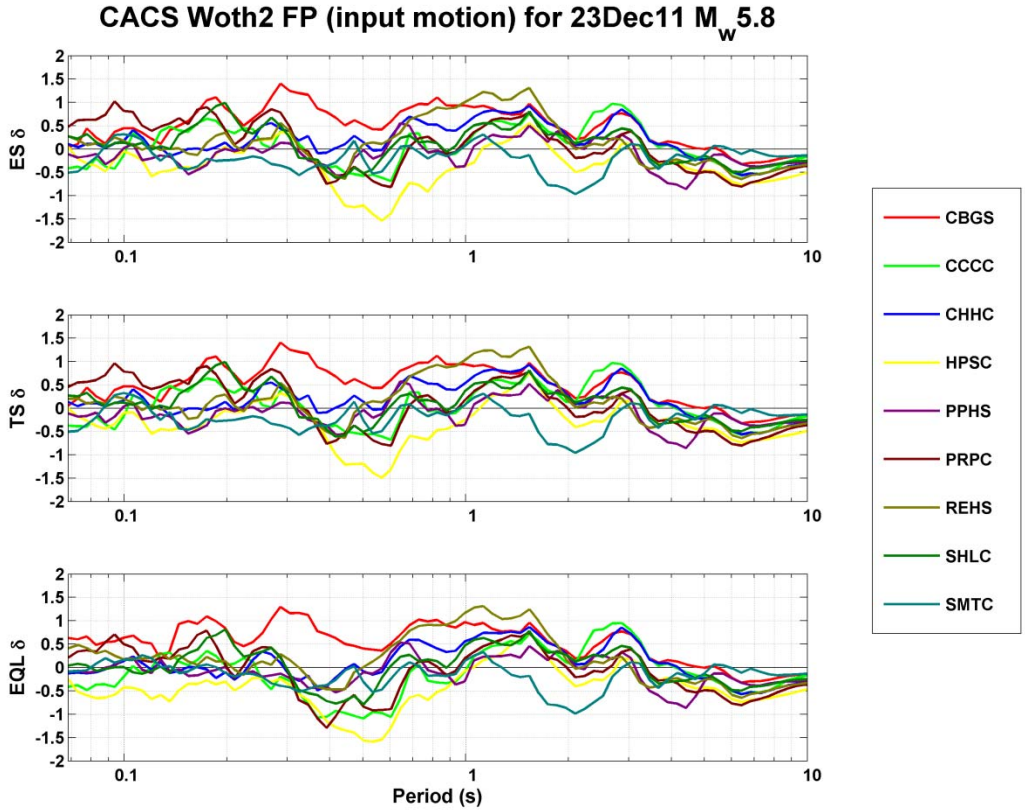
CACS Woth2 FP (input motion) for 23Dec11 M$_w$5.8
ES δ
TS δ
EQL δ
Period (s)
CBGS
CCCC
CHHC
HPSC
PPHS
PRPC
REHS
SHLC
SMTC

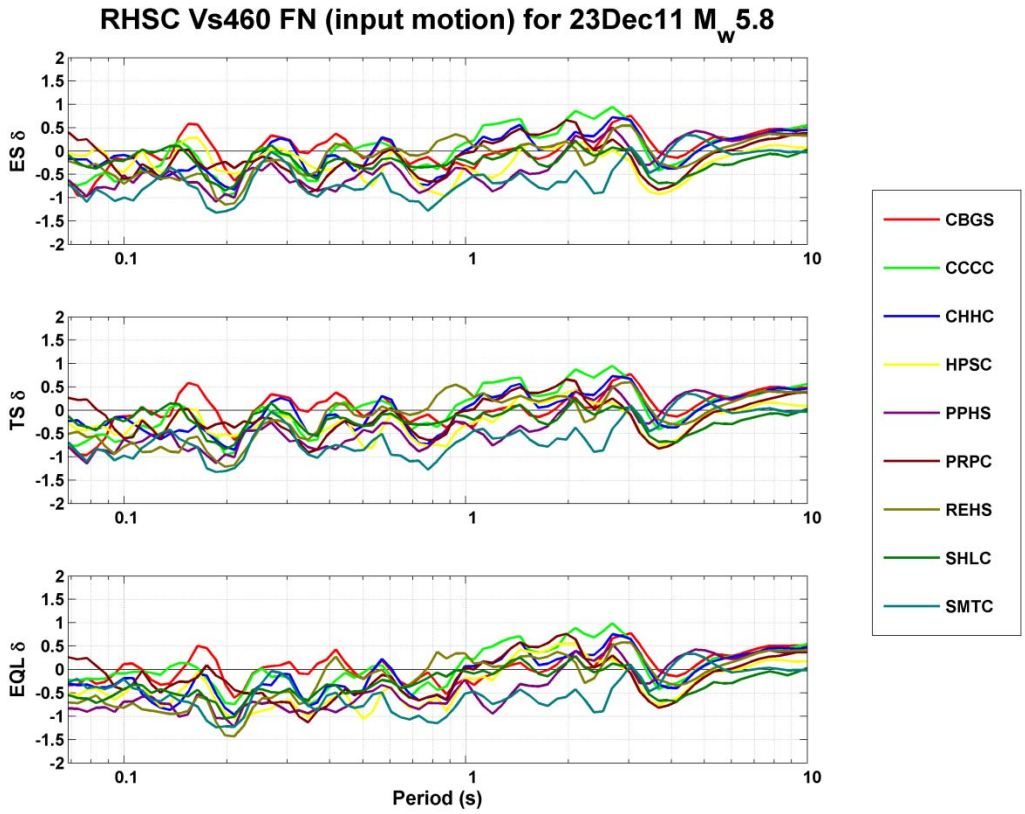
RHSC Vs460 FN (input motion) for 23Dec11 M_w5.8
ES δ
TS δ
EQL δ
Period (s)
CBGS
CCCC
CHHC
HPSC
PPHS
PRPC
REHS
SHLC
SMTC

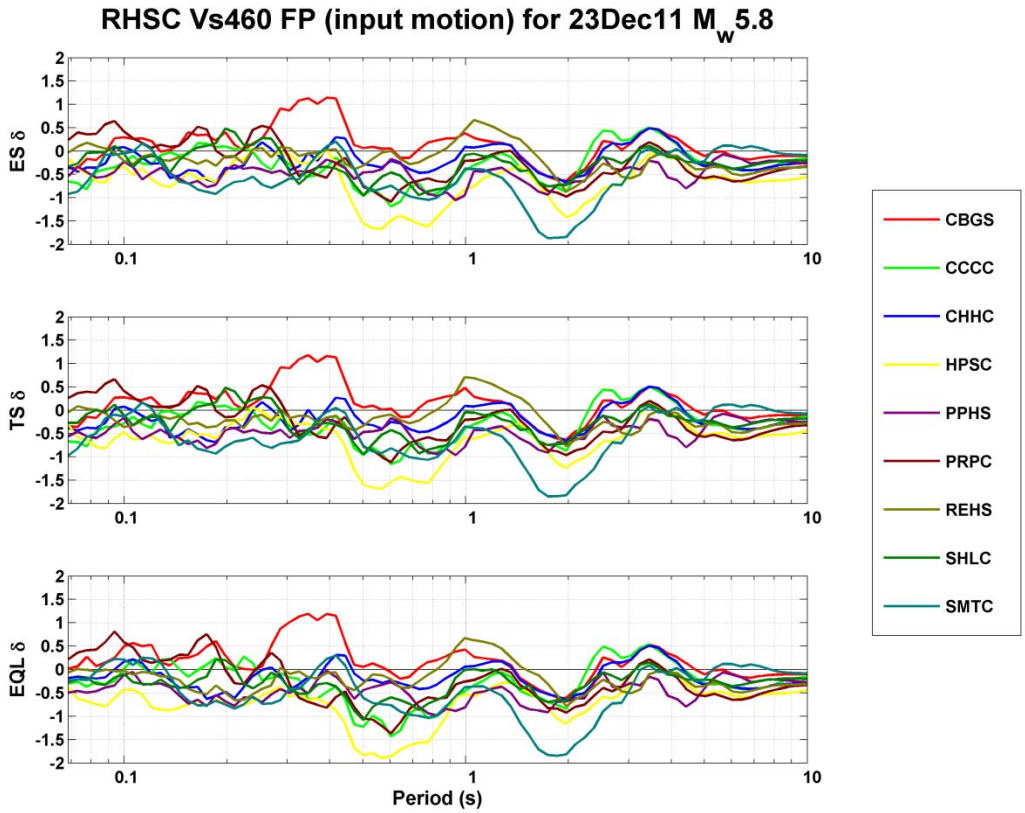
RHSC Vs460 FP (input motion) for 23Dec11 M_w5.8
ES δ
TS δ
EQL δ
Period (s)
CBGS
CCCC
CHHC
HPSC
PPHS
PRPC
REHS
SHLC
SMTC

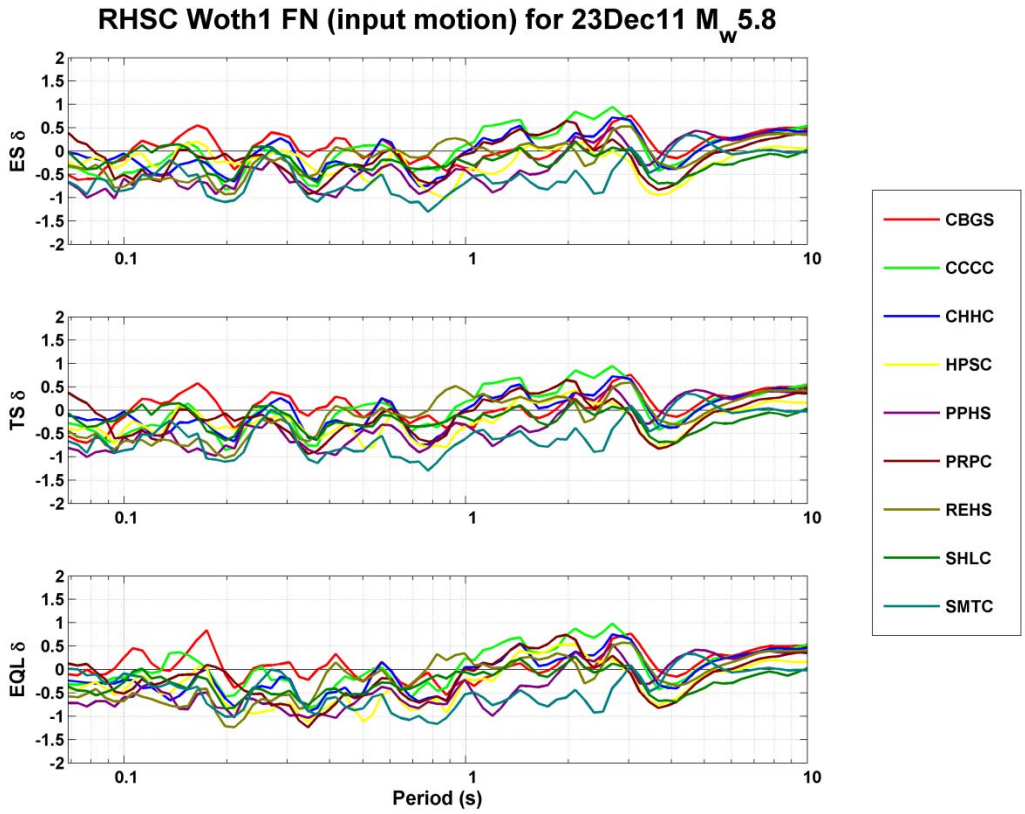
RHSC Woth1 FN (input motion) for 23Dec11 M$_w$5.8
ES δ
TS δ
EQL δ
Period (s)
CBGS
CCCC
CHHC
HPSC
PPHS
PRPC
REHS
SHLC
SMTC

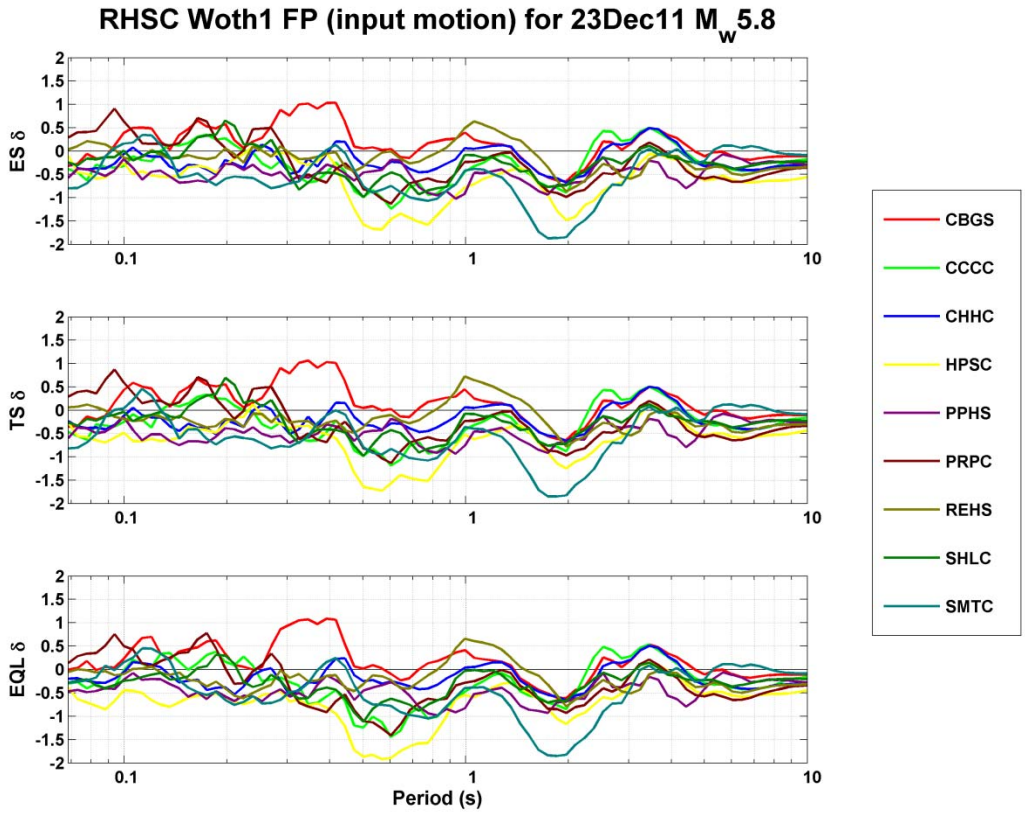
RHSC Woth1 FP (input motion) for 23Dec11 M$_w$5.8
ES δ
TS δ
EQL δ
Period (s)
CBGS
CCCC
CHHC
HPSC
PPHS
PRPC
REHS
SHLC
SMTC

Appendix A.7.5

Residuals for 23 December 2011 M_w 5.9 Event

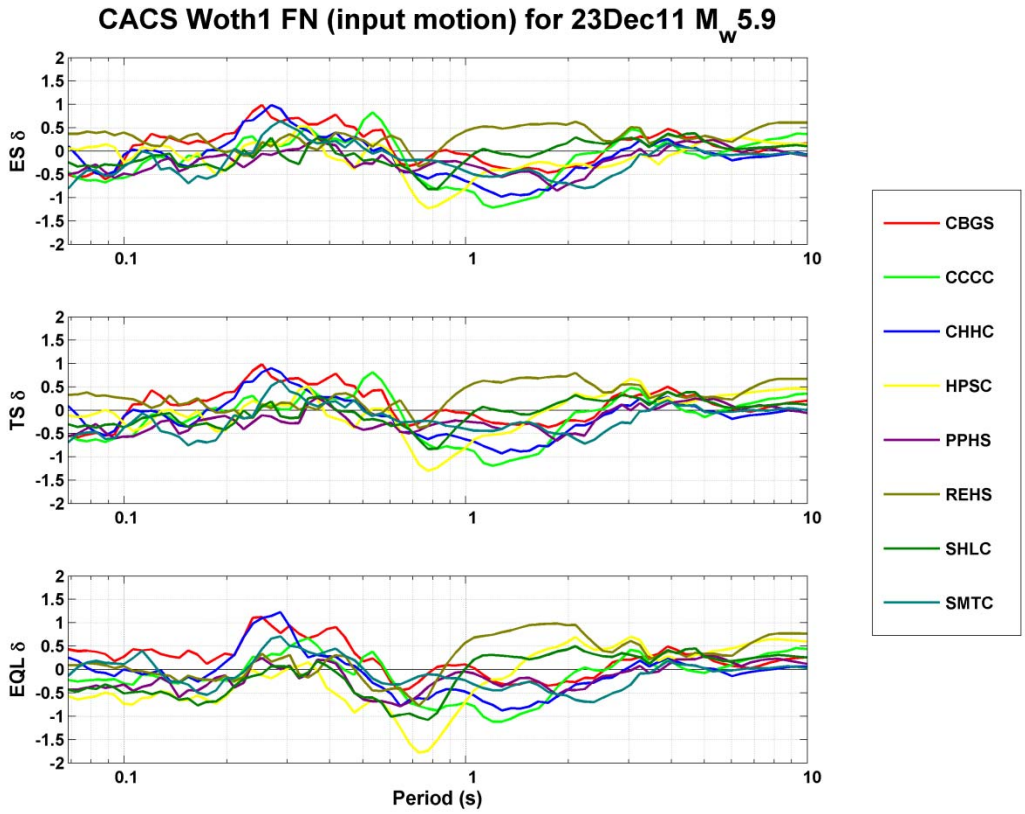
CACS Woth1 FN (input motion) for 23Dec11 M$_w$5.9
ES δ
TS δ
EQL δ
Period (s)
CBGS
CCCC
CHHC
HPSC
PPHS
REHS
SHLC
SMTC

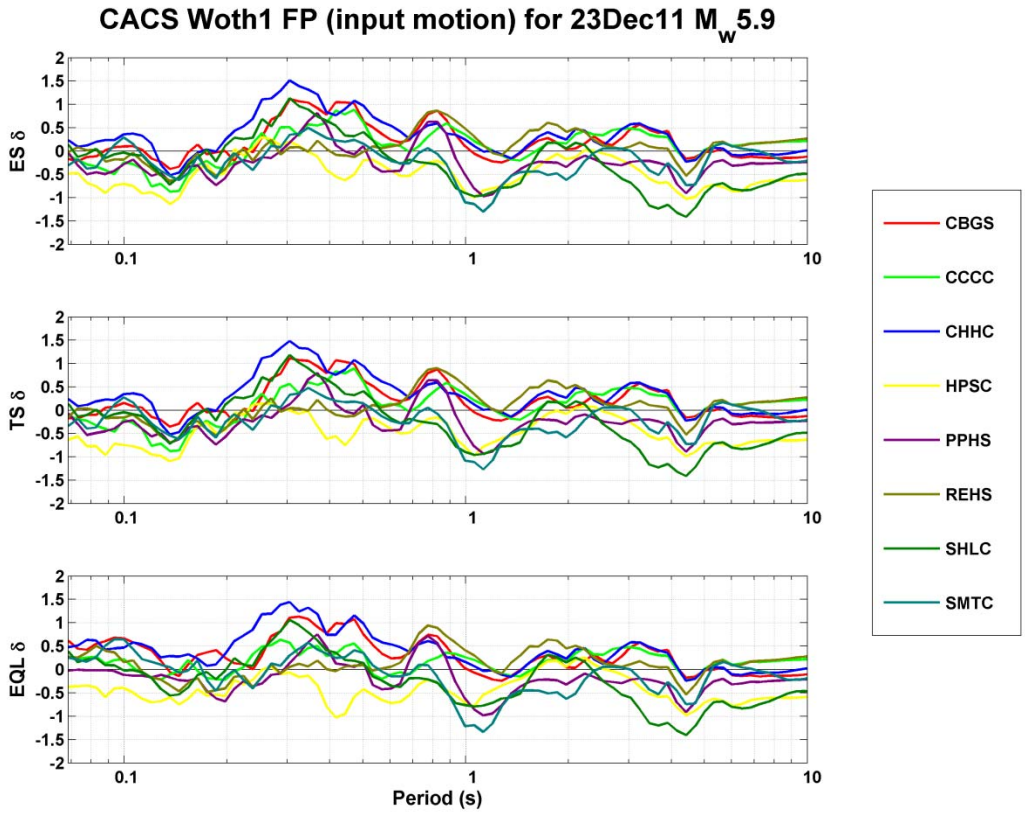
CACS Woth1 FP (input motion) for 23Dec11 M$_w$5.9
ES δ
TS δ
EQL δ
Period (s)
CBGS
CCCC
CHHC
HPSC
PPHS
REHS
SHLC
SMTC

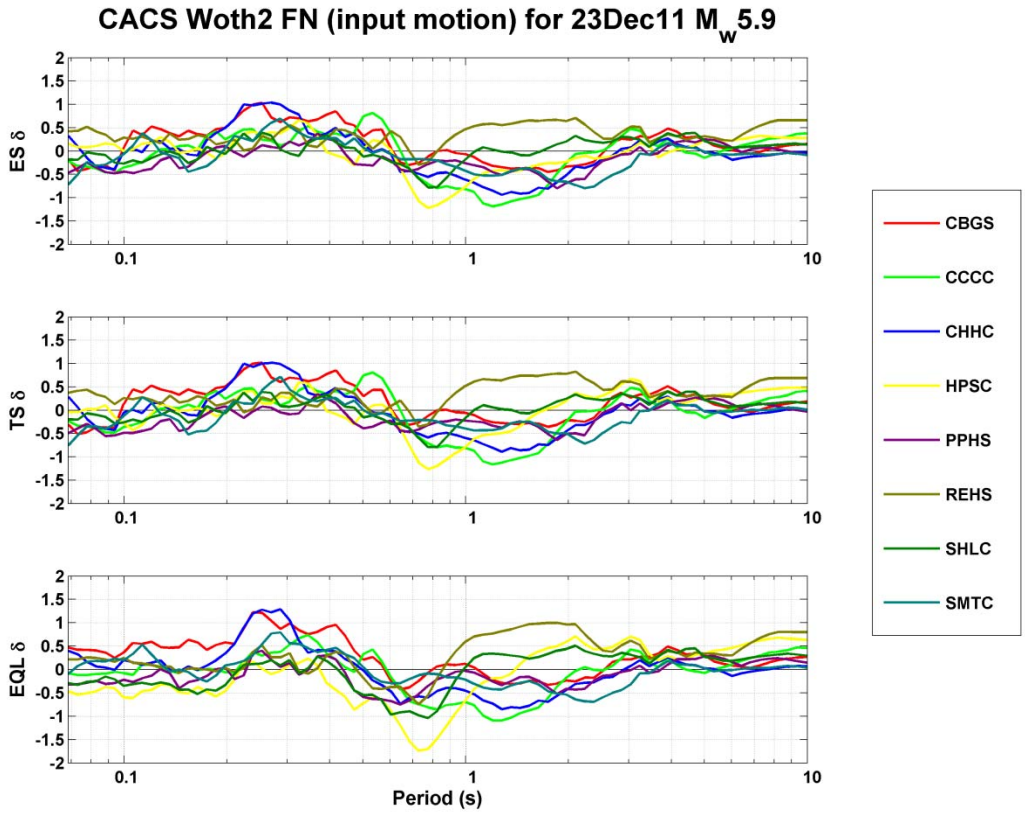
CACS Woth2 FN (input motion) for 23Dec11 M$_w$5.9
ES δ
TS δ
EQL δ
Period (s)
CBGS
CCCC
CHHC
HPSC
PPHS
REHS
SHLC
SMTC

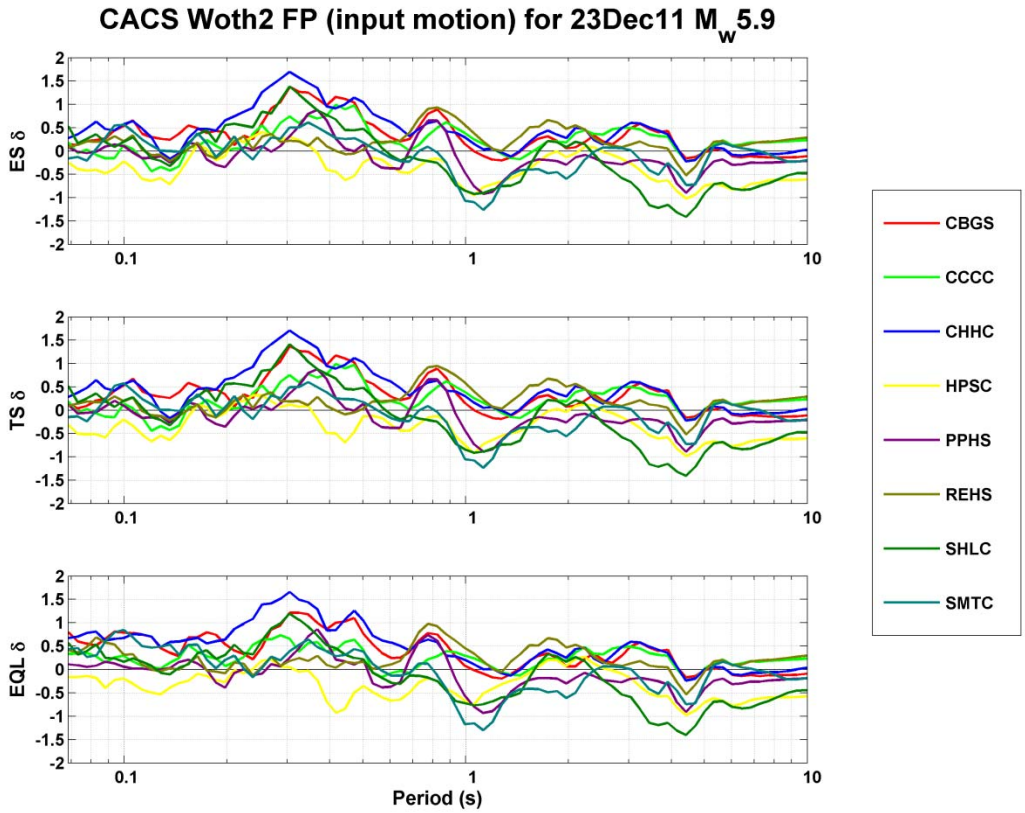
CACS Woth2 FP (input motion) for 23Dec11 M$_w$5.9
ES δ
TS δ
EQL δ
Period (s)
CBGS
CCCC
CHHC
HPSC
PPHS
REHS
SHLC
SMTC

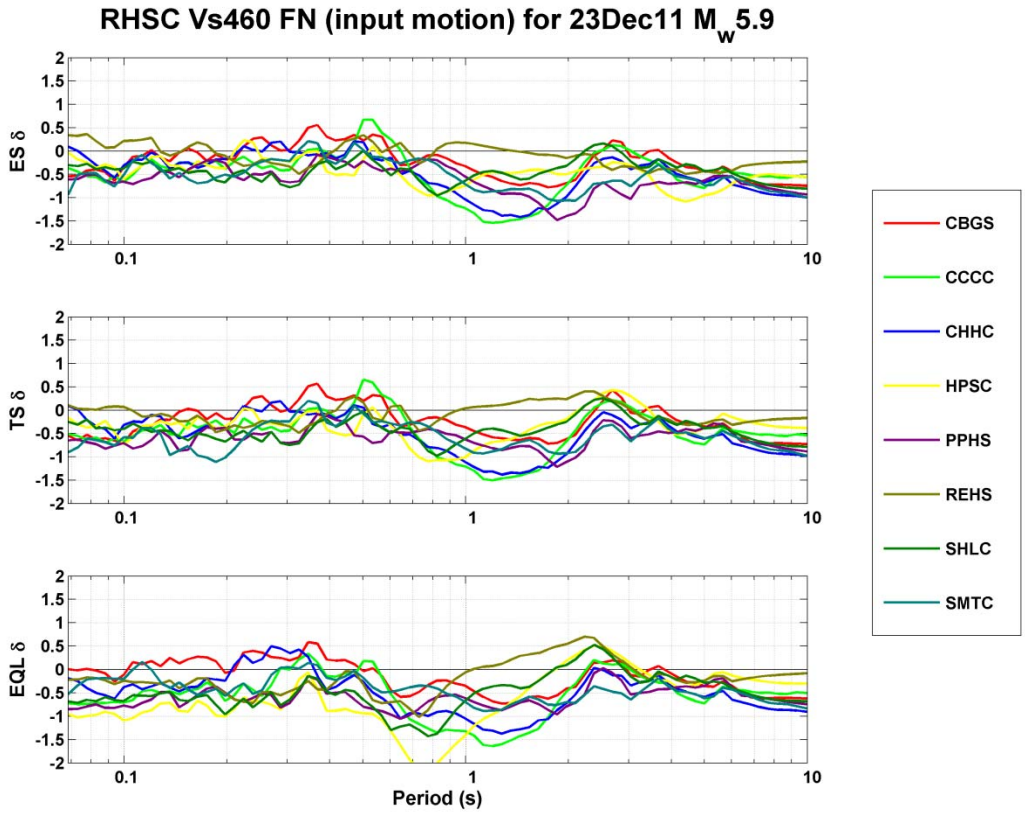
RHSC Vs460 FN (input motion) for 23Dec11 M_w5.9
ES δ
TS δ
EQL δ
Period (s)
CBGS
CCCC
CHHC
HPSC
PPHS
REHS
SHLC
SMTC

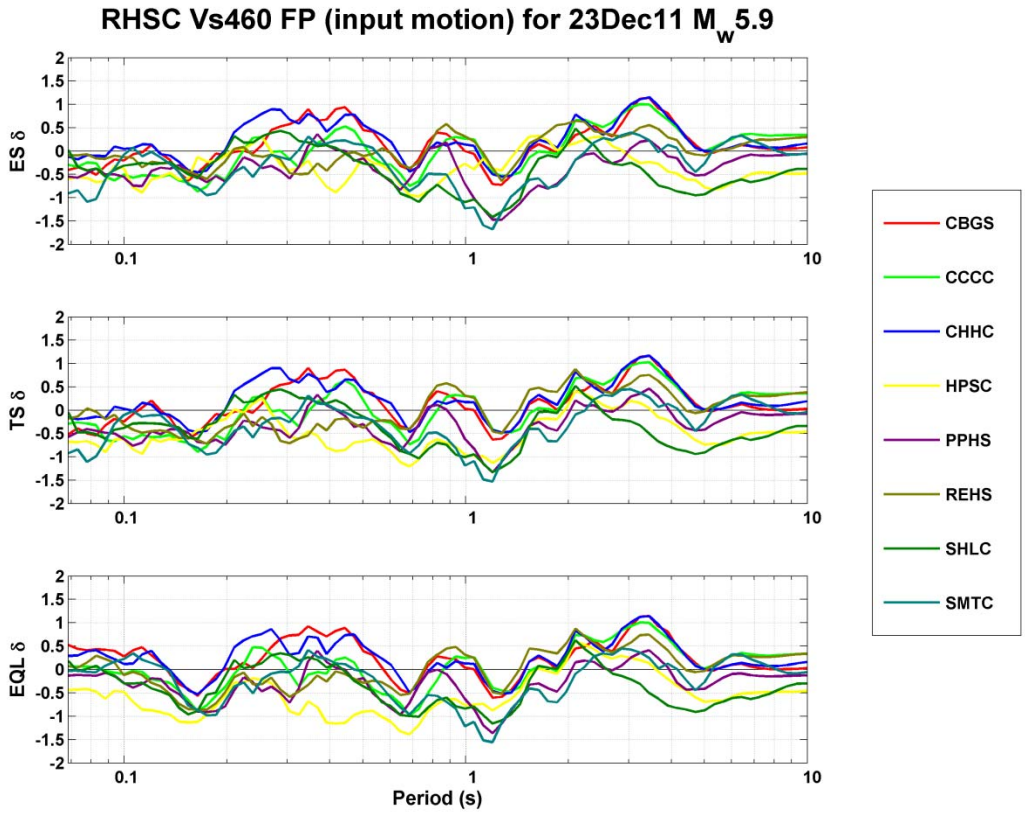
RHSC Vs460 FP (input motion) for 23Dec11 M_w5.9
ES δ
TS δ
EQL δ
Period (s)
CBGS
CCCC
CHHC
HPSC
PPHS
REHS
SHLC
SMTC

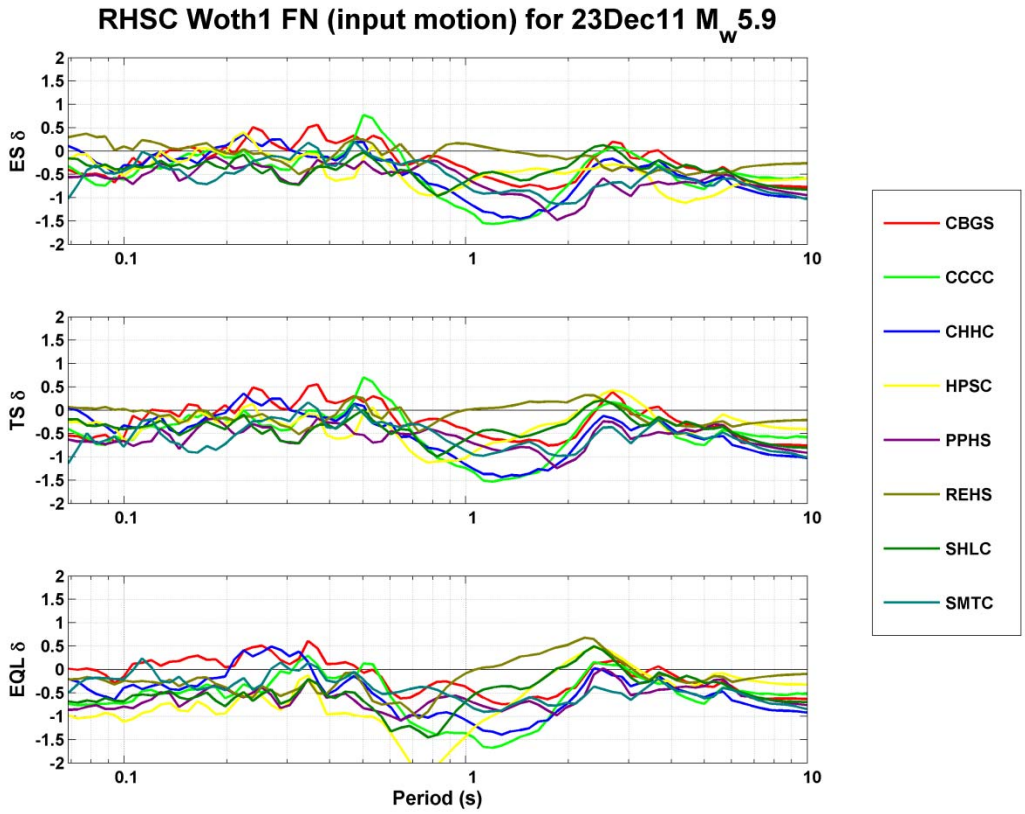
RHSC Woth1 FN (input motion) for 23Dec11 M_w5.9
ES δ
TS δ
EQL δ
Period (s)
CBGS
CCCC
CHHC
HPSC
PPHS
REHS
SHLC
SMTC

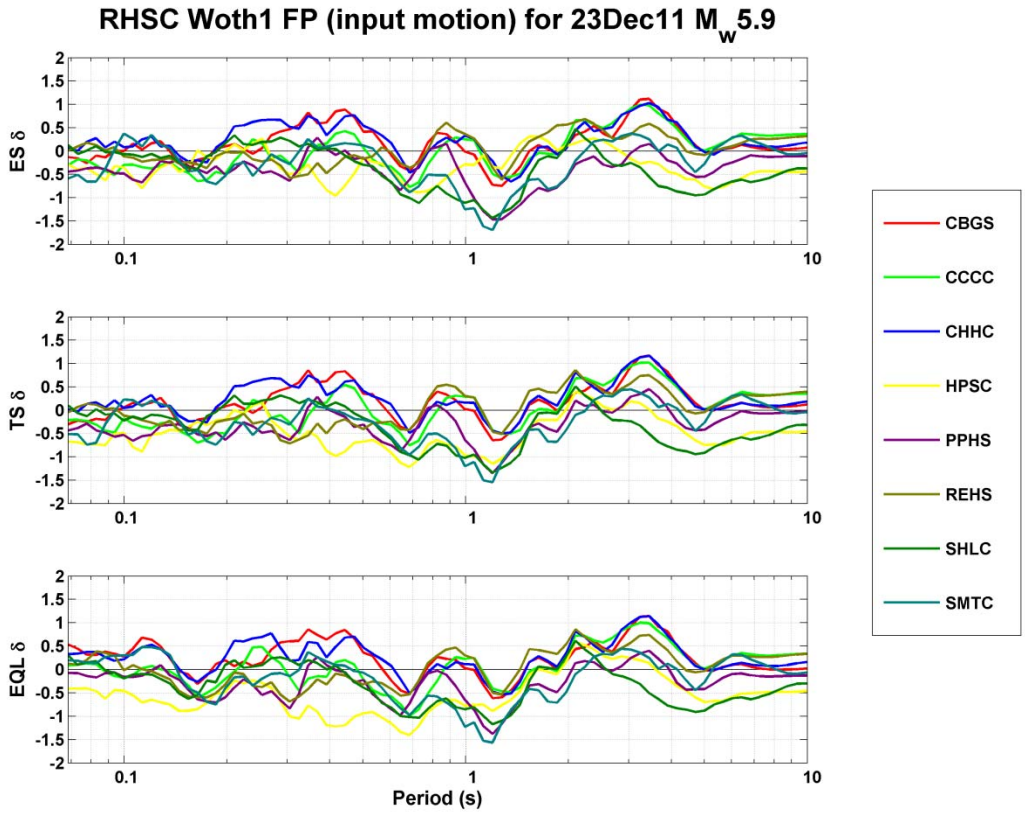
RHSC Woth1 FP (input motion) for 23Dec11 M_w5.9
ES δ
TS δ
EQL δ
Period (s)
CBGS
CCCC
CHHC
HPSC
PPHS
REHS
SHLC
SMTC

Appendix A.7.6

Residuals for 26 December 2010 M_w 4.7 Event

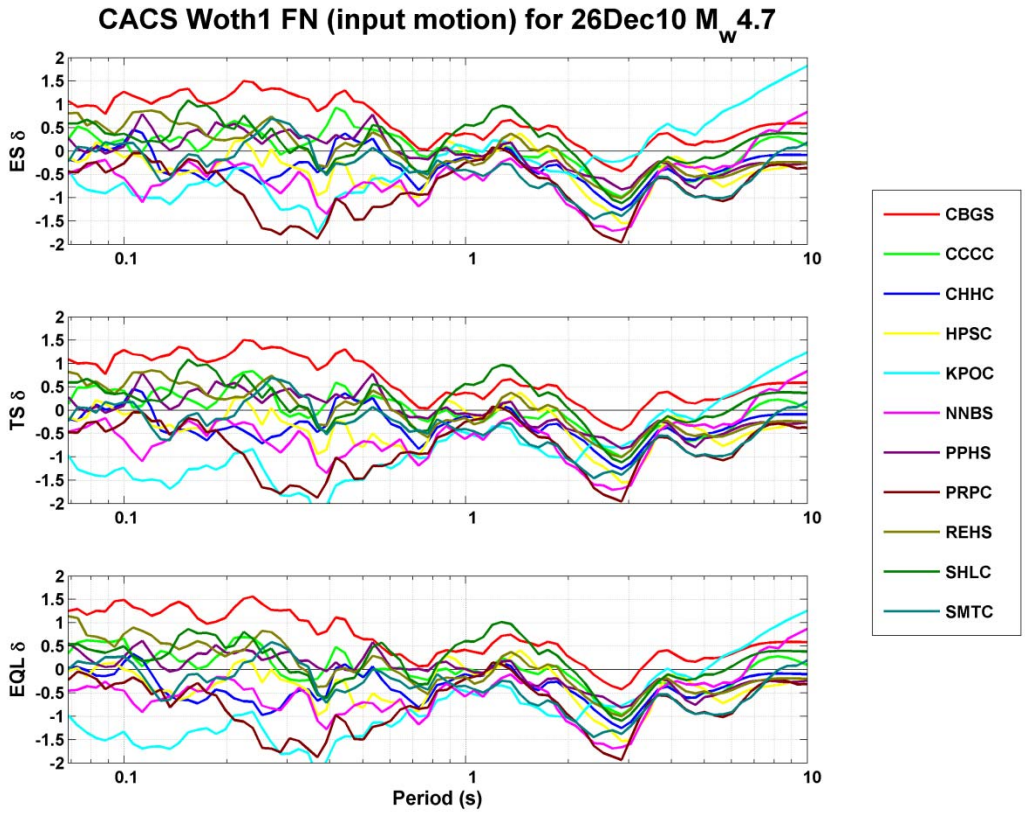
CACS Woth1 FN (input motion) for 26Dec10 M$_w$4.7
ES δ
TS δ
EQL δ
Period (s)
CBGS
CCCC
CHHC
HPSC
KPOC
NNBS
PPHS
PRPC
REHS
SHLC
SMTC

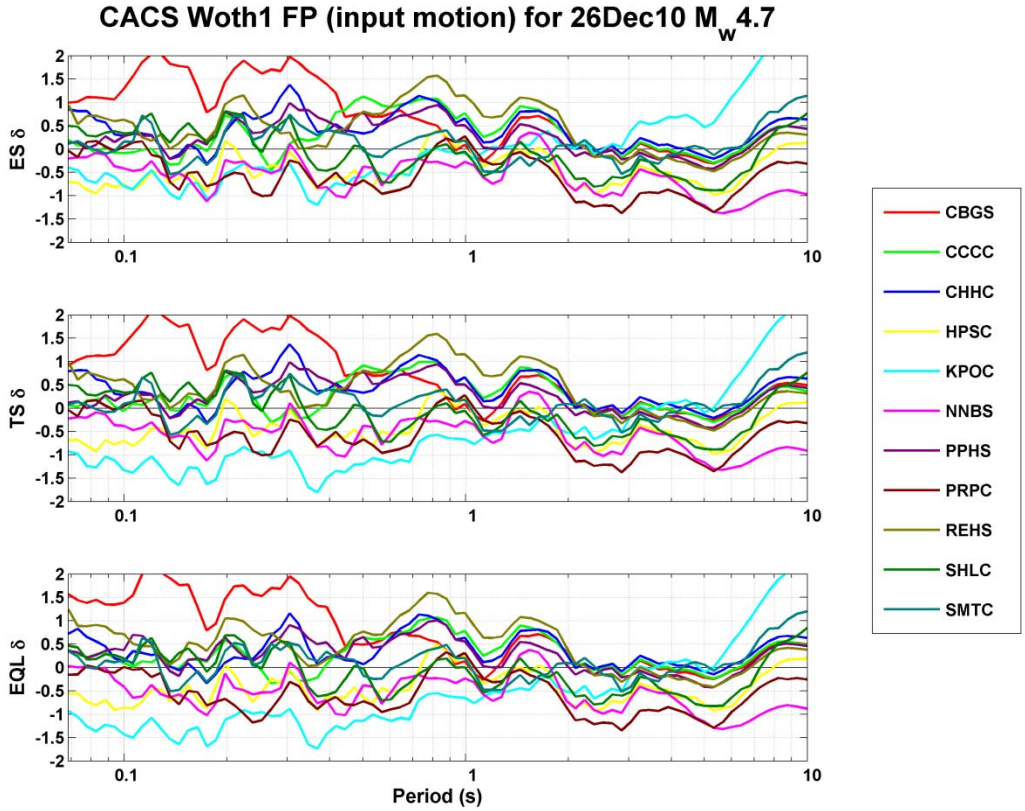
CACS Woth1 FP (input motion) for 26Dec10 M$_w$4.7
ES δ
TS δ
EQL δ
Period (s)
CBGS
CCCC
CHHC
HPSC
KPOC
NNBS
PPHS
PRPC
REHS
SHLC
SMTC

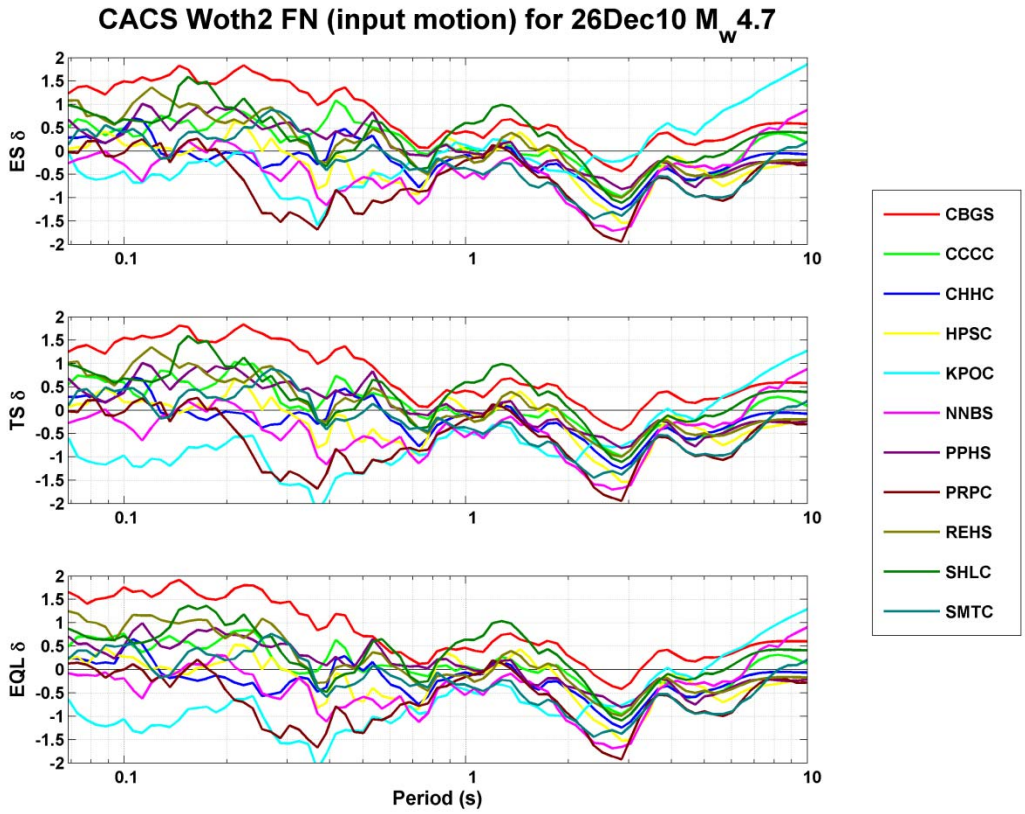
CACS Woth2 FN (input motion) for 26Dec10 M$_w$4.7
ES δ
TS δ
EQL δ
Period (s)
CBGS
CCCC
CHHC
HPSC
KPOC
NNBS
PPHS
PRPC
REHS
SHLC
SMTC

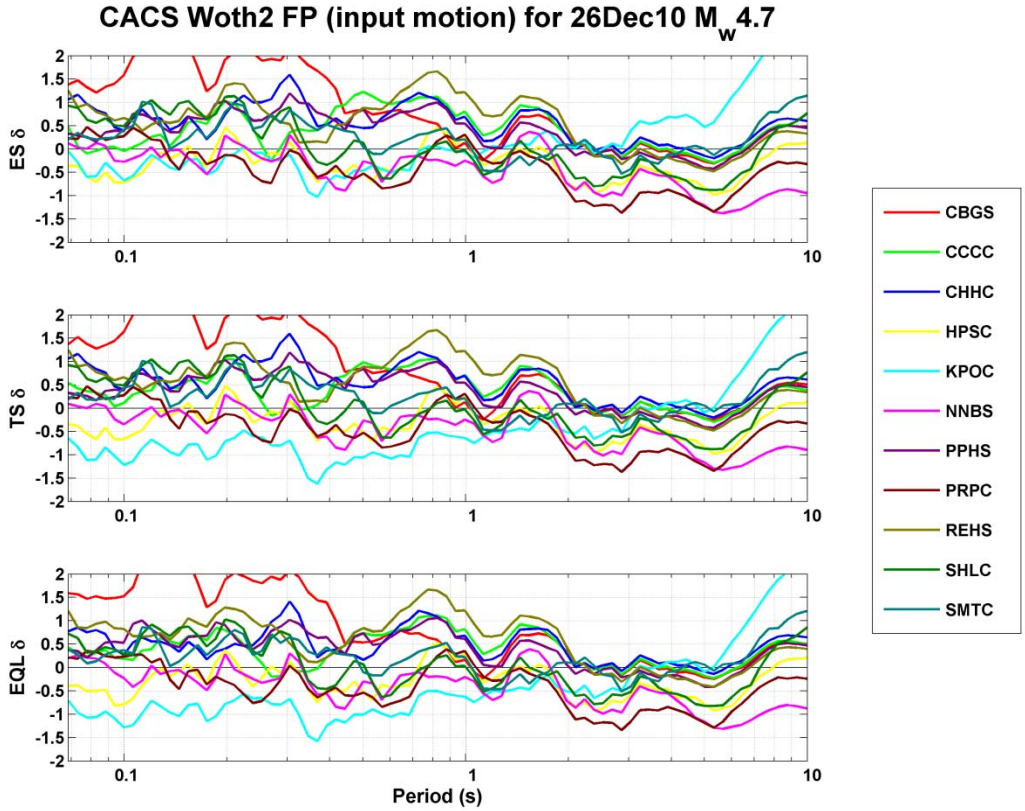
CACS Woth2 FP (input motion) for 26Dec10 M$_w$4.7
ES δ
TS δ
EQL δ
Period (s)
CBGS
CCCC
CHHC
HPSC
KPOC
NNBS
PPHS
PRPC
REHS
SHLC
SMTC

Appendix B

Additional Insights from Triaxial Testing

APPENDIX B: ADDITIONAL INSIGHTS FROM TRIAXIAL TESTING

B.1 INTRODUCTION

Chapters 3 and 4 include materials presented in technical papers submitted to archival journals. They provide the key details and insights regarding the "undisturbed" sampling and laboratory testing program undertaken to investigate critical shallow soil deposits at selected building sites in the CBD of Christchurch, NZ. These chapters focused on describing the procedures used to obtain samples and to test retrieved "undisturbed" soil specimens in the laboratory as well interpreting the results of these tests with an emphasis on understanding the undrained loading response of these soils. Triaxial testing (primarily cyclic triaxial testing, CTX) of high quality test specimens was used to examine the liquefaction susceptibility of soils that proved problematic for building performance during the 2010-11 Canterbury earthquake sequence.

This appendix provides additional details and insights not included in the technical papers presented in Chapters 3 and 4 regarding the interpretation of data and results from triaxial testing of "undisturbed" soil specimens. The following information and data are presented and discussed:

- Summary tables of pertinent information regarding the testing of "undisturbed" specimens are provided for both monotonic and cyclic triaxial tests. This information includes: 1) sites/locations and depths of tested specimens; 2) testing data such as isotropic consolidation stresses (σ'_c), pre-test void ratios (e_{con}) and relative densities (D_r), applied cyclic stress ratios (CSR) for CTX tests, as well as index testing results for tested specimens (G_s, PI, FC, void ratio limits, and USCS); 3) number of cycles to obtain specific axial strain levels (N_c 3% S.A and N_c 5% D.A. ε_{ax}) during CTX testing; and 4) interpreted CPT data that corresponds to each tested specimen (e.g., I_c, q_{c1N}, and K_σ). Also provided are data pertaining to post-CTX testing, with an emphasis on the data from post-liquefaction reconsolidation testing.
- Plots of CSR versus $N_{c\text{-}3\%\ S.A.\varepsilon}$ are presented for each studied site in the Christchurch CBD. Labels are provided that provide information regarding each specimen (e.g., specimen identifier, void ratio and D_r, corresponding CPT data, and FC) that corresponds to the respective data points; interpreted CRR curves are drawn following the same power function fit described in Chapters 3 and 4 (i.e., $CRR=a\cdot N^{-b}$). Included with each plot of CSR vs. N_c are the corresponding grain size distribution plots for the tested CTX specimens.
- Plots of CSR versus $N_{c\text{-}3\%\ S.A.\varepsilon}$ for the various soil types tested across all the CBD sites studied are provided with interpreted CRR curves. These plots are similar to the plots presented in Chapter 4, but with further supporting data provided through the use of labels for individual specimens.

- Plots of CSR versus $N_{c\text{-}3\%\ S.A.\varepsilon}$ for the various soil types are presented in a similar fashion as described above with a range of estimated CRR curves resulting from the Robertson and Wride (1998) and Boulanger and Idriss (2014) CPT-based liquefaction triggering correlations. These plots are provided to better compare the results of the CTX testing to two commonly used empirically based liquefaction triggering procedures. Also provided are potential ranges of estimated CSR values for the 3 largest earthquakes from the Canterbury events (Darfield, Christchurch, and 13 JUN 2011 M_w6.0 events).
- Volumetric strain ($\varepsilon_{vol\text{-}rec}$) is plotted against the maximum level of shear strain ($\gamma_{max}=1.5\cdot\varepsilon_{ax}$) for specimens that were reconsolidated post-CTX testing (post-liquefaction reconsolidation).
- Researchers (e.g., Robertson and Wride, 1998; Robinson et al., 2013) have examined the correlation between soil behavior type index (I_c; Robertson and Wride, 1998) and fines content (FC). As adjacent CPT data was available for the sampled soils, I_c is compared to values of FC for the studied CBD soils.
- A more detailed comparison of relative density (D_r) estimated in the lab for triaxial specimens to D_r estimated from CPT data is presented.

B.2 SUMMARY TABLES OF TRIAXIAL TESTING

Table B.1 and Table B.2 provide information regarding the cyclic and monotonic triaxial test specimens, respectively. This information is used in the plots and information presented in subsequent sections of Appendix B. Beneath each table is an explanation of the data presented. As noted, the CPT data for the LS-II site does not correspond with the data found during the sampling and testing process—i.e., for a given specimen depth the CPT data and interpretations do not agree with the information found from interpreting the lab results (mainly I_c and corresponding USCS/soil type significantly disagree). Data from the nearest CPT investigation is provided for the LS-II site for reference purposes only and should not be used for comparison purposes unless future work proves this data is reasonable. Void ratio limits were found using the Japanese Standard method (JIS A 1224:2000) for SP, SP-SM, and SM soil specimens; ML soils have too high of a fines content for this method to return reasonable results.

Table B.3 provides a summary of the post-liquefaction tests completed on specimens following cyclic triaxial testing. A total of 10 post-liquefaction monotonic tests and 21 post-liquefaction reconsolidation tests were completed. Post-liquefaction reconsolidation tests were completed for the specimens tested from the CTUC site and all but one of the specimens from the CTH site; however, after this testing was complete it was realized that there was an issue with the transducer used to measure volume change. Therefore, no post-liquefaction test data are reported for these specimens. This issue with the transducer was corrected prior to testing for the remaining sites.

B.3 SITE SPECIFIC CSR VS. $N_{C\text{-}3\%\ S.A.\varepsilon}$

Figure B.1 through Figure B.7 provide plots of CSR vs. $N_{c\text{-}3\%\ S.A.\varepsilon}$ for the sites studied in the CBD of Christchurch. Each data point is labelled with the borehole where the specimen was

obtained, the depth of the specimen, and pertinent information from the nearest CPT corresponding to the depth of the specimen (q_{c1N} and I_c). Also included are data regarding important index test results (FC, e_{con}, and D_r). Values of CSR are not corrected to field conditions but instead represent the applied cyclic stress ratio in CTX conditions; however CSR values are normalized to atmospheric pressure using K_σ suggested by Boulanger and Idriss 2014. Interpreted cyclic resistance curves are provided as well. Beneath each plot of CSR vs. $N_{c\text{-}3\%\ S.A.\varepsilon}$ is a plot of the various grain size distribution (GSD) curves for the specimens tested at each site. Specimens were grouped based on similar depth and GSD for the CRR curves presented in each figure of CSR vs. $N_{c\text{-}3\%\ S.A.\varepsilon}$. A brief description of the data and results for each site is provided below.

- CTH site (86-100 Kilmore St.): As discussed in Chapters 3 and 4, three main soil units were studied at the CTH site: a shallow layer of silt and a shallow layer of sand, both of which overly a layer of gravelly material, and a layer of sand that underlies the gravelly soil. Based on the CRR curves presented in Figure B.1, the lowest sand layer is slightly more resistant than the upper sand layer, which is slightly stronger than the shallowest silt layer. As shown in Chapter 4, though, when these CSR values are corrected to field conditions using the assumed values of C_r' for the various soil types, these CRR curves are more similar, suggesting similar liquefaction resistances.
- FTG-7 site (151 Kilmore St.): The FTG-7 site has a slightly more variable soil profile than the CTH site; however, three soil units could be identified from the field and laboratory testing program so that CRR curves could be interpreted. These soil units include a silt layer from 3.5 to 3.8 m, a silty sand layer from 4.7 to 5.54 m, and a lower unit of sand from about 10.24 to 11.18 m. Multiple tests were carried out on specimens that did not match specimens from similar depth with regards to the USCS, highlighting some of the soil variability at this site. Two tests were completed on specimens from the shallowest samples obtained from this site—corresponding to specimens from 2.57 m and 2.72 m. As shown in Figure B.2, though, the trend of these two tests represents a much steeper CRR curve compared to the other soil units; as further testing was unable to be completed for this unit, a CRR curve was not fitted to these data.
- CTUC site (199 Armagh St.): The CTUC site consists of a layer of silty sand (SM) underlain by a layer of cleaner sand (SP-SM). These two layers make up the upper 4-5 m of the soil profile and overlie a layer of gravelly material, which is underlain by a layer of sandy material. Three specimens were tested from both the upper silty sand unit from 2.75 to 3.40 m and the upper layer of sand from 3.41 to 4.05 m, as shown in Figure B.3, while only one high-quality specimen was able to be obtained and tested from the lower sand layer. It should be noted that the q_{c1N} values for the specimens from the shallow sand layers are all less than 34. As discussed in Chapters 3 and 4, specimens of clean sand (SP and SP-SM) with $q_{c1N}<60$ were most likely disturbed during the sampling and testing procedures; therefore, the results shown in Figure B.3 for the shallow SP-SM soil are for informational purposes only and should not be used to estimate the liquefaction susceptibility of these soils.
- PWC site (119 Armagh St.): Shallow gravelly soil at the PWC site inhibited high quality samples from being obtained in the upper 12 to 13 m of the subsurface. However, as the PWC building was founded on a mat foundation, the bottom of which was located at a

depth of about 3.8 m below the ground surface (Zupan 2014), the sandy material below this gravelly soil was the focus of the CTX testing. Figure B.4 shows that the grain size distributions of all the sampled soil specimens were close; hence, one unit of soil was interpreted for the PWC site. Specimens from 12.75 to 14.89 were tested to derive a single CRR curve.

- VT site (90 Armagh St.): Similar to the PWC site, the VT site consists of shallow gravelly soil in the upper portion of the profile, which was not sampled using the D&M sampler. All of the tested soil from this site was sandy, with a unit from 7.37 to 7.99 m being the shallowest. Two specimens were tested from a deeper unit, one from a depth of 13.77 m and one from a depth of 13.92 m; however, as shown in Figure B.5, a reasonable trend in the CSR vs. $N_{c\text{-}3\%\ S.A.\varepsilon}$ was not observed for this soil unit based on these two test results.
- LS-II site (48 Lismore St.): Characterizing the shallow soils was the focus of investigations carried out at the LS-II site. As shown in Figure B.6, a large range of grain size distributions were observed in the upper subsurface profile of the LS-II site. Only one test was carried out on the shallowest layer of ML material, while two tests each were completed on a layer of sand from 4.2 to 4.49 m and a layer of sand from 5.25 to 6.33 m. The CRR curve for the shallower sand unit did not follow the observed slope of similar soil types (i.e., it is much steeper than was typically observed); the slope of the slightly deeper sand layer was more consistent with other units of similar soil type, however, the vertical position of the curve was much higher than all other tested sands. As previously noted, the CPT data for the LS-II site did not agree with the data from "undisturbed" sampling and laboratory testing so that in-situ estimations of D_r are not possible from q_{c1N} values; however, a possible explanation for the much higher interpreted liquefaction resistance of this soil layer could be that the specimens were significantly densified during sampling and specimen preparation.
- SA site (193 Armagh St.): Only one sand specimen was able to be obtained from the SA site due to the presence of stiff soils in the shallow subsurface (e.g., stiff sands and gravels). Therefore, no CRR curves were interpreted for this site. Furthermore, the q_{c1N} value for the single test shown in Figure B.7 was approximately 41, which is below the threshold for high quality sampling and testing of sands described previously (i.e., loose sands with $q_{c1N}<60$ were most likely disturbed during sampling and testing).

B.4 CSR VS. $N_{C\text{-}3\%\ S.A.\varepsilon}$ FOR VARIOUS SOIL TYPES

To supplement the results of CTX testing presented in Chapter 4, Figure B.8 through Figure B.12 provide plots of CSR vs. $N_{c\text{-}3\%\ S.A.\varepsilon}$ for the various soil types tested from the Christchurch CBD. Each data point is labelled to provide information regarding the tested specimens, similar to the information described in Section B.3. Figure B.8 to Figure B.10 provide plots of CSR vs. $N_{c\text{-}3\%\ S.A.\varepsilon}$ for all sand specimens (SP and SP-SM); each of these figures presents the same data but with different data labels provided for different the ranges of q_{c1N} values. Also shown are the interpreted CRR curves using a power function fit. As was discussed in Chapters 3 and 4, the CRR values for the very loose to loose sand specimens ($q_{c1N}<60$) plot above the denser sand specimens, which implies a higher liquefaction resistance for these loose sands. This higher

implied resistance coupled with the larger spread of CRR values for the loose sands when compared to the denser sands (i.e., do not display as good of a power function fit) suggests the loose sand specimens were significantly densified during sampling and specimen preparation. The data points that correspond to testing of sand specimens from the LS-II site are assumed to have $q_{c1N}<60$. It can be seen that the specimens tested from a depth of about 5.32 and 6.26 m at the LS-II site plot significantly above all the other data points, which most likely suggest that these specimens were significantly densified.

Figure B.11 provides a plot of CSR vs. $N_{c\text{-}3\%\ S.A.\varepsilon}$ for all silty sand (SM) soil specimens. The interpreted q_{c1N} for these specimens ranged from 17 to 35. Unlike the cleaner sands, the interpreted CRR curve from CTX testing of SM specimens shows a clear trend that agrees with the expected power regression fit. Figure B.12 shows a plot of CSR vs. $N_{c\text{-}3\%\ S.A.\varepsilon}$ for all silt specimens. It can be seen that there is considerably more scatter around the interpreted CRR curve for the ML specimens when compared to the medium dense sands and silty sands. Further CTX testing of "undisturbed" silts from the CBD would be warranted to supplement the data presented in Figure B.12, especially at lower values of CSR to extend the CRR curve to higher values of N_c.

Figure B.8 to Figure B.12 contain shading of labels to indicate specimens that originated from D&M samples that were sampled using drilling mud (labelled as "Sampled using mud to advance D&M sampler"). The reason for this identification is to differentiate specimens that were obtained using either of the following two set-ups for the D&M sampler: 1) after drilling to a specific sample depth using mud-rotary techniques, the D&M sampler was lowered to the bottom of the borehole using different rods than the rods used during drilling and advanced using fresh water with a different pump from the pump used to circulate drilling mud (referred to hereafter as set-up 1), and 2) after drilling to a specific sample depth using mud-rotary techniques, the D&M sampler was lowered to the bottom of the borehole using the same rods used during the drilling process and advanced using drilling mud and the same pump used to circulate the drilling mud (referred to hereafter as set-up 2). The specimens labelled with shading correspond to the latter of these two set-ups. Set-up 1 was used during the beginning phases of sampling, while set-up 2 was used during the latter phases of sampling. The differentiation between the two sampling techniques was originally made due to a suspicion that set-up 1 may have been leading to further disturbance of soil specimens compared to set-up 2; however, after examining the CTX test results, this was shown to not be the case. This differentiation is provided for reference purposes.

B.5 CSR VS. $N_{C\text{-}3\%\ S.A.\varepsilon}$ FOR VARIOUS SOIL TYPES WITH CPT-BASED TRIGGERING CORRELATIONS

Figure B.13 to Figure B.15 presents similar data discussed in Section B.4 with the addition of CRR curves interpreted from two CPT-based liquefaction triggering procedures: the Boulanger and Idriss (2015) procedure (for P_L=50%; referred to as BI15) and the Robertson and Wride (1998) procedure (RW98). The RW98 procedure is only used for a FC ≤ 35 as this corresponds to an $I_c \leq 2.6$, which is recommended as the maximum soil behavior type index for using the RW98 procedure to evaluate liquefaction triggering. As these procedures are used to estimate the $CRR_{M7.5,\ 1atm}$ for a given q_{c1Ncs} value. To convert these CRR values to various N_c values, the

relationship proposed by Idriss (1999) was used to convert various earthquake magnitudes to equivalent number of stress cycles (N_c). The magnitude scaling factor (MSF) proposed by Boulanger and Idriss (2014) was then used to convert $CRR_{M7.5}$ to CRR for a given magnitude/N_c value (i.e., $CRR_{M\neq7.5}=CRR_{M7.5}$*MSF) for both triggering procedures. The CSR values from CTX testing were converted to field conditions using the following factors of C_r' (so that $CSR_{Field}=CSR_{CTX}\cdot C_r$'): 0.57 for SP and SP-SM soils, 0.6 for SM soils, and 0.66 for ML soils. A range of q_{c1N} (BI15) and Q_{tn} (RW98) and FC values were used to generate the CRR curves shown in Figure B.13 to Figure B.15 to compare to the CRR curves interpreted from CTX testing.

Also shown in Figure B.13 to Figure B.15 are ranges of potential CSR values from the three largest events of the 2010-11 Canterbury earthquake sequence (M_w7.1 Darfield, M_w6.2 Christchurch, and 13 JUN 2011 M_w6.0 events). CSR values were calculated for these events using the equation

$$CSR = 0.65 * PGA * \left(\frac{\sigma_v}{\sigma_v'}\right) * r_d \quad \text{(B.1)}$$

A peak ground acceleration (PGA) of 0.21, 0.50, and 0.22 g was used for the Darfield, Christchurch, and 13 JUN 2011 M_w6.0 events, respectively; these PGA values are representative of the level of shaken experienced in the CBD of Christchurch for these events. Three values of overburden effective stress were chosen that corresponded to the approximate range and average effective confining pressure used during CTX testing: 38, 119, and 210 kPa. The groundwater table (GWT) was assumed to be 2 m. The shear stress reduction factor, r_d, was calculated based on the expression provided by Idriss (1999), which depends on both the depth and the earthquake magnitude. Depths were back calculated from the three values of σ'_v by assuming a total unit weight of soil (γ_T) of 17.3 kN/m^3 and 19.6 kN/m^3 for soil above and below the GWT, respectively.

The ranges of CSR for the three largest events of the Canterbury earthquakes are provided to illustrate the demand witnessed by each of the events; they do not necessarily represent all possible seismically-induced stresses in the CBD of Christchurch. One noticeable detail of the CSR values shown is the significantly larger applied stresses witnessed during the Christchurch event compared to both the Darfield and 13 JUN 2011 events, which is due to the PGA of the Christchurch event being more than double (on average) that of the other two events. Also apparent is the similarity of CSR for the Darfield and 13 JUN 2011 M_w6.0 events, which is due to these two events having similar shaking intensities; however, since the Darfield event has a larger magnitude, the equivalent number of applied uniform stress cycles is considerably higher when compared to the 13 JUN 2011 event.

.

B.6 VOLUMETRIC STRAINS FROM POST-LIQUEFACTION RECONSOLIDATION TESTS

As discussed in Section B.2, post-liquefaction reconsolidation tests were carried out on several specimens following the completion of CTX testing. These were completed by allowing the specimens to drain and return to the initial effective consolidation pressure after cyclic loading. Figure B.16 provides a plot of the volumetric strain achieved during reconsolidation ($\varepsilon_{vol\text{-}rec}$) versus the maximum shear strain achieved during CTX testing ($\gamma_{max\text{-}CTX}$) for all post-liquefaction reconsolidation tests. There is not necessarily a noticeable trend in Figure B.16; however, when results are plotted separately for specimens above and below the I_c=2.05 threshold (I_c is the soil behavior type index proposed by Robertson and Wride, 1998) a positive trend of $\varepsilon_{vol\text{-}rec}$ with increasing $\gamma_{max\text{-}CTX}$ is noticed in the more silt-like soil specimens (I_c>2.05), which is shown in Figure B.17. This trend is not necessarily shown for the sand-like specimens (I_c<2.05) in Figure B.18. Sancio (2003) reported a similar positive trend of $\varepsilon_{vol\text{-}rec}$ with increasing $\gamma_{max\text{-}CTX}$ for silty and clayey soils tested from Adapazari, Turkey.

B.7 I_C AND FC FOR CTX SPECIMENS

Figure B.19 examines the relationship between I_c and FC for the triaxial specimens tested from the Christchurch CBD. Also included in this plot is data from previous studies completed by Merrick Taylor (Univ. of Canterbury) and Josh Zupan (Univ. of California, Berkeley) following the Canterbury earthquakes; these data were shared via personal communication by Josh Zupan. The data between both studies compares relatively well. The values of I_c are slightly higher on average for the cleaner sands (FC≤12%) for the data obtained in this study when compared to the Zupan and Taylor data; furthermore, the Zupan and Taylor study has more data in the FC>12% range when compared to the data from this study. A regression of the Zupan and Taylor data is provided, which is described by the equation $FC = (0.125 \cdot I_c)^8 - 10$. When the data for both studies is used to regress FC against I_c using the functional form

$$FC = 80 * \left(I_c + C_{fc}\right) - 137 \tag{B.2}$$

suggested by Boulanger and Idriss (2014), a C_{fc} = 0.07 was found. Equation B.2 is plotted in Figure B.19, both with a C_{fc} value of 0.07 and 0. Also plotted are the correlations proposed by Robertson and Wride (1998) for comparison purposes.

Figure B.20 shows a plot of I_c vs. FC for the data compiled from the study presented in this dissertation. These data are plotted with the correlation proposed by Robinson et al. (2013), which follows the following functional form:

$$FC = 47.53 * I_c - 60.56 \pm \sigma \geq 20 \tag{B.3}$$

where σ = 23%. The CBD data for the most part plots within +/- one standard deviation of the median correlation from Robinson et al. (2013); however, as this correlation is restricted to FC≥20%, it cannot be compared to the low fines content sands tested from the CBD as a part of

this study. Figure B.21 to Figure B.27 provide plots similar to Figure B.20 but on a site-by-site basis.

B.8 D_r AND q_{c1Ncs} FOR CTX SPECIMENS

Chapter 3 provided a discussion regarding the comparison of relative density (D_r) of triaxial specimens compared to D_r obtained from CPT-based correlations. CPT data for each triaxial specimen was examined using adjacent CPT investigations over the depth of each specimen, as previously discussed. Figure B.28 shows D_r of all triaxial specimens tested in this study plotted against q_{c1Ncs}, while Figure B.29 to Figure B.35 shows similar plots on a site-by-site basis. Also provided are four correlations of D_r calculated from q_{c1Ncs}. It can be seen that in general, the Baldi et al. (1986) correlation plots higher than the other three correlations (Jamiolkowski et al. 2001, Salgado et al. 1997, and Kulhawy and Mayne 1990) and is in better agreement with the data compiled as a part of this study. As discussed in Chapter 3, specimens with $q_{c1Ncs} < 80$ plot above even the Baldi et al. (1986), which suggests that these soils were potentially densified during the sampling and specimen preparation procedures.

Table B.1: CTX Specimen Data and Information

Site	Bore Name	Samp. No.	Spec. Depth (m)	σ'_c[1] (kPa)	e_{con}[2]	CSR[3]	N_c 3% S.A.[4]	N_c 5% D.A.[5]	G_s[6]	PI[7] (%)	FC[8] (%)	USCS[9]	$I_{c\text{-}10}$ ave	$q_{c1N\text{-}11}$ ave	K_σ[12]	D_r (%)	e_{min}	e_{max}
86-100 Kil. St	DM BH1	3U	3.07	54.7	0.718	0.316	6	11	2.69	4	72.1	ML	2.34	26.3	1.06	--	--	--
86-100 Kil. St	DM BH1	3U	3.23	64.9	0.767	0.356	4	6.5	2.7	--	--	--	2.11	35.9	1.04	--	--	--
86-100 Kil. St	DM BH1	4U	3.67	58.0	0.804	0.269	9	14	2.69	4	79.7	ML	2.06	36.1	1.06	--	--	--
86-100 Kil. St	DM BH1	5U	4.27	51.0	0.774	0.365	6	8	2.69	NP	5.9	SP-SM	1.79	92.5	1.07	76	0.660	1.138
86-100 Kil. St	DM BH1	5U	4.43	49.3	0.757	0.289	15	21	2.67	NP	7	SP-SM	1.81	95.9	1.07	77	0.645	1.133
86-100 Kil. St	DM BH2	4U	14.23	116.6	0.732	0.364	7	9	2.67	NP	5.7	SP-SM	1.81	127.9	0.98	74	0.611	1.075
86-100 Kil. St	DM BH2	5U	14.86	123.1	0.736	0.319	9	10	2.7	NP	8.5	SP-SM	1.93	111.4	0.98	73	0.608	1.086
86-100 Kil. St	DM BH2	6U	15.36	126.0	0.755	0.276	9	11	2.69	NP	5.2	SP-SM	2.01	91.9	0.98	73	0.629	1.096
86-100 Kil. St	DM BH2	6U	15.51	126.0	0.746	0.214	69	72	2.68	NP	3.8	SP	2.02	95.9	0.98	71	0.620	1.061
151 Kil. St	DM BH1	2U	2.57	55.9	0.779	0.302	17	19	2.69	3	72	ML	2.40	18.9	1.05	--	--	--
151 Kil. St	DM BH1	2U	2.72	54.3	0.782	0.371	13	15	2.68	3	65	ML	2.28	22.3	1.05	--	--	--
151 Kil. St	DM BH1	3U	3.57	60.9	0.690	0.390	3	6	2.71	5	93	CL-ML	2.45	29.0	1.05	--	--	--
151 Kil. St	DM BH1	3U	3.72	61.6	0.670	0.296	17	25	2.75	2	--	ML	2.43	31.1	1.05	--	--	--
151 Kil. St	DM BH1	4U	4.77	66.9	0.735	0.360	13	14	2.71	4	43.6	SM	2.22	34.0	1.04	--	--	--
151 Kil. St	DM BH1	4U	4.92	71.3	0.697	0.303	37	42.5	2.67	NP	28.8	SM	2.26	32.0	1.03	83	0.590	1.201
151 Kil. St	DM BH1	5U	5.57	74.8	0.781	0.439	1	2	2.66	NP	44.8	SM	2.26	34.9	1.03	74	0.607	1.279
151 Kil. St	DM BH1	7U	10.31	116.8	0.684	0.315	8	11	2.65	NP	2.9	SP	1.79	100.1	0.98	75	0.583	0.980

Site	Bore Name	Samp. No.	Spec. Depth (m)	σ'_c[1] (kPa)	e_{con}[2]	CSR[3]	N_c 3% S.A.[4]	N_c 5% D.A.[5]	G_s[6]	PI[7] (%)	FC[8] (%)	USCS[9]	$I_{c\text{-}10}$ ave	$q_{c1N\text{-}11}$ ave	K_σ[12]	D_r (%)	e_{min}	e_{max}
151 Kil. St	DM BH2	4U	5.88	84.7	0.759	0.304	14	16.5	2.68	NP	12	SP-SM	2.24	37.2	1.01	77	0.640	1.148
151 Kil. St	DM BH2	6U	6.38	86.8	0.832	0.354	2	3	2.7	--	--	--	2.35	31.9	1.01	--	--	--
151 Kil. St	DM BH2	7U	6.72	88.0	0.831	0.317	2	3	2.71	3	78.4	ML	2.60	19.1	1.01	--	--	--
151 Kil. St	DM BH2	11U	10.97	125.2	0.719	0.363	13	14.5	2.68	NP	4.4	SP	1.81	107.9	0.97	74	0.610	1.035
151 Kil. St	DM BH2	11U	11.11	126.2	0.697	0.420	3	4.5	2.68	NP	7.2	SP-SM	1.82	105.3	0.97	70	0.552	1.030
199 Arm. St	DM BH1	2U	2.82	72.6	0.866	0.392	1	1.5	2.73	NP	25.7	SM	2.34	26.7	1.03	--	--	--
199 Arm. St	DM BH1	2U	2.98	74.2	0.869	0.216	122	124	2.72	2	22.6	SM	2.31	27.1	1.02	--	--	--
199 Arm. St	DM BH1	3U	3.33	72.8	0.810	0.239	15	--	2.69	NP	22.3	SM	2.57	16.9	1.02	68	0.623	1.205
199 Arm. St	DM BH1	3U	3.48	72.9	0.745	0.271	>82	>87	2.67	NP	8.3	SP-SM	2.45	20.4	1.02	75	0.625	1.105
199 Arm. St	DM BH1	4U	3.82	74.3	0.723	0.387	6	10	2.68	NP	6	SP-SM	2.34	28.5	1.02	80	0.624	1.113
199 Arm. St	DM BH1	4U	3.98	74.6	0.701	0.354	12	18	2.69	NP	3.6	SP	2.23	34.0	1.02	83	0.625	1.063
199 Arm. St	DM BH1	7U	13.67	146.3	0.709	0.320	4	6	2.68	NP	7.7	SP-SM	2.09	79.8	0.96	--	--	--
119 Arm. St	DM BH1a	7U	14.27	197.3	0.748	0.285	6	9	2.67	NP	4.4	SP	2.03	61.9	0.95	80	0.655	1.120
119 Arm. St	DM BH1b	3U	12.82	182.2	0.794	0.347	2	3	2.68	NP	5.2	SP-SM	1.85	90.5	0.94	67	0.641	1.101
119 Arm. St	DM BH1b	5U	13.81	198.1	0.725	0.288	8	10.5	2.67	NP	4	SP	1.95	72.7	0.94	73	0.617	1.023
119 Arm. St	DM BH1b	6U	14.32	197.9	0.668*	0.264	26	29.5	2.67	NP	2.6	SP	1.90	80.3	0.94	79	0.584	0.988
119 Arm. St	DM BH1b	7U	14.57	204.2	0.782	0.266	7	9.5	2.69	NP	5.1	SP-SM	1.93	73.2	0.94	75	0.664	1.138
119 Arm. St	DM BH1b	7U	14.82	210.0	0.671	0.240	14	18	2.66	NP	3.6	SP	1.98	74.7	0.94	84	0.606	1.002

Site	Bore Name	Samp. No.	Spec. Depth (m)	σ'_c[1] (kPa)	e_{con}[2]	CSR[3]	N_c 3% S.A.[4]	N_c 5% D.A.[5]	G_s[6]	PI[7] (%)	FC[8] (%)	USCS[9]	$I_{c\text{-}10}$ ave	$q_{c1N\text{-}11}$ ave	K_σ[12]	D_r (%)	e_{min}	e_{max}
90 Arm. St	DM BH2	1U	7.44	99.2	0.735	0.371	8	10.5	2.69	NP	4.2	SP	1.80	106.6	1.00	82	0.651	1.113
90 Arm. St	DM BH2	2U	7.77	103.0	0.763	0.307	8	8.5	2.7	NP	4.5	SP	1.62	136.7	1.00	74	0.646	1.104
90 Arm. St	DM BH2	2U	7.92	105.2	0.735	0.251	49.5	47	2.69	NP	4.9	SP	1.67	135.3	0.99	80	0.645	1.103
90 Arm. St	DM BH2	5U	11.32	152.4	0.792	0.298	6	8	2.66	NP	11.7	SP-SM	2.22	40.4	0.97	72	0.640	1.175
90 Arm. St	DM BH2	10U	13.77	153.6	0.733	0.296	9	10.5	2.69	NP	5.3	SP-SM	1.81	86.0	0.96	76	0.625	1.083
48 Lis. St	DM BH1	1U	1.82	38.8	0.841	0.342	8	9.5	2.71	NP	94.7	ML	2.51+	22.0+	1.09	--	--	--
48 Lis. St	DM BH1	4U	4.27	57.0	0.749	0.355	8	9	2.67	NP	10.6	SP-SM	2.47+	23.7+	1.03	78	0.630	1.184
48 Lis. St	DM BH1	4U	4.42	60.0	0.714	0.302	12	12	2.67	NP	16.9	SM	2.54+	17.2+	1.03	78	0.590	1.147
48 Lis. St	DM BH1	5U	5.32	67.2	0.737	0.410	31	27.5	2.68	NP	4.8	SP	2.27+	33.1+	1.02	87	0.676	1.145
48 Lis. St	DM BH1	7U	6.26	72.6	0.698	0.480	6	5.5	2.67	NP	5.5	SP-SM	2.02+	59.9+	1.02	76	0.608	0.985
193/195 Pet. St	DM BH1	1U	1.82	37.6	0.777	0.349	10	11.5	2.68	NP	3.7	SP	2.32	40.9	1.06	73	0.656	1.097

1. Pressure for isotropic consolidation phase prior to triaxial test
2. Void ratio of specimen after consolidation (before triaxial test) ; reported to three decimal places for comparison purposes.
3. Cyclic stress ratio used for CTX test; CSR = $\sigma_d/(2\sigma'_c)$
4. Number of cycles to 3% single amplitude (S.A.) axial strain
5. Number of cycles to 5% double amplitude (D.A.) axial strain
6. Specific gravity of specimen's soil solids (ASTM D854-14)
7. Plasticity index of specimen's soil (ASTM D4318-10e1)
8. Fines content of specimen's soil (ASTM D422-63(07)e2)
9. Unified soil classification system for specimen's soil (ASTM D2487-11)
10. Average soil behavior type index (Robertson 2009); calculated using data from closest CPT investigation to borehole over height of specimen (nominal height = 14 cm)
11. Average normalized tip resistance (Boulanger and Idriss 2014); calculated using data from closest CPT investigation to borehole over height of specimen (nominal height = 14 cm)
12. K_σ calculated using relationship from Boulanger and Idriss (2014)

*There is error in the calculated void ratio prior to testing for the BH1b specimen at 14.32 m at 119 Armagh St., because correct weights of solids were not measured; instead it was estimated based on reasonable values from other specimens

+CPT data does not support borehole data for 48 Lismore St. and may not accurately represent the field conditions at the borehole location

Table B.2: Monotonic Triaxial Specimen Data and Information

Site	Boring Name	Sample No.	Spec. Depth (m)	σ'_c[1] (kPa)	e_{con}[2]	G_s[3]	PI[4] (%)	FC[5] (%)	USCS[6]	$I_{c\text{-}ave}$[7]	$q_{c1N\text{-}ave}$[8]	D_r	e_{min}	e_{max}
86-100 Kil. St	DM BH1	4U	3.83	55.3	0.758	2.67	4	68.4	ML	2.24	31.4	--	--	--
151 Kil. St	DM BH2	10U	10.37	120.8	0.791	2.71	NP	4.6	SP	1.81	105.2	68	0.652	1.091
90 Arm. St	DM BH2	10U	13.92	97.6	0.728	2.67	NP	8.1	SP-SM	1.73	97.6	74	0.601	1.096
48 Lis. St	DM BH1	2U	2.17	41.4	0.883	2.68	NP	30.9	SM	2.32[+]	30.6[+]	63	0.621	1.328

1. Pressure for isotropic consolidation phase prior to triaxial test
2. Void ratio of specimen after consolidation (before triaxial test); reported to three decimal places for comparison purposes.
3. Specific gravity of specimen's soil solids (ASTM D854-14)
4. Plasticity index of specimen's soil (ASTM D4318-10e1)
5. Fines content of specimen's soil (ASTM D422-63(07)e2)
6. Unified soil classification system for specimen's soil (ASTM D2487-11)
7. Average soil behavior type index (Robertson 2009); calculated using data from closest CPT investigation to borehole over height of specimen (nominal height = 14 cm)
8. Average normalized tip resistance (Boulanger and Idriss 2014); calculated using data from closest CPT investigation to borehole over height of specimen (nominal height = 14 cm)

[+]CPT data does not support borehole data for 48 Lismore St. and may not accurately represent the field conditions at the borehole location

Table B.3: Post-Liquefaction Test Summary and Data

Site	Boring Name	Samp No.	Spec Depth (m)	Post-Liq Test[1]	ε_{vol} Reconsol.[2] (%)	γ_{max} CTX[3] (%)
86-100 Kil. St	DM BH1	3U	3.07	--	--	--
86-100 Kil. St	DM BH1	3U	3.23	--	--	--
86-100 Kil. St	DM BH1	4U	3.67	--	--	--
86-100 Kil. St	DM BH1	5U	4.27	--	--	--
86-100 Kil. St	DM BH1	5U	4.43	--	--	--
86-100 Kil. St	DM BH2	4U	14.23	--	--	--
86-100 Kil. St	DM BH2	5U	14.86	--	--	--
86-100 Kil. St	DM BH2	6U	15.36	--	--	--
86-100 Kil. St	DM BH2	6U	15.51	Mono	--	--
151 Kil. St	DM BH1	2U	2.57	Recon	1.77	6.11
151 Kil. St	DM BH1	2U	2.72	Recon	1.71	5.88
151 Kil. St	DM BH1	3U	3.57	Recon	1.44	7.69
151 Kil. St	DM BH1	3U	3.72	Recon	1.76	6.89
151 Kil. St	DM BH1	4U	4.77	Recon	1.91	5.77
151 Kil. St	DM BH1	4U	4.92	Mono	--	--
151 Kil. St	DM BH1	5U	5.57	Mono	--	--
151 Kil. St	DM BH1	7U	10.31	Recon	1.36	6.57
151 Kil. St	DM BH2	4U	5.88	Mono	--	--
151 Kil. St	DM BH2	6U	6.38	Mono	--	--
151 Kil. St	DM BH2	7U	6.72	Recon	2.16	8.04
151 Kil. St	DM BH2	11U	10.97	Recon	1.57	5.22
151 Kil. St	DM BH2	11U	11.11	Mono	--	--
199 Arm. St	DM BH1	2U	2.82	--	--	--
199 Arm. St	DM BH1	2U	2.98	--	--	--
199 Arm. St	DM BH1	3U	3.33	--	--	--
199 Arm. St	DM BH1	3U	3.48	--	--	--
199 Arm. St	DM BH1	4U	3.82	--	--	--
199 Arm. St	DM BH1	4U	3.98	--	--	--
199 Arm. St	DM BH1	7U	13.67	--	--	--
119 Arm. St	DM BH1a	7U	14.27	Recon	1.81	7.37
119 Arm. St	DM BH1b	3U	12.82	Recon	1.5	10.64
119 Arm. St	DM BH1b	5U	13.81	Recon	1.33	6.96
119 Arm. St	DM BH1b	6U	14.32	Recon	1.46	6.59
119 Arm. St	DM BH1b	7U	14.57	Mono	--	--
119 Arm. St	DM BH1b	7U	14.82	Recon	1.56	6.52

Site	Boring Name	Samp No.	Spec Depth (m)	Post-Liq Test[1]	ε_{vol} Reconsol.[2] (%)	γ_{max} CTX[3] (%)
90 Arm. St	DM BH2	1U	7.44	Mono	--	--
90 Arm. St	DM BH2	2U	7.77	Recon	2.24	5.46
90 Arm. St	DM BH2	2U	7.92	Recon	2.1	5.00
90 Arm. St	DM BH2	5U	11.32	Recon	1.91	6.56
90 Arm. St	DM BH2	10U	13.77	Mono	--	--
48 Lis. St	DM BH1	1U	1.82	Recon	1.84	6.44
48 Lis. St	DM BH1	4U	4.27	Recon	1.54	5.45
48 Lis. St	DM BH1	4U	4.42	Mono	--	--
48 Lis. St	DM BH1	5U	5.32	Recon	1.32	4.58
48 Lis. St	DM BH1	7U	6.26	Recon	1.42	4.96
193/195 Pet. St	DM BH1	1U	1.82	Recon	1.32	6.33

1. Post-liquefaction test performed: reconsolidation (recon) or monotonic (mono)
2. Volumetric strain measured during post-liquefaction reconsolidation test
3. Maximum shear strain during CTX test ($\gamma_{max} = 1.5 \cdot \varepsilon_{ax\text{-}max}$)

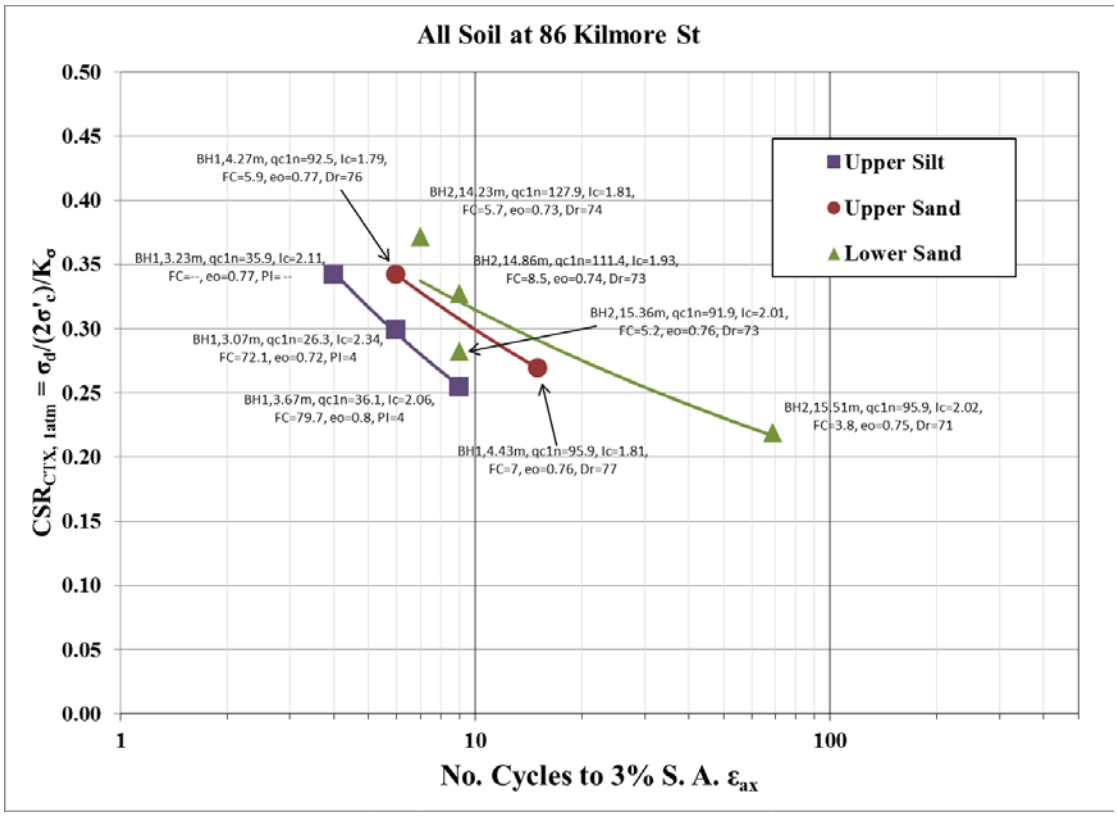

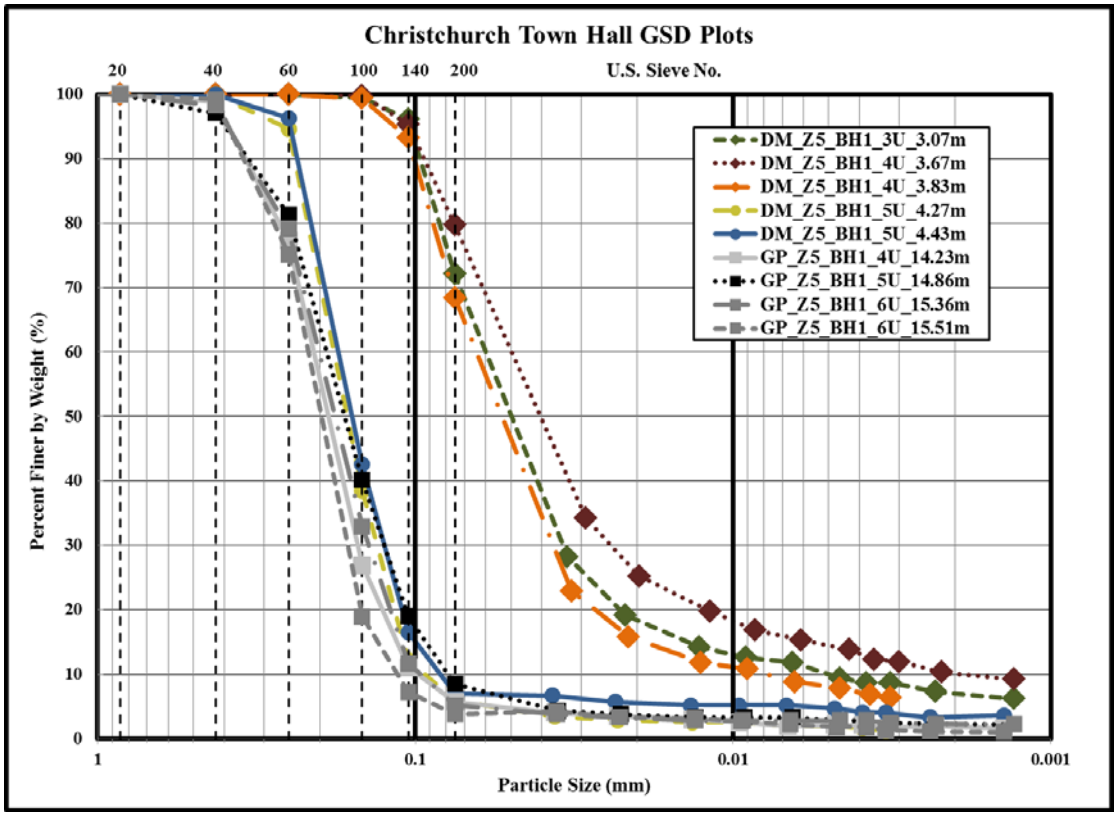

Figure B.1: CSR vs. $N_{c\text{-}3\%\ S.A.\varepsilon}$ and GSD plot for CTH site

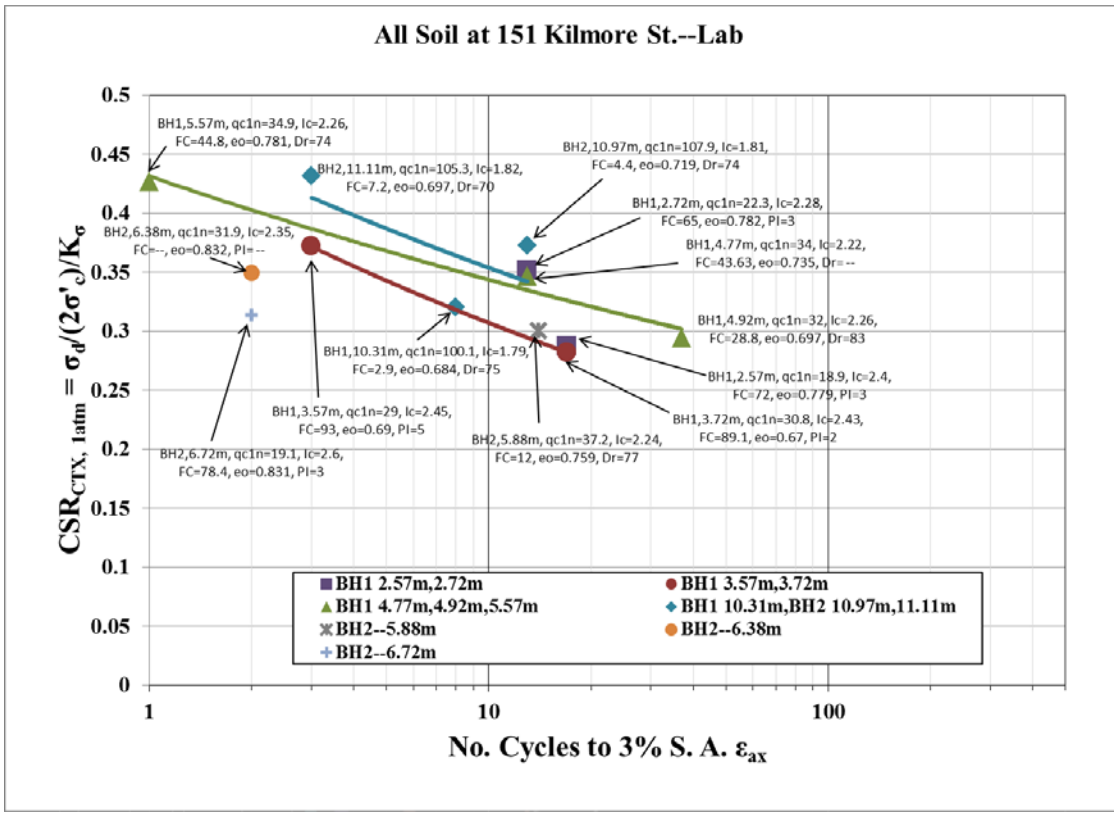

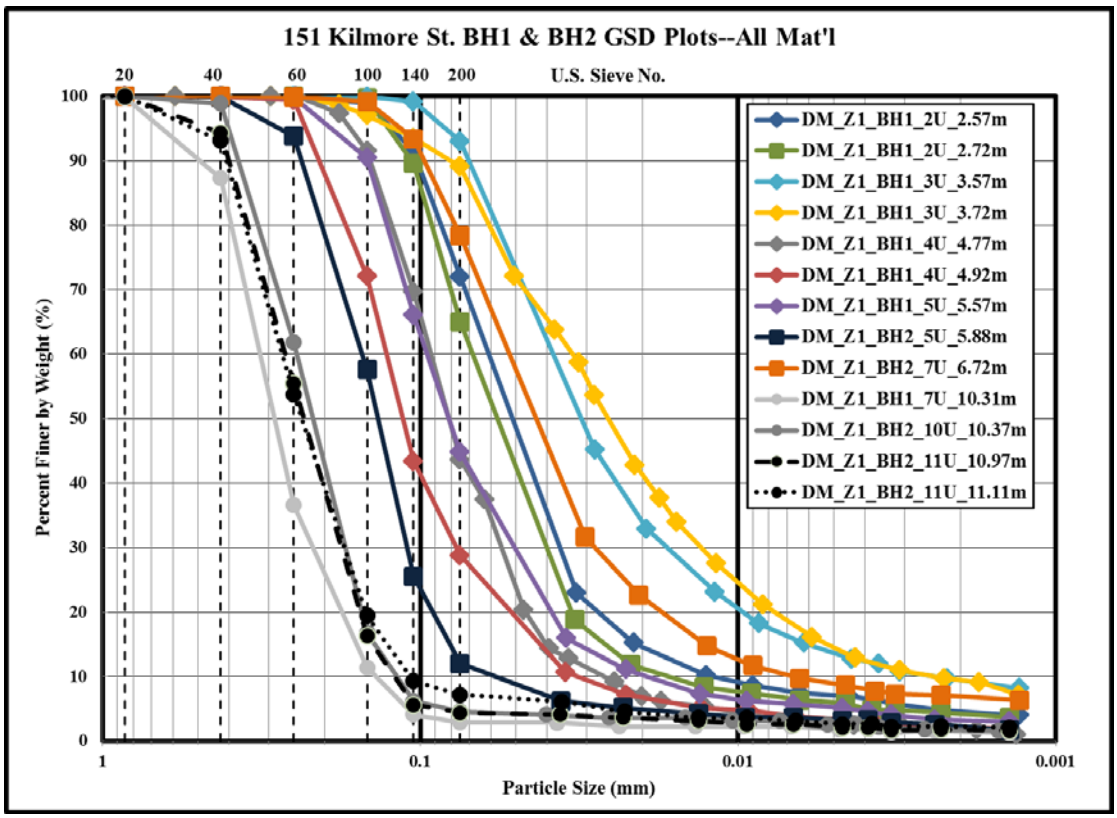

Figure B.2: CSR vs. $N_{c\text{-}3\%\ S.A.\varepsilon}$ and GSD plot for FTG-7 site

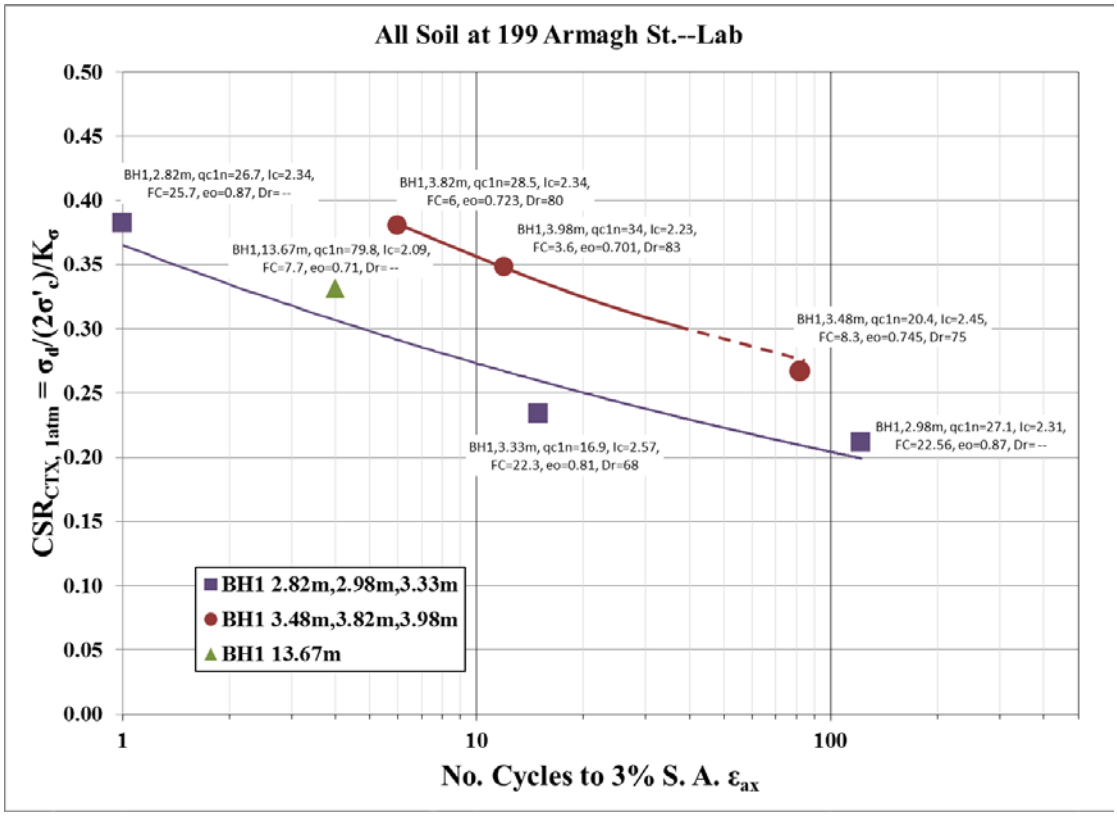

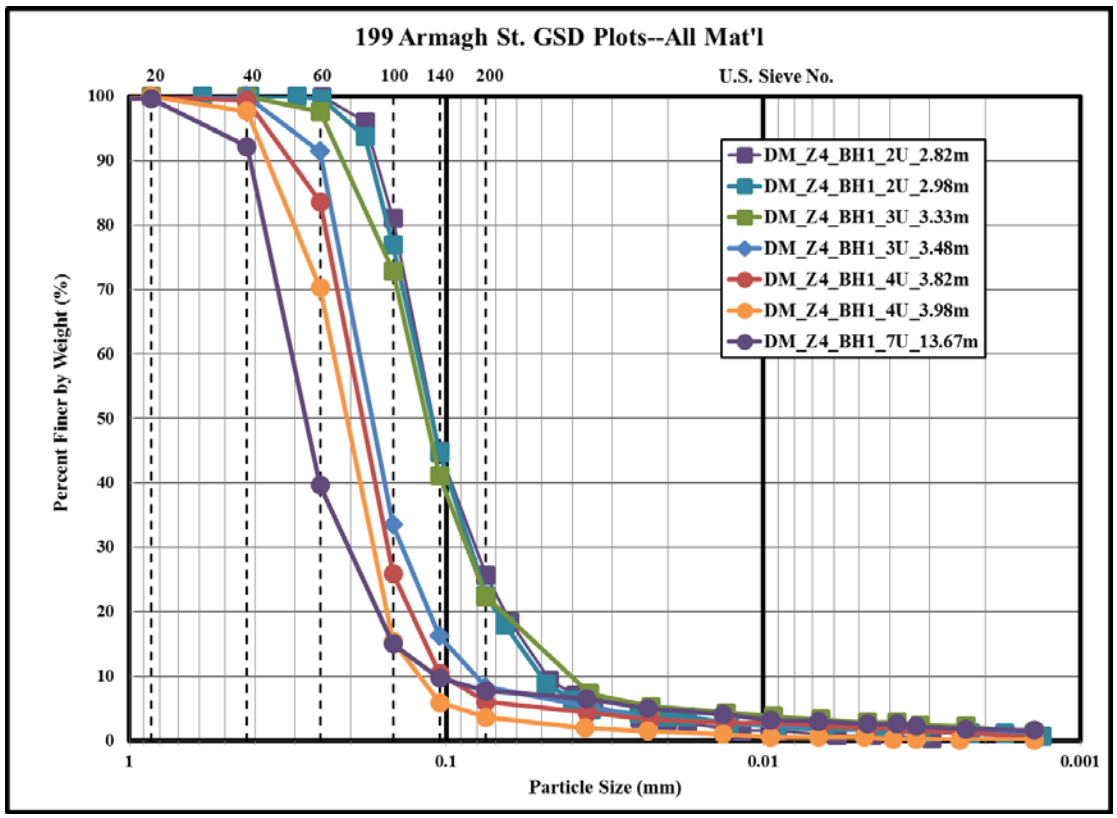

Figure B.3: CSR vs. $N_{c\text{-}3\%\ S.A.\varepsilon}$ and GSD plot for CTUC site

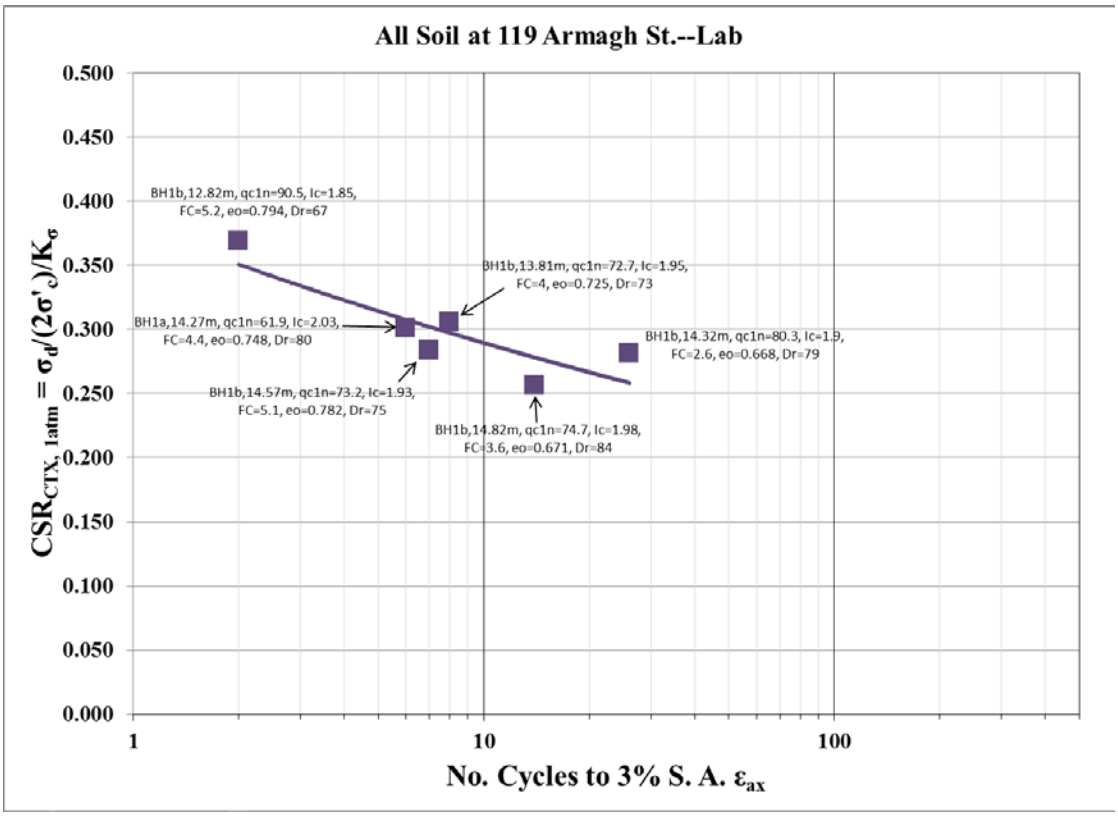

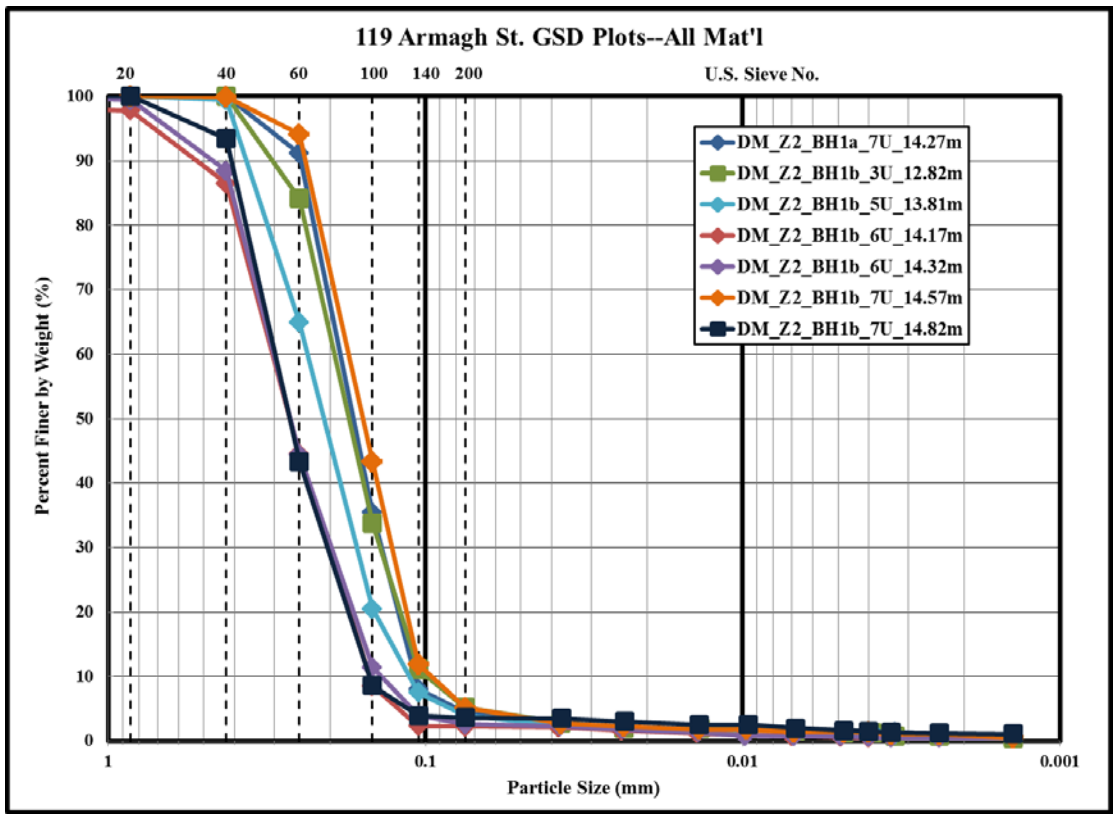

Figure B.4: CSR vs. $N_{c\text{-}3\%\ S.A.\varepsilon}$ and GSD plot for PWC site

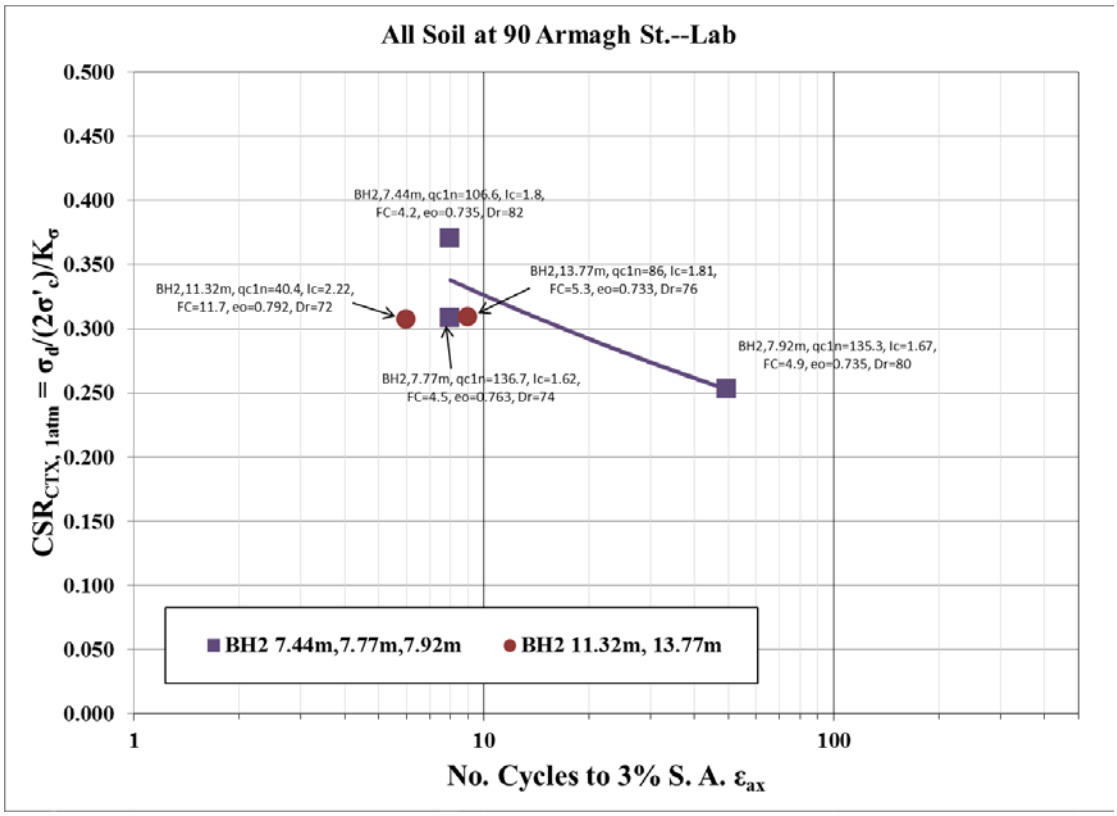

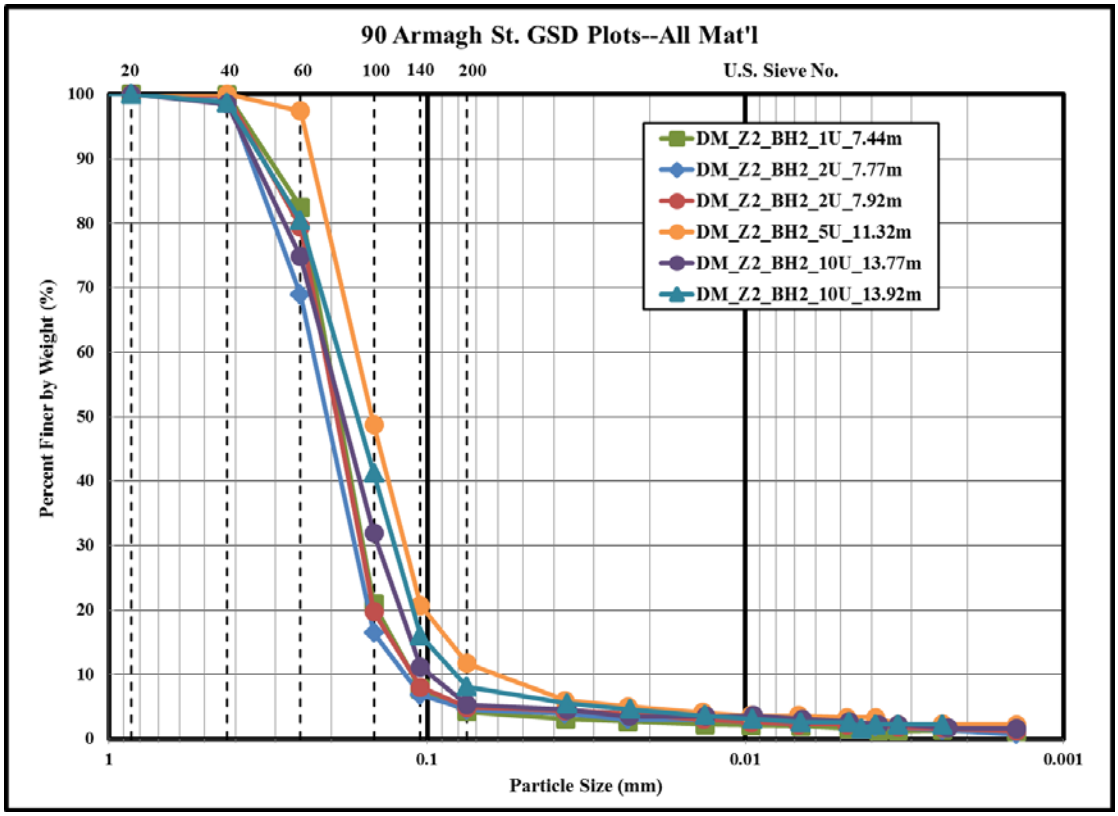

Figure B.5: CSR vs. $N_{c\text{-}3\%\ S.A.\varepsilon}$ and GSD plot for VT site

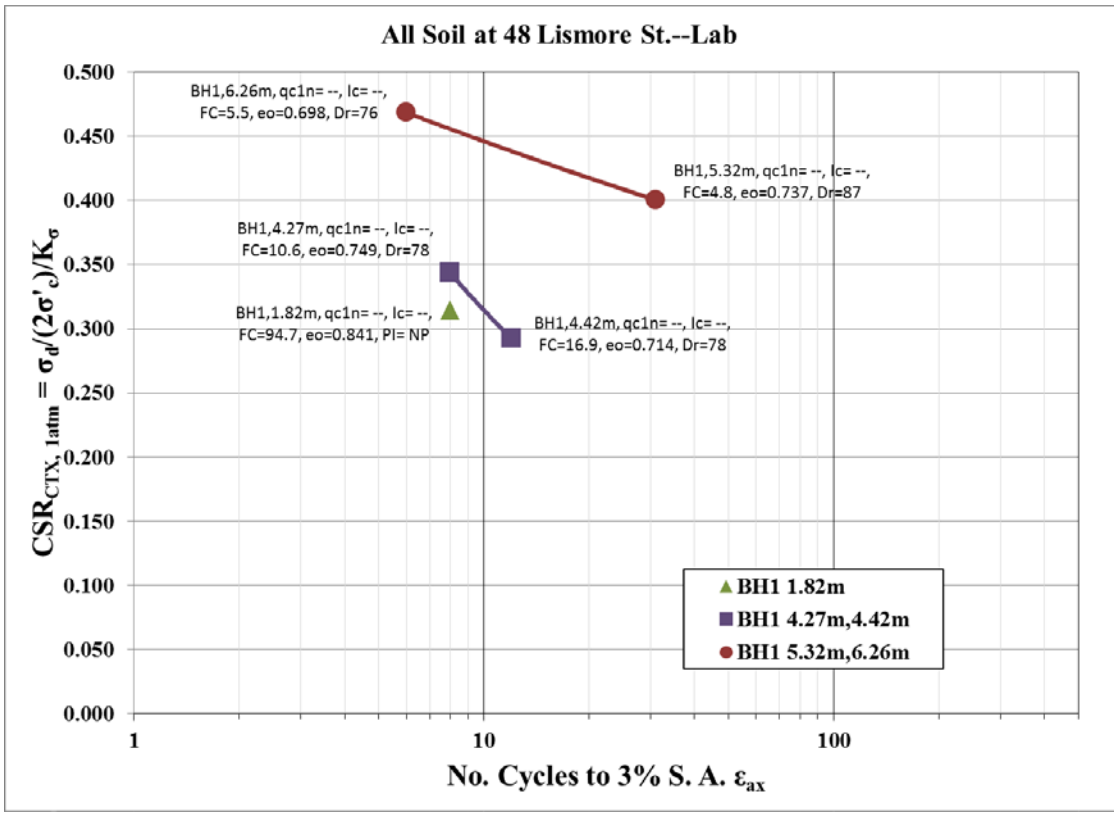

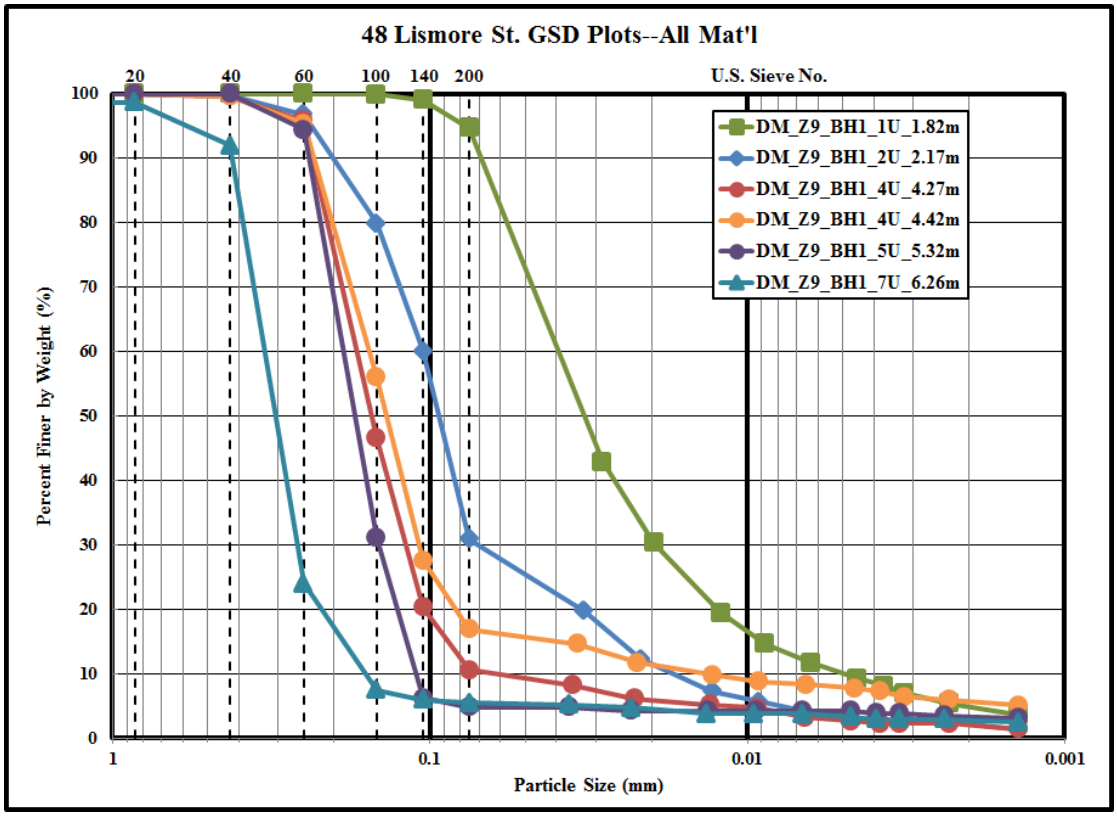

Figure B.6: CSR vs. $N_{c\text{-}3\%\ S.A.\varepsilon}$ and GSD plot for LS-II site

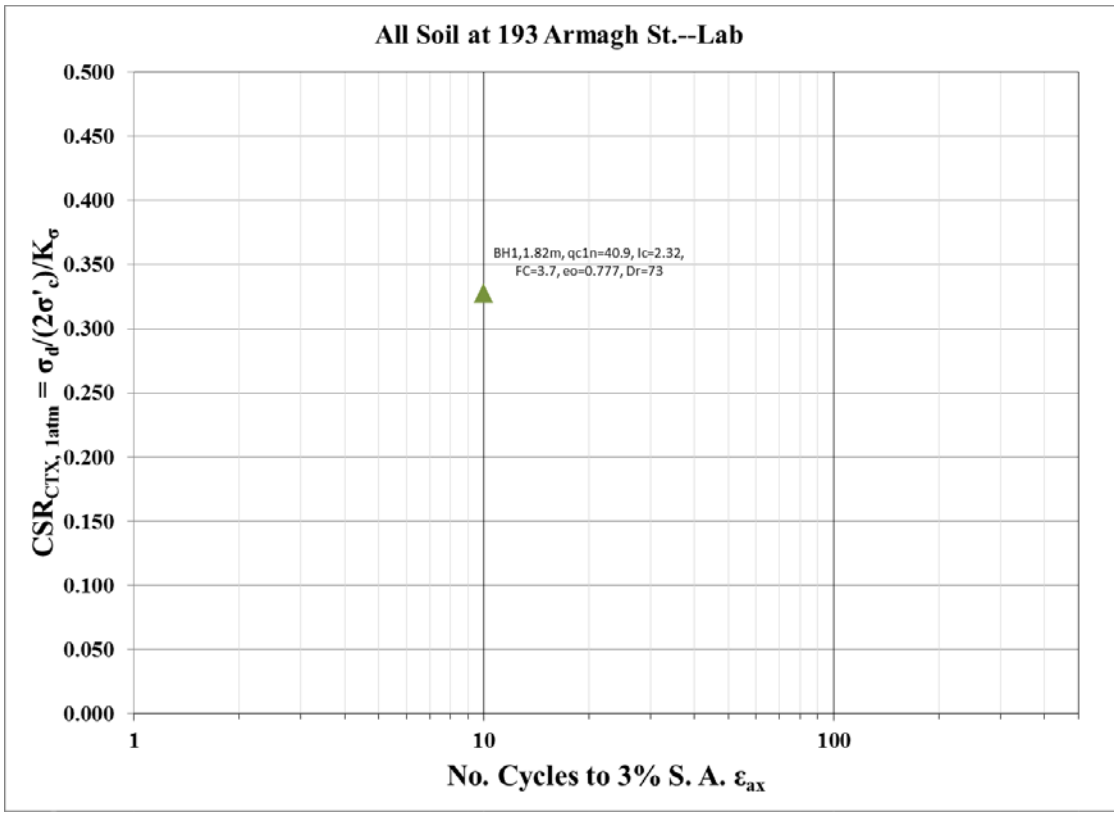

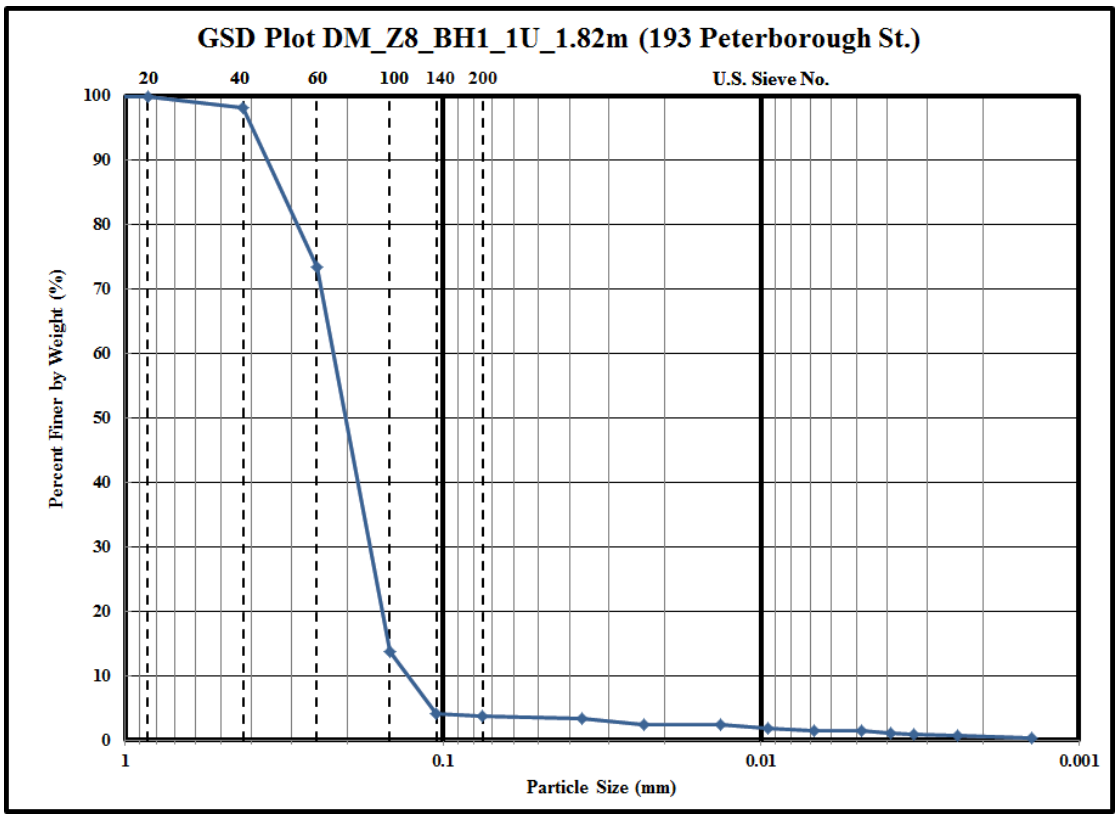

Figure B.7: CSR vs. $N_{c\text{-}3\%\ S.A.\varepsilon}$ and GSD plot for SA site

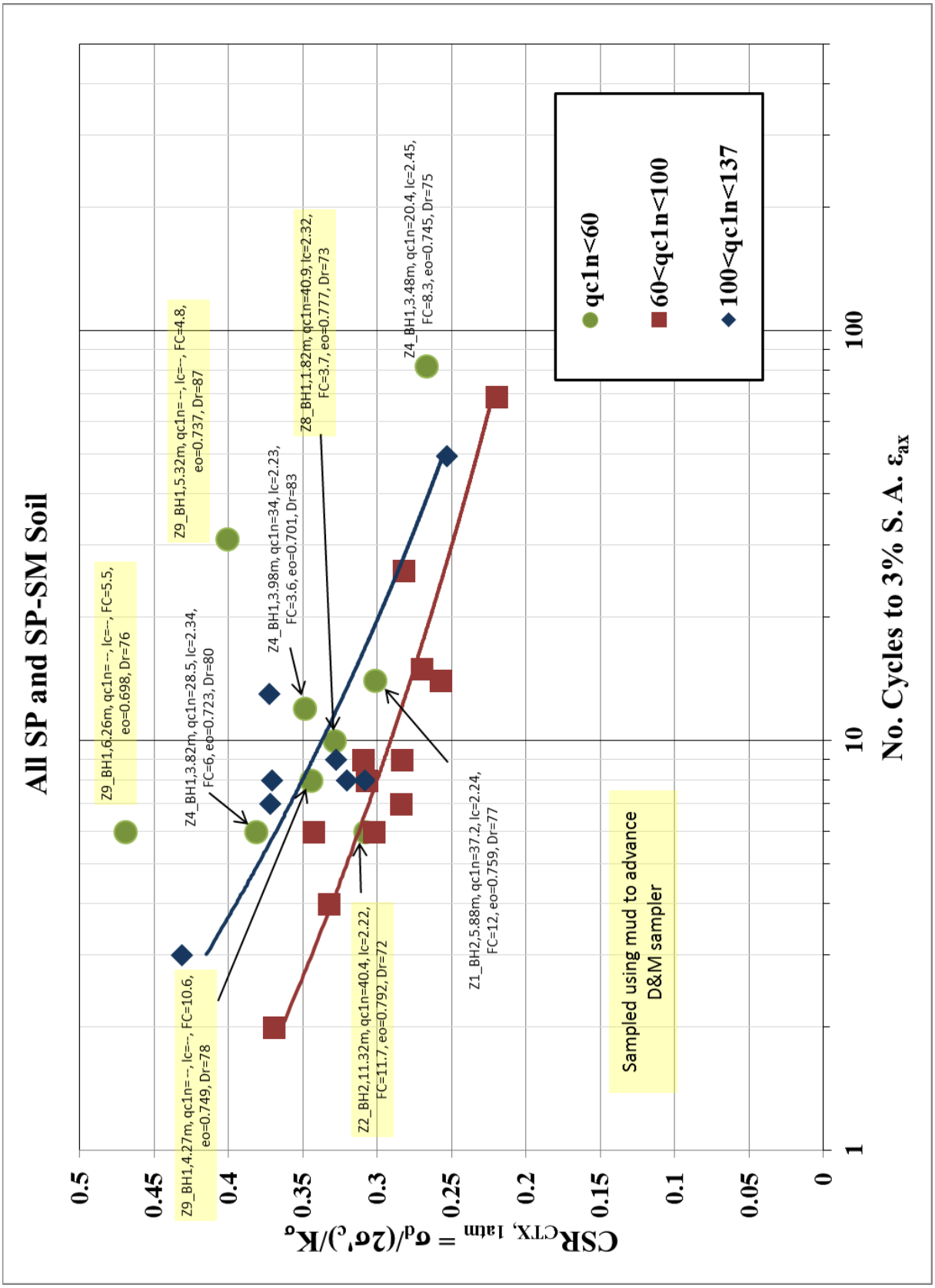

Figure B.8: CSR vs. $N_{c\text{-}3\%\ S.A.\varepsilon}$ for SP and SP-SM soils; specimens with q_{c1N}<60 labelled

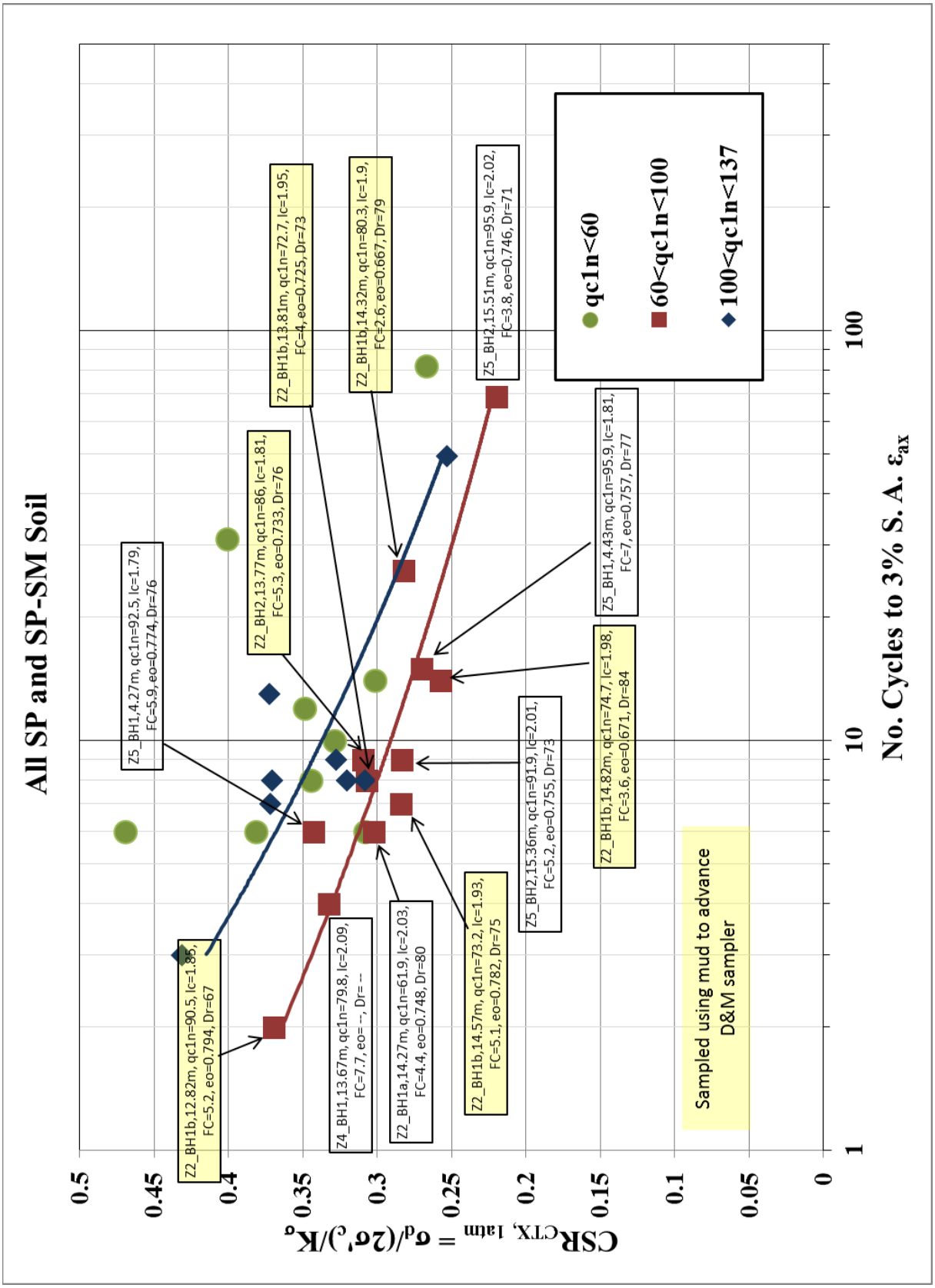

Figure B.9: CSR vs. $N_{c\text{-}3\%\ S.A.\varepsilon}$ for SP and SP-SM soils; specimens with $60<q_{c1N}<100$ labelled

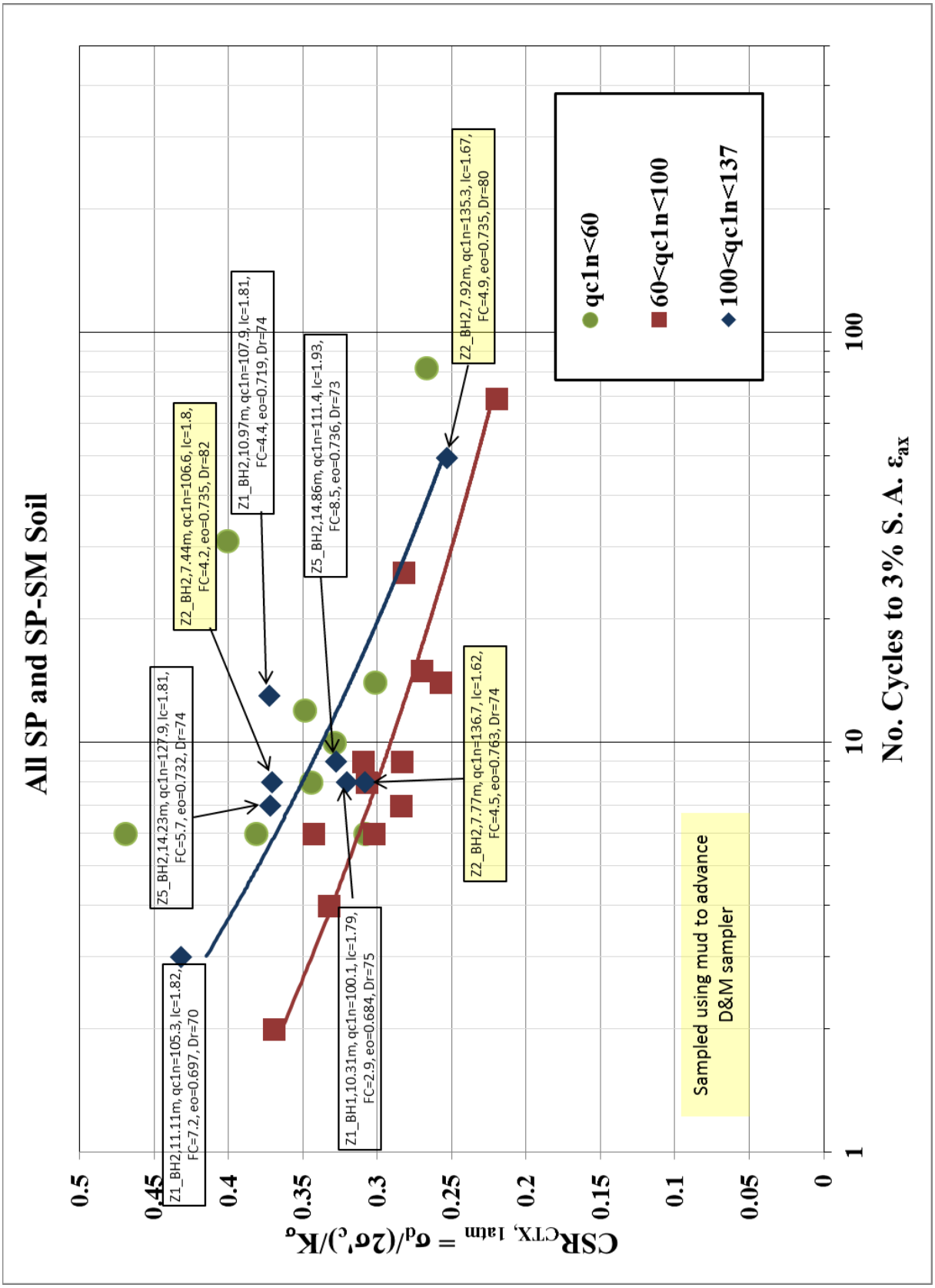

Figure B.10: CSR vs. $N_{c\text{-}3\%\ S.A.\varepsilon}$ for SP and SP-SM soils; specimens with $100<q_{c1N}<137$ labelled

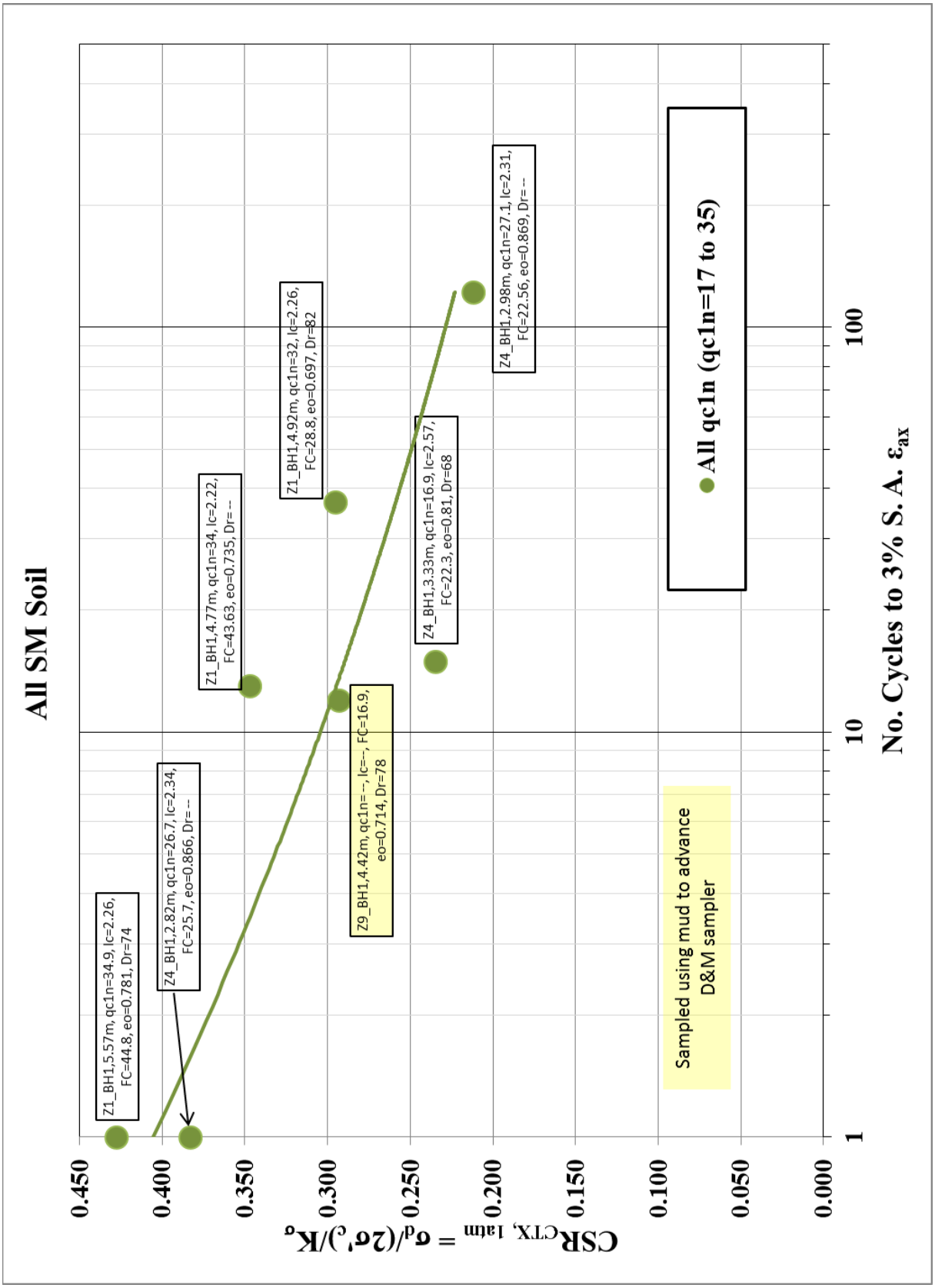

Figure B.11: CSR vs. $N_{c\text{-}3\%\ S.A.\varepsilon}$ for SM soil specimens

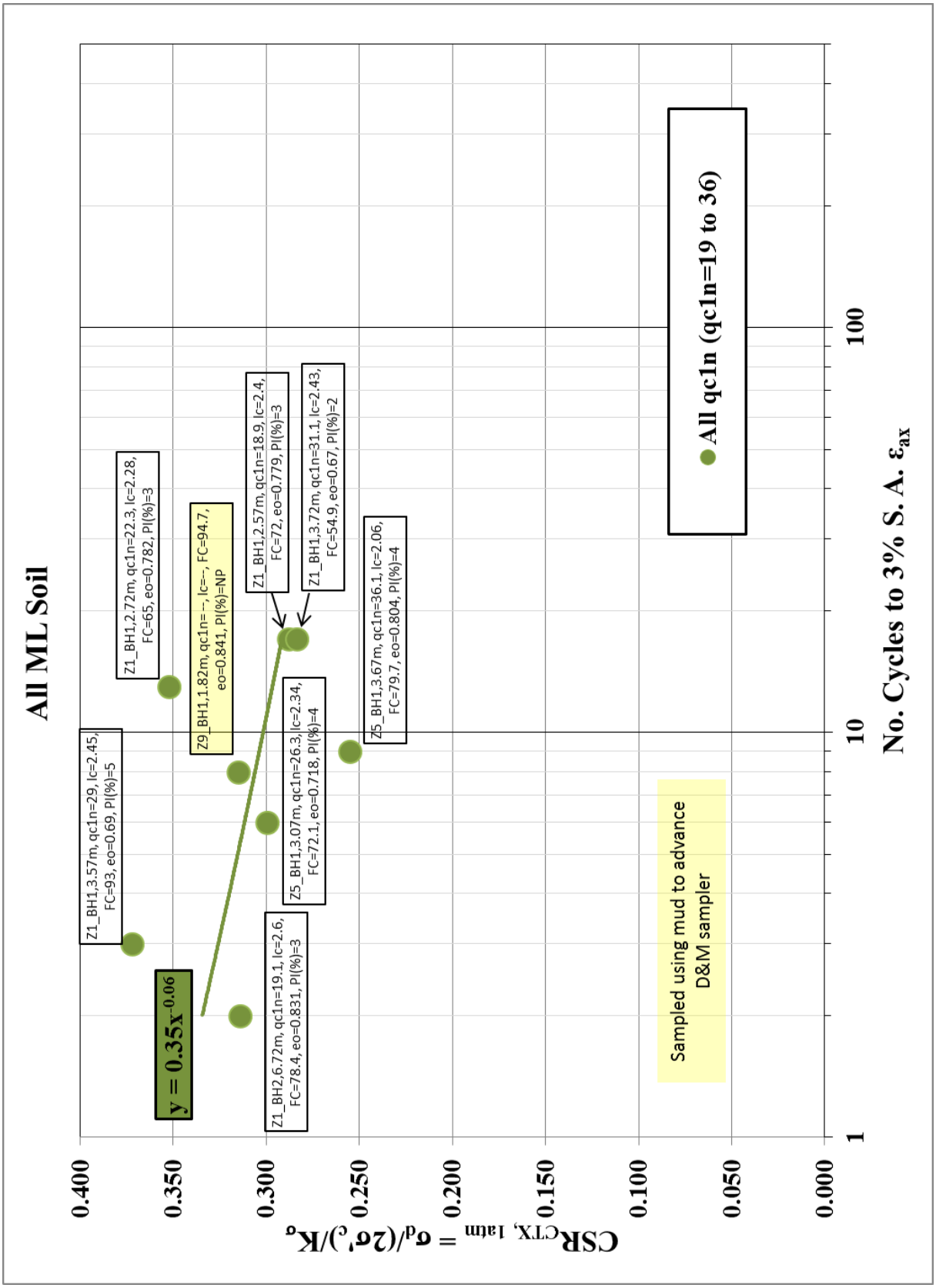

Figure B.12: CSR vs. $N_{c\text{-}3\%\ S.A.\varepsilon}$ for ML soil specimens

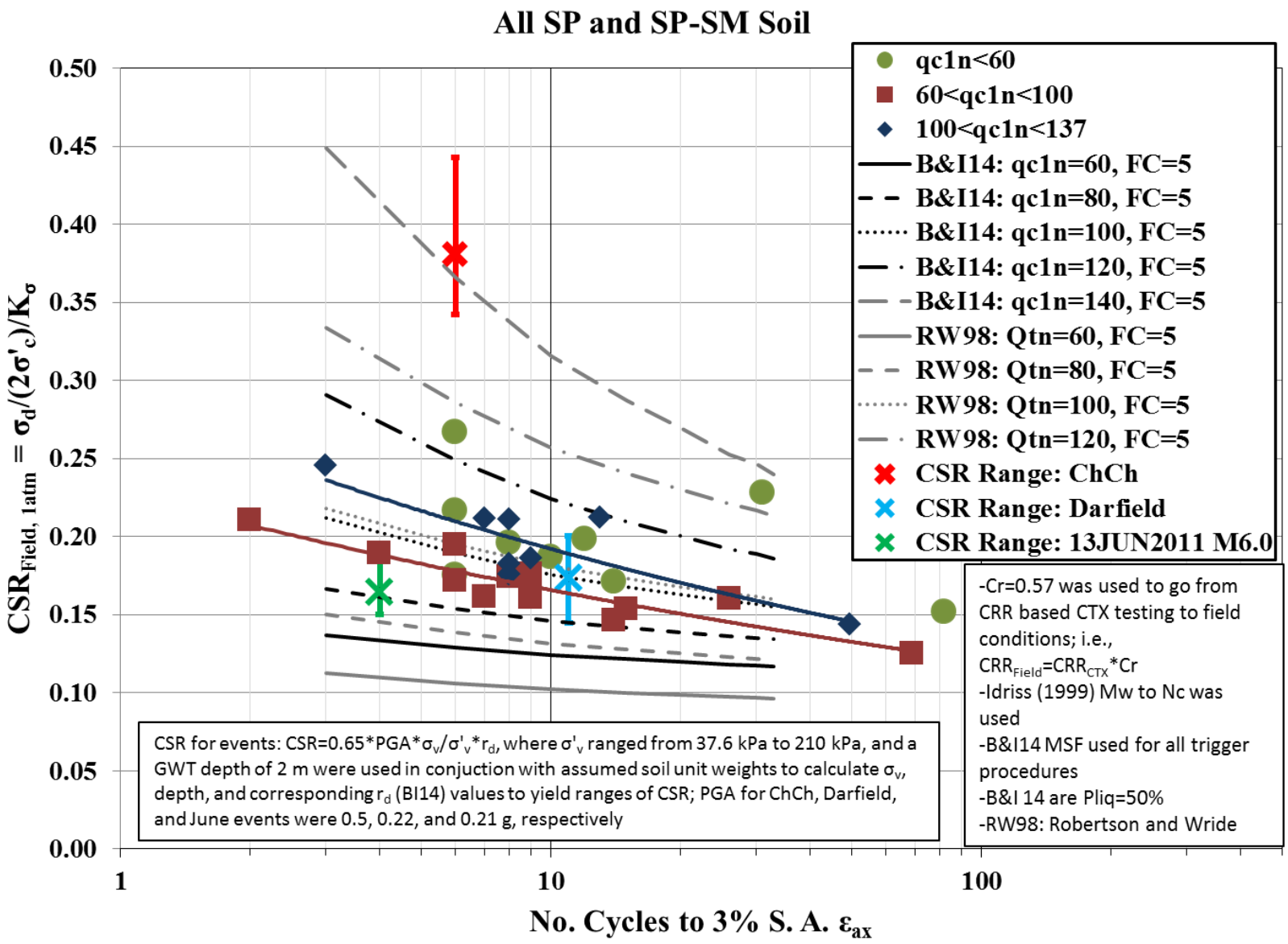

Figure B.13: CSR vs. $N_{c\text{-}3\%\ S.A.\varepsilon}$ for SP and SP-SM specimens with CPT-based liquefaction triggering correlation CRR curves

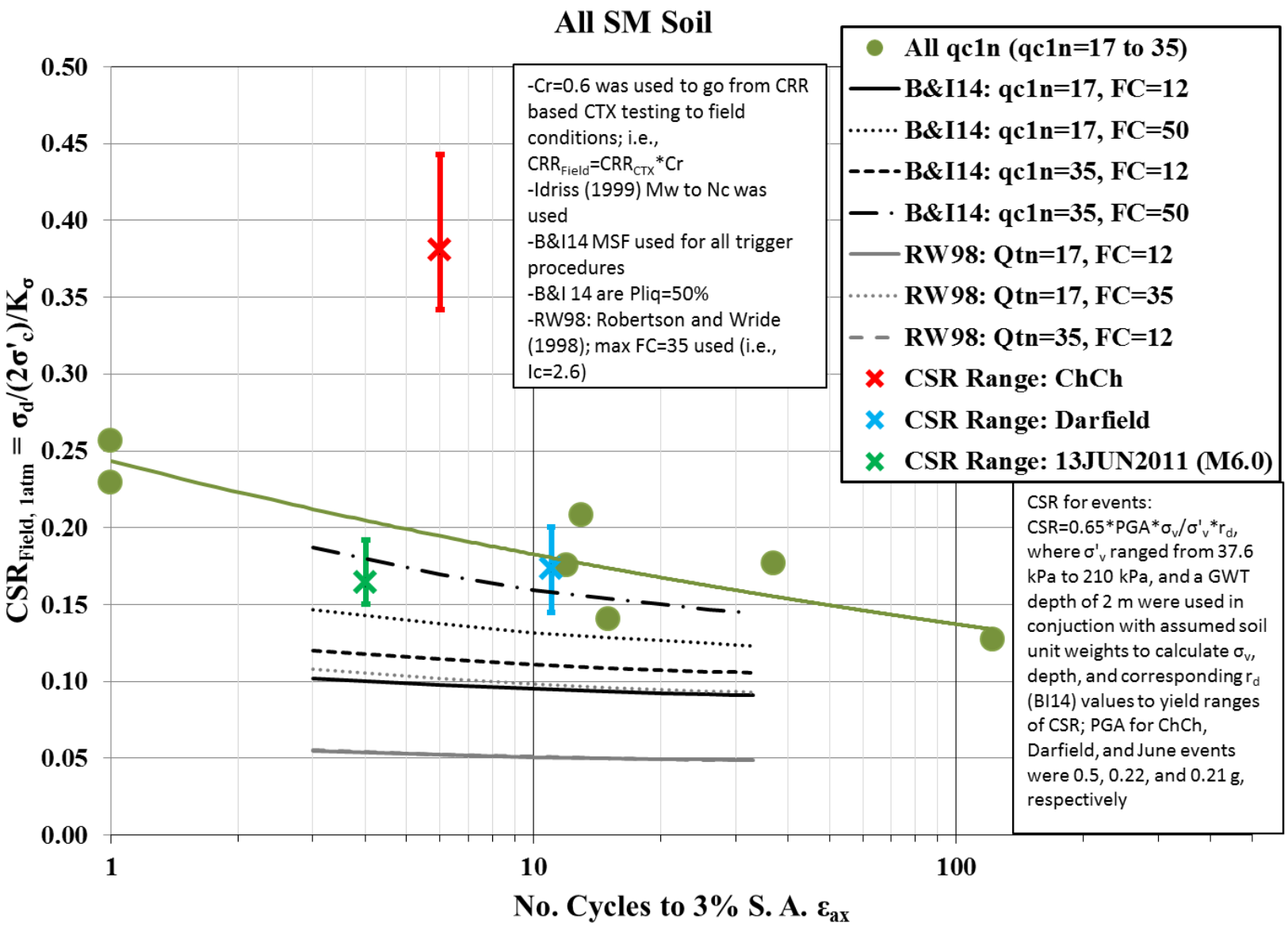

Figure B.14: CSR vs. $N_{c\text{-}3\%\ S.A.\varepsilon}$ for SM specimens with CPT-based liquefaction triggering correlation CRR curves

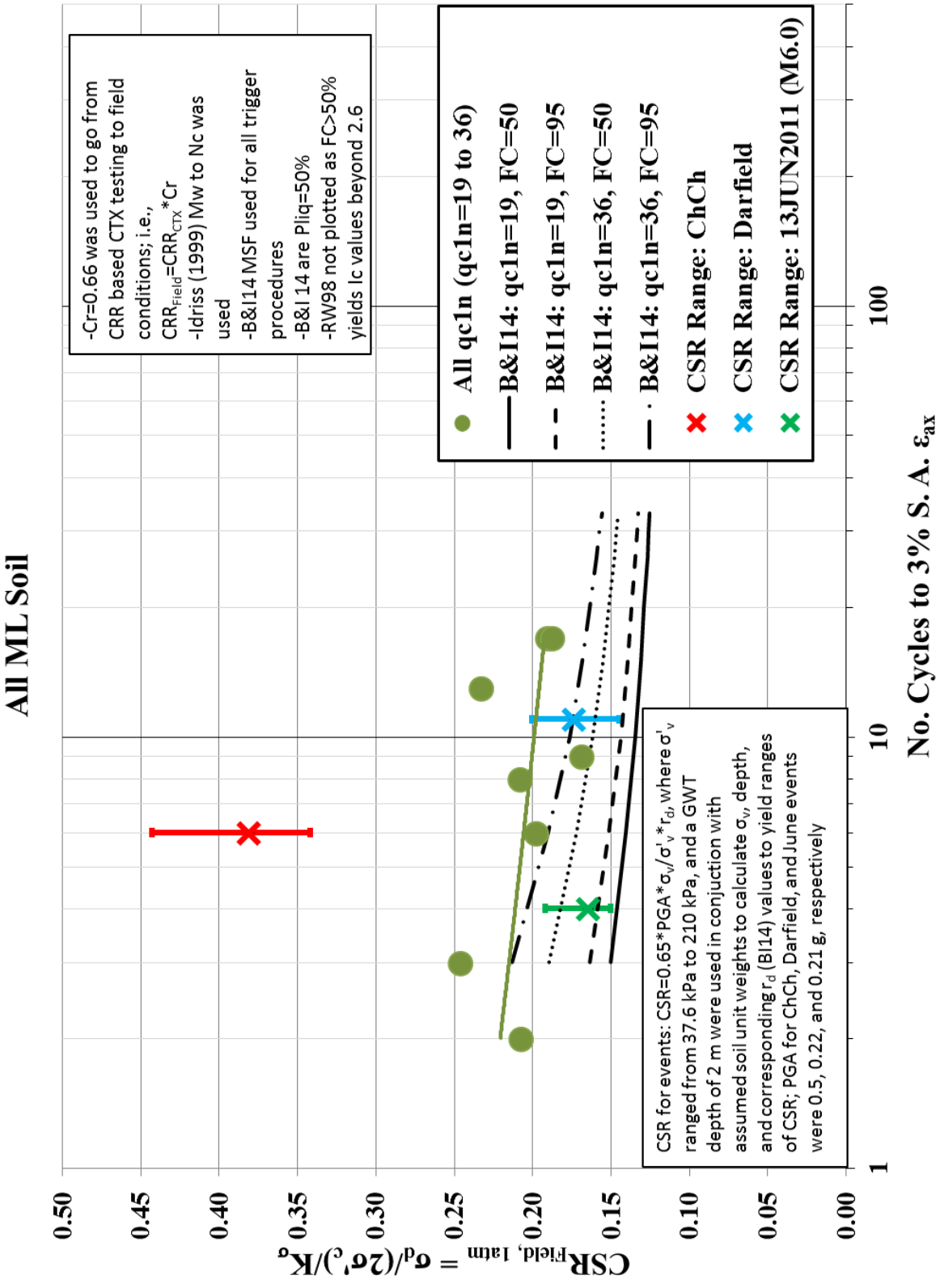

Figure B.15: CSR vs. $N_{c\text{-}3\%\ S.A.\varepsilon}$ for ML specimens with CPT-based liquefaction triggering correlation CRR curves

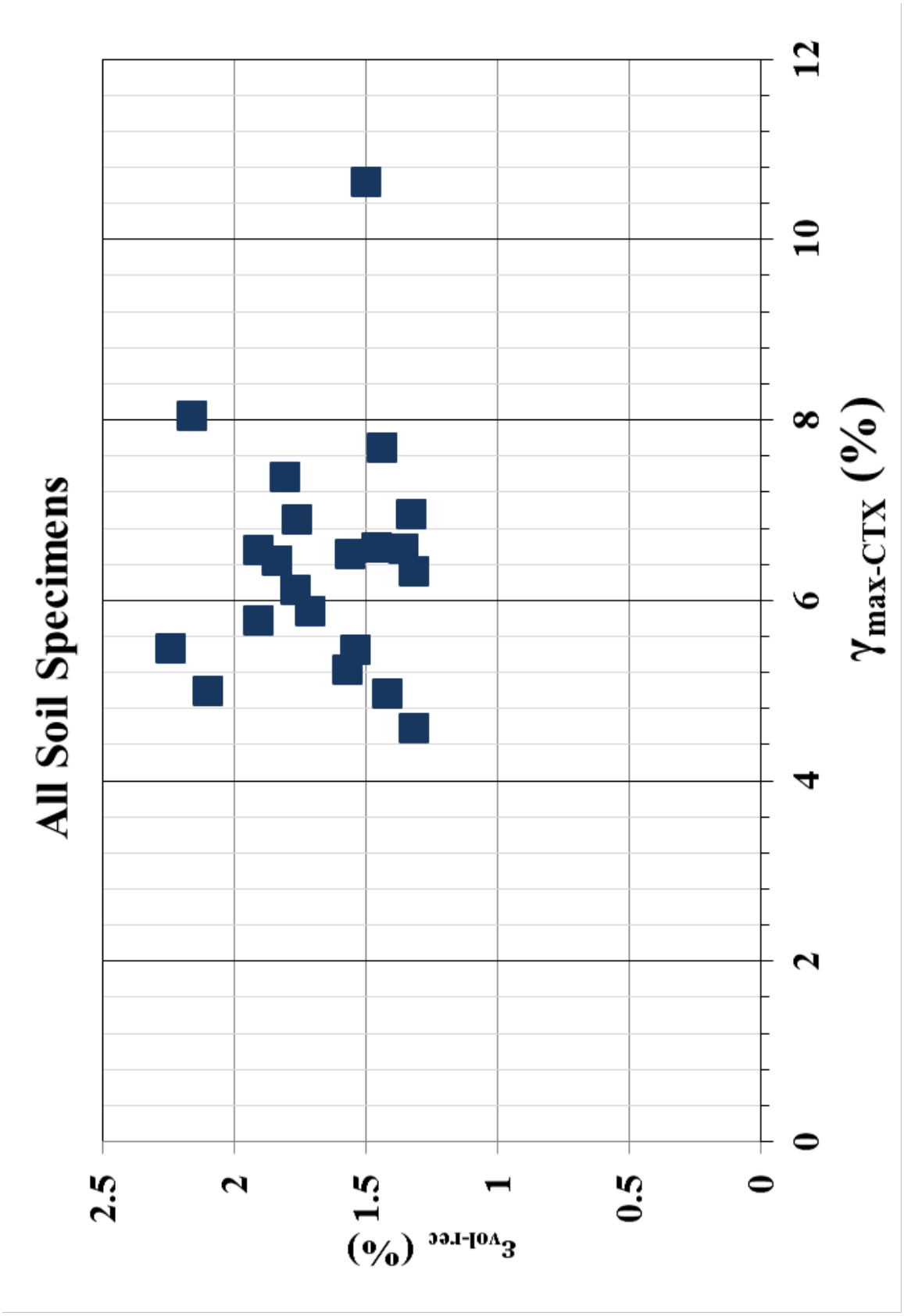

Figure B.16: $\varepsilon_{vol\text{-}rec}$ vs. $\gamma_{max\text{-}CTX}$ for all CTX test specimens

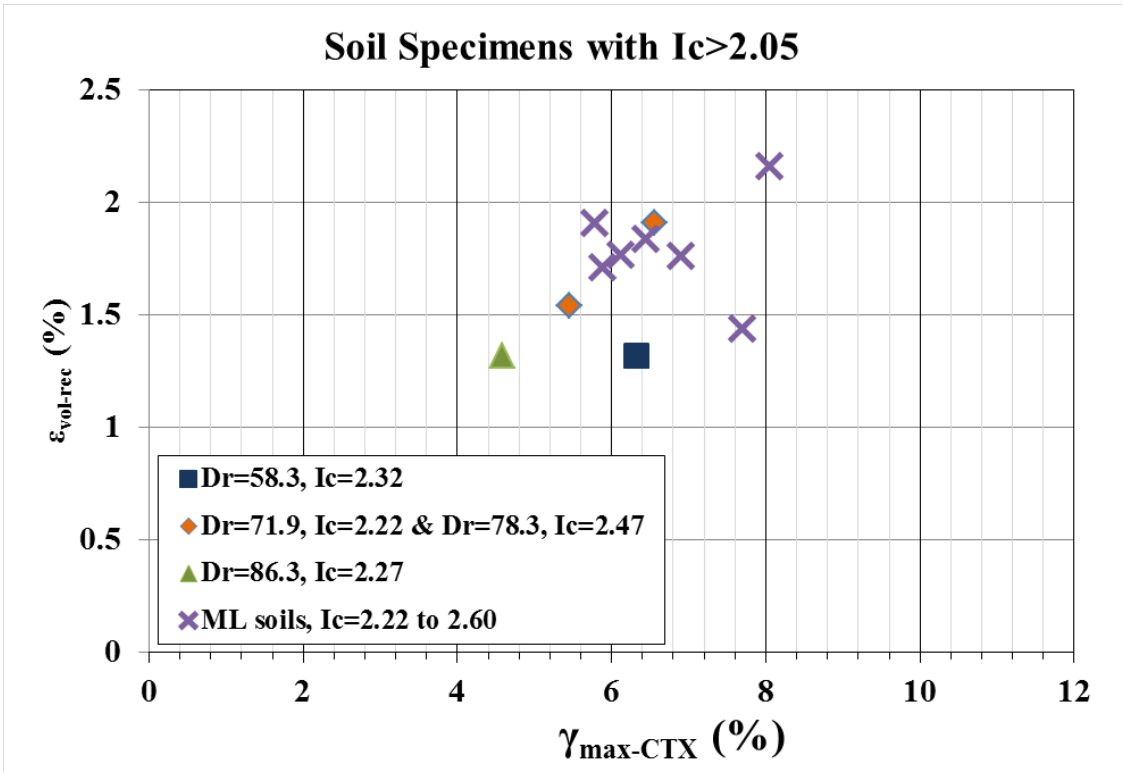

Figure B.17: $\varepsilon_{vol\text{-}rec}$ vs. $\gamma_{max\text{-}CTX}$ for CTX test specimens with I_c>2.05 (silt-like behavior type)

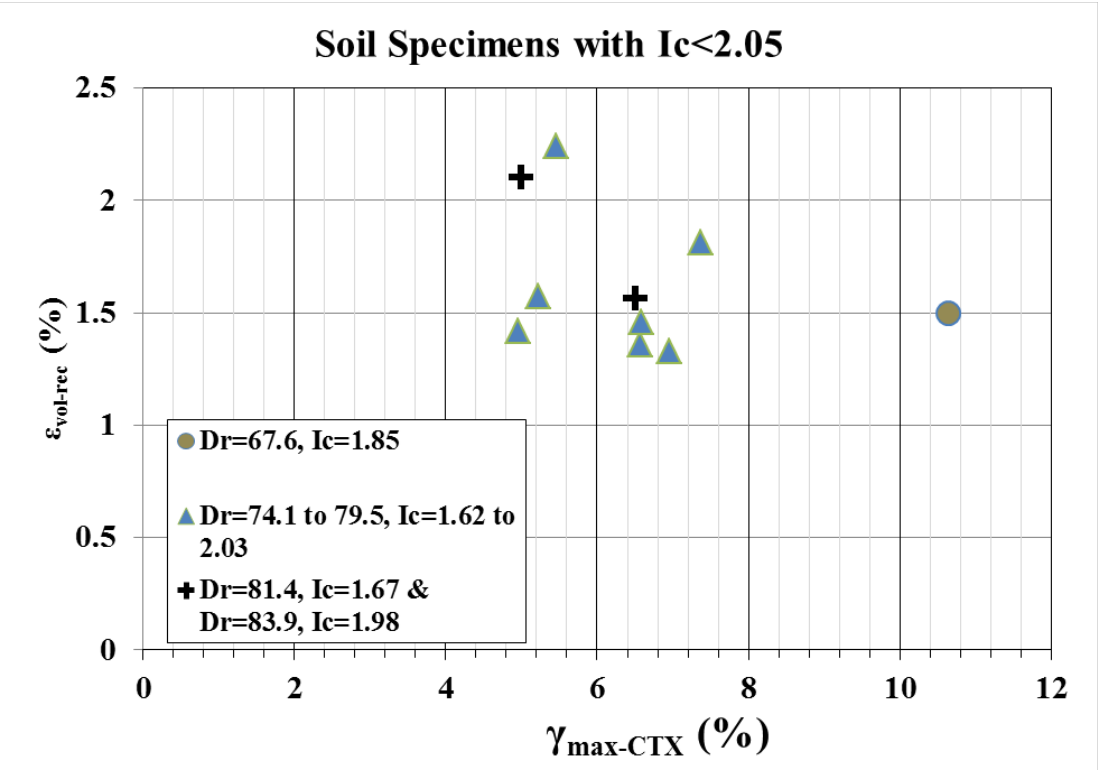

Figure B.18: $\varepsilon_{vol\text{-}rec}$ vs. $\gamma_{max\text{-}CTX}$ for CTX test specimens with I_c<2.05 (sand-like behavior type)

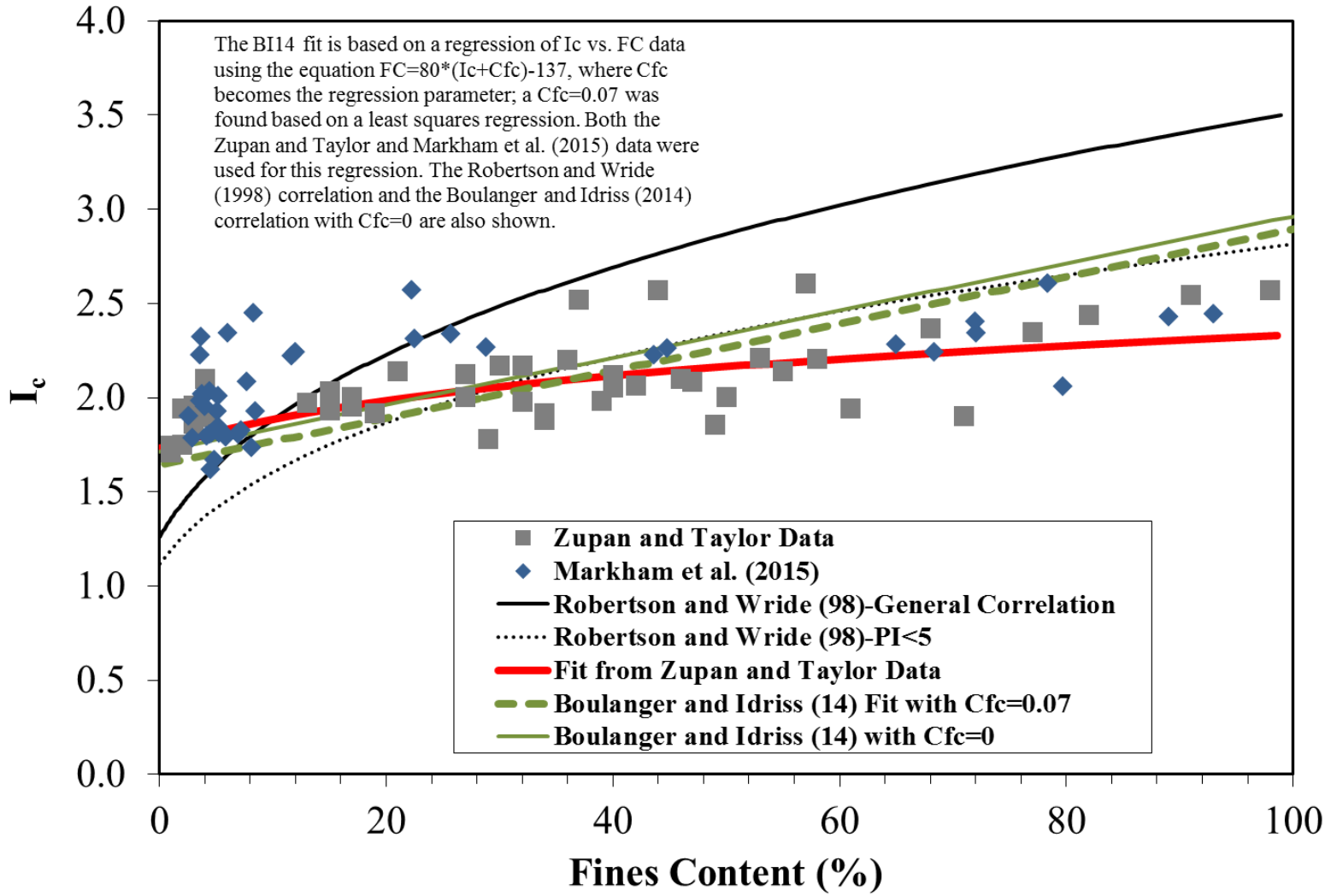

Figure B.19: I_c vs. FC for current study (Markham et al. 2015) and previous studies (Zupan and Taylor); also plotted with various correlations of I_c as a function of FC

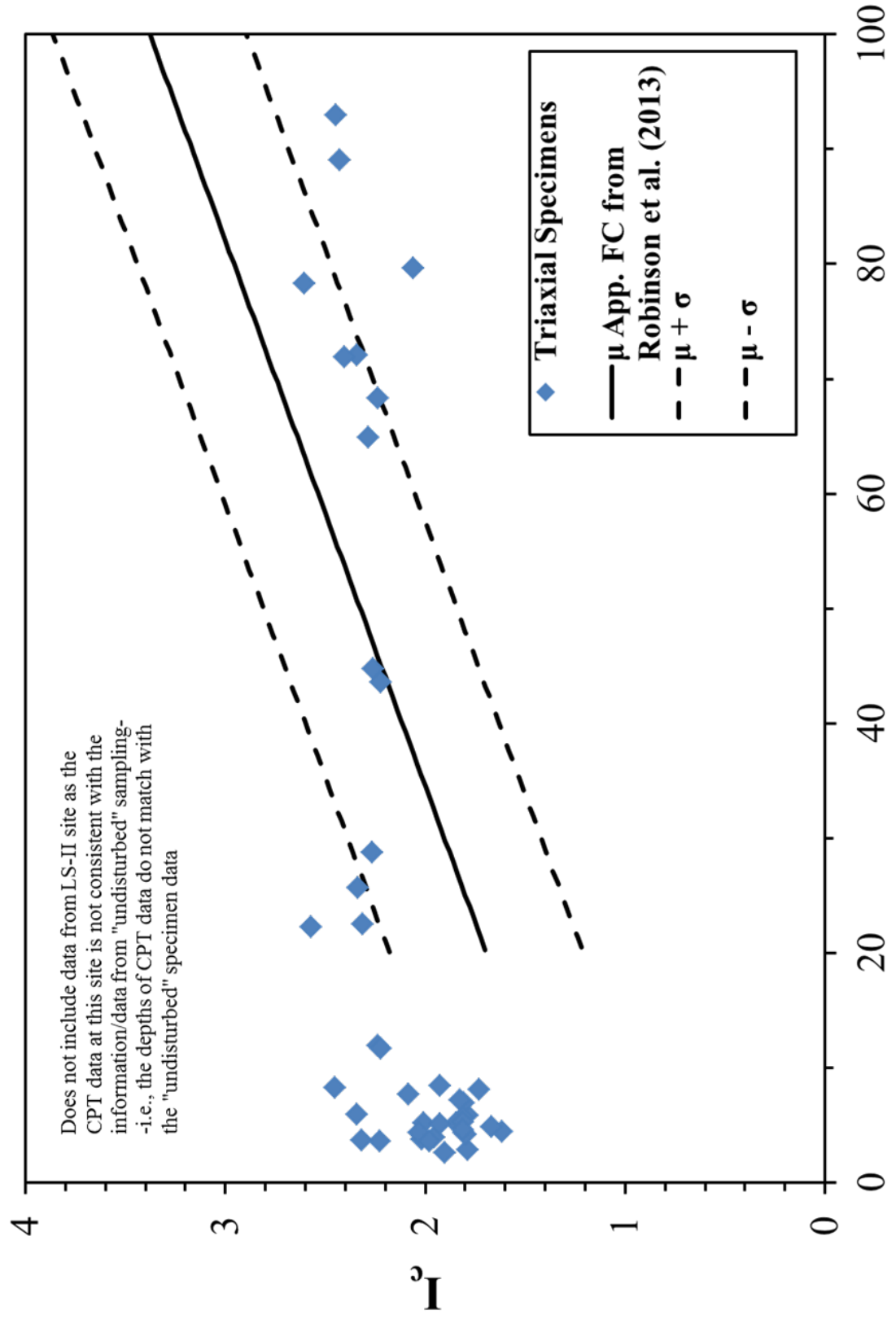

Figure B.20: I_c vs. FC for triaxial specimens; plotted with Robinson et al. (2013) correlation

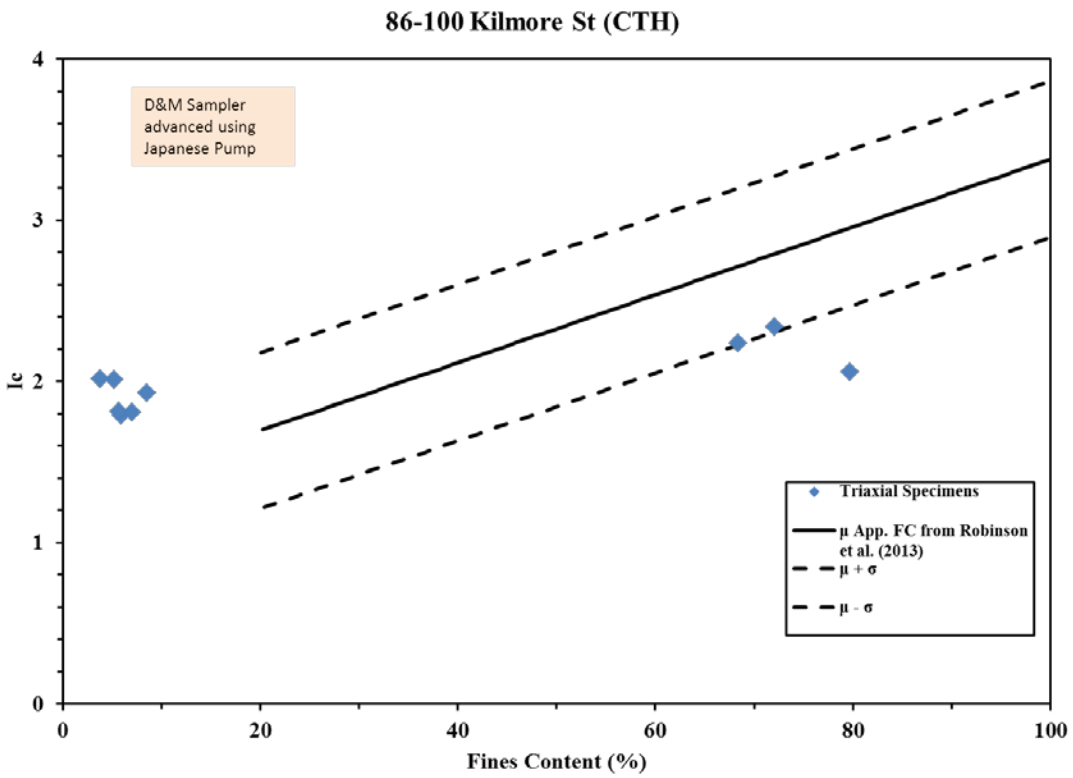

Figure B.21: I_c vs. FC for the CTH site triaxial specimens

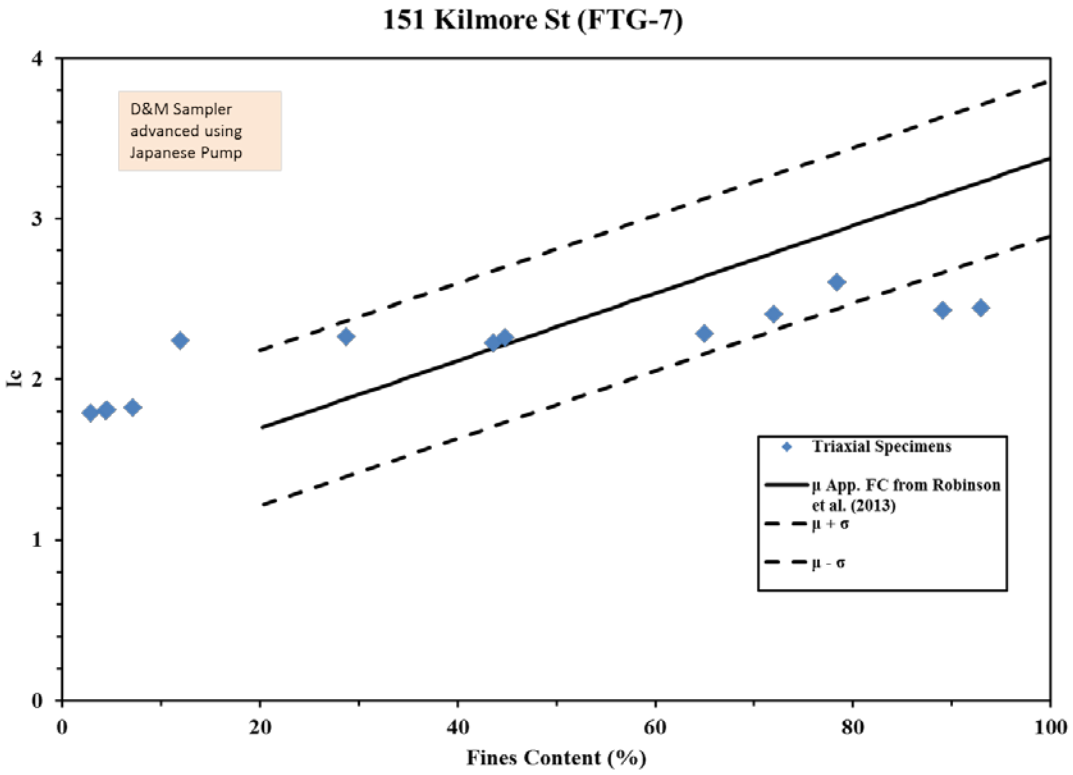

Figure B.22: I_c vs. FC for the FTG-7 site triaxial specimens

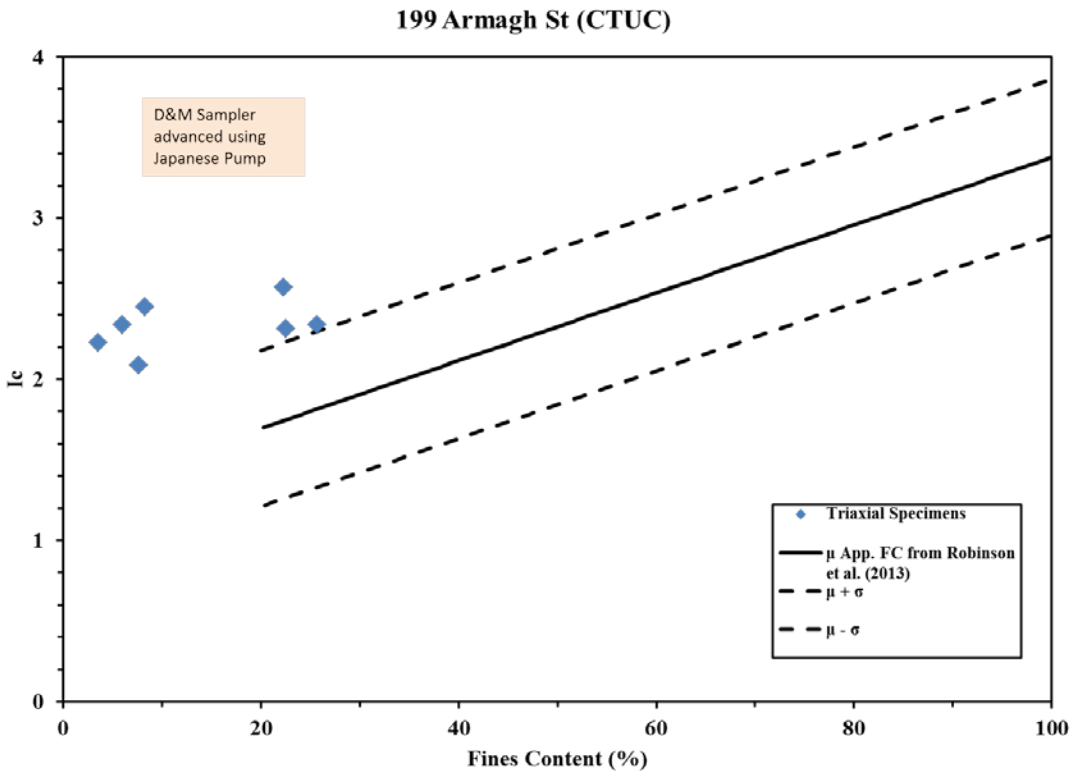

Figure B.23: I_c vs. FC for the CTUC site triaxial specimens

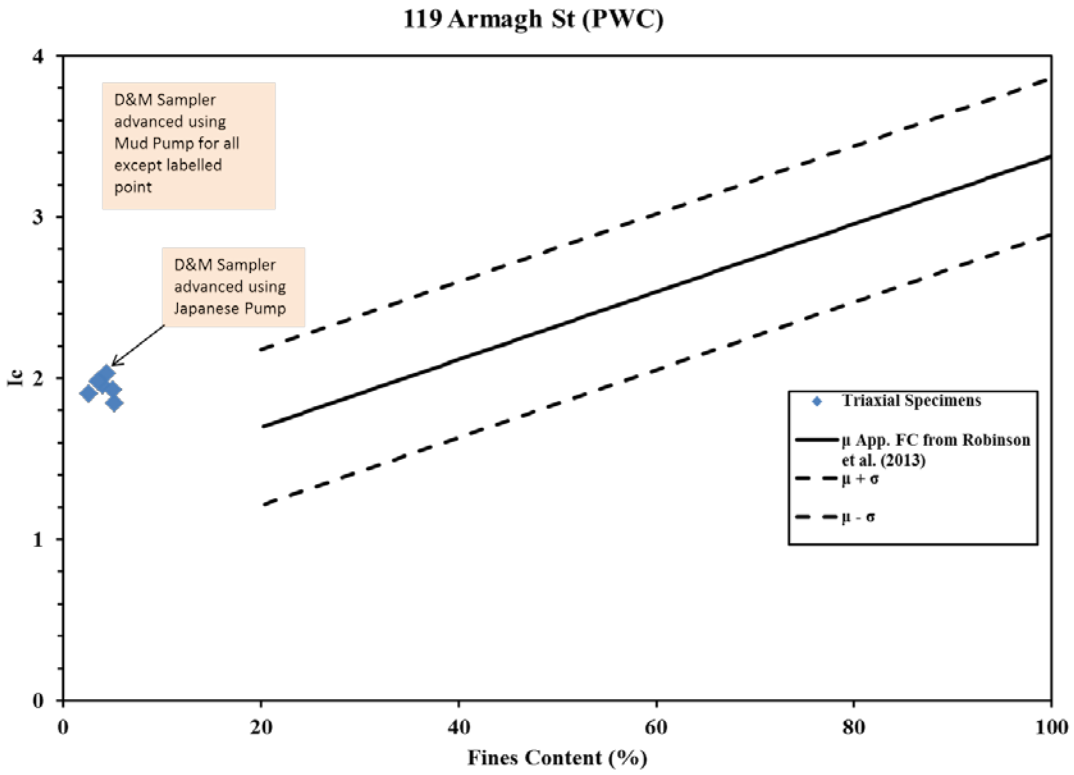

Figure B.24: I_c vs. FC for the PWC site triaxial specimens

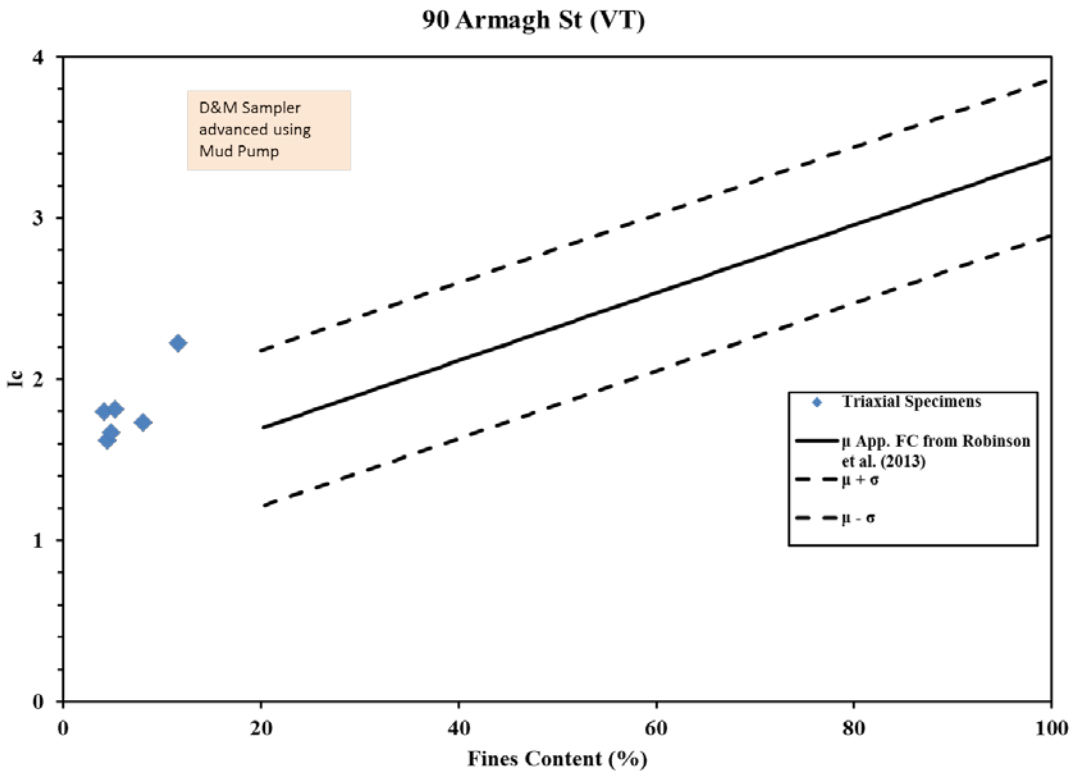

Figure B.25: I_c vs. FC for the VT site triaxial specimens

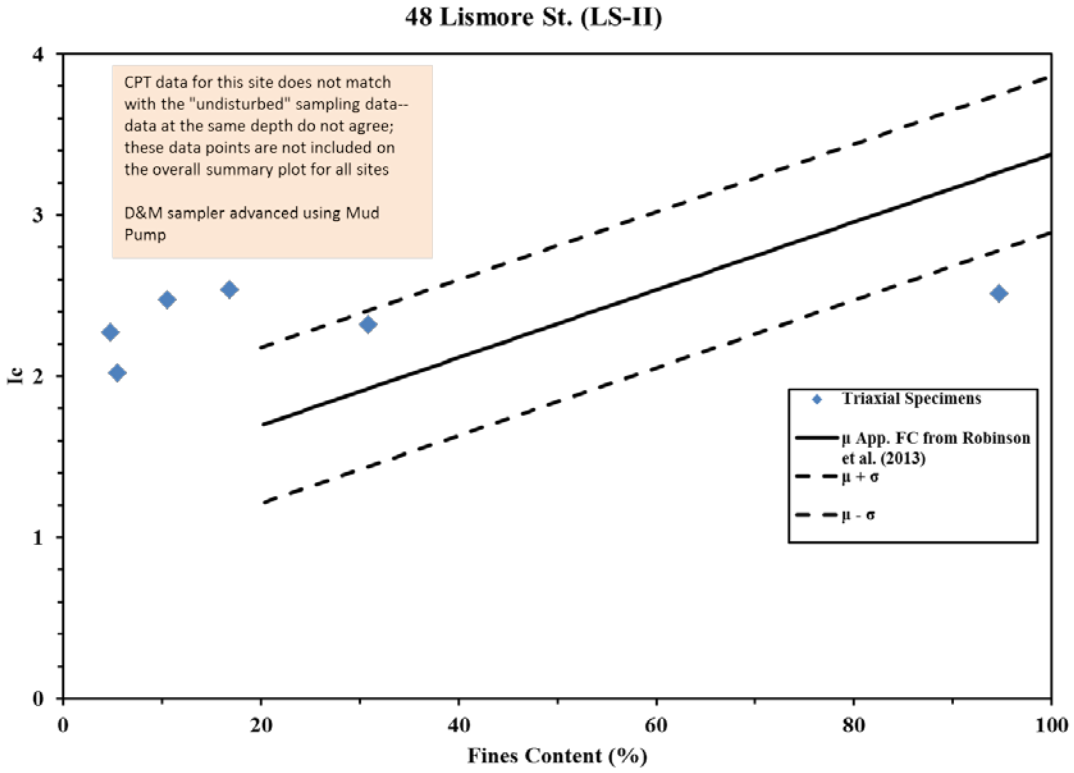

Figure B.26: I_c vs. FC for the LS-II site triaxial specimens

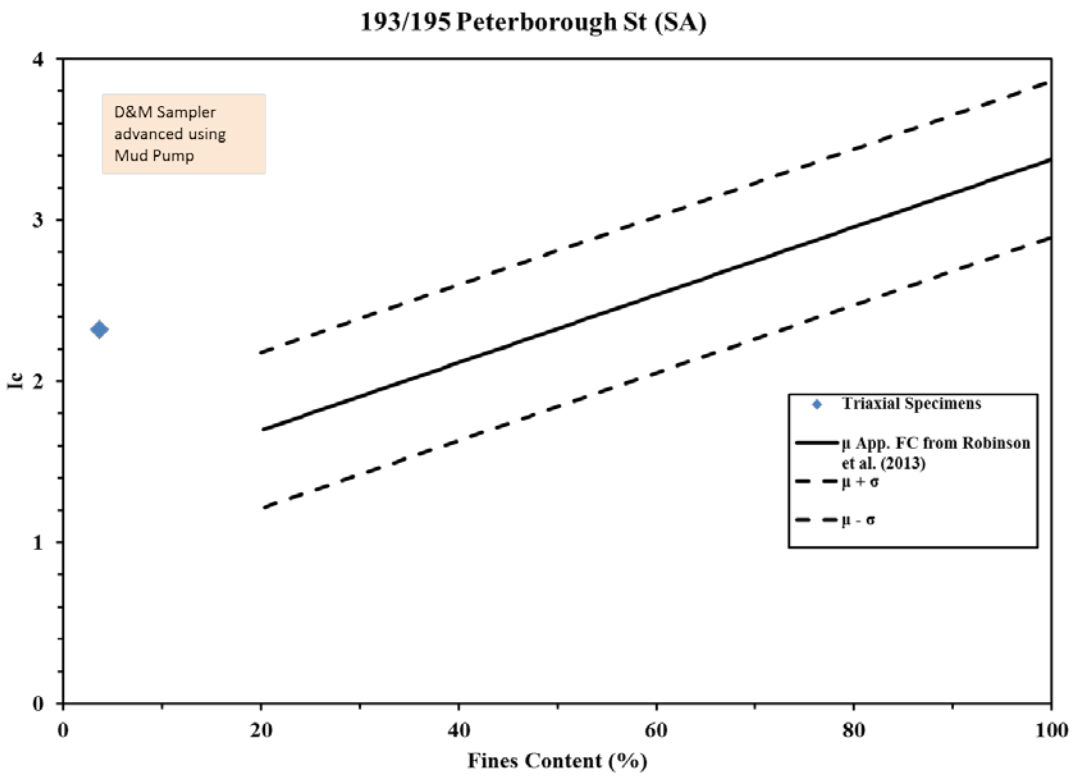

Figure B.27: I_c vs. FC for the SA site triaxial specimen

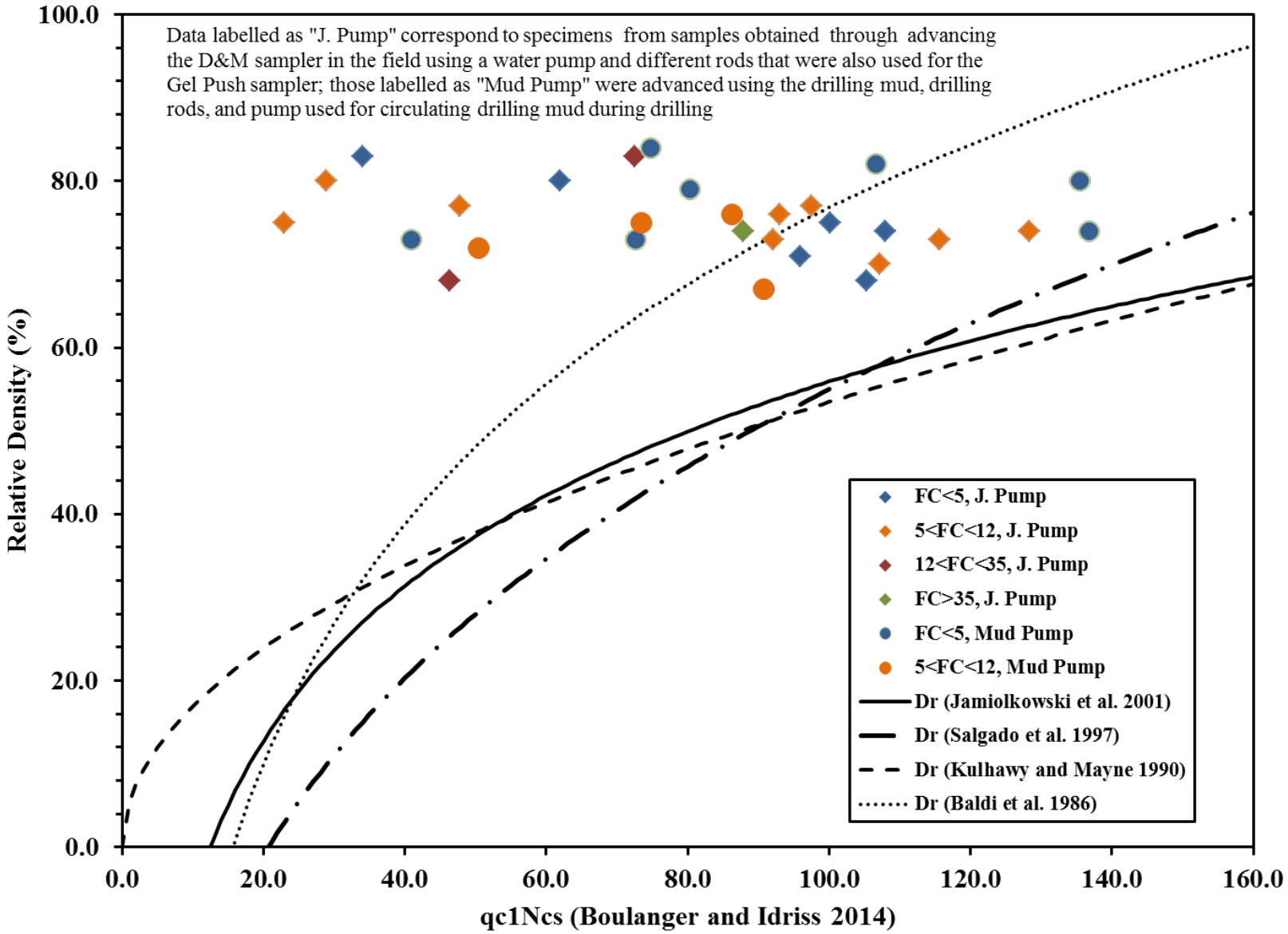

Figure B.28: D_r vs. q_{c1Ncs} for all triaxial soil specimens; multiple CPT-based correlations are also plotted

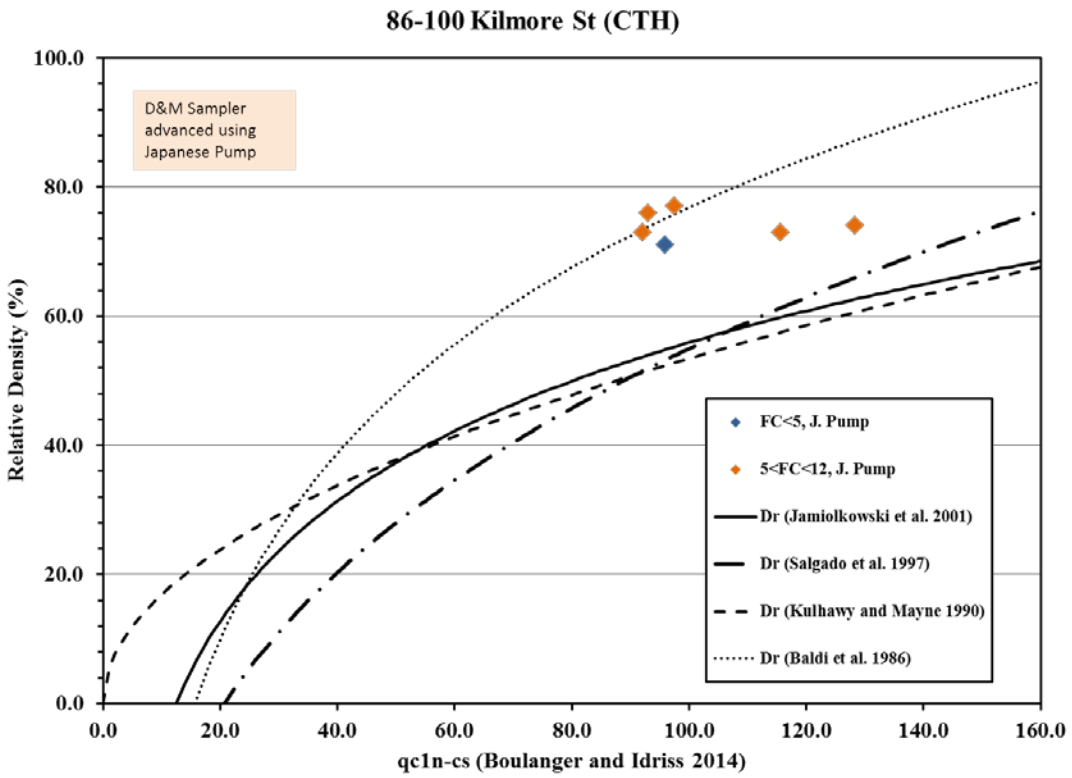

Figure B.29: D_r vs. q_{c1Ncs} for the CTH site

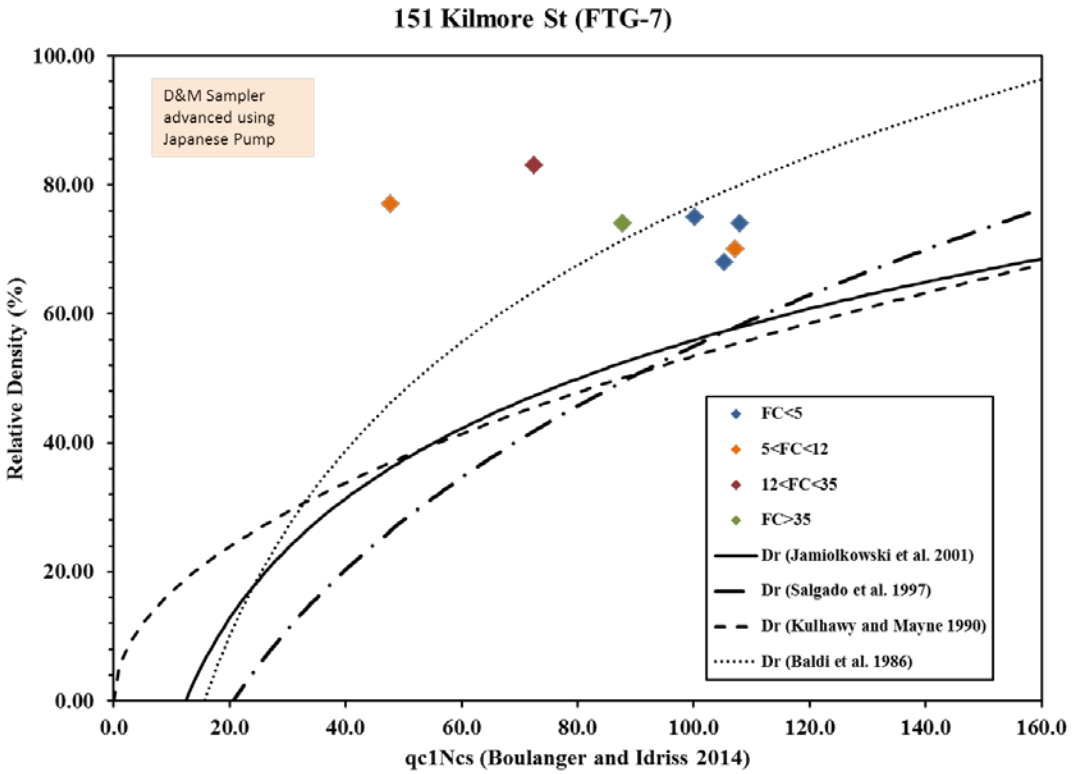

Figure B.30: D_r vs. q_{c1Ncs} for the FTG-7 site

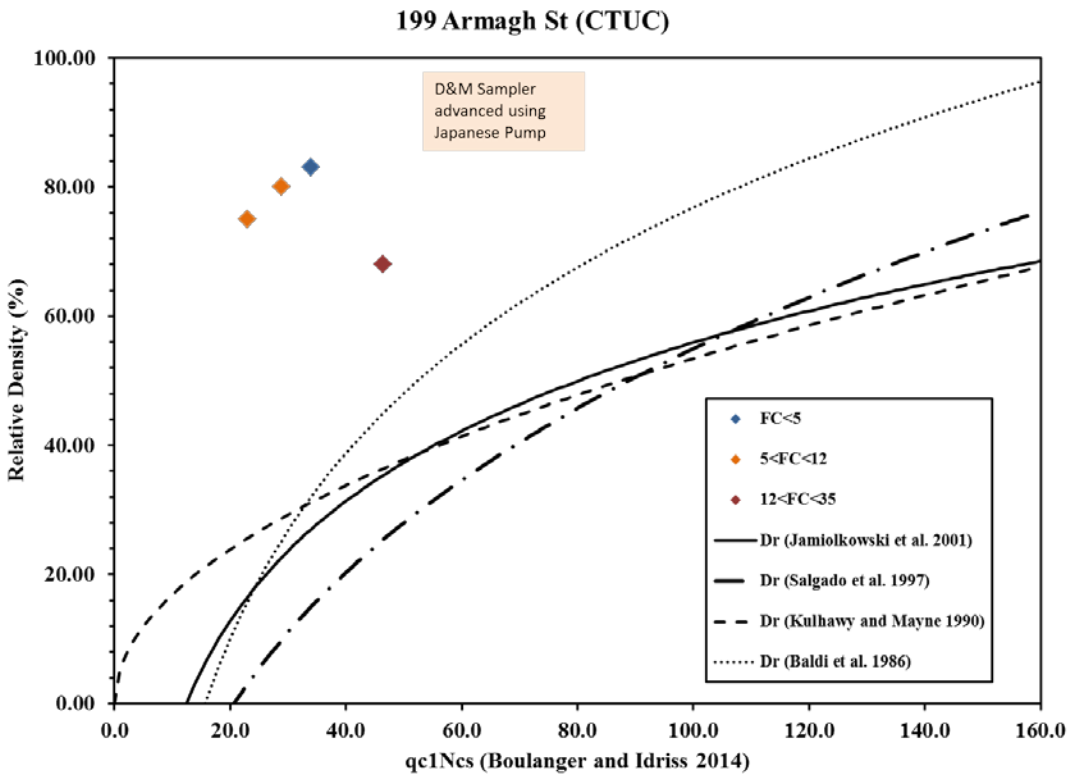

Figure B.31: D_r vs. q_{c1Ncs} for the CTUC site

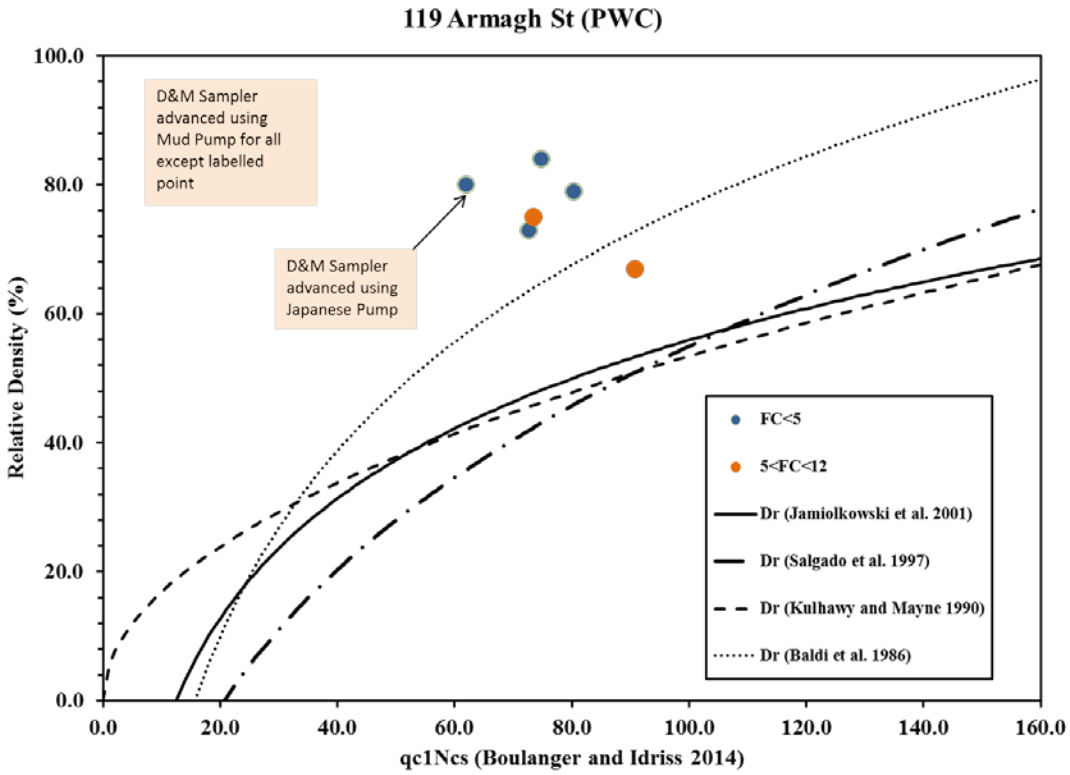

Figure B.32: D_r vs. q_{c1Ncs} for the PWC site

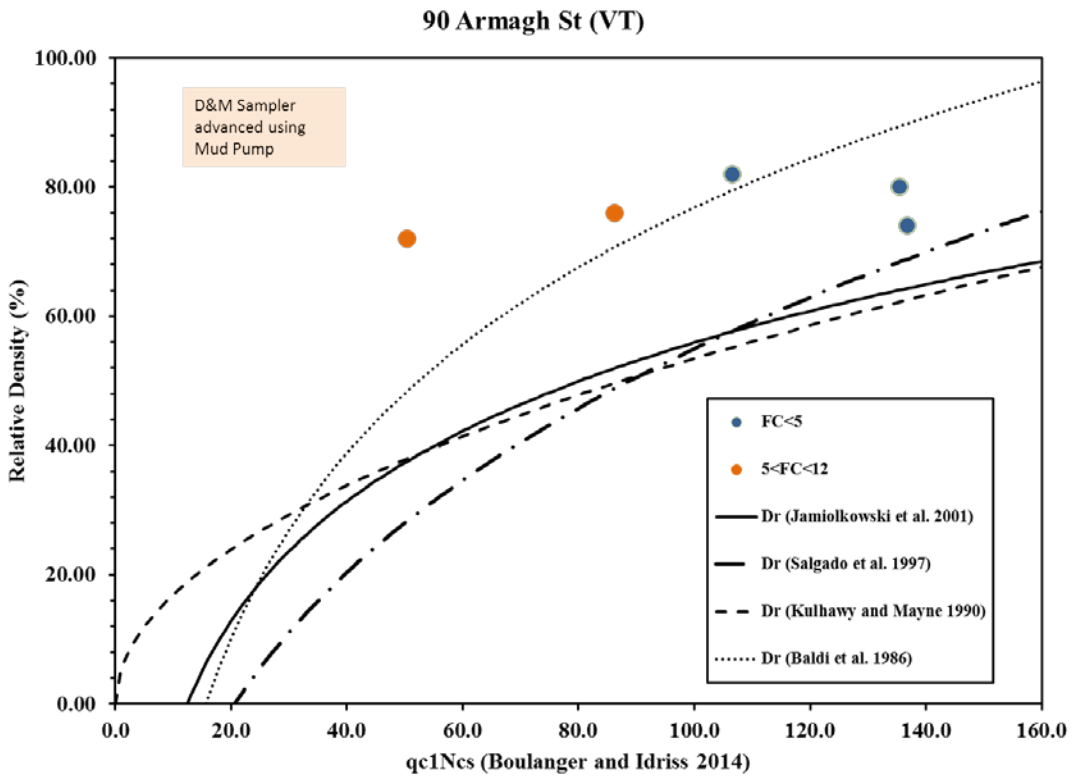

Figure B.33: D_r vs. q_{c1Ncs} for the VT site

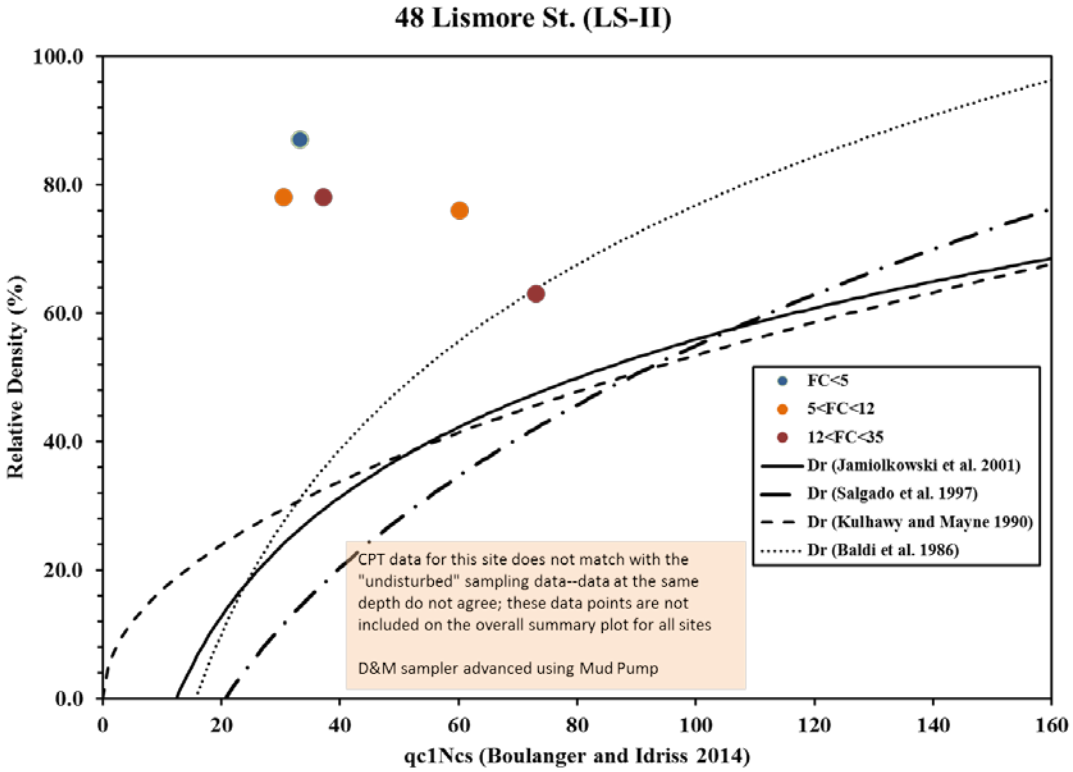

Figure B.34: D_r vs. q_{c1Ncs} for the LS-II site

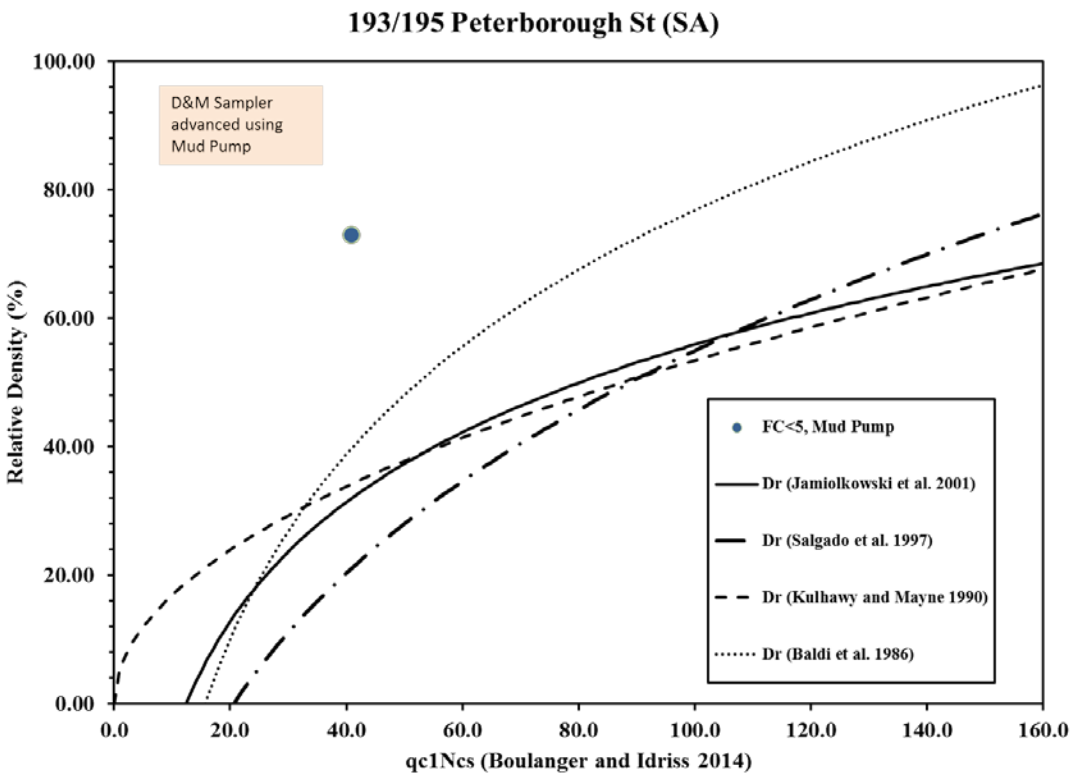

Figure B.35: D_r vs. q_{c1Ncs} for the SA site

Appendix C

Supporting Data and Information for Undistubed Soil Sampling and Laboratory Testing

Appendix C.1

Boring Locations and Logs for Undisturbed Sampling at CBD Sites

Appendix C.1.1

Christchurch Town Hall (CTH) Site—86-100 Kilmore St.

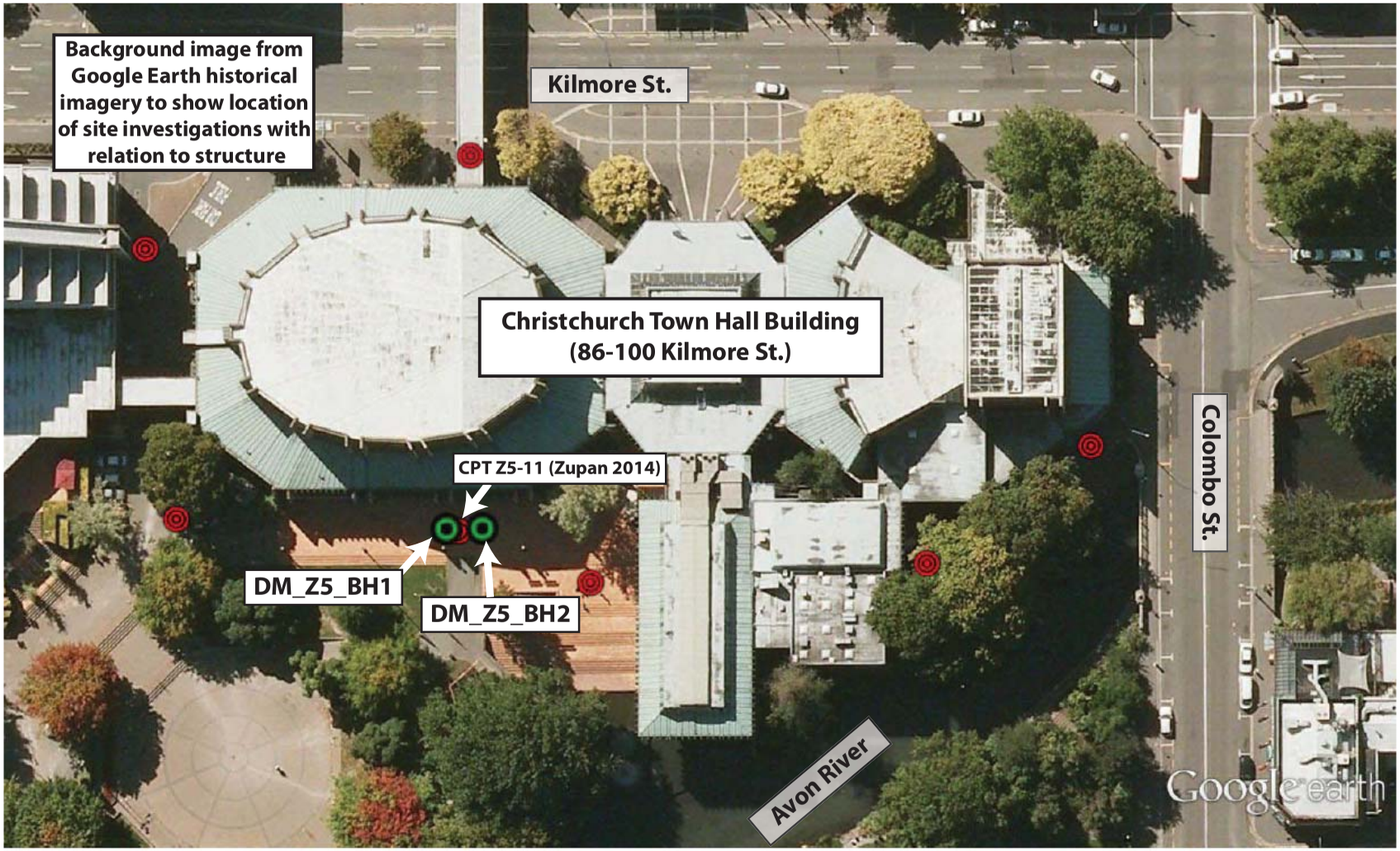

Google earth

feet 300

meters 100

SOIL BORING LOG

Project No:	Boring Number
	DM_BH1

General Comments: **Page 1 of 3**

Project Name: CBD Project	**Location:** 86 Kilmore St. (Town Hall)
Elevation:	**Drilling Contractor:** McMillan
Drilling Method and Equipment:	Rotary wash mud drilling and Hollow Stem Auger
Water Level: N/A	**Start/Finish:** May 5 to May 7, 2014
Loggers: Chris Markham	

Depth below Surface (m)	Sample: Interval	Sample: Number and Type	Sample: Recovery (m)		Soil Description (From extrusion of sample in lab)	Comments (Depth of Casing, Drilling Rate, Drilling Fluid Loss, Tests and Instrumentation)
1						From the ground surface had to carefully remove tiles and saw through about 15-20cm of concrete to allow for bath to be placed and boring to be started
2		D&M Sample 1U 1.7-2.15m	44.2cm		Primarily sandy silt; pieces of wood and rootlets present; some rust color (sample near assumed GWT)	Casing Depth: 1.185m bgs
3		D&M Sample 2U 2.3-2.75m	45 cm (Full)		Sandy silt; grey; very moist; many rootlets and small twigs	Casing Depth: 1.185m bgs
		D&M Sample 3U 2.9-3.35m	45 cm (Full)		Sandy silt to silty sand (fine sand); grey; very moist; transistion to coarser sandy silt at bottom of sample	Casing Depth: 1.185m bgs
4		D&M Sample 4U 3.5-3.95m	45 cm (Full)		sandy silt to silty sand (very fine sand); grey; moist	Casing Depth: 1.185m bgs
5		D&M Sample 5U 4.1-4.55m	45 cm (Full)		primarily fine sand with some silt; dark grey; some light brown (almost rust colored) spots along outside of specimen, but very faint	Casing Depth: 1.185m bgs After Sample 5U was taken, the 6" casing and mud rotary bath was removed and hollow-stem auger was advanced to about 11.9 m bgs
6						Drilling "soft" to about 5.5m bgs--most likely the upper SM/ML mat'l At about 5.5 m auger hit stiffer mat'l--most likely gravelly soil
7						

SOIL BORING LOG

Project No:	Boring Number
	DM_BH1

General Comments: **Page 2 of 3**

Project Name: CBD Project	**Location:** 86 Kilmore St. (Town Hall)
Elevation:	**Drilling Contractor:** McMillan
Drilling Method and Equipment:	Rotary wash mud drilling and Hollow Stem Auger
Water Level: N/A	**Start/Finish:** May 5 to May 7, 2014
Loggers: Chris Markham	

Depth below Surface (m)	Sample: Interval	Sample: Number and Type	Sample: Recovery (m)		Soil Description (From extrusion of sample in lab)	Comments (Depth of Casing, Drilling Rate, Drilling Fluid Loss, Tests and Instrumentation)
8						
9						
10						
11						
12						Hollow stem augering completed at 11.9 m bgs; auger left in place to be used as casing for mud rotary drilling to obtain deeper samples
13						
14						

SOIL BORING LOG

Project No:	Boring Number
	DM_BH1

General Comments: **Page 3 of 3**

Project Name: CBD Project	**Location:** 86 Kilmore St. (Town Hall)
Elevation:	**Drilling Contractor:** McMillan
Drilling Method and Equipment:	Rotary wash mud drilling and Hollow Stem Auger
Water Level: N/A	**Start/Finish:** May 5 to May 7, 2014
Loggers: Chris Markham	

Depth below Surface (m)	Sample: Interval	Sample: Number and Type	Sample: Recovery (m)		Soil Description (From extrusion of sample in lab)	Comments (Depth of Casing, Drilling Rate, Drilling Fluid Loss, Tests and Instrumentation)
15		D&M Sample 6U 14.57-15.02m	43 cm		fine sand; maybe some silt; grey; moist	Hollow stem auger was stopped at 11.9 m; from here the auger was used as casing to peform "conventional" mud rotary drilling; fall-in was experienced at bottom of hole and a hollow barrel was pushed to clean out slough/fall-in to allow for Sample 6U to be taken; had to apply pressure to sampling rods to advance sampler through 10-15cm of slough at bottom of hole to target depth
		D&M Sample 7U 15.1-15.55m	No Recovery		fine sand; maybe some silt; grey; moist	D&M brass tube crushed during attempt to obtain Sample 7U; most likely due to the presence of a cobble or large piece of gravel
16						
17						
18						
19						
20						
21						

SOIL BORING LOG

Project No:	Boring Number
	DM_BH2

General Comments: **Page 1 of 3**

Project Name: CBD Project
Location: 86 Kilmore St. (Town Hall)
Elevation:
Drilling Contractor: McMillan
Drilling Method and Equipment: Rotary wash mud drilling and Hollow Stem Auger
Water Level: N/A
Start/Finish: May 8 to May 9, 2014
Loggers: Chris Markham

Depth below Surface (m)	Sample: Interval	Sample: Number and Type	Sample: Recovery		Soil Description (From extrusion of sample in lab)	Comments (Depth of Casing, Drilling Rate, Drilling Fluid Loss, Tests and Instrumentation)
1						From the ground surface had to carefully remove tiles and saw through about 15-20cm of concrete to allow for bath to be placed and boring to be started
2		GP Sample 1U 1.7-2.65m	93.8 cm			Casing Depth: 1.175m bgs GP: Gel-Push Samples taken
3		GP Sample 1U 2.7-3.65m	87.8 cm			Casing Depth: 1.175m bgs
4		GP Sample 1U 3.7-4.65m	57.8 cm			Casing Depth: 1.175m bgs
5						
6						Used hollow stem auger to advance hole after Sample 3U through gravelly soil to a depth of about 13.6 m bgs
7						

SOIL BORING LOG

Project No:	Boring Number
	DM_BH2

General Comments: **Page 2 of 3**

Project Name: CBD Project	**Location:** 86 Kilmore St. (Town Hall)
Elevation:	**Drilling Contractor:** McMillan
Drilling Method and Equipment:	Rotary wash mud drilling and Hollow Stem Auger
Water Level: N/A	**Start/Finish:** May 8 to May 9, 2014
Loggers: Chris Markham	

Depth below Surface (m)	Sample: Interval	Sample: Number and Type	Sample: Recovery		Soil Description	Comments
					(From extrusion of sample in lab)	Depth of Casing, Drilling Rate, Drilling Fluid Loss, Tests and Instrumentation
8						
9						
10						
11						
12						
13						
14						Hollow stem augering completed at 13.6 m bgs; auger left in place to be used as casing for mud rotary drilling to obtain deeper samples

SOIL BORING LOG

Project No:	Boring Number
	DM_BH2

General Comments: **Page 3 of 3**

Project Name: CBD Project	**Location:** 86 Kilmore St. (Town Hall)
Elevation:	**Drilling Contractor:** McMillan
Drilling Method and Equipment:	Rotary wash mud drilling and Hollow Stem Auger
Water Level: N/A	**Start/Finish:** May 8 to May 9, 2014
Loggers: Chris Markham	

Depth below Surface (m)	Sample: Interval	Sample: Number and Type	Sample: Recovery		Soil Description (From extrusion of sample in lab)	Comments (Depth of Casing, Drilling Rate, Drilling Fluid Loss, Tests and Instrumentation)
15		D&M Sample 4U 14.06-14.51m	45 cm (Full)		fine sand; maybe some silt; grey; moist	Casing Depth: 13.58 m bgs D&M sampler used to obtain samples below the termination of the hollow stem auger as GP sampler's outer diamter larger than inner diamter of auger
		D&M Sample 5U 14.69-15.14m	45 cm (Full)		fine sand; maybe some silt; grey; moist	Casing Depth: 13.58 m bgs
16		D&M Sample 6U 15.19-15.64m	43.9 cm		fine sand; maybe some silt; grey; moist	Casing Depth: 13.58 m bgs
17						
18						
19						
20						
21						

Appendix C.1.2

FTG-7 Building Site—151 Kilmore St.

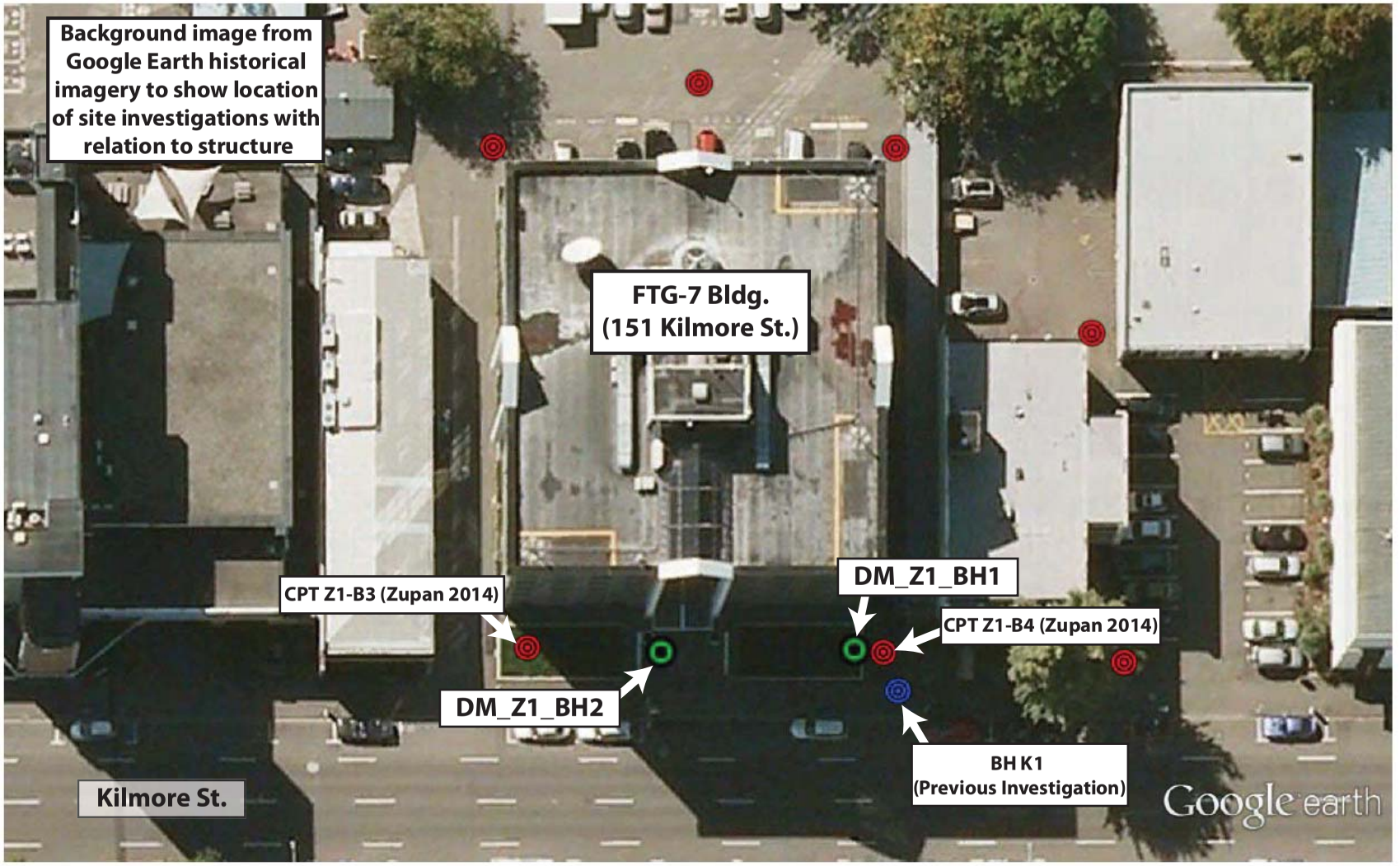

Google earth

feet 100

meters 50

SOIL BORING LOG

Project No:	Boring Number
	DM_BH1

General Comments: **Page 1 of 2**

Project Name: CBD Project	**Location:** 151 Kilmore St
Elevation:	**Drilling Contractor:** McMillan
Drilling Method and Equipment:	Rotary wash mud drilling and Hollow Stem Auger
Water Level: N/A	**Start/Finish:** May 15 to May 16, 2014
Loggers: Chris Markham	

Depth below Surface (m)	Sample: Interval	Sample: Number and Type	Sample: Recovery (m)		Soil Description (From extrusion of sample in lab)	Comments (Depth of Casing, Drilling Rate, Drilling Fluid Loss, Tests and Instrumentation)
1						There was about 0.25m of fill that raised the property above the surface adjacent to the street. The area near the street was where the initial CPT (Z1-B4) was completed and target depths for sampling were based on. Therefore, about 0.25m was added on to each depth to get actual depths from the drilling surface, but reported depths are from "natural" ground surface where CPT was performed
2		D&M Sample 1U 1.8-2.25m	44.8cm		Primarily silt; grey to light brown with some rust color; rootlets present	Casing Depth: N/A No Casing for first sample
3		D&M Sample 2U 2.4-2.85m	44.0cm		sandy silt to silty sand (fine sand); grey to light brown with some rust coloring	Casing Depth: 2.0m bgs
4		D&M Sample 3U 3.4-3.85m	44.0cm		primarily silt (maybe some fine sand) in upper part of sample; grey; Lower part of sample transitioned to sandy silt to silty sand (fine sand); grey	Casing Depth: 2.0m bgs
5		D&M Sample 4U 4.6-5.05m	45.0cm (Full)		sample showed mostly a silty sand mat'l (fine sand) with layers of primarily silty mat'l; grey	Casing Depth: 2.0m bgs
6		D&M Sample 5U 5.4-5.85m	45.0cm (Full)		sandy silt; grey; some small rootlets present	Casing Depth: 5.04m bgs
7						

SOIL BORING LOG

Project No:	Boring Number
	DM_BH1

General Comments: **Page 2 of 2**

Project Name: CBD Project	**Location:** 151 Kilmore St
Elevation:	**Drilling Contractor:** McMillan
Drilling Method and Equipment:	Rotary wash mud drilling and Hollow Stem Auger
Water Level: N/A	**Start/Finish:** May 15 to May 16, 2014
Loggers: Chris Markham	

Depth below Surface (m)	Sample Interval	Sample Number and Type	Sample Recovery (m)		Soil Description (From extrusion of sample in lab)	Comments (Depth of Casing, Drilling Rate, Drilling Fluid Loss, Tests and Instrumentation)
8						
9						
		D&M Sample 6U 9-9.45m	15.3cm		med. To fine sand with some silt; light brown to grey	Casing Depth: 8.08m bgs
10						
		D&M Sample 7U 10-10.45m	43.1cm		fairly clean, fine sand; brown to grey	Casing Depth: 8.08m bgs
11						
12						
		D&M Sample 8U 12-12.45m	12.3cm		fairly clean sand; light brown	Casing Depth: 8.08m bgs
13						
		D&M Sample 9U 13.2-13.65m	27.4cm		sample contained layers of both silty sand and sandy silt mat'l; some rust coloring in layers; mostly light brown to grey	Casing Depth: 8.08m bgs
		D&M Sample 10U 13.7-14.15m	24.4cm		silty sand (fine sand) to sandy silt; light brown	Casing Depth: 8.08m bgs
14						

SOIL BORING LOG

Project No:	Boring Number
	DM_BH2

General Comments: **Page 1 of 2**

Project Name: CBD Project	**Location:** 151 Kilmore St
Elevation:	**Drilling Contractor:** McMillan
Drilling Method and Equipment:	Rotary wash mud drilling and Hollow Stem Auger
Water Level: N/A	**Start/Finish:** May 14 to May 15, 2014
Loggers: Chris Markham	

Depth below Surface (m)	Sample: Interval	Sample: Number and Type	Sample: Recovery (m)		Soil Description (From extrusion of sample in lab)	Comments (Depth of Casing, Drilling Rate, Drilling Fluid Loss, Tests and Instrumentation)
1						There was about 0.45m of fill that raised the property above the surface adjacent to the street. The area near the street was where the initial CPT (Z1-B3) was completed and target depths for sampling were based on. Therefore, about 0.45m was added on to each depth to get actual depths from the drilling surface, but reported depths are from "natural" ground surface where CPT was performed
		D&M Sample 1U 1.2-1.65m	45.0cm (Full)		sandy silt to silty sand; grey to brown; some rust coloring	Casing Depth: 0.28m bgs
2		D&M Sample 2U 1.9-2.35m	30.8cm		debris (brick, small pieces of concrete) at top of sample; interlayered sandy silt with primarily silt mat'l; vertical discolorations/intrusions throughout sample; rootlets prevalent	Casing Depth: 0.28m bgs during sampling the tube did not fully extend and the tube was slightly damaged/dinged; This was the first sample that was affected by a cobble (probably fall in due to casing being too high) that disallowed high quality sample being obtained in upper material
		D&M Sample 3U 2.6-3.05m	37.0cm		debris (brick and small pieces of gravel and concrete) present at top of sample; primarily silty mat'l; rootlets present throughout sample; grey with some rust coloring throughout	Casing Depth: 0.28m bgs Tube was crushed/pushed in at the bottom due to cobble
3						
		D&M Sample 4U 3.3-3.75m	38.3cm		Large piece of cobble at top of tube (maybe part of cobble that was affecting Samples 2u and 3U)--8-9cm long; mat'l similar to sample 3U	Casing Depth: 1.8m bgs (approx.) Tube was crushed the full length of sample; very difficult to get tube off of sampler once pulled to surface after taking sample; this was the last sample that was affected by cobble mentioned above
4						
5						Decided to use non-side discharge bit (bottom discharge) to attempt to push the cobble to the side of the hole--this didn't work; used sonic core barrel to try and "grab" the cobble, which initially didn't work; attempted to use side discharge (typical) tri-cone bit to drill through the cobble; at a certain point drilling fluid was spilling out from the top of the hole, so hole had to be sealed with bentonite; at about 5.55m below the natural ground we were able to grab the piece of cobble that was affecting the quality of the samples; decided to take a D&M sample at 5.55m below natural ground
		D&M Sample 5U 5.55-6.0m	45.0cm (Full)		Bottom of sample contained silty sand (fine sand); grey	Casing Depth: 4.95m bgs
6		D&M Sample 6U 6.05-6.5m	45.0cm (Full)		layers of sandy silt and silty sand throughout sample; grey	Casing Depth: 4.95m bgs
		D&M Sample 7U 6.55-7.0m	43.1cm		top part of sample was primarily silt--very compressible and soft; grey	Casing Depth: 4.95m bgs
7						

SOIL BORING LOG

Project No:	Boring Number
	DM_BH2

General Comments: **Page 2 of 2**

Project Name: CBD Project	**Location:** 151 Kilmore St
Elevation:	**Drilling Contractor:** McMillan
Drilling Method and Equipment:	Rotary wash mud drilling and Hollow Stem Auger
Water Level: N/A	**Start/Finish:** May 14 to May 15, 2014
Loggers: Chris Markham	

Depth below Surface (m)	Sample: Interval	Sample: Number and Type	Sample: Recovery (m)		Soil Description (From extrusion of sample in lab)	Comments (Depth of Casing, Drilling Rate, Drilling Fluid Loss, Tests and Instrumentation)
8						
9						
		D&M Sample 8U 9.0-9.45m	44.3cm		mostly a clean sand; med. To fine; grey to brown	Casing Depth: 8.335m bgs
10		D&M Sample 9U 9.6-10.05m	39.2cm		silty sand; grey	Casing Depth: 8.335m bgs
		D&M Sample 10U 10.2-10.65m	37.3cm		fairly clean sand; grey	Casing Depth: 8.335m bgs
11		D&M Sample 11U 10.8-11.25m	42.6cm		fairly clean, fine sand; brown to grey	Casing Depth: 8.335m bgs
12						
13						
14						

Appendix C.1.3

CTUC Building Site—199 Armagh St.

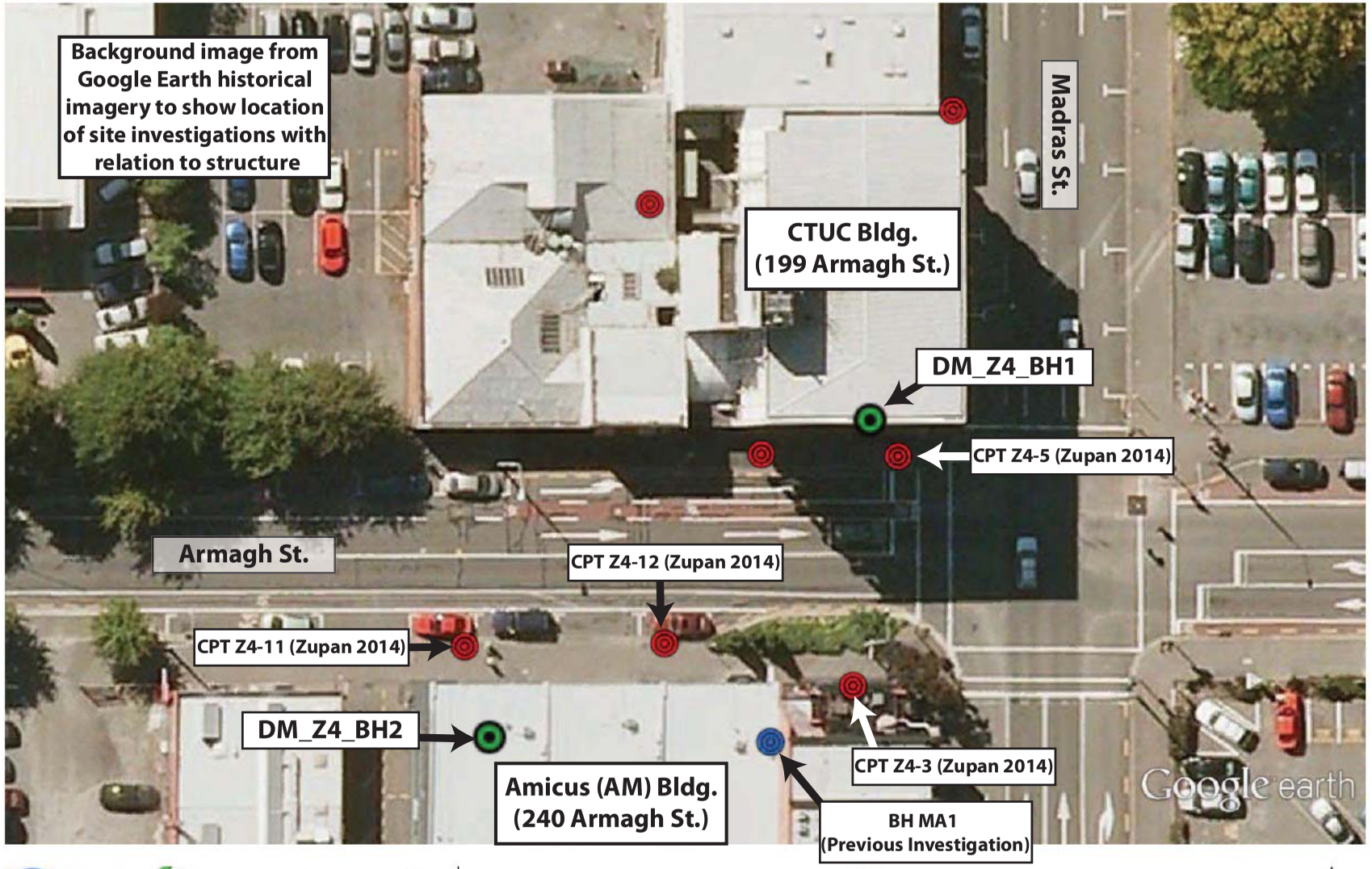
Background image from Google Earth historical imagery to show location of site investigations with relation to structure
Madras St.
CTUC Bldg. (199 Armagh St.)
DM_Z4_BH1
CPT Z4-5 (Zupan 2014)
Armagh St.
CPT Z4-12 (Zupan 2014)
CPT Z4-11 (Zupan 2014)
DM_Z4_BH2
CPT Z4-3 (Zupan 2014)
Amicus (AM) Bldg. (240 Armagh St.)
BH MA1 (Previous Investigation)
Google earth
Google earth
feet
meters
100
50

SOIL BORING LOG

Project No:	Boring Number
	DM_BH1

General Comments: **Page 1 of 4**

Project Name: CBD Project	**Location:** 199 Armagh St.
Elevation:	**Drilling Contractor:** McMillan
Drilling Method and Equipment:	Rotary wash mud drilling
Water Level: N/A	**Start/Finish:** April 10 to April 14, 2014
Loggers: Chris Markham	

Depth below Surface (m)	Sample: Interval	Sample: Number and Type	Sample: Recovery (m)		Soil Description (From extrusion of sample in lab and field observations during drilling)	Comments (Depth of Casing, Drilling Rate, Drilling Fluid Loss, Tests and Instrumentation)
1						
2						
3		D&M Sample 1U 2.15-2.6m	45cm (Full)		Sandy silt with some layering of sandier material (silty sand); Brown to grey; moist	Casing Depth: 1.2m bgs
		D&M Sample 2U 2.65-3.1m	45cm (Full)		silty sand (fine to med. Sand); brown to grey;	Casing Depth: 2.25m bgs
4		D&M Sample 3U 3.15-3.6m	45cm (Full)		silty sand; grey to brown	Casing Depth: 2.25m bgs
		D&M Sample 4U 3.65-4.1m	45cm (Full)		silty sand to primiarily sandy material with some silt (fine to med. Sand); dark grey to brown	Casing Depth: 2.705m bgs
5					Primarily sandy material with maybe some silt Transitioned to gravelly, much stiffer material	attempted to take D&M sample at 4.15m bgs but the tube crushed due to gravelly, firm soil within the stroke of the D&M tube
6						drilling mud lost due to gravelly material from about 5.5 to 6.0m bgs
7						

SOIL BORING LOG

Project No:	Boring Number
	DM_BH1

General Comments: **Page 2 of 4**

Project Name: CBD Project	**Location:** 199 Armagh St.
Elevation:	**Drilling Contractor:** McMillan
Drilling Method and Equipment:	Rotary wash mud drilling
Water Level: N/A	**Start/Finish:** April 10 to April 14, 2014
Loggers: Chris Markham	

Depth below Surface (m)	Sample: Interval	Sample: Number and Type	Sample: Recovery (m)		Soil Description (From extrusion of sample in lab)	Comments (Depth of Casing, Drilling Rate, Drilling Fluid Loss, Tests and Instrumentation)
8						
9						Lost driling fluid still at a depth of 8-8.5m bgs after we used sonic to get through some of the gravelly material
10						Attempted to tri-cone at a depth of about 9.9m bgs, but still lost drilling fluid due to pervious gravelly mat'l; had to revert back to sonic drilling
11						
12						Based on the sonic barrel samples from the sonic drilling, realized that we were in sandy material at about 11.7m bgs; started conventional mud rotary from this point onwards to obtain deeper samples
13		D&M Sample 6U 12.5-12.95m	45cm (Full)		Primarily wood and rootlets; some Cohesive, slightly to med. Plastic silt material	Organic material on tri-cone around 12.5m bgs Casing Depth: 11.445 m bgs Sample was much lighter in the field than previous samples, so could tell there was something different compared to other samples (wood)
14		D&M Sample 7U 13.5to 13.95m	45cm (Full)		Upper part of sample was silty sand, grey; lower part of sample was primarily cohesive silty material	Casing Depth: 11.445 m bgs Sample was much lighter in the field than previous samples, so could tell there was something different compared to other samples (wood)

SOIL BORING LOG

Project No:	Boring Number
	DM_BH1

General Comments: **Page 3 of 4**

Project Name: CBD Project	**Location:** 199 Armagh St.
Elevation:	**Drilling Contractor:** McMillan
Drilling Method and Equipment:	Rotary wash mud drilling
Water Level: N/A	**Start/Finish:** April 10 to April 14, 2014
Loggers: Chris Markham	

Depth below Surface (m)	Sample: Interval	Sample: Number and Type	Sample: Recovery (m)		Soil Description (From extrusion of sample in lab)	Comments: Depth of Casing, Drilling Rate, Drilling Fluid Loss, Tests and Instrumentation
15						Organic material still present at 15m bgs, as could be seen by cuttings coming to surface during ciruclation of drilling mud
16						
17						
18						
19						
20						
21						

SOIL BORING LOG

Project No:	Boring Number
	DM_BH1

General Comments: **Page 4 of 4**

Project Name: CBD Project	**Location:** 199 Armagh St.
Elevation:	**Drilling Contractor:** McMillan
Drilling Method and Equipment:	Rotary wash mud drilling
Water Level: N/A	**Start/Finish:** April 10 to April 14, 2014
Loggers: Chris Markham	

Depth below Surface (m)	Sample: Interval	Sample: Number and Type	Sample: Recovery (m)		Soil Description	Comments
					(From extrusion of sample in lab)	Depth of Casing, Drilling Rate, Drilling Fluid Loss, Tests and Instrumentation
22						Tri-cone getting clogged up at about 22m bgs due to cohesive, plastic material that looked and felt like clay; shells present
23		D&M Sample 8U 22.1-22.75m			Cohesive, plastic material at top of sample that felt like clay (upper 2-3cm); non-cohesive, silty material in lower part of sample; the soil had dried out quite a bit as it wasn't extruded until approx. 6-7 months after the sample was taken for sample 8U	Casing depth: 11.445m bgs no casing was advanced beyond sample 7U--i.e. boring was open holed to get sample 8U
24						
25						
26						
27						
28						

SOIL BORING LOG

Project No:	Boring Number
	DM_BH2

General Comments: **Page 1 of 1**

Project Name: CBD Project	**Location:** 240 Armagh St
Elevation:	**Drilling Contractor:** McMillan
Drilling Method and Equipment:	Rotary wash mud drilling
Water Level: N/A	**Start/Finish:** April 9 to April 10, 2014
Loggers: Chris Markham	

Depth below Surface (m)	Sample Interval	Sample Number and Type	Recovery (m)		Soil Description (From extrusion of sample in lab and field observations during drilling)	Comments (Depth of Casing, Drilling Rate, Drilling Fluid Loss, Tests and Instrumentation)
1						
		D&M Sample 1U 1.0-1.45m	45cm (Full)		sandy silt to silty sand; light brown; sample not very moist, though the soil had been in the tube 6-7 months prior to extrusion in the lab	No Casing used for first sample
		D&M Sample 2U 1.5-1.95m	45cm (Full)		sandy silt to silty sand; light brown; some rust color; sample not very moist, though the soil had been in the tube 6-7 months prior to extrusion in the lab	Casing Depth: 0.74m bgs
2		D&M Sample 3U 2.0-2.45m	45cm (Full)		Top of sample showed sandy silt to silty sand; grey	Casing Depth: 1.605m bgs
		D&M Sample 4U 1.5-1.95m	44.1cm			Casing Depth: 1.605m bgs
3		D&M Sample 5U 3.0-3.45m	44.6cm		Top part of sample showed sandy silt mat'l with some silty sand mat'l; brown, grey, and some rust color; Bottom part of sample was cohesive, med. Plastic silt (maybe clay??); smells like organics present; brown to grey	Casing Depth: 2.26m bgs
4						
		D&M Sample 6U 4.27-4.72m	44.9cm		Top of sample was primarily silty mat'l; grey with some rust/light brown coloring;	Casing Depth: 3.7m bgs
5		D&M Sample 7U 4.77-5..22m	44.1cm		Cohesive (some plasticity) silt; grey with some rust coloring; rootlets prevalent throughout sample	Casing Depth 4.235m bgs
		D&M Sample 8U 5.5-5.95m	45cm (Full)		Similar mat'l as 6U and 7U; cohesive with some plasticity silt; rootlets prevalent throughout the sample; soil primarily grey with some rust coloring	Casing Depth: 4.235m bgs
6		D&M Sample 9U 6.1-6.55m	45cm (Full)		primarily silt at top of specimen; grey with some rust coloring; Sandy silt to silty sand layers near bottomo of sample; rootlets prevalent throughout; brown/rust coloring prevalent throughout sample	Casing Depth: 5.745m bgs
		D&M Sample 10U 6.7-7.15m	44.6cm		Primarily silt sand with some sandy silt; grey;	Casing Depth: 5.745m bgs
7						

Appendix C.1.4

PWC Building Site—119 Armagh St.

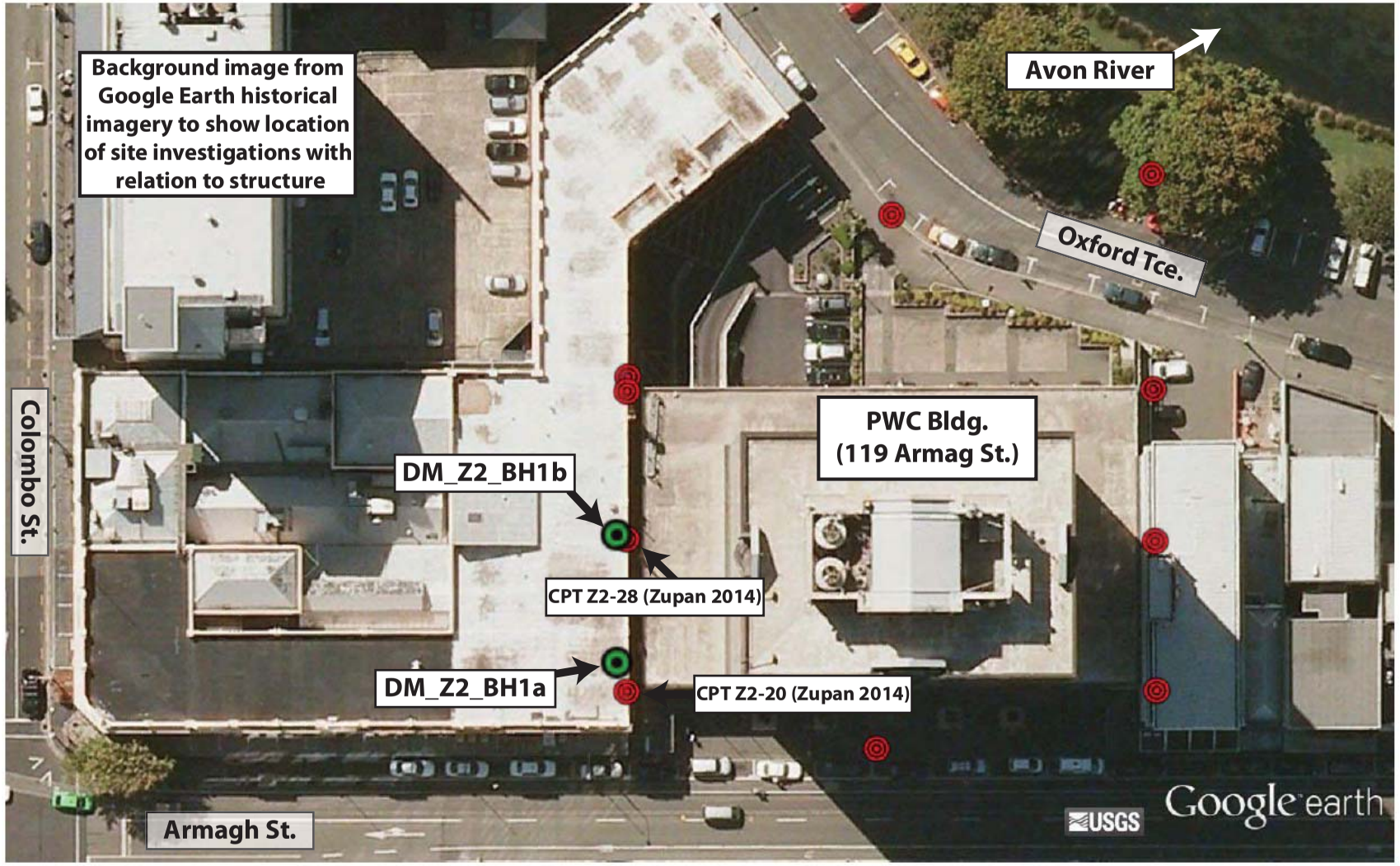

Google earth

feet 200

meters 70

SOIL BORING LOG

Project No:	Boring Number
	DM_BH1a

General Comments: **Page 1 of 3**

Project Name: CBD Project	**Location:** 119 Armagh St
Elevation:	**Drilling Contractor:** McMillan
Drilling Method and Equipment:	Rotary wash mud drilling and Sonic Drilling
Water Level: N/A	**Start/Finish:** June 9 to June 10, 2014
Loggers: Chris Markham	

Depth below Surface (m)	Sample: Interval	Sample: Number and Type	Sample: Recovery (m)		Soil Description (From extrusion of sample in lab)	Comments (Depth of Casing, Drilling Rate, Drilling Fluid Loss, Tests and Instrumentation)
1						
2		D&M Sample 1U 1.9-2..35m	43.8cm		debris (small pieces of concrete, brick, and gravel) at top and bottom of sample; Primarily silty sand; brown to grey	Casing Depth: 0.66m bgs
		D&M Sample 2U 2.4-2.85m	44.0cm		top 5cm (approx) of sample was rubble/debris, then about 12-13cm of silt with maybe some fine sand; the rest of the sample (bottom part) was silty sand, grey	Casing Depth: 0.66m bgs
3		Sonic Sample (collected in plastic liner) 2.85-8.85m			based on sonic sample, from 3.19-3.46m bgs, primarily a sandy mat'l, dark grey	Sonic Sampling was completed by advancing the sonic core barrel along with 4" casing to obtain samples in plastic liners; once the sonic sampling was completed, the 6" casing was able to be advanced via wash drilling to the end depth of the sonic sampling; sonic drilling was used to get through the thick layer of gravelly material from about 3m to about 9m
4					from 3.46 to about 6.0m bgs, the soil looked to be a gravelly sand to sandy gravel; a sieve analysis was completed on this mat'l--results still being processed	
5		Continuous sampling with each sample being about 1.52m in length				
6						
7						

SOIL BORING LOG

Project No:	Boring Number
	DM_BH1a

General Comments: **Page 2 of 3**

Project Name: CBD Project	**Location:** 119 Armagh St
Elevation:	**Drilling Contractor:** McMillan
Drilling Method and Equipment:	Rotary wash mud drilling and Sonic Drilling
Water Level: N/A	**Start/Finish:** June 9 to June 10, 2014
Loggers: Chris Markham	

Depth below Surface (m)	Sample: Interval	Sample: Number and Type	Sample: Recovery (m)		Soil Description (From extrusion of sample in lab)	Comments (Depth of Casing, Drilling Rate, Drilling Fluid Loss, Tests and Instrumentation)
8						
9						
10						
11		D&M Sample 3U attempted 10.45m				Casing Depth: 9.79m D&M Sample was attempted, but the tube crushed; still too gravelly and stiff to obtain a sample
12		D&M Sample 4U Skipped due to gravelly soil (too stiff)				
13						
14		D&M Sample 5U 13-13.45m	43.3cm		fine to med. sand (maybe some silt); sample still hasn't been extruded as of 10/29/14	Casing Depth: 12.75m (for 5U and 6U) Due to fall in the sampler had to be excessively pushed to get it to the target depth; also, casing only 0.25m above target depth instead of the minimum 0.3m
		D&M Sample 6U 13.5-13.95m	44.3cm		fine to med. sand (maybe some silt); sample still hasn't been extruded as of 10/29/14	when replacing free draining bottom cap in lab with non draining cap, the soil in the tube slid down about 3cm, which is unusual

SOIL BORING LOG

Project No:	Boring Number
	DM_BH1a

General Comments: **Page 3 of 3**

Project Name: CBD Project	**Location:** 119 Armagh St
Elevation:	**Drilling Contractor:** McMillan
Drilling Method and Equipment:	Rotary wash mud drilling and Sonic Drilling
Water Level: N/A	**Start/Finish:** June 9 to June 10, 2014
Loggers: Chris Markham	

Depth below Surface (m)	Sample: Interval	Sample: Number and Type	Sample: Recovery (m)		Soil Description (From extrusion of sample in lab)	Comments (Depth of Casing, Drilling Rate, Drilling Fluid Loss, Tests and Instrumentation)
15		D&M Sample 7U 14.0-14.45m	41.8cm		fine to med. sand (maybe some silt); light brown to grey	Casing Depth: 12.75m bgs
16						
17						
18						
19						
20						
21						

SOIL BORING LOG

Project No:	Boring Number
	DM_BH1b

General Comments: **Page 1 of 3**

Project Name: CBD Project	**Location:** 119 Armagh St
Elevation:	**Drilling Contractor:** McMillan
Drilling Method and Equipment:	Rotary wash mud drilling and Hollow Stem Auger
Water Level: N/A	**Start/Finish:** Sept. 30 to Oct 1, 2014
Loggers: Chris Markham	

Depth below Surface (m)	Sample: Interval	Sample: Number and Type	Sample: Recovery (m)		Soil Description (From extrusion of sample in lab)	Comments (Depth of Casing, Drilling Rate, Drilling Fluid Loss, Tests and Instrumentation)
1						The hole was hand cleared down to 1.34m bgs and 6" casing was placed in the hole and advanced a minimial distance to allow for mud to be used to weight the hole so that samples could be taken; original target depth for sample was 1.1m but debris present down to 1.34m bgs so that
2		D&M Sample 1U 1.5-1.95m	45.0cm (Full)		top part of sample contained layers of primarily silty mat'l and layers of sandy silt to silty sand; light brown with some rust coloring; bott. part of sample contained similar mat'l to top part of sample	Casing Depth: N/A
3		D&M Sample 2U 1.95-2.4m	26.3cm		silty sand to sandy silt; light brown to grey	Casing Depth: N/A After sample 2U was taken, hollow stem auger was advanced to a depth of approximately 9.5-10.0 m bgs; the hollow stem auger was then reversed (pulled up) while backfilling the hole with sand that was brought to the site; in the end, the gravelly soil present from about 2.2-2.4m bgs to about 9-9.5m bgs was replaced with sand so that mud rotary could be used without sonic drilling to obtain samples of the sandy soil below the gravel
4						
5						
6						
7						

SOIL BORING LOG

Project No:	Boring Number
	DM_BH1b

General Comments: **Page 2 of 3**

Project Name: CBD Project	**Location:** 119 Armagh St
Elevation:	**Drilling Contractor:** McMillan
Drilling Method and Equipment:	Rotary wash mud drilling and Hollow Stem Auger
Water Level: N/A	**Start/Finish:** Sept. 30 to Oct 1, 2014
Loggers: Chris Markham	

Depth below Surface (m)	Sample Interval	Sample Number and Type	Sample Recovery (m)		Soil Description (From extrusion of sample in lab)	Comments (Depth of Casing, Drilling Rate, Drilling Fluid Loss, Tests and Instrumentation)
8						
9						
10						
11						
12						
13		D&M Sample 3U 12.5-12.95m	43.8cm		primarily sand (maybe some silt); grey; med. to fine	Casing Depth: 11.9m bgs
		D&M Sample 4U 13-13.45m	40.8cm		primarily sand (maybe some silt); grey; med. to fine wood at bottom of the sample	Casing Depth: 11.9m bgs wood at the bottom of the sample caused the tube to crush during sampling
14		D&M Sample 5U 13.5-13.95m	45.0cm (Full)		primarily sand (maybe some silt); grey to light brown; med. to fine	Casing Depth: 13.0m bgs

SOIL BORING LOG

Project No:	Boring Number
	DM_BH1b

General Comments: **Page 3 of 3**

Project Name: CBD Project	**Location:** 119 Armagh St
Elevation:	**Drilling Contractor:** McMillan
Drilling Method and Equipment:	Rotary wash mud drilling and Hollow Stem Auger
Water Level: N/A	**Start/Finish:** Sept. 30 to Oct 1, 2014
Loggers: Chris Markham	

Depth below Surface (m)	Sample: Interval	Sample: Number and Type	Sample: Recovery (m)		Soil Description (From extrusion of sample in lab)	Comments (Depth of Casing, Drilling Rate, Drilling Fluid Loss, Tests and Instrumentation)
15		D&M Sample 6U 14.0-14.45m	45.0cm (Full)		primarily sand (maybe some silt); grey to light brown; med. to fine	Casing Depth: 13.4m bgs
		D&M Sample 6U 14.5-14.95m	45.0cm (Full)		silty sand (more silty than samples above it); light brown to grey	Casing Depth: 13.4m bgs
16						
17						
18						
19						
20						
21						

Appendix C.1.5

VT Building Site—90 Armagh St.

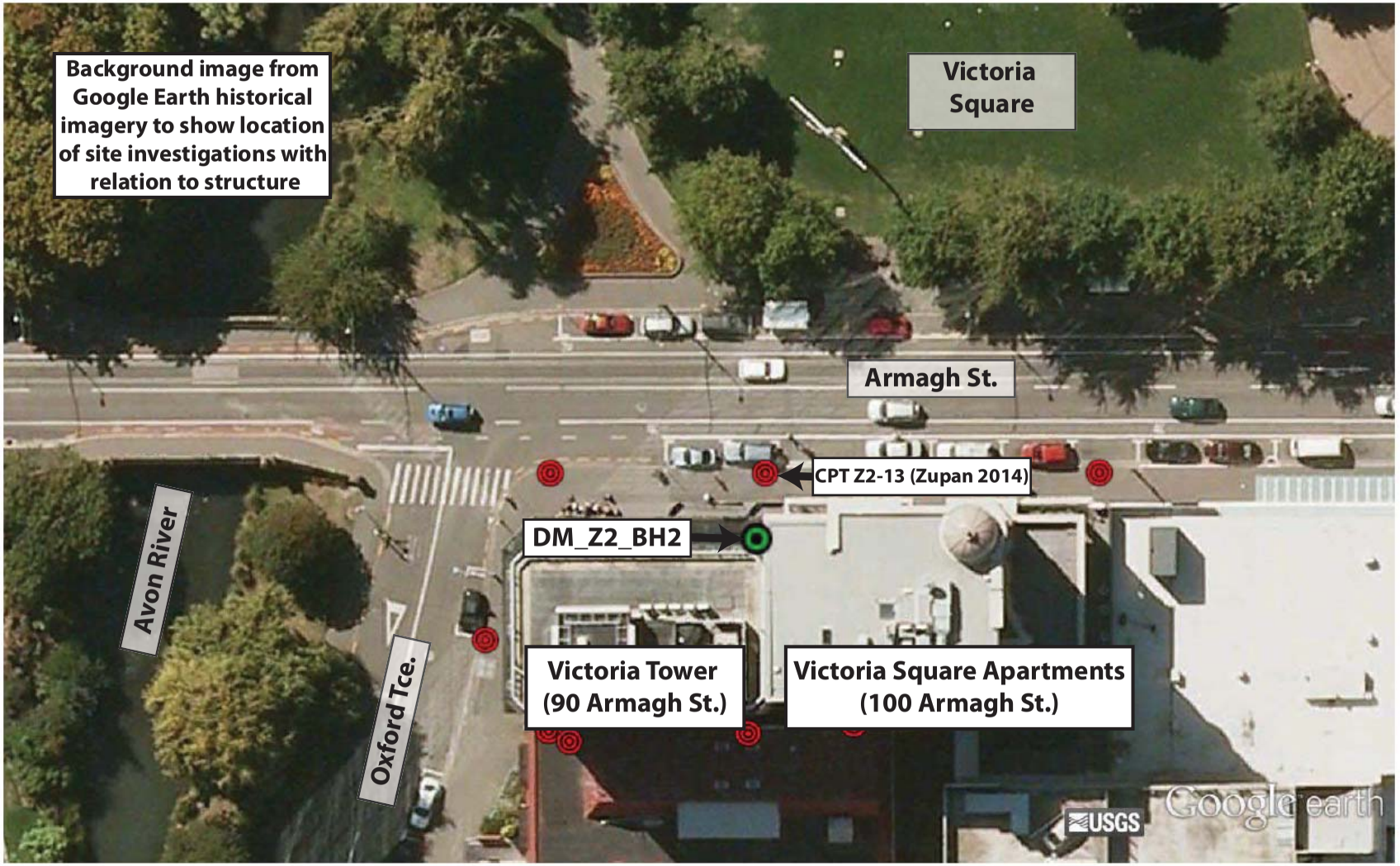

Google earth

feet 200
meters 60

SOIL BORING LOG

Project No:	Boring Number
	DM_BH2

General Comments: **Page 1 of 2**

Project Name: CBD Project	**Location:** 119 Armagh St
Elevation:	**Drilling Contractor:** McMillan
Drilling Method and Equipment:	Rotary wash mud drilling and Hollow Stem Auger
Water Level: N/A	**Start/Finish:** Jun 12 to Jun 16, 2014
Loggers: Chris Markham	

Depth below Surface (m)	Sample: Interval	Sample: Number and Type	Sample: Recovery (m)		Soil Description (From extrusion of sample in lab or observations in the field)	Comments (Depth of Casing, Drilling Rate, Drilling Fluid Loss, Tests and Instrumentation)
1						Used Sonic drilling to get through the upper gravelly soil; also had some concrete from previous foundation in the upper ~1.5m - 3m; wood debris was also present in the upper part of the subsurface and at deeper parts (see below)
						this hole was the first hole where drilling mud and the drilling rods were used to advance sampler; prior to this used water and different rods (similar to GP set-up); used this technique from here on
2						Did not get good recovery until sonic sample at 2.82 m; debris etc.
3						
						hit something hard that made drilling very difficult at ~3 m (debris, old foundation, wood?)
4						
					gravelly sand from ~4.3 to 5.0 m	inner plastic liner in sonic sampler was warped inside sampler for sonic samples from 4.34 to 5.86 m and 5.86 to 6.5 m; could not get liner out of tube and had to vibrate material out of core barrel and then pull platic liner out separately
5					sandy gravel from ~5 to 5.9 m	
6					sandy gravel from ~5.9 to 6.3 m	
					Silty sand from 6.3 to 6.5 m	
7						

SOIL BORING LOG

Project No:	Boring Number
	DM_BH2

General Comments: **Page 2 of 2**

Project Name: CBD Project	**Location:** 90 Armagh St
Elevation:	**Drilling Contractor:** McMillan
Drilling Method and Equipment:	Rotary wash mud drilling
Water Level: N/A	**Start/Finish:** Jun 12 to Jun 16, 2014
Loggers: Chris Markham	

Depth below Surface (m)	Sample: Interval	Sample: Number and Type	Sample: Recovery (m)		Soil Description (From extrusion of sample in lab)	Comments (Depth of Casing, Drilling Rate, Drilling Fluid Loss, Tests and Instrumentation)
8		D&M Sample 1U 7.1-7.55m	45cm (Full)		Wood at bottom of specimen from 7.2 to 7.34 m Some wood for specimen from 7.37 to 7.51 m but able to test; fine sand, dark grey with some silt	Casing Depth: 6.8m
		D&M Sample 2U 7.6-8.05m	44.8cm		Fine sand; grey	Casing Depth: 6.8m
9						
		D&M Sample 3U 9-9.45m	N/A			Casing Depth: 8.65m No sample actually attempted at this point due to presence of gravels (could tell from drilling resistance); kept sample numbering so showing as place holder
10						Found some wood at about 9.8m
		D&M Sample 4U 10.2-10.65m	N/A			Casing Depth: 9.72m Tube crushed; no recovery; either due to wood or gravel
11		D&M Sample 5U 11-11.45m	44.1cm		specimen from 11.1 to 11.24 m of too poor quality to test silty sand from 11.25 to 11.39 m specimen; grey	Casing Depth: 9.72m
		D&M Sample 6U 11.5-11.95	N/A		sand with maybe some silt; dark grey (field observation)	Casing Depth: 9.72m tube crushed; probably from hiting wood because found piece of wood at bottom of tube; no recovery--bagged sample
12		D&M Sample 7U 12-12.45m	N/A		sand with maybe some silt (field observation)	Casing Depth: 9.72m very little recovery so just bagged sample
		D&M Sample 8U 12.55-13m	N/A		mostly sand	Casing Depth: 9.72m hydraulic pressure during sampler advancement got very high; tube crushed and sampler head became stuck in D&M sampler; switched out Deme's sampler for UCB sampler with o-rings on sampler instead of split seals
13		D&M Sample 9U 13.1-13.55m	40.8cm		specimen too poor to test from 13.2 to 13.34 m; grey sand; fine to almost medium particles	Casing Depth: 9.72m
		D&M Sample 10U 13.6-14.05m	44.8cm		grey, fine sand for 13.7 to 13.74 m grey fine sand for 13.85 to 13.99 m	Casing Depth: 9.72m
14						

Appendix C.1.6

LS-II Building Site—48 Lismore St.

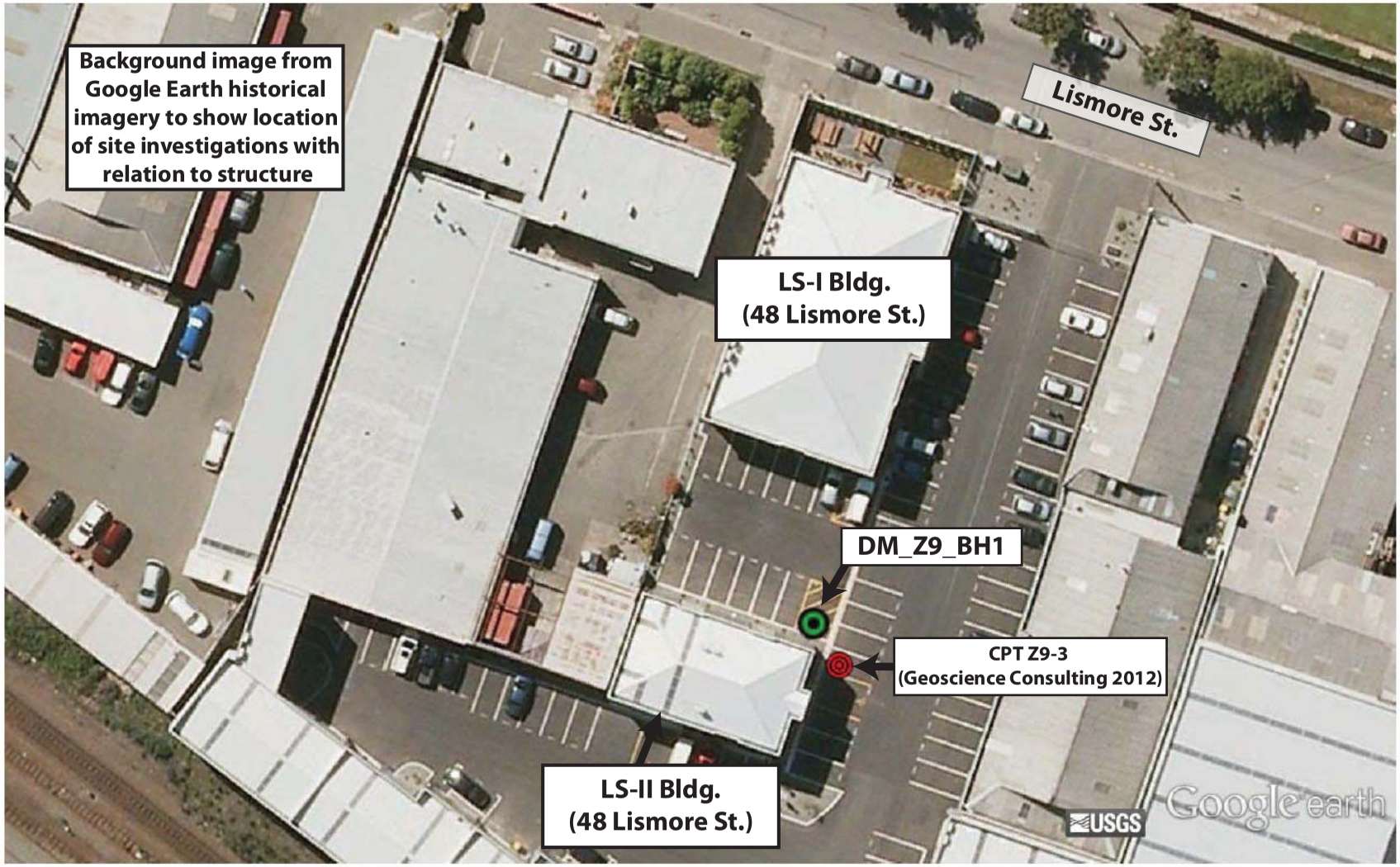

Google earth

feet 200

meters 70

SOIL BORING LOG

Project No:	Boring Number
	DM_BH1

General Comments: **Page 1 of 2**

Project Name: CBD Project	**Location:** 48 Lismore St. (Unit 2)
Elevation:	**Drilling Contractor:** McMillan
Drilling Method and Equipment:	Rotary wash mud drilling
Water Level: N/A	**Start/Finish:** Sept. 29, 2014
Loggers: Chris Markham	

Depth below Surface (m)	Sample: Interval	Sample: Number and Type	Sample: Recovery (m)		Soil Description (From extrusion of sample in lab)	Comments (Depth of Casing, Drilling Rate, Drilling Fluid Loss, Tests and Instrumentation)
1						
2		D&M Sample 1U 1.5-1.95m	45 cm (Full)			Casing Depth: 1.15m bgs
		D&M Sample 2U 2-2.45m	45 cm (Full)			Casing Depth: 1.15m bgs
3		D&M Sample 3U 2.5-2.95m	45 cm (Full)			Casing Depth: 2.2m bgs
4						
5		D&M Sample 4U 4.1-4.55m	45 cm (Full)			Casing Depth: 3.7m bgs some wood on tri-cone right above this sample may have some wood in sample
		D&M Sample 5U 5-5.45m	45 cm (Full)			Casing Depth: 4.15m bgs
6		D&M Sample 6U 5.64-6.09m	41.8cm			Casing Depth: 5.2m bgs
		D&M Sample 7U 6.1-6.55m	40.1cm			Casing Depth: 5.65m bgs Tube crushed at bottom some loss of drilling mud above this sample during drilling
7						

SOIL BORING LOG

Project No:	Boring Number
	DM_BH1

General Comments: **Page 2 of 2**

Project Name: CBD Project	**Location:** 48 Lismore St. (Unit 2)
Elevation:	**Drilling Contractor:** McMillan
Drilling Method and Equipment:	Rotary wash mud drilling
Water Level: N/A	**Start/Finish:** Sept. 29, 2014
Loggers: Chris Markham	

Depth below Surface (m)	Sample: Interval	Sample: Number and Type	Sample: Recovery (m)		Soil Description (From extrusion of sample in lab)	Comments (Depth of Casing, Drilling Rate, Drilling Fluid Loss, Tests and Instrumentation)
8						
9						Target depth for Sample 8U was 8.5m bgs; at about 8.3m bgs the drill rods started to "jump"; this was most likely due to the presense of gravelly soils at this depth, which was not evident from the CPT data; this very stiff material was encountered to a depth of 10.1m bgs, which is where it was decided to end the borehole; samples 8U-10U were unable to be taken due to the presence of this very stiff material
10						the sonic core barrel was lowered down the hole to attempt to "grab" some of this material to identify it; almost no material was retrieved as it was too difficult to advance the barrell through the stiff soil; a couple of very small (3-5mm) gravel pieces were retrieved by the barrell
11						
12						
13						
14						

Appendix C.1.7

SA Building Site—193 Peterborough St.

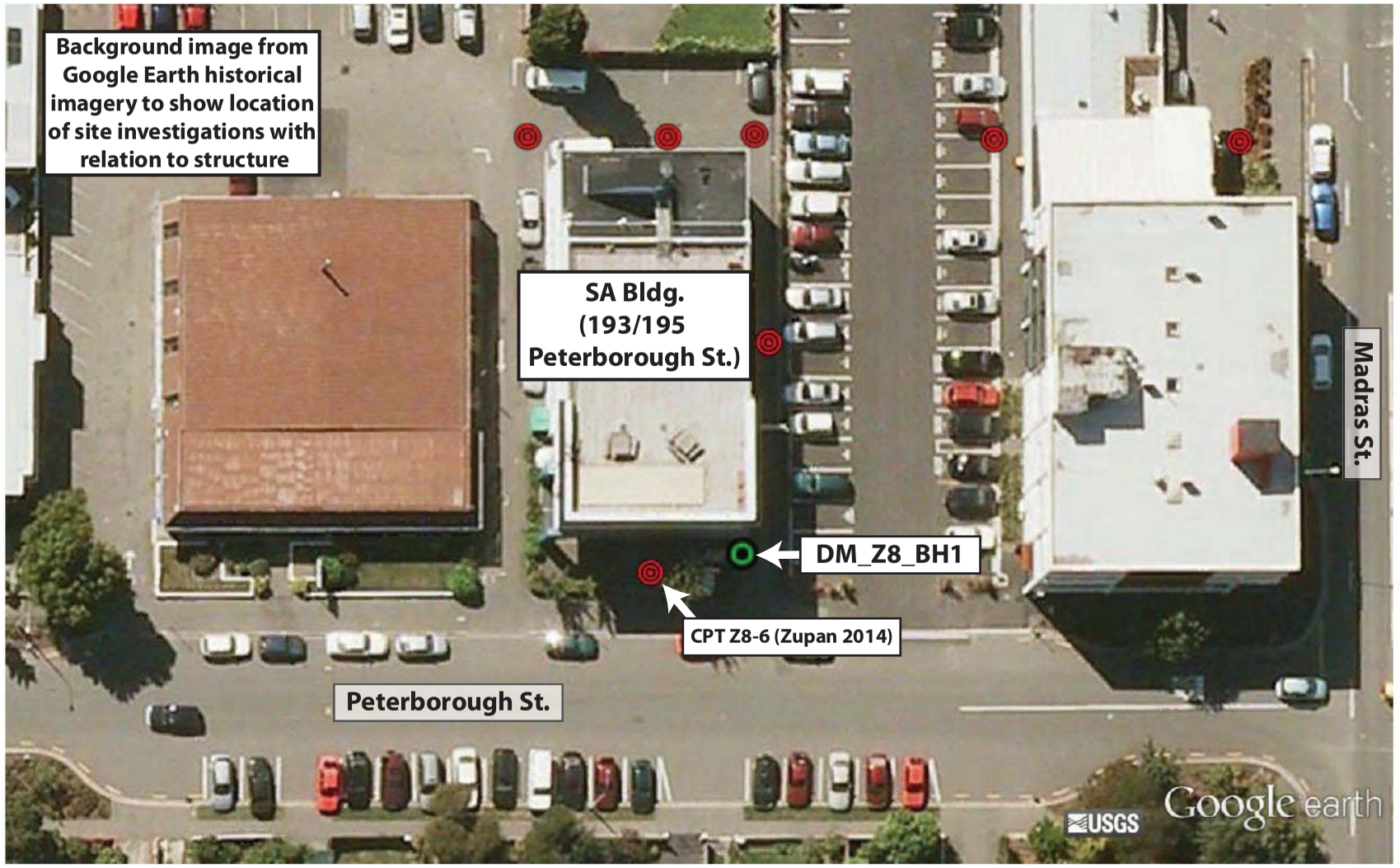

Google earth

feet 100

meters 50

SOIL BORING LOG

Project No:	Boring Number
	DM_BH1

General Comments: **Page 1 of 1**

Project Name: CBD Project
Location: 193/195 Peterborough St
Elevation:
Drilling Contractor: McMillan
Drilling Method and Equipment: Rotary wash mud drilling
Water Level: N/A
Start/Finish: October 15, 2014
Loggers: Chris Markham

Depth below Surface (m)	Sample Interval	Sample Number and Type	Sample Recovery (m)		Soil Description (From extrusion of sample in lab and field observations during drilling)	Comments (Depth of Casing, Drilling Rate, Drilling Fluid Loss, Tests and Instrumentation)
1						
2		D&M Sample 1U 1.5-1.95 m	44.3cm		poor quality specimen with sandy silt in top 2/3 and silty sand in bottom 1/3 of specimen and split at transition for 1.6 to 1.74 m silty sand; light brown to grey; med to fine for specimen 1.75 to 1.89 m	Casing Depth: 1.15 m bgs small pieces of gravel in tri-cone above 2U
3		D&M Sample 2U 1.97 to 2.42m	33.3cm		specimen from 2.07 to 2.21 m had sandy with some silt in upper half of specimen and primarily silt in bottom half of specimen; only specimen that could be obtained from this tube so not tested	Casing Depth: 1.15 m bgs sample advanced but then maxed out the hydraulic pressure of the rig; probably hit gravelly or very hard soil; recovered soil in upper part of tube loss of drilling mud through gravels starting at 2.2-2.3 m
4						sonic sampling (did not take samples) through gravelly soil till about 6.0 m
5						
6						
7		D&M Sample 3U 6 to 6.45m	N/A		silty sand; dark grey (field observation)	Casing Depth: 5.26 m bgs tube crushed due to gravels; expected to see sandy material at this depth based on CPT but turned out to be much stiffer started hitting gravel at 6.2 m and decided to end drilling on this hole as we were already deeper than the material of interest

Appendix C.2

Processed Undisturbed CTX Test Results

The following corrections were made to the triaxial test data presented in Appendices C.2 and C.3:

Membrane correction

Axial stresses were corrected for loads carried by the membrane (i.e., not the soil) in both cyclic and monotonic triaxial tests using the following equation proposed by Duncan and Seed (1967):

$$\Delta\sigma_{ax-m} = -C_{am} * \left(\frac{2}{3}\right) * E_m \frac{4t_{om}}{D_{os}}$$

Where $\Delta\sigma_{ax\text{-}m}$ is the portion of the applied stress attributed to the membrane,

$$C_{am} = \left(\frac{1 + 2\varepsilon_{at} - \sqrt{\frac{1-\varepsilon_v}{1-\varepsilon_{at}}}}{1-\varepsilon_v}\right)$$

E_m is the Young's modulus of the membrane (assumed as 14 kg/cm^2=1373.4 kPa)
t_{om} is the initial thickness of the membrane prior to testing
D_{os} is the initial diameter of the specimen prior to testing
ε_{at} is the total axial strain during the test
ε_{vol} is the total volumetric strain during the test

Because of the negative sign in the calculation of $\Delta\sigma_{ax\text{-}m}$, this values should be added to the total applied stress if positive ε_{ax} represents compression (i.e., the specimen gets shorter) and negative ε_{ax} represents extension (i.e., the specimen gets taller). In this way, the axial stress being applied to the actual soil is less than the total axial stress being applied to the specimen and membrane in compression (i.e., $\Delta\sigma_{ax\text{-}m}$ is negative) and higher than the total axial stress in extension (i.e., $\Delta\sigma_{ax\text{-}m}$ is positive).

Area Correction

CTX and monotonic triaxial testing was completed using the CKC electropneumatic triaxial device with the Automated Triaxial Testing System software developed by Li et al. (1998). This software automatically applies an area correction based on the assumption that the soil specimen deforms as a right cylinder during testing, which allows for an axial stress calculation based on this corrected area.

Appendix C.2.1

Christchurch Town Hall (CTH) Site—86-100 Kilmore St.

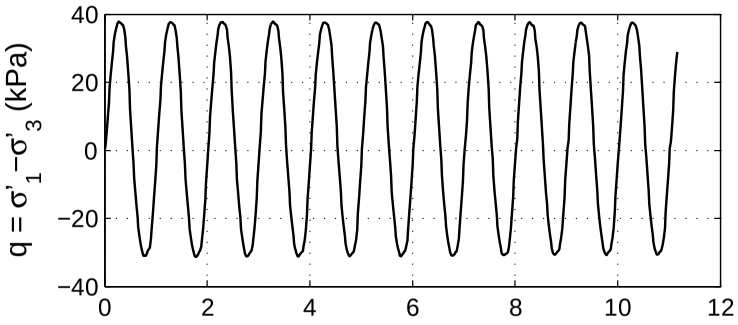

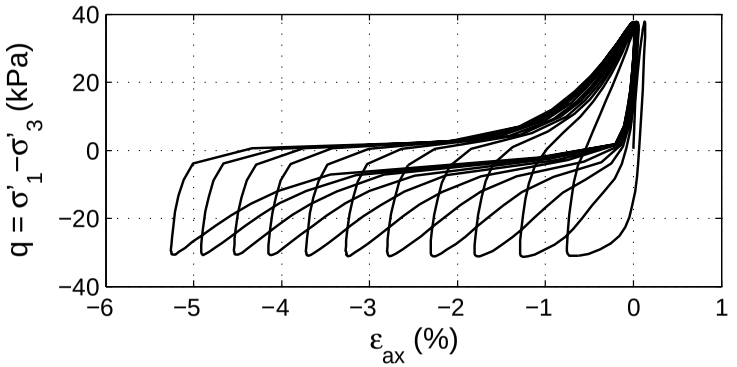

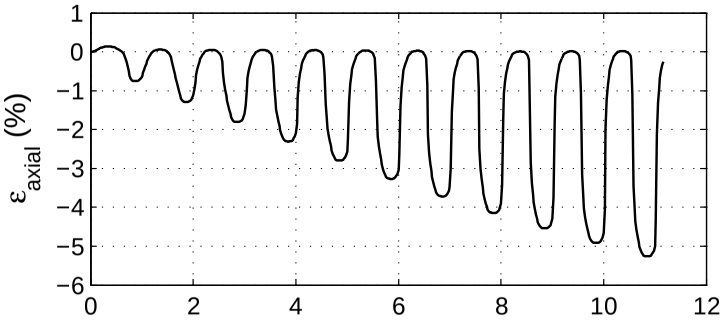

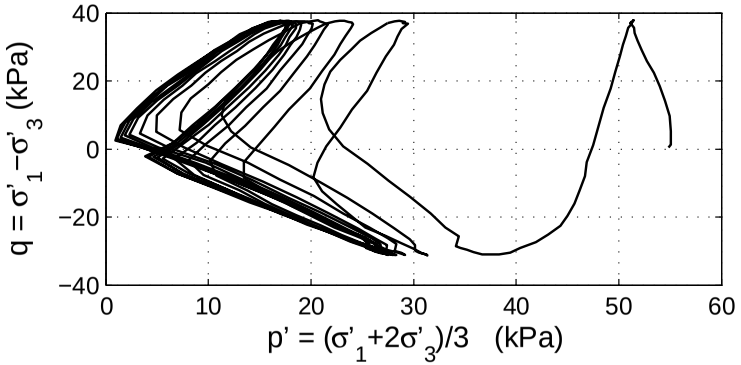

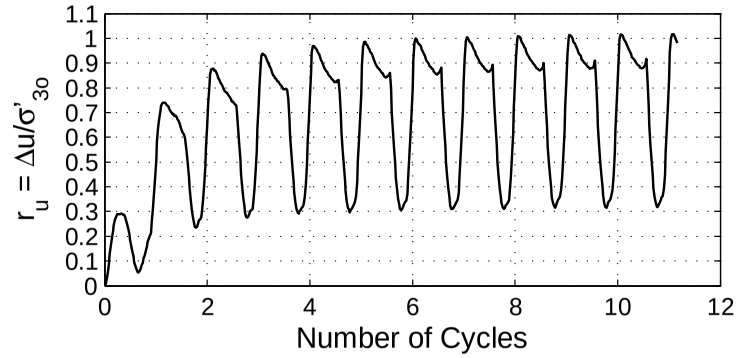

Specimen & Isotropic Cyclic Triaxial Test Data

Site:	86 Kil. St	**Loading Freq (Hz):**	0.1
Borehole:	DM BH1	**B−Value:**	0.985
Sample No.:	3U	**CSR:**	0.316
Sampler Type:	D&M	**N to $\varepsilon_{Ax-S.A.}$=3%:**	6
Spec. Depth (m):	3.07	**N to $\varepsilon_{Ax-D.A.}$=5%:**	11
Date Tested:	05/26/14	**Post−Cyclic Test:**	−−
Date Sampled:	05/05/14		
Spec. Ht. (mm):	139.5		
Spec. Diam. (mm):	60.9		
Dry Mass (g):	635.40		
Gs:	2.69		
e_o:	0.72		
σ'_{3o} (kPa):	54.7		
PI (%):	4		
USCS:	ML		

Isotropic Consolidation Test

Site:	86 Kil. St
Borehole:	DM BH1
Sample No.:	3U
Sampler Type:	D&M
Spec. Depth (m):	3.07
Date Tested:	05/26/14
Date Sampled:	05/05/14

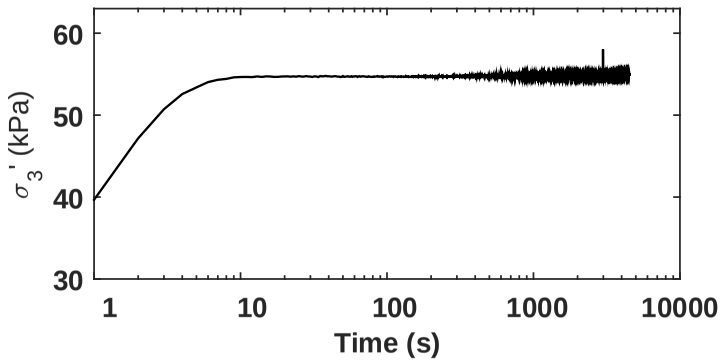

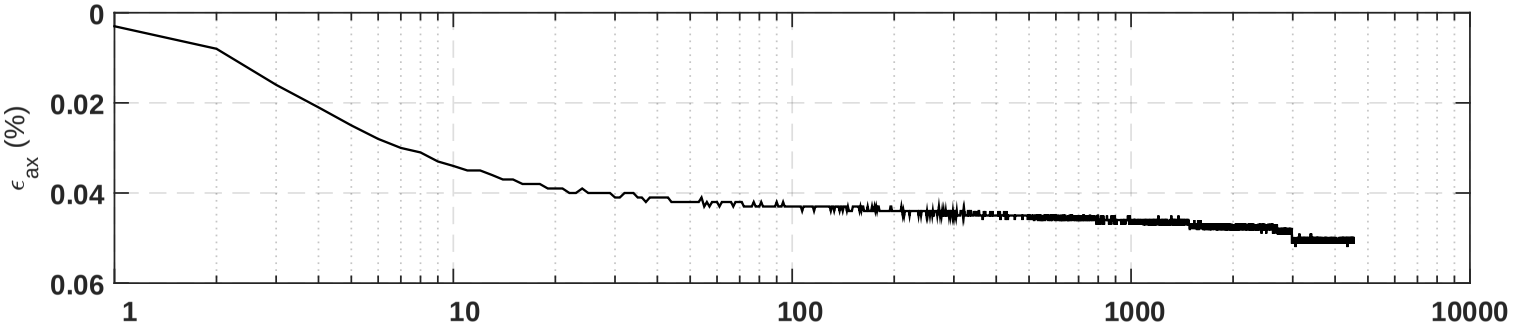

Post CTX Reconsolidation Test

Site:	86 Kil. St
Borehole:	DM BH1
Sample No.:	3U
Sampler Type:	D&M
Spec. Depth (m):	3.07
Date Tested:	05/26/14
Date Sampled:	05/05/14

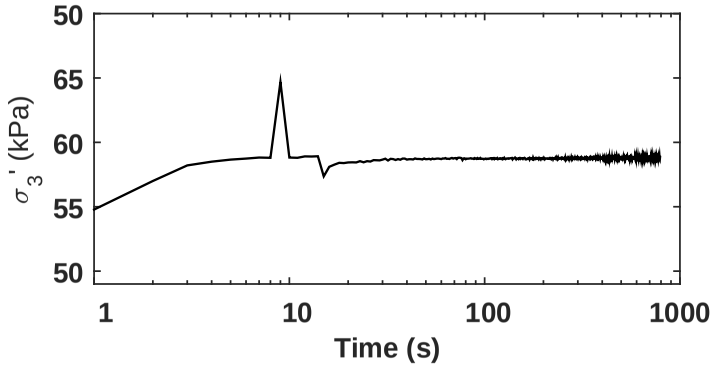

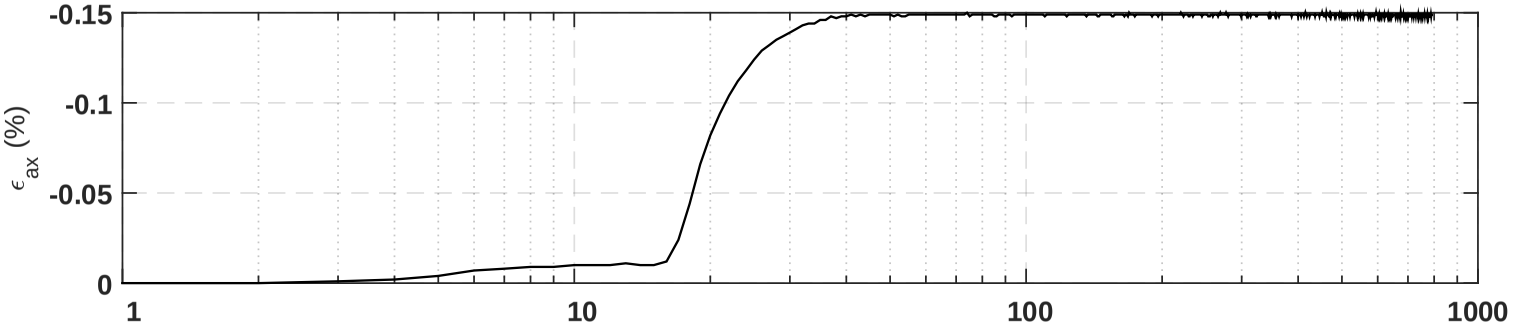

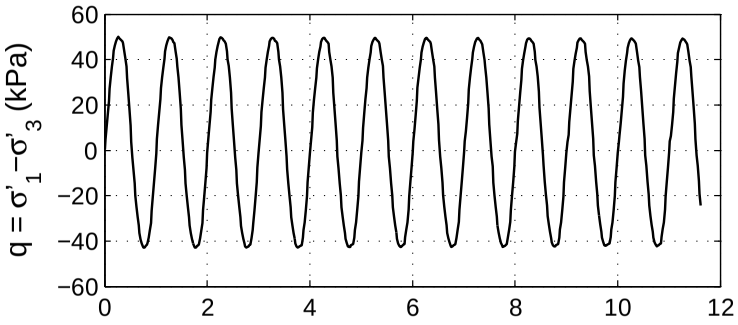

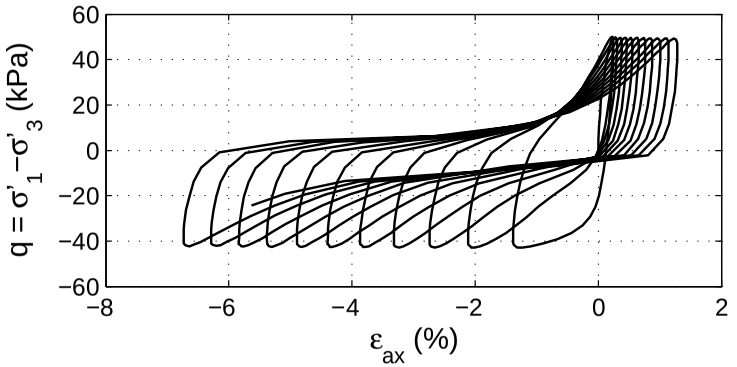

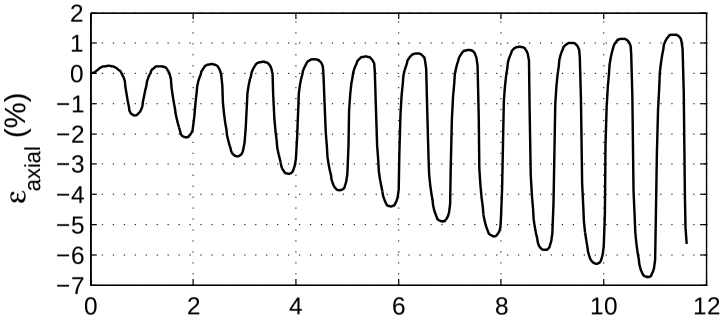

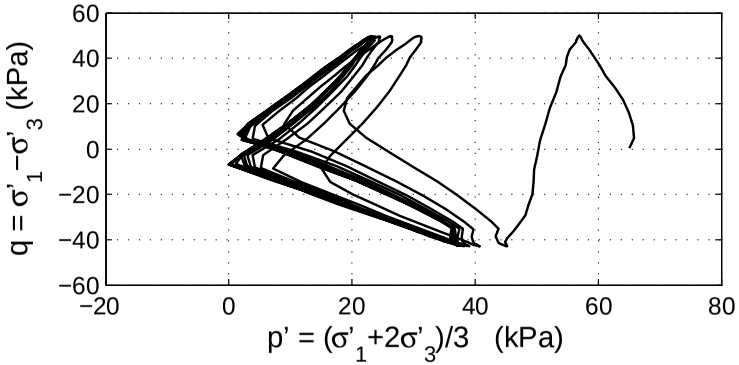

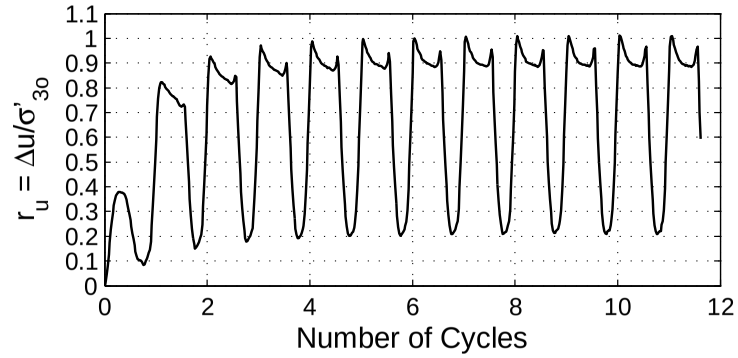

Specimen & Isotropic Cyclic Triaxial Test Data

Site:	86 Kil. St	**Loading Freq (Hz):**	0.1
Borehole:	DM BH1	**B−Value:**	0.994
Sample No.:	3U	**CSR:**	0.356
Sampler Type:	D&M	**N to $\varepsilon_{Ax-S.A.}$=3%:**	4
Spec. Depth (m):	3.23	**N to $\varepsilon_{Ax-D.A.}$=5%:**	6.5
Date Tested:	05/27/14	**Post−Cyclic Test:**	−−
Date Sampled:	05/05/14		
Spec. Ht. (mm):	142.7		
Spec. Diam. (mm):	60.9		
Dry Mass (g):	635.78		
Gs:	2.7		
e_o:	0.77		
σ'_{3o} (kPa):	64.9		
PI (%):	−−		
USCS:	−−		

Isotropic Consolidation Test

Site:	86 Kil. St
Borehole:	DM BH1
Sample No.:	3U
Sampler Type:	D&M
Spec. Depth (m):	3.23
Date Tested:	05/27/14
Date Sampled:	05/05/14

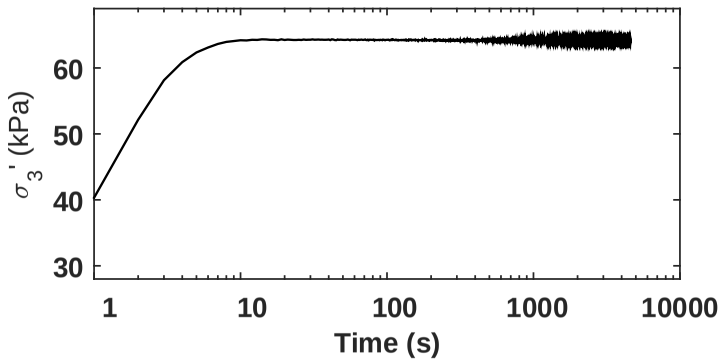

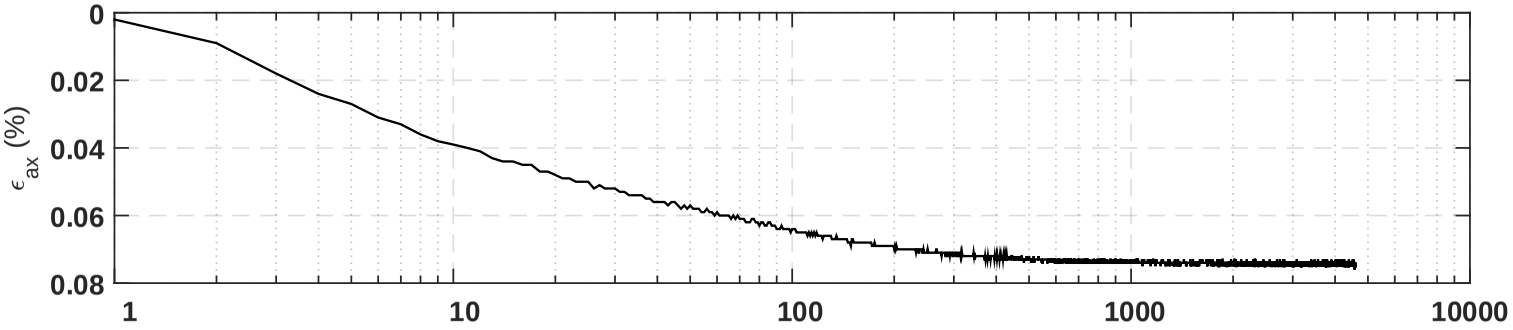

Post CTX Reconsolidation Test

Site:	86 Kil. St
Borehole:	DM BH1
Sample No.:	3U
Sampler Type:	D&M
Spec. Depth (m):	3.23
Date Tested:	05/27/14
Date Sampled:	05/05/14

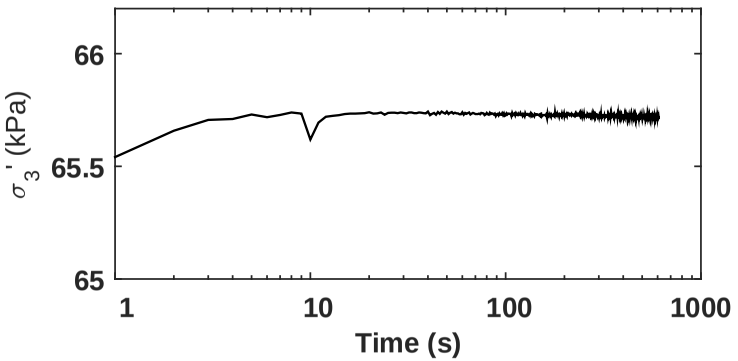

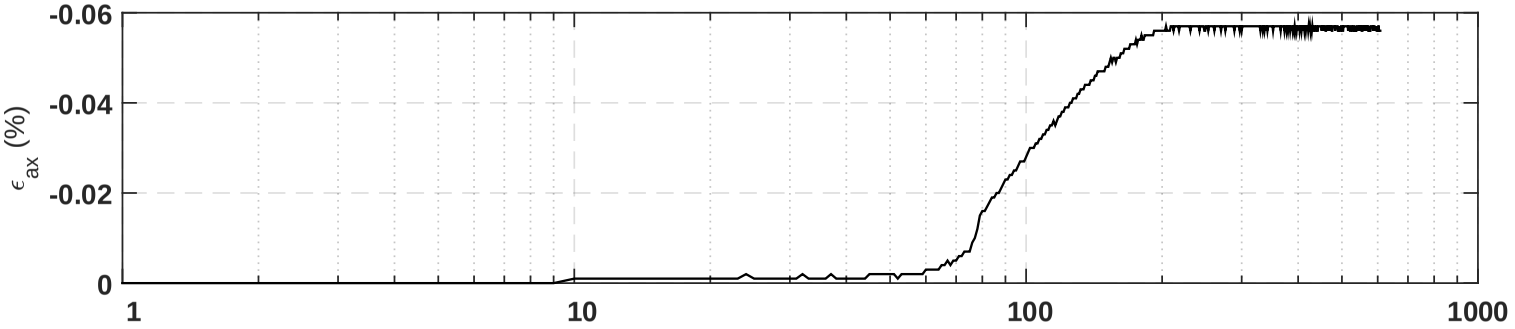

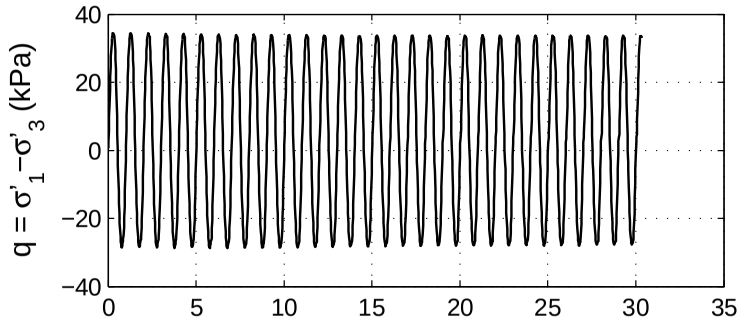

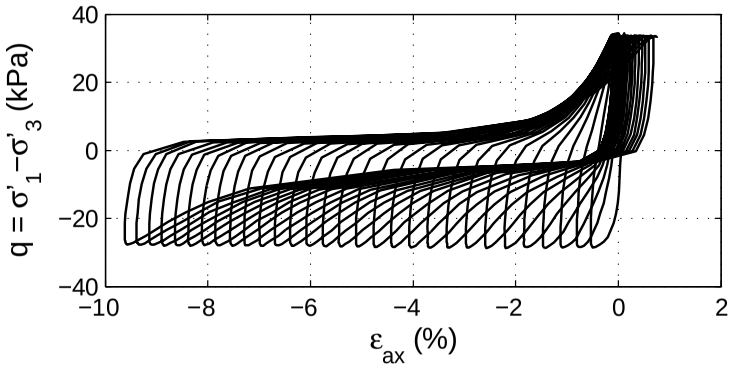

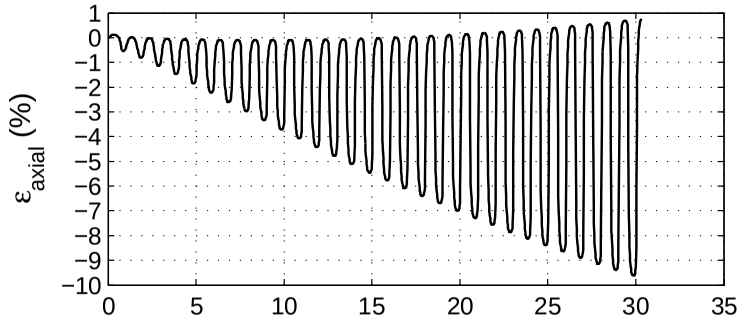

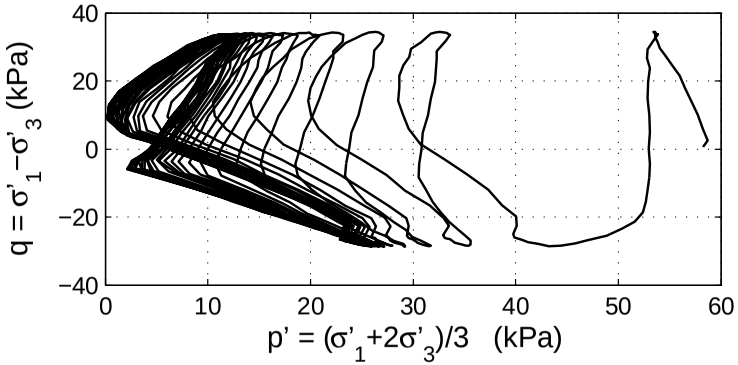

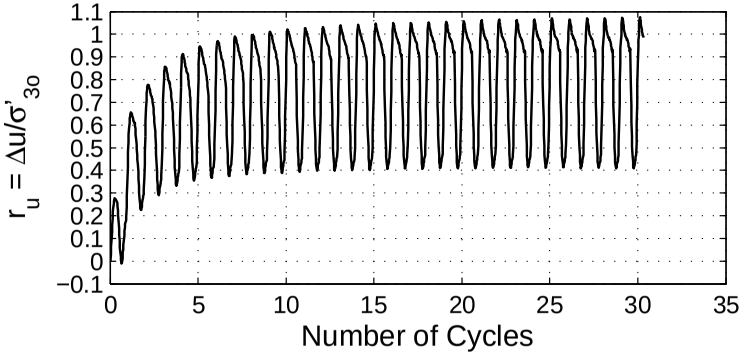

Specimen & Isotropic Cyclic Triaxial Test Data

Site:	86 Kil. St	**Loading Freq (Hz):**	0.1
Borehole:	DM BH1	**B−Value:**	0.990
Sample No.:	4U	**CSR:**	0.269
Sampler Type:	D&M	**N to $\varepsilon_{Ax-S.A.}$=3%:**	9
Spec. Depth (m):	3.67	**N to $\varepsilon_{Ax-D.A.}$=5%:**	14
Date Tested:	05/28/14	**Post−Cyclic Test:**	−−
Date Sampled:	05/06/14		
Spec. Ht. (mm):	139.8		
Spec. Diam. (mm):	60.9		
Dry Mass (g):	608.10		
Gs:	2.69		
e_o:	0.80		
σ'_{3o} (kPa):	58.0		
PI (%):	4		
USCS:	ML		

Isotropic Consolidation Test

Site:	86 Kil. St
Borehole:	DM BH1
Sample No.:	4U
Sampler Type:	D&M
Spec. Depth (m):	3.67
Date Tested:	05/28/14
Date Sampled:	05/06/14

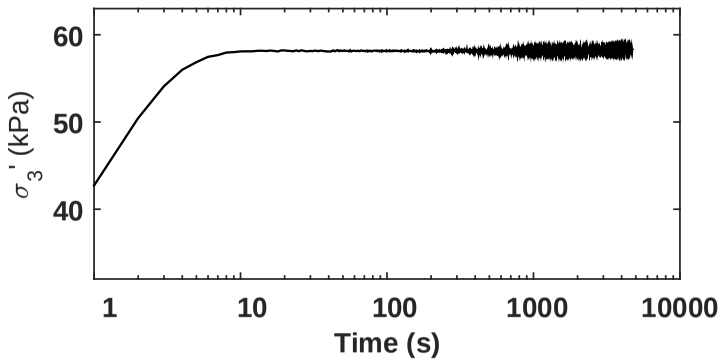

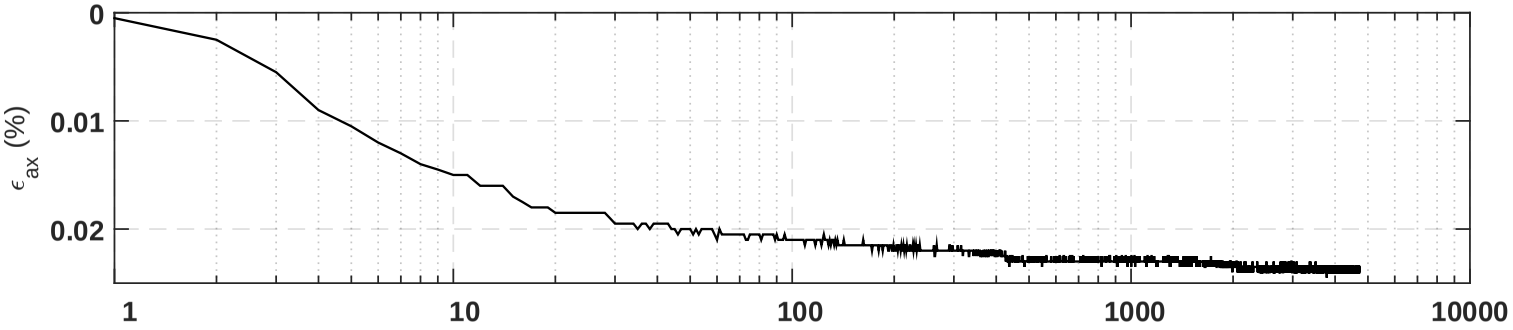

Post CTX Reconsolidation Test

Site:	86 Kil. St
Borehole:	DM BH1
Sample No.:	4U
Sampler Type:	D&M
Spec. Depth (m):	3.67
Date Tested:	05/28/14
Date Sampled:	05/06/14

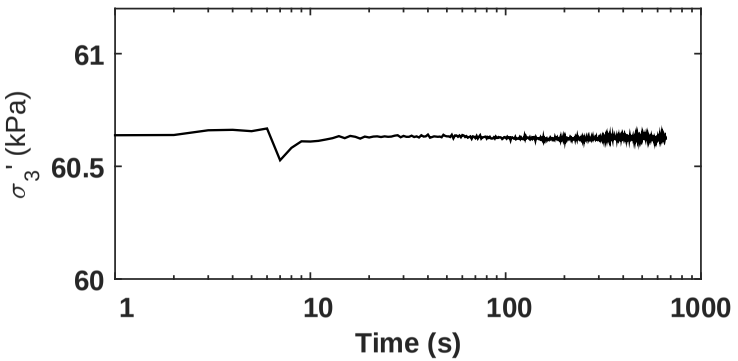

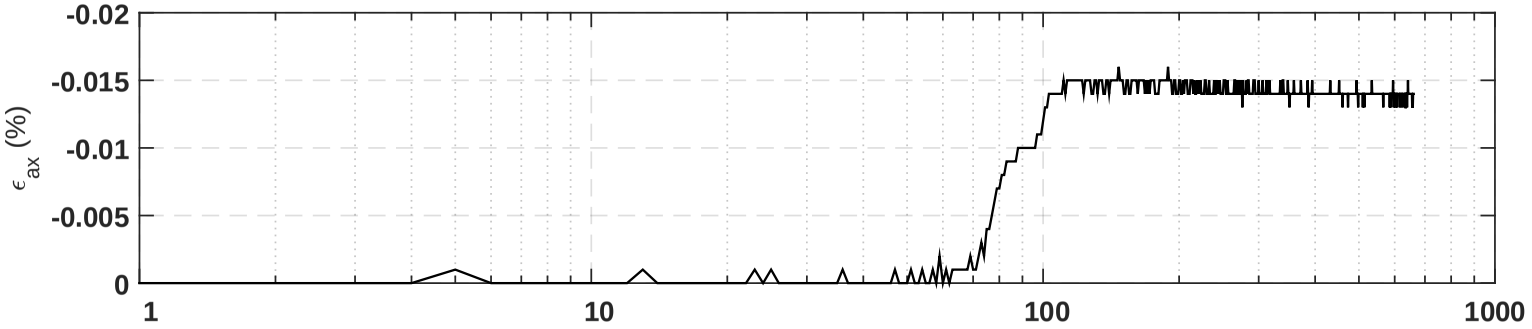

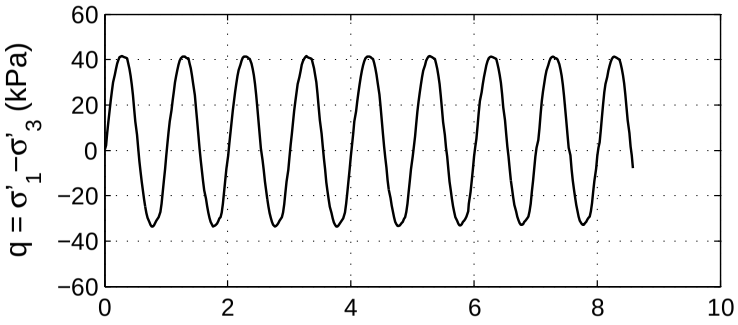

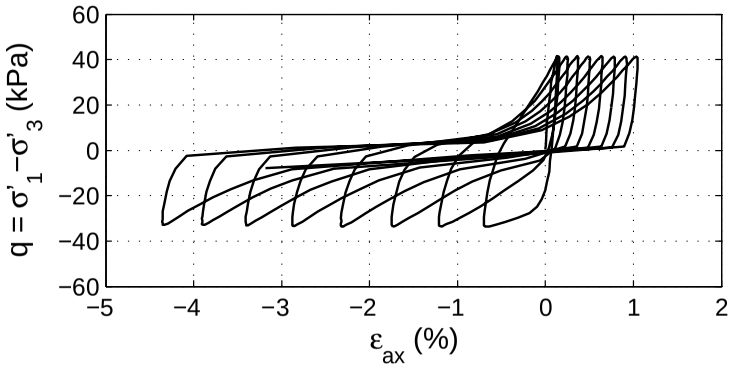

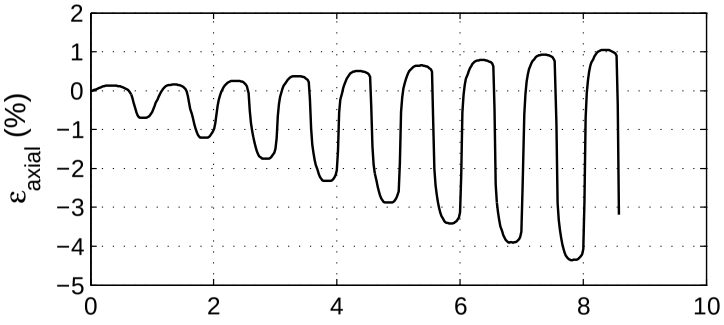

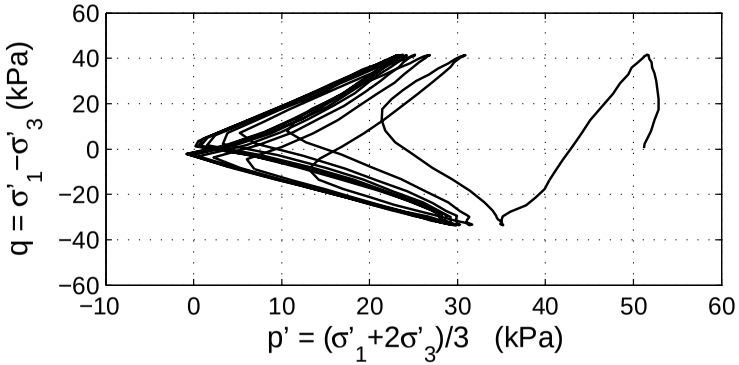

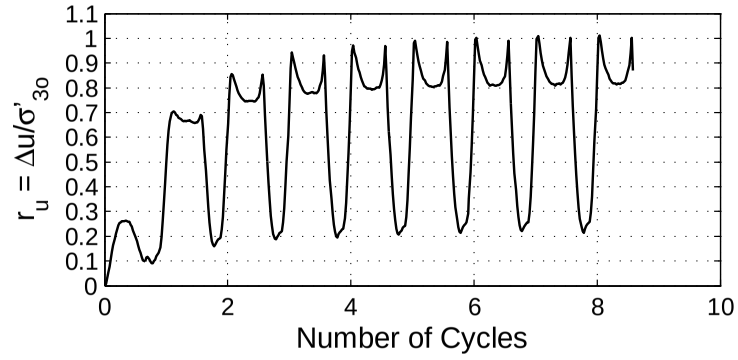

Specimen & Isotropic Cyclic Triaxial Test Data

Site:	86 Kil. St	**Loading Freq (Hz):**	0.1
Borehole:	DM BH1	**B−Value:**	0.991
Sample No.:	5U	**CSR:**	0.365
Sampler Type:	D&M	**N to $\varepsilon_{Ax-S.A.}$=3%:**	6
Spec. Depth (m):	4.27	**N to $\varepsilon_{Ax-D.A.}$=5%:**	8
Date Tested:	05/29/14	**Post−Cyclic Test:**	−−
Date Sampled:	05/06/14		
Spec. Ht. (mm):	140.4		
Spec. Diam. (mm):	60.9		
Dry Mass (g):	619.78		
Gs:	2.69		
e_o:	0.77		
σ'_{3o} (kPa):	51.0		
PI (%):	NP		
USCS:	SP−SM		

Isotropic Consolidation Test

Site:	86 Kil. St
Borehole:	DM BH1
Sample No.:	5U
Sampler Type:	D&M
Spec. Depth (m):	4.27
Date Tested:	05/29/14
Date Sampled:	05/06/14

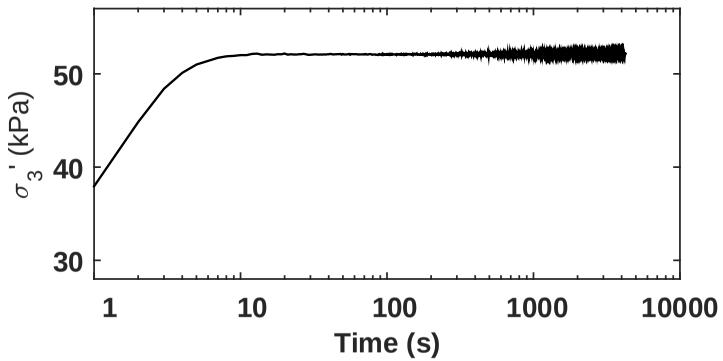

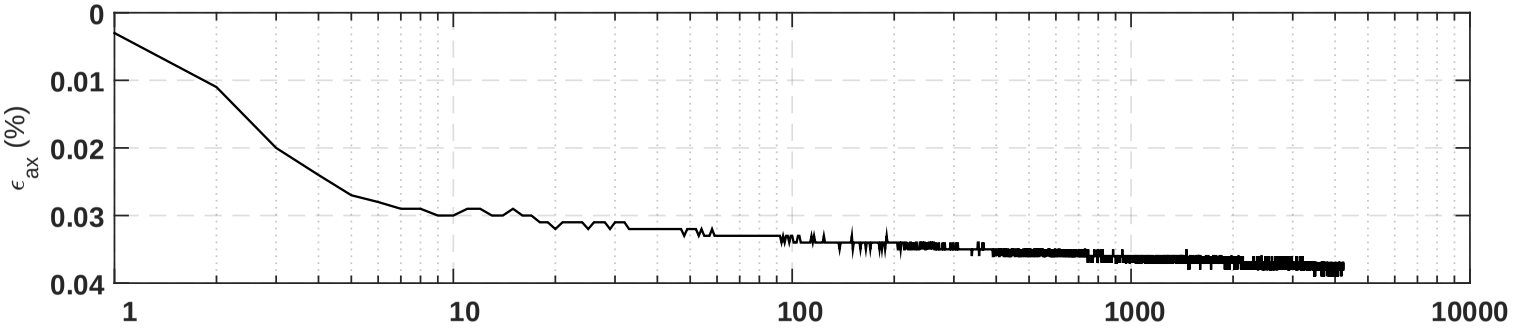

Post CTX Reconsolidation Test

Site:	86 Kil. St
Borehole:	DM BH1
Sample No.:	5U
Sampler Type:	D&M
Spec. Depth (m):	4.27
Date Tested:	05/29/14
Date Sampled:	05/06/14

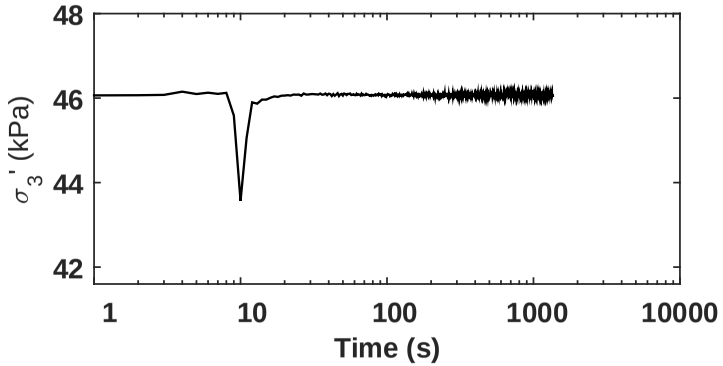

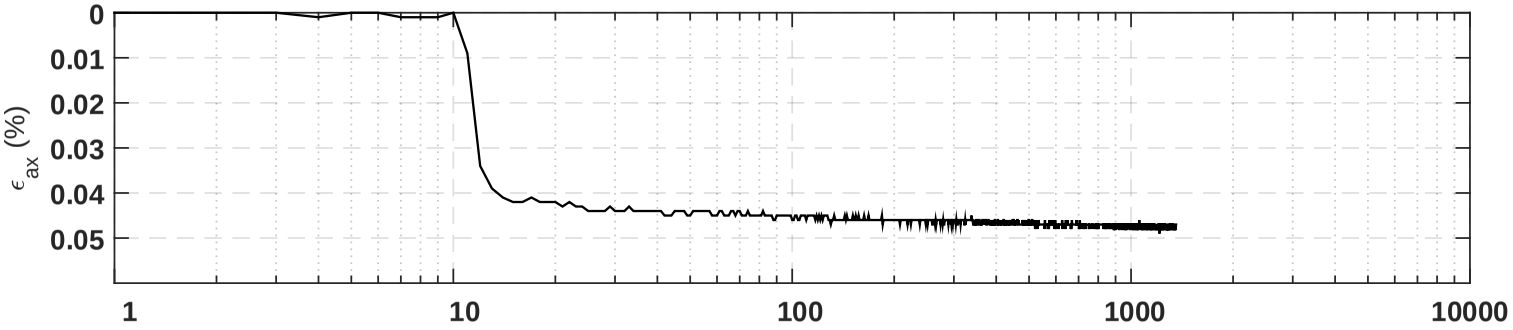

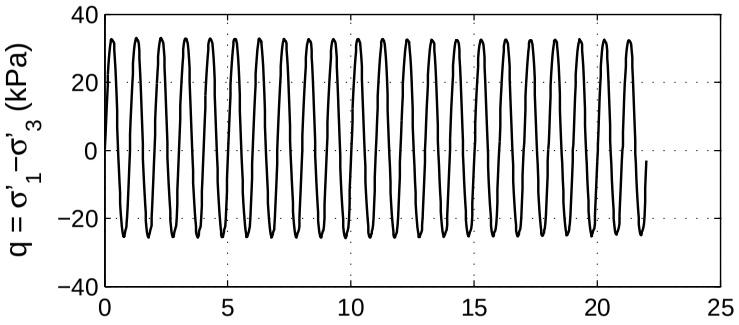

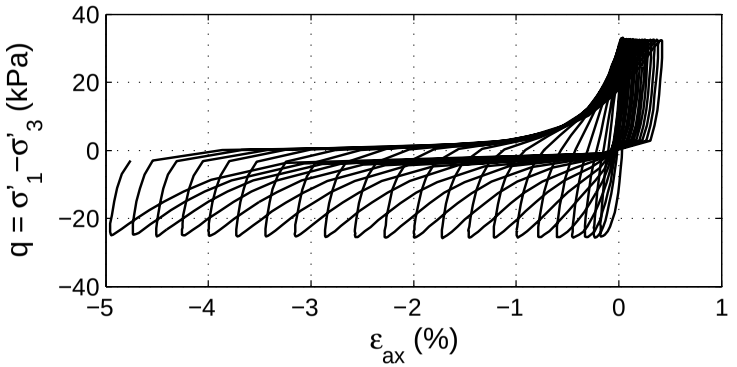

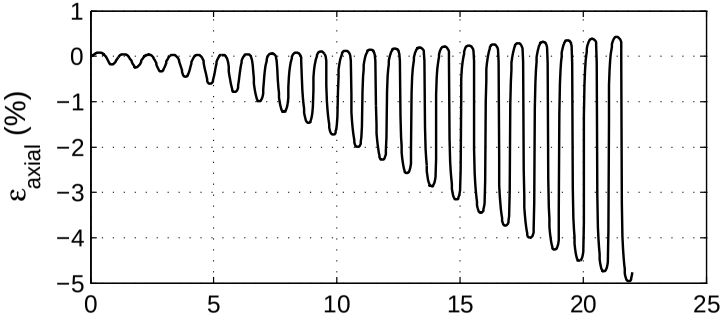

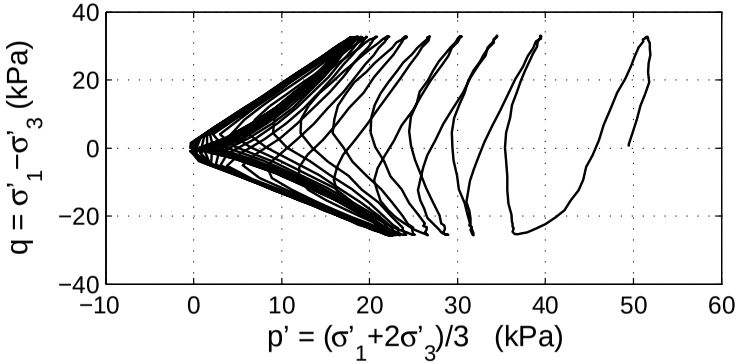

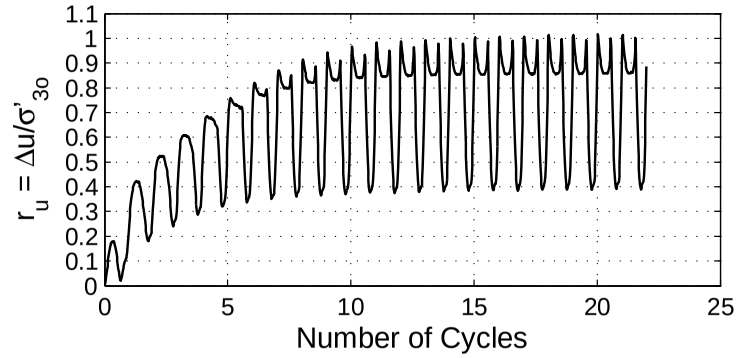

Specimen & Isotropic Cyclic Triaxial Test Data

Site:	86 Kil. St	**Loading Freq (Hz):**	0.1
Borehole:	DM BH1	**B−Value:**	0.987
Sample No.:	5U	**CSR:**	0.289
Sampler Type:	D&M	**N to $\varepsilon_{Ax-S.A.}$=3%:**	15
Spec. Depth (m):	4.43	**N to $\varepsilon_{Ax-D.A.}$=5%:**	21
Date Tested:	05/06/14	**Post−Cyclic Test:**	−−
Date Sampled:	05/06/14		
Spec. Ht. (mm):	139.3		
Spec. Diam. (mm):	61.1		
Dry Mass (g):	619.96		
Gs:	2.67		
e_ρ:	0.76		
σ'_{3o} (kPa):	49.3		
PI (%):	NP		
USCS:	SP−SM		

Isotropic Consolidation Test

Site:	86 Kil. St
Borehole:	DM BH1
Sample No.:	5U
Sampler Type:	D&M
Spec. Depth (m):	4.43
Date Tested:	05/06/14
Date Sampled:	05/06/14

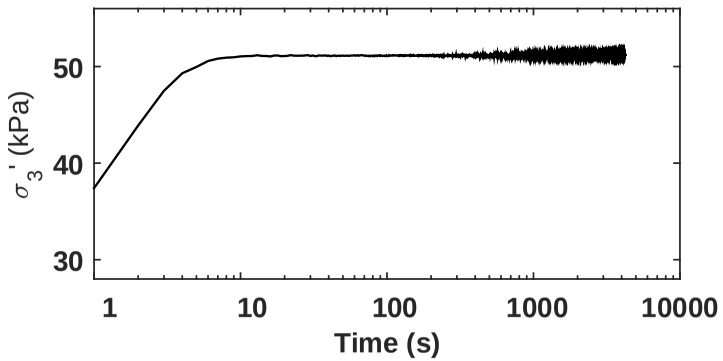

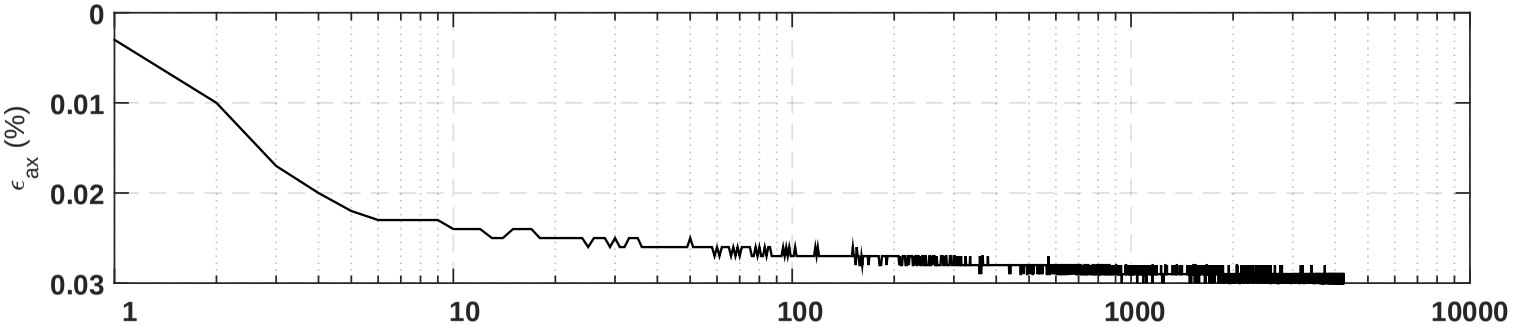

Post CTX Reconsolidation Test

Site:	86 Kil. St
Borehole:	DM BH1
Sample No.:	5U
Sampler Type:	D&M
Spec. Depth (m):	4.43
Date Tested:	05/06/14
Date Sampled:	05/06/14

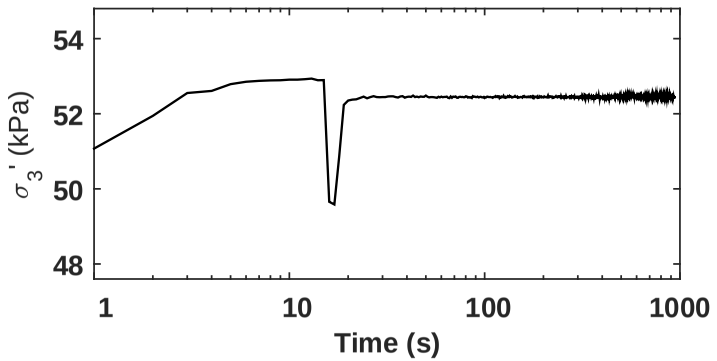

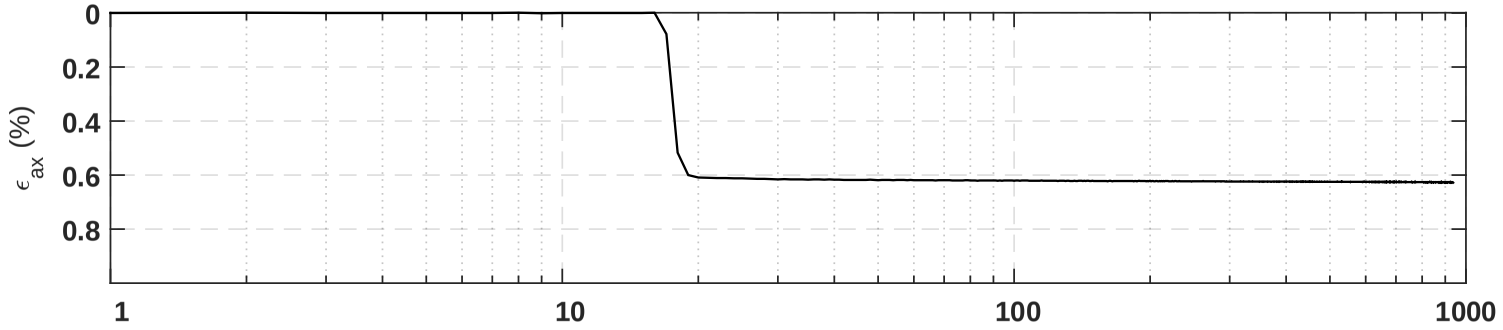

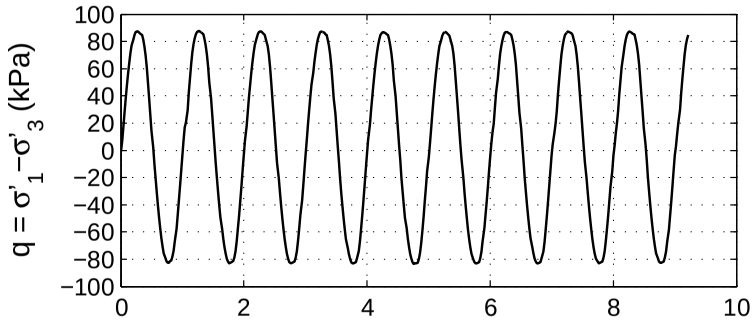

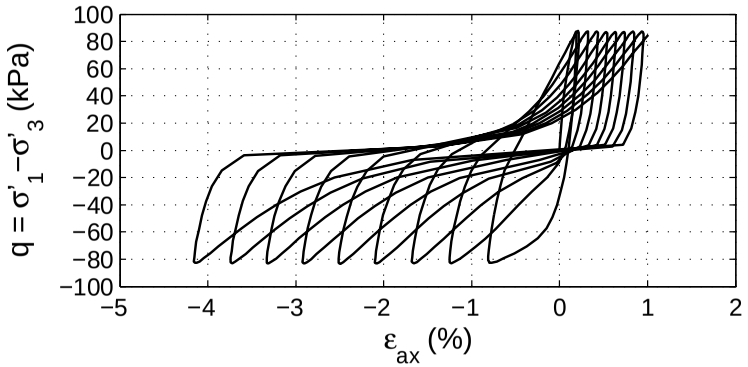

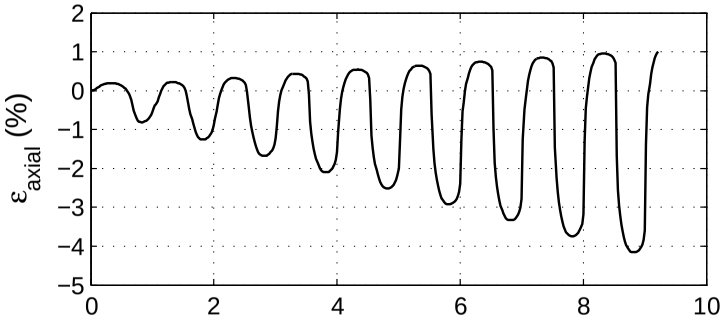

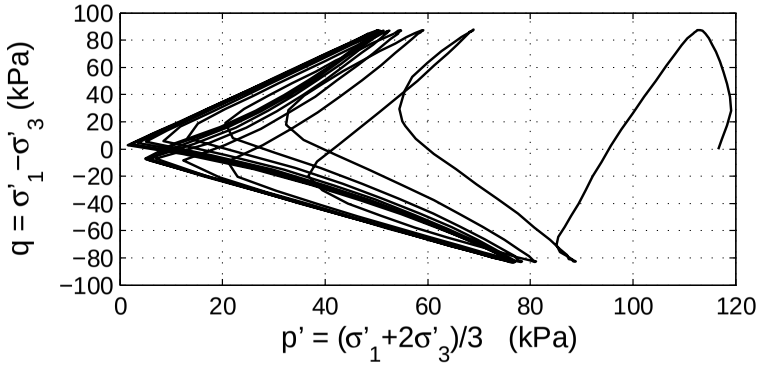

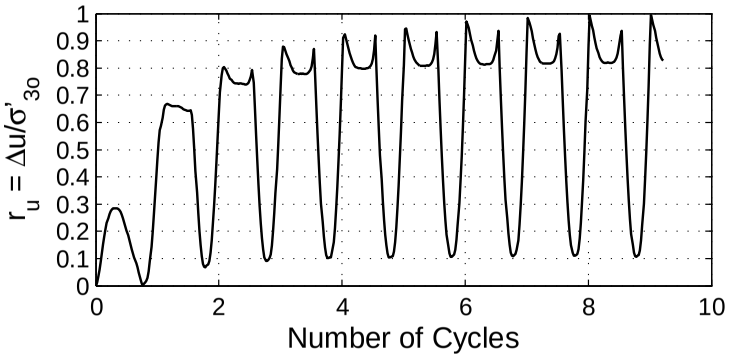

Specimen & Isotropic Cyclic Triaxial Test Data

Site:	86 Kil. St	**Loading Freq (Hz):**	0.1
Borehole:	DM BH2	**B−Value:**	0.983
Sample No.:	4U	**CSR:**	0.364
Sampler Type:	D&M	**N to $\varepsilon_{Ax-S.A.}$=3%:**	7
Spec. Depth (m):	14.23	**N to $\varepsilon_{Ax-D.A.}$=5%:**	9
Date Tested:	05/30/14	**Post−Cyclic Test:**	−−
Date Sampled:	05/09/14		
Spec. Ht. (mm):	139.4		
Spec. Diam. (mm):	60.9		
Dry Mass (g):	626.35		
Gs:	2.67		
e_o:	0.73		
σ'_{3o} (kPa):	116.6		
PI (%):	NP		
USCS:	SP−SM		

Isotropic Consolidation Test

Site:	86 Kil. St
Borehole:	DM BH2
Sample No.:	4U
Sampler Type:	D&M
Spec. Depth (m):	14.23
Date Tested:	05/30/14
Date Sampled:	05/09/14

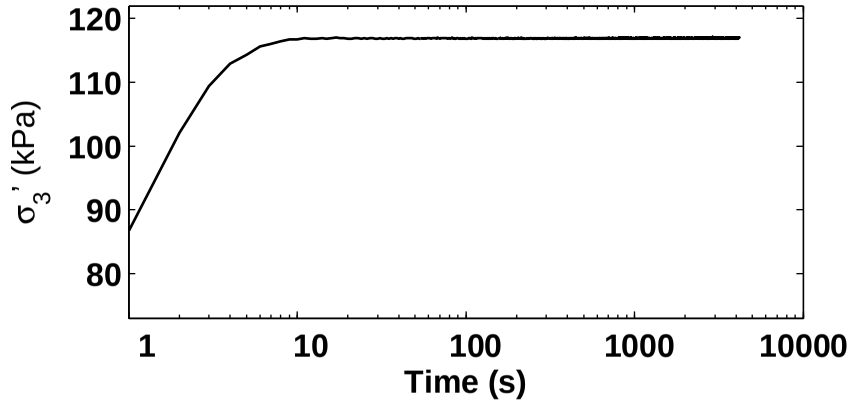

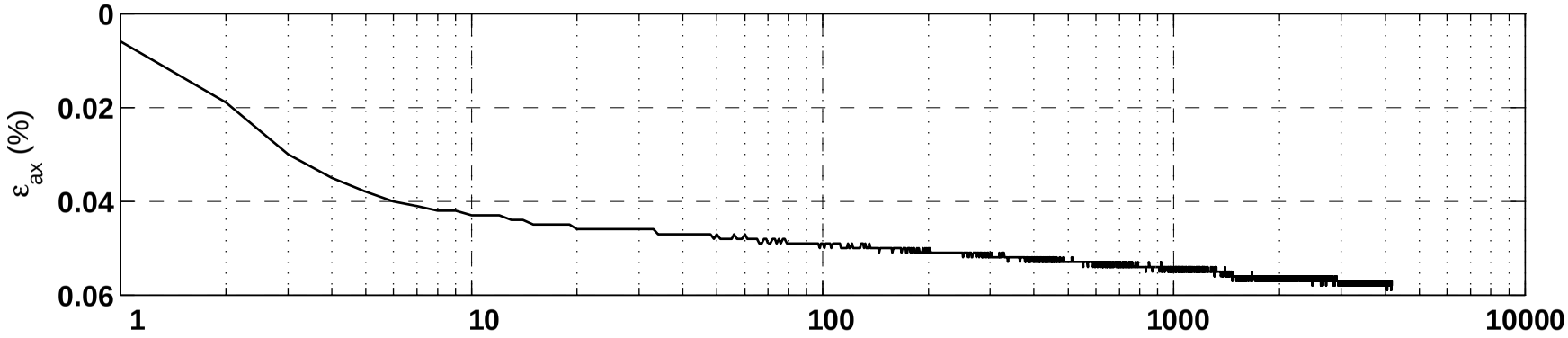

Post CTX Reconsolidation Test

Site:	86 Kil. St
Borehole:	GP BH1
Sample No.:	4U
Sampler Type:	D&M
Spec. Depth (m):	14.23
Date Tested:	05/30/14
Date Sampled:	05/09/14

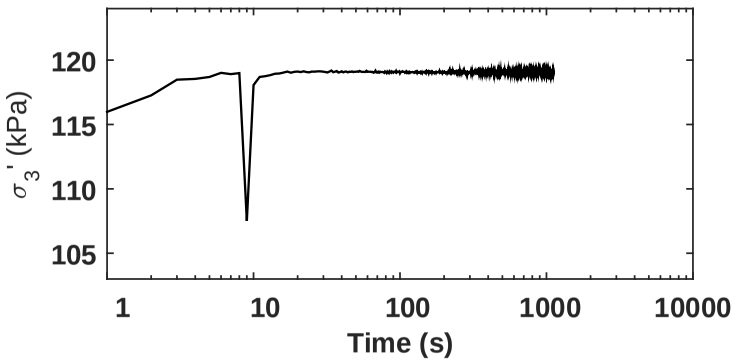

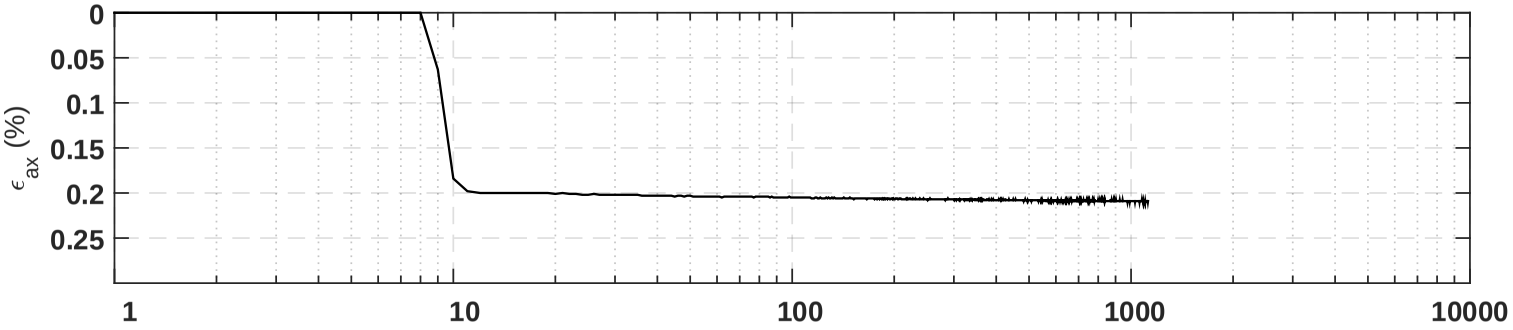

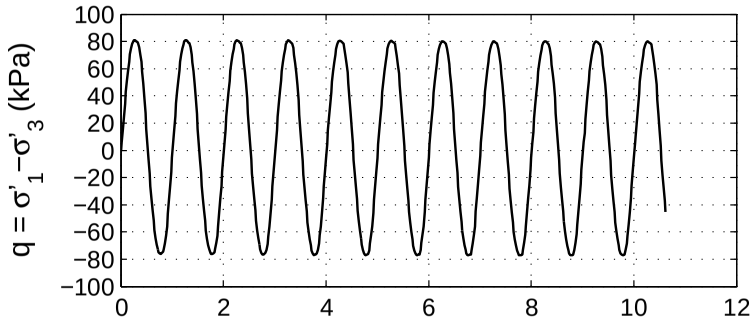

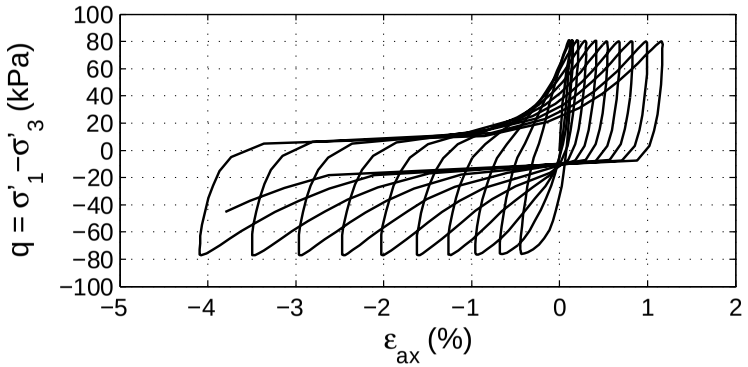

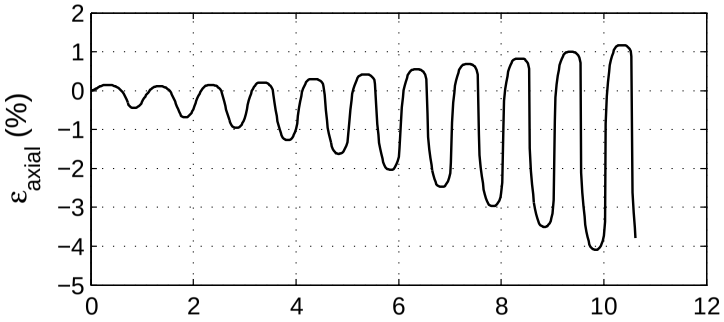

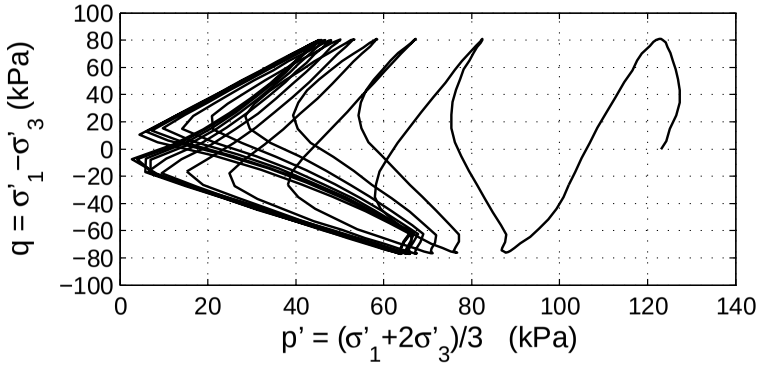

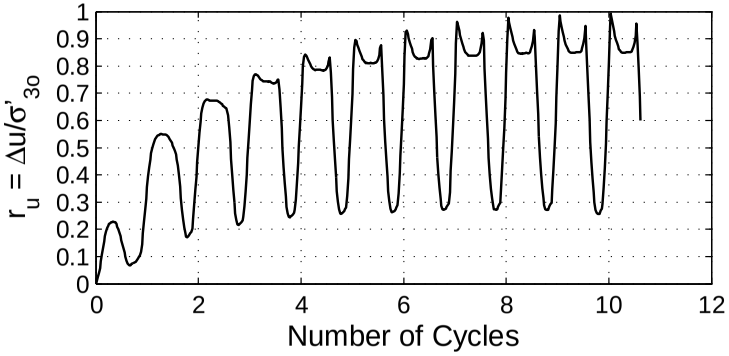

Specimen & Isotropic Cyclic Triaxial Test Data

Site:	86 Kil. St	**Loading Freq (Hz):**	0.1
Borehole:	DM BH2	**B−Value:**	0.984
Sample No.:	5U	**CSR:**	0.319
Sampler Type:	D&M	**N to $\varepsilon_{Ax-S.A.}$=3%:**	9
Spec. Depth (m):	14.86	**N to $\varepsilon_{Ax-D.A.}$=5%:**	10
Date Tested:	05/31/14	**Post−Cyclic Test:**	−−
Date Sampled:	05/09/14		
Spec. Ht. (mm):	140.4		
Spec. Diam. (mm):	60.8		
Dry Mass (g):	633.85		
Gs:	2.7		
e_o:	0.74		
σ'_{3o} (kPa):	123.1		
PI (%):	NP		
USCS:	SP−SM		

Isotropic Consolidation Test

Site:	86 Kil. St
Borehole:	DM BH2
Sample No.:	5U
Sampler Type:	D&M
Spec. Depth (m):	14.86
Date Tested:	05/31/14
Date Sampled:	05/09/14

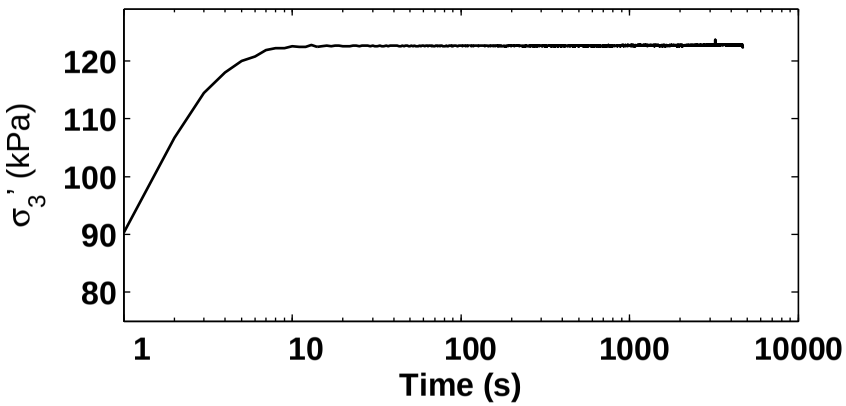

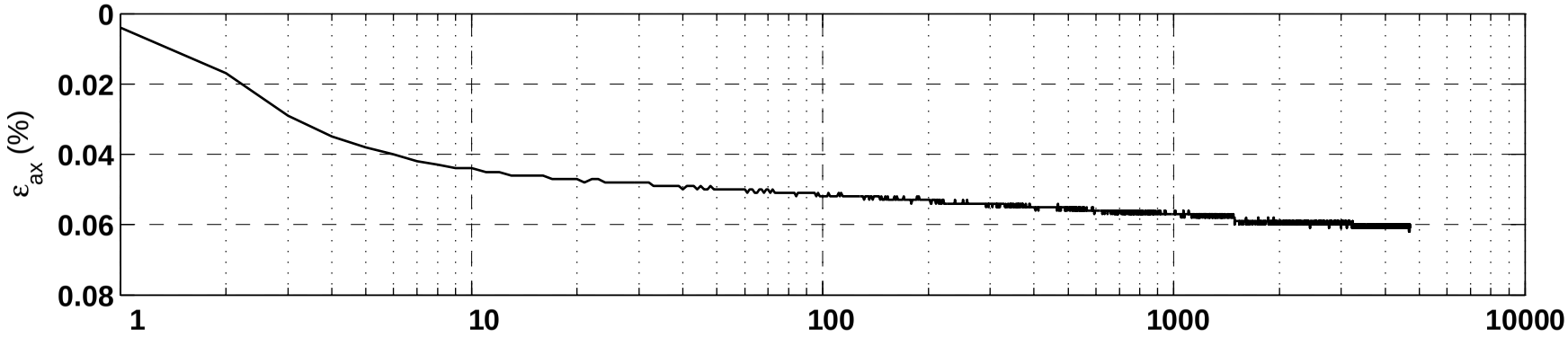

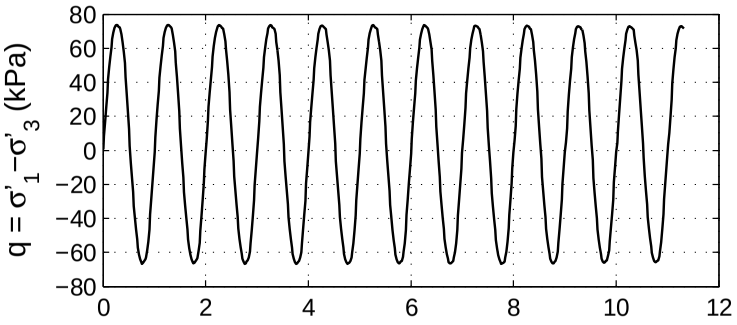

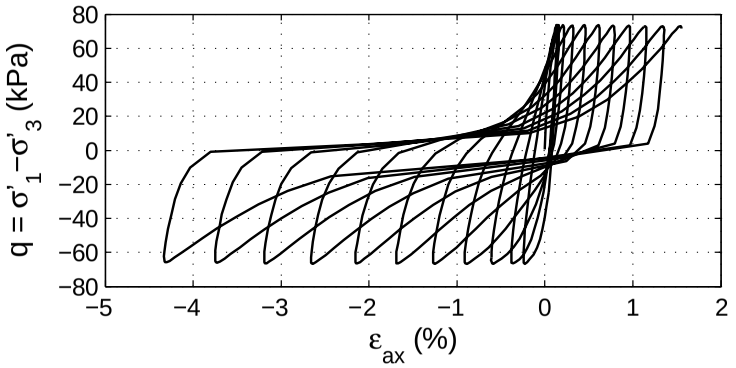

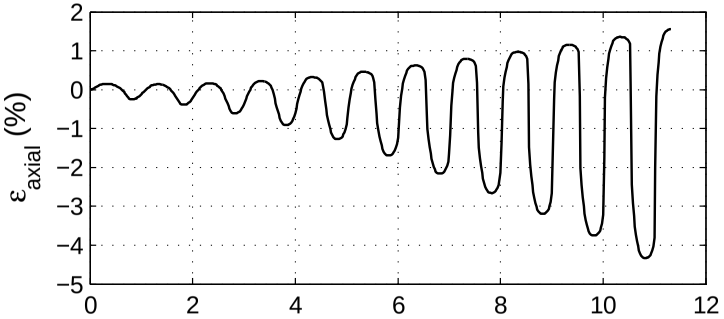

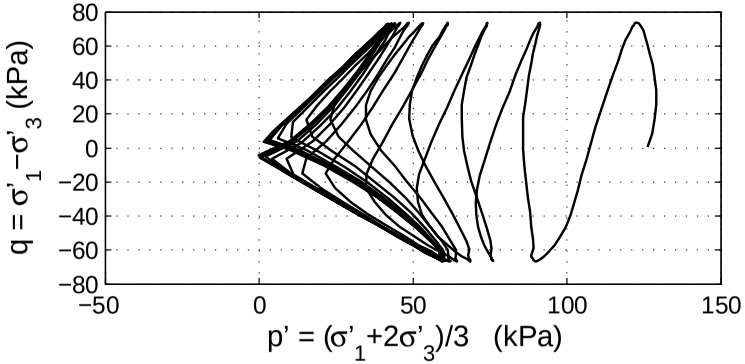

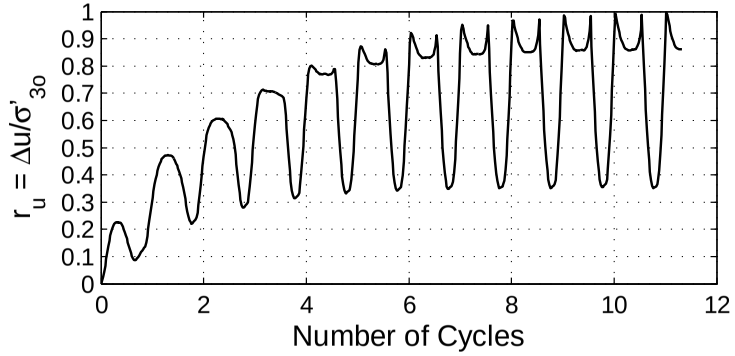

Specimen & Isotropic Cyclic Triaxial Test Data

Site:	86 Kil. St	**Loading Freq (Hz):**	0.1
Borehole:	DM BH2	**B−Value:**	0.991
Sample No.:	6U	**CSR:**	0.276
Sampler Type:	D&M	**N to $\varepsilon_{Ax-S.A.}$=3%:**	9
Spec. Depth (m):	15.36	**N to $\varepsilon_{Ax-D.A.}$=5%:**	11
Date Tested:	06/02/14	**Post−Cyclic Test:**	−−
Date Sampled:	05/09/14		
Spec. Ht. (mm):	139.0		
Spec. Diam. (mm):	60.7		
Dry Mass (g):	616.83		
Gs:	2.69		
e_ρ:	0.76		
σ'_{3o} (kPa):	126.0		
PI (%):	NP		
USCS:	SP−SM		

Isotropic Consolidation Test

Site:	86 Kil. St
Borehole:	DM BH2
Sample No.:	6U
Sampler Type:	D&M
Spec. Depth (m):	15.36
Date Tested:	06/02/14
Date Sampled:	05/09/14

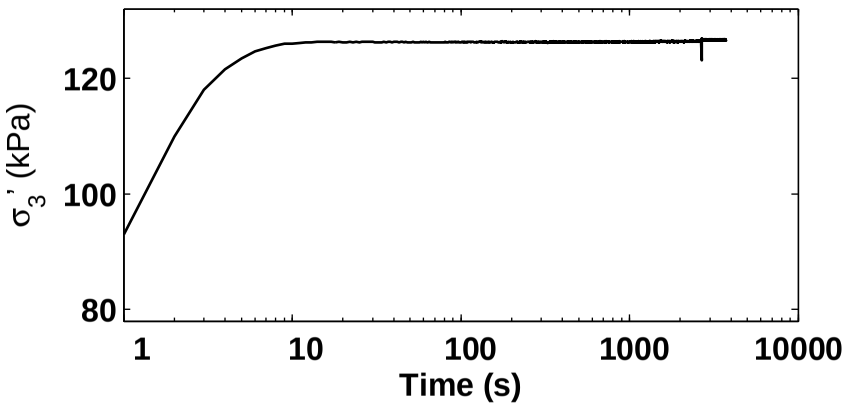

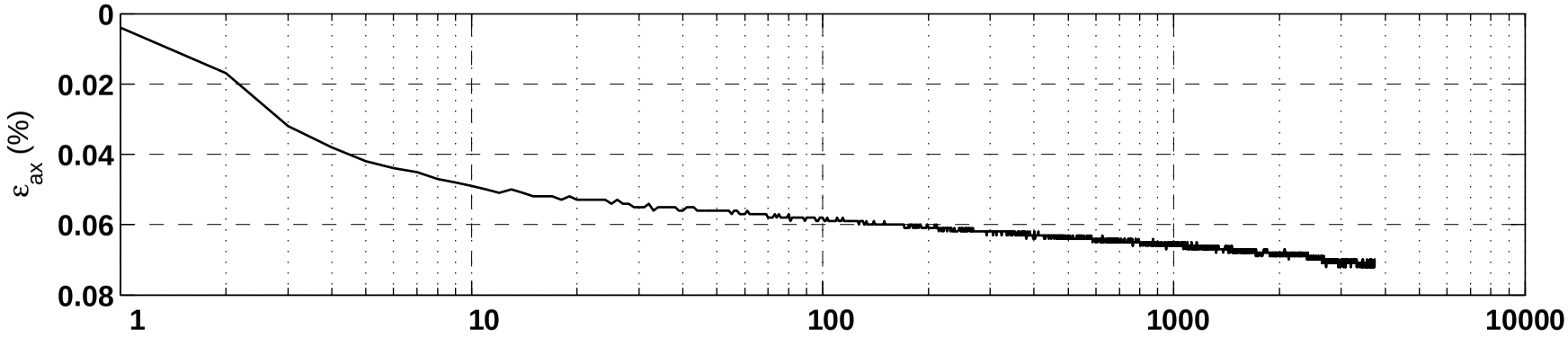

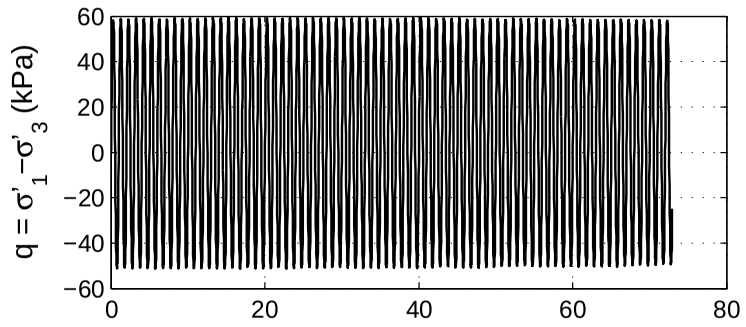

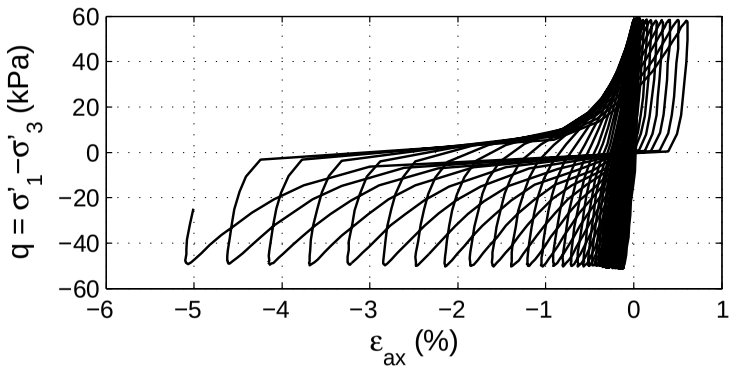

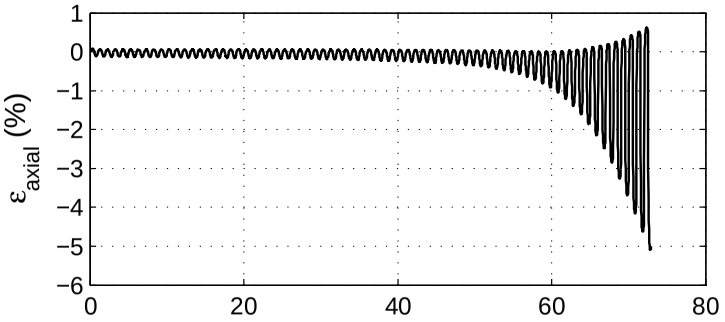

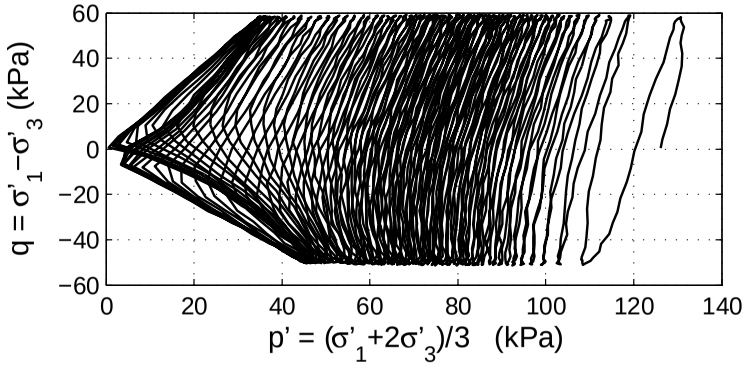

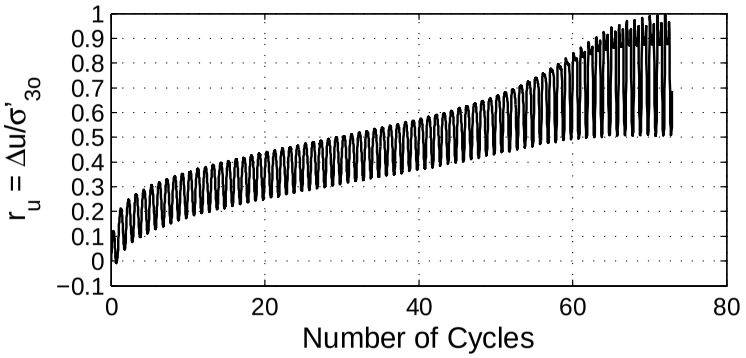

Specimen & Isotropic Cyclic Triaxial Test Data

Site:	86 Kil. St	**Loading Freq (Hz):**	0.1
Borehole:	DM BH2	**B−Value:**	0.980
Sample No.:	6U	**CSR:**	0.214
Sampler Type:	D&M	**N to $\varepsilon_{Ax-S.A.}$=3%:**	69
Spec. Depth (m):	15.51	**N to $\varepsilon_{Ax-D.A.}$=5%:**	72
Date Tested:	06/04/14	**Post−Cyclic Test:**	Monotonic
Date Sampled:	05/09/14		
Spec. Ht. (mm):	139.8		
Spec. Diam. (mm):	60.9		
Dry Mass (g):	625.24		
Gs:	2.68		
e_o:	0.75		
σ'_{3o} (kPa):	126.0		
PI (%):	NP		
USCS:	SP		

Isotropic Consolidation Test

Site:	86 Kil. St
Borehole:	DM BH2
Sample No.:	6U
Sampler Type:	D&M
Spec. Depth (m):	15.51
Date Tested:	06/04/14
Date Sampled:	05/09/14

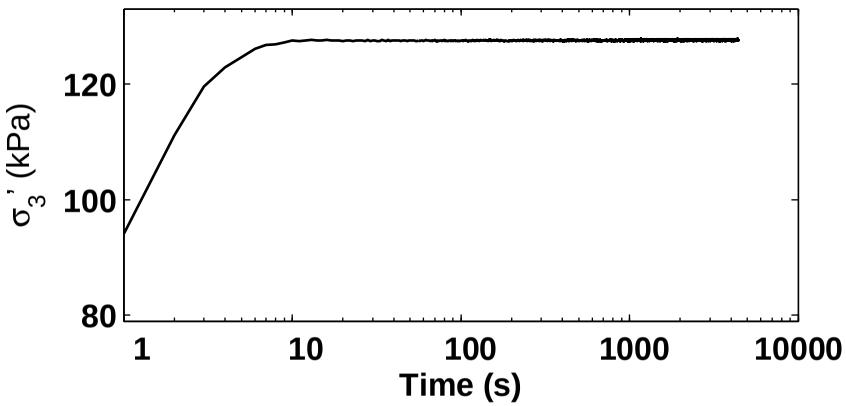

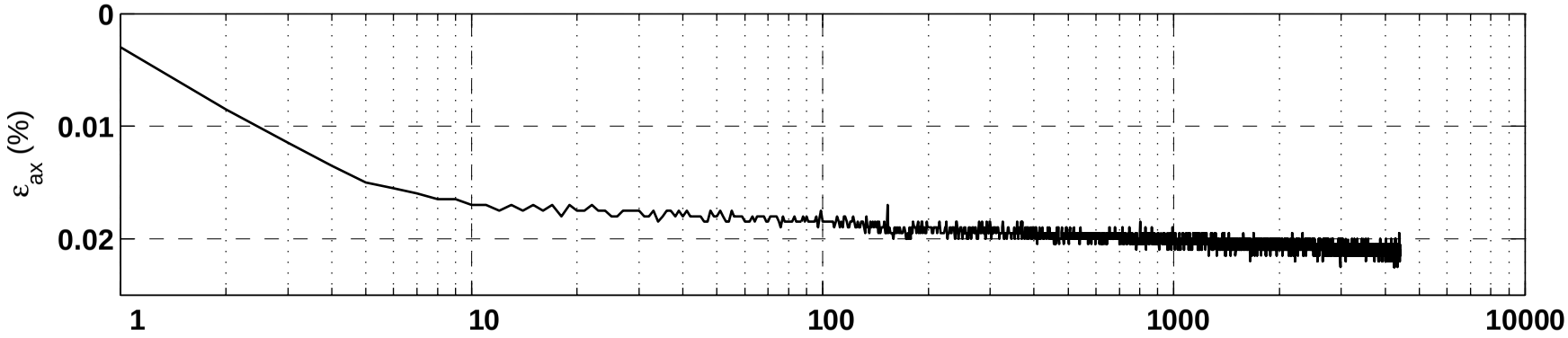

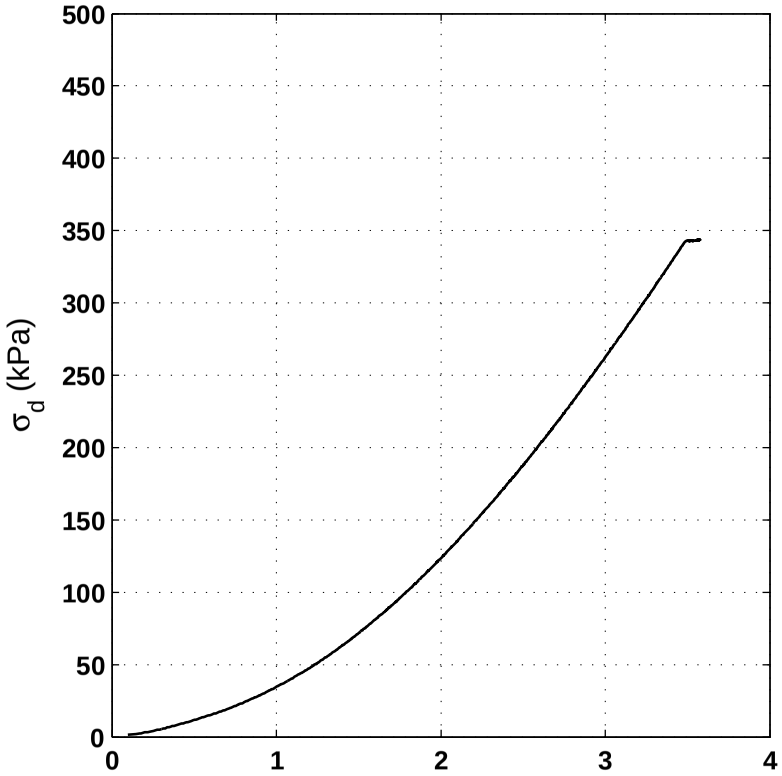

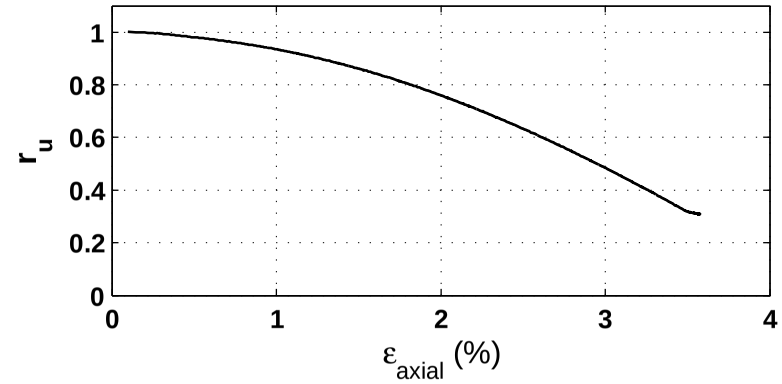

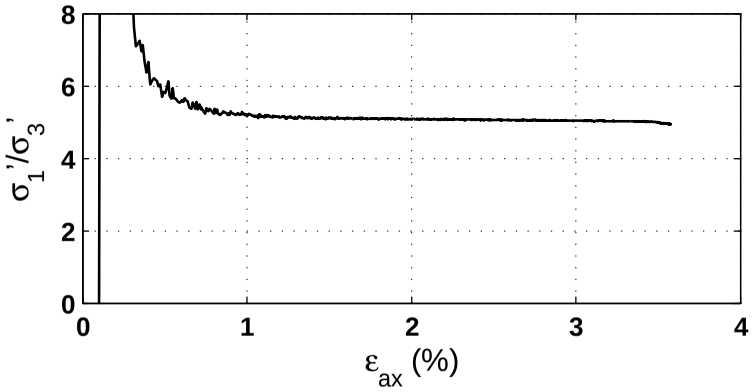

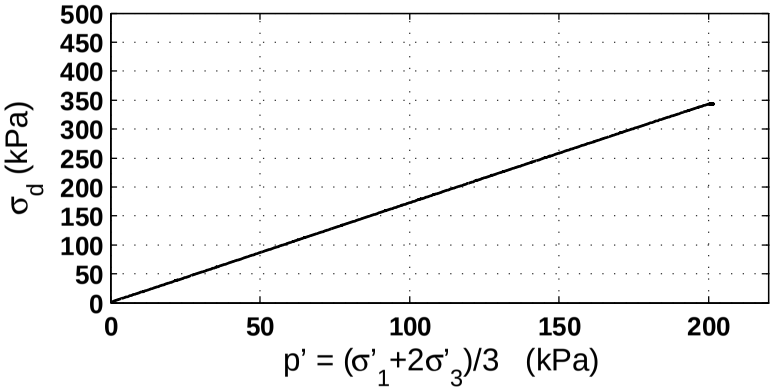

Post CTX Monotonic Comp. Test

Site:	86 Kil. St	**Rate (kPa/min):**	20
Borehole:	DM BH2		
Sample No.:	6U		
Sampler Type:	D&M		
Spec. Depth (m):	15.51		
Date Tested:	06/04/14		
Date Sampled:	05/09/14		

Appendix C.2.2

FTG-7 Building Site—151 Kilmore St.

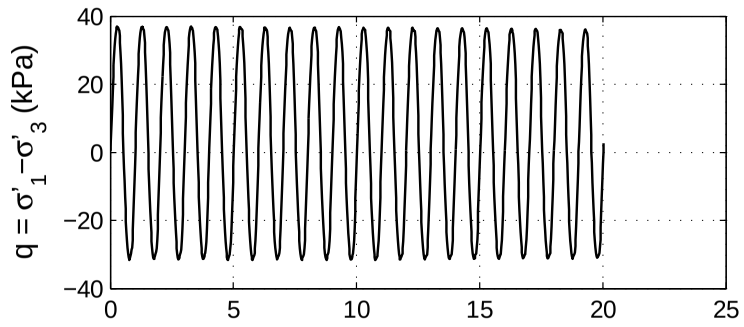

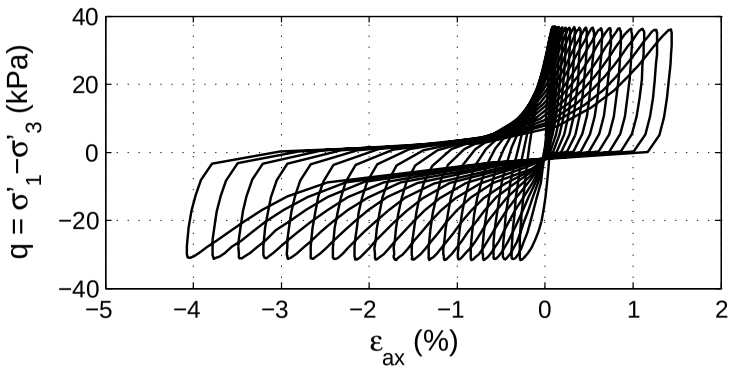

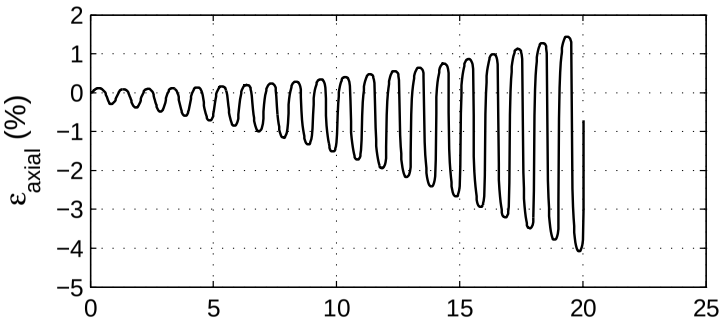

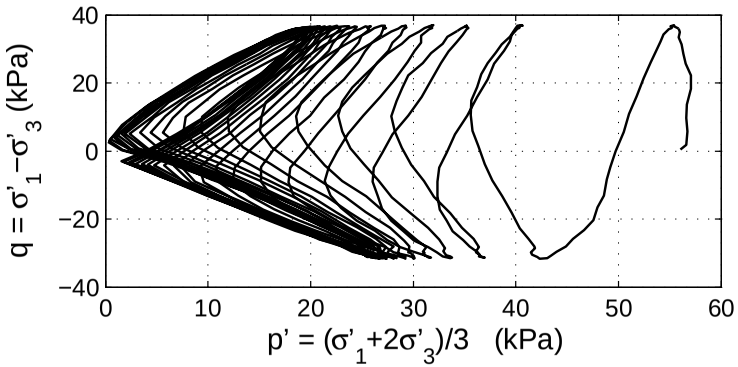

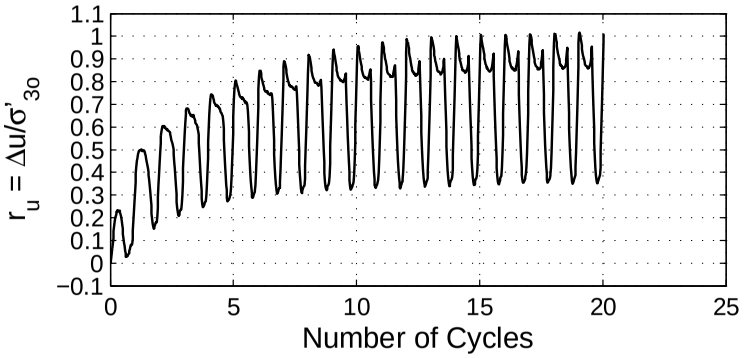

Specimen & Isotropic Cyclic Triaxial Test Data

Site:	151 Kil. St	**Loading Freq (Hz):**	0.1
Borehole:	DM BH1	**B−Value:**	0.985
Sample No.:	2U	**CSR:**	0.302
Sampler Type:	D&M	**N to $\varepsilon_{Ax-S.A.}$=3%:**	17
Spec. Depth (m):	2.57	**N to $\varepsilon_{Ax-D.A.}$=5%:**	19
Date Tested:	06/13/14	**Post−Cyclic Test:**	Reconsol.
Date Sampled:	05/15/14		
Spec. Ht. (mm):	141.5		
Spec. Diam. (mm):	61.1		
Dry Mass (g):	626.49		
Gs:	2.69		
e_o:	0.78		
σ'_{3o} (kPa):	55.9		
PI (%):	3		
USCS:	ML		

Isotropic Consolidation Test

Site:	151 Kil. St
Borehole:	DM BH1
Sample No.:	2U
Sampler Type:	D&M
Spec. Depth (m):	2.57
Date Tested:	06/13/14
Date Sampled:	05/15/14

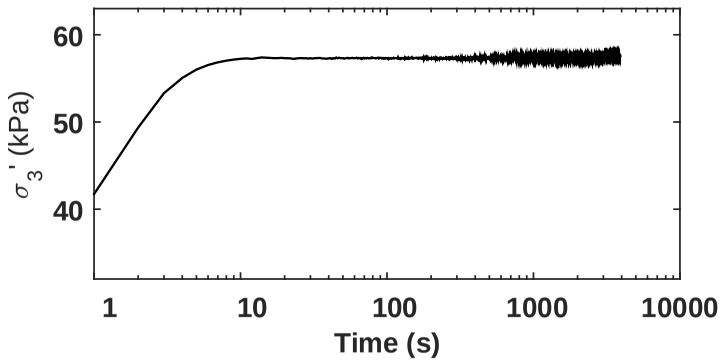

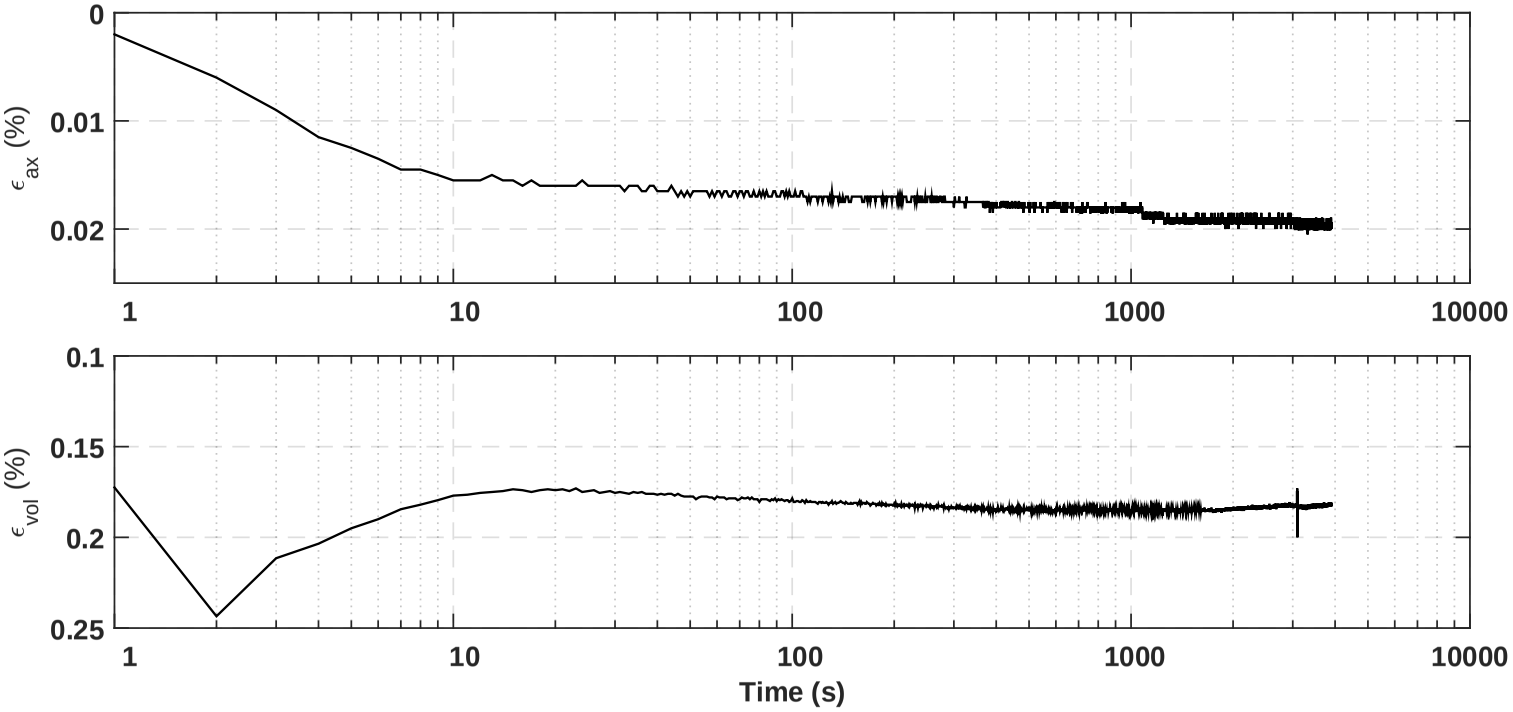

Post CTX Reconsolidation Test

Site:	151 Kil. St
Borehole:	DM BH1
Sample No.:	2U
Sampler Type:	D&M
Spec. Depth (m):	2.57
Date Tested:	06/13/14
Date Sampled:	05/15/14

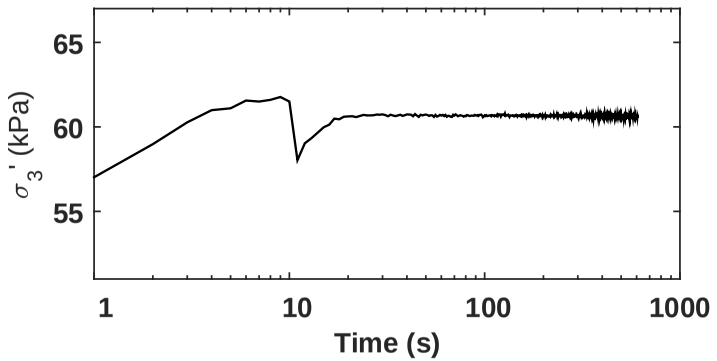

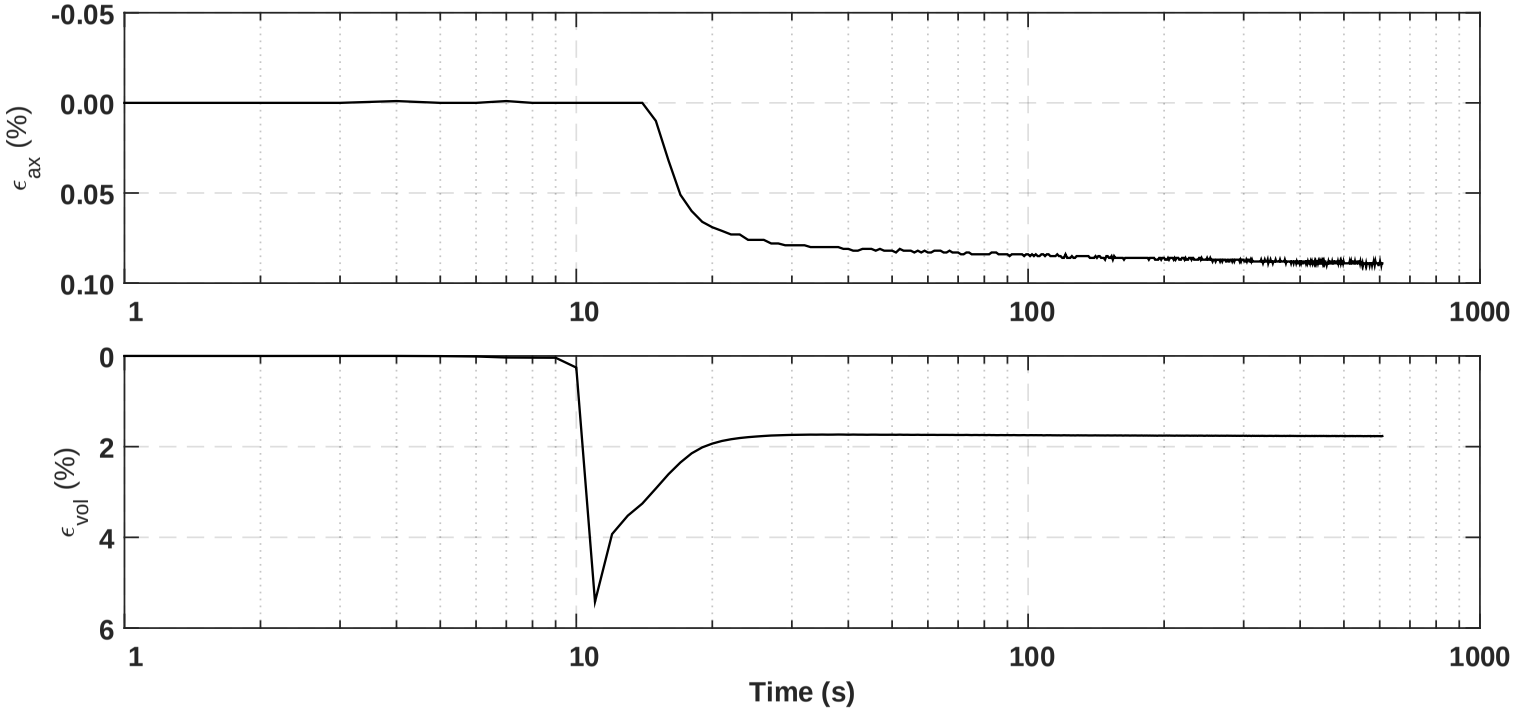

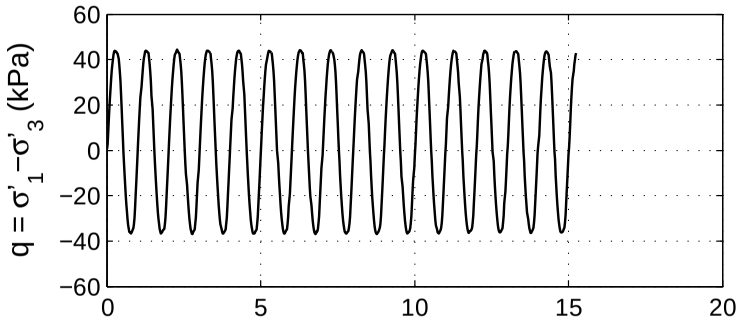

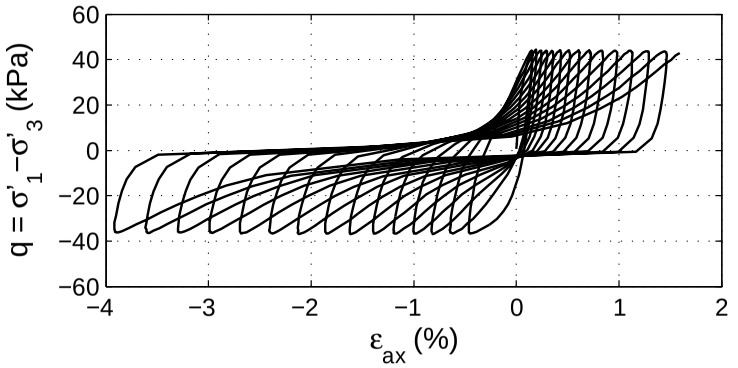

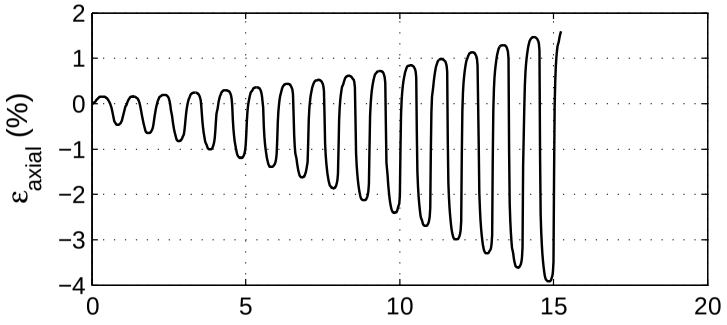

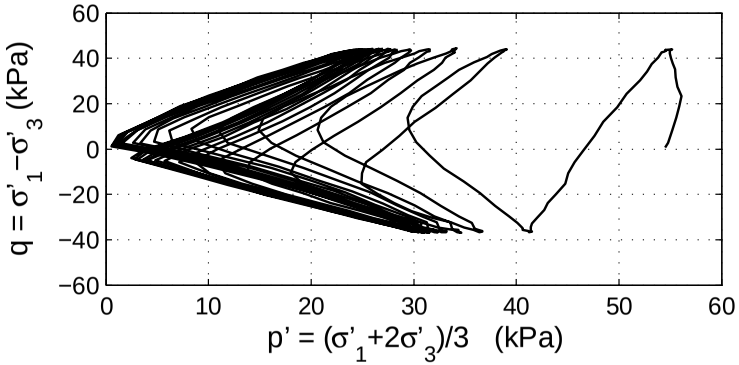

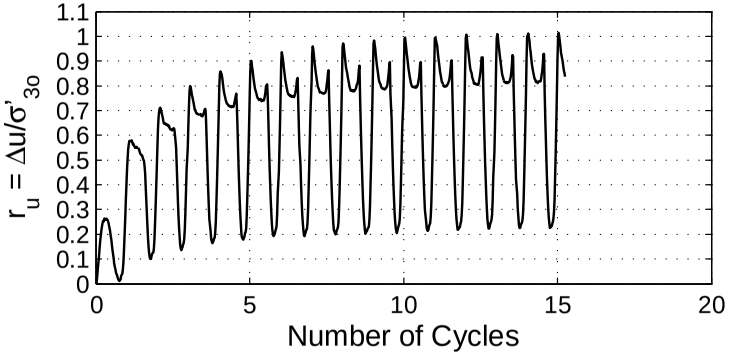

Specimen & Isotropic Cyclic Triaxial Test Data

Site:	151 Kil. St	**Loading Freq (Hz):**	0.1
Borehole:	DM BH1	**B−Value:**	0.981
Sample No.:	2U	**CSR:**	0.371
Sampler Type:	D&M	**N to $\varepsilon_{Ax-S.A.}$=3%:**	13
Spec. Depth (m):	2.72	**N to $\varepsilon_{Ax-D.A.}$=5%:**	15
Date Tested:	06/14/14	**Post−Cyclic Test:**	Reconsol.
Date Sampled:	05/15/14		
Spec. Ht. (mm):	133.2		
Spec. Diam. (mm):	61.0		
Dry Mass (g):	586.13		
Gs:	2.68		
e_o:	0.78		
σ'_{3o} (kPa):	54.3		
PI (%):	3		
USCS:	ML		

Isotropic Consolidation Test

Site:	151 Kil. St
Borehole:	DM BH1
Sample No.:	2U
Sampler Type:	D&M
Spec. Depth (m):	2.72
Date Tested:	06/14/14
Date Sampled:	05/15/14

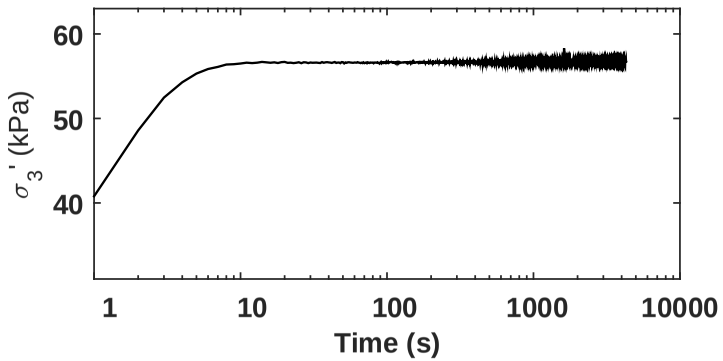

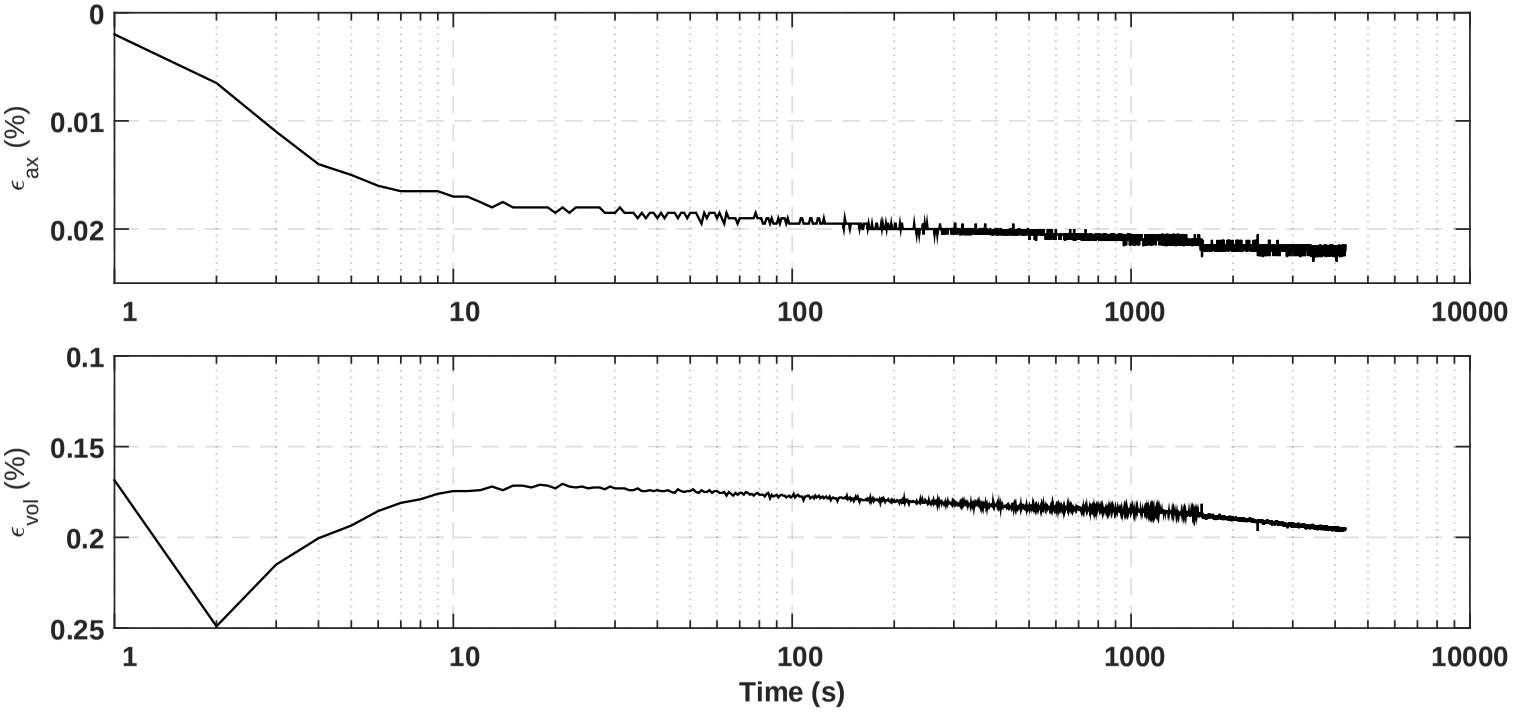

Post CTX Reconsolidation Test

Site:	151 Kil. St
Borehole:	DM BH1
Sample No.:	2U
Sampler Type:	D&M
Spec. Depth (m):	2.72
Date Tested:	06/14/14
Date Sampled:	05/15/14

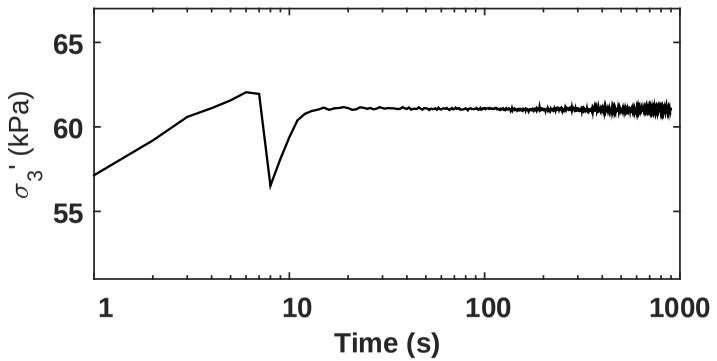

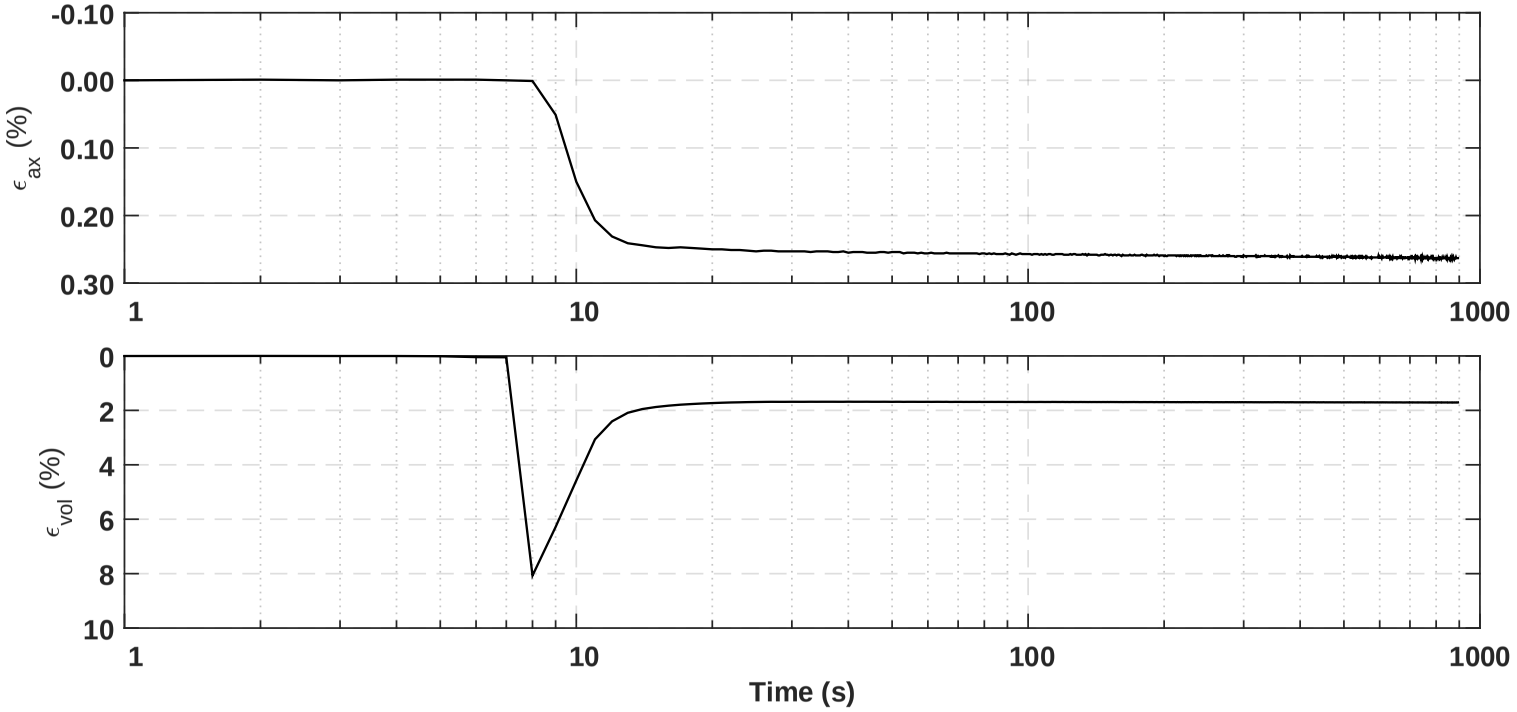

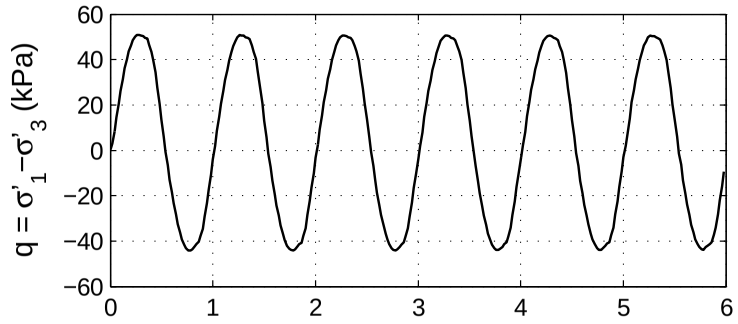

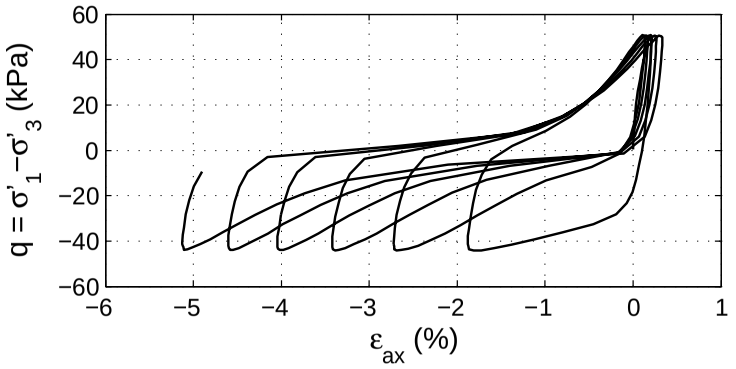

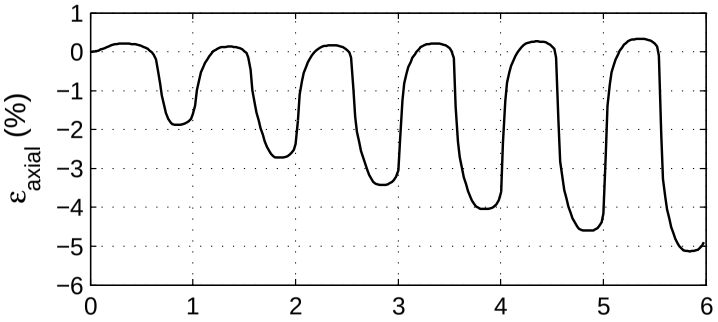

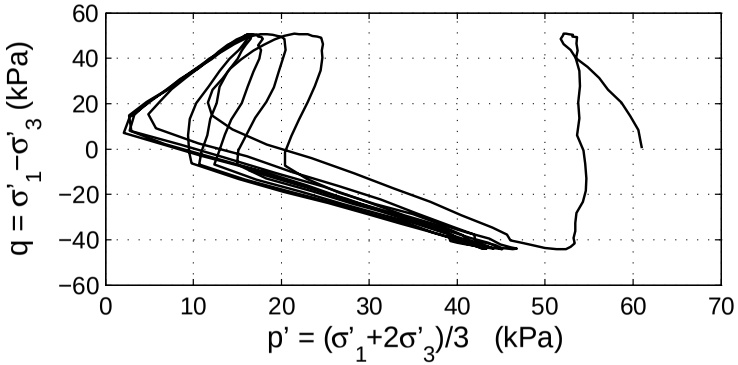

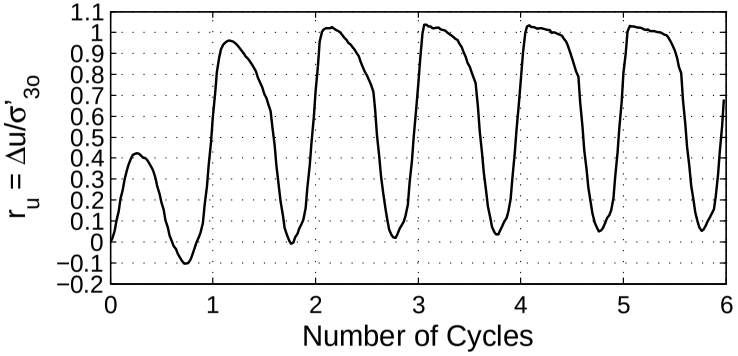

Specimen & Isotropic Cyclic Triaxial Test Data

Site:	151 Kil. St	**Loading Freq (Hz):**	0.1
Borehole:	DM BH1	**B−Value:**	0.985
Sample No.:	3U	**CSR:**	0.390
Sampler Type:	D&M	**N to $\varepsilon_{Ax-S.A.}$=3%:**	3
Spec. Depth (m):	3.57	**N to $\varepsilon_{Ax-D.A.}$=5%:**	6
Date Tested:	06/14/14	**Post−Cyclic Test:**	Reconsol.
Date Sampled:	05/15/14		
Spec. Ht. (mm):	138.9		
Spec. Diam. (mm):	61.0		
Dry Mass (g):	651.57		
Gs:	2.71		
e_o:	0.69		
σ'_{3o} (kPa):	60.9		
PI (%):	5		
USCS:	CL−ML		

Isotropic Consolidation Test

Site:	151 Kil. St
Borehole:	DM BH1
Sample No.:	3U
Sampler Type:	D&M
Spec. Depth (m):	3.57
Date Tested:	06/14/14
Date Sampled:	05/15/14

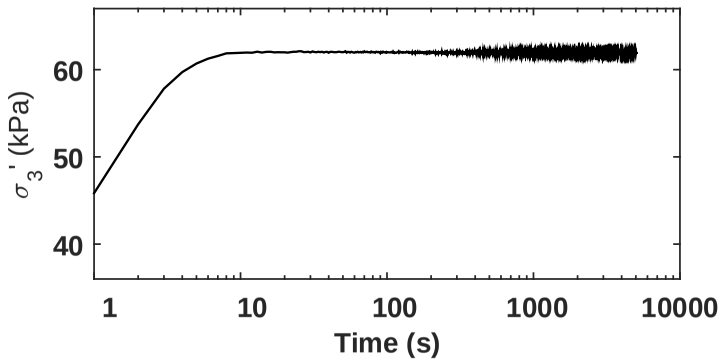

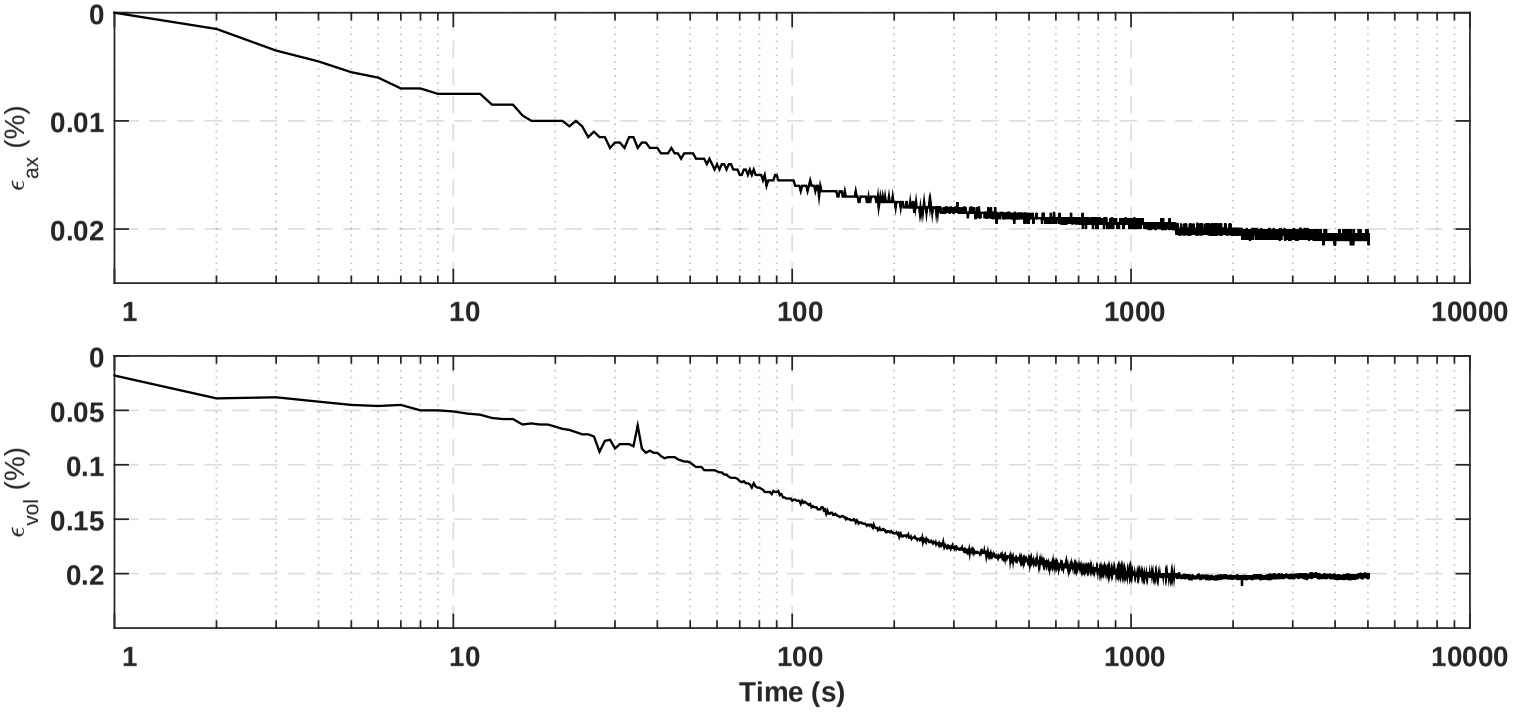

Post CTX Reconsolidation Test

Site:	151 Kil. St
Borehole:	DM BH1
Sample No.:	3U
Sampler Type:	D&M
Spec. Depth (m):	3.57
Date Tested:	06/14/14
Date Sampled:	05/15/14

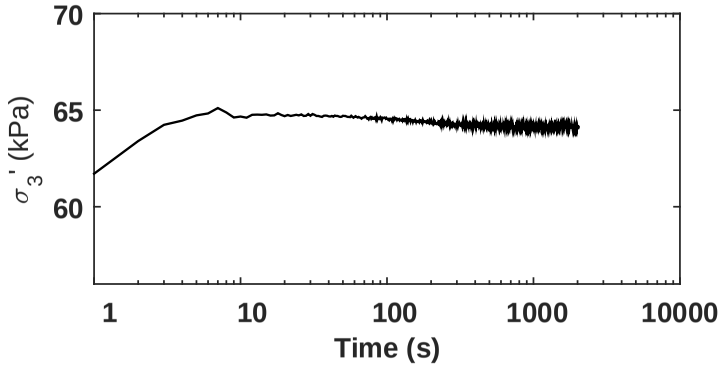

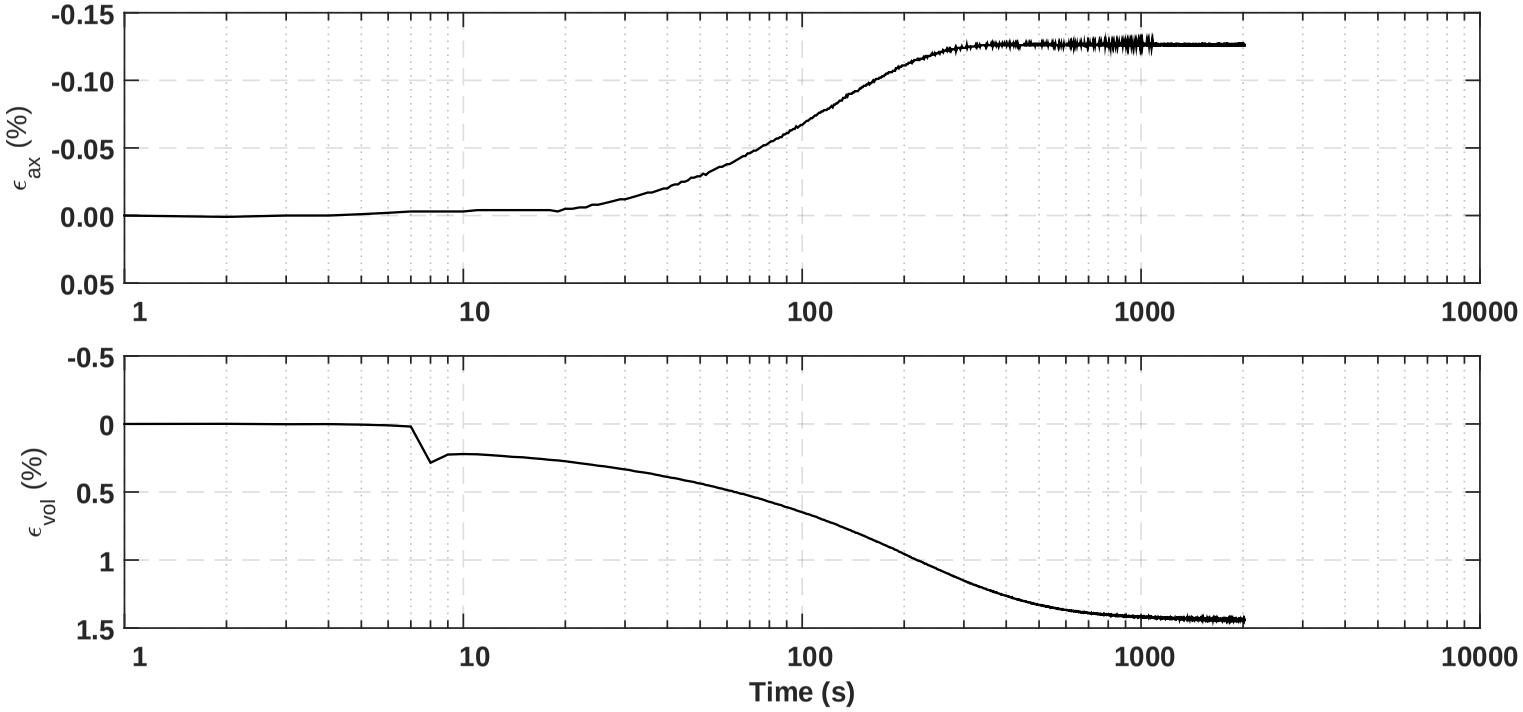

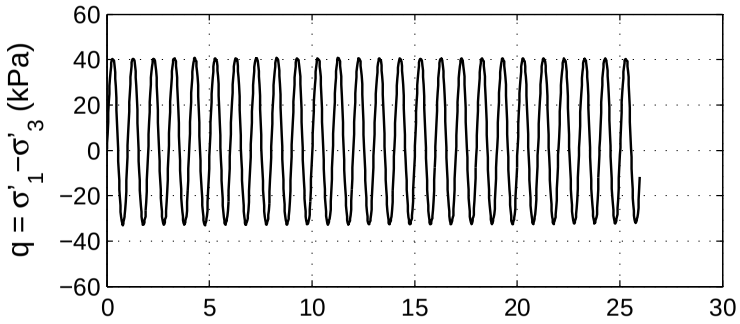

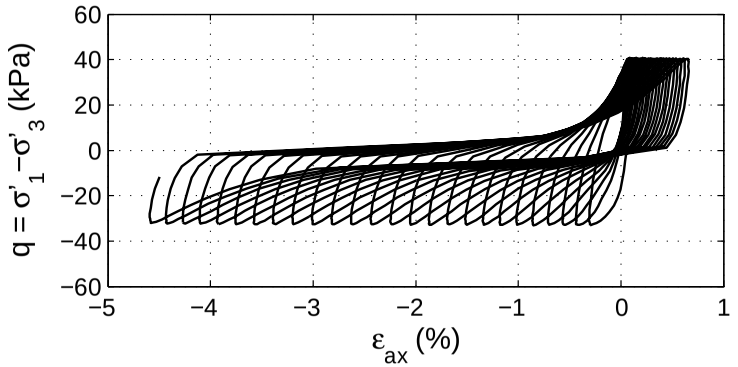

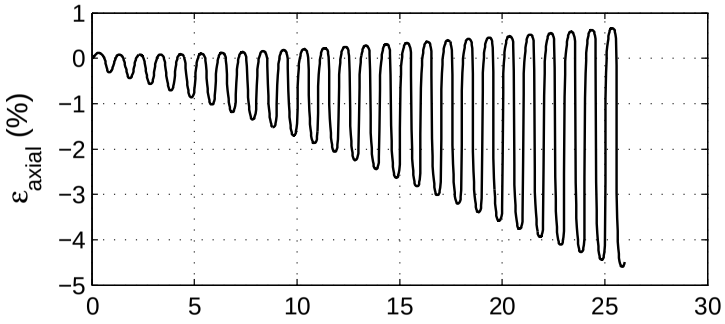

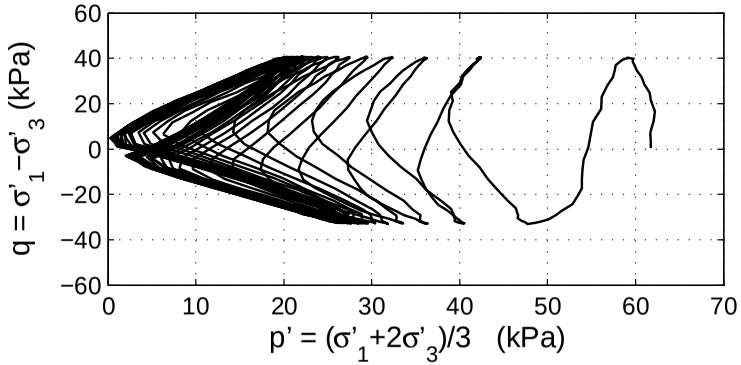

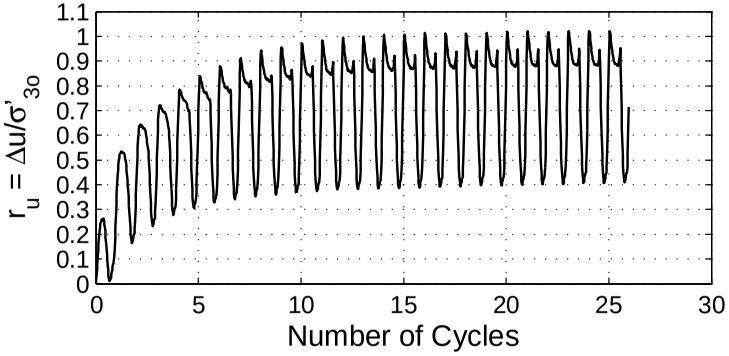

Specimen & Isotropic Cyclic Triaxial Test Data

Site:	151 Kil. St	**Loading Freq (Hz):**	0.1
Borehole:	DM BH1	**B−Value:**	0.984
Sample No.:	3U	**CSR:**	0.296
Sampler Type:	D&M	**N to $\varepsilon_{Ax-S.A.}$=3%:**	17
Spec. Depth (m):	3.72	**N to $\varepsilon_{Ax-D.A.}$=5%:**	25
Date Tested:	06/15/14	**Post−Cyclic Test:**	Reconsol.
Date Sampled:	05/15/14		
Spec. Ht. (mm):	135.2		
Spec. Diam. (mm):	61.0		
Dry Mass (g):	649.96		
Gs:	2.75		
e_o:	0.67		
σ'_{3o} (kPa):	61.6		
PI (%):	2		
USCS:	ML		

Isotropic Consolidation Test

Site:	151 Kil. St
Borehole:	DM BH1
Sample No.:	3U
Sampler Type:	D&M
Spec. Depth (m):	3.72
Date Tested:	06/15/14
Date Sampled:	05/15/14

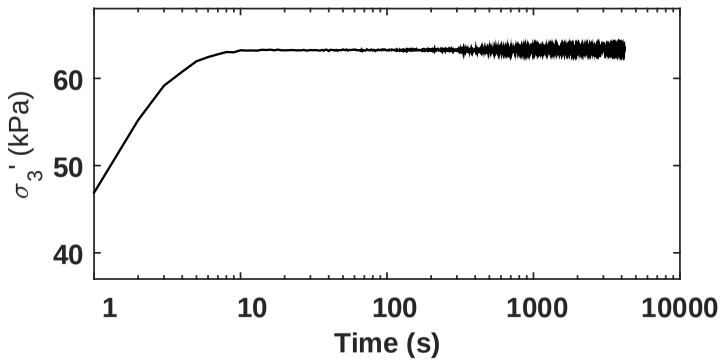

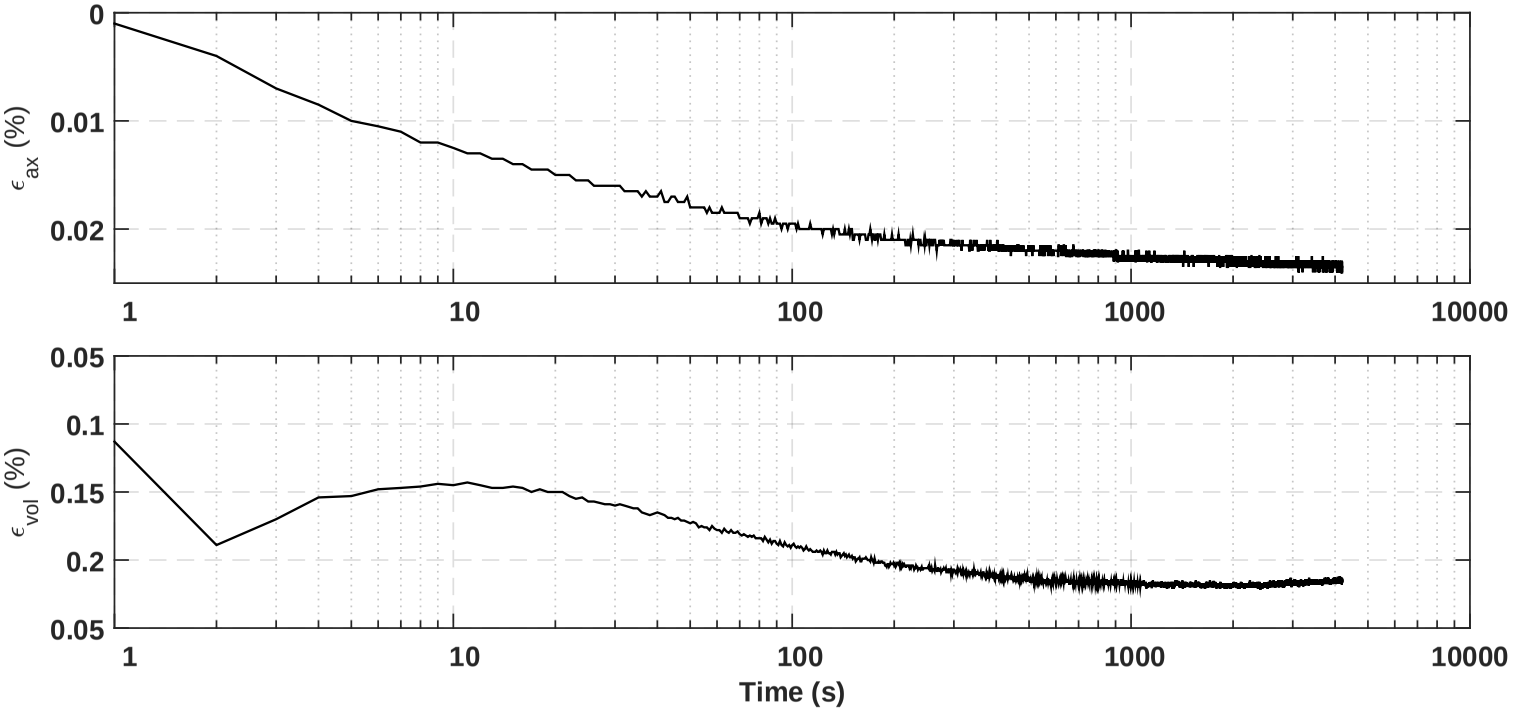

Post CTX Reconsolidation Test

Site:	151 Kil. St
Borehole:	DM BH1
Sample No.:	3U
Sampler Type:	D&M
Spec. Depth (m):	3.72
Date Tested:	06/15/14
Date Sampled:	05/15/14

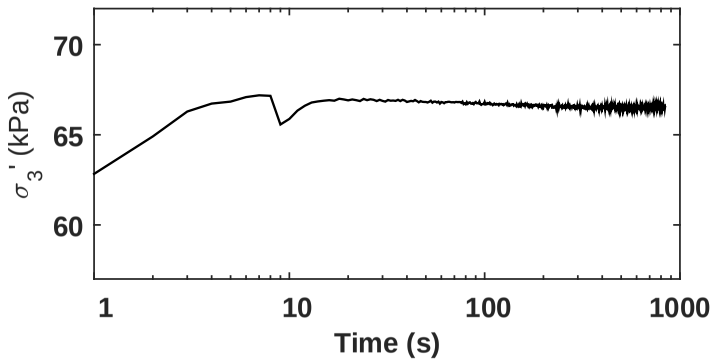

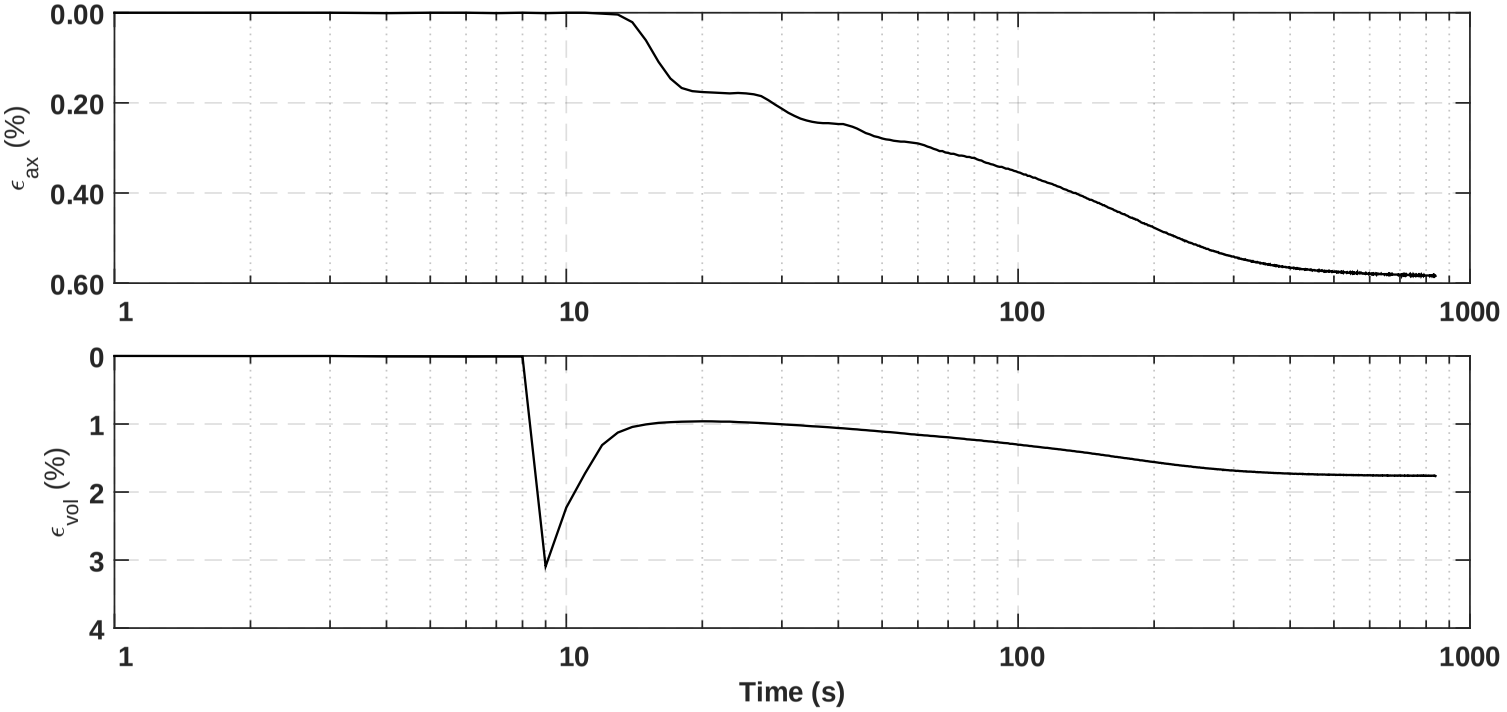

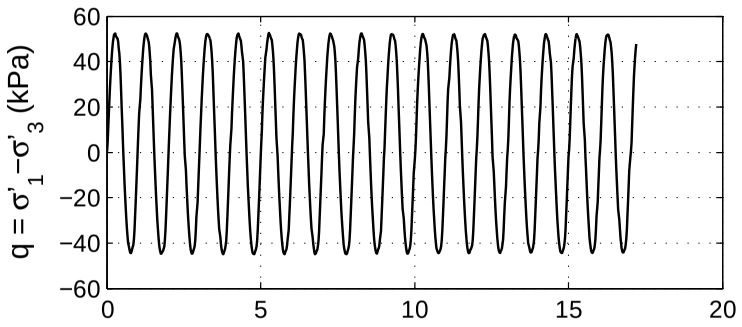

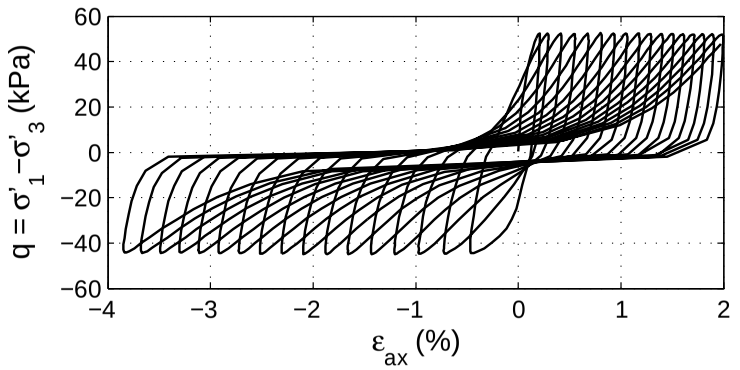

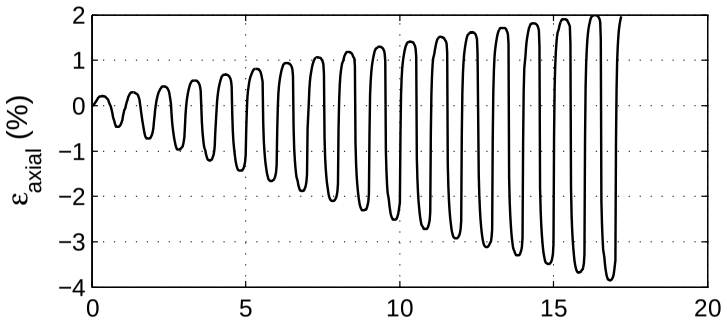

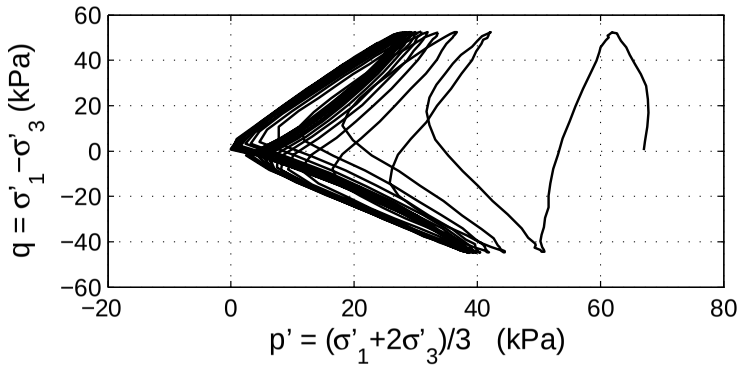

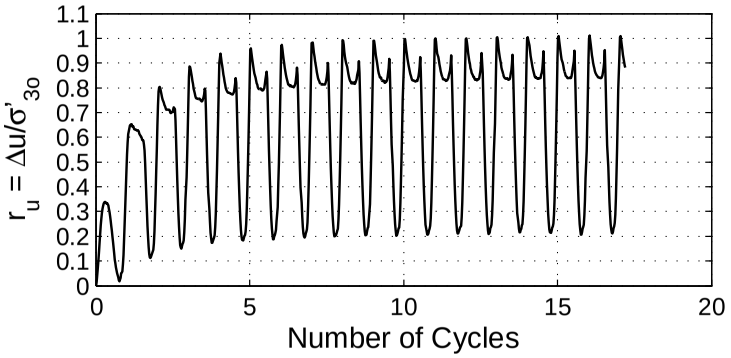

Specimen & Isotropic Cyclic Triaxial Test Data

Site:	151 Kil. St	**Loading Freq (Hz):**	0.1
Borehole:	DM BH1	**B−Value:**	0.983
Sample No.:	4U	**CSR:**	0.360
Sampler Type:	D&M	**N to $\varepsilon_{Ax-S.A.}$=3%:**	13
Spec. Depth (m):	4.77	**N to $\varepsilon_{Ax-D.A.}$=5%:**	14
Date Tested:	06/16/14	**Post−Cyclic Test:**	Reconsol.
Date Sampled:	05/16/14		
Spec. Ht. (mm):	138.8		
Spec. Diam. (mm):	61.0		
Dry Mass (g):	632.76		
Gs:	2.71		
e_o:	0.73		
σ'_{3o} (kPa):	66.9		
PI (%):	4		
USCS:	SM		

Isotropic Consolidation Test

Site:	151 Kil. St
Borehole:	DM BH1
Sample No.:	4U
Sampler Type:	D&M
Spec. Depth (m):	4.77
Date Tested:	06/16/14
Date Sampled:	05/16/14

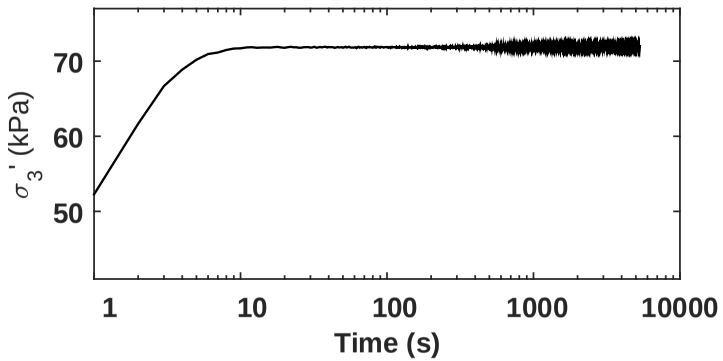

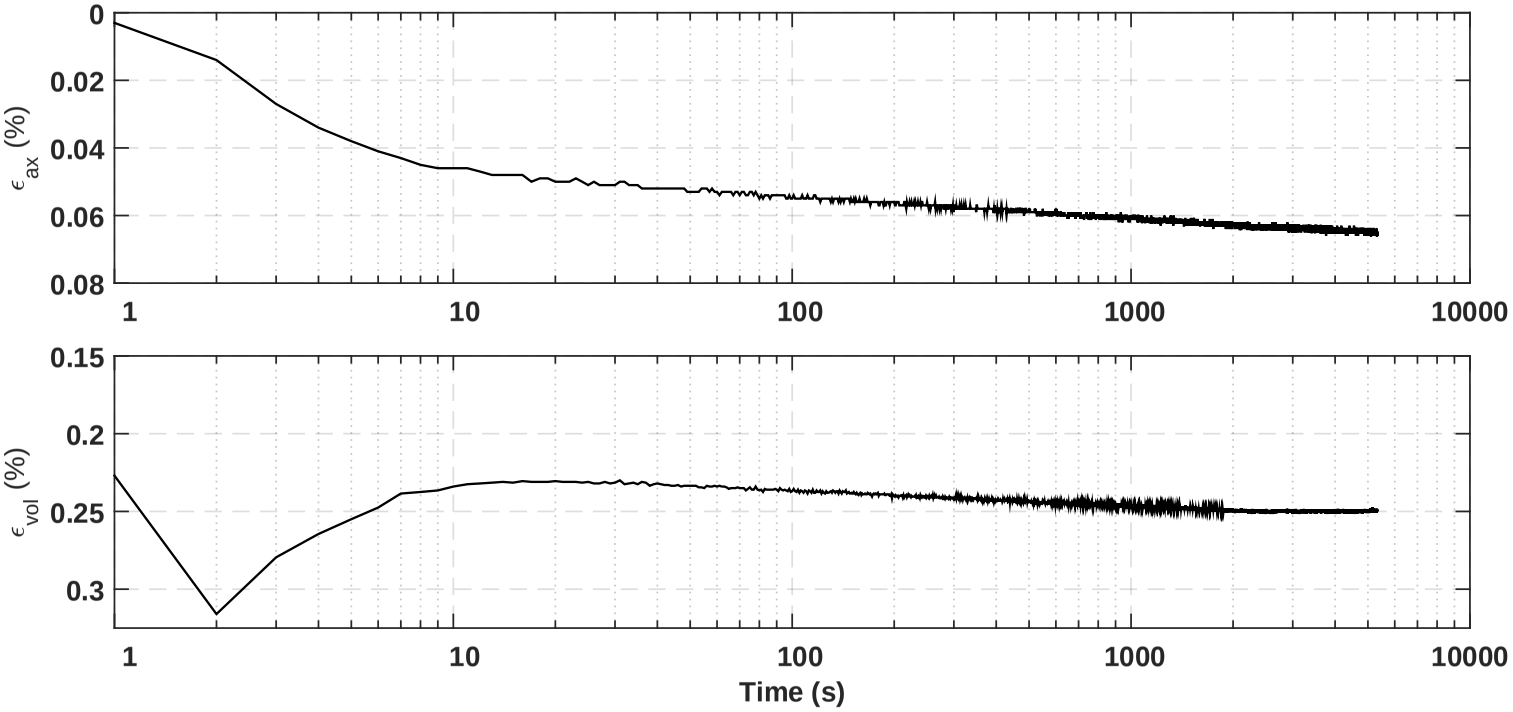

Post CTX Reconsolidation Test

Site:	151 Kil. St
Borehole:	DM BH1
Sample No.:	4U
Sampler Type:	D&M
Spec. Depth (m):	4.77
Date Tested:	06/16/14
Date Sampled:	05/16/14

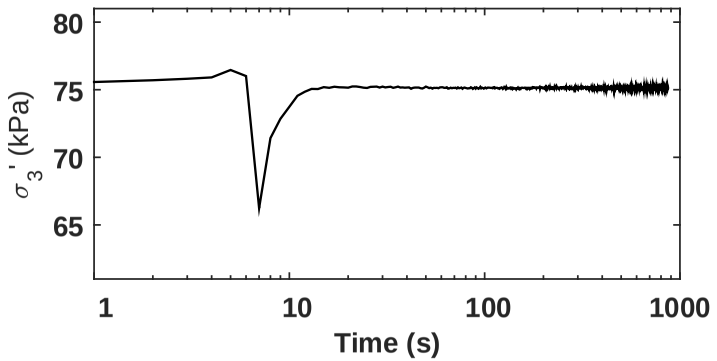

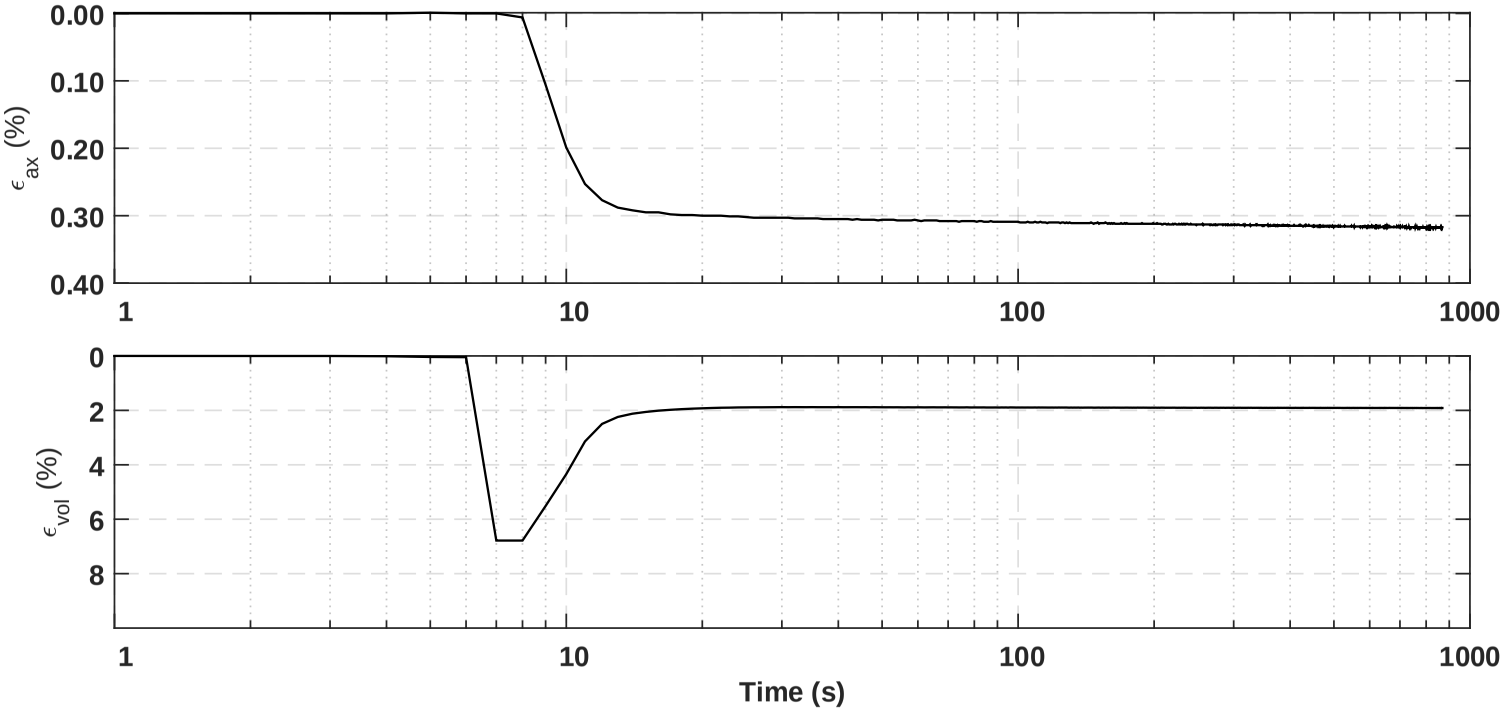

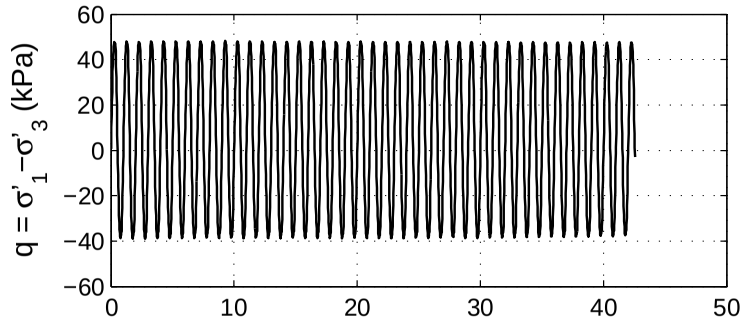

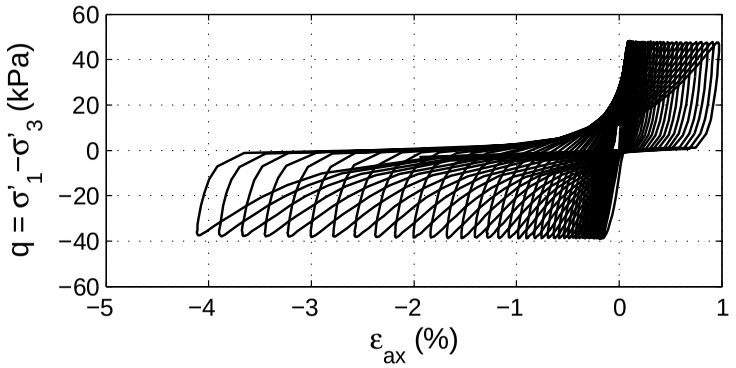

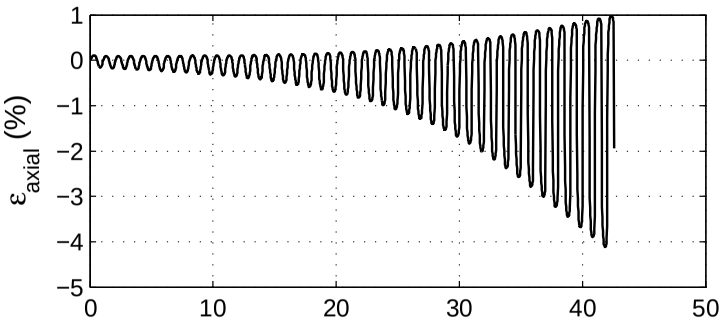

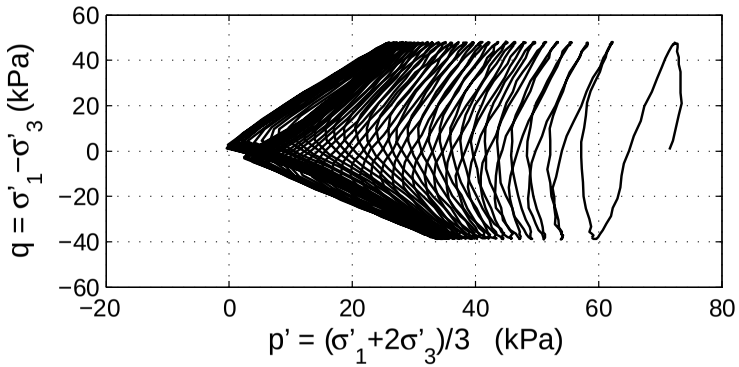

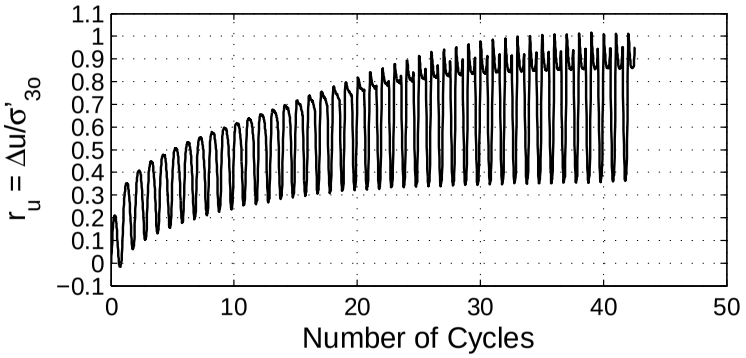

Specimen & Isotropic Cyclic Triaxial Test Data

Site:	151 Kil. St	**Loading Freq (Hz):**	0.1
Borehole:	DM BH1	**B−Value:**	0.987
Sample No.:	4U	**CSR:**	0.303
Sampler Type:	D&M	**N to $\varepsilon_{Ax-S.A.}$=3%:**	37
Spec. Depth (m):	4.92	**N to $\varepsilon_{Ax-D.A.}$=5%:**	42.5
Date Tested:	06/16/14	**Post−Cyclic Test:**	Monotonic
Date Sampled:	05/16/14		
Spec. Ht. (mm):	139.0		
Spec. Diam. (mm):	61.0		
Dry Mass (g):	638.75		
Gs:	2.67		
e_o:	0.70		
σ'_{3o} (kPa):	71.3		
PI (%):	NP		
USCS:	SM		

Isotropic Consolidation Test

Site:	151 Kil. St
Borehole:	DM BH1
Sample No.:	4U
Sampler Type:	D&M
Spec. Depth (m):	4.92
Date Tested:	06/16/14
Date Sampled:	05/16/14

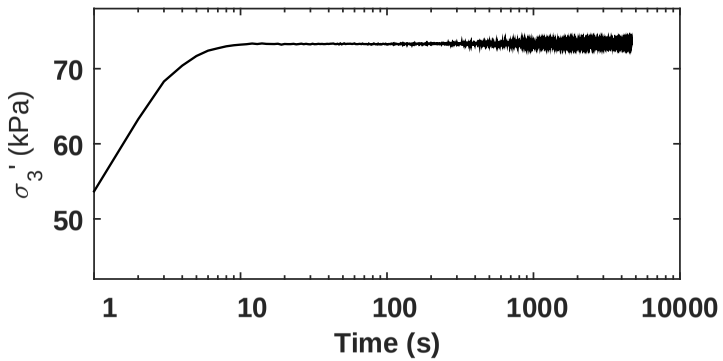

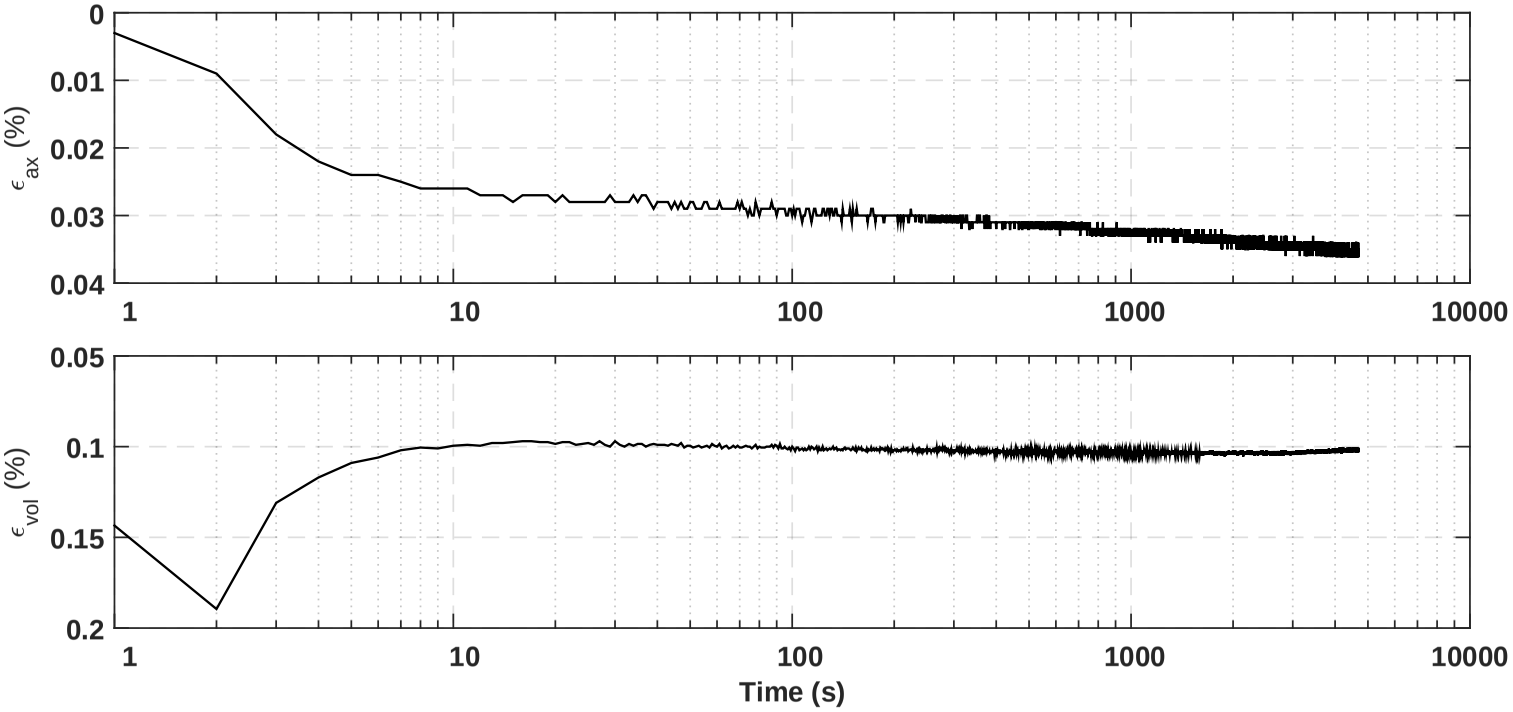

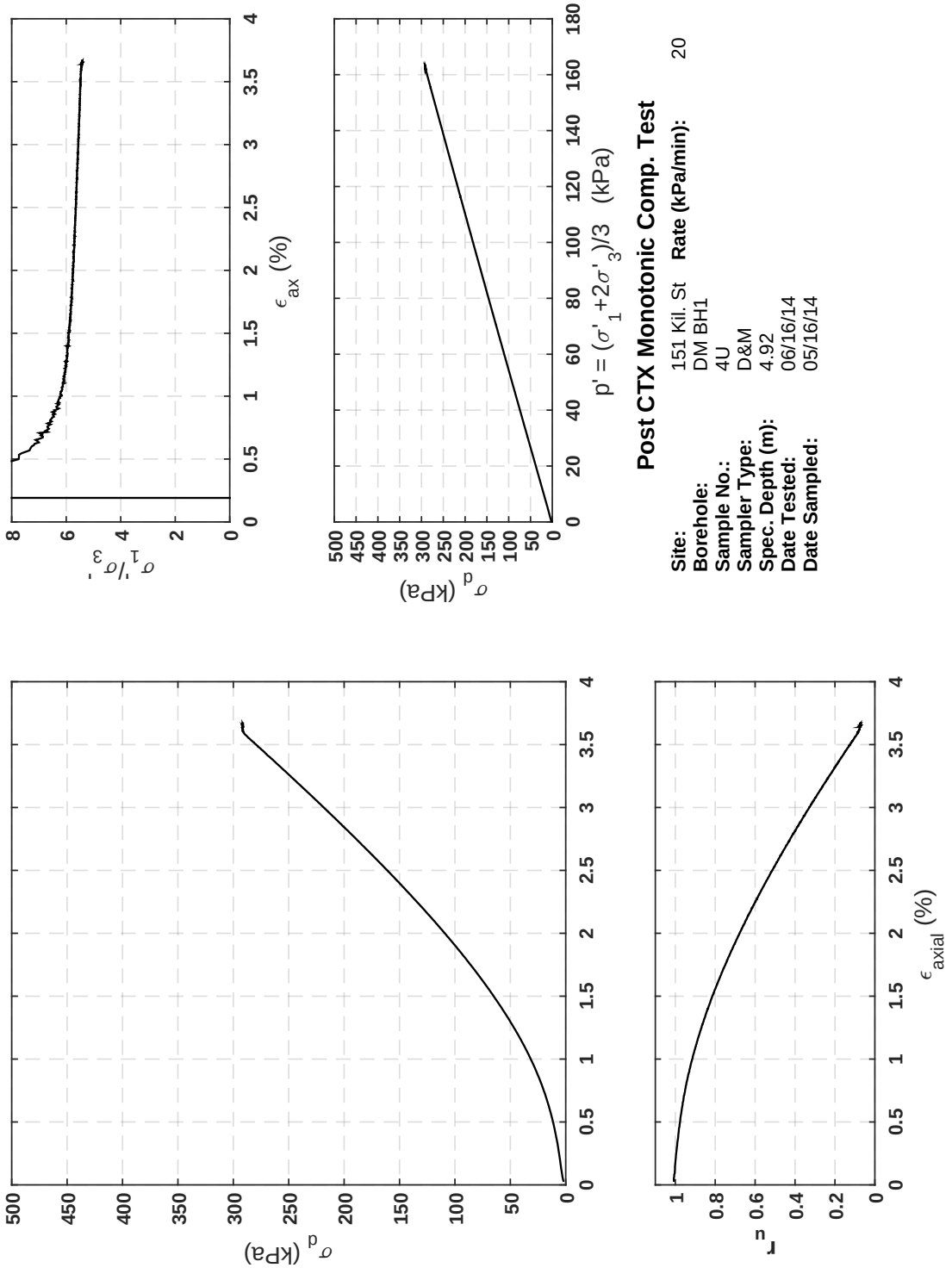
Post CTX Monotonic Comp. Test
Site: 151 Kil. St
Borehole: DM BH1
Sample No.: 4U
Sampler Type: D&M
Spec. Depth (m): 4.92
Date Tested: 06/16/14
Date Sampled: 05/16/14
Rate (kPa/min): 20
σ'1/σ'3
ϵax (%)
σd (kPa)
p' = (σ'1+2σ'3)/3 (kPa)
σd (kPa)
ru
ϵaxial (%)

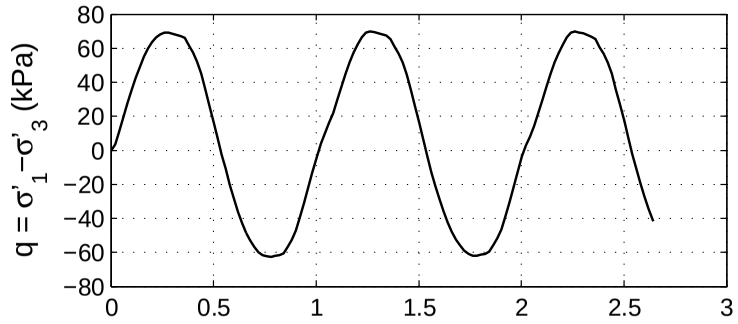

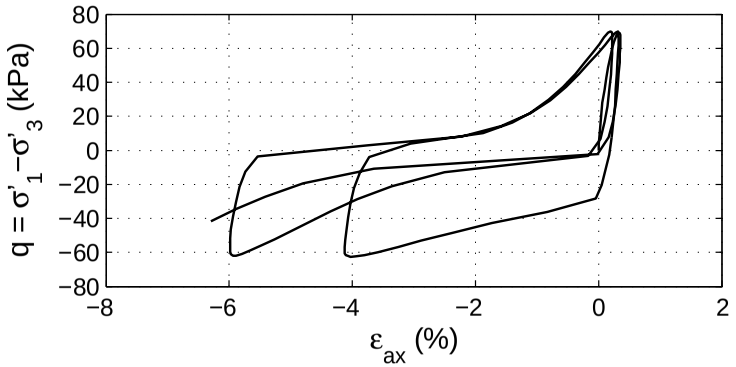

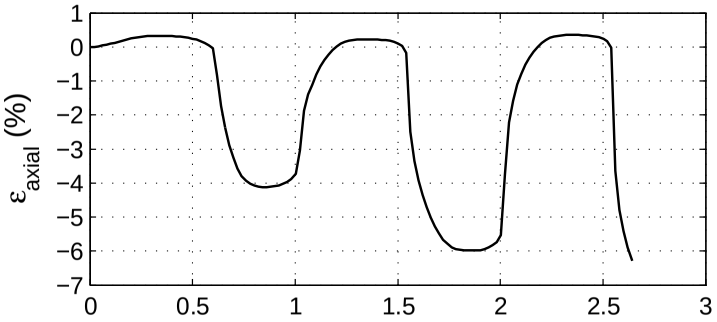

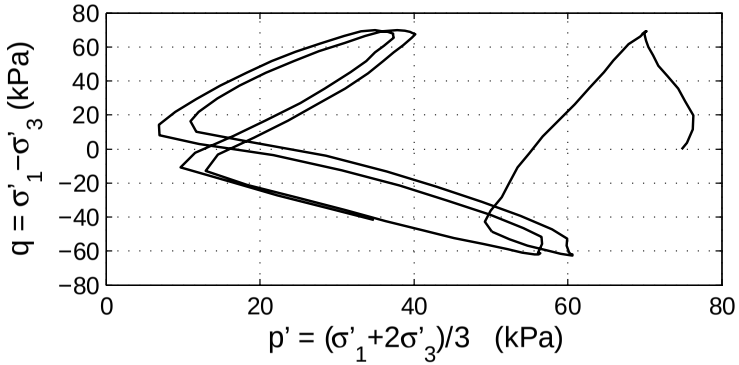

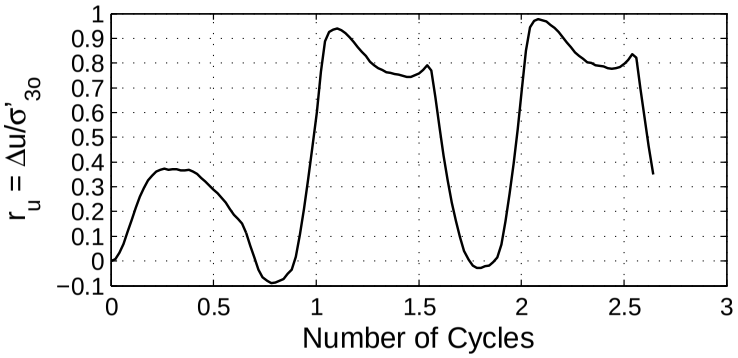

Specimen & Isotropic Cyclic Triaxial Test Data

Site:	151 Kil. St	**Loading Freq (Hz):**	0.1
Borehole:	DM BH1	**B−Value:**	0.967+
Sample No.:	5U	**CSR:**	0.439
Sampler Type:	D&M	**N to $\varepsilon_{Ax-S.A.}$=3%:**	1
Spec. Depth (m):	5.57	**N to $\varepsilon_{Ax-D.A.}$=5%:**	2
Date Tested:	10/21/14	**Post−Cyclic Test:**	Monotonic
Date Sampled:	05/16/14		
Spec. Ht. (mm):	134.9		
Spec. Diam. (mm):	60.8		
Dry Mass (g):	584.16		
Gs:	2.66		
e_o:	0.78		
σ'_{3o} (kPa):	74.8		
PI (%):	NP		
USCS:	SM		

Isotropic Consolidation Test

Site:	151 Kil. St
Borehole:	DM BH1
Sample No.:	5U
Sampler Type:	D&M
Spec. Depth (m):	5.57
Date Tested:	10/21/14
Date Sampled:	05/16/14

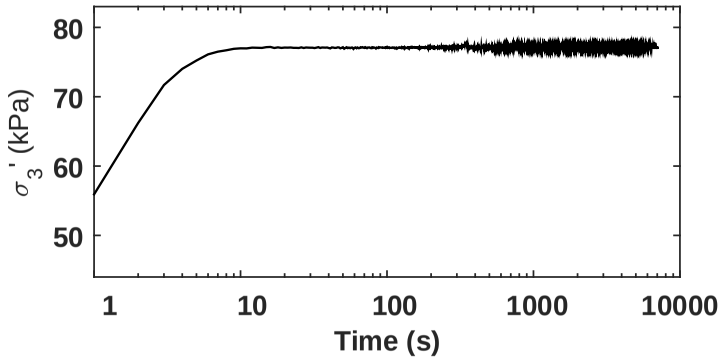

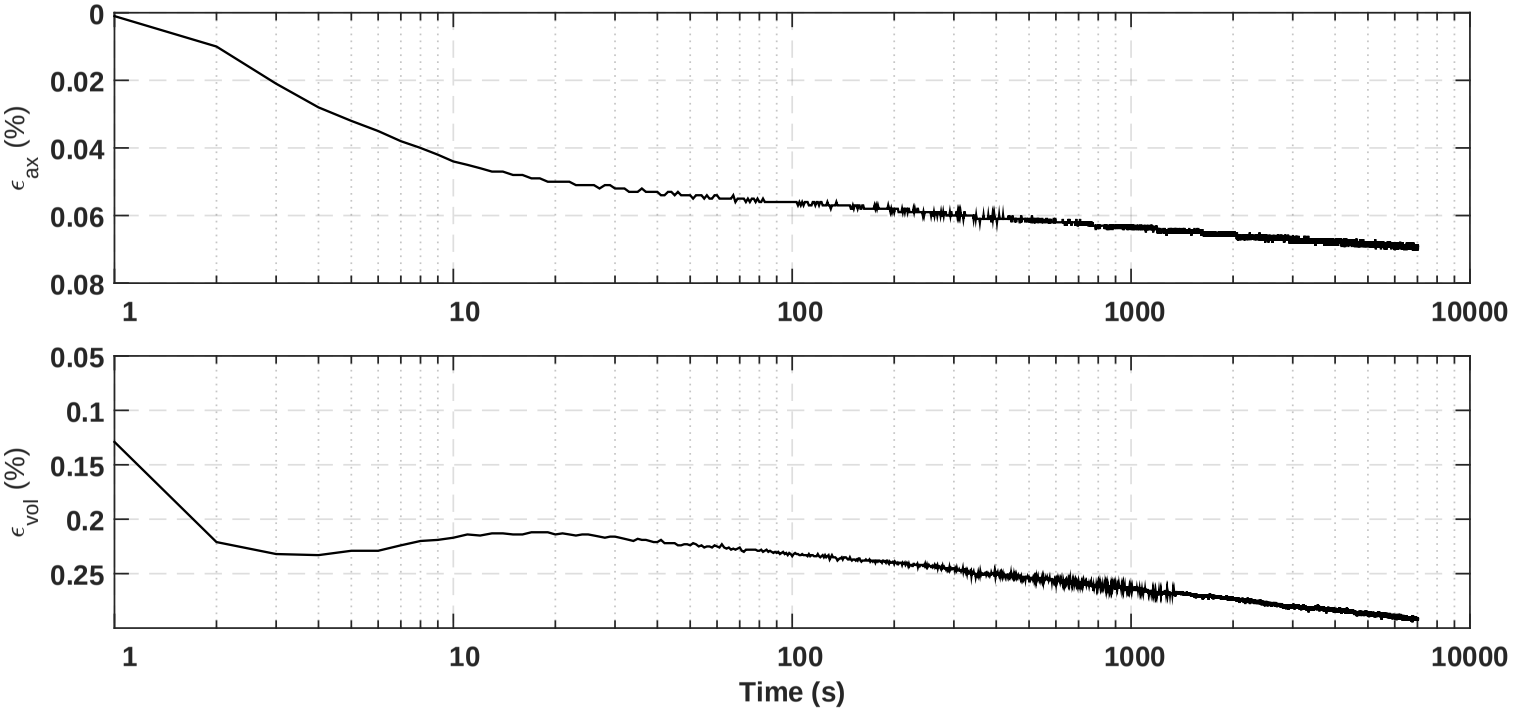

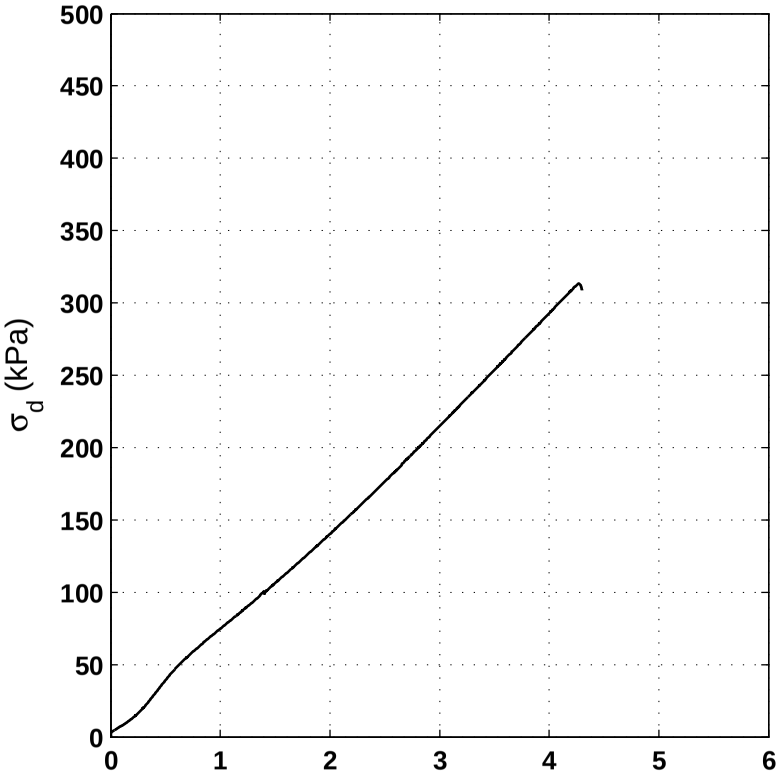

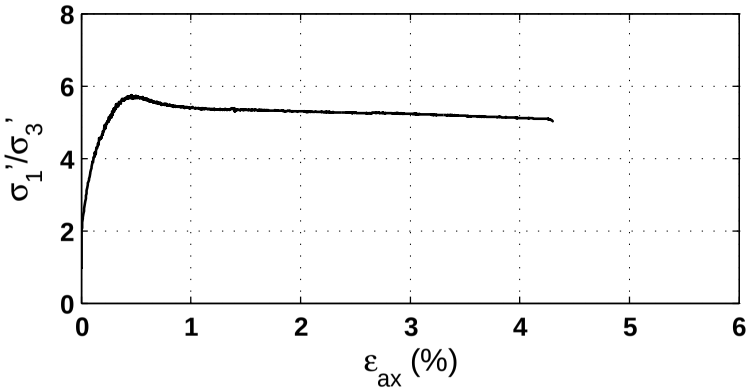

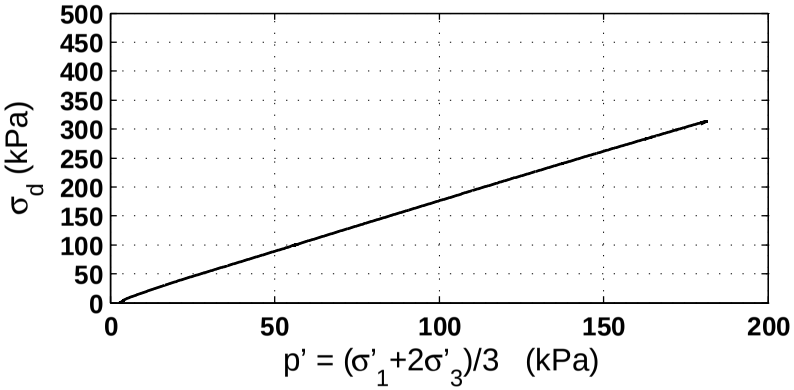

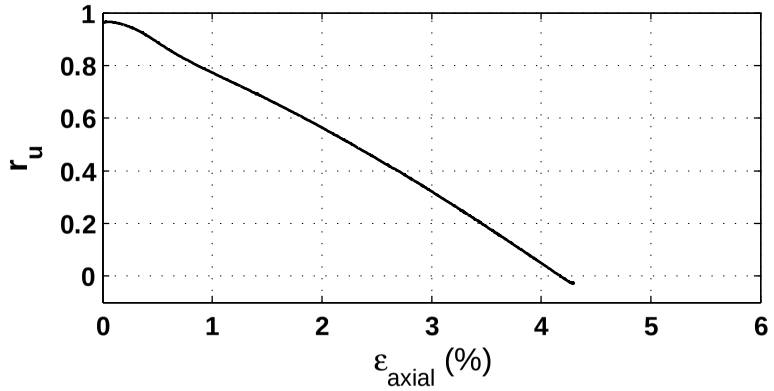

Post CTX Monotonic Comp. Test

Site:	151 Kil. St	**Rate (kPa/min):**	10
Borehole:	DM BH1		
Sample No.:	5U		
Sampler Type:	D&M		
Spec. Depth (m):	5.57		
Date Tested:	10/21/14		
Date Sampled:	05/16/14		

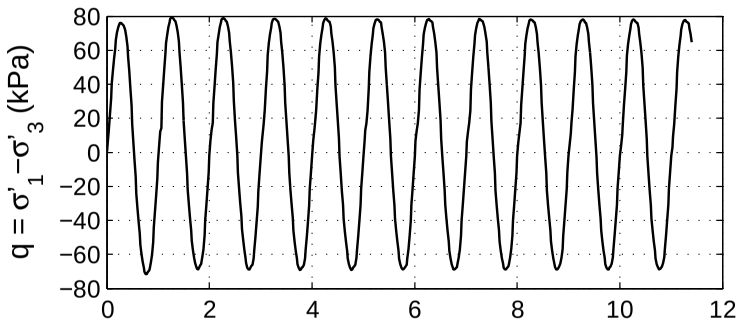

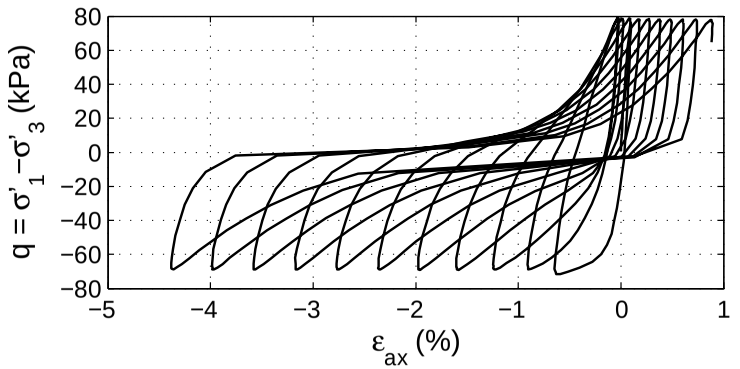

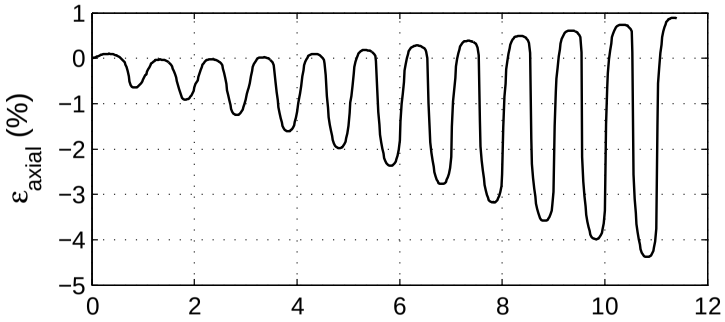

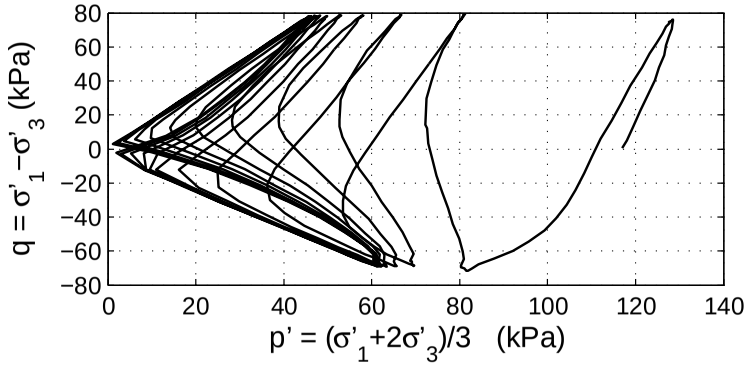

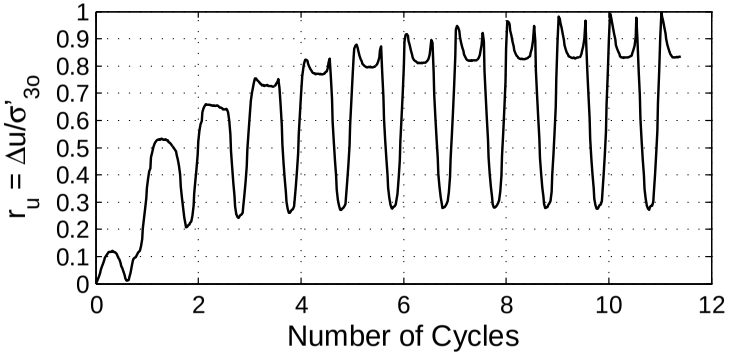

Specimen & Isotropic Cyclic Triaxial Test Data

Site:	151 Kil. St	**Loading Freq (Hz):**	0.1
Borehole:	DM BH1	**B−Value:**	0.983
Sample No.:	7U	**CSR:**	0.315
Sampler Type:	D&M	**N to $\varepsilon_{Ax-S.A.}$=3%:**	8
Spec. Depth (m):	10.31	**N to $\varepsilon_{Ax-D.A.}$=5%:**	11
Date Tested:	06/19/14	**Post−Cyclic Test:**	Reconsol.
Date Sampled:	05/16/14		
Spec. Ht. (mm):	134.7		
Spec. Diam. (mm):	60.9		
Dry Mass (g):	618.36		
Gs:	2.65		
e_o:	0.68		
σ'_{3o} (kPa):	116.8		
PI (%):	NP		
USCS:	SP		

Isotropic Consolidation Test

Site:	151 Kil. St
Borehole:	DM BH1
Sample No.:	7U
Sampler Type:	D&M
Spec. Depth (m):	10.31
Date Tested:	06/19/14
Date Sampled:	05/16/14

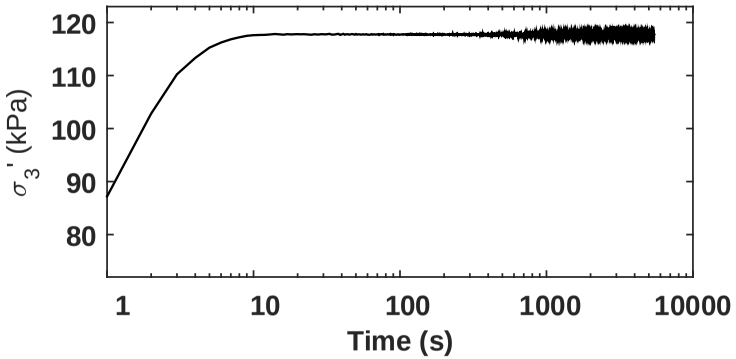

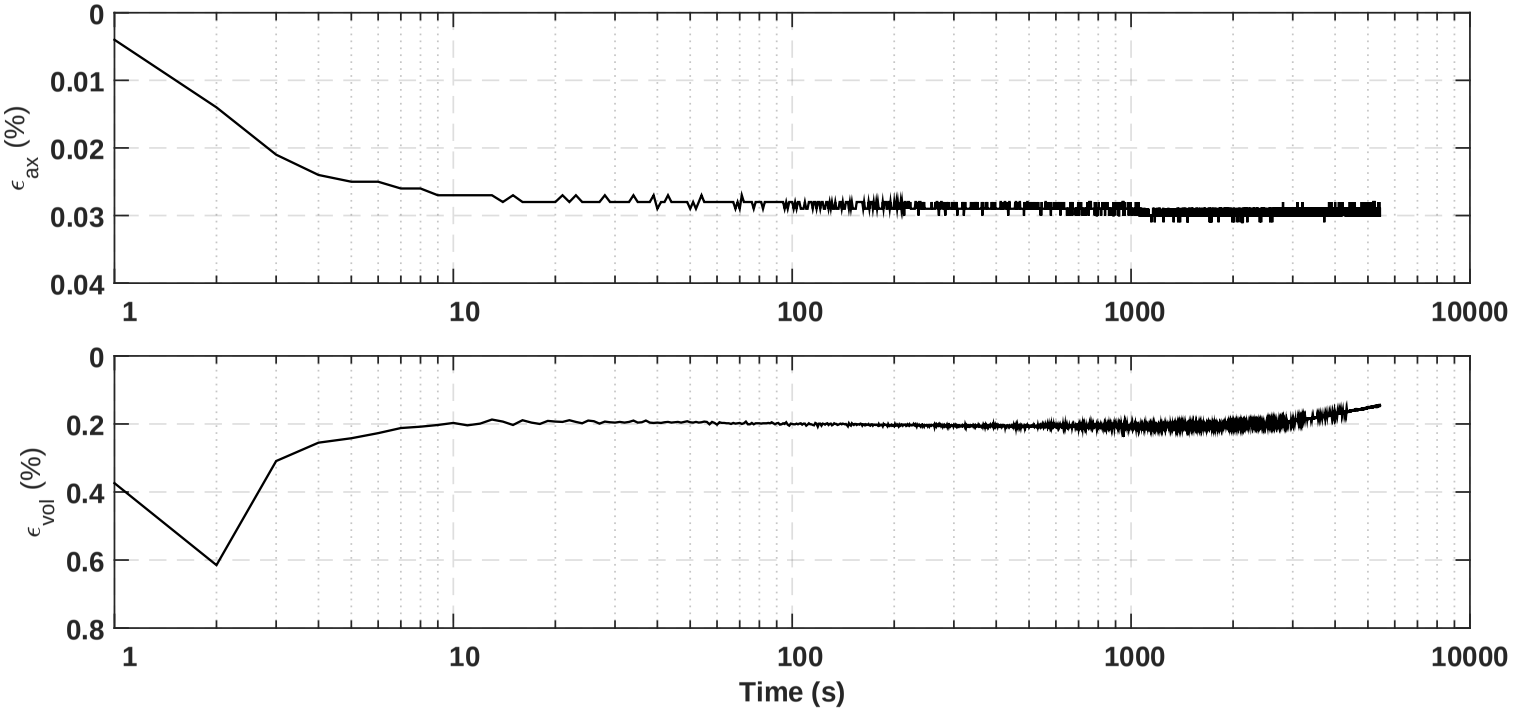

Post CTX Reconsolidation Test

Site:	151 Kil. St
Borehole:	DM BH1
Sample No.:	7U
Sampler Type:	D&M
Spec. Depth (m):	10.31
Date Tested:	06/19/14
Date Sampled:	05/16/14

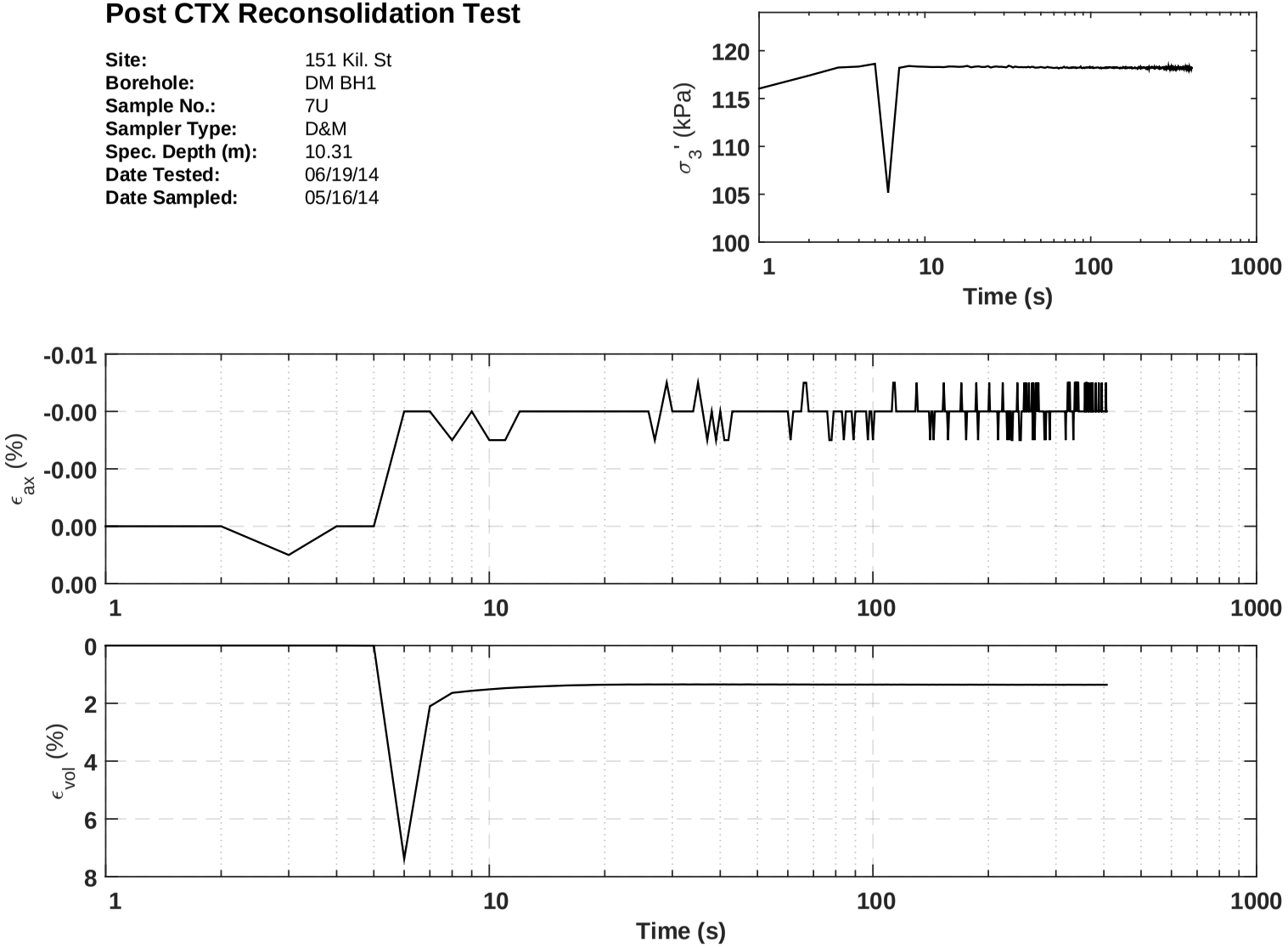

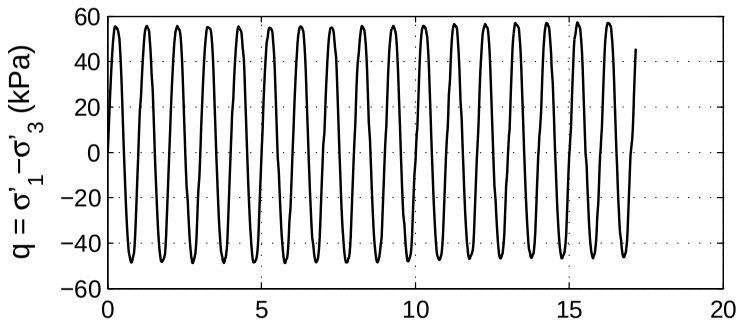

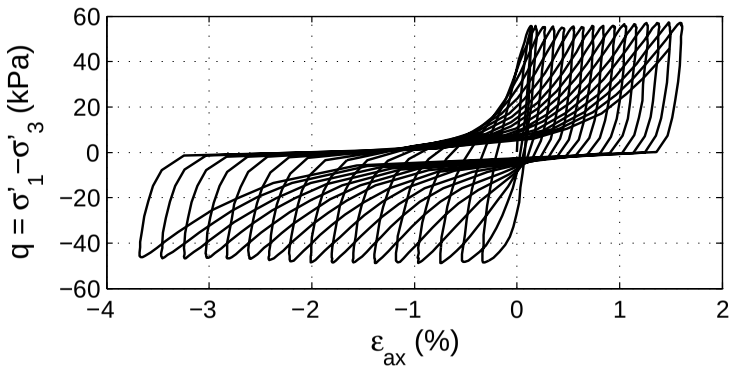

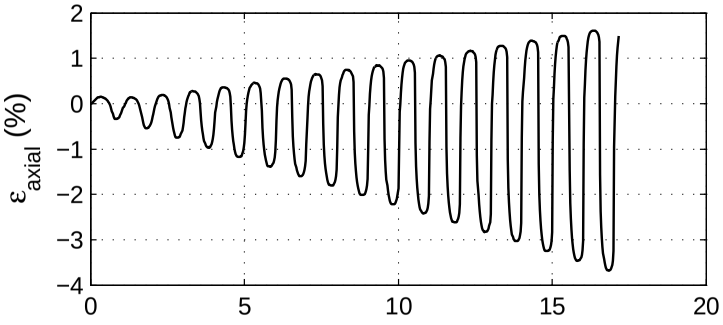

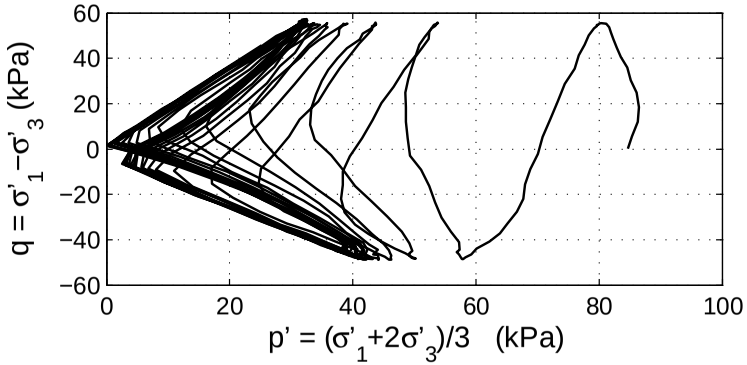

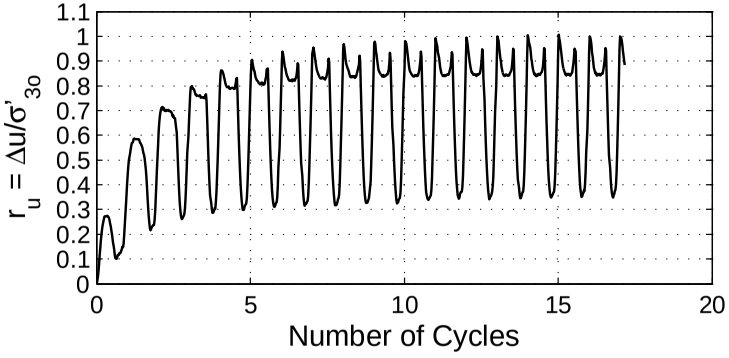

Specimen & Isotropic Cyclic Triaxial Test Data

Site:	151 Kil. St	**Loading Freq (Hz):**	0.1
Borehole:	DM BH2	**B−Value:**	0.988
Sample No.:	5U	**CSR:**	0.304
Sampler Type:	D&M	**N to $\varepsilon_{Ax-S.A.}$=3%:**	14
Spec. Depth (m):	5.88	**N to $\varepsilon_{Ax-D.A.}$=5%:**	16.5
Date Tested:	06/08/14	**Post−Cyclic Test:**	Monotonic
Date Sampled:	05/14/14		
Spec. Ht. (mm):	140.0		
Spec. Diam. (mm):	60.9		
Dry Mass (g):	622.42		
Gs:	2.68		
e_o:	0.76		
σ'_{3o} (kPa):	84.7		
PI (%):	NP		
USCS:	SP−SM		

Isotropic Consolidation Test

Site:	151 Kil. St
Borehole:	DM BH2
Sample No.:	4U
Sampler Type:	D&M
Spec. Depth (m):	5.88
Date Tested:	06/08/14
Date Sampled:	05/14/14

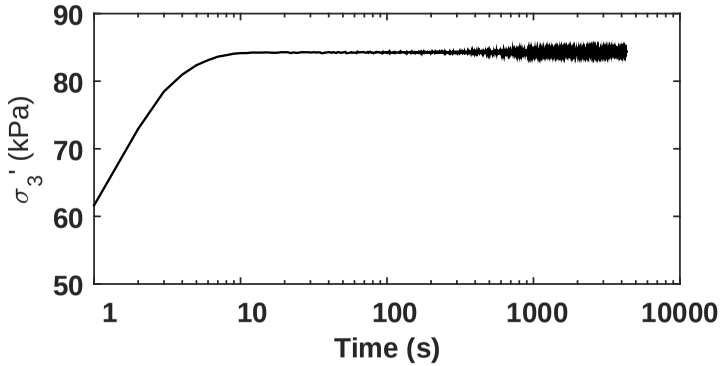

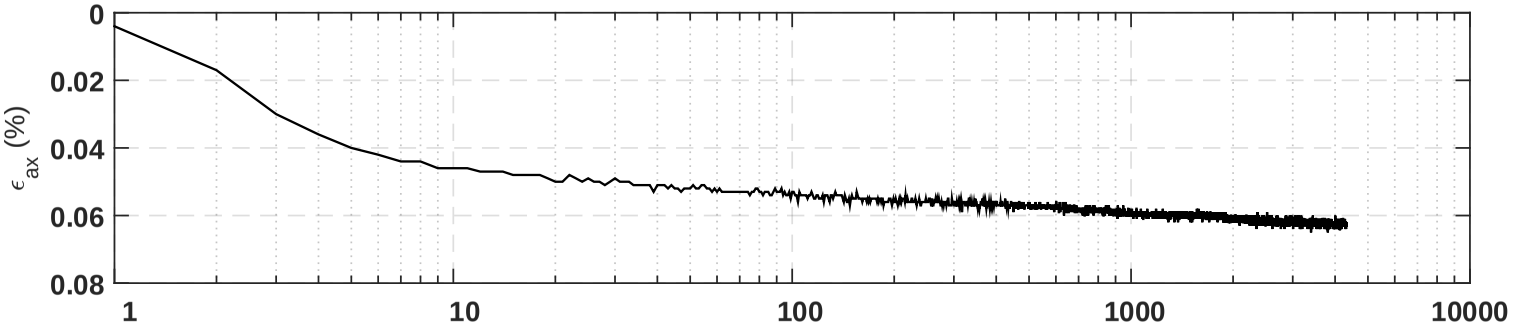

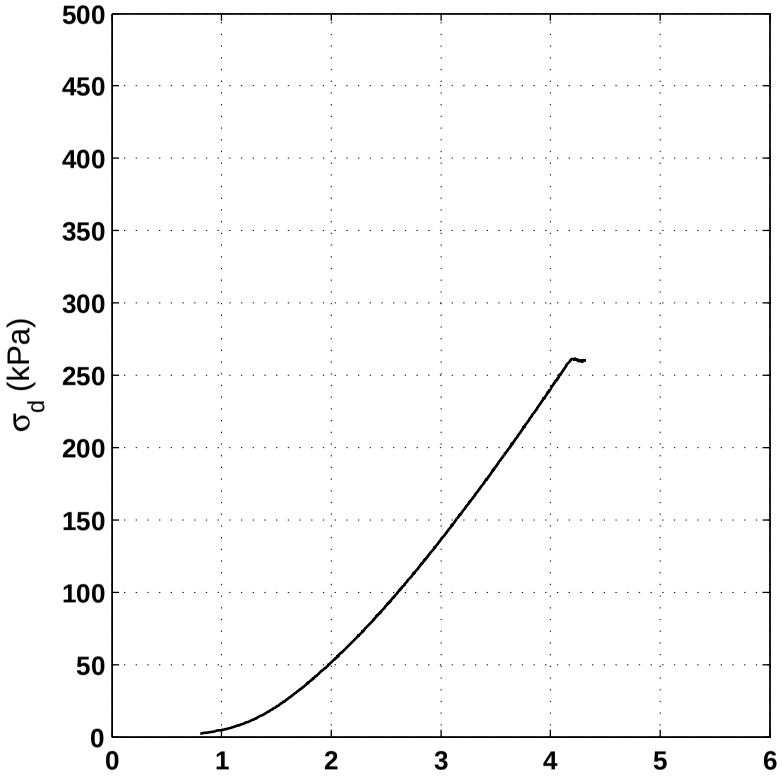

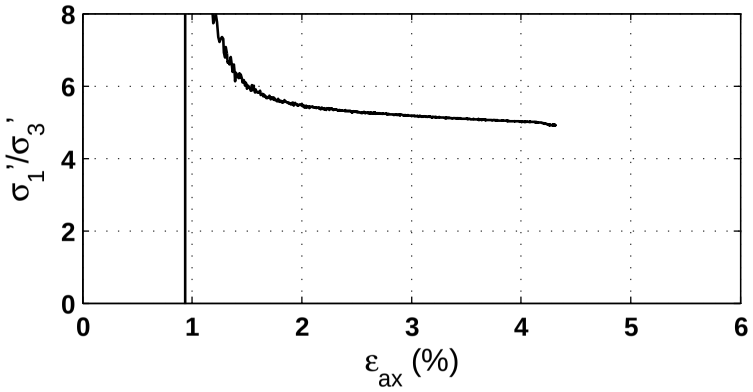

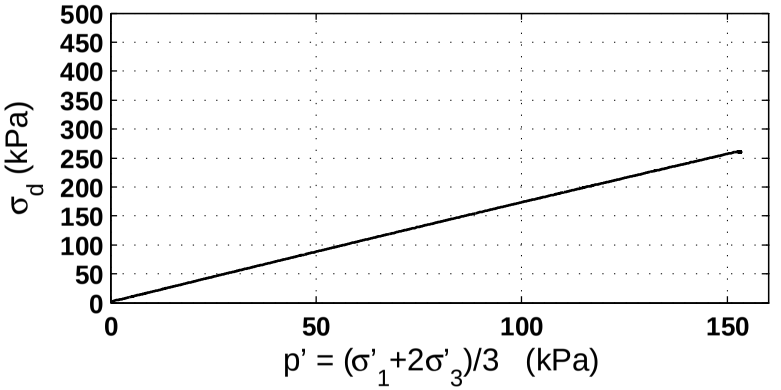

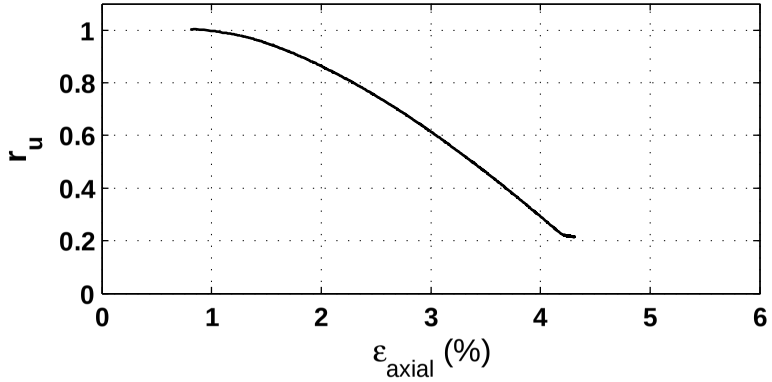

Post CTX Monotonic Comp. Test

Site:	151 Kil. St	**Rate (kPa/min):**	20
Borehole:	DM BH2		
Sample No.:	4U		
Sampler Type:	D&M		
Spec. Depth (m):	5.88		
Date Tested:	06/08/14		
Date Sampled:	05/14/14		

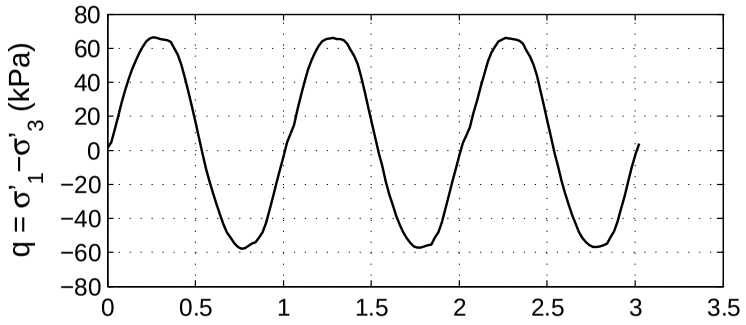

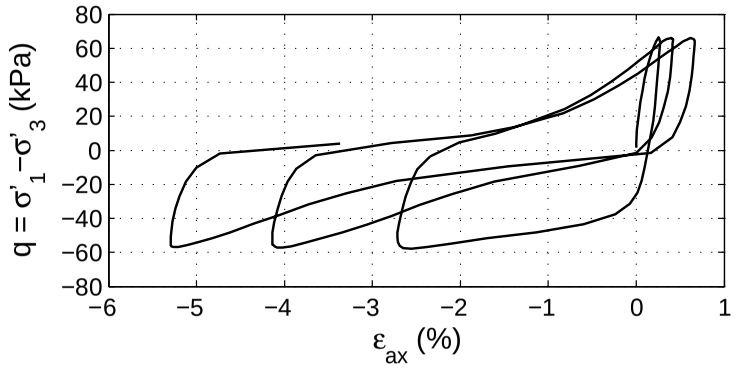

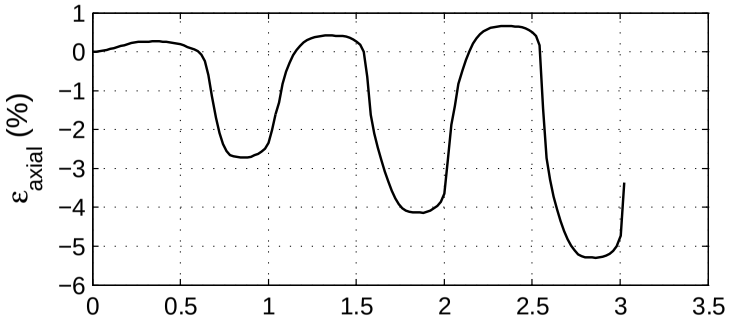

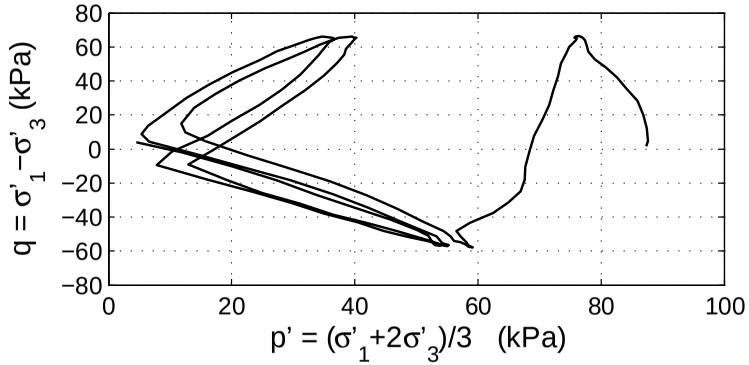

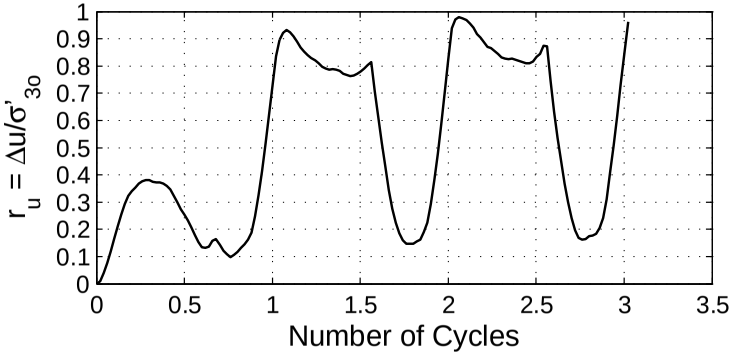

Specimen & Isotropic Cyclic Triaxial Test Data

Site:	151 Kil. St	**Loading Freq (Hz):**	0.1
Borehole:	DM BH2	**B−Value:**	0.980
Sample No.:	6U	**CSR:**	0.354
Sampler Type:	D&M	**N to $\varepsilon_{Ax-S.A.}$=3%:**	2
Spec. Depth (m):	6.38	**N to $\varepsilon_{Ax-D.A.}$=5%:**	3
Date Tested:	06/07/14	**Post−Cyclic Test:**	Monotonic
Date Sampled:	05/14/14		
Spec. Ht. (mm):	139.4		
Spec. Diam. (mm):	60.8		
Dry Mass (g):	596.90		
Gs:	2.7		
e_o:	0.83		
σ'_{3o} (kPa):	86.8		
PI (%):	−−		
USCS:	−−		

Isotropic Consolidation Test

Site:	151 Kil. St
Borehole:	DM BH2
Sample No.:	6U
Sampler Type:	D&M
Spec. Depth (m):	6.38
Date Tested:	06/07/14
Date Sampled:	05/14/14

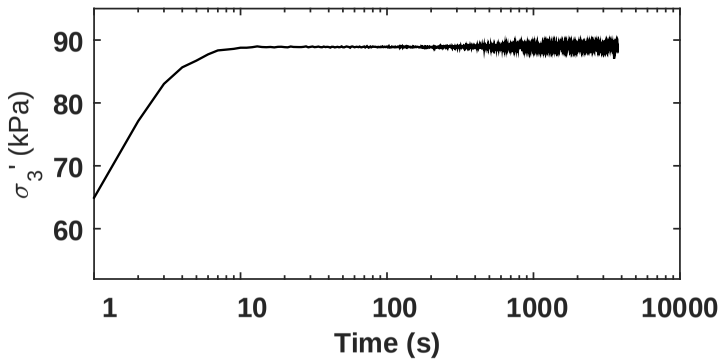

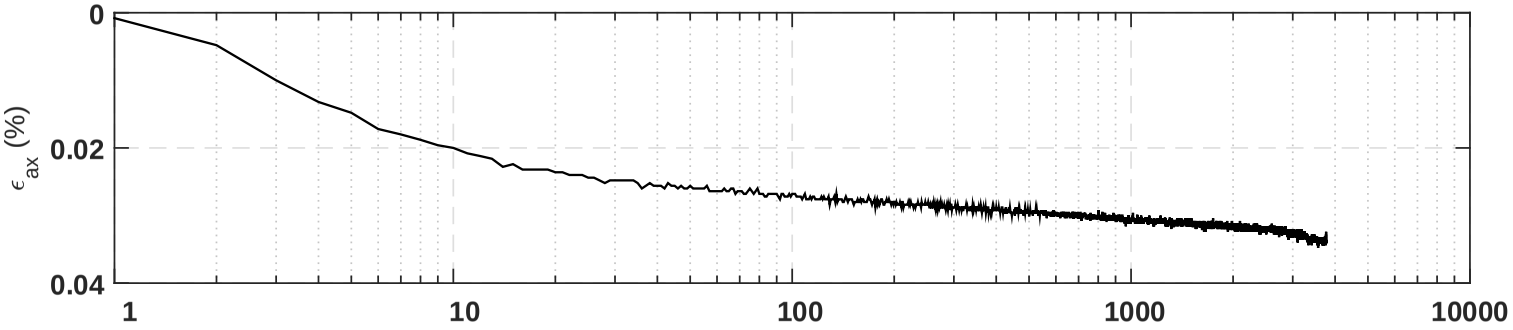

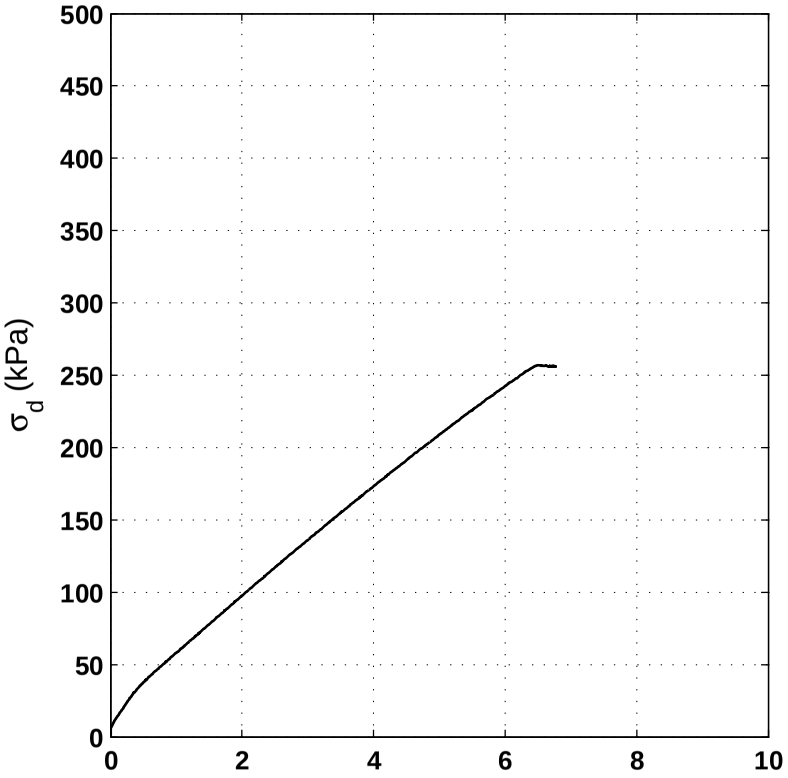

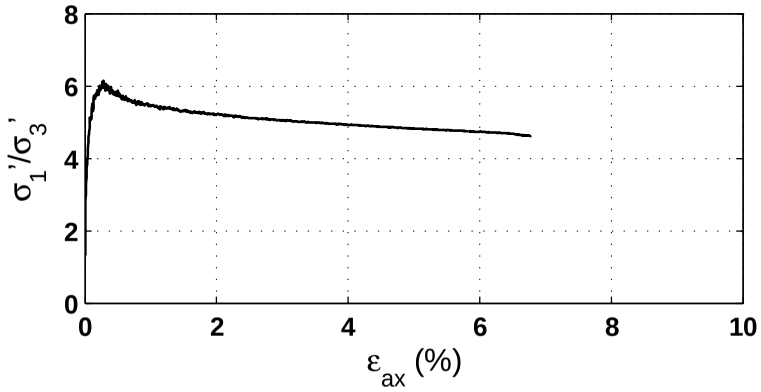

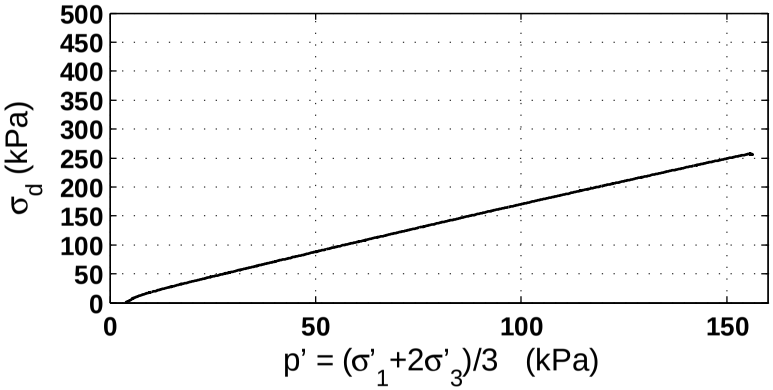

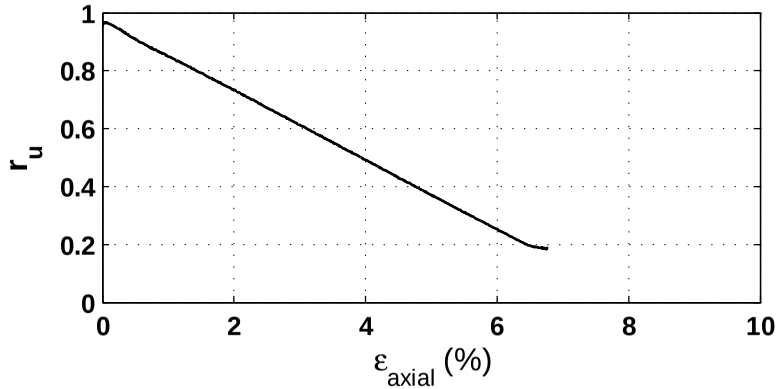

Post CTX Monotonic Comp. Test

Site:	151 Kil. St	**Rate (kPa/min):**	20
Borehole:	DM BH2		
Sample No.:	6U		
Sampler Type:	D&M		
Spec. Depth (m):	6.38		
Date Tested:	06/07/14		
Date Sampled:	05/14/14		

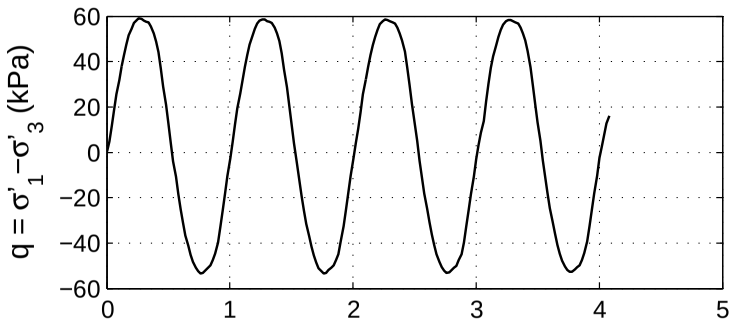

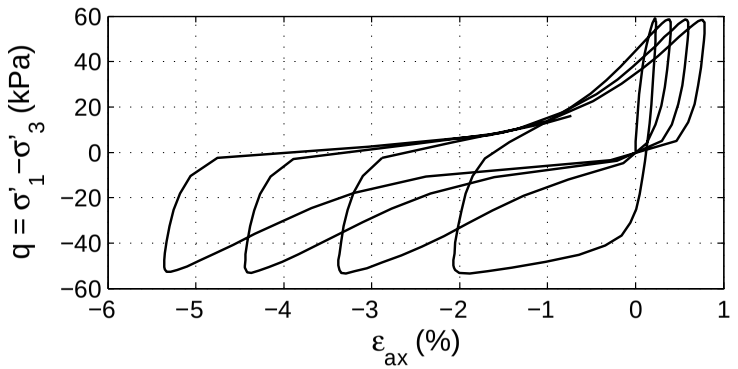

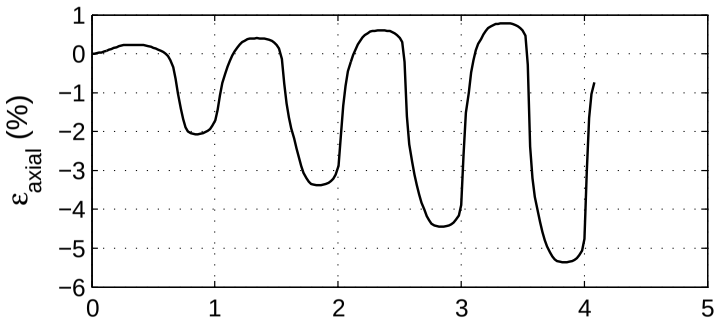

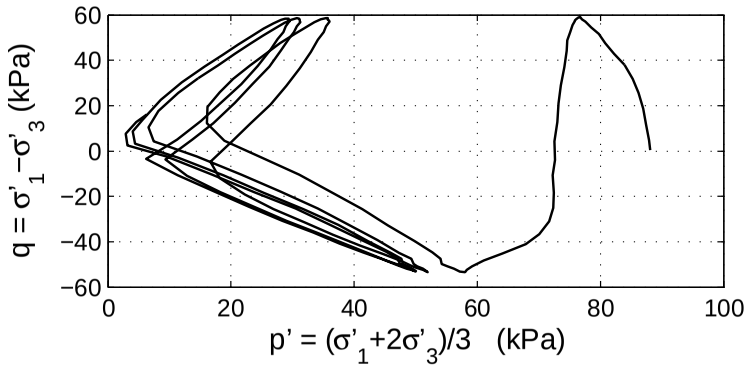

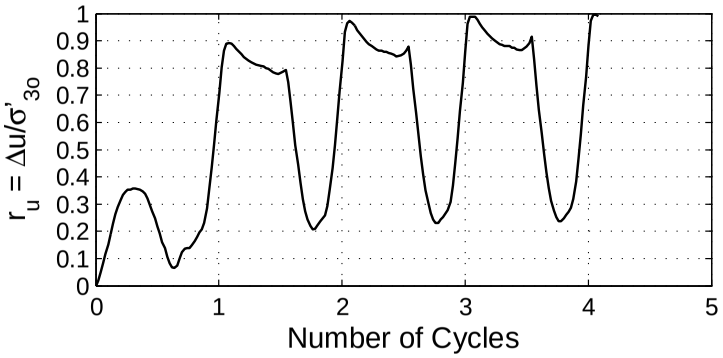

Specimen & Isotropic Cyclic Triaxial Test Data

Site:	151 Kil. St	**Loading Freq (Hz):**	0.1
Borehole:	DM BH2	**B−Value:**	0.989
Sample No.:	7U	**CSR:**	0.317
Sampler Type:	D&M	**N to $\varepsilon_{Ax-S.A.}$=3%:**	2
Spec. Depth (m):	6.72	**N to $\varepsilon_{Ax-D.A.}$=5%:**	3
Date Tested:	06/20/14	**Post−Cyclic Test:**	Reconsol.
Date Sampled:	05/15/14		
Spec. Ht. (mm):	138.2		
Spec. Diam. (mm):	60.6		
Dry Mass (g):	590.63		
Gs:	2.71		
e_o:	0.83		
σ'_{3o} (kPa):	88.0		
PI (%):	3		
USCS:	ML		

Isotropic Consolidation Test

Site:	151 Kil. St
Borehole:	DM BH2
Sample No.:	7U
Sampler Type:	D&M
Spec. Depth (m):	6.72
Date Tested:	06/20/14
Date Sampled:	05/15/14

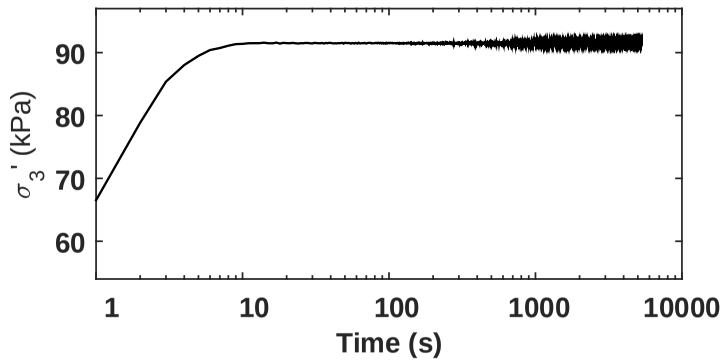

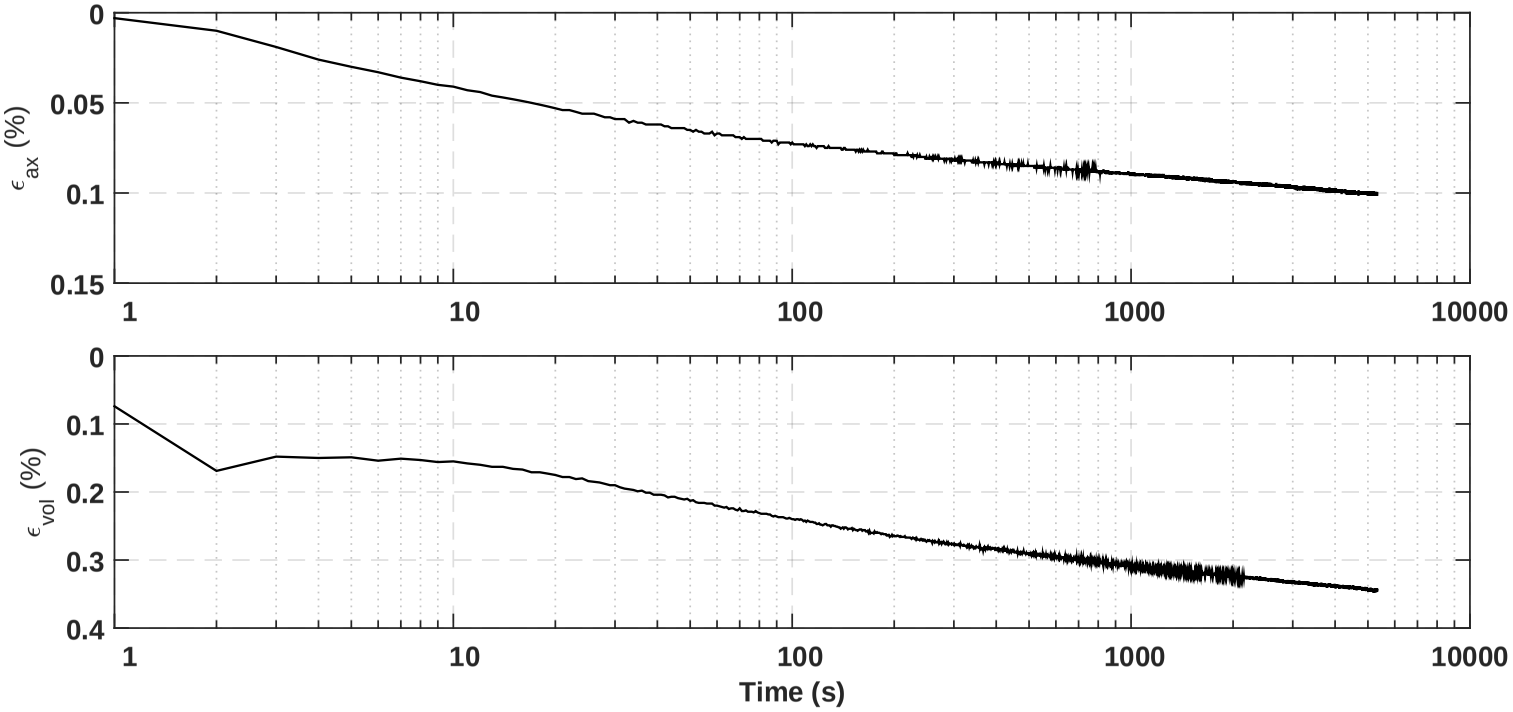

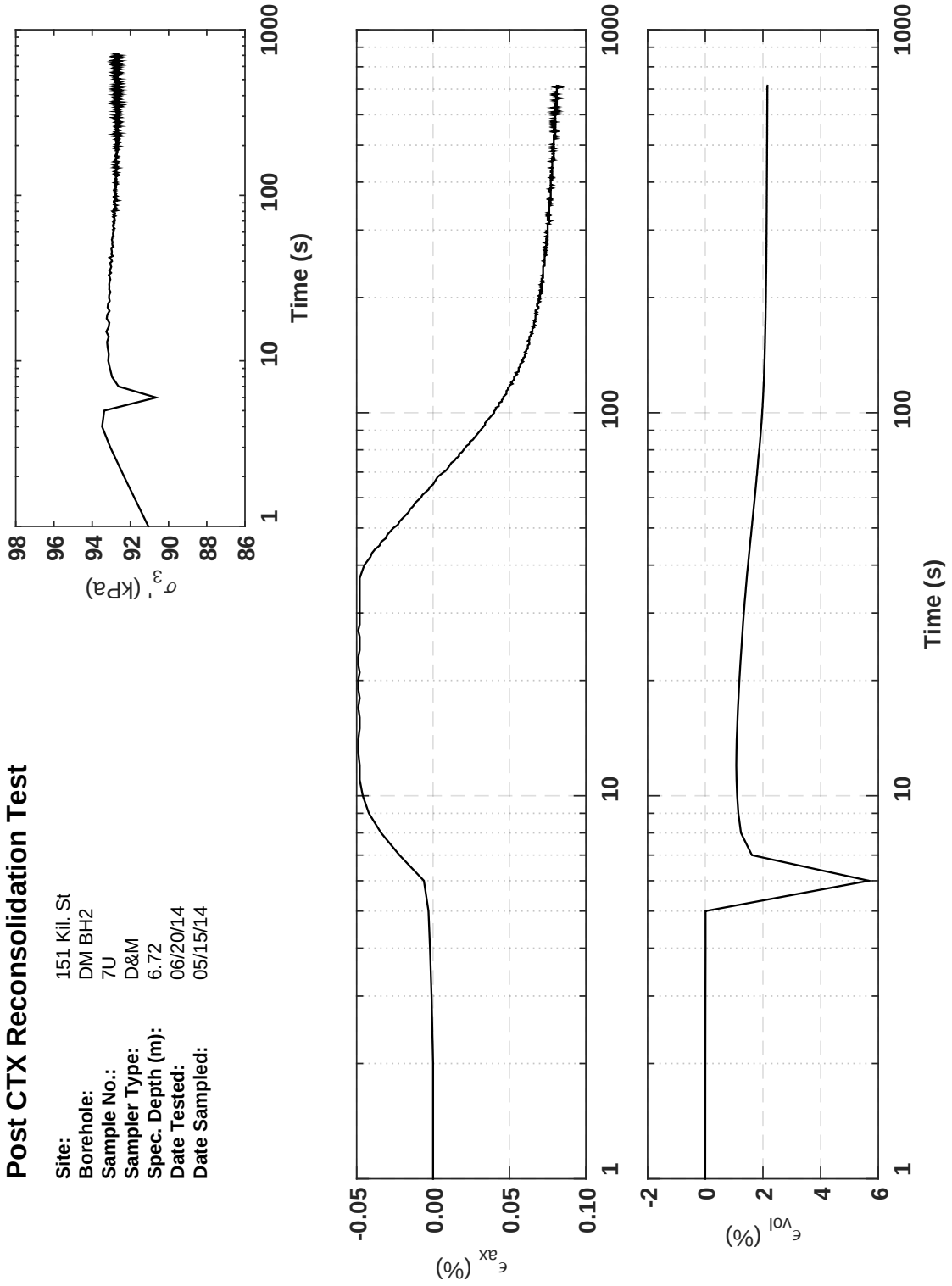
Post CTX Reconsolidation Test
Site: 151 Kil. St
Borehole: DM BH2
Sample No.: 7U
Sampler Type: D&M
Spec. Depth (m): 6.72
Date Tested: 06/20/14
Date Sampled: 05/15/14
σ3' (kPa)
Time (s)
εax (%)
εvol (%)
Time (s)

Specimen & Isotropic Cyclic Triaxial Test Data

Site:	151 Kil. St	**Loading Freq (Hz):**	0.1
Borehole:	DM BH2	**B–Value:**	0.974
Sample No.:	11U	**CSR:**	0.363
Sampler Type:	D&M	**N to $\varepsilon_{Ax-S.A.}$=3%:**	13
Spec. Depth (m):	10.97	**N to $\varepsilon_{Ax-D.A.}$=5%:**	14.5
Date Tested:	06/18/14	**Post–Cyclic Test:**	Reconsol.
Date Sampled:	05/15/14		
Spec. Ht. (mm):	134.9		
Spec. Diam. (mm):	61.1		
Dry Mass (g):	628.20		
Gs:	2.68		
e_o:	0.72		
σ'_{3o} (kPa):	125.2		
PI (%):	NP		
USCS:	SP		

Isotropic Consolidation Test

Site:	151 Kil. St
Borehole:	DM BH2
Sample No.:	11U
Sampler Type:	D&M
Spec. Depth (m):	10.97
Date Tested:	06/18/14
Date Sampled:	05/15/14

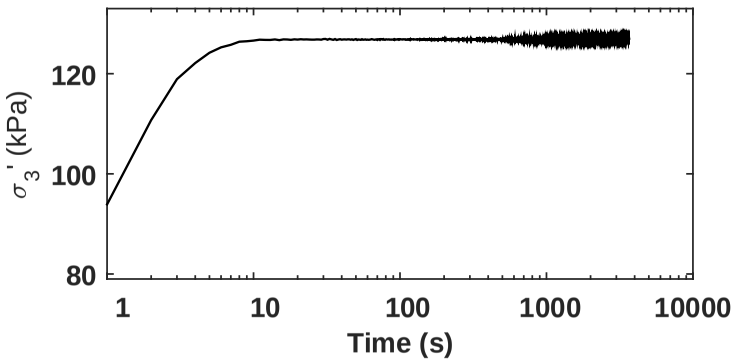

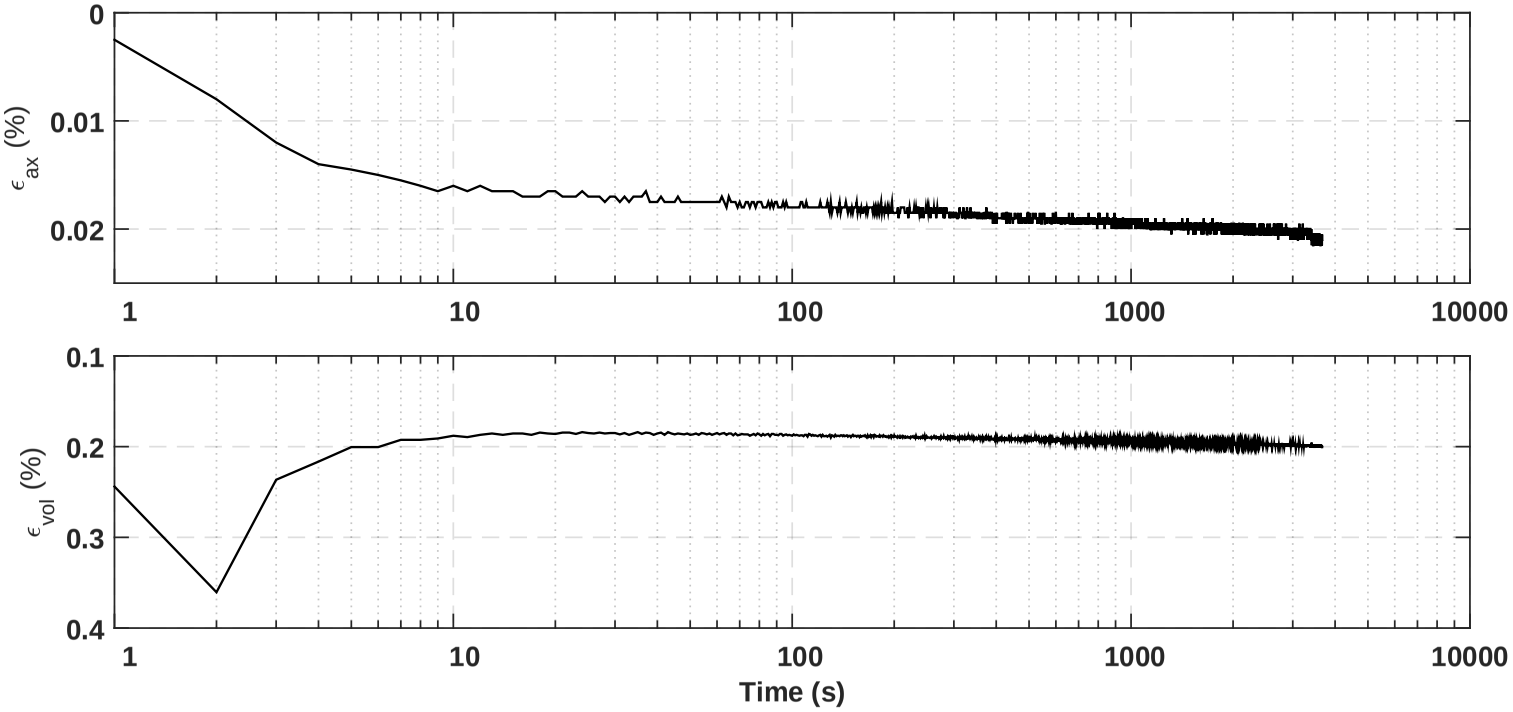

Post CTX Reconsolidation Test

Site:	151 Kil. St
Borehole:	DM BH2
Sample No.:	11U
Sampler Type:	D&M
Spec. Depth (m):	10.97
Date Tested:	06/18/14
Date Sampled:	05/15/14

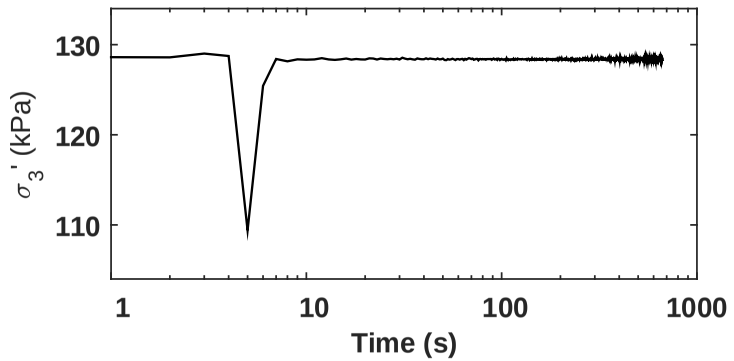

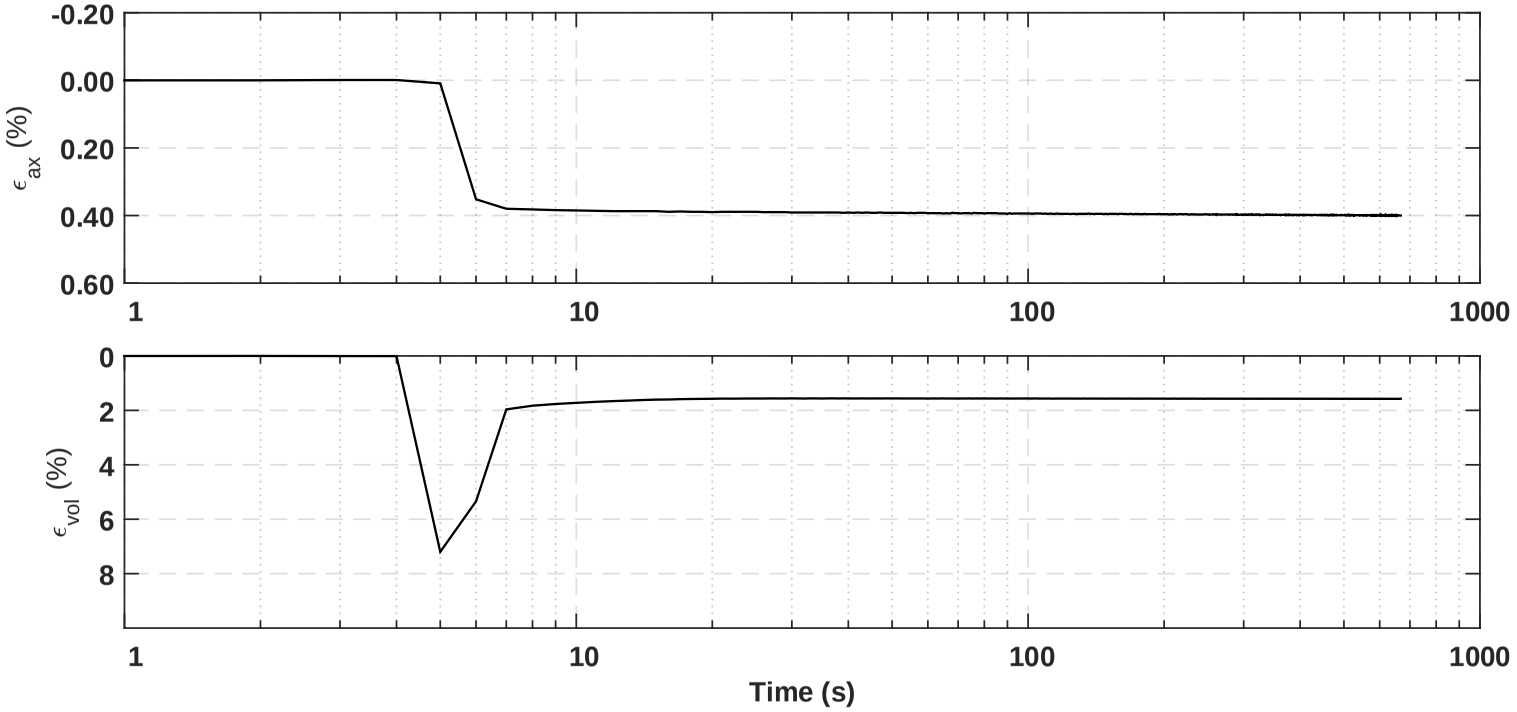

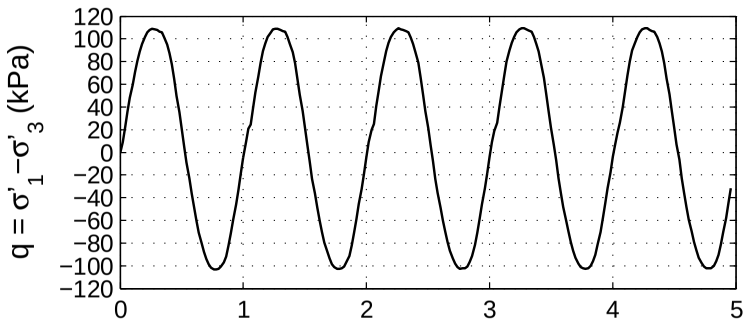

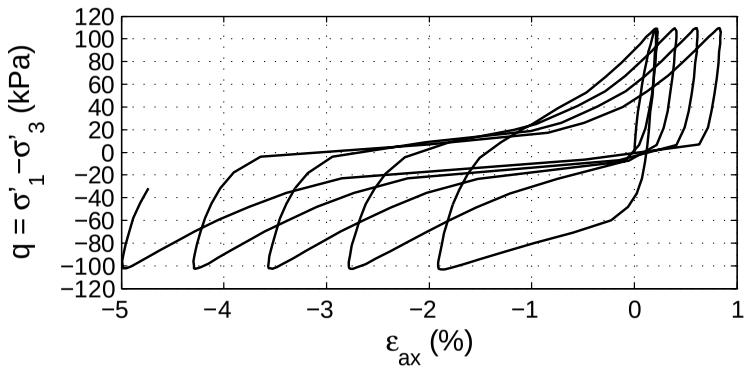

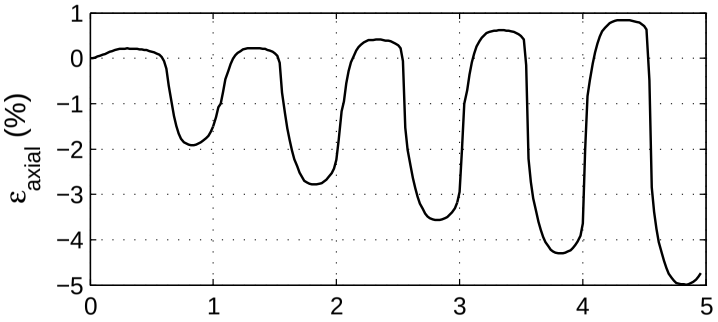

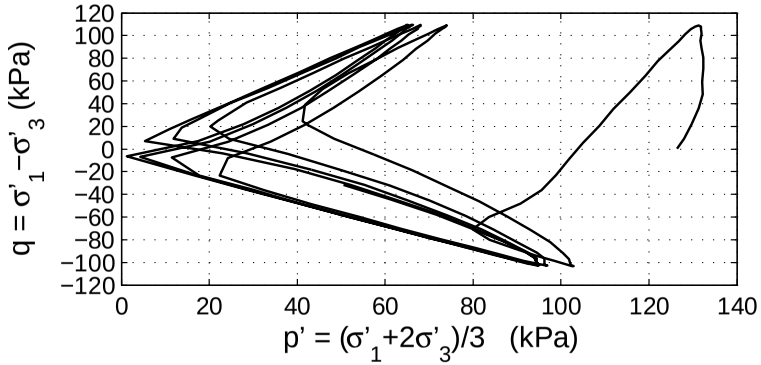

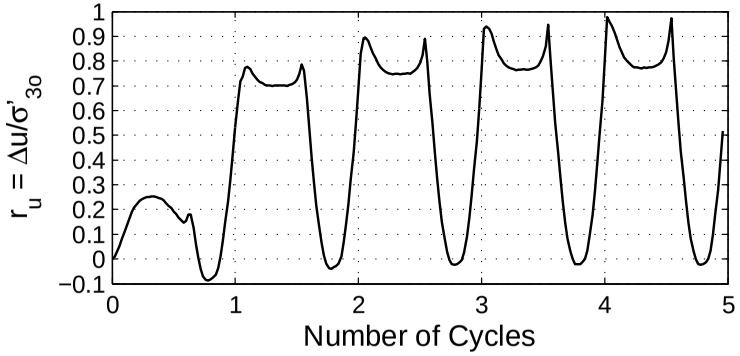

Specimen & Isotropic Cyclic Triaxial Test Data

Site:	151 Kil. St	**Loading Freq (Hz):**	0.1
Borehole:	DM BH2	**B−Value:**	0.990
Sample No.:	11U	**CSR:**	0.420
Sampler Type:	D&M	**N to $\varepsilon_{Ax-S.A.}$=3%:**	3
Spec. Depth (m):	11.11	**N to $\varepsilon_{Ax-D.A.}$=5%:**	4.5
Date Tested:	06/19/14	**Post−Cyclic Test:**	Monotonic
Date Sampled:	05/15/14		
Spec. Ht. (mm):	133.2		
Spec. Diam. (mm):	61.1		
Dry Mass (g):	615.86		
Gs:	2.68		
e_o:	0.70		
σ'_{3o} (kPa):	126.2		
PI (%):	NP		
USCS:	SP−SM		

Isotropic Consolidation Test

Site:	151 Kil. St
Borehole:	DM BH2
Sample No.:	11U
Sampler Type:	D&M
Spec. Depth (m):	11.11
Date Tested:	06/19/14
Date Sampled:	05/15/14

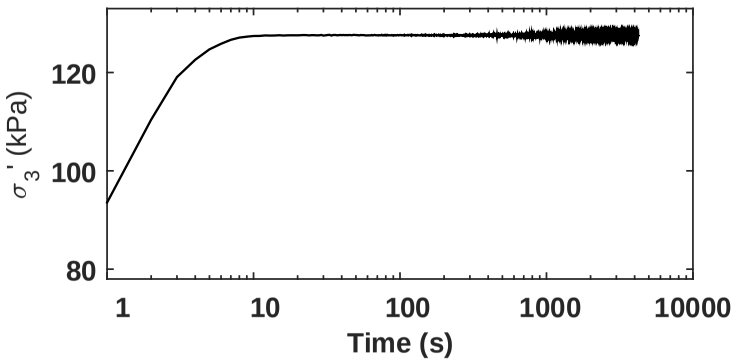

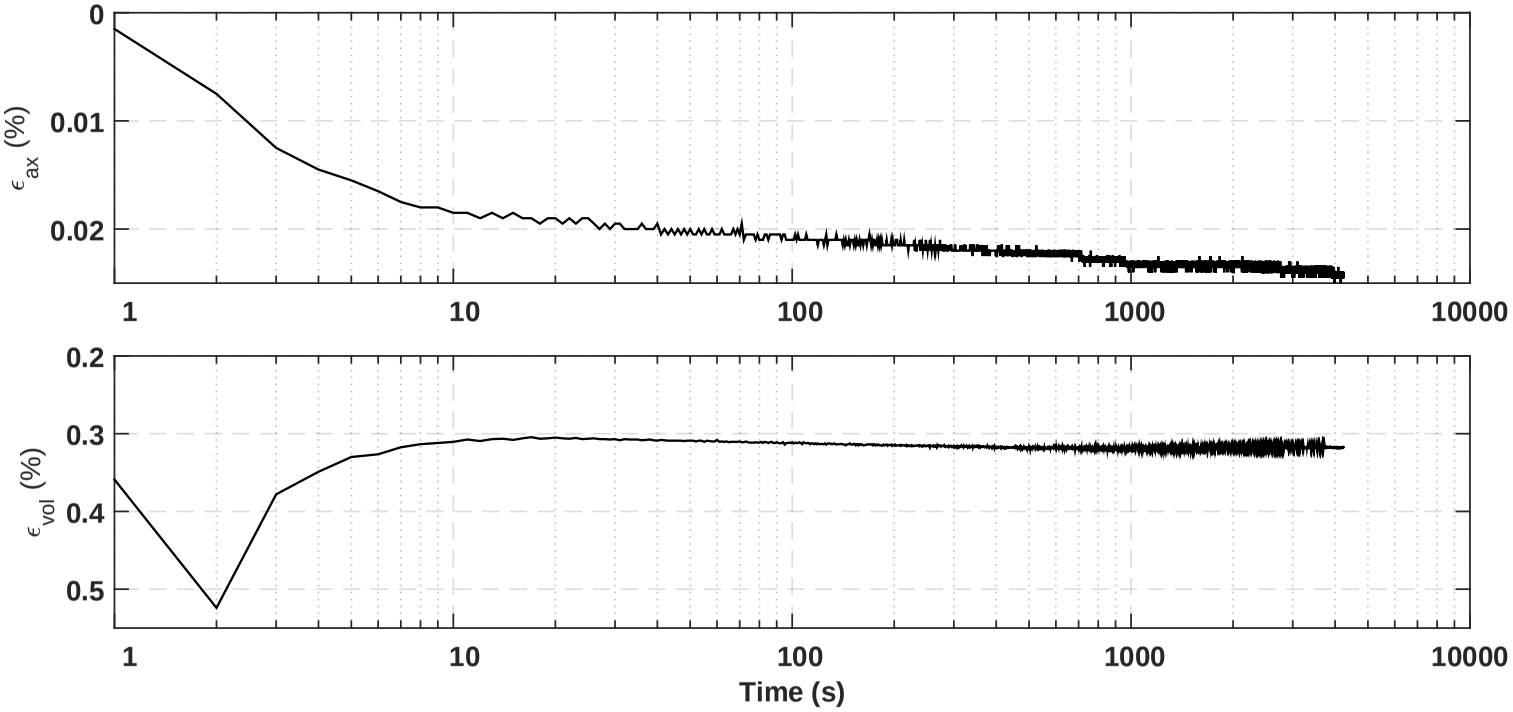

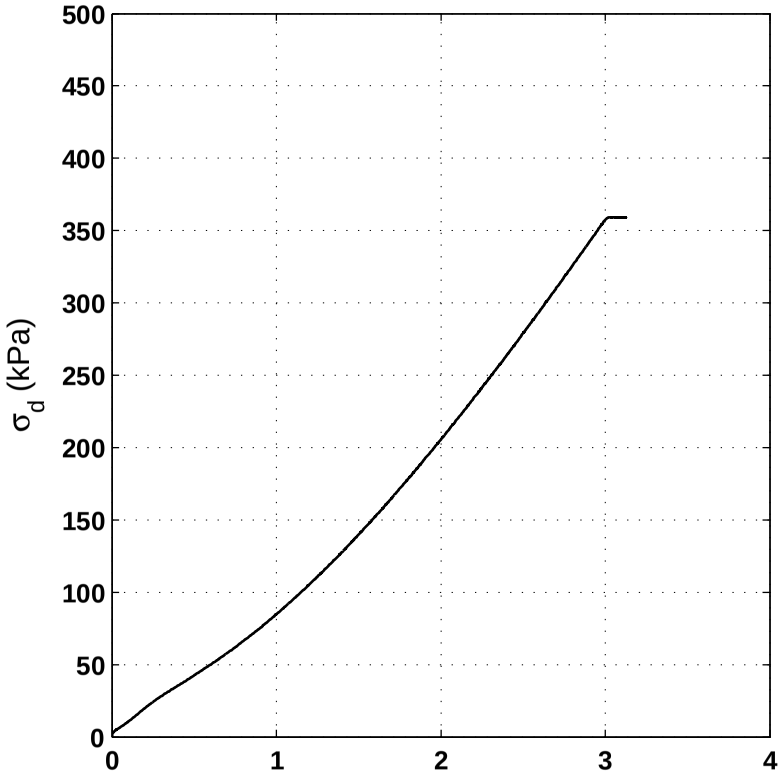

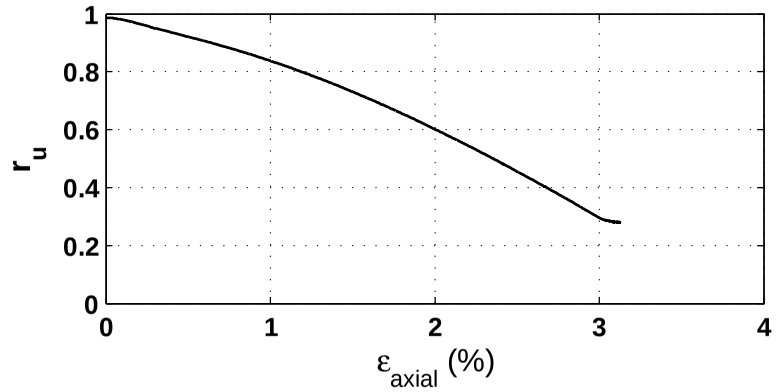

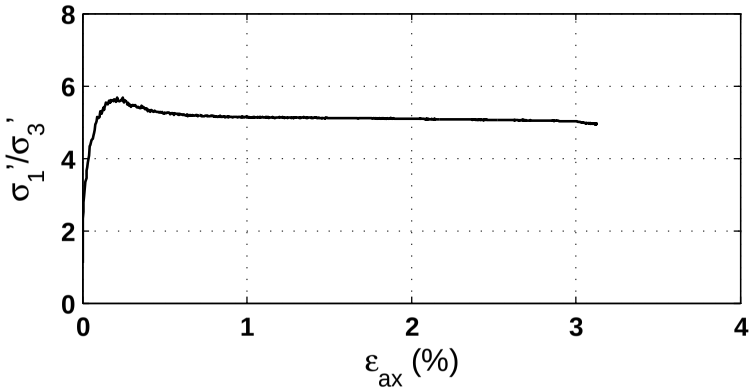

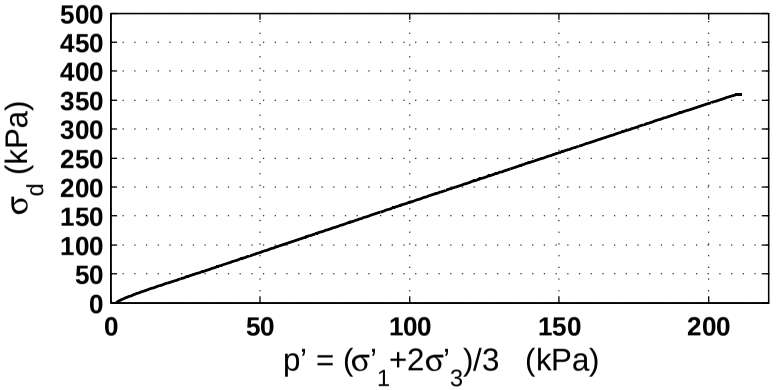

Post CTX Monotonic Comp. Test

Site:	151 Kil. St	**Rate (kPa/min):**	20
Borehole:	DM BH2		
Sample No.:	11U		
Sampler Type:	D&M		
Spec. Depth (m):	11.11		
Date Tested:	06/19/14		
Date Sampled:	05/15/14		

Appendix C.2.3

CTUC Building Site—199 Armagh St.

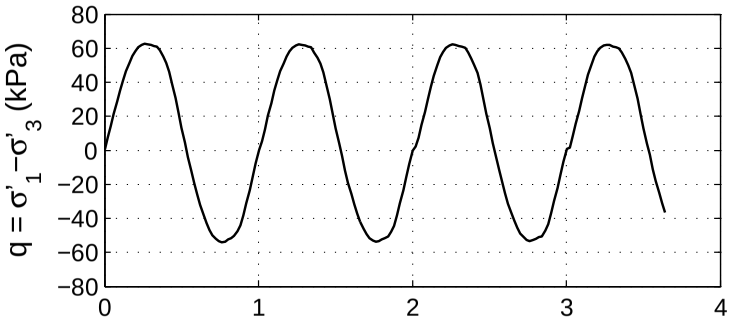

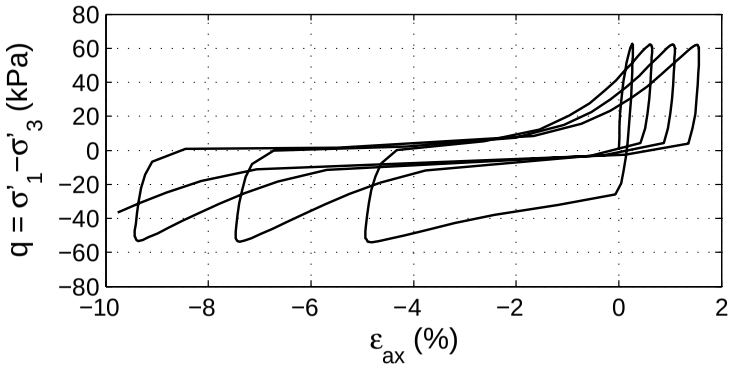

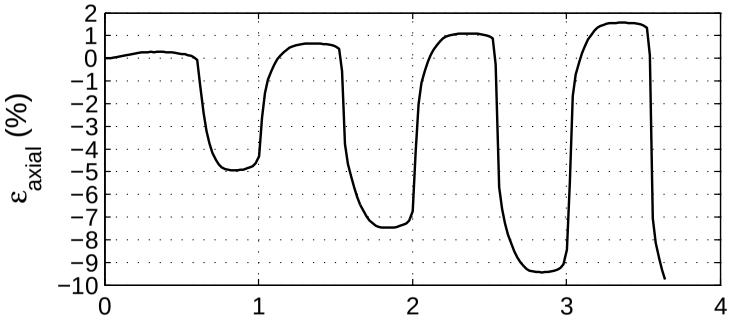

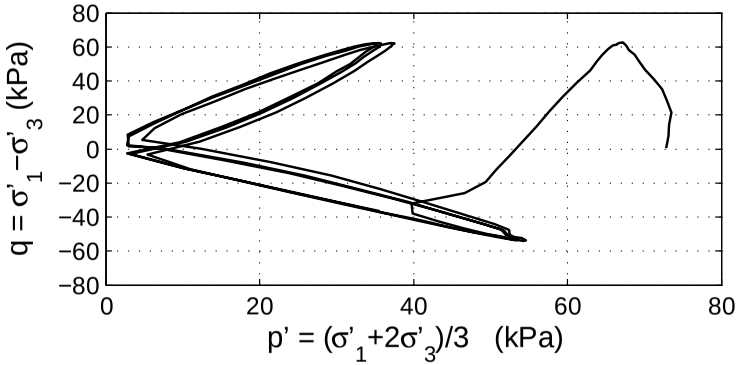

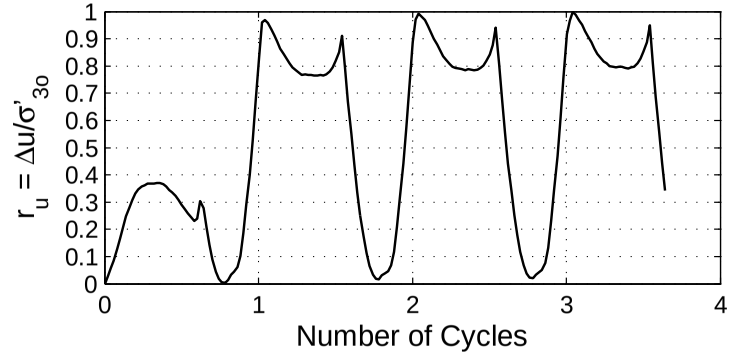

Specimen & Isotropic Cyclic Triaxial Test Data

Site:	199 Arm. St	**Loading Freq (Hz):**	0.1
Borehole:	DM BH1	**B−Value:**	0.986
Sample No.:	2U	**CSR:**	0.392
Sampler Type:	D&M	**N to $\varepsilon_{Ax-S.A.}$=3%:**	1
Spec. Depth (m):	2.82	**N to $\varepsilon_{Ax-D.A.}$=5%:**	1.5
Date Tested:	05/22/14	**Post−Cyclic Test:**	−−
Date Sampled:	04/11/14		
Spec. Ht. (mm):	136.7		
Spec. Diam. (mm):	60.8		
Dry Mass (g):	580.47		
Gs:	2.73		
e_ρ:	0.87		
σ'_{3o} (kPa):	72.6		
PI (%):	NP		
USCS:	SM		

Isotropic Consolidation Test

Site:	199 Arm. St
Borehole:	DM BH1
Sample No.:	2U
Sampler Type:	D&M
Spec. Depth (m):	2.82
Date Tested:	05/22/14
Date Sampled:	04/11/14

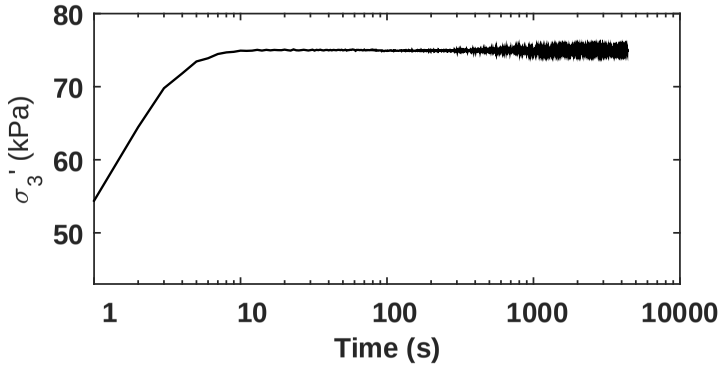

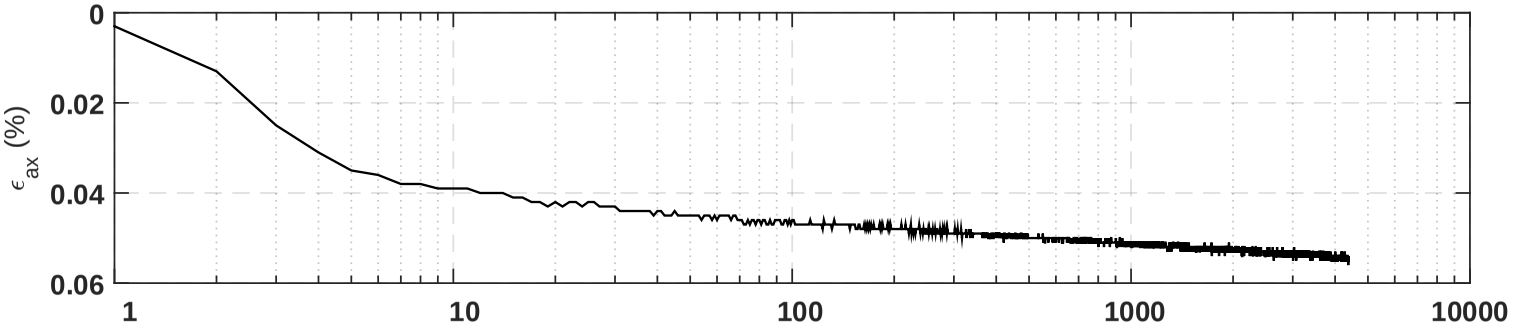

Post CTX Reconsolidation Test

Site:	199 Arm. St
Borehole:	DM BH1
Sample No.:	2U
Sampler Type:	D&M
Spec. Depth (m):	2.82
Date Tested:	05/22/14
Date Sampled:	04/11/14

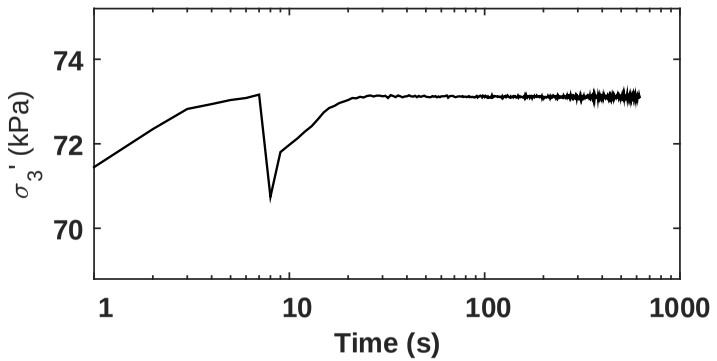

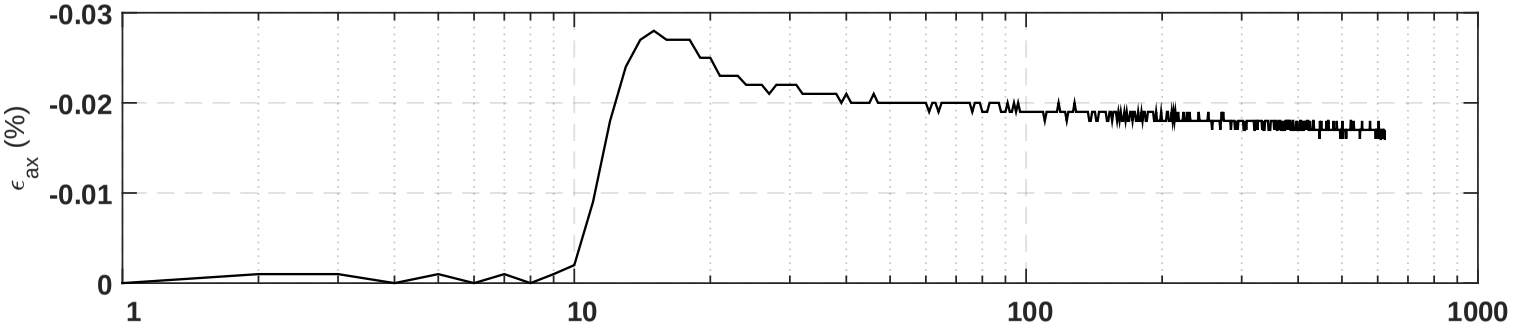

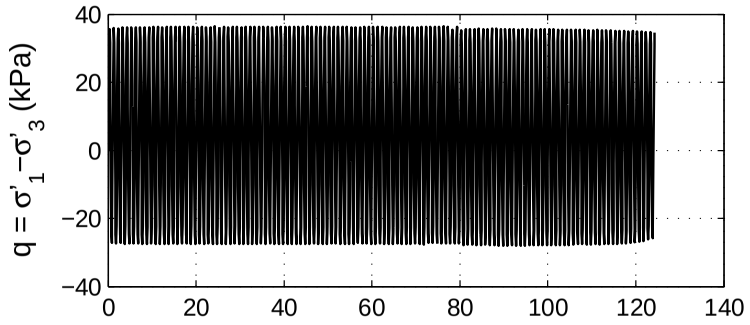

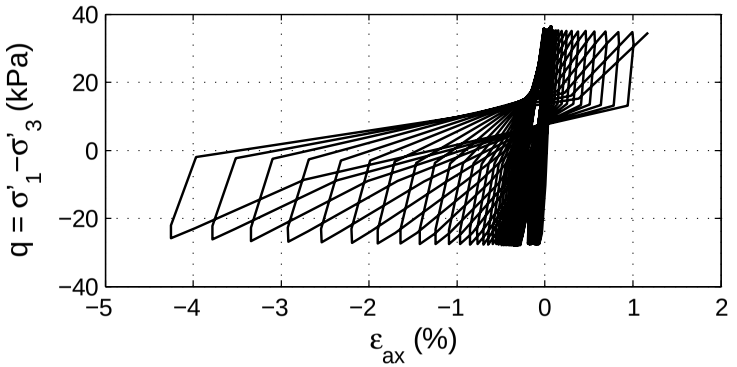

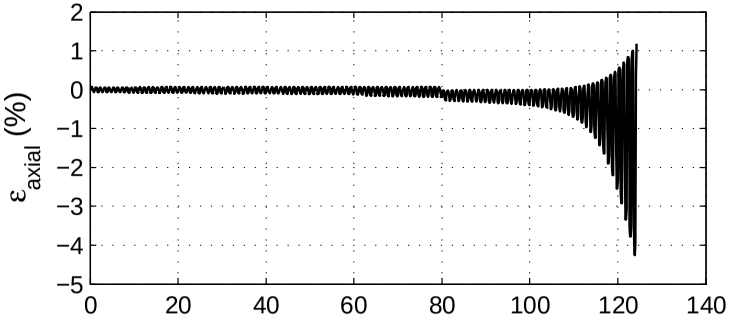

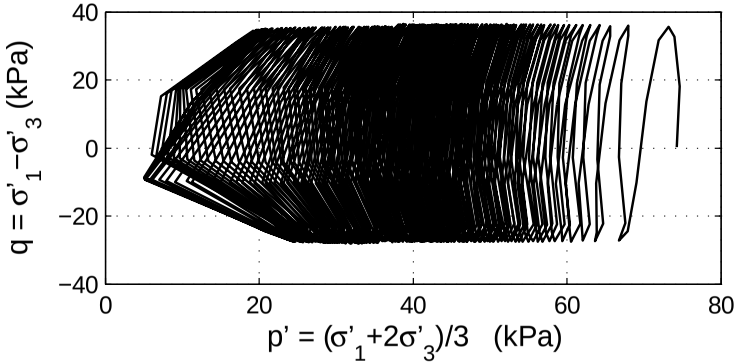

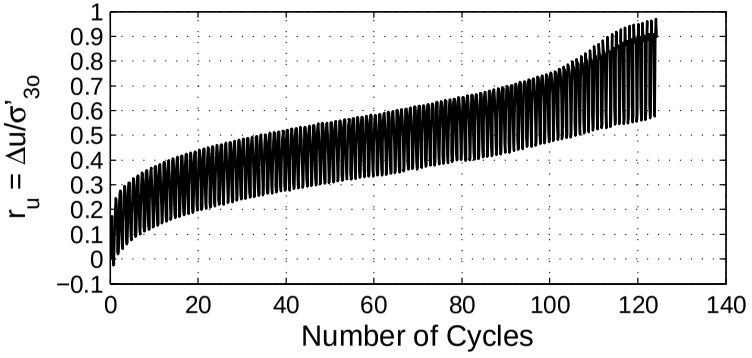

Specimen & Isotropic Cyclic Triaxial Test Data

Site:	199 Arm. St	**Loading Freq (Hz):**	0.1
Borehole:	DM BH1	**B−Value:**	0.975
Sample No.:	2U	**CSR:**	0.216
Sampler Type:	D&M	**N to $\varepsilon_{Ax-S.A.}$=3%:**	122
Spec. Depth (m):	2.98	**N to $\varepsilon_{Ax-D.A.}$=5%:**	124
Date Tested:	05/03/14	**Post−Cyclic Test:**	−−
Date Sampled:	04/11/14		
Spec. Ht. (mm):	140.1		
Spec. Diam. (mm):	60.8		
Dry Mass (g):	591.45		
Gs:	2.72		
e_o:	0.87		
σ'_{3o} (kPa):	74.2		
PI (%):	2		
USCS:	SM		

Isotropic Consolidation Test

Site:	199 Arm. St
Borehole:	DM BH1
Sample No.:	2U
Sampler Type:	D&M
Spec. Depth (m):	2.98
Date Tested:	05/03/14
Date Sampled:	04/11/14

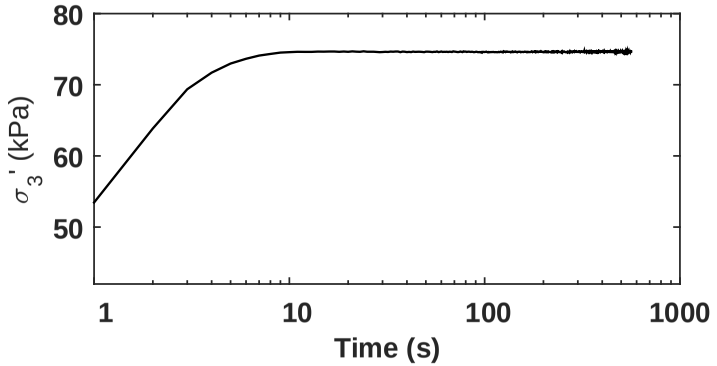

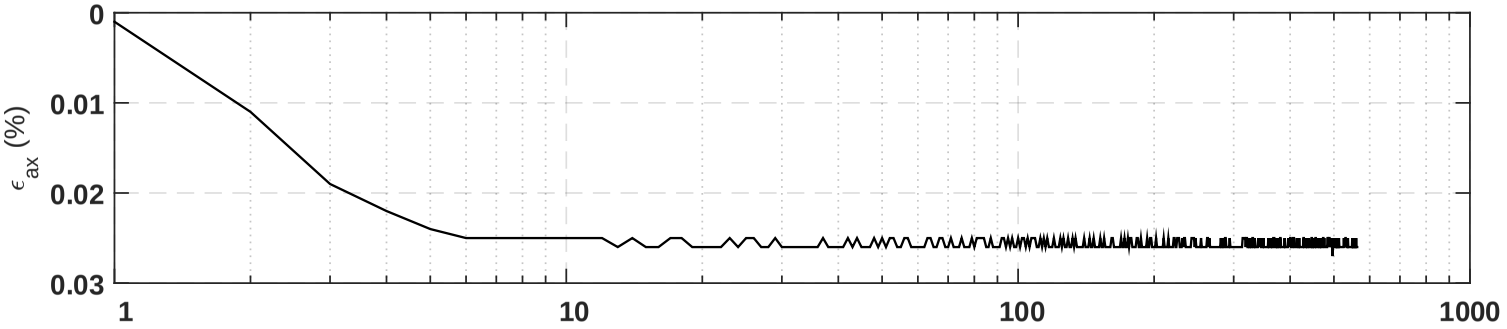

Post CTX Reconsolidation Test

Site:	199 Arm. St
Borehole:	DM BH1
Sample No.:	2U
Sampler Type:	D&M
Spec. Depth (m):	2.98
Date Tested:	05/03/14
Date Sampled:	04/11/14

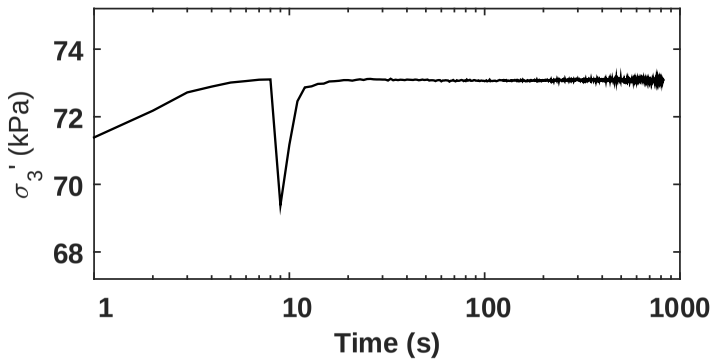

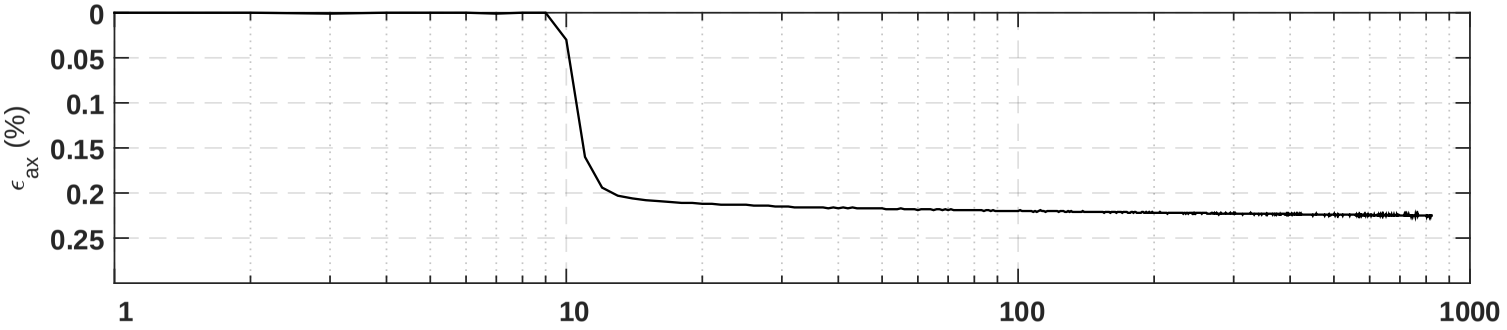

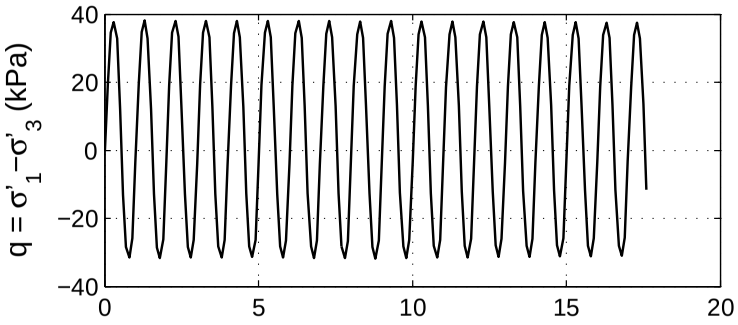

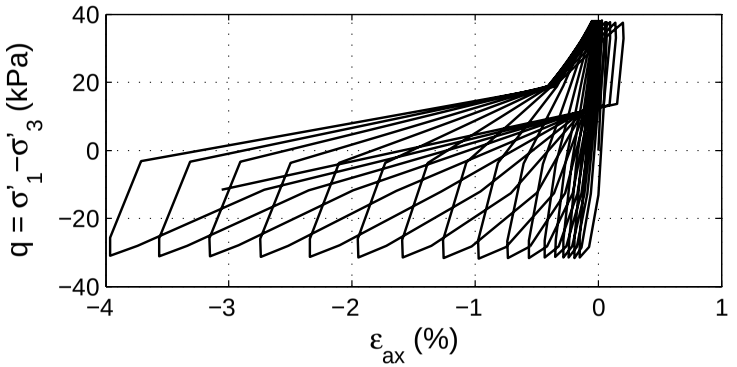

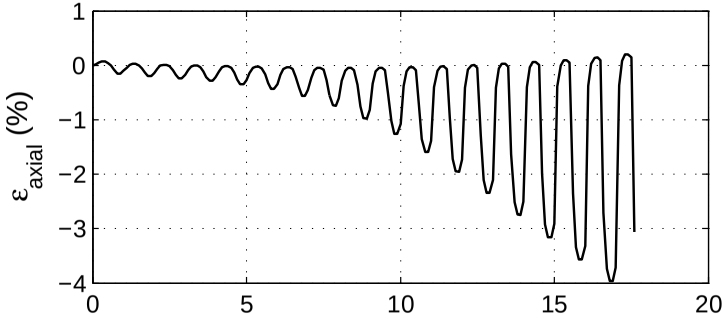

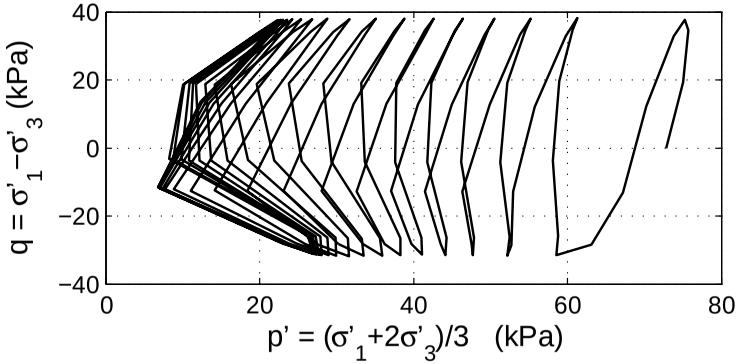

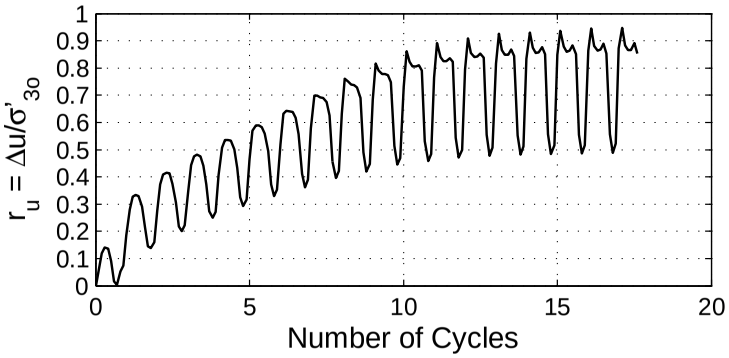

Specimen & Isotropic Cyclic Triaxial Test Data

Site:	199 Arm. St	**Loading Freq (Hz):**	0.1
Borehole:	DM BH1	**B−Value:**	0.954
Sample No.:	3U	**CSR:**	0.239
Sampler Type:	D&M	**N to $\varepsilon_{Ax-S.A.}$=3%:**	15
Spec. Depth (m):	3.33	**N to $\varepsilon_{Ax-D.A.}$=5%:**	−−
Date Tested:	04/30/14	**Post−Cyclic Test:**	−−
Date Sampled:	04/11/14		
Spec. Ht. (mm):	133.5		
Spec. Diam. (mm):	61.6		
Dry Mass (g):	592.11		
Gs:	2.69		
e_ρ:	0.81		
σ'_{3o} (kPa):	72.8		
PI (%):	NP		
USCS:	SM		

Isotropic Consolidation Test

Site:	199 Arm. St
Borehole:	DM BH1
Sample No.:	3U
Sampler Type:	D&M
Spec. Depth (m):	3.33
Date Tested:	04/30/14
Date Sampled:	04/11/14

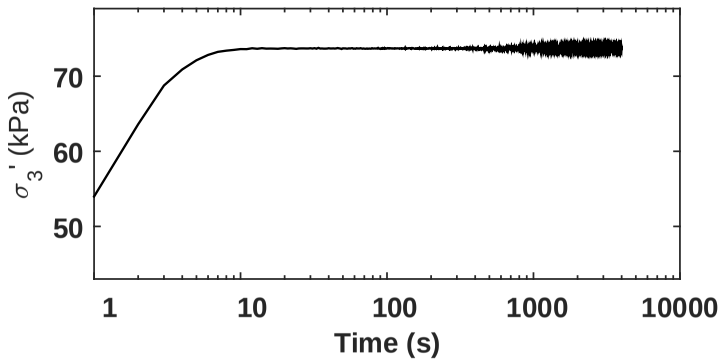

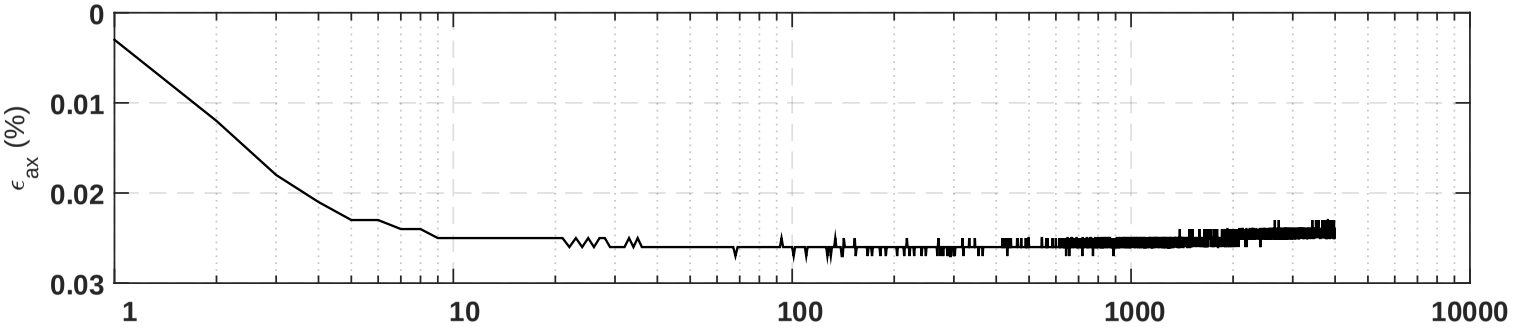

Post CTX Reconsolidation Test

Site:	199 Arm. St
Borehole:	DM BH1
Sample No.:	3U
Sampler Type:	D&M
Spec. Depth (m):	3.33
Date Tested:	04/30/14
Date Sampled:	04/11/14

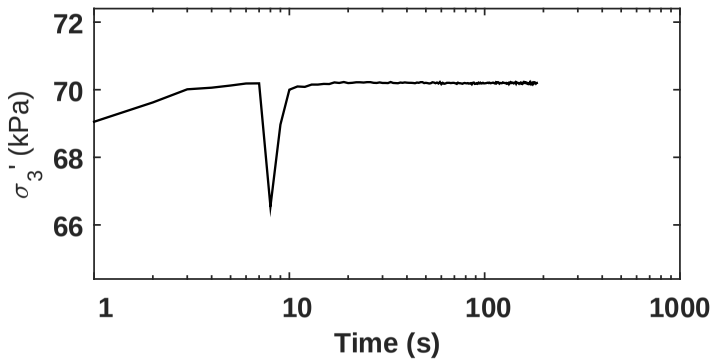

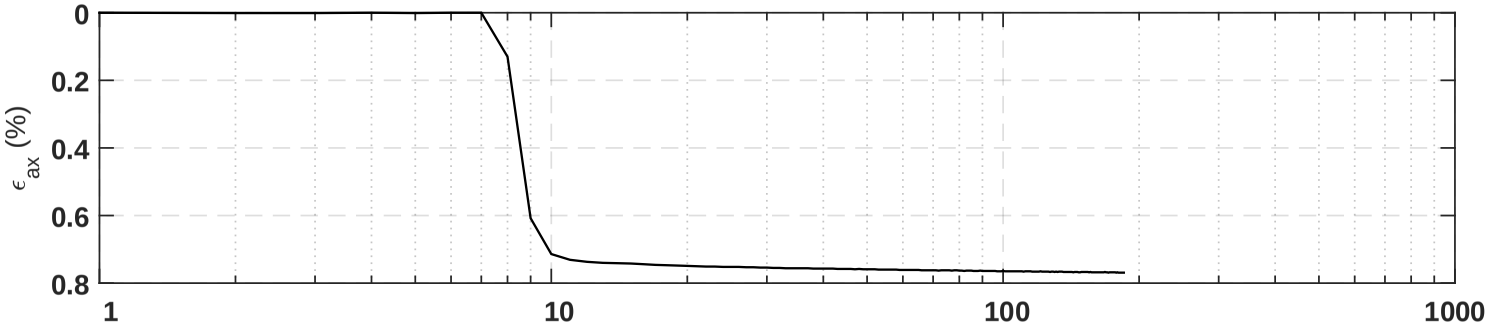

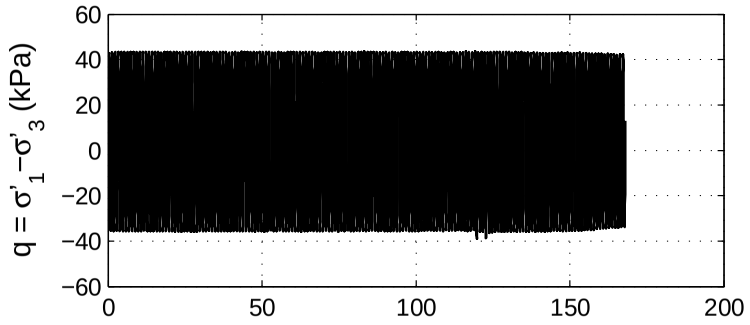

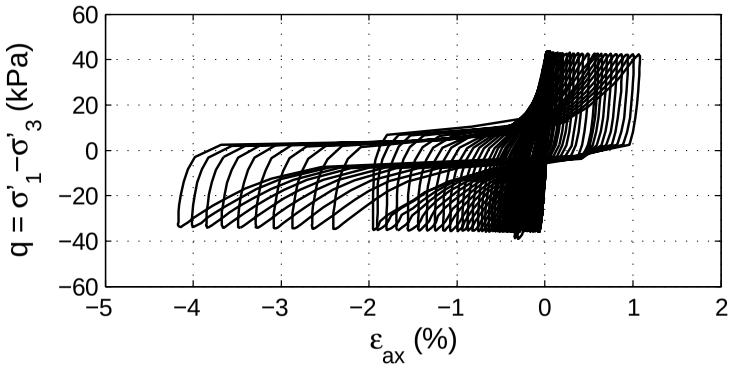

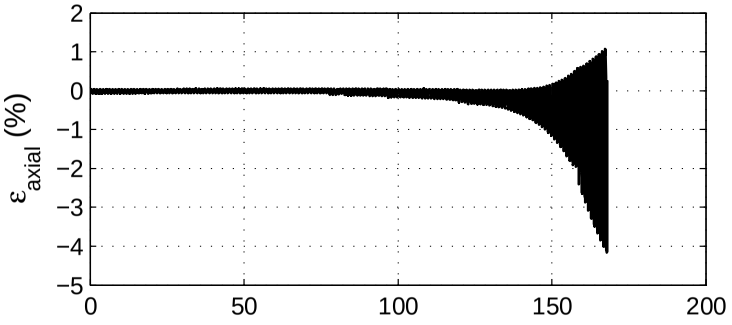

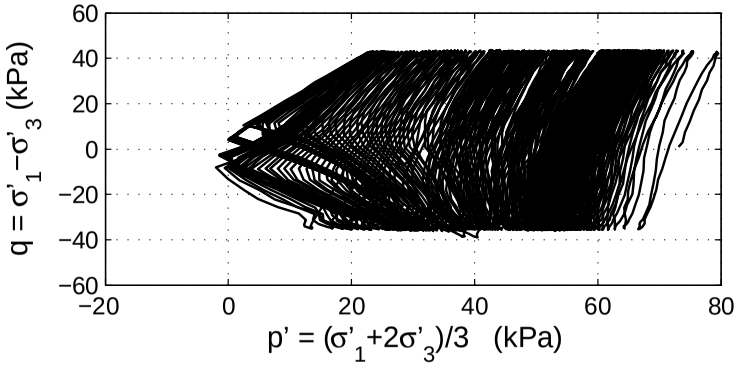

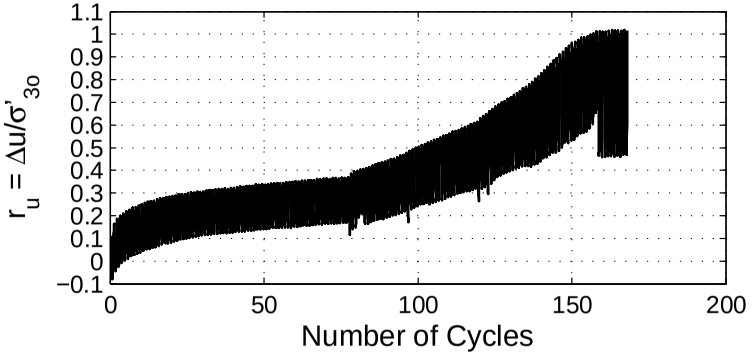

Specimen & Isotropic Cyclic Triaxial Test Data

Site:	199 Arm. St	**Loading Freq (Hz):**	0.1
Borehole:	DM BH1	**B−Value:**	0.959
Sample No.:	3U	**CSR:**	0.271
Sampler Type:	D&M	**N to $\varepsilon_{Ax-S.A.}$=3%:**	>82
Spec. Depth (m):	3.48	**N to $\varepsilon_{Ax-D.A.}$=5%:**	>87
Date Tested:	05/20/14	**Post−Cyclic Test:**	−−
Date Sampled:	04/11/14		
Spec. Ht. (mm):	138.7		
Spec. Diam. (mm):	61.1		
Dry Mass (g):	621.62		
Gs:	2.67		
e_o:	0.75		
σ'_{3o} (kPa):	72.9		
PI (%):	NP		
USCS:	SP−SM		

Isotropic Consolidation Test

Site:	199 Arm. St
Borehole:	DM BH1
Sample No.:	3U
Sampler Type:	D&M
Spec. Depth (m):	3.48
Date Tested:	05/20/14
Date Sampled:	04/11/14

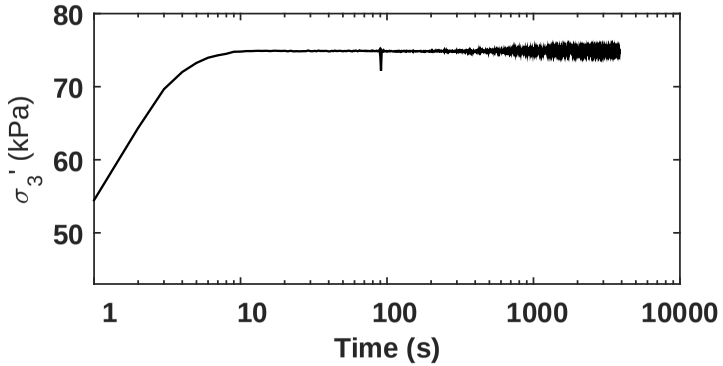

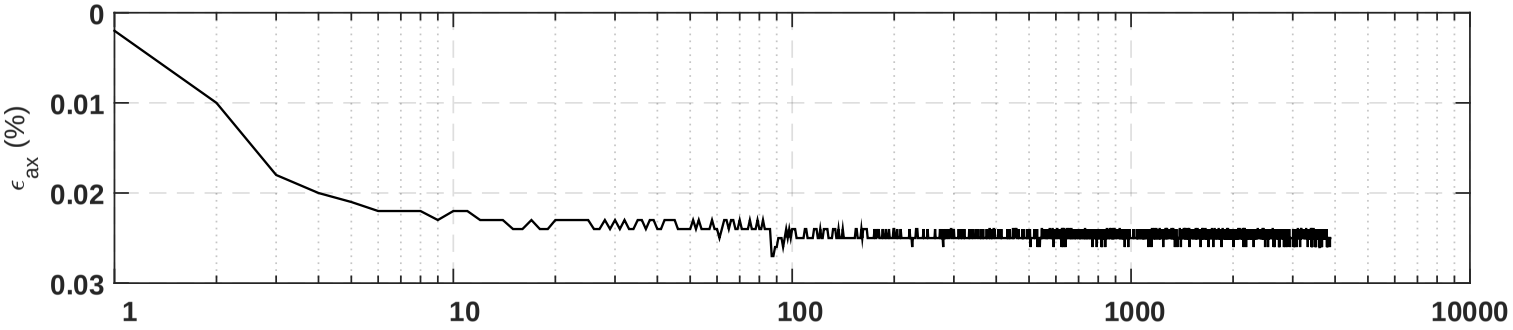

Post CTX Reconsolidation Test

Site:	199 Arm. St
Borehole:	DM BH1
Sample No.:	3U
Sampler Type:	D&M
Spec. Depth (m):	3.48
Date Tested:	05/20/14
Date Sampled:	04/11/14

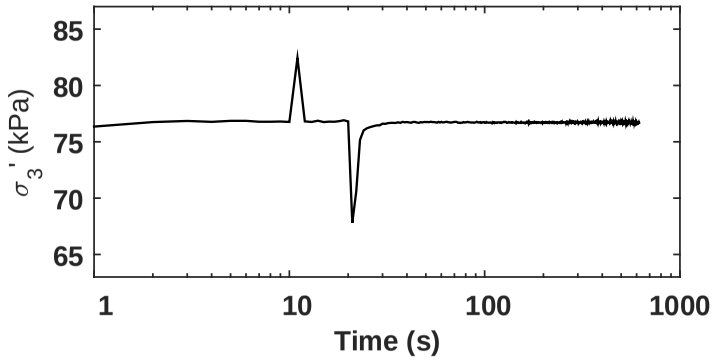

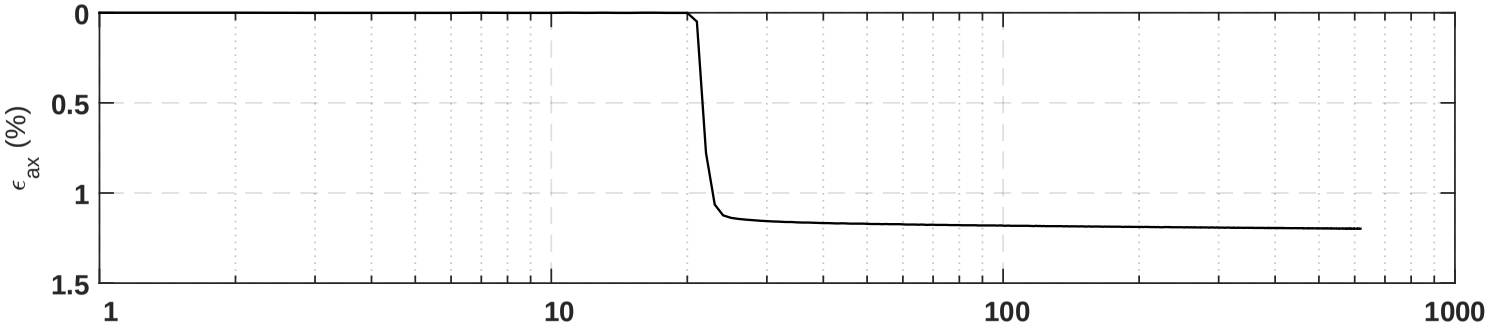

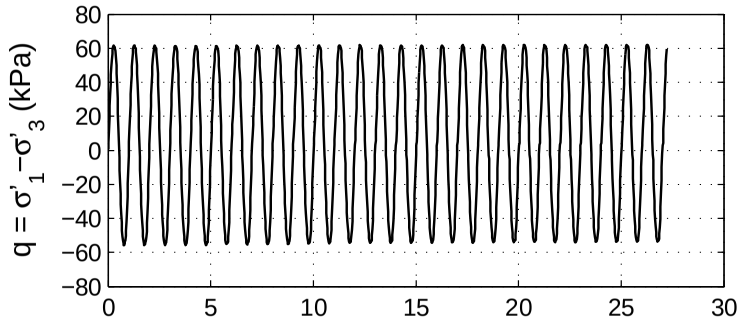

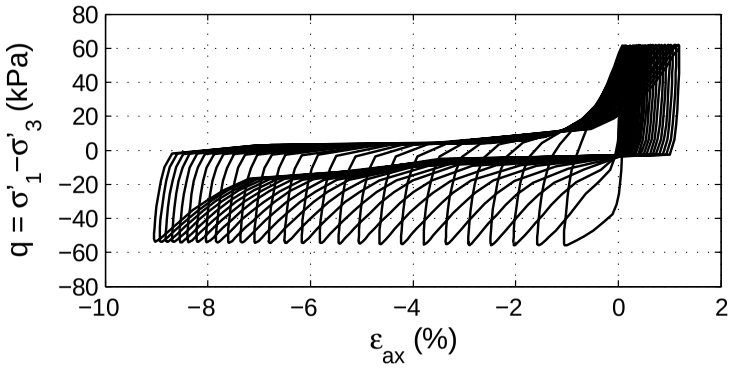

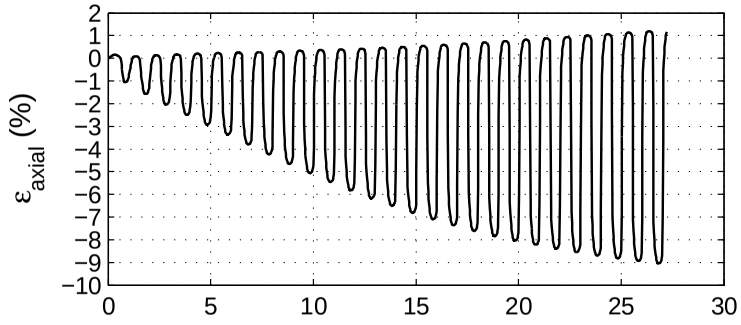

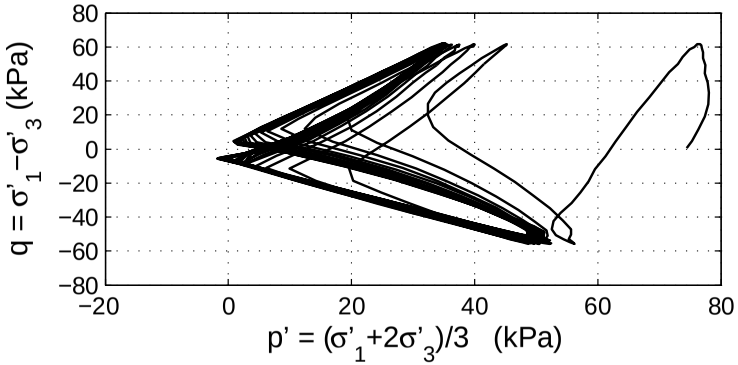

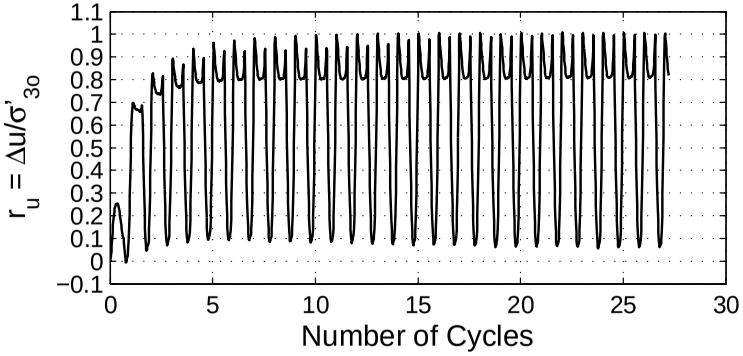

Specimen & Isotropic Cyclic Triaxial Test Data

Site:	199 Arm. St	**Loading Freq (Hz):**	0.1
Borehole:	DM BH1	**B−Value:**	0.984
Sample No.:	4U	**CSR:**	0.387
Sampler Type:	D&M	**N to $\varepsilon_{Ax-S.A.}$=3%:**	6
Spec. Depth (m):	3.82	**N to $\varepsilon_{Ax-D.A.}$=5%:**	10
Date Tested:	05/23/14	**Post−Cyclic Test:**	−−
Date Sampled:	04/11/14		
Spec. Ht. (mm):	141.7		
Spec. Diam. (mm):	60.9		
Dry Mass (g):	641.52		
Gs:	2.68		
e_o:	0.72		
σ'_{3o} (kPa):	74.3		
PI (%):	NP		
USCS:	SP−SM		

Isotropic Consolidation Test

Site:	199 Arm. St
Borehole:	DM BH1
Sample No.:	4U
Sampler Type:	D&M
Spec. Depth (m):	3.82
Date Tested:	05/23/14
Date Sampled:	04/11/14

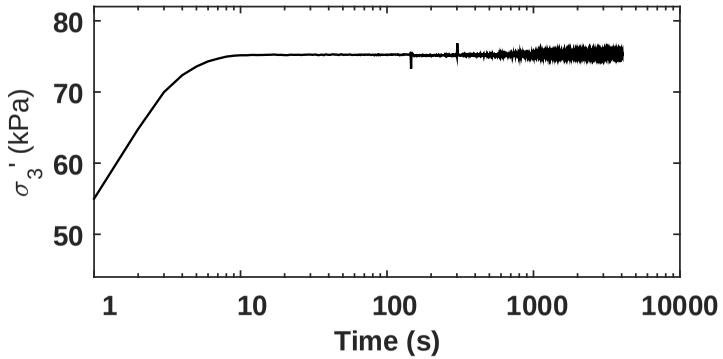

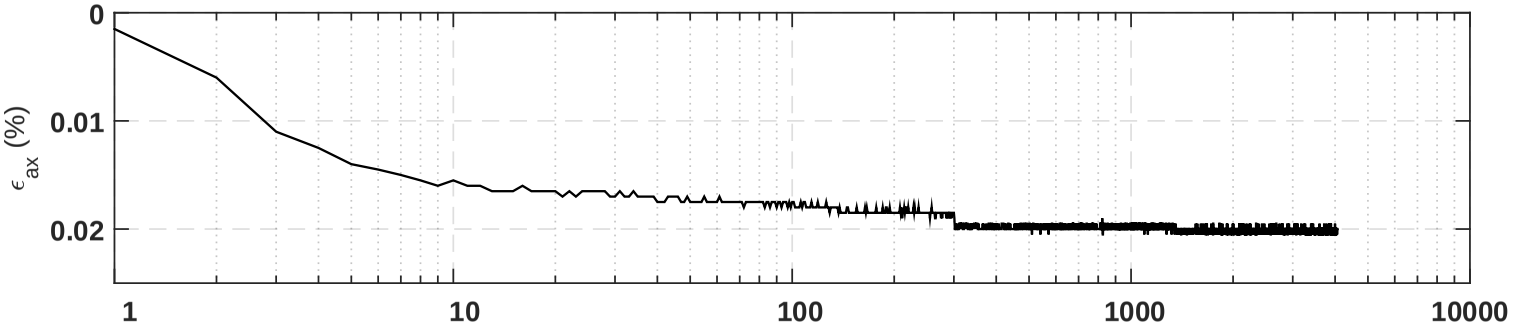

Post CTX Reconsolidation Test

Site:	199 Arm. St
Borehole:	DM BH1
Sample No.:	4U
Sampler Type:	D&M
Spec. Depth (m):	3.82
Date Tested:	05/23/14
Date Sampled:	04/11/14

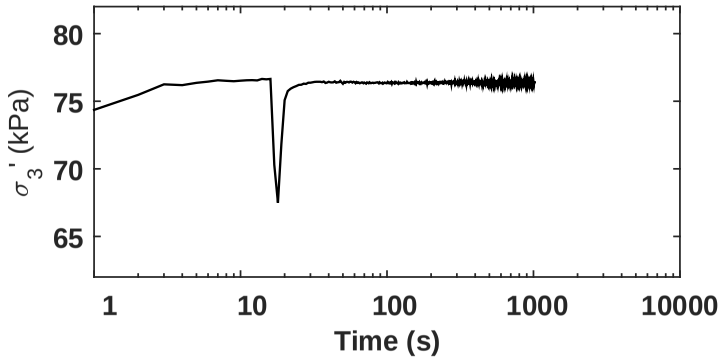

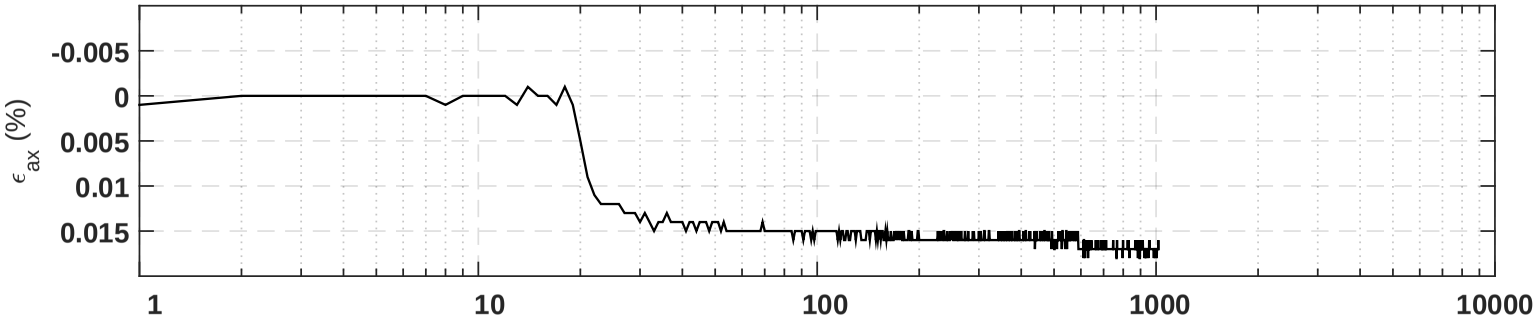

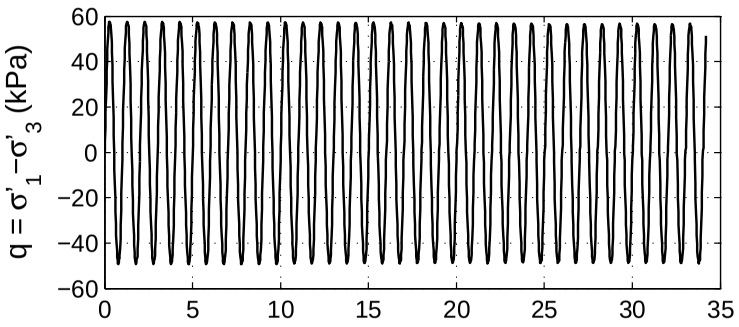

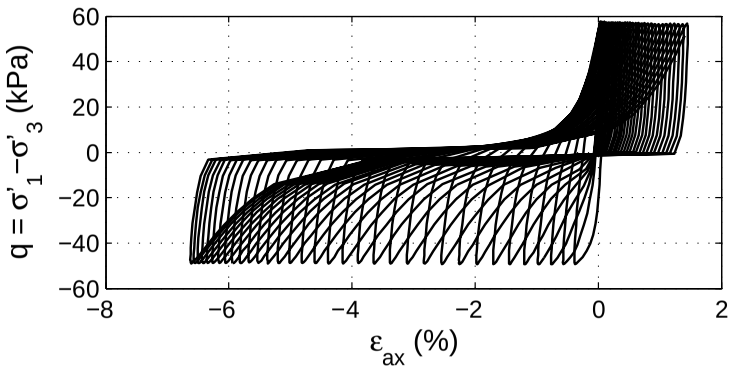

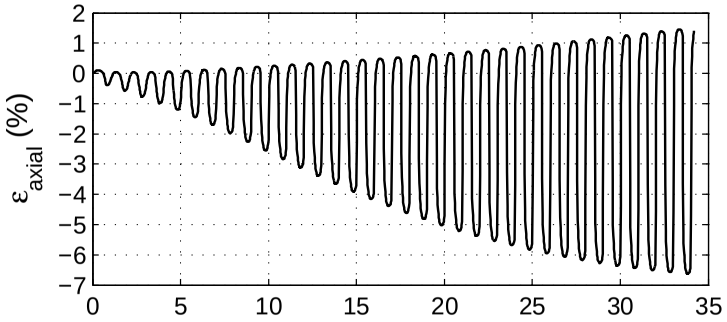

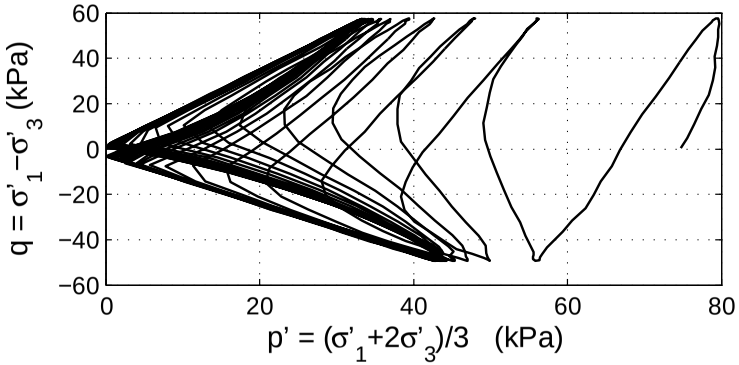

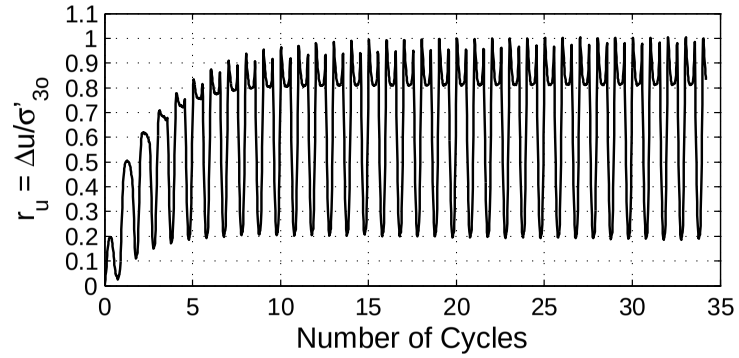

Specimen & Isotropic Cyclic Triaxial Test Data

Site:	199 Arm. St	**Loading Freq (Hz):**	0.1
Borehole:	DM BH1	**B−Value:**	0.985
Sample No.:	4U	**CSR:**	0.354
Sampler Type:	D&M	**N to $\varepsilon_{Ax-S.A.}$=3%:**	12
Spec. Depth (m):	3.98	**N to $\varepsilon_{Ax-D.A.}$=5%:**	18
Date Tested:	05/22/14	**Post−Cyclic Test:**	−−
Date Sampled:	04/11/14		
Spec. Ht. (mm):	140.8		
Spec. Diam. (mm):	61.0		
Dry Mass (g):	651.25		
Gs:	2.69		
e_o:	0.70		
σ'_{3o} (kPa):	74.6		
PI (%):	NP		
USCS:	SP		

Isotropic Consolidation Test

Site:	199 Arm. St
Borehole:	DM BH1
Sample No.:	4U
Sampler Type:	D&M
Spec. Depth (m):	3.98
Date Tested:	05/22/14
Date Sampled:	04/11/14

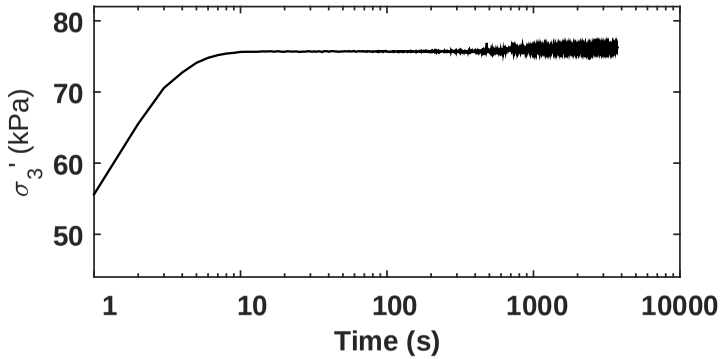

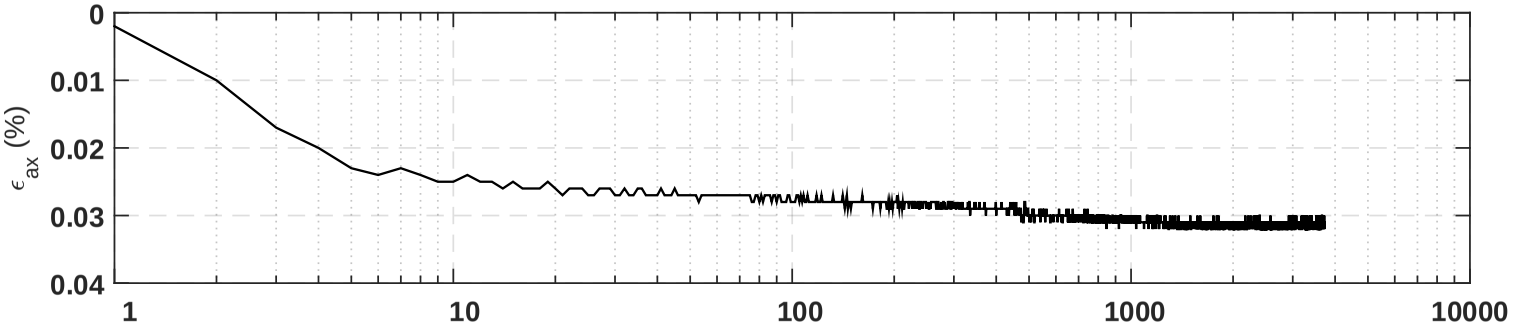

Post CTX Reconsolidation Test

Site:	199 Arm. St
Borehole:	DM BH1
Sample No.:	4U
Sampler Type:	D&M
Spec. Depth (m):	3.98
Date Tested:	05/22/14
Date Sampled:	04/11/14

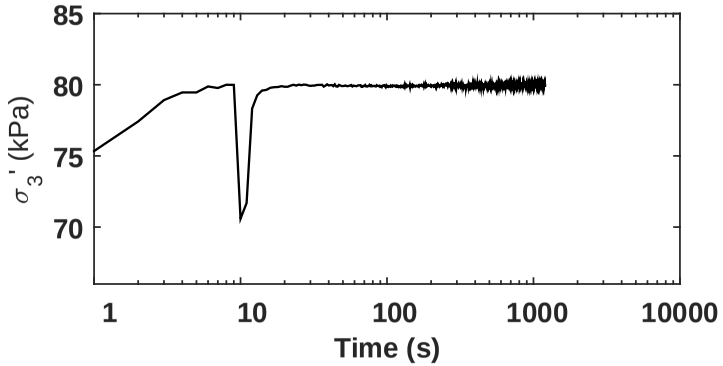

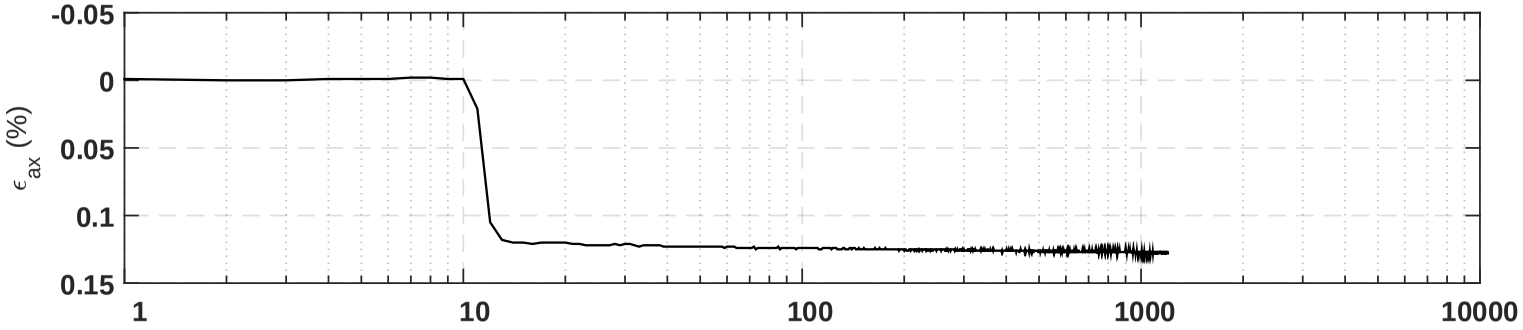

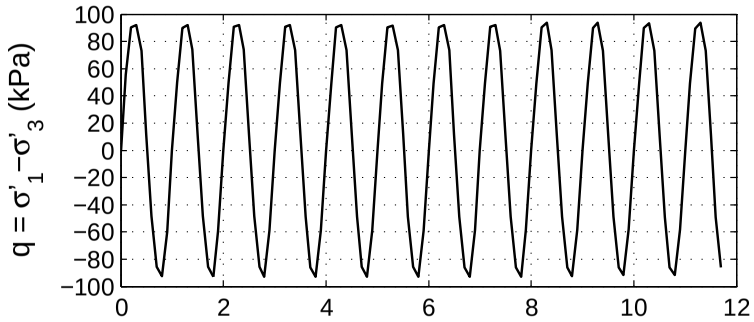

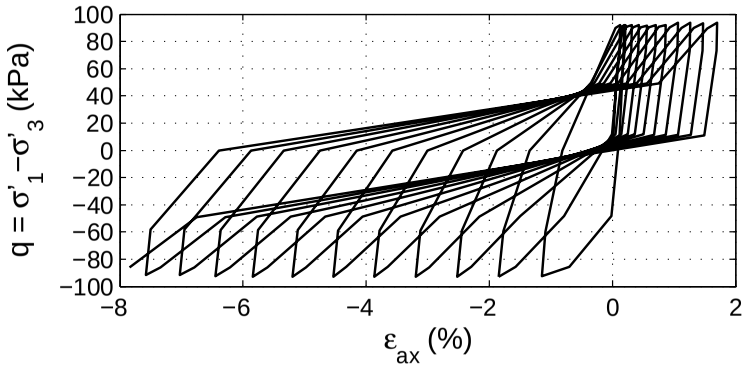

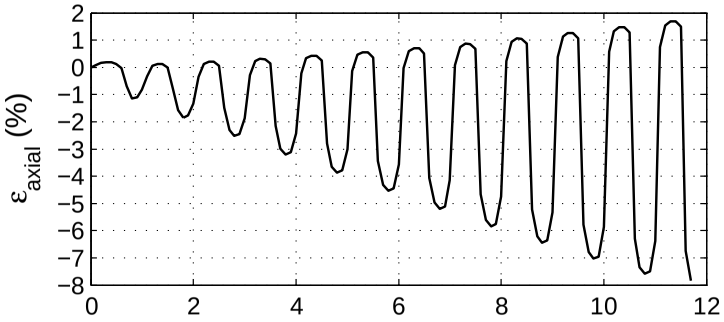

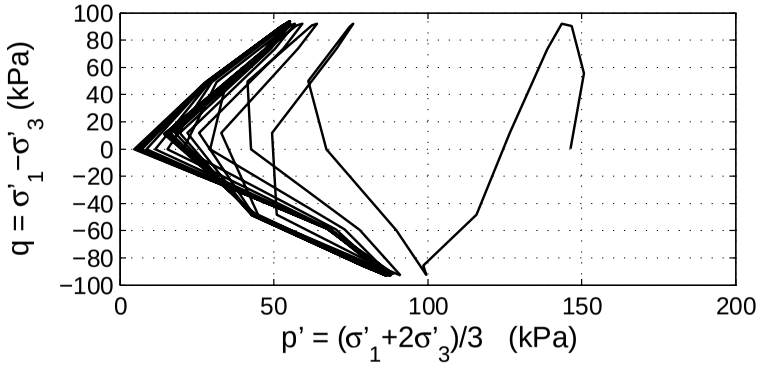

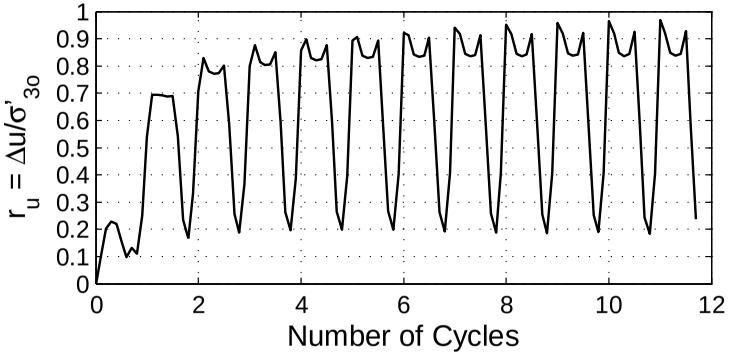

Specimen & Isotropic Cyclic Triaxial Test Data

Site:	199 Arm. St	**Loading Freq (Hz):**	0.1
Borehole:	DM BH1	**B−Value:**	0.971
Sample No.:	7U	**CSR:**	0.320
Sampler Type:	D&M	**N to $\varepsilon_{Ax-S.A.}$=3%:**	4
Spec. Depth (m):	13.67	**N to $\varepsilon_{Ax-D.A.}$=5%:**	6
Date Tested:	04/28/14	**Post−Cyclic Test:**	−−
Date Sampled:	04/15/14		
Spec. Ht. (mm):	140.5		
Spec. Diam. (mm):	61.0		
Dry Mass (g):	642.74		
Gs:	2.68		
e_o:	0.71		
σ'_{3o} (kPa):	146.3		
PI (%):	NP		
USCS:	SP−SM		

Isotropic Consolidation Test

Site:	199 Arm. St
Borehole:	DM BH1
Sample No.:	7U
Sampler Type:	D&M
Spec. Depth (m):	13.67
Date Tested:	04/28/14
Date Sampled:	04/15/14

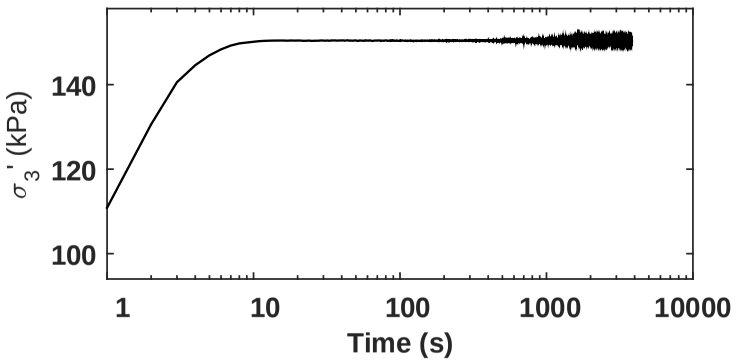

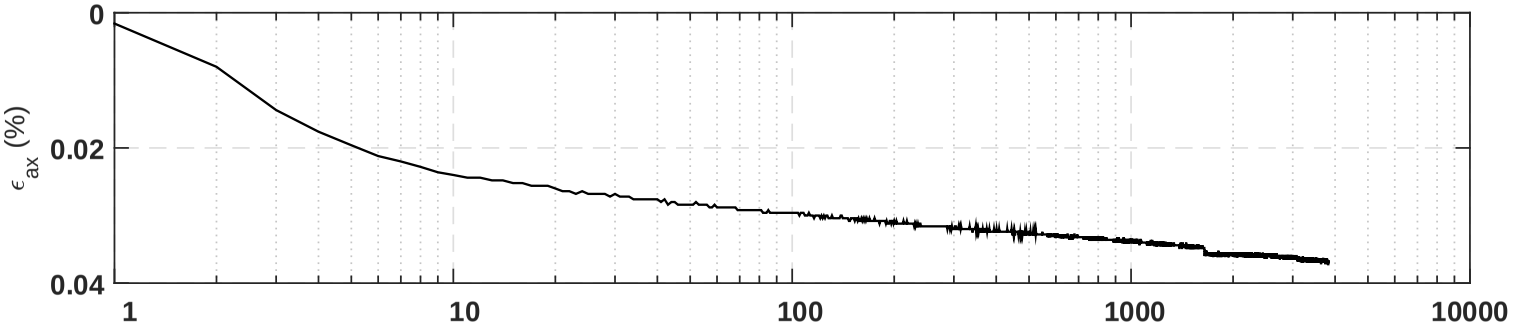

Post CTX Reconsolidation Test

Site:	199 Arm. St
Borehole:	DM BH1
Sample No.:	7U
Sampler Type:	D&M
Spec. Depth (m):	13.67
Date Tested:	04/28/14
Date Sampled:	04/15/14

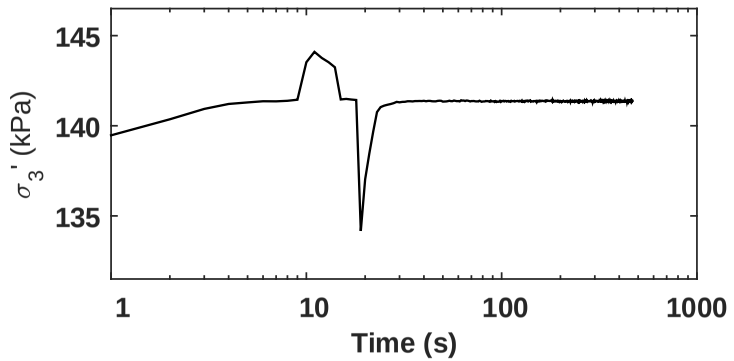

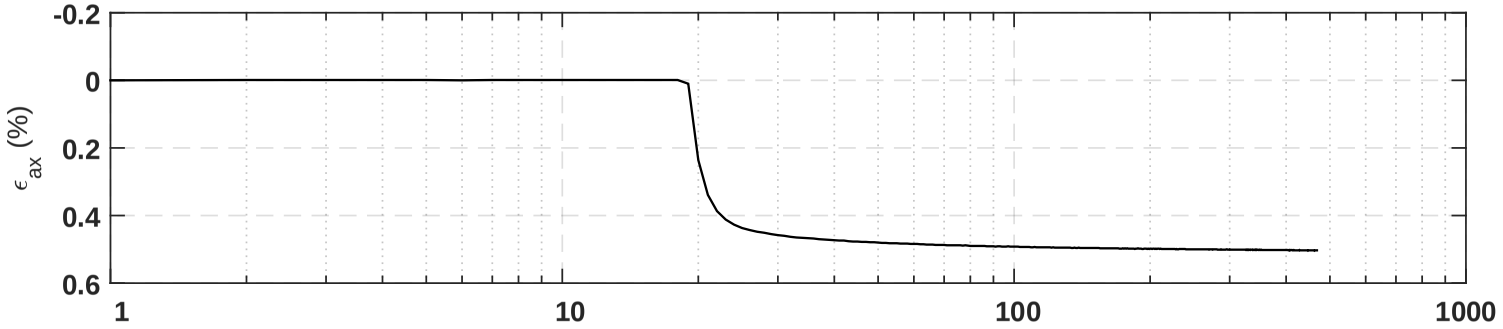

Appendix C.2.4

PWC Building Site—119 Armagh St.

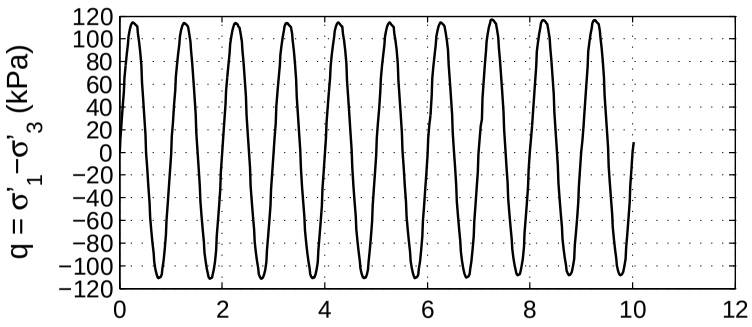

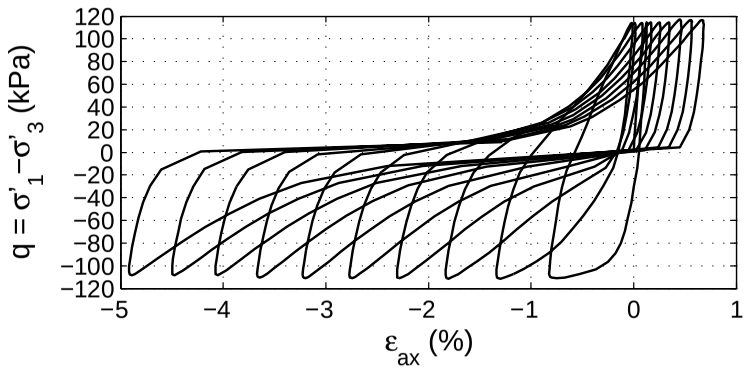

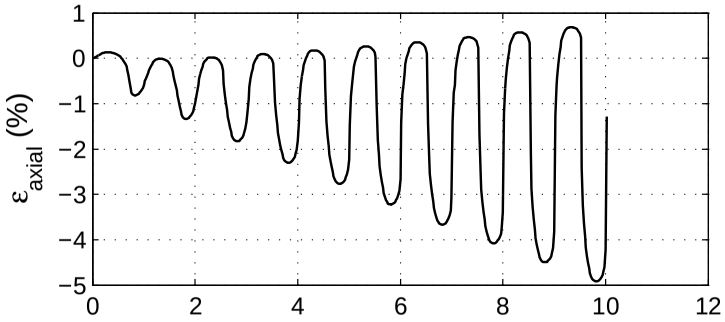

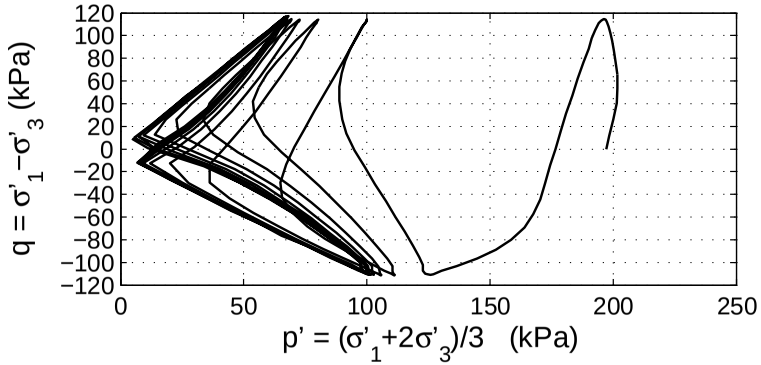

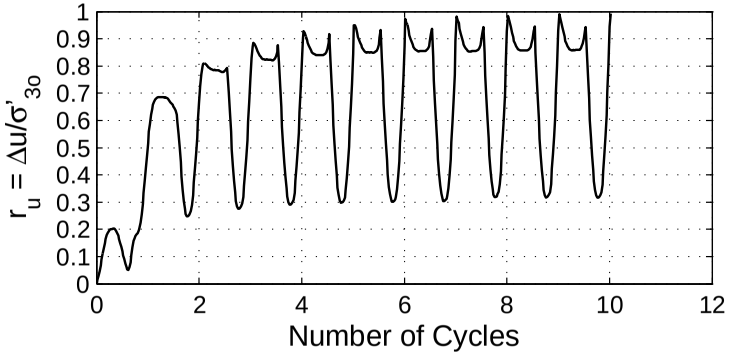

Specimen & Isotropic Cyclic Triaxial Test Data

Site:	119 Arm. St	**Loading Freq (Hz):**	0.1
Borehole:	DM BH1a	**B−Value:**	0.974
Sample No.:	7U	**CSR:**	0.285
Sampler Type:	D&M	**N to $\varepsilon_{Ax-S.A.}$=3%:**	6
Spec. Depth (m):	14.27	**N to $\varepsilon_{Ax-D.A.}$=5%:**	9
Date Tested:	06/24/14	**Post−Cyclic Test:**	Reconsol.
Date Sampled:	06/10/14		
Spec. Ht. (mm):	139.9		
Spec. Diam. (mm):	60.8		
Dry Mass (g):	619.53		
Gs:	2.67		
e_o:	0.75		
σ'_{3o} (kPa):	197.3		
PI (%):	NP		
USCS:	SP		

Isotropic Consolidation Test

Site:	119 Arm. St
Borehole:	DM BH1a
Sample No.:	7U
Sampler Type:	D&M
Spec. Depth (m):	14.27
Date Tested:	06/24/14
Date Sampled:	06/10/14

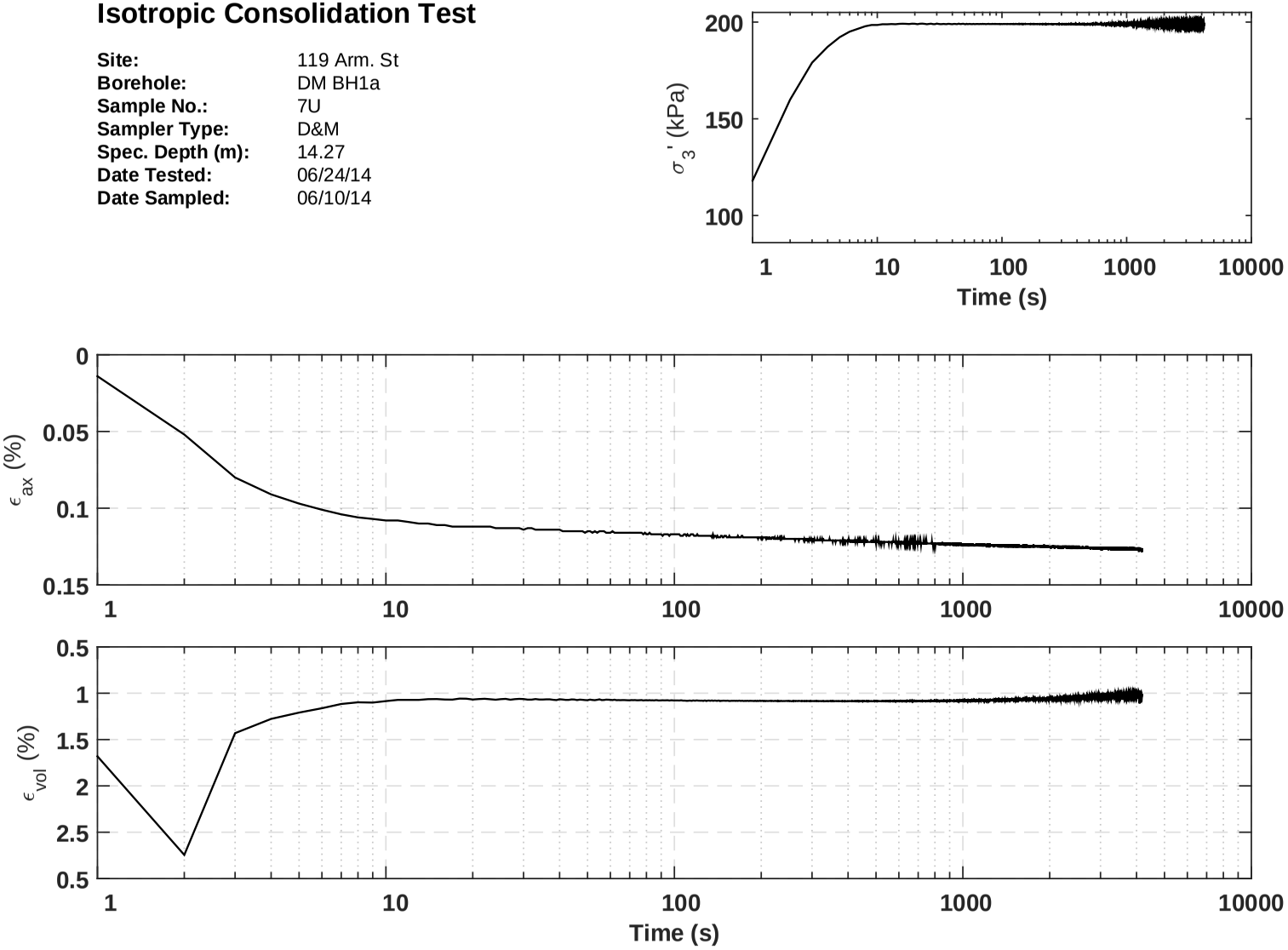

Post CTX Reconsolidation Test

Site:	119 Arm. St
Borehole:	DM BH1a
Sample No.:	7U
Sampler Type:	D&M
Spec. Depth (m):	14.27
Date Tested:	06/24/14
Date Sampled:	06/10/14

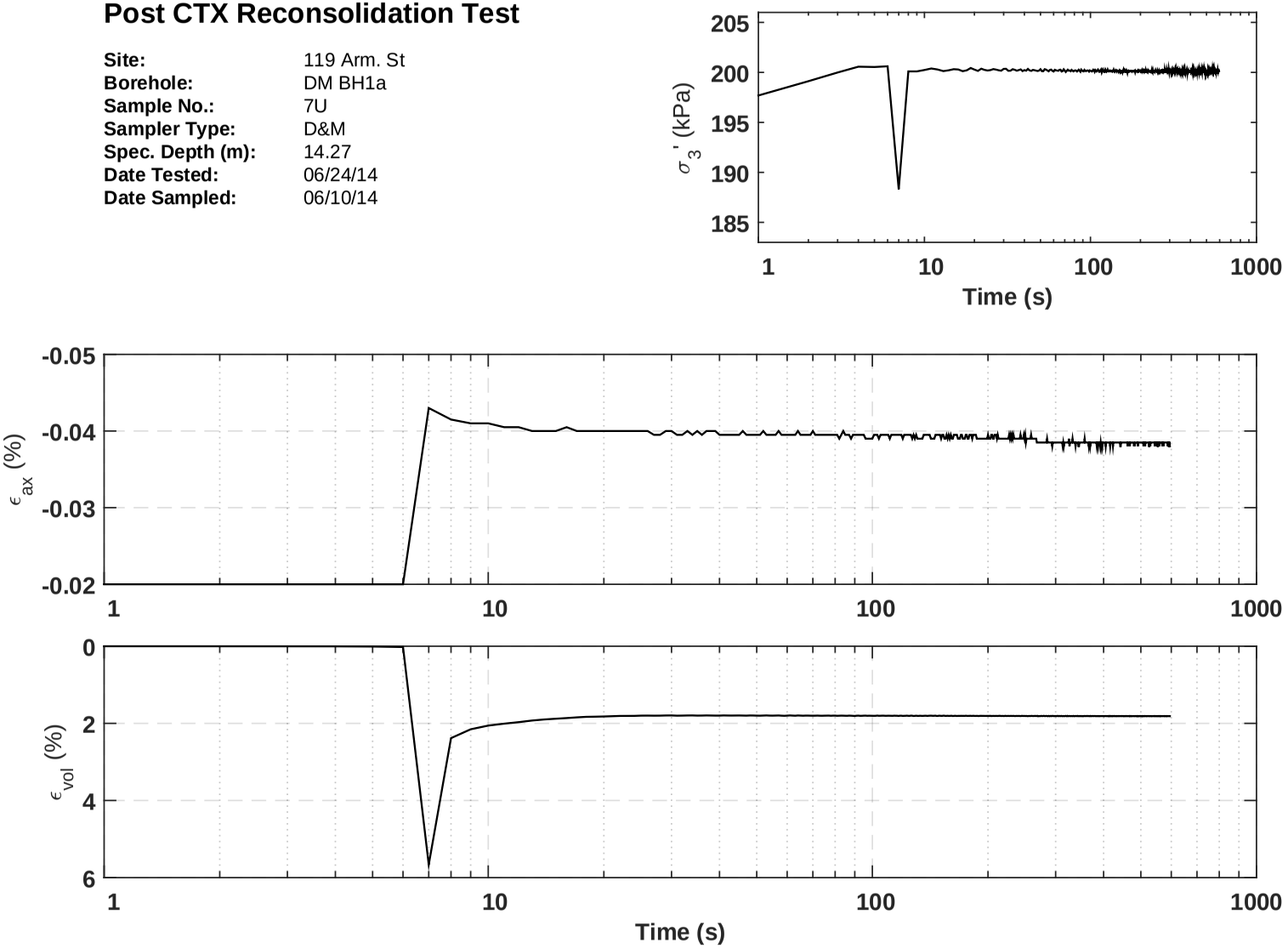

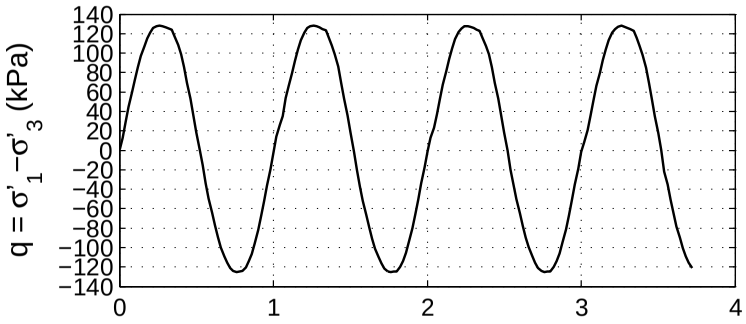

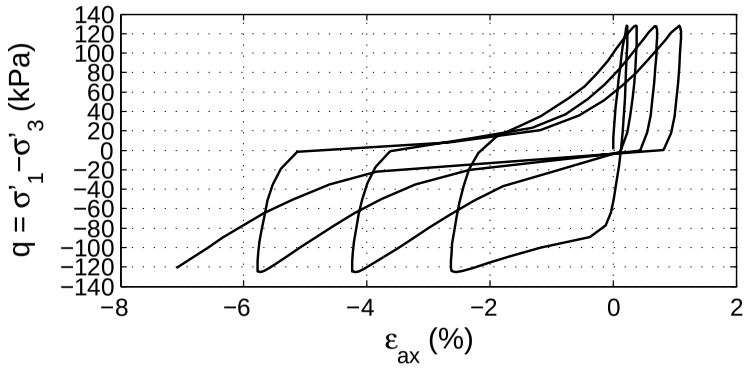

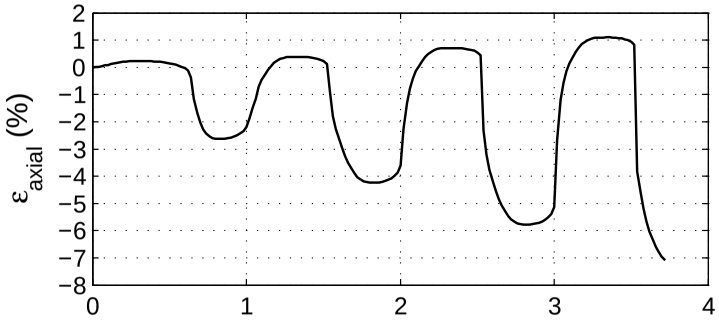

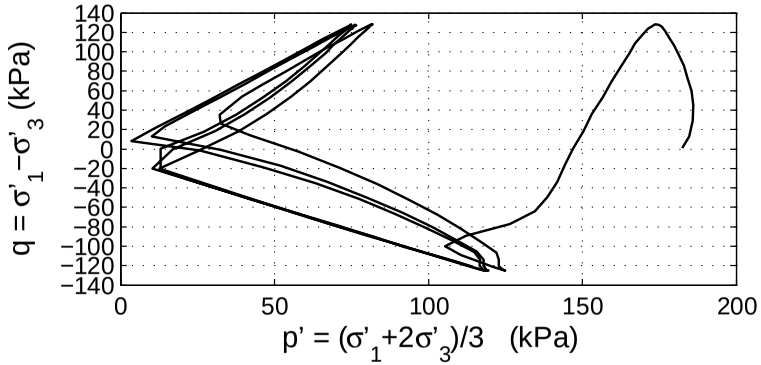

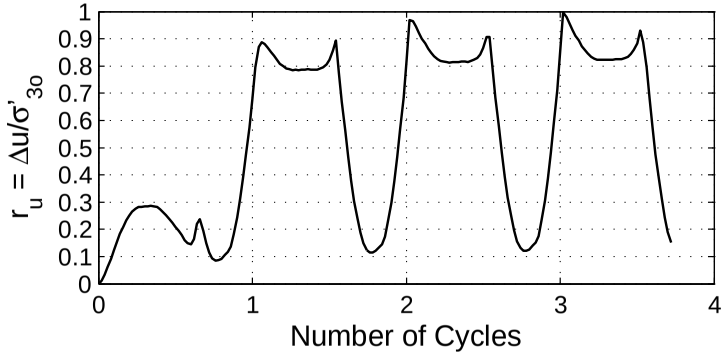

Specimen & Isotropic Cyclic Triaxial Test Data

Site:	119 Arm. St	**Loading Freq (Hz):**	0.1
Borehole:	DM BH1b	**B−Value:**	0.969
Sample No.:	3U	**CSR:**	0.347
Sampler Type:	D&M	**N to $\varepsilon_{Ax-S.A.}$=3%:**	2
Spec. Depth (m):	12.82	**N to $\varepsilon_{Ax-D.A.}$=5%:**	3
Date Tested:	10/03/14	**Post−Cyclic Test:**	Reconsol.
Date Sampled:	10/01/14		
Spec. Ht. (mm):	137.4		
Spec. Diam. (mm):	60.6		
Dry Mass (g):	592.96		
Gs:	2.68		
e_o:	0.79		
σ'_{3o} (kPa):	182.2		
PI (%):	NP		
USCS:	SP−SM		

Isotropic Consolidation Test

Site:	119 Arm. St
Borehole:	DM BH1b
Sample No.:	3U
Sampler Type:	D&M
Spec. Depth (m):	12.82
Date Tested:	10/03/14
Date Sampled:	10/01/14

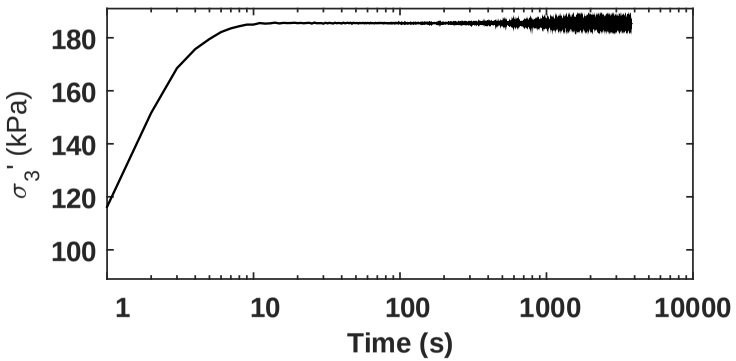

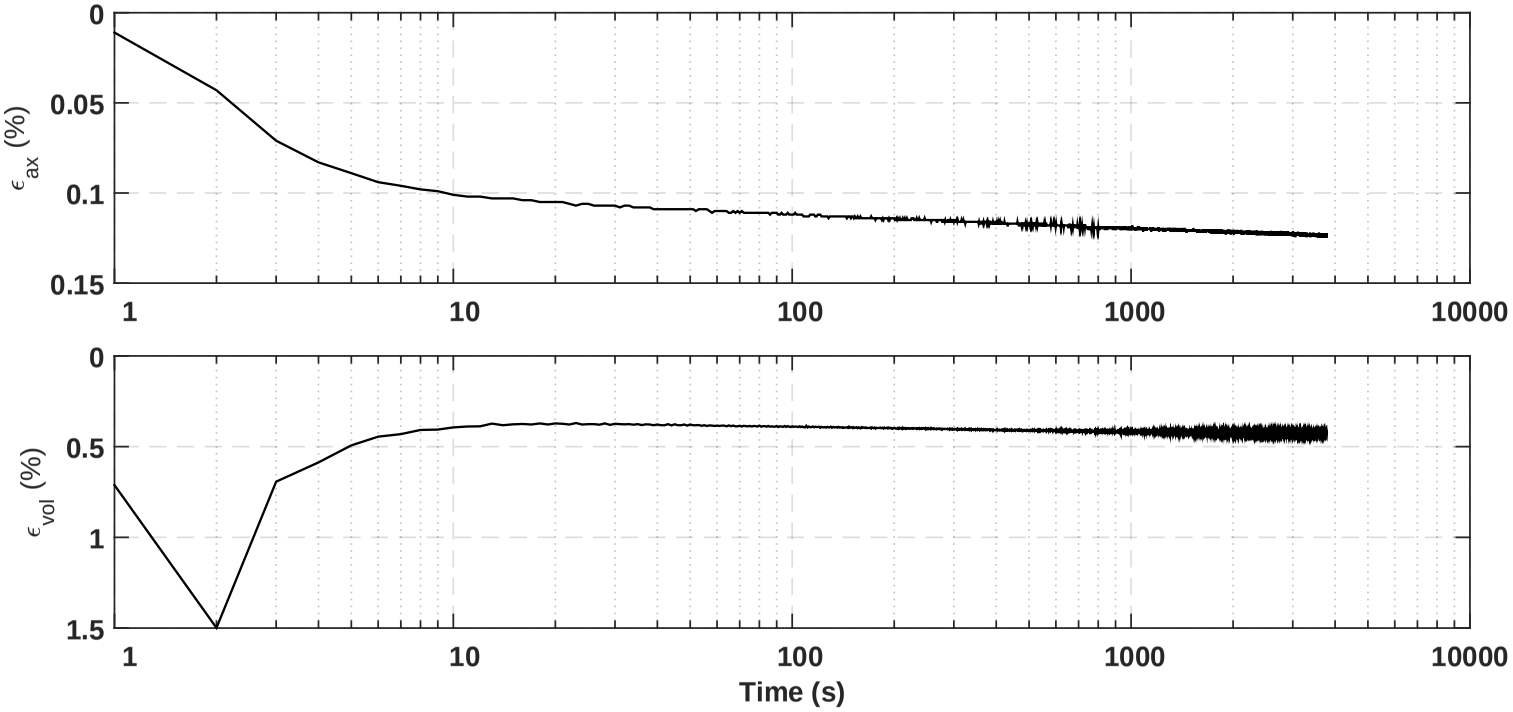

Post CTX Reconsolidation Test

Site:	119 Arm. St
Borehole:	DM BH1b
Sample No.:	3U
Sampler Type:	D&M
Spec. Depth (m):	12.82
Date Tested:	10/03/14
Date Sampled:	10/01/14

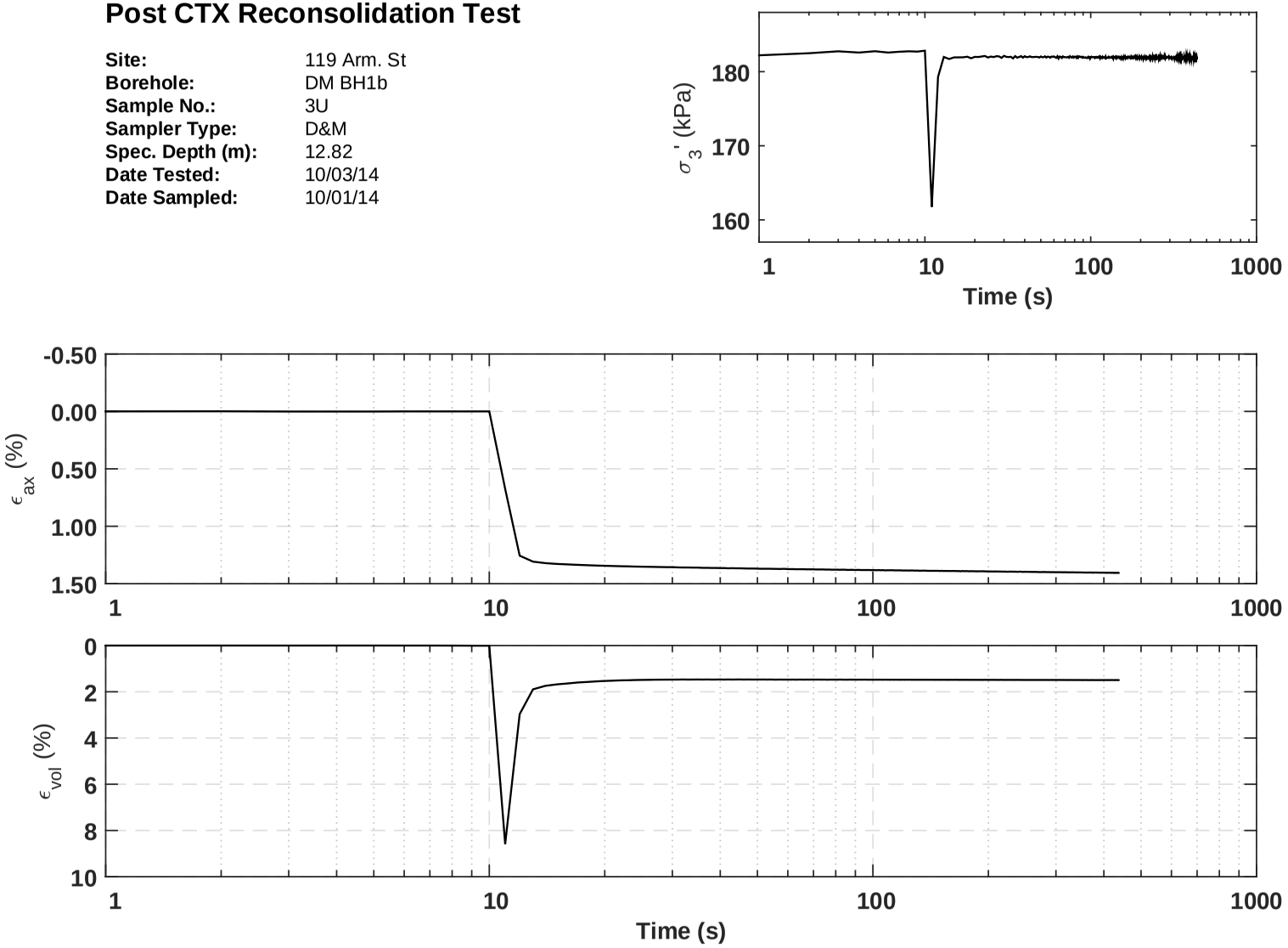

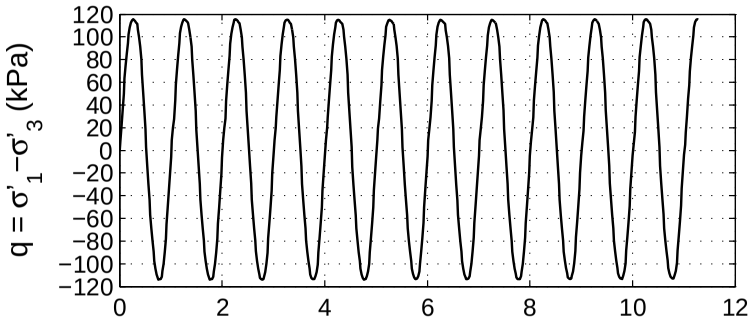

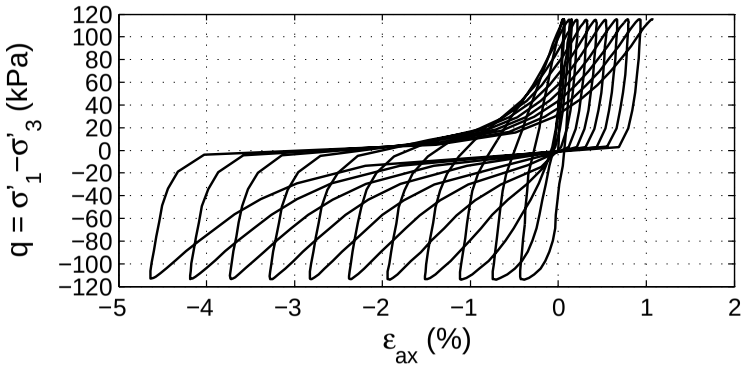

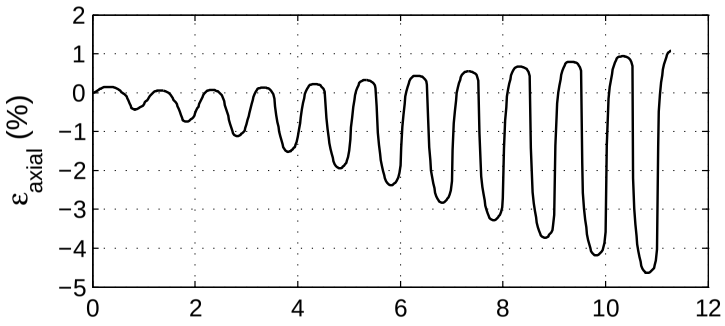

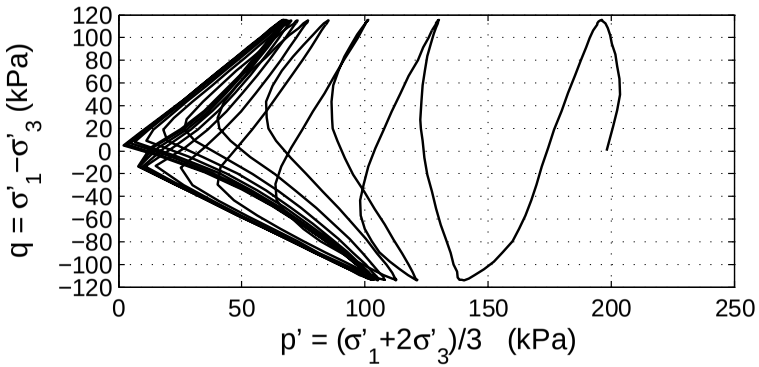

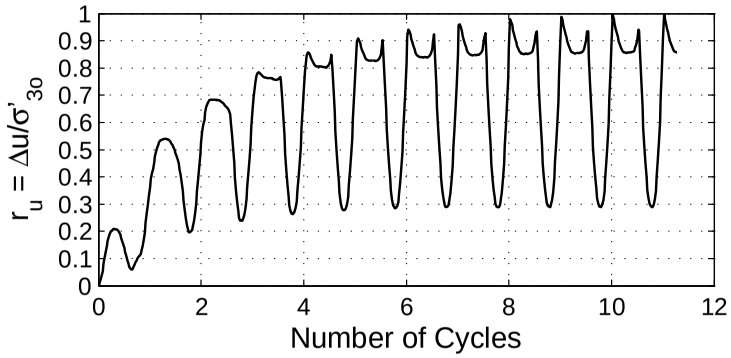

Specimen & Isotropic Cyclic Triaxial Test Data

Site:	119 Arm. St	**Loading Freq (Hz):**	0.1
Borehole:	DM BH1b	**B−Value:**	0.953
Sample No.:	5U	**CSR:**	0.288
Sampler Type:	D&M	**N to $\varepsilon_{Ax-S.A.}$=3%:**	8
Spec. Depth (m):	13.81	**N to $\varepsilon_{Ax-D.A.}$=5%:**	10.5
Date Tested:	10/04/14	**Post−Cyclic Test:**	Reconsol.
Date Sampled:	10/01/14		
Spec. Ht. (mm):	137.7		
Spec. Diam. (mm):	60.8		
Dry Mass (g):	618.82		
Gs:	2.67		
e_o:	0.72		
σ'_{3o} (kPa):	198.1		
PI (%):	NP		
USCS:	SP		

Isotropic Consolidation Test

Site:	119 Arm. St
Borehole:	DM BH1b
Sample No.:	5U
Sampler Type:	D&M
Spec. Depth (m):	13.81
Date Tested:	10/04/14
Date Sampled:	10/01/14

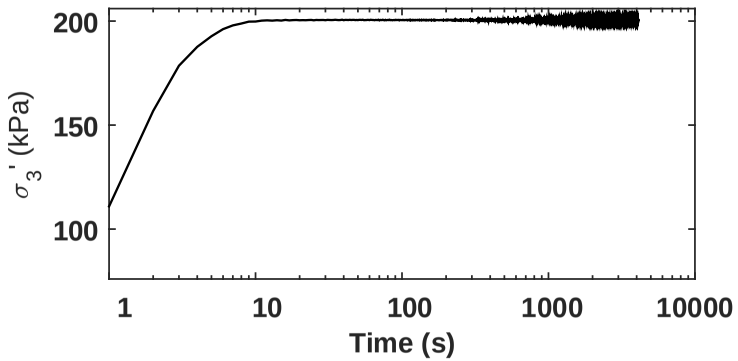

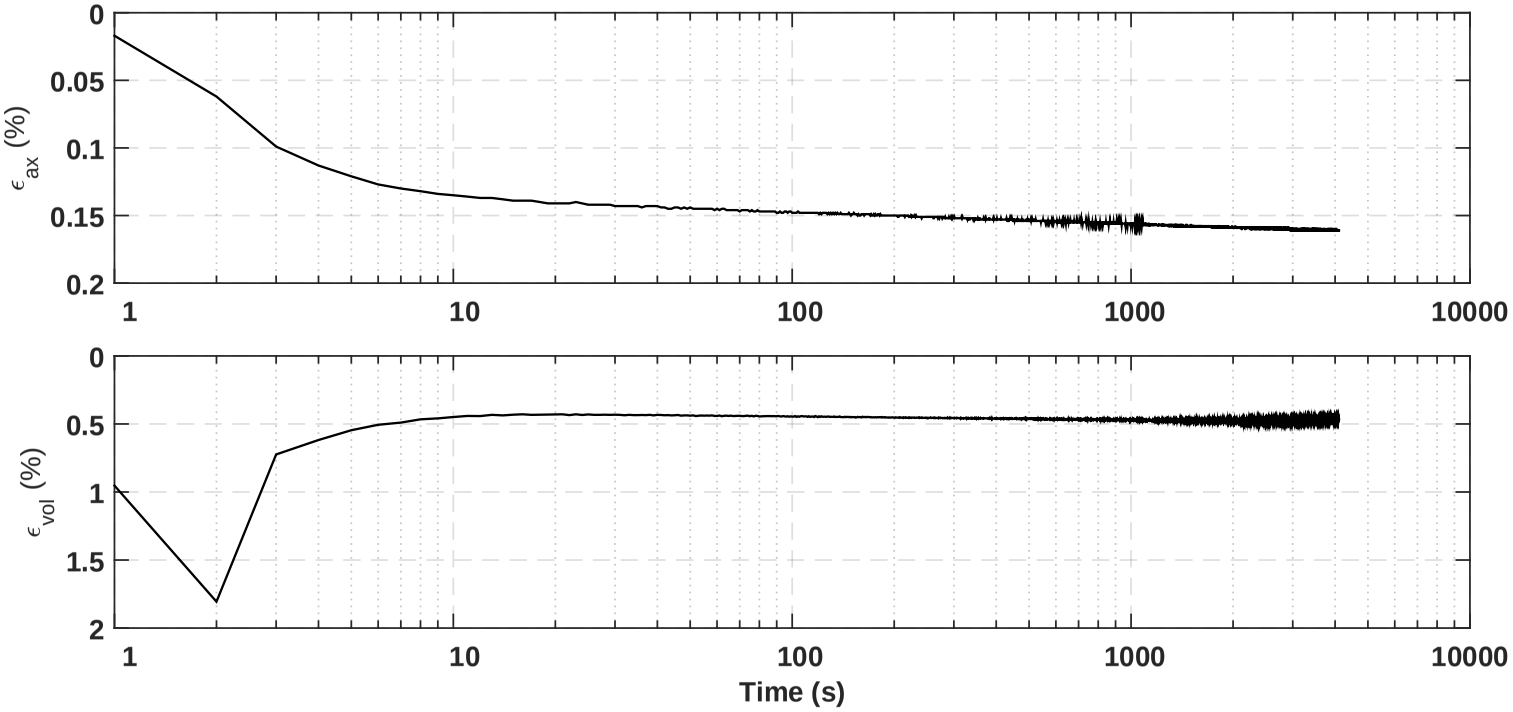

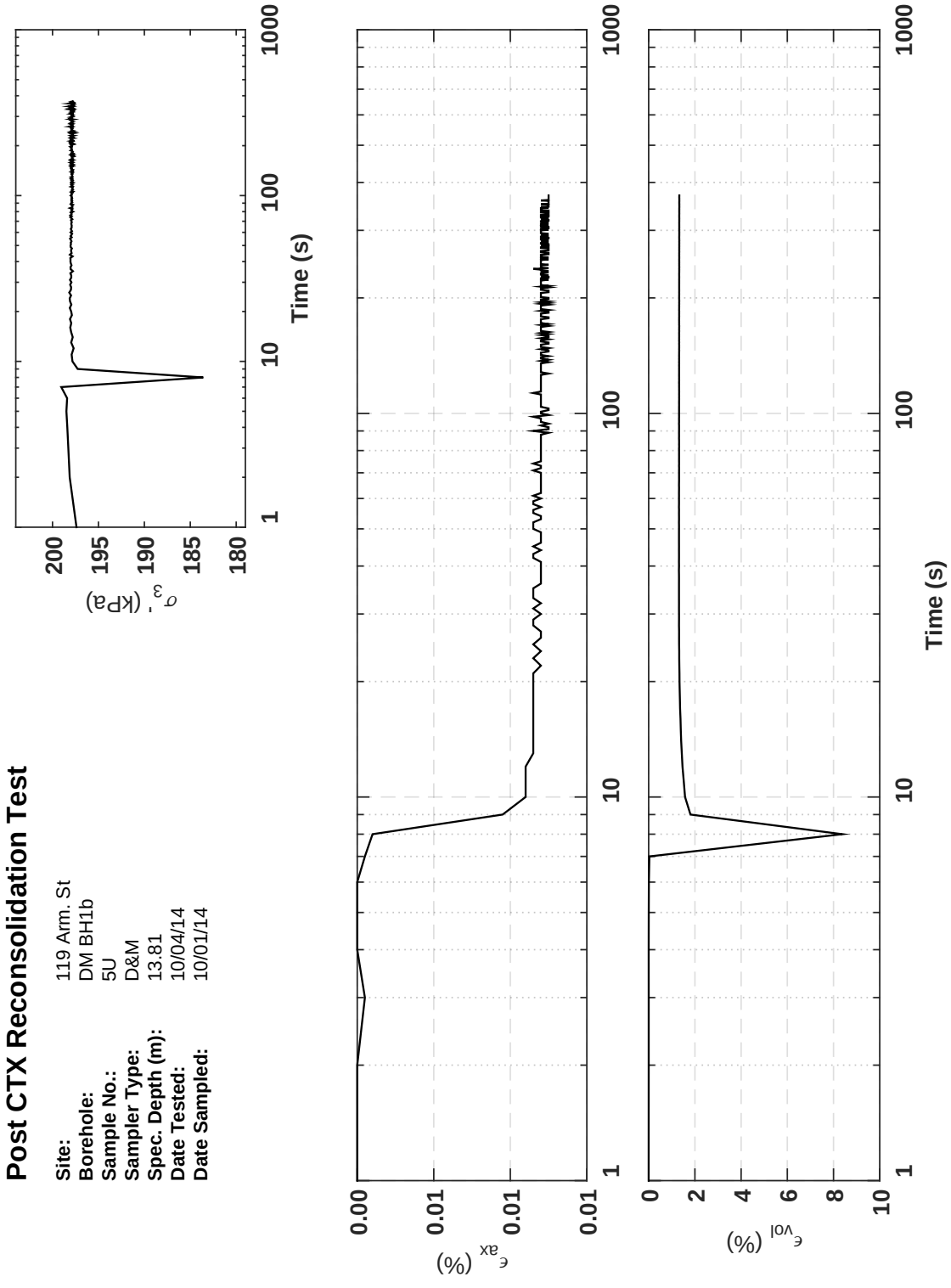
Post CTX Reconsolidation Test
Site: 119 Arm. St
Borehole: DM BH1b
Sample No.: 5U
Sampler Type: D&M
Spec. Depth (m): 13.81
Date Tested: 10/04/14
Date Sampled: 10/01/14
σ3' (KPa)
200
195
190
185
180
1
10
100
1000
Time (s)
εax (%)
0.00
0.01
0.01
0.01
εVol (%)
0
2
4
6
8
10
Time (s)

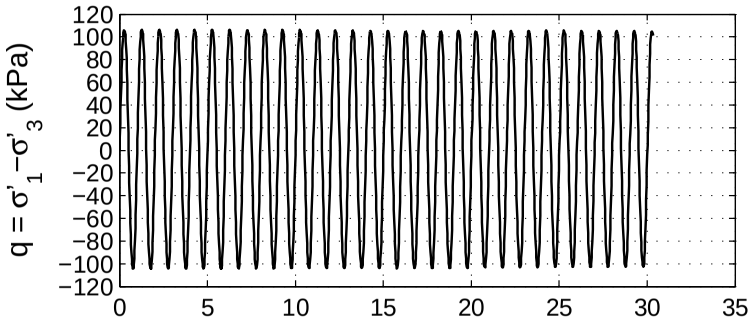

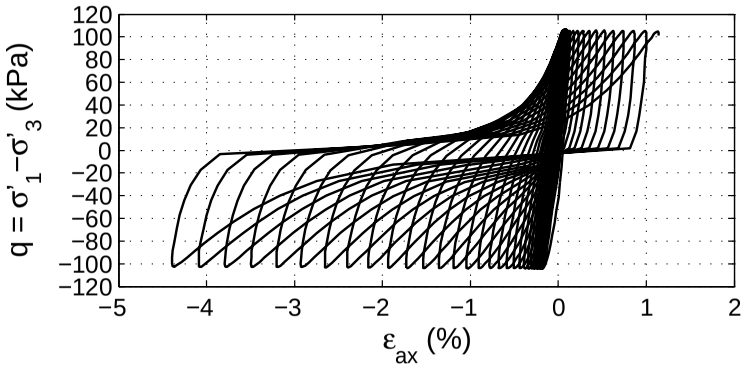

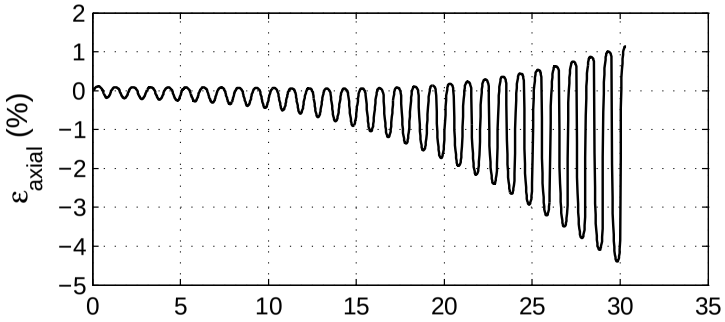

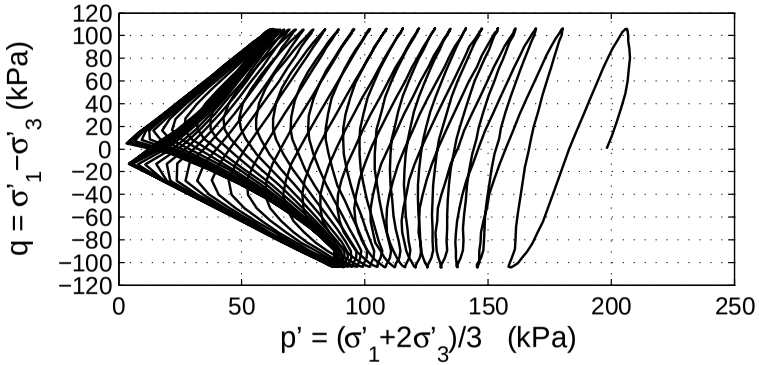

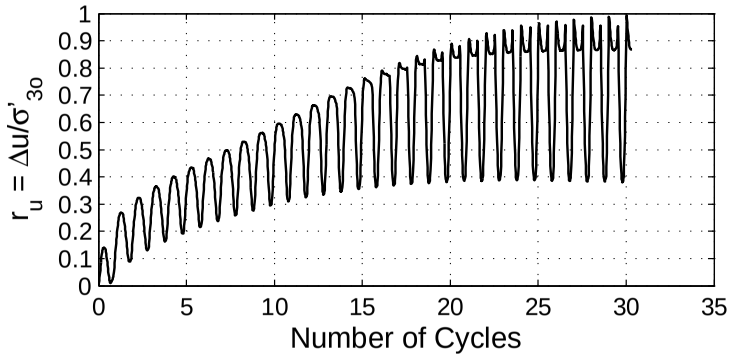

Specimen & Isotropic Cyclic Triaxial Test Data

Site:	119 Arm. St	**Loading Freq (Hz):**	0.1
Borehole:	DM BH1b	**B−Value:**	0.946+
Sample No.:	6U	**CSR:**	0.264
Sampler Type:	D&M	**N to $\varepsilon_{Ax-S.A.}$=3%:**	26
Spec. Depth (m):	14.32	**N to $\varepsilon_{Ax-D.A.}$=5%:**	29.5
Date Tested:	10/10/14	**Post−Cyclic Test:**	Reconsol.
Date Sampled:	10/01/14		
Spec. Ht. (mm):	136.4		
Spec. Diam. (mm):	60.8		
Dry Mass (g):	634.36*		
Gs:	2.67		
e_o:	0.67*		
σ'_{3o} (kPa):	197.9		
PI (%):	NP		
USCS:	SP		

Isotropic Consolidation Test

Site:	119 Arm. St
Borehole:	DM BH1b
Sample No.:	6U
Sampler Type:	D&M
Spec. Depth (m):	14.32
Date Tested:	10/10/14
Date Sampled:	10/01/14

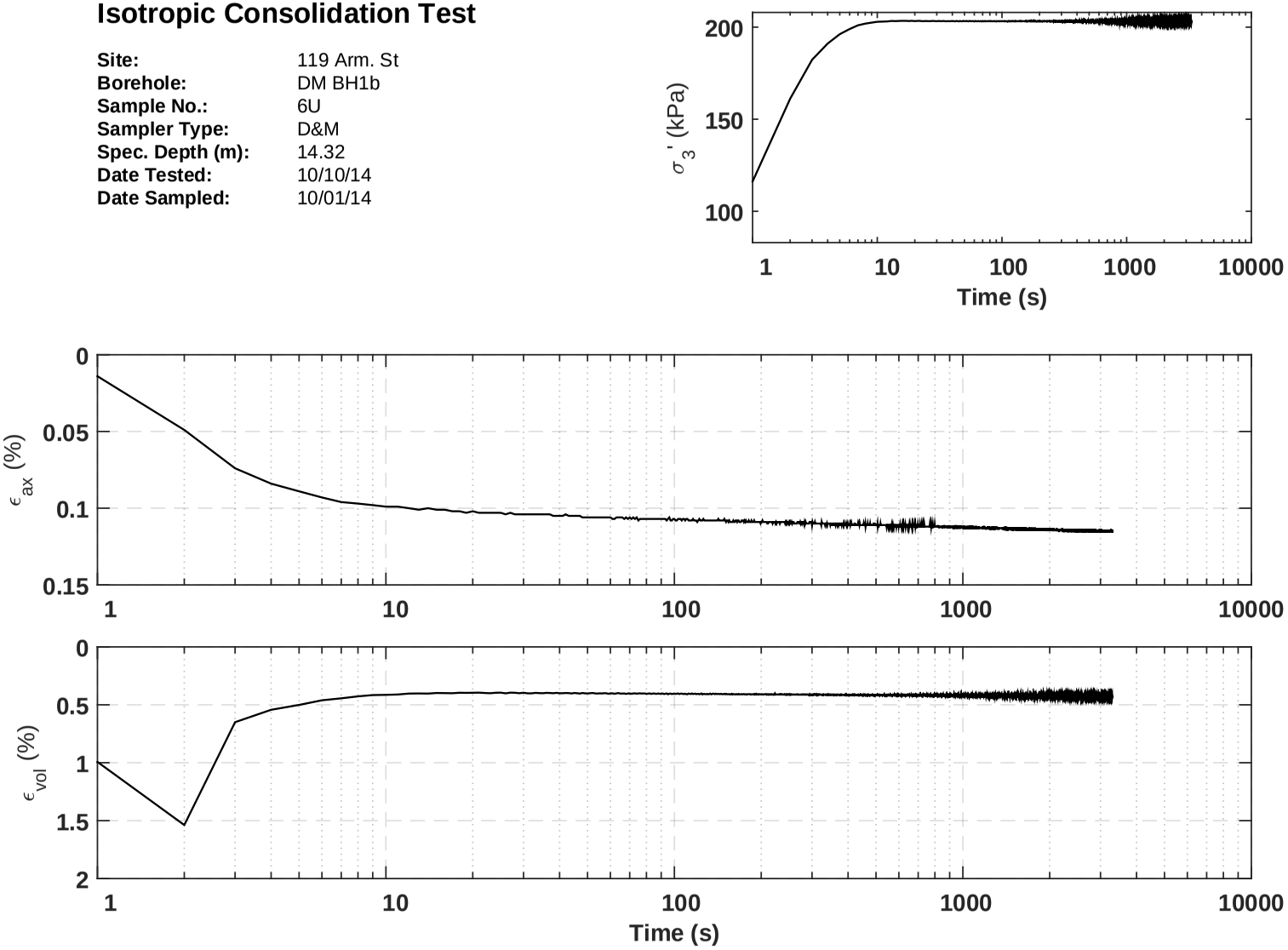

Post CTX Reconsolidation Test

Site:	119 Arm. St
Borehole:	DM BH1b
Sample No.:	6U
Sampler Type:	D&M
Spec. Depth (m):	14.32
Date Tested:	10/10/14
Date Sampled:	10/01/14

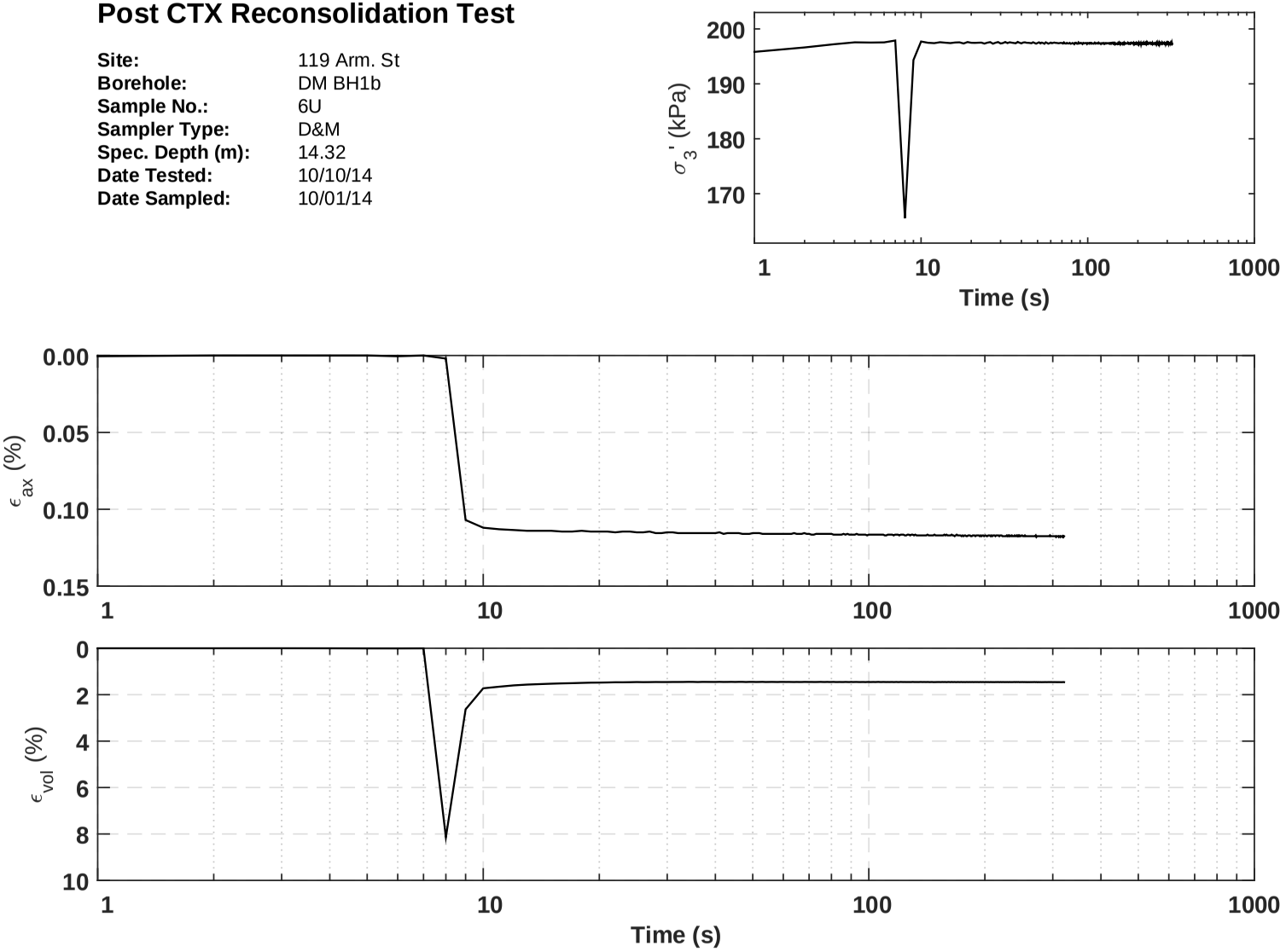

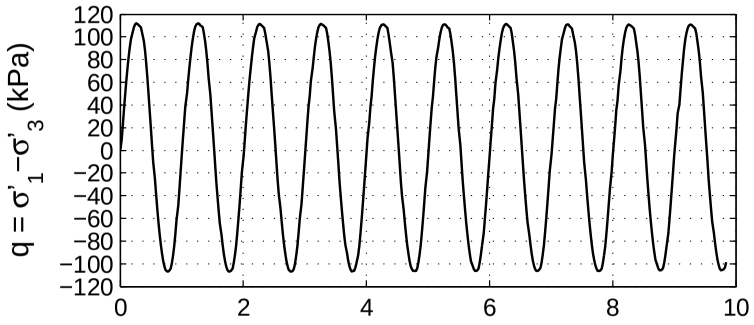

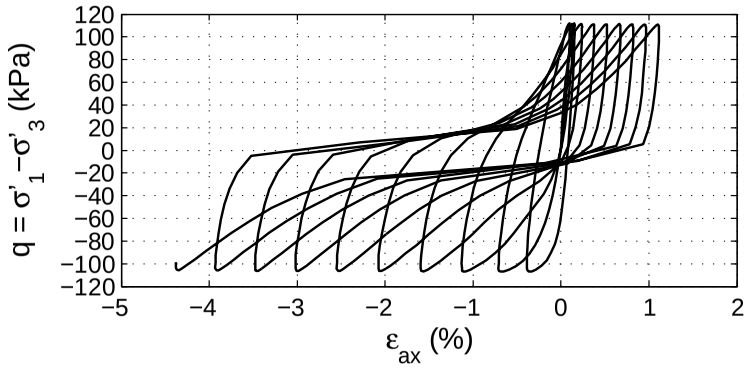

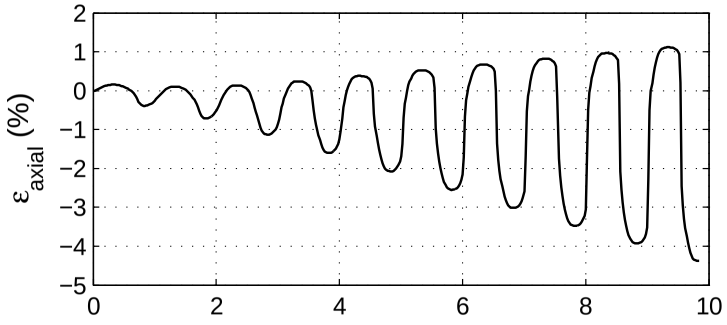

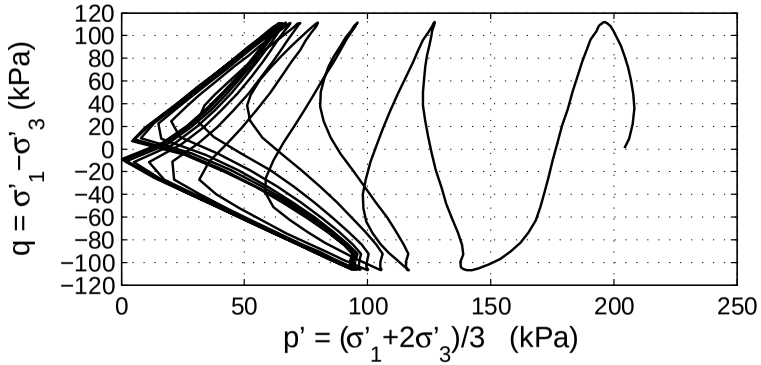

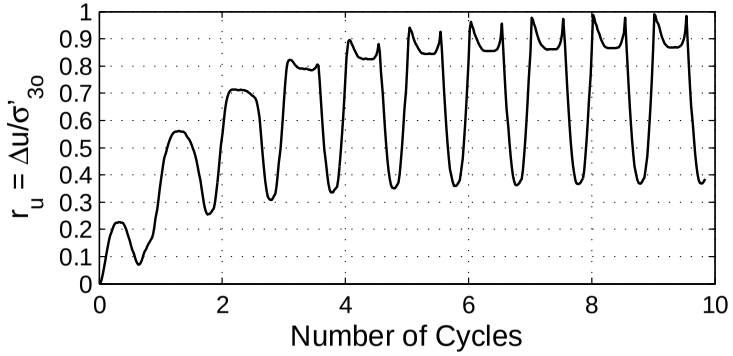

Specimen & Isotropic Cyclic Triaxial Test Data

Site:	119 Arm. St	**Loading Freq (Hz):**	0.1
Borehole:	DM BH1b	**B−Value:**	0.960
Sample No.:	7U	**CSR:**	0.266
Sampler Type:	D&M	**N to $\varepsilon_{Ax-S.A.}$=3%:**	7
Spec. Depth (m):	14.57	**N to $\varepsilon_{Ax-D.A.}$=5%:**	9.5
Date Tested:	10/10/14	**Post−Cyclic Test:**	Monotonic
Date Sampled:	10/01/14		
Spec. Ht. (mm):	139.0		
Spec. Diam. (mm):	60.8		
Dry Mass (g):	608.95		
Gs:	2.69		
e_ρ:	0.78		
σ'_{3o} (kPa):	204.2		
PI (%):	NP		
USCS:	SP−SM		

Isotropic Consolidation Test

Site:	119 Arm. St
Borehole:	DM BH1b
Sample No.:	7U
Sampler Type:	D&M
Spec. Depth (m):	14.57
Date Tested:	10/10/14
Date Sampled:	10/01/14

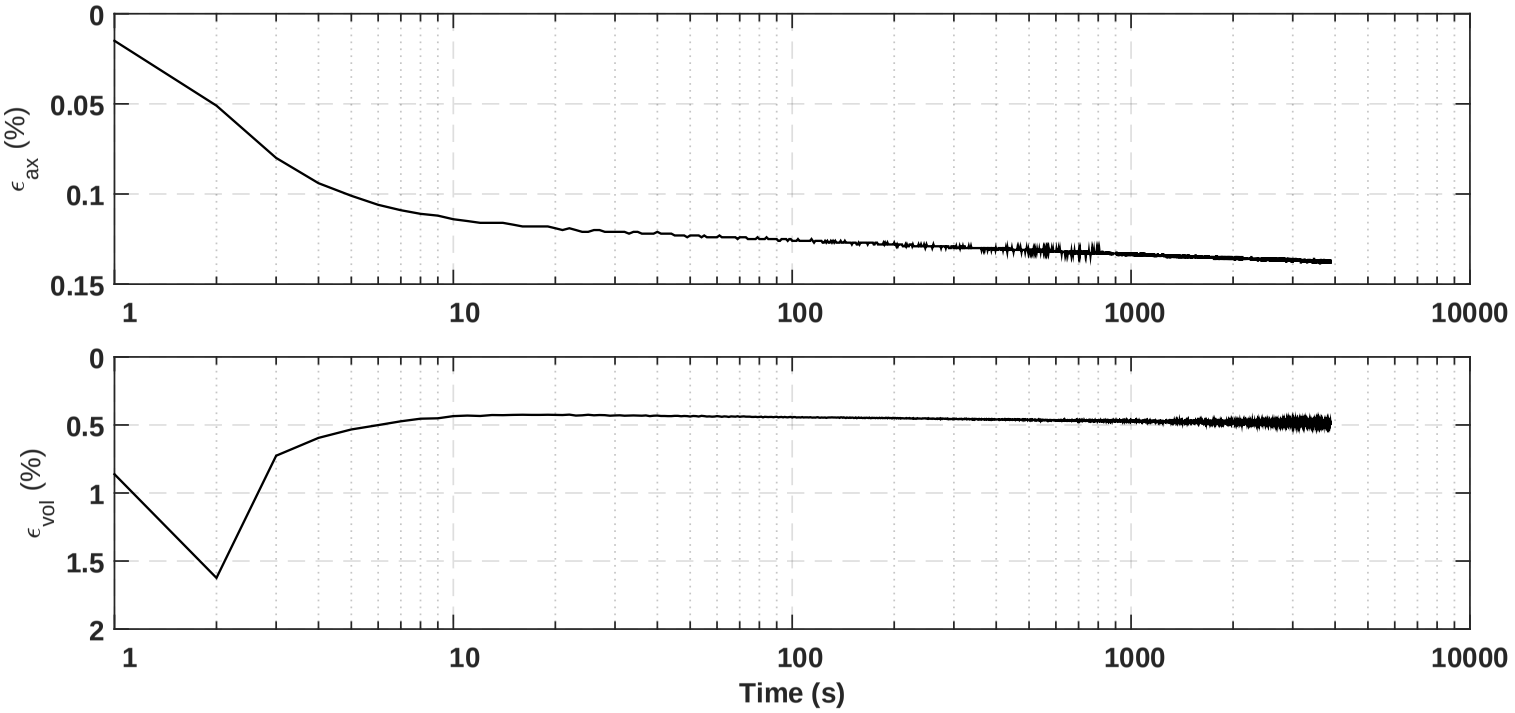

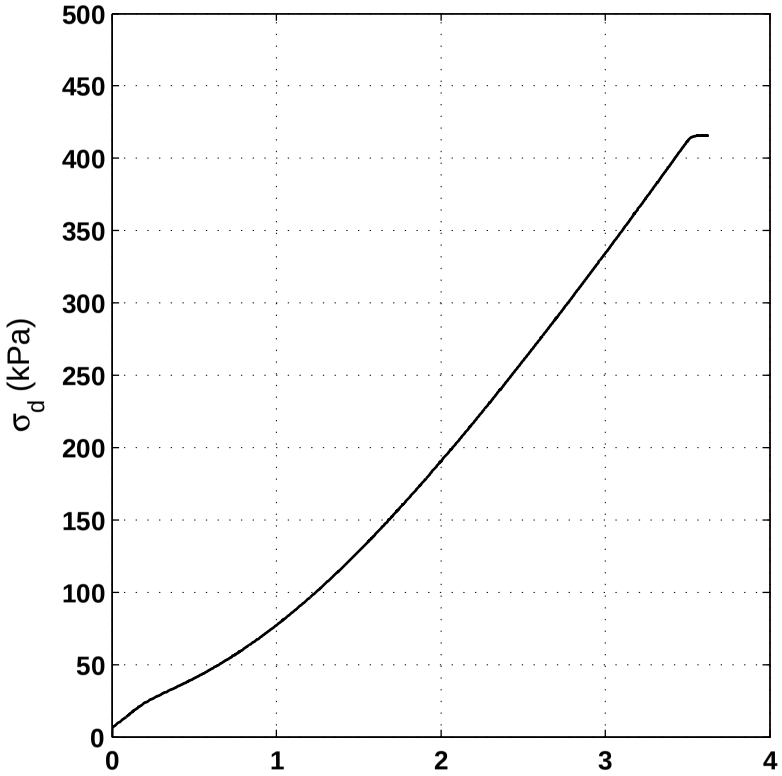

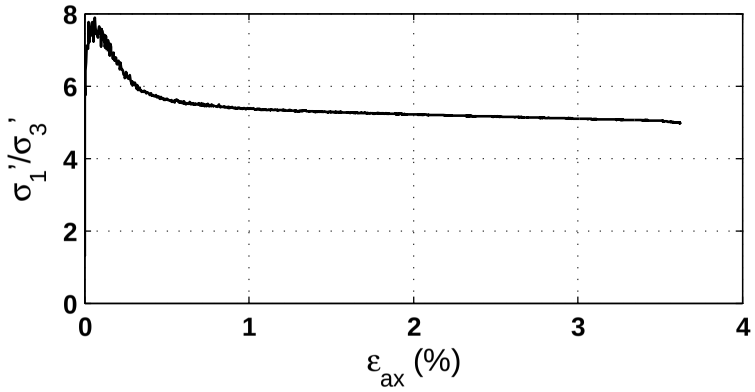

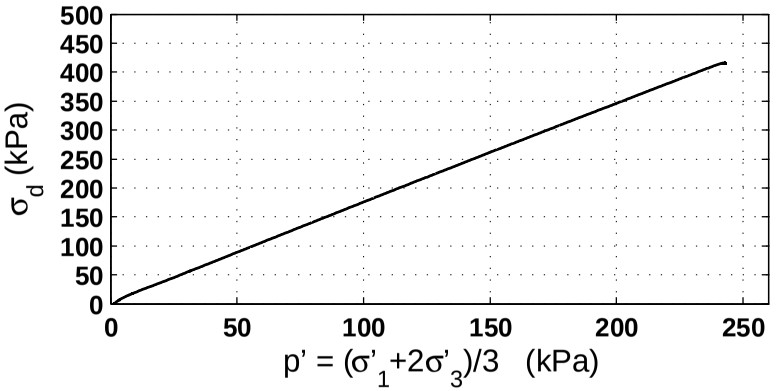

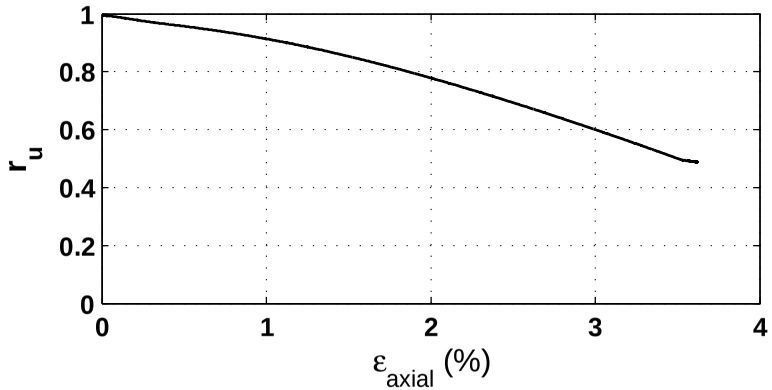

Post CTX Monotonic Comp. Test

Site:	119 Arm. St	**Rate (kPa/min):**	12
Borehole:	DM BH1b		
Sample No.:	7U		
Sampler Type:	D&M		
Spec. Depth (m):	14.57		
Date Tested:	10/10/14		
Date Sampled:	10/01/14		

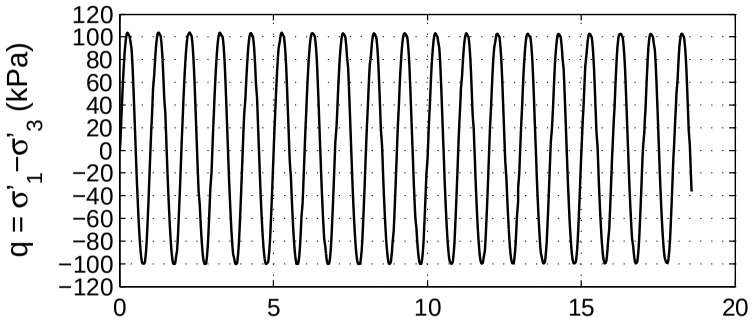

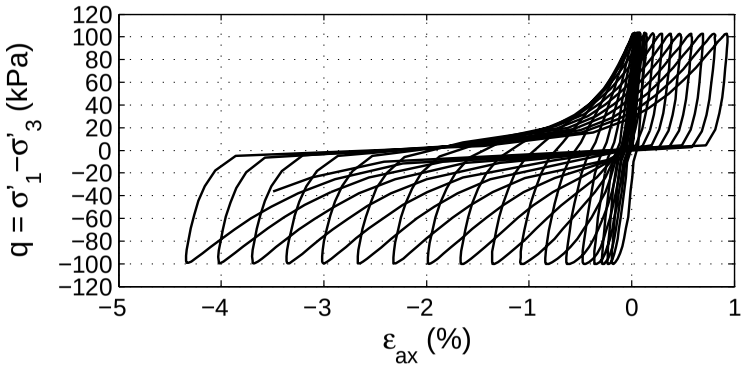

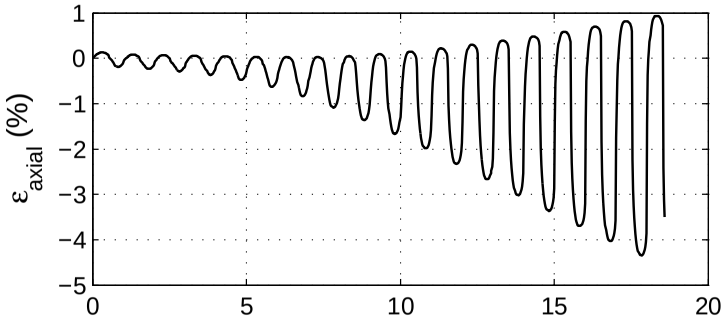

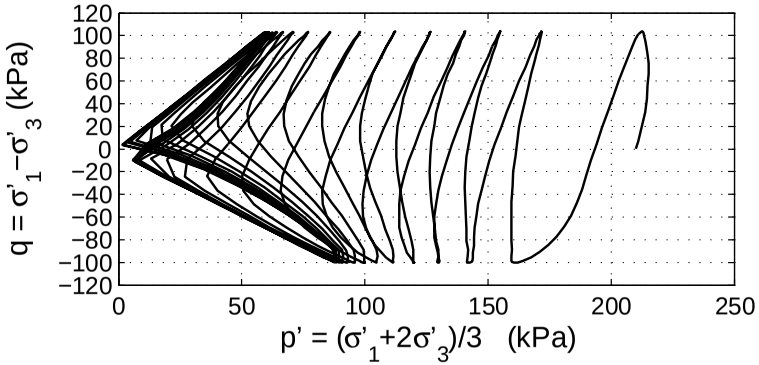

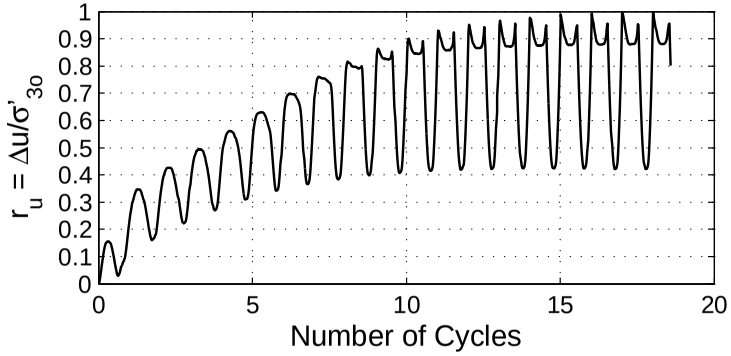

Specimen & Isotropic Cyclic Triaxial Test Data

Site:	119 Arm. St	**Loading Freq (Hz):**	0.1
Borehole:	DM BH1b	**B−Value:**	0.980
Sample No.:	7U	**CSR:**	0.240
Sampler Type:	D&M	**N to $\varepsilon_{Ax-S.A.}$=3%:**	14
Spec. Depth (m):	14.82	**N to $\varepsilon_{Ax-D.A.}$=5%:**	18
Date Tested:	10/14/14	**Post−Cyclic Test:**	Reconsol.
Date Sampled:	10/01/14		
Spec. Ht. (mm):	143.2		
Spec. Diam. (mm):	60.8		
Dry Mass (g):	661.74		
Gs:	2.66		
e_o:	0.67		
σ'_{3o} (kPa):	210.0		
PI (%):	NP		
USCS:	SP		

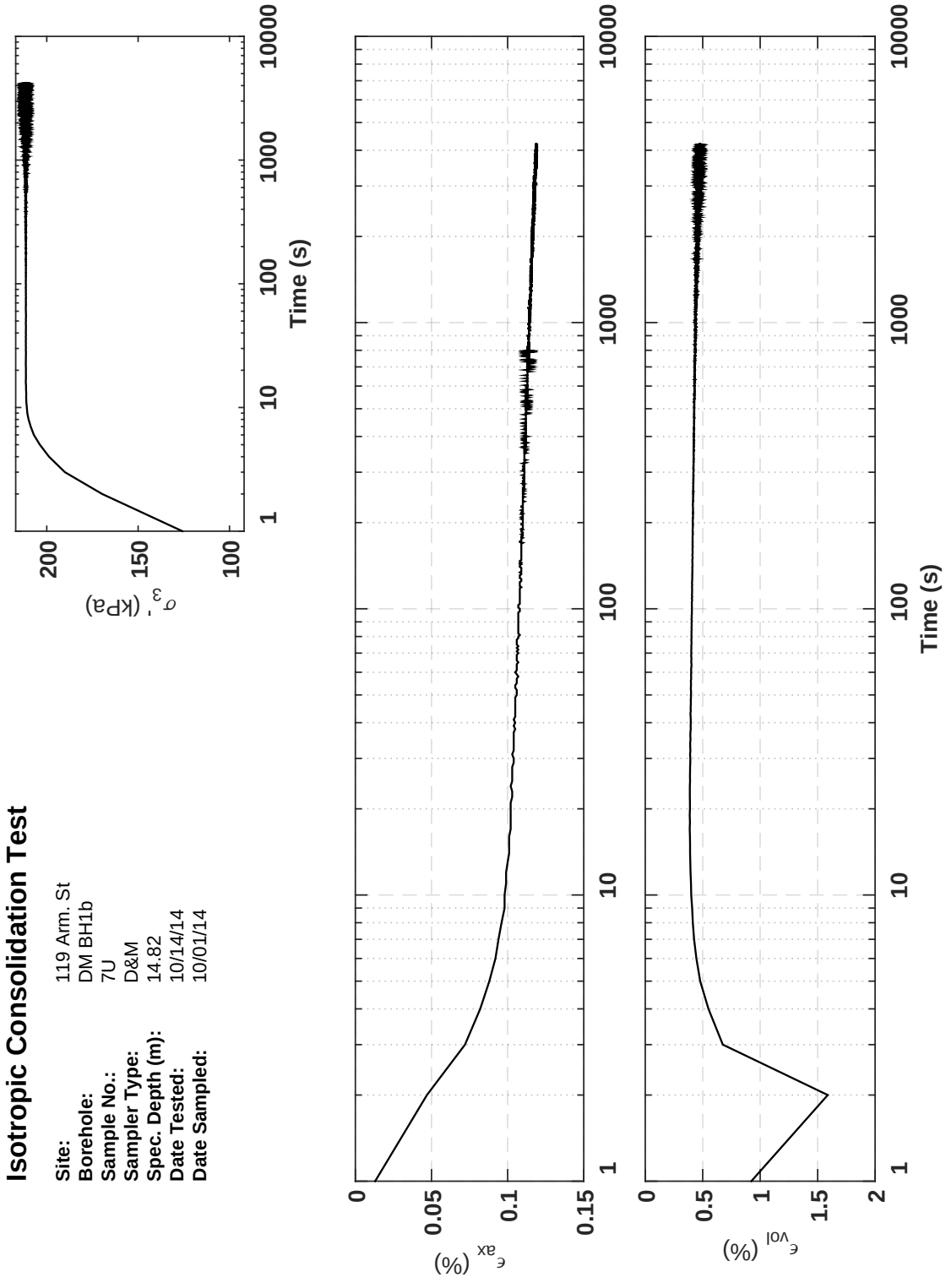
Isotropic Consolidation Test
Site: 119 Arm. St
Borehole: DM BH1b
Sample No.: 7U
Sampler Type: D&M
Spec. Depth (m): 14.82
Date Tested: 10/14/14
Date Sampled: 10/01/14
σ3' (KPa)
200
150
100
1
10
100
1000
10000
Time (s)
εax (%)
0
0.05
0.1
0.15
εvol (%)
0
0.5
1
1.5
2

Post CTX Reconsolidation Test

Site:	119 Arm. St
Borehole:	DM BH1b
Sample No.:	7U
Sampler Type:	D&M
Spec. Depth (m):	14.82
Date Tested:	10/14/14
Date Sampled:	10/01/14

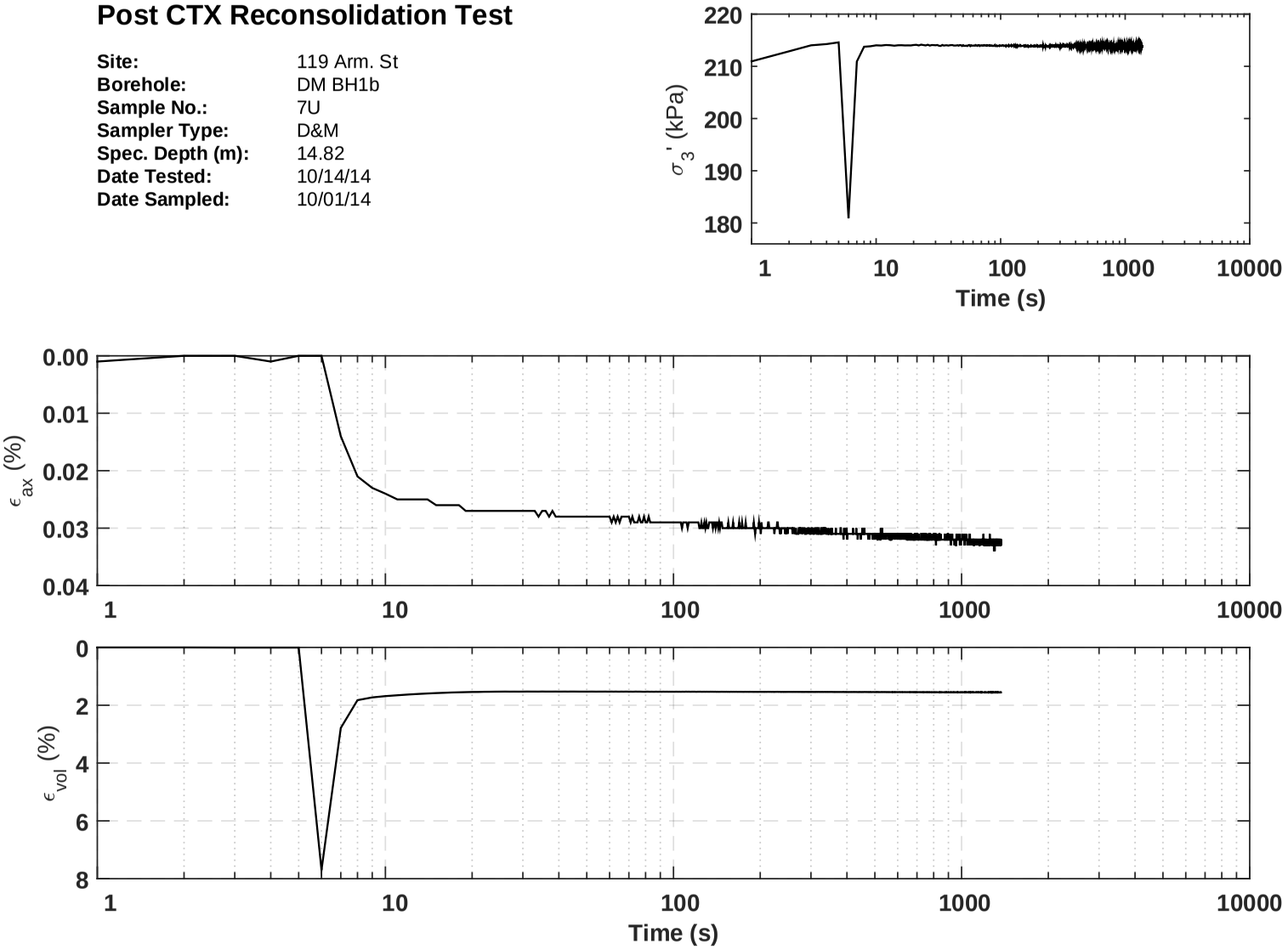

Appendix C.2.5

VT Building Site—90 Armagh St.

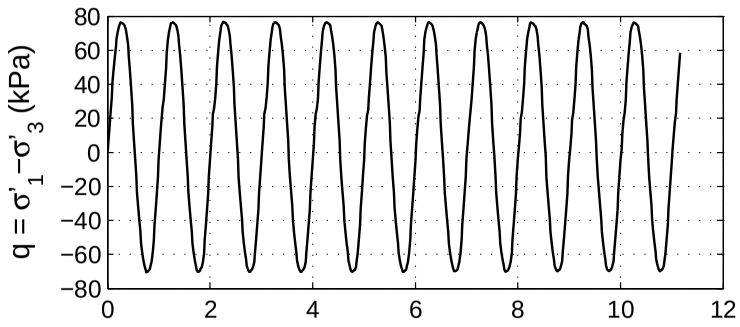

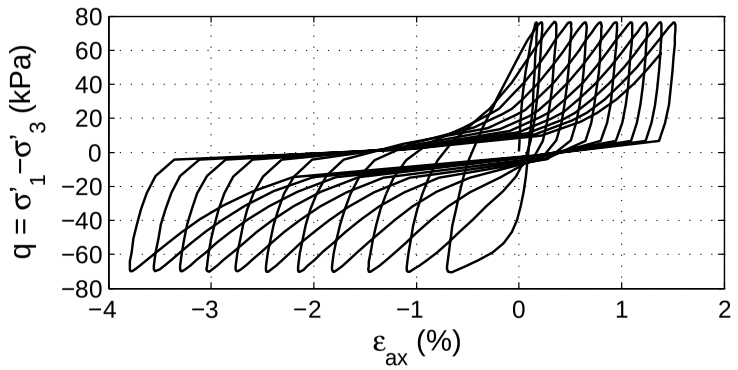

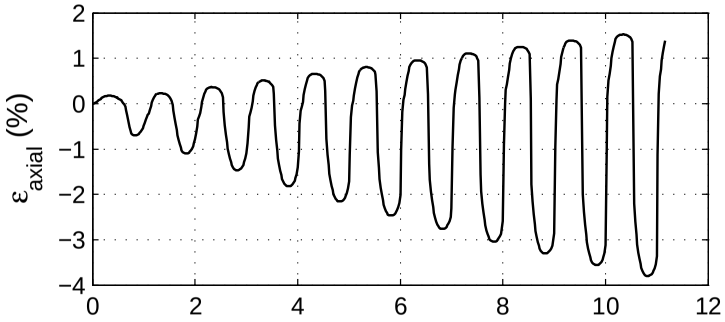

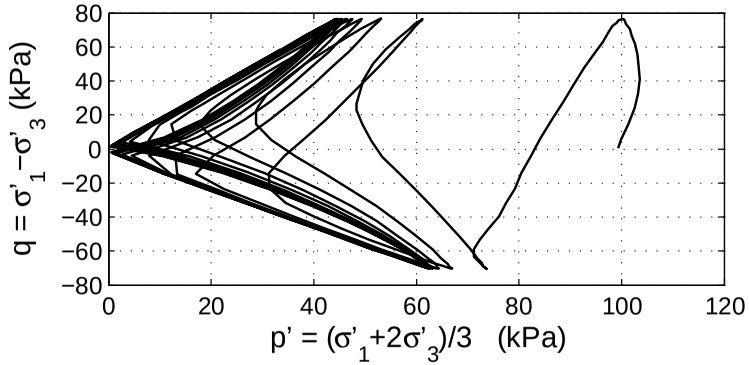

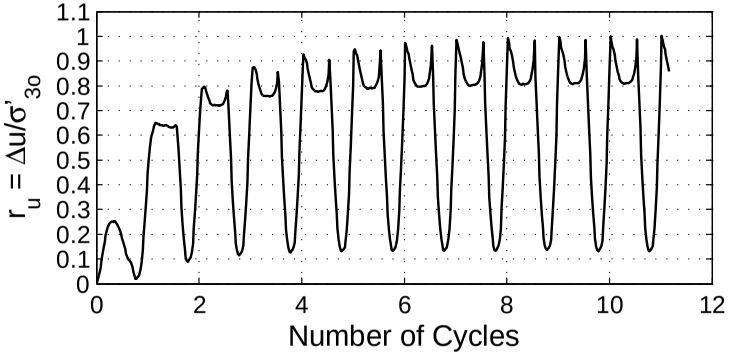

Specimen & Isotropic Cyclic Triaxial Test Data

Site:	90 Arm. St	**Loading Freq (Hz):**	0.1
Borehole:	DM BH2	**B−Value:**	0.986
Sample No.:	1U	**CSR:**	0.371
Sampler Type:	D&M	**N to $\varepsilon_{Ax-S.A.}$=3%:**	8
Spec. Depth (m):	7.44	**N to $\varepsilon_{Ax-D.A.}$=5%:**	10.5
Date Tested:	06/21/14	**Post−Cyclic Test:**	Monotonic
Date Sampled:	06/13/14		
Spec. Ht. (mm):	143.0		
Spec. Diam. (mm):	60.9		
Dry Mass (g):	645.38		
Gs:	2.69		
e_o:	0.74		
σ'_{3o} (kPa):	99.2		
PI (%):	NP		
USCS:	SP		

Isotropic Consolidation Test

Site:	90 Arm. St
Borehole:	DM BH2
Sample No.:	1U
Sampler Type:	D&M
Spec. Depth (m):	7.44
Date Tested:	06/21/14
Date Sampled:	06/13/14

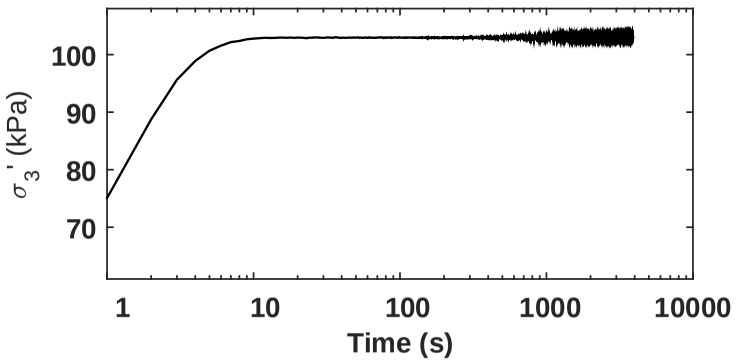

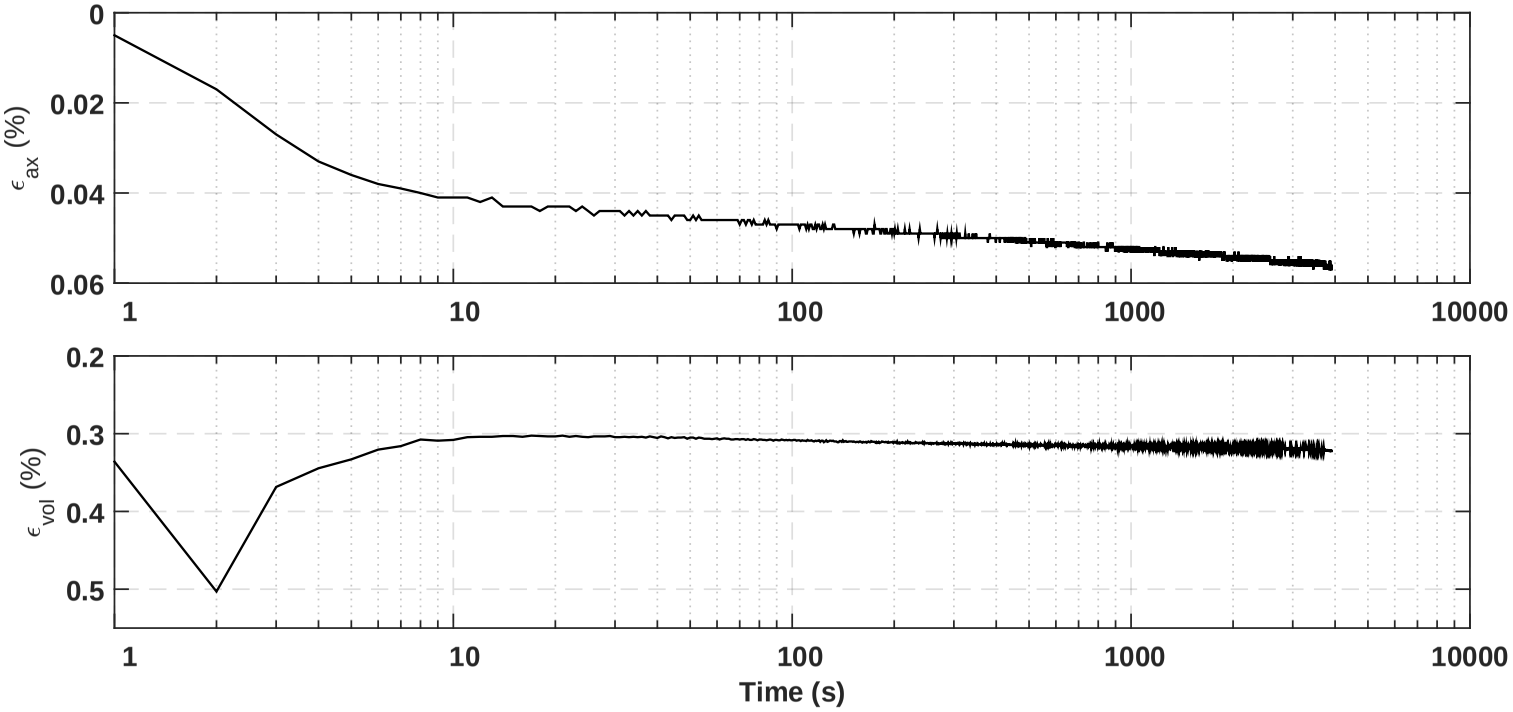

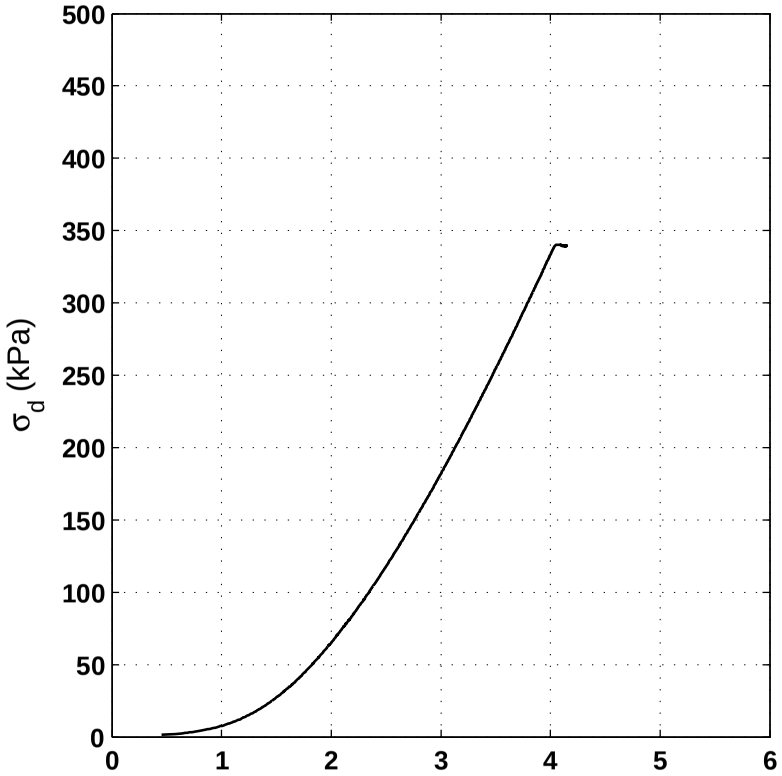

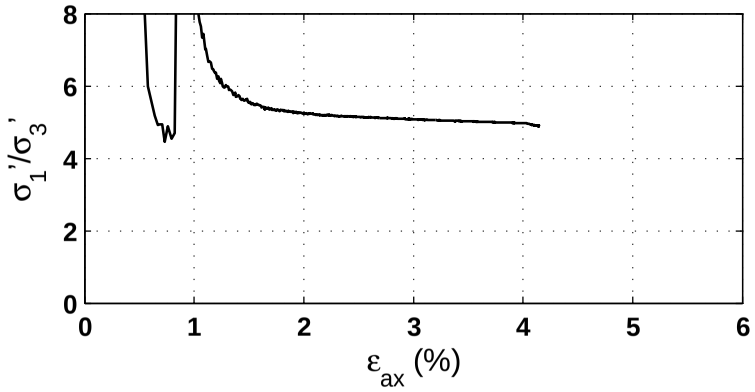

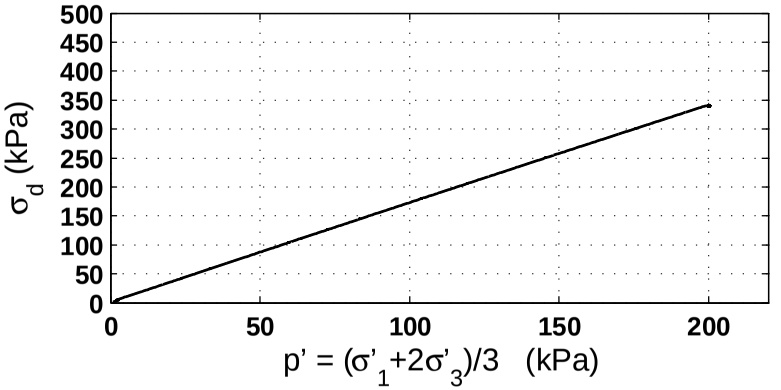

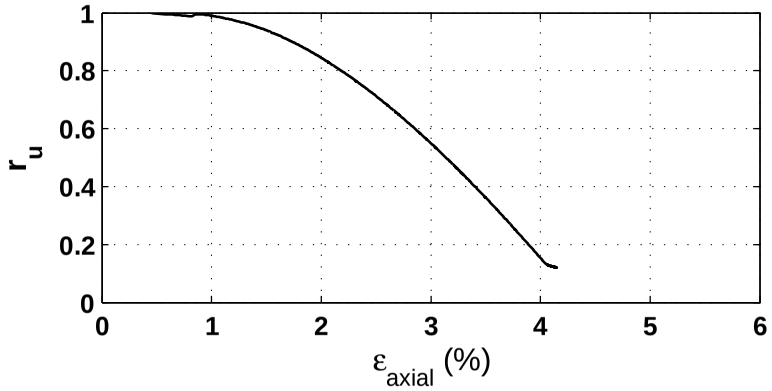

Post CTX Monotonic Comp. Test

Site:	90 Arm. St	**Rate (kPa/min):**	20
Borehole:	DM BH2		
Sample No.:	1U		
Sampler Type:	D&M		
Spec. Depth (m):	7.44		
Date Tested:	06/21/14		
Date Sampled:	06/13/14		

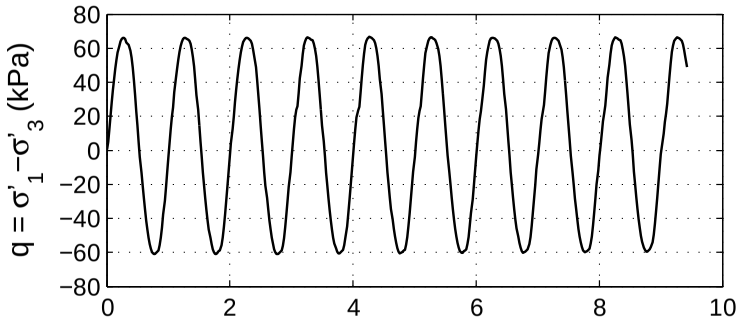

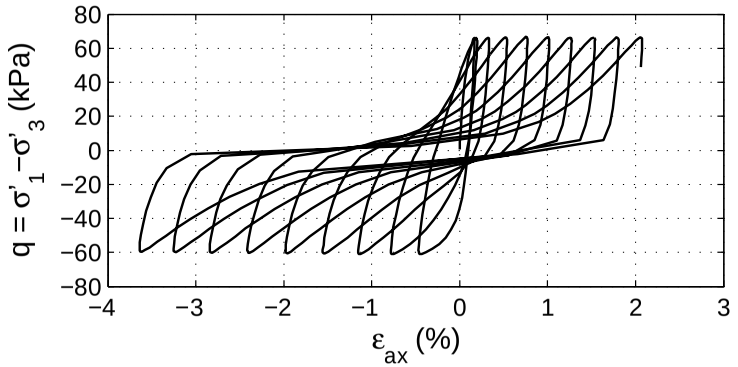

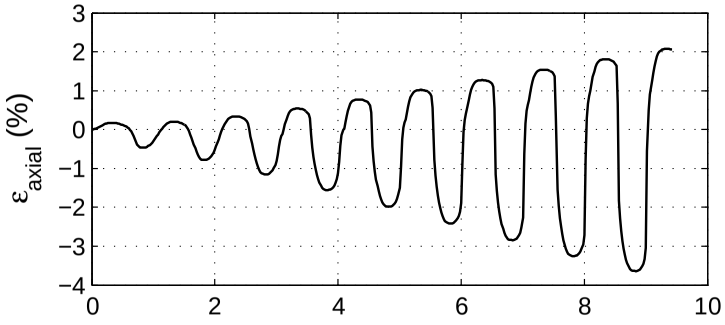

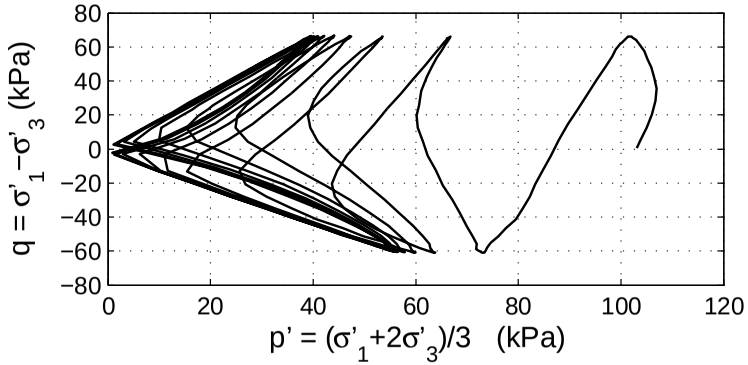

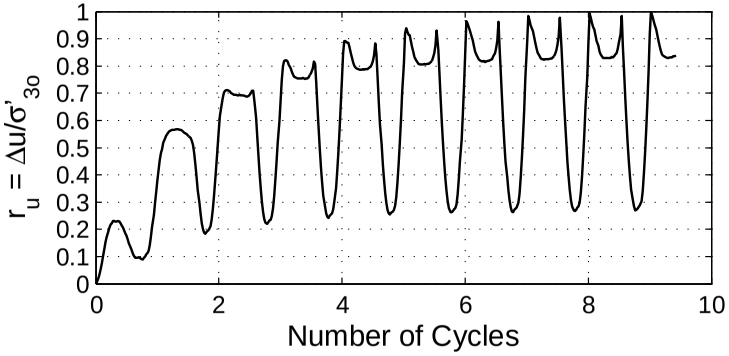

Specimen & Isotropic Cyclic Triaxial Test Data

Site:	90 Arm. St	**Loading Freq (Hz):**	0.1
Borehole:	DM BH2	**B−Value:**	0.984
Sample No.:	2U	**CSR:**	0.307
Sampler Type:	D&M	**N to $\varepsilon_{Ax-S.A.}$=3%:**	8
Spec. Depth (m):	7.77	**N to $\varepsilon_{Ax-D.A.}$=5%:**	8.5
Date Tested:	06/21/14	**Post−Cyclic Test:**	Reconsol.
Date Sampled:	06/13/14		
Spec. Ht. (mm):	139.4		
Spec. Diam. (mm):	60.9		
Dry Mass (g):	622.68		
Gs:	2.7		
e_o:	0.76		
σ'_{3o} (kPa):	103.0		
PI (%):	NP		
USCS:	SP		

Isotropic Consolidation Test

Site:	90 Arm. St
Borehole:	DM BH2
Sample No.:	2U
Sampler Type:	D&M
Spec. Depth (m):	7.77
Date Tested:	06/21/14
Date Sampled:	06/13/14

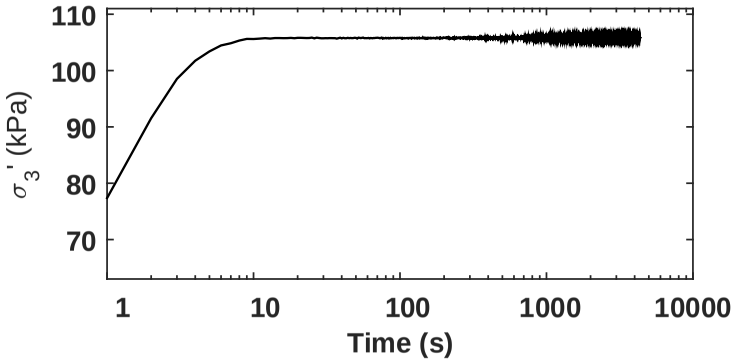

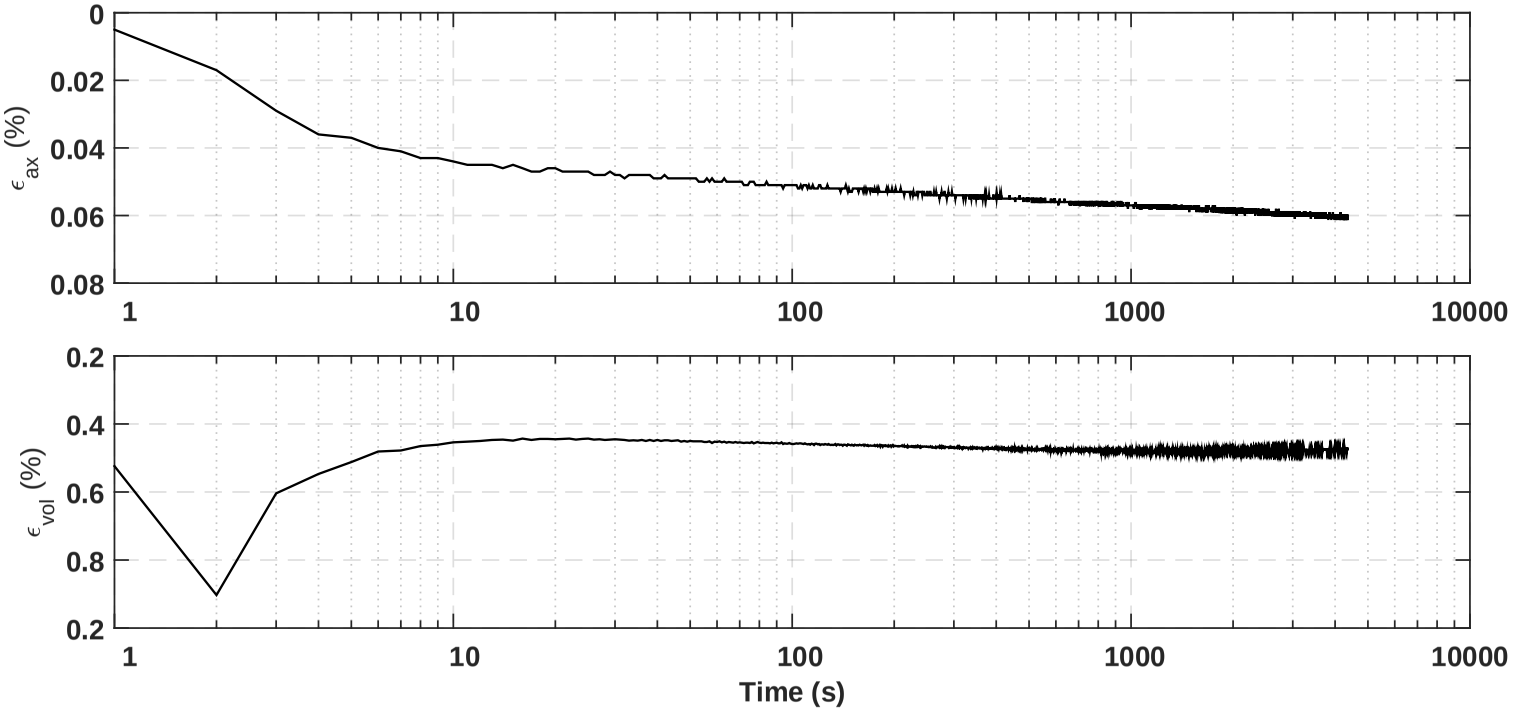

Post CTX Reconsolidation Test

Site:	90 Arm. St
Borehole:	DM BH2
Sample No.:	2U
Sampler Type:	D&M
Spec. Depth (m):	7.77
Date Tested:	06/21/14
Date Sampled:	06/13/14

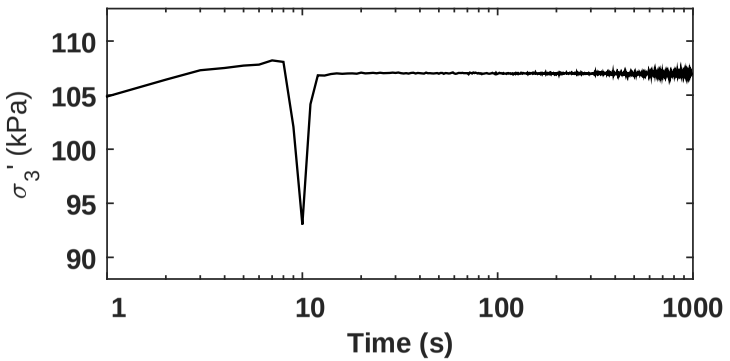

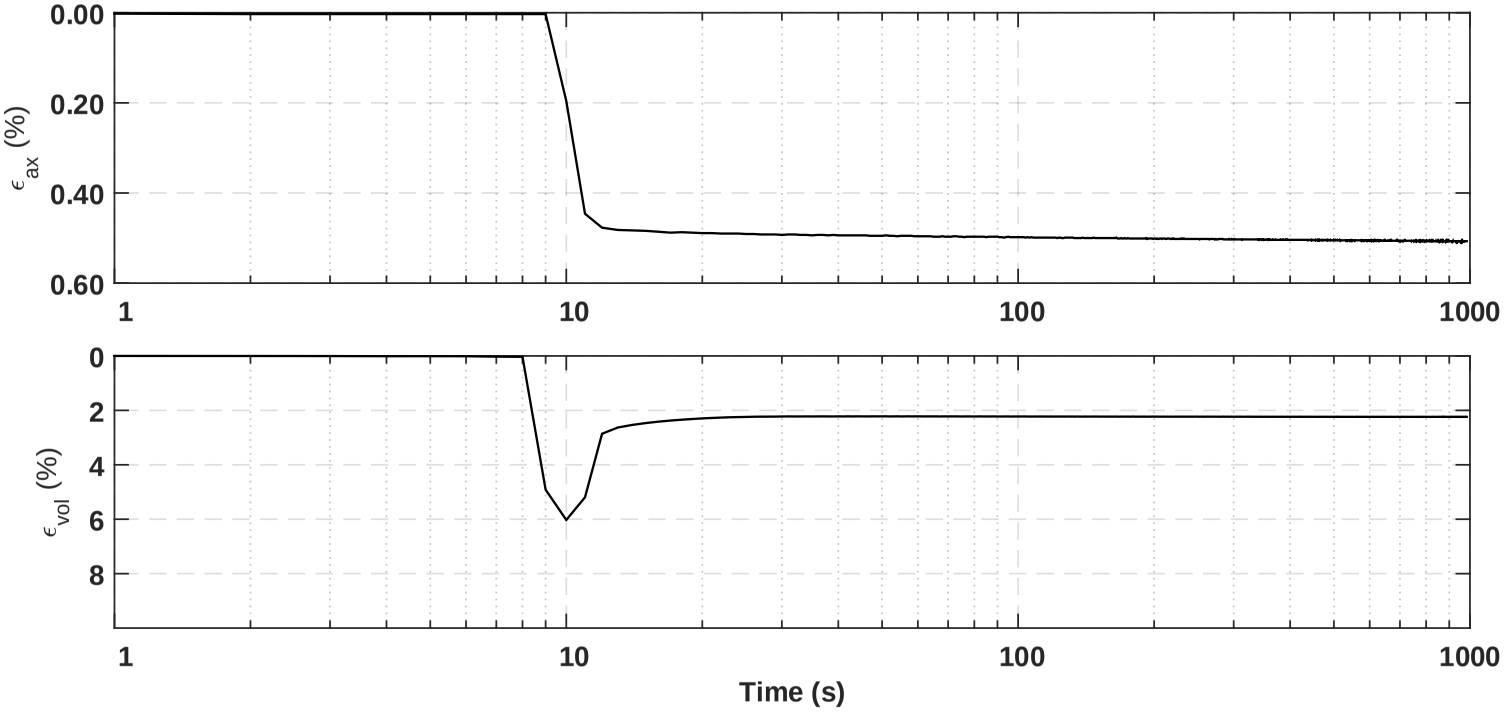

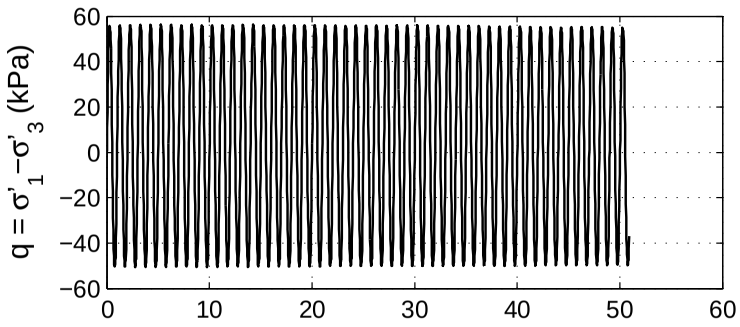

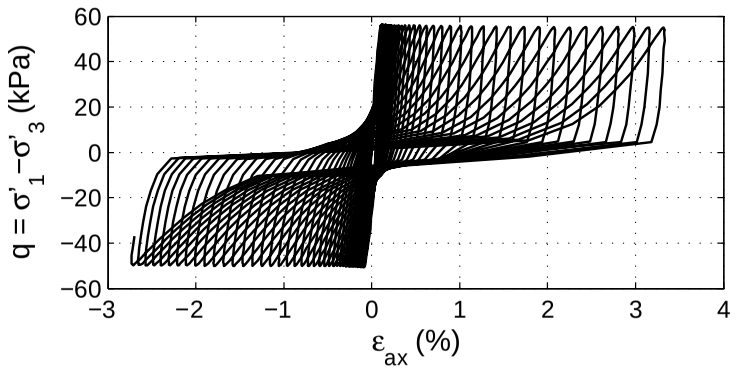

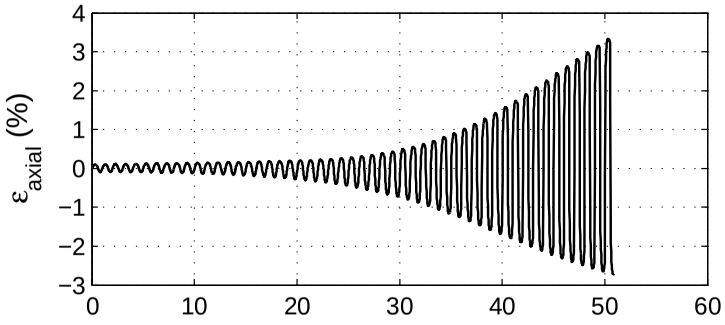

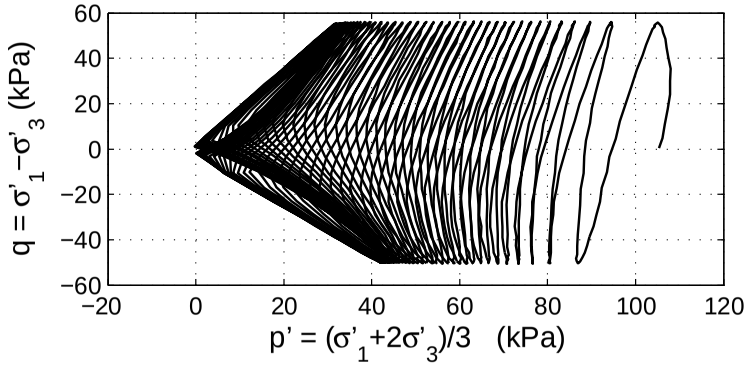

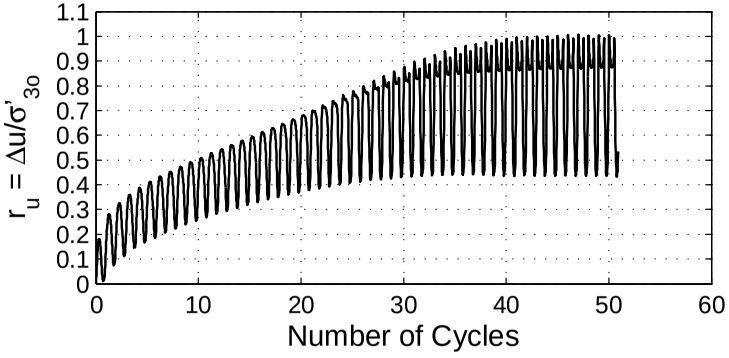

Specimen & Isotropic Cyclic Triaxial Test Data

Site:	90 Arm. St	**Loading Freq (Hz):**	0.1
Borehole:	DM BH2	**B−Value:**	0.986
Sample No.:	2U	**CSR:**	0.251
Sampler Type:	D&M	**N to $\varepsilon_{Ax-S.A.}$=3%:**	49.5
Spec. Depth (m):	7.92	**N to $\varepsilon_{Ax-D.A.}$=5%:**	47
Date Tested:	06/22/14	**Post−Cyclic Test:**	Reconsol.
Date Sampled:	06/13/14		
Spec. Ht. (mm):	139.3		
Spec. Diam. (mm):	60.9		
Dry Mass (g):	630.13		
Gs:	2.69		
e_o:	0.73		
σ'_{3o} (kPa):	105.2		
PI (%):	NP		
USCS:	SP		

Isotropic Consolidation Test

Site:	90 Arm. St
Borehole:	DM BH2
Sample No.:	2U
Sampler Type:	D&M
Spec. Depth (m):	7.92
Date Tested:	06/22/14
Date Sampled:	06/13/14

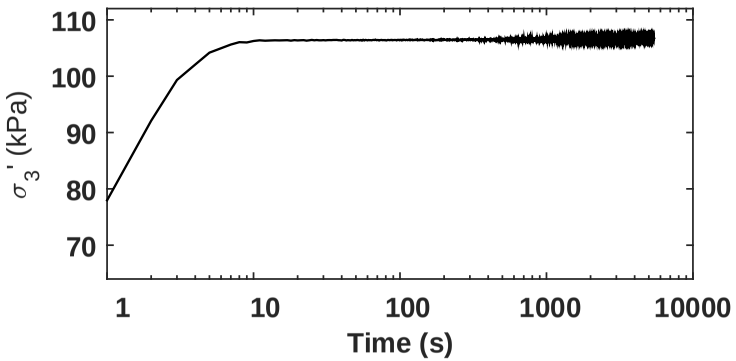

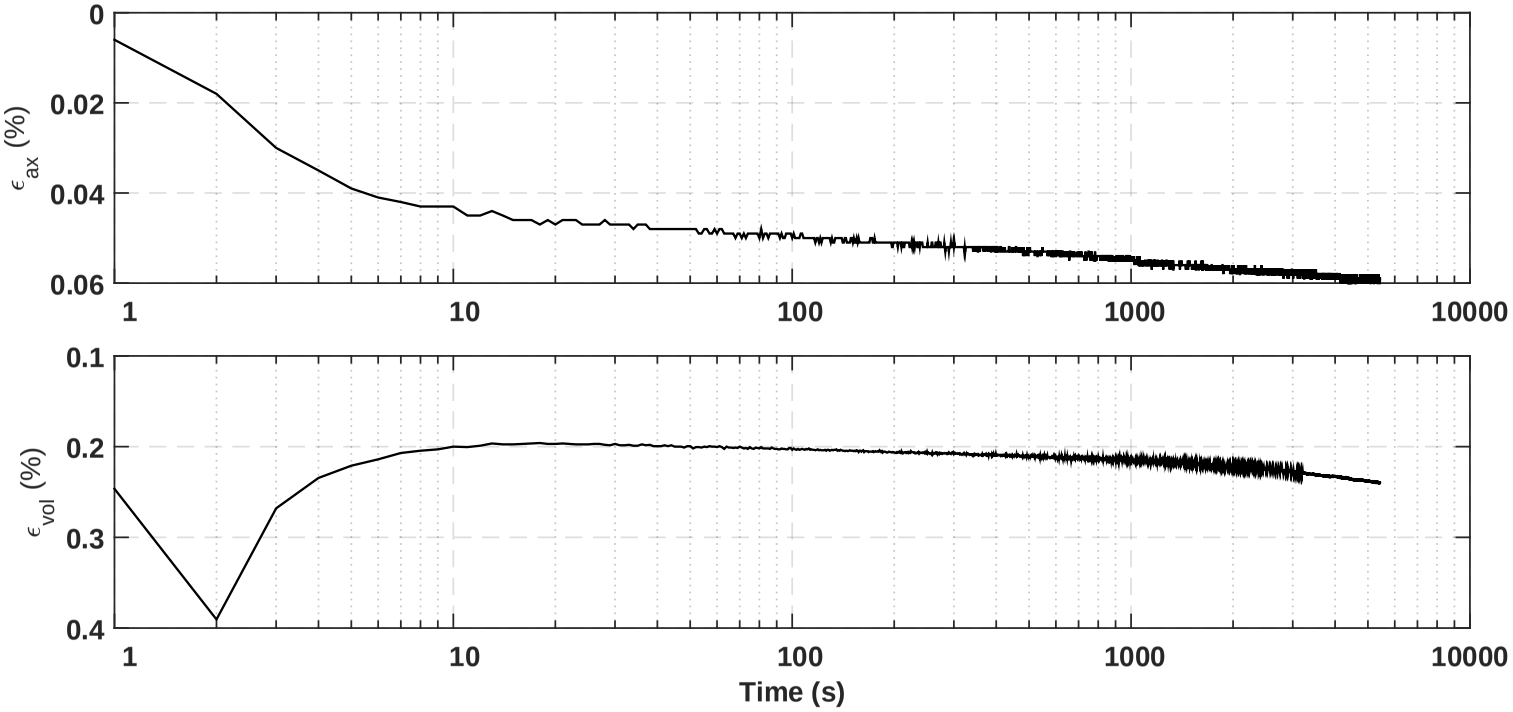

Post CTX Reconsolidation Test

Site:	90 Arm. St
Borehole:	DM BH2
Sample No.:	2U
Sampler Type:	D&M
Spec. Depth (m):	7.92
Date Tested:	06/22/14
Date Sampled:	06/13/14

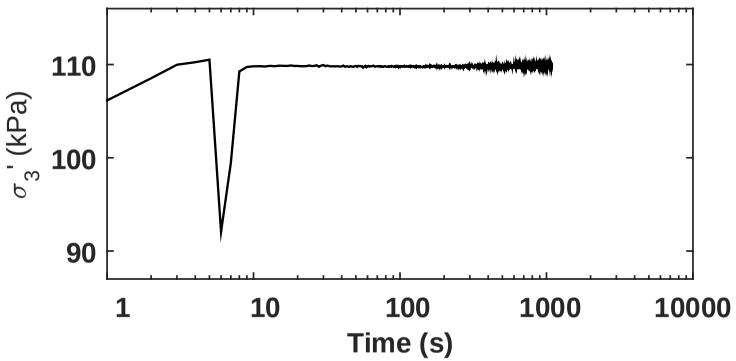

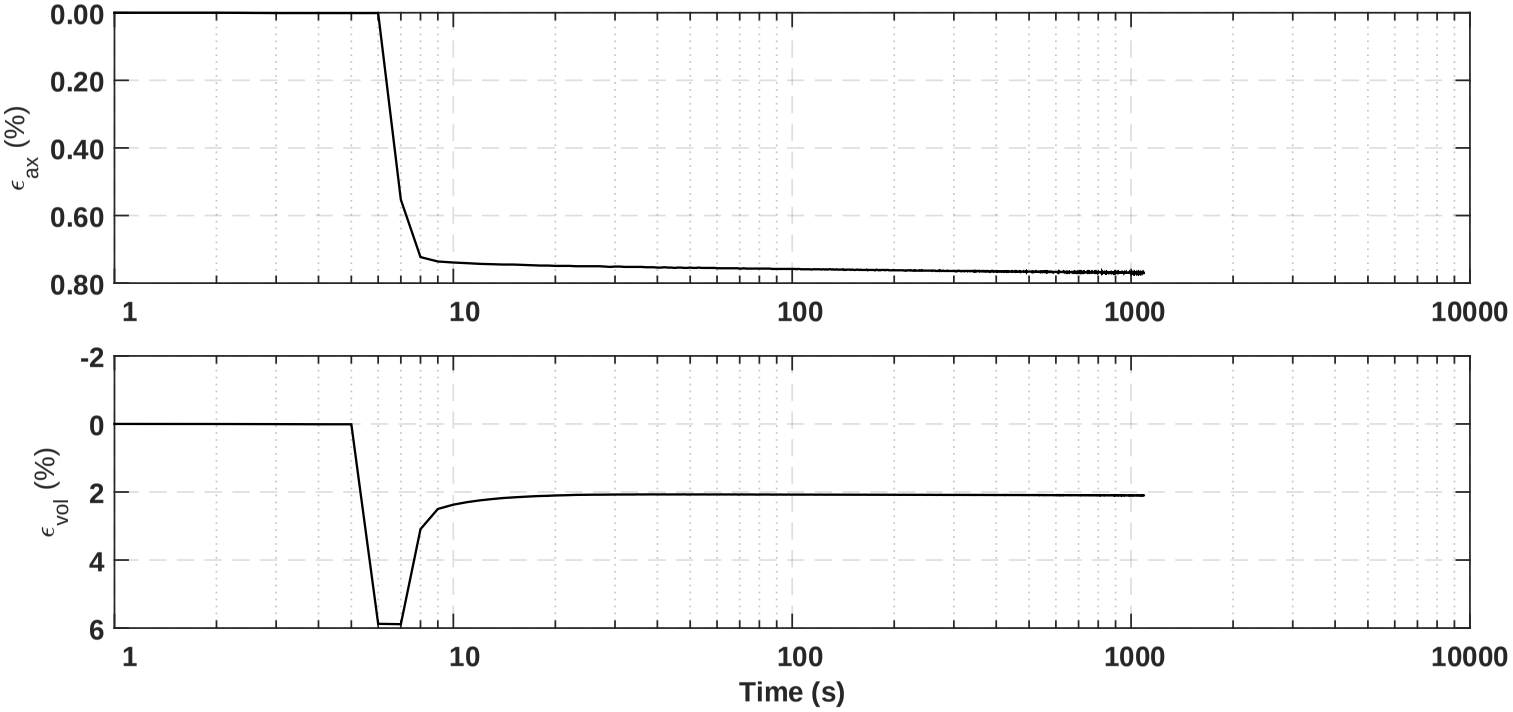

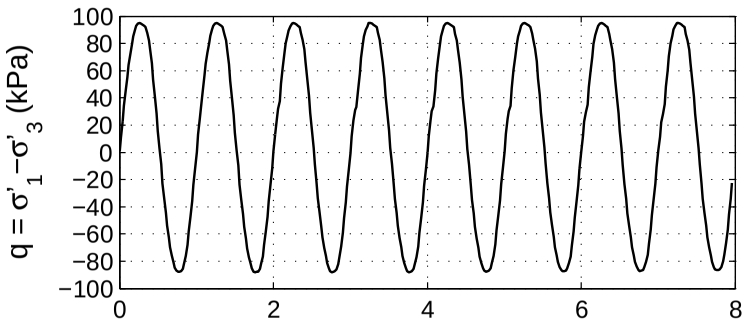

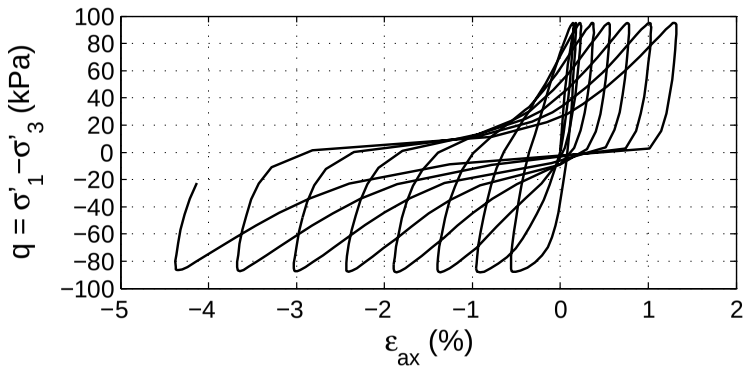

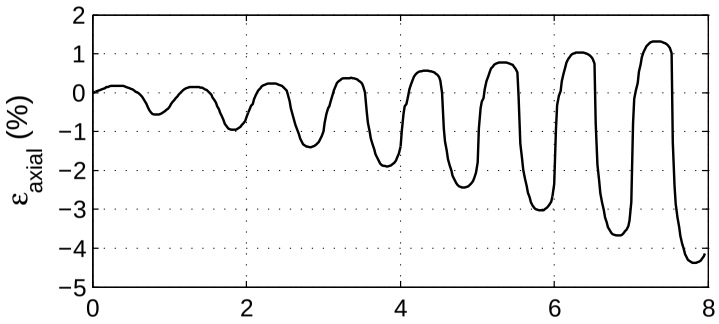

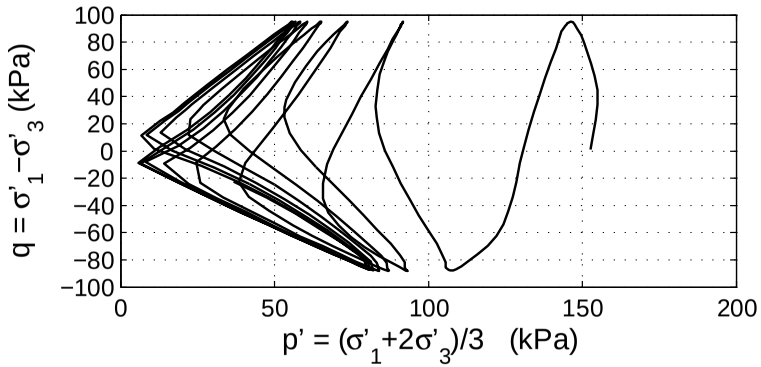

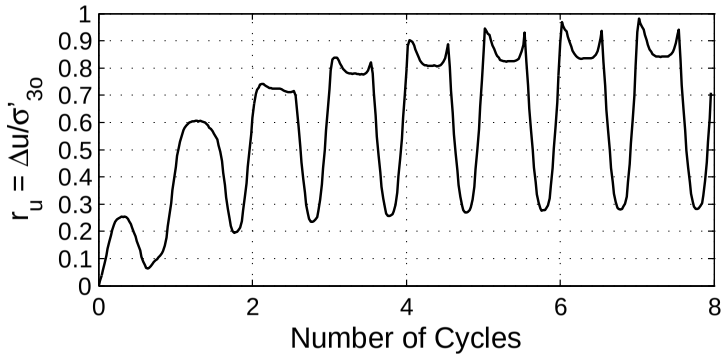

Specimen & Isotropic Cyclic Triaxial Test Data

Site:	90 Arm. St	**Loading Freq (Hz):**	0.1
Borehole:	DM BH2	**B−Value:**	0.984
Sample No.:	5U	**CSR:**	0.298
Sampler Type:	D&M	**N to $\varepsilon_{Ax-S.A.}$=3%:**	6
Spec. Depth (m):	11.32	**N to $\varepsilon_{Ax-D.A.}$=5%:**	8
Date Tested:	06/22/14	**Post−Cyclic Test:**	Reconsol.
Date Sampled:	06/13/14		
Spec. Ht. (mm):	138.2		
Spec. Diam. (mm):	60.8		
Dry Mass (g):	595.99		
Gs:	2.66		
e_o:	0.79		
σ'_{3o} (kPa):	152.4		
PI (%):	NP		
USCS:	SP−SM		

Isotropic Consolidation Test

Site:	90 Arm. St
Borehole:	DM BH2
Sample No.:	5U
Sampler Type:	D&M
Spec. Depth (m):	11.32
Date Tested:	06/22/14
Date Sampled:	06/13/14

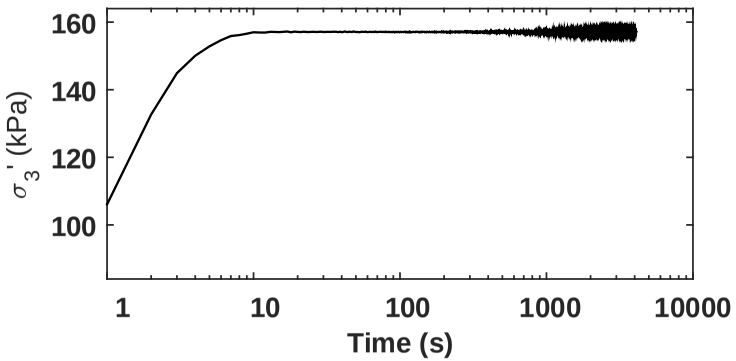

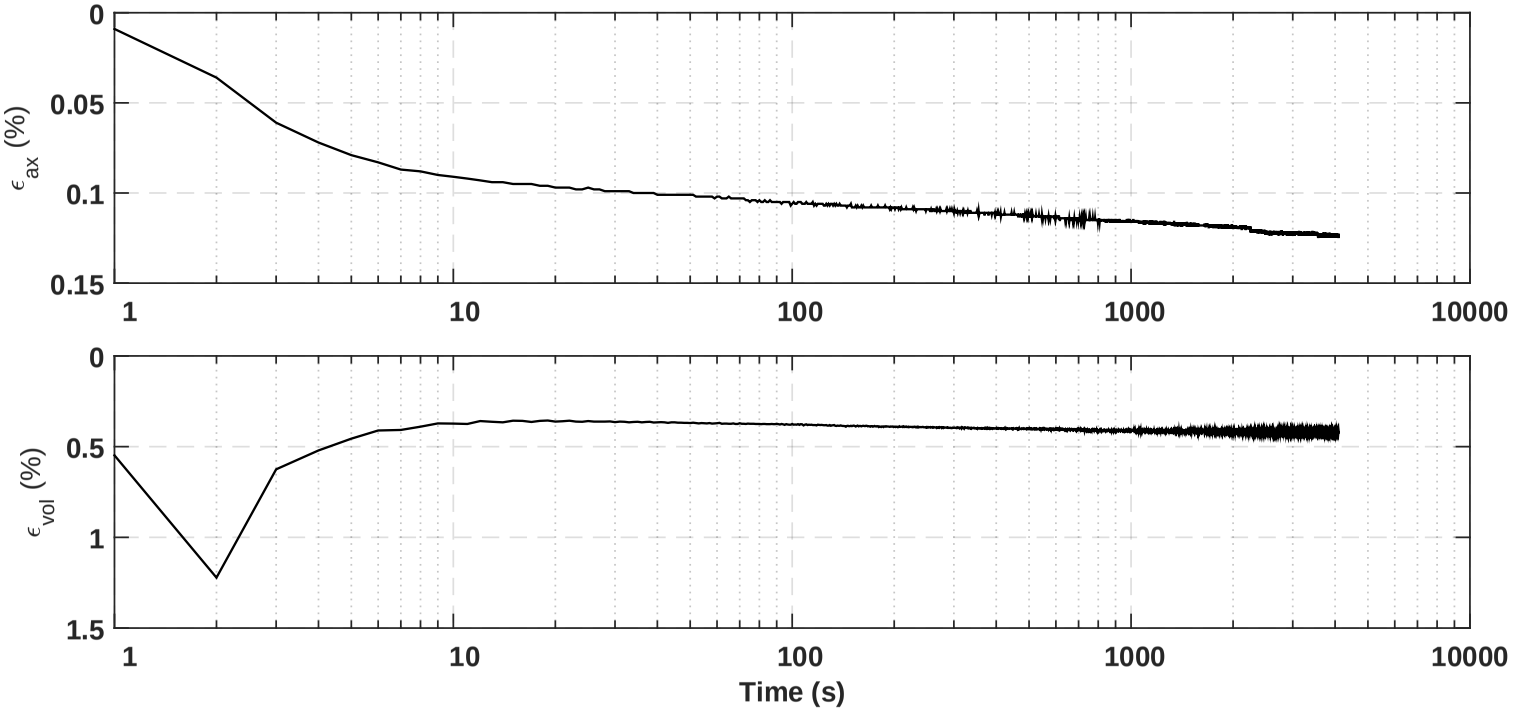

Post CTX Reconsolidation Test

Site:	90 Arm. St
Borehole:	DM BH2
Sample No.:	5U
Sampler Type:	D&M
Spec. Depth (m):	11.32
Date Tested:	06/22/14
Date Sampled:	06/13/14

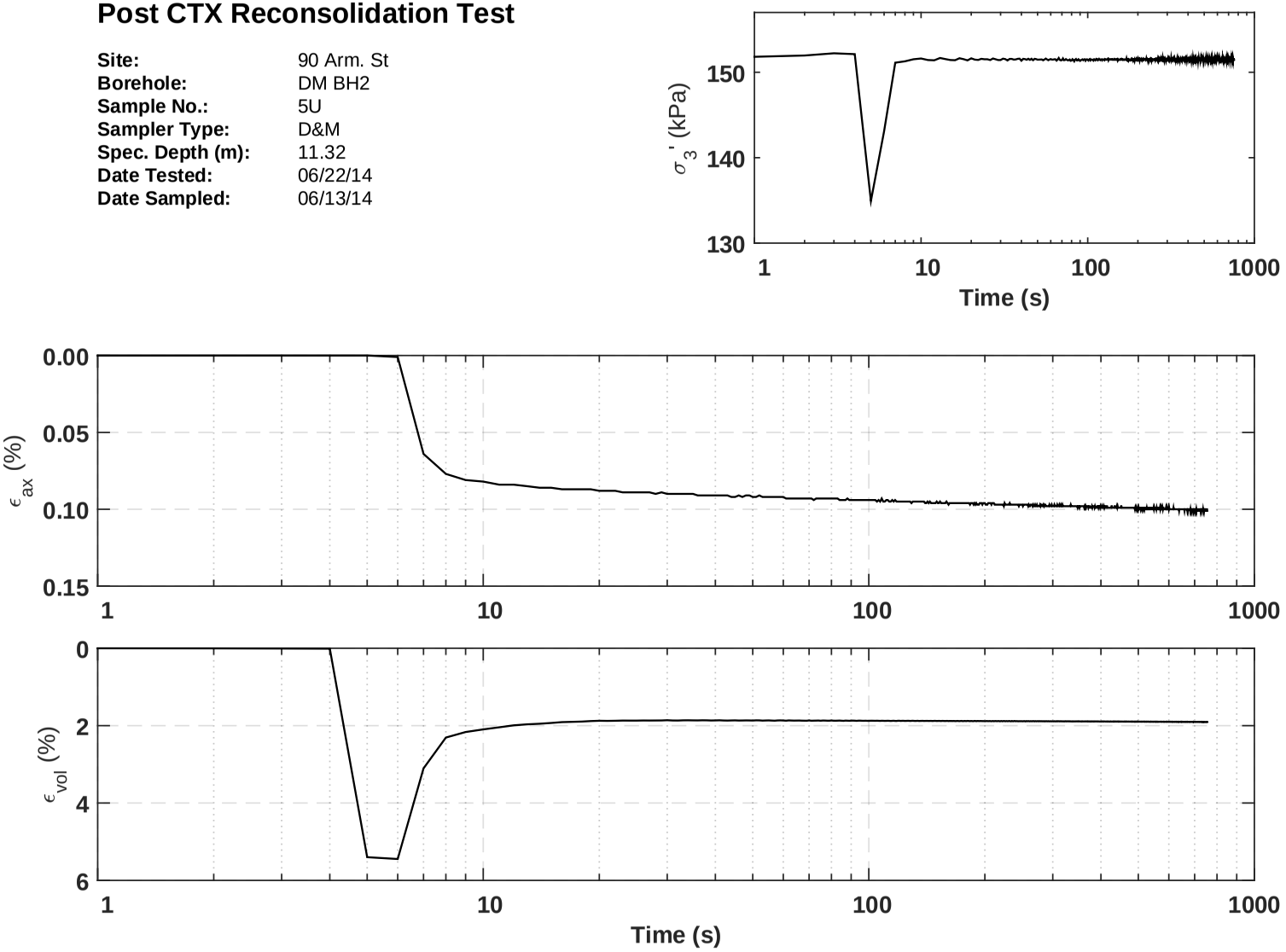

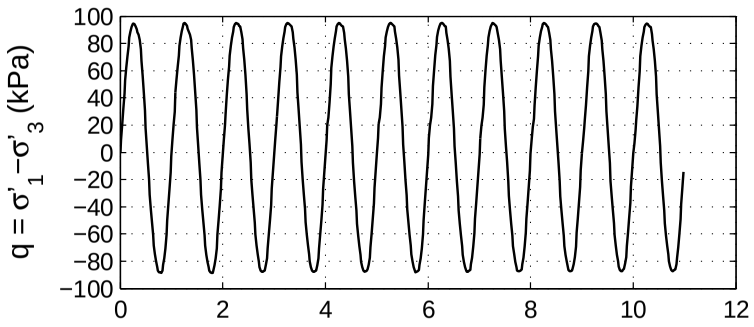

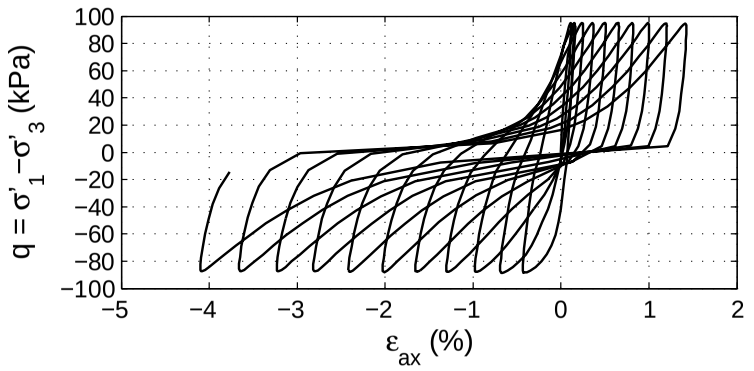

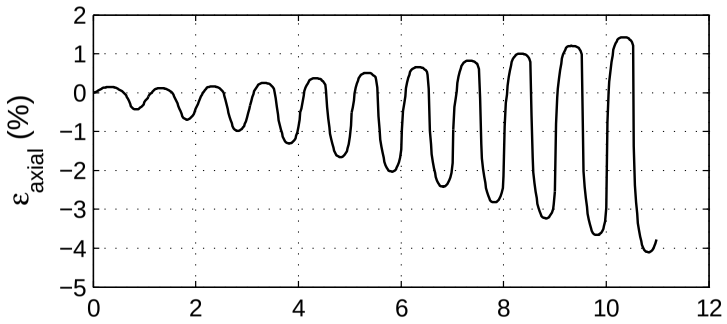

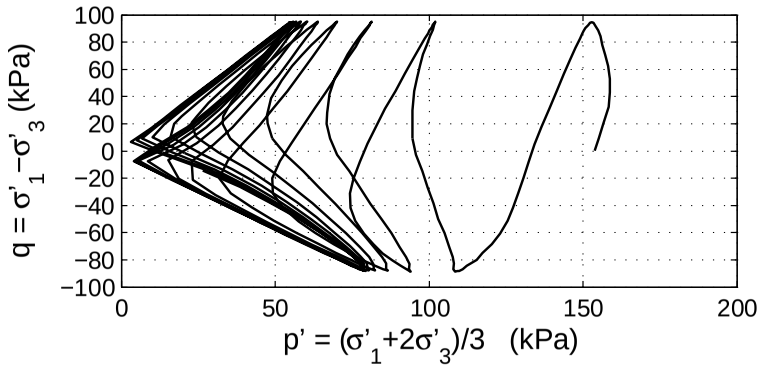

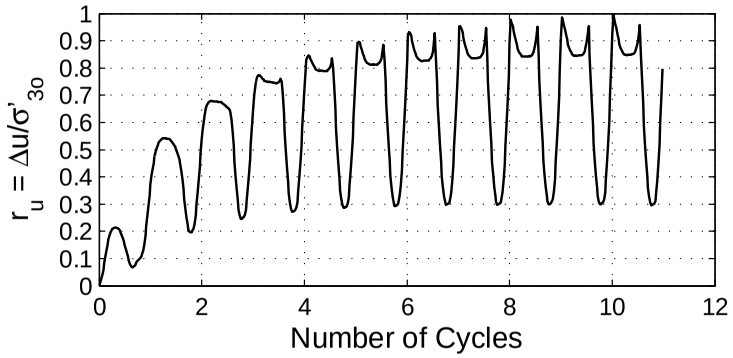

Specimen & Isotropic Cyclic Triaxial Test Data

Site:	90 Arm. St	**Loading Freq (Hz):**	0.1
Borehole:	DM BH2	**B−Value:**	0.983
Sample No.:	10U	**CSR:**	0.296
Sampler Type:	D&M	**N to $\varepsilon_{Ax-S.A.}$=3%:**	9
Spec. Depth (m):	13.77	**N to $\varepsilon_{Ax-D.A.}$=5%:**	10.5
Date Tested:	06/23/14	**Post−Cyclic Test:**	Monotonic
Date Sampled:	06/16/14		
Spec. Ht. (mm):	140.0		
Spec. Diam. (mm):	60.8		
Dry Mass (g):	631.08		
Gs:	2.69		
e_o:	0.73		
σ'_{3o} (kPa):	153.6		
PI (%):	NP		
USCS:	SP−SM		

Isotropic Consolidation Test

Site:	90 Arm. St
Borehole:	DM BH2
Sample No.:	10U
Sampler Type:	D&M
Spec. Depth (m):	13.77
Date Tested:	06/23/14
Date Sampled:	06/16/14

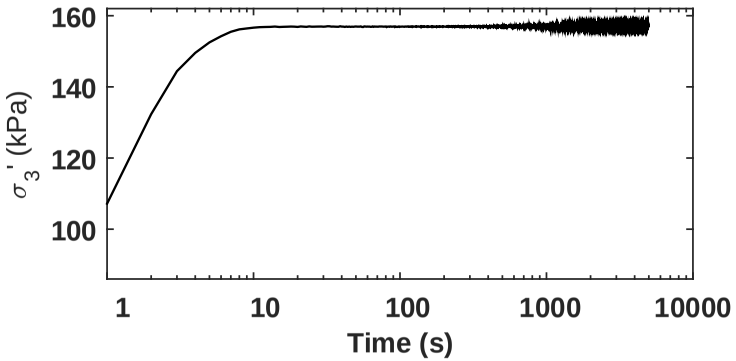

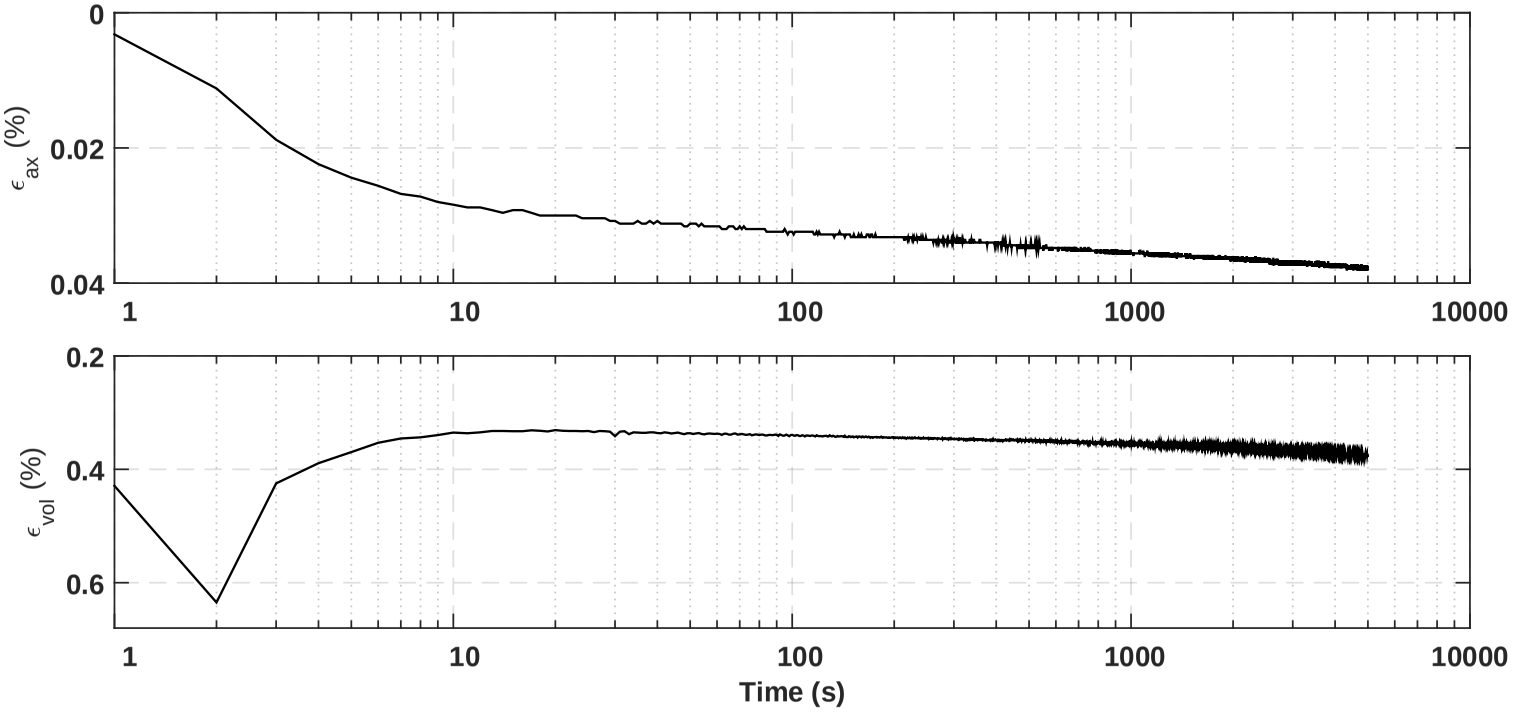

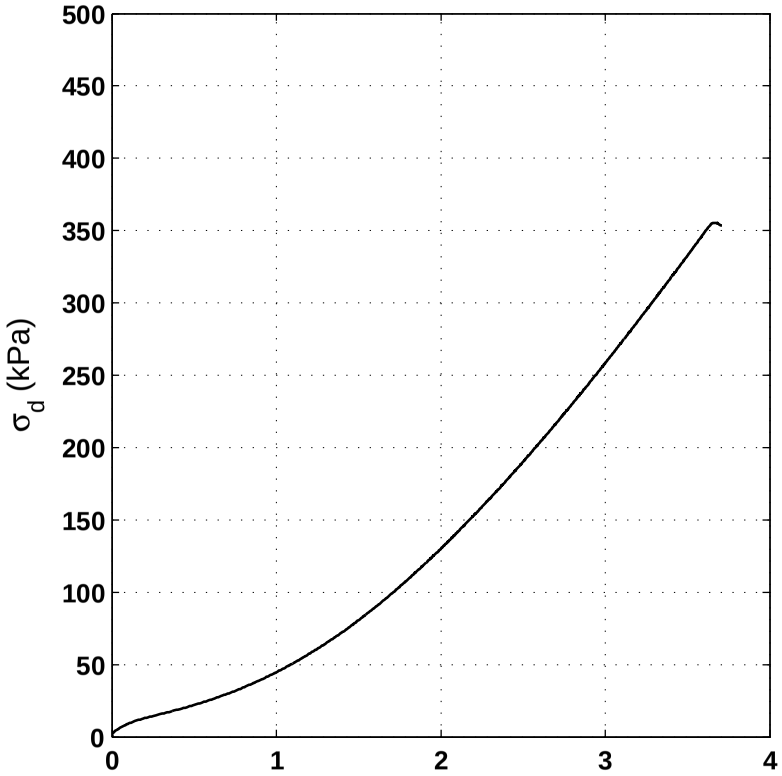

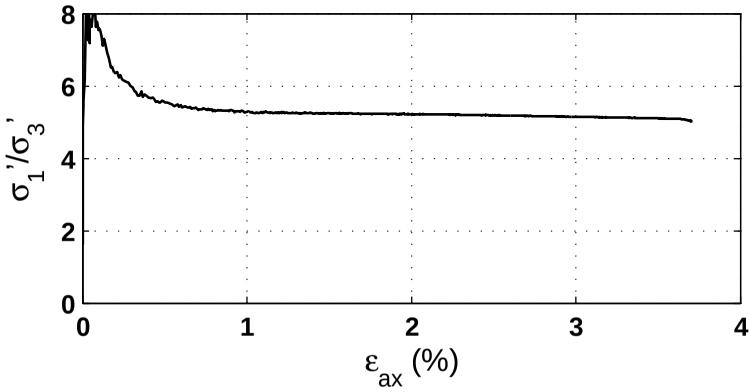

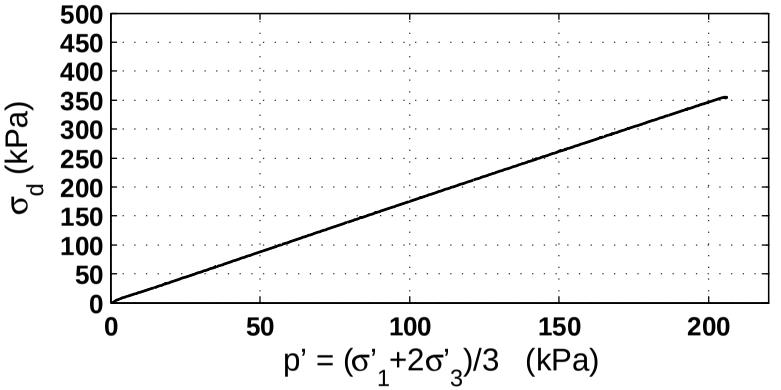

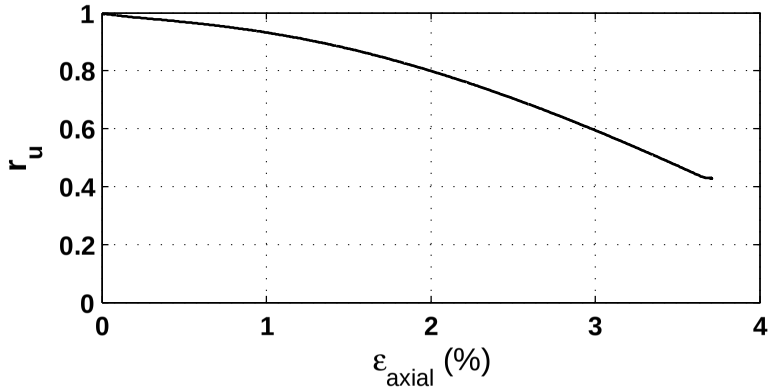

Post CTX Monotonic Comp. Test

Site:	90 Arm. St	**Rate (kPa/min):**	20
Borehole:	DM BH2		
Sample No.:	10U		
Sampler Type:	D&M		
Spec. Depth (m):	13.77		
Date Tested:	06/23/14		
Date Sampled:	06/16/14		

Appendix C.2.6

LS-II Building Site—48 Lismore St.

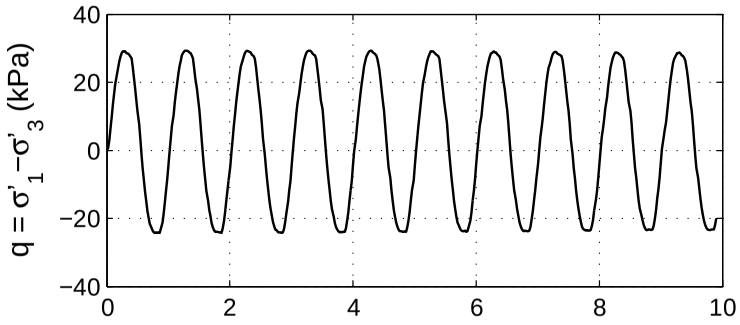

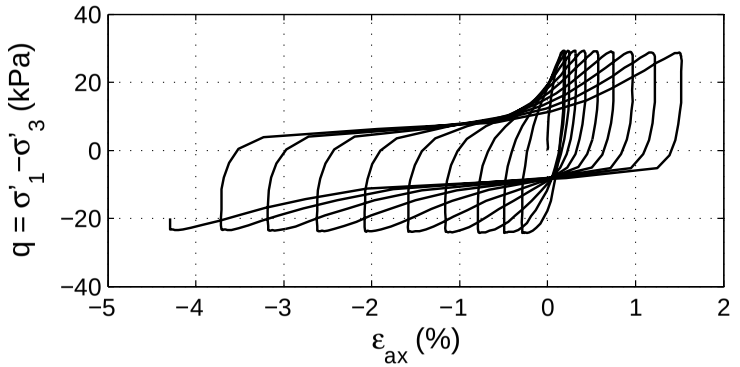

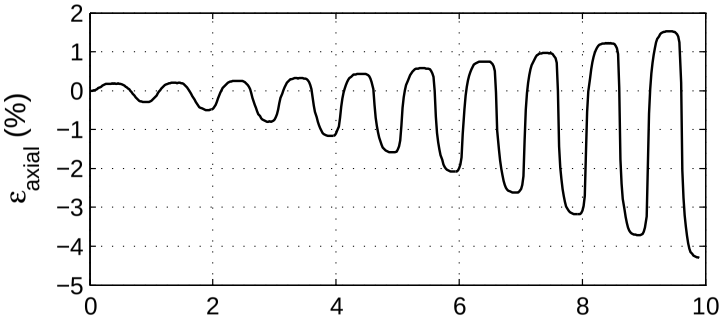

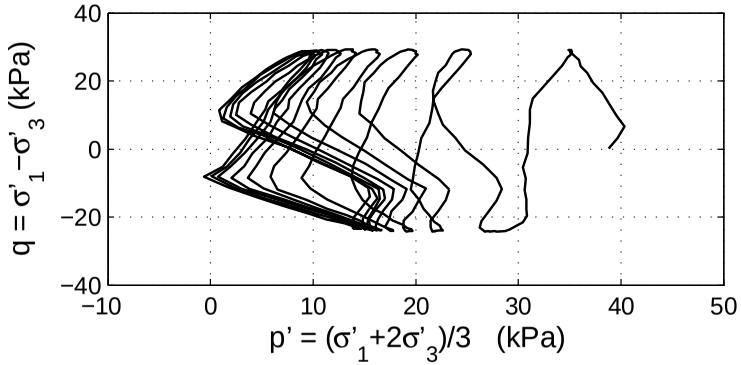

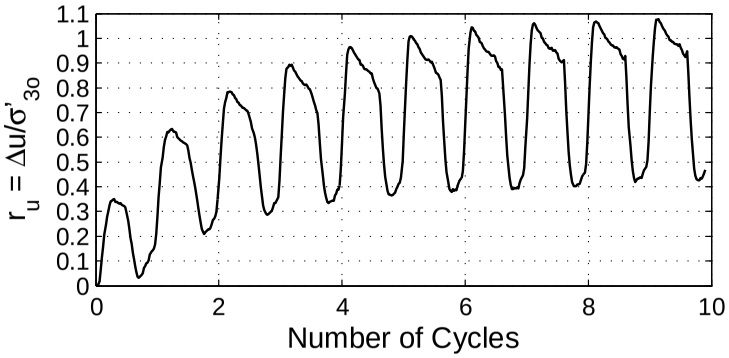

Specimen & Isotropic Cyclic Triaxial Test Data

Site:	48 Lis. St	**Loading Freq (Hz):**	0.1
Borehole:	DM BH1	**B−Value:**	0.987
Sample No.:	1U	**CSR:**	0.342
Sampler Type:	D&M	**N to $\varepsilon_{Ax-S.A.}$=3%:**	8
Spec. Depth (m):	1.82	**N to $\varepsilon_{Ax-D.A.}$=5%:**	9.5
Date Tested:	10/05/14	**Post−Cyclic Test:**	Reconsol.
Date Sampled:	09/29/14		
Spec. Ht. (mm):	136.6		
Spec. Diam. (mm):	60.7		
Dry Mass (g):	581.52		
Gs:	2.71		
e_o:	0.84		
σ'_{3o} (kPa):	38.8		
PI (%):	NP		
USCS:	ML		

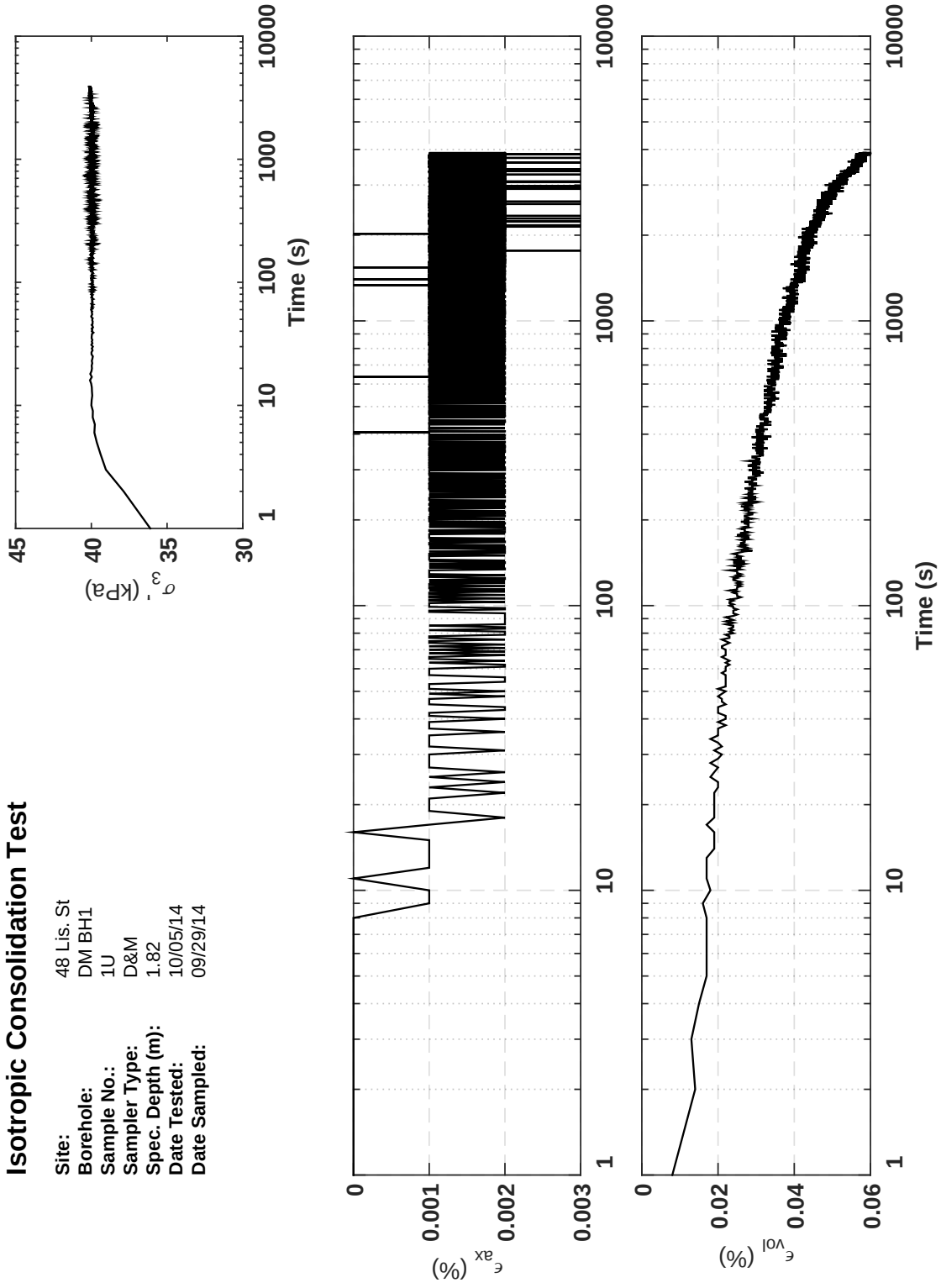
Isotropic Consolidation Test
Site: 48 Lis. St
Borehole: DM BH1
Sample No.: 1U
Sampler Type: D&M
Spec. Depth (m): 1.82
Date Tested: 10/05/14
Date Sampled: 09/29/14
σ3' (kPa)
45
40
35
30
1
10
100
1000
10000
Time (s)
εax (%)
0
0.001
0.002
0.003
εvol (%)
0.02
0.04
0.06

Post CTX Reconsolidation Test

Site:	48 Lis. St
Borehole:	DM BH1
Sample No.:	1U
Sampler Type:	D&M
Spec. Depth (m):	1.82
Date Tested:	10/05/14
Date Sampled:	09/29/14

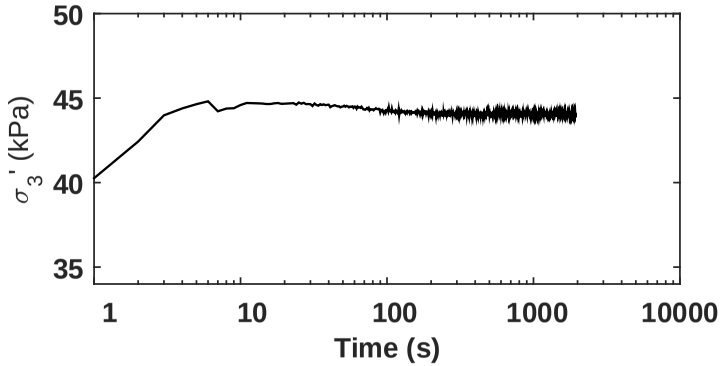

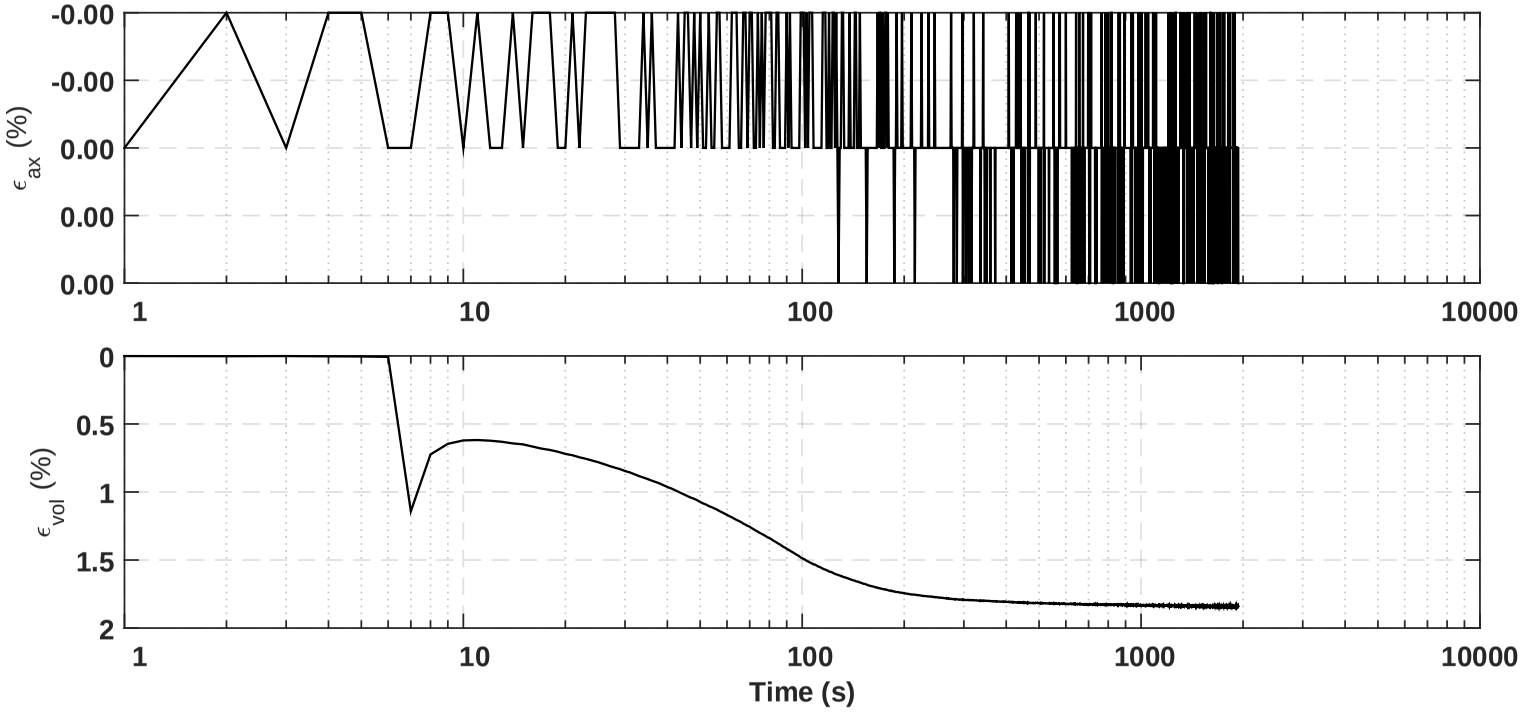

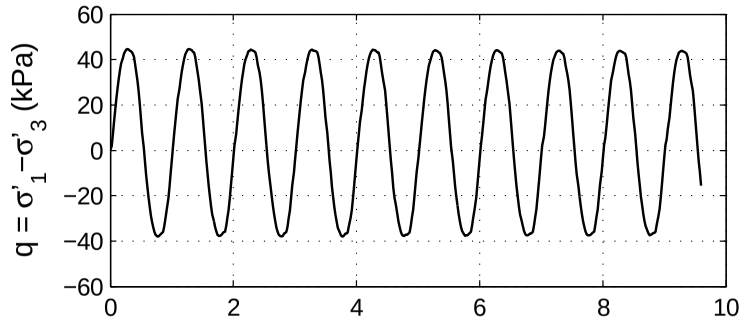

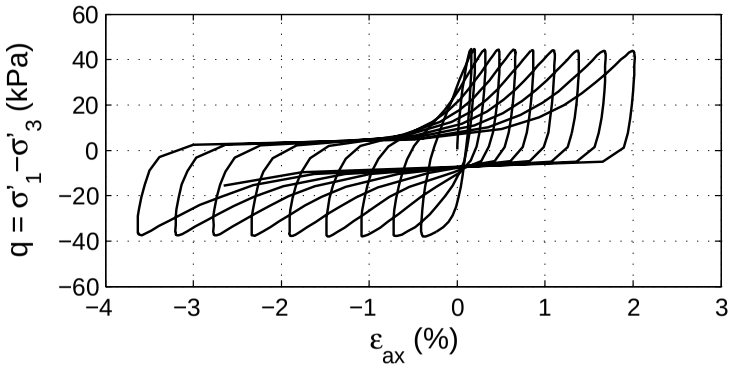

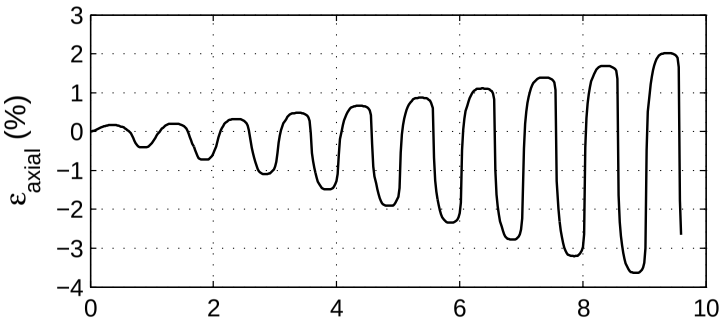

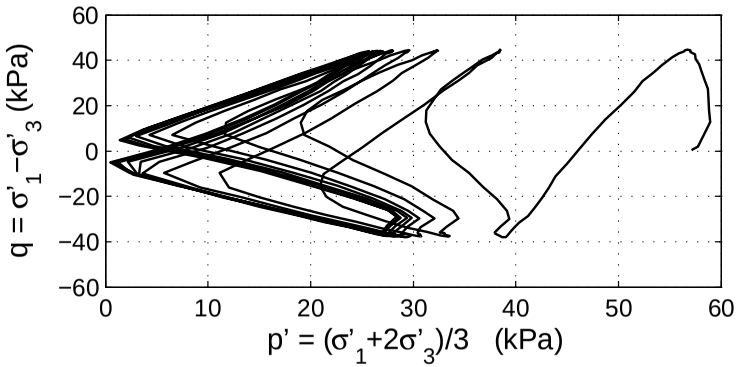

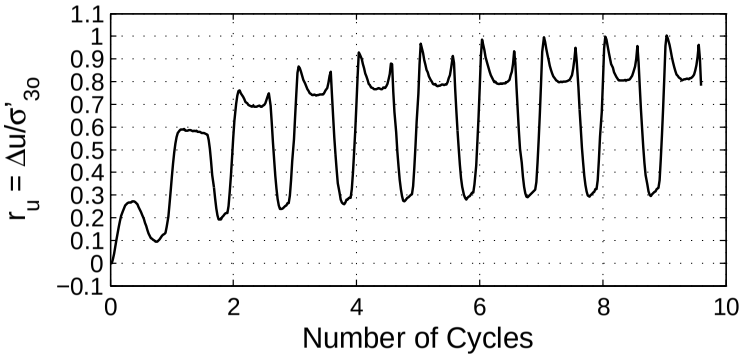

Specimen & Isotropic Cyclic Triaxial Test Data

Site:	48 Lis. St	**Loading Freq (Hz):**	0.1
Borehole:	DM BH1	**B−Value:**	0.970
Sample No.:	4U	**CSR:**	0.355
Sampler Type:	D&M	**N to $\varepsilon_{Ax-S.A.}$=3%:**	8
Spec. Depth (m):	4.27	**N to $\varepsilon_{Ax-D.A.}$=5%:**	9
Date Tested:	10/07/14	**Post−Cyclic Test:**	Reconsol.
Date Sampled:	09/29/14		
Spec. Ht. (mm):	137.3		
Spec. Diam. (mm):	60.8		
Dry Mass (g):	608.55		
Gs:	2.67		
e_o:	0.75		
σ'_{3o} (kPa):	57.0		
PI (%):	NP		
USCS:	SP−SM		

Isotropic Consolidation Test

Site:	48 Lis. St
Borehole:	DM BH1
Sample No.:	4U
Sampler Type:	D&M
Spec. Depth (m):	4.27
Date Tested:	10/07/14
Date Sampled:	09/29/14

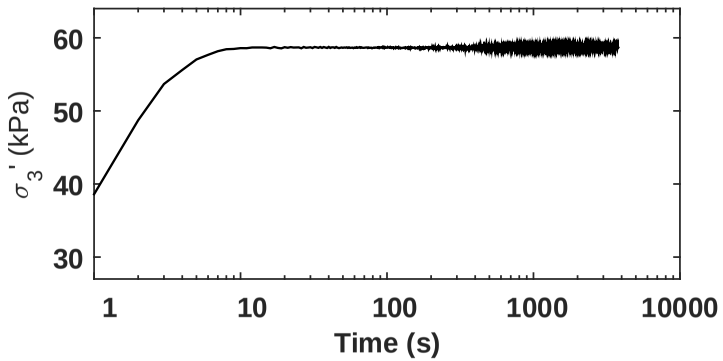

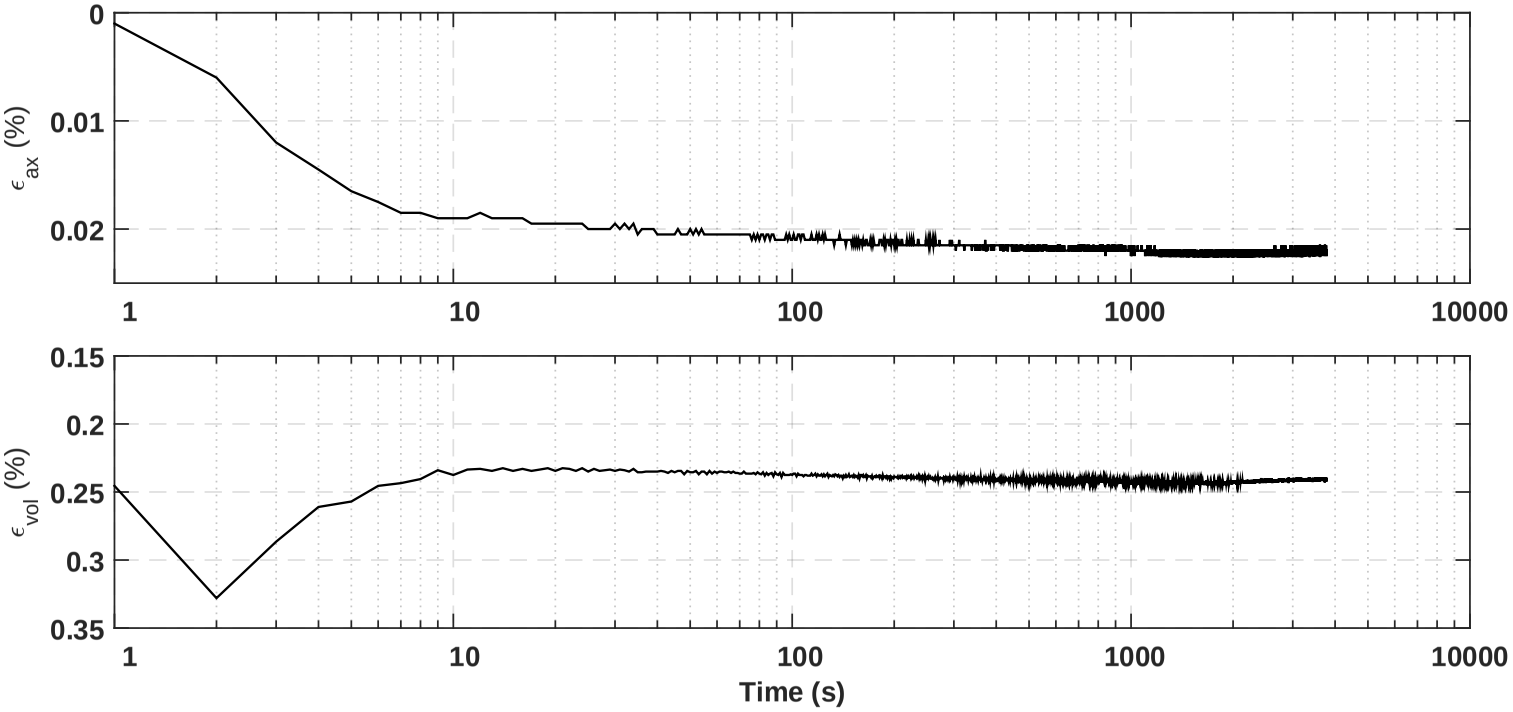

Post CTX Reconsolidation Test

Site:	48 Lis. St
Borehole:	DM BH1
Sample No.:	4U
Sampler Type:	D&M
Spec. Depth (m):	4.27
Date Tested:	10/07/14
Date Sampled:	09/29/14

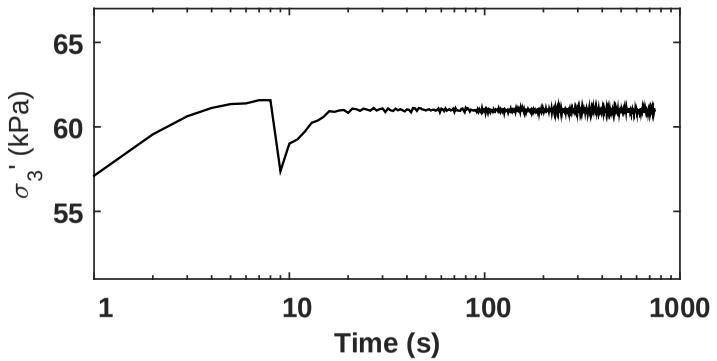

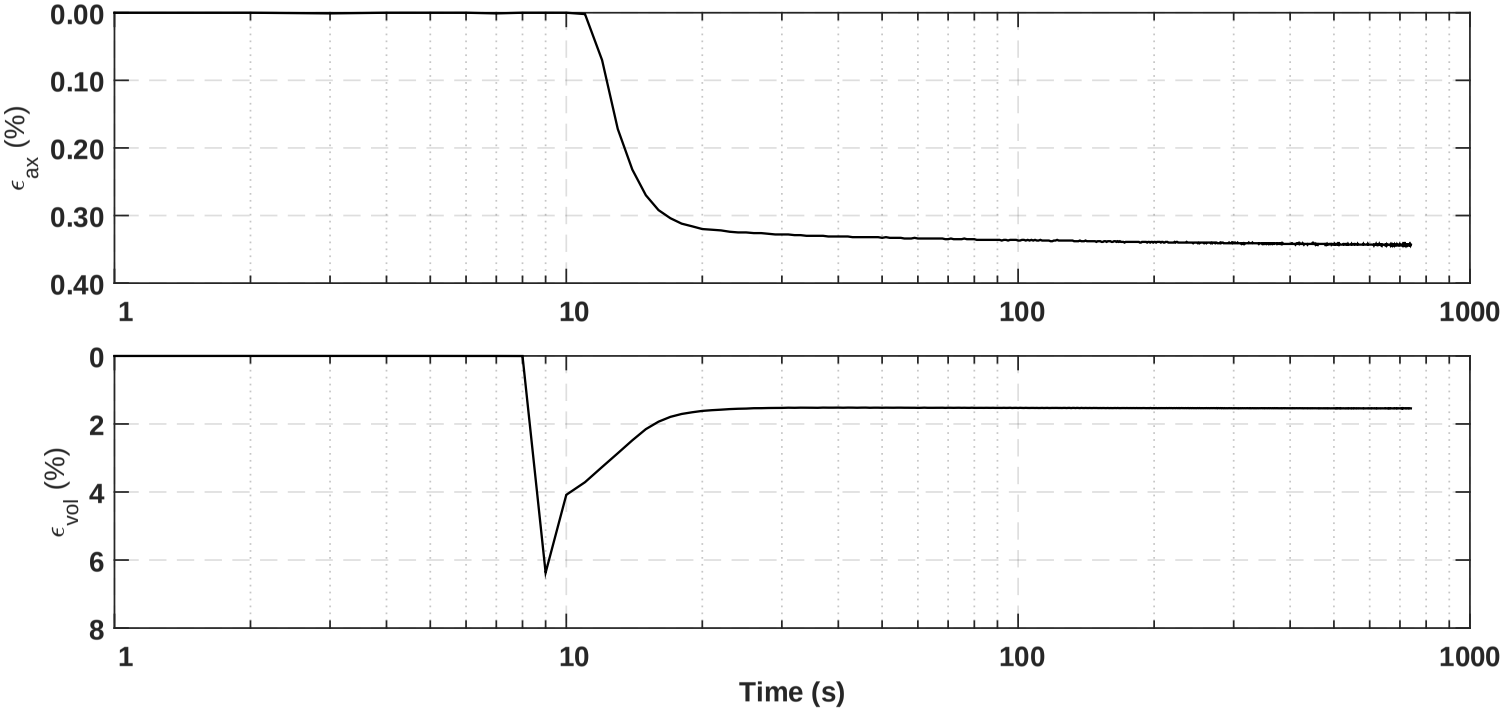

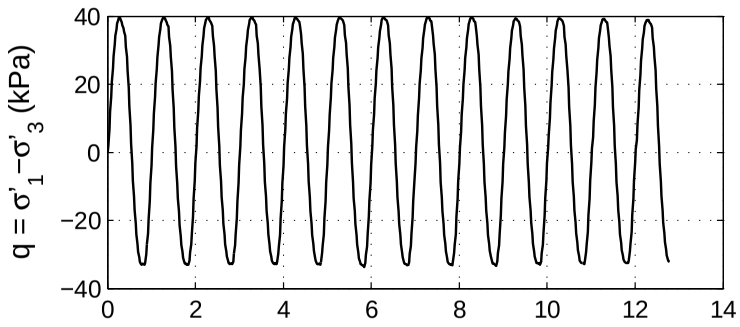

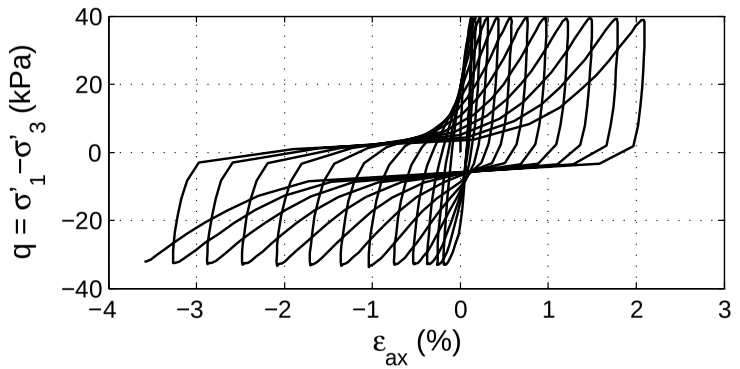

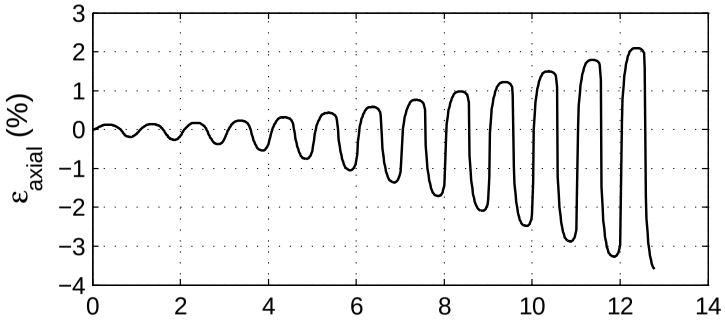

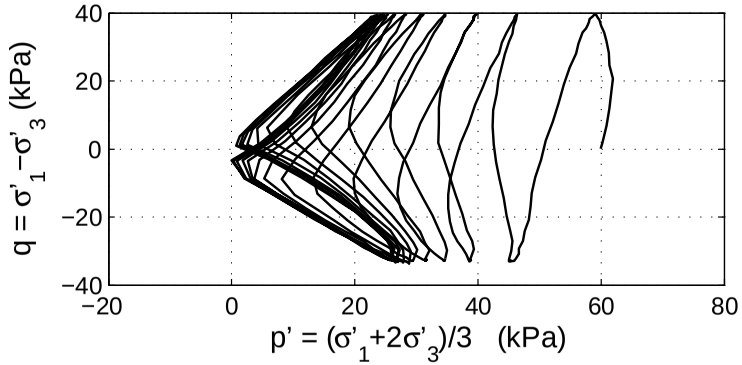

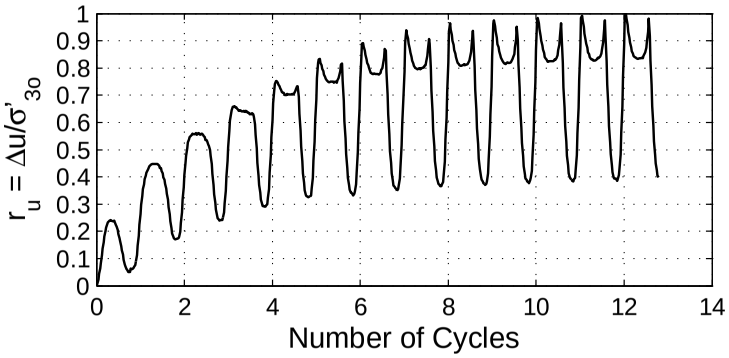

Specimen & Isotropic Cyclic Triaxial Test Data

Site:	48 Lis. St	**Loading Freq (Hz):**	0.1
Borehole:	DM BH1	**B−Value:**	0.971
Sample No.:	4U	**CSR:**	0.302
Sampler Type:	D&M	**N to $\varepsilon_{Ax-S.A.}$=3%:**	12
Spec. Depth (m):	4.42	**N to $\varepsilon_{Ax-D.A.}$=5%:**	12
Date Tested:	10/08/14	**Post−Cyclic Test:**	Monotonic
Date Sampled:	09/29/14		
Spec. Ht. (mm):	135.4		
Spec. Diam. (mm):	60.9		
Dry Mass (g):	613.40		
Gs:	2.67		
e_o:	0.71		
σ'_{3o} (kPa):	60.0		
PI (%):	NP		
USCS:	SM		

Isotropic Consolidation Test

Site:	48 Lis. St
Borehole:	DM BH1
Sample No.:	4U
Sampler Type:	D&M
Spec. Depth (m):	4.42
Date Tested:	10/08/14
Date Sampled:	09/29/14

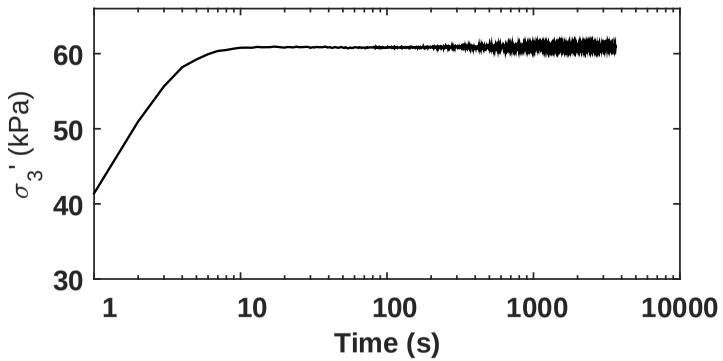

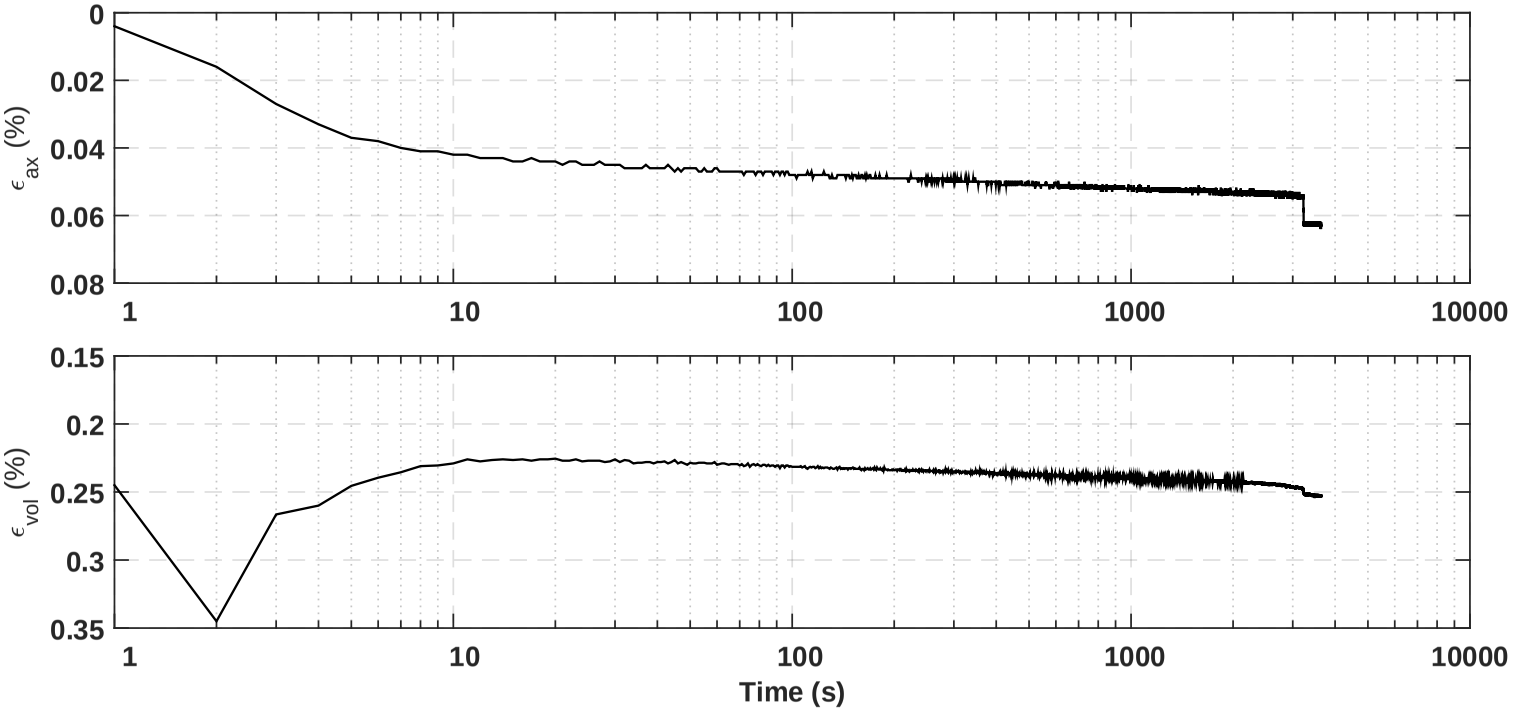

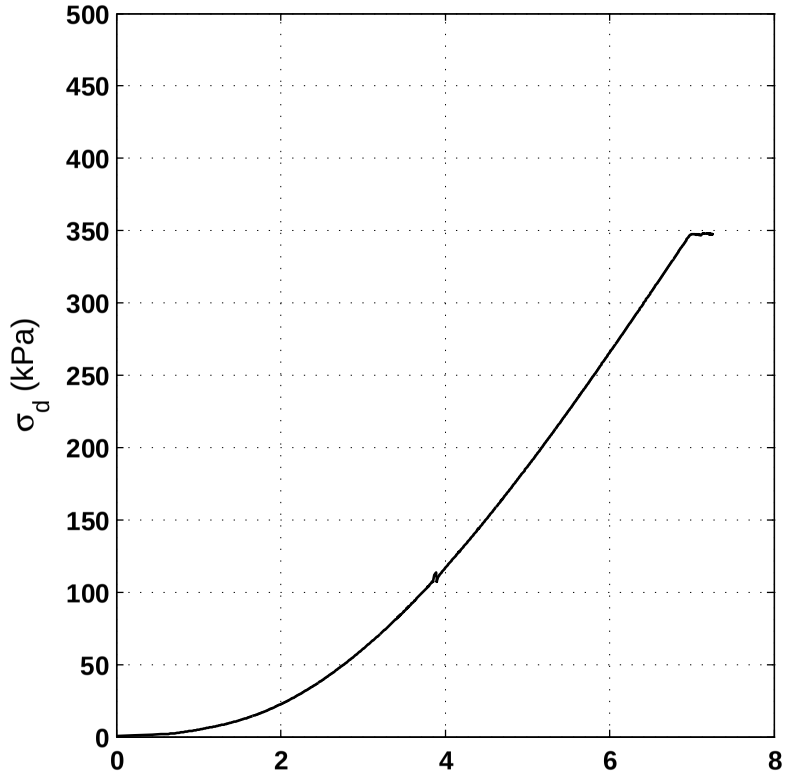

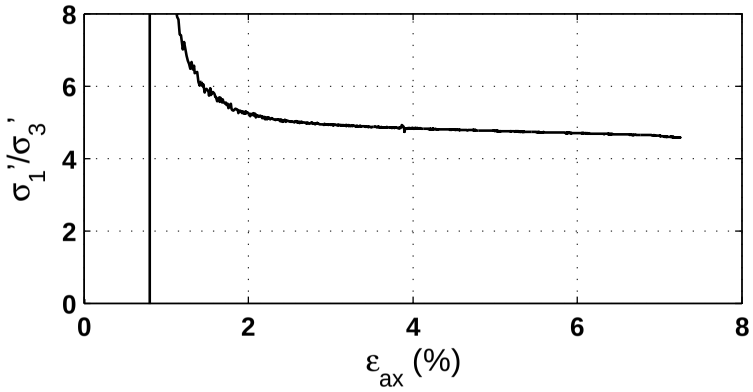

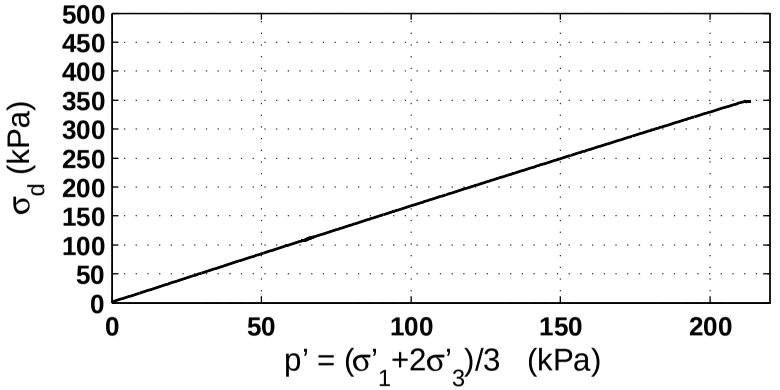

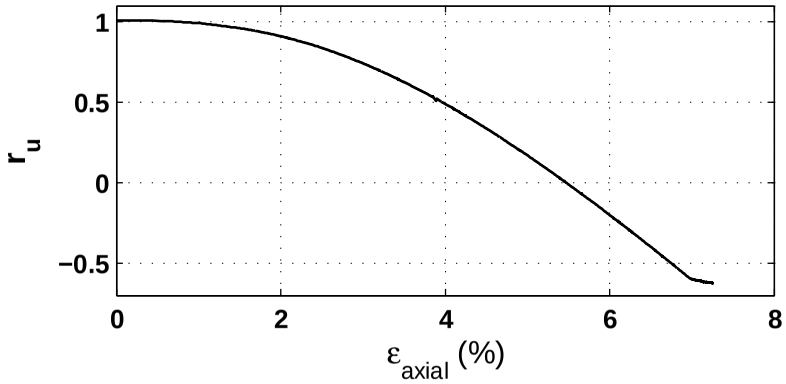

Post CTX Monotonic Comp. Test

Site:	48 Lis. St	**Rate (kPa/min):**	12
Borehole:	DM BH1		
Sample No.:	4U		
Sampler Type:	D&M		
Spec. Depth (m):	4.42		
Date Tested:	10/08/14		
Date Sampled:	09/29/14		

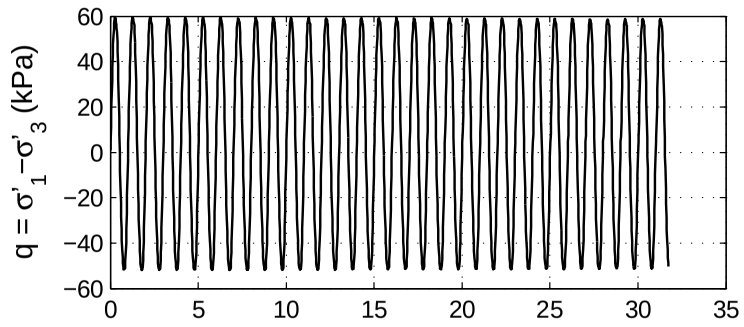

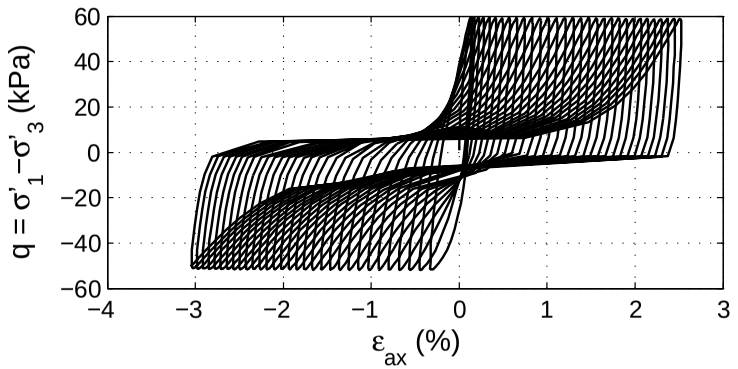

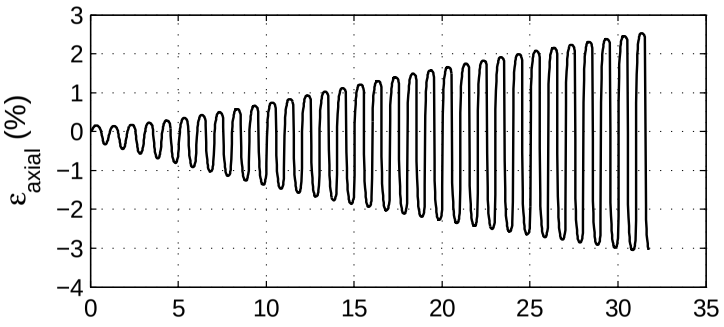

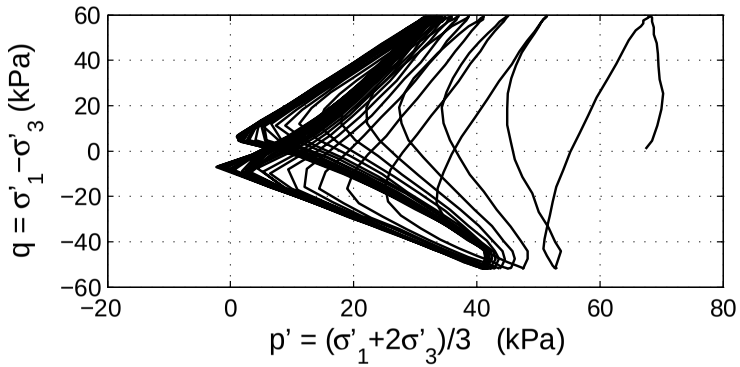

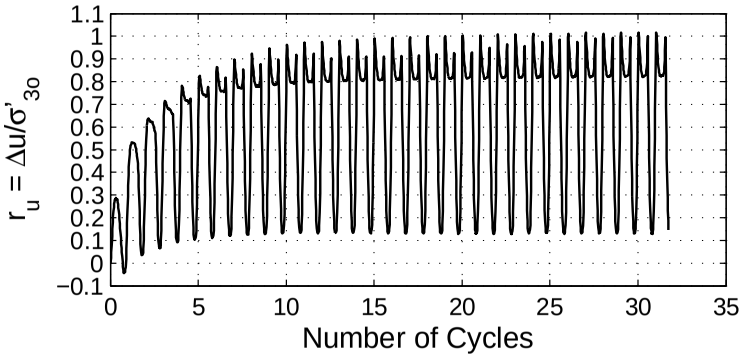

Specimen & Isotropic Cyclic Triaxial Test Data

Site:	48 Lis. St	**Loading Freq (Hz):**	0.1
Borehole:	DM BH1	**B−Value:**	0.981
Sample No.:	5U	**CSR:**	0.410
Sampler Type:	D&M	**N to $\varepsilon_{Ax-S.A.}$=3%:**	31
Spec. Depth (m):	5.32	**N to $\varepsilon_{Ax-D.A.}$=5%:**	27.5
Date Tested:	10/12/14	**Post−Cyclic Test:**	Reconsol.
Date Sampled:	09/29/14		
Spec. Ht. (mm):	139.6		
Spec. Diam. (mm):	61.0		
Dry Mass (g):	628.68		
Gs:	2.68		
e_o:	0.74		
σ'_{3o} (kPa):	67.2		
PI (%):	NP		
USCS:	SP		

Isotropic Consolidation Test

Site:	48 Lis. St
Borehole:	DM BH1
Sample No.:	5U
Sampler Type:	D&M
Spec. Depth (m):	5.32
Date Tested:	10/12/14
Date Sampled:	09/29/14

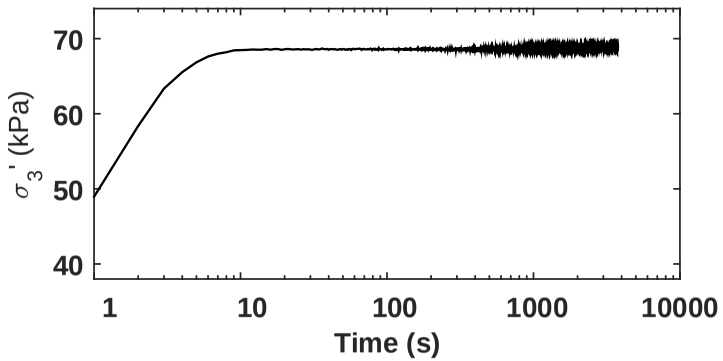

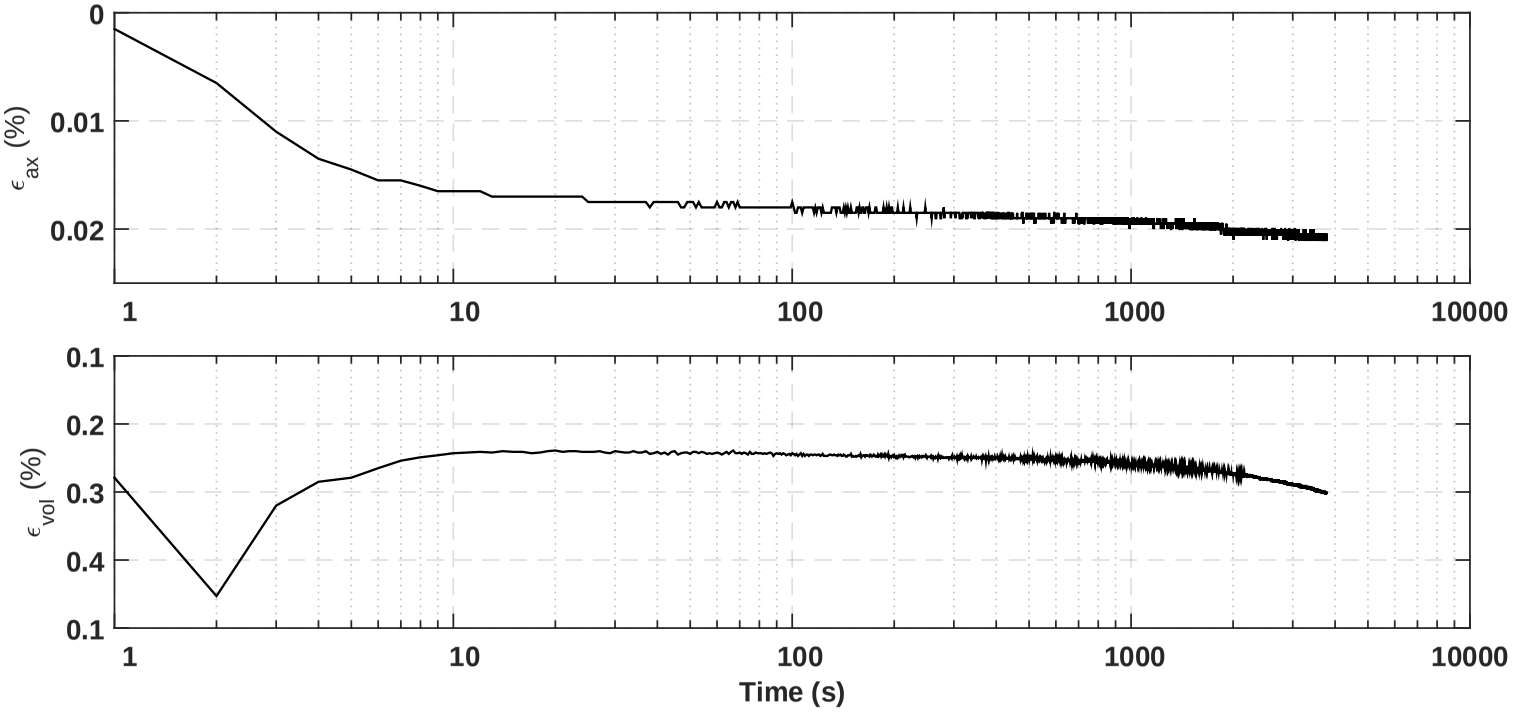

Post CTX Reconsolidation Test

Site:	48 Lis. St
Borehole:	DM BH1
Sample No.:	5U
Sampler Type:	D&M
Spec. Depth (m):	5.32
Date Tested:	10/12/14
Date Sampled:	09/29/14

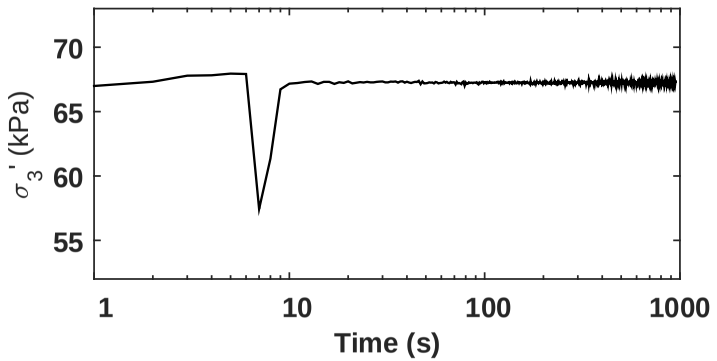

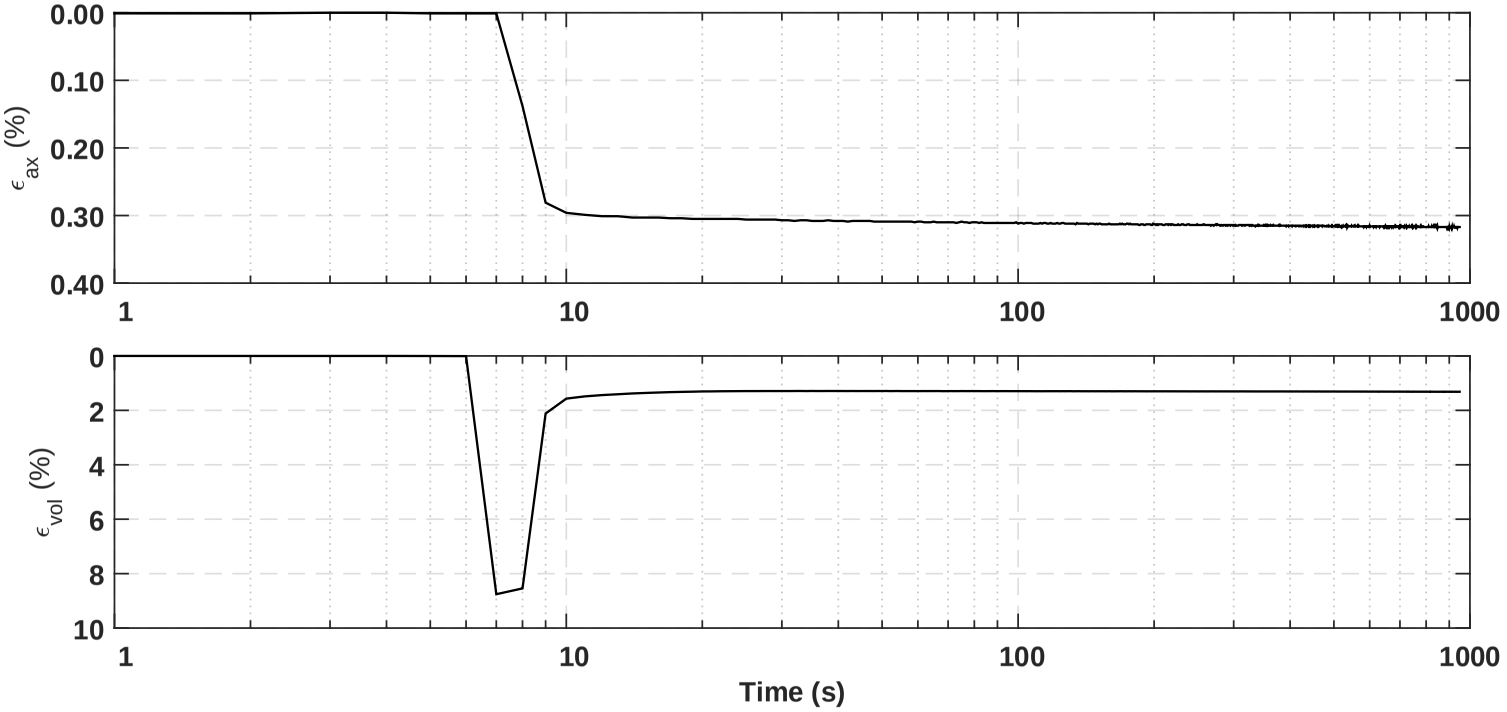

Specimen & Isotropic Cyclic Triaxial Test Data

Site:	48 Lis. St	**Loading Freq (Hz):**	0.1
Borehole:	DM BH1	**B–Value:**	0.983
Sample No.:	7U	**CSR:**	0.480
Sampler Type:	D&M	**N to $\varepsilon_{Ax-S.A.}$=3%:**	6
Spec. Depth (m):	6.26	**N to $\varepsilon_{Ax-D.A.}$=5%:**	5.5
Date Tested:	10/20/14	**Post–Cyclic Test:**	Reconsol.
Date Sampled:	09/29/14		
Spec. Ht. (mm):	138.8		
Spec. Diam. (mm):	60.9		
Dry Mass (g):	634.68		
Gs:	2.67		
e_o:	0.70		
σ'_{3o} (kPa):	72.6		
PI (%):	NP		
USCS:	SP–SM		

Isotropic Consolidation Test

Site:	48 Lis. St
Borehole:	DM BH1
Sample No.:	7U
Sampler Type:	D&M
Spec. Depth (m):	6.26
Date Tested:	10/20/14
Date Sampled:	09/29/14

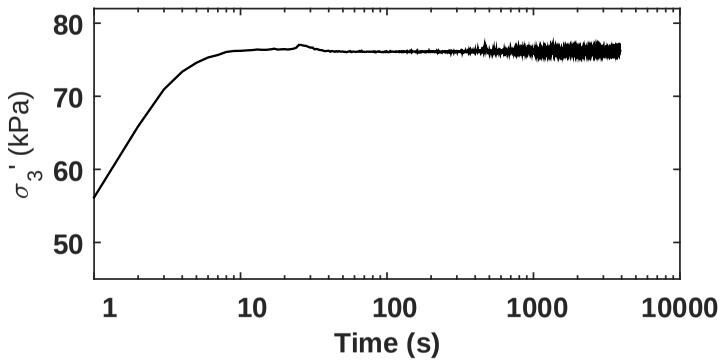

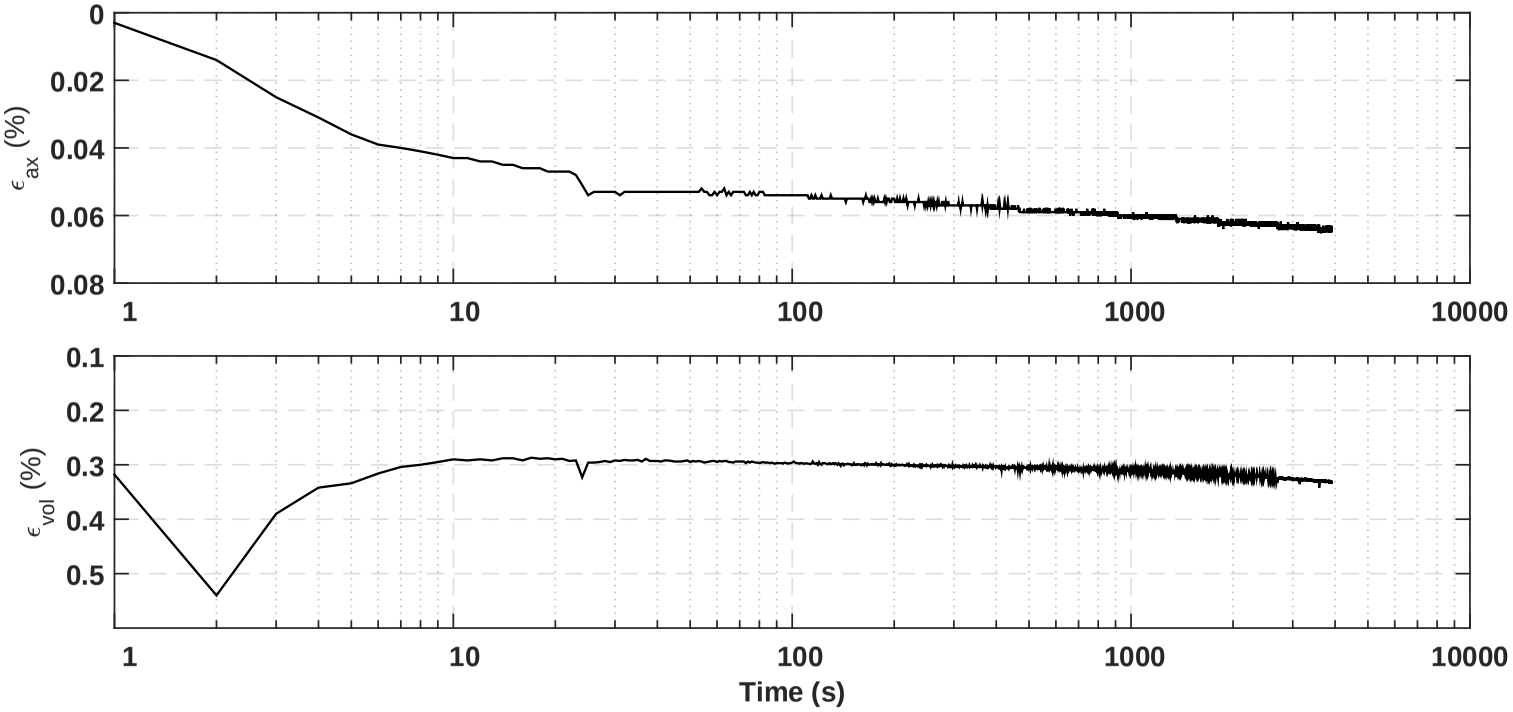

Post CTX Reconsolidation Test

Site:	48 Lis. St
Borehole:	DM BH1
Sample No.:	7U
Sampler Type:	D&M
Spec. Depth (m):	6.26
Date Tested:	10/20/14
Date Sampled:	09/29/14

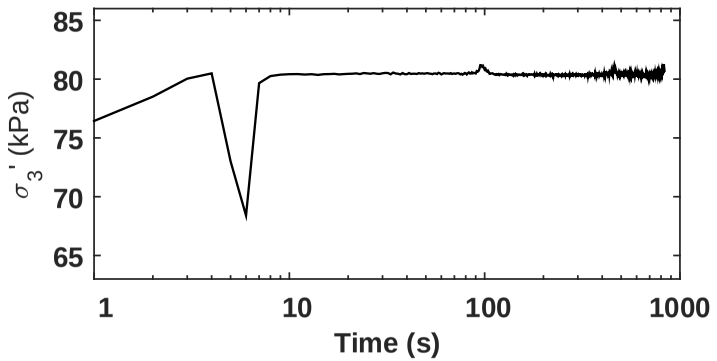

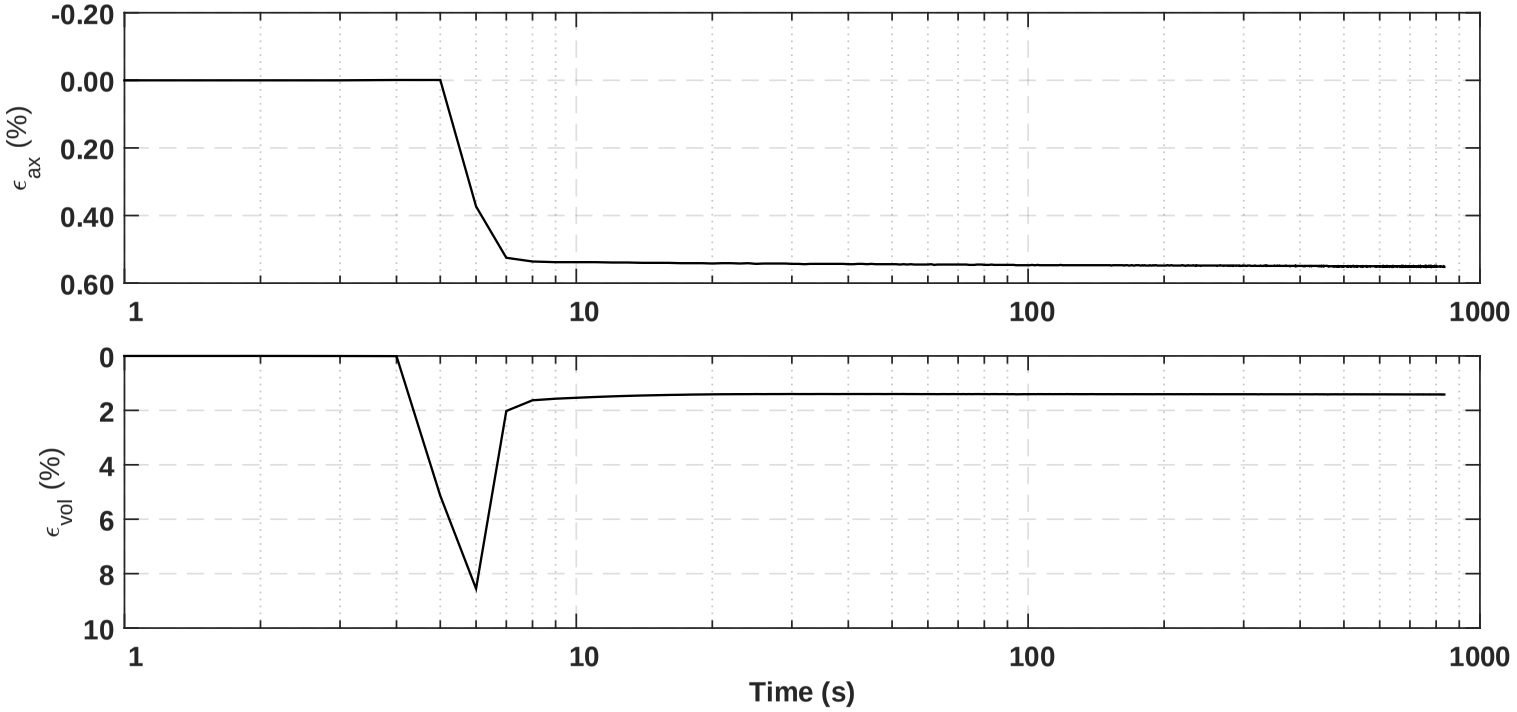

Appendix C.2.7

SA Building Site—193 Peterborough St.

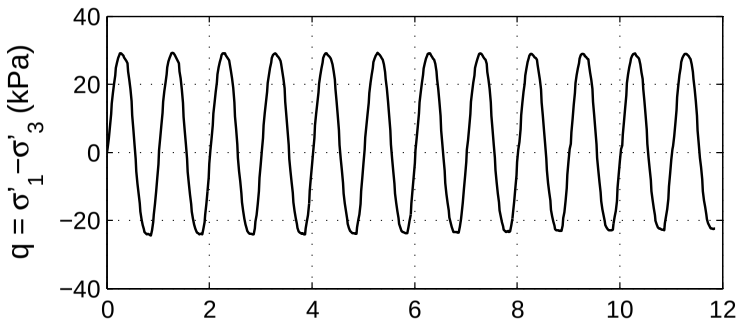

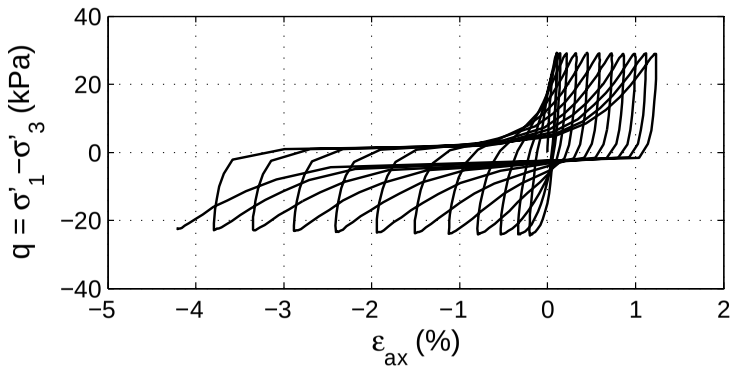

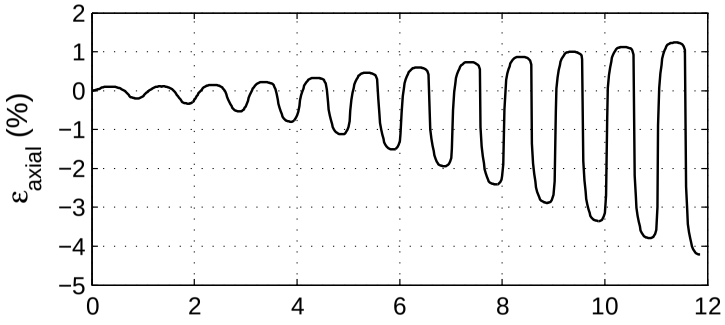

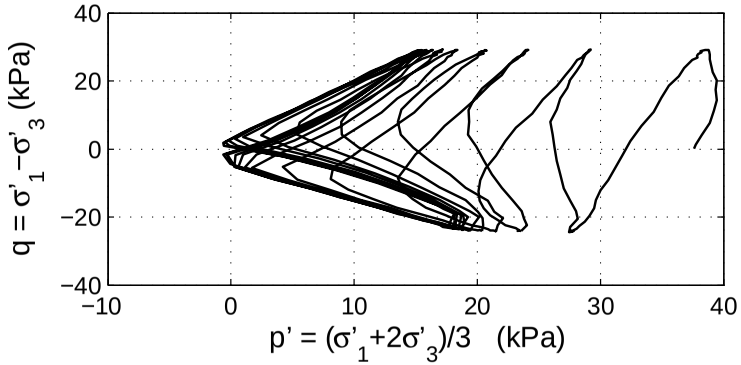

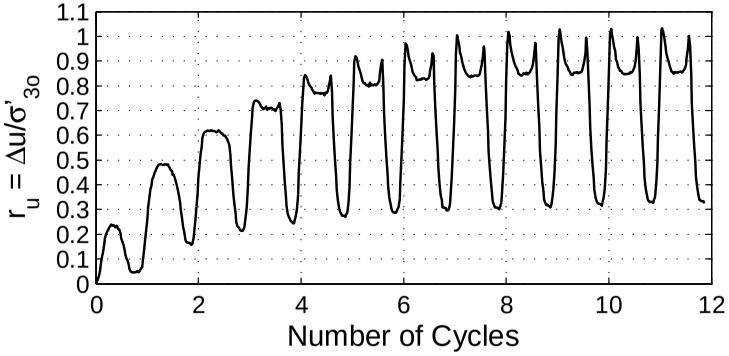

Specimen & Isotropic Cyclic Triaxial Test Data

Site:	193 Pet. St	**Loading Freq (Hz):**	0.1
Borehole:	DM BH1	**B−Value:**	0.987
Sample No.:	1U	**CSR:**	0.349
Sampler Type:	D&M	**N to $\varepsilon_{Ax-S.A.}$=3%:**	10
Spec. Depth (m):	1.82	**N to $\varepsilon_{Ax-D.A.}$=5%:**	11.5
Date Tested:	10/18/14	**Post−Cyclic Test:**	Reconsol.
Date Sampled:	10/15/14		
Spec. Ht. (mm):	143.9		
Spec. Diam. (mm):	60.9		
Dry Mass (g):	632.23		
Gs:	2.68		
e_o:	0.78		
σ'_{3o} (kPa):	37.6		
PI (%):	NP		
USCS:	SP		

Post CTX Reconsolidation Test

Site:	193 Pet. St
Borehole:	DM BH1
Sample No.:	1U
Sampler Type:	D&M
Spec. Depth (m):	1.82
Date Tested:	10/18/14
Date Sampled:	10/15/14

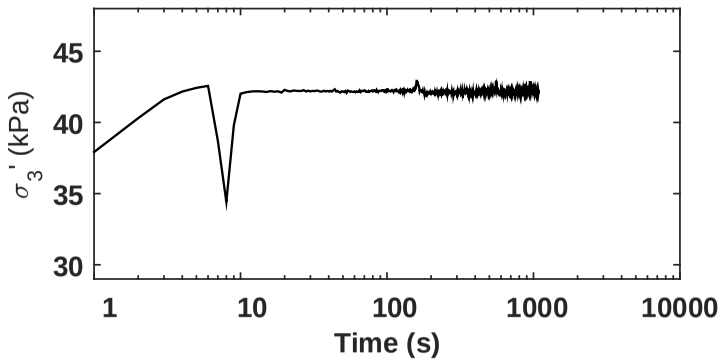

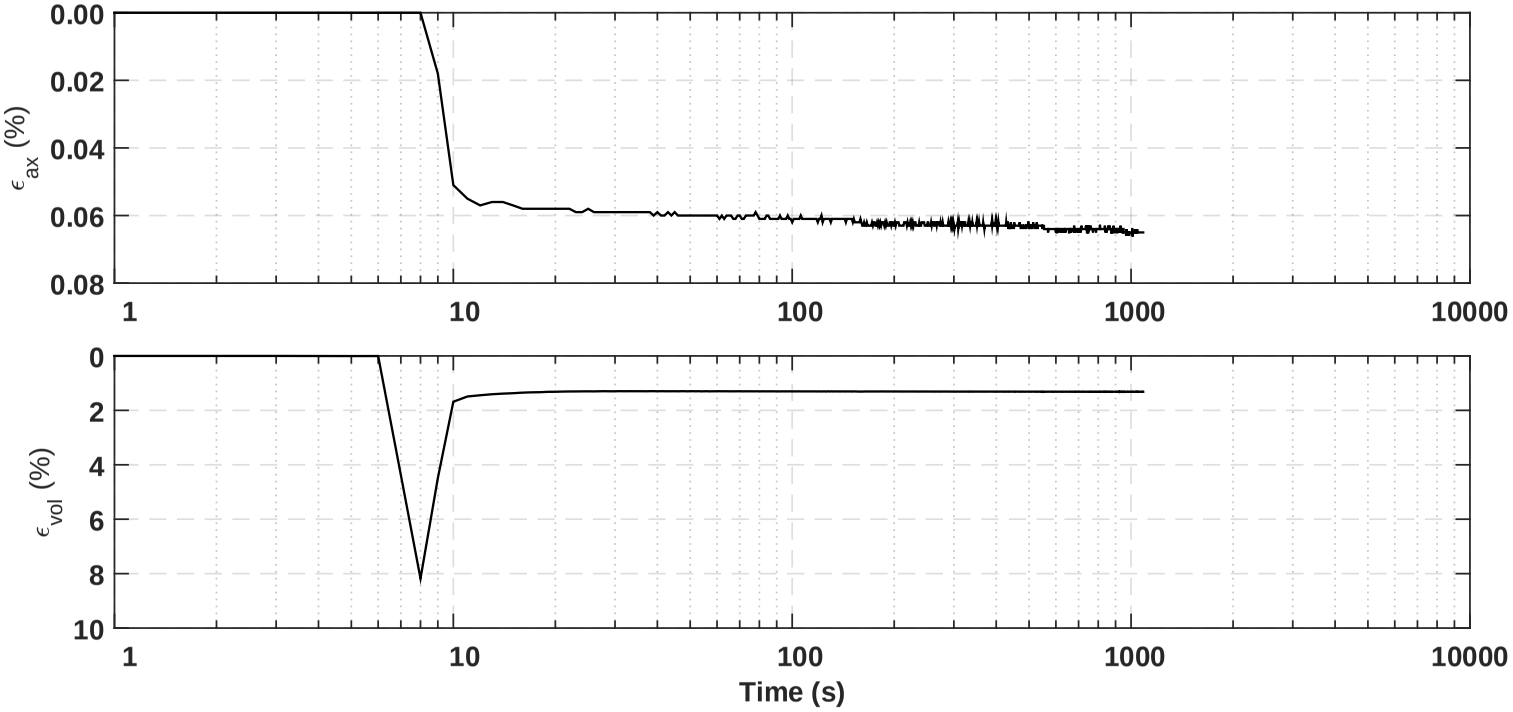

Appendix C.3

Processed Undisturbed Monotonic Triaxial Test Results

The following corrections were made to the triaxial test data presented in Appendices C.2 and C.3:

Membrane correction

Axial stresses were corrected for loads carried by the membrane (i.e., not the soil) in both cyclic and monotonic triaxial tests using the following equation proposed by Duncan and Seed (1967):

$$\Delta\sigma_{ax-m} = -C_{am} * \left(\frac{2}{3}\right) * E_m \frac{4t_{om}}{D_{os}}$$

Where $\Delta\sigma_{ax\text{-}m}$ is the portion of the applied stress attributed to the membrane,

$$C_{am} = \left(\frac{1 + 2\varepsilon_{at} - \sqrt{\frac{1-\varepsilon_v}{1-\varepsilon_{at}}}}{1-\varepsilon_v}\right)$$

E_m is the Young's modulus of the membrane (assumed as 14 kg/cm^2=1373.4 kPa)
t_{om} is the initial thickness of the membrane prior to testing
D_{os} is the initial diameter of the specimen prior to testing
ε_{at} is the total axial strain during the test
ε_{vol} is the total volumetric strain during the test

Because of the negative sign in the calculation of $\Delta\sigma_{ax\text{-}m}$, this values should be added to the total applied stress if positive ε_{ax} represents compression (i.e., the specimen gets shorter) and negative ε_{ax} represents extension (i.e., the specimen gets taller). In this way, the axial stress being applied to the actual soil is less than the total axial stress being applied to the specimen and membrane in compression (i.e., $\Delta\sigma_{ax\text{-}m}$ is negative) and higher than the total axial stress in extension (i.e., $\Delta\sigma_{ax\text{-}m}$ is positive).

Area Correction

CTX and monotonic triaxial testing was completed using the CKC electropneumatic triaxial device with the Automated Triaxial Testing System software developed by Li et al. (1998). This software automatically applies an area correction based on the assumption that the soil specimen deforms as a right cylinder during testing, which allows for an axial stress calculation based on this corrected area.

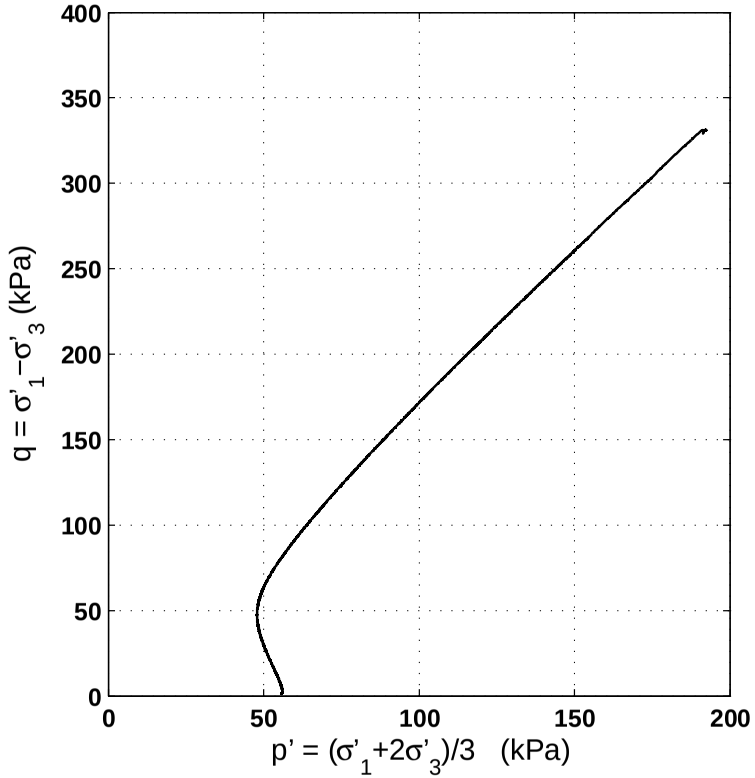

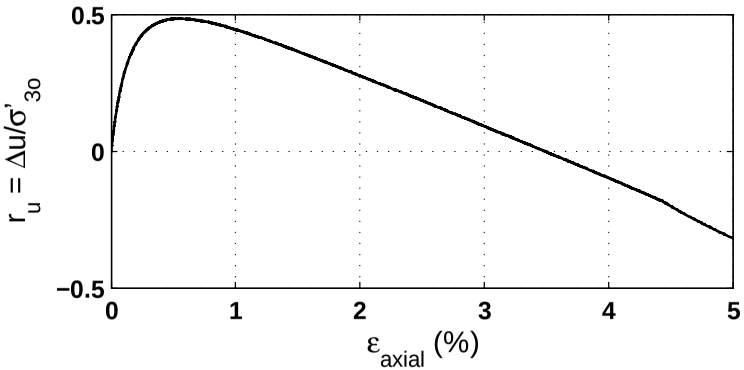

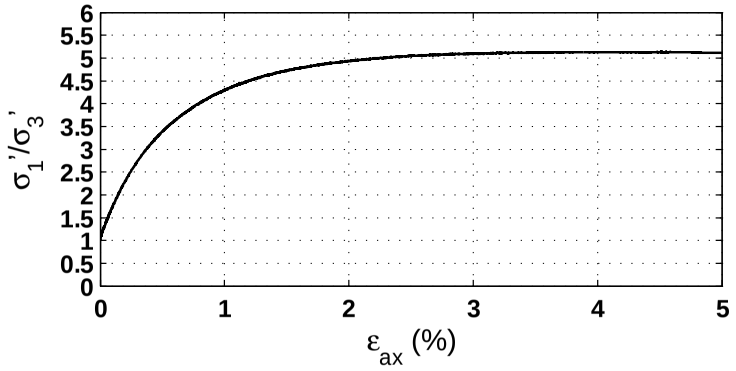

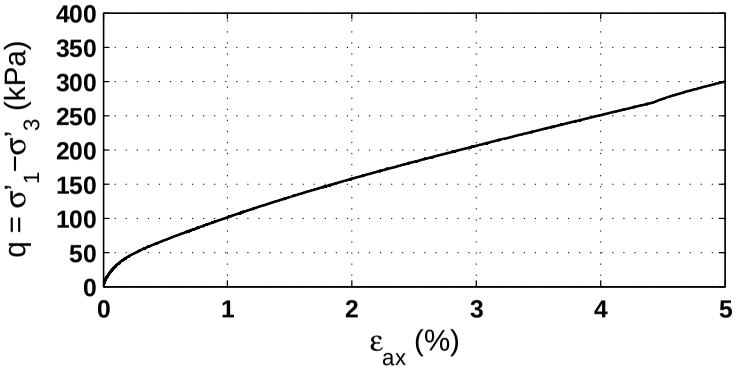

Specimen and ICU Static Triaxial Compression Test Data

Site:	86 Kil. St	**Rate (kPa/min):**	2
Borehole:	DM BH1	**B−Value:**	0.975
Sample No.:	4U		
Sampler Type:	D&M		
Spec. Depth (m):	3.83		
Date Tested:	06/02/14		
Date Sampled:	05/06/14		
Spec. Ht. (mm):	137.9		
Spec. Diam. (mm):	61.0		
Dry Mass (g):	611.40		
Gs:	2.67		
e_ρ:	0.76		
σ'_{3o} (kPa):	55.3		
PI (%):	4		
USCS:	ML		

Isotropic Consolidation Test

Site:	86 Kil. St
Borehole:	DM BH1
Sample No.:	4U
Sampler Type:	D&M
Spec. Depth (m):	3.83
Date Tested:	06/02/14
Date Sampled:	05/06/14

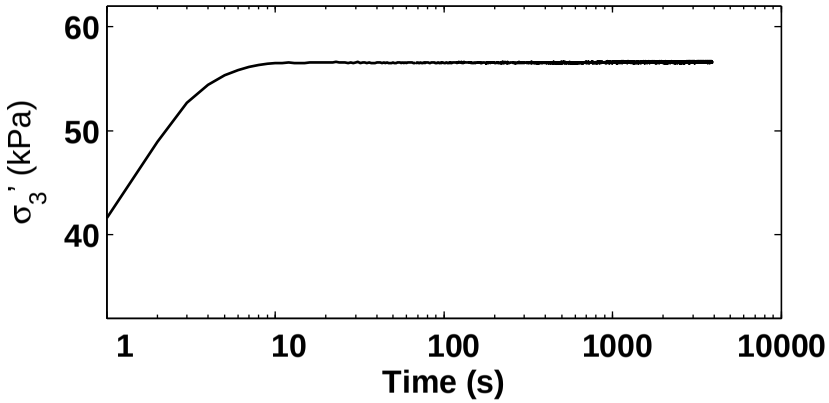

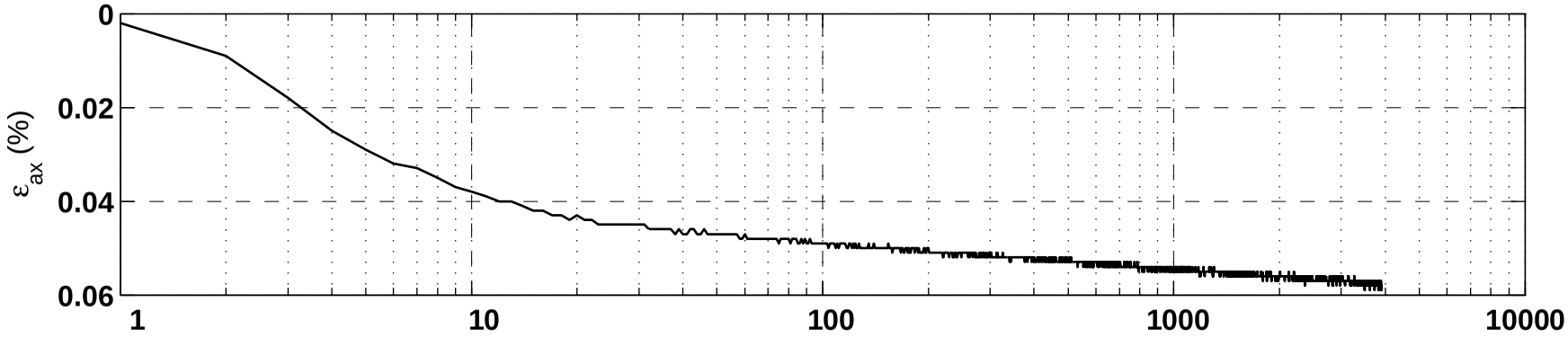

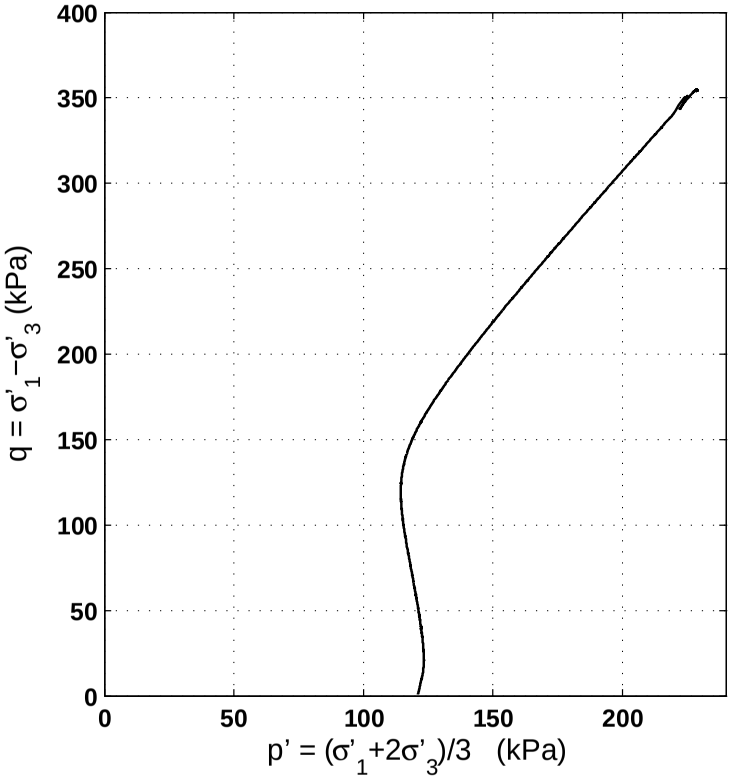

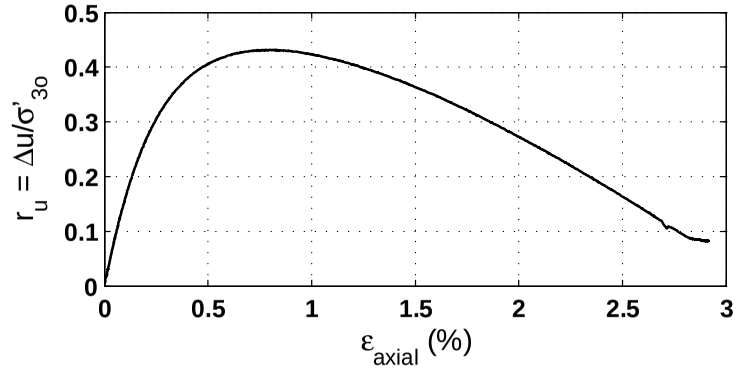

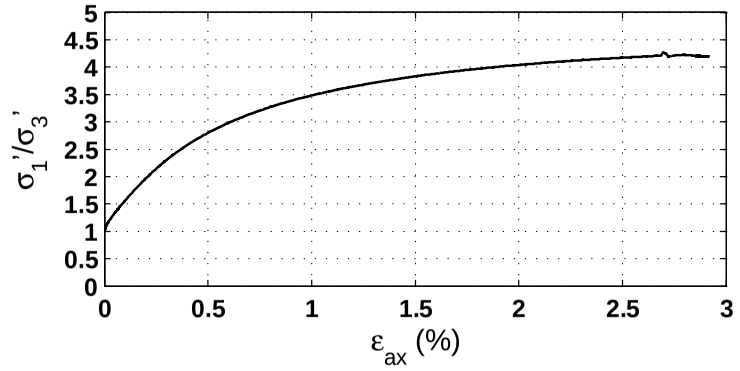

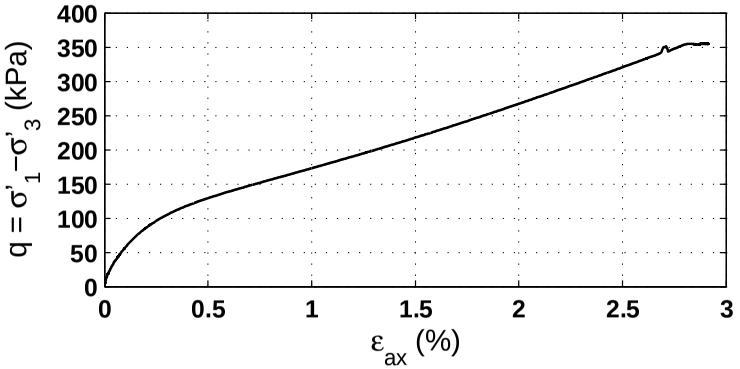

Specimen and ICU Static Triaxial Compression Test Data

Site:	151 Kil. St	**Rate (kPa/min):**	12
Borehole:	DM BH2	**B−Value:**	0.988
Sample No.:	10U		
Sampler Type:	D&M		
Spec. Depth (m):	10.37		
Date Tested:	06/20/14		
Date Sampled:	05/15/14		
Spec. Ht. (mm):	139.6		
Spec. Diam. (mm):	60.9		
Dry Mass (g):	630.33		
Gs:	2.71		
e_o:	0.79		
σ'_{3o} (kPa):	120.8		
PI (%):	NP		
USCS:	SP		

Isotropic Consolidation Test

Site:	151 Kil. St
Borehole:	DM BH2
Sample No.:	10U
Sampler Type:	D&M
Spec. Depth (m):	10.37
Date Tested:	06/20/14
Date Sampled:	05/15/14

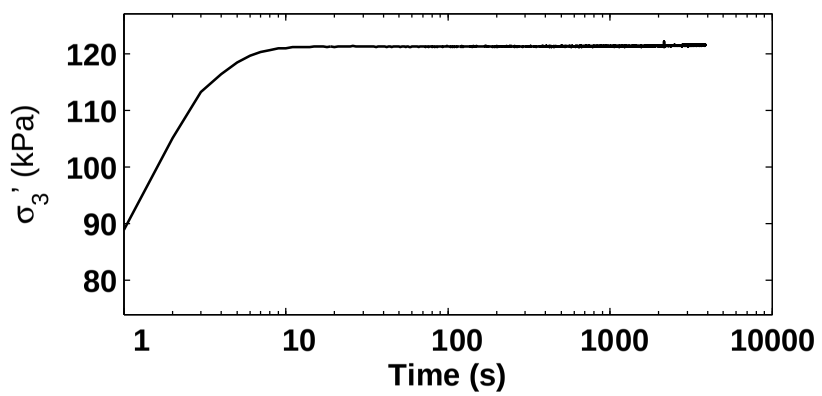

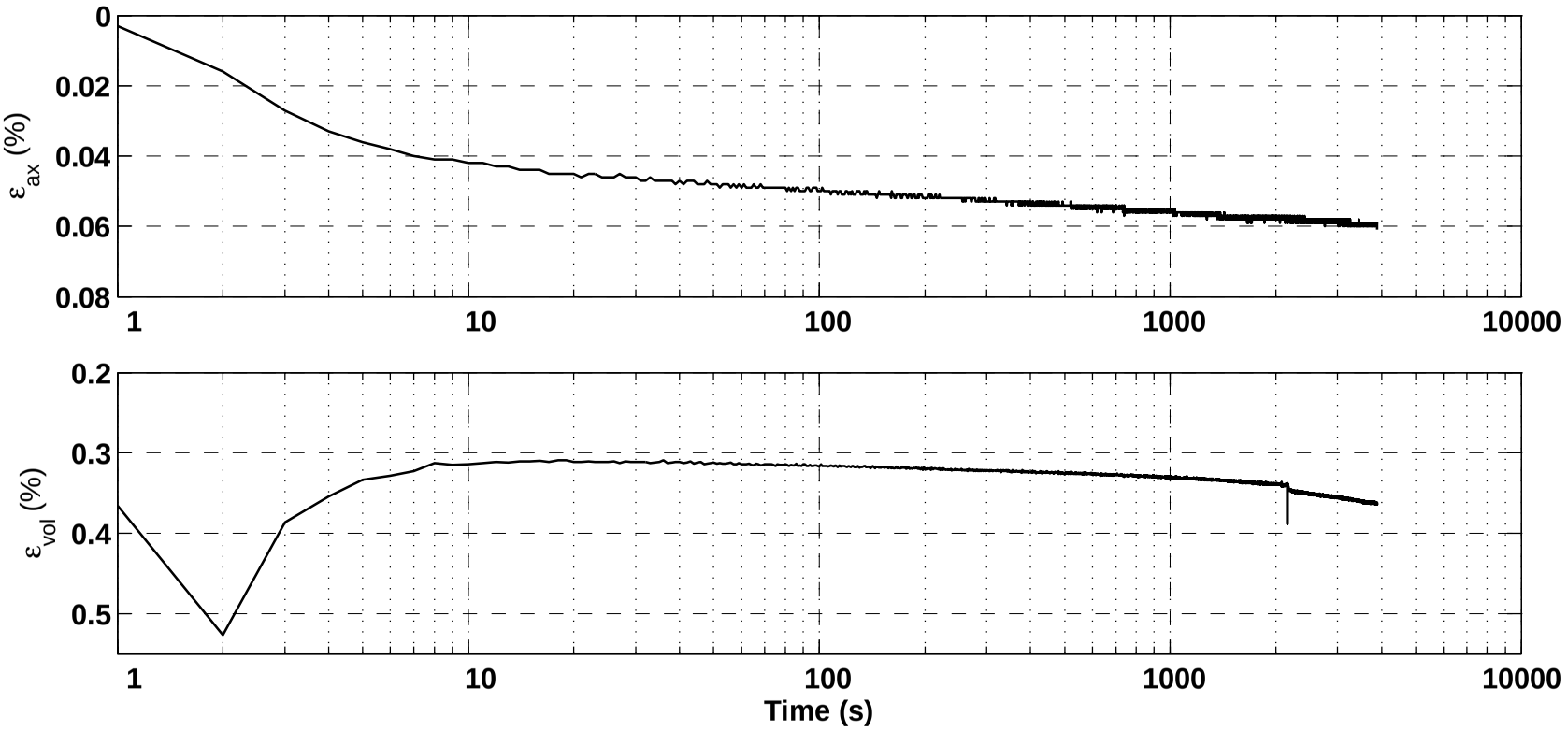

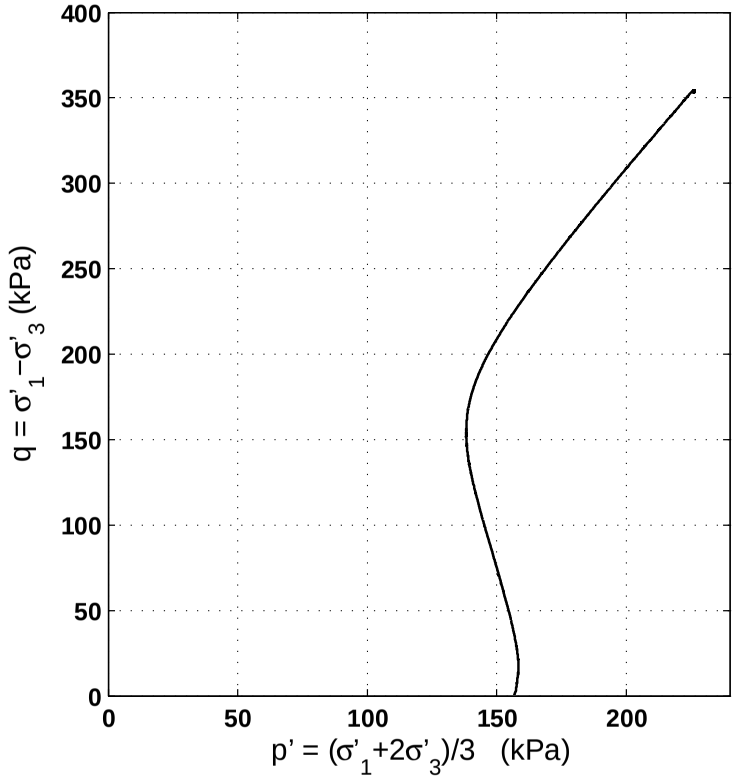

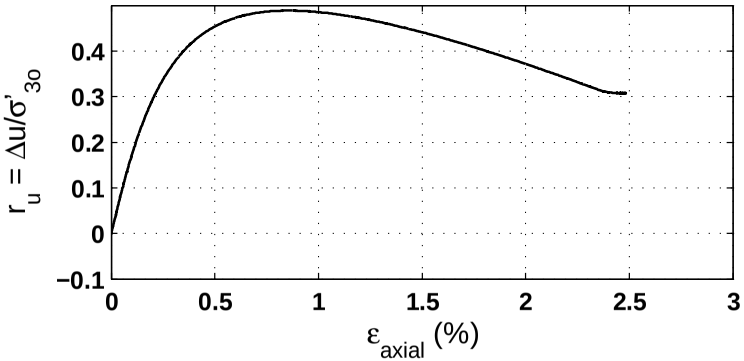

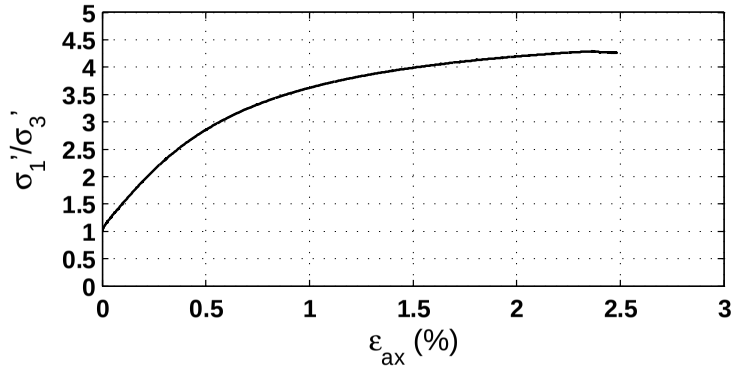

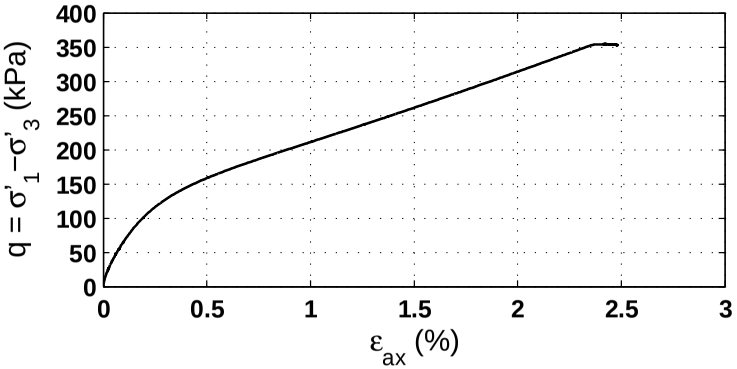

Specimen and ICU Static Triaxial Compression Test Data

Site:	90 Arm. St	**Rate (kPa/min):**	12
Borehole:	DM BH2	**B−Value:**	0.989
Sample No.:	10U		
Sampler Type:	D&M		
Spec. Depth (m):	13.92		
Date Tested:	06/23/14		
Date Sampled:	06/16/14		
Spec. Ht. (mm):	139.0		
Spec. Diam. (mm):	60.6		
Dry Mass (g):	620.63		
Gs:	2.67		
e_ρ:	0.73		
σ'_{3o} (kPa):	156.5		
PI (%):	NP		
USCS:	SP−SM		

Isotropic Consolidation Test

Site:	90 Arm. St
Borehole:	DM BH2
Sample No.:	10U
Sampler Type:	D&M
Spec. Depth (m):	13.92
Date Tested:	06/23/14
Date Sampled:	06/16/14

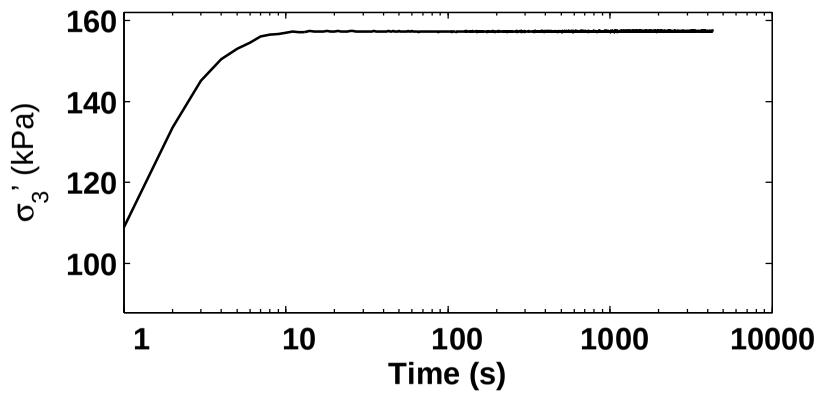

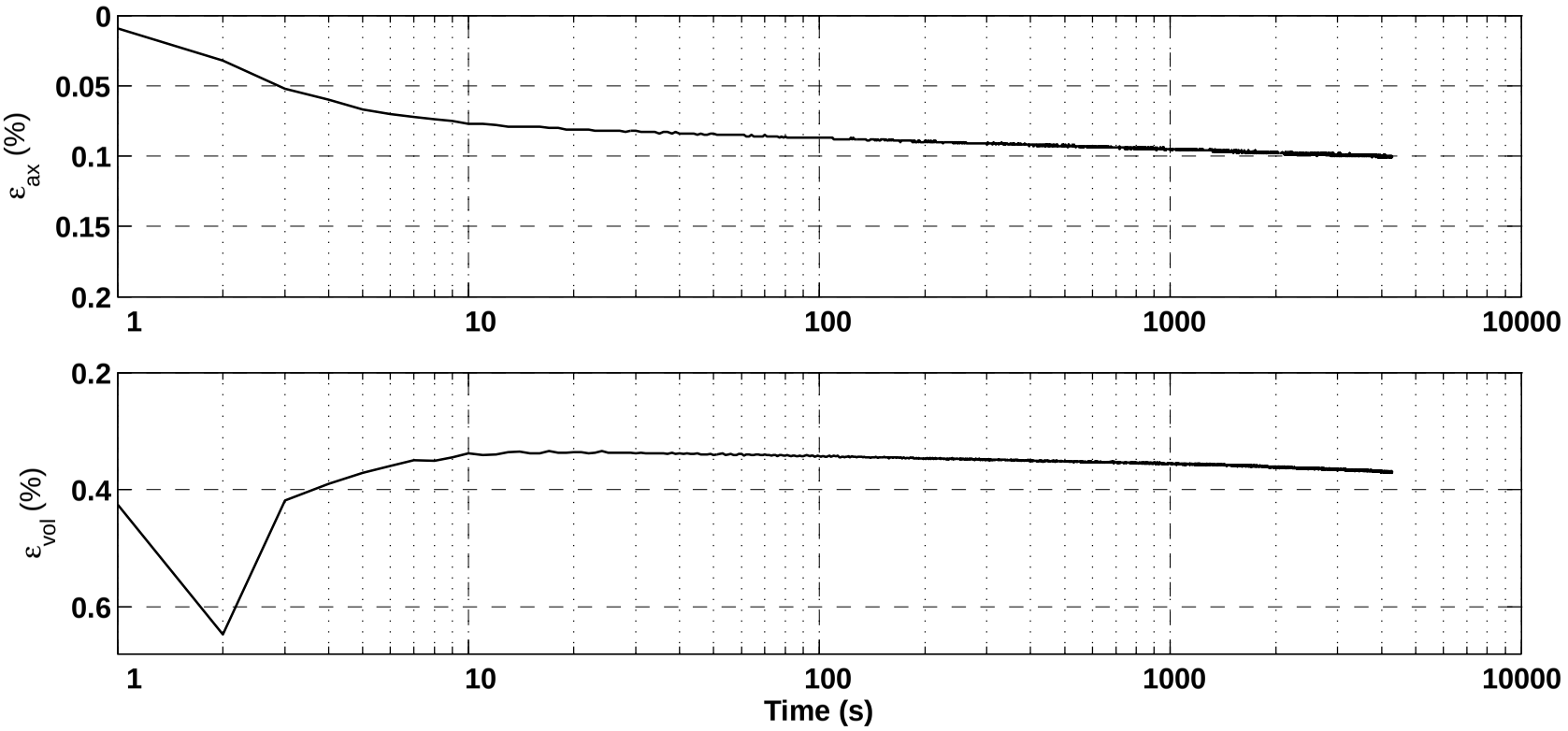

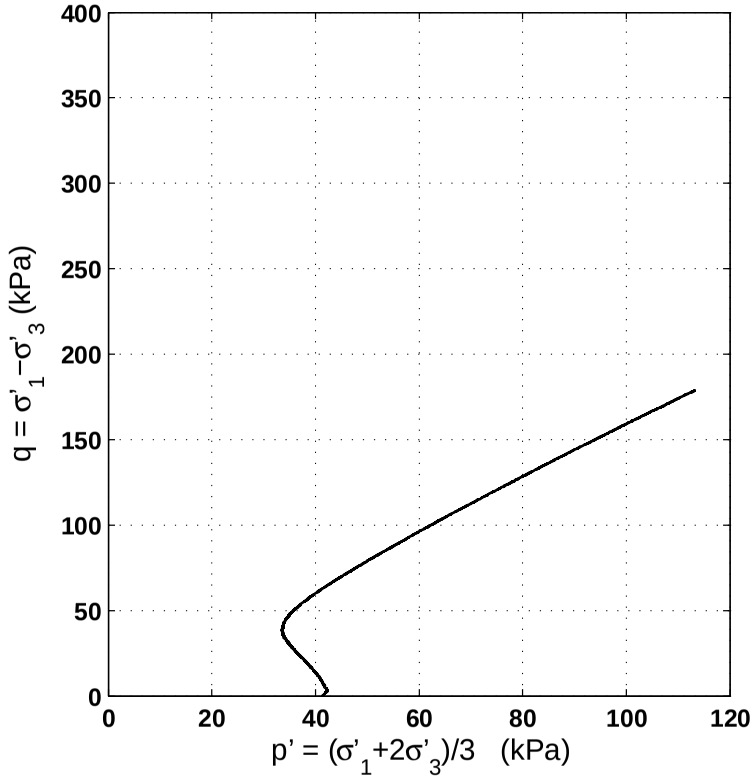

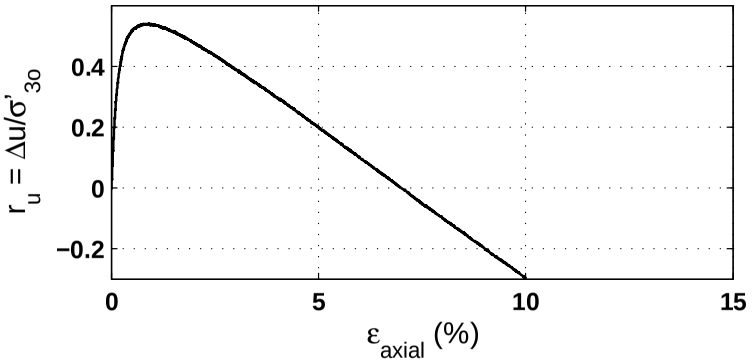

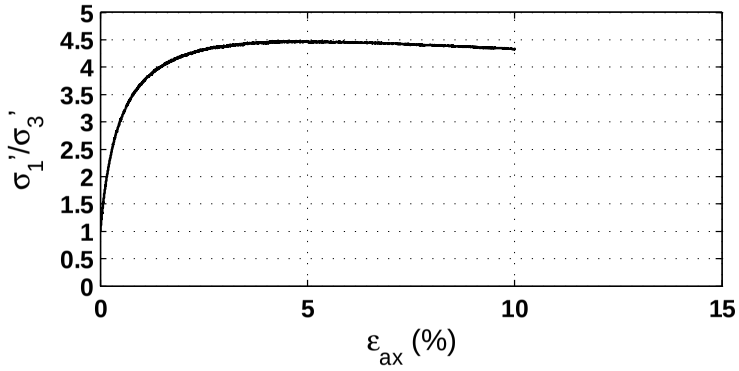

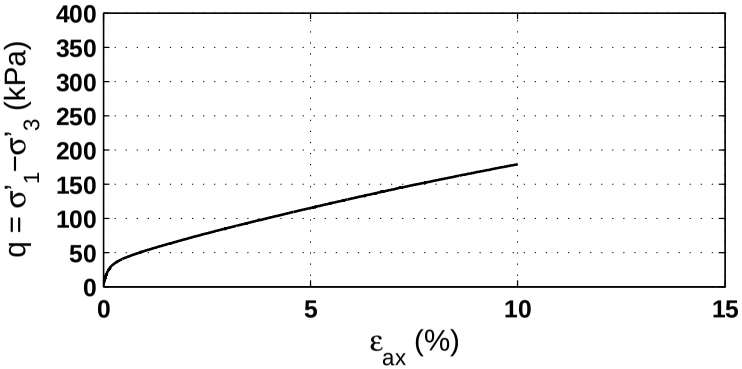

Specimen and ICU Static Triaxial Compression Test Data

Site:	48 Lis. St	**Rate (kPa/min):**	2
Borehole:	DM BH1	**B−Value:**	0.970
Sample No.:	2U		
Sampler Type:	D&M		
Spec. Depth (m):	2.17		
Date Tested:	10/06/14		
Date Sampled:	09/29/14		
Spec. Ht. (mm):	137.6		
Spec. Diam. (mm):	60.7		
Dry Mass (g):	566.71		
Gs:	2.68		
e_ρ:	0.88		
σ'_{3o} (kPa):	41.4		
PI (%):	NP		
USCS:	SM		

Isotropic Consolidation Test

Site:	48 Lis. St
Borehole:	DM BH1
Sample No.:	2U
Sampler Type:	D&M
Spec. Depth (m):	2.17
Date Tested:	10/06/14
Date Sampled:	09/29/14

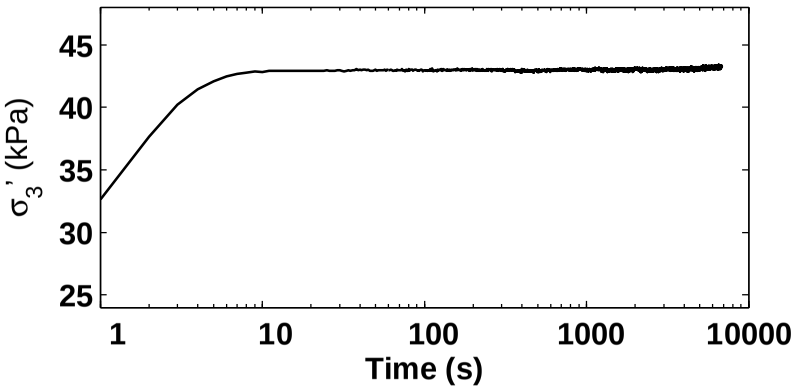

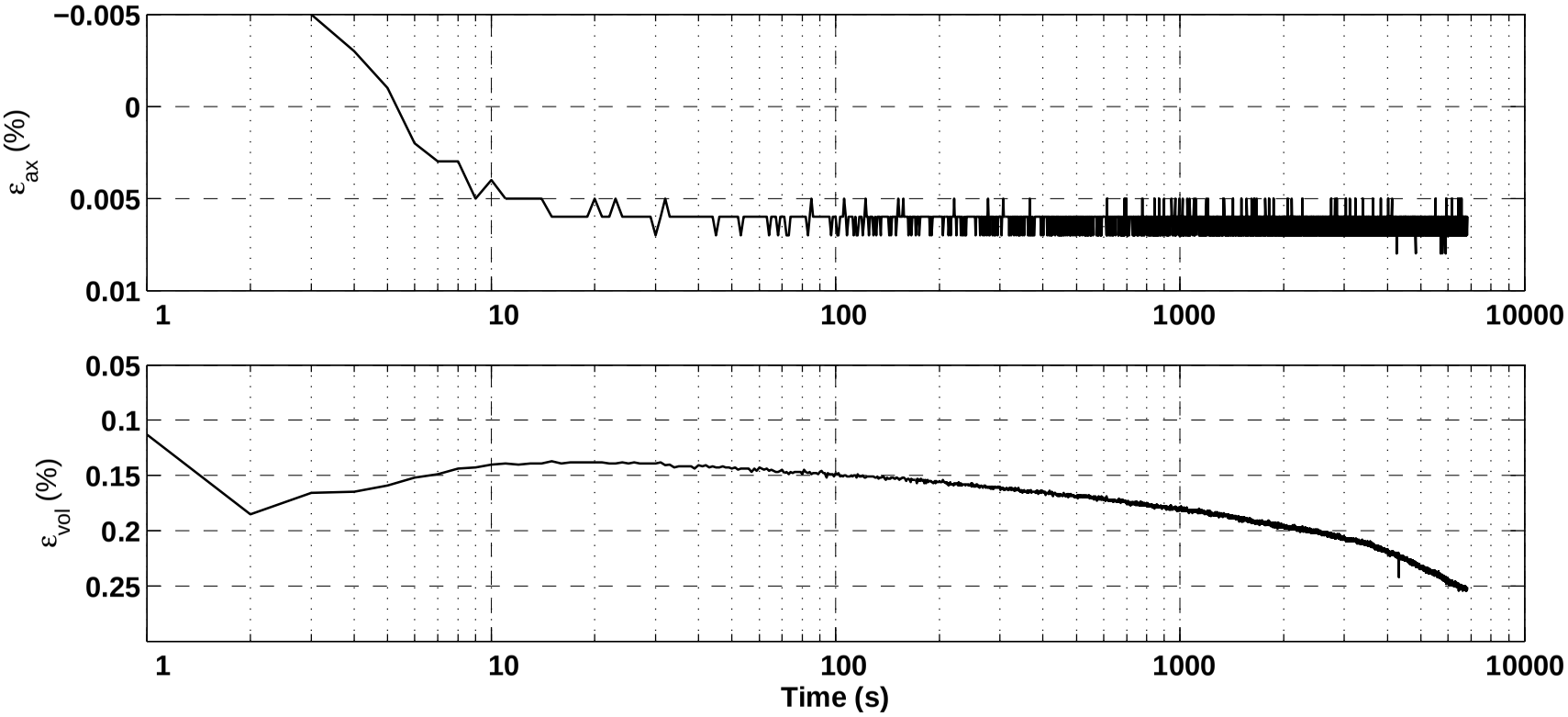

Appendix C.4

Undisturbed Triaxial Specimen Photos

Town Hall DM BH1 Sample_3U 3.07m

Town Hall DM BH1 Sample_3U 3.23m

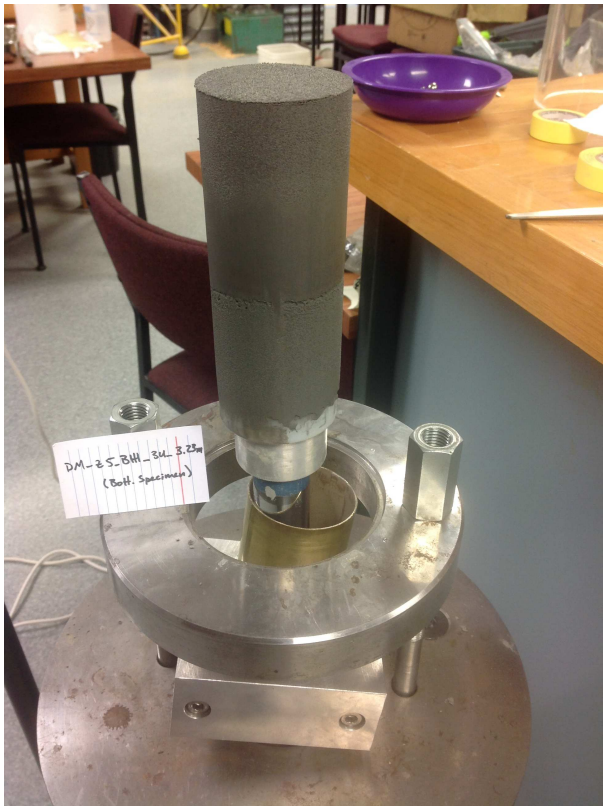

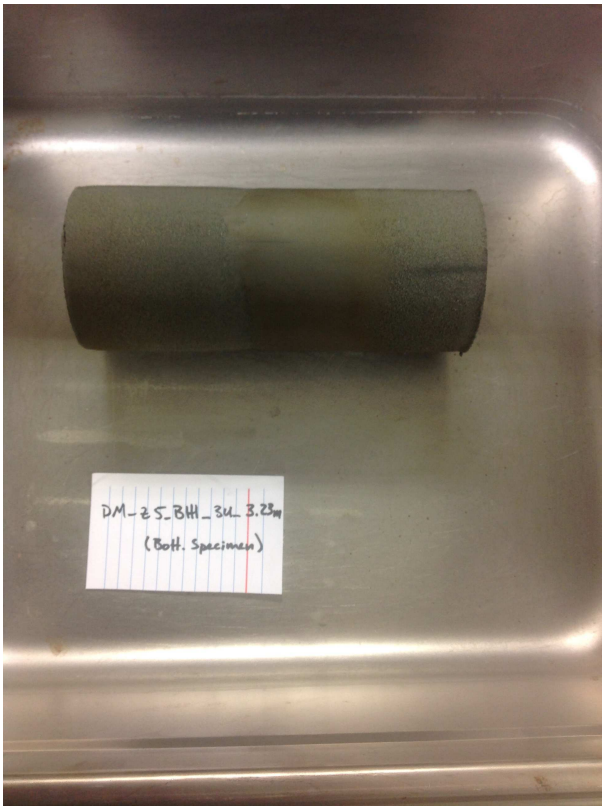

Town Hall DM BH1 Sample_4U 3.67m

Town Hall DM BH1 Sample_4U 3.83m

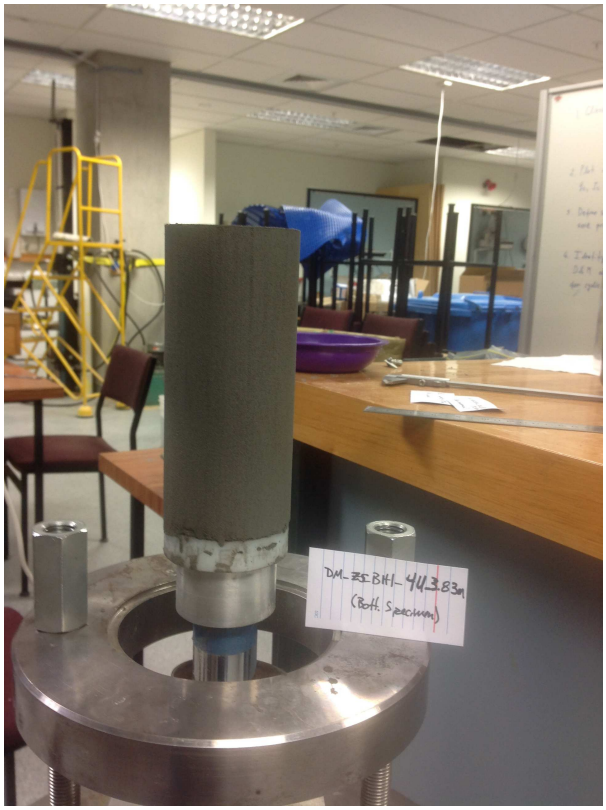

Town Hall DM BH1 Sample_5U 4.27m

Town Hall DM BH1 Sample_5U 4.43m

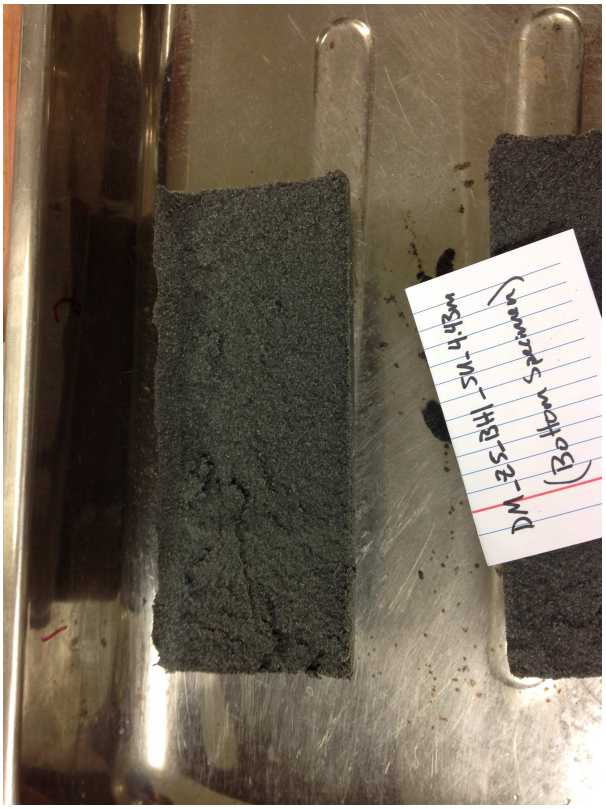

Town Hall DM BH2 Sample_4U 14.23m

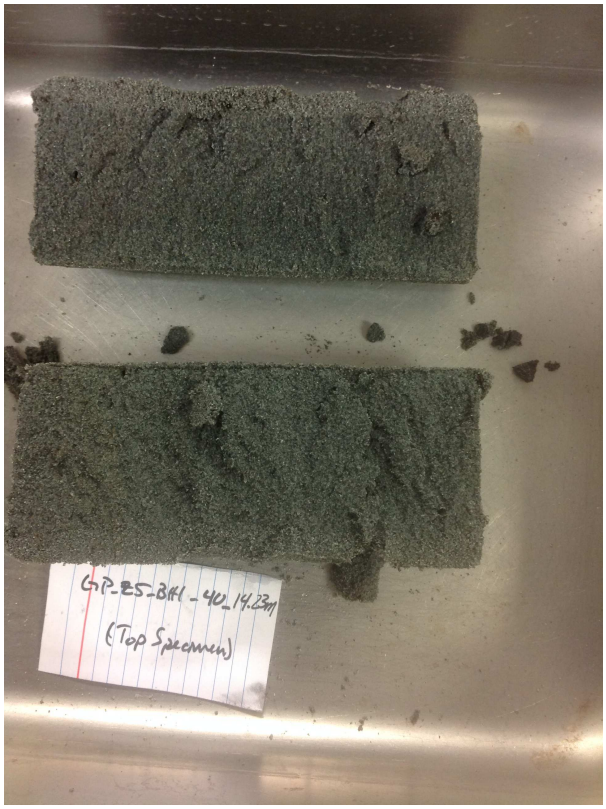

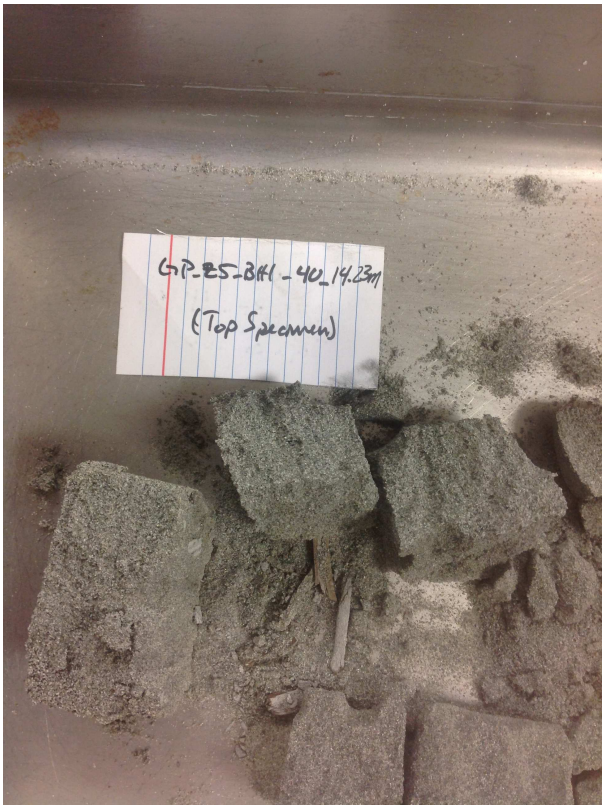

Town Hall DM BH2 Sample_5U 14.86m

Town Hall DM BH2 Sample_6U 15.36m

Town Hall DM BH2 Sample_6U 15.51m

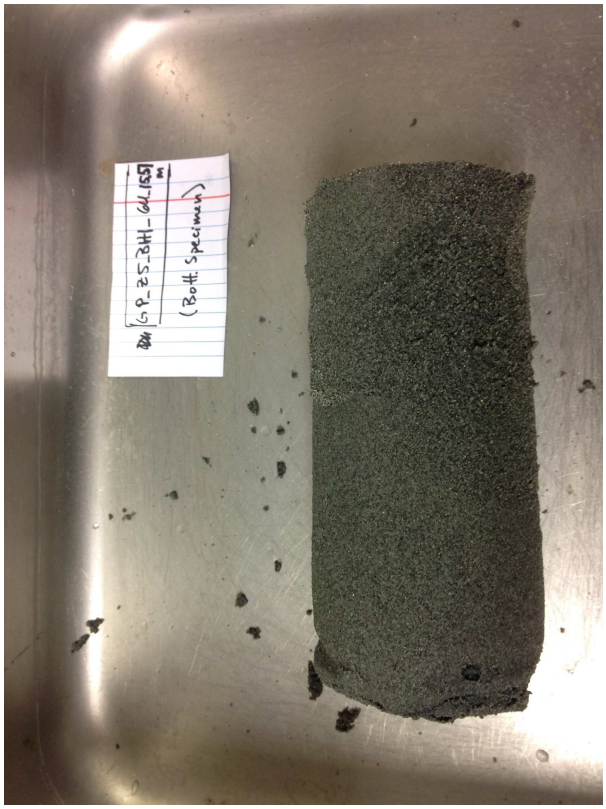

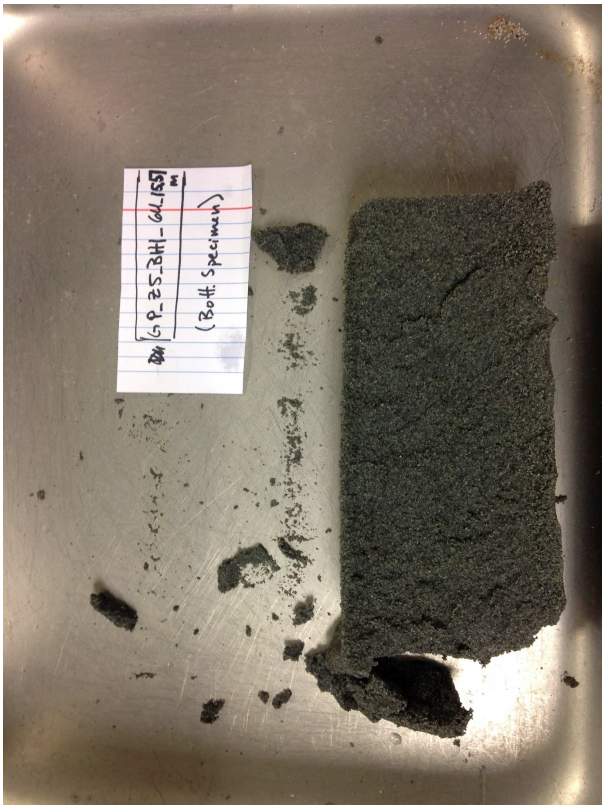

151 Kilmore St (FTG−7) DM BH1 Sample_2U 2.57m

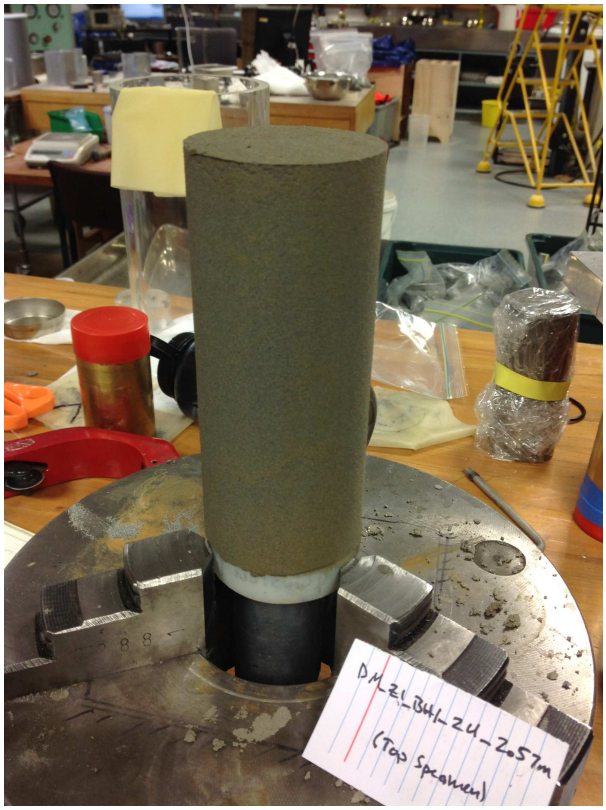

151 Kilmore St (FTG−7) DM BH1 Sample_2U 2.72m

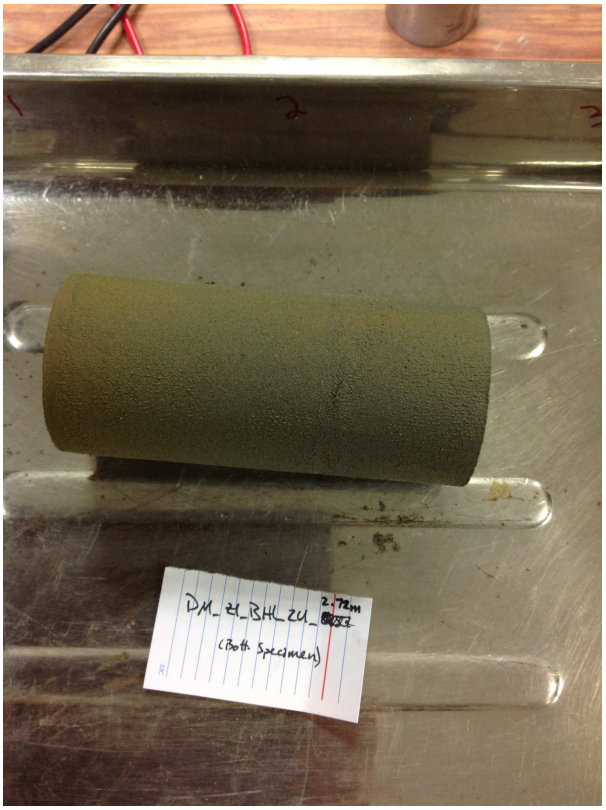

151 Kilmore St (FTG−7) DM BH1 Sample_3U 3.57m

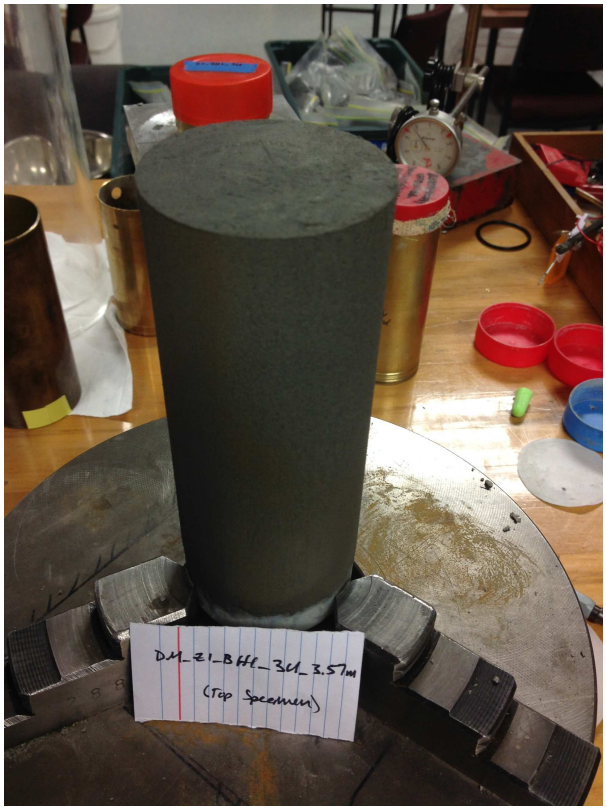

151 Kilmore St (FTG−7) DM BH1 Sample_3U 3.72m

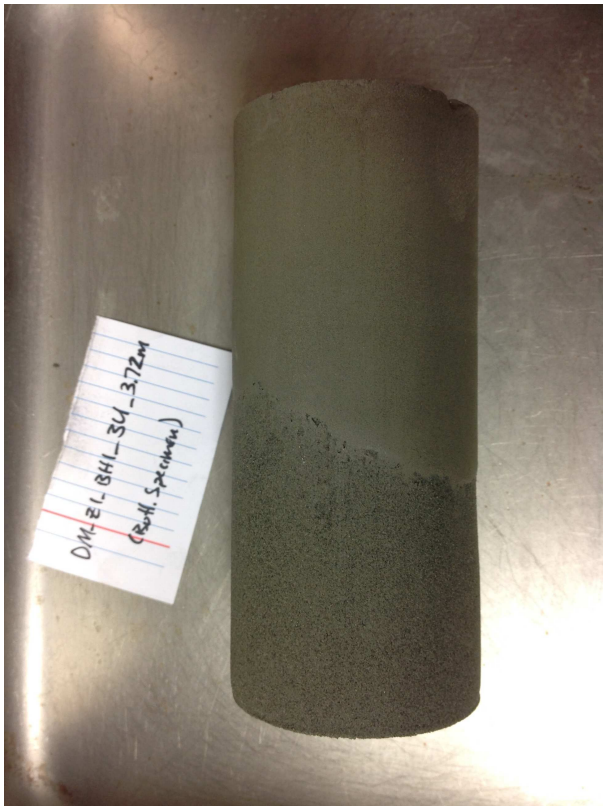

151 Kilmore St (FTG−7) DM BH1 Sample_4U 4.77m

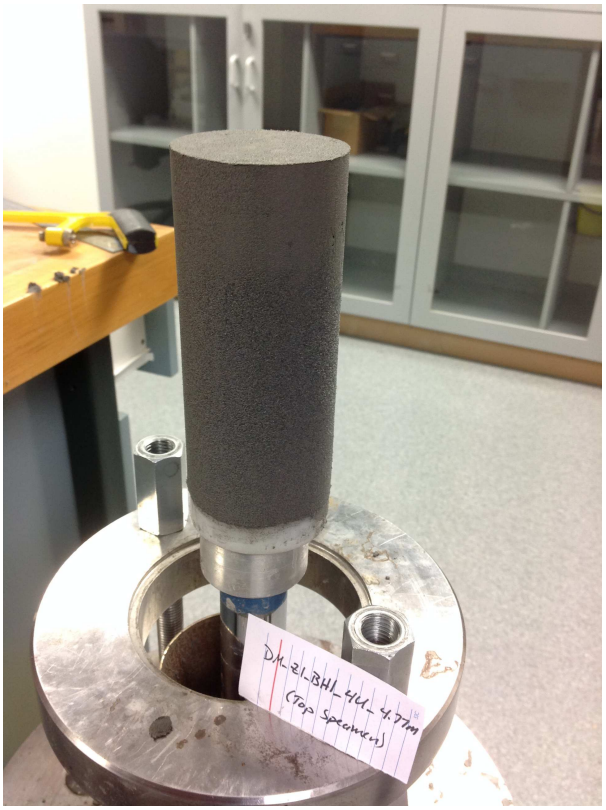

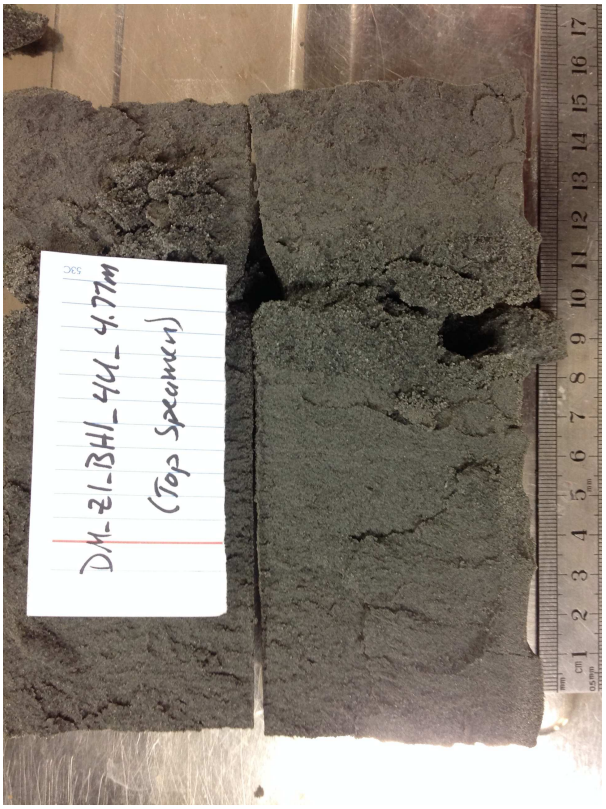

151 Kilmore St (FTG−7) DM BH1 Sample_4U 4.92m

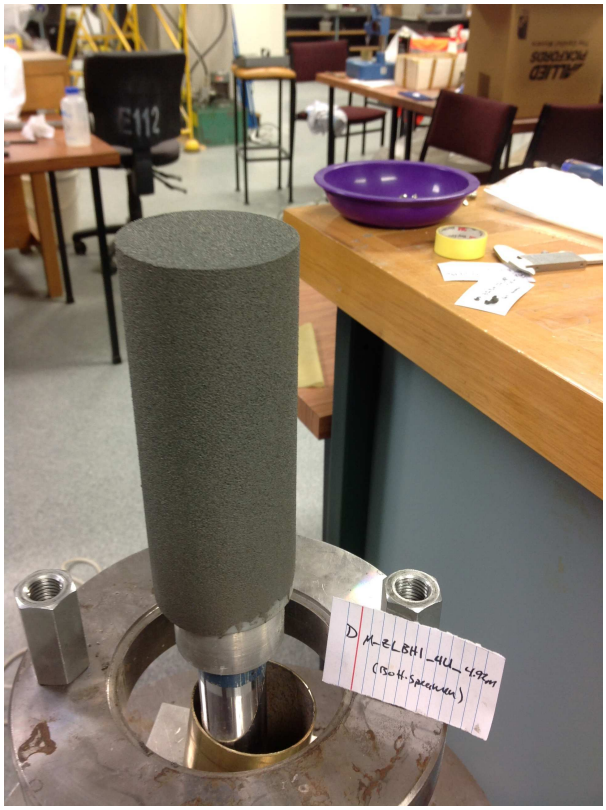

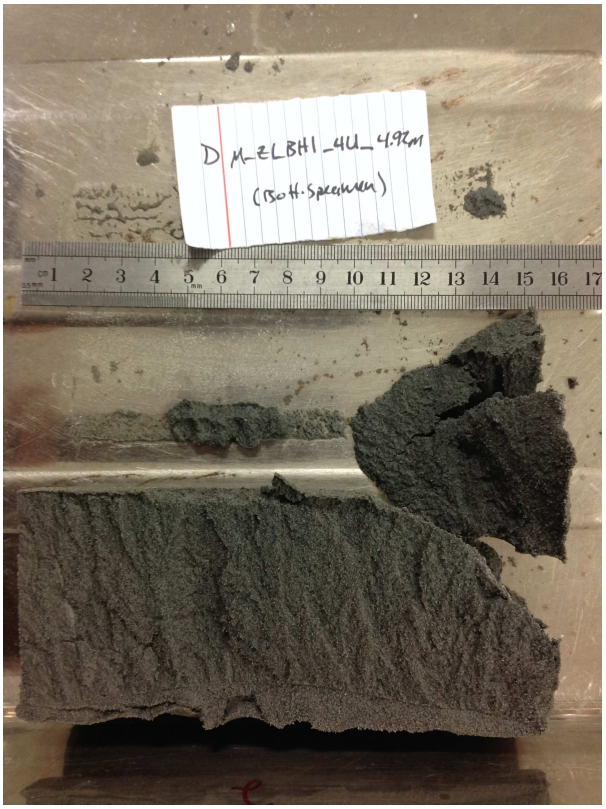

151 Kilmore St (FTG−7) DM BH1 Sample_5U 5.57m

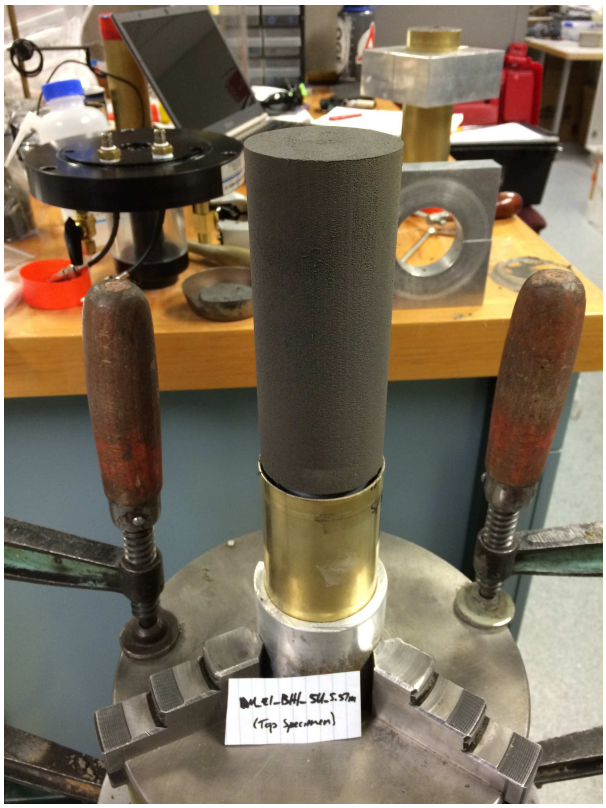

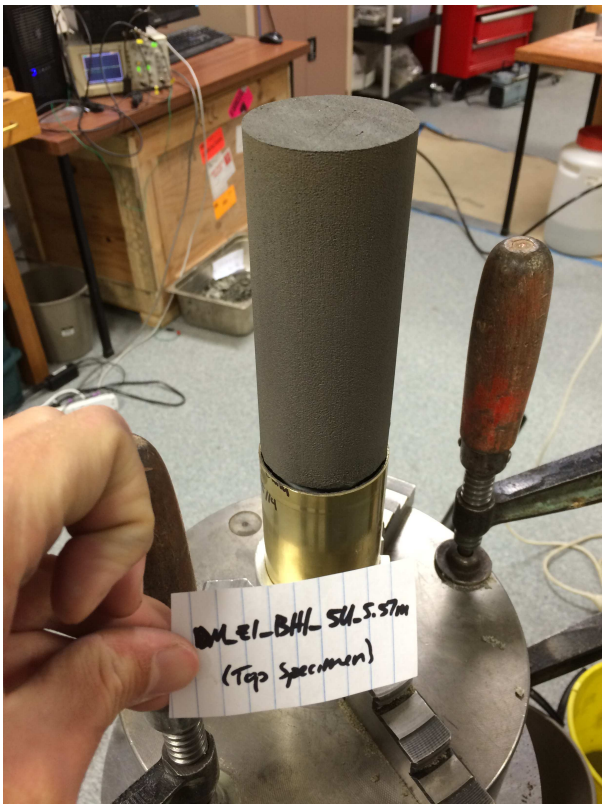

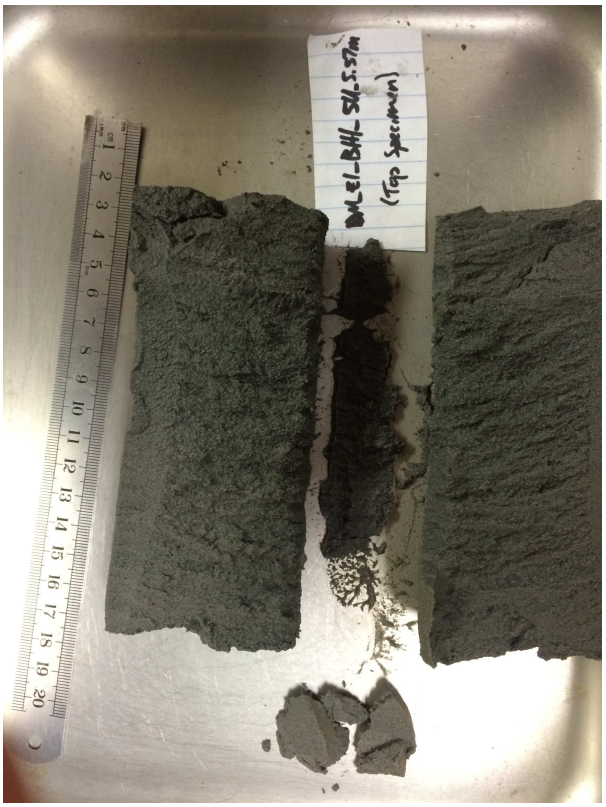

151 Kilmore St (FTG−7) DM BH2 Sample_4U 5.88m

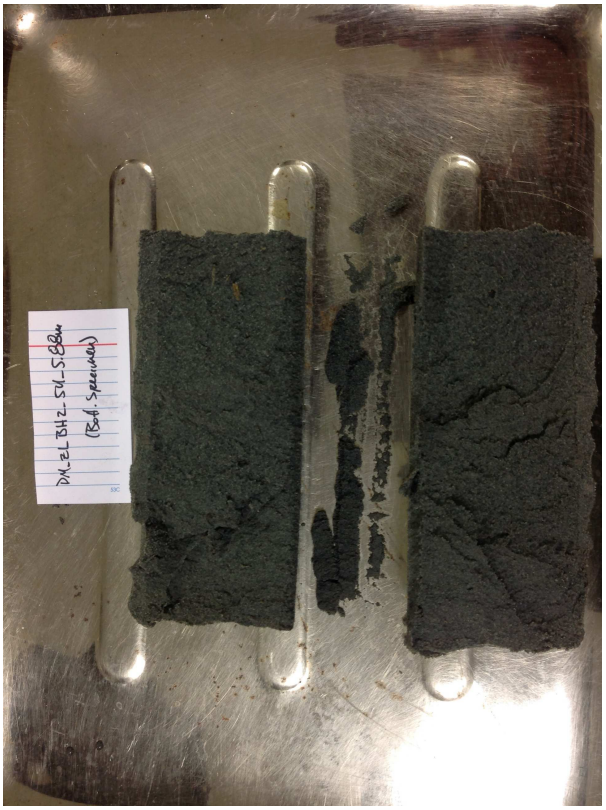

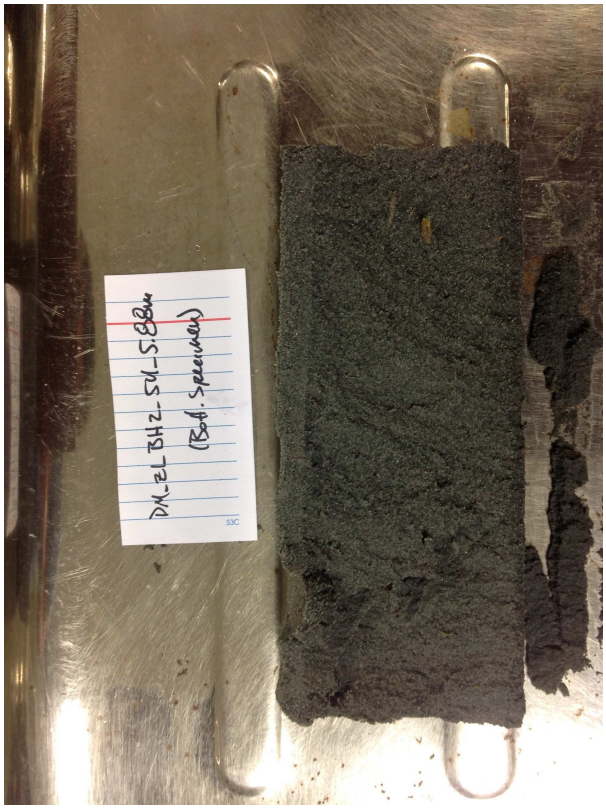

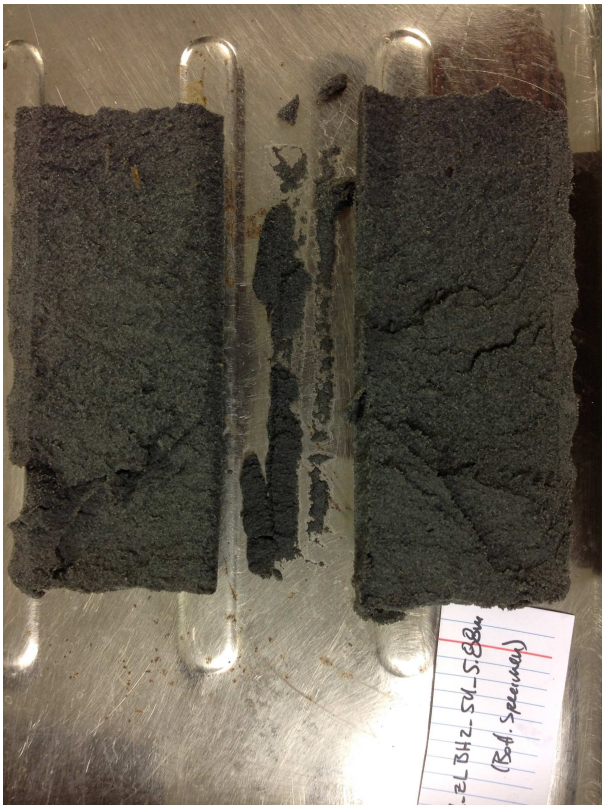

151 Kilmore St (FTG−7) DM BH2 Sample_6U 6.38m

151 Kilmore St (FTG−7) DM BH2 Sample_7U 6.72m

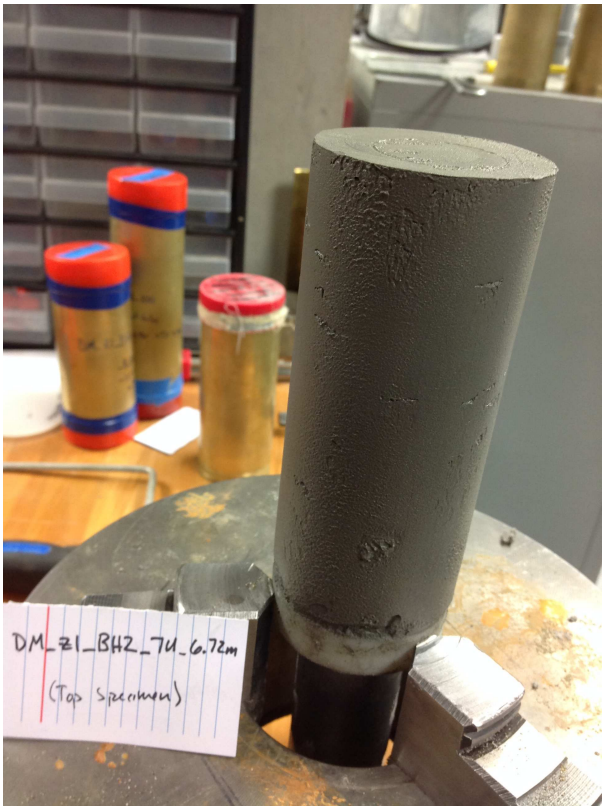

151 Kilmore St (FTG−7) DM BH1 Sample_7U 10.31m

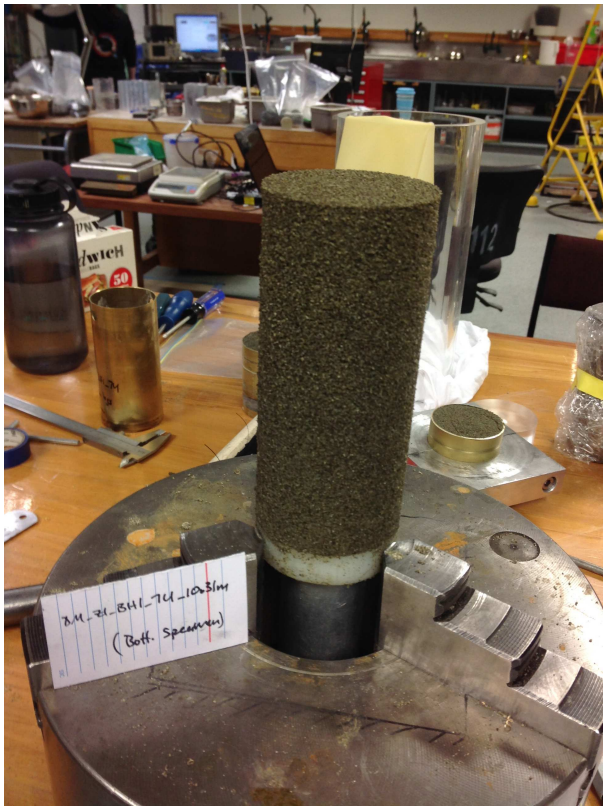

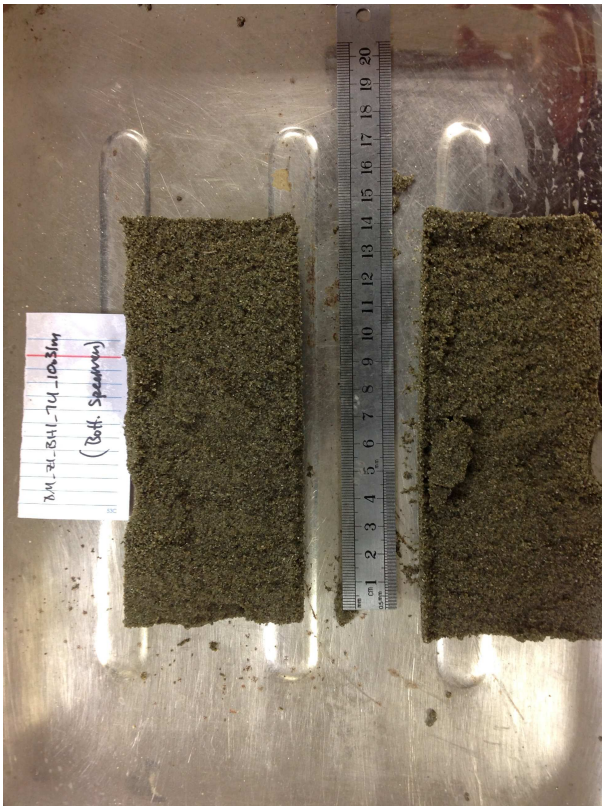

151 Kilmore St (FTG−7) DM BH2 Sample_10U 10.37m

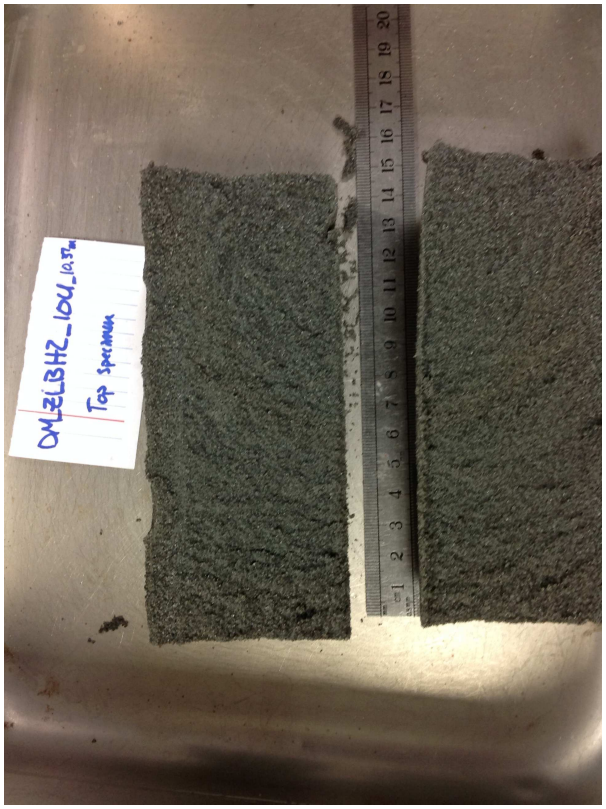

151 Kilmore St (FTG−7) DM BH2 Sample_11U 10.97m

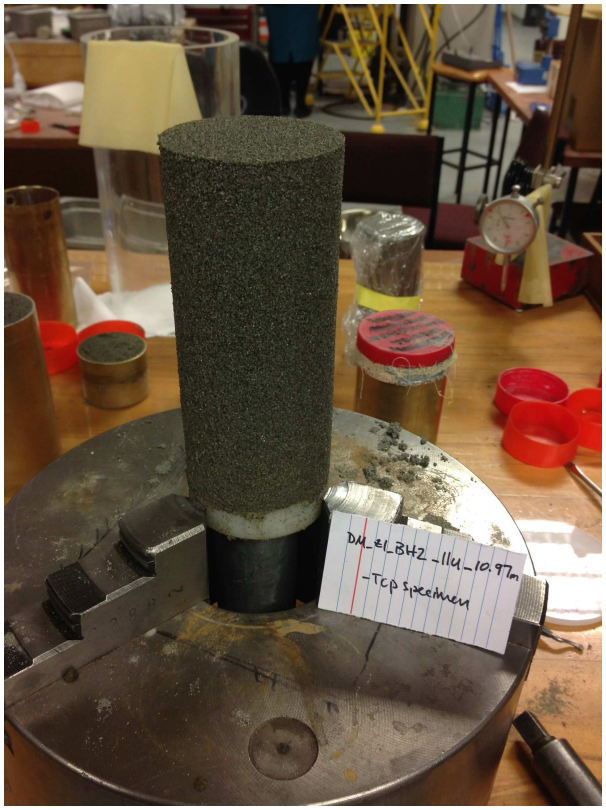

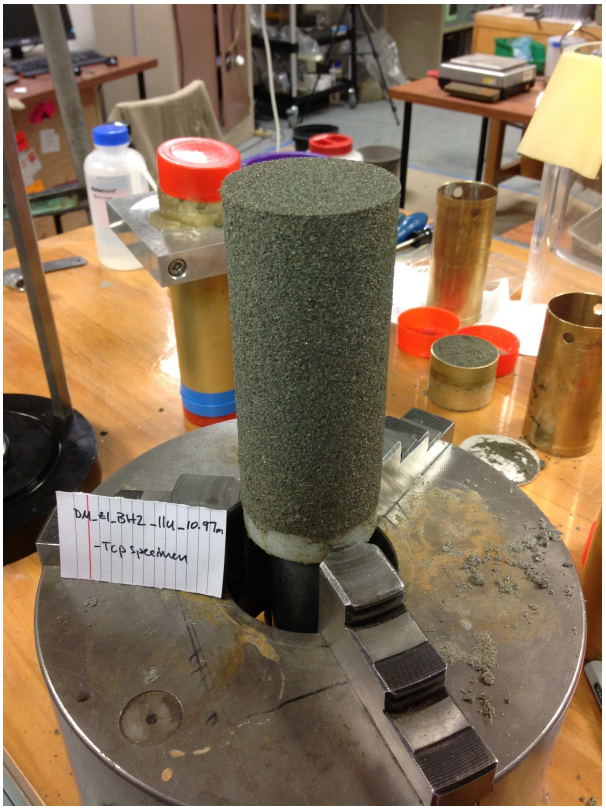

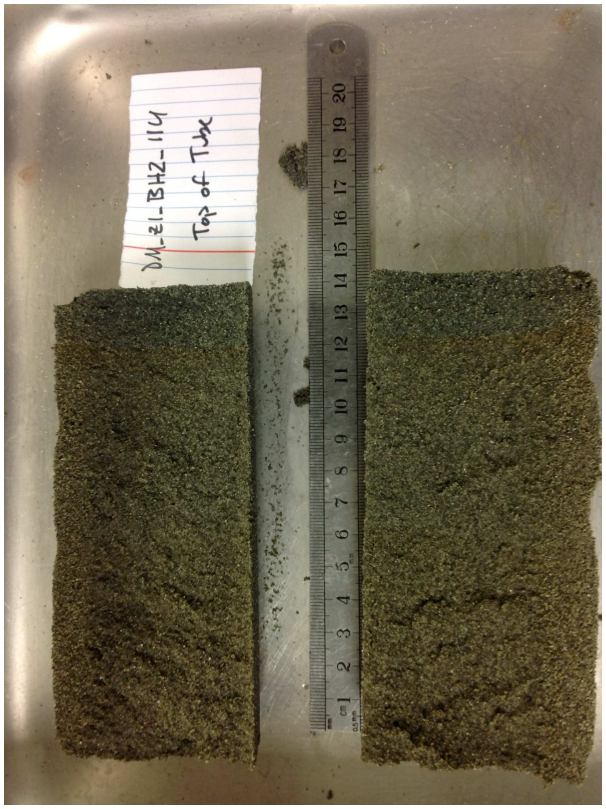

151 Kilmore St (FTG−7) DM BH2 Sample_11U 11.11m

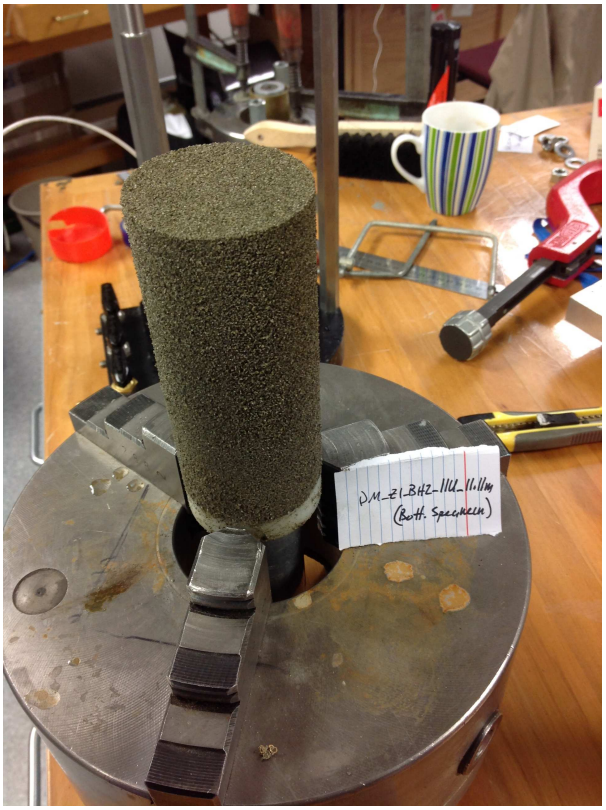

199 Armagh St (CTUC Bldg.) DM BH1 Sample_2U 2.82m

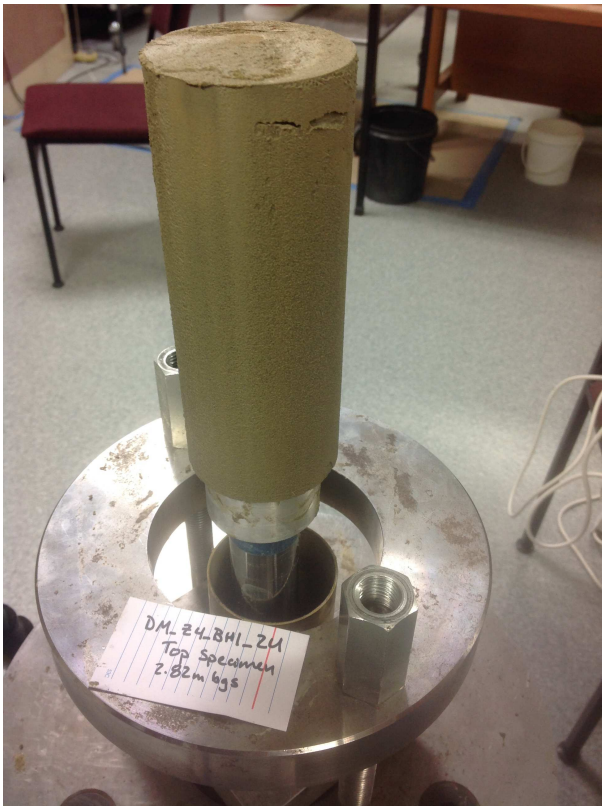

199 Armagh St (CTUC Bldg.) DM BH1 Sample_2U 2.98m

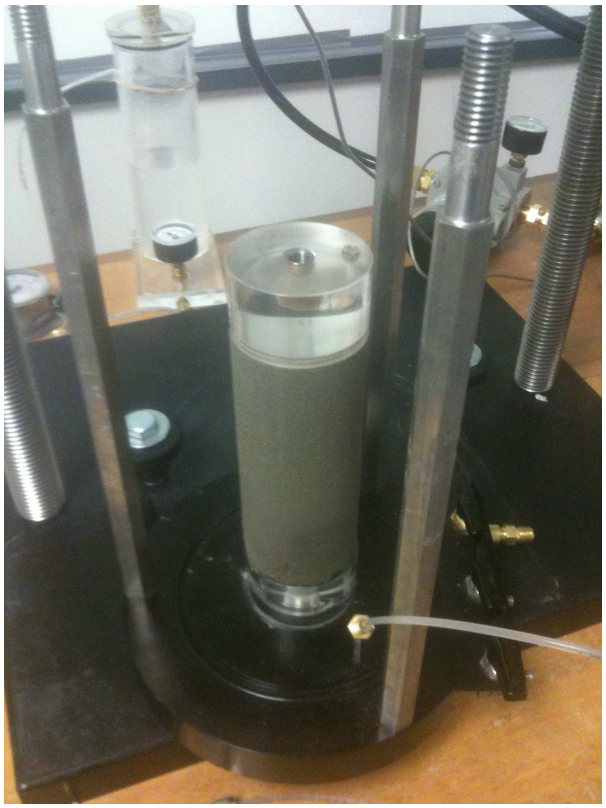

199 Armagh St (CTUC Bldg.) DM BH1 Sample_3U 3.33m

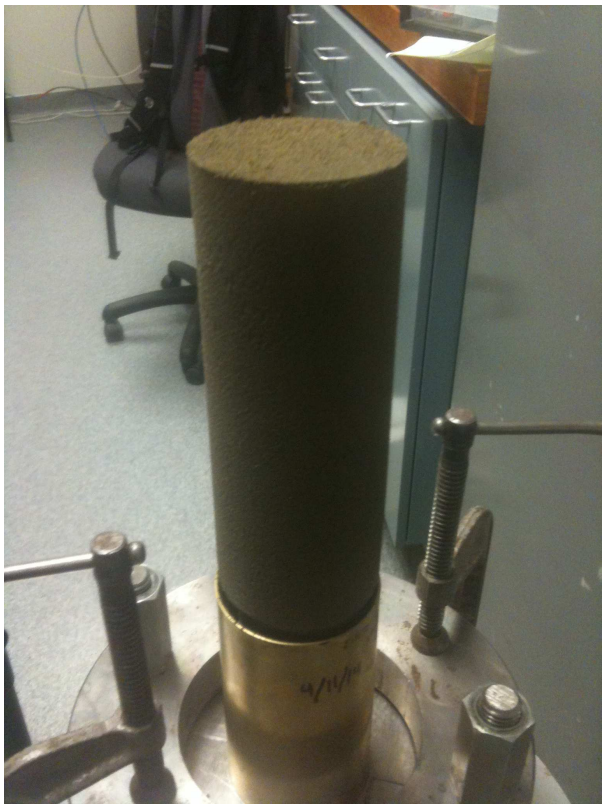

199 Armagh St (CTUC Bldg.) DM BH1 Sample_3U 3.48m

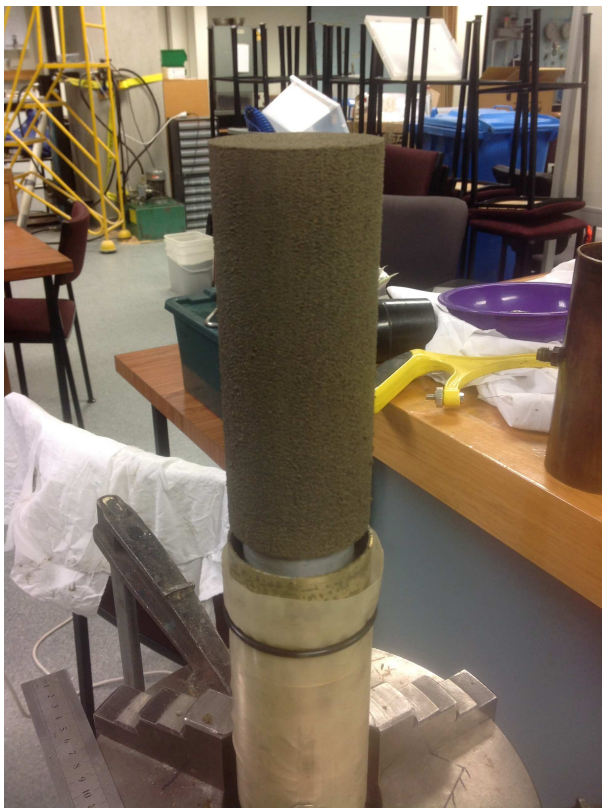

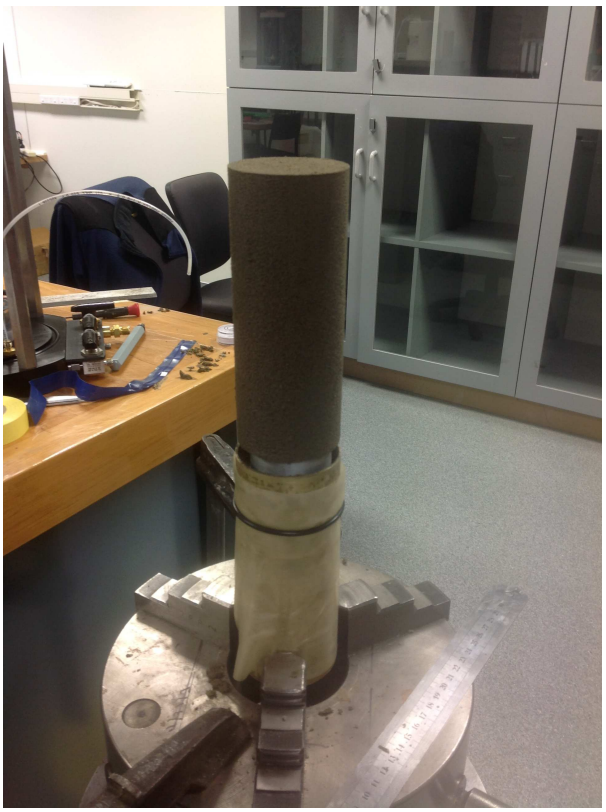

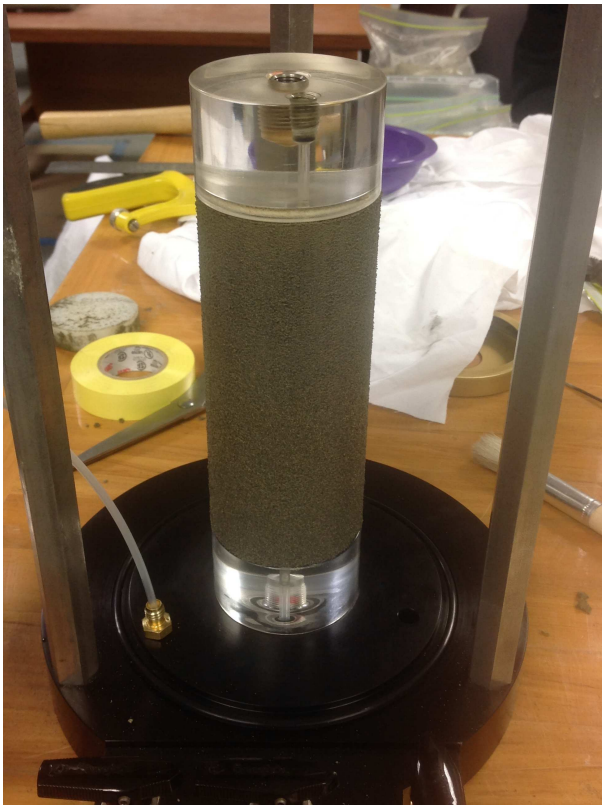

199 Armagh St (CTUC Bldg.) DM BH1 Sample_4U 3.82m

199 Armagh St (CTUC Bldg.) DM BH1 Sample_4U 3.98m

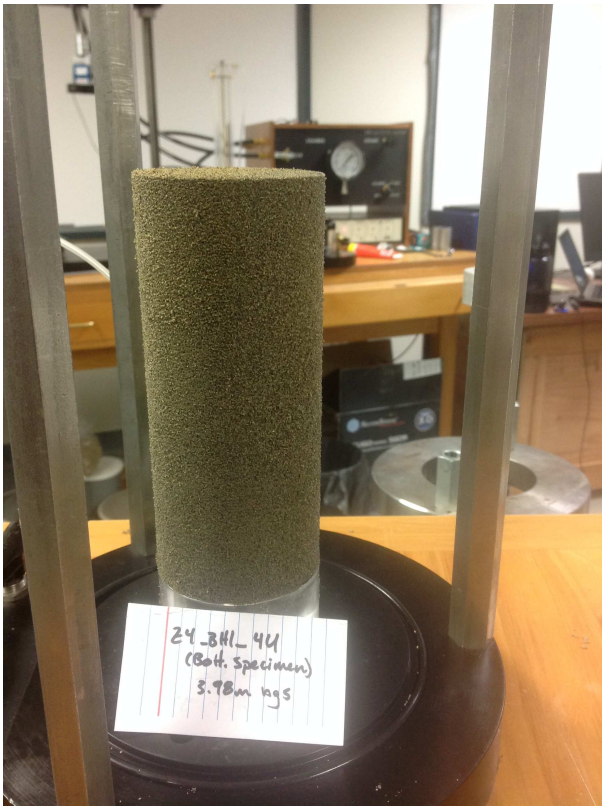

199 Armagh St (CTUC Bldg.) DM BH1 Sample_7U 13.67m

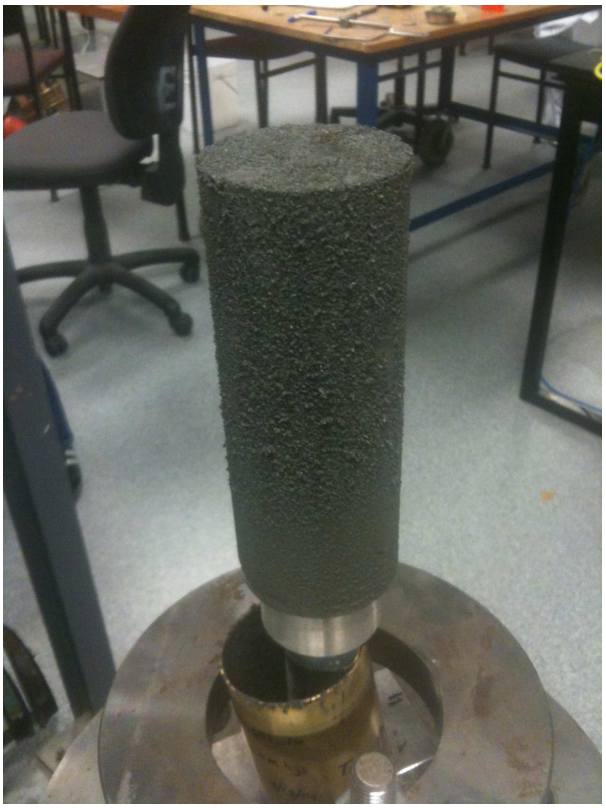

119 Armagh St. (PWC Bldg.) DM BH1b Sample_3U 12.82m

119 Armagh St. (PWC Bldg.) DM BH1b Sample_5U 13.81m

119 Armagh St. (PWC Bldg.) DM BH1a Sample_7U 14.27m

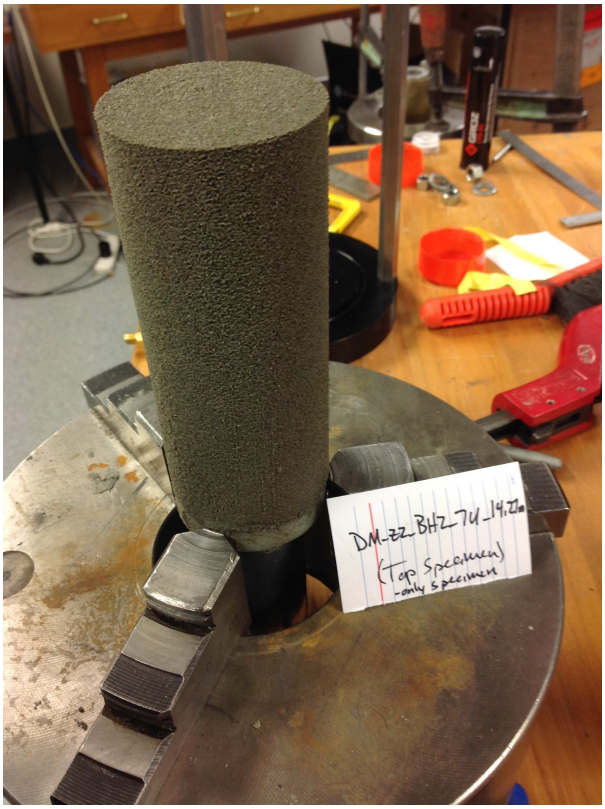

119 Armagh St. (PWC Bldg.) DM BH1b Sample_6U 14.32m

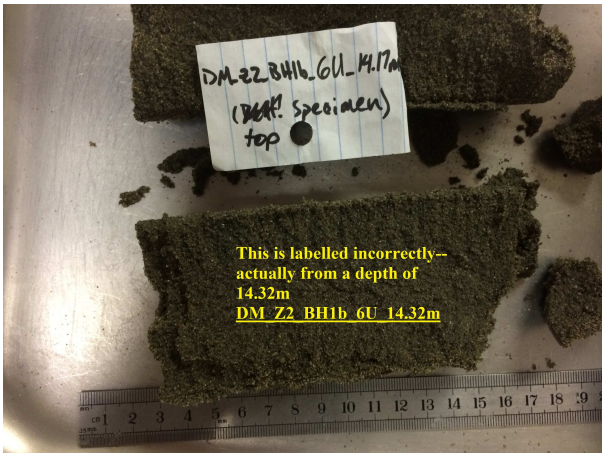

119 Armagh St. (PWC Bldg.) DM BH1b Sample_7U 14.57m

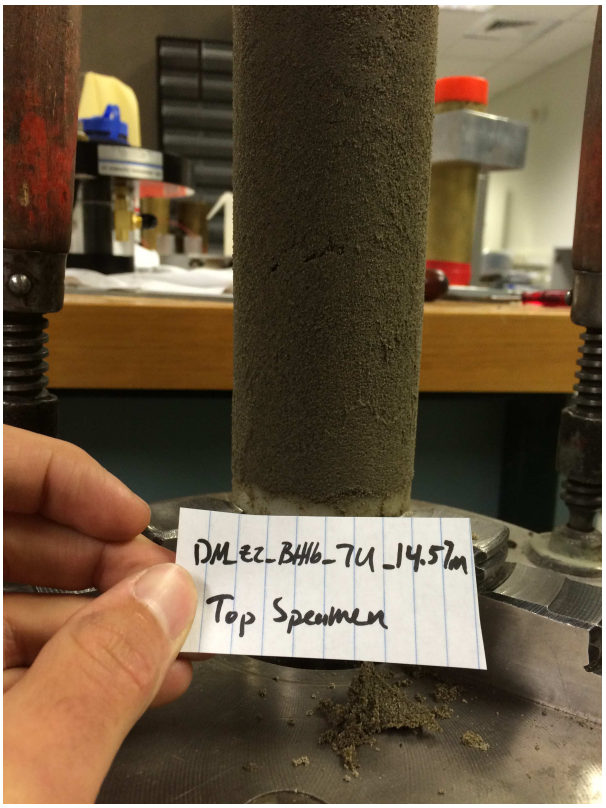

119 Armagh St. (PWC Bldg.) DM BH1b Sample_7U 14.82m

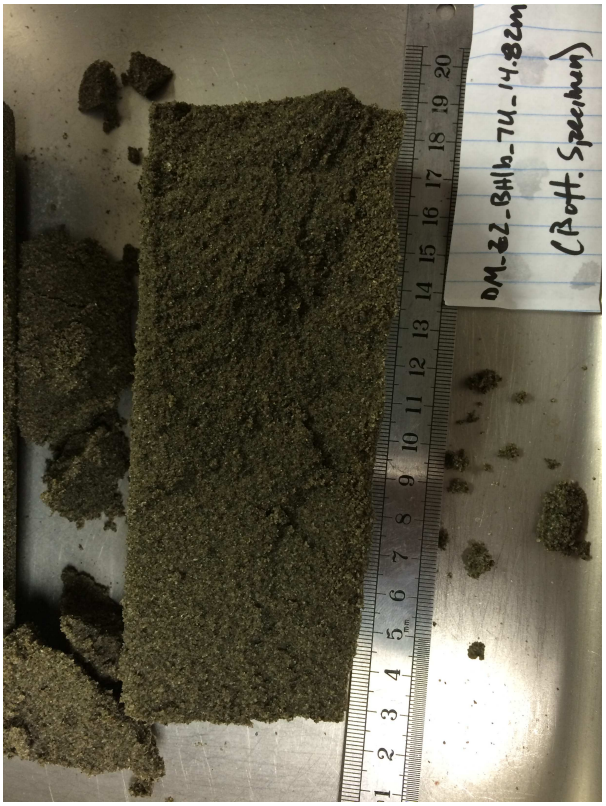

90 Armagh St. (VT/VSA Bldg.) DM BH2 Sample_1U 7.44m

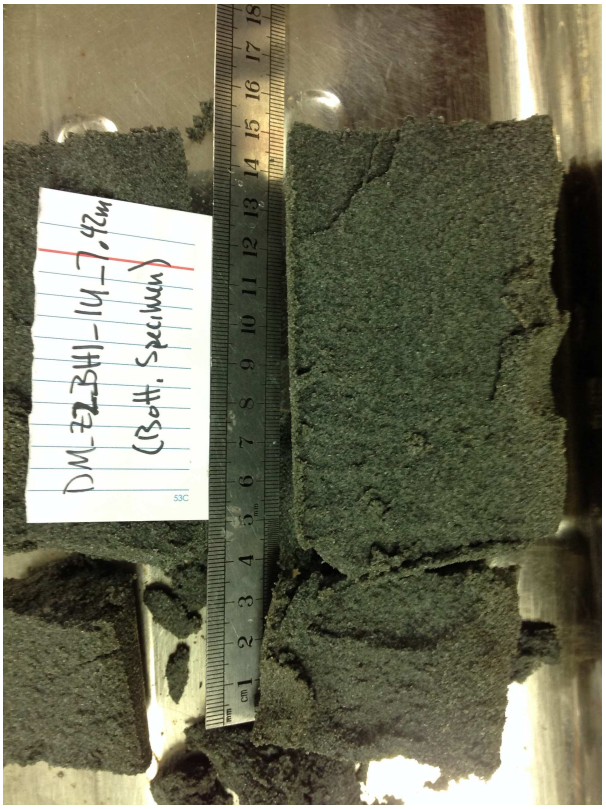

90 Armagh St. (VT/VSA Bldg.) DM BH2 Sample_2U 7.77m

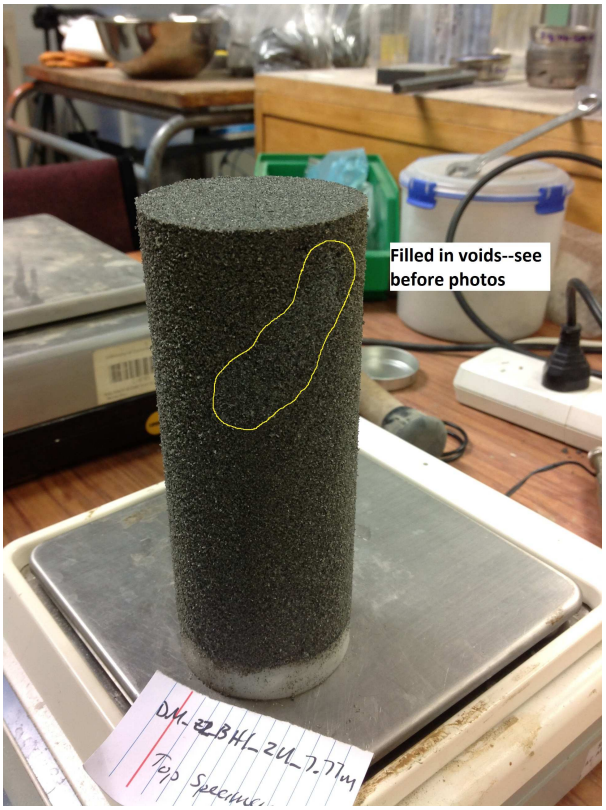

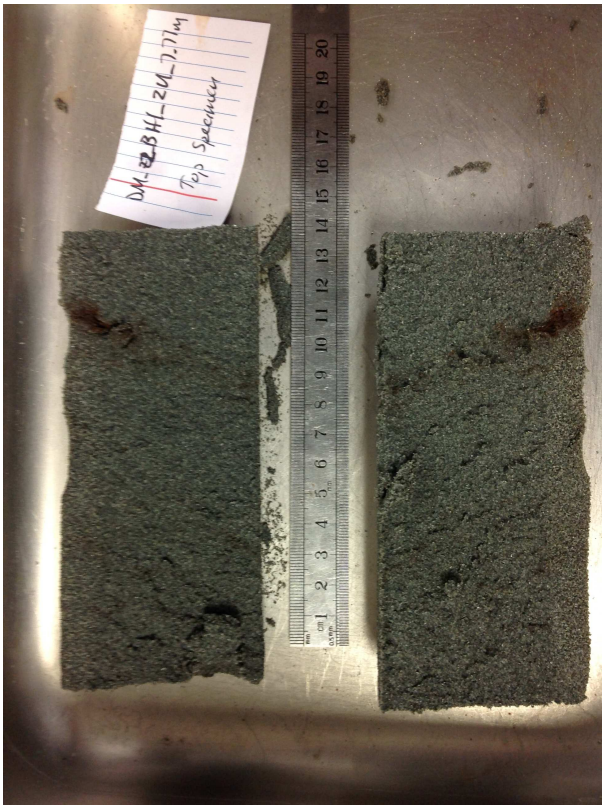

90 Armagh St. (VT/VSA Bldg.) DM BH2 Sample_2U 7.92m

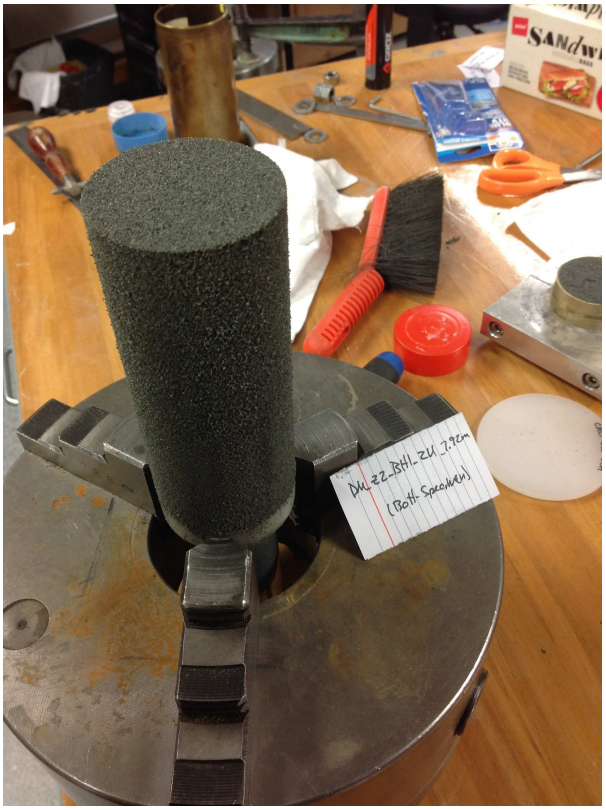

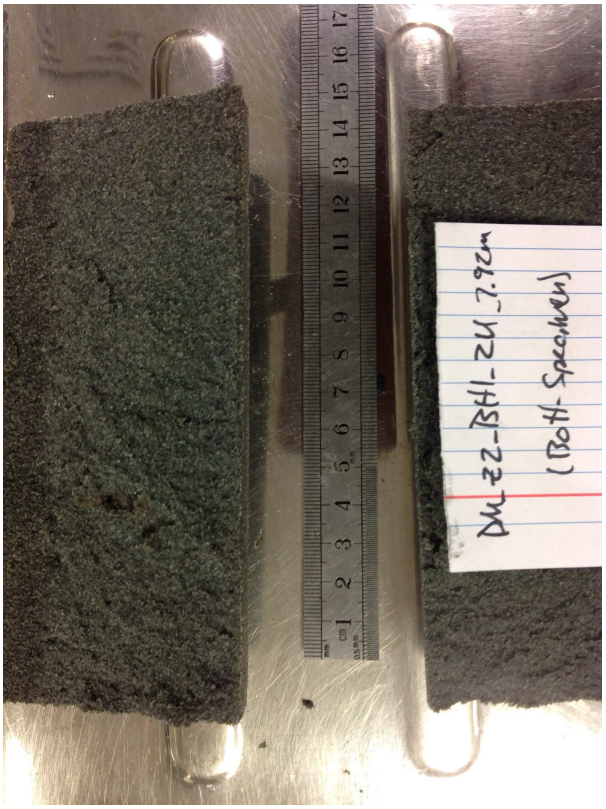

90 Armagh St. (VT/VSA Bldg.) DM BH2 Sample_5U 11.32m

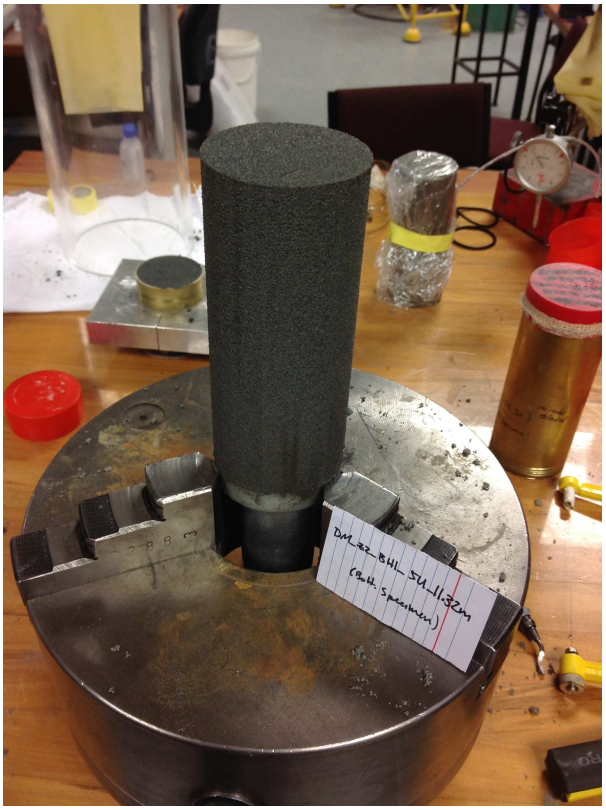

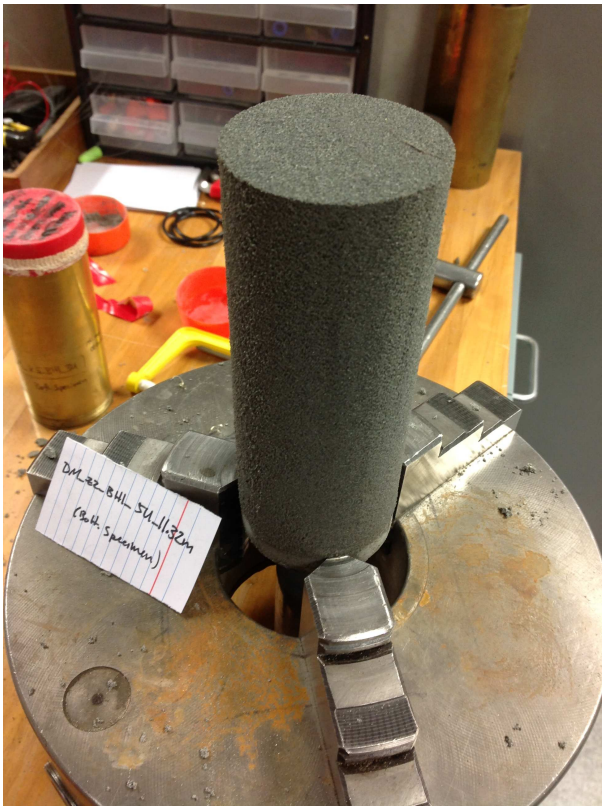

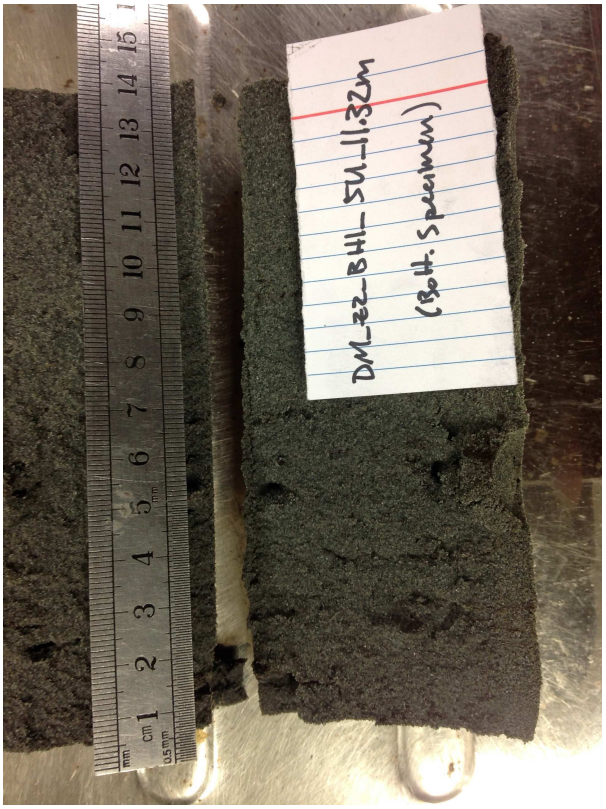

90 Armagh St. (VT/VSA Bldg.) DM BH2 Sample_10U 13.77m

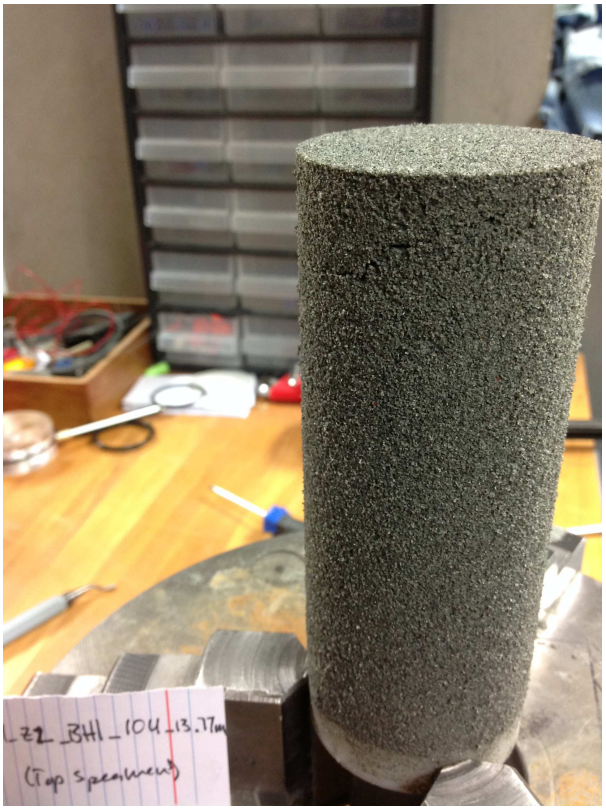

90 Armagh St. (VT/VSA Bldg.) DM BH2 Sample_10U 13.92m

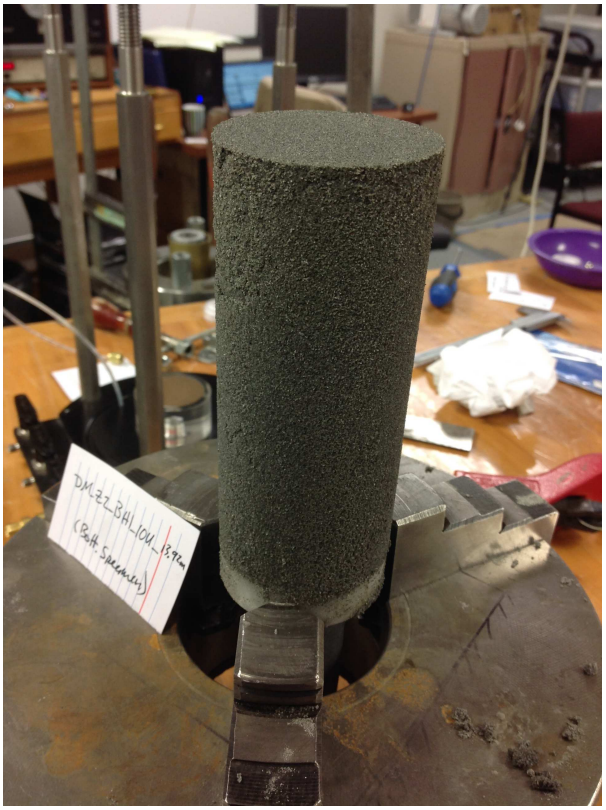

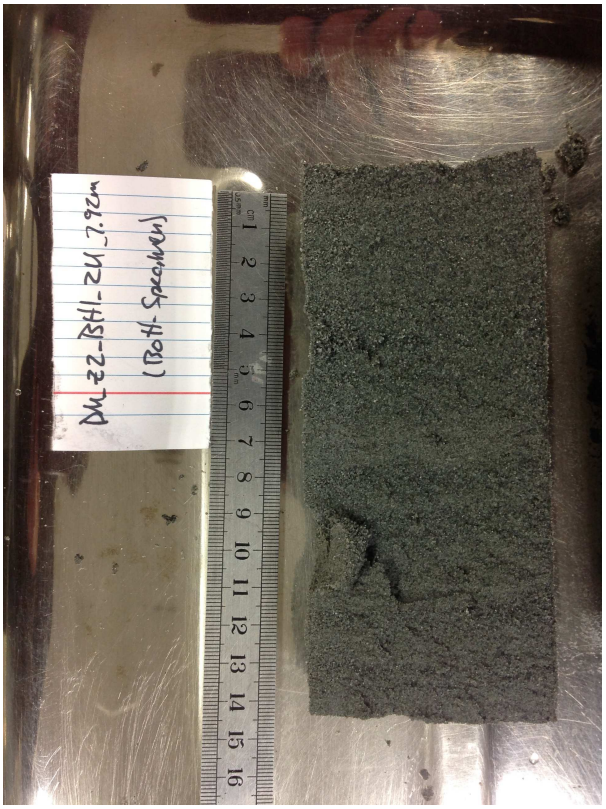

48 Lismore St. (LS−II Bldg.) DM BH1 Sample_1U 1.82m

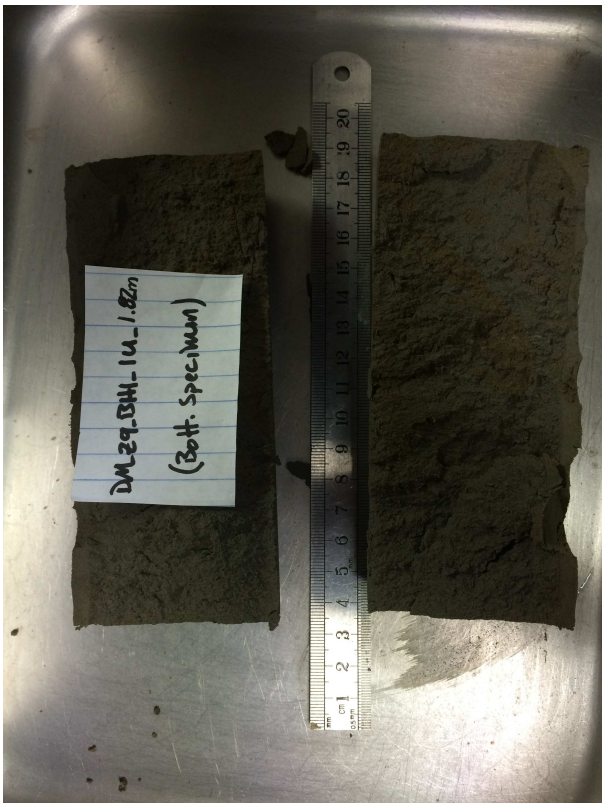

48 Lismore St. (LS−II Bldg.) DM BH1 Sample_2U 2.17m

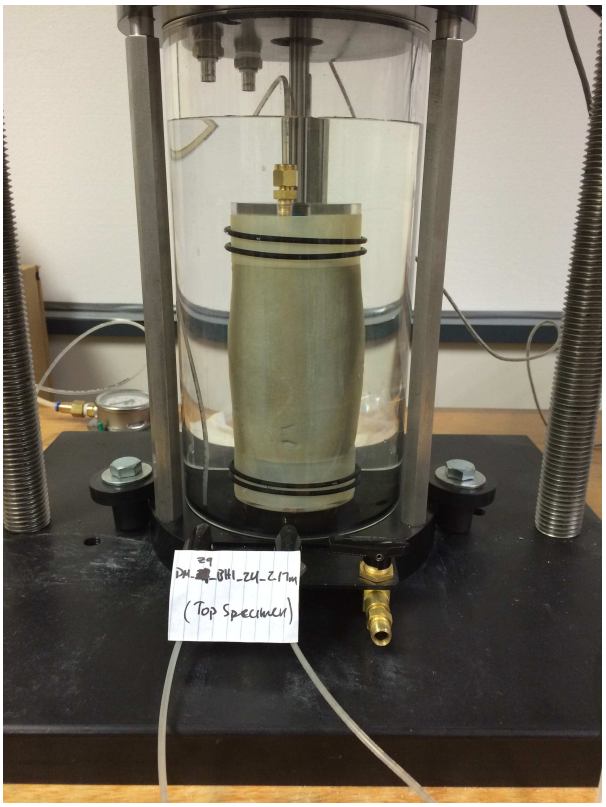

48 Lismore St. (LS−II Bldg.) DM BH1 Sample_4U 4.27m

48 Lismore St. (LS−II Bldg.) DM BH1 Sample_4U 4.42m

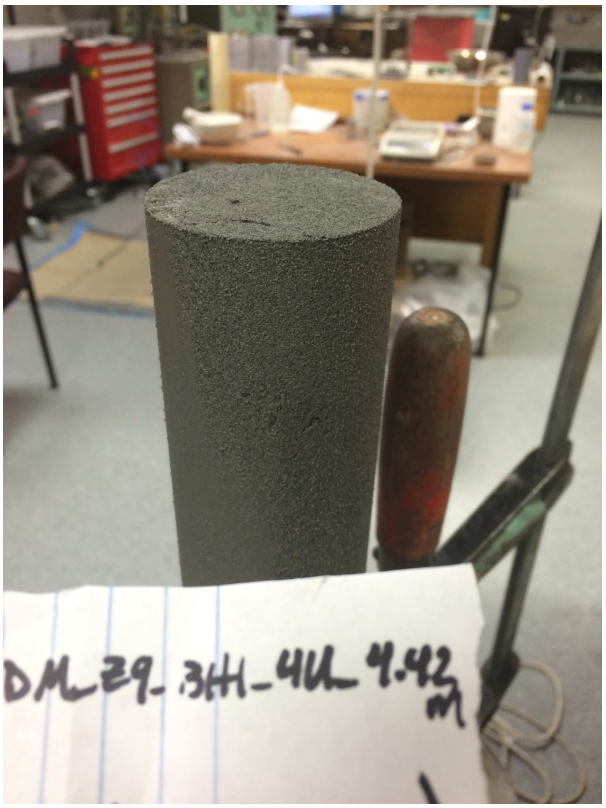

48 Lismore St. (LS−II Bldg.) DM BH1 Sample_5U 5.32m

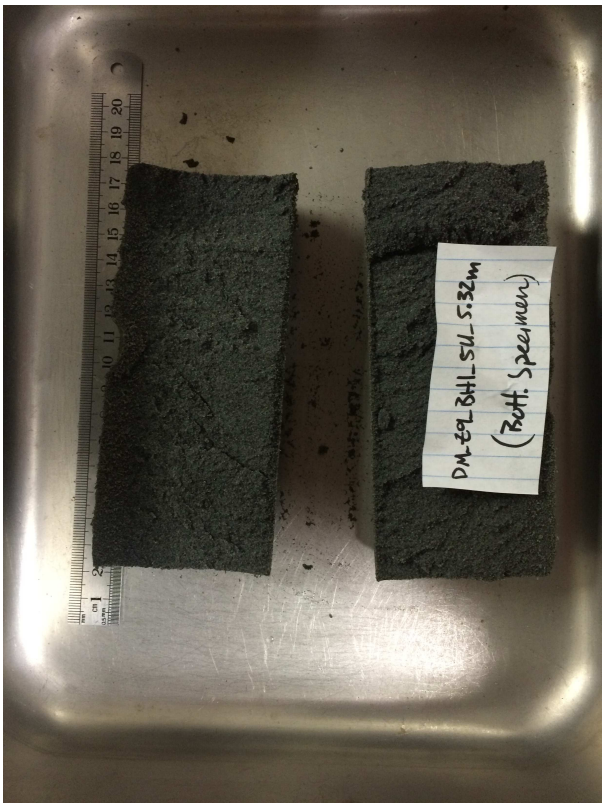

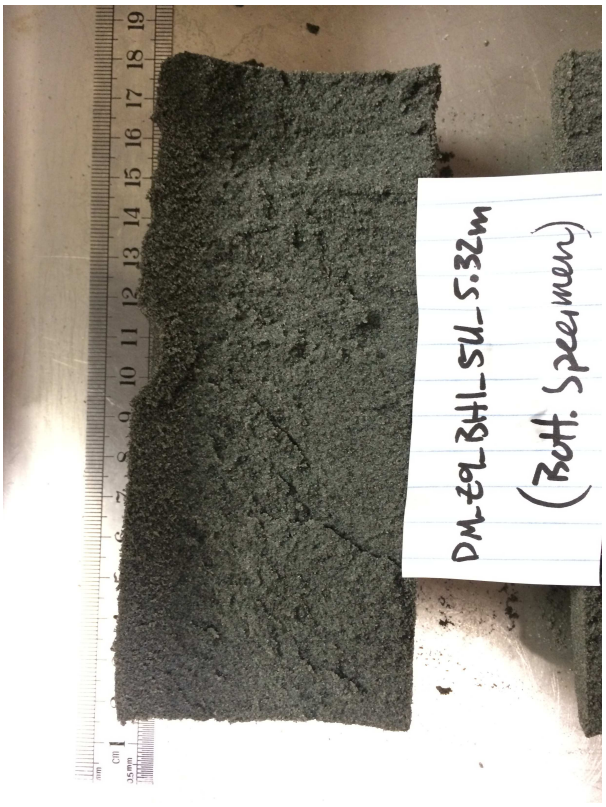

48 Lismore St. (LS−II Bldg.) DM BH1 Sample_7U 6.26m

193/195 Peter. St (SA Bldg.) DM BH1 Sample_1U 1.82m

Appendix C.5

Raw Triaxial Test Data

Triaxial test data from “undisturbed” specimen testing are included as separate electronic files attached to this dissertation

Appendix D

Test Results for Steady State Testing of Reconstituted Specimens

The following corrections were made to the triaxial test data presented in Appendix D:

Membrane correction

Axial stresses were corrected for loads carried by the membrane (i.e., not the soil) in both cyclic and monotonic triaxial tests using the following equation proposed by Duncan and Seed (1967):

$$\Delta\sigma_{ax-m} = -C_{am} * \left(\frac{2}{3}\right) * E_m \frac{4t_{om}}{D_{os}}$$

Where $\Delta\sigma_{ax\text{-}m}$ is the portion of the applied stress attributed to the membrane,

$$C_{am} = \left(\frac{1 + 2\varepsilon_{at} - \sqrt{\frac{1-\varepsilon_v}{1-\varepsilon_{at}}}}{1-\varepsilon_v}\right)$$

E_m is the Young's modulus of the membrane (assumed as 14 kg/cm^2=1373.4 kPa)
t_{om} is the initial thickness of the membrane prior to testing
D_{os} is the initial diameter of the specimen prior to testing
ε_{at} is the total axial strain during the test
ε_{vol} is the total volumetric strain during the test

Because of the negative sign in the calculation of $\Delta\sigma_{ax\text{-}m}$, this values should be added to the total applied stress if positive ε_{ax} represents compression (i.e., the specimen gets shorter) and negative ε_{ax} represents extension (i.e., the specimen gets taller). In this way, the axial stress being applied to the actual soil is less than the total axial stress being applied to the specimen and membrane in compression (i.e., $\Delta\sigma_{ax\text{-}m}$ is negative) and higher than the total axial stress in extension (i.e., $\Delta\sigma_{ax\text{-}m}$ is positive).

Area Correction

The monotonic triaxial tests conducted on reconstituted specimens for steady state testing were tested in a strain controlled loading frame different from the CKC triaxial apparatus used for testing "undisturbed" soil specimens; the same assumption was made regarding the deformation of the specimen as a right cylinder during shearing. The corrected area of the specimen was calculated as follows:

$$A_c = A_o * \left(\frac{1-\varepsilon_v}{1-\varepsilon_a}\right)$$

where A_c is the corrected area of the specimen, A_o is the initial area of the specimen, ε_v is the volumetric strain, and ε_a is the axial strain. See Germaine and Ladd (1988).

Appendix D.1

Results for CTH Site

D.1.1 Upper Silt Layer

D.1.2 Upper Sand Layer

D.1.3 Lower Sand Layer

Appendix D.1.1

Upper Silt Layer

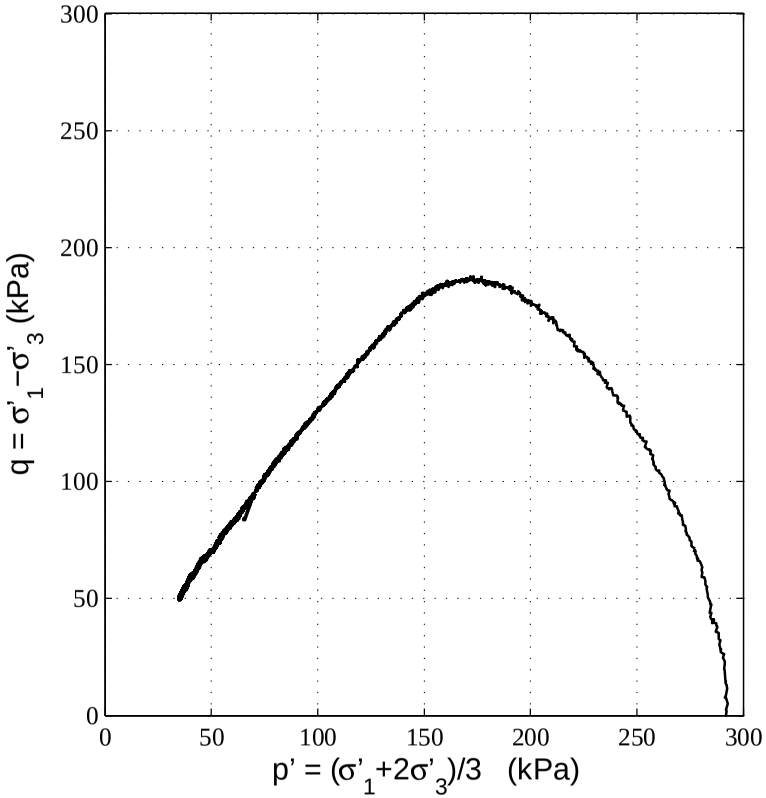

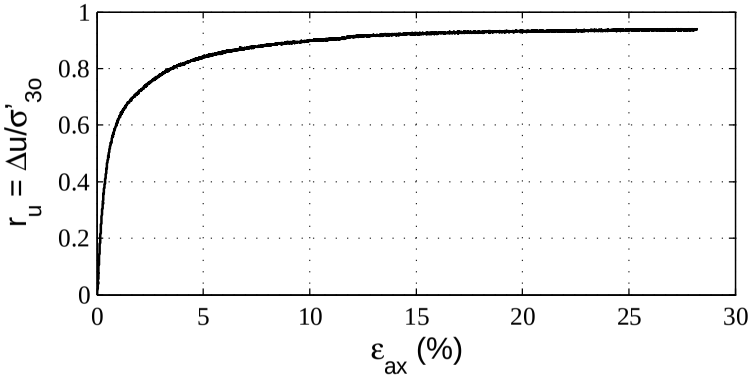

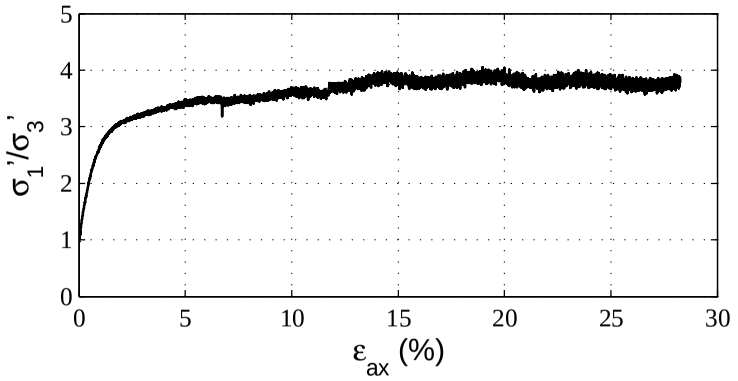

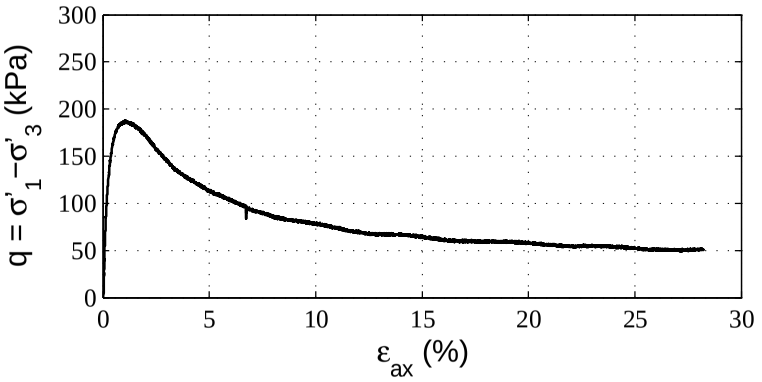

Steady State ICU Monotonic Triaxial Compression Test Data

Site:	CTH
Soil Unit:	Upp. Silt
Specimens Mixed:	DM_Z5_BH1_3U_3.07m DM_Z5_BH1_4U_3.67m DM_Z5_BH1_4U_3.83m
Test:	Test 1
σ'_{3o} (kPa):	295.3
e_o:	0.84
D_r (%)	––

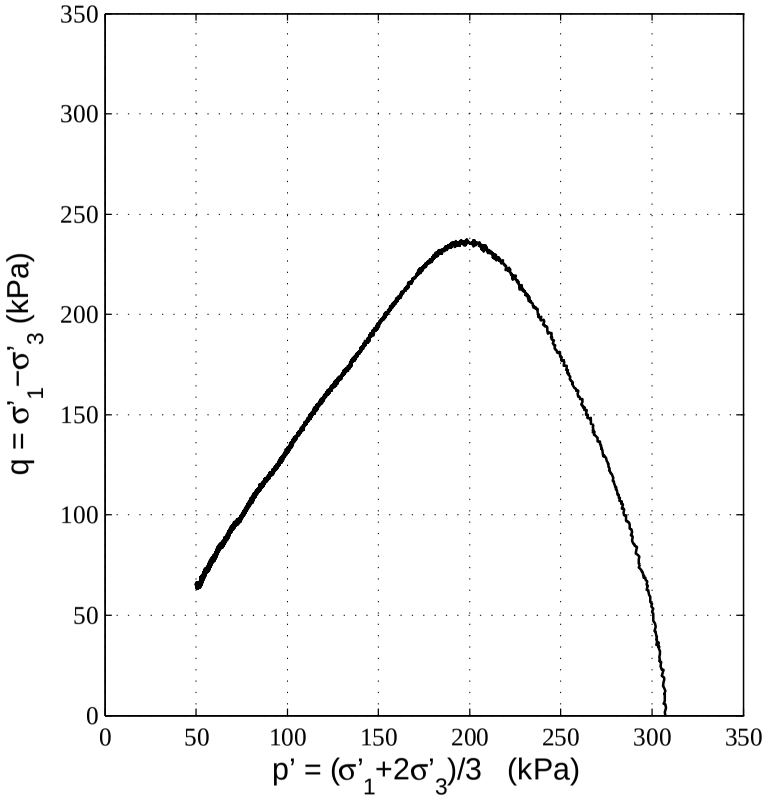

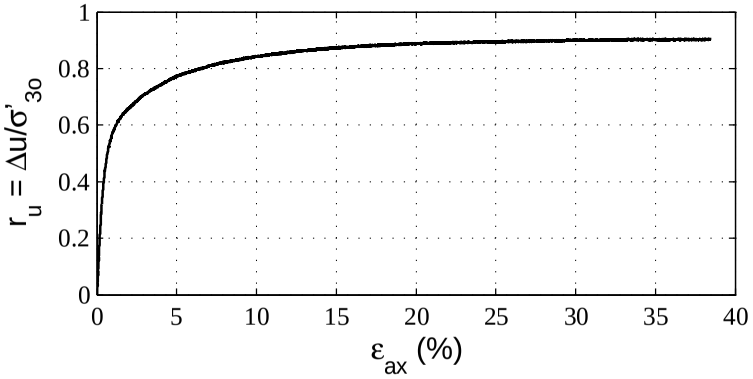

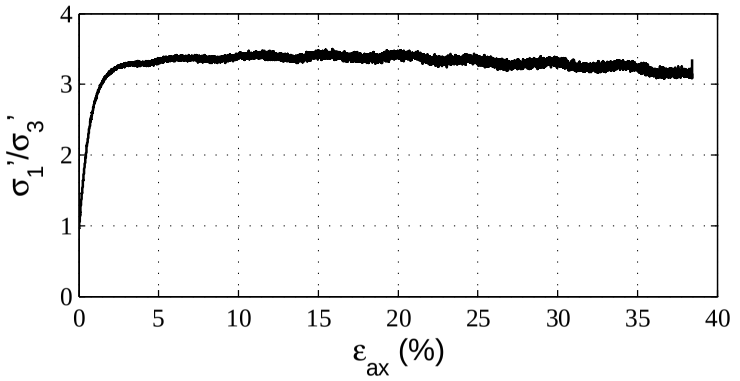

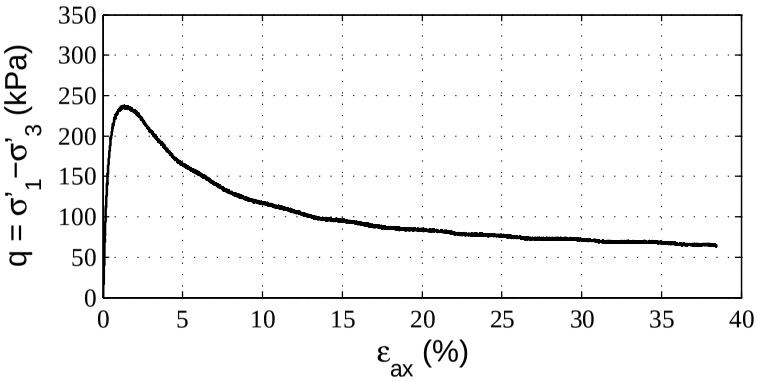

Steady State ICU Monotonic Triaxial Compression Test Data

Site:	CTH
Soil Unit:	Upp. Silt
Specimens Mixed:	DM_Z5_BH1_3U_3.07m DM_Z5_BH1_4U_3.67m DM_Z5_BH1_4U_3.83m
Test:	Test 2
σ'_{3o} (kPa):	310.4
e_o:	0.82
D_r (%)	––

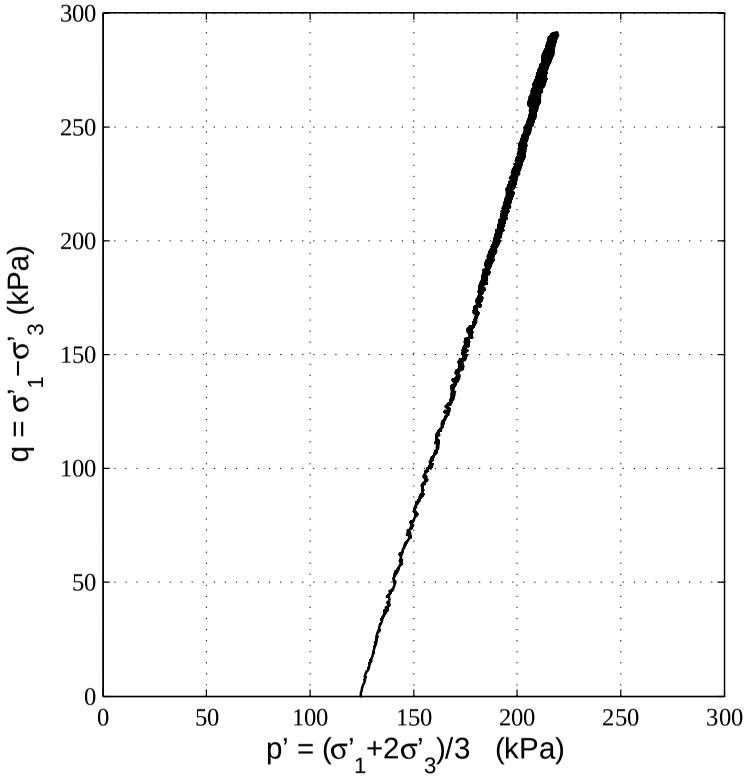

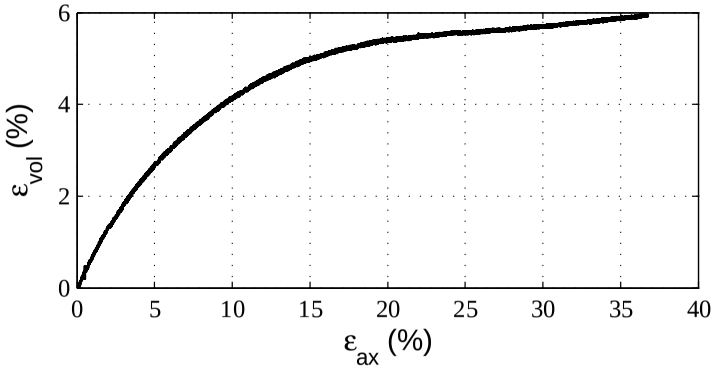

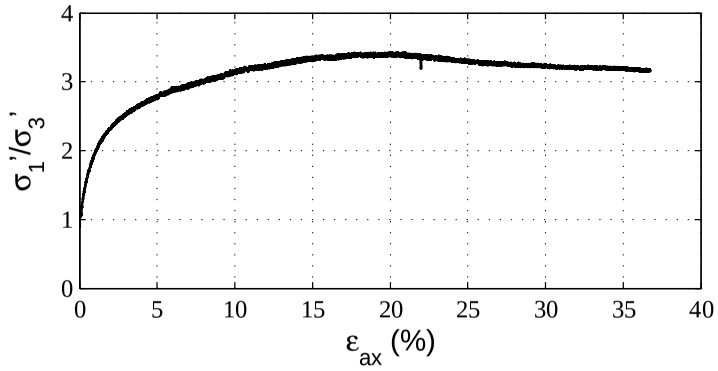

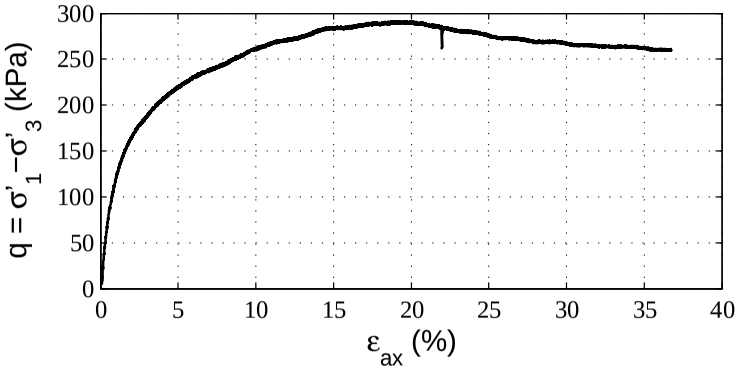

Steady State CD Monotonic Triaxial Compression Test Data

Site:	CTH
Soil Unit:	Upp. Silt
Specimens Mixed:	DM_Z5_BH1_3U_3.07m DM_Z5_BH1_4U_3.67m DM_Z5_BH1_4U_3.83m
Test:	Test 3
σ'_{3o} (kPa):	124.1
e_o:	0.87
e_{ss}	0.76
D_r (%)	––

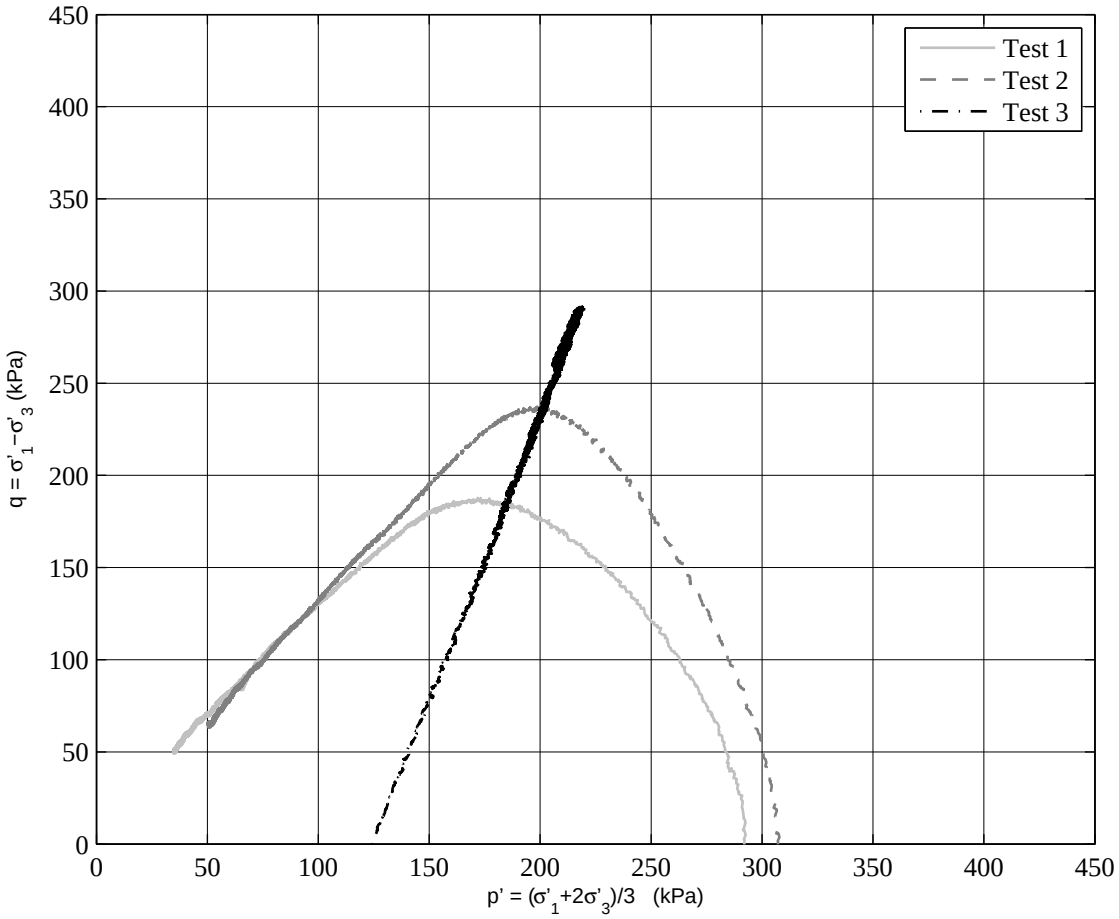
Test 1
Test 2
Test 3
q = σ'1−σ'3 (kPa)
p' = (σ'1+2σ'3)/3 (kPa)
0
50
100
150
200
250
300
350
400
450

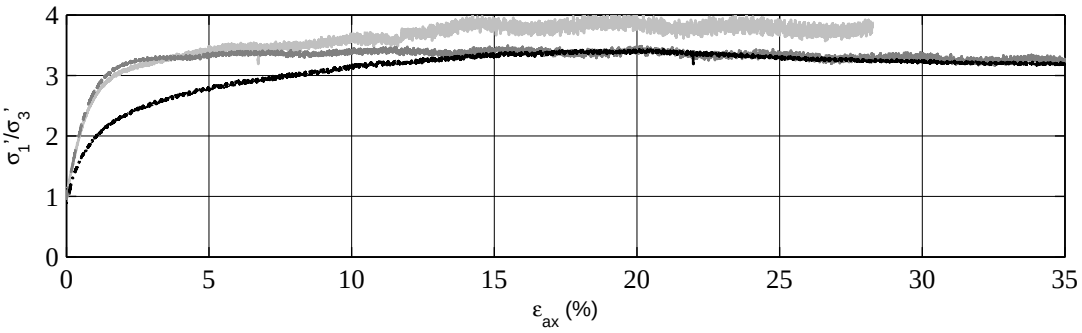
σ1'/σ3'
εax (%)
0
1
2
3
4
5
10
15
20
25
30
35

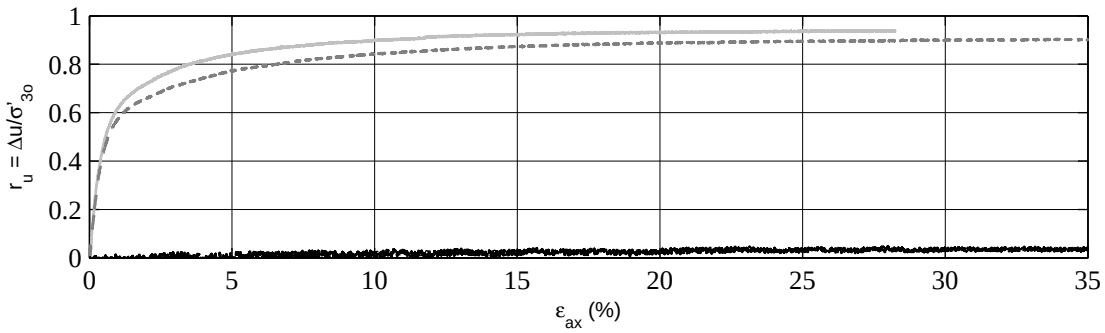
ru = Δu/σ'3o
εax (%)
0
0.2
0.4
0.6
0.8
1
5
10
15
20
25
30
35

Appendix D.1.2

Upper Sand Layer

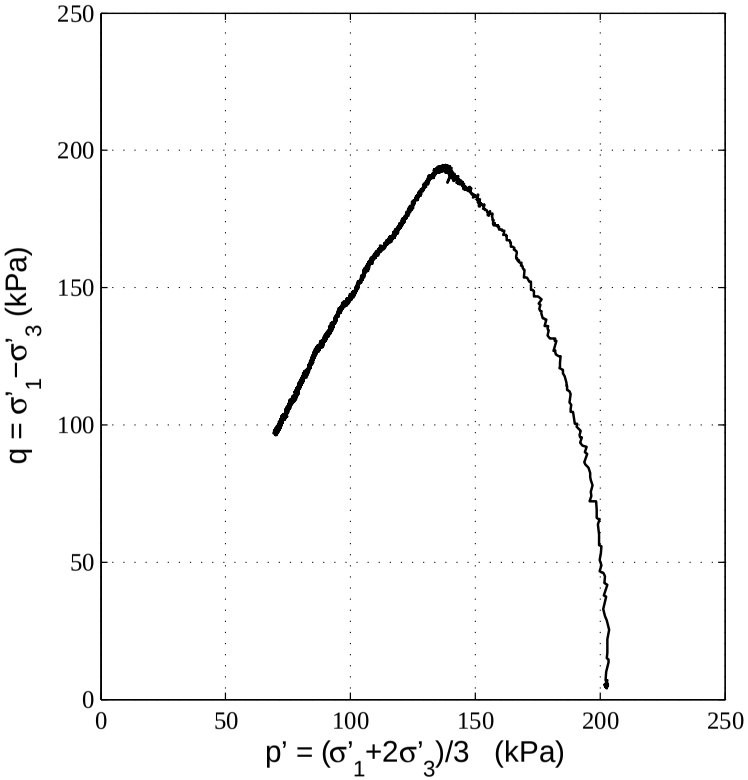

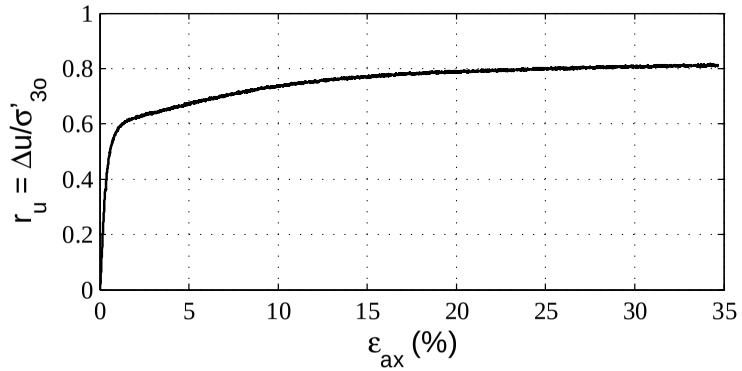

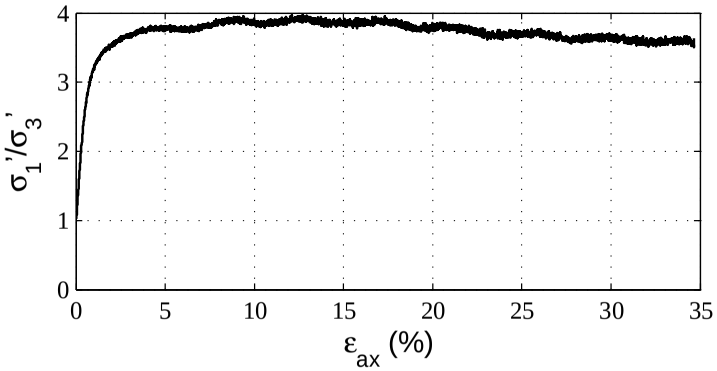

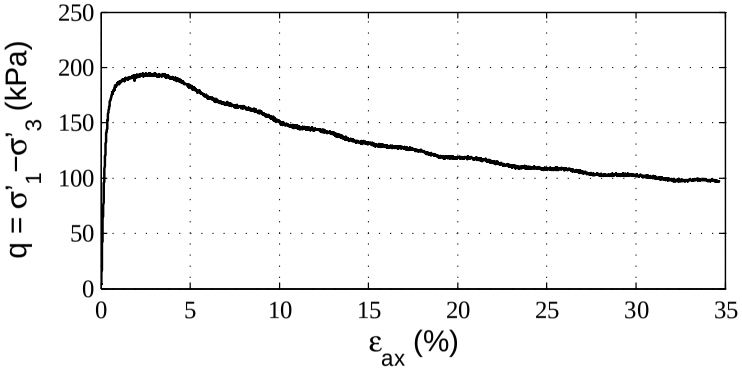

Steady State ICU Monotonic Triaxial Compression Test Data

Site:	CTH
Soil Unit:	Upp. Sand
Specimens Mixed:	DM_Z5_BH1_5U_4.27m DM_Z5_BH1_5U_4.43m
Test:	Test 1
σ'_{3o} (kPa):	200.7
e_o:	1.03
D_r (%)	22

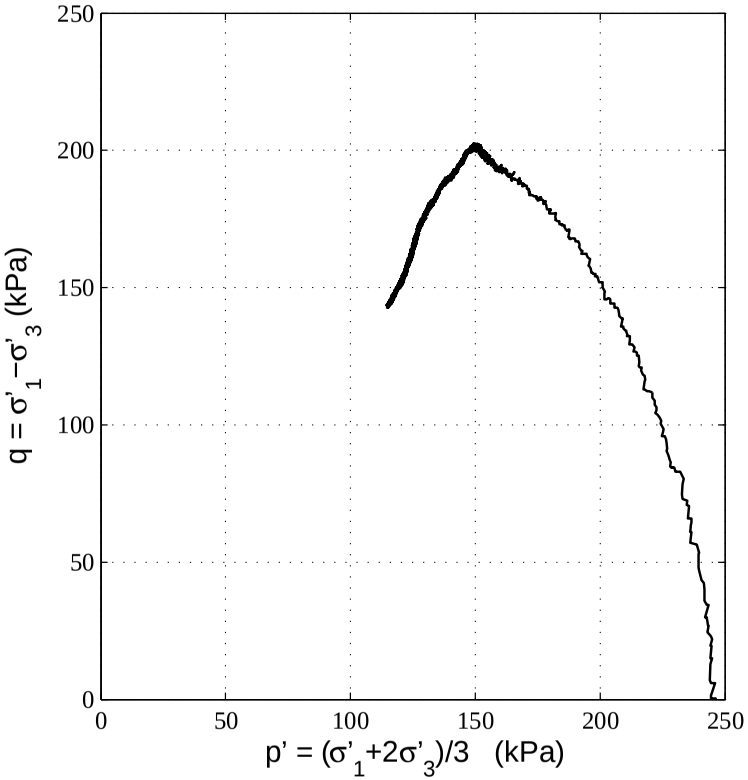

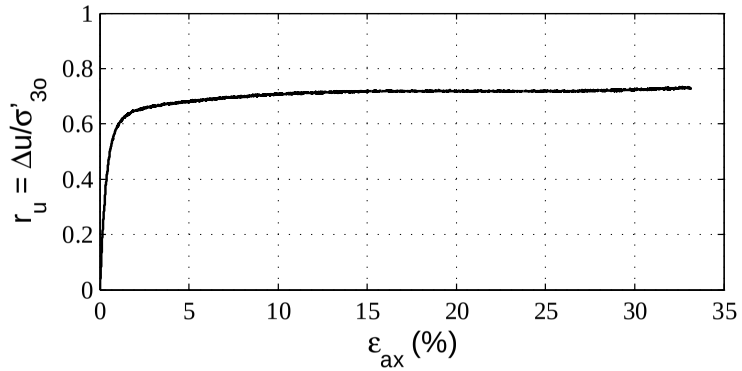

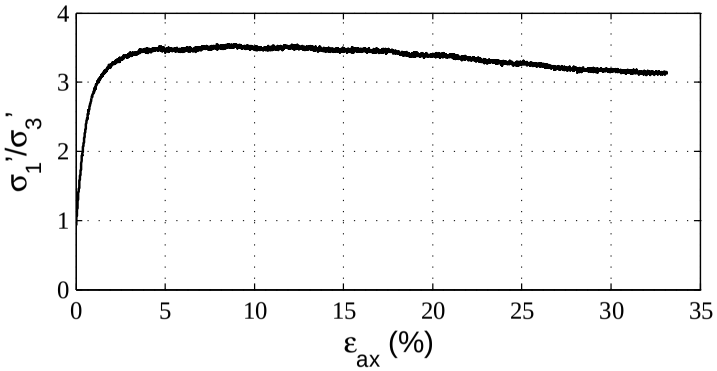

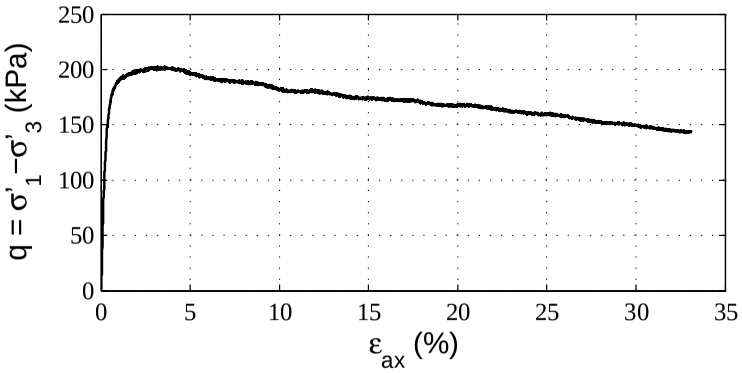

Steady State ICU Monotonic Triaxial Compression Test Data

Site:	CTH
Soil Unit:	Upp. Sand
Specimens Mixed:	DM_Z5_BH1_5U_4.27m DM_Z5_BH1_5U_4.43m
Test:	Test 2
σ'_{3o} (kPa):	249.6
e_o:	0.98
D_r (%)	33

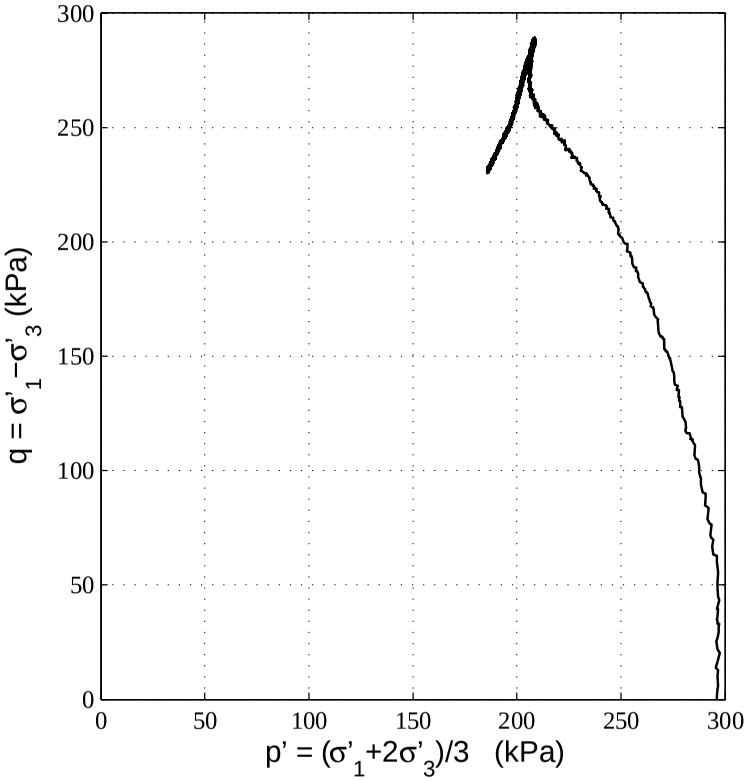

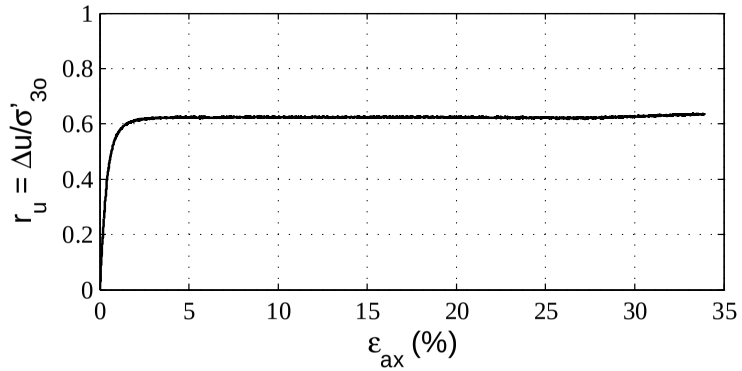

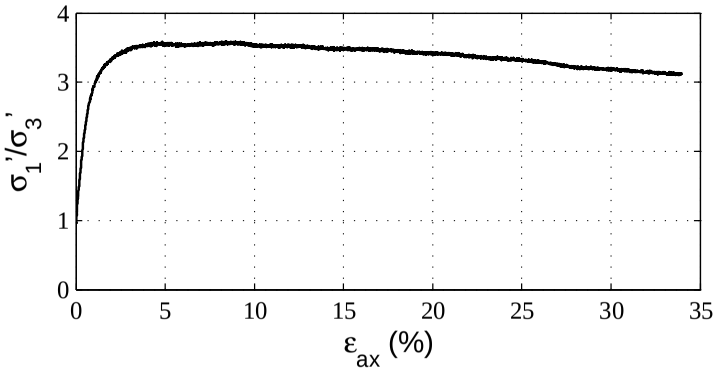

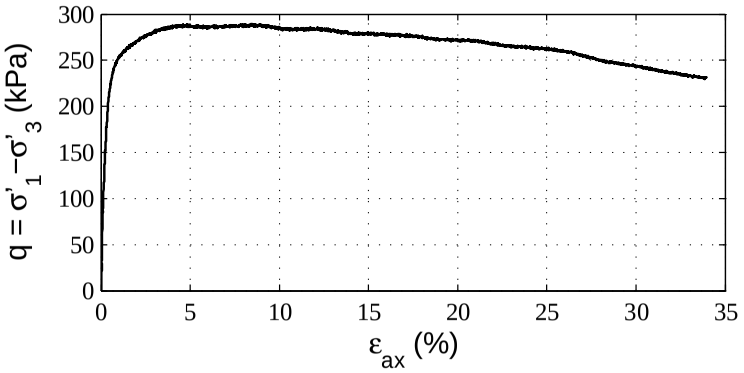

Steady State ICU Monotonic Triaxial Compression Test Data

Site:	CTH
Soil Unit:	Upp. Sand
Specimens Mixed:	DM_Z5_BH1_5U_4.27m DM_Z5_BH1_5U_4.43m
Test:	Test 3
σ'_{3o} (kPa):	298.6
e_o:	0.95
D_r (%)	39

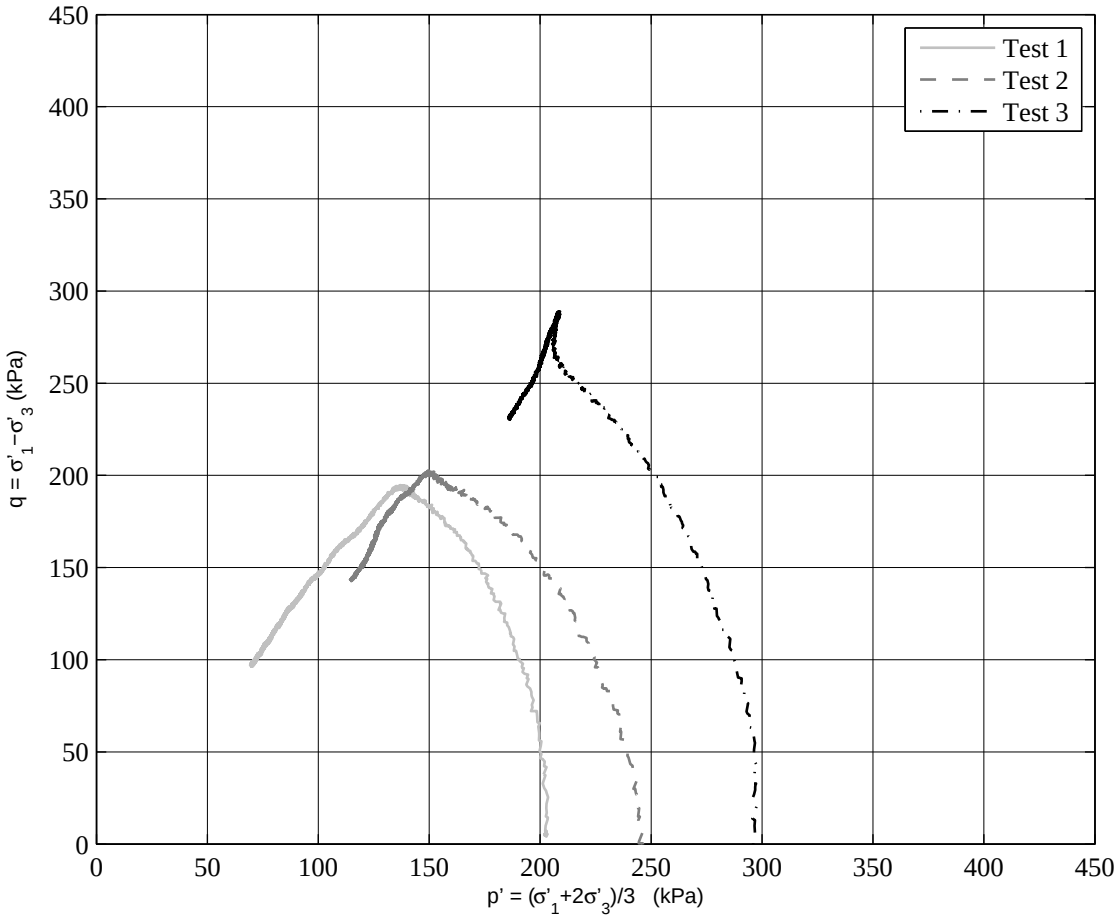
Test 1
Test 2
Test 3
q = σ'1−σ'3 (kPa)
p' = (σ'1+2σ'3)/3 (kPa)
0
50
100
150
200
250
300
350
400
450

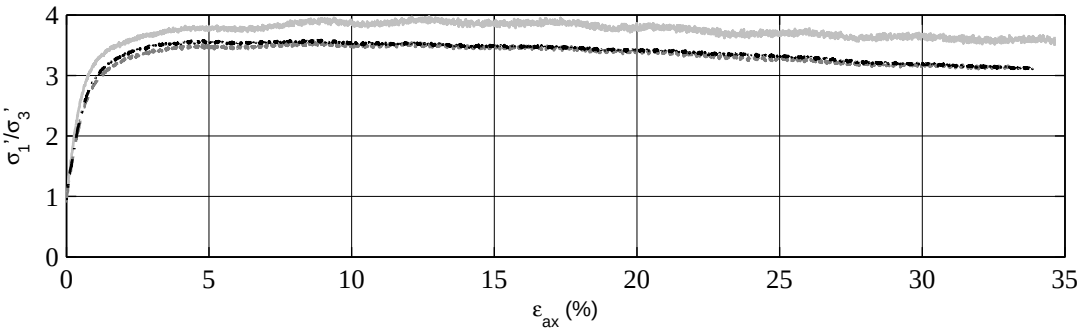
σ1'/σ3'
εax (%)
0
1
2
3
4
5
10
15
20
25
30
35

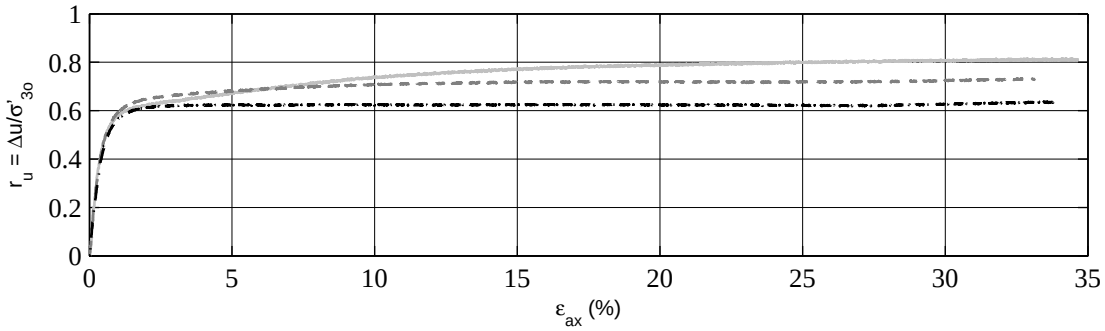
ru = Δu/σ'3o
εax (%)
0
0.2
0.4
0.6
0.8
1
5
10
15
20
25
30
35

Appendix D.1.3

Lower Sand Layer

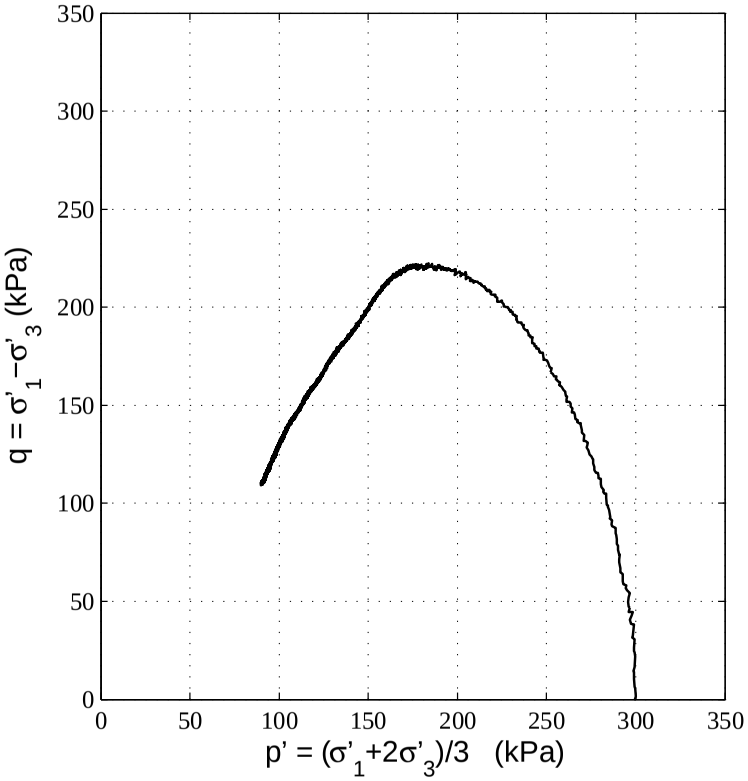

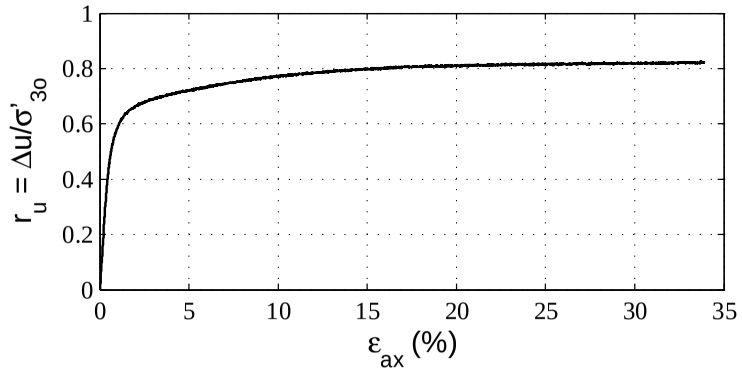

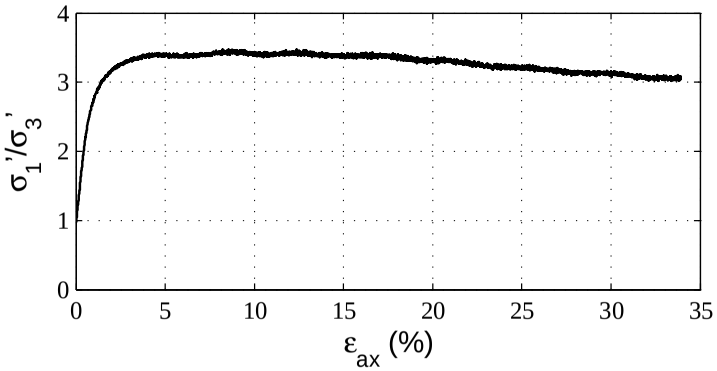

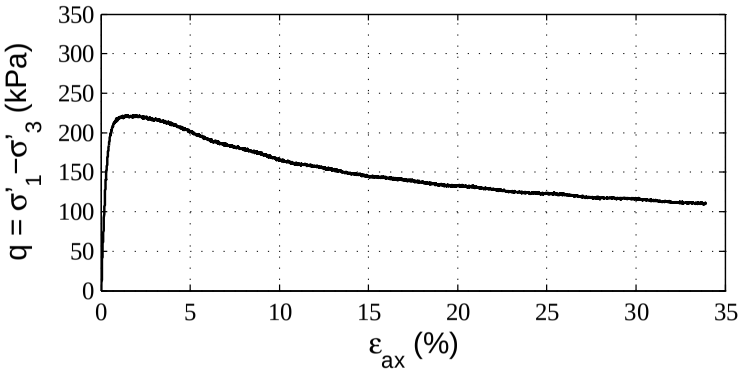

Steady State ICU Monotonic Triaxial Compression Test Data

Site:	CTH
Soil Unit:	Lower Sand
Specimens Mixed:	DM_Z5_BH2_4U_14.23m DM_Z5_BH2_6U_15.36m
Test:	Test 1
σ'_{3o} (kPa):	301.9
e_o:	0.96
D_r (%)	28

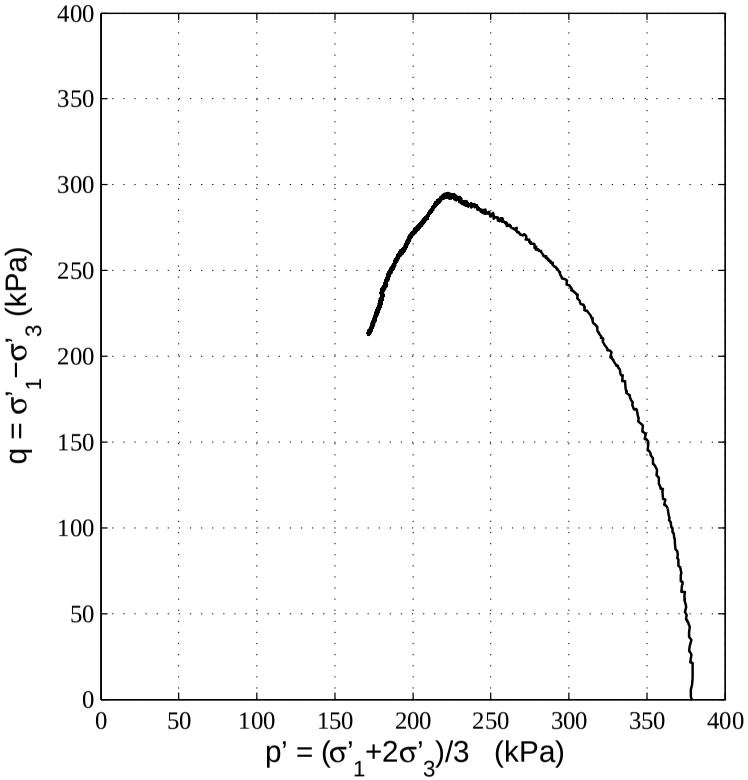

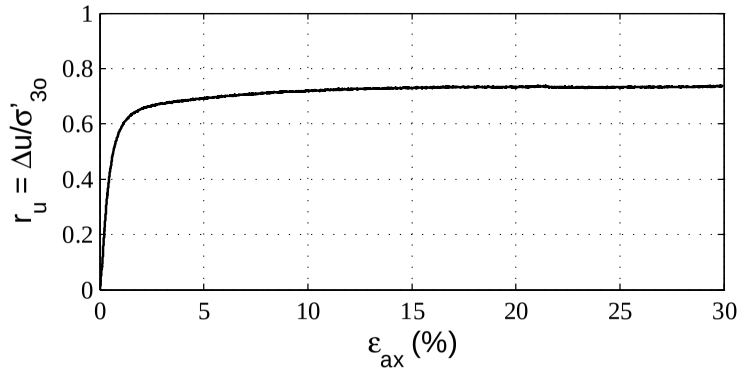

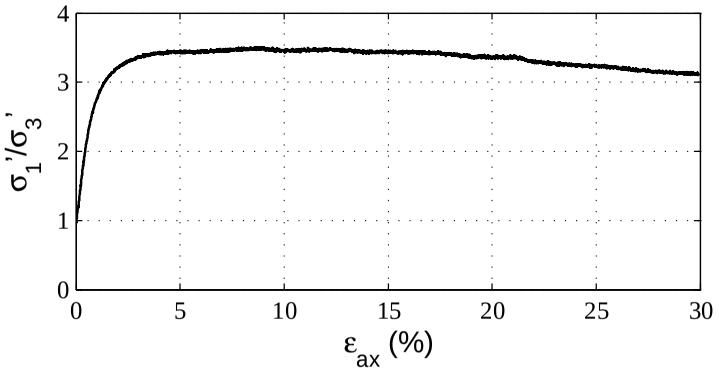

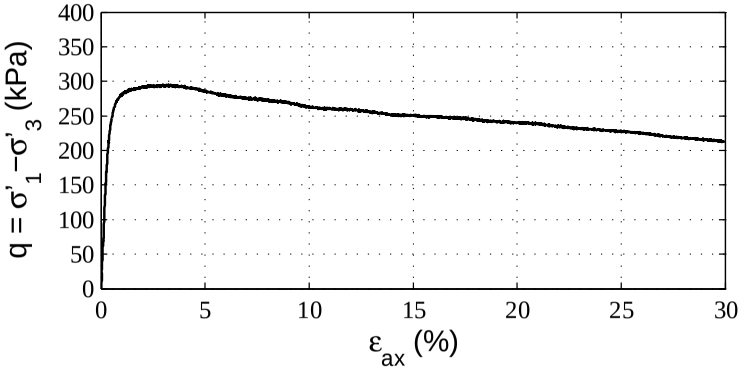

Steady State ICU Monotonic Triaxial Compression Test Data

Site:	CTH
Soil Unit:	Lower Sand
Specimens Mixed:	DM_Z5_BH2_4U_14.23m DM_Z5_BH2_6U_15.36m
Test:	Test 2
σ'_{3o} (kPa):	381.3
e_o:	0.94
D_r (%)	32

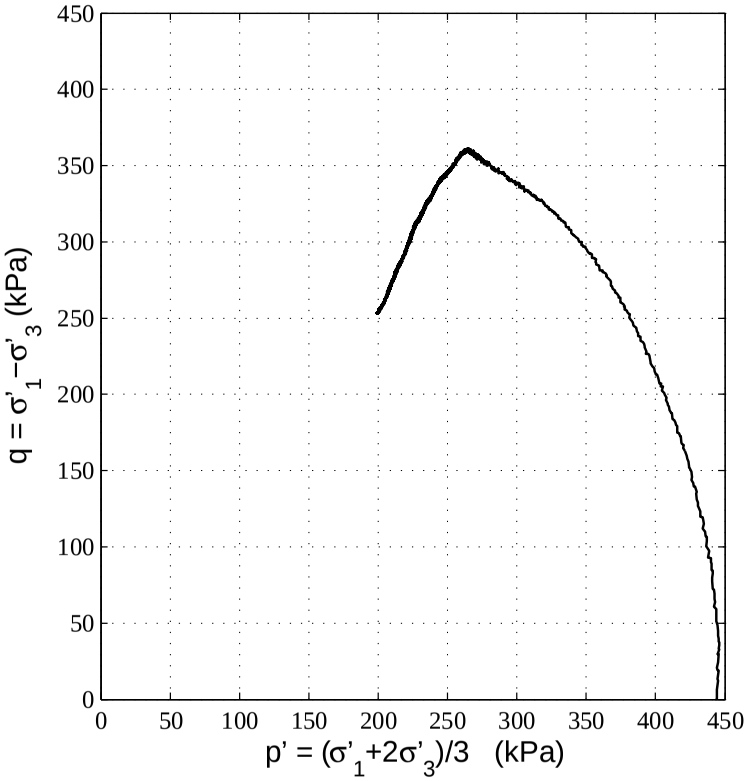

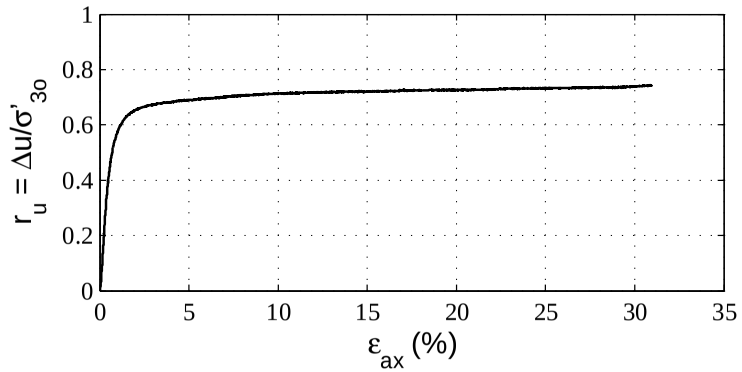

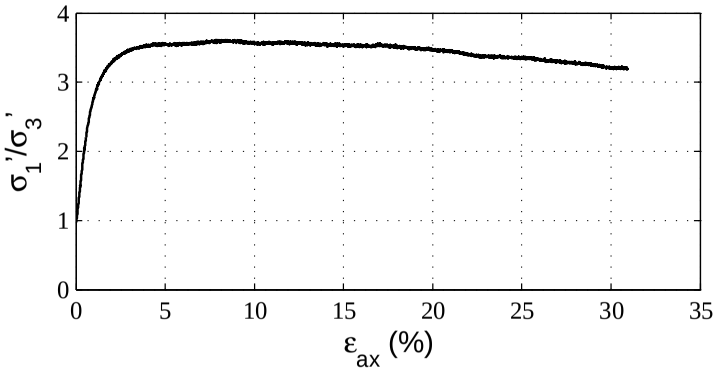

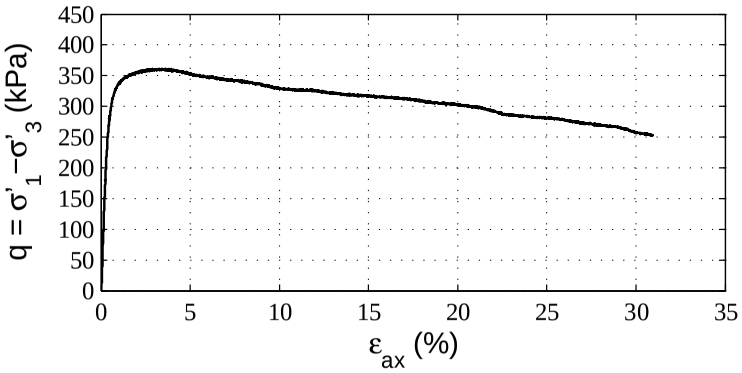

Steady State ICU Monotonic Triaxial Compression Test Data

Site:	CTH
Soil Unit:	Lower Sand
Specimens Mixed:	DM_Z5_BH2_4U_14.23m DM_Z5_BH2_6U_15.36m
Test:	Test 3
σ'_{3o} (kPa):	447.1
e_o:	0.90
D_r (%)	40

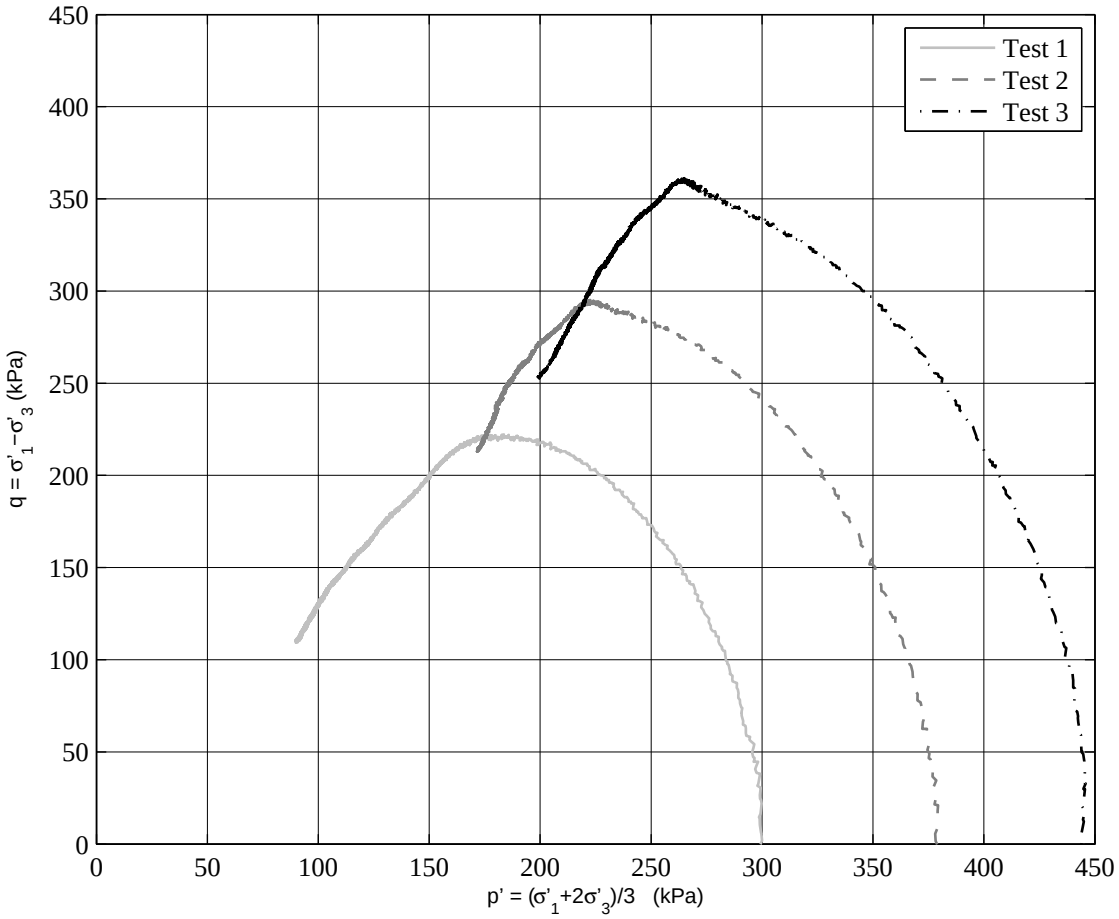
Test 1
Test 2
Test 3
q = σ'1−σ'3 (kPa)
p' = (σ'1+2σ'3)/3 (kPa)
0
50
100
150
200
250
300
350
400
450

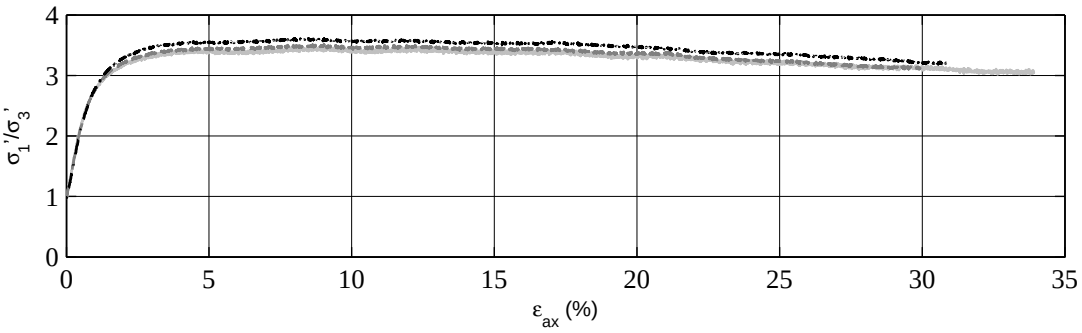
σ1'/σ3'
εax (%)
0
1
2
3
4
5
10
15
20
25
30
35

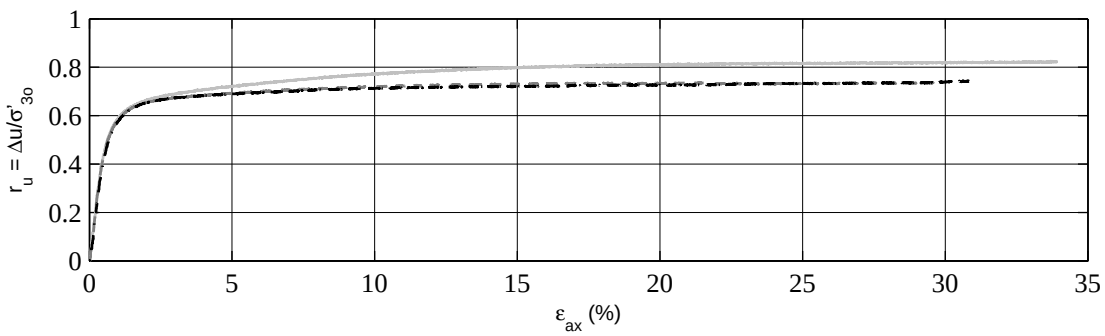
ru = Δu/σ'3o
εax (%)
0
0.2
0.4
0.6
0.8
1
5
10
15
20
25
30
35

Appendix D.2

Results for FTG-7 Site

D.2.1 Upper Silty Sand

D.2.2 Lower Sand Layer

Appendix D.2.1

Upper Silty Sand

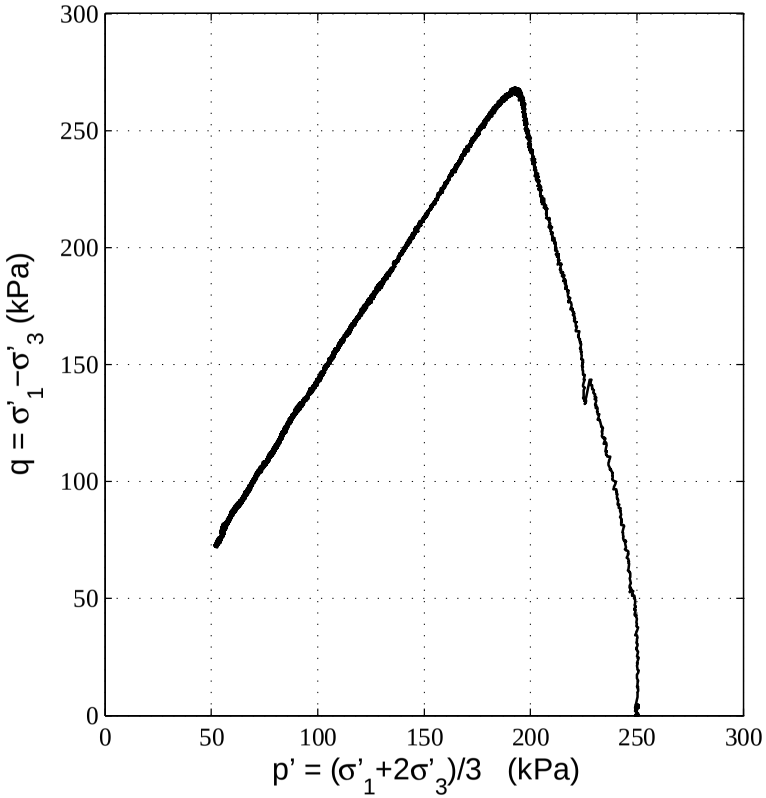

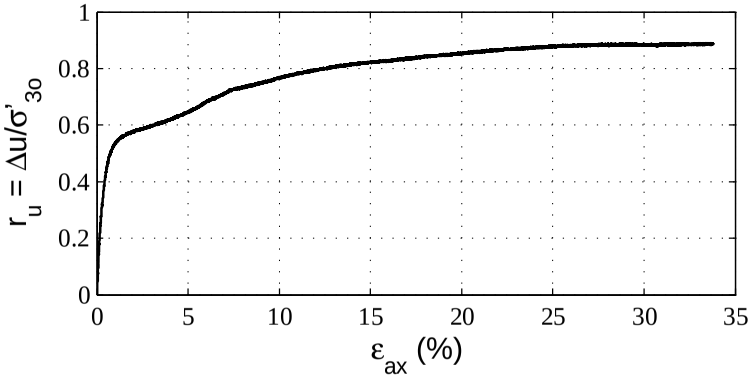

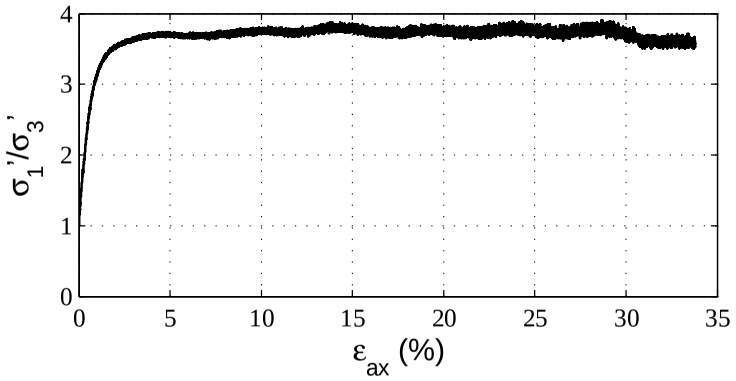

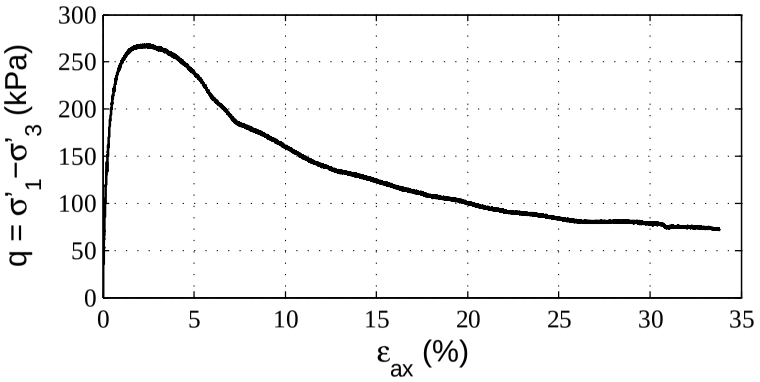

Steady State ICU Monotonic Triaxial Compression Test Data

Site:	FTG−7
Soil Unit:	Upp. Silty Sand
Specimens Mixed:	DM_Z1_BH1_4U_4.77m DM_Z1_BH1_4U_4.92m DM_Z1_BH1_5U_5.57m
Test:	Test 1
σ'_{3o} (kPa):	249.1
e_o:	0.84
D_r (%)	63

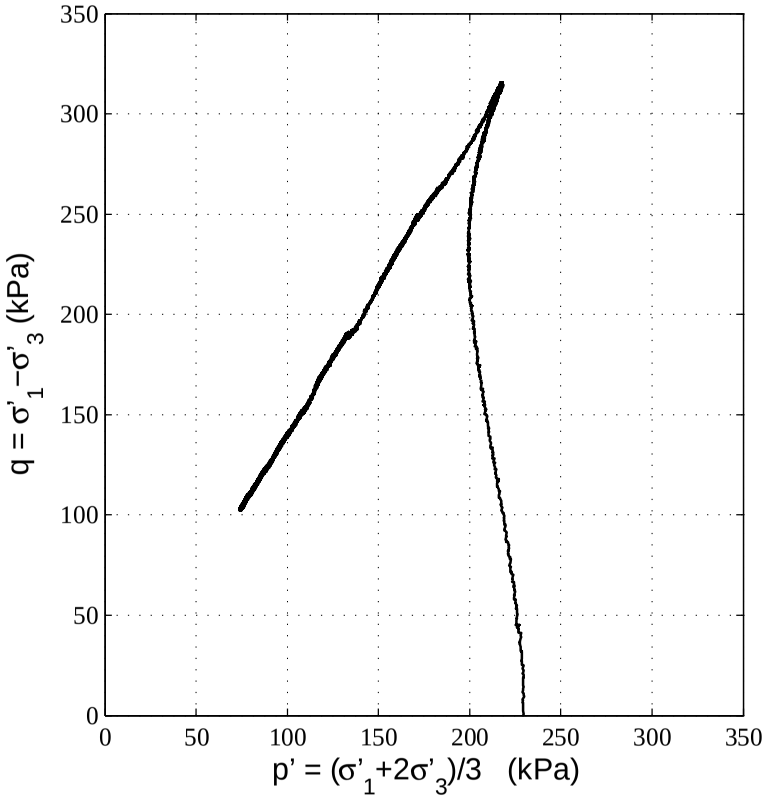

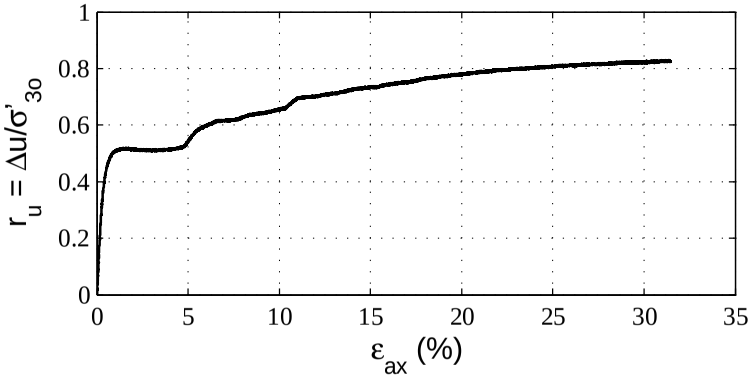

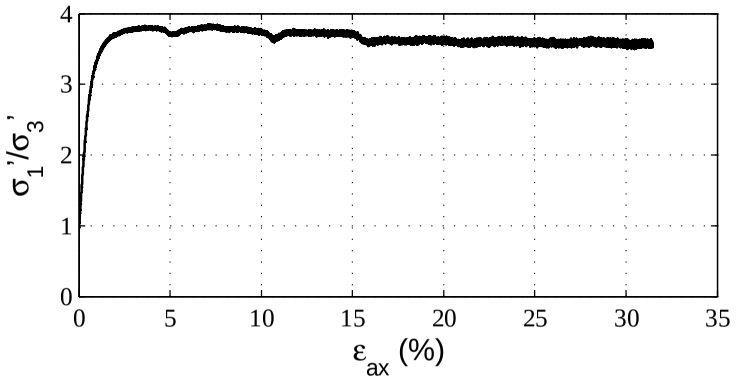

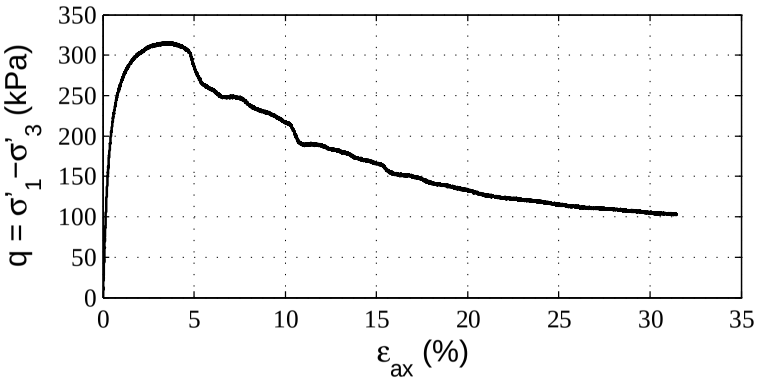

Steady State ICU Monotonic Triaxial Compression Test Data

Site:	FTG−7
Soil Unit:	Upp. Silty Sand
Specimens Mixed:	DM_Z1_BH1_4U_4.77m DM_Z1_BH1_4U_4.92m DM_Z1_BH1_5U_5.57m
Test:	Test 2
σ'_{3o} (kPa):	230.5
e_o:	0.82
D_r (%)	66

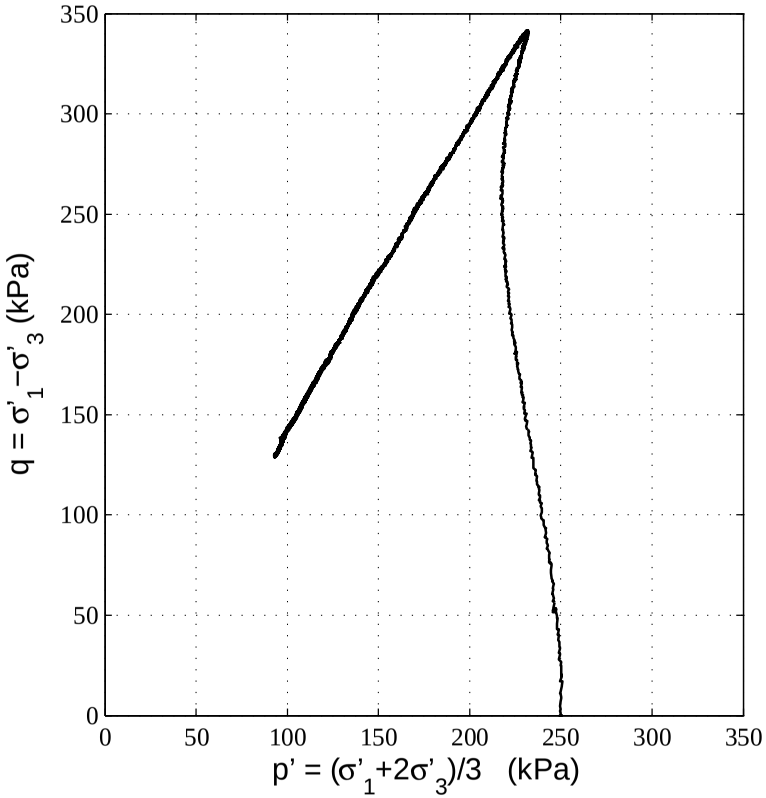

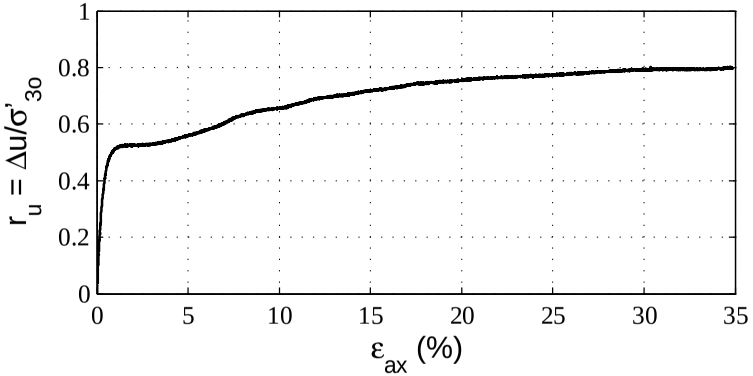

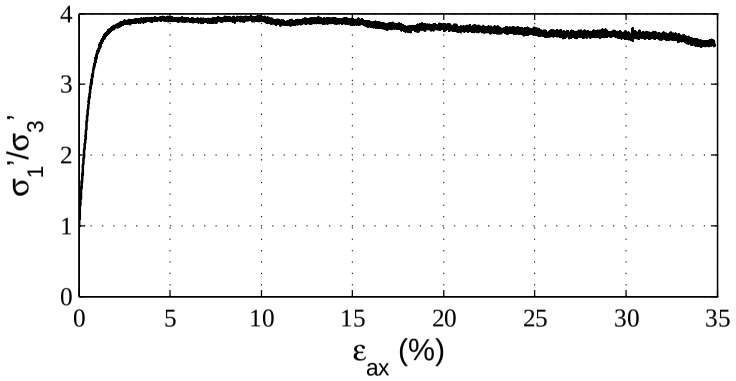

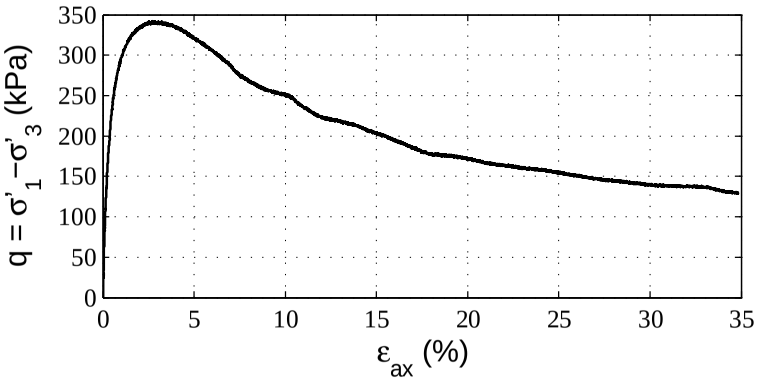

Steady State ICU Monotonic Triaxial Compression Test Data

Site:	FTG−7
Soil Unit:	Upp. Silty Sand
Specimens Mixed:	DM_Z1_BH1_4U_4.77m DM_Z1_BH1_4U_4.92m DM_Z1_BH1_5U_5.57m
Test:	Test 3
σ'_{3o} (kPa):	249.6
e_o:	0.79
D_r (%)	70

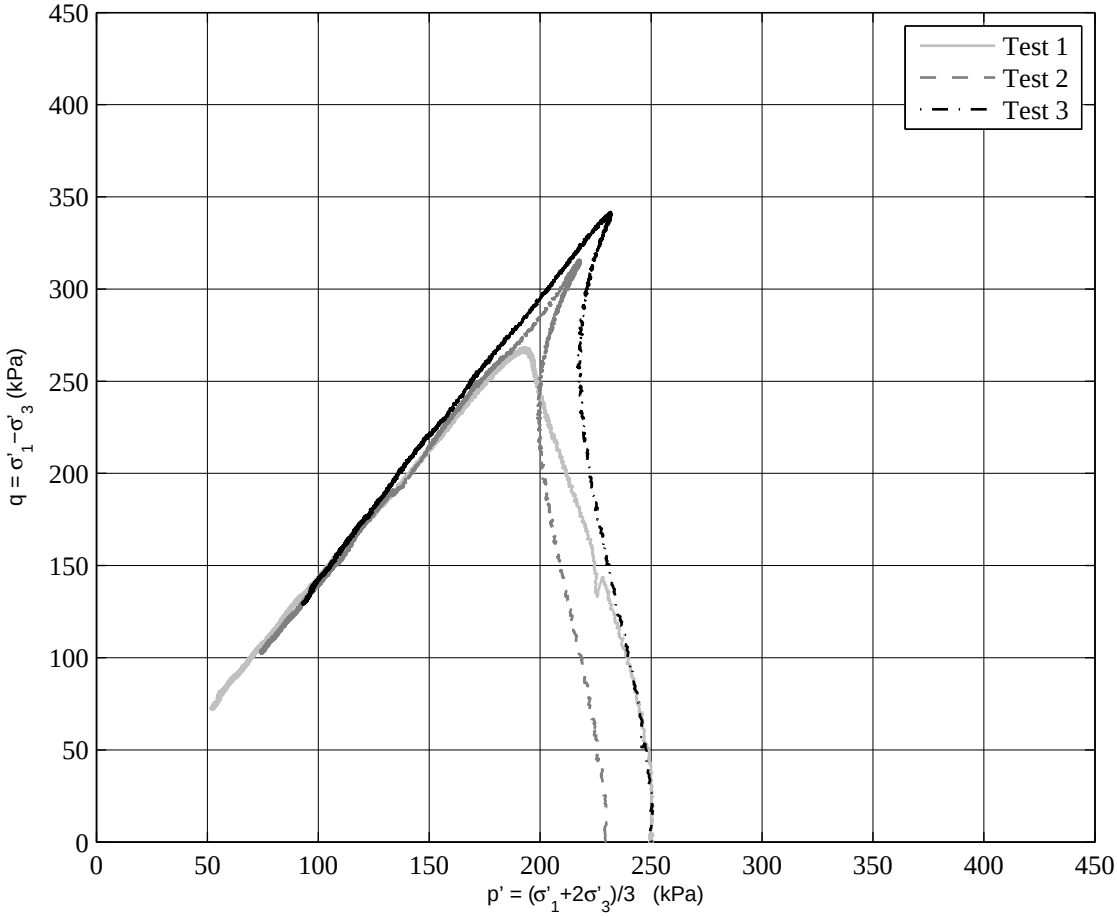
Test 1
Test 2
Test 3
q = σ'1−σ'3 (kPa)
p' = (σ'1+2σ'3)/3 (kPa)
0
50
100
150
200
250
300
350
400
450

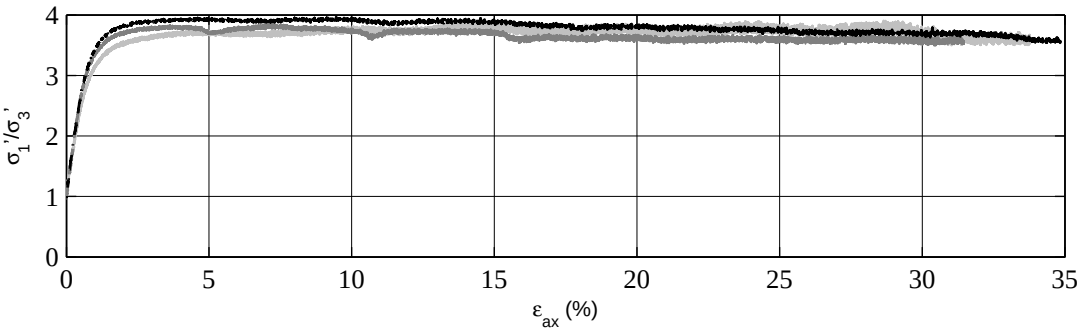
σ1'/σ3'
εax (%)
0
1
2
3
4
5
10
15
20
25
30
35

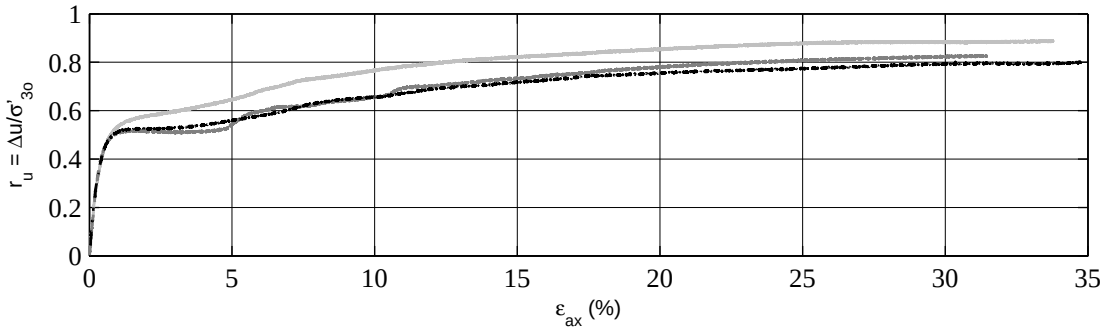
ru = Δu/σ'3o
εax (%)
0
0.2
0.4
0.6
0.8
1
5
10
15
20
25
30
35

Appendix D.2.2

Lower Sand Layer

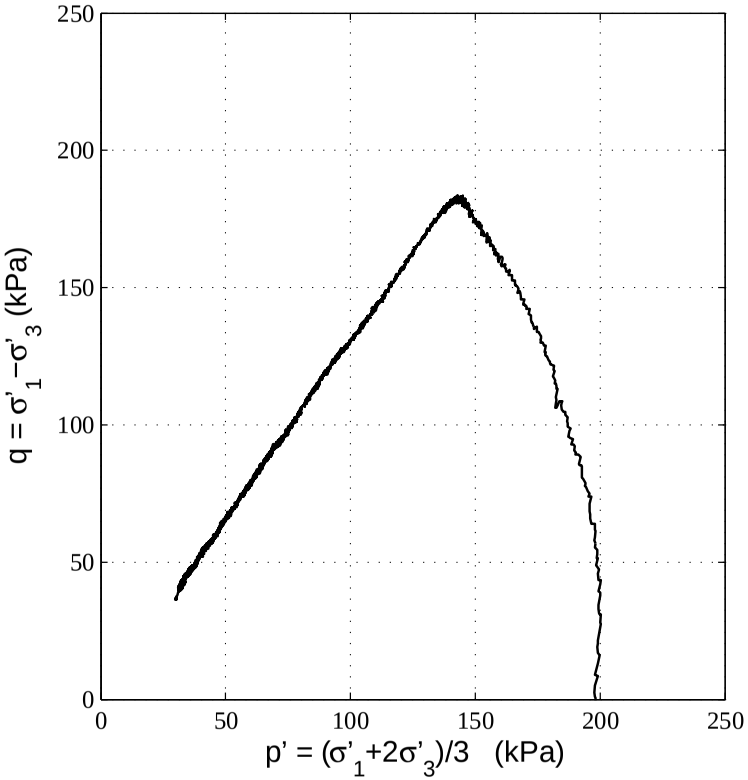

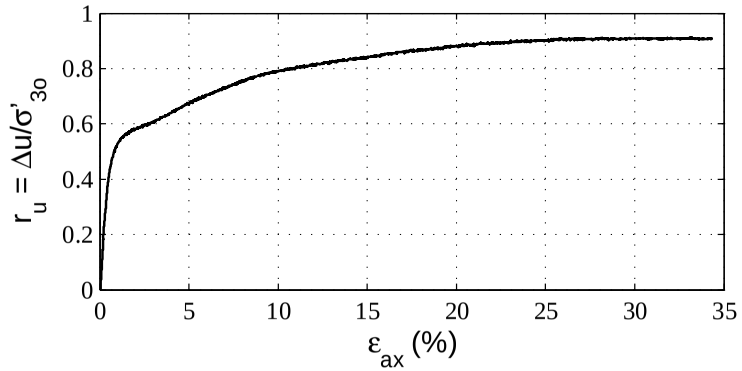

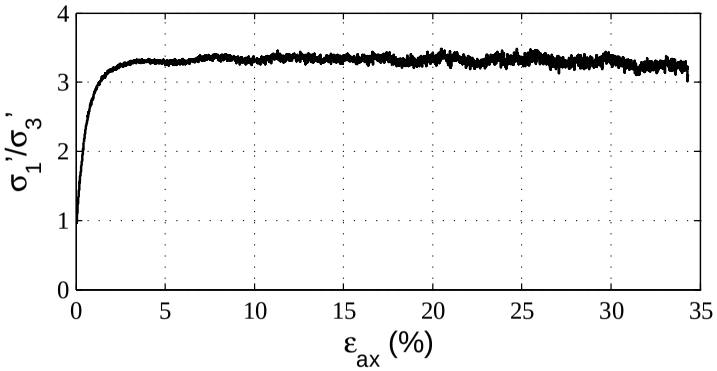

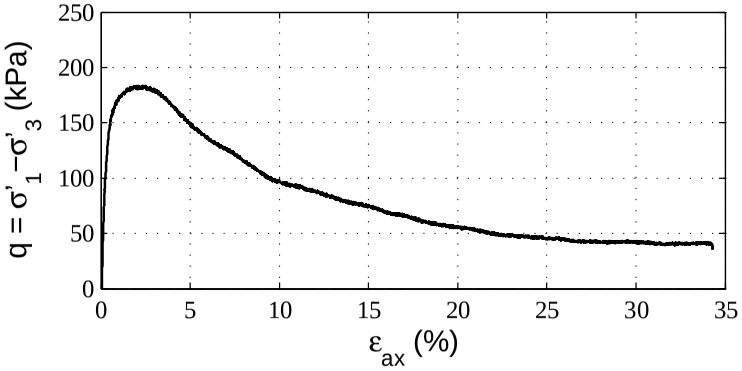

Steady State ICU Monotonic Triaxial Compression Test Data

Site:	FTG−7
Soil Unit:	Lower Sand
Specimens Mixed:	DM_Z1_BH2_11U_10.97m DM_Z1_BH2_11U_11.11m
Test:	Test 1
σ'_{3o} (kPa):	199.6
e_o:	0.93
D_r (%)	24

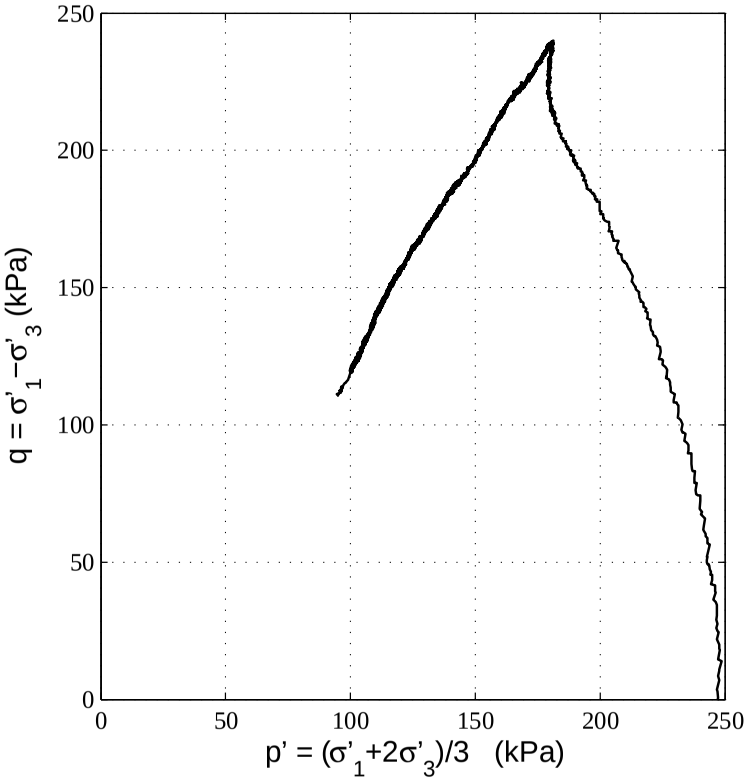

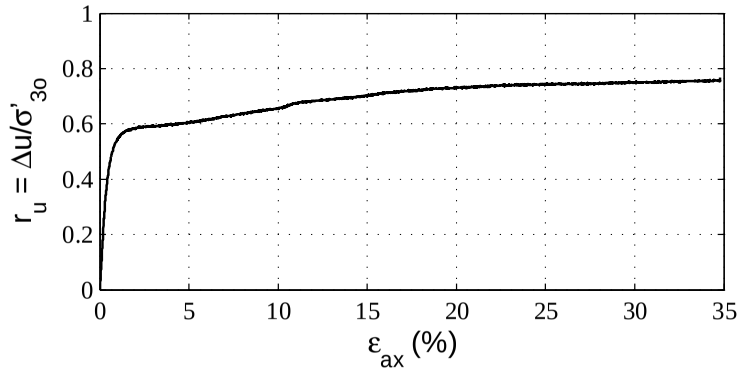

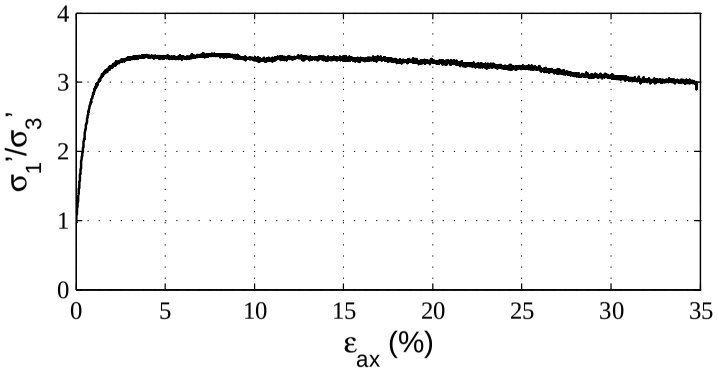

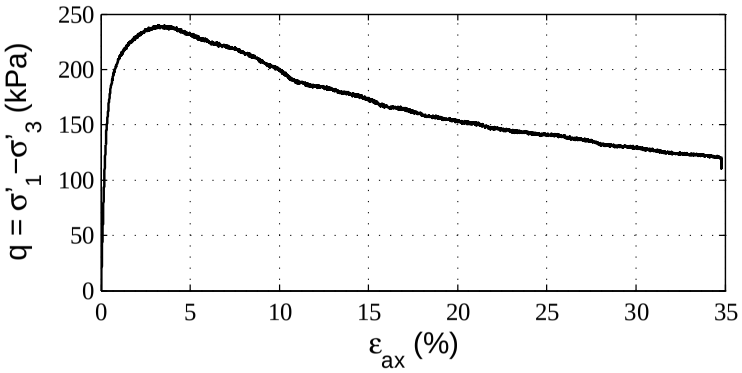

Steady State ICU Monotonic Triaxial Compression Test Data

Site:	FTG−7
Soil Unit:	Lower Sand
Specimens Mixed:	DM_Z1_BH2_11U_10.97m DM_Z1_BH2_11U_11.11m
Test:	Test 2
σ'_{3o} (kPa):	248.2
e_o:	0.90
D_r (%)	30

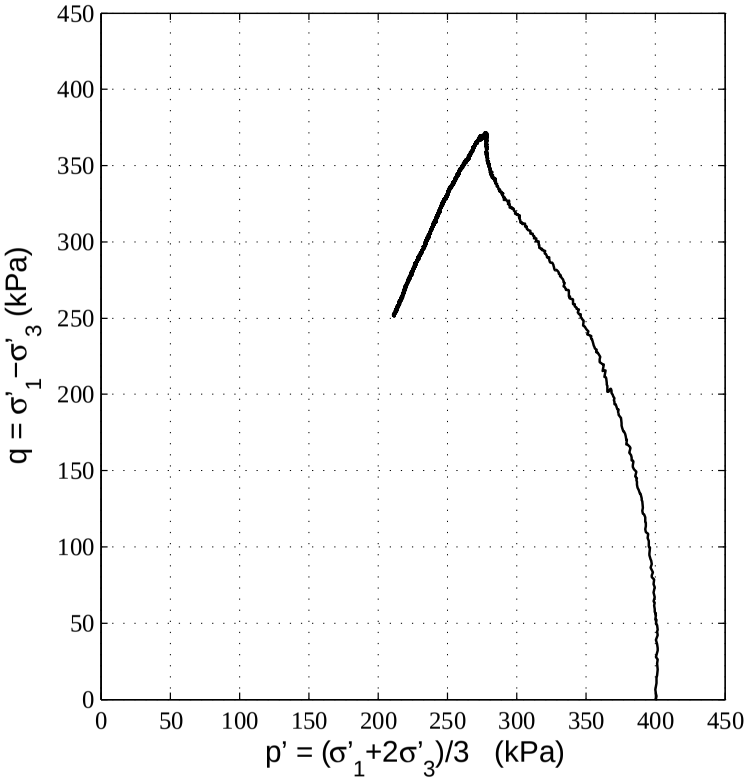

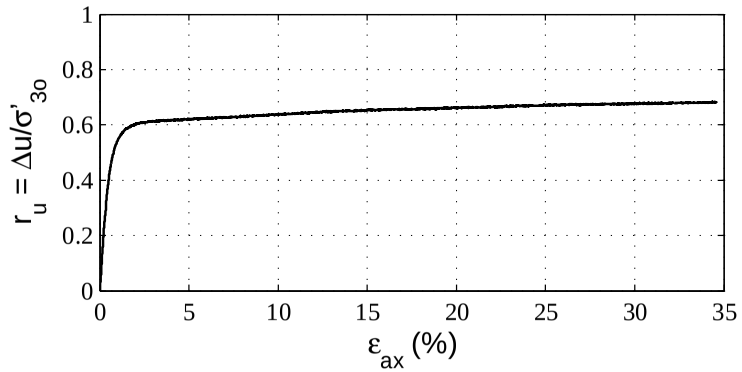

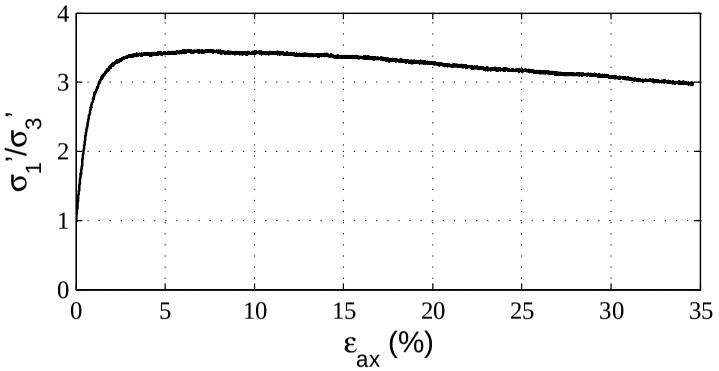

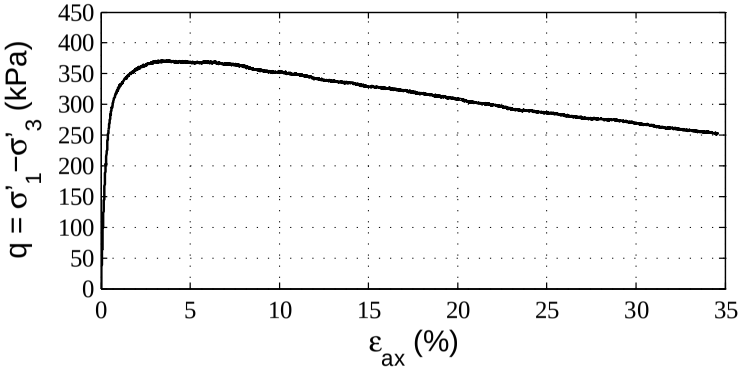

Steady State ICU Monotonic Triaxial Compression Test Data

Site:	FTG−7
Soil Unit:	Lower Sand
Specimens Mixed:	DM_Z1_BH2_11U_10.97m DM_Z1_BH2_11U_11.11m
Test:	Test 3
σ'_{3o} (kPa):	400.9
e_o:	0.86
D_r (%)	39

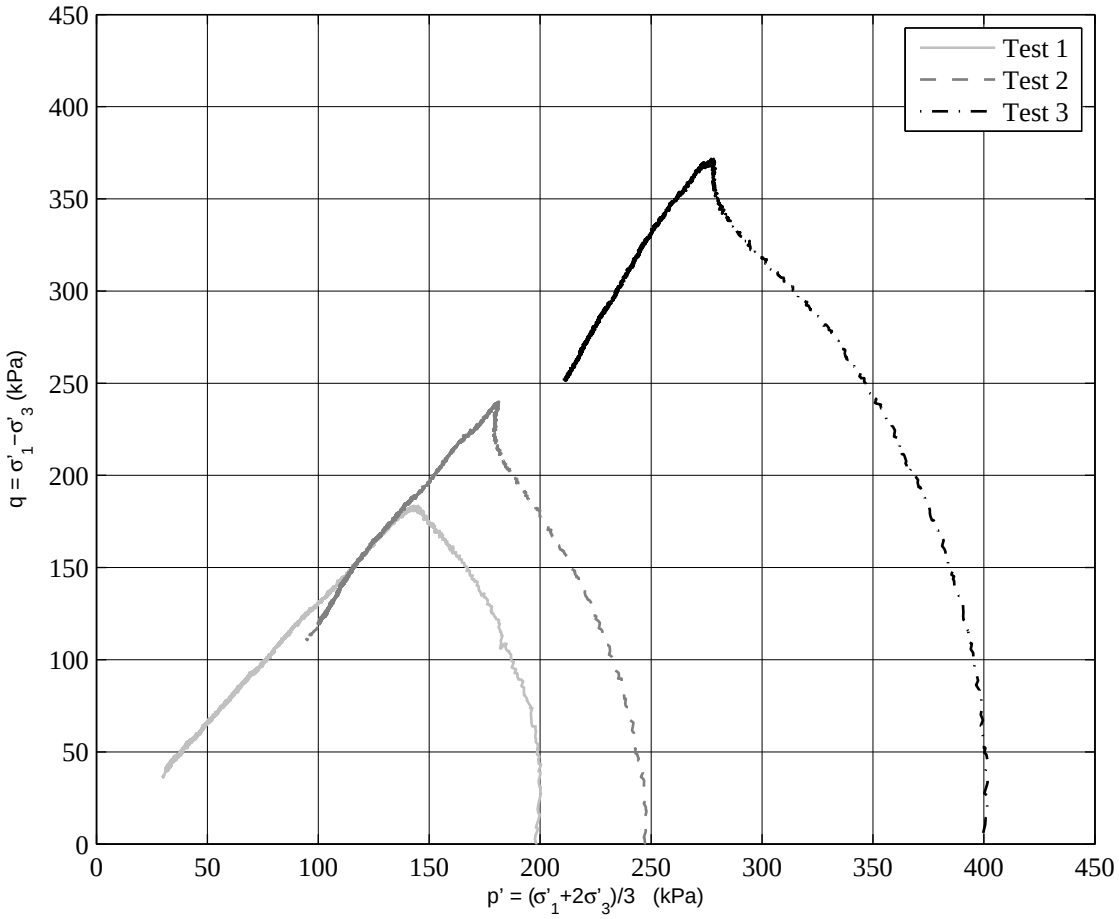
Test 1
Test 2
Test 3
q = σ'1−σ'3 (kPa)
p' = (σ'1+2σ'3)/3 (kPa)
0
50
100
150
200
250
300
350
400
450

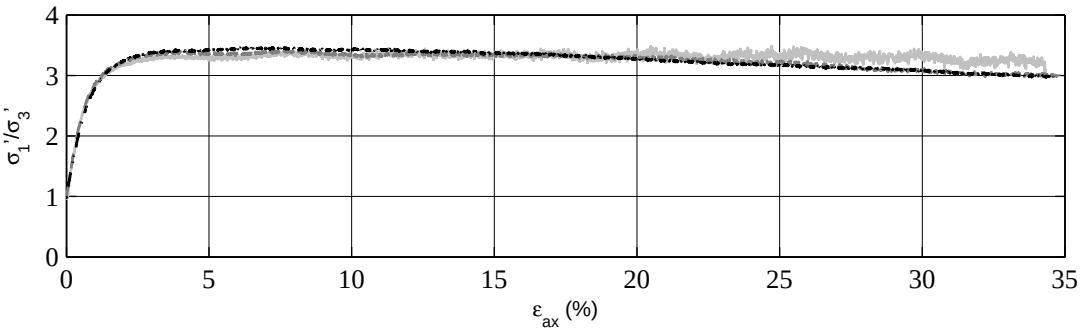
σ1'/σ3'
εax (%)
0
1
2
3
4
5
10
15
20
25
30
35

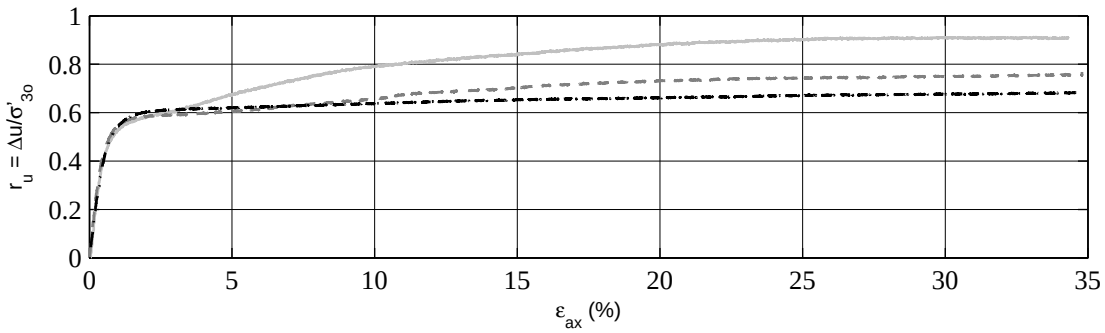
ru = Δu/σ'3o
εax (%)
0
0.2
0.4
0.6
0.8
1
5
10
15
20
25
30
35

Appendix D.3

Results for CTUC Site

D.3.1 Upper Sand Layer

Appendix D.3.1

Upper Sand Layer

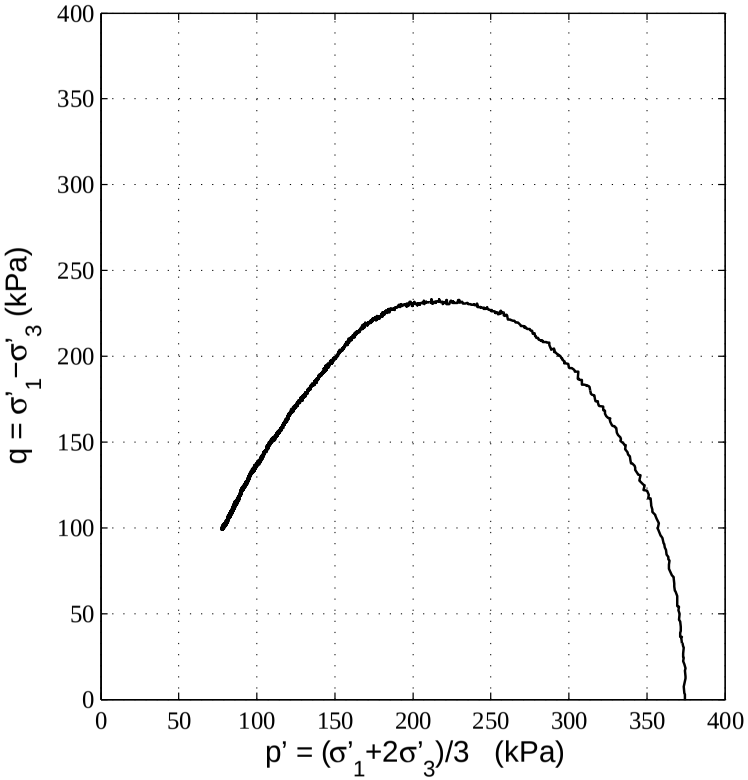

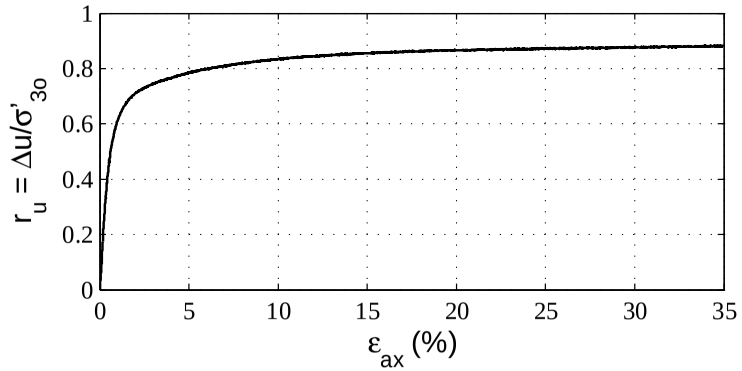

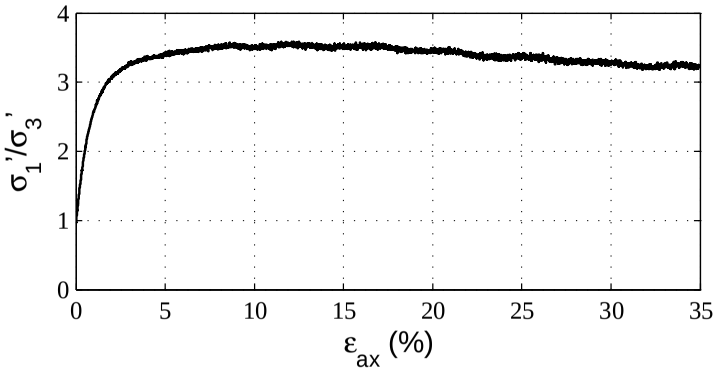

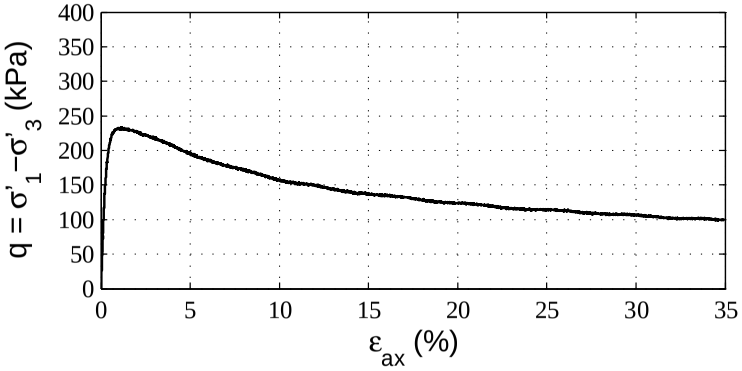

Steady State ICU Monotonic Triaxial Compression Test Data

Site:	CTUC
Soil Unit:	Upp. Sand
Specimens Mixed:	DM_Z4_BH1_3U_3.48m DM_Z4_BH1_4U_3.82m
Test:	Test 1
σ'_{3o} (kPa):	377.7
e_o:	0.97
D_r (%)	29

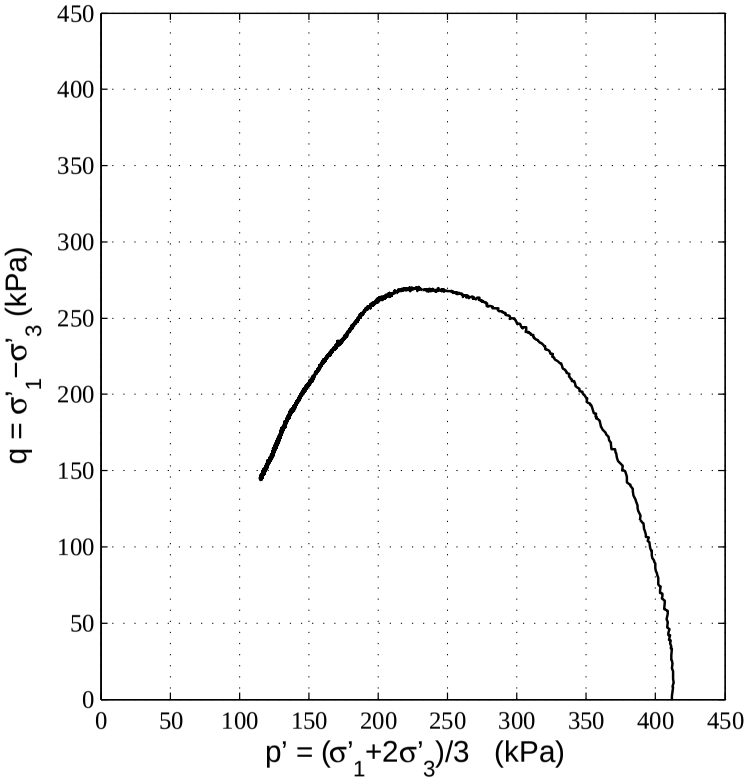

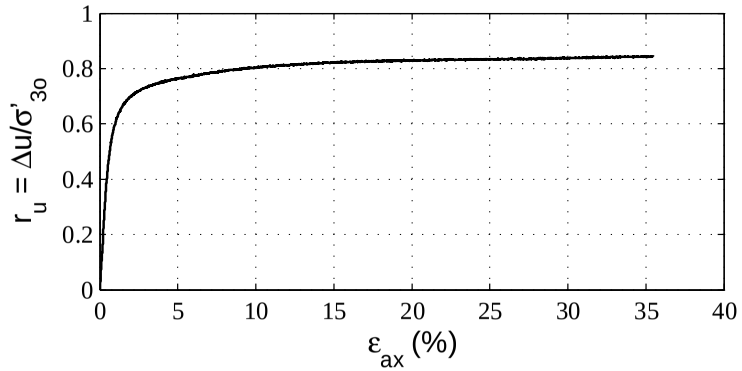

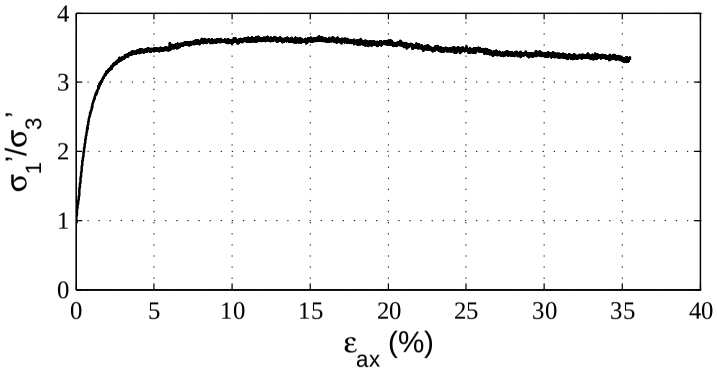

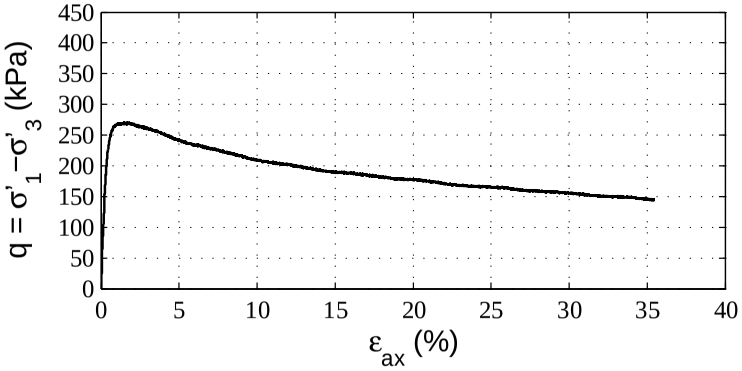

Steady State ICU Monotonic Triaxial Compression Test Data

Site:	CTUC
Soil Unit:	Upp. Sand
Specimens Mixed:	DM_Z4_BH1_3U_3.48m DM_Z4_BH1_4U_3.82m
Test:	Test 2
σ'_{3o} (kPa):	415.5
e_o:	0.93
D_r (%)	37

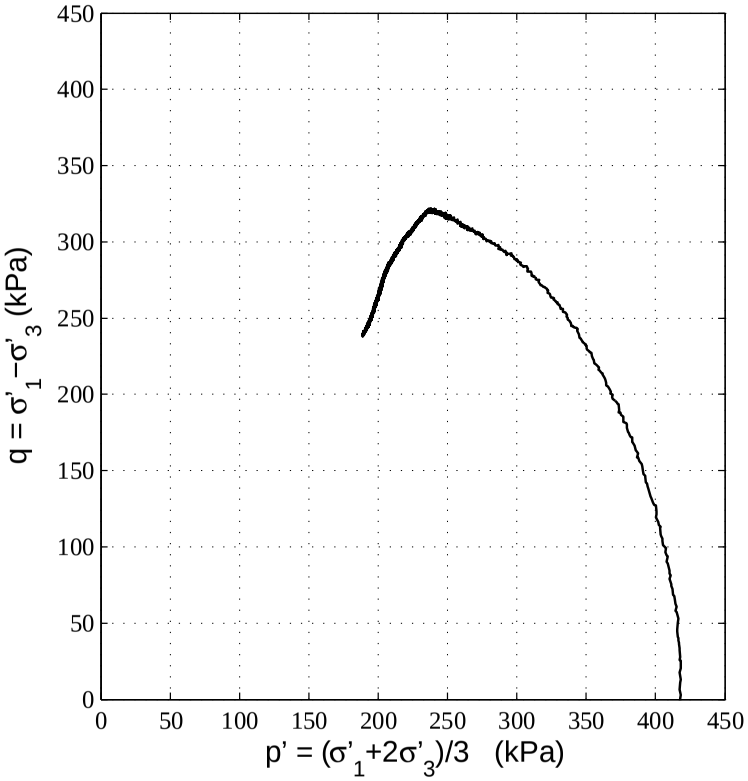

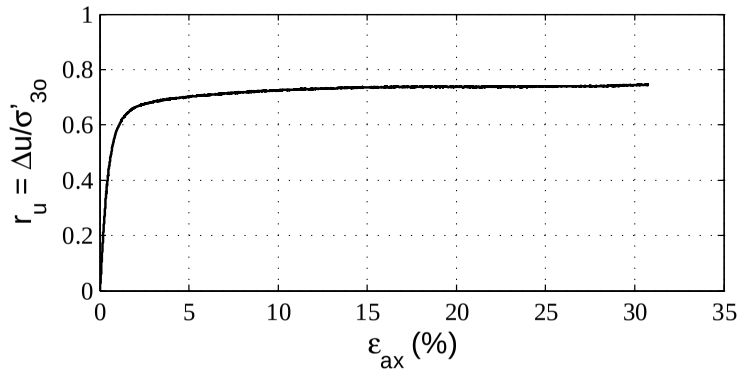

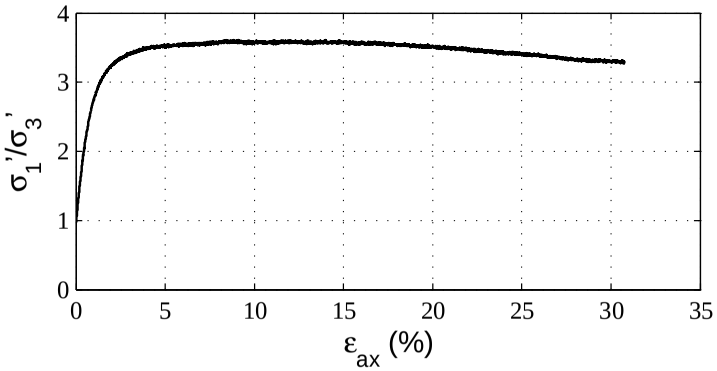

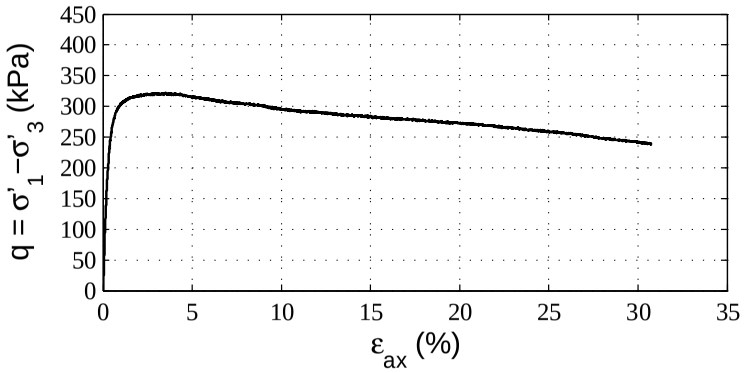

Steady State ICU Monotonic Triaxial Compression Test Data

Site:	CTUC
Soil Unit:	Upp. Sand
Specimens Mixed:	DM_Z4_BH1_3U_3.48m DM_Z4_BH1_4U_3.82m
Test:	Test 3
σ'_{3o} (kPa):	420.6
e_o:	0.89
D_r (%)	45

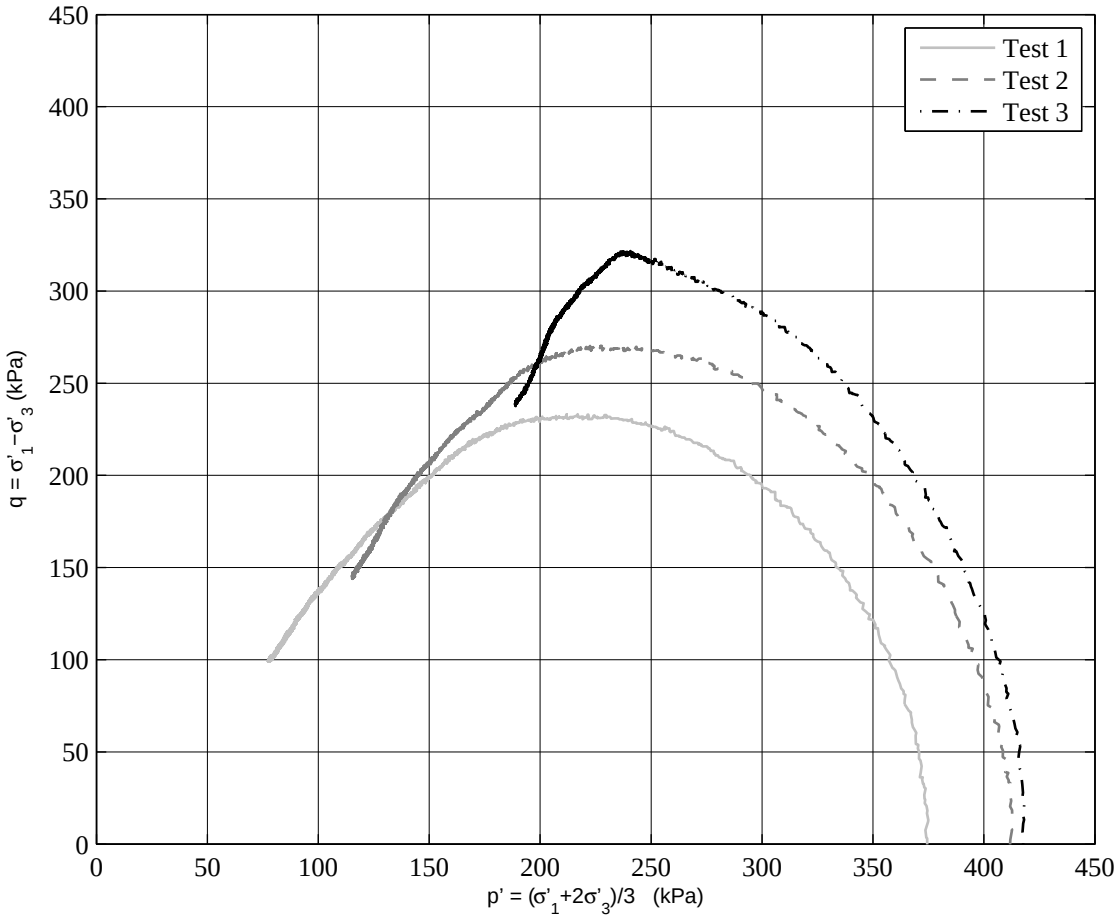
Test 1
Test 2
Test 3
q = σ'1−σ'3 (kPa)
p' = (σ'1+2σ'3)/3 (kPa)
0
50
100
150
200
250
300
350
400
450

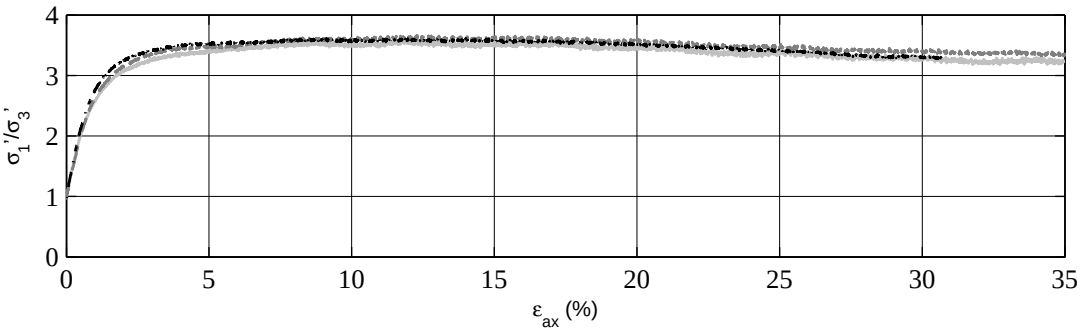
σ1'/σ3'
εax (%)
0
1
2
3
4
5
10
15
20
25
30
35

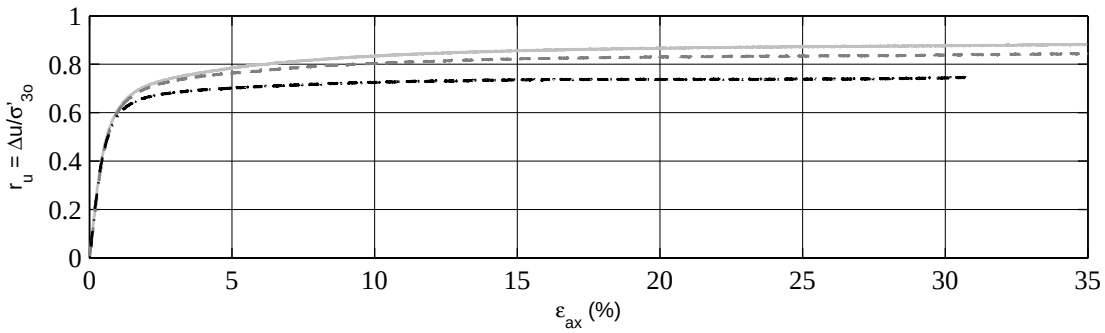
ru = Δu/σ'3o
εax (%)
0
0.2
0.4
0.6
0.8
1
5
10
15
20
25
30
35

Appendix D.4

Results for PWC Site

D.4.1 Sand Layer

Appendix D.4.1

Sand Layer

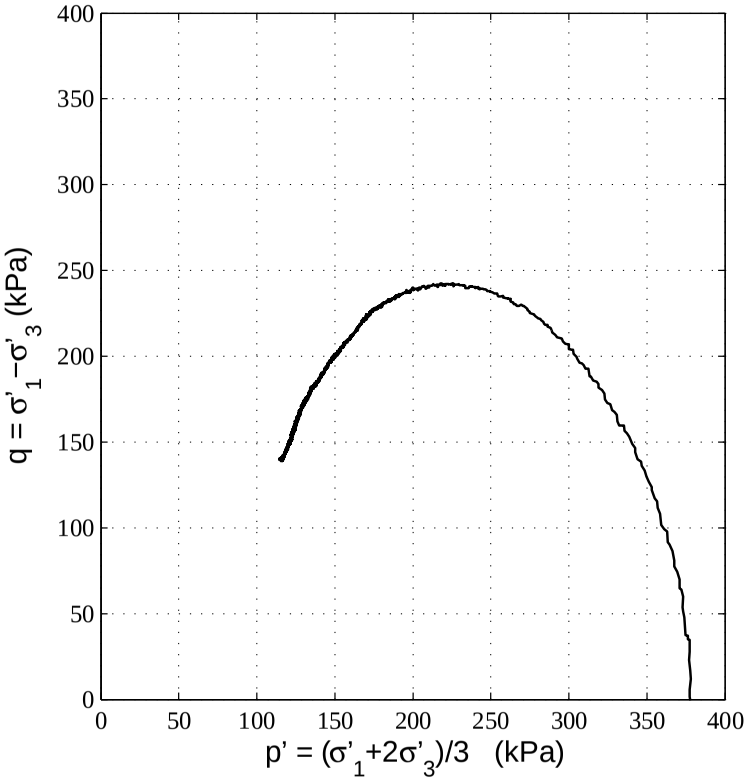

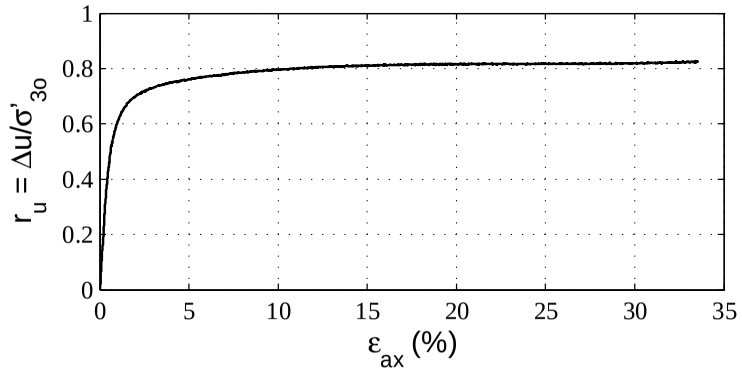

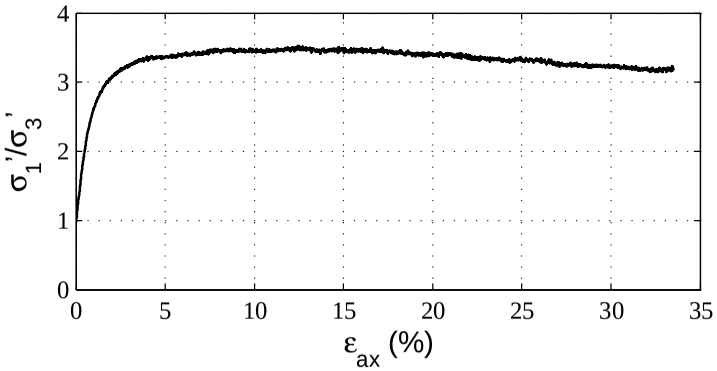

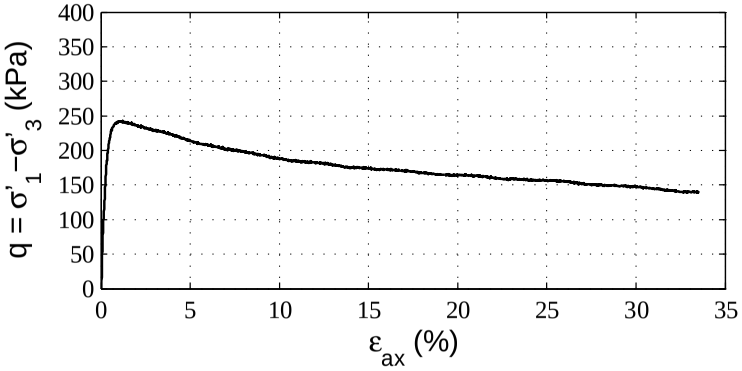

Steady State ICU Monotonic Triaxial Compression Test Data

Site:	PWC
Soil Unit:	Sand
Specimens Mixed:	DM_Z2_BH1b_3U_12.82m DM_Z2_B1b_7U_14.57m
Test:	Test 1
σ'_{3o} (kPa):	380.5
e_o:	0.98
D_r (%)	30

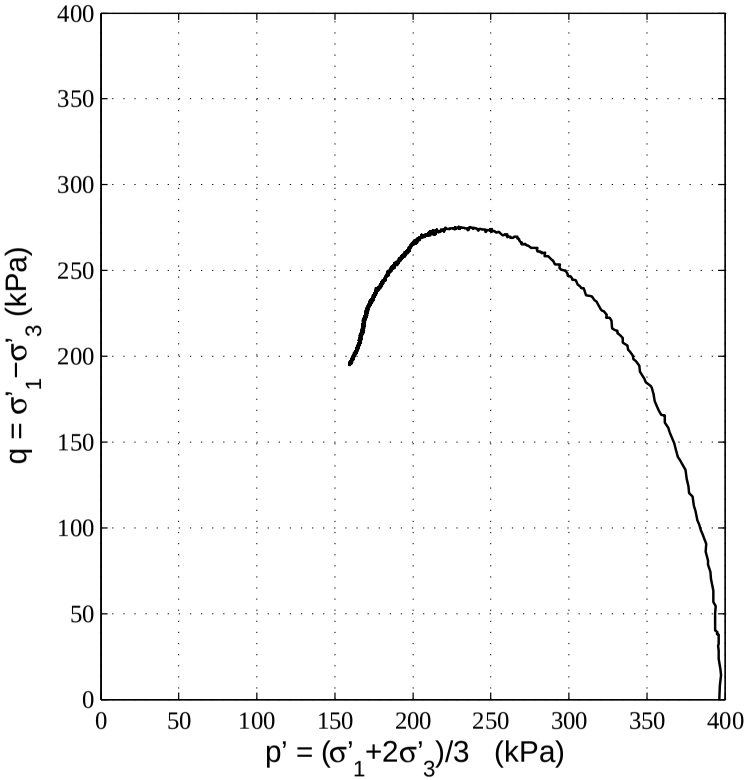

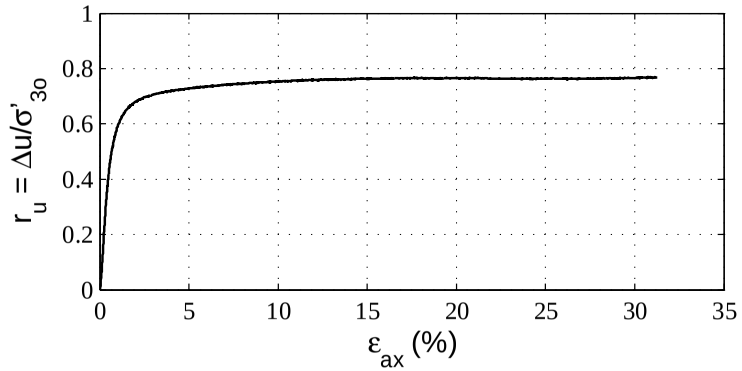

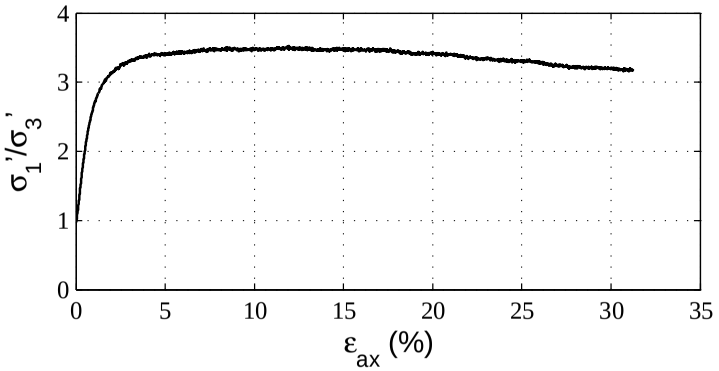

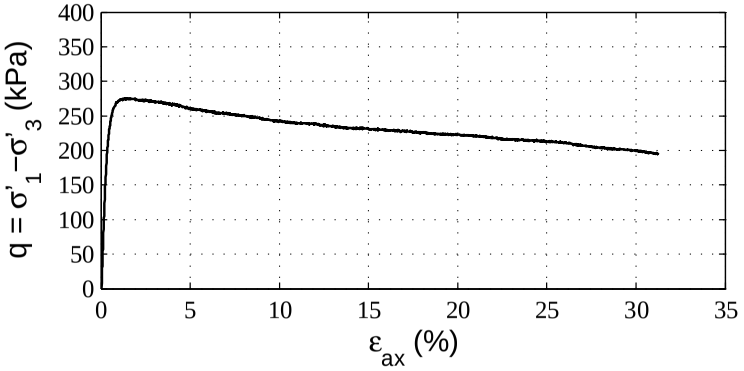

Steady State ICU Monotonic Triaxial Compression Test Data

Site:	PWC
Soil Unit:	Sand
Specimens Mixed:	DM_Z2_BH1b_3U_12.82m DM_Z2_B1b_7U_14.57m
Test:	Test 2
σ'_{3o} (kPa):	399.9
e_o:	0.96
D_r (%)	34

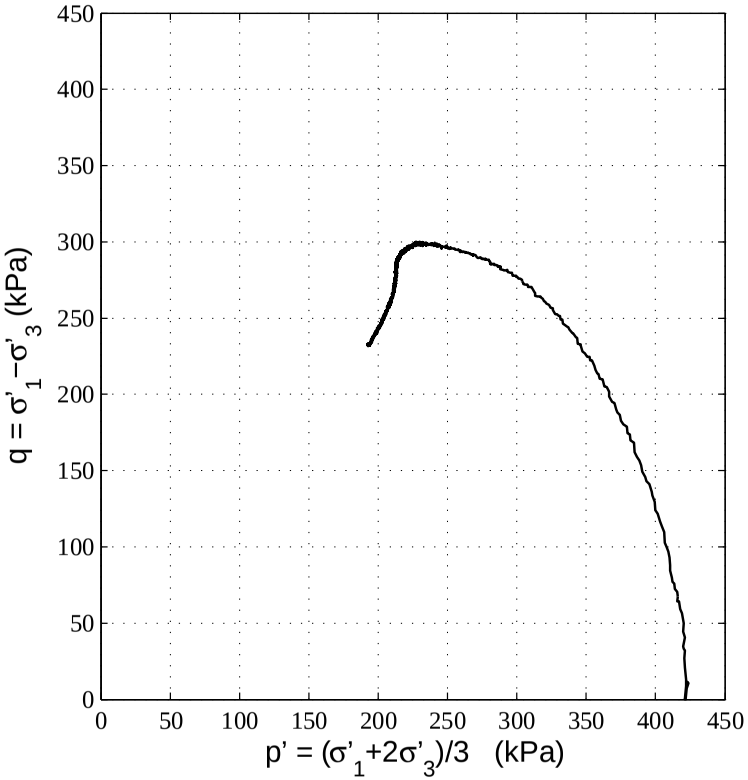

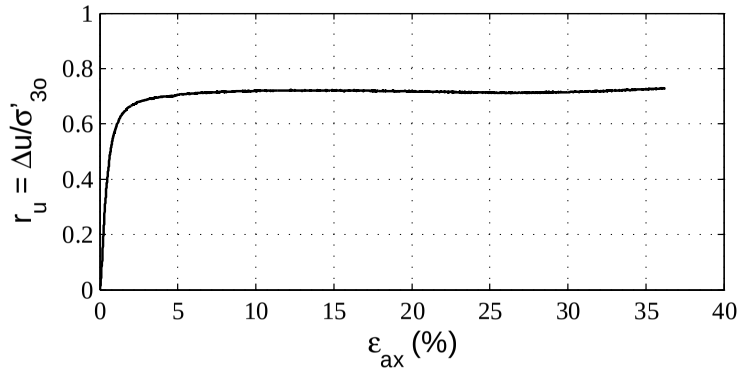

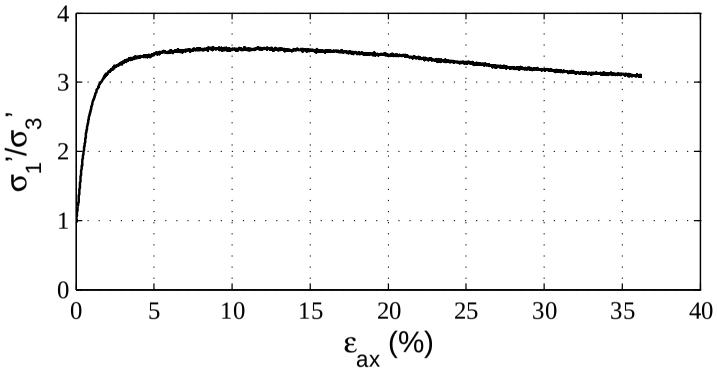

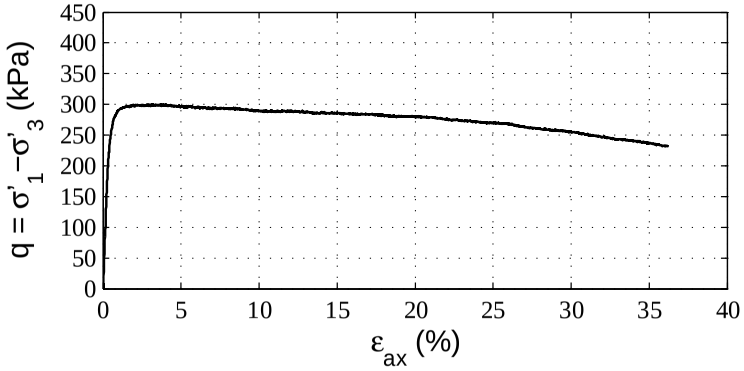

Steady State ICU Monotonic Triaxial Compression Test Data

Site:	PWC
Soil Unit:	Sand
Specimens Mixed:	DM_Z2_BH1b_3U_12.82m DM_Z2_B1b_7U_14.57m
Test:	Test 3
σ'_{3o} (kPa):	419.0
e_o:	0.93
D_r (%)	40

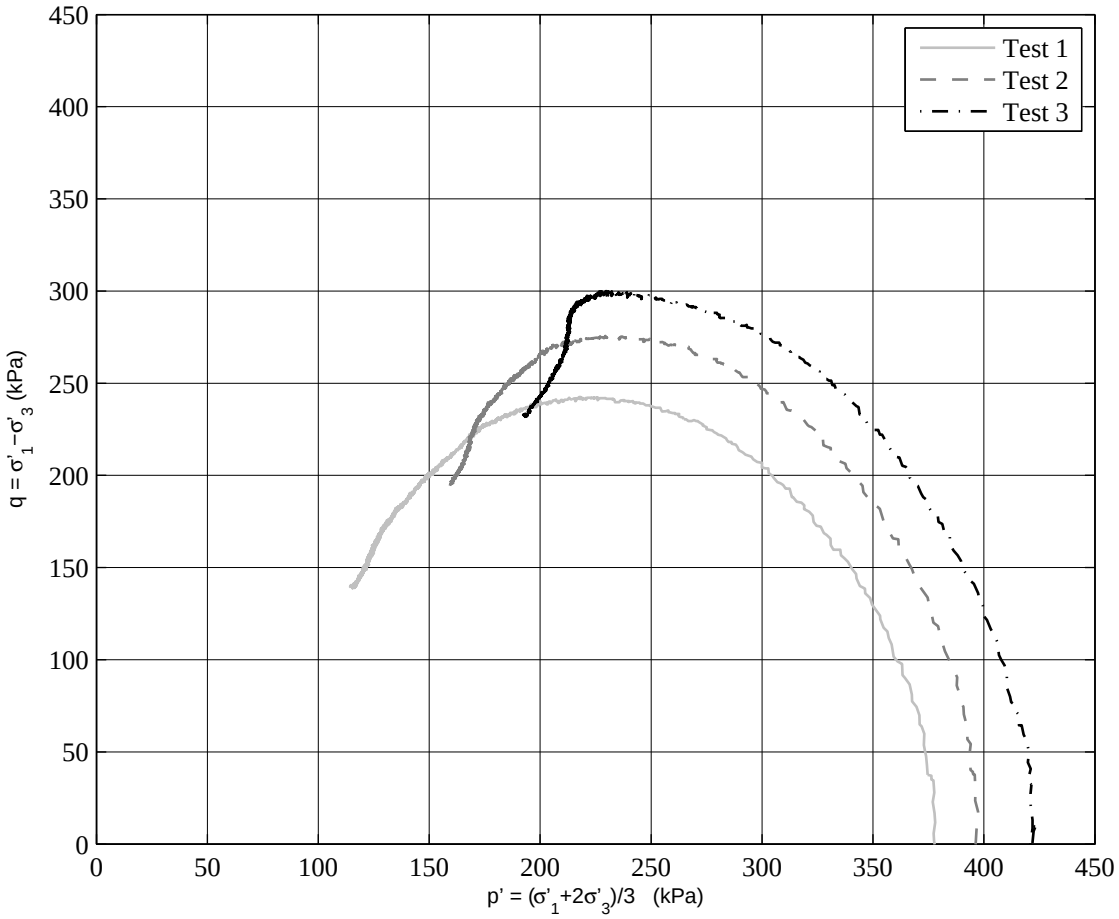
Test 1
Test 2
Test 3
q = σ'1−σ'3 (kPa)
p' = (σ'1+2σ'3)/3 (kPa)
0
50
100
150
200
250
300
350
400
450

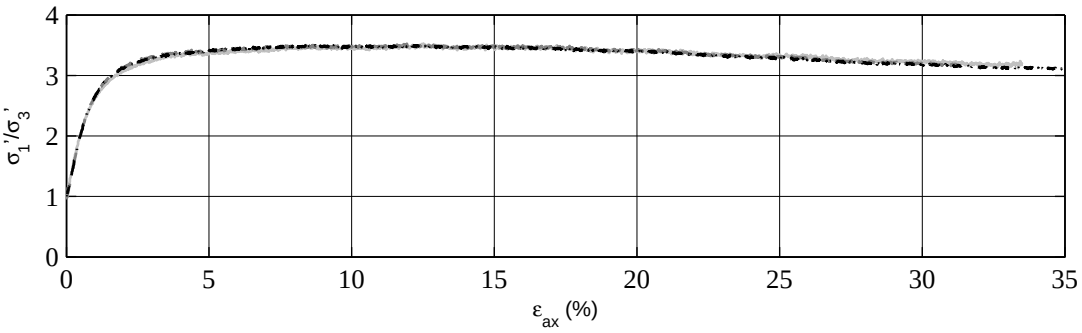
σ1'/σ3'
εax (%)
0
1
2
3
4
5
10
15
20
25
30
35

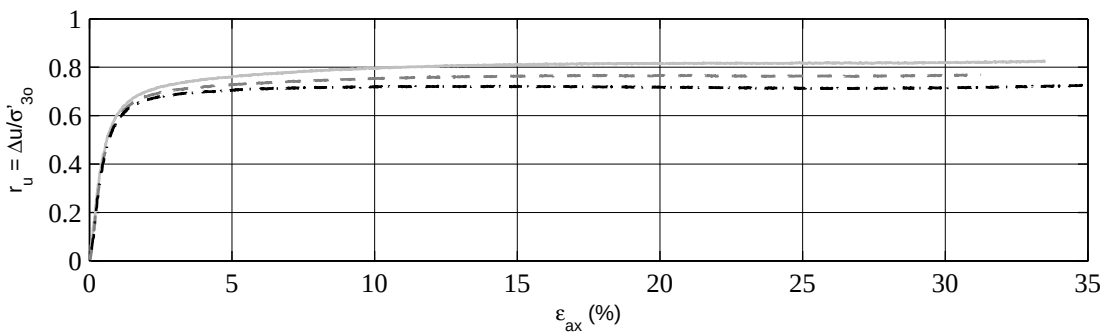
ru = Δu/σ'3o
εax (%)
0
0.2
0.4
0.6
0.8
1
5
10
15
20
25
30
35

Appendix D.5

Results for VT Site

D.5.1 Upper Sand Layer

Appendix D.5.1

Upper Sand Layer

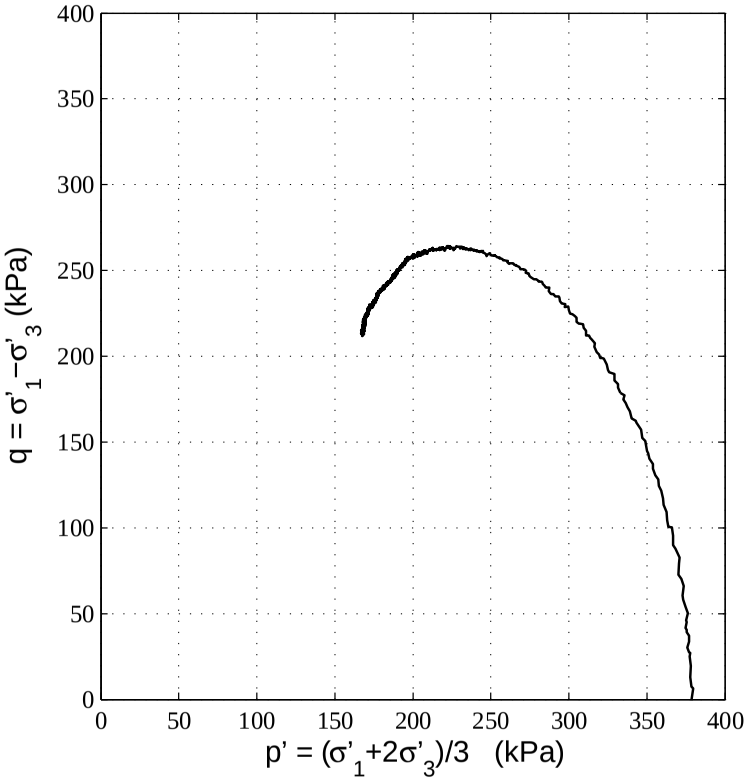

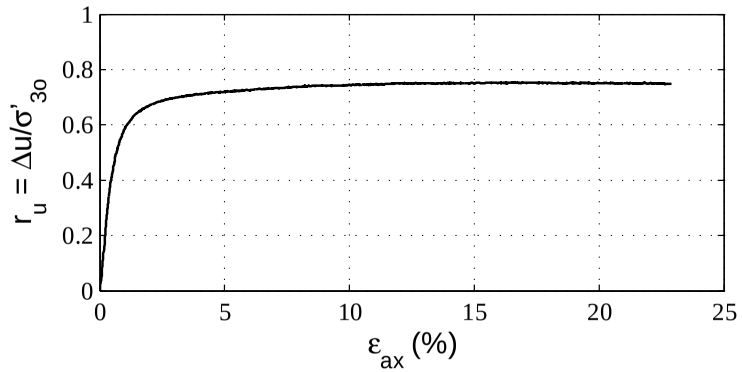

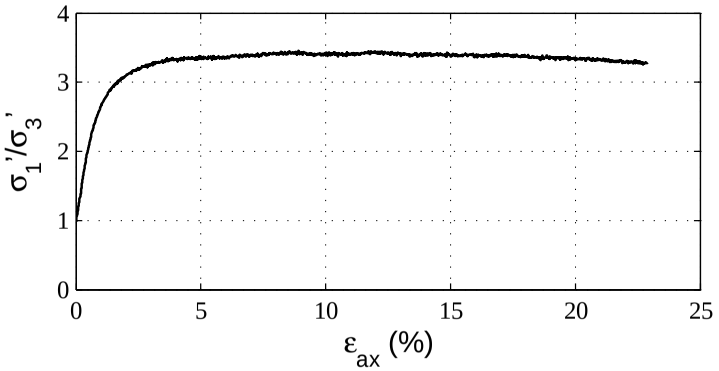

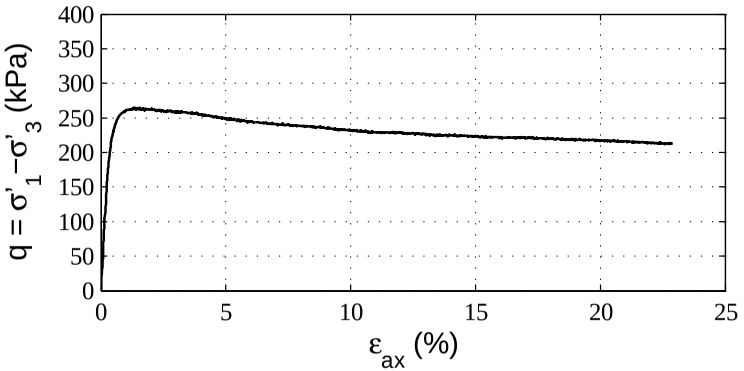

Steady State ICU Monotonic Triaxial Compression Test Data

Site:	VT
Soil Unit:	Upp. Sand
Specimens Mixed:	DM_Z2_BH2_1U_7.44m DM_Z2_B2_2U_7.92m
Test:	Test 1
σ'_{3o} (kPa):	379.8
e_o:	0.99
D_r (%)	26

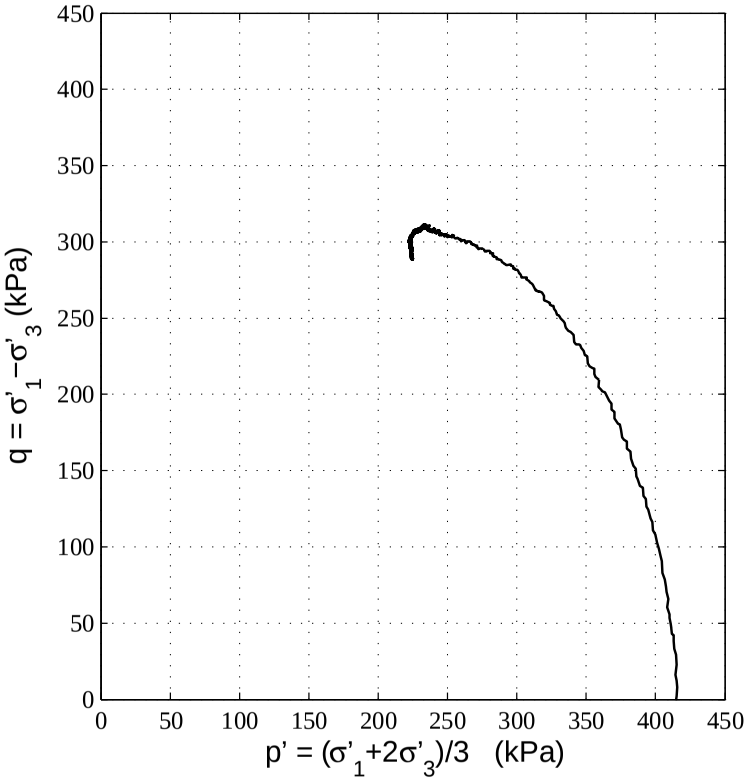

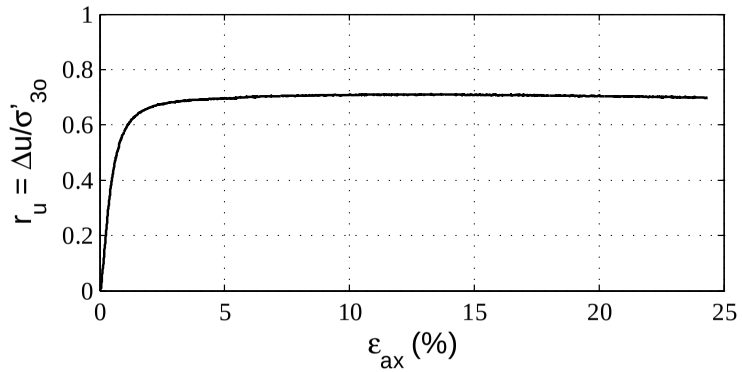

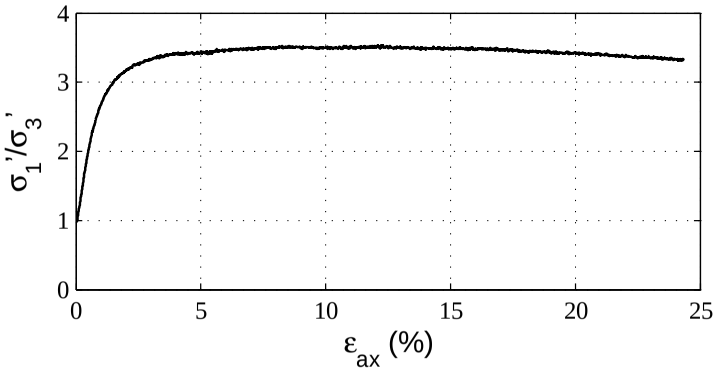

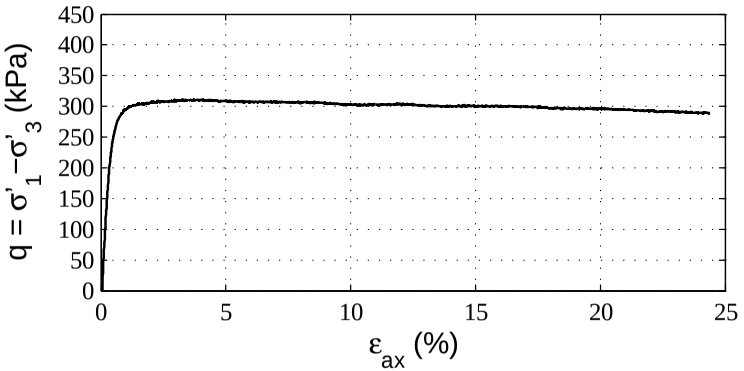

Steady State ICU Monotonic Triaxial Compression Test Data

Site:	VT
Soil Unit:	Upp. Sand
Specimens Mixed:	DM_Z2_BH2_1U_7.44m DM_Z2_B2_2U_7.92m
Test:	Test 2
σ'_{3o} (kPa):	418.8
e_o:	0.95
D_r (%)	35

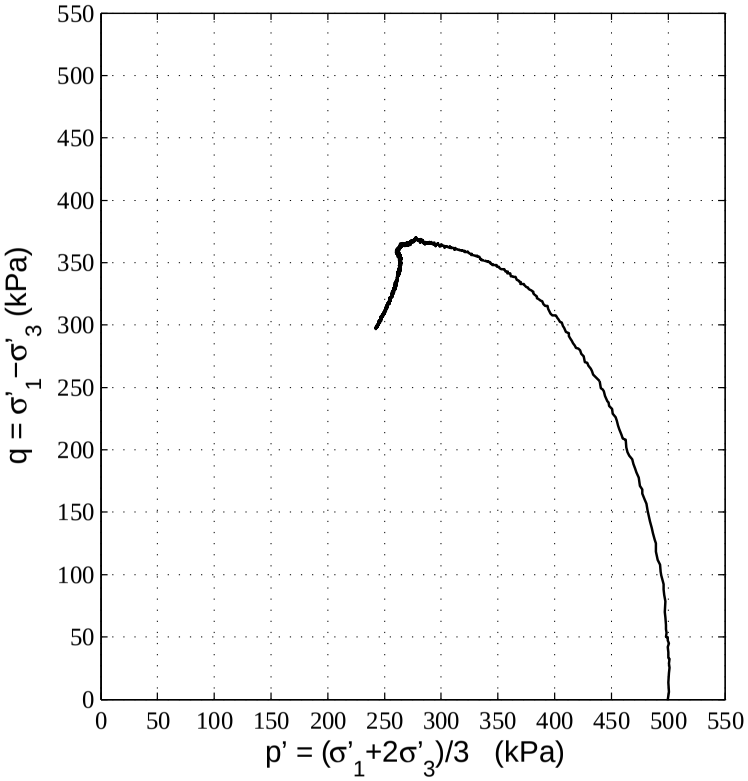

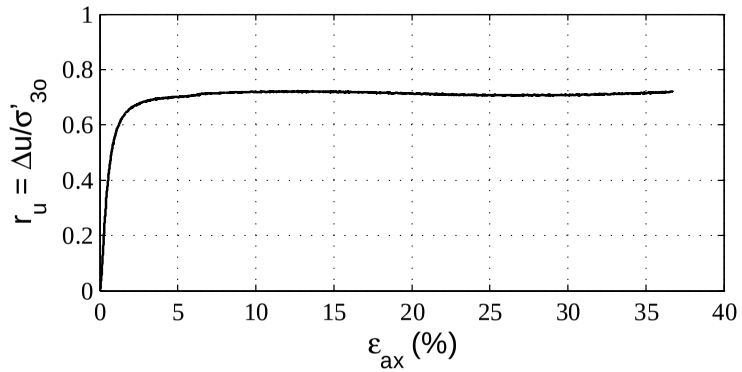

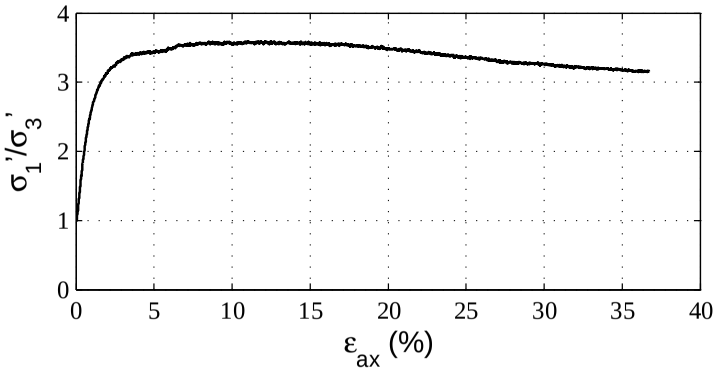

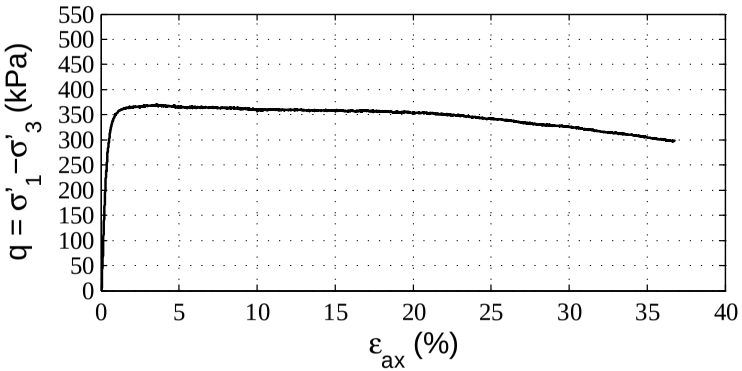

Steady State ICU Monotonic Triaxial Compression Test Data

Site:	VT
Soil Unit:	Upp. Sand
Specimens Mixed:	DM_Z2_BH2_1U_7.44m DM_Z2_B2_2U_7.92m
Test:	Test 3
σ'_{3o} (kPa):	503.0
e_o:	0.93
D_r (%)	39

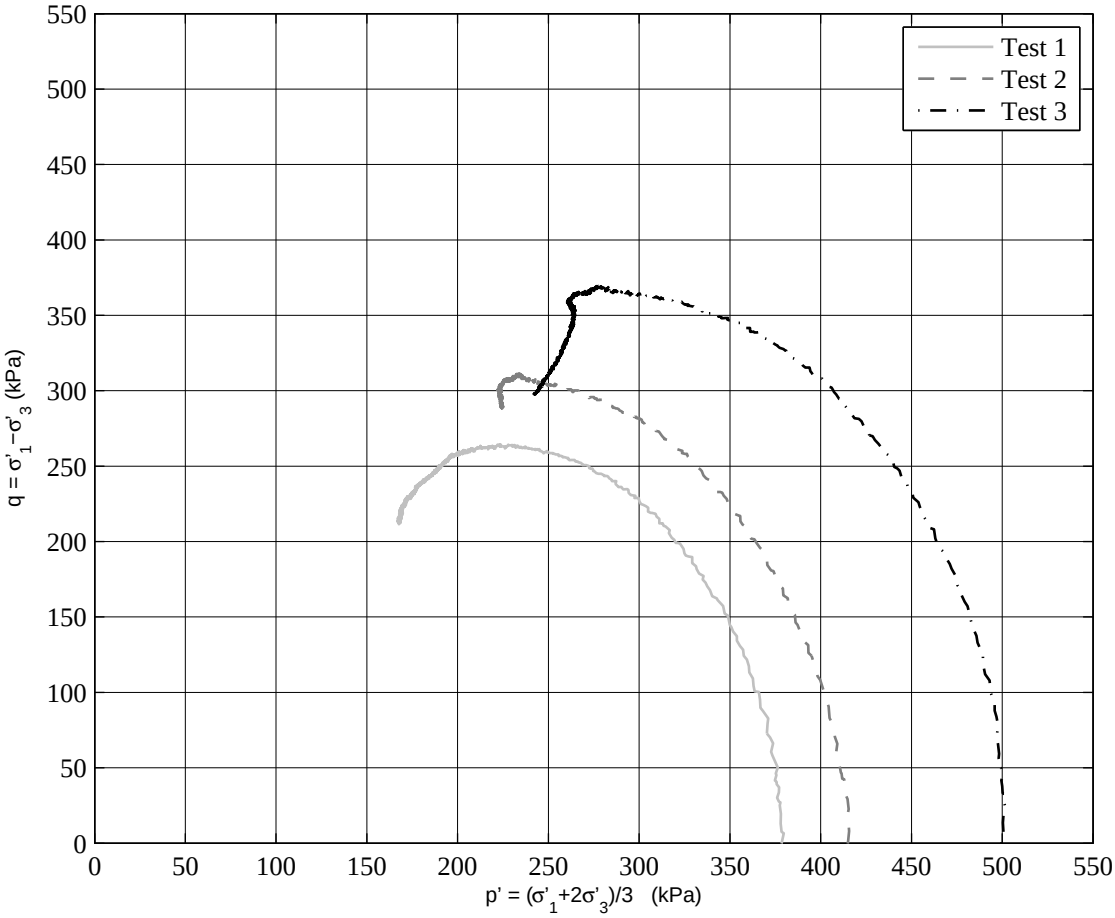
Test 1
Test 2
Test 3
q = σ'1−σ'3 (kPa)
p' = (σ'1+2σ'3)/3 (kPa)
0
50
100
150
200
250
300
350
400
450
500
550

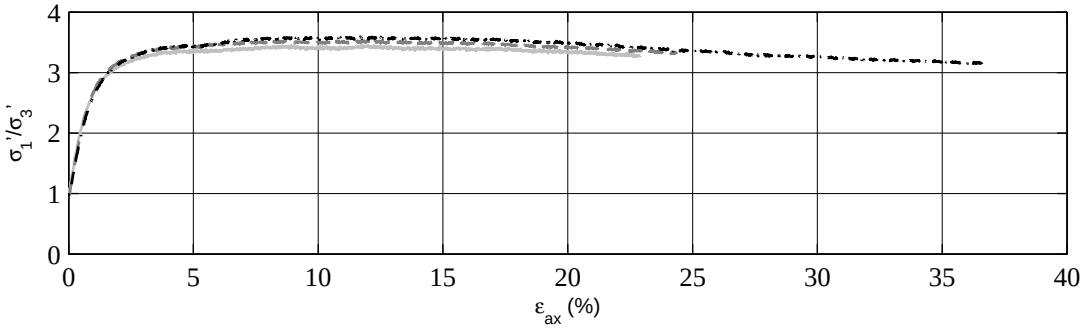
σ1'/σ3'
εax (%)
0
1
2
3
4
5
10
15
20
25
30
35
40

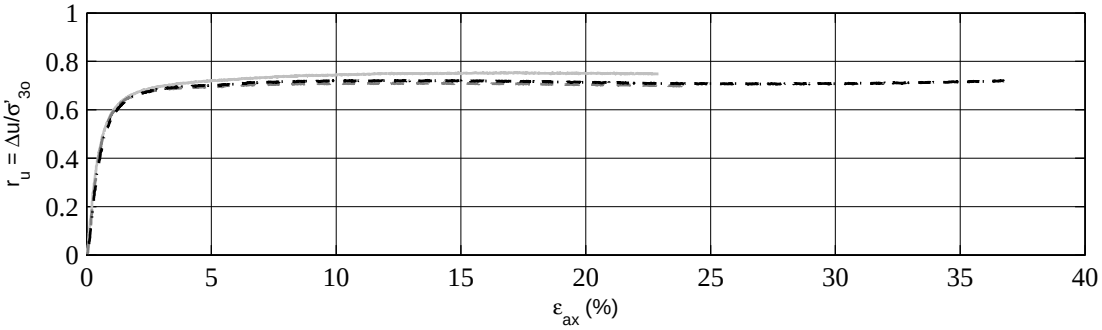
ru = Δu/σ'3o
εax (%)
0
0.2
0.4
0.6
0.8
1
5
10
15
20
25
30
35
40